

**CLINICAL VECTORCARDIOGRAPHY
AND ELECTROCARDIOGRAPHY**

EDWARD MASSIE, A.B., M.D., F.A.C.P., F.A.C.C.

*Associate Professor of Clinical Medicine, Washington University School of Medicine,
Director of Heart Stations, Barnes Hospital and Jewish Hospital, St. Louis,
Director, Cardiovascular Clinic, Washington University Clinics;
Area Consultant in Cardiology to the Veterans Administration*

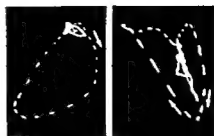
THOMAS J. WALSH, B.S., M.D., F.A.C.C.

*Instructor of Clinical Medicine, Washington University School of Medicine;
Associate Director of Heart Station, Barnes Hospital, Visiting Physician, Jewish Hospital,
Attending Physician, Washington University Service, Veterans Administration Hospital, St. Louis*

Published by

THE YEAR BOOK PUBLISHERS • INC.

200 EAST ILLINOIS STREET, CHICAGO



T



CLINICAL VECTORCARDIOGRAPHY AND ELECTROCARDIOGRAPHY

© COPYRIGHT 1960 BY THE YEAR BOOK PUBLISHERS, INC.

Library of Congress Catalog Card Number 59-12151

PRINTED IN U.S.A.

To Our Families

FELICE, HENRY *and* BARRY MASSIE
and DOROTHY V. *and* JAMES W. WALSH

Preface

PUBLICATIONS IN THE FIELD of clinical and experimental vectorcardiography have increased greatly in number in the past few years. This is a reflection of the widespread and growing interest in the clinical application of this new diagnostic procedure. Vectorcardiography and the vector approach to electrocardiography have proved their clinical value and have contributed immeasurably to the fundamental understanding of the electrical activities of the heart.

In this text we have endeavored to present in a relatively simple and direct manner the principles, methodology, and clinical applications of vectorcardiography and, wherever possible, have correlated the vectorcardiogram with the scalar electrocardiogram. In this way, we hope to help the reader bridge the gap between conventional electrocardiography, vector electrocardiography, and vectorcardiography.

It must be admitted that the ideal spatial vectorcardiogram most accurately representing the electromotive forces of the heart cannot be obtained as yet, although rapid progress is being made toward the attainment of this objective. It is equally true that the enthusiastic upsurge of investigative studies in the field of vectorcardiography has brought with it an unfortunate multiplicity of proposed vectorcardiographic lead systems which yield somewhat differing results. This train of events in turn has led to much confusion. To circumvent this difficulty, we have utilized Grishman's cube system of electrode placement to record the vectorcardiograms appearing in this text. In our experience, it has proved to be a most satisfactory vectorcardiographic method.

The text proper is divided into four principal sections: PART I, "The Normal Electrocardiogram and Vectorcardiogram"; PART II, "The Abnormal Electrocardiogram and Vectorcardiogram"; PART III, "The Cardiac Arrhythmias"; and PART IV, "Other Conditions Affecting the Electrocardiogram." Each of the chapters forming these sections contains many illustrative electrocardiograms and vectorcardiograms. Numerous additional records have been collected and are presented for study in PART V.

We wish to extend our sincere thanks to Drs. Gonzalo T. Roman, Jr., and

Edgar J. Mills, Fellows in Cardiology in the Department of Medicine, Washington University School of Medicine, who helped a great deal in obtaining and interpreting many of the vectorcardiograms, and to Dr. James W. Walsh of the Barnes Hospital Resident Staff, who *reviewed much of the manuscript and made many worthwhile suggestions.*

A number of the Fellows, including Drs. Ralph Copp, Jr., William H. Danforth, Gerald A. Diettert, Charles E. Hogancamp, Milton Kardesch, Brent M. Parker, Ernest E. Pund, Jr., Celestino Sanchez, Porfirio M. Tiongson, and Herbert B. Zimmerman, who worked in the Barnes Hospital Heart Station with us during the past several years, have contributed much and stimulated interest in the vector field. We are grateful for the co-operation of Dr. Carl V. Moore, Busch Professor and Chairman of the Department of Medicine, and Drs. John R. Smith, Bernard A. Bereu, and Sidney Jick, members of the Barnes Hospital Medical Staff, and the House Officers who rotated through the Heart Station.

We want to express our deep gratitude to Miss Marilyn J. Harris, Medical Illustrator of the Washington University Medical School, for her most skillful and able handling of the illustrations, which are so important in a publication such as this. We are very indebted to Miss Edna M. Edwards, Head Technician at the Barnes Hospital Heart Station, who has been of immeasurable help in mounting the vectorcardiograms and electrocardiograms with meticulousness and for her invaluable help with the galley proofs. The Heart Station Technicians, especially Mrs. Eileen R. Gerner, Miss Dorothy M. Hollander, Mrs. Martha Ann Oellermann, and Miss Glenna M. Gambill, *deserve our thanks for their work in enabling us to secure the vectorcardiograms and electrocardiograms.* We also had the valuable help and advice of Messrs. K. Cramer Lewis and Walter J. Coerver, Medical Photographers of the Department of Illustration, Washington University School of Medicine, which we greatly appreciate. In addition, we wish to thank Mrs. Wanda Coburn, Mrs. Jacqueline Nelson, Mrs. Alice Marshall, Miss Ardeth Burrill, and Mrs. Laura Shanklin for their patience in typing the text and legends. Miss Margaret E. Peteler, Head Technician of the Jewish Hospital Heart Station, helped very much in obtaining some of the electrocardiograms showing complex rhythms. Mr. William C. Wetzig of the Sanborn Company co-operated fully in providing technical consultation. Finally, for the consideration and unfailing co-operation of the Year Book Publishers, we wish to express our special thanks.

EDWARD MASSIE
THOMAS J. WALSH

Table of Contents

PART I

THE NORMAL ELECTROCARDIOGRAM AND VECTORCARDIOGRAM

1. BASIC CONSIDERATIONS 3

Electrical Activity of a Single Myocardial Cell, 7. Potential Variations in the Electrical Field of a Myocardial Cell, 11. Vector Representation of the Cardiac Dipole, 13.

2. ELECTROCARDIOGRAPHIC LEADS AND LEAD REFERENCE SYSTEMS 17

Extremity Leads and Frontal Plane Reference Systems, 19. Einthoven's Equilateral Triangle Hypothesis, 21. Unipolar Precordial Leads and Horizontal Reference Frame, 29

3. INSTRUMENTATION, TERMINOLOGY, AND TIME AND VOLTAGE MEASUREMENTS; CONSTRUCTION OF MEAN VECTORS 32

Instrumentation, 32. String Galvanometer, 32. Amplifier Tube and Coil Wire Electrocardiograph, 32. Direct-Writing Electrocardiograph, 32. Oscilloscope Tube Electrocardiograph, 34. Terminology and Time and Voltage Measurements, 34. Electrocardiographic Deflections, 35. Voltage, 35. Time, 35. Heart Rate, 35. Construction of Mean Vectors, 36. Frontal Plane Mean Vectors, 37. Horizontal Plane Mean Vectors, 39

4. THEORETICAL BASES OF THE ELECTROCARDIOGRAPHIC AND VECTORCARDIOGRAPHIC LEADS 43

Equivalent Dipole and Semidirect Lead Hypotheses, 43. Lead Vector, Vector Image, and Lead Field Concepts, 45.

5. THE NORMAL ELECTROCARDIOGRAM 52

General Features of the Normal ECG, 53. The P Wave, 53. The P-R Interval, 54. The Electrical Axes of Rotation, 60. Electrocardiographic Characteristics of the Normal Scalar Electrocardiogram, 61.

6. VENTRICULAR REPOLARIZATION, VENTRICULAR GRADIENT AND SPATIAL QRS-T ANGLE 70

Ventricular Repolarization, 70. The S-T Segment and T Wave, 70. The U Wave, 71. Ventricular Gradient and Spatial QRS-T Angle, 71. The Monophasic Curves and Ventricular Gradient in Myocardial Ischemia, 87. The Spatial QRS-T Angle, 88.

7. VECTORCARDIOGRAPHY

92

Instrumentation, 92. Electrode Placement and Lead Systems, 93. Equilateral Tetrahedron Lead System, 93. Grishman's Cube Lead System, 94. Derivation of Scalar Lead Deflections from the Vectorcardiogram, 99. Construction of Vector Loops from the Electrocardiogram, 102. The Normal Vectorcardiogram, 105. P sE Loop, 108. QRS sE Loop, 108. T sE Loop, 113.

PART II

THE ABNORMAL ELECTROCARDIOGRAM AND VECTORCARDIOGRAM

8. VENTRICULAR HYPERTROPHY: GENERAL CONSIDERATIONS

117

Review of the Pertinent Anatomy and Septal-Ventricular Activation Sequence, 117. Interventricular Septum, 117. Free Walls of Left and Right Ventricles, 117. Electrical Effects of Ventricular Hypertrophy, 118. The Electrocardiogram in Ventricular Hypertrophy, 123

9. LEFT VENTRICULAR HYPERTROPHY

125

The Instantaneous VA Vectors, 125. Ventricular Repolarization, 128. General Electrocardiographic Findings and Related Diagnostic Criteria in Left Ventricular Hypertrophy, 129. Limitations in Diagnostic Specificity of the Criteria in Left Ventricular Hypertrophy, 130. Vectorcardiographic Findings in Left Ventricular Hypertrophy, 131.

10. RIGHT VENTRICULAR HYPERTROPHY

138

The Instantaneous VA Vectors, 138. The Tall R and RSR' Patterns of Right Ventricular Hypertrophy, 139. QRS Configuration in the Precordial Leads in the Tall R and RSR' Patterns of Right Ventricular Hypertrophy, 143. Ventricular Repolarization, 146. General Electrocardiographic Findings in Right Ventricular Hypertrophy, 146. Vectorcardiographic Findings in Right Ventricular Hypertrophy, 148. Vectorcardiographic Tall R P, 148. Vectorcardiographic S-T Vector and T sE Loop, 155

11. COMBINED VENTRICULAR HYPERTROPHY; VENTRICULAR HYPERTROPHY IN CHILDREN

156

Combined Ventricular Hypertrophy, 156. Ventricular Strain Patterns, 158. Ventricular Hypertrophy in Infancy and Early Childhood, 159. The Electrocardiographic Diagnosis of Right Ventricular Hypertrophy, 163. The Electrocardiographic Diagnosis of Left Ventricular Hypertrophy, 164

12. CONGENITAL HEART DISEASE, MITRAL STENOSIS, AND COR PULMONALE: GENERAL CONSIDERATIONS

165

Factors Affecting the Frequency and Prominence of the Patterns of Right Ventricular Hypertrophy, 166. Manner of Transmission of QRS Forces to the Lead Electrode, 166. Duration, Degree, and Type of Right Ventricular Overloading, 167. Presence or Absence of Coexisting Left Ventricular Overloading, 168.

13. CONGENITAL HEART DISEASE

169

Types of Congenital Heart Disease, 169. Stenotic Lesions Causing Systolic Left Ventricular Overloading, 170. Coarctation of the Aorta, 170. Congenital Aortic and Subaortic Stenosis, 172. Stenotic Lesions Causing Systolic Right Ventricular Overloading, 172. Pulmonic Stenosis (Isolated with Normal Aortic Root), 173. Cardiac Shunts Causing Diastolic Left Ventricular Overloading with or without Systolic Right Ventricular Overloading, 174. Interventricular Septal Defect, 174. Patent Ductus Arteriosus, 176. Cardiac Shunts Causing Diastolic Right Ventricular Overloading, 178. Interventricular Septal Defect (with Left-to-Right Shunt), 178. Atrial Septal Defect (with Right-to-Left Shunt), 179. Multiple Cardiac Anomalies or Cardiac Anomalies Accompanied by Other Developmental Defects, 180. Dextrocardia, 180. Tetralogy of Fallot, 182.

14. MITRAL STENOSIS

183

Electrocardiographic Findings, 184. Cardiac Rhythm, 184. The Electrocardiographic and Vectorcardiographic P Mitrale Pattern, 184. Right Ventricular Hypertrophy, 187. Vectorcardiographic Findings, 188. Type A QRS sE Loop Pattern, 189. Type B QRS sE Loop Pattern, 189. Type C QRS sE Loop Pattern, 191.

15. COR PULMONALE AND PULMONARY EMPHYSEMA

192

Clinical Forms of Cor Pulmonale, 192. Genesis of Electrocardiographic Findings in Chronic Cor Pulmonale Due to Pulmonary Emphysema, 193. Chronic Cor Pulmonale and Chronic Pulmonary Disease without Detectable Cor Pulmonale, 194. The Electrocardiographic and Vectorcardiographic Findings in Chronic Cor Pulmonale and in Pulmonary Emphysema without Cor Pulmonale, 195. Right Atrial Enlargement, 195. The Electrocardiographic and Vectorcardiographic P Pulmonale Pattern, 195. Right-Axis Deviation of a QRS, 195. Pre-cordial QRS Pattern of "Marked Clockwise Rotation," 197. Electrocardiographic and Vectorcardiographic Findings in Acute Cor Pulmonale, 211. Acute Pulmonary Embolism with Acute Cor Pulmonale, Electrocardiographic and Vectorcardiographic Findings, 218.

16. LEFT BUNDLE BRANCH BLOCK

221

General Considerations, 221. Mechanisms, 222. The Instantaneous V4 Vectorcardiographic Findings, 227. Incomplete Left Bundle Branch Block, 236.

17. RIGHT BUNDLE BRANCH BLOCK

241

General Considerations, 241. Mechanisms, 241. The Instantaneous V4 Vectorcardiographic Findings, 247. Vectorcardiographic Findings, 247. Diagnosis of Coexisting Ventricular Hypertrophy, 252. Other Types of Intraventricular Block, 254. Focal or Post-infarction Intraventricular Block, 254. Diffuse Intraventricular Block, 254.

18. MYOCARDIAL ISCHEMIA, INJURY, AND INFARCTION: GENERAL CONSIDERATIONS	255
<i>Ischemia, 255. Subendocardial Ischemia, 255. Transmural (Epicardial) Ischemia, 255. Injury, 258. Diastolic Current of Injury, 256. Systolic Current of Injury, 256. Subendocardial and Subepicardial Injury, 259. The -I or S-T Vector of the Vectorcardiogram, 259. Infarction, 259. Mechanism of the QRS Abnormalities of Infarction, 261. Criteria of Q Wave Abnormality, 263. Evolution of an Infarction, 263. Terminology and Classification of Infarction Patterns, 265.</i>	
19. ANTERIOR MYOCARDIAL INFARCTION	268
<i>Anteroseptal Infarction, 268. Strictly Anterior Infarction, 272. Anterolateral Infarction, 278. Extensive Anterior Infarction, 283. S-T Vector and Ventricular Repolarization in Acute Phase of Anterior Infarction, 287</i>	
20. INFEROPOSTERIOR MYOCARDIAL INFARCTION	289
<i>Diaphragmatic (Inferior) Infarction, 289. Posterolateral Infarction, 299. Strictly Posterior Infarction, 308.</i>	
21. MISCELLANEOUS CARDIAC ABNORMALITIES	317
<i>Infarctions in Combined Locations, 317. Myocardial Infarction with Bundle Branch Block, 320. Infarction of the Interventricular Septum, 331. Fibrosis of the Interventricular Septum, 332. Subendocardial Myocardial Infarction, 333. Ventricular Aneurysm, 333. Perinfarction Block, 335. Pericarditis and Myocarditis, 338.</i>	
22. MYOCARDIAL DAMAGE, CORONARY INSUFFICIENCY, AND STRESS TESTS	340
<i>Myocardial Damage and Coronary Insufficiency, 340. Stress Tests, 342. The Anoxemia Test, 342. The Exercise Test, 343</i>	

PART III

THE CARDIAC ARRHYTHMIAS

23. DISTURBANCES OF IMPULSE FORMATION AND CONDUCTION. GENERAL CONSIDERATIONS	353
<i>General Introduction, 353. Atrioventricular Interference and Dissociation, 355. Atrioventricular Block, 356. Autonomic Nervous Tone, 359. Classification of Disturbances of Impulse Formation, 359. Normal Sinus (Sinoatrial) Rhythm, 360. Variant Types of Sinus Rhythm, 360. Sinus Tachycardia and Sinus Bradycardia, 360. Sinus Arrhythmia, 361. "Coronary Nodal Rhythm," 361.</i>	
24. ATRIOVENTRICULAR NODAL AND IDIOVENTRICULAR ESCAPE BEATS AND RHYTHMS	363
<i>The Electrocardiographic Features of Atrioventricular Nodal Beats, 363. Atrioventricular Nodal Escape, 367. Atrioventricular Nodal Escape Rhythms, 369. Persisting Atrioventricular Nodal Rhythm with Complete Atrial Capture, 371. Atrioventricular Nodal Rhythms with Intermittent Atrial Interference (Wandering Supraventricular Pacemaker), 373. Atrioventricular Nodal Rhythms without Atrial Capture (with Atrioventricular Dissociation), 374. Clinical Significance of Atrioventricular Dissociation, 379. Ventricular Aberration of Atrioventricular Nodal Escape Beats, 381. Idioventricular Escape Rhythm, 382</i>	

25 ECTOPIC BEATS AND RHYTHMS

Terminology and General Considerations, 393. Coupled Ectopic Beats, 396. Mechanisms, 396. Coupled Ectopic Atrial Beats, 398. Coupled Ectopic Atrioventricular Nodal Beats, 392. Coupled Ectopic Ventricular Beats, 393. Postectopic T Wave Changes, 398. Clinical Significance of Coupled Ectopic Beats, 400. Automatic Ectopic Beats (Parasyctole), 402.

26 ECTOPIC TACHYCARDIAS; FLUTTER AND FIBRILLATION

407

Paroxysmal Ectopic Tachycardia, 407. Mechanisms, 407. General Considerations, 407. Paroxysmal Supraventricular Tachycardia, 409. Paroxysmal Ventricular Tachycardia, 427. Atrial Flutter and Atrial Fibrillation, 430. Atrial Flutter, 432. Impure Atrial Flutter or Atrial Flutter-Fibrillation, 436. Atrial Fibrillation, 436. Effect of Vagal Stimulation in Flutter and Fibrillation, 439. Clinical Aspects of Atrial Flutter and Fibrillation, 439. Mechanism of Atrial Flutter and Atrial Fibrillation, 442. Ventricular Flutter and Fibrillation, 443.

27 ATRIOVENTRICULAR BLOCK AND SINODIAL BLOCK

446

Atrioventricular Block, 446. Electrocardiographic Features of Atrioventricular Block, 446. Clinical Aspects of Atrioventricular Block, 455. Sinodial Pause, Sinodial Arrest, and Sinodial Block, 455. Clinical Aspects of Sinodial Pause, Sinodial Arrest, and Sinodial Block, 460.

PART IV

OTHER CONDITIONS AFFECTING THE ELECTROCARDIOGRAM

28 DIGITALIS, QUINIDINE, AND PRONESTYL; ELECTROLYTE IMBALANCE

463

Effect of Digitalis on Impulse Formation and Transmission, 463. Digitalis Action, 463. Digitalis Effect on the Electrocardiogram, 465. Quinidine and Pronestyl, 469. Actions of Quinidine and Pronestyl, 469. The Electrocardiographic Changes Due to Quinidine and Pronestyl, 469. Electrolyte Imbalance, 470. Potassium, 470. Calcium, 470.

29 VENTRICULAR PRE-EXCITATION (WOLFF-PARKINSON-WHITE SYNDROME)

480

Mechanism, 480. Accessory Atrioventricular Pathway Theory, 480. Accelerated Atrioventricular Conduction Theory, 481. Validity of the Foregoing Theories of Ventricular Pre-excitation, 481. Electrocardiographic Findings, 483. Production and Termination of Ventricular Pre-excitation, 487. Vectorcardiographic Findings, 489. Paroxysmal Rapid Heart Action in the Wolff-Parkinson-White Syndrome, 489. Clinical Aspects of Wolff-Parkinson-White Syndrome, 493.

PART V

ILLUSTRATIVE VECTORCARDIOGRAMS AND ELECTROCARDIOGRAMS

ILLUSTRATIONS

497

BIBLIOGRAPHY

573

INDEX

583

PART I

The Normal Electrocardiogram and Vectorcardiogram

Basic Considerations

ELECTROCARDIOGRAPHY AND VECTORCARDIOGRAPHY are two related methods of studying the bioelectrical potentials generated by heart muscle. Much has been learned within recent years about the manner in which the myocardial cell produces electromotive force, but many questions still remain unanswered. Briefly summarized, the facts relating to the production of bioelectrical potentials in a single cell are these:

1 Extracellularly, sodium ions are present in high concentration and potassium ions in low concentration, while the reverse is true intracellularly (Fig. 1). The concentration gradient of the sodium ions favors their flow into the cell, and the concentration gradient of the potassium ions encourages diffusion of the latter ions out of the cell. The effect of the concentration gradients of the ions on their diffusion tends to be counterbalanced by electrostatic forces exerted by the ions.

2 The resting cell membrane is impermeable to the sodium ions. However, when the membrane is stimulated, its ionic permeability is increased. This increase is probably related in some way to the release of acetylcholine from the storage form in which it exists in the resting cell. Once released, the free ester acts intracellularly on a specific protein receptor and, perhaps by changing the configuration of this protein, brings about an increase in membrane permeability.

3 Initially, sodium ions flow with the concentration gradient across the membrane into the cell, and this continues until an equilibrium is established. This flow of sodium current has been observed to coincide with the rising phase of the action potential, and the sodium influx is followed by an outflow of potassium ions from the cell during the falling phase of the action potential. When the flow of potassium

current exceeds the sodium current, repolarization of the membrane commences.

4. The triggering agent, acetylcholine, is promptly inactivated by acetylcholine esterase, with the result that the receptor protein returns to its resting state and the ionic impermeability of the membrane is restored.

As a working concept of cellular electrical activity, the electrochemical mechanism just described is less satisfactory, because of its complexity, than the mechanism proposed by Bernstein (Bernstein's membrane theory) in 1913. According to the latter concept, the resting cell membrane (Fig. 2, A) is a non-conductor which accumulates negative ions along its inner surface and positive ions along its outer surface. Every positive charge is paired with and balanced by a negative charge. Current flow between the two charges is prevented by the high electrical resistance of the cellular membrane. A single pair of positive and negative charges lying in close proximity to each other constitutes a dipole. The resting cell membrane with its double layer of balanced positive and negative charges or dipoles is said to be in the polarized state.

If an excitatory stimulus is applied to a point on the cell surface, the electrical resistance of the cell membrane is lowered at the site of stimulation. In effect, a short circuit is created across the stimulated membrane which enables the positive charge of the local dipole to flow into the cell and neutralize its companion negative charge (Fig. 2, B). The local flow of current resulting from stimulation of the resting cell membrane is analogous to the flow of electrical current from positive pole to negative pole of a one-cell battery when the two poles are connected by a conductor. The flow of electrical current from positive charge to negative charge can be considered to reflect the greater pressure or potential of the former; and the force responsible for the current flow,

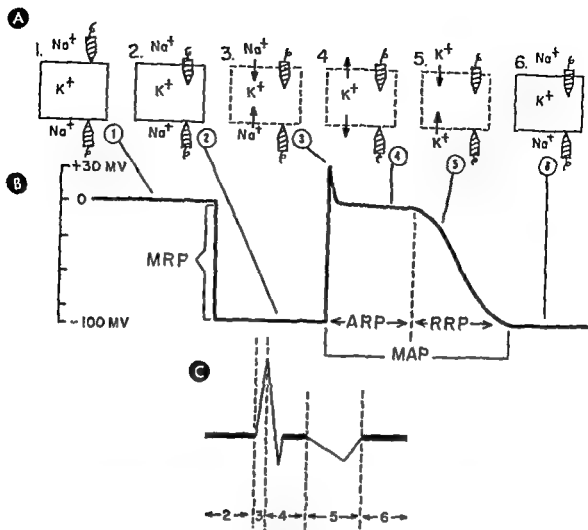
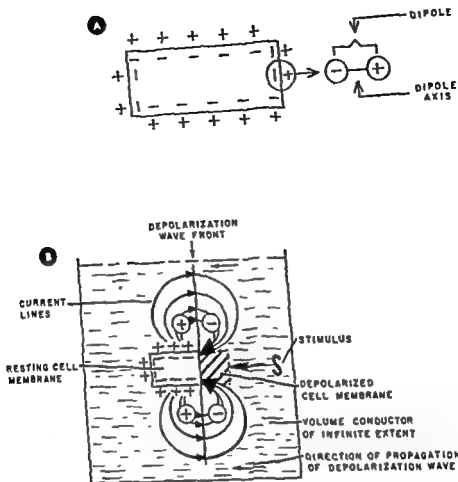


Fig. 1.—Depolarization and repolarization of heart muscle cell. In A, a single heart muscle cell is depicted schematically during the resting phase, depolarization, and repolarization. The transmembrane flow of sodium and potassium ions during these changes in polarization of the schematic muscle cell corresponds to a flow of electrical current in the surrounding conducting medium and results in changes in the potential recorded by two electrodes of a galvanometer. In stage 1, the two electrodes are applied to the surface of the hypothetical cell so that there is no difference in potential between the two electrodes, the galvanometer registering zero voltage, as shown in B. In stage 2, the top electrode is plunged into the interior of the cell, and immediately it gains a negative potential with reference to the lower electrode. This is reflected in the voltage curve, which corresponds to the membrane resting potential, as shown in B. In stage 3, Na ions pass into the cell because of the increased "permeability" with an abrupt rise of the voltage curve and a positive overshoot, as indicated in B. The positive overshoot coincides with the upstroke of the H wave in the electrogram in C. With the subsequent flow of K ions out of the cell, the voltage curve returns to the same level as that in stage 2. Simultaneously, the electrogram in C writes a T wave. The entire period from the upstroke and positive overshoot occurring in stage 3 to the eventual return of the monophasic curve to the same base line as in stage 2 represents the duration of the monophasic action potential (MAP). At stage 6, the schematic heart muscle cell is once again polarized and in the resting phase. The abbreviations ARP and RRP refer to the absolute and relative refractory phases of the cell (See text for detailed discussion.) (After Pick, A., *Digitalis and the electrocardiogram*, Circulation 15:603, 1957.)



rounding conducting medium at a single instant during right-to-left depolarization of the cell

the electromotive force, is derived from the difference in potential between the two dipole charges

Although the transient flow of current resulting from stimulation of cell membrane leaves the local cell membrane in a discharged state, the flow of current also stimulates adjacent resting membrane and, in so doing, lowers the electrical resistance of the latter. As a consequence, a new membrane current appears, which in turn initiates discharge of the next point along the cell surface. This sequence is repeated over and over again until depolarization has spread from one end of the cell to the other. At any instant during cellular depolarization or activation, membrane current flows out of the cell ahead of the depolarization wave front and back into the cell behind it, so that the direction of current flow is from resting

membrane toward neutralized or activated membrane. The greatest amount of current outflow and positive potential exists immediately in front of the depolarization wave front, the greatest amount of current inflow and negative potential, immediately behind the wave front. Consequently, a dipole is created in the conducting medium in close proximity to the membrane surface. The dipole axis, which can be visualized as a straight line connecting positive and negative charges of the dipole, parallels the direction of physiologic activity—that is, the long axis of the cell. The positive pole of the dipole is oriented toward resting membrane, the negative pole, toward activated membrane. The depolarization process can be visualized, therefore, as a self-propagated wave front of surface dipoles which extend around the circumference of the cell in a

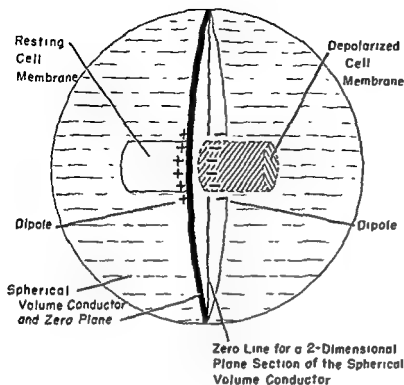
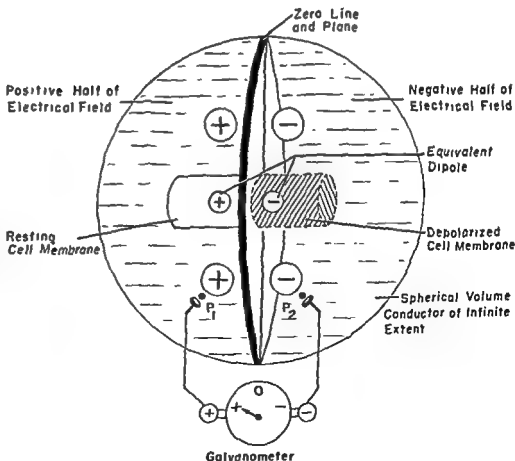


Fig. 3.—A three-dimensional depolarizing cell situated in a spherical volume conductor. At a given instant, the activation wave front consists of a ring of surface dipoles encircling the circumference of the cell. An imaginary perpendicular plane (the zero plane) through the midpoints of the dipole axes divides the cell into a positively charged resting portion and a relatively negatively charged neutralized portion. It also divides the electrical field of the cell into correspondingly charged halves.

Fig. 4.—Equivalent dipole representation of the electrical field of a depolarizing cell. The surface dipoles of the activation wave front are represented by a single equivalent dipole, expressing the net electrical effect of all component dipoles. The electrical field is likewise represented by equivalent dipoles arranged along the zero plane. Thus, if the positive and negative electrodes of a galvanometer are placed at points P_1 and P_2 in the conducting medium, a positive potential difference or positive voltage is registered by the galvanometer.



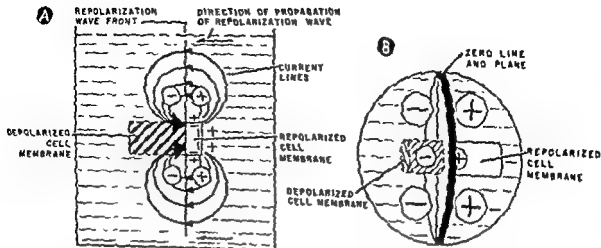


Fig. 5.—Equivalent dipole representation of cellular repolarization. A—cross-section of the cell; B—top-down view.

plane perpendicular to its long axis (Fig 3). All of the dipoles are oriented in the same direction and produce an electrical field of intense positivity in front of the depolarization front and a field of equally intense negativity just behind it. If the cell is situated in a volume conductor (Fig 4), the flow of current through the conducting medium creates an electrical field in which a potential difference exists between any two field points located on opposite sides of a perpendicular line through the dipole center, the zero potential line.

With the completion of depolarization, all membrane surfaces of the cell are uniformly discharged so that the potential difference and electrical field disappear. Restoration of the membrane charges, called repolarization (Fig 5), is accomplished by

cellular metabolism, and in the isolated muscle cell begins at the site first stimulated. As was the case with the depolarization process, the repolarization process can also be considered to spread along the cell membrane as a self-propagated wave front of surface dipoles. However, during repolarization the membrane current flows out of the cell from behind and back into the cell ahead of the wave front. The negative charges of the dipoles along the repolarization wave front precede the positive charges, and the repolarization process advances toward neutralized membrane surfaces, leaving in its wake polarized resting membrane.

ELECTRICAL ACTIVITY OF A SINGLE MYOCARDIAL CELL

As a necessary preface to a discussion concerning the electrical field of a single muscle cell and the distribution of potential in this electrical field, a brief explanation of the galvanometer is necessary.

The galvanometer is basically a very sensitive galvanometer. A galvanometer has two terminals, one of which

is connected to the positive electrode and the other to the negative electrode. The electrodes, when placed at any two points in an electrical field, conduct field currents to the galvanometer terminals, across which is produced a potential difference corresponding to that existing between the field points themselves. The electrical circuit between the galvanometer and the field points where the electrodes are situated con-

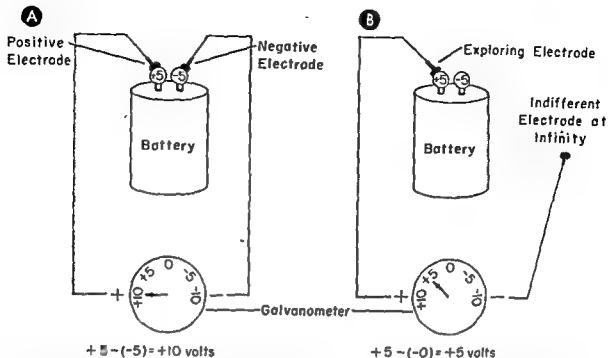


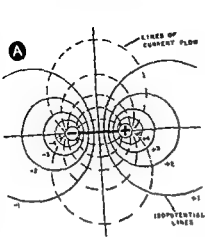
Fig. 6.—Simple examples of bipolar (A) and unipolar (B) leads. In A, the lead wires of the voltmeter are connected to the battery poles so as to form a bipolar lead, and the voltmeter records only the difference in potential between the poles

polar lead

stitutes a *lead*. If the positive lead electrode is either more positive or less negative than the negative electrode, the voltage registered by the galvanometer is positive in sign; if the positive electrode is more negative or relatively less positive than the negative electrode, a negative potential difference is recorded. Leads in which the negative electrode is at zero potential (because the position of the negative electrode is electrically remote from the dipole) are known as *unipolar leads* (Fig. 6). In leads of this type, the positive electrode is called the *exploring electrode*, the negative electrode, the *indifferent electrode*. The potential difference between the exploring and indifferent electrodes of a unipolar lead equals the potential present at the former electrode, since the indifferent electrode is at zero potential. Leads in which the negative electrode and the positive electrode are both at measurable potentials are known as *bipolar leads*. In a bipolar lead (Fig. 6), the voltage registered by the galvanometer is not the potential present at the positive or negative electrode but is, instead, the potential difference between the two electrodes.

It will be recalled that depolarization or repolarization of a single muscle cell immersed in a volume conductor is accompanied by the appearance of membrane currents and an electrical field in the surround-

ing medium. In this electrical field the intense positivity and equally intense negativity existing at a given instant on opposite sides of the depolarization or repolarization wave front are equivalent to the net electrical effect of all surface dipoles present at the time. Consequently, the net effective electromotive force produced at a given instant during depolarization or repolarization of a single muscle cell can be represented by a single resultant or equivalent dipole (Fig. 4). In the case of the single muscle cell, the magnitude or *moment*⁶ of the equivalent dipole equals simply the sum total of the magnitudes of all elementary dipoles, since the dipole forces are exerted in a parallel direction along the long axis of the cell and are therefore directly additive in effect. However, in the case of dipole forces not acting in parallel directions, the effects of the component forces are not directly additive. Thus, to determine the resultant or equivalent dipole force representing the net effective electromotive force of all dipoles of differing directions present, the elementary dipole forces are expressed as vector quantities and are then added vectorially. Vector representation of electrical forces and



A Plane of the Electrical Field of a Single Dipole

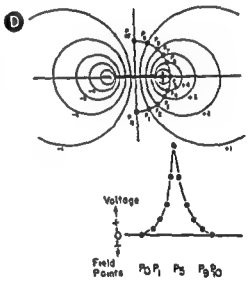
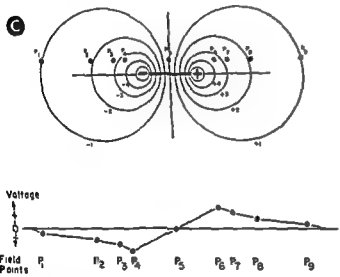
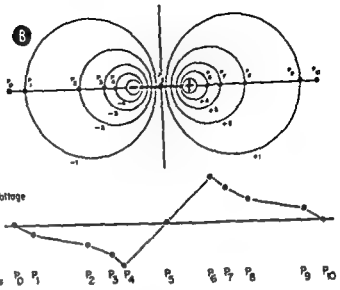


Fig 7.—Diagram of electrical field of a single dipole

field of a si
given arbitr
other point
electrode al

vector mathematics are discussed later in this chapter.

Before discussing the potential variations produced by depolarization and repolarization of a single muscle cell and recorded at various field points, it will be well first to consider the characteristic distribution of potential in the electrical field surrounding a hypothetical dipole and the way this factor influences the potentials recorded at various points in the electrical field. For simplification, the explanation can be presented in the form of a hypothetical experiment, which will entail mapping out in a general way the electrical field* of a dipole (Fig. 7, A). This can be done by placing the indifferent or negative electrode of the galvanometer at electrical infinity and then recording the potential at first one point and then another. In keeping with the purpose of this experiment, the points selected for the measurement of electrical potential will differ by one or both of the following variables: (1) the distance between field point and dipole center, and (2) the angle subtended by the dipole axis and a straight line (r) drawn from the field point to the center of the dipole axis. (By convention, this angle is designated θ and is measured toward the positive pole of the dipole, using as a reference frame a transverse line coinciding with the dipole axis and a perpendicular line through the center of the dipole axis. The positive half of the transverse line is at 0° and the negative half at 180° , while the superior half of the perpendicular line is at 90° .)

The hypothetical experiment alluded to above will be presented in two parts.

Part I.—In this part of the hypothetical experiment (see Fig. 7, B), the electrical field will first be explored from left to right along a line coinciding with the dipole axis. At the periphery of the field, the exploring electrode is so far distant from the dipole that it is essentially at zero potential. However, as the electrode is moved to the right, it gradually approaches the negative charge of the dipole, and a greater and greater negative potential is recorded. The maximal negative potential is registered when the electrode lies nearest or at the negative pole of the dipole. As the electrode is then moved further to the right, the negative potential decreases abruptly, and at a point halfway between the two dipole charges, the electrode is at zero potential. Immediately thereafter, an abrupt rise in positive potential is

recorded which reaches its maximal value when the electrode arrives at a point nearest or coinciding with the positive pole of the dipole. Afterward the positive potential falls off gradually as the electrode moves away from the dipole and approaches the periphery of the field on the right.

If the electrode next explores field points lying along a line at some distance from, but parallel to, the dipole axis (Fig. 7, C), the changes in potential will follow much the same sequence as was just described, although the voltages registered will be smaller. If the exploring electrode is then used to test points situated along a line perpendicular to the dipole axis and passing through its center, the galvanometer registers zero voltage consistently for each point tested, since all points on the perpendicular line through the dipole center lie equidistant from positive and negative charges.

Conclusion.—1 The potential at any field point varies inversely with the distance (r) of the point in question from the dipole center.

2. Zero potential is recorded at all field points located on a perpendicular line through the center of the dipole axis, or, phrased somewhat differently, when a perpendicular to the dipole axis, zero potential is registered

greatest, and the isopotential lines are most closely bunched, along the line coinciding with the dipole axis.

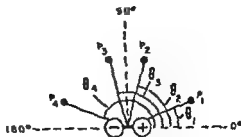
4 The sign of the potential registered at a field point depends on the relative proximity of the positive and negative charges. In other words, if the point tested lies on the negative side of the zero potential line, the voltage registered has a negative sign. If situated on the positive side, a positive sign.

Part II.—If the distance (r) between the exploring electrode and dipole center remains constant (Fig. 7, D), as the electrode is shifted on an arc from the zero potential line gradually toward the line of maximal potential coinciding with the dipole axis, the potential recorded at successive field points increases progressively, while the reverse holds true if the exploring electrode moves in the opposite direction toward the zero potential line. The potential is positive in sign if the electrode is approaching the positive pole of the dipole and negative if it moves toward the negative pole.

Conclusion.—1. If r remains of constant length for all field points tested, but varies with respect to the angle θ it subtends with the dipole axis, the potentials recorded decrease as angle θ approaches 90° and increase as the angle approaches 0° or 180° . In the first instance,

*To simplify the explanation, the following conditions are assumed: (1) a planar section of a perfectly symmetrical electrical field, (2) a single dipole, centrally situated in a homogeneous volume conductor of infinite extent or spherical contour.

the voltage will be positive in sign, in the second, it will be negative.



The relationships outlined in the conclusions of Parts I and II of the hypothetical experiment can be expressed more succinctly in equation form

$$(1) \quad V_p = \frac{e \cdot \cos \theta}{r^2}$$

where V_p is the potential at point P , e is the dipole moment or magnitude; r is the distance of point P from the dipole center, measured along a straight line (r) between the two, and θ is the angle subtended by the dipole axis and r . If r is dropped from the equation, then

$$(2) \quad V_p = e \cdot \cos \theta$$

Since, in actuality, V_p varies inversely with angle θ when the latter is between 0° and 90° , and directly with angle θ when it is between 90° and 180° , it is more convenient to utilize the cosine function of angle θ , which bears a direct relationship to V_p regardless of the size of the angle. Thus,

$$(3) \quad V_p \propto \cos \theta$$

The significance of the preceding equation is illustrated in the accompanying drawing

$$\left. \begin{array}{l} V_{P_1} \\ V_{P_2} \\ V_{P_3} \end{array} \right\} \sim L\theta \quad \left. \begin{array}{l} V_{P_1} \\ V_{P_2} \\ V_{P_3} \end{array} \right\} \sim \frac{1}{L\theta} \quad \text{or, } V_p \sim \cos \theta$$

Equation 2 expresses, in a simple way, the manner in which the physical laws governing the distribution of lines of current flow and isopotential lines in the hypothetical electrical field of a single dipole determine the potentials recorded at any point in that field.

raphy is constructed, and an attempt is made to determine the relationship between the electrical field of the human heart and the electrical field of a single dipole.

eral way, to the electrical field of the human heart by making certain assumptions concerning the characteristics of the human body as a volume conductor. In fact, it will be shown in Chapter 2 that Equation 2 provides the basis for the explanation of the manner in which body surface leads respond to the electrical forces of the heart.

POTENTIAL VARIATIONS IN THE ELECTRICAL FIELD OF A MYOCARDIAL CELL

In the preceding hypothetical experiment, the exploring electrode was placed in the electrical field at different positions with respect to a dipole of fixed location. However, during depolarization or repolarization of a single cell, the dipole does not remain in a fixed position but travels from one end of the cell to the other.

galvanometer (Fig. 8) The indifferent electrode of

the unipolar lead is placed at a great distance from the muscle cell and remains at a uniform zero potential during the period of electrical activity. To compare the potentials present simultaneously at three field points—one point at each end of the cell (Fig. 8, points A and C) and the third at its midpoint (Fig. 8, B)—it will be supposed that the galvanometer has three exploring electrodes with recording channels for each, just as a multichannel electrocardiograph has. The potential variations from instant to instant are recorded graphically by the galvanometer as curves or deflections of a moving base line, these wave forms representing voltage plotted against time (paper speed). The size of the deflection measured from

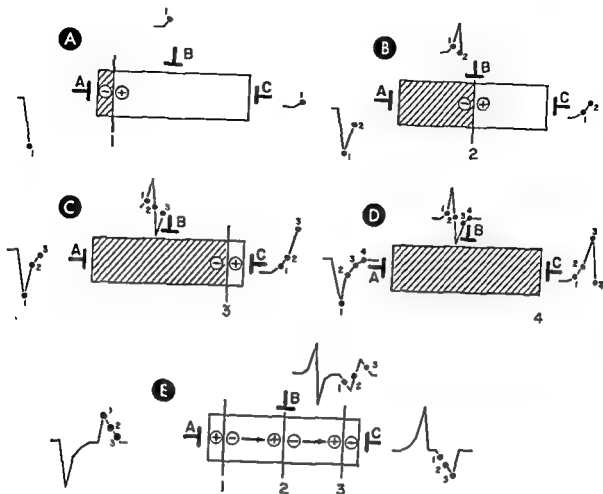


Fig. 8. The potential wave at one electrode (A, B, or C) as a dipole moves past it (A, B, and C) and repolarization (E). The

the isoelectric base line is determined by the magnitude of the voltage, and the direction of the deflection, by the voltage sign. Positive voltage causes an upswing of the base line, negative voltage, a downswing. If the muscle cell is stimulated at its left end, membrane current begins to flow and a field of electromotive force, represented by a resultant or equivalent dipole, appears. At this instant, electrode A facing the stimulated end of the cell is in closer proximity to the negative charge of the dipole than at any time subsequently. Therefore, electrode A is at maximal negative potential, and this is evidenced graphically by a sharp downward deflection of the voltage curve. The other two electrodes lie in the positive field of the dipole. Since electrode B, overlying the center of the cell, is closer to the positive dipole charge than is electrode C at the distal end of the cell, electrode B is at a greater positive potential and shows a more prominent upward deflection of its voltage curve. As depolarization continues and the equivalent dipole

moves farther away from electrode A and nearer to electrodes B and C, the negative potential at A steadily diminishes while the positive potential at electrodes B and C increases. Thus, as the downward voltage curve for electrode A gradually drifts upward, the upright curves for electrodes B and C become taller. The maximum positive voltage and the peak of the voltage curve for electrode B are reached shortly before the dipole arrives directly under electrode B. At this instant, the electrode lies equidistant from positive and negative dipole charges, and it is therefore at zero potential, the voltage curve for electrode B falling to the isoelectric or zero line. Shortly thereafter, the potential at electrode B suddenly plunges to a maximum negative potential, and the voltage curve drops to the nadir of a downward deflection, because of the close proximity of the electrode to the negative charge of the dipole. During the remainder of depolarization, the dipole moves steadily away from electrodes A and B (which record pro-

gressively smaller negative potentials) and approaches electrode C. The increasing positive po-

completion of depolarization. When this occurs, the dipole is abruptly extinguished and the voltage curve for each electrode returns to the isoelectric line.

Conclusion—The voltage deflections representing graphically the potential variations at electrodes A, B, and C during depolarization of a single cell (see Fig. 8) are as follows:

plus-minus (negative deflection is assumed) at

two minus components.

3. At electrode C, overlying the opposite end of the cell, an upward deflection of maximum size, an R wave, is recorded. The curve gradually ascends to its peak and

case of electrode C. This abrupt downstroke from the peak of the voltage deflection is called the intrinsic deflection and, in research electrocardiography, is thought to signify the arrival of the activation wave in the tissues underlying an electrode applied directly to the epicardial surface of the heart. The importance of the intrinsic deflection, or intrinsicoid deflection, as it is designated in clinical electrocardiography, will be discussed later.

Repolarization commences at the left end of the cell and proceeds along the membrane in the same direction as depolarization. However, the resultant dipole produced by repolarization membrane current is so oriented that the negative charge precedes the

depolarization except that they are oppositely directed and longer voltage the de-

rection produced by depolarization except that in repolarization the downward deflection of the diphasic complex is written before the upward component, while the reverse holds true in depolarization.

In clinical electrocardiography, the voltage deflections recorded when the atria depolarize and then repolarize are labeled, respectively, the P and Tp or Ta waves, and the corresponding ventricular deflections are the QRS and T waves.

VECTOR REPRESENTATION OF THE CARDIAC DIPOLE

Any quantity which has direction and magnitude is a vector quantity. A scalar quantity is one having only magnitude, not direction. Thus, temperature, weight, and potential are scalar quantities, while force, specifically the electromotive force represented by a dipole, is a vector quantity (Fig. 9). The direction in which a force is acting is indicated by the direction the vector arrow points, the magnitude of the force, by the length of the arrow. When the electrical force of a dipole is being depicted, the length of the vector represents the strength of the vector.

It

ties (these with scalar quantities). Vector addition, or, more correctly, vector composition, is the process by which two or more vector quantities are combined geometrically. For purpose of explanation, it will be supposed that two vectors representing forces of known magnitude and direction

are to be added to each other. The two vectors are laid off from the same point (O), and a parallelogram is constructed using the vectors as two sides.

single

It is possible to use the triangle method of vector addition, the triangle method can also be used to determine the resultant of two or more vectors. In this method, the two vectors are laid off so that the tail of the second vector coincides with the tip of the first. A line drawn from the tail of the first vector to the tip of the second depicts the resultant.

order in which the line drawn from the vector added to all the vectors,

represents the resultant of

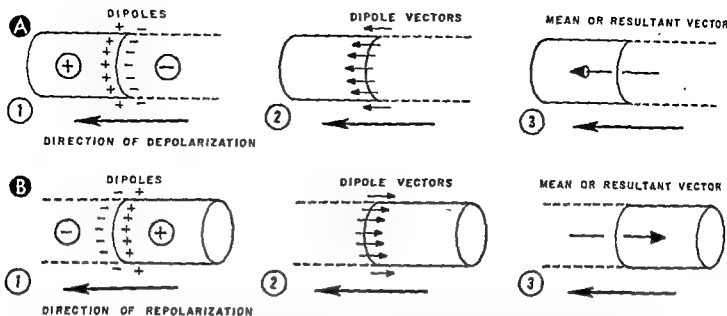


Fig. 9.—Resultant or mean vector representation of electrical activity of heart muscle cell. The drawings show that the electrical field and dipoles produced by depolarization (A) and repolarization (B) of an isolated heart cell can be represented by a single resultant vector. Note, in B, 2 and 3, that the head of the vector points toward the field of electrical positivity, not in the direction in which the cell is being repolarized.

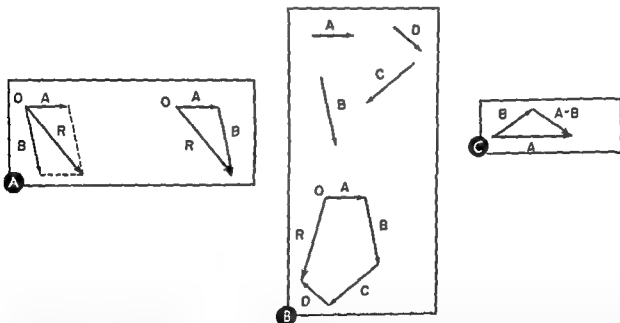


Fig. 10.—Vector mathematics. The resultant vector (R) of two or more component vectors is calculated in A and B by two methods of vector addition or vector composition, the more useful of the two being the parallelogram method in A. In C, the method of subtracting two vectors is shown—in this instance, vector B being subtracted from vector A .

Fig. 11.—The trigonometric basis of vector projection
A, the law of cosines. This law states that the square on any side of a triangle is equal to the sum of the square on the other two sides diminished by twice their product into the cosine of the included angle, or

$$A^2 = B^2 + C^2 - 2BC \cos (180^\circ - \alpha)$$

Since $\cos (180^\circ - \alpha) = -\cos \alpha$,

$$A^2 = B^2 + C^2 + 2BC \cos \alpha$$

Let it be supposed that two forces represented by vec-

demonstrated

1 If the magnitude of vector B is 4 units, the magnitude of vector C is 3 units, and angle α equals 90° , then

$$A^2 = 16 + 9 + 24 (\cos 90^\circ)$$

but the cosine of 90° is 0. Therefore,

$$A^2 = 25, A = 5$$

2 If angle α equals 0° and $\cos 0^\circ = 1$, then $\cos \alpha$ equals 1. Therefore, substituting the known value of 1 for $\cos \alpha$ in equation $A^2 = B^2 + C^2 + 2BC \cos \alpha$, then

$$A^2 = B^2 + 2BC + C^2, \text{ or}$$

$$A^2 = (B + C)^2$$

$$A^2 = (4 + 3)^2, \text{ or } A = 7$$

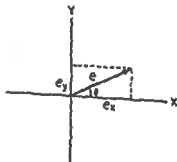
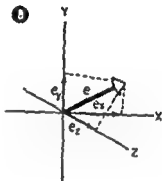
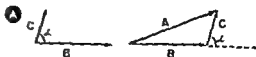
3 If angle α equals 180° , then $\cos 180^\circ = -1$

$$A^2 = B^2 - 2BC + C^2 = (B - C)^2$$

Therefore, $A = B - C = 1$.

This simple trigonometric problem demonstrates that, when forces are directed parallel to each other and in the same direction, the magnitude of the resultant vector is the sum of the magnitudes of the two component vectors, when parallel forces act in the opposite direction, the magnitude of their resultant is the difference between the magnitudes of the two component vectors. When they act in perpendicular directions, the magnitude of their resultant is intermediate between these two extremes.

B , the X , Y , and Z components of a cardiac spatial vector. The magnitude of the cardiac spatial vector is equal to the vectorial sum of its X , Y , and Z components (See text for details.)



A single force can be defined in terms of its components (Fig. 11, B). The component of a force in any particular direction is defined as the effective magnitude of the force in that direction.

In electrocardiography and vectorcardiography, the equivalent dipole vector is often described in terms of its effective magnitude along the three natural co-ordinate axes of the body, namely, the transverse (X), vertical (Y), and sagittal (Z) axes. The dipole vector can therefore be resolved into its X , Y , and Z components, or, conversely, the dipole vector is equal to the vectorial sum of its X , Y , and Z components. To find the magnitude of the X and Y components of the dipole vector, for example

The length and direction of the resultant of two vectors can be computed more exactly by means of the law of cosines (see Fig. 11, A) and the trigonometric rule that the sides of a triangle are respectively proportional to the sines of the angles opposite the sides. This simple trigonometric problem indicates that, when forces are directed parallel to each other and in the same direction, their resultant is equal to the sum of their magnitudes.

When two vectors directed along the same straight line is their algebraic sum.*

*To subtract two vectors directed along the same straight line is to subtract their magnitudes.

tors are indicated by the end of -

(assuming that the direction and magnitude of the dipole vector were known), lines are drawn from the tip of the vector to the X and Y axes so as to complete a parallelogram having the dipole vector as its diagonal (Fig. 11, B). The diagonal divides the parallelogram into two right-angle triangles having the dipole vector as their hypotenuse. The length of the dipole vector equals the dipole moment. Angle θ is the angle between the dipole vector and the X axis; the side adjacent to angle θ is the X component of the dipole vector; and the side adjacent to the angle $(90^\circ - \theta)$ is the Y component. However, components X and Y in the figure are simply the lengths demarcated by perpendiculars from the tip of the dipole vector on lines coinciding with the X and Y co-ordinate axes. Therefore, the effective magnitude of the dipole vector along the X or Y axis, or along the axis of a given lead, is equal to the projection of the dipole vector on that axis. Since other factors enter into determination of the lead voltage in electrocardiography, this rela-

tionship must be rephrased as follows: The voltage recorded in a given lead varies directly with the projection of the cardiac vector on the lead axis. This is the vectorial equivalent of the relationship: The voltage recorded in a given lead varies directly with the dot product of e and $\cos \theta$ ($e \cdot \cos \theta$), where e is the dipole moment and θ the angle subtended by the lead axis and dipole axis.

To project a vector on a lead axis, perpendiculars are dropped from the ends of the vector to the axis. If the vector projects on the positive half of the lead axis, the voltage registered by the lead has a positive sign, if the vector projects on the negative portion of the lead axis, the lead voltage has a negative sign. If the vector parallels or coincides with the lead axis, it projects maximal voltage on the lead. A vector directed perpendicular to a lead axis does not project on the lead axis, and so the galvanometer shows zero voltage.

Electrocardiographic Leads and Lead Reference Systems

IN CHAPTER 1 it was indicated that during depolarization or repolarization of a single muscle cell the electrical forces produced at any given instant can be represented by a single equivalent dipole or mean vector, which expresses the sum total effect of all elementary dipole forces present. According to the

assumed that excitation spreads radially through the atria at a uniform speed, in marked contrast with ventricular excitation. Not only are the free walls of the ventricles much thicker than those of the atria, but the ventricles possess a specialized conducting system, the Purkinje system. This system consists of an

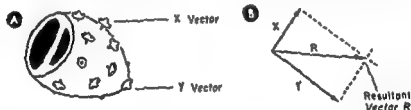


Fig. 12.—Vector representation of electrical activity. The electrical activity of the heart, as manifested at the body surface, can also be represented at any given instant by a single equivalent dipole or its corresponding mean vector. However, the processes of depolarization and repolarization are much more complex in heart muscle than in the single muscle cell. This is especially true of ventricular muscle. Atrial myocardium, on the other hand, behaves much like an isolated muscle strip. Therefore, atrial excitation and recovery are believed to begin in the same region and to proceed through the atria in the same direction. In addition, since the atria have not been demonstrated to have a specialized conducting apparatus and because of the thinness of atrial muscle, it is generally

assumed that excitation spreads radially through the atria at a uniform speed, in marked contrast with ventricular excitation. Not only are the free walls of the ventricles much thicker than those of the atria, but the ventricles possess a specialized conducting system, the Purkinje system. This system consists of an

extensive network of conducting fibers which are distributed throughout the entire subendocardium of both ventricles and penetrate deeply into the inner two thirds of the ventricular wall. As a consequence, subendocardial muscle is the first to undergo activation, and does so quite rapidly. The excitation wave then spreads outward more slowly through the ventricular wall.

Since the electrical effects of ventricular depolarization and repolarization are a function of the electrical effects at the endocardial and epicardial surfaces, it is a permissible and useful simplification to visualize a segment of ventricular wall as if it consisted of a single muscle fiber extending from endocardium to epicardium. Thus, with this supposition,

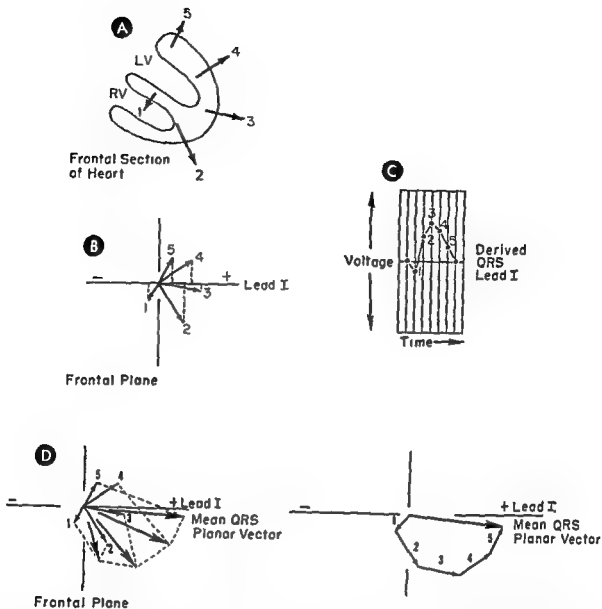


Fig. 13.—The mean instantaneous QRS vectors and the mean QRS vector of the electrocardiogram. **A**, schematic frontal section of the ventricles. The numbered vectors represent successive mean instantaneous QRS planar vectors through instantaneous vector on the axis of lead I, plotted against time, reproducing the electrocardiographic QRS deflection which would be recorded by lead I. It is evident that the changing projection of the vectors on the axis of derivation of lead I is responsible for the detailed features of the QRS deflection. **D**, two methods of vector addition of the mean instantaneous QRS planar vectors to obtain the mean QRS planar vector. The mean QRS vector expresses the net effective or resultant magnitude, polarity, and direction of the five mean instantaneous vectors and is related to the resultant voltage and direction of the QRS deflection in lead I.

the electrical forces produced by activation of such a segment of ventricular wall are directed outward, inasmuch as

produced during activation of different portions of ventricular free wall vary widely in direction, electrical sense, and magnitude (Fig. 12). Some of the forces act in much the same direction and therefore augment one another, others act in opposite directions and counterbalance one another. The balance arrived at between opposing forces determines the electrical field of the heart at a given instant, as represented at the body surface, and can be visualized as a single equivalent dipole or mean instantaneous spatial vector. It is as if the electrocardiograph in effect calculates the projection of the mean instantaneous spatial vector on its lead axis by the electronic equivalent of vector addition.

Depolarization and repolarization do not occur simultaneously in every region of the heart but spread successively through the myocardium from one point to the next. Since the electrical forces existing at each instant during depolarization or repolarization arise in a different portion of the heart,

(Fig. 13, A) It is the changing projections of these vectors on a given lead axis (Fig. 13, B), plotted against time (paper speed), which produce the P, QRS, and T deflections recorded by the lead (Fig. 13, C and D). Since the heart is a three-dimensional structure situated in a volume conductor, the body torso, the electrical forces produced by the heart must necessarily be spatially oriented forces and, accordingly, must be represented as spatial vectors.

graph the instantaneous cardiac spatial vectors.

Since, as previously indicated, a cardiac spatial vector is equal to the vectorial sum of its projections on the transverse (X), vertical (Y), and sagittal (Z) axes (i.e., the sum of its X, Y, and Z components)—in theory at least—one could define the spatial characteristics of such a vector by recording its projections on three leads whose axes coincide with the natural co-ordinate axes of the body. In reality, the components of a cardiac vector cannot be determined accurately from the voltages recorded in body surface leads. The reasons for this are inherent in the characteristics of the body as a volume conductor: (a) the body is not electrically homogeneous, nor is it symmetrical in contour; (b) the electrical center of the heart is not centrally placed in the torso, and (c) the body is not a volume conductor of infinite extent. Therefore, since no body surface lead is electrically remote from the heart, the voltages recorded are significantly influenced by the distance of the lead electrodes from the electrical center of the heart, the voltages varying inversely with the cube of the distance between heart and electrode. For these reasons, the voltage registered in any surface lead is directly proportional but not equal to the projection of the vector on the axis of the lead, since the factors cited above modify the lead voltage. Nevertheless, the direction and magnitude of a spatial vector can be approximated, at least, by recording three or more leads which contain the X, Y, and Z components of the vector. This is equivalent to determining the projections of the vector on two body planes, since the frontal plane contains components X and Y, the horizontal plane contains components X and Z, and the

respond to the six extremity leads which on the front record the

EXTREMITY LEADS AND FRONTAL PLANE REFERENCE SYSTEMS

The standard bipolar limb leads (Fig. 14)—leads I, II and III—were developed originally by Einthoven and his associates, and their usefulness has diminished little over the years. In recording these leads, the positive and negative terminals of the electrocardiograph are connected to the left arm, and the right arm, and the foot. Neither electrode is connected to the ground potential, in contrast to

unipolar leads. The polarity of lead I is such that an upright or positive deflection of the electrocardiographic base line occurs when the potential at the left arm is relatively positive with reference to that at the right arm, and a downward or negative deflection is written when the left arm potential is relatively negative with respect to the right arm potential. If LA signifies the potential at the left arm, and RA the potential at the right arm, then Lead I = LA - RA

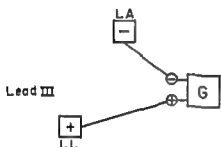
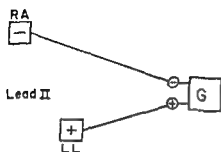
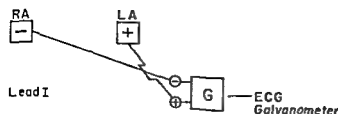
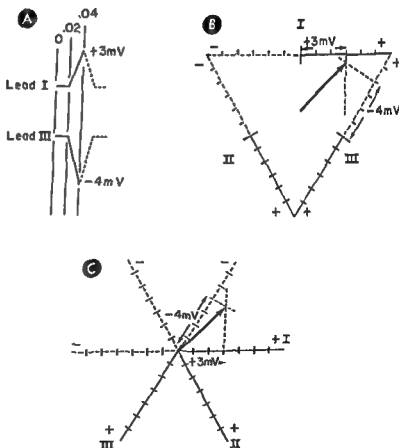


Fig. 14.—Lead wire connections and galvanometer (G) polarity in the three standard bipolar extremity leads leads I, II, and III. RA, right arm, LA, left arm; LL, left leg

Fig. 15.—Method of constructing a mean instantaneous QRS vector from the electrocardiogram. The voltages registered by leads I and III at 0.04 second of the QRS interval (A) are plotted along the appropriate lead axes of the reference figures in B and C, the former being Einthoven's equilateral triangle and the latter, the triaxial reference frame. Perpendiculars are then dropped from the plotted points. The vector drawn from the center of the reference frame to the point of intersection of the perpendicular lines is the frontal (plane) mean 0.04-second instantaneous QRS vector or mean instantaneous electrical axis of QRS at 0.04 second of the QRS interval.



Lead II—The positive electrode is connected to the left leg, and the negative electrode to the right arm. If LL represents the potential at the left leg, then $\text{Lead II} = LL - RA$

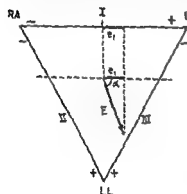
Lead III—The positive electrode is connected to the left leg, and the negative electrode to the left arm. Therefore, $\text{Lead III} = LL - LA$

If the three bipolar limb leads are considered to form a closed circuit, then, according to Kirchhoff's law, the algebraic sum of all the potential differences

is. This is referred to as *Einthoven's law*, though it is not based on his equilateral triangle theory. In fact, the relationship between the potentials in leads I, II, and III remains the same even if the triangle formed by the axes of these leads is not an equilateral triangle.

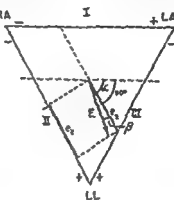
Einthoven's Equilateral Triangle Hypothesis

Almost a half century ago, Einthoven and his associates formulated certain postulates which contained



$$\cos \alpha = \frac{e_1}{E} \text{ or}$$

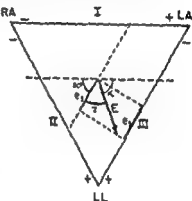
$$e_1 = E \cos \alpha$$



$$\cos \beta = \frac{e_2}{E}$$

$$\text{but } \beta = \alpha - 60^\circ$$

$$\therefore e_2 = E \cos (\alpha - 60^\circ)$$



$$\cos \gamma = \frac{e_3}{E}$$

$$\text{but } \gamma = 180^\circ - (\alpha + 60^\circ)$$

$$\text{or } \gamma = 120^\circ - \alpha$$

$$\therefore e_3 = E \cos (120^\circ - \alpha)$$

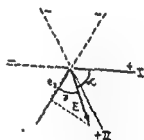
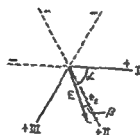
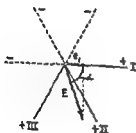


Fig. 16—Continued.

e trigonometric
or the triaxial

in a closed circuit is zero, and therefore, $\text{Lead I} + \text{lead II} + \text{lead III} = 0$

However, Einthoven reversed the galvanometer connections for lead II so that the deflections recorded in this lead would be upright in most individuals. Therefore, $\text{Lead I} + (-\text{lead II}) + \text{lead III} = 0$, or $\text{Lead I} + \text{lead III} = \text{lead II}$. Thus the sum of the potentials in leads I and III equals the potential in lead

the nucleus of the present-day equivalent dipole, or mean vector, concept of electrocardiography. These postulates, which in the aggregate are referred to as *Einthoven's triangle hypothesis*, are as follows:

1. Einthoven proposed to treat the bipolar limb leads as if the electrodes at the left and right shoulders (the extremities acting merely as extensions of the lead wires of the electrodes) and at the pubis were

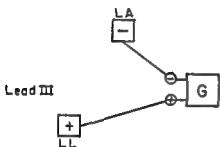
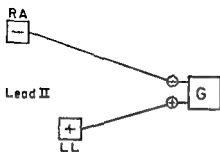
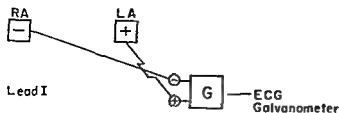
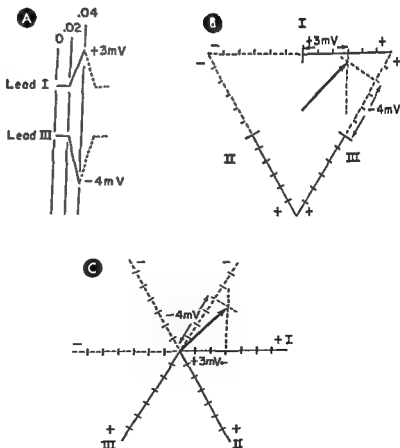


Fig. 14.—Lead wire connections and galvanometer (G) polarity in the three standard bipolar extremity leads: leads I, II, and III RA, right arm, LA, left arm, LL, left leg

Fig. 15.—Method of constructing a mean instantaneous QRS vector from the electrocardiogram. The voltages registered by leads I and III at 0.04 second of the QRS interval (A) are plotted along the appropriate lead axes of the reference figures in B and C, the former being Einthoven's equilateral triangle and the latter, the triaxial reference frame. Perpendiculars are then dropped from the plotted points. The vector drawn from the center of the reference frame to the point of intersection of the perpendicular lines is the frontal (plane) mean 0.04-second instantaneous QRS vector or mean instantaneous electrical axis of QRS at 0.04 second of the QRS interval.



frame is equidistant from the positive and negative electrodes of each lead and is therefore at zero potential. Since the lead axes are transposed without changing their orientation (or their polarity), they form a triaxial reference frame, divided into 60° angles and into sextants numbered I to VI in a counterclockwise direction from the positive axis of lead I.

Einthoven used the equilateral triangle to determine the frontal plane orientation of the mean manifest vector. The qualifying term *manifest* can be used whenever reference is made to the planar projection of a cardiac spatial vector, but is not so used in this

text except in the discussion of electrical axis and the ventricular gradient.

If the voltage deflections in the bipolar limb leads (or any leads) are used to construct a vector representing the orientation and magnitude of an instantaneous manifest vector, the constructed vector can be designated the *instantaneous electrical axis*. The mean or average of all vectors depicting the instant-to-instant change in the instantaneous electrical axis during a given interval of the cardiac cycle is called the *mean electrical axis* for the interval in question. The foregoing terms will be used interchangeably in

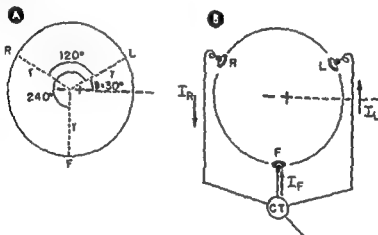


Fig 18 — Mathematical proof that the central point is at zero potential.

tions of Einthoven's triangle.

remembered that the central point is at zero potential.

pressed by the

of the dipole axis, and θ , the angle between a line drawn from p to the dipole center and a line coinciding with the dipole axis. In A,

$$V_L = \frac{K \cos \theta}{r^2}, V_R = \frac{K \cos (\theta + 120^\circ)}{r^2}, \text{ and } V_F = \frac{K \cos (\theta + 240^\circ)}{r^2}$$

Inasmuch as the values for K and r^2 are the same in each of the three equations, the value of $\cos \theta$ is the same in each of the three equations. Inasmuch as the value of $\cos \theta$ is the same in each of the three equations, the value of $\cos \theta$ is the same in each of the three equations. Thus,

Therefore,

$$\cos 150^\circ = -\cos 30^\circ, \text{ and } \cos 270^\circ = 0$$

$$V_L + V_R + V_F = \cos 30^\circ + (-\cos 30^\circ) + 0$$

$$V_L + V_R + V_F = 0$$

$$V_L + V_R + V_F = 0$$

$$V_L + V_R + V_F = 0$$

$$V_L + V_R + V_F = 0$$

$$V_L + V_R + V_F = 0$$

$$V_L + V_R + V_F = 0$$

... of the network can be rewritten as follows: $V_R - V_{CT} = V_{CT} - V_L + V_{CT} - V_F$, or $3V_{CT} = V_R + V_L + V_F$. Therefore, $V_{CT} = \frac{V_R + V_L + V_F}{3}$. However, as shown in A, $V_R + V_L + V_F = 0$, then $V_{CT} = 0$.

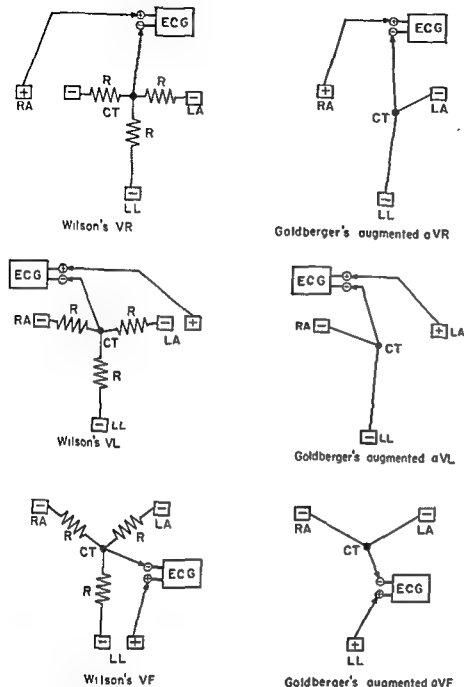


Fig. 17.—The lead-wire connections and galvanometer polarity in Wilson's unipolar limb leads (VR, VL, and VF) and in Goldberger's augmented unipolar limb leads (aVR, aVL, and aVF).

situated at the apices of an equilateral triangle, the sides of which were formed by imaginary lines connecting the electrode positions (Fig. 15, B). Each line connecting the two electrode positions of a lead represented the lead axis for the lead in question

2 According to Einthoven, the electromotive forces generated by the heart at any given instant can be represented by a resultant or equivalent dipole located at the center of the equilateral triangle.

3. Einthoven further proposed that the equilateral triangle be considered to be situated in a homogeneous volume conductor of infinite extent, or, as an alternate postulate, that the dipole be visualized as

if it were lying at the center of a large sphere, at the surface of which were located the apices of the equilateral triangle

The midpoint of each bipolar lead axis divides the axis into positive and negative halves. Perpendicular lines drawn through the centers of the lead axes of leads I, II, and III intersect at the center of the equilateral triangle, and from this point the dipole vector can be considered to originate. For convenience, the equilateral triangle can be rearranged into a triaxial reference figure by superimposing the lead axes of leads I, II, and III so that their midpoints coincide (Fig. 15, C). The center point of this reference

the Einthoven triangle will be used (see Fig 16) to demonstrate the calculation of the components of the vector (E) along leads I, II, and III (components e_1 , e_2 , and e_3). In Figure 16, E represents the manifest dipole vector, and e_1 , e_2 , and e_3 , the projections of E on the axes of leads I, II, and III, respectively. Angle α is the angle formed by the manifest vector with a horizontal line through the dipole center. Angle β is the angle subtended by E with the lead axis of lead II, and angle γ , the angle between E and the axis of lead III. As the figure indicates, the components of the manifest vector, i.e., the projections of the vector on

the bipolar lead axes, can be described in terms of angle α as follows:

$$\begin{aligned}e_1 &= E \cdot \cos \alpha \\e_2 &= E \cdot \cos (\alpha - 60^\circ) \\e_3 &= E \cdot \cos (120^\circ - \alpha)\end{aligned}$$

It will be recalled that a unipolar lead is distinguished from a bipolar lead by the fact that its negative or indifferent electrode is at zero potential. In the hypothetical unipolar leads previously described, the indifferent electrode was placed at electrical infinity and therefore at zero potential. Obviously, this is not possible in electrocardiography because the body is a

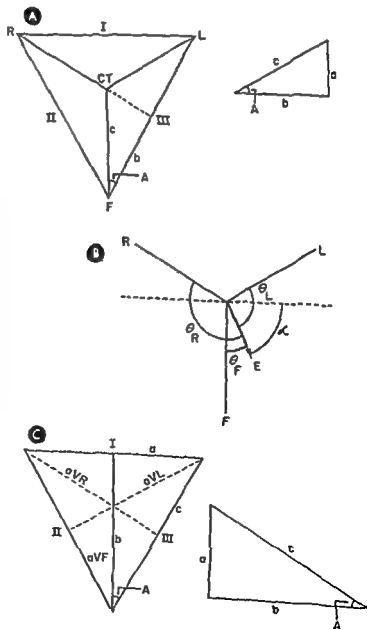


Fig 20.—Calculation of the correction factors of the unipolar leads A, calculation of the correction factors for Wilson's unipolar limb leads—VR, VL, and VF B, projections of a manifest vector (E) on the lead axes of the unipolar limb leads C, calculation of the correction factors for Goldberger's augmented unipolar limb leads— aVR , aVL , and aVF .

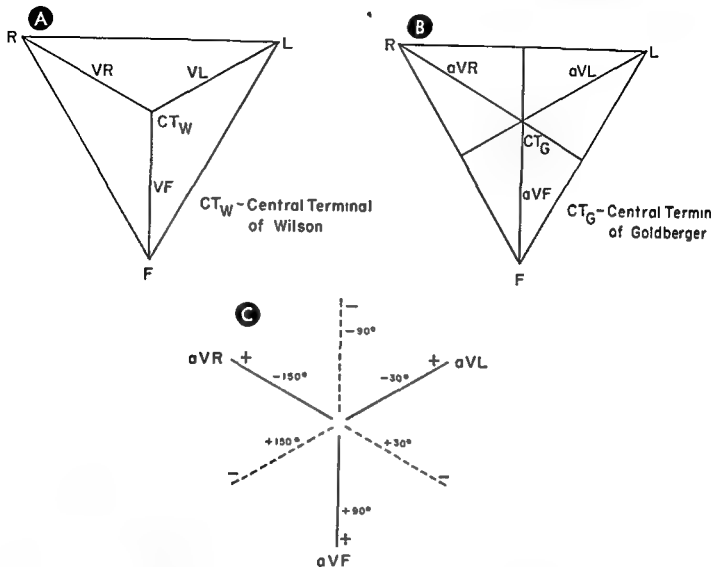


Fig. 19.—Axes of derivation of Wilson's unipolar extremity leads (A) and Goldberger's augmented unipolar limb leads (B), as related to Einthoven's equilateral triangle C, triaxial reference frame formed by the lead axes of the augmented unipolar limb leads

this text with the terms *instantaneous spatial vector* and *mean spatial vector*. The distinction between vectors representing actual cardiac electromotive forces and vectors calculated from the electrocardiogram or recorded in the vectorcardiogram will be evident from the context. The methods by which instantaneous and mean vectors can be constructed will be described later, in conjunction with vector analysis of the electrocardiogram (pp. 36-42). However, a brief résumé of the method of constructing an instantaneous vector (Fig. 15) follows:

1. The potentials recorded at a given instant in at least two of the three bipolar limb leads are plotted as positive or negative values on the corresponding portions of the lead axes of the two leads

⌚ Perpendicular lines are then dropped from these

points on the lead axes and are extended until they intersect

3. A line drawn from the center of the triaxial reference frame (or Einthoven triangle) to the point of intersection of the perpendicular lines represents the mean instantaneous vector or electrical axis

It is evident that the method outlined above is simply the reverse of that used to determine the components or projections of a vector on the three coordinate axes or on the lead axis of any lead. In the discussion of vector methods, it was stated that the component of a vector along a given lead, or the projection of the vector on the lead (e_L), was equal to the product of the magnitude (E) of the projected vector and the cosine of the angle (θ) subtended by the vector and lead axis, that is $e_L = E \cdot \cos \theta$. To simplify the presentation, the triaxial modification of

the Einthoven triangle will be used (see Fig. 16) to demonstrate the calculation of the components of the vector (E) along leads I, II, and III (components e_1 , e_2 , and e_3). In Figure 16, E represents the manifest dipole vector, and e_1 , e_2 , and e_3 , the projections of E on the axes of leads I, II, and III, respectively. Angle α is the angle formed by the manifest vector with a horizontal line through the dipole center. Angle β is the angle subtended by E with the lead axis of lead II, and angle γ , the angle between E and the axis of lead III. As the figure indicates, the components of the manifest vector, i.e., the projections of the vector on

the bipolar lead axes, can be described in terms of angle α as follows:

$$e_1 = E \cdot \cos \alpha$$

$$e_2 = E \cdot \cos (\alpha - 60^\circ)$$

$$e_3 = E \cdot \cos (120^\circ - \alpha)$$

It will be recalled that a unipolar lead is distinguished from a bipolar lead by the fact that its negative or indifferent electrode is at zero potential. In the hypothetical unipolar leads previously described, the indifferent electrode was placed at electrical infinity and therefore at zero potential. Obviously, this is not possible in electrocardiography because the body is a

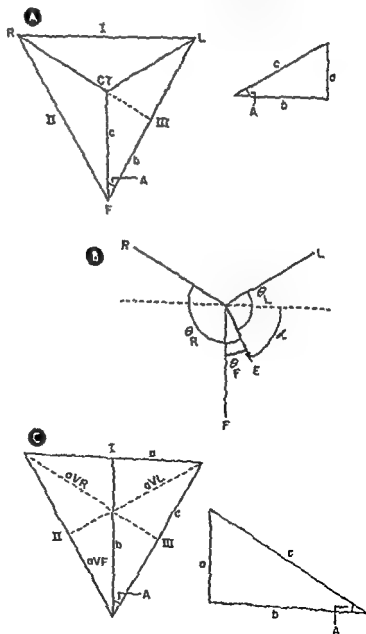


Fig 20.—Calculation of the correction factors of the unipolar leads A, calculation of the correction factors for Wilson's unipolar limb leads—VR, VL, and VF. B, projections of a manifest vector (E) on the lead axes of the unipolar limb leads C, calculation of the correction factors for Goldberger's augmented unipolar limb leads— aVR , aVL , and aVF

volume conductor of finite extent. However, from Kirchoff's law the sum of potentials of the three extremities is equal to zero throughout the cardiac cycle. Wilson utilized this principle to construct a central terminal by connecting together at one point the lead wires from electrodes attached to the left and right arms and the left leg (Fig. 17). The indifferent electrode is attached to this central terminal and is therefore at approximately zero potential (Fig. 18). The exploring electrode is applied to an extremity and connected to the positive pole of the galvanometer. Inasmuch as the central terminal in effect places the negative terminal of the electrocardiograph (or the indifferent electrode) at the zero point of the electrical field, or, in other words, at the center of the dipole axis, a unipolar lead axis can be visualized as an

from the center of the triangle to the lead axis of lead III.

If the length of lead III is given a value of 1, then b , which is one half the length of III, equals $\frac{1}{2}$. The lead axis of VF (c) bisects the 60° angle at F, and so angle $A = 30^\circ$, $\cos A = b/c$, $\cos 30^\circ = \frac{1}{2}/c$, and $\cos 30^\circ = \frac{1}{2}\sqrt{3}$.

By substitution, $\frac{1}{2}\sqrt{3} = \frac{1}{2}/c$, or $c/2\sqrt{3} = \frac{1}{2}$. Therefore, $c = 1/\sqrt{3} = 1/1.73 = 0.58$.

In theory at least, this means that the voltage recorded in a unipolar lead—whether the lead is VF, VL, or VR—is only 58% of the voltage projected on the lead axis by the manifest vector, while in a bipolar limb lead the recorded and projected voltages are theoretically equal. This relationship can be expressed mathematically (Fig. 20, B). As will be recalled, the

TABLE 1.—LEAD CONNECTIONS FOR THE WILSON AND GOLDBERGER UNIPOLAR LIMB LEADS

WILSON			GOLDBERGER		
Lead	Exploring Electrode	Central Terminal	Lead	Exploring Electrode	Central Terminal
VR	Right arm	Right arm Left arm Left leg	aVR	Right arm	Left arm Left leg
VL	Left arm	Left arm Right arm Left leg	aVL	Left arm	Right arm Left leg
VF	Left leg	Left arm Right arm Left leg	aVF	Left leg	Left arm Right arm

imaginary line in space extending from the position of the positive electrode to the center of the dipole axis. In clinical electrocardiography, the unipolar limb leads are formed by placing the exploring electrode on the right arm (VR), left arm (VL), and the left leg (VF). Thus the lead axes of VR, VL, and VF extend from the apices of Einthoven's triangle to its center, and are therefore the medians of the equilateral triangle (Fig. 19).

It is evident by inspection that the unipolar lead axes are shorter than the axes of bipolar leads I, II, and III, and, for this reason, the unipolar leads register lower voltages if not corrected. The correction factor for the unipolar leads can be determined in a simple manner, using lead VF as an example (Fig. 20, A). The lead axis of VF is added as a median to the equilateral triangle, and a perpendicular line is drawn

projection (e) of a manifest vector (E) on a given lead axis is defined by the following equation: $e = E \cdot \cos \theta$. Thus, if angle θ is expressed in terms of angle α subtended by the manifest vector and a horizontal line through the center of the dipole axis, then

$$e_I = E \cdot \cos \theta_I = E \cdot \cos (90^\circ - \alpha)$$

$$e_{II} = E \cdot \cos \theta_{II} = E \cdot \cos (210^\circ - \alpha)$$

$$e_I = E \cdot \cos \theta_I = E \cdot \cos (120^\circ - \alpha)$$

However, the voltages recorded in the unipolar leads, in comparison with the voltages registered by the bipolar leads, would be as follows.

$$vI = E \cdot \cos \alpha \quad vR = \frac{E \cdot \cos (210^\circ - \alpha)}{\sqrt{3}}$$

$$vII = E \cdot \cos (\alpha - 60^\circ) \quad vL = \frac{E \cdot \cos (120^\circ - \alpha)}{\sqrt{3}}$$

$$vIII = E \cdot \cos (120^\circ - \alpha) \quad vF = \frac{E \cdot \cos (90^\circ - \alpha)}{\sqrt{3}}$$

Thus, in order to compare corresponding deflections registered in the bipolar limb leads and in the unipolar

limb leads of Wilson, the voltage values in the latter

giving two
in the elec-

trodes, Wilson placed a 5,000-ohm resistor in each of the three extremity wires forming the central terminal, in order to minimize or eliminate such skin currents. However, because of the small amplitude deflections obtained with Wilson's unipolar leads, Goldberger modified them by removing the resistors from the central terminal and disconnecting the limb attached to the exploring electrode. He designated these modified unipolar leads augmented leads, and with the prefix "a" they became aVR, aVL, and aVF (Figs. 17 and 19). The lead connections for the Wilson and Goldberger unipolar limb leads (Fig. 17) are given in Table 1.

The unipolar and bipolar limb leads can be mathematically interrelated as follows:

$$(1) VL_L = VL - CT \text{ or } VL - \frac{(VL + VR + VF)}{3}$$

where VL_L is the potential in the lead and VL is the potential at the left arm.

But,

$$(2) VL + VR + VF = 0$$

Therefore, $VL_L = VL$. Thus, VL will designate both

$$(3) I = VL - VR \text{ or } VL = I + VR \\ III = VF - VL \text{ or } VL = -III + VF \\ 2VL = I - III + VR + VF$$

But,

$$(4) VR + VL + VF = 0 \text{ or } -VL = VR + VF$$

Therefore,

$$(5) 2VL = I - III - VL \text{ or } VL = \frac{I - III}{3}$$

In a similar manner, VR or VF can be obtained by adding the two bipolar leads containing one or the other, and then solving the equation for the unknown, as demonstrated above. It will be found that,

$$VR = \frac{-I + III}{3} \text{ and } VF = \frac{I + III}{3}$$

These relationships hold true for unipolar leads in which Wilson's central terminal of zero potential is used. In Goldberger's unipolar limb leads, however, the central terminal is not at zero potential but at a potential which is the average of those present at the two extremities connected to the central terminal. Thus,

$$aVL = VL - \frac{(VR - VF)}{2}$$

$$2aVL = 2VL - (VR - VF)$$

$$2aVL = 2VL - VR + VF$$

but

$$-VL = VR + VF$$

Therefore,

$$2aVL = 2VL - (-VL)$$

$$2aVL = 3VL$$

$$aVL = \frac{3VL}{2} = 1.5 VL$$

Also,

$$aVR = 1.5 VR \text{ and } aVF = 1.5 VF$$

From the foregoing calculations it is evident that the recorded voltage deflections at a given extremity are 50% larger in an augmented unipolar limb lead than in the unipolar lead with Wilson's central terminal.

The lead axis of an augmented unipolar limb lead can be visualized in the Einthoven triangle as a line which bisects the angle at an apex and passes through the center of the triangle to form a perpendicular with the opposite side. The correction factor for an augmented lead (Fig. 20, C) can be computed as follows

$$\cos A \text{ (or } 30^\circ) = \frac{c}{b} = \frac{c}{1}$$

$$\cos 30^\circ = \frac{\sqrt{3}}{2} = \frac{c}{1}$$

$$\frac{\sqrt{3}}{2} = \frac{c}{1}$$

$$c = \frac{\sqrt{3}}{2} = \frac{1.73}{2} = 0.87$$

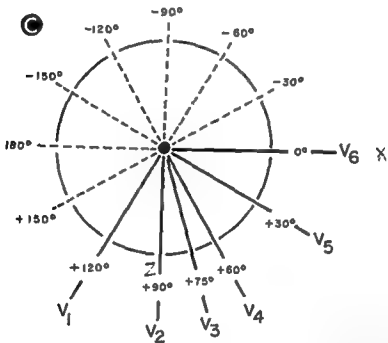
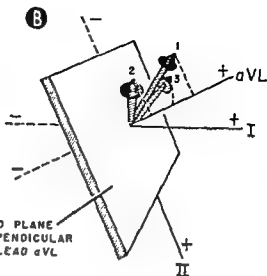
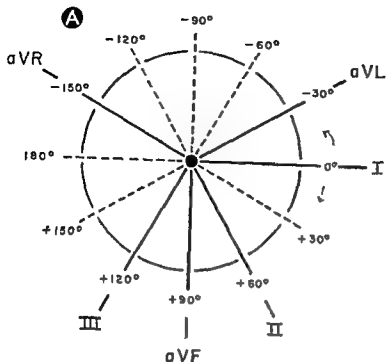
or

$$aVF = 0.87 VF$$

Theoretically, the voltage recorded in an augmented unipolar limb lead is 87% of the voltage projected on the lead axis by the manifest voltage.

Unipolar limb leads routinely recorded in clinical electrocardiography are ordinarily the augmented leads aVR, aVL, and aVF, although the latter differ from Goldberger's original augmented leads in that the 5,000-ohm resistances in the lead wires are usually retained. The lead axes of the augmented leads form a triaxial reference figure which is rotated 30° from the bipolar reference frame. By superimposing the center points of the two reference figures, a hexaxial reference frame is obtained which is divided into 30° segments (Fig. 21, A and B). The figure is scaled off from 0° at the positive end of the lead I axis.

counterclockwise direction



horizontal reference frame formed by the lead axes of the unipolar leads (I, II, and aVL) so that the midpoints of the lead positive halves of the lead axes, the interrupted lines, the vector I, in all subsequent figures depicting either the frontal reference frame (lead II in the frontal reference frame) the line projects on or lies entirely in the horizontal reference frame as depicted, vector I is the orientation of vector I of lead aVL. C, the

above the lead I axis. It should be noted that each bipolar lead is perpendicular to one of the unipolar leads and divides its lead axis into positive and negative halves. Similarly, each unipolar lead demarcates the

positive and negative components of a bipolar lead axis. In this text, the hexaxial reference figure just described will be used to orient all frontal plane vectors and the frontal projection of the spatial vector loop.

UNIPOLAR PRECORDIAL LEADS AND HORIZONTAL REFERENCE FRAME

As will be recalled, a mean instantaneous cardiac vector is a spatial vector and can therefore be defined in terms of its projections on the transverse (X), sagittal (Z), and vertical (Y) co-ordinate axes of the body. The components of the vector along these axes—the X , Y , and Z components—determine the projection of the vector on the frontal, sagittal, and horizontal planes of the body. The limb leads respond to the X and Y components of the vector and can therefore be used to calculate, in an approximate way, the magnitude and orientation of the frontal plane projection of the spatial vector. However, the more anterior or posterior the orientation of a spatial dipole vector of given magnitude (i.e., the larger the Z component of the vector), the less is its projection on the frontal plane leads and the smaller the deflections recorded in these leads (Fig. 21, B). This follows from the fact that a cardiac vector is the vectorial sum of its components, consequently, as one component becomes larger, the sum of the other two must become smaller. It is evident that the characteristics of the dipole vector cannot be determined from leads measuring only the X and Y components of the vector. Theoretically, a single third lead is required having its lead axis oriented perpendicularly to the frontal plane in an anteroposterior direction. Such a lead would provide the necessary information about the Z , or sagittal, component of the vector. In actuality, not one, but six or more chest leads are recorded routinely, each lead responding somewhat differently to the Z component of the spatial vector.

Before the development of the Wilson central terminal the chest leads employed were bipolar leads.

These leads have been supplanted almost entirely by the unipolar (V) leads. With the indifferent electrode attached to the central terminal, different unipolar (V) precordial leads are recorded by applying the exploring electrode to different points on the chest.

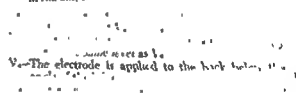
These leads are not augmented in the manner of aVR,

aVL, and aVF. However, for the purpose of visualization, the axes of the unipolar leads can be extended through and beyond the dipole center to form the negative portions of these axes. The lead axes of the precordial leads approximately define a horizontal plane, upon which project the anteroposterior (Z) and transverse (X) components of the dipole vector (Fig. 22, A). The unipolar precordial leads (Fig. 22, B and C) are as follows:

V_1 —The positive or exploring electrode is placed in the fourth intercostal space at the right sternal border.



V_2 —The electrode is placed at the same level as V_1 , but in the mid-clavicular line.



V_3 —The electrode is applied to the left chest at the level of the V2 electrode.



V_4 —The electrode is placed on the right chest at a position corresponding to that of V_3 on the left.

The precordial leads routinely recorded usually consist of leads V_1 to V_6 ; but it may prove advantageous, under certain circumstances, to record additional chest leads in higher or lower interspaces, from the right precordium or left posterior chest. An upward deflection is written in a chest lead if the electrical force (or vector) is directed toward the lead electrode—or, in other words, along the positive axis of the lead. A negative deflection is inscribed if the field of electrical positivity (indicated by the direction the arrow points) is directed away from the electrode or along the negative axis of the lead. There are several facts of special pertinence to the precordial leads which should be kept in mind:

1. The axes of the precordial leads vary in direction from subject to subject because of differences in

chest contour. It follows without saying that the precordial leads bear no predetermined mathematical relationship to one another, in contrast with the limb leads. Of equal significance is the fact that, although electrode placement is standardized, the precordial leads vary rather widely from individual to individual, regarding the direction of their anatomic lead axes. Thus, in patients with long thin chests, the conductivity of the tissues underlying the electrode and the position of the electrode relative to that of the dipole may differ markedly from the conditions found in subjects with short, thick chests. More will be said of this later.

2 The proximity of the precordial electrode to the heart affects the electrocardiogram according to Polson's formula, which states that "the potential of a given dipole as determined at a certain point within its electromotive field will vary in inverse relationship to the cube of the distance of this point from the center of the dipole." The extremity lead electrodes can be considered electrically remote and are not influenced greatly by variations in their distance from the dipole center. On the other hand, minor changes in the distance between heart and recording chest electrode can produce marked alterations in the voltage of the deflections registered in the precordial leads.

3 The lead axes of leads V_1 and V_2 are almost perpendicular to the frontal plane, so that these leads respond negligibly to the X and Y components of the vector and maximally to the Z component (Fig. 22). However, lead V_3 is virtually a frontal plane lead, which from next to the

patient's chest habitus. As a result, the axes of leads V_1 and V_2 may lie in the horizontal plane while the axes of the remaining precordial leads slant downward from the dipole center. Occasionally this circumstance may have important consequences, as will be seen later.

Even though the precordial leads depart considerably from what would be theoretically ideal leads for measuring the Z component of the dipole vector, they have the advantage of extensive clinicopathologic correlation. However, if it is assumed that the axes of the precordial leads lie approximately in a horizontal plane through the dipole center, then they can serve as a horizontal reference frame for calculating mean planar vectors from the electrocardiogram or for deriving the precordial lead deflections from the vectorcardiogram (Fig. 21, C). The reference figure is scaled off in degrees in the same manner as described for the frontal reference system, that is, positive degrees are marked off in a clockwise direction anteriorly (in the lower half of the figure) and minus degrees in a counterclockwise direction posteriorly (in the upper half of the figure). Because of individual variation in the orientation of the precordial lead axes, the location of these lead axes in the reference figure can only be an approximation, but for the sake of uniformity, the directions cited below will be adhered to in this text.

V_1 —The lead axis of lead V_1 is placed along the $+120^\circ$, -60° axis of the reference frame

V_2 —The axis of lead V_2 is oriented along the anteroposterior or $+90^\circ$, -90° axis of the reference figure. The anatomic axis of this lead can be visualized as oriented

V_3 —The lead axis of lead V_3 is placed along the $+0^\circ$, -180° axis of the reference frame

V_4 —The axis of lead V_4 has been situated on the $+30^\circ$, -150° axis of the reference figure

V_5 —The axis of lead V_5 approximates the $+30^\circ$, -150° axis of the reference figure

V_6 —The lead axis of V_6 coincides with the transverse co-ordinate axis X and lies along the 0° , 180° axis

The positive half of the axis of each of the above leads is situated anterior to the dipole center.

precordial leads (V_3 , V_4 , and V_5) are intermediate in direction between V_2 and V_3 and show a mixed response to all three components (X, Y, and Z) of the dipole vector.

4 During ventricular depolarization and repolarization, the cardiac dipole center is probably at the level of the fourth intercostal space and slightly to the left of the sternal margin in most, but not all, individuals. In all likelihood, it moves upward during atrial activation. Therefore, not only are the routine six precordial leads recorded at three different thoracic levels, but leads V_3 to V_6 are taken at points inferior to the dipole center to an extent varying with the pa-

Instrumentation, Terminology, and Time and Voltage Measurements; Construction of Mean Vectors

INSTRUMENTATION

String Galvanometer

THE STRING GALVANOMETER, one type of electrocardiograph, consists of a metal-plated (gold or platinum) quartz string which terminates in lead wires at its two extremities (Fig. 23, A). The quartz string is suspended under proper tension (so that 1 mv input through the string causes it to be deflected 1 cm) between the poles of an electromagnet or in a permanent magnetic field. Current flow through the quartz string sets up a magnetic field which opposes the permanent magnetic field and produces movement of the string. Displacement of the string follows Fleming's left-hand rule, which states that, if the thumb, forefinger, and second finger are held at right angles to one another, the forefinger representing the direction of the magnetic field from its north to south pole and the second finger the direction of current flow in the string, the thumb will point in the direction the wire will move. The string interrupts a beam of light focused on it. Thus, displacement of the string projects a moving shadow on the exposed photographic paper. A grid lens containing opaque lines also interrupts the light beam to project, on the record, horizontal lines 1 mm. apart, every fifth line being heavier than those intervening. A revolving five-spoked wheel, one spoke of which is broader than the others, interrupts the light beam at intervals of 0.04 second, as indicated by vertical lines. Every fifth line is heavier than the others and corresponds to a time interval of 0.2 second. Since the quartz string has little inertia, the string galvanometer is capable of recording very accurate electro-

cardiograms. However, the low resistance of this instrument, compared with the skin resistance, makes the recording susceptible to distortion if the lead electrodes are not applied properly.

Amplifier Tube and Coil Wire Electrocardiograph

The amplifier tube and coil wire electrocardiograph differs from the string galvanometer in that there is suspended between the poles of the magnet a coil of wire to which a mirror is attached (Fig. 23, B). The ends of the wire coil are connected to two lead wires which pass to the patient. Electrical potentials arising in the heart are amplified by electronic vacuum tubes and then flow through the coil, producing lines of force and rotation of the coil according to Fleming's left-hand rule. Light focused on the mirror is reflected on photographic paper along with the linear shadow cast by an unsilvered vertical segment of the mirror surface. This shadow is displaced with rotation of the mirror.

Direct-Writing Electrocardiograph

The direct-writing electrocardiograph has a lever or stylus attached directly to the conducting unit, suspended between the magnet poles (Fig. 23, C). A vacuum tube is required to amplify the cardiac potentials sufficiently to enable the heavy writing arm to move with proper speed. Some of the instruments have ink-writing points. However, most direct-writing

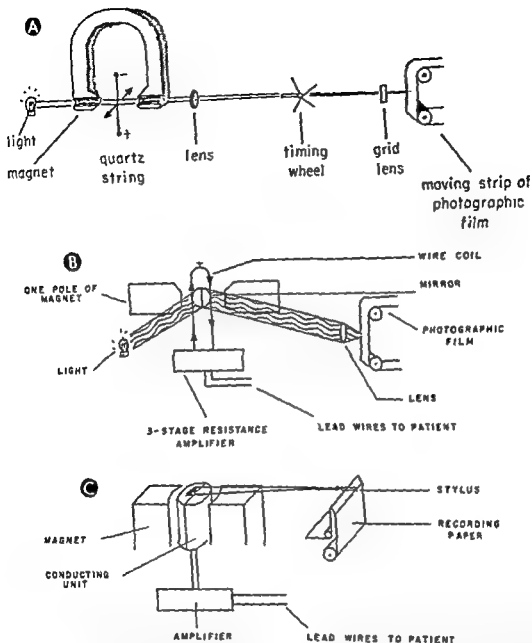


Fig 23.—A, the string galvanometer electrocardiograph B, the amplifier tube and wire coil electrocardiograph C, the direct-writing electrocardiograph. (The oscilloscope electrocardiograph is described in Chapter 7, on Vectorcardiography.)

electrocardiographs utilize a heated stylus and a special type of electrocardiograph paper. The recording surface of this paper consists of a layer of carbon coated with wax, which the heated stylus melts, thereby disclosing the carbon beneath. The recording paper usually has horizontal amplitude lines and vertical time lines marked on it prior to use. Since the timing is not synchronized automatically with the paper speed, the latter must be checked periodically.

Directions for checking the paper speed are contained in the manufacturer's instruction manual.

Oscilloscope Tube Electrocardiograph

The oscilloscope tube electrocardiograph will be discussed later (Chapter 7) in conjunction with the vectorcardiograph, because of the close relationship between the two instruments.

TERMINOLOGY AND TIME AND VOLTAGE MEASUREMENTS

The electrocardiographic tracing is superimposed on a co-ordinate grid consisting of horizontal and vertical lines. Each vertical line indicates a 0.04-second interval of time, and every fifth vertical line, in heavier print than the others, demarcates a 0.2-second time period (Fig. 24, A). The horizontal lines are 1 mm.

apart, every fifth line being heavier than the others and corresponding to a length of 5 mm. (Fig. 24, A). If the electrocardiograph is properly standardized, then 1 mm, as indicated by each horizontal line, equals 0.1 mv. (Fig. 24, B). The string galvanometer projects, on photographic paper, time lines which are

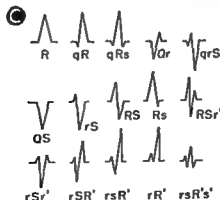
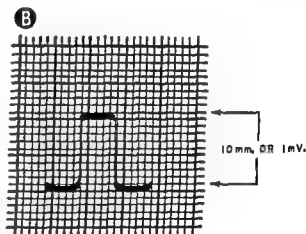
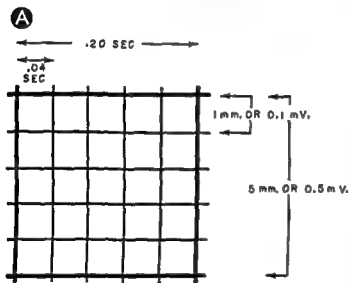


Fig. 24. A, time lines of the electrocardiogram. B, the standardization deflection is 10-mm (mv) of a properly standardized electrocardiogram. C, method of relative sizes of their component waves

synchronized automatically with the paper speed so that, regardless of paper speed, the time markings have the same meaning. However, the direct-writing electrocardiograph uses paper on which the time lines have already been printed. This makes it essential that the paper speed of such an instrument be checked frequently according to the instructions accompanying the individual instrument.

Electrocardiographic Deflections

Every cardiac cycle is accompanied in the electrocardiogram by deflections representing depolarization and repolarization of first the atria and then the ventricles. The cardiac cycle is initiated by the appearance of a small upward deflection called the P wave.

Following the P wave and directed oppositely to it, the Ta (or Tp) wave. Ordinarily the Ta wave is buried in, and obscured by, the large deflection which occurs at about the same time, the QRS complex. The latter complex is related to ventricular depolarization and is generally the largest deflection to be recorded during the cardiac cycle. The QRS complex is normally upright in leads I, V₄, and V₆ and downwardly directed in leads aVR, V₁, and V₂. The segment which intervenes between the termination of the QRS complex and the onset of the T wave is called the S-T segment and is normally isoelectric. The junction of the terminal component of the QRS deflection with the S-T segment is called the S-T junction, or J. The T wave, which is usually intermediate in amplitude between the P and QRS deflections, is normally upright in leads I and inverted in lead aVR. More will be said of this later.

The R wave is the earliest upward deflection of the QRS complex. The R wave may be preceded by a negative wave, the Q wave. The first downward deflection after the R is called the S wave. Occasionally the S wave is followed by a second positive deflection, R'. A negative wave following R' is termed S'. This method of labeling can be extended to R'', R''', S'', S''', etc. Small letters and capital letters are often used in labeling the QRS complex in order to indicate the magnitude of one of its components relative to another (Fig. 24, C). For example, the symbol qR implies that the Q wave is relatively small and the R wave relatively prominent. The T and P waves may

be upright, downwardly directed (negative or inverted), or *diphasic*, the latter term meaning that the wave has both an upward and downward component (either +— or —+).

Voltage

All deflections above the base line should be measured from the top of the base line to their highest point, while downward deflections should be measured from their deepest point to the bottom of the base line. To compute the total amplitude of a complex having upward and downward components, these components are measured separately, as just described, and their individual values are then added. To obtain the net or resultant amplitude of the complex, the above-mentioned values are added algebraically.

The reference level for measurement of the P, Ta, ST, and T deflections is the T-P segment, all other deflections having the P-R segment as reference base line. Amplitude may be expressed in terms of millimeters or millivolts (1 mm. = 0.1 mv.).

Time

The lead in which time-interval measurements are to be performed should be the one containing the largest deflections, because in such a lead the component to be measured is more likely to be clearly demarcated by definitive points of beginning and ending. A lead exhibiting complexes of smaller amplitude is likely to have some deflections whose curves of onset and offset merge gradually and indistinguishably with the base line. These low-amplitude deflections may even be isoelectric during early and terminal portions of their inscription. Under such circumstances, time-interval measurements may be erroneous. With reference particularly to P-R and QRS intervals, the longest interval found in the six extremity leads should be measured.

Heart Rate

If the number of large squares (0.2-second intervals) counted in a single R-R interval, n , is known, the heart rate can be calculated as follows:

1. By dividing into 300 the number of large squares (0.2-second intervals) counted in a single R-R interval.

$$\text{Heart rate/min} = \frac{300}{\text{Number of 0.2-sec squares in single R-R interval}}$$

2. By dividing the R-R or P-P cycle length (in seconds) into 60.

In the presence of an irregular rhythm the heart rate can be determined by the following methods:

1. Inasmuch as the graph paper moves about 1 inch in a 1-second period, the heart rate can be obtained by counting the number of QRS complexes in a 6-inch strip of record and multiplying this by 10.

2. If several R-R intervals are counted together with the number of 0.2-second intervals over the same distance, the heart rate may be calculated from the following formula:

$$\frac{\text{Number of R-R intervals} \times 300}{\text{Number of 0.2-sec. intervals}} = \text{heart rate/min.}$$

CONSTRUCTION OF MEAN VECTORS

The electrocardiograph reacts to the infinite number of elementary electromotive forces produced by

Various tables have also been devised from which the rate can be read for a given R-R interval. The normal heart rate ranges from 60 to 100 beats per minute. According to present terminology, a heart rate of 60-100 beats per minute with a sinus node pacemaker is called *normal sinus rhythm*. A heart rate faster than 100 in adults is designated *sinus tachycardia*, less than 60, *sinus bradycardia*. Actually, the normal heart rate often exceeds these limits, particularly in infants and children.

the heart at any instant as if they were resolved into a single equivalent dipole, and the latter, in turn, is

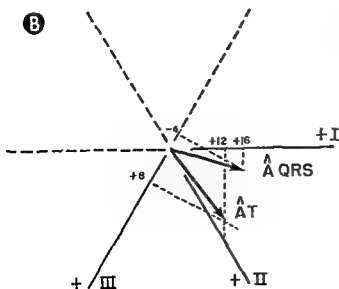
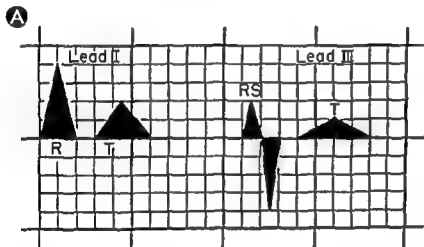


Fig. 25.—Construction of the frontal plane mean QRS and mean T vectors (A QRS and A T), utilizing the net or resultant areas of the QRS and T waves in Leads I and III of the ECG tracing (A). The values for the areas are expressed in microvolt-seconds (B). For example, the R wave in lead I has a duration of 0.08 second and an amplitude of 4 mm, or 400 microvolts. To get the area in microvolt-

of lead I in B, the same is applied to the T waves

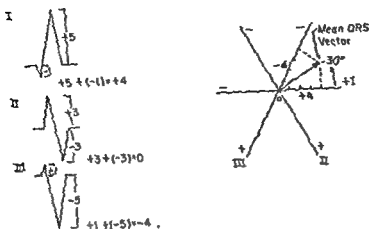


Fig. 26.—Construction of the frontal plane mean QRS vector (\bar{A} QRS) from the three leads utilizing similar methods shown in Fig. 25.

On the minus (-) side of the axis, the complexes recorded in the leads I, II, and III are represented by an instantaneous resultant or mean cardiac spatial vector. This vector changes in direction and magnitude from instant to instant during electrical systole and diastole as first one region of heart muscle and then another undergoes depolarization and repolarization. The changing projection of the instantaneous mean cardiac spatial vector on the axis of a given lead determines, in large part, the deflection recorded in the lead. For example, during ventricular depolarization the instant-to-instant change in the characteristics of the mean instantaneous QRS vectors determines whether the ventricular complex is to have QR, qR, Rr, RS or rS.

represented by an instantaneous resultant or mean cardiac spatial vector. This vector changes in direction and magnitude from instant to instant during electrical systole and diastole as first one region of heart muscle and then another undergoes depolarization and repolarization. The changing projection of the instantaneous mean cardiac spatial vector on the axis of a given lead determines, in large part, the deflection recorded in the lead. For example, during ventricular depolarization the instant-to-instant change in the characteristics of the mean instantaneous QRS vectors determines whether the ventricular complex is to have QR, qR, Rr, RS or rS.

in space by the tips of all mean instantaneous spatial vectors appearing in succession during the QRS interval. The vector constructed more commonly from the ventricular deflections in the electrocardiogram is the mean QRS spatial vector or its planar projection.

sum of all instantaneous spatial vectors appearing during the QRS interval, while the planar mean vectors represent the planar projections of the mean spatial vectors.

Frontal Plane Mean Vectors

The frontal plane mean QRS vector is constructed from the mean instantaneous spatial vectors of the bipolar limb leads I, II, and III, utilizing the triaxial reference figure derived from Einthoven's triangle. The most accurate method of constructing the mean QRS vector* (Fig. 25) is as follows:

*The methods described for constructing the mean QRS vector can be applied similarly to the construction of the mean P or T vectors from the bipolar limb leads.

... which depict, in a very approximate way, the direction and magnitude of the instantaneous cardiac vectors. However, the procedure is time consuming and requires that the leads be recorded at a constant speed. As a result, to record the spatial loop, which is in essence the planar projection of the pathway traced

1. In each of two bipolar limb leads, the area of each wave component of the QRS deflection is measured (area in microvolt-seconds equals one half the width in seconds times the amplitude in microvolts), and the value obtained for each component is given a plus sign if the wave is upwardly directed and a minus sign if downwardly directed. Then the areas of all components of the QRS deflection in a given lead are added algebraically. In this manner, the net QRS area is determined for each of the two bipolar limb leads and is plotted on the appropriate positive or negative half of the axis of the lead in question.

2. Perpendicular lines are dropped from the points plotted.

3. A line drawn from the center of the reference figure to the intersection of the two perpendicular lines represents the mean manifest electrical axis of the QRS (\bar{A} QRS) or the frontal mean QRS vector.

A less exact method of constructing the mean vector entails the use of the net amplitude of the QRS complexes in the bipolar limb leads (Fig. 26). However, this procedure, as well as that described in the preceding paragraph, has the disadvantage of being too cumbersome for routine clinical use. Another method, to be described in the following paragraphs, permits rapid and reasonably accurate calculation of the orientation of the mean QRS vector in the frontal plane merely by inspection of the ventricular deflections in the three bipolar leads (Fig. 26). Although the absolute magnitude of the mean vector is not obtained with this latter method, the magnitude of the mean vector is of less importance than the orientation of the vector.

Construction of vectors by inspection is based on

the fact, already discussed, that the projection of a vector on a lead (e_L) is equal to the product of the magnitude of the projected vector (E) and the cosine of the angle (θ) subtended by the vector and lead axis, or $e_L = E \cdot \cos \theta$. Since the voltage registered in the lead is directly proportional to the projection of the vector on the lead axis, then $V_L \propto E \cdot \cos \theta$.

This relationship holds true both for instantaneous and mean vectors. For a given magnitude of the mean QRS vector, therefore, the resultant QRS voltage in the lead varies directly with cosine θ . If the mean vector is directed perpendicularly to the lead axis, angle θ is 90° and the cosine of 90° is zero; and, consequently, the lead records a QRS deflection whose net area is zero (i.e., an isoelectric or very small complex or one consisting of upward and downward components whose algebraic sum is zero—the so-called *transitional*, *equipotential*, or *equiphase complex*). When the mean QRS vector parallels the lead axis, angle θ is 0° and the cosine of 0° is 1, or maximal; and, consequently, a ventricular deflection of maximum area or size is recorded by the lead. Conversely, a lead deflection with a net area of zero indicates that the mean vector is perpendicular to the axis of the lead, while a lead deflection of maximum area signifies that the vector tends to parallel the lead axis. This relationship can be utilized in conjunction with the hexaxial reference frame to determine in an approximate way the orientation of the frontal plane projection of the mean spatial vector (Fig. 27). The method used is as follows.

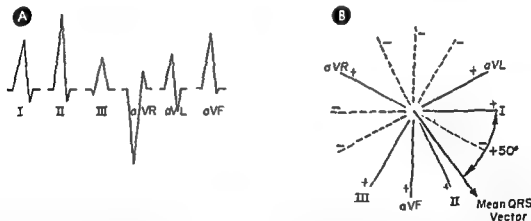


Fig. 27.—Construction of frontal plane mean QRS vector by the inspection method. By inspection of the QRS complexes recorded in the six extremity leads (A), the electrical axis of QRS (\bar{A} QRS) or the orientation of the mean QRS vector in the frontal plane can be defined quite accurately. Leads II and aVR register the largest QRS complexes, the

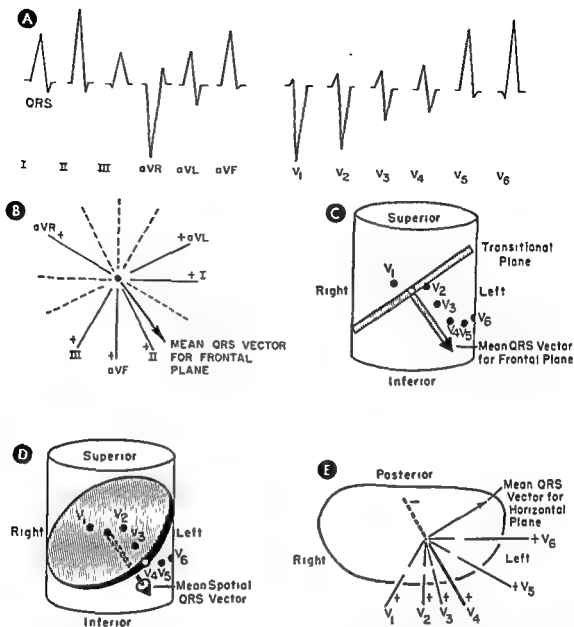


Fig. 29.—Construction of the frontal and horizontal plane mean QRS vectors and the mean QRS spatial vector. In A, the QRS complexes are depicted as recorded by each of the six extremity leads and six precordial leads. The extremity leads are recorded in the frontal plane (B). In Figure 27, the chest is visualized as a cylinder on which are superimposed small black circles representing the points of application of the chest electrodes. The frontal plane mean QRS vector (C) is placed in this cylinder without changing its frontal plane orientation. The transitional plane for the QRS vector is also depicted in C, as visualized in an edge-on view, since the vector to which it is perpendicular is oriented entirely in the frontal plane at this point in the procedure. Inasmuch as any lead having its axis situated within the transitional plane records a transitional QRS complex, the frontal plane mean QRS vector can be transformed into the mean spatial QRS vector (sA QRS) by tilting the transitional plane and QRS vector (without changing its frontal plane orientation) so that the perimeter of the plane passes through the precordial lead registering the transitional QRS complex (D). In A, it can be seen that lead V₁ displays the transitional QRS. Therefore, by properly tilting the transitional plane, the mean spatial QRS vector is obtained and is directed from such a sketch, but if actual vector models are used, the posterior orientation of the spatial vector can be measured readily.

1. In D, the chest is visualized as a cylinder on which are superimposed small black circles representing the points of application of the chest electrodes. The frontal plane mean QRS vector (C) is placed in this cylinder without changing its frontal plane orientation. The transitional plane for the QRS vector is also depicted in C, as visualized in an edge-on view, since the vector to which it is perpendicular is oriented entirely in the frontal plane at this point in the procedure. Inasmuch as any lead having its axis situated within the transitional plane records a transitional QRS complex, the frontal plane mean QRS vector can be transformed into the mean spatial QRS vector (sA QRS) by tilting the transitional plane and QRS vector (without changing its frontal plane orientation) so that the perimeter of the plane passes through the precordial lead registering the transitional QRS complex (D). In A, it can be seen that lead V₁ displays the transitional QRS. Therefore, by properly tilting the transitional plane, the mean spatial QRS vector is obtained and is directed from such a sketch, but if actual vector models are used, the posterior orientation of the spatial vector can be measured readily.

2. In E, a horizontal section of the chest is depicted, as viewed from above. The lead axes of the six precordial leads are shown. The mean QRS vector for the horizontal plane is shown, but the negative axes are not shown. The mean QRS vector for the horizontal plane is shown, but the negative axes are not shown. The mean QRS vector for the horizontal plane is shown, but the negative axes are not shown.

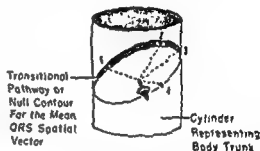
figure in the same manner as for the frontal hexaxial figure (Fig 28). Thus, the positive half of the lead axis of V_4 forms the 0° axis, and the negative half of the lead, the 180° axis. The lead axis of V_2 is considered to form the anteroposterior (or $+90^\circ$, -90°) axis. If, for example, lead V_4 registers the transitional complex and lead V_2 shows an RS or resultantly negative deflection, then the horizontal mean QRS vector is directed along the -90° axis—that is, straight posteriorly. If lead V_4 shows a transitional RS deflection and lead V_2 records an R or resultantly upright de-

which Grant utilizes this concept to determine the orientation of a mean spatial vector is described in the following paragraphs in terms of the mean QRS spatial vector, although the discussion is equally relevant to the construction of mean P and T spatial vectors (Fig 29).

1. The chest is represented as a cylinder on which are superimposed the approximate positions of the precordial electrodes
2. The projection of the mean QRS spatial vector on the frontal plane is constructed from the three standard

Fig 30.—Transitional pathway or null contour for the mean QRS spatial vector. The exploring electrodes of unipolar leads (1, 2, 3, and 4) lie on the perimeter of the

mean spatial vector. Consequently, each lead registers a resultantly zero QRS potential (i.e., a transitional RS or QR deflection or a QRS of very low amplitude).



flexion, as may occur in right ventricular hypertrophy, then the mean vector lies perpendicular to the lead axis of V_4 and along the $+90^\circ$ axis, the vector being directed straight anteriorly.

This method yields only the planar projection of the mean QRS spatial vector, but in most instances this information is quite sufficient for diagnostic purposes. However, the frontal and horizontal planar mean QRS vectors can be used to compute the spatial vector mathematically or to measure its position directly in a vector model. Grant uses the horizontal orientation of the QRS vector to convert the frontal projection into the mean spatial vector. According to Grant, the axis of the precordial lead recording a transitional QRS defines a plane perpendicular to the mean QRS spatial vector which coincides with the zero potential line perpendicular to the equivalent dipole axis and passing through its center. The intersection of this plane with the body surface traces around the chest the transitional pathway, or null contour (Fig 30). At any point on the null contour where the exploring electrode of a unipolar lead happens to be placed, a plus-minus or minus-plus transitional complex will be recorded, since the axis of that lead is perpendicular to the cardiac vector. The manner in

limb leads, as previously described. The vector is plotted in the hexaxial reference figure and it then transferred to the cylinder without changing its orientation.

3. Each of the unipolar precordial leads is examined until the lead recording a transitional QRS complex is identified. The

spatial vector which has as its center the origin of the vector in the midline of the cylinder slightly below the level of leads V_1 and V_4 .

4. Without altering its orientation, the QRS spatial vector is projected onto the frontal plane perpendicular to the null contour, or the mean QRS spatial vector in terms of its actual, three-dimensional orientation in space.

Grant and Estes, Urschel and Abbey, and others have devised vector models which have had great value as teaching aids. In general, these models consist of a plastic cylinder representing the chest, upon which is etched or painted the precordial electrode positions. Mounted on this cylinder is a pointer and, attached to it, a plate

complex. The QRS

po

V_1

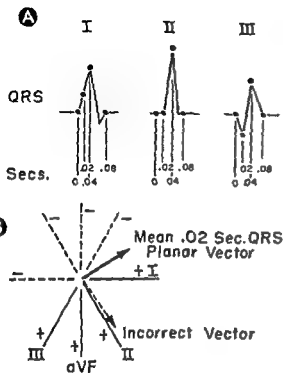


Fig. 31.—Construction of mean 0.02-second vectors from the routine electrocardiogram. In A, the QRS complexes are registered in leads I, II, and III with corresponding points (measured from the actual onset of ventricular activation) on the deflections identically numbered and separated from each other by 0.02-second intervals. It is evident that at 0.02 second after onset of the QRS interval, lead II registers zero potential, so that the mean vector for the initial 0.02-second period is perpendicular to the lead axis of II, as shown in B. If the above leads were recorded consecutively rather than simultaneously, the phasic relationship indicated in the figure would not be apparent. Hasty inspection of the three leads might lead to the conclusion that point 2 in lead II occurs at 0 second, and point 3 at 0.02 second, after onset of depolarization. Thus the mean 0.02-second QRS vector might be thought erroneously to parallel the positive lead axis of II. As far as the extremity leads are concerned, this error can be avoided by application of Einthoven's law. For example, the error of identifying point 2 in lead II as the 0.02-second deflection is evident because the corresponding deflections in leads I and III, when added (Einthoven's law $I + III = II$), yield a zero value instead of a positive value for the voltage of the 0.02-second deflection in lead II. Unfortunately, no such mathematical relationship exists between the deflections recorded by the precordial leads, and so there is no way to compensate for the lack of phase relationship in these leads.

Frontal Plane

tor with its perpendicular transitional plane. The "vector" can be rotated freely within the cylinder except at its fixed point, which in the model is equivalent to the electrical center of the heart. Urschel and Abbey have attempted to quantitate the information obtainable from vector models by mounting degree scales in the bottom of the cylinder (for the horizontal plane) and on the side of the cylinder (for the sagittal plane). The hexaxial reference figure is depicted on a plastic surface behind the cylinder.

The QRS complex can also be divided into 0.02-

second portions, which can then be treated in each of the standard limb and precordial leads as individual deflections. From these values can be derived a mean spatial vector for each 0.02- or 0.04-second interval of the QRS complex. The construction of mean vectors for such short intervals of the QRS deflection is likely to involve significant errors unless leads are recorded simultaneously at increased paper speed (Fig. 31). This problem will be considered in more detail in a later section concerning the construction of vector loops from the electrocardiogram (see pp. 102-104).

Theoretical Bases of the Electrocardiographic and Vectorcardiographic Leads

EQUIVALENT DIPOLE AND SEMI-DIRECT LEAD HYPOTHESES

THE SINGLE EQUIVALENT dipole theory, which has been developed in the preceding chapters proposes that, in terms of body surface potentials, (a) the electrical field produced by heart muscle can be represented at any instant by a single equivalent dipole, and this in turn by a mean instantaneous spatial vector, and (b) the voltage registered in any given lead is directly proportional to the projection of the instantaneous vector on the axis of the lead but is inversely proportional to the cube of the distance between the dipole and lead electrode. This concept implies that the scalar deflection registered by an electrocardiographic lead—whether it is an extremity, precordial, back, or esophageal lead—merely reflects the manner in which the lead taps a single dipole vector. The validity of the single equivalent dipole concept is fundamental to vectorcardiography and to the vector method of electrocardiographic interpretation. Although vectorcardiography in its present form appeared soon after the development of the cathode ray oscilloscope in the 1930's, the vector concept and its implications were known to Einthoven and associates and to some of his contemporaries. In fact, Einthoven utilized lead axes and the vector projection method to determine the mean electrical axis (vector) of the scalar deflections recorded in leads I, II, and III. The extremity leads were considered compatible with Einthoven's hypothesis and the equivalent dipole theory because the points of application of the lead electrodes to the body surfaces were accepted as being "electrically remote" from the heart. However, with the development of the precordial leads a new concept emerged, which has been variously termed the *semidirect lead concept* or the *localized, regional, or*

proximity potentials concept. This theory stressed the relative proximity of the precordial lead electrodes to the heart and was based on Wilson's observations in animal experiments that unipolar precordial leads and leads which were applied directly to the epicardial surface of the heart recorded QRS complexes quite similar except for size. From this experimental observation was derived the concept that the potential variations of a precordial lead reflect to a great extent the potential variations of the epicardial surface closest to the lead electrode. Thus, because of their apparent similarity to direct leads, the unipolar precordial leads were designated *semidirect leads*.

The semidirect lead, or proximity potentials, hypothesis was next extended to include the unipolar limb leads, whose potential variations were thought to be influenced chiefly by the potential variations of the surface of the heart they faced. The corollary to this proposal was that the potential variations of the unipolar limb leads must necessarily be governed by the position of the heart in the chest. Conversely, if the configuration characteristic of the lead deflection recorded from each different aspect of the heart is established, then the electrocardiogram should indicate the "electrical" position of the heart. This concept carried with it the implication that anatomic heart position and rotation could be determined electrocardiographically, but, as will be indicated later, in both theory and practice the semidirect lead hypothesis is probably of limited validity in light of more recent studies. The results of some of these studies are, in brief, as follows:

1. Schwartz, Levine, and Simonson have carried out electrocardiographic mirror-pattern cancellation

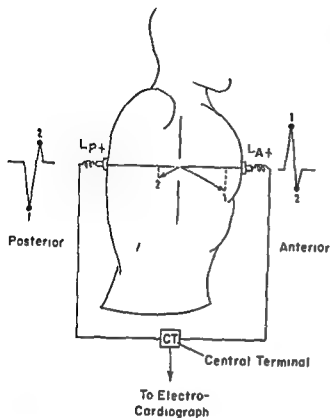


Fig. 32.—Simplified illustration of the manner in which electrocardiographic mirror-pattern cancellation studies are performed. If the dipole concept is correct and the electrical forces of the heart can be represented by instantaneous resultant vectors, then for a lead such as lead LA_1 , whose exploring electrode is placed on the anterior surface of the chest, there must be another lead, LP_1 , on the opposing surface of the back, which records QRS complexes having a mirror-image relationship to those recorded by lead LA_1 . Thus, vector 1 projects positivity on lead LA_1 and equal negativity on LP_1 . Vector 2 projects negativity on lead LA_1 and equal positivity on lead LP_1 . These two leads are unipolar leads, since their indifferent or negative electrodes are attached to a central terminal (CT). For this reason, their lead axes pass through the dipole center. Inasmuch as the two leads register mirror-image deflections, their positive lead axes lie on the anterior and posterior portions of a single line extending through the dipole center. Their mirror-image potentials cancel out each other when passed into the central terminal, so that, theoretically, zero voltage would be recorded from the latter. If localized potentials significantly influence the electrocardiogram, anterior chest lead LA_1 would be dominated by potentials from the anterior surface of the heart, and lead LP_1 would respond mainly to potentials from the posterior aspect of the heart. In consequence, mirror patterns could not be recorded and cancellation of potentials would be impossible.

studies designed to prove or disprove the dipole theory (Fig 32). In normal subjects and patients with heart disease they measured potential variations from electrode sites connected to form an electrical bridge circuit. This circuit was so arranged that potentials referred from two electrode sites to a central terminal could be canceled out if the heart behaved as a true dipole. Along a line passing through the dipole position the magnitudes of electrical potential referred to a central terminal have a fixed distribution, increasing as the distance from the dipole lessens, changing polarity or sign as the dipole is passed, and then decreasing as the distance from the dipole becomes greater. Therefore, leads recorded from the opposite points of this line, when it is extended to the body surface, should exhibit mirror patterns of each other if the dipole theory is valid. In normal subjects and patients with myocardial infarction, Schmitt, Levine, and Simonson found that, on the average, only 9% of any pair of mirror patterns failed to cancel. There were poorer degrees of cancellation in patients with bundle branch block, and this was attributed to migration of the cardiac dipole. In brief, the results of the studies by these investigators were in agreement with the dipole theory. The influence of localized potentials on

the electrocardiogram was thought to be a very minor one. Frank and other investigators have performed similar studies with results almost identical to those above.

2. If the dipole theory is correct, it should be possible to derive, from the vectorcardiogram, scalar lead deflections which resemble those actually recorded at the various precordial lead points. The electrical and manual methods for deriving scalar leads are discussed later. The lead electrodes of the vectorcardiogram are relatively remote from the heart, compared with the electrodes of the unipolar precordial leads. Therefore, if local potentials play a significant role in the genesis of the precordial electrocardiogram, the deflections in the scalar precordial leads, as derived from the horizontal plane vectorcardiogram, should differ from those actually recorded, while the deflections should be similar if the dipole concept is valid. Milnor and his co-workers, and Grishman and Scherlis, Duchosal and Grosgrain, and others, have found the resemblance between derived and recorded scalar lead deflections to be quite close, even in the case of the diagnostic Q waves of myocardial infarction. According to the semidirect lead hypothesis, the abnormal Q waves produced by myocardial infarction

result from the transmission of negativity from the left ventricular cavity through a "window" of necrotic myocardium, and are therefore a manifestation of the semidirect nature of the precordial leads. However, scalar lead deflections derived manually or electronically from vectorcardiograms recorded (with electrically remote leads) in instances of myocardial infarction show diagnostic Q waves. This common observation would seem to indicate that the Q waves of infarction are representative of a general disturbance in the balance of electrical forces, which in turn leads to the appearance of mean instantaneous QRS spatial vectors of abnormal direction and/or magnitude.

Although these two conflicting theories continue to

be a source of controversy, the weight of evidence at present is preponderantly in support of the validity of the equivalent dipole theory when applied to body surface potentials and surface leads. Some authorities admit the validity of this evidence only insofar as it pertains to the extremity leads, but they retain the semidirect lead hypothesis as the explanation of the manner in which the unipolar precordial leads respond to the cardiac forces. Occasional reference will be made in this text to the semidirect lead approach to the electrocardiogram, particularly in the section on electrical heart position and cardiac rotation (pp 60-64), but otherwise the text will adhere strictly to the equivalent dipole or resultant vector concept.

LEAD VECTOR, VECTOR IMAGE, AND LEAD FIELD CONCEPTS

Let it be supposed that a hypothetical experiment is being performed to determine the relationship between the voltage recorded in a lead and the orientation of the dipole axis with respect to the anatomic axis of the lead (Fig 33). A plaster model of the body torso has been filled with saline solution, and electrodes have been attached at positions on the model corresponding to the left shoulder (L), right shoulder (R), and the junction of the left leg with the trunk (F). An artificial dipole vector is placed in the torso model.

term
cordex
therefore, the anatomic axes of these leads can be considered to form an equilateral triangle. An artificial dipole vector mounted on a pivot has been placed in the model. The dipole vector is at variance with the actual cardiac axis in the human chest. The experiment will consist of (a) rotating the dipole vector

since the artificial dipole is of constant strength, and its projection on each lead axis is maximal and therefore the same.

However, it is found that the maximal deflection is recorded in lead I when the artificial dipole vector points superiorly.

lead I, instead of lead I recording a deflection of resultant zero voltage, as would be anticipated, the lead registers a negative deflection. It becomes evident from these findings that the lead voltage can be correlated with the orientation of the dipole vector only if one assumes that, in addition to its anatomic axis, lead I has an effective axis directed differently. The effective axis of lead I can be visualized as an imaginary line drawn parallel to the dipole vector of the torso model.

Thus, even though the experiment has not yet been completed, it can already be seen that the effective lead axes of the bipolar limb leads form a scalene or Burrows triangle.

reasons of the model, although other factors, such as the location of the lead electrode, the irregular contour of the torso model, and the finite size of the model as a volume conductor (and, in the human torso, additional variables such as the uneven conductivity of the body tissues), would influence the orientation of the effective lead axes.

The second unexpected finding in the hypothetical

entirely valid, the following results would be expected (a) At the time each lead registers its maximal deflection, the dipole vector should lie parallel to the anatomic axis of the lead—along the 0° , -180° axis for lead I, the $+60^\circ$, -120° axis for lead II, and the $+120^\circ$, -60° axis for lead III. (b) The magnitude of the maximal deflection in each lead should be equal,

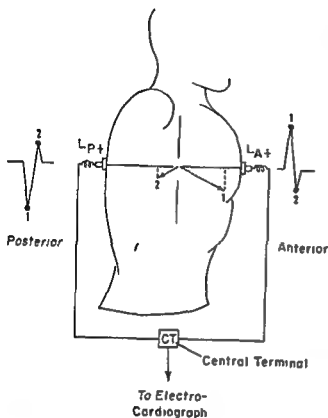


Fig. 32.—Simplified illustration of the manner in which electrocardiographic mirror-pattern cancellation studies are performed. If the dipole concept is correct and the electrical forces of the heart can be represented by instantaneous resultant vectors, then for a lead such as lead L_A , whose exploring electrode is placed on the anterior surface of the chest, there must be another lead, L_P , on the opposing surface of the back, which records QRS complexes having a mirror-image relationship to those recorded by lead L_A . Thus, vector 1 projects positivity on lead L_A and equal negativity on L_P . Vector 2 projects negativity on lead L_A and equal positivity on lead L_P . These two leads are unipolar leads, since their indifferent or negative electrodes are attached to a central terminal (CT). For this reason, their lead axes pass through the dipole center. Inasmuch as the two leads register mirror-image deflections, their positive lead axes lie on the anterior and posterior portions of a single line extending through the dipole center. Their mirror-image potentials cancel out each other when passed into the central terminal, so that, theoretically, zero voltage would be recorded from the latter. If localized potentials significantly influence

potentials from the posterior aspect of the heart. In consequence, mirror patterns could not be recorded and cancellation of potentials would be impossible

studies designed to prove or disprove the dipole theory (Fig. 32). In normal subjects and patients with heart disease they measured potential variations from electrode sites connected to form an electrical bridge circuit. This circuit was so arranged that potentials referred from two electrode sites to a central terminal could be canceled out if the heart behaved as a true dipole. Along a line passing through the dipole position the magnitudes of electrical potential referred to a central terminal have a fixed distribution, increasing as the distance from the dipole lessens, changing polarity or sign as the dipole is passed, and then decreasing as the distance from the dipole becomes greater. Therefore, leads recorded from the opposite points of this line, when it is extended to the body surface, should exhibit mirror patterns of each other if the dipole theory is valid. In normal subjects and patients with myocardial infarction, Schmitt, Levine, and Simonson found that, on the average, only 9% of any pair of mirror patterns failed to cancel. There were poorer degrees of cancellation in patients with bundle branch block, and this was attributed to migration of the cardiac dipole. In brief, the results of the studies by these investigators were in agreement with the dipole theory. The influence of localized potentials on

the electrocardiogram was thought to be a very minor one. Frank and other investigators have performed similar studies with results almost identical to those above.

2. If the dipole theory is correct, it should be possible to derive, from the vectorcardiogram, scalar lead deflections which resemble those actually recorded at the various precordial lead points. The electrical and manual methods for deriving scalar leads are discussed later. The lead electrodes of the vectorcardiogram are relatively remote from the heart, compared with the electrodes of the unipolar precordial leads. Therefore, if local potentials play a significant role in the genesis of the precordial electrocardiogram, the deflections in the scalar precordial leads, as derived from the horizontal plane vectorcardiogram, should differ from those actually recorded, while the deflections should be similar if the dipole concept is valid. Milnor and his co-workers, and Grishman and Scherlis, Duchosal and Groscurin, and others, have found the resemblance between derived and recorded scalar lead deflections to be quite close, even in the case of the diagnostic Q waves of myocardial infarction. According to the semidirect lead hypothesis, the abnormal Q waves produced by myocardial infarction

experiment is that the magnitudes of the maximal deflections in leads I, II, and III are different. Evidently, the leads must be weighted differently in terms of their lengths. The concept of lead weight or length was shown previously to apply to the bipolar and unipolar limb leads. By calculations based on the Einthoven equilateral triangle, it was possible to demonstrate that the bipolar lead axes are longer than the axes of the augmented unipolar limb leads, while the

since the dipole vector parallels the lead vector when the maximal deflection is recorded. Therefore, the above equation can be restated as follows. The size of the maximal deflection in a given lead is proportional to the magnitude or length of the lead vector; or, the voltage equivalent or value of each unit length of the projected component of the dipole vector is proportional to the length of the lead axis. Thus, the lengths of the lead vectors of leads I, II, and III in the experi-

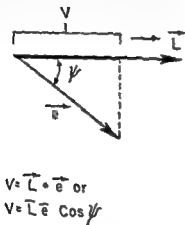


Fig. 34 - Relationship of the lead deflection to the magnitude and accompanying equation of the projection of the

- \vec{L} — LEAD VECTOR
- L — MAGNITUDE OR LENGTH OF LEAD VECTOR
- \vec{e} — DIPOLE VECTOR
- e — LENGTH OF DIPOLE VECTOR OR DIPOLE MOMENT
- ψ — ANGLE SUBTENDED BY LEAD AND DIPOLE VECTORS
- V — PROJECTION OF DIPOLE VECTOR ON LEAD VECTOR OR VOLTAGE PROJECTED ON LEAD

axes of the Wilson unipolar leads are the shortest of all. It was also shown that, with reference to the magnitude of a cardiac vector, the unit of amplitude in the augmented unipolar leads is equivalent to only 87% of an equal deflection in the standard bipolar leads, and the percentage drops to 58% in the case of the Wilson unipolar leads.

Like the extremity leads, the Wilson unipolar leads also have the same direction (or direction of deflection) as the vector quantities or lead vectors. The directions of the lead vectors have already been established in this experiment. To determine the relative lengths of these lead vectors, a concept by Burger and van Milam can be utilized (Fig. 34). This proposes that the deflection in a given lead is the dot product of the dipole vector and lead vector and can be calculated by multiplying the magnitudes of these vectors by the cosine of the angle (ψ) they subtend, or $V = \vec{e} \cdot \vec{L} = e \cdot L \cos \psi$. In this experiment, the magnitude of the dipole vector is ignored, and the lead vector is considered as the lead axis.

ment can be made proportional to the magnitude of the maximal deflection in each of these leads.

With the information provided by the experimental observations, it is now possible to construct a triangle $R'L'F'$ having as its sides the lead vectors of leads I, II, and III.

The image point of L , Apex R' lies inferiorly and anteriorly to R , the site of the right shoulder electrode, and is the image point of R , while F' is the image point of F . In fact, for every point on the surface of the torso model there is a corresponding image point, in other words, the anatomic torso surface can be represented electrically by an image surface. According to Frank, who advanced this theory of the image vector, the projection of the cardiac dipole vector on a second vector originating at the dipole center and extending to a point on the image surface, multiplied by the length of this vector, gives a result which is proportional to the true unipolar potential measured at the corresponding point on the torso surface. If an electrode is relatively near the di-

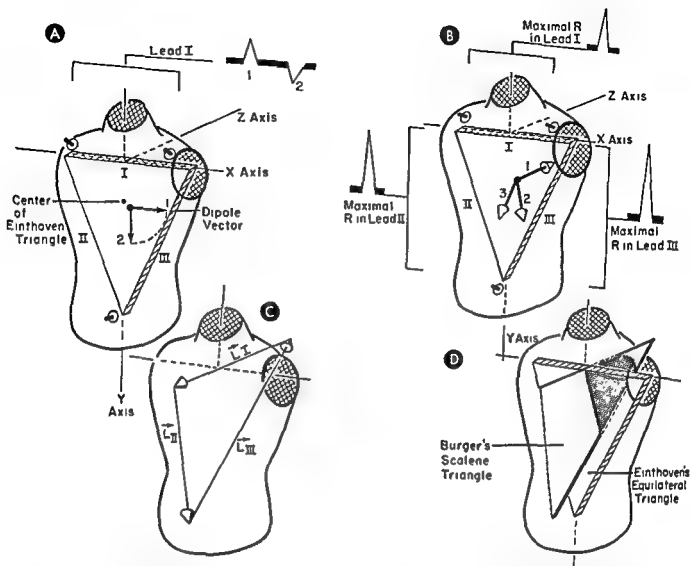
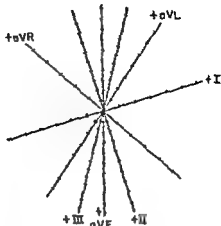


Fig. 33.—Schematic diagram of an experiment with torso model and artificial dipole illustrating the basis of the lead vector concept. In A, with the dipole vector at position I, lead I records an R wave of unexpectedly low amplitude in-

terior, and inferior (C). In a similar manner, the directions of the lead vectors of leads II and III can be determined from the directions of the dipole vector when it projects maximally on lead II (vector 2) and on lead III (vector 3). In B, it should be noted that the maximal R waves for leads I, II, and III are not equal in size. Consequently, the three of leads I, II, and III is a scalene triangle which does not lie entirely in the frontal plane.



Fig. 36.—Four nonequilateral triangles representing variations in the Burger triangle, as the result of differing locations of the dipole center in a torso model (After Langner.)



Leads	Millimeters per Scale Unit	Proportionality Factors
I	7.5	1
II	4.5	0.6
III	3.75	0.5
aVR	8.25	1.1
aVL	6	0.8
aVF	4.5	0.6

Fig. 37.—Hexaxial reference figure formed by lead vectors calculated from torso model studies. The effective directions of the various lead axes are shown, and the differing lengths or magnitudes of the lead vectors have been corrected for by the use of proportionality factors. Thus, since the lead vector of lead III is twice the length of that of lead I, it is assigned a proportionality factor only one-half that of lead I. As a result, the scale unit of lead III is one-half the length of that of lead I.

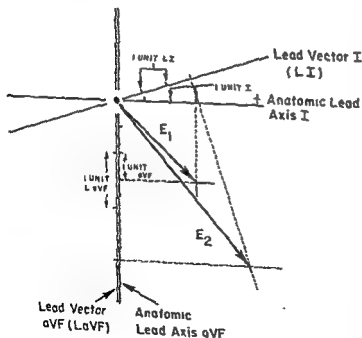


Fig. 38.—Reference figure consisting of the anatomic lead axes of I (labeled lead I) and aVF (labeled lead aVF), the line on the right in the vertical double line) and the lead vectors of lead I (lead vector I or L I) and of aVF (lead vector aVF or L aVF, the left line of the vertical double line). The anatomic lead axes are marked off in equal scale units, and, for convenience, the scale units in lead vector I are the same as those in the anatomic lead axes. Since lead vector aVF has a length or magnitude approximately twice that of lead vector I, its scale units are twice as large as those in the other axis. If the lead vectors had the same direction and magnitude as their corresponding anatomic lead axes, a cardiac vector I (E_1) projecting equally on both would be accurately reproduced in the vectorcardiogram or could be accurately constructed from the electrocardiographic deflections in the two leads. However, because of the differing magnitudes of the lead vectors and the altered direction of lead vector I, there is an exaggeration of the vertical projection of the cardiac vector in the frontal plane vectorcardiogram and the electrocardiographic deflections recorded by these leads, as indicated by vector II (E_2).

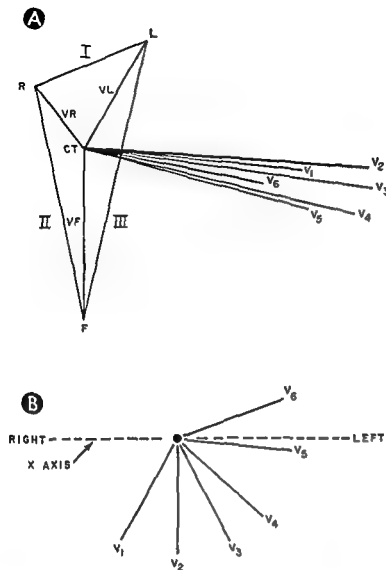


Fig. 35.—Lead vectors of the conventional twelve electrocardiographic leads **A**, the lead vectors of the standard bipolar and unipolar limb leads (frontal view), as calculated from data obtained from torso model studies. The lead vectors of the unipolar precordial leads originate from point CT (Wilson's central terminal). The precordial lead vectors are visualized in the frontal plane in order to demonstrate their respective magnitudes and their angles of declination from the horizontal **B**, the positions of the precordial lead vectors in the horizontal plane shown in relation to the transverse axis (X) representing the intersection of the frontal and horizontal planes of the body. The magnitude of these lead vectors is not indicated in **B**. (After Helm)

pole, its image point is far from the dipole, if the electrode is situated far from the dipole, the image point is near the dipole.

The closely related concepts of the lead vector and image vector are actually based on studies which resemble, although in a more complicated form, the hypothetical experiment described in the preceding paragraphs. At present, these concepts are being used to study the electrical qualities of the body as a volume conductor and the effects of dipole eccentricity. One of the most promising applications of the lead vector and image vector concepts has been suggested by the investigations of Burger and van Milaan, Frank, Helm, and others. As already indicated in the hypothetical experiment described above, it has been shown that the Einthoven triangle is not equilateral but is scalene or nonequilateral (Burger triangle) because of the differing lengths and directions of the bipolar lead vectors. Attempts have been

made to calculate Burger triangles for the human body and to calculate the lead vectors of the other routine leads (Fig. 35). While data obtained so far is not definitive, it seems likely that reasonably accurate Burger triangles will eventually be constructed, possibly for each type of body habitus (Fig. 36). At present, however, it is felt that the use of the "average" scalene Burger triangle, such as that constructed from the data of Frank and Kay, probably introduces less error in most subjects than the conventional Einthoven triangle. It is worthy of note that Einthoven's law (Lead I + lead III = Lead II) is applicable to the Burger triangle. A revised hexaxial reference figure for the frontal plane based on the lead vectors, has been calculated from torso models (Fig. 37).

In order to calculate more accurately the various frontal plane vectors from the electrocardiogram, the differing lengths of the lead vectors can be corrected for by means of proportionality factors. These are ob-

system (X, Y, and Z axes of the body). This type of lead system, called an orthogonal lead system, was thought to offer some advantage over systems based on the Einthoven triangle. However, if these rectangular systems are reconstructed, using the appropriate lead vectors, their geometric configurations can also be shown to be distorted to varying degree.

Another approach to the problem of devising more satisfactory leads has been that of McFee and Johnston. These investigators utilized models of selected planes of the body through which water was made to flow in sheets. The models were so constructed that

the course of flow encountered resistances analogous to the electrical resistances in the body. Thus, by causing the water to flow between points corresponding to different electrode positions, the flow lines could be mapped out for combinations of points. These flow lines were considered to approximate the lines of current flow in the body, so that the pattern of flow lines for a given lead represented the lead field for the lead (Fig. 41). McFee and Johnston are now attempting to devise improved leads by selecting combinations of electrodes in which the undesirable features of the flow lines tend to cancel out one another.

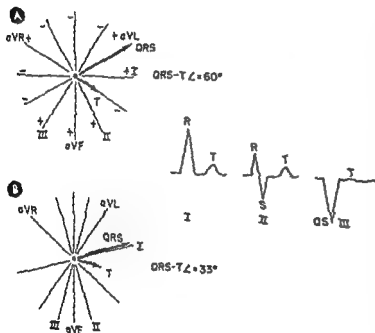


Fig. 40.—The influence of the different directions of the lead vectors as opposed to the anatomic lead axes, the magnitude variations in the leads being ignored. From the schematic complexes labeled leads I, II, and III, it can be seen that the mean QRS vector is perpendicular to the lead axis of II and the mean T vector is perpendicular to the axis of lead III. If these vectors are constructed in the ordinary hexaxial reference figure (A), the QRS-T angle obtained is 60° , which is borderline abnormal. However, if these vectors are plotted in the reference frame (B) formed by the effective axes of the various leads, the QRS-T angle resulting is only 33° , a value well within normal limits.

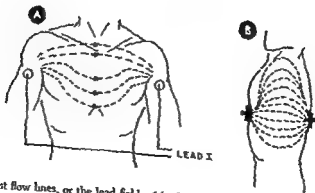


Fig. 41.—Pattern of current flow lines, or the lead field, of lead I (A) and of an anteroposterior bipolar chest lead (B).

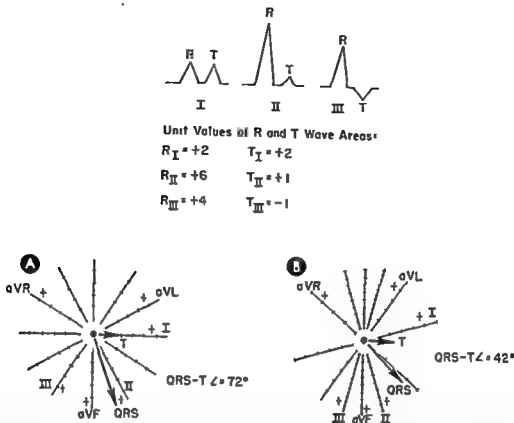


Fig. 39.—Application of the corrected hexaxial reference figure to the calculation of the frontal plane QRS-T angle. It will be assumed, in this figure, that a planar QRS-T angle greater than 60° means that the corresponding spatial QRS-T angle also exceeds the upper limit of normal of 60° . Similarly, a planar QRS-T angle less than 60° implies that the spatial QRS-T angle is also less than 60° . In actual fact, this assumption is usually a valid one in the interpretation of normal and abnormal electrocardiograms.

In A, the mean QRS and T vectors are plotted on the usual hexaxial reference frame, based on the equilateral Einthoven triangle. (The vectors are constructed from the relative values for the areas of the diagrammatic QRS and T complexes in leads I, II, and III, given above.) The frontal plane QRS-T angle obtained is approximately 72° and therefore is abnormally wide.

If, however, the vectors are plotted on the hexaxial reference frame in B, which corrects for the differing lengths of the leads, the frontal plane QRS-T angle is

1 amplitude unit = 4 mm.

1 scale unit in A and in lead I of B = 5 mm

The scalar units of the remaining leads in B are obtained by multiplying the proportionality factors of the leads times 5 mm

tained by dividing the length of lead I by the length of every other frontal plane lead. The proportionality factors are used to mark off properly the scale on each lead axis so that the longer the lead vector the smaller are its scalar units.

The following correction values have been calculated by Langner:

Lead I 1	Lead aVR 1.1
Lead II 0.6	Lead aVL 0.8
Lead III 0.5	Lead aVF 0.6

It is evident from the above proportionality factors that the lead vectors of II, III, and aVF are about twice as long as the lead vector of lead I. Thus, in the electrocardiogram there tends to be an exaggeration

of the vertical component of the heart vector (Figs 38, 39, and 40)

Like the preceding scalar leads, the vectocardiographic leads also are modified by the shape, dimensions, and conductivity of the trunk and by the electrode positions. Thus, the anatomic lead axes and corresponding lead vectors of the vectocardiographic leads differ in length and direction. For example, since the Einthoven triangle is not equilateral, systems of electrode placement based on it must necessarily have lead vectors differing significantly from the anatomic lead axes. Several of the lead systems have been so constructed as to have their anatomic lead axes parallel to the axes of the "natural" co-ordinate

THE P WAVE

Unlike the ventricles, the atria do not have a specialized conduction apparatus. Instead, the excitation wave initiated by a sinus impulse fans out radially from the sinoatrial node and spreads uniformly in this manner through the atrial muscle. The elementary electrical forces produced by activation of the atria

vertically downward, so that the P wave in lead I becomes smaller and the P waves in leads II, III, and aVF larger. On the other hand, in short stocky individuals, the frontal orientation of the mean P vector may approach the 0° axis or positive axis of lead I, in which case the P wave in lead I tends to be larger than

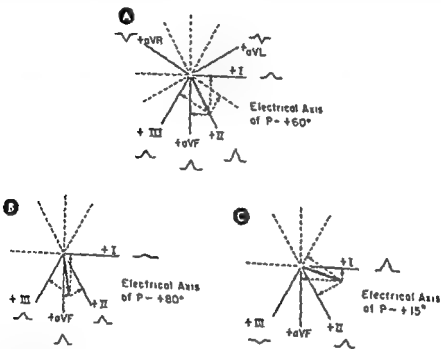


Fig 43.—Variations in orientation of the mean manifest electrical axis of P (A P) in a normal individual. The hexaxial reference system is shown in each diagram.

in all directions from the sinus node. However, the net effective or average direction of these instantaneous P vectors in the frontal plane—in other words, the mean manifest electrical axis of P (A P) or the frontal mean P vector—approximates the $+60^\circ$ axis of the frontal hexaxial reference figure or the positive half of the axis of lead II (Fig 43). Consequently, the P waves tend to be tallest normally in lead II, isoelectric, or diphasic, in lead aVL, and upright in leads I and aVF. Inverted P waves are normally present in lead aVR. In normal subjects of tall and slender body habitus, the frontal mean P vector is sometimes oriented more

usual and the P wave in lead III may be diphasic or inverted.

The horizontal plane mean P vector is relatively variable in orientation, ranging from 0° to $+60^\circ$ in general. In some individuals, the P wave in lead I is slightly inverted, and in some it is almost inverted. Inasmuch as the P wave in lead I is almost inverted in normal subjects, the P wave in lead I may show t

With the completion of atrial depolarization, the

The Normal Electrocardiogram

GENERAL SEQUENCE OF CARDIAC EXCITATION

THE SPREAD OF EXCITATION through the heart follows a sequence which is largely determined by the site of origin of the excitation impulse, the anatomic distribution of the specialized conducting pathways, and the speed of conduction in the different parts of the heart. The sinoatrial node, which is located in the wall of the right atrium near the entrance of the superior vena cava, normally is the most rhythmical focus in the heart, and therefore is the site of origin of the excitation impulse and the dominant cardiac pacemaker. Sinus node discharge per se produces no detectable deflection in the electrocardiogram, although the sinus impulse initiates atrial activation, the latter

producing, in turn, the electrocardiographic P wave. In the course of its spread through the atrial myocardium, the excitation impulse arrives at the atrioventricular node. This structure consists of a bundle of longitudinal conducting fibers which merge inferiorly with the common bundle of His situated in the upper portion of the interventricular septum. The atrioventricular node picks up the atrial excitation impulse and transmits it to the intraventricular conducting pathways. The bundle of His is relatively short and soon divides into two main branches—the left and right bundle branches—which descend subendocardially on either side of the interventricular septum. The bundle branches terminate by branching profusely to form an extensive network of conducting fibers, the Purkinje system, which is distributed widely throughout the subendocardium of both ventricles and the lower two thirds of the interventricular septum.

The subendocardial spread of excitation through the myocardial syncytium takes place about 5–10 times more rapidly than its subsequent radial passage outward through the ventricular wall. In addition, substantial evidence, accumulated by various investigators, supports the belief that the subendocardium and inner layers of ventricular myocardium are normally “electrocardiographically silent” during depolarization. As an explanation of this finding, it has been suggested tentatively that the Purkinje fibers may extend more deeply into the inner ventricular wall than previously supposed (Fig. 42). This may result in the inner ventricular wall being activated too rapidly and in too many directions for any measurable potentials to be produced. Thus, in effect at least, the electrical forces arising during ventricular depolarization are generated almost entirely by the outer subepicardial one third of the ventricular wall.

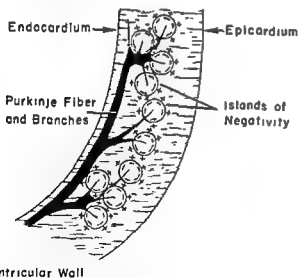
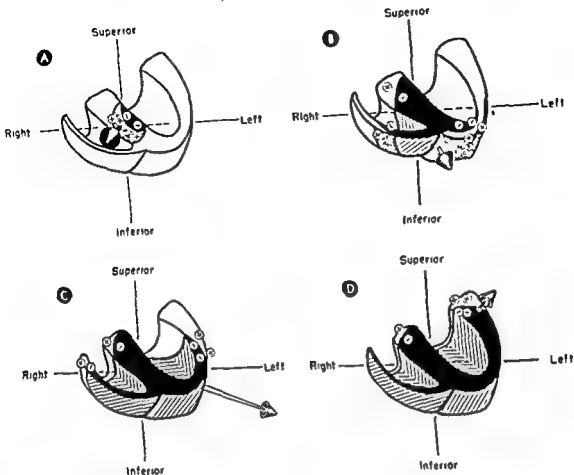


Fig. 42.—Schematic section of the ventricular wall showing the Purkinje fibers shortly after onset of ventricular depolarization. Since the Purkinje fibers penetrate the inner two thirds of the ventricular wall, excitation begins as scattered “islands of negativity” at the termini of the Purkinje fibers. Measurable activation potentials are not



activation of the apical walls of the left and right ventricles (C) and activation of the basal walls of the left and right ventricles (D).

branches. The excitation process then passes rapidly over the endocardial surfaces of both ventricles and shortly thereafter begins to spread transmurally through the apical walls of the left and right ventricles.

✓ **0.02-second apicoanterior VA vector**—Within 0.02 second of onset of the QRS interval, the activation wave has passed through the lower two thirds of the septum, but it continues to spread in an apex-to-base direction over the right septal surface and basal one third of the septal myocardium. Meanwhile, the activation wave front has penetrated to the epicardial surface of the apical right ventricular wall and is now moving through the lateral wall of the right ventricle and through the apicoanterior wall of the left ventricle. The rapid extension of the excitation process through the apical myocardium is probably due to the relatively thin layer of muscle in this region or per-

haps to the deeper penetration of the Purkinje fibers into the apical myocardium. The electrical forces produced by activation of the free walls of the left and right ventricles can be represented by two vectors, directed to the left and right of the long axis of the heart. Since the left ventricular forces and their representative vector are of greater magnitude than their right ventricular counterparts, the resultant of the two vectors, which is called the 0.02-second apicoanterior VA vector in this text, is oriented along the long axis of the heart—i.e., anteriorly, to the left, and somewhat inferiorly (Fig. 44, B). The frontal plane projection of the apicoanterior vector is directed approximately along the $+60^\circ$ axis or the positive half of the axis of lead II. If the 0.02-second VA vector is superimposed on the frontal and horizontal reference frames, it projects positivity on leads I, V_6 , aVF and V_1 and V_2 , causing all leads but V_2 to inscribe the upstroke of an

downstroke of the P wave reaches the isoelectric line. In cases of complete heart block or atrioventricular dissociation, it is sometimes possible to discern a negative deflection following the P wave. This deflection represents the atrial T (repolarization) wave and is called the Ta (or Tp) wave. When seen, it is usually directed oppositely to the P wave. In most instances, however, the Ta-wave is buried in the following QRS complex. With rapid heart rates, the Ta wave can cause an apparent depression of the ST segment.

The P-R Interval

The P-R interval extends from the beginning of the P wave to the onset of the first component of the QRS complex (Q or initial R) and usually does not exceed 0.20 seconds in normal adults. After inscription of the P wave, the base line of the electrocardiogram usually

remains isoelectric, inasmuch as the electrical potentials formed during the remainder of the P-R interval are of relatively insignificant magnitude. The P-R interval is used primarily as a measure of the conduction time through the atrioventricular node, although in fact it represents the total time required for the impulse to travel from the region of the atria near the sinus node to the ventricles. This apparent discrepancy between fact and clinical usage arises because the atrioventricular node has such a very slow rate of conductivity that it constitutes the main conduction bottleneck between sinus node and ventricles. Thus the major portion of the P-R interval is required normally for passage of the impulse through the atrioventricular node. While changes in intra-atrial conduction time can also alter the P-R interval, such changes are infrequently encountered, in contrast with disturbances of atrioventricular conduction.

THE QRS COMPLEX

In the following paragraphs the spread of depolarization through septal and ventricular myocardium, and the electrical forces of differing direction and magnitude thereby produced, will be schematized in terms of a series of hypothetical instantaneous cardiac spatial vectors. These vectors will here be designated ventricular activation vectors (VA vectors) to distinguish them from manifest vectors determined from the electrocardiogram or vectorcardiogram and from vectors representing actual cardiac forces (as opposed to those recorded). However, the direction and relative magnitude of each of these VA vectors conform more or less to the characteristics of comparable instantaneous vectors in the normal vectorcardiogram and to the facts known regarding the course of ventricular activation. These VA vectors are assumed to be resultant or mean vectors, each representing the average direction and magnitude of all electrical forces produced at a given instant by the heart, and for this very reason, they can be related only in a general way to activation of a specific region of the heart.

Since the original investigations of Lewis and Rothschild many years ago, septal activation has been thought to occur first on the left septal surface and thereafter to spread as a double wave of envelopment from above downward and from without inward. This concept of septal depolarization has been modified

✓ 0.01-second septal VA vector.—An isopotential line is written in the electrocardiogram while the excitation impulse is passing through the atrioventricular node and the common bundle of His. The left septal surface is the first to be activated and this occurs in its upper third because of the early ramification of the left bundle branch in this region. Inasmuch as the septum lies relatively parallel, not perpendicular, to the frontal plane, the VA vector representing this phase of septal depolarization is directed anteriorly as well as to the right (Fig. 44, A). In intermediate and vertical spatial positions of the heart, the septal vector is thought to pass upward, in horizontal heart position, to pass downward. Purely septal depolarization is exceedingly transient, probably not much longer than 0.01 second in duration. If this septal vector were to be projected on the extremity and

V_6 , which normally records small initial Q waves, and (b) initial positivity in lead V_1 , which usually displays a small initial R wave. Either a small Q wave or positive deflection may be written in lead aVF, depending on whether the septal vector is directed somewhat superiorly or inferiorly.

After onset of septal depolarization, the excitation wave spreads rapidly over the entire left septal surface, and at the same time it emerges on the right septal surface initially near the base of the anterior papillary muscle where the right bundle gives off its first

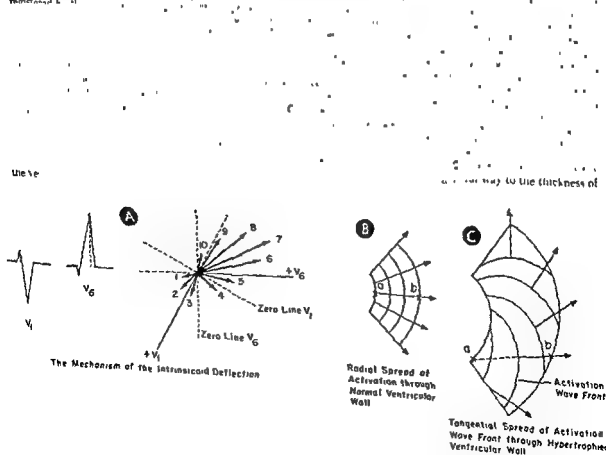
second VA vectors would project maximal positive voltage on leads V_1 and V_2 , and the 0.04-second VA vector would do the same in the case of lead V_6 . Thus, for each lead from V_1 to V_6 , the instantaneous vector projecting maximal positivity tends to appear later and to project greater positive voltage. Not only is this circumstance the basis for the normal transition from resultant QRS negativity in right precordial leads to resultant positivity in left precordial leads, but it is also responsible for the different times of onset of the intrinsicoid deflection in leads V_1 and V_6 , as will be explained later (Fig. 46).

In the normal precordial electrocardiogram, the change from resultant QRS negativity to resultant positivity can occur gradually, so that one or more intervening leads record *transitional* or *equiphase*, *RS deflections*. The precordial lead registering the

transitional RS deflection is termed the *transitional lead*. Not infrequently the transition from resultant negativity to positivity takes place abruptly between two adjacent leads, in this case, the transitional lead can be visualized as situated intermediate between the two leads in question.

One of the concepts which evolved from the semi-direct lead hypothesis was that rotation of the heart on its longitudinal axis could be recognized by certain changes in the precordial QRS transition. It was thought that the transitional RS deflection was recorded by the precordial lead whose exploring electrode was situated over the interventricular septum. Lead electrodes to the right of this point were believed to record primarily right ventricular potentials and electrodes to the left, left ventricular potentials. If the transitional QRS complex was registered by a

Fig. 46.—The present concept of the intrinsicoid deflection. The time of onset of the intrinsicoid deflection in leads V_1 and V_6 is measured from the onset of the QRS deflection in each lead to the points where the perpendicular (dashed) lines dropped from the peaks of the R waves intersect the horizontal axis. The nature of the deflection, as to the nature of the deflection, are representative during the QRS interval.



R wave (Fig. 45). In the case of lead V_1 , the 0.02-second VA vector contributes to the downstroke of the R wave, since the positive voltage projected on V_1 by the 0.02-second vector is usually of lesser magnitude than that produced by the initial septal vector.

0.04-second left ventricular VA vector.—At about 0.04 second after onset of septal depolarization, the

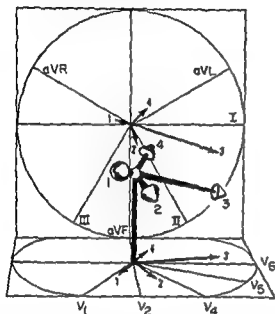


Fig. 45.—The planar projections of the four normal instantaneous VA vectors. Vector 1 represents initial septal activation, vector 2, apicoanterior left ventricular wall depolarization, vector 3, principally left ventricular depolarization, and vector 4, terminal activation of basal portions of the left ventricle. If the four QRS vectors described in Figure 44 are depicted as above, their projections on the frontal plane lead axes and horizontal plane lead axes would cause leads I and V_6 to register a small Q wave followed by a large R wave, and leads aVR and V_1 to write a small initial R wave and then a deep S wave.

septum and most of the lateral wall of the right ventricle have completed depolarization. Except for a small posterobasal segment of the right ventricular walls, the activation process is confined entirely to the left ventricle, where it continues to spread through the thick lateral wall. This gives rise to electrical forces of maximal strength which dominate the small right ventricular forces so completely that the resultant 0.04-second vector is almost identical with its left ventricular component. Thus the 0.04-second vector is the largest of the VA vectors and is directed at almost a right angle to the long axis of the heart—i.e., to the left, posteriorly, and slightly inferiorly (approximately along the -5° or -10° axis of the frontal reference frame) (Fig. 44, C). The appearance of this

vector coincides with the inscription of the peak of the R wave in leads I and V_6 and the nadir of the S wave in V_1 (Fig. 45).

0.06-second terminal, or basal, VA vector.—The terminal vector is produced mainly by activation of the thick posterolateral and basal wall of the left ventricle. Depolarization of the pulmonary conus also occurs at about this time, but its over-all contribution to the electrical field of the heart is ordinarily negligible. The terminal vector is directed to the left and superiorly (approximately along the -40° axis in the frontal reference frame) and more posteriorly than the preceding vectors (Fig. 44, D), and it projects smaller positive voltages on leads I and V_6 and smaller negative voltage on lead V_1 (Fig. 45).

Although a mean cardiac spatial vector exists for each and every instant of the QRS interval, for simplification only the four instantaneous VA vectors just described will be utilized hereafter to schematize ventricular activation. In relating these spatial vectors to certain features of the electrocardiogram, it should be kept in mind that the precordial lead deflections are largely determined by the projections of the cardiac vectors on the horizontal plane, the limb lead deflections, by the projections of the vectors on the frontal plane.

Precordial transition of the QRS configuration—

The normal precordial electrocardiogram is characterized by a progressive right-to-left increase in the relative amplitude of the R waves and a decrease in depth of the S waves. The explanation offered for this finding by proponents of the unipolar or semidirect lead concept of electrocardiography is summarized later in this section. As previously indicated, the growing preponderance of left ventricular forces during the first half of the QRS interval tends to be paralleled by an increasing magnitude and more leftward and posterior orientation of each successive instantaneous vector. This trend culminates in the appearance of the maximal mean instantaneous QRS vector (corresponding to the 0.04-second VA vector), after which subsequent instantaneous vectors tend to decrease in length. In other words, as the instantaneous vectors lengthen, they also rotate toward the positive halves of the lead axes of left precordial leads and away from the negative halves of the axes of right precordial leads. If the horizontal projections of all the instantaneous cardiac vectors were evident rather than just those of the four VA vectors described, it would become apparent that for each precordial lead there is an instantaneous vector which projects maximal positivity on the lead. For example, the 0.01- or 0.02-

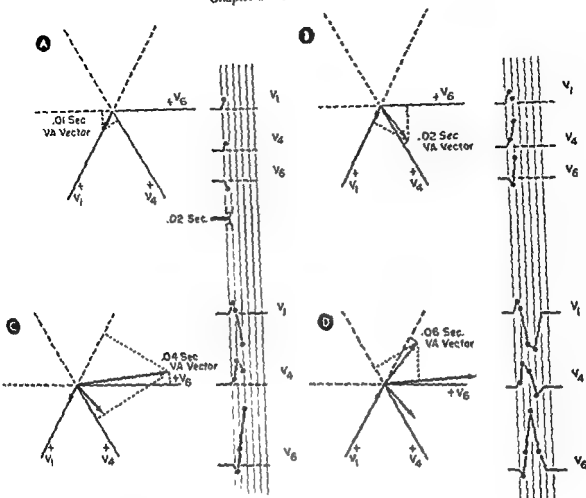


Fig 47.—A-D, projections of the four normal instantaneous VA vectors on precordial leads V_1 , V_4 , and V_6 . The voltages projected by these vectors on the lead axis of the three leads are shown. The peak of the R wave in V_6 coincides with the 0.04-second VA vector, the peak of the R wave in V_4 coincides with the 0.02-second VA vector, and the peak of the R wave in V_1 coincides with the 0.01-second VA vector. The onset of the intrinsic deflection occurs later in lead V_6 than in V_4 , but this merely indicates that the maximal positive instantaneous vector for V_6 appears later in the QRS interval than the corresponding vector for V_4 . Moreover, the appearance of the maximal positive vector for a given lead cannot be considered indicative of the completion of depolarization in the heart muscle facing the lead, and this holds true whether ven-

tricular activation takes place in a normal or abnormal manner. One reason for this is that radial spread of the activation wave through the ventricular wall, a prerequisite of Wilson's concept of the intrinsic deflection, may not be characteristic of the abnormal or normal heart. Tamm¹ has shown that the intrinsic deflection occurs in a normal or abnormal manner. One reason for this is that radial spread of the activation wave through the ventricular wall, a prerequisite of Wilson's concept of the intrinsic deflection, may not be characteristic of the abnormal or normal heart. Tamm¹ has shown that the intrinsic deflection occurs in a normal or abnormal manner. One reason for this is that radial spread of the activation wave through the ventricular wall, a prerequisite of Wilson's concept of the intrinsic deflection, may not be characteristic of the abnormal or normal heart. Tamm¹ has shown that the intrinsic deflection occurs in a normal or abnormal manner.

tricular activation takes place in a normal or abnormal manner. One reason for this is that radial spread of the activation wave through the ventricular wall, a prerequisite of Wilson's concept of the intrinsic deflection, may not be characteristic of the abnormal or normal heart. Tamm¹ has shown that the intrinsic deflection occurs in a normal or abnormal manner. One reason for this is that radial spread of the activation wave through the ventricular wall, a prerequisite of Wilson's concept of the intrinsic deflection, may not be characteristic of the abnormal or normal heart. Tamm¹ has shown that the intrinsic deflection occurs in a normal or abnormal manner. One reason for this is that radial spread of the activation wave through the ventricular wall, a prerequisite of Wilson's concept of the intrinsic deflection, may not be characteristic of the abnormal or normal heart. Tamm¹ has shown that the intrinsic deflection occurs in a normal or abnormal manner.

lead to the left of leads V_3 and V_4 , it was reasoned that clockwise rotation of the heart on its longitudinal axis must have occurred to bring the septum into this position. Conversely, counterclockwise rotation was implicated when the transitional lead was shifted to the right of leads V_3 and V_4 . While there are many theoretical and practical objections to the electrocardiographic diagnosis of cardiac rotation, it is quite conceivable that in an occasional instance anatomic rotation of the heart can be largely responsible for the pattern of "clockwise" or "counterclockwise" rotation* in the precordial leads.

As already indicated in Chapter 3, it has been demonstrated that the lead recording the transitional QRS deflection is not necessarily the lead overlying the septum, but rather the lead whose axis is perpendicular to the horizontal mean QRS vector. If, for example, the instantaneous VA vectors were added vectorially, the horizontal mean VA vector expressing the average direction and magnitude of the instantaneous vectors would be found to lie along the -15° axis. Since the lead axis of V_3 is situated at about $+75^\circ$ in the horizontal reference frame, the mean VA vector is perpendicular to this lead axis and lead V_3 would record the transitional QRS complex. Therefore, in the precordial electrocardiogram, the location of the lead registering the transitional QRS complex depends on the orientation of the horizontal mean QRS vector, and this vector, in turn, ordinarily approximates the orientation of the maximal instantaneous QRS vector in the horizontal plane.

Intrinsicoid deflection.—If the exploring electrode of a unipolar lead is applied directly to the epicardial surface of the heart to form a *direct lead*, the lead records an R wave as the ventricular activation wave moves toward the electrode. At the exact moment that the epicardial muscle underlying the electrode becomes depolarized, the activation potentials disappear and an abrupt downstroke is inscribed, extending from the peak of the R wave to the base line, or to the nadir of the S wave, if present. This is called the *intrinsic deflection*. If muscle in contact with the electrode is the last to be depolarized, then the intrinsic

deflection ends at the base line and forms the final limb of the QRS complex in the lead. However, if the underlying muscle is not the last to be activated, the intrinsic deflection terminates at the nadir of the following S wave. Wilson considered the interval extending from the onset of the QRS complex to the onset of the intrinsic deflection in a direct lead to be related both to the thickness of muscle between the exploring electrode and the ventricular cavity and to the speed of conduction of the activation impulse through this muscle. Thus, onset of the intrinsic deflection would be expected to occur later in the QRS interval in leads recorded over the thick left ventricular wall than in leads overlying the right ventricle. Wilson and his associates believed, with some reservations, that the so-called *intrinsicoid deflection* in the indirect unipolar precordial leads used in clinical electrocardiography corresponded to the intrinsic deflection of the direct epicardial leads (Fig. 46, A). The interval from onset of the QRS to onset of the intrinsicoid deflection (sometimes designated the *ventricular activation time* or *pre-intrinsicoid deflection time*) was considered normal if it did not exceed a maximum of 0.035 second in precordial leads facing the epicardial surface of the right ventricle and 0.055 second in leads overlying the epicardial surface of the left ventricle. Seemingly, Wilson's concept of the intrinsicoid deflection was justified by the observation of the delayed onset of the intrinsicoid deflection in ventricular hypertrophy and intraventricular conduction disturbances.

Since the intrinsicoid deflection concept outlined above is based on the semidirect lead hypothesis, its validity for surface leads, such as those utilized in clinical electrocardiography, is open to serious question. According to the equivalent dipole or vector concept of surface lead electrocardiography, the intrinsicoid deflection in an indirect lead is produced by the instantaneous QRS vector which projects maximal positivity on the lead and is not related directly to the state of activation of the muscle nearest the electrode (Figs. 46, A, and 47). This concept can be simply illustrated by considering the 0.01-, 0.02-, 0.04-, and 0.06-second VA vectors. The times of onset of the intrinsicoid deflection in leads V_1 and V_6 are measured along the base line of the electrocardiogram, from the beginning of the QRS interval to the point demarcated on the base line by a perpendicular dropped from the peak of the R wave in each lead. In this hypothetical example, the peak of the R wave in

*Hereafter, in this text, "clockwise rotation" and "counterclockwise rotation" will be enclosed by quotation marks only when these terms refer to the so-designated electrocardiographic patterns. By this means, the authors hope to convey to the reader their doubts concerning the relationship between anatomic and electrocardiographic "rotation."

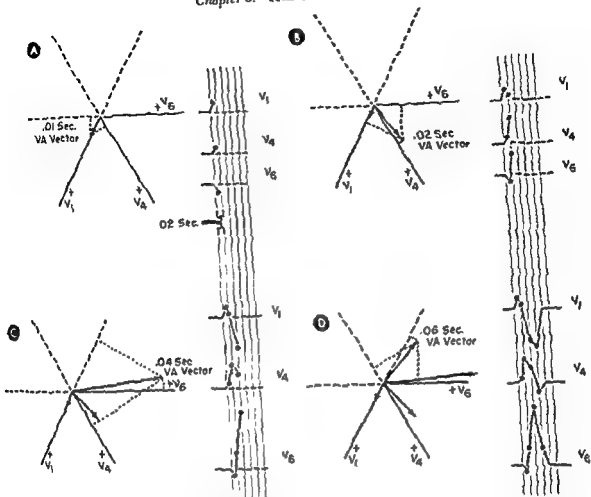


Fig 47.—A-D, projections of the four normal instantaneous VA vectors on precordial leads V_1 , V_4 , and V_6 . The voltages projected by these vectors on the lead axes of the above leads plotted in the ECG which in lead V_1 the .01-second VA vector is projected as a small r wave, in lead V_4 as a small r wave, and in lead V_6 as a small r wave.

of ventricular activation

lead V_1 coincides with the appearance of the 0.01-second VA vector, which is the maximal positive vector for the lead. In contrast, the peak of the R wave in V_6 coincides with the 0.04-second VA vector, the

tricular activation takes place in a normal or abnormal manner. One reason for this is that radial spread of the activation wave through the ventricular wall, a prerequisite of Wilson's concept of the intrinsicoid deflection, may not be characteristic of the abnormal or normal heart. Tangential spread of excitation certainly occurs in the hypertrophied heart and may also occur in the normal heart (Fig 48, B and C). This circumstance in itself invalidates Wilson's concept of the intrinsicoid deflection. In actuality the authors have not found measurement of the ventricular activation time to be of much value in the clinical interpretation of electrocardiograms.

maximal instantaneous vector for V_6 appears later in the QRS interval than the corresponding vector for V_1 . Moreover, the appearance of the maximal positive vector for a given lead cannot be considered indicative of the completion of depolarization in the heart muscle facing the lead, and this holds true whether ven-

ELECTRICAL HEART POSITION

The relationship existing between the QRS configuration and the anatomic position of the heart in the chest has been recognized for many years. With the advent of unipolar electrocardiography, Wilson and his associates devised, and later authors further developed, a method by which five different *electrical* heart positions (the qualification "electrical" is deserving of emphasis) could be defined according to the particular combination of QRS complexes found in the unipolar limb and precordial leads. It is important to stress that Wilson regarded these electrocardiographic positions of the heart as being only generally related to the anatomic heart position and not necessarily dependent on it. The belief that a unipolar electrode records a QRS complex whose contour is relatively specific for the region of the heart facing the electrode was only one of the many applications of the semidirect lead hypothesis. Conversely, it was reasoned that, if a QRS complex recorded by a given lead displays a configuration identified with a certain region of the heart, then the lead may be assumed to face this area. According to this concept, which has also been termed the *unipolar method* for electrocardiographic interpretation, potential variations of the anterolateral epicardial surface of the left ventricle are transmitted to the left precordium (leads V_5 and V_6 therefore recording qR complexes), and those of the epicardial surface of the right ventricle are transmitted to the right precordium (leads V_1 and V_2 regis-

tering rS deflections). The right arm (lead aVR) is thought usually to face the ventricular cavities, and registers their negative potential variations as predominantly downward deflections (Qr , QS , rS , or rSr'). The electrocardiographic positions of the heart, and hence the configuration of the QRS complexes in aVL and aVF , are thought to be expressions of rotation of the heart primarily on its longitudinal axis.

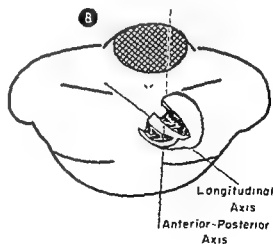
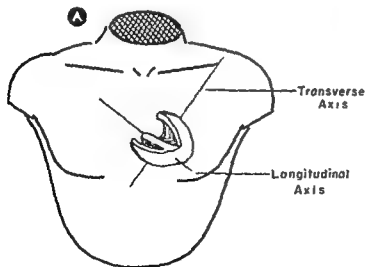
Electrical Axes of Rotation

The axes of the heart have been defined as the longitudinal, the anteroposterior, and the transverse axes.

Longitudinal axis—This axis is a line connecting the apex with the midpoint of the ventricles (Fig. 48, A and B.) Rotation on this axis is described as if the heart were visualized in an apex-to-base direction, clockwise rotation causing the right ventricle to move superiorly and counterclockwise rotation moving the left ventricle superiorly.

Anteroposterior axis—This is a horizontal line running through the center of the heart in an anteroposterior direction (Fig. 48, B) Rotation of the heart on this axis causes its apex to face either the left shoulder (horizontal) or the left hip (vertical).

Transverse axis—This is a line in the frontal plane perpendicular to and bisecting the longitudinal axis midway between apex and base of the heart (Fig. 48,



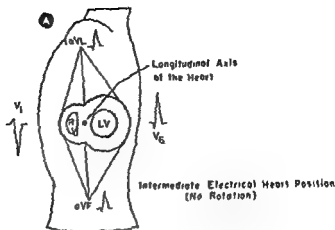
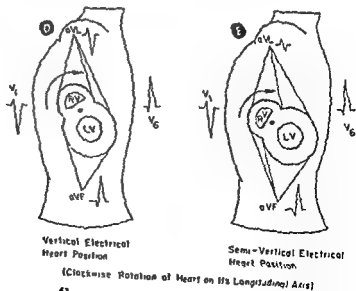
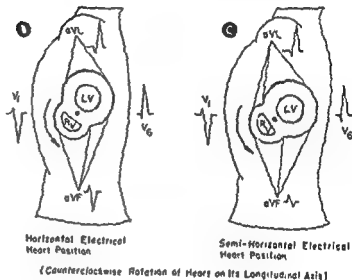


Fig. 49.—Illustrating the genesis of the QRS patterns in the electrocardiographic heart positions in terms of the semidirect lead, or unipolar, concept. According to this concept, a lead facing only the right ventricle registers an rS complex, one facing only the left ventricle, a QR complex. Leads facing portions of both ventricles record QRS complexes which are intermediate in configuration between the rS and the QR complexes. The heart is depicted in cross-section through the ventricles, as viewed through the left sagittal surface of the body—i.e., in an apex-to-base direction. The longitudinal axis of the heart is seen end-on as a point lying in the interventricular septum. Lead V_1 is depicted as a posterior lead, since it faces the posterolateral aspect of the left ventricle, almost directly across the chest from lead V_6 . (After Barker, J M)



A). Rotation on this axis swings the apex of the heart forward or backward.

Electrocardiographic Heart Positions

The following electrocardiographic heart positions are described in terms of the unipolar, or semidirect lead, concept (Fig. 49):

Intermediate heart position.—No rotation of the heart is considered to exist in the intermediate heart position (Fig. 49, A), the right ventricle being anteriorly placed and the left ventricle posteriorly placed. Leads aVL and aVF subtend equal angles* with the left ventricular surface, whose potential variations dominate those from the right ventricle. Consequently, the QRS deflections recorded in these two leads tend to resemble those registered in leads from the left side of the precordium (V_5 and V_6).

Horizontal heart position.—Counterclockwise rotation of the heart on its longitudinal axis swings the

*When the source of electrical potential is a charged surface, the potential at a field point (P) is proportional to the solid angle subtended by a cone drawn from P to include all surface dipoles on a sphere of unit radius about the point.

left ventricle above the right ventricle, which comes to occupy more of the diaphragmatic surface of the heart (Fig. 49, B). Lead aVL therefore records potential variations conducted to it from the epicardial surface of the left ventricle, so that its QRS deflections are similar to those recorded in leads V_5 and V_6 . Lead aVF records electrical potentials from the right ventricle and exhibits QRS complexes resembling those in leads V_1 and V_2 .

Semihorizontal heart position.—Less-marked counterclockwise rotation results in lead aVL facing the left ventricle as above, but lead aVF records potentials of about equal magnitude from those portions of the right and left ventricles resting on the diaphragm (Fig. 49, C). Accordingly, lead aVL registers complexes resembling those in leads V_5 and V_6 , while lead aVF records very small complexes not resembling those of either side of the precordium.

Vertical heart position.—Clockwise rotation swings the right ventricle above the left ventricle, which now comes to occupy more of the diaphragmatic surface of the heart (Fig. 49, D). Lead aVL, which faces the right ventricle, records complexes resembling those in leads V_1 and V_2 , while lead aVF records QRS de-

Intermediate Electrical Heart Position

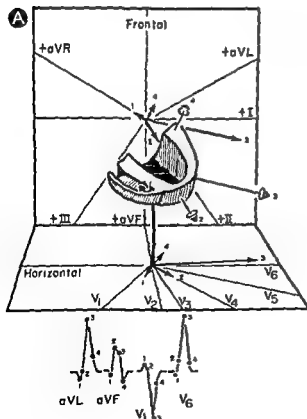
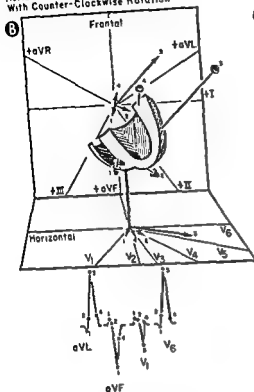


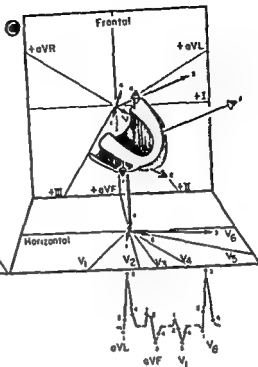
Fig. 50.—Illustrating the genesis of the QRS patterns in the electrocardiographic heart positions in terms of the resultant vector concept. In Figure 49 the QRS deflections in leads aVL and aVF and in leads V_1 and V_6 were explained in terms of the semidirect lead concept and were related to electrical heart position. In the present

which these vectors emanate in A through E has been depicted as if rotated in the same direction as the VA vectors. This was done to indicate more clearly the direction of rotation of the vectors and should not be thought to imply that the heart itself actually shows such marked rotational changes.

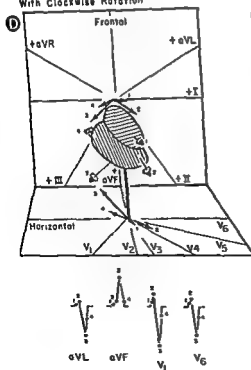
Horizontal Electrical Heart Position
With Counter-Clockwise Rotation



Semi-Horizontal Electrical Heart Position



Vertical Electrical Heart Position
With Clockwise Rotation



Semi-Vertical Electrical Heart Position

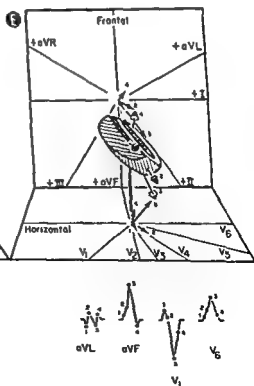


Fig. 50.—Legend on facing page

deflections similar to those in precordial leads V_5 and V_6 .

Semivertical heart position.—With less-marked clockwise rotation, lead aVL faces portions of both left and right ventricles (Fig. 49, E). Thus lead aVF records ventricular complexes resembling those in V_5 and V_6 , while aVL registers deflections which are small and nondescript.

Indeterminate position.—There is no apparent relationship between the QRS complexes of the limb leads and those of the precordial leads.

In terms of the equivalent dipole or vector concept, the relationship between the configuration of the QRS complex in leads aVL , aVF , V_1 , and V_6 can be explained by varying degrees of rotation of the instan-

aneous vectors, which may or may not be due to anatomic rotation of the heart (Fig. 50). Thus, the 0.02-second VA vector approximating the long axis of the interventricular septum can serve as the axis around which the other instantaneous vectors can be rotated in a clockwise or counterclockwise direction. It will be found that the projections of the four instantaneous VA vectors on the lead axes of the frontal and horizontal reference frames reproduce the electrocardiographic features described for the various electrical heart positions. However, rotation of the instantaneous vectors does not necessarily mean that the heart itself has rotated, as will be explained in Chapter 8, on ventricular hypertrophy.

GENERAL CHARACTERISTICS OF THE NORMAL SCALAR ELECTROCARDIOGRAM

EXTREMITY LEADS	PRECORDIAL LEADS
P WAVE	
1. Direction	In normal electrocardiograms, the mean P spatial vector is situated to the left, inferiorly, and somewhat anteriorly
The frontal mean P vector ($\bar{A}P$) lies approximately along the positive half of the lead axis of lead II ($+60^\circ$). Therefore, upright P waves are projected on leads I, II, and aVF ; inverted P waves, on lead aVR . Inasmuch as the frontal mean P vector lies more or less perpendicular to the lead axes of leads III and aVL , minor variations in the position of the vector can completely reverse the direction of the P waves recorded in these leads. Thus, leads III and aVL can normally display upright, inverted, or diphasic P waves.	The horizontal mean P vector usually is oriented slightly to the right of the positive half of the lead axis of lead V_4 ($+30^\circ$) or, less frequently, slightly to the left of this point. Thus, in the normal electrocardiogram, precordial leads V_2 through V_4 register upright P waves, while lead V_1 records a low upright P wave if the mean P vector lies to the right of $+30^\circ$, an inverted P wave if the vector lies to the left of $+30^\circ$, and a diphasic P wave ($+-$) if the mean P vector is oriented along the $+30^\circ$ axis, perpendicular to the lead axis of V_1 .
2. Amplitude	The amplitude of the P wave is not usually
Lead II generally records a taller P wave than leads I and III, but in none of these leads does the normal P wave in children or adults equal or exceed 3 mm., with only rare exceptions	In children and adults, the amplitude of the normal P wave in lead V_1 does not exceed 2.5 mm., with only rare exceptions
3. Duration	The maximum normal duration of the P waves measured in the bipolar limb leads is 0.10 second. P waves of 0.12-second duration
broad P waves	

4. Comments

are recorded properly or not

4 Lead aVF

While the

ing in the atr

tion of retrog

right, rarely

hypertrophy

observed in d

Slight notching of st

... and occasional exceptions

P-R INTERVAL

The P-R interval is measured from the beginning of the P wave to the onset of the first component of the QRS deflection. The lead selected for measuring the P-R interval should be the bipolar limb lead with the longest P-R interval.

Comments

... percentage of normal subjects the P-R

the same in

... second or more

QRS COMPLEX

1 Direction

In normal adults, the mean QRS spatial vector is directed to the left, inferiorly, and slightly posteriorly (Fig 51).

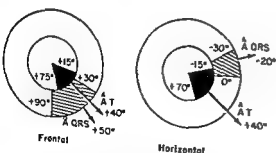


Fig. 51.—The range of variation and average orientation of sA QRS and sA T in the frontal plane and horizontal plane, calculated from the electrocardiograms of normal subjects.

The frontal mean QRS vector is usually located between $+30^\circ$ and $+90^\circ$ and tends, on the average, to lie along the $+50^\circ$ axis. Thus the main component of the QRS deflection is upright in leads I and II and is downwardly directed in lead aVR. Leads III, aVL, and aVF

The horizontal mean QRS vector is normally oriented between 0° and -30° , its average position approximating -15° . Its transitional

may normally record diphasic, resultantly positive, or resultantly negative QRS deflections. The main component of the QRS should be upright in at least two of the three bipolar limb leads for any position of the frontal mean QRS vector between -30° and $+150^\circ$. In occasional normal obese adults, the frontal mean QRS vector may be situated above $+30^\circ$ (left-axis deviation), while in occasional tall slender adults and in children, the mean frontal QRS vector may be situated to the right of $+90^\circ$ (right-axis deviation).

and leads to the left recording resultantly upright qR or qRs deflections. In normal subjects with the precordial lead pattern of clockwise rotation, the transitional RS deflection may be recorded by a lead farther to the left (V_4), while counterclockwise rotation shifts the transitional lead to the right of V_4 .

2. Duration

In adults, the QRS interval or width varies between 0.08 and 0.10 second in the limb leads. In general, the QRS duration tends to vary inversely with the heart rate and directly with the age of the patient. Thus, in children under 14 years of age, the upper limit of normal for the QRS duration is 0.09 second, in children under 5 years, it is 0.08 second. About 3% of normal adult subjects may have QRS deflections wider than 0.10 second.

The QRS interval or duration is not ordinarily measured in the precordial leads. This is

that the QRS interval can show such wide variation in the precordial leads of serial electrocardiograms recorded from the same individual.

3 Amplitude

The criteria for high QRS voltage in the limb leads are discussed in later chapters (see Chapter 9, on Left Ventricular Hypertrophy, and Chapter 10, on Right Ventricular Hypertrophy) in conjunction with the diagnostic criteria of ventricular hypertrophy. In brief, a

The criteria for high QRS voltage in the precordial leads are somewhat complicated and are best deferred for discussion along with the criteria for the diagnosis of ventricular hypertrophy. Low QRS voltage is present in the precordial leads if the amplitude of the largest QRS deflection is 8 mm. or less.

mm can be considered abnormally high voltage. High QRS voltage is usually not diagnosed from the bipolar limb leads.

Abnormally low QRS voltage exists if none of the three bipolar limb leads displays upwardly or downwardly directed QRS deflections exceeding 5 mm in amplitude (using the top or bottom of the baseline, as the case may be, for reference).

4 Comments

Low QRS voltage can be observed in either the limb leads or the precordial leads of normal subjects and is usually due to the fact that the cardiac forces are oriented more or less perpendicular to the frontal plane or, as the case may be, the horizontal plane. On the other hand, when the QRS voltage is low in both limb and precordial leads, then it can generally be inferred either that the magnitude of the cardiac forces is less than normal or that the cardiac forces are not transmitted to the surface electrode as well as normally, whether because of decreased conductivity of the lungs as the result of emphysema or pleural or pericardial effusion or because of anasarca, myxedema, etc.

As the chest electrode is moved from right to left across the precordium, the R/S amplitude

chest electrodes and the heart, since the exploring electrode of leads V_3 and V_4 are closer to the heart than the exploring electrode of leads V_1 and V_2 . Electrocardiograms not infrequently show so gradual a decrease in the R/S ratio involving one or more leads that the finding frequently indicates anterior myocardial hypertrophy.

reference level for measuring S-T segment displacement is the T-P segment, but in the presence of sinus tachycardia, the P-R segment may offer a more accurate base line for comparison. When S-T segment elevation occurs as a normal variation, the S-T segment is often less likely to be a normal variant of relatively low amplitude. C S wave of large area, elevated S—since they probably do not signify subepicardial myocardial injury. S-T segment elevation occurring as a normal variation tends to appear more commonly in leads V_1 and V_2 than in any of the other leads of the routine electrocardiogram.

T WAVE

1. Duration

0.10–0.25 second Just as in the case of the S-T interval, the duration of the T wave is generally not measured specifically but is included in the Q-T interval.

2. Direction

The T waves are normally upright in leads I and II but may be flat or biphasic in lead III. In leads aVR and aVL, the T wave is not upright, although occasional exceptions to the rule are noted.

Usually the T waves are upright in precordial leads V_1 through V_4 , but normal adults under 30 years of age may show inverted T waves in leads V_1 through V_4 , and sometimes in V_5 . However, in adults over 30, T wave inversion is usually confined to lead V_1 . Inverted T waves in leads V_1 and V_2 have the same significance as in lead I, although in none of these leads does an inverted T wave per se necessarily constitute an abnormality.

3. Amplitude

Although it is stated that the amplitude of the normal T wave in the limb leads only rarely exceeds 8 mm, there is rather marked individual variation. In fact, amplitude criteria for T wave normality or abnormality have not been established.

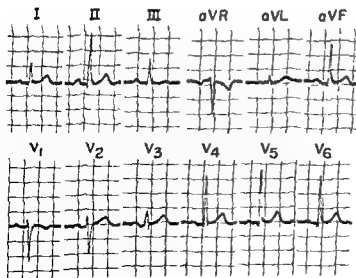
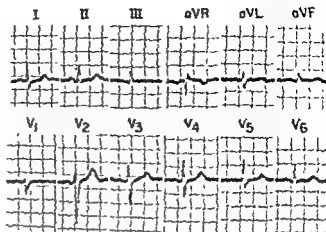


Fig. 52.—Normal electrocardiogram In the frontal plane, $\angle P = +60^\circ$, $\angle QRS = +80^\circ$, and $\angle T = +45^\circ$. In the horizontal plane, $\angle QRS = -10^\circ$ and $\angle T = +20^\circ$. The orientation of aVR and aVL in the horizontal plane can only be determined if one of the routine precordial leads records the transition from resultantly upright QRS and T deflections to resultantly inverted deflections, or vice versa. In the above electrocardiogram, the transitional lead for QRS is situated between leads V_2 and V_3 . Since aVR must be perpendicular to the transitional lead, the orientation of the vector is approximately -10° to -15° . The transition lead for T is located between leads V_1 and V_2 , upright T waves being recorded to the left and inverted T waves to the right. Again, since $\angle T$ must be

Fig 53.—Normal electrocardiogram. In the frontal plane, Δ QRS is situated at about $+60^\circ$ and Δ T is located at $+30^\circ$. In the horizontal plane the Δ QRS is at -25° and Δ T is at $+35^\circ$. Although this electrocardiogram shows semivertical heart position, as a rule, electrical heart position will not appear in the interpretation of any subsequent electrocardiograms in this text.



4 Comments

The ECG shows a normal sinus rhythm with a heart rate of approximately 75 bpm. The P waves are upright and of normal amplitude in leads I, II, III, aVL, aVF, and V4-V6. The QRS complex is narrow and has a duration of approximately 0.08 seconds. The T waves are upright and of normal amplitude in leads I, II, III, aVL, aVF, and V4-V6. The ST segment is isoelectric in all leads. The overall impression is of a normal ECG.

Ventricular Repolarization; Ventricular Gradient and Spatial QRS-T Angle

VENTRICULAR REPOLARIZATION

The S-T Segment and T Wave

THE *ISOELECTRIC SEGMENT* which is written immediately following termination of the QRS deflection and extends into the T wave is called the *RS-T segment* or *S-T segment*, and the corresponding time interval is referred to as the *S-T interval*. Electrophysiologically, the S-T segment is the earliest part of the T wave. Normally, recovery begins in some regions of the heart before depolarization is completed in other areas. However, these early repolarization forces which are produced during the S-T interval do not normally reach sufficient magnitude to displace the S-T segment from the isoelectric base line. In the occasional normal exceptions to this rule, minor degrees of S-T segment elevation (usually not exceeding 2.5 mm) are observed, most commonly in leads V_1 to V_3 . The predilection of this normal variation for leads V_1 through V_3 is probably explained by one or more of the following three factors.

1 The closer proximity of the exploring chest electrodes of leads V_1 to V_3 to the heart would tend to magnify all the electrical forces produced by the heart, and among these the early repolarization forces. This may actually represent one of the few instances in which the precordial leads respond in part to *proximity* or *localized potentials*.

2 In the discussion of the ventricular gradient later in this chapter, an important relationship is explained which is pertinent to the present subject, namely, that the larger the resultant area of the QRS deflection the greater will be the tendency for the S-T segment and T wave to be displaced in a direction opposite to that of the QRS deflection. Thus, since leads V_1 through V_3 normally record QRS deflections with relatively large terminal S waves, the

S-T segments in these leads are more likely to be elevated than the S-T segments in other leads.

3. Occasional instances of apparent S-T segment elevation appearing in lead V_1 , or less frequently in lead V_2 , may, we believe, actually represent a small terminal R' which merges indistinguishably with the S-T segment. In such cases, we have observed rSr' deflections in leads V_1 and/or V_2 of electrocardiograms recorded prior or subsequent to the tracing showing the apparent S-T segment elevation. Vectorcardiograms obtained in a few cases have not shown an S-T vector but instead have displayed terminal QRS vectors which were directed slightly to the right

attributed to late depolarization in the region of the pulmonary conus.

As will be recalled, a vector representing elementary repolarization forces points away from the direction in which the repolarization process is spreading,

the positive charges of the dipoles along the wave front precede the negative charges. It so happens that in depolarization the orientation of electrical positivity, and thus the direction the vector points, coincides with the direction of physiological activity.

In the isolated cell or muscle strip, repolarization and depolarization begin at the same point on the cell surface and proceed in the same direction. However, the intact heart muscle cell in situ and, in a more

of depolarization. The fact that, unlike the recovery process in the isolated cell, repolarization of the muscle of the ventricular wall is initiated in the layer of muscle last activated has been attributed to sub-endocardial recovery delay resulting from the great pressure applied to the inner ventricular wall during dynamic cardiac systole. The delayed onset of sub-endocardial repolarization permits epicardial muscle to recover first, even though it was the last activated, and, as a consequence, the repolarization wave moves toward the endocardial surface of the heart. Since the repolarization wave advances toward depolarized muscle and leaves polarized muscle in its wake, the instantaneous repolarization forces and representative mean instantaneous T vectors point in a direction the opposite of that in which repolarization is spreading. Parenthetically, one might add that atrial myocardium, unlike ventricular muscle, behaves in the same manner as the isolated muscle strip, in that repolarization begins in the same region and proceeds in the same direction as depolarization. For this reason, the P wave of atrial depolarization and the atrial T wave (Ta wave) are oppositely directed.

The average direction and magnitude of all mean instantaneous T spatial vectors which produce the electrocardiographic T wave can be represented by a single vector, the mean T spatial vector (sAT). Usually, the mean T spatial vector of normal subjects points to the left, inferiorly, and either anteriorly or slightly posteriorly. It is more likely to have a verti-

cally inferior orientation in younger persons and a horizontal and leftward orientation in older subjects. The most constant feature of the normal mean T spatial vector is its approximately parallel orientation with respect to the mean QRS spatial vector. The spatial QRS-T angle subtended by the two mean spatial vectors, which is described later in this chapter, rarely exceeds 50° - 60° in the absence of detectable heart disease. This accounts for the fact that the T waves are normally upright in leads I, V_3 , and V_6 , since these leads record resultant upright QRS deflections in most instances.

The U Wave

The U wave is usually a minor upright wave which follows the T wave or is fused with it. The exact cause of this deflection is not known, but there is reason to believe that it is produced by potentials elicited by the stretching of ventricular muscle during the period of rapid blood inflow into the ventricles. A negative U wave is never present in normal subjects in leads I and II but may be seen in the

vascul. Appar is observed characteristically in many of the electrocardiographic leads when the serum potassium concentration is quite low. This is discussed more fully in a later chapter.

VENTRICULAR GRADIENT AND SPATIAL QRS-T ANGLE

In the presence of a ventricular gradient, the depolarization wave front in that the negative charges of the dipoles along the repolarization wave front precede the positive charges, the reverse being true in the case of depolarization. Useful as this simplification may have been, repolarization of heart muscle is such a protracted process compared to depolarization that, except at the beginning and end, recovery is occurring at the same time throughout most of the muscle. It is evident from this that the electrical effects of repolarization of some portions of heart muscle or, in the case of a single muscle cell, of some areas of the cell membrane tend to offset the effects of repolarization occurring simultaneously at other sites. In other words, there is *opposition* of effects in repolarization. This is not the case in depolarization, for the latter process can be visualized

as a wave front of dipoles involving at any instant only a small strip of cell membrane or of muscle tissue. From a practical standpoint, however, only the potential variations at the endocardial and epicardial surfaces of a heart muscle cell need be considered, since the electrical effects of depolarization and repolarization of a single myocardial cell—or, for that matter, the entire thickness of ventricular muscle—are equal to the algebraic sum of the electrical effects of these processes at the endocardial and epicardial surfaces of the cell or ventricular wall. For this reason, it is a permissible simplification to imagine the ventricular muscle to be a single muscle fiber extending from the endocardium to the epicardium of the heart.

That only the surface effects of depolarization and repolarization need be considered is generally accepted by most authorities in the field of electrocardiography. This premise has been the basis of a number

Ventricular Repolarization; Ventricular Gradient and Spatial QRS-T Angle

VENTRICULAR REPOLARIZATION

The S-T Segment and T Wave

THE ISOELECTRIC SEGMENT which is written immediately following termination of the QRS deflection and extends into the T wave is called the RS-T segment or S-T segment, and the corresponding time interval is referred to as the S-T interval. Electrophysiologically, the S-T segment is the earliest part of the T wave. Normally, recovery begins in some regions of the heart before depolarization is completed in other areas. However, these early repolarization forces which are produced during the S-T interval do not normally reach sufficient magnitude to displace the S-T segment from the isoelectric base line. In the occasional normal exceptions to this rule, minor degrees of S-T segment elevation (usually not exceeding 2.5 mm.) are observed, most commonly in leads V_1 to V_3 . The predilection of this normal variation for leads V_1 through V_3 is probably explained by one or more of the following three factors:

1. The closer proximity of the exploring chest electrodes of leads V_1 to V_3 to the heart would tend to magnify all the electrical forces produced by the heart, and among these the early repolarization forces. This may actually represent one of the few instances in which the precordial leads respond in part to proximity or localized potentials

2. In the discussion of the ventricular gradient later in this chapter, an important relationship is explained which is pertinent to the present subject, namely, that the larger the resultant area of the QRS deflection the greater will be the tendency for the S-T segment and T wave to be displaced in a direction opposite to that of the QRS deflection. Thus, since leads V_1 through V_3 normally record QRS deflections with relatively large terminal S waves, the

S-T segments in these leads are more likely to be elevated than the S-T segments in other leads.

3. Occasional instances of apparent S-T segment elevation appearing in lead V_1 , or less frequently in lead V_2 , may, we believe, actually represent a small terminal R' which merges indistinguishably with the S-T segment. In such cases, we have observed rS' deflections in leads V_1 and/or V_2 of electrocardiograms recorded prior or subsequent to the tracing showing the apparent S-T segment elevation. Vectorcardiograms obtained in a few cases have not shown an S-T vector but instead have displayed terminal QRS vectors which were directed slightly to the right and posteriorly. The latter finding and the corresponding rS' deflection in leads V_1 of the electrocardiogram usually represent a normal variation and have been attributed to late depolarization in the region of the pulmonary conus.

As will be recalled, a vector representing elementary repolarization forces points away from the direction in which the repolarization process is spreading, since the negative charges of the dipoles along the repolarization wave front precede the positive charges. This is to be contrasted with depolarization in which the positive charges of the dipoles along the wave front precede the negative charges. It so happens that in depolarization the orientation of electrical positivity, and thus the direction the vector points, coincides with the direction of physiological activity.

In the isolated cell or muscle strip, repolarization and depolarization begin at the same point on the cell surface and proceed in the same direction. However, the intact heart muscle cell in situ and, in a more general sense, the ventricular myocardium as a whole undergo repolarization in an epicardial-to-endocardial direction, this being just the reverse of the direction

B Cooled Endocardial Surface of Cell

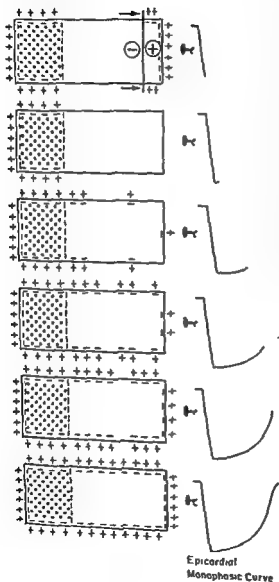
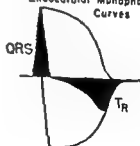


Fig. 54 (cont.).—In B, the endocardial surface of the cell has been cooled. Consequently, the downwardly directed curve recorded at the epicardial surface represents solely potential variations at the latter surface, the curve being designated the *epicardial monophasic curve*. Because the same number of dipoles have been involved in depolarization and repolarization of the epicardial surface and of the endocardial surface and because of the uniform rate of recovery throughout the cell, it follows that the endocardial and epicardial monophasic curves have the same configuration and enclose equal areas even though they are opposite in sign or direction.

If the upright endocardial monophasic curve and downwardly directed epicardial curves described in A and B are plotted on the positive and negative sides of the same base line (as in C), with the endocardial curve slightly preceding the epicardial curve (since depolarization and repolarization of the cell are assumed to start first at its endocardial surface), the potential variations between the two cell surfaces during depolarization and repolarization can be obtained by algebraic addition of corresponding points on the two curves. The values obtained, plotted against time according to their voltage and sign, yield an upright R wave and inverted T wave of equal area but opposite sign. The T wave obtained when there is uniform rate of recovery is:



C Algebraic Addition of Epicardial and Endocardial Monophasic Curves



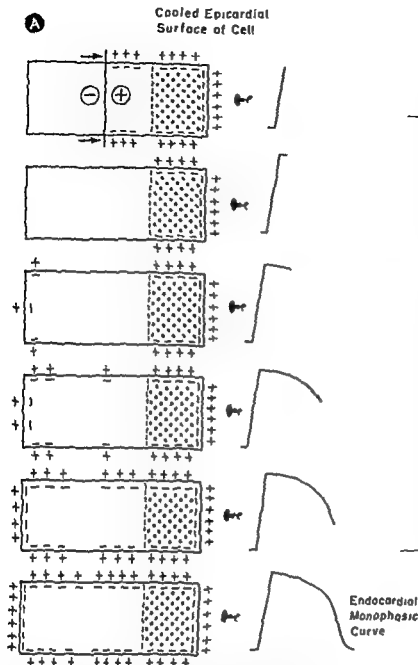


Fig. 54.—The endocardial and epicardial monophasic curves recorded from a heart muscle cell and their relationship to the QRS deflection and regression T wave. In A, the cooled epicardial surface of the cell undergoes no

boundary of the cooled region, which therefore retains its dipoles. As a consequence, the monophasic curve recorded by the electrode overlying the epicardial end of the cell reflects entirely potential variations at the endocardial surface of the cell and is called the *endocardial monophasic curve*. Note that repolarization is occurring more or less simultaneously throughout the cell. It begins at the endocardial surface, and, since the rate of recovery is uniform throughout the cell, the endocardial region regains all of its dipoles sooner than regions of the cell nearer the epicardial surface. Thus the repolarization process moves in an endocardial-to-epicardial direction but does not produce a wave front (continued)

of classic studies by Wilson and his associates and by Bayley, Ashman, Gardberg, Byer, and others. The results of these investigations can be summarized in the form of the following hypothetical experiment.

Part I (Fig. 54, A) —If one first cools the epicardial surface of the cell and then stimulates the endocardial surface, the depolarization wave spreads from the site stimulated toward the epicardial end of the cell. (The direction of physiologic activity in the cell will be assumed, in this experiment, to parallel the axis of a unipolar lead whose exploring electrode lies in close proximity to the epicardial membrane surface.) However, the activation wave is blocked at the boundary of the cooled region, which therefore re-

tains its membrane dipoles even though the rest of the cell surface has been discharged. With discharge of the endocardial aspect of the cell, the epicardial surface becomes intensely positive by comparison, so that an abrupt upward deflection of the electrocardiographic base line occurs. The summit of this curve persists until repolarization commences at the endocardial surface. With the appearance of the first dipoles on the endocardial surface, the relative positivity of the cooled epicardial surface begins to decline. As recovery through the cell continues, the number of dipoles on the endocardial surface increases progressively, and, as they approach in number those present during the resting phase, the

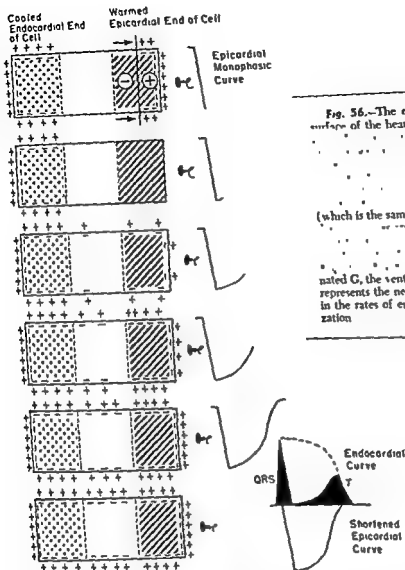


Fig. 56.—The effect of warming the epicardial surface of the heart muscle cell on the recorded T

(which is the same as in figures 54 and 55). \mathcal{L} is the net electrical effect of the difference in the rates of endocardial and epicardial repolarization

of two waves the first, the QRS, which represents the net electrical effects of depolarization and is upright in this experiment, and the second, the T wave, which represents the net electrical effects of repolarization and is, in this instance, downwardly directed. When there is a uniform rate of recovery throughout the cell, as is assumed in this phase of the hypothetical experiment, the T wave is equal in area but opposite in direction to the QRS deflection and is called the regression T wave (T_R). It follows from the definition of a regression T wave that $A_{QRS} + A_{T_R} = 0$, where A equals area. This important relationship should be kept in mind during the remainder of the hypothetical experiment.

Part III (Fig. 56).—In this phase of the experiment, the epicardial surface of the cell is warmed and the endocardial surface cooled. Depolarization is blocked at the boundary of the cooled cell membrane, the endocardial surface retains its dipoles, and, consequently, discharge of the epicardial surface of the cell causes a sharp downstroke of the electrocardiogram tracing, just as occurred in Part II. However, because the epicardial end of the cell has been warmed, it recovers more quickly than previously. The greater rapidity with which the epicardial surface of the cell regains its dipoles during repolarization is reflected in the more rapid return of the monophasic curve to the isoelectric base line, the duration

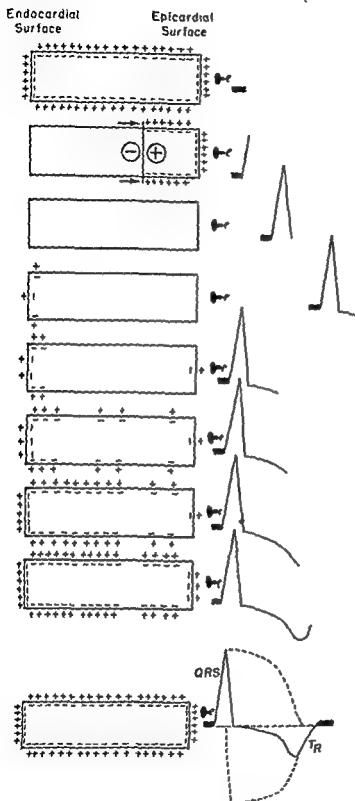
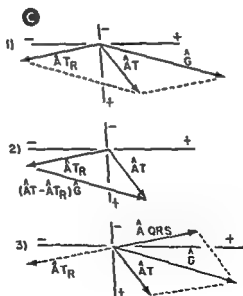
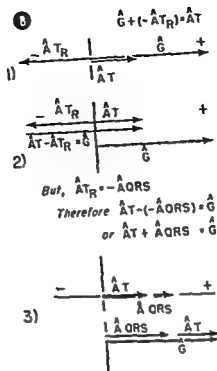
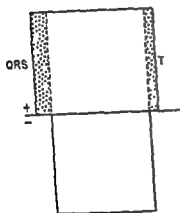
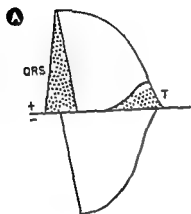


Fig. 55.—The QRS complex and regression T wave recorded at the epicardial surface of a heart muscle cell in which the endocardial surface is uniform throughout. The endocardial surface has been cooled.

electrocardiogram curve returns gradually to the isoelectric base line. When repolarization is completed, the endocardial and epicardial surfaces are equally charged and the curve reaches the isoelectric base line. Inasmuch as there has been no change in the number of dipoles at the epicardial surface of the cell during this period, the monophasic curve recorded must therefore represent the electrical effects of depolarization and repolarization of the endocardial end of the cell. The duration of the endocardial monophasic curve is a function of the rate of recovery at the endocardial surface of the cell.

*Part II. (Fig. 54, B).—*If one next cools the endocardial end of the cell, an electrode overlying the opposite end records an abrupt downward deflection at the time the epicardial surface of the cell becomes negatively charged relative to the cooled endocardial surface, which has retained its dipoles, for the reason previously cited. With the reappearance of the first dipoles on the epicardial surface, the electrocardiographic tracing begins its ascent to the base line. As the dipoles increase in number, the positivity of the endocardial surface with reference to the epicardial surface declines progressively and a rising curve is inscribed which reaches the isoelectric base line with completion of repolarization. In this instance, the monophasic curve obtained is exactly like that recorded when the epicardial surface was cooled, except that in the latter case the curve was upright while the curve just recorded is downwardly directed. This negative monophasic curve represents the electrical effects of epicardial depolarization and repolarization, since the degree of polarization of the endocardial surface of the cell did not change significantly during the activation and recovery processes.

The two monophasic curves obtained in Parts I and II of the experiment are now plotted on the positive and negative sides of the same base line, with the endocardial curve slightly preceding but overlapped terminally by the epicardial curve, since the endocardial surface of the cell was the first to be activated and the first to recover (Fig. 54, C). Each monophasic wave represents the depolarization and repolarization potentials existing at one or the other cell surface, plotted against time. The potential variations between the two cell surfaces can be determined by algebraically adding pairs of corresponding points on the monophasic curves. The values obtained are plotted according to their voltage and sign and yield a biphasic deflection. This derived deflection is identical with the deflection which would be recorded if neither cell surface were cooled (Fig. 55). It consists



1, 2, 3 The relationship of the vectors \hat{A}_{QRS} , \hat{A}_{Tz} , and \hat{A}_T . In A are shown the same axes of monophase.

(B, sec 3) The same relationships between \hat{A}_{QRS} , \hat{A}_{Tz} , and \hat{A}_T are demonstrated in parts 1-3 of C, in which the vectors do not lie along the axis of the electrocardiographic lead recording the monophasic curves.

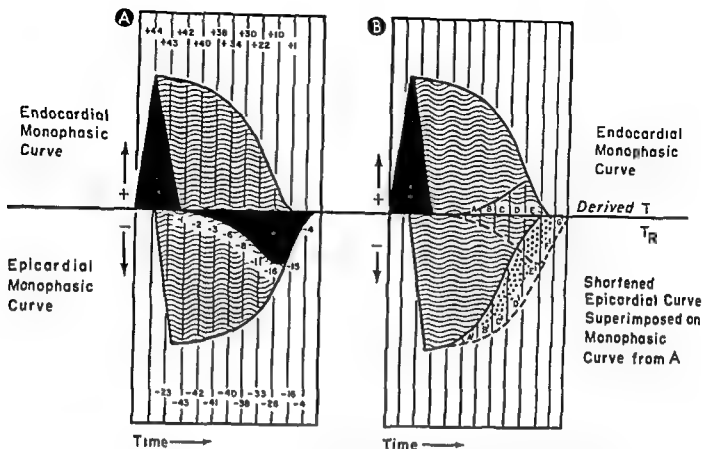


Fig. 57.—The ventricular gradient and its relationship to the endocardial and epicardial monophasic curves. In A, the two monophasic curves obtained when there is uniform rate of recovery throughout the cell have been added algebraically. In B, the endocardial curve is the same as the endocardial curve and the shortened epicardial curve (as represented by lines A' to G' of B) equals the total area enclosed by the upright T wave and the regression T wave (represented by lines A to G extending between the two T waves, lines which are equal in length to corresponding lines between the two superimposed monophasic curves). The sum of A T_A + A T is designated the gradient, or G. Therefore, A T_A + A T = G.

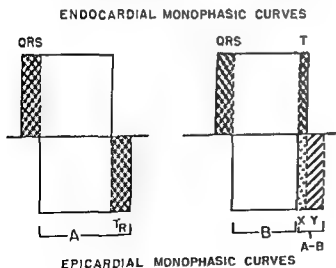


Fig. 58.—The relationships described in Figure 57 can be expressed more simply by substituting rectangles, as here, for the monophasic curves. Rectangle A = the epicardial curve, yielding the

$$\text{Area (A)} - \text{Area (B)} = A(X) + A(Y) = A T + A T_A = G.$$

of the curve being shortened to a corresponding degree. Since the endocardial surface of the cell has not been warmed, the rate of recovery there is the same as before, and so the endocardial monophasic curve remains unchanged from that recorded in Part II. As a result, the endocardial and epicardial monophasic curves are no longer equal in area and, when added algebraically, yield QRS and T waves of differing areas. Thus, the sum of (A QRS) and (A T) does not equal zero but instead equals a measurable quantity, G , designated by Wilson the *ventricular gradient*. Clearly, the ventricular gradient represents the net electrical effect of the difference in the rates of repolarization at the endocardial and epicardial surfaces of the cell. To reduce the ventricular gradient concept to more tangible terms, it is defined in the following paragraph as a function of the monophasic curves obtained in Parts II and III of the hypothetical experiment.

If the epicardial monophasic curve from which the inverted regression T wave was derived and the shortened monophasic curve of the upright T wave last recorded are superimposed on each other, the difference in their areas, which will be found to equal the total area enclosed by the two T waves, is identical with the ventricular gradient (Figs 57 and 58). In other words, the ventricular gradient represents the repolarization potentials which, added to the regression T potentials, yield the potentials producing the upright T wave (Fig 59). If these electrical forces are depicted as vector quantities, vector addition of the regression T vector and ventricular gradient vector yields, as the resultant of the two component vectors, the recorded T vector. Theoretically, it is possible to calculate the ventricular gradient by subtracting vectorially the regression T vector from the recorded T vector. In actuality, however, there is no way to record the regression T wave of heart muscle because the rate of repolarization is not uniform throughout the ventricular muscle. Nevertheless, since the QRS area and the regression T area are of equal size, although of opposite sign, the ventricular gradient can be determined by vector addition of A QRS and A T.

As stated earlier, the axis of derivation of the

Consequently, in determining the ventricular gradient the vectors representing A QRS and A T must be laid off along the lead axis. In Parts I and II of this experiment, the rate of repolarization was uniform throughout the cell, and the epicardial and endocardial monophasic curves obtained enclosed equal areas of opposite sign. Added algebraically, the two monophasic curves yield QRS and T deflections which are also equal in area but opposite in sign. If A QRS and A T are plotted along the positive half of the axis of derivation of the lead recorded, the resultant of the two vectors (which in this instance equals the sum of A QRS and A T laid off head to tail, since the vectors coincide exactly in direction) is not zero, as was previously the case, but instead is a third vector, the gradient vector G . This gradient vector has a specific magnitude and is directed away from the region in which the duration of the excited state is longest (i.e., recovery slowest) toward the region where it is shortest. In this phase of the experiment, the gradient vector is found to be directed from the endocardial surface of the cell toward the epicardial surface.

Part IV (Fig. 60).—In this portion of the hypothetical experiment, the muscle cell is stimulated at its epicardial surface, and so the direction in which the cell undergoes depolarization is the reverse of that described previously. Repolarization will again be assumed to occur at a uniform rate throughout the cell, so that the epicardial and endocardial monophasic curves recorded are equal in area but oppositely directed. Since depolarization and repolarization both commence first at the epicardial surface of the cell, the epicardial monophasic curve precedes the endo-

cardial curve in equal area, whereas previously, when activation of the cell occurred in an endocardial-to-epicardial direction, an upright QRS and inverted T wave were obtained. It is evident that this reversal in the direction of the QRS and T deflections can be attributed entirely to the reversed direction of depolarization. Because there has been no change in the uniform duration of the excited state throughout the cell, one is not surprised to find, on plotting A QRS and A T on the axis of derivation of the electrocardiographic lead, that, once again, the ventricular gradient is zero.

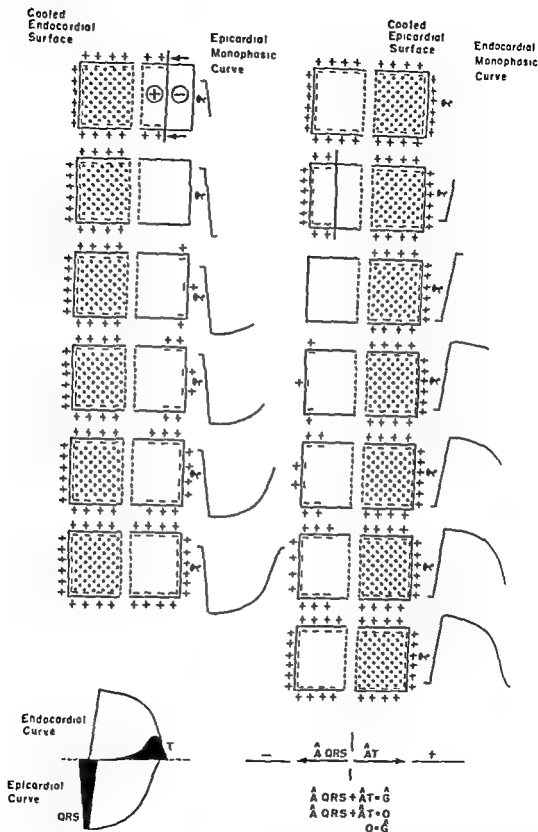


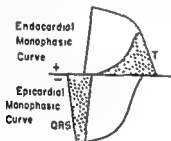
Fig. 60.—The effect of reversal in the direction of cellular depolarization on the monophasic curves and on ΔQRS and ΔT_n . Here the cell has been stimulated at its epicardial surface, so that depolarization and repolarization of the endocardial surface. Repolarization occurs at a uniform monophasic curves are equal but their time relationship to epicardial curve precedes the endocardial curve, with the

No matter how great may be the discrepancy between the times of onset of depolarization and repolarization at the endocardial and epicardial surfaces of the cell, as long as the rate of repolarization remains uniform through the cell the areas enclosed by the epicardial and endocardial monophasic curves remain equal and the ventricular gradient continues to be zero (Fig. 61). Thus, as onset of depolarization at one surface of the cell lags farther and farther behind the time of onset of depolarization at the other surface, the derived QRS and T deflections enclose larger and larger areas of equal size but opposite sign,

and $\Delta QRS + \Delta T = G = 0$. One can demonstrate the preceding facts for himself in the following simple way

To obviate the necessity of having to add algebraically two monophasic curves, the latter are represented as two rectangles of equal dimensions. The "endocardial rectangle" is drawn above the isoelectric base line, the "epicardial rectangle," below the base line (Fig. 61). The left side of each rectangle cor-

A Uniform Rate of Repolarization Throughout Cell



Slower Rate of Repolarization at the Epicardial Surface of Cell

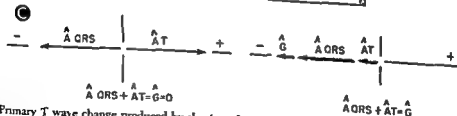
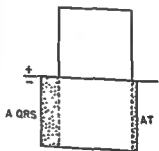
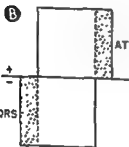
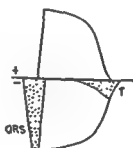
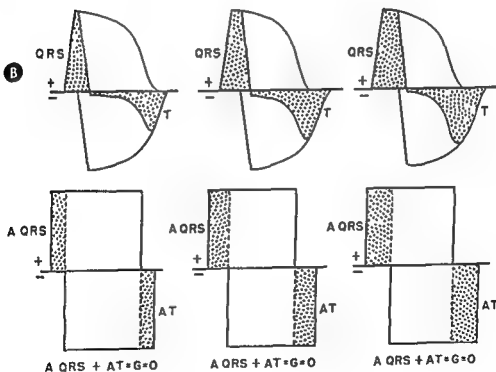
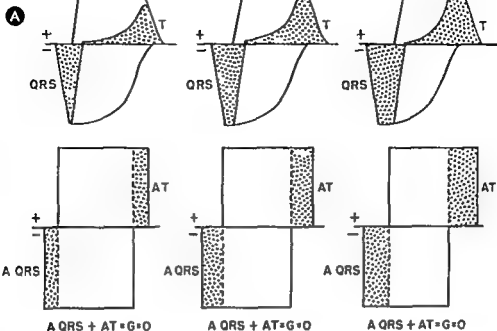


Fig. 62—Primary T wave change produced by slowing of repolarization at the epicardial surface of the cell. The monophasic curves are represented as rectangles of equal dimensions. The addition of ΔQRS to ΔT results in a T wave of zero magnitude.

addition of ΔQRS and ΔT derived from the clinical electrocardiogram.



gradient continues to be zero. In A, epicardial repolarization precedes the onset of depolarization. In B, the time of onset of depolarization precedes the time of onset of repolarization. In C, the time of onset of depolarization and repolarization are simultaneous.

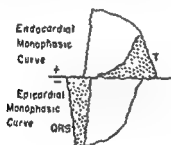
No matter how great may be the discrepancy between the times of onset of depolarization and repolarization at the endocardial and epicardial sur-

faces, the ventricular gradient G remains to be zero (Fig. 61). Thus, as onset of depolarization at one surface of the cell lags farther and farther behind the time of onset of depolarization at the other surface, the derived QRS and T deflections enclose larger and larger areas of equal size but opposite sign,

and $\Delta QRS + \Delta T = G = 0$. One can demonstrate the preceding facts for himself in the following simple way:

To obviate the necessity of having to add algebraically two monophasic curves, the latter are represented as two rectangles of equal dimensions. The "endocardial rectangle" is drawn above the isoelectric base line, the "epicardial rectangle," below the base line (Fig. 61). The left side of each rectangle corresponds to the initial limb of the monophasic curve, while the right side corresponds to the terminal limb of the curve. When one rectangle precedes the other,

A Uniform Rate of Repolarization Throughout Cell



B Slower Rate of Repolarization in the Epicardial Surface of Cell

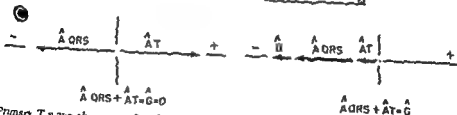
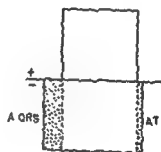
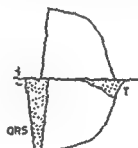


Fig. 62—Primary T wave change produced by slowing of repolarization at the epicardial surface of the cell.

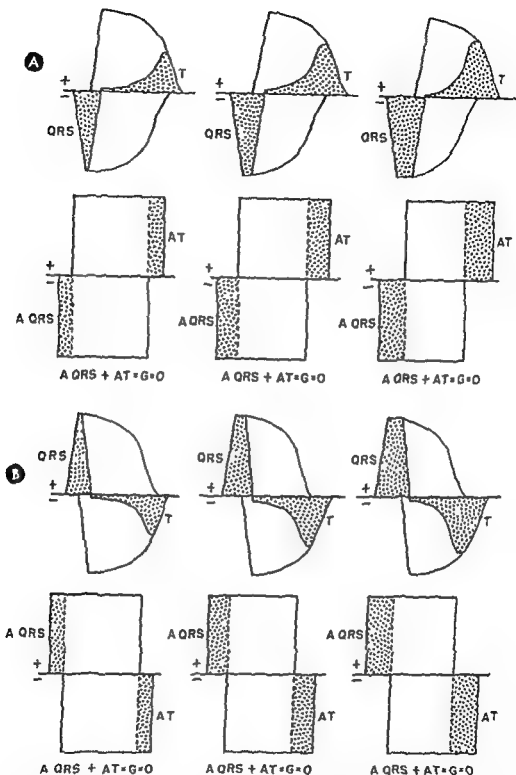


Fig. 61.—Demonstration of the fact that, no matter how marked the discrepancy between the times of onset of depolarization and repolarization at the two surfaces of the cell, as long as the rate of repolarization remains uniform throughout the cell the areas enclosed by the epicardial and endocardial monophasic curves remain equal and the ventricular gradient continues to be zero. In **A**, epicardial depolarization precedes endocardial depolarization, while in **B** the reverse holds true.

the overlapping portion of the former (on the left) is analogous to the QRS deflection, similarly, if the right end of one rectangle extends beyond the other, the overlapping area corresponds to the T wave.

1 If the endocardial rectangle precedes (extends to the left of) the epicardial rectangle, the overlapping part of the former is situated above the base line and corresponds to an upright QRS deflection. Since the dimensions of the two rectangles are equal, it is obvious that the epicardial rectangle must necessarily overlap the right end of the endocardial rectangle to the same extent that its left end is overlapped by the latter. Thus, the overlapping portion of the epicardial rectangle corresponds to a T wave enclosing the same area as the QRS but directed oppositely. Hence, $A_{QRS} + A_T = C = 0$.

2 If the endocardial rectangle continues to be advanced farther and farther ahead of (i.e. to the left of) the epicardial rectangle, the overlapping portions of the two rectangles, representing the QRS and T deflections, increase in size but maintain their original directions and equal areas. Thus, the gradient is still zero, just as in the above paragraph.

3 To determine the effect on the gradient of a complete reversal in the time sequence of depolarization, initial stimulation of the epicardial surface of the cell will be simulated by moving the epicardial rectangle ahead of, or to the left of, the endocardial rectangle. In this instance, the left end of the epicardial rectangle situated below the base line overlaps the left end of the endocardial rectangle, while the right end of the latter overlaps to an equal extent the right end of the epicardial rectangle. The overlapping portions of the two rectangles are analogous to downwardly directed QRS and upright T deflections of equal area. Here too, $A_{QRS} + A_T = C = 0$, despite the fact that the directions of the QRS and T deflections are completely reversed, compared to their directions in the preceding two paragraphs.

The salient fact to emerge from the above discussion, and one which is the very core of the ventricular gradient concept, is this: An alteration in the relationship between the heart muscle is not accompanied by an alteration in the ventricular gradient.

Part V (Fig. 62) - In continuation of the hypothetical experiment with the equally hypothetical heart muscle cell (which extends from the endocardial to the epicardial surface of the ventricular wall), the next step will be to cool the epicardial surface

of the cell to a degree sufficient to delay recovery in the cooled region without blocking depolarization. The stimulus is applied to the epicardial surface of the cell just as was done in the preceding phase of the experiment. Since onset of depolarization occurs at the epicardial surface of the cell before its occurrence at the endocardial surface, the direction of depolarization is the reverse of normal and the overlying lead electrode records a downwardly directed QS deflection. However, because the epicardial end of the cell has been cooled, its rate of recovery is slowed relative to that of the endocardial surface, which, although the last activated, reaccumulates its dipoles at a faster rate. This reverses the general order of repolarization, and so the epicardial surface and overlying lead electrode are at a relatively negative potential with respect to the endocardial end of the cell throughout the entire period of repolarization. The T wave recorded is therefore directed downwardly (is inverted), like the QS deflection that preceded it. Consequently, if one were to record monophasic curves from the two surfaces of the cell, one would note the following: (1) Onset of the epicardial curve precedes onset of the endocardial curve. (2) The epicardial curve is prolonged beyond the termination of the endocardial monophasic curve as the result of the slower rate of epicardial repolarization. (3) Thus, the endocardial curve is overlapped by the epicardial curve at both its beginning and end, and obviously encloses a smaller area than the latter. (4) The overlapping portions of the epicardial curve correspond, on algebraic addition of the two curves, to the downwardly directed QS and T deflections of differing areas which were previously recorded. (5) The areas enclosed by the QS and T deflections can be represented by vectors which differ in length but point in the same direction. If these vectors, A_{QRS} and A_T , are laid off along the negative half of the axis of derivation of the lead recorded and are then added vectorially, the resultant $A_{QRS} + A_T$ is a vector

Whatever the relationship between the epicardial and endocardial monophasic curves may be, provided that the areas enclosed by the two curves maintain their same relative proportions (Fig. 63). In other words, the presence of a gradient initially is indicative, not of the fact that the direction of depolarization is reversed, but of the fact that there is a difference in the rate of recovery or in the duration of the excited state at the endocardial and epicardial surfaces of the cell. As long as there is no further change

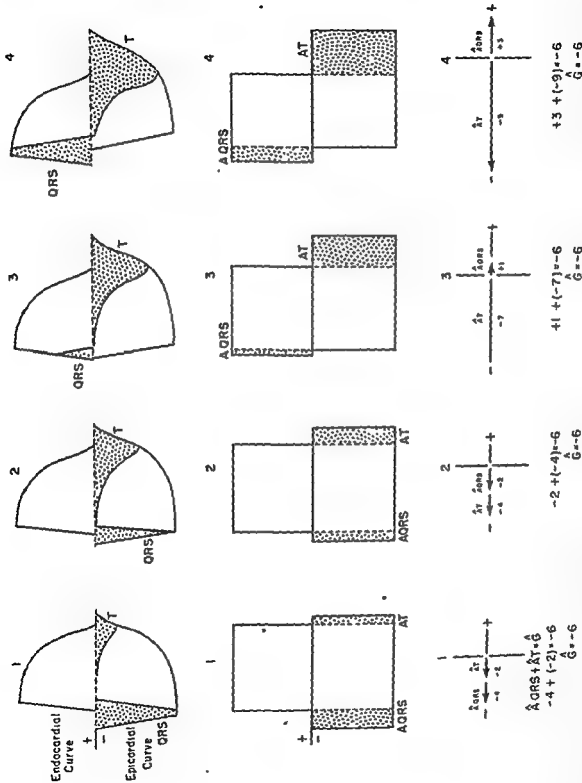


Fig. 63.—The effect of changing time relationships of the epicardial and endocardial monophasic curves on the gradient. In this figure, each pair of monophasic curves, numbered 1 through 4, is represented by a corresponding pair of rectangles to simplify calculation of the gradient, G . Thus the monophasic curves in column 1, if depicted as rectangles having the same area, relatively, as the monophasic curves themselves, yield ΔQRS and ΔT , which can be assigned the unit values of -4 and -2 . Vector addition or algebraic addition of these values yields a gradient vector of -6 units. As long as the areas enclosed by the two rectangles remain unchanged, the time relationship between epicardial and endocardial curves or rectangles can be varied widely, to produce marked changes in the direction and area of ΔQRS and ΔT (columns 2, 3, and 4). However, in every instance, the gradient remains -6 units in magnitude and has the same direction as in column 1. Therefore, the ΔT changes in this figure are all secondary ΔT changes, consequent to alterations in cellular depolarization.

polarization countless elementary QRS and T forces of differing magnitude and direction are produced by all the minute wedges of muscle forming the ventricular wall. For each pair of QRS and T forces or vectors so produced, there exists a corresponding gradient vector which expresses the net electrical effect of the different rate of recovery throughout the wedge of muscle.

However, in terms of body surface potentials, as previously explained, the elementary QRS and T

By the same token, for each succeeding pair of mean instantaneous QRS and T vectors, there is a mean instantaneous ventricular gradient vector which represents the net electrical effects of the different rates of recovery in all muscle units of the ventricular wall simultaneously undergoing first depolarization and then repolarization. Since the processes of depolarization and repolarization do not occur simultaneously in all portions of the ventricular muscle but involve the different regions sequentially, the mean instantaneous QRS, T, and ventricular gradient spatial vectors vary somewhat in direction and magnitude from instant to instant during the cardiac cycle. At present there is no practicable way to determine the instant-to-instant change in the mean instantaneous ventricular gradient vector.

likewise, the spatial vector of the mean T spatial vector ($\bar{A}T$) the mean ventricular gradient spatial vector (\bar{G}). The spatial vector of the ventricular gradient has been studied primarily in its frontal plane projection (\bar{G}), which is the vectorial sum of the vectors representing the mean manifest electrical axis of QRS ($\bar{A}QRS$) and the mean electrical axis of T ($\bar{A}T$). The method used to calculate the mean ventricular gradient (\bar{G}) from the electrocardiogram (see Fig. 64) is outlined below

1 The amplitude and duration of the QRS deflection and T wave are measured in at least two standard leads of a

2 The product of the amplitude of a deflection multiplied by one half its duration or width equals the area of the deflection in microvolt-seconds. This value is then converted into Ashman units (1 Ashman unit = 4 microvolt-seconds). If either the QRS or the

T deflection has two or more wave components, the areas of these waves are measured separately and then added algebraically, according to their sign, to obtain the resultant area of the deflection.

3. The values for the areas of the QRS and T deflections in the two leads are plotted on the appropriate lead axes of the triaxial reference frame, and perpendiculars are dropped from the plotted points.

4. Lines drawn from the center of the reference figure to the point of intersection of each pair of perpendicular lines represent the mean manifest electrical axes of QRS and T, or $\bar{A}QRS$ and $\bar{A}T$.

5. The parallelogram method of vector addition is utilized to obtain the gradient vector which is the resultant of $\bar{A}QRS$ and $\bar{A}T$. Thus, $\bar{A}QRS$ and $\bar{A}T$ serve as two sides of the parallelogram, and the other two sides are formed by lines drawn parallel to the former. A diagonal line drawn from the center of the reference figure represents the mean ventricular gradient (\bar{G}).

Normally, the mean ventricular gradient vector \bar{G} lies within 30° and to the left or right of $\bar{A}QRS$ in the frontal plane, depending on whether the heart is in horizontal or vertical heart position. In neither case, does \bar{G} normally deviate from $\bar{A}QRS$ by an angle greater than 30° .

It must be added to that of the T wave if S-T segment deviations are present, since the period during which the ventricles repolarize corresponds to both the S-T and the T intervals. It is evident, however, that S-T segment deviations due to the current of injury produce significant error when introduced into the calculation of the ventricular gradient.

The practical, as well as theoretical, importance of the ventricular gradient concept is that it provides a means of differentiating primary and secondary T wave variations. These two types of T wave changes were explained earlier in terms of the hypothetical heart muscle cell, but the basis for distinguishing one from the other is the same in clinical electrocardiography. Thus the important relationship of $\bar{A}QRS + \bar{A}T = \bar{G}$ which can be rearranged to $\bar{A}T = \bar{G} - \bar{A}QRS$ which can be

altered by a change either in the mean ventricular gradient vector \bar{G} or in the mean electrical axis of QRS. Primary T wave changes result solely from a

in the duration of the excited state at these two surfaces, the gradient remains the same despite variations in the time sequence of onset of depolarization throughout the cell.

The concepts demonstrated in this hypothetical experiment are of great importance in clinical electrocardiography and can be stated in a simplified way, as follows: (1) T wave (repolarization) changes which are not accompanied by a change in the ventricular gradient are due to some alteration in the time sequence of onset of depolarization throughout the cell or, more generally, throughout heart muscle.

trical effects of depolarization and repolarization at the epicardial and endocardial surfaces of heart muscle need be considered. During ventricular depolarization and repolarization, for each tiny wedge of ventricular muscle involved there are produced QRS and T forces which represent the algebraic sum of paired endocardial and epicardial monophasic curves specific for the muscle segment in question. However, in the heart muscle cell in situ the duration of the excited state or the rate of recovery is not uniform through the cell, as was the case in the hypothetical cell considered previously, nor is the duration of the

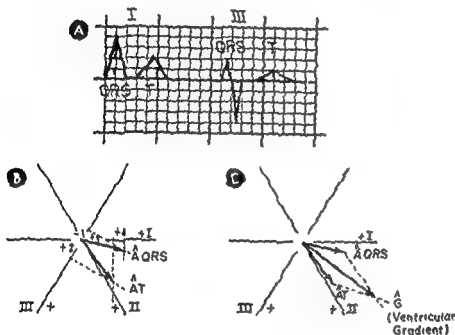


Fig. 64.—Construction of the mean ventricular gradient vector, \bar{C} , from the standard limb leads of the electrocardiogram. The area of each QRS and T deflection in at least two of the three bipolar limb leads is calculated (A), utilizing the formula, $\text{Area} = \frac{1}{2} \text{Width} \times \text{Height}$, and is expressed either in microvolt-seconds or in Ashman units (1 Ashman unit = 4 microvolt-seconds). In B, the values for the QRS deflections in leads I and III are plotted on appropriate axes of the triaxial reference frame, and perpendiculars are dropped from the two points. The vector drawn from the center of the reference figure to the point of intersection of the perpendicular lines represents $\bar{A} \text{ QRS}$. The same procedure is followed in determining $\bar{A} \text{ T}$. In C, $\bar{A} \text{ QRS}$ and $\bar{A} \text{ T}$ are added vectorially by the parallelogram method to yield the resultant vector, \bar{C} , the mean ventricular gradient vector.

They are designated *secondary T wave changes*. (2) T wave (repolarization) changes which are accompanied by an alteration in the direction and magnitude of the gradient vector are *primary T wave abnormalities* and reflect a change in the duration of the excited state in some region of the cell or of the heart muscle.

Up to this point in the discussion, the gradient concept has been considered only in its application to the rudimentary electrical activities of a single muscle cell. However, as will be recalled, the hypothetical muscle cell is essentially the equivalent of a minute wedge of muscle extending through the entire thickness of ventricular wall, since only the elec-

trical effects of depolarization and repolarization at the epicardial and endocardial surfaces of heart muscle need be considered. During ventricular depolarization and repolarization, for each tiny wedge of ventricular muscle involved there are produced QRS and T forces which represent the algebraic sum of paired endocardial and epicardial monophasic curves specific for the muscle segment in question. However, in the heart muscle cell in situ the duration of the excited state or the rate of recovery is not uniform through the cell, as was the case in the hypothetical cell considered previously, nor is the duration of the

case when the hypothetical cell was stimulated at its epicardial end, so also in bundle branch block, the change in the depolarization process must inevitably produce a secondary change in the repolarization process and therefore a change in the T wave.

tions producing primary T wave changes, Δ QRS and Δ T show an equal but oppositely directed increment in size. Thus the ventricular gradient vector \bar{G} does not change in direction, and, if normal before onset of the bundle branch block, it remains so. If it should be horizontal before onset of the bundle branch block, it remains horizontal.

co) In this event, the presence of primary T wave abnormalities, in addition to the secondary T wave changes of bundle branch block, can be assumed. This fact in particular potentially provides one of the more valuable applications of the ventricular gradient concept.

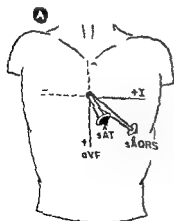
Unfortunately, there are at present limitations, inherent to the methods used to determine the ventricular gradient, which greatly impair its clinical usefulness. The accuracy and reliability of frontal plane ventricular gradient calculations can be assured, to some extent, only by the most tedious and time-consuming measurements of specially recorded electrocardiograms.

The manual construction of the horizontal mean ventricular gradient vector and the mean ventricular gradient spatial vector introduces even greater inaccuracies. However, Briller and his associates have constructed an electronic analogue computer which automatically calculates from the vectorcardiogram the magnitude and direction of the spatial ventricular gradient in terms of its projection on each of the three recording planes of the body.

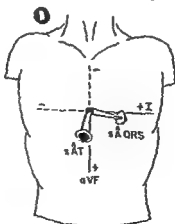
The Monophasic Curves and Ventricular Gradient in Myocardial Ischemia

As already indicated, one can imagine that there exists a pair of monophasic curves for each minute wedge of ventricular muscle. Thus, for a given area of the ventricle or for the ventricular muscle mass as a whole, there are endocardial and epicardial monophasic curves which represent the algebraic summation of all the monophasic curves of the component muscle units. Since normally the rate of recovery is more rapid in epicardial muscle, even though it is activated last, the epicardial monophasic curve is therefore of shorter duration than the endocardial curve and is preceded by it. Accordingly, the QRS deflection and T wave recorded in a lead overlying the electrically dominant left ventricle tend to have the same upright direction. Since subendocardial ischemia prolongs the endocardial monophasic curve so

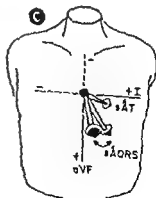
Fig 66
a) QRS as
emphified,
b) Δ T
ob
yo
ter
a



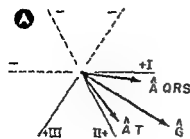
Normal Adult



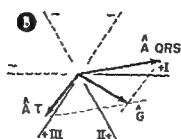
Normal Elderly Adult



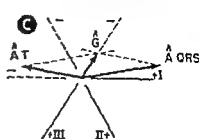
Normal Child



Frontal Plane



Frontal Plane



Frontal Plane

corded in lead I, they would constitute secondary T and the orientation of the ventricular gradient vector has complicated the previously existent left bundle b_1 was the case in B; however, in this instance the ventricular gradient would be abnormal and the T wave abnormalities would be categorized as primary T wave changes (due to myocardial ischemia, for example)

change in the direction or magnitude of the mean ventricular gradient vector, i.e., from some change in the rate of recovery and duration of the excited state in various portions of the ventricular muscle. Consequently, a primary T wave change which is identified by the abnormal direction and/or magnitude of \bar{C} is usually indicative of some myocardial abnormality. A secondary change in the size or direction of the T wave is consequent to an alteration in the process of ventricular depolarization and is evidenced by a change in the mean electrical axis of QRS and by a normal ventricular gradient. A secondary T wave change is not in itself indicative of myocardial abnormality, although the basic disturbance of depolarization responsible for the T wave change may well imply this.

Primary T wave changes include T wave abnormalities noted in the following: myocardial ischemia, electrolyte imbalance, ventricular hypertrophy, according to some authors, quinidine and digitalis therapy, and miscellaneous conditions like hypothyroidism, beriberi, and other diseases not primarily involving the heart.

The lowering of the T wave amplitude or T wave inversion which is produced in normal subjects by digitalis, and occasionally by exercise, is somewhat unique in that it probably results from an increase in the rate of recovery of ventricular muscle, the effect being more marked in regions with a slower rate of recovery normally. Thus, as the rate of recovery in subendocardial layers of ventricular muscle increases and approaches that of subepicardial myocardium, the normal gradient in the duration of the excited state across the ventricular wall diminishes. This is accompanied by a progressive decrease in the magni-

tude of the mean ventricular gradient vector (without any change in its direction), which in turn causes progressive lowering, and finally inversion, of the T waves in leads previously registering upright T waves. For the same reason, leads previously recording inverted T waves show upright T waves. These T wave changes must, of necessity, occur, because $\bar{A}T = \bar{C} - \bar{A}QRS$. In this equation $\bar{A}QRS$ does not change but \bar{C} becomes smaller, so that $\bar{A}T$ must also become smaller until, when finally $\bar{A}QRS$ exceeds \bar{C} , the direction of $\bar{A}T$ is reversed. By and large, changes in $\bar{A}T$ which are due to changes in magnitude of the ventricular gradient with essentially no change in its direction have much less significance in terms of cardiac disease than do directional changes in the gradient when these are not the result of changes in cardiac position.

Secondary T wave changes are perhaps best illustrated by the T wave abnormalities characterizing bundle branch block. From a theoretical standpoint, bundle branch block is roughly analogous to the hypothetical cell with a normal gradient in duration of the excited state which is stimulated at its epicardial surface rather than at its endocardial surface. This changes the time sequence of onset of depolarization throughout the cell. The same end-result is effected in bundle branch block, but in this condition, the causative mechanism is blocked impulse conduction down one of the main bundle branches. Excitation can only reach the ventricular muscle on the blocked side by spreading from the intact bundle branch via the muscle fibers. Consequently, the time sequence of onset of depolarization in the blocked ventricle differs from that present during normal intraventricular conduction. Just as was found to be the

case when the hypothetical cell was stimulated at its epicardial end, so also in bundle branch block, the change in the depolarization process must inevitably produce a secondary change in the repolarization process and therefore a change in the appearance of the T wave. However, if the bundle branch block is not complicated by cardiac disease or by other conditions producing primary T wave changes, A QRS and A T show an equal but oppositely directed increment in size. Thus the ventricular gradient vector \bar{C} does not change in direction, and, if normal before onset of the bundle branch block, it remains normal.

trocardiograms. The manual construction of the horizontal mean ventricular gradient vector and the mean ventricular gradient spatial vector introduces even greater inaccuracies. However, Briller and his associates have constructed an electronic analogue computer which automatically calculates from the vectorcardiogram the magnitude and direction of the spatial ventricular gradient in terms of its projection on each of the three recording planes of the body.

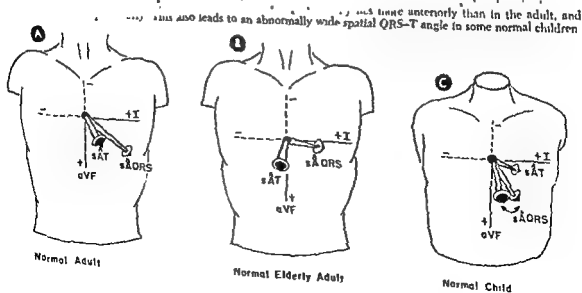
The Monophasic Curves and Ventricular Gradient in Myocardial Ischemia

As already indicated, one can imagine that there exists a pair of monophasic curves for each minute wedge of ventricular muscle. Thus, for a given area of the ventricle or for the ventricular muscle mass as a whole, there are endocardial and epicardial monophasic curves which represent the algebraic summation of all the monophasic curves of the component muscle units. Since normally the rate of recovery is more rapid in epicardial muscle, even though it is activated last, the epicardial monophasic curve is therefore of shorter duration than the endocardial curve and is preceded by it. Accordingly, the QRS deflection and T wave recorded in a lead overlying the electrically dominant left ventricle tend to have the same upright direction. Since subendocardial ischemia prolongs the endocardial monophasic curve so

63]. In this event, the presence of primary T wave abnormalities, in addition to the secondary T wave changes of bundle branch block, can be assumed. This fact in particular potentially provides one of the more valuable applications of the ventricular gradient concept.

Unfortunately, there are at present limitations, inherent to the methods used to determine the ventricular gradient, which greatly impair its clinical usefulness. The accuracy and reliability of frontal plane ventricular gradient calculations can be assured, to some extent, only by the most tedious and time-consuming measurements of specially recorded elec-

Fig 66 The spatial QRS-T angle in



that it extends even farther behind the epicardial curve, algebraic addition of the two curves yields a T wave of greater size but of unchanged direction. As will be seen later, in Chapter 18, this is, indeed, what occurs in subendocardial ischemia; that is, an overlying lead registers a taller T wave. This is a primary T wave. When the lead is moved to a position where it changes in direction. On the other hand, when ischemia becomes transmural and extends to the epicardium, the epicardial monophasic curve is prolonged beyond the endocardial curve, so that algebraic addition of the two yields a T wave which is directed just the opposite of the QRS deflection; that is to say, an overlying lead will register an upright QRS deflection and an inverted T wave. The greater the degree of slowing of recovery at the epicardial surface, the larger and the more deeply inverted is the T wave in this lead.

As will be indicated in Chapter 18, the S-T segment deviation which signals the appearance of muscle injury has much the same mechanism of production as the monophasic curves recorded from the single cell in the hypothetical experiment at the beginning of this chapter. It will be recalled that a monophasic curve was recorded when depolarization was blocked at one or the other surface of the cell by cooling. In the case of muscle injury, the injury process itself has the same blocking effect on depolarization, so that at the end of the QRS interval the injured region retains its dipoles and assumes a positive charge with respect to uninjured depolarized muscle elsewhere. Consequently, an overlying lead records an upward displacement of the base line during the S-T interval. When at times the R wave, S-T segment, and T wave fuse to form a single wave, the latter is often referred to as a *monophasic curve*. Ischemia and injury will be discussed in greater detail later, in Chapter 18, but there the electrical effects of these processes will be explained in vector terms rather than in terms of monophasic curves. However, the two approaches to the subject of ischemia and injury are fundamentally equivalent.

The Spatial QRS-T Angle

From previous considerations of the ventricular repolarization process in the human heart and the ventricular gradient concept, it readily follows that mean instantaneous T spatial vectors normally are oriented more or less in the same direction as the mean instantaneous QRS spatial vectors. Accordingly, the resultants of these instantaneous vectors, the mean

T and mean QRS spatial vectors (sA T and sA QRS), normally subtend a relatively narrow angle. Grant and Estes have applied this fact to the clinical interpretation of electrocardiograms by utilizing their "cylinder method" of constructing mean spatial vectors from the electrocardiographic lead deflections to calculate the spatial QRS-T angle. They found that in normal adult subjects the calculated spatial QRS-T angle is usually less than 40° and rarely exceeds 50° (Fig 66). The exceptions to this rule are "normal" elderly subjects whose spatial QRS-T angles will occasionally exceed 60° in the absence of detectable heart disease. The spatial QRS-T angle in children and in many adolescents normally exceeds 60° . Grant and Estes maintain that, if the spatial QRS-T angle is used in interpreting electrocardiograms, there is little to be gained from calculating the mean (frontal plane) ventricular gradient, but this is open to question. As these investigators themselves admit, the spatial QRS-T angle does not distinguish between primary and secondary T wave abnormalities, which is one of the prime functions of the ventricular gradient. On the other hand, the practical usefulness of the ventricular gradient is at present limited by the cumbersome calculations required for its determination, although this handicap will undoubtedly be overcome in the future by the development of methods of electronically computing the ventricular gradient.

For the present, determination of the spatial QRS-T angle provides a practicable means of applying certain principles of the ventricular gradient concept to the clinical interpretation of the electrocardiogram. However, one should not conceive of the spatial QRS-T angle as representing the complete realization of the potentialities of the ventricular gradient concept, although it does teach one to evaluate, for example, the T waves in relationship to the QRS deflections appearing in the same lead. By computing the spatial QRS-T angle, the electrocardiographer will find it much easier to differentiate normal T waves from abnormal T waves. Granting these advantages of the spatial QRS-T angle, one must at the same time call attention to certain disadvantages of this approach.

- 1 Sometimes the null contour or transitional pathway for the mean T spatial vector does not pass through the electrode positions of any of the six precordial leads routinely recorded. In this instance, upright T waves are registered in all six chest leads. For this to happen, the horizontal mean T (planar) vector must lie in the $+30^\circ$ to $+90^\circ$ segment of the horizontal reference frame (this is as precise a localiza-

tion of the vector as one can make with any degree of certainty). Obviously, the spatial QRS-T angle would have relatively little reliability in this situation unless one were to record additional precordial leads so that the null contour for the mean T spatial vector might be mapped out.

2. When the method of Grant and Estes is used to determine the spatial QRS-T angle, there must be available a vector model of the type used by these investigators.

3. If, on the other hand, the orientations of ΣA QRS and ΣA T in the frontal and horizontal planes are determined separately for each plane, these values must then be used to calculate trigonometrically the spatial QRS-T angle by means of tables of the type devised by Helm (see Table 2).

In either case, determination of the spatial QRS-T angle is time consuming.

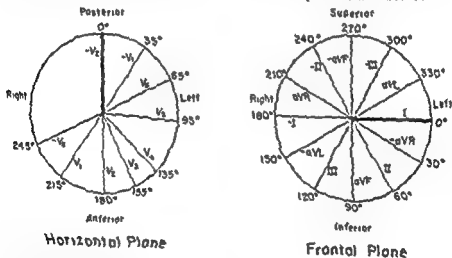
4. In determining the spatial QRS-T angle, the effective direction and length of each individual lead

is not taken into consideration. The implications of this fact have already been considered in Chapter 4, dealing with the lead vector concept. Suffice to say, the use of reference systems based on the anatomic lead axes, rather than on the corresponding lead vectors, introduces some error into the construction of mean vectors from the electrocardiogram. Admittedly, this factor may have relatively little significance except in cases of borderline wide spatial QRS-T angles.

5. Not all investigators will agree as to the correctness of the normal limits of the spatial QRS-T angle proposed by Grant and Estes; in fact, some have found rather marked variation in the width of the spatial QRS-T angle in normal subjects.

Despite the objections just listed, the spatial QRS-T angle represents a major step away from the empiricism with which the electrocardiographic T waves were interpreted in previous years.

TABLE 2—CALCULATION OF THE SPATIAL ANGLE SUBTENDED BY ΣA QRS AND ΣA T ON THE LONG AXIS (MAXIMAL INSTANTANEOUS SPATIAL VECTORS) OF THE QRS AND T WAVES



	0°	5°	10°	15°	20°	25°	30°	35°	40°	45°	50°	55°	60°	65°	70°	75°	80°	85°	90°	95°	100°	105°	110°	115°	120°	125°	130°	135°	140°	145°	150°	155°	160°	165°	170°	175°	180°	185°	190°	195°	200°	205°	210°	215°	220°	225°	230°	235°	240°	245°	250°	255°	260°	265°	270°	275°	280°	285°	290°	295°	300°	305°	310°	315°	320°	325°	330°												
0°	0	1	2	3	4	5	6	7	8	9	10	11	12	13	14	15	16	17	18	19	20	21	22	23	24	25	26	27	28	29	30	31	32	33	34	35	36	37	38	39	40	41	42	43	44	45	46	47	48	49	50	51	52	53	54	55	56	57	58	59	60																		
5°	1	2	3	4	5	6	7	8	9	10	11	12	13	14	15	16	17	18	19	20	21	22	23	24	25	26	27	28	29	30	31	32	33	34	35	36	37	38	39	40	41	42	43	44	45	46	47	48	49	50	51	52	53	54	55	56	57	58	59	60	61	62	63	64	65	66	67	68	69	70									
10°	2	3	4	5	6	7	8	9	10	11	12	13	14	15	16	17	18	19	20	21	22	23	24	25	26	27	28	29	30	31	32	33	34	35	36	37	38	39	40	41	42	43	44	45	46	47	48	49	50	51	52	53	54	55	56	57	58	59	60	61	62	63	64	65	66	67	68	69	70	71	72	73	74	75	76	77	78	79	80
15°	3	4	5	6	7	8	9	10	11	12	13	14	15	16	17	18	19	20	21	22	23	24	25	26	27	28	29	30	31	32	33	34	35	36	37	38	39	40	41	42	43	44	45	46	47	48	49	50	51	52	53	54	55	56	57	58	59	60	61	62	63	64	65	66	67	68	69	70	71	72	73	74	75	76	77	78	79	80	
20°	4	5	6	7	8	9	10	11	12	13	14	15	16	17	18	19	20	21	22	23	24	25	26	27	28	29	30	31	32	33	34	35	36	37	38	39	40	41	42	43	44	45	46	47	48	49	50	51	52	53	54	55	56	57	58	59	60	61	62	63	64	65	66	67	68	69	70	71	72	73	74	75	76	77	78	79	80		
25°	5	6	7	8	9	10	11	12	13	14	15	16	17	18	19	20	21	22	23	24	25	26	27	28	29	30	31	32	33	34	35	36	37	38	39	40	41	42	43	44	45	46	47	48	49	50	51	52	53	54	55	56	57	58	59	60	61	62	63	64	65	66	67	68	69	70	71	72	73	74	75	76	77	78	79	80			
30°	6	7	8	9	10	11	12	13	14	15	16	17	18	19	20	21	22	23	24	25	26	27	28	29	30	31	32	33	34	35	36	37	38	39	40	41	42	43	44	45	46	47	48	49	50	51	52	53	54	55	56	57	58	59	60	61	62	63	64	65	66	67	68	69	70	71	72	73	74	75	76	77	78	79	80				
35°	7	8	9	10	11	12	13	14	15	16	17	18	19	20	21	22	23	24	25	26	27	28	29	30	31	32	33	34	35	36	37	38	39	40	41	42	43	44	45	46	47	48	49	50	51	52	53	54	55	56	57	58	59	60	61	62	63	64	65	66	67	68	69	70	71	72	73	74	75	76	77	78	79	80					
40°	8	9	10	11	12	13	14	15	16	17	18	19	20	21	22	23	24	25	26	27	28	29	30	31	32	33	34	35	36	37	38	39	40	41	42	43	44	45	46	47	48	49	50	51	52	53	54	55	56	57	58	59	60	61	62	63	64	65	66	67	68	69	70	71	72	73	74	75	76	77	78	79	80						
45°	9	10	11	12	13	14	15	16	17	18	19	20	21	22	23	24	25	26	27	28	29	30	31	32	33	34	35	36	37	38	39	40	41	42	43	44	45	46	47	48	49	50	51	52	53	54	55	56	57	58	59	60	61	62	63	64	65	66	67	68	69	70	71	72	73	74	75	76	77	78	79	80							
50°	10	11	12	13	14	15	16	17	18	19	20	21	22	23	24	25	26	27	28	29	30	31	32	33	34	35	36	37	38	39	40	41	42	43	44	45	46	47	48	49	50	51	52	53	54	55	56	57	58	59	60	61	62	63	64	65	66	67	68	69	70	71	72	73	74	75	76	77	78	79	80								
55°	11	12	13	14	15	16	17	18	19	20	21	22	23	24	25	26	27	28	29	30	31	32	33	34	35	36	37	38	39	40	41	42	43	44	45	46	47	48	49	50	51	52	53	54	55	56	57	58	59	60	61	62	63	64	65	66	67	68	69	70	71	72	73	74	75	76	77	78	79	80									
60°	12	13	14	15	16	17	18	19	20	21	22	23	24	25	26	27	28	29	30	31	32	33	34	35	36	37	38	39	40	41	42	43	44	45	46	47	48	49	50	51	52	53	54	55	56	57	58	59	60	61	62	63	64	65	66	67	68	69	70	71	72	73	74	75	76	77	78	79	80										
65°	13	14	15	16	17	18	19	20	21	22	23	24	25	26	27	28	29	30	31	32	33	34	35	36	37	38	39	40	41	42	43	44	45	46	47	48	49	50	51	52	53	54	55	56	57	58	59	60	61	62	63	64	65	66	67	68	69	70	71	72	73	74	75	76	77	78	79	80											
70°	14	15	16	17	18	19	20	21	22	23	24	25	26	27	28	29	30	31	32	33	34	35	36	37	38	39	40	41	42	43	44	45	46	47	48	49	50	51	52	53	54	55	56	57	58	59	60	61	62	63	64	65	66	67	68	69	70	71	72	73	74	75	76	77	78	79	80												
75°	15	16	17	18	19	20	21	22	23	24	25	26	27	28	29	30	31	32	33	34	35	36	37	38	39	40	41	42	43	44	45	46	47	48	49	50	51	52	53	54	55	56	57	58	59	60	61	62	63	64	65	66	67	68	69	70	71	72	73	74	75	76	77	78	79	80													
80°	16	17	18	19	20	21	22	23	24	25	26	27	28	29	30	31	32	33	34	35	36	37	38	39	40	41	42	43	44	45	46	47	48	49	50	51	52	53	54	55	56	57	58	59	60	61	62	63	64	65	66	67	68	69	70	71	72	73	74	75	76	77	78	79	80														
85°	17	18	19	20	21	22	23	24	25	26	27	28	29	30	31	32	33	34	35	36	37	38	39	40	41	42	43	44	45	46	47	48	49	50	51	52	53	54	55	56	57	58	59	60	61	62	63	64	65	66	67	68	69	70	71	72	73	74	75	76	77	78	79	80															
90°	18	19	20	21	22	23	24	25	26	27	28	29	30	31	32	33	34	35	36	37	38	39	40	41	42	43	44	45	46	47	48	49	50	51	52	53	54	55	56	57	58	59	60	61	62	63	64	65	66	67	68	69	70	71	72	73	74	75	76	77	78	79	80																
95°	19	20	21	22	23	24	25	26	27	28	29	30	31	32	33	34	35	36	37	38	39	40	41	42	43	44	45	46	47	48	49	50	51	52	53	54	55	56	57	58	59	60	61	62	63	64	65	66	67	68	69	70	71	72	73	74	75	76	77	78	79	80																	
100°	20	21	22	23	24	25	26	27	28	29	30	31	32	33	34	35	36	37	38	39	40	41	42	43	44	45	46	47	48	49	50	51	52	53	54	55	56	57	58	59	60	61	62	63	64	65	66	67	68	69	70	71	72	73	74	75	76	77	78	79	80																		
105°	21	22	23	24	25	26	27	28	29	30	31	32	33	34	35	36	37	38	39	40	41	42	43	44	45	46	47	48	49	50	51	52	53	54	55	56	57																																										

that it extends even farther behind the epicardial curve, algebraic addition of the two curves yields a T wave of greater size but of unchanged direction. As will be seen later, in Chapter 18, this is, indeed, what occurs in subendocardial ischemia; that is, an overlying lead registers a taller T wave. This is a primary T wave change, since \bar{A} QRS does not change in area while \bar{A} T does—hence the ventricular gradient also changes in direction. On the other hand, when ischemia becomes transmural and extends to the epicardium, the epicardial monophasic curve is prolonged beyond the endocardial curve, so that algebraic addition of the two yields a T wave which is directed just the opposite of the QRS deflection, that is to say, an overlying lead will register an upright QRS deflection and an inverted T wave. The greater the degree of slowing of recovery at the epicardial surface, the larger and the more deeply inverted is the T wave in this lead.

As will be indicated in Chapter 18, the S-T segment deviation which signals the appearance of muscle injury has much the same mechanism of production as the monophasic curves recorded from the single cell in the hypothetical experiment at the beginning of this chapter. It will be recalled that a monophasic curve was recorded when depolarization was blocked at one or the other surface of the cell by cooling. In the case of muscle injury, the injury process itself has the same blocking effect on depolarization, so that at the end of the QRS interval the injured region retains its dipoles and assumes a positive charge with respect to uninjured depolarized muscle elsewhere. Consequently, an overlying lead records an upward displacement of the base line during the S-T interval. When at times the R wave, S-T segment, and T wave fuse to form a single wave, the latter is often referred to as a *monophasic curve*. Ischemia and injury will be discussed in greater detail later, in Chapter 18, but there the electrical effects of these processes will be explained in vector terms rather than in terms of monophasic curves. However, the two approaches to the subject of ischemia and injury are fundamentally equivalent.

The Spatial QRS-T Angle

From previous considerations of the ventricular repolarization process in the human heart and the ventricular gradient concept, it readily follows that mean instantaneous T spatial vectors normally are oriented more or less in the same direction as the mean instantaneous QRS spatial vectors. Accordingly, the resultants of these instantaneous vectors, the mean

T and mean QRS spatial vectors (\bar{sA} T and \bar{sA} QRS), normally subtend a relatively narrow angle. Grant and Estes have applied this fact to the clinical interpretation of electrocardiograms by utilizing their "cylinder method" of constructing mean spatial vectors from the electrocardiographic lead deflections to calculate the *spatial QRS-T angle*. They found that in normal adult subjects the calculated spatial QRS-T angle is usually less than 40° and rarely exceeds 50° (Fig. 66). The exceptions to this rule are "normal" elderly subjects whose spatial QRS-T angles will occasionally exceed 60° in the absence of detectable heart disease. The spatial QRS-T angle in children and in many adolescents normally exceeds 60° . Grant and Estes maintain that, if the spatial QRS-T angle is used in interpreting electrocardiograms, there is little to be gained from calculating the mean (frontal plane) ventricular gradient, but this is open to question. As these investigators themselves admit, the spatial QRS-T angle does not distinguish between primary and secondary T wave abnormalities, which is one of the prime functions of the ventricular gradient. On the other hand, the practical usefulness of the ventricular gradient is at present limited by the cumbersome calculations required for its determination, although this handicap will undoubtedly be overcome in the future by the development of methods of electronically computing the ventricular gradient.

For the present, determination of the spatial QRS-T angle provides a practicable means of applying certain principles of the ventricular gradient concept to the clinical interpretation of the electrocardiogram. However, one should not conceive of the spatial QRS-T angle as representing the complete realization of the potentialities of the ventricular gradient concept, although it does teach one to evaluate, for example, the T waves in relationship to the QRS deflections appearing in the same lead. By computing the spatial QRS-T angle, the electrocardiographer will find it much easier to differentiate normal T waves from abnormal T waves. Granting these advantages of the spatial QRS-T angle, one must at the same time call attention to certain disadvantages of this approach.

1 Sometimes the null contour or transitional pathway for the mean T spatial vector does not pass through the electrode positions of any of the six precordial leads routinely recorded. In this instance, upright T waves are registered in all six chest leads. For this to happen, the horizontal mean T (planar) vector must lie in the $+30^\circ$ to $+90^\circ$ segment of the horizontal reference frame (this is as precise a localiza-

tion of the vector as one can make with any degree of certainty). Obviously, the spatial QRS-T angle would have relatively little reliability in this situation unless one were to record additional precordial leads so that the null contour for the mean T spatial vector might be mapped out.

2 When the method of Grant and Estes is used to determine the spatial QRS-T angle, there must be available a vector model of the type used by these investigators

3 If, on the other hand, the orientations of sA QRS and sA T in the frontal and horizontal planes are determined separately for each plane, these values must then be used to calculate trigonometrically the spatial QRS-T angle by means of tables of the type devised by Helm (see Table 2).

In either case, determination of the spatial QRS-T angle is time consuming.

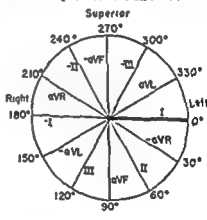
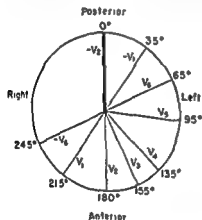
4 In determining the spatial QRS-T angle, the effective direction and length of each individual lead

is not taken into consideration. The implications of this fact have already been considered in Chapter 4, dealing with the lead vector concept. Suffice to say, the use of reference systems based on the anatomic lead axes, rather than on the corresponding lead vectors, introduces some error into the construction of mean vectors from the electrocardiogram. Admittedly, this factor may have relatively little significance except in cases of borderline wide spatial QRS-T angles.

5. Not all investigators will agree as to the correctness of the normal limits of the spatial QRS-T angle proposed by Grant and Estes, in fact, some have found rather marked variation in the width of the spatial QRS-T angle in normal subjects

Despite the objections just listed, the spatial QRS-T angle represents a major step away from the empiricism with which the electrocardiographic T waves were interpreted in previous years.

TABLE 2—CALCULATION OF THE SPATIAL ANGLE SUBTENDED BY sA QRS AND sA T OR BY THE LONG AXES (MAXIMAL INSTANTANEOUS SPATIAL VECTORS) OF THE QRS SE AND T SE LOOPS



Horizontal Plane												Interior												Frontal Plane															
0°	5°	10°	15°	20°	25°	30°	35°	40°	45°	50°	55°	60°	65°	70°	75°	80°	85°	90°																					
(+ +)	(+ +)	(+ +)	(+ +)	(+ +)	(+ +)	(+ +)	(+ +)	(+ +)	(+ +)	(+ +)	(+ +)	(+ +)	(+ +)	(+ +)	(+ +)	(+ +)	(+ +)	(+ +)																					
180°	175°	170°	165°	160°	155°	150°	145°	140°	135°	130°	125°	120°	115°	110°	105°	100°	95°	90°																					
(- -)	(- -)	(- -)	(- -)	(- -)	(- -)	(- -)	(- -)	(- -)	(- -)	(- -)	(- -)	(- -)	(- -)	(- -)	(- -)	(- -)	(- -)	(- -)																					
180°	185°	190°	195°	200°	205°	210°	215°	220°	225°	230°	235°	240°	245°	250°	255°	260°	265°	270°																					
360°	355°	350°	345°	340°	335°	330°	325°	320°	315°	310°	305°	300°	295°	290°	285°	280°	275°	270°																					
(+ -)	(+ -)	(+ -)	(+ -)	(+ -)	(+ -)	(+ -)	(+ -)	(+ -)	(+ -)	(+ -)	(+ -)	(+ -)	(+ -)	(+ -)	(+ -)	(+ -)	(+ -)	(+ -)																					
0°	5°	10°	15°	20°	25°	30°	35°	40°	45°	50°	55°	60°	65°	70°	75°	80°	85°	90°																					
180°	175°	170°	165°	160°	155°	150°	145°	140°	135°	130°	125°	120°	115°	110°	105°	100°	95°	90°																					
(- -)	(- -)	(- -)	(- -)	(- -)	(- -)	(- -)	(- -)	(- -)	(- -)	(- -)	(- -)	(- -)	(- -)	(- -)	(- -)	(- -)	(- -)	(- -)																					
180°	185°	190°	195°	200°	205°	210°	215°	220°	225°	230°	235°	240°	245°	250°	255°	260°	265°	270°																					
360°	355°	350°	345°	340°	335°	330°	325°	320°	315°	310°	305°	300°	295°	290°	285°	280°	275°	270°																					
(+ -)	(+ -)	(+ -)	(+ -)	(+ -)	(+ -)	(+ -)	(+ -)	(+ -)	(+ -)	(+ -)	(+ -)	(+ -)	(+ -)	(+ -)	(+ -)	(+ -)	(+ -)	(+ -)																					

cos = 1 000	0°	5°	10°	15°	20°	25°	30°	35°	40°	45°	50°	55°	60°	65°	70°	75°	80°	85°	90°																				
180°	175°	170°	165°	160°	155°	150°	145°	140°	135°	130°	125°	120°	115°	110°	105°	100°	95°	90°																					
360°	355°	350°	345°	340°	335°	330°	325°	320°	315°	310°	305°	300°	295°	290°	285°	280°	275°	270°																					
cos = 999	0°	5°	10°	15°	20°	25°	30°	35°	40°	45°	50°	55°	60°	65°	70°	75°	80°	85°	90°																				
180°	175°	170°	165°	160°	155°	150°	145°	140°	135°	130°	125°	120°	115°	110°	105°	100°	95°	90°																					
360°	355°	350°	345°	340°	335°	330°	325°	320°	315°	310°	305°	300°	295°	290°	285°	280°	275°	270°																					
cos = 999	0°	5°	10°	15°	20°	25°	30°	35°	40°	45°	50°	55°	60°	65°	70°	75°	80°	85°	90°																				
180°	175°	170°	165°	160°	155°	150°	145°	140°	135°	130°	125°	120°	115°	110°	105°	100°	95°	90°																					
360°	355°	350°	345°	340°	335°	330°	325°	320°	315°	310°	305°	300°	295°	290°	285°	280°	275°	270°																					
cos = 999	0°	5°	10°	15°	20°	25°	30°	35°	40°	45°	50°	55°	60°	65°	70°	75°	80°	85°	90°																				
180°	175°	170°	165°	160°	155°	150°	145°	140°	135°	130°	125°	120°	115°	110°	105°	100°	95°	90°																					
360°	355°	350°	345°	340°	335°	330°	325°	320°	315°	310°	305°	300°	295°	290°	285°	280°	275°	270°																					

(Continued on next page)

(Continued on next page)

TABLE 2 (Continued)

[illegible]

TABLE II (Continued)

The orientations of sA QRS and sA T, as expressed in terms of the reference frames used throughout this text,

the spatial angle between the QRS and T vectors, the orientation of the QRS vector in the horizontal plane is located in the horizontal marginal columns at the top of the table, while the orientation of the QRS vector in the frontal plane is located in the vertical marginal column at the left of the table. The three numbers appearing at the intersection of the columns are read directly from the table, and positive or negative signs are inserted before the middle and

respectively. The two signs obtained from the vertical marginal columns are inserted before the middle and

lower numbers, respectively. The sign of the middle number should be the same in both instances, or some error in the orientations of the vectors has been made. The same procedure is followed with reference to the T vector. Thus, one is left with two sets of three values. The paired upper values, the paired middle values, and the paired lower values are multiplied, and the three products are then added algebraically according to their signs. The result is the cosine of the angle between the two spatial vectors. In the table, cosines for values midway between the groups of angles given in the vertical marginal columns are listed. By locating in these columns the position of the calculated cosine, the spatial angle can be determined to the nearest 5°. If the calculated cosine is positive, the angle chosen must be between 0° and 90°. If the calculated cosine has a negative value, the angle chosen must be between 90° and 180°, since the angle between two spatial vectors cannot exceed 180°.

EXAMPLE (Fig 53, Chap 5):

Orientation° of sA QRS	Horizontal Plane	Frontal Plane
	85°	60°
Orientation° of sA T	125°	30°
QRS T $+0.23 \times -0.52 = -0.1196$ $+0.49 \times +0.74 = +0.3626$ $+0.84 \times +0.43 = +0.3612$ $\hline +0.6042$		

Cosine of spatial angle subtended by sA QRS and sA T = +0.6042.
Spatial QRS-T angle = approximately 53°

EXAMPLE (Fig 83, A, Chap. 7)

Orientation° of long axis of QRS sE loop	Horizontal Plane	Frontal Plane
	80°	45°
Orientation° of long axis of T sE loop	100°	40°
QRS T $+0.12 \times -0.13 = -0.0156$ $+0.70 \times +0.76 = +0.5320$ $+0.70 \times +0.64 = +0.4480$ $\hline +0.9644$		

+0.9644

cosine of spatial angle = +0.9644 in terms of the reference frames depicted in the above table

Vectorcardiography

INSTRUMENTATION

THE CATHODE RAY TUBE of the oscilloscope electrocardiograph and vectorcardiograph functions in the following way: An electrically heated filament enclosed in an evacuated glass tube heats a metal plate cathode covered with some substance capable of emitting electrons freely when hot. A second plate, the anode, is maintained at a high positive potential by an outside current source. As a result, a strong electrical field exists between the cathode and anode, and in this field the electrons emitted by the cathode are accelerated to a high velocity. The electrons pass through a small hole in the anode and emerge beyond as a fine beam of cathode rays. This electron beam passes between two sets of deflection plates at right angles to each other and strikes a fluorescent viewing screen on the inner surface of the oscilloscope tube. As long as the deflection plates remain uncharged, the electron beam remains focused at a single point on the screen, but once a potential difference appears between the two pairs of plates, the electron beam is drawn toward the positively charged plate of each pair and deflected away from the negatively charged plate. Superior-inferior displacement of the beam is governed by the potential difference across the vertical, (Y) deflecting, plates, and side-to-side displacement of the beam, by the potential difference across the transverse or horizontal (X) plates.

When the oscilloscope is used to record an electrocardiogram, electrical currents from the patient are transmitted by lead wires to the oscilloscope, where, after considerable amplification, they produce a potential difference across the vertical deflection plates. If the superior plate is relatively positively charged with respect to the inferior plate, the electron beam is displaced upward, if the inferior plate is more positive or less negative than the superior plate, the beam moves downward. At the same time that the potential variations across the plates deflect the

beam vertically upward and/or downward, a positive charge is placed intermittently on the left horizontal deflection plate, causing the electron beam to sweep at a given speed horizontally from right to left across the screen (i.e., from the observer's left to right). Thus the voltage recorded in a single electrocardiographic lead is depicted as a function of time.

When the oscilloscope is used as a vectorcardiograph, the horizontal beam sweep is turned off, and two leads preferably with perpendicular lead axes, are connected to the vertical and horizontal pairs of deflection plates. Thus, at a given instant during electrical systole or diastole, the electron beam is displaced according to the resultant of the cardiac forces acting along the two perpendicular leads being recorded and across the two pairs of deflection plates. If one visualizes the cardiac forces acting along the leads as vectors, then, in a general sense, the distance (translated into millivolts, according to the standardization factors used for the two leads) the electron beam is displaced and the direction of displacement correspond roughly to the magnitude and direction of the resultant or mean instantaneous planar vector. The instantaneous planar vector itself can be visualized as extending from the point of origin, or resting point of the beam, to the position of the beam following displacement.

The instant-to-instant change in the direction and magnitude of the instantaneous cardiac vectors during atrial and ventricular depolarization and during ventricular repolarization is accompanied in the vectorcardiogram by the inscription of three successive closed loops—the P sE,* QRS sE, and T sE loops, respectively. To provide a means of timing in the vectorcardiogram, the electron beam is interrupted by an

*E = equivalent cardiac dipole, Σ = E expressed as vector quantity, and sE = Σ expressed as spatial vector quantity

oscillator circuit which breaks the loops into dashes. In the vectorcardiograms appearing in this text, the dashes occur at intervals of 0.0025 second. Each dash is modulated into the form of a teardrop, the blunt end of which indicates the direction of inscription of a given loop. The distance between the dashes indicates the speed of inscription. Closely spaced dashes signify a slow rate of inscription, widely spaced and elongated dashes, a rapid speed of inscription.

Since only two leads can be connected to the deflection plates of the oscilloscope at any single time, the three loops traced on the oscilloscope screen during the cardiac cycle represent the projections of the P sE, QRS sE, and T sE (spatial) loops on the plane

defined by the axes of the leads being recorded. In this text the loops visualized on the screen of the oscilloscope will be referred to either as the *planar loops* or, more specifically, as *frontal QRS loops* (sagittal R loop, horizontal T loop, etc.) or the *QRS sE loop in the frontal projection*. To obtain the frontal projection of the vectorcardiogram, two leads which define the frontal plane are recorded, preferably leads paralleling the transverse (X) and vertical (Y) co-ordinate axes of the body. Similarly, the horizontal projection can be obtained by recording a transverse lead and an anteroposterior lead (Z), and the sagittal projection can be obtained by recording vertical and anteroposterior leads.

ELECTRODE PLACEMENT AND LEAD SYSTEMS

The lead systems used most commonly in vectorcardiography are of two types. The first type includes all lead systems based on the Einthoven equilateral triangle, such as those devised by Milovanovich, Jouve, Vastesaeger, and the "equilateral tetrahedron" system suggested by Wilson and used most extensively by Burch and his associates. The second general type of electrode arrangement consists of the orthogonal lead systems. Of these, the most widely used are Duchosal and Sulzer's rectangular system and Grishman's cube system, a modification of the former. Orthogonal lead systems differ from those based on the equilateral triangle in that the lead electrodes are applied in such a way that the leads formed are perpendicular to one another.

Equilateral Tetrahedron Lead System

In the equilateral tetrahedron system, electrodes are placed on the left—

... the oscilloscope so as to record each of the planar projections of the vectorcardiogram (see Fig. 63) is described below.

Frontal plane—1. The lead wires from the left and right arms are connected to the horizontal deflection plates in such a way that, when the right arm (RA) electrode is relatively negative with respect to the left arm (LA) electrode, the electron beam is displaced to the subject's and screen's left (the observer's right).

2. The lead wire from the left leg (LL) is connected to the inferior deflection plate of the vertical set, and Wilson's central terminal (CT) is connected

to the superior deflecting plate. When electrode LL is relatively positive with respect to CT, the electron beam is deflected vertically downward.

Left sagittal plane—1. Wilson's central terminal (CT) is connected to the horizontal deflection plate on the screen's right (the observer's left), and the lead wire from the back electrode (B) is connected to the other horizontal plate. When B is relatively negative with respect to CT, the electron beam is shifted anteriorly or to the screen's right (the observer's left).

2. The left leg electrode (LL) is connected to the inferior deflecting plate, and CT to the superior plate,

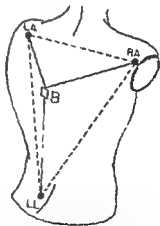


Fig. 67.—Equilateral tetrahedron system of electrode placement used by Burch and his associates. The vectorcardiogram is recorded in the frontal plane (defined by points LA, RA, and LL), in the left sagittal plane (defined by points LA, LL, and B, the back electrode), and in the superior plane (defined by points LA, RA, and B).

Vectorcardiography

INSTRUMENTATION

THE CATHODE RAY TUBE of the oscilloscope electrocardiograph and vectorcardiograph functions in the following way: An electrically heated filament enclosed in an evacuated glass tube heats a metal plate cathode covered with some substance capable of emitting electrons freely when hot. A second plate, the anode, is maintained at a high positive potential by an outside current source. As a result, a strong electrical field exists between the cathode and anode, and in this field the electrons emitted by the cathode are accelerated to a high velocity. The electrons pass through a small hole in the anode and emerge beyond as a fine beam of cathode rays. This electron beam passes between two sets of deflection plates at right angles to each other and strikes a fluorescent viewing screen on the inner surface of the oscilloscope tube. As long as the deflection plates remain uncharged, the electron beam remains focused at a single point on the screen, but once a potential difference appears between the two pairs of plates, the electron beam is drawn toward the positively charged plate of each pair and deflected away from the negatively charged plate. Superior-inferior displacement of the beam is governed by the potential difference across the vertical, (Y) deflecting, plates, and side-to-side displacement of the beam, by the potential difference across the transverse or horizontal (X) plates.

When the oscilloscope is used to record an electrocardiogram, electrical currents from the patient are transmitted by lead wires to the oscilloscope, where, after considerable amplification, they produce a potential difference across the vertical deflection plates. If the superior plate is relatively positively charged with respect to the inferior plate, the electron beam is displaced upward, if the inferior plate is more positive or less negative than the superior plate, the beam moves downward. At the same time that the potential variations across the plates deflect the

beam vertically upward and/or downward, a positive charge is placed intermittently on the left horizontal deflection plate, causing the electron beam to sweep at a given speed horizontally from right to left across the screen (i.e., from the observer's left to right). Thus the voltage recorded in a single electrocardiographic lead is depicted as a function of time.

When the oscilloscope is used as a vectorcardiograph, the horizontal beam sweep is turned off, and two leads preferably with perpendicular lead axes, are connected to the vertical and horizontal pairs of deflection plates. Thus, at a given instant during electrical systole or diastole, the electron beam is displaced according to the resultant of the cardiac forces acting along the two perpendicular leads being recorded and across the two pairs of deflection plates. If one visualizes the cardiac forces acting along the leads as vectors, then, in a general sense, the distance (translated into millivolts, according to the standardization factors used for the two leads) the electron beam is displaced and the direction of displacement correspond roughly to the magnitude and direction of the resultant or mean instantaneous planar vector. The instantaneous planar vector itself can be visualized as extending from the point of origin, or resting point of the beam, to the position of the beam following displacement.

The instant-to-instant change in the direction and magnitude of the instantaneous cardiac vectors during atrial and ventricular depolarization and during ventricular repolarization is accompanied in the vectorcardiogram by the inscription of three successive closed loops—the P sE, *QRS sE, and T sE loops, respectively. To provide a means of timing in the vectorcardiogram, the electron beam is interrupted by an

*E = equivalent cardiac dipole, E = E expressed as vector quantity, and sE = E expressed as spatial vector quantity

nomenclature used by Grishman and his associates to designate the leads will be changed so as to emphasize the relationship of the leads to the co-ordinate axes of the body. Thus, the three bipolar leads of the cube system will be assigned the symbols X_c , Y_c , and Z_c . Lead X_c is the transverse lead (Grishman's

lead A); lead Y_c is the vertical lead (Grishman's lead C); and lead Z_c is the sagittal lead (Grishman's lead B). The corresponding body axes will be referred to as the X, Y, and Z axes, just as in preceding chapters.

The positions of the electrodes in the cube system and the polarity of the electrodes (Fig. 69) follow:

Lead Electrode

"Common electrode" (serves as the negative electrode for leads X_c and Z_c and the positive electrode for lead Y_c)

Positive electrode for lead X_c (transverse lead)

Positive electrode for lead Z_c (sagittal or anteroposterior lead)

Negative electrode for lead Y_c (vertical lead)

Position

Right posterior axillary line at level of first or second lumbar vertebra (point 1 in Fig. 69, A).

Left posterior axillary line at same level as the above (point 2 in Fig. 69, A)

Right anterior axillary line at same level as the above (point 3 in Fig. 69, A)

Over right scapula in the right posterior axillary line (point 4 in Fig. 69, A)

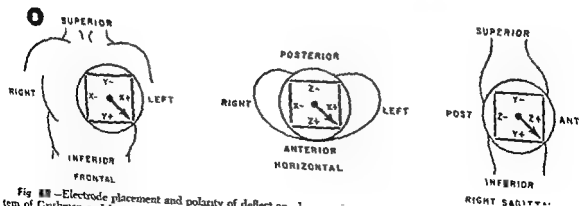
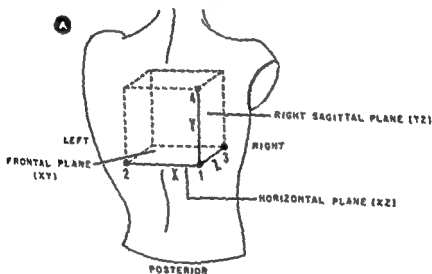


Fig. 69—Electrode placement and polarity of electrode system of Grishman.

Cube system of electrode placement

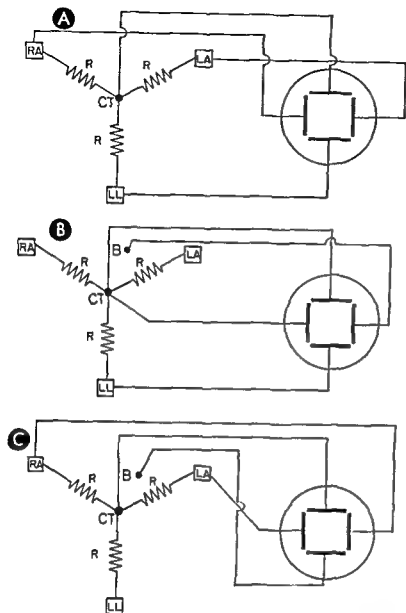


Fig. 68.—Equilateral tetrahedron system of electrode placement. The electrodes are connected to the deflection plates of the oscilloscope as follows: **A**, in recording the frontal projection of the vectorcardiogram, **B**, in recording the left sagittal plane projection, and **C**, in recording the superior projection. **CT**, central terminal of Wilson, **B**, a unipolar back lead placed at a point 12 cm. to the left of the seventh dorsal vertebra. Note that in recording the superior projection the connections of the left and right arms to the right and left deflection plates of the oscilloscope are the reverse of those utilized to record the frontal projection, and that the normal QRS $\pm E$ loop, as recorded with this system, tends to be situated to the observer's right in the frontal projection and to his left in the superior projection.

the beam moving downward when **LL** is positive with respect to **CT**.

Superior plane—The lead wire connections to the oscilloscope in recording the superior projection of the vectorcardiogram are shown in Figure 68, **C**, and will not be described here.

Standardizing factors—1 Horizontal deflection in frontal plane (**R-L**) is 1 unit (usually 1 inch) for 1 mv. potential difference between electrodes **R** and **L**. (See Chapter 2 for calculation of correction factors for unipolar leads when bipolar leads are assigned a value of 1.)

2. Vertical deflection in frontal plane (**C-F**) is 1.7 units (or inches) per 1 mv. potential difference between electrode **F** and Wilson's central terminal (See Chapter 2 for calculation of standardization factor for lead **VF**.)

3 Horizontal deflection in sagittal plane (**C-B**) is 1.2 units (or inches) for 1 mv. potential difference between the back electrode (**B**) and the Wilson's central terminal.*

Grishman's Cube Lead System

Grishman's cube system of electrode placement, a modification of the rectangular system of Duchosal and Sulzer, is one of the orthogonal systems more commonly used in this country. It was the lead system utilized to record virtually all of the vectorcardiograms appearing in this text. In the following description of the cube method of electrode placement, the

*Abildskov, J. A., Burch, G. E., and Cronqvist, J. A.: The validity of the equilateral tetrahedron as a spatial reference system, *Circulation* 2:122, 1950.

nomenclature used by Grishman and his associates to designate the leads will be changed so as to emphasize the relationship of the leads to the co-ordinate axes of the body. Thus, the three bipolar leads of the cube system will be assigned the symbols X_c , Y_c , and Z_c . Lead X_c is the transverse lead (Grishman's

lead A); lead Y_c is the vertical lead (Grishman's lead C), and lead Z_c is the sagittal lead (Grishman's lead B). The corresponding body axes will be referred to as the X, Y, and Z axes, just as in preceding chapters.

The positions of the electrodes in the cube system and the polarity of the electrodes (Fig. 69) follow:

Lead Electrode

"Common electrode" (serves as the negative electrode for leads X_c and Z_c and the positive electrode for lead Y_c)

Positive electrode for lead X_c (transverse lead)

Positive electrode for lead Z_c (sagittal or anteroposterior lead)

Negative electrode for lead Y_c (vertical lead)

Position

Right posterior axillary line at level of first or second lumbar vertebra (point 1 in Fig. 69, A).

Left posterior axillary line at same level as the above (point 2 in Fig. 69, A)

Right anterior axillary line at same level as the above (point 3 in Fig. 69, A)

Over right scapula in the right posterior axillary line (point 4 in Fig. 69, A)

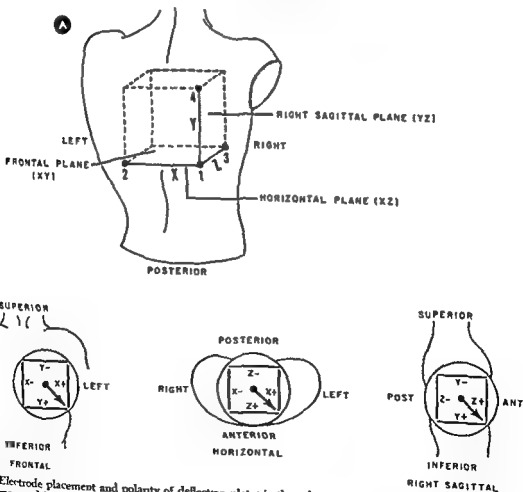


Fig. 69.—Electrode placement and polarity of deflection plates in the cube orthogonal vectorcardiographic lead system of Grishman and his associates. A, positions of the electrodes. B, polarity of deflection plates of oscilloscope and standardization deflection.

* X_c = transverse lead in the cube system of electrode placement

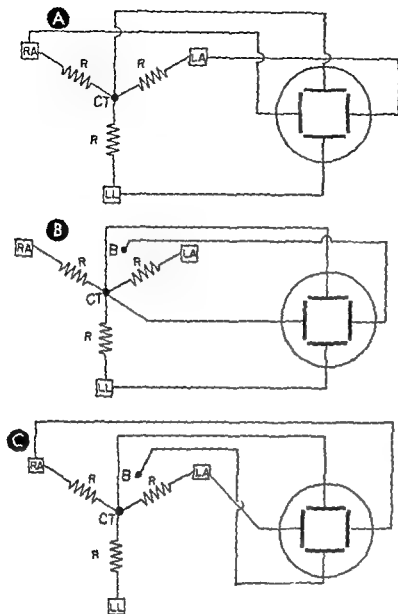


Fig. 68.—Equilateral tetrahedron system of electrode placement. The electrodes are connected to the deflection plates of the oscilloscope as follows, **A**, in recording the frontal projection of the vectorcardiogram; **B**, in recording the left sagittal plane projection; and **C**, in recording the superior projection. **CT**, central terminal of Wilson, **B**, a unipolar back lead placed at a point 2 cm. to the left of the seventh dorsal vertebra. Note that in recording the superior projection the connections of the left and right arms to the right and left deflection plates of the oscilloscope are the reverse of those utilized to record the frontal projection, and that the normal QRS sE loop, as recorded with this system, tends to be situated to the observer's right in the frontal projection and to his left in the superior projection.

the beam moving downward when LL is positive with respect to CT.

Superior plane.—The lead wire connections to the oscilloscope in recording the superior projection of the vectorcardiogram are shown in Figure 68, C, and will not be described here.

Standardizing factors—1. Horizontal deflection in frontal plane (R-L) is 1 unit (usually 1 inch) for 1 mv. potential difference between electrodes R and L. (See Chapter 2 for calculation of correction factors for unipolar leads when bipolar leads are assigned a value of 1.)

2 Vertical deflection in frontal plane (C-F) is 1.7 units (or inches) per 1 mv. potential difference between electrode F and Wilson's central terminal. (See Chapter 2 for calculation of standardization factor for lead VF.)

3 Horizontal deflection in sagittal plane (C-B) is 1.2 units (or inches) for 1 mv. potential difference between the back electrode (B) and the Wilson's central terminal.*

Grishman's Cube Lead System

Grishman's cube system of electrode placement, a modification of the rectangular system of Duchosal and Sulzer, is one of the orthogonal systems more commonly used in this country. It was the lead system utilized to record virtually all of the vectorcardiograms appearing in this text. In the following description of the cube method of electrode placement, the

*Abildskov, J. A., Burch, G. E., and Cronin, J. A. The validity of the equilateral tetrahedron as a spatial reference system, *Circulation* 2:122, 1950

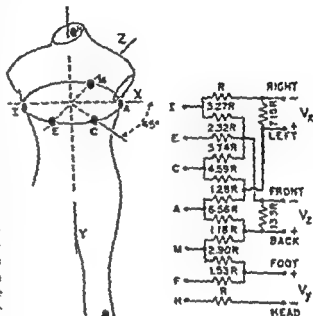
of the oscilloscope, as can be seen in Figure 70.

The theory underlying Grishman's cube lead system is as follows: If the electrical center of the heart (E) is visualized as occupying the center of a sphere, eight points on the surface of this sphere can be selected which are equidistant from the dipole center (E) and form the corners of a cube (Fig. 71). In the cube method, three bipolar leads are applied to the thorax so as to form (in theory at least) three adjoining sides of a cube having E as its center. The electrical center of the heart is assumed to occupy the center of a sagittal plane passing just to the left of the sternum in the fourth intercostal space. Since the lengths of the leads, their distances from the electrical center of the heart (E), and the angle each subtends with E were at one time all thought to be the equal, this system was originally considered by some authorities to be the most accurate method of recording the vectorcardiogram, but this is certainly not the case.

No attempt will be made in this text to evaluate the comparative merits of the equilateral tetrahedron and cube systems other than to point out that the equilateral tetrahedron is said to yield frontal plane vector loops which conform better with the findings in the limb leads of the scalar electrocardiogram. On the other hand, the horizontal projection in the cube system correlates better with the precordial electrocardiogram. Actually, both the cube and tetrahedron lead systems are being superseded by lead systems which correctly record the magnitude and direction of the components of the spatial vector. The theoretical basis of corrected lead systems, such as the SVEC system of Schmitt and his associates and the vectorcardiographic system of Frank, was outlined in limited detail in Chapter 4. The fact deserves emphasis that the corrected lead systems such as those just cited were devised, for the most part, from data obtained from torso model studies. Nevertheless, there is reason to believe that the information derived from these investigations—and, for that matter, the corrected lead systems as well—are valid when applied to the human torso and electrical potentials generated by the heart.

Of the corrected lead systems which have been advocated, we have favored the system proposed by Frank (Fig. 72), since it entails the use of only seven electrodes as contrasted with the fourteen electrodes required by the SVEC system of Schmitt and his co-workers. Moreover, in our limited experience, the Frank system has yielded quite satisfactory results. In this system, electrodes A , C , E , I , and M are situated at the same transverse level (approximately the

fifth intercostal space). Electrode A is placed in the left midaxillary line; electrode I is placed in the right midaxillary line; electrodes E and M are applied in the midlines anteriorly and posteriorly, respectively; and, finally, electrode C , is situated at an angle of 45° between anterior midline and left midaxillary line. Electrode F is placed on the left leg, and electrode H on



the back of the neck. The X component of the spatial vector in the Frank lead system is derived from electrodes A , C , and I , electrode C serving to introduce a correction for the backward slant of the image line or lead vector, I - A . The Z , or anteroposterior, component of the spatial vector is derived from all five transverse electrodes, while the Y , or vertical, component of the spatial vector is derived from electrodes H , M , and F (potential difference V_F appearing between electrode H and a junction of two resistors joining M and F). These electrodes are connected directly

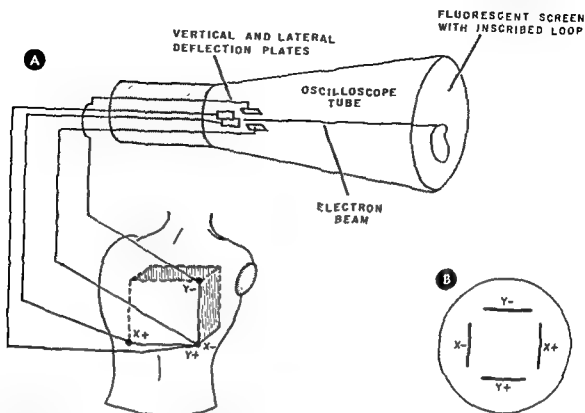


Fig. 70.—Relationship between the lead electrodes and the deflection plates of the oscilloscope in the cube system of lead electrode placement. A, electrode placement. B, polarity of deflection plates viewed from the face of the oscilloscope tube

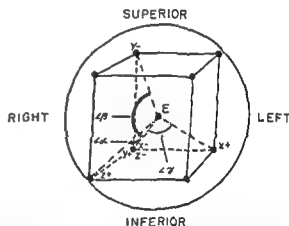


Fig. 71.—Theoretical basis of Grishman's cube system of lead electrode placement. Note that $\angle \alpha$ subtended by lead Zc with E, $\angle \beta$ subtended by lead Yc with E, and $\angle \gamma$ subtended by lead Xc with E are equal to one another. (See text for details.)

If transverse lead Xc and vertical lead Yc are attached to the two pairs of deflection plates, the oscilloscope records the projection of the cardiac spatial vector on the frontal plane. Similarly, lead Xc and sagittal lead Zc define the projection of the vector on the horizontal plane, and leads Yc and Zc, the projection of the vector on the right sagittal plane. The polarity of the deflection plates and the standardization of the component leads are the same for each planar projection in the cube system of electrode placement. Consequently, regardless of the plane

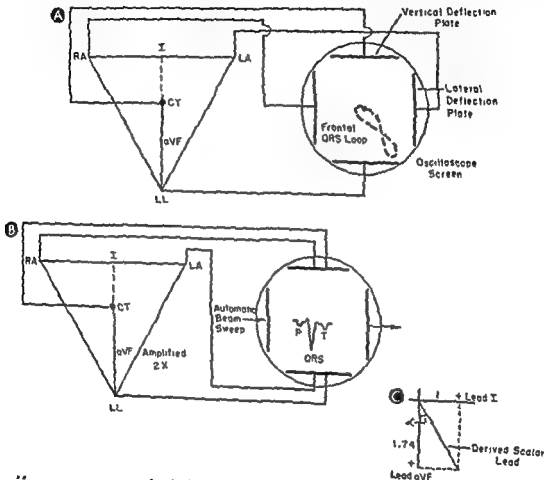
being recorded, a 1-mv. input into the circuit causes the electron beam to descend at a 45° angle inferiorly and to the observer's right or the screen's left (Hereafter, the direction will be stipulated in terms of the screen's left or right.)

The two electrodes of each vectorcardiographic lead are attached to a pair of deflection plates in such a way that the relationship of the lead electrodes to the point source of potential in the body (the heart) is duplicated in the relationship of the deflection plates to the resting position of the electron beam

DERIVATION OF SCALAR LEAD DEFLECTIONS FROM THE VECTORCARDIOGRAM

to be recorded. The vectorcardiographic leads can be accomplished electronically or manually (or by visual inspection).

Electronic method of derivation — In this method (Fig 74), the axes of the component vectorcardiographic leads are treated as lead vectors having a definite magnitude or length and an effective direc-



perpendiculars dropped from the assigned lengths of these leads, and, second, by calculating the angle subtended by the diagonal and either of the two lead axes. In this instance, lead aVF was selected. Therefore,

$$\tan \alpha = \frac{\text{Opposite side}}{\text{Adjacent side}} = \frac{1}{1.74}$$

$$\tan \alpha = 0.577$$

$$0.577 = \tan 30^\circ$$

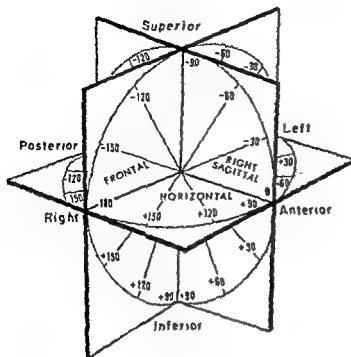


Fig. 73.—Reference frames for the horizontal, right

axis is situated to the left in the horizontal and frontal reference frames and anteriorly in the right sagittal plane

to computing and compensating networks, the outputs of which are V_x , V_y , and V_z , which are proportional to the corresponding components of the dipole with equal standardization factors. An important advantage claimed by advocates of the Frank system (though not all authorities agree) is its relative insensitivity to variations in dipole position within the limits usually encountered in clinical vectorcardiography.

Our experience with the Frank system of recording vectorcardiograms has not been extensive as yet, but our preliminary impressions of this system, compared with the cube system of lead electrode placement, are as follows: (1) The QRS sE loops recorded with the two systems from the same subject generally show surprisingly close agreement in their predominant features. (2) With the Frank system, the QRS sE loops tend to have a more posterior and inferior orientation than corresponding loops recorded from the same persons with the cube lead system. In addition, normal QRS sE loops recorded with the Frank lead system quite frequently exhibit rightward, posterior, and sometimes superior terminal deflections, in contrast with the relative infrequency of this finding in normal QRS sE loops obtained with the cube lead system. (3) On the whole, the QRS sE loops recorded with the Frank system show closer agreement with the

electrocardiogram than loops obtained with the cube system. (4) Perhaps the most striking and frequently observed difference in the vectorcardiograms recorded with the two systems of lead placement is the wider spatial angle subtended by the long axes of the QRS sE and T sE loops recorded with the Frank system in comparison with the spatial angle of the QRS sE—T sE loops obtained with the cube system. The authors have not yet determined the normal range of variation of the spatial angle of the QRS sE and T sE loops in vectorcardiograms recorded with the Frank lead system.

As previously indicated, most of the vectorcardiograms presented in this text were recorded with the cube lead system, and so the descriptions of normal and abnormal vectorcardiograms will pertain mainly to records obtained with this reference system and will apply only in a general sense to vectorcardiograms obtained by other methods of electrode placement.

The reference frame used to indicate descriptively the orientation of the vector loops in a body plane (see Fig. 73) is the same as that utilized in earlier chapters to describe the orientation of mean vectors. This reference frame can be used for each body plane, zero degrees in the figure lying to the left in the frontal and horizontal planes and anteriorly in the right sagittal plane. The upper half of the reference figure is marked off in -30° segments from 0° on the screen's left to 180° on the screen's right, while the lower half of the figure is marked off in $+30^\circ$ segments clockwise from the screen's left to right. Thus $+90^\circ$ is located inferiorly in the sagittal and frontal planes and anteriorly in the horizontal, and -90° lies superiorly in the sagittal and frontal planes and posteriorly in the horizontal. For convenience and simplicity, in this text the reference frames will be visualized in terms of the familiar scalar leads, as shown in Table 3.

TABLE 3—PLANAR VECTORCARDIOGRAPHIC REFERENCE FRAMES EXPRESSED IN TERMS OF SCALAR LEADS

AXIS	HORIZONTAL	RIGHT SAGITTAL	FRONTAL
0° to 180°	Lead V_x	Lead V_z	Lead I
$+90^\circ$ to -90°	Lead V_x	Lead aVF	Lead aVF
$+30^\circ$ to -150°	Lead V_x		Lead aVR
$+60^\circ$ to -120°	Lead V_x		Lead II
$+75^\circ$ to -105°	Lead V_x		
$+120^\circ$ to -60°	Lead V_x		Lead III
$+135^\circ$ to -45°	Lead V_{xR}		Lead aVL
$+150^\circ$ to -30°	Lead V_{xL}		



dial leads can also be derived

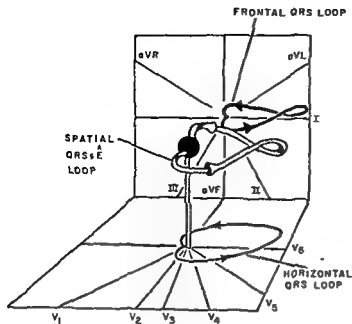


Fig. 75.—Schematic diagram of QRS sE loop showing its projections on the frontal and horizontal reference frames formed by scalar leads I through aVF and V_1 through V_6 .

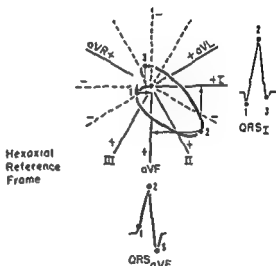
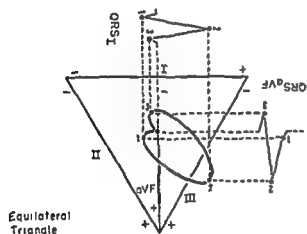


Fig. 76. Projection of the QRS deflections in leads I and aVF from a schematic frontal QRS loop, using the

us vectors drawn from the origin of the loop to the points in question. Note that the point (or electrical null point) is always superimposed on the center of the appropriate reference frame. The projection of

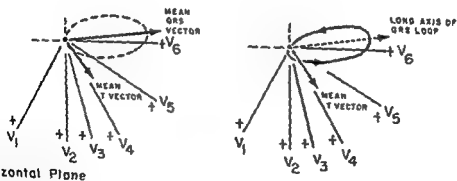
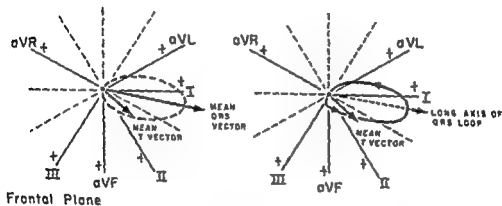
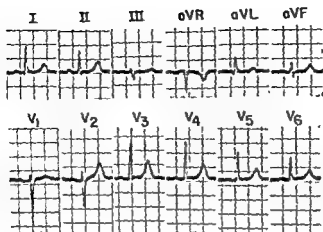


Fig 78 —Construction of vector QRS loops from the electrocardiogram. (The method is described in detail in the text.)

tion. As vector quantities, the two lead axes can be added electronically to yield a third, resultant lead vector. For example, if the outputs of the transverse lead X_c and vertical lead Y_c (or leads I and aVF, as in Fig. 74) were to be added electronically and then applied to the vertical pair of oscilloscope plates, the electron beam would respond to potential variations across the vertical plates as if, in effect, a single scalar lead intermediate between the two component leads were being recorded. Moreover, by amplifying one of the component leads more than the other, the axis of the derived lead could then be rotated toward or away from either of the component vectorcardiographic leads. Thus, if the amplification of the two component vectorcardiographic leads is varied according to the appropriate amplification coefficients, which have been calculated, lead deflections can be derived for any scalar lead whose axis is situated in the plane defined by the component leads.

Manual method of derivation—Scalar lead deflections can also be derived manually from the vectorcardiogram, but, in actual practice, mere inspection

of the vectorcardiogram is usually sufficient to translate the vector loops into their scalar electrocardiographic equivalents. As will be recalled, a vectorcardiographic loop is, in essence, the planar projection of the pathway traced in space by the tips of all instantaneous resultant vectors generated in sequence during the P, QRS, or T intervals (see Fig. 75). Thus, a line drawn from the cardiac dipole center to any point on the QRS loop represents the planar projection of the resultant spatial vector for a given instant of the QRS interval. These instantaneous vectors, or the points on the loop corresponding to the termini of the vectors, can be projected on any lead axis passing through the origin of the loop. The positions of these projected points on the axis of the lead concerned can then be plotted on an ordinate, and their times of occurrence on an abscissa, to form the derived electrocardiographic deflection (Figs. 76 and 77). With increased proficiency in the use of this method, the scalar leads can be derived merely by inspection of the vector loop and by superimposing it mentally on the frontal, horizontal, or sagittal reference frames

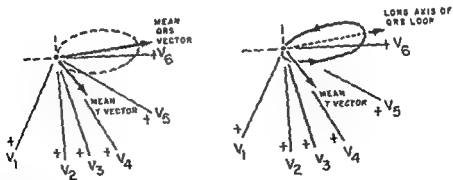
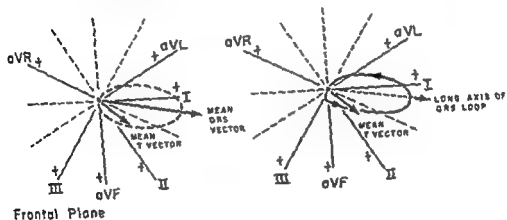
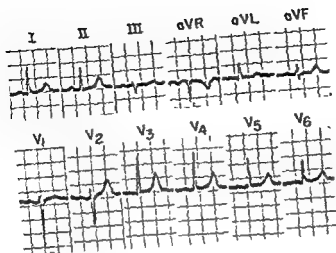
CONSTRUCTION OF VECTOR LOOPS FROM THE ELECTROCARDIOGRAM

To construct from the electrocardiogram a vector loop resembling at all closely one actually recorded by the vectorcardiograph is a formidable procedure. The two scalar leads selected for the construction of the frontal or horizontal projection of the spatial vector loop must record the two components of the dipole vector in this plane. The frontal plane components of a cardiac vector are the transverse (X) and vertical (Y), components, and the horizontal plane components are the sagittal (Z) component and transverse components. In addition, the two scalar leads must be recorded simultaneously at rapid speed so that corresponding points on the same deflection in each of the two leads can be identified by their timing with reference to the onset of the deflection. The voltage values for many such points are plotted on the axes of the leads, and from these points perpendiculars are dropped. The intersection of each pair of perpendicular lines corresponds to the tip of an instantaneous planar vector drawn from the center of the reference figure. If the calculated positions of successive instantaneous vectors are connected by a line beginning and ending at the center of the planar reference frame, a planar vector loop is obtained. Obviously, the greater the number of points on the lead deflection plotted on the lead axes, the more

accurate will be the construction of the vector loop.

If the manual construction of vector loops from the electrocardiogram is to have any practical merit in clinical electrocardiography, the method should utilize the extremity and precordial leads recorded routinely (Fig. 78). For example, the frontal plane vector loop would be constructed from any two of the bipolar or unipolar extremity leads, and the horizontal vector loop, from any two precordial leads (or from lead I and lead V_2). A number of objections can be raised to the use of the unipolar precordial leads for this purpose, one of the foremost being the proximity of the exploring electrodes to the heart. Moreover, there is no consistent mathematical relationship between the individual precordial leads themselves and between the extremity and precordial leads. And so, for this reason, the magnitude of the anteroposterior component (Z) of the dipole vector, as determined in the precordial lead, cannot be correlated quantitatively with the magnitudes of the transverse and vertical components determined from the extremity leads.

The most serious shortcoming of the routine electrocardiographic leads, if used to construct the vector loop, is that the leads are recorded, not simultaneously, but sequentially. This lack of phase relation-



Horizontal Plane

Fig 78 -Construction of vector QRS loops from the electrocardiogram. (The method is described in detail in the text.)

ship in the various leads is discussed below. In short, to achieve a high degree of accuracy in the manual construction of loops from the routine electrocardiographic leads is an obvious impracticality, if not an impossibility. However, if the inaccuracy of the method is recognized, the attempt to visualize the routine electrocardiogram in terms of vector loops can be of advantage in several respects. (1) It tends to promote a broader understanding of the relationship between vectorcardiography, vector projection methods of electrocardiographic analysis, and routine electrocardiography. (2) It represents an approach, albeit an approximate one, to the application of vectorcardiographic observations and data to the interpretation of scalar electrocardiograms. (3) It permits a more detailed and a more complete application of vector principles to the teaching of electrocardiography.

The method described and used effectively by Grant and Estes to construct QRS loops is based on calculation of the mean QRS vector for each 0.02 second of the QRS interval. The objection has been raised that the lack of phase relationship between consecutively recorded scalar leads precludes accurate construction of mean vectors for such short time intervals. Grant and Estes answer this objection by pointing out that the mathematical relationship between the individual deflections or portions of deflections in the different extremity leads (Lead I + Lead III = Lead II, and, Lead aVR + Lead aVL + Lead aVF = 0) makes it possible to determine the onset of the QRS interval without having to record the leads simultaneously. However, this means of determining phase relationship has at least two limitations. (1) It cannot be applied to the precordial leads, since they are not mathematically interrelated, nor can they be related to the extremity leads. (2) As regards the extremity leads, the inertia of the direct-writing stylus, the relatively slow paper speed routinely used, and other physical limitations imposed on recording accuracy—all can lead to error in the construction of vector loops, despite the use of the above formulas.

Since, at best, calculated vector loops display merely a rough similarity to those actually recorded, it would seem advantageous to use the simplest method of construction yielding satisfactory results. The method described in this section entails merely (a) inspection of the scalar leads and (b) estimation of the approximate orientation of the initial deflection, the maximal deflection (corresponding to the

long axis of the QRS loop and the mean QRS vector), and the terminal deflection of the QRS loop.

Method of constructing vector loops (Fig. 78).—1. The mean QRS vector for the frontal plane is determined from the bipolar limb leads, and the horizontal mean QRS vector is determined from the precordial leads, as previously described. The orientation of these vectors roughly corresponds to that of the maximal deflection or long axes of the frontal and horizontal QRS loops.

2. The QRS loop ordinarily projects fairly symmetrically on either side of the mean QRS planar vector (corresponding to the maximal mean instantaneous QRS vector of the QRS loop), as one might anticipate, since the lead whose axis is perpendicular to the mean vector (the transitional lead) registers an equiphasic RS deflection. This implies that a perpendicular line through the midpoint of the axis of derivation of the transitional lead bisects the planar QRS loop into two limbs, the efferent limb and the afferent limb.

The *efferent limb* is the first limb of the loop to be written. It is inscribed away from the point of origin of the loop and normally projects entirely on the positive half of the axis of derivation of the transitional lead.

The *afferent limb* is inscribed toward the point of origin of the QRS loop and normally projects entirely on the negative half of the axis of derivation of the transitional lead.

With these points in mind, one can sketch the loop in preliminary form so that it is oriented symmetrically along the axis of the mean QRS planar vector.

3. This crude QRS loop can then be altered in its initial and terminal portions (and, if necessary, in the efferent and afferent limbs as well) until the schematic loop conforms approximately to the relative magnitude and direction of the initial, maximal, and terminal components of the QRS complex in each lead. The direction of inscription of the constructed frontal and horizontal QRS loops is often evident from the way the estimated instantaneous vectors develop, but occasionally it is not possible to deduce this information from abnormal electrocardiograms, particularly those showing marked alterations in ventricular depolarization, such as right bundle branch block, right ventricular hypertrophy, and myocardial infarction.

4. There is probably no advantage to be gained by construction of P and T loops. The mean P and T vectors provide sufficient information.

THE NORMAL VECTORCARDIOGRAM

The spatial vectorcardiogram consists of three spatial loops which appear in close succession during a single cardiac cycle. The vector loops are produced by mean instantaneous P, QRS, and T spatial forces. To indicate that these loops depict the instantaneous change in the direction and magnitude of the equivalent dipole (E), treated as a spatial vector (sE), they are designated the P sE, QRS sE, and T sE loops. It is not possible to record these spatial loops directly, but wire models of the loops can be constructed from their horizontal, sagittal, and frontal projections in the vectorcardiogram. However, this is seldom necessary in clinical vectorcardiography, since most vectorcardiograms can be interpreted with reasonable accuracy from the planar projections themselves. For this reason, the vectorcardiographic descriptions given in this and subsequent chapters will deal with each planar projection more or less individually. The fact should be borne in mind, however, that the horizontal, sagittal, and frontal projections of a given vectorcardiogram represent merely different "views" of the same spatial loop or loops (P sE, QRS sE, and T sE loops). For the sake of convenience, the following terms will frequently be used hereafter in this text:

Horizontal P loop—The projection of the P sE loop on the horizontal plane.

Sagittal P loop—The projection of the P sE loop on the sagittal plane.

Frontal P loop—The projection of the P sE loop on the frontal plane.

(The same terminology will be applied to the planar projections of the QRS sE and T sE loops. In more general terms, the projection of a spatial loop (or loops) on a plane will sometimes be referred to as a planar loop (or loops).)

The orientation of a planar loop will be expressed in plus or minus degrees of the appropriate reference frames. However, the magnitudes of the planar loops, if described, will be defined largely in relative or qualitative terms rather than quantitatively. The reason for this is that there are too few quantitative studies of the normal and abnormal spatial vectorcardiogram available to provide any reliable standards for the magnitudes of the loops. Moreover, until more satisfactory lead systems are devised, there seems little to be gained from attempting to quantitate vector magnitude.

Although we have recorded vectorcardiograms from many normal subjects, the description of the normal vectorcardiogram

series is due to the fact that we found that our preliminary results agreed with data obtained previously by other investigators with larger study series.

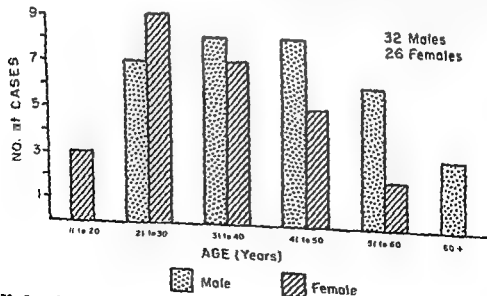
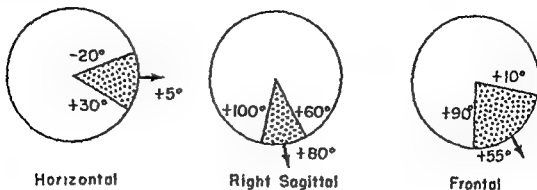
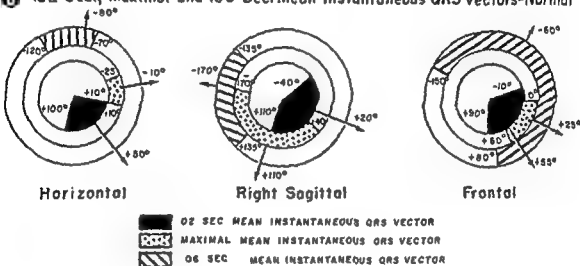


Fig. 79. Horizontal P loop in normal subjects. The presence of an

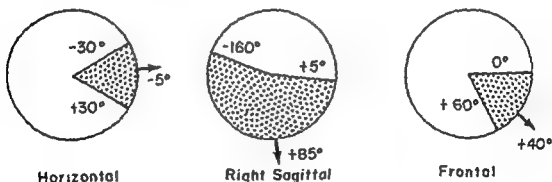
A Maximal Mean Instantaneous P Vector — Normal



B .02 Sec., Maximal and .06 Sec. Mean Instantaneous QRS Vectors—Normal



C Maximal Mean Instantaneous T Vector — Normal



D Spatial Angle of Divergence of QRSs^A and Ts^A — Normal

% of Normal VCGs	Spatial Angle
50 %	10° or Less
35 %	11° to 30°
15 %	31° to 45°

Average Spatial Angle 17°

Fig. 80.—Legend on facing page

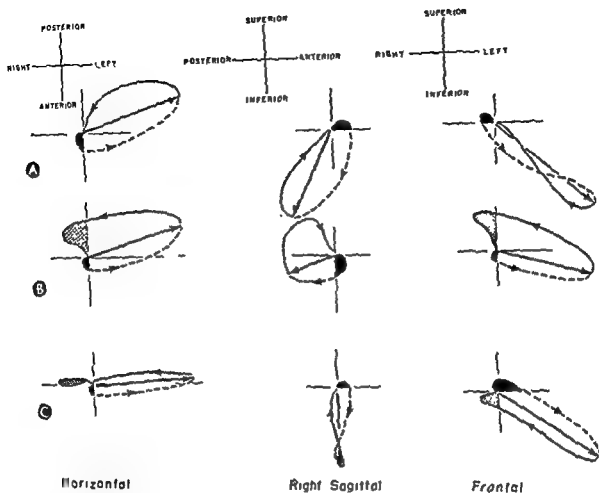


Fig. 81.—A, B, and C, the schematic planar orientation of the QRS loop. The solid portion of the loop corresponds to the long axis or minimal mean instantaneous vector, etc. The dashed portion represents the QRS loop.

Fig. 80.—The normal orientations of the various mean leads.

TABLE 4.—PLANAR PROJECTIONS OF THE P sE LOOP OF THE NORMAL VECTORCARDIOGRAM

PLANE	ORIENTATION OF THE MAXIMAL MEAN INSTANTANEOUS VECTOR OF THE P sE LOOP*			DIRECTION OF INSCRIPTION	GENERAL CONFIGURATION
	Extreme Range†	Av	Usual Range‡		
Horizontal	-20° to +30°	+5°	0° to +5°	Counter-clockwise	The P sE loop tends to be smaller and perhaps more variable in contour in this projection than in the frontal and sagittal projections. It may be triangle shaped, oval, or elongated, or show a figure-of-eight configuration
Right sagittal	+60° to +100°	+80°	+80° to +90°	Clockwise	The P sE loop in the sagittal projection is usually oval and elongated, although occasionally it is triangle shaped
Frontal	+10° to +90°	+55°	+20° to +60°	Counter-clockwise	The P sE loop in the frontal projection can be thin and elongated as in the sagittal projection, or it can be triangle shaped

*The range in orientation, as expressed in degrees by paired values, is always to be read in a clockwise direction in the appropriate reference frame. This convention will be adhered to throughout the text.

†Extreme range = the extreme limits of the range in orientation of a given vector, usual range = the range in orientation of a given vector in 85% of the cases studied

P sE LOOP

The P sE loop in its planar projections has been studied very little as yet, probably because it is technically the most difficult component of the vectorcardiogram to record satisfactorily. The general features of the planar P loops of the vectorcardiogram, as observed by us, are presented in Table 4 (see also Fig 80, A).

In summary, the P sE loop normally is oriented spatially to the left, inferiorly, and slightly anteriorly and is counterclockwise inscribed in the horizontal and frontal projections and clockwise inscribed in the right sagittal projection

QRS sE LOOP

In describing the planar projections of the normal QRS spatial loop, it will be necessary frequently to refer to specific portions or components of the loop. In such instances the following terminology (see also Fig. 81) will be used.

Initial deflection.—This is arbitrarily defined as the very first deflection of the QRS sE loop to the right and/or superiorly. Normally the initial deflection is also directed anteriorly and can be considered to be produced by instantaneous forces or vectors appearing during the first 0.015 second of the QRS interval. This portion of the loop reflects primarily initial left-to-right septal activation and

subsequent beginning activation of the apicoanterior region of the right and left ventricles. The initial deflection therefore corresponds roughly to the 0.01-second septal VA vector and the 0.02-second apicoanterior VA vector described in Chapter 5.

"Long axis," or "maximal vector," of the QRS sE loop.—As the term implies, the longest diameter of the loop drawn from the point of origin is the long axis or maximal vector of the loop. Ordinarily, the terminus of the maximal vector coincides with the turning point of the loop with respect to leads I and V₆. The orientation of the maximal QRS vector in the vectorcardiogram corresponds roughly to the direction of the

Efferent (centrifugal or outgoing) limb of the loop.—The efferent limb of the QRS sE loop is inscribed as the electron beam moves away from the point of origin, and

Afferent (centripetal or returning) limb.—The afferent limb is inscribed as the electron beam moves back toward its point of origin. It is related to activation of the lateral

to the last segment of the loop to be written before the loop returns to the point of origin. If this portion of the loop deviates from its expected course to form a distinct

TABLE 5.—PLANAR PROJECTIONS OF THE QRS SE LOOP OF THE NORMAL VECTOCARDIOGRAM

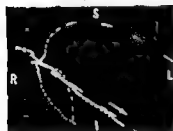
	HORIZONTAL				RIGHT SACCTAL				FRONTAL	
	Right, anterior		Left, sometimes right, posterior		Anterior, superior, or sometimes inferior		Right, superior, or inferior		If the minimal instantaneous QRS vector of the frontal QRS loop lies between 0° and +10°, the loop usually has a counterclockwise direction of inscription, while loops with a maximal instantaneous QRS vector to the right of +40° are generally clockwise inscribed	
	Extreme Range	Av	Usual Range	Extreme Range	Av	Usual Range	Extreme Range	Av	Usual Range	
0.02-second mean instantaneous QRS vector	+10° to +100°	+50°	+20° to +85°	-40° to +110°	+20°	0° to +50°	-10° to +90°	+55°	0° to +60°	
Maximal mean instantaneous QRS vector	-25° to +10°	-10°	-15° to +10°	+40° to -170°	+110°	+80° to +140°	0° to +60°	+25°	0° to +40°	
0.06-second mean instantaneous QRS vector	-120° to -70°	-80°	-95° to -70°	+135° to -135°	-170°	+145° to +150°	-150° to +80°	-60°	-85° to +80°	
Initial deflection of QRS se	Right, anterior				Anterior, superior, or sometimes inferior				Right, superior, or inferior	
Direction of inscription	Invariably counterclockwise				Invariably clockwise					
Terminal instantaneous QRS vectors	Left, sometimes right, posterior				Posterior, inferior, or sometimes superior				The terminal vectors may lie superiorly, in which case they tend to be located also to the right. When the terminal vectors are situated inferiorly, they can be either to the right or to the left.	



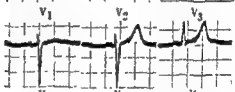
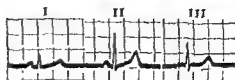
HORIZONTAL
(Ampl. 2X)



RIGHT SAGITTAL
(Ampl. 2X)



FRONTAL
(Ampl. 2X)



enlargement, and (2) the long axis. The electrocardiogram shows a normal vectorcardiogram, even though its orientation is still within the limits of normal variation. Note that the P, QRS, and T wave loops in each projection tend to be concordant in orientation.

deflection situated to the right and/or superiorly late in the QRS interval, the term *terminal deflection* or *appendage* will be used.

PLANAR QRS LOOPS OF THE NORMAL VECTORCARDIOGRAM—The ranges of variation and average orientations of the 0.02-second, maximal, and 0.06-second mean instantaneous QRS vectors in each projection of the normal QRS sE loop are shown in Figure 80, B.

HORIZONTAL QRS LOOP—Usually the normal QRS sE loop in the horizontal projection tends to be more or less oval, elliptical, or triangle shaped. The length, or long diameter, of the loop is usually 1½–3 times the width (or anteroposterior dimension). In normal

adults, the terminal portion of the horizontal QRS loop extended slightly to the right and posteriorly before returning to the point of origin.

RIGHT SAGITTAL QRS LOOP—The normal QRS sE loop in the sagittal projection can be oval, elliptical,

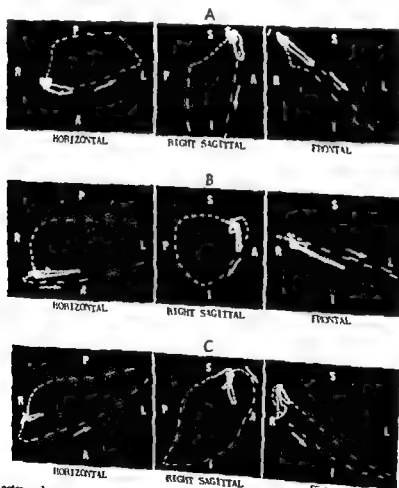


Fig. 83.—A, vectorcardiogram
25 units.

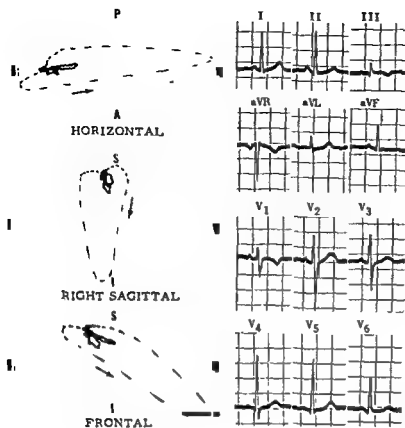
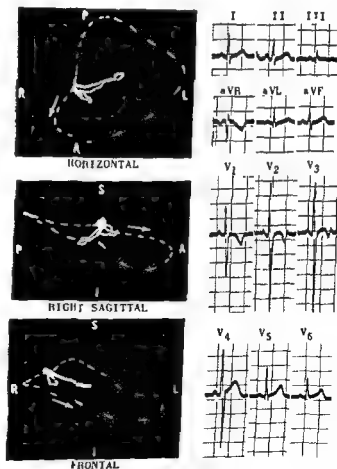


Fig. 84.—Normal electrocardiogram and vectorcardiogram in a pregnant woman, 28, without heart disease. The smaller of the two small loops in each projection of the vectorcardiogram is the planar P loop, the other being the planar T loop.

Fig. 85.—Normal electrocardiogram and vectorcardiogram in girl, 18, without heart disease. The tall R wave in lead V_1 of the electrocardiogram can be related to the early, relatively large anterior deflection of the QRS sE loop, which projects larger positive voltages on lead V_1 than are normally observed in adults. These related features of the electrocardiogram and vectorcardiogram are persisting characteristics of the "juvenile" type of electrocardiographic and vectorcardiographic patterns. The large RS deflections in the midprecordial leads of the electrocardiogram can be related to the wide anteroposterior diameter of the horizontal and sagittal QRS loops. In other words, the mean instantaneous QRS spatial vectors forming the efferent limb of the QRS sE loop extend far anteriorly, while the vectors of the afferent limb of the loop extend even farther posteriorly, the maximal positive and negative voltages being projected on those precordial leads responding primarily to the anteroposterior component of the cardiac vectors (leads V_1 through V_6).



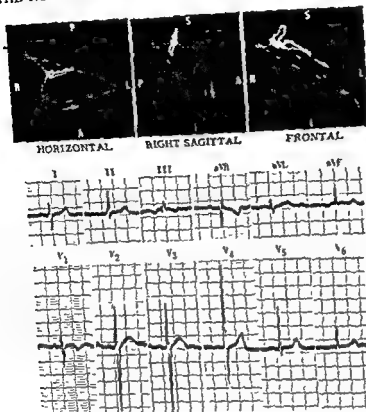


Fig. 86—Normal electrocardiogram and vectorcardiogram in box 4 without any lead.

or triangle shaped. Normally, there is an initial deflection of the loop anteriorly and usually superiorly, sometimes inferiorly. The efferent limb then is written in an anterosuperior to posteroinferior direction, the long axis of the sagittal loop lying inferior and slightly posterior. The afferent limb subsequently returns in a clockwise direction posteriorly and inferiorly to the point of origin. Occasionally the terminal returning limb extends slightly superiorly.

FRONTAL QRS LOOP.—In contrast with the horizontal and sagittal projections, the direction of inscription of the QRS sE loop in the frontal projection can be either clockwise or counterclockwise, depending (in part at least) on the location of the loop. As a broad generalization, it can be said that QRS sE loops lying above the $+40^\circ$ axis of the frontal reference frame tend to be inscribed in a counterclockwise direction, while loops situated below the $+40^\circ$ axis are ordinarily clockwise inscribed. In normal vectorcardiograms the frontal QRS loops observed by us were, on the average, located at about $+25^\circ$ but

ranged between 0° and $+60^\circ$. The configuration of the frontal loop also was variable in that some loops were elongated, others elliptical shaped; and not infrequently loops having a figure-of-eight contour were observed. On comparing the limb leads of the electrocardiogram, we noted that there was the tendency for the long axis of the frontal QRS loop recorded with the cube lead system to be situated more horizontally than the mean frontal QRS vector constructed from the electrocardiogram.

Since the normal QRS sE loop returns to its point of origin, an S-T vector is not observed. The S-T vectors are discussed in a later section.

T sE LOOP

The normal T sE loop is usually elongated or elliptical shaped, sometimes almost linear in configuration.

The spatial angle* (see Table 6) between the two loops ordinarily does not exceed 60° in normal subjects (Fig. 80, D), and, as a general rule, the same holds true for the planar angle subtended by the long axes of the QRS sE and T sE loops projected on the horizontal or frontal plane.

The outgoing or efferent limb of the normal T sE loop is almost always inscribed more slowly than the returning limb, and this is reflected in the fact that the initial limbs of the electrocardiographic T waves have more gentle slopes than the terminal limbs, which either descend abruptly or rise rapidly to the base line. As would be expected, the direction of inscription of the T sE loop in each projection tends to be the same as that of the QRS sE loop, although this can be somewhat variable. Generally, the T sE loop in the horizontal projection is counterclockwise

is determined by means of the trigonometric table compiled by Helm and Fowler, which is reproduced, with the permission of these authors, at the end of Chapter 6

TABLE 6—T sE LOOP AND SPATIAL QRS sE—T sE ANGLE

ORIENTATION OF THE MAXIMAL MEAN INSTANTANEOUS VECTOR OF THE T sE LOOP	RANGE	AVERAGE
Horizontal	-30° to $+30^\circ$	-5°
Right sagittal	$+5^\circ$ to -160°	$+85^\circ$
Frontal	0° to $+60^\circ$	$+40^\circ$
Spatial QRS sE—T sE angle* (angular divergence of long axes of QRS sE and T sE loops)	0° to 45°	17°

*The spatial QRS—T angles in the vectorcardiograms of the authors' series of normal patients showed the following approximate percentage distribution

Percentage of vectorcardiograms	50	93	13
Spatial QRS sE—T sE angle	10° or less	11° — 30°	31° — 45°

inscribed, and in the sagittal projection clockwise inscribed, while in the frontal projection the T sE loop can be written in either direction (Figs 82–86).

PART II

The Abnormal Electrocardiogram
and Vectorcardiogram

Ventricular Hypertrophy:

General Considerations

REVIEW OF THE PERTINENT ANATOMY AND SEPTAL-VENTRICULAR ACTIVATION SEQUENCE

Interventricular Septum

THE INTERVENTRICULAR SEPTUM is situated almost parallel to the frontal plane of the body, its apical portion lying slightly anterior and inferior to its basal portion. The thickness of the septal muscle mass approximates that of the basal wall of the left ventricle. Both septum and free wall of the left ventricle decrease in thickness in a tapering manner as they approach the apex.

downward. The left division branches early and profusely, but the right does not branch until it reaches the vicinity of the base of the anterior papillary muscle. The left bundle branch distributes the excitation impulse to those regions of the muscular septum derived from the left ventricle, the septal muscle contributed by the right ventricle being activated via the right bundle branch. For all intents and purposes, the right basal region of the septum is the only electronically significant contribution of the right ventricle to the septal muscle mass, while the major portion of the septal muscle is depolarized in a left posterior to right anterior direction via ramifications of the left bundle branch. Since conduction via the Purkinje fibers takes place very rapidly, activation of the septal musculature, despite the latter's thickness, normally produces electrical forces of small magnitude. As will be seen later, when septal activation occurs in an abnormal fashion it is capable of generating potentials of considerable magnitude. In any event, with the single exception of the right basal portion of the septum, which is derived from the right

ventricle, the remainder of the septal muscle can be considered to form the anteromedial wall of the left ventricle. The significance of the foregoing facts will become evident in later discussions.

Free Walls of Left and Right Ventricles

The effective sites, or electrical locations, of the right and left ventricles are determined by various factors—for example, the anatomic location of the ventricles, the sequence of ventricular activation, and the relative magnitudes of the potentials generated in the two ventricles. The effective site of the left ventricle is posterior, to the left, and superior, the effective site of the right ventricle is to the right, anterior, and inferior or superior. The free wall of the right ventricle is relatively thinner than that of the left ventricle, and the right ventricle itself is shorter than the left. The apical or trabecular walls of both right and left ventricles are thinner, and the basal walls of the two ventricles thicker, than other portions of the free walls, and there also tends to be a parallel relationship between the magnitudes of the electrical forces generated in basal and trabecular walls. The fact that the trabecular portions of the two ventricles give rise to forces of small magnitude can perhaps be attributed to another factor, in addition to the thinness of the trabecular muscle, and that is, the deeper penetration of the Purkinje fibers into the apical myocardium. Thus, activation of the inner muscle occurs very rapidly via the Purkinje fibers, and consequently generates negligible forces. Only later, when a

bounded wave front is formed during activation of outer layers of apical muscle, are there produced electrical forces of significant magnitude.

The hypothetical instantaneous VA (ventricular activation) vectors previously used to schematize ventricular activation in the normal heart will serve the same function in subsequent discussions of the activation process in ventricular hypertrophy, bundle branch block, and myocardial infarction. The magnitude of these vectors normally increases until the

maximal VA vector appears at about 0.04 second after onset of ventricular activation, and tends to decrease thereafter. The normal orientation, timing, and significance of each of these vectors were described in detail in Chapter 5, to which the reader is referred. Let it suffice to say that, normally, the instantaneous VA vectors reflect predominantly the electrical effects of left ventricular activation, since the activation forces generated by the right ventricle are comparatively small.

ELECTRICAL EFFECTS OF VENTRICULAR HYPERTROPHY

Pathologically, the basic abnormality of the heart muscle in ventricular hypertrophy consists of an increased cross-sectional area of the individual muscle fibers without any change in their total number. The altered morphology of the hypertrophied muscle fibers can have electrical effects which lead to recognizable changes in the electrocardiogram, although this is not an invariable rule. The three general electrical effects of ventricular hypertrophy are: (1) increased magnitude and rotation of the mean instantaneous QRS spatial vectors toward the effective electrical site of the hypertrophied ventricle, (2) lengthening of the time required for activation of the hypertrophied ventricle, and (3) rotation of the mean instantaneous T spatial vectors away from the mean instantaneous QRS spatial vectors. The mechanisms by which anatomic ventricular hypertrophy is translated into the foregoing electrical effects are depicted in Figure 87 and discussed in the following paragraphs.



OF THE HYPERTROPHIED VENTRICLE

It will be recalled that each instantaneous QRS spatial vector produced during simultaneous activation of the ventricular free walls can be considered to be the resultant of two component vectors which represent the electrical forces generated in opposing walls of the left and right ventricles (Fig 88). If the electrical forces produced by the left ventricle increase in magnitude without any change in the magnitude of the right ventricular forces, then, obviously, the resultant of the left and right ventricular forces (the mean instantaneous QRS spatial vector) not only lengthens but also assumes more nearly the same direction as the left ventricular component vector. Con-

versely, if the magnitude of the right ventricular forces increases while the left ventricular forces remain unchanged, the mean instantaneous QRS spatial vector rotates in the direction of the right ventricular component vector and then becomes larger.

It is evident, therefore, that in ventricular hypertrophy the larger forces arising in the affected ventricle can lead both to an increased magnitude of the mean instantaneous QRS spatial vector and to rotation of the vector toward the effective site of the hypertrophied ventricle. Some of the factors responsible for the increased magnitude of the forces generated by the hypertrophied ventricle are the following.

1. When the cross-sectional area of a muscle fiber increases, the fiber's internal resistance to current flow decreases (Fig. 89). According to the circuit equation, $I = e/(R + r)$, the current flow (I) in any closed circuit equals the electromotive force (e) of the current source divided by the sum of the resistances in the external (R) and internal (r) circuits. If the electromotive force of the membrane current of a heart muscle cell is assumed to be constant, it follows that a decrease in the internal resistance (r) must necessarily result in an increased current flow in the external circuit in the conducting medium surrounding the cell. The increased current flow is transmitted to the galvanometer and produces a larger voltage drop across its terminals.

2. As the result of the increased breadth of the muscle fibers in the hypertrophied ventricle, the surface area and the thickness of the ventricular wall are increased, and therefore the hypertrophied ventricle produces QRS forces of greater magnitude. In addition, for reasons to be explained below, the increased thickness of the ventricular wall may result in tangential, rather than radial, spread of the activation wave through the involved muscle, and this gives rise to larger QRS forces.

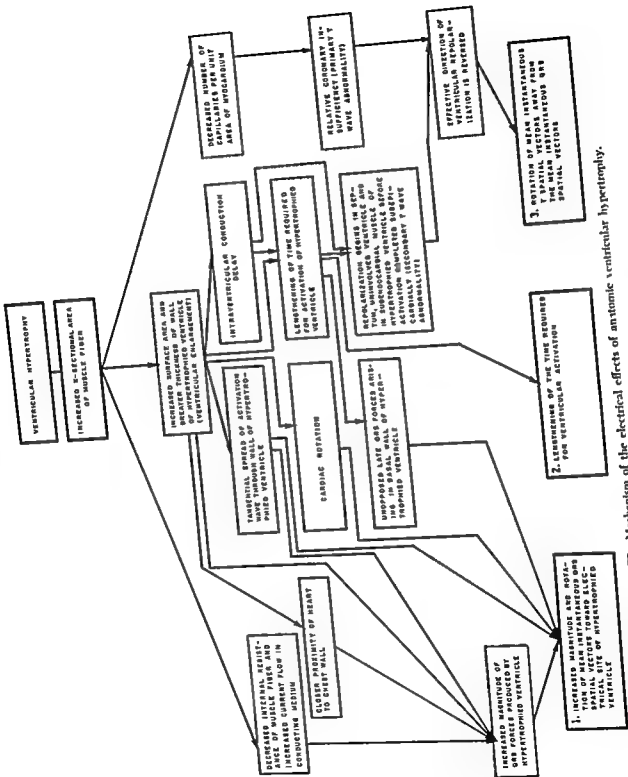


Fig. 87.—Mechanism of the electrical effects of anatomic ventricular hypertrophy.

and to the right, superiorly, and either anteriorly or slightly posteriorly in right ventricular hypertrophy.

2. The mean instantaneous spatial vectors produced relatively late in the QRS interval may be rotated from their usual position, owing to the fact that late QRS forces arising in the thick basal wall of the hypertrophied ventricle are unopposed by potentials from the other ventricle. Such an abnormality can be attributed to the increased thickness of the wall of the hypertrophied ventricle, which results in the lengthening of the time required for completion of activation in the affected ventricle. This factor, occasionally in conjunction with a co-existing intraventricular conduction disturbance, may result in activation being completed in the unaffected ventricle before basal regions of the hypertrophied ventricle have completed activation. Thus, late QRS forces are produced in the thickest portion of the hypertrophied ventricle and are virtually unopposed. The late instantaneous vectors may represent primarily forces arising in the basal wall of the hypertrophied ventricle.

3. Some authorities believe that anatomic cardiac rotation is one of the factors responsible for the displacement of the instantaneous QRS spatial vectors toward the effective electrical site of the hypertrophied ventricle. For example,

a) According to some authorities, the mechanical effect of right ventricular hypertrophy may lead to extreme clockwise rotation of the heart on its longitudinal axis, so that the left and right ventricles exchange positions. Thus, in right ventricular hypertrophy, the instantaneous QRS vectors are oriented just as normally, toward the electrically dominant left ventricle, but the left ventricle is located anteriorly and to the right. This explanation of the rightward and anterior orientation of the instantaneous QRS vectors in right ventricular hypertrophy has been severely criticized.

b) The posterior, superior, and leftward orientation of the instantaneous QRS vectors in left ventricular hypertrophy has been attributed to counterclockwise rotation of the heart on its longitudinal axis. In several recent studies, no consistent correlation could be demonstrated between anatomic heart position and orientation of the mean QRS spatial vector or the long axis of the vectorcardiographic QRS sE loop. It would seem, therefore, that in left ventricular hypertrophy cardiac rotation is not the primary mechanism responsible for the characteristic orientation of the instantaneous vectors.

LENGTHENING OF THE TIME REQUIRED FOR ACTIVATION OF THE HYPERTROPHIED VENTRICLE

Several different mechanisms, jointly or individually, may be responsible for the lengthening of the time required for ventricular activation. They are as follows.

1. Because the wall of the hypertrophied ventricle is thicker than normal, the distance the activation wave must travel to reach the epicardium is increased. Thus, onset of the intrinsicoid deflection or the appearance of the maximal vector in a lead facing the hypertrophied ventricle is delayed. The greater muscle mass of the hypertrophied ventricle also causes an overall lengthening of the time required for ventricular activation, as evidenced by an increased duration of the QRS interval.

2. Another factor which has been implicated by some investigators is lengthening of the conduction time required for spread of excitation over the endocardium as the result of ventricular dilatation and hypertrophy.

3. A localized conduction disturbance, such as incomplete bundle branch block, may also contribute to the prolonged QRS interval. The conduction defect can result from coronary artery disease or from compression of blood vessels supplying the subendocardium, owing to increased intraventricular pressure.

ROTATION OF THE MEAN INSTANTANEOUS T SPATIAL VECTORS AWAY FROM THE MEAN INSTANTANEOUS QRS SPATIAL VECTORS

The mechanisms, in ventricular hypertrophy, which cause the mean instantaneous T spatial vectors to diverge from the corresponding QRS vectors are described below, according to the type of T wave abnormality produced in the electrocardiogram, whether secondary or primary. As will be recalled, an abnormally wide divergence of the instantaneous QRS and T vectors, which produces secondary T wave changes, is not associated with an abnormal ventricular gradient, since it results from a primary change in the depolarization process. When the displacement of the instantaneous T spatial vectors produces primary T wave abnormalities, the ventricular gradient is abnormal. Consequently, the underlying mechanism must entail some change in the process of recovery in the hypertrophied ventricle.

Secondary abnormality of the mean instantaneous T spatial vectors.—Because of the increased thickness of the ventricular wall, a longer time is required for

the activation wave to pass from the endocardium to the epicardium. Therefore, repolarization begins in the endocardium before epicardial depolarization has been completed, and the direction in which repolarization spreads thereafter is the reverse of normal. Since the hypertrophied ventricle tends to be electrically preponderant during both ventricular depolarization and repolarization, the reversed order of recovery in the layers of the hypertrophied ventricular wall affects the over-all balance of T forces. As a result, the instantaneous T vectors rotate away from the instantaneous QRS vectors, causing the QRS deflections and the accompanying T waves in a given lead to be oppositely directed. Because of the overlapping of the depolarization and repolarization processes in ventricular hypertrophy, the larger T forces produced by the hypertrophied ventricle manifest themselves early in the S-T interval by displacing the base line of the electrocardiogram. The effect of these early repolarization forces can be visualized as an S-T vector, which, for obvious reasons, parallels the instantaneous T vectors, in the absence of true injury S-T vectors. Thus, scalar leads showing inverted T waves record depressed S-T segments, while leads with upright T waves show S-T segment elevation. Secondary ST-T wave changes of this type presumably result from the altered ventricular activation process in ventricular hypertrophy.

Primary abnormality of the mean instantaneous QRS spatial vectors—This type of repolarization abnormality, as it occurs in ventricular hypertrophy, is usually due to myocardial ischemia. The latter condi-

tion can result from coronary artery disease or possibly from relative coronary insufficiency. The concept of relative coronary insufficiency rests on the fact that ventricular hypertrophy leads to a decrease in the number of capillaries per unit volume of myocardium. Moreover, the cross-sectional area of the muscle fibers is increased so that the inside of each cell becomes farther removed from the capillaries. As a result, the interchange of oxygen and metabolites is impeded and ischemia ensues.

Myocardial ischemia prolongs the recovery process in all layers of ventricular wall, and so repolarization begins at the endocardial surface and proceeds in the same direction as depolarization. The instantaneous T vectors swing away from the effective region of ischemia; and, since this usually coincides with the site of the hypertrophied ventricle, the angular divergence of the QRS and T vectors becomes abnormally wide. (Myocardial ischemia will be discussed in more detail in Chapter 18.)

The ECG in Ventricular Hypertrophy

Although the electrocardiographic findings in ventricular hypertrophy are described in full detail in the individual sections dealing with hypertrophy of one or the other ventricle, it is appropriate to conclude the introductory comments by relating the specific electrical effects of left and right ventricular hypertrophy to the electrocardiogram (see also Fig 87), under the following headings:

LEFT VENTRICULAR HYPERTROPHY

In left ventricular hypertrophy, the mean instantaneous QRS spatial vectors of increased magnitude —

RIGHT VENTRICULAR HYPERTROPHY

In right ventricular hypertrophy, the mean instantaneous QRS spatial vectors of increased —

Thus the electrocardiogram shows the following general abnormalities—

1. Leads I and aVL record tall upright R waves and leads II, III, and aVF record RS deflections. The limb leads usually show left-axis deviation of the mean manifest electrical axis of QRS.

2. Leads I and aVL show tall R waves and leads II, III, and aVF show RS deflections. The limb leads usually show right-axis deviation of the mean manifest electrical axis of QRS.

and to the right, superiorly, and either anteriorly or slightly posteriorly in right ventricular hypertrophy.

2. The mean instantaneous spatial vectors produced relatively late in the QRS interval may be rotated from their usual position, owing to the fact that late QRS forces arising in the thick basal wall of the hypertrophied ventricle are unopposed by potentials from the other ventricle. Such an abnormality can be attributed to the increased thickness of the wall of the hypertrophied ventricle, which results in the lengthening of the time required for completion of activation in the affected ventricle. This factor, occasionally in conjunction with a co-existing intraventricular conduction disturbance, may result in activation being completed in the unaffected ventricle before basal regions of the hypertrophied ventricle have completed activation. Thus, late QRS forces are produced in the thickest portion of the hypertrophied ventricle and are virtually unopposed. The late instantaneous vectors may represent primarily forces arising in the basal wall of the hypertrophied ventricle.

3. Some authorities believe that anatomic cardiac rotation is one of the factors responsible for the displacement of the instantaneous QRS spatial vectors toward the effective electrical site of the hypertrophied ventricle. For example.

a) According to some authorities, the mechanical effect of right ventricular hypertrophy may lead to extreme clockwise rotation of the heart on its longitudinal axis, so that the left and right ventricles exchange positions. Thus, in right ventricular hypertrophy, the instantaneous QRS vectors are oriented just as normally, toward the electrically dominant left ventricle, but the left ventricle is located anteriorly and to the right. This explanation of the rightward and anterior orientation of the instantaneous QRS vectors in right ventricular hypertrophy has been severely criticized.

b) The posterior, superior, and leftward orientation of the instantaneous QRS vectors in left ventricular hypertrophy has been attributed to counterclockwise rotation of the heart on its longitudinal axis. In several recent studies, no consistent correlation could be demonstrated between anatomic heart position and orientation of the mean QRS spatial vector or the long axis of the vectorcardiographic QRS sE loop. It would seem, therefore, that in left ventricular hypertrophy cardiac rotation is not the primary mechanism responsible for the characteristic orientation of the instantaneous vectors

LENGTHENING OF THE TIME REQUIRED FOR ACTIVATION OF THE HYPERTROPHIED VENTRICLE

Several different mechanisms, jointly or individually, may be responsible for the lengthening of the time required for ventricular activation. They are as follows:

1. Because the wall of the hypertrophied ventricle is thicker than normal, the distance the activation wave must travel to reach the epicardium is increased. Thus, onset of the intrinsicoid deflection or the appearance of the maximal vector in a lead facing the hypertrophied ventricle is delayed. The greater muscle mass of the hypertrophied ventricle also causes an overall lengthening of the time required for ventricular activation, as evidenced by an increased duration of the QRS interval.

2. Another factor which has been implicated by some investigators is lengthening of the conduction time required for spread of excitation over the endocardium as the result of ventricular dilatation and hypertrophy.

3. A localized conduction disturbance, such as incomplete bundle branch block, may also contribute to the prolonged QRS interval. The conduction defect can result from coronary artery disease or from compression of blood vessels supplying the subendocardium, owing to increased intraventricular pressure.

ROTATION OF THE MEAN INSTANTANEOUS T SPATIAL VECTORS AWAY FROM THE MEAN INSTANTANEOUS QRS SPATIAL VECTORS

The mechanisms, in ventricular hypertrophy, which cause the mean instantaneous T spatial vectors to diverge from the corresponding QRS vectors are

normally wide divergence of the instantaneous QRS and T vectors, which produces secondary T wave changes, is not associated with an abnormal ventricular gradient, since it results from a primary change in the depolarization process. When the displacement of the instantaneous T spatial vectors produces primary T wave abnormalities, the ventricular gradient is abnormal. Consequently, the underlying mechanism must entail some change in the process of recovery in the hypertrophied ventricle.

Secondary abnormality of the mean instantaneous T spatial vectors—Because of the increased thickness of the ventricular wall, a longer time is required for

Left Ventricular Hypertrophy

NORMALLY, THE LEFT VENTRICLE contributes approximately three quarters of the potentials which produce the QRS deflection. With hypertrophy of the left ventricle, this electrical predominance of left over right ventricle becomes all the more accentuated. The greater the disparity between left and right ventricular forces, the more closely the electrocardiogram resembles a levocardiogram, in that the mean instantaneous QRS vectors more nearly represent pure left ventricular forces. Thus, the mean instantaneous QRS spatial vectors in left ventricular hypertrophy tend to increase in magnitude as they develop in an abnormally posterior, superior, and leftward direction.

THE INSTANTANEOUS VA VECTORS

Q01-SECOND SEPTAL VA VECTOR

In left ventricular hypertrophy, the septal VA vector is usually relatively normal in direction and magnitude, however, sometimes it has a larger magnitude than normal and extends farther anteriorly, inferiorly, and to the right. The greater size of the Q01-second VA vector possibly is a reflection of septal hypertrophy. The septum anatomically is a part of the hypertrophy process just like the ventricular free wall. In other cases of left ventricular hypertrophy, the Q01-second VA vector may be oriented in a more left-to-right direction and less anteriorly. This has been attributed, by some investigators to counterclockwise rotation of the heart on its longitudinal axis.

VARIATIONS IN THE Q01-SECOND SEPTAL VA VECTOR.—The three types of variations follow.

1. There may be normal direction and magnitude of the vector with the following results in the electrocardiogram

The ventricular activation sequence will be schematized, below, in terms of hypothetical instantaneous VA (ventricular activation) vectors which represent a synthesis of the findings in a typical case of left ventricular hypertrophy (see also Fig. 90). The description of the VA vectors in left ventricular hypertrophy to be given in the following paragraphs should be compared with the earlier description of the instantaneous VA vectors in the typical normal heart (pp 54-59). These VA vectors in the typical normal heart re-
vectors
trophy.

Leads I and V_4 .—The vector projects small Q waves on these leads, just as normally.

Leads III, aVF, and V_1 .—On these leads, the vector projects the initial part of a small R wave.

2. There may be increased magnitude but normal direction of the vector, so that the following deflections are written:

Leads I and V_4 .—The vector projects deep but narrow Q waves on these leads.

Leads III, aVF, and V_1 .—The vector projects the initial portion of a relatively tall R wave on these leads. Ordinarily, however, the R/S amplitude ratio in lead V_1 merely approaches but does not equal 1, the S wave remaining the larger component of the RS deflection in this lead.

3. The vector may be oriented more to the right and less anteriorly:

Leads I and V_4 .—The vector may project narrow Q waves on these leads.

2. Leads V_1 through V_3 or V_4 display large rS deflections; and leads V_4 and V_6 tall R waves. The transition point for the QRS deflection tends to be shifted to the left of its usual position near the electrode position of lead V_3 or V_4 .

2. Leads V_{3R} through V_5 or V_6 record QRS deflections of varying configuration (e.g., rR', qR, rsR', etc.) whose net voltage is positive, while precordial leads to the left record QRS deflections of diminishing positive and increasing negative voltage. There is therefore a reversal in the precordial QRS transition.

Lengthening of the time required for activation of the hypertrophied ventricle.—The prolonged ventricular activation time of the hypertrophied ventricle causes:

LEFT VENTRICULAR HYPERTROPHY

1. Delayed onset of the intrinsicoid deflection in lead V_4 .

2. An over-all lengthening of the time required for activation of the ventricle so that the QRS interval is often prolonged to 0.11 or 0.12 second.

RIGHT VENTRICULAR HYPERTROPHY

1. Delayed onset of the intrinsicoid deflection in lead V_1 .

Rotation of the mean instantaneous T spatial vectors away from the mean instantaneous QRS spatial vectors—The greater angular divergence of the mean instantaneous QRS and T spatial vectors means that the QRS deflections and T waves in any lead tend to be directed oppositely, while normally they usually have the same direction. The resulting findings are as follows.

LEFT VENTRICULAR HYPERTROPHY

Leads I, aVL, V_4 , and V_6 record inverted T waves, and leads II, III, aVF, and V_1 through V_3 or V_5 record upright T waves.

RIGHT VENTRICULAR HYPERTROPHY

Leads II, III, aVF, and V_{3R} through V_4 or V_6 record inverted T waves, and leads I, aVL, V_5 , and V_6 register upright T waves.

Left Ventricular Hypertrophy

NORMALLY, THE LEFT VENTRICLE contributes approximately three quarters of the potentials which produce the QRS deflection. With hypertrophy of the left ventricle, this electrical predominance of left over

sembles a levocardiogram, in that the mean instantaneous QRS vectors more nearly represent pure left ventricular forces. Thus, the mean instantaneous QRS spatial vectors in left ventricular hypertrophy tend to increase in magnitude as they develop in an abnormally posterior, superior, and leftward direction.

THE INSTANTANEOUS VA VECTORS

0.01-SECOND SEPTAL VA VECTOR

In left ventricular hypertrophy, the septal VA vector is usually relatively normal in direction and magnitude, however, sometimes it has a larger magnitude than normal and extends farther anteriorly, inferiorly, and to the right. The greater size of the 0.01-second VA vector possibly is a reflection of septal hypertrophy. The septum anatomically is a part of the left ventricle and can therefore participate in the hypertrophy process just like the ventricular free wall. In other cases of left ventricular hypertrophy, the 0.01-second VA vector may be oriented in a more left-to-right direction and less anteriorly. This has been attributed, by some investigators to counterclockwise rotation of the heart on its longitudinal axis.

VARIATIONS IN THE 0.01-SECOND SEPTAL VA VECTOR—The three types of variations follow

1. There may be normal direction and magnitude of the vector with the following results in the electrocardiogram

The ventricular activation sequence will be schematized, below, in terms of hypothetical instantaneous VA (ventricular activation) vectors which represent a synthesis of the findings in a typical case of left ventricular hypertrophy (see also Fig. 90). The description of the VA vectors in left ventricular hypertrophy to be given in the following paragraphs should be compared with the earlier description of the instantaneous VA vectors in the typical normal heart (pp 54-59). These VA vectors in the typical normal heart resemble closely those actually recorded in the vectorcardiographic pattern of left ventricular hypertrophy.

Leads I and V_4 —The vector projects small Q waves on these leads, just as normally

Leads III, aVF, and V_1 —On these leads, the vector projects the initial part of a small R wave.

2 There may be increased magnitude but normal direction of the vector, so that the following deflections are written

Leads I and V_4 —The vector projects deep but narrow Q waves on these leads

Leads III, aVF, and V_1 —The vector projects the initial portion of a relatively tall R wave on these leads. Ordinarily, however, the R/S amplitude ratio in lead V_1 merely approaches but does not equal 1, the S wave remaining the larger component of the RS deflection in this lead.

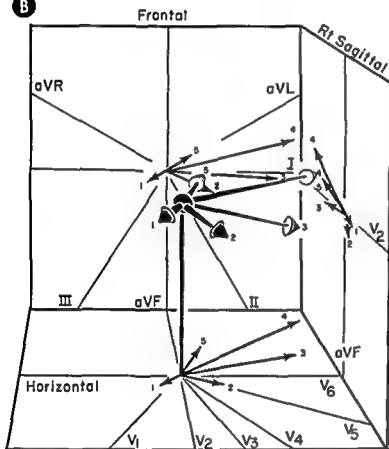
3 The vector may be oriented more to the right and less anteriorly

Leads I and V_4 —The vector may project somewhat deeper Q waves than normal on leads I and V_4 . These Q waves are usually not particularly striking, in contrast with the preceding variant, probably because

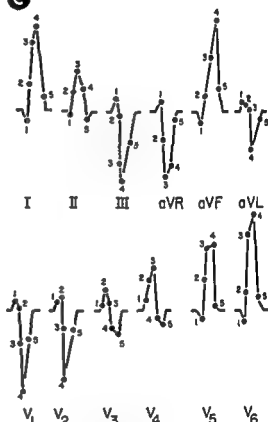
A

Sequence of Ventricular Activation in LVH

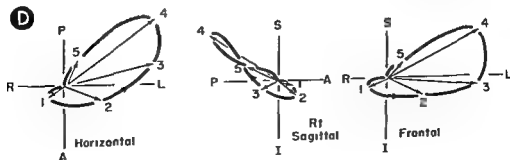
- 1 LEFT SEPTAL SURFACE
- 2 APICO-ANTERIOR WALLS OF LEFT AND RIGHT VENTRICLES
- 3 VENTRICULAR FREE WALL
- 4 BASAL SEPTUM AND RIGHT VENTRICULAR FREE WALL AND LATERAL ASPECT OF LEFT VENTRICLE
- 5 BASAL LEFT VENTRICULAR FREE WALL

B

Instantaneous VA Vectors in LVH

C

QRS Deflections Projected on Scalar Leads

D

Planar QRS Loops in LVH

Fig. 90.—Instantaneous VA vectors in left ventricular hypertrophy (LVH). **A**, sequence of septal-ventricular activation. **B**, the instantaneous VA spatial vectors. These vectors are numbered so that they can be related, in an approximate

the R waves in leads I and V_4 are larger than normal, and so the relative (though not the absolute) size of the Q and R waves in these leads may differ little from normal.

Leads III, aVF, and V_1 .—The more rightward and the less anterior and inferior the orientation of the vector, the less is its projection on the lead axes of leads III, aVF, and V_1 . A smaller anterior component

hypertrophy (see below)

0.02-SECOND APICOANTERIOR VA VECTOR

In left ventricular hypertrophy, the marked electrical predominance of the left ventricle can be manifested as early as 0.02 second after onset of the QRS interval. In this event, the apicoanterior VA vector is larger than normal and directed more to the left and either less anteriorly and inferiorly or somewhat posteriorly or superiorly just as was the case with the 0.01-second septal VA vector, and for the same reason, the 0.02-second vector sometimes may have an exaggerated anterior and rightward projection.

1 The initial septal VA vector may be oriented more to the right and less anteriorly and inferiorly than normal, and the 0.02-second apicoanterior VA vector, more to the left, posteriorly, and superiorly.

Leads I and V_4 .—On these leads, the vectors project a Q wave and the upstroke of an R wave, both deflections being larger than normal but of normal relative proportions.

Leads III, aVF, and V_1 .—Very small initial R waves are often produced. In some cases, lead III displays a Q wave and lead V_1 a QS deflection.

2 Both the 0.01- and 0.02-second VA vectors may have an exaggerated anterior, rightward and

No satisfactory explanation has as yet been offered for the fact that initial R waves may be absent in lead V_1 in 10–30% of cases of left ventricular hypertrophy and in lead V_2 in 1–17% of the cases. In all probability, antecedent anteroapical myocardial infarction is responsible for this finding in some cases, but certainly not in all.

0.04-SECOND LEFT VENTRICULAR VA VECTOR

This vector reflects the accentuated electrical preponderance of the left ventricle in left ventricular hypertrophy more clearly than do the preceding vectors. Thus, the magnitude of the 0.04-second VA vector in left ventricular hypertrophy is greater than normal, and the orientation of the vector, more posterior and superior, and to the left.

Leads I and V_4 .—The projection of this vector on the axes of leads I and V_4 contributes to the tall R waves inscribed in these leads.

Leads III, aVF, and V_1 .—The vector projects deep S waves on leads V_1 and V_2 and smaller S waves on leads III and aVF.

Despite the greater magnitude of the 0.04-second VA vector in left ventricular hypertrophy, it is not the maximal vector to appear during ventricular activation. The maximal vector appears 0.01–0.02 second later, the delay possibly being the result of either or both of the following factors: (1) the over-all lengthening of the time required for ventricular activation, owing to the marked thickening of the left ventricular wall, and (2) the relatively greater hypertrophy of the basal and posterolateral walls of the left ventricle. These regions are activated late in the QRS interval normally. Inasmuch as they generate the maximal forces in left ventricular hypertrophy and may be activated even later than in the normal heart, the maximal vector is also delayed in onset.

0.06-SECOND BASAL VA VECTOR

The abnormal magnitude and orientation of the 0.06-second VA vector are indicative of the delayed onset of the maximal ventricular activation forces in left ventricular hypertrophy.

by

Griffiths, 1950

Leads III, aVF, and V_1 .—R waves which are taller than normal but of normal duration. Lead V_1 is particularly likely to show this finding.

vector can be visualized as extending farther to the left and lying more posterior and superior than all the foregoing VA vectors. The basal VA vector tends to parallel the negative portion of the lead V_1 axis and may project maximal positivity on lead V_6 .

Leads I and V_4 .—This vector coincides approximately with the peak of the tall R waves in lead V_6 and contributes to the tall R wave registered in lead I.

Leads III, aVF, and V_1 .—The vector coincides approximately with the nadir of the S wave in leads III, aVF, and V_1 .

Since the peak of the R wave in lead V_6 corresponds to the time of onset of the intrinsicoid deflection in this lead, it is evident that the fact that the 0.06-second VA vector is the maximal VA vector to appear during ventricular activation (rather than the 0.04-second VA vector, as is normally the case) means that there is a delayed onset of the intrinsicoid deflection in lead V_6 . On the other hand, onset of the intrinsicoid deflection occurs at the normal time in lead V_1 .

As will be recalled, the maximal instantaneous VA (or QRS) vector in the horizontal plane corresponds roughly to the horizontal mean QRS vector calculated from the precordial leads of the electrocardiogram. The orientation of the mean QRS vector is established by identifying the precordial lead which registers the equiphasic or transitional RS deflection, the so-called *transitional lead*. Precordial leads located to the right of the transitional lead register low R waves and deep S waves in left ventricular hypertrophy, since they lie in the negative field of the mean QRS vector, leads to the left of the transitional lead record tall R waves, because they are situated in the positive field of the vector. The marked posterior orientation

of the instantaneous vectors and horizontal mean vector, which characterizes left ventricular hypertrophy, is responsible for the fact that the transitional or equiphasic RS deflection frequently is recorded by a lead situated to the left of the normal transitional zone between leads V_3 and V_4 . If, for example, the horizontal mean QRS vector lies between -60° and -90° in the horizontal reference frame, a lead intermediate between leads V_3 and V_6 would record the transitional deflection, leads V_1 through V_3 displaying resultantly negative or downwardly directed QRS deflections. This is the conventional electrocardiographic pattern of "clockwise rotation." However, when there is marked "clockwise rotation" with RS deflections in lead V_3 or V_6 , the QRS voltage in the latter leads may not meet the criteria for voltage of left ventricular hypertrophy.

0.08-SECOND TERMINAL VA VECTOR

For a prolonged interval after completion of right ventricular activation, basal portions of the left ventricle continue to depolarize. Accordingly, the QRS interval in left ventricular hypertrophy is usually prolonged, sometimes to 0.12 second, and the terminal VA vector appears later than normal. Since the forces produced by activation of basal portions of the left ventricle are unopposed by forces arising elsewhere, the terminal VA vector is directed even farther posteriorly but less superiorly than the VA vectors preceding it.

Leads I and V_6 .—This vector projects diminishing positivity on leads I and V_6 .

Leads III, aVF, and V_1 .—On these leads, the vector projects diminishing negativity.

VENTRICULAR REPOLARIZATION

Before depolarization in the basal regions of the left ventricle is completed, repolarization begins at the endocardial surface of the left ventricle (see Chapter 8). In the right ventricle, recovery begins at the epicardial surface, just as normally, although the resulting T forces are negligible compared to the repolarization forces arising in the left ventricle. The reversal in the direction of repolarization in the electrically dominant left ventricle causes the instantaneous T vectors to rotate away from the instantaneous VA vectors. Thus, electrocardiographic leads registering upright QRS deflections usually record inverted T waves (leads I, aVL, V_3 , and V_6), while leads displaying deep S waves have upright T waves (leads

V_1 and V_2). Because of the overlapping of the depolarization and repolarization processes, repolarization forces begin to act on the electrocardiograph before the QRS forces have subsided. Since these repolarization forces, which appear early in the S-T interval, are identical with the forces producing the T wave and have the same direction, the S-T segments tend to be depressed in leads recording inverted T waves and slightly elevated in leads registering upright T waves. Sometimes the QRS deflections and T waves in left ventricular hypertrophy are concordant, in such cases the authors phrase the interpretations "left ventricular hypertrophy" on the basis of high QRS voltage alone (to be discussed later).

GENERAL ECG FINDINGS AND RELATED DIAGNOSTIC CRITERIA IN LEFT VENTRICULAR HYPERTROPHY

Increased magnitude and a more posterior, superior, and leftward orientation of the mean instantaneous QRS spatial vectors:

EXTREMITY LEADS

1. Leads I and aVL record tall upright QRS deflections, while leads II, III, and aVF display rS deflections. The S wave in lead III is usually deep.

$R_I + S_{III} \geq 25 \text{ mm}$.

$R_{aVL} > 11 \text{ mm}$

$R_{aVF} > 20 \text{ mm}$

Comment: QRS in leads I and aVL is usually tall and upright.

2. There is often left-axis deviation of the mean momentary electrical axis of QRS (A QRS). When this is the case,

PRECORDIAL LEADS

1. Leads V_1 through V_4 or V_5 record small initial R waves followed by very deep S waves, while leads V_5 and/or V_6 register small Q waves followed by very tall R waves.

QRS VOLTAGE CRITERIA

$S_{r_1} \geq 24 \text{ mm}$.

R_{r_5} or $R_{r_6} > 26 \text{ mm}$.

R_{r_5} or $R_{r_6} + S_{r_1} > 35 \text{ mm}$

2. Since the mean instantaneous QRS spatial vectors in left ventricular hypertrophy are often directed posteriorly, superiorly, and leftward, the QRS complex in leads V_1 through V_4 is often a deep rS or RS pattern, while in leads V_5 and V_6 it is often a tall R wave.

ORIENTATION OF A QRS (FIG. 91, A)

Frontal Plane

Range: -80° to $+90^\circ$

Average: $+3^\circ$

Horizontal Plane

Range: -60° to 0°

Average: -25°

Over-all lengthening of the time required for ventricular activation.

EXTREMITY LEADS

Increased QRS duration 0.11–0.12 second

CRITERIA

PRECORDIAL LEADS

Delayed onset of the intrinsicoid deflection in lead V_1 : 0.05 second, or later after onset of the QRS interval. Normal time of onset of intrinsicoid deflection in lead V_1 .

Rotation of the mean instantaneous T spatial vectors to the right, anteriorly, and inferiorly, away from the mean instantaneous QRS spatial vectors.

EXTREMITY LEADS

1. Lead aVL or aVF 0.5 mm or more depression of S-T segment (representing early abnormally directed T wave forces)

2. Lead aVL or aVF Flat, diphasic, or inverted T wave (with an R wave of 6 mm, or more amplitude) plus 0.5 mm, or more depression of S-T segment

3. Lead aVR Upright T wave

CRITERIA

PRECORDIAL LEADS

1. Lead V_4 or V_5 S-T segment depression and/or low or inverted T waves.

ORIENTATION OF $\bar{A}T$ (FIG. 91, A)

Frontal Plane

Range: $+10^{\circ}$ to -140°
 Average: $+120^{\circ}$

Horizontal Plane

Range: $+45^{\circ}$ to $+170^{\circ}$
 Average: $+135^{\circ}$

Comment. The transition from upright T waves and elevated S-T segments to inverted T waves and depressed S-T segments usually occurs just to the left or right of, or in the same lead as, that recording the transitional, equiphasic RS deflection. However, in the presence of digitalis effect or of superimposed myocardial ischemia, precordial leads to the right of the transition point for the QRS may record inverted T waves.

LIMITATIONS IN DIAGNOSTIC SPECIFICITY OF THE CRITERIA
IN LEFT VENTRICULAR HYPERTROPHY

The diagnostic accuracy of the electrocardiogram in left ventricular hypertrophy leaves much to be desired. In the first place, left ventricular hypertrophy merely exaggerates the normal electrical preponderance of the left ventricle without otherwise causing any marked disturbance in the orientation of the mean instantaneous QRS spatial vectors. For this reason, the configuration of the QRS deflections in left ventricular hypertrophy, aside from the large voltage, is not particularly distinctive, while abnormalities of the QRS configuration usually figure prominently in the diagnosis of conditions such as right ventricular hypertrophy, bundle branch block, and myocardial infarction. Since characteristic changes in QRS configuration are lacking in left ventricular hypertrophy, the electrocardiographic diagnosis must therefore depend on other criteria—namely, QRS voltage, orientation of the planar mean QRS vectors, the QRS duration and pre-intrinsicoid deflection time, and, finally, the angular divergence of the QRS and T forces. Each of these categories of diagnostic criteria deserves critical scrutiny.

QRS VOLTAGE CRITERIA—The QRS voltage registered by a body surface lead depends not only on the magnitude of the cardiac vector but also on the conductivity of the body tissues and the distance of the lead electrode from the heart. Thus, left ventricular hypertrophy occurring in a patient with emphysema, which increases the distance between electrode and heart and decreases the conductivity of the lungs, may fail to produce large amplitude QRS deflections. Anasarca can have the same result. On the other hand, large QRS deflections may be recorded not infrequently in subjects with normal hearts and with thin chest walls, particularly in adolescents and young adults.

CRITERIA RELATING TO ORIENTATION OF PLANAR

MEAN QRS VECTORS OR MEAN QRS SPATIAL VECTOR:

Left-axis deviation—Of the patients with left ventricular hypertrophy studied by Grishman and his associates, only one fourth showed left-axis deviation. On the other hand, left-axis deviation is observed in some subjects with normal hearts and a short stocky physique. In brief, left ventricular hypertrophy is far from being the only factor causing left-axis deviation. For example, Grant has presented evidence suggesting that anterolateral infarction can be responsible for the occurrence of left-axis deviation in the electrocardiogram.

Leftward and posterior (clockwise) rotation of the mean horizontal QRS vector—This is commonly observed in acute and chronic cor pulmonale, in which anatomic rotation of the heart on its longitudinal axis is believed to occur. Clockwise rotation can also represent a normal variation in some individuals.

CRITERIA PERTAINING TO QRS DURATION AND TIME OF ONSET OF INTRINSICOID DEFLECTION—Lengthening of the time required for ventricular activation can result from various types of intraventricular conduction delay in the left ventricle. In fact, it can be quite difficult at times to distinguish left ventricular hypertrophy with a prolonged ventricular activation time from incomplete left bundle branch block or peri-infarction block.

ABNORMALLY WIDE ANGULAR DIVERGENCE OF MEAN QRS AND MEAN T SPATIAL VECTORS—Neither the location of the leads recording depressed S-T segments and inverted T waves nor the morphology of the S-T segments and T waves has diagnostic specificity for left ventricular hypertrophy alone. Certainly, the S-T segment deviation and T wave changes produced by digitalis, coronary insufficiency, hypokalemia, or numerous other factors are usually indis-

tinguishable from ST segment and T wave abnormalities occurring in left ventricular hypertrophy.

Since none of the above criteria can individually be considered diagnostically specific for left ventricular

hypertrophy, it follows that the electrocardiographic diagnosis of left ventricular hypertrophy gains in reliability in direct proportion to the number of criteria satisfied.

VECTOCARDIOGRAPHIC FINDINGS IN LEFT VENTRICULAR HYPERTROPHY

QRS sE LOOP

In the patients with left ventricular hypertrophy whom we studied vectorcardiographically (see Fig 91 and Table 7), the magnitude of the maximal instantaneous QRS spatial vector and the relative size of the spatial loop were only estimated qualitatively, not measured precisely. The maximal mean instantaneous QRS vector in left ventricular hypertrophy tends to be longer than that in the normal subject, and the QRS sE loop usually encloses a larger area. The configuration of the QRS sE loop in the frontal and horizontal projections is perhaps more variable than in the sagittal projection. Thus the horizontal and frontal QRS loops sometimes have an oval-shaped configuration in which the long and short dimensions of the loop are almost equal, at other times, the loops display a figure-of-eight configuration or they are extremely long and narrow.

HORIZONTAL QRS LOOP—In left ventricular hypertrophy, the initial deflection of the horizontal QRS loop is usually written to the right and anteriorly, just as occurs normally, and the instantaneous vectors forming the initial deflection generally are of essentially normal magnitude. However, it is not uncommon to observe

QRS vectors and a decrease in the anterior component of these vectors. In this event, the initial R waves recorded in leads V_1 and V_2 may be extremely low and may even appear to be absent, but in either case, leads V_3 and V_6 display normal Q waves. Ordinarily, when QS deflections in leads V_1 and V_2 represent residuals of an old antero-septal myocardial infarction, the normal septal Q waves are absent in leads V_3 and V_6 , and this fact is often quite helpful in differentiating left ventricular hypertrophy and antero-septal infarction.

After inscription of the initial deflection, the horizontal QRS loop in left ventricular hypertrophy is written farther posteriorly and extends farther to the left than is normally the case. While this feature is present fairly constantly in most cases of left ventricular hypertrophy, there is considerable variability in the configuration of the horizontal QRS loop (Fig 92). We have arbitrarily separated the various types of QRS loop configuration which we have observed in left ventricular hypertrophy into the following

1. The "figure-eight" type, in which the loop is inscribed in a counterclockwise direction.

2. The "figure-eight" type, in which the loop is inscribed in a clockwise direction. This type of contour is observed not infrequently in left ventricular hypertrophy. The proximal loop of the "figure-eight" is inscribed counterclockwise, and the distal loop is clockwise.

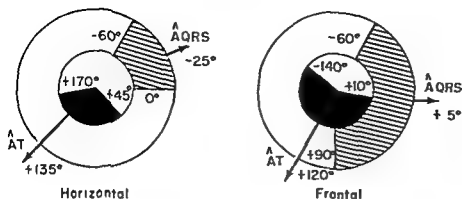
3. The "figure-eight" type, in which the loop is inscribed in a clockwise direction. More often than not, the initial deflection in loops showing this type of configuration is written to the left and anteriorly, or, less frequently, posteriorly. The electrocardiograms in these cases often show slurring of the upstroke of the R waves in leads I and V_6 and absent Q waves in these leads, in addition to the findings of left ventricular hypertrophy. These features would be interpreted by some authorities as indicating incomplete left bundle branch block superimposed on left ventricular hypertrophy. In support of such an interpretation is the similarity of the QRS loops which we have observed, and just described, in

adults with left ventricular hypertrophy than in older adults with this condition, and the same seems to hold true for the corresponding electrocardiographic abnormality, which consists of relatively deep, narrow Q waves in leads I, aVL, V_1 , and V_6 and relatively tall initial R waves in lead V_3 (followed by the deep S waves characteristic of left ventricular hypertrophy).

Another variation in the initial deflection of the

of the efferent limb almost directly to the left and posteriorly. In other words, there is a relative increase in the left-right component of the initial instantaneous

A Δ QRS and Δ T - Left Ventricular Hypertrophy



B .02 Sec. and Maximal Mean Instantaneous QRS Vectors and Max T Vector - Left Ventricular Hypertrophy

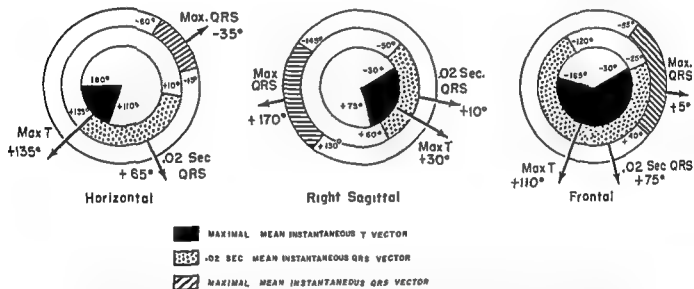


Fig. 91.—A, orientations of Δ QRS and Δ T in the horizontal and frontal planes, as calculated from electrocardiograms in cases of left ventricular hypertrophy studied by the authors of this text. The ranges of variation in orientation of Δ QRS in the two planes are indicated by the striped segment of the outer ring of each circle, of Δ T in the two planes, by the solid black section of the inner circle. B, orientations of the mean .02-second instantaneous vector, and of the maximal mean instantaneous vector of the vectorcardiographic QRS e loop in left ventricular hypertrophy. The data presented in B were derived from the vectorcardiograms recorded by the authors from 35 patients with radiologic and electrocardiographic evidence of left ventricular hypertrophy.

TABLE 7 -VECTOR ANGIOGRAPHIC FINDINGS IN LEFT VENTRICULAR HYPERTROPHY (SEE FIG. 91, B)

	HORIZONTAL			RIGHT SAGITTAL			FRONTAL		
	Extreme Range	Av	Usual Range	Extreme Range	Av	Usual Range	Extreme Range	Av	Usual Range
QRS sL Loop									
Maximal mean instantaneous QRS vector	-60° to -15°	-35°	-45° to -15°	+130° to -145°	+170°	+155° to -170°	-55° to +40°	+5°	-5° to +20°
0.02-second mean instantaneous QRS vector	+10° to +135°	+65°	+20° to +100°	-50° to +60°	+10°	...	-25° to -120°	+75°	+30° to 160°
Maximal mean instantaneous T vector	+110° to 160°	+135°		-30° to +75°	+30°	-30° to +20°	-30° to -105°	+110°	+160° to -165°
Direction of initial deflection of the planar QRS loop	Right, anterior					Usually anterior, inferior, sometimes superior			Right, inferior or, less often, superior
Direction of inversion of planar QRS loop	1. Counterclockwise usually 2. Less frequently in figure-of-eight loops, the proximal loop of the "eight" is counterclockwise inscribed and the distal loop, clockwise inscribed					Clockwise			Counterclockwise, particularly if the initial deflection of the QRS loop is directed inferiorly
Direction of S-T vector	Right, anterior			Anterior, inferior					Right, inferior or, occasionally, superior
Spatial QRS vector angle	65° to 175°	155°	...						
Time of appearance of maximal leftward mean instantaneous QRS vector	0.04-0.075 second	0.0175 second	0.015-0.0525 second						

those recorded in cases of incomplete left bundle branch block without associated left ventricular hypertrophy.

Rare left ventricular hypertrophy pattern.—In an occasional case of left ventricular hypertrophy, a figure-of-eight horizontal QRS loop is observed. It differs from those described above in that the initial deflection of the QRS loop forms the proximal loop of the "eight" while the distal portion includes the remainder of the clockwise inscribed QRS loop.

may be written in a clockwise or counterclockwise direction. Burch and his associates found that some of the atypical frontal plane loops which were clockwise inscribed displayed a slight uptwist of their distal tips. These investigators felt that this finding may be one of the earliest indications of left ventricular hypertrophy and may represent a transition stage between the normal-appearing loops with clockwise inscription and the counterclockwise-inscribed loops typical of left ventricular hypertrophy. We have

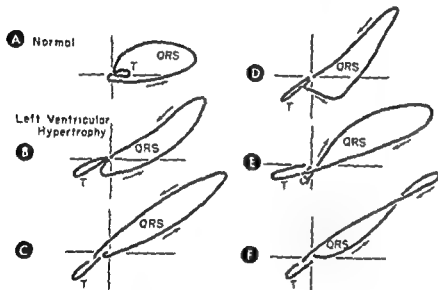


Fig 92.—Horizontal QRS loop pattern variants in left ventricular hypertrophy. In A, normal horizontal QRS and T loops are shown for purposes of comparison. The QRS loops in B, C, and D are commonly noted in vectorcardiograms of patients with left ventricular hypertrophy. The QRS loop pattern in E is rarely observed, at least in the experience of the authors of this text. The authors suspect that the QRS loop pattern in F may reflect combined left ventricular hypertrophy and incomplete left bundle branch block. Note that in all the QRS loops shown in B through F the planar T loop is almost 180° discordant to the QRS loop.

RIGHT SAGITTAL QRS LOOP—Usually, the sagittal loop is initially inscribed anteriorly and inferiorly and then is written in a clockwise direction posteriorly and superiorly.

FRONTAL QRS LOOP—The initial deflection of the frontal QRS loop is usually directed to the right and inferiorly, and the remainder of the loop is then written in a counterclockwise direction far to the left and superiorly. This produces left-axis deviation of a QRS in the electrocardiogram. Sometimes the frontal and sagittal QRS loops are located inferiorly and to the left, and in these cases the frontal loop may be written in a clockwise direction.

Burch and his co-workers, using the equilateral tetrahedron system of electrode placement, observed that the typical frontal QRS loop in left ventricular hypertrophy has a smooth configuration, encloses a relatively wide area, is inscribed in a counterclockwise direction, and is located in the 0° to -60° segment of the frontal reference frame (Fig 93). The less typical loops observed in left ventricular hypertrophy are located in the 0° to +60° segment and tend to have a relatively normal appearance. They

rarely observed transitional frontal QRS loops (recorded with the cube system) in left ventricular hypertrophy

T sE LOOP AND S-T VECTOR

The spatial T loop is usually directed oppositely to the QRS sE loop, in most cases being situated to the right, anteriorly, and inferiorly, or sometimes superiorly. The angular deviation of the long axes of the QRS sE and T sE loops ordinarily exceeds the normal 45°, ranging from 65° to 175° in the series which we studied, and averaging about 153°.

In left ventricular hypertrophy, the QRS sE loop often fails to return to its point of origin after inscription, an arrow drawn from the origin to the termination of the loop indicating the direction and approximate magnitude of the S-T vector. The S-T vector tends to parallel the long axis of the T sE loop in left ventricular hypertrophy, for reasons already discussed, and is therefore directed to the right, anteriorly, and inferiorly or superiorly (Figs 94-96).

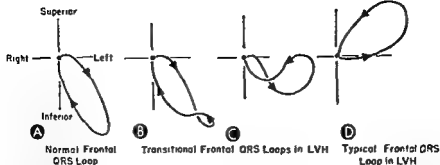


Fig 93.—Frontal QRS loop patterns recorded with the tetrahedron lead system in left ventricular hypertrophy

and his co-workers suggest that the up-twist of the tips of these loops may be an early vectorcardiographic sign of left ventricular hypertrophy, which may, with progression, develop into the typical pattern shown in D. It should be borne in mind that these observations were made from vectorcardiograms recorded with the equilateral tetrahedron reference system rather than with the cube system.

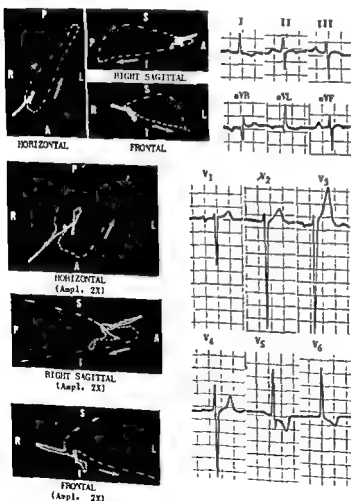


Fig 94.—Electrocardiographic and vectorcardiographic patterns of left ventricular hypertrophy.

The salient diagnostic features in the electrocardiogram are: (1) Left-axis deviation of Δ QRS = -40° . (2) $S_{r1} + R_{r4} = 39$ mm (upper limits of normal, 35 mm). (3) the spatial QRS-T angle is abnormally wide, and there are inverted T waves following upright R waves in leads I, V_4 , and V_6 and upright T waves following the large downwardly directed RS deflections in the right precordial leads.

The diagnostic vectorcardiographic findings are. (1) Although the exact amplification of the vectorcardiogram is not stated above, the smaller planar loops were recorded at a lower degree of amplification than normally, indicating an increased magnitude of the mean instantaneous QRS spatial vectors. (2) The posterior rotation of the long axes of the horizontal and sagittal QRS loops and the left-axis deviation of the frontal loop are typical features of left ventricular hypertrophy. (3) The planar QRS loops remain open after their inscription, indicating an S-T vector directed to the right, anteriorly, and slightly superiorly. (4) The long axis of the T sE loop is almost 160° discordant to that of the QRS sE loop.

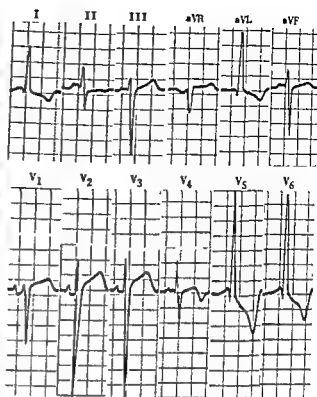
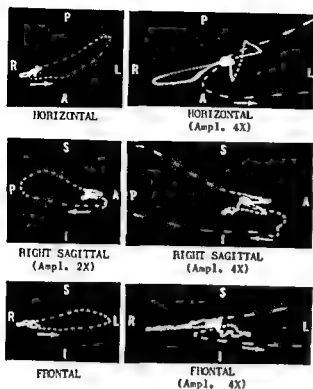


Fig. 95. Electrocardiogram and vectorcardiogram.

hypertrophy in lead aVL are also satisfied (R wave amplitude exceeding 11 mm, with S-T depression and/or inverted T wave), and $R_1 + S_{II}$ exceeds 25 mm. Similarly, the vectorcardiogram displays most of the features described in Figure 94 except that there is no S-T vector.

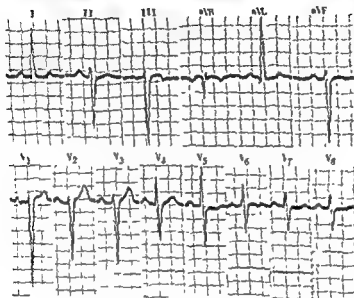
hypertrophy. The electrocardiogram voltages in leads V_5 and V_6 are the criteria for left ventricular



HORIZONTAL

RIGHT SAGITTAL

FRONTAL



ne electro-
R waves in
15 mm. (4)
plane mean
R waves in
act that left

The
these
corda;

Right Ventricular Hypertrophy

REFERENCE HAS already been made to the fact that the normal electrocardiogram is, in essence, a levo-cardiogram, the reason being that the electrical forces produced by the left ventricle determine, for the most part, the characteristics of the QRS and T deflections in the normal electrocardiogram. Left ventricular hypertrophy simply exaggerates the normal electrical preponderance of left over right ventricle, so that the general form of the QRS deflections in the various leads is not strikingly altered, although ordinarily the size of the QRS complexes is greatly increased (The shortcomings of QRS voltage criteria for the diagnosis of the left ventricular hypertrophy were considered in Chapter 9).

Right ventricular hypertrophy, on the other hand, tends to cause a marked change in the balance of cardiac forces and therefore, typically at least, is accompanied by characteristic alterations in the appearance of the QRS deflections. Thus, by and large, the typical features of right ventricular hypertrophy are more readily recognized and are more reliable diagnostic signs than those of left ventricular hypertrophy. However, for right ventricular hypertrophy to produce recognizable changes in the electrocardiogram

and vectorcardiogram, it is not enough that the right ventricular potentials merely increase in magnitude. The increment in the magnitude of the right ventricular forces must be such that the normal electrical predominance of the left ventricle is abolished, or at least reduced to the degree that specific changes in QRS configuration or voltage appear in the electrocardiogram. This being the case, it is not surprising that right ventricular "overloading" must exist for a considerable period of time if the pattern of right ventricular hypertrophy is to develop in the electrocardiogram and vectorcardiogram; even then, often enough, diagnostic changes may fail to appear.

The prominence of the electrocardiographic and vectorcardiographic manifestations of right ventricular hypertrophy, when present, depends on, among other things, how early in the QRS interval and to what degree right ventricular forces offset and eventually dominate forces arising in the left ventricle. While these factors are related, to a great extent, to the type of cardiac lesion producing the right ventricular hypertrophy, for the present the discussion will be limited to the general patterns of right ventricular hypertrophy without regard to their specific etiology.

THE INSTANTANEOUS VA VECTORS

The instant-to-instant changes in the balance of cardiac forces in right ventricular hypertrophy and the manifestations of these changes in the electrocardiogram can be illustrated in a simplified fashion by utilizing the hypothetical instantaneous VA vectors to schematize the ventricular activation process, as was done in the preceding chapter on left ventricular hypertrophy. To relate better this general discussion of typical electrocardiographic findings to subsequent more specific descriptions of the electro-

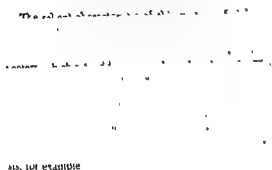
cardiogram and vectorcardiogram in right ventricular hypertrophy, two patterns or series of VA vectors will be considered, each having its electrocardiographic and vectorcardiographic counterpart, as will be seen later. We have arbitrarily designated these two patterns as the *RSR'* and the *tall R* patterns of right ventricular hypertrophy, with the purpose of suggesting by these terms the characteristics of the instantaneous VA or QRS vectors which produce *RSR'* deflections in electrocardiographic lead V_1 in some cases of right

ventricular hypertrophy and tall R waves in that same lead in other cases. For the same reason, these terms

will be applied to the corresponding vectorcardiographic patterns of right ventricular hypertrophy.

The Tall R and the RSR' Patterns of Right Ventricular Hypertrophy

TALL R PATTERN OF RIGHT VENTRICULAR HYPERTROPHY



also, for example

RSR' PATTERN OF RIGHT VENTRICULAR HYPERTROPHY

In this pattern of right ventricular hypertrophy (Fig. 98), the instantaneous mean vectors appearing during the first 0.01 second of the QRS interval are essentially normal in direction and magnitude and project an RS deflection on lead V_1 . Subsequent instantaneous vectors develop in a rightward and anterior direction but do not attain a magnitude comparable to that of the earlier leftward vectors, even though they produce a prominent terminal R' wave in lead V_1 . Lead V_1 therefore registers an RSR' deflection. The RSR' pattern of right ventricular hypertrophy tends to be observed electrocardiographically and vectorcardiographically when, anatomically, there is selective hypertrophy of basal portions of the right ventricle and of the trabecular network, as opposed to concentric hypertrophy of the entire right ventricular wall. The dilatation of the right ventricle which usually accompanies selective hypertrophy may be an additional factor in the production of the RSR' pattern of right ventricular hypertrophy.

0.01-SECOND SEPTAL VA VECTOR

1 Initially, the interventricular septum is activated just as normally, so that the septal VA vector is directed to the right, anteriorly, and inferiorly or superiorly

Leads I and V_4 Small, normal Q wave

Lead aVF Small, normal Q wave if the septal vector is directed superiorly, or the beginning upstroke of an R wave if the vector is directed inferiorly

Lead V_1 Beginning upstroke of an initial R wave.

2 Occasionally in the tall R pattern, the initial vector is directed to the right, anteriorly, and inferiorly or superiorly

Leads I and V_4 Beginning upstroke of an initial R wave

Lead aVF (As in paragraph 1 above)

Lead V_1 Small Q wave

0.02-SECOND VA VECTOR

thi
of t
ma
inf
the
ventricular hypertrophy

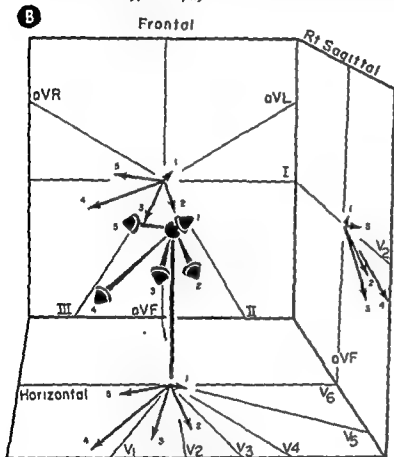
During activation of the apicoanterior and apicobasilar walls of the left and right ventricles, the left ventricular forces are electrically preponderant to much the same degree as normally. Thus, the 0.02-second VA vector is directed inferiorly, anteriorly, and to the left.

(Continued on p. 142)

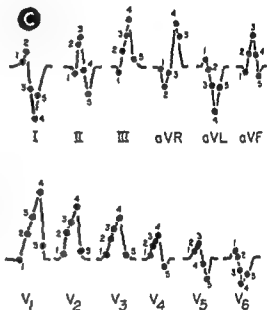


Sequence of Septal-Ventricular Activation in Right Ventricular Hypertrophy

1. INITIAL ACTION OF LEFT SEPTAL SURFACE
2. CONTINUED SEPTAL ACTIVATION AND ACTIVATION OF APICO-ANTERIOR FREE WALL OF BOTH VENTRICLES
3. ACTIVATION OF ANTEROLATERAL FREE WALL OF BOTH VENTRICLES
4. CONTINUED ACTIVATION OF ANTEROLATERAL WALL OF RIGHT VENTRICLE AND SEPTUM, AND ACTIVATION OF BASAL WALL OF LEFT VENTRICLE
5. COMPLETION OF ACTIVATION OF BASAL SEPTUM AND RIGHT VENTRICLE FREE WALL



Instantaneous VA Vectors in Right Ventricular Hypertrophy — Tail R Pattern



QRS Deflections Projected on Scalar Leads

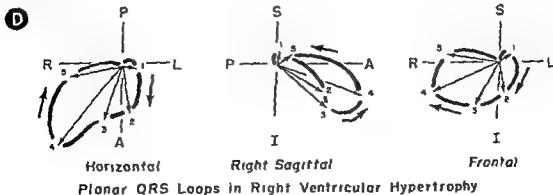


Fig. 97.—Legend on facing page

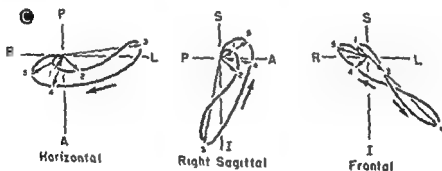
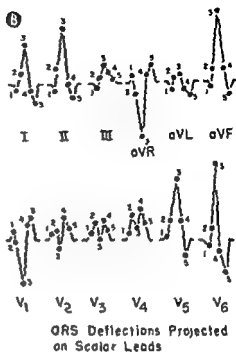
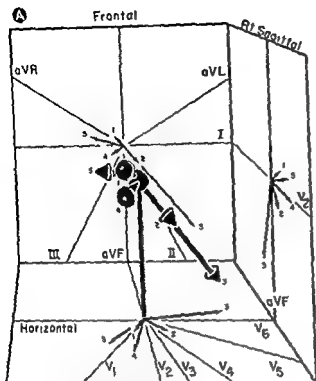


Fig 111 - Instantaneous VA vectors in the RSR' pattern

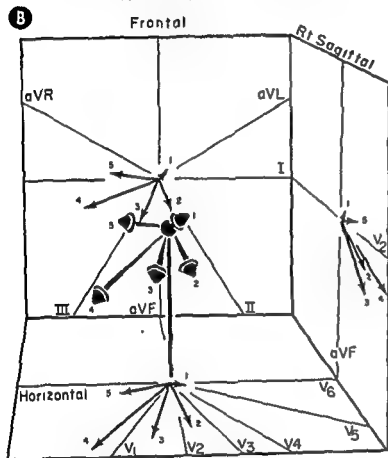
see
the
loop

description of the sagittal loop, and the anterior and rightward orientation of the planar

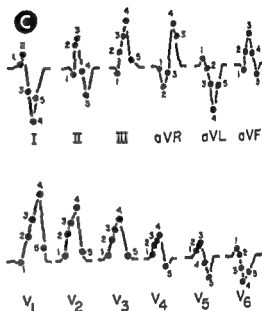


Sequence of Septal-Ventricular Activation in Right Ventricular Hypertrophy

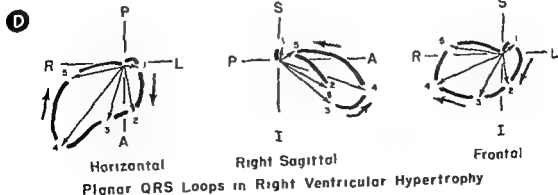
- 1 INITIAL ACTION OF LEFT SEPTAL SURFACE
- 2 CONTINUED SEPTAL ACTIVATION AND ACTIVATION OF APICO-ANTERIOR FREE WALL OF BOTH VENTRICLES
- 3 ACTIVATION OF ANTEROLATERAL FREE WALL OF BOTH VENTRICLES
- 4 CONTINUED ACTIVATION OF ANTEROLATERAL WALL OF RIGHT VENTRICLE AND SEPTUM, AND ACTIVATION OF BASAL WALL OF LEFT VENTRICLE
- 5 COMPLETION OF ACTIVATION OF BASAL SEPTUM AND RIGHT VENTRICLE FREE WALL



Instantaneous VA Vectors in Right Ventricular Hypertrophy — Tall R Pattern



QRS Deflections Projected on Scalar Leads



Planar QRS Loops in Right Ventricular Hypertrophy

Fig 97.—Legend on facing page

SUMMARY OF QRS CONFIGURATIONS

Leads I and V_1 : qR_s , rS
 Lead aVF: qR_s , qR_s , RS , Rs
 Lead V_1 : rS^r , rR^r , qR

Leads I and V_1 : qR_s
 Lead aVF: qR_s , qR_s , RS , Rs
 Lead V_1 : rS^r , rR^r

QRS Configuration in the Precordial Leads in the Tall R and RS^r Patterns of Right Ventricular Hypertrophy

The orientation of the 0.01-second septal VA vector and 0.02-second apicoanterior VA vector with respect to the lead axis of V_1 determines whether the tall R wave in this lead is preceded by a small initial R wave (rR^r complex), by a small Q wave (qR complex), or by embryonic R and S waves (rSR^r), or merely displays slurring or notching of its upstroke (Fig. 89). Sometimes the tall R wave in lead V_1 is followed by a small S wave.

Lead V_1 , such as those cited above, are discussed in greater detail in the section dealing with the vectorcardiographic tall R pattern.

While the specific mechanism responsible, in right ventricular hypertrophy, for the rotation of the instantaneous VA vectors to the right and anteriorly, or, less commonly, posteriorly, is not known, the effects of this rotation are readily apparent.

1 As indicated previously, the fact that the VA

2 Normally, right ventricular activation is dominated almost completely by the depolarization forces of the left ventricle, so that, with the exception of the 0.01- and 0.02-second VA vectors, virtually all of the VA vectors tend to be directed to the left and posteriorly.

ized by a del.
vector for le:

dominance of the right ventricle does not usually make its appearance until later in the QRS interval. Accordingly, onset of the intrinsicoid deflection in lead V_1 is also late (0.04 second or more).

3 As will be seen later, the displacement of the VA vectors increasingly to the right, anteriorly and in a superior direction produces the two vectorcardiographic findings most consistently present in right

ventricular hypertrophy—namely, clockwise inscription of the QRS ΣE loop in the horizontal projection and counterclockwise inscription of the spatial loop in the sagittal projection.

As previously indicated, qR complexes may occasionally be recorded in lead V_1 in right ventricular hypertrophy. Sometimes the Q wave in this lead can be attributed to the fact that the initial 0.01-second VA vector is oriented relatively perpendicular to the lead axis of V_1 . Thus, the initial R wave of what would

leftward initial deflection of the QRS ΣE loop in the vectorcardiogram. Some of the mechanisms which have been proposed in explanation of this latter finding are as follows.

1. The leftward deflection of the QRS ΣE loop has been interpreted as signifying initial excitation of the right septal surface and subsequent septal activation in a direction the reverse of normal. The proponents of this theory believe that right-to-left septal depolarization also occurs in a small percentage of normal subjects.

2. On the other hand, the leftward orientation of the initial QRS vectors has been attributed by other authorities to increasing degrees of clockwise rotation of a vertical heart around its longitudinal axis.

3. It has also been postulated that the initial negativity of the right septal surface may be due to a decrease in certain areas of the density of the union between Purkinje fibers and muscle fibers as the result of dilatation of the ventricle.

4. Still another theory proposes that potentials arising in the high basal portion of the septum are transmitted to the right precordium through a dilated right atrium. This region of the septum is activated late in systole and dominated earlier in the QRS interval by potentials produced by activation of free ventricular wall, the former factor accounting for the late R wave and the latter for the Q wave in lead V_1 .

In the tall R pattern of right ventricular hypertrophy the chest leads show a reversal of the normal precordial QRS transition, that is to say, instead of the normal progressive increase in the R/S amplitude ratio from right to left across the precordium, the

Leads I and V₄: Beginning upstroke of an R wave.

Lead aVF: Upstroke of an R wave.

Lead V₁: Isoelectric segment or a minor upward or downward deflection, depending on minor differences in the position of the 0.02-second VA vector.

Leads I and V₆: Beginning upstroke of an R wave.

Lead aVF: Upstroke of an R wave or beginning upstroke of an R wave following a small Q wave

Lead V₁: Descending limb of a small initial R wave or the beginning downstroke of the following S wave.

0.04-SECOND VA VECTOR

Shortly before the appearance of the 0.04-second VA vector, and much earlier in the period of ventricular activation than is the rule in the RSR' pattern of right ventricular hypertrophy, the hypertrophied right ventricle in the tall R pattern of right ventricular hypertrophy begins to assert its electrical predominance, as evidenced by the development of subsequent instantaneous vectors in a superior, anterior, and rightward direction. Thus, the 0.04-second VA vector in this right ventricular hypertrophy pattern extends only slightly inferiorly and to the left or extends slightly to the right. In either case, it projects far anteriorly.

Although the electrical predominance of the left ventricle continues to be maintained, it is not so complete as is normally the case, since the opposing right ventricular forces of increasing magnitude counterbalance a larger and larger fraction of the left ventricular forces, in contrast with the normal course of events. In consequence, the resultant of the component left and right ventricular forces, the 0.04-second VA vector, is of lesser magnitude than normal and extends less to the left and posteriorly, or may even lie slightly anteriorly. Generally, however, this vector remains the maximal mean instantaneous VA vector, just as it is normally

Leads I and V₆: Beginning downstroke of a deep S wave if the vector lies to the right, or the descending limb of an R wave if it lies to the left

Lead aVF: Descending limb of the R wave

Lead V₁: Beginning upstroke of a tall R wave

Leads I and V₆: Peak of the R wave.

Lead aVF: Completion of the upstroke or descending limb of R wave.

Lead V₁: Nadir of S wave (The S wave in V₁ may be shallower than the normal S wave in this lead because of the more anterior orientation of the 0.04-second VA vector in the RSR' pattern of right ventricular hypertrophy)

0.06-SECOND VA VECTOR

As the relative strength of the left ventricular potentials continues to wane, the preponderance of right ventricular forces becomes increasingly marked. As a result, the 0.06- and 0.08-second VA vectors are of increased magnitude and come to be oriented more and more toward the effective electrical site of the right ventricle—i.e., superiorly, to the right, and anteriorly

During the terminal half of the ventricular activation period, right ventricular forces begin to exceed left ventricular forces, and, as this progresses, the instantaneous VA vectors rotate anteriorly, superiorly or upward, and to the right. Thus, the 0.06- and 0.08-second VA vectors assume an anterior, inferior, and slightly leftward or increasingly rightward position

Leads I and V₆: Terminal deep S wave of greater size than the preceding R wave

Lead aVF: Terminal S wave, which may or may not be larger than the preceding R wave

Lead V₁: Completion of tall, terminal R wave, which is the sole component wave or the dominant component of the ventricular deflection in lead V₁

Leads I and V₆: Terminal S wave, which is smaller than the preceding R wave.

Lead aVF: Completion of R wave or small terminal S wave

Lead V₁: Completion of terminal R' wave, which may or may not be larger than the preceding S wave

R/S ratio is greater in V_1 than in V_6 and decreases from right to left across the precordium (Fig 100). The reversed precordial transition in right ventricular hypertrophy results from the displacement of the instantaneous vectors toward the right and anteriorly, away from their normal location to the left and pos-

teriorly. This abnormality becomes increasingly obvious in the precordial electrocardiogram as the orientation of the maximal V_A vector (or \bar{A} QRS in the horizontal plane) approaches the positive axis of lead V_2 ($+90^\circ$), and quite marked when the maximal vector shifts to the right of this point

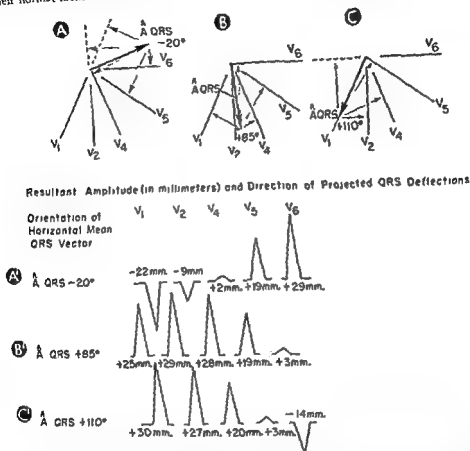
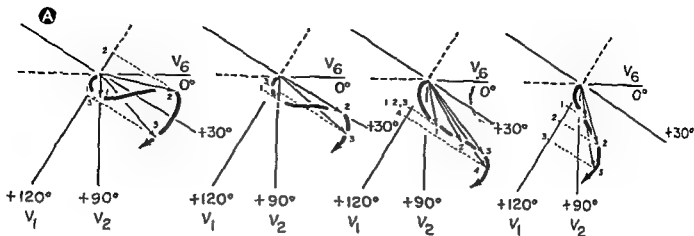
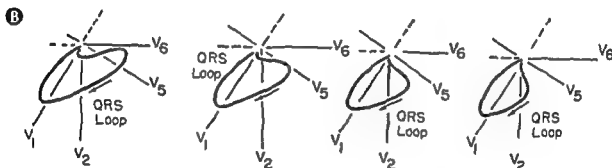


Fig 100.—Explanation of reversed precordial QRS transition in right ventricular hypertrophy. It should be remembered that the projection of a mean vector on a lead axis yields information only in terms of the net polarity and net area or voltage of QRS. In A, the mean QRS vector occupies a normal position in the horizontal plane, at about -20° , and, as can be seen in A', projects a normal precordial QRS transition on the chest leads. From V_1 to V_6 , there is a steadily increasing net positivity.

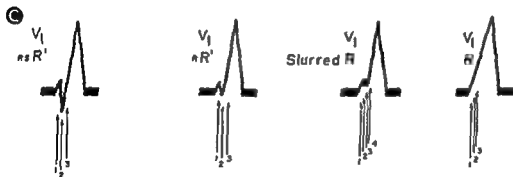
maximal resultant positivity on right precordial leads (C') and resultant negativity on left precordial leads, the result being a striking reversal in the precordial QRS transition. The arbitrarily selected length of the mean QRS vector is the same in A, B, and C. The measured projection of the mean QRS vector on each lead axis is expressed in millimeters. From the latter values were derived the resultant amplitudes of the schematic deflections depicted in A', B', and C'.



Variations in course of the early efferent limb of the horizontal QRS loop in RVH



Corresponding configurations of the horizontal QRS loops in RVH



Related variations in the initial portion of the QRS deflection in Lead V_1

Fig 99.—The effect of variations in the course of the efferent limb of the horizontal QRS loop in right ventricular hypertrophy on the QRS configuration in lead V_1 . A planar vectors, and their projections on the lead from which the projections of that, in the first there is a slur on the upstroke of the R wave, and in the last striking changes in QRS configuration in lead V_1 characteristics of vectors 1-3 and corresponding parts of the QRS loop wave recorded in lead V_1 . Note the R deflection in the third.

ORIENTATION OF A QRS

Frontal Plane

The orientation of A QRS in the frontal plane was calculated by the authors of this text from electrocardiograms of 90 patients with vectorcardiographic right ventricular hypertrophy due to congenital heart disease, mitral stenosis, or chronic cor pulmonale

	RANGE	AVERAGE
Congenital heart disease	+75° to -150°	+130°
Mitral stenosis	0° to +140°	+100°
Chronic cor pulmonale	+120° to -90°	+145°

Horizontal Plane

The orientation of A QRS in the horizontal plane was not calculated by the authors because it was not possible to do so with any degree of accuracy in many instances *

Lengthened activation time of the hypertrophied right ventricle



Rotation of the mean instantaneous T spatial vectors away from the mean instantaneous QRS spatial vectors

EXTREMITY LEADS

Leads I and aVL record upright T waves, and leads II, III, aVR, and aVF usually register inverted T waves and depressed ST segments

PRECORDIAL LEADS

Lead V₁ usually displays inverted T waves and depressed ST segments, while the T waves are upright in lead V₆

RELATED T WAVE CRITERIA

Leads V₁ and V₂ record inverted T waves with R waves of 5 mm or more amplitude

QRS criteria for the diagnosis of right ventricular hypertrophy recommended by Milnor

1 R/S or R'/S ratio in V₁ greater than 1 with R or R' greater than 0.5 mv, and a QRS duration less than 0.12 second

2 Milnor considers right-axis deviation of A QRS to be diagnostic of right ventricular hypertrophy if A QRS is situated to the right and between +110° and -91°

QRS criteria for the diagnosis of right ventricular hypertrophy recommended by the authors of this text.

1. An R/S, R'/S or an R/Q ratio of 1 or greater

3 Right axis deviation of A QRS to the right of +110°.

4 An R/Q ratio of 1 or greater

*The reason for this is that the orientation of A QRS in the horizontal plane was not calculated by the authors because it was not possible to do so with any degree of accuracy in many instances *

VENTRICULAR REPOLARIZATION

For essentially the same reasons as applied in the case of left ventricular hypertrophy, secondary and, less commonly, primary T wave abnormalities occur in right ventricular hypertrophy. When the right ventricular myocardium is hypertrophied, a longer time is required for activation to spread from endocardium to epicardium. Consequently, endocardial layers of muscle are able to recover earlier than subepicardial muscle, with the result that repolarization spreads through the right ventricular wall in a direction the reverse of normal. Repolarization forces arising in the right ventricle therefore summate with those produced in the left ventricle and cause the instantaneous T vectors almost always to be directed away from the terminal instantaneous VA (QRS) vectors, and, less

frequently, away from the maximal instantaneous VA (QRS) vector. Thus, the mean or maximal T vector is usually directed to the left, posteriorly, and superiorly in the RSR' pattern, and less to the left and more posteriorly and inferiorly in the tall R pattern.

In short, when there is an upright terminal component of the QRS deflection in V_1 , the following T wave is generally inverted, when there is a terminal S wave in V_1 , the T wave may be upright. Prominent S-T segment depression in right precordial leads is not so common in right ventricular hypertrophy as is S-T segment depression in the left precordial leads in left ventricular hypertrophy; but, when present in the former, it is usually associated with the tall R pattern of right ventricular hypertrophy.

GENERAL ECG FINDINGS AND RELATED DIAGNOSTIC CRITERIA IN RIGHT VENTRICULAR HYPERTROPHY

Increased magnitude and/or more anterior, superior, and rightward orientation of the mean instantaneous QRS spatial vectors

EXTREMITY LEADS

1. Leads I and aVL record RS or rS deflections, while leads II, III, and aVF commonly record qR, qRs, or R_s deflections, or, less commonly, in marked right-axis deviation, these leads display rS complexes. There is usually a tall terminal R wave in lead aVR.

R in aVR ≥ 5 mm

2. There is usually right-axis deviation of the mean manifest electrical axis of QRS. Thus, lead I usually registers an essentially downward ventricular deflection. If leads II and III record upright QRS deflections, then the electrical axis or mean frontal QRS vector is situated in

the right half of the frontal reference frame, and the QRS deflection in QRS vector lies to the right and above the -150° axis of the frontal reference frame. In such an instance, the bipolar limb leads show the $S_1-S_2-S_3$ pattern, each lead recording a QRS deflection whose largest component is an S wave.

PRECORDIAL LEADS

1. Although the configuration of the QRS complex recorded in lead V_1 may vary widely from case to case in right ventricular hypertrophy, nevertheless, in virtually every diagnosable case the resultant voltage of the deflection has a positive sign. In other words, whether the QRS deflection in lead V_1 has an rSR', qR, Rs, or rR' configuration, in each instance the QRS deflection is predominantly upright. Lead V_6 may record a QRS deflection of essentially normal size and configuration in right ventricular hypertrophy, but when the electrocardiographic pattern of right ventricular hypertrophy is well developed, this lead generally registers an equiphasic RS deflection or an rS or qrS deflection.

RELATED QRS VOLTAGE CRITERIA

R in $V_1 \geq 7$ mm
 S to $V_1 \leq 1$ mm
 R/S ratio in $V_1 > 1$
 R in $V_1 + S$ in V_6 or $V_6 > 10.5$ mm
 R in V_6 or $V_6 \leq 1$ mm
 S in V_6 or $V_6 \geq 7$ mm
 R/S ratio in V_6 or $V_6 \leq 1$

2. Since the mean instantaneous QRS spatial vectors are displaced to the right and anteriorly in right ventricular hypertrophy, the corresponding mean horizontal QRS vector is rotated accordingly and tends to assume a position almost 180° away from its normal location. Consequently, in right ventricular hypertrophy there is a reversed precordial QRS transition, as evidenced by a right-to-left progressive decrease in the R/S amplitude ratio.

tion of the loop, a relatively minor limb is then written to the left and anteriorly, its limited leftward extent reflecting earlier onset of right ventricular preponderance in comparison with the RSR' pattern of right ventricular hypertrophy. If the leftward limb of the loop extends into the 0° to +30° segment of the horizontal reference frame, lead V_1 records a small S wave, if it reaches the +30° axis without passing beyond, the initial R wave in V_1 is followed by a notch which does not descend below the isoelec-

tric base line (Fig. 99); if the leftward deflection is written almost perpendicular to the lead axis of V_1 , a slur appears on the upstroke of the tall R wave subsequently inscribed in this lead, and, finally, if the deflection continues to be written increasingly anteriorly as well as momentarily to the left, lead V_1 registers the beginning of the upstroke of a tall R wave. After inscription of the short leftward segment, the loop abruptly swings more anteriorly and to the right and returns in a clockwise direction to

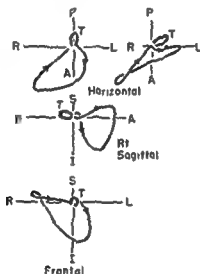
TABLE 8—QRS sE AND T sE LOOP FINDINGS IN THE TALL R AND RSR' PATTERNS OF RIGHT VENTRICULAR HYPERTROPHY

Projection	INITIAL DEFLECTION OF QRS sE LOOP	MAXIMUM MEAN INSTANTANEOUS QRS VECTOR		DIRECTION OF INSCRIPTION OF QRS sE LOOP	CONFIGURATION OF QRS sE LOOP	TERMINAL MEAN INSTANTANEOUS VECTOR OF QRS sE LOOP	MAXIMUM MEAN INSTANTANEOUS T VECTOR
		Range	AV				
Horizontal	Right, anterior, or left, anterior	Tall R +15° to +170°	+120°	Clockwise	Triangular or oval	Right, anterior or posterior	Left, posterior
		RSR' -10° to +10°	+5°	1 Clockwise 2 Counter-clockwise-clockwise	1. J-shaped efferent and afferent limbs 2 Figure-of-eight loop configuration	Anterior, right	Left, posterior
Right sagittal	Anterior, superior, or anterior, inferior	Tall R -75° to +80°	+40°	1 Clockwise-counter-clockwise 2 Counter-clockwise	1. Figure-of-eight with small proximal loop 2. Elongated or oval	Anterior, inferior, or anterior, superior	Posterior, inferior, or posterior, superior
		RSR' +70° to +115°	+80°	Clockwise-counter-clockwise	Figure-of-eight	Anterior, inferior	Posterior, inferior or superior
Frontal	Right, inferior, or right, superior Occasionally left, inferior, or left, superior	Tall R +20° to -130°	+130°	Clockwise	Variable	Right, inferior; or right, superior	Left, inferior, or left, superior
		RSR' +10° to +90°	+80°	Counter-clockwise or clockwise	Variable		

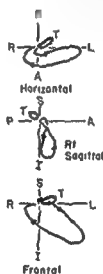
VECTORCARDIOGRAPHIC FINDINGS IN RIGHT VENTRICULAR HYPERTROPHY

Before considering the QRS sE loop configurations which correspond to the two arbitrary patterns of right ventricular hypertrophy sketched earlier in this chapter in terms of the instantaneous VA vectors and electrocardiogram, it is well to preview the vectorcardiographic abnormalities most typically and consistently observed in right ventricular hypertrophy (see also Fig. 101 and Table 8). By and large, all of the variant QRS sE loop patterns produced by right ventricular hypertrophy share in common the following general abnormalities:

1. The QRS sE loop is situated more anteriorly than is normally the case
2. The long axis of the QRS sE loop tends to be rotated medially or to the right.



Tall R Configuration



RSR' Configuration

Fig. 101.—Schematic planar QRS and T loops depicting the vectorcardiographic characteristics of the RSR' and tall R patterns of right ventricular hypertrophy.

3. The farther to the right the rotation of the QRS sE loop, the less inferior or the more superior is its location, as a general rule
4. The afferent limb of the QRS sE loop, either in whole or in part, is written in a rightward, anterior, and superior direction, and this causes corresponding portions of the horizontal and right sagittal QRS loops to be inscribed in clockwise and counterclockwise directions, respectively

Vectorcardiographic Tall R Pattern

The essential characteristics of this QRS sE loop pattern of right ventricular hypertrophy (see also

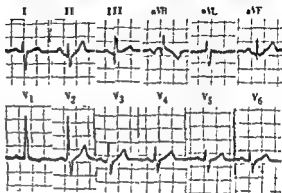
Figs. 101 and 102) can be listed as follows:

1. The long axis or maximal mean instantaneous vector of the QRS sE loop is oriented either far to the right and somewhat anteriorly (occasionally posteriorly) or almost directly anteriorly and slightly to the right.
2. Alternatively, the mean instantaneous vectors of the QRS sE loop may extend anteriorly and equally to the left and right of the midline.
3. The mean instantaneous vectors of the QRS sE loop which lie to the right and anteriorly are of much greater magnitude than corresponding vectors in the RSR' loop pattern of right ventricular hypertrophy, which will be described later. These large rightward and anterior vec-

tors are responsible for the tall R wave recorded in lead V₁ of the electrocardiogram

The planar QRS loops of the vectorcardiogram in

projection, the QRS sE loop can have an initial deflection directed to the right and anteriorly or one directed to the left and slightly anteriorly or posteriorly. (Some of the theories which have been proposed to account for the apparent reversed direction of the septal activation forces were considered earlier.) Following the initial deflec-



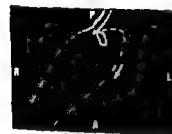
septal activation produces forces directed to the left and posteriorly (a not infrequent finding in right ventricular hypertrophy).

teriorly, as is the maximal mean instantaneous QRS vector.

sequently (2) the frontal QRS loop is rotated inferiorly and medially and lies at about $+75^\circ$.



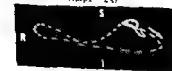
HORIZONTAL



HORIZONTAL
(Ampl. 2X)



RIGHT SAGITTAL
(Ampl. 2X)



FRONTAL
(Ampl. 2X)

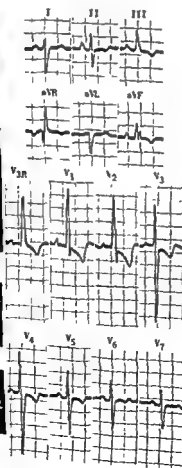


Fig. 104.—Electrocardiographic and vectorcardiographic findings supporting the diagnosis of right ventricular hypertrophy in a man, 30, with cyanotic congenital heart disease of unknown type.

Electrocardiographic findings supporting the diagnosis of right ventricular hypertrophy are: (1) There is right-axis deviation of Λ QRS ($+150^\circ$). (2) The terminal R of the QR deflection in aVR is greater than 5-mm amplitude. (3) There are small Q and tall R waves (18 mm) with late onset of intrinsoid deflection (0.07 second) in lead V_1 and a reversed precordial QRS transition. (4) The T waves are inverted in the precordial leads showing upright QRS deflections, which signifies an abnormally wide QRS-T spatial angle.

The diagnostic vectorcardiographic abnormalities are: (1) After the initial inscription of the QRS sE loop to the left, slightly posteriorly and inferiorly, the loop is written primarily anteriorly and to the right, in a clockwise direction in the horizontal projection and in a counterclockwise direction in the sagittal projection. The maximal mean instantaneous QRS spatial vector is situated to the right, anteriorly, and inferiorly. (2) There is a small S-T vector directed to the right. (3) The T sE loop is almost 150° discordant to the QRS sE loop. (4) The anterior orientation of the P sE loop is suggestive of right atrial enlargement.

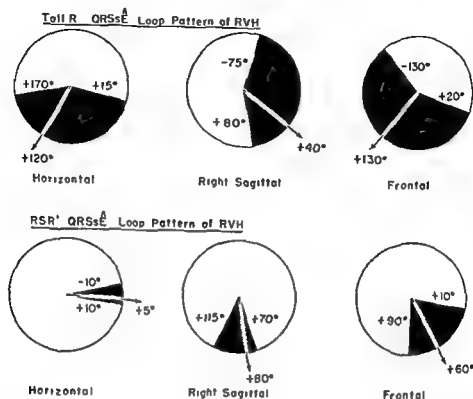


Fig. 102.—Extreme range of variation and average orientations of the maximal mean instantaneous QRS planar vectors of the QRS sE loops in the tall R and the RSR' vectorcardiographic patterns of right ventricular hypertrophy.

its point of origin. The maximal instantaneous QRS vector tends to lie in the right anterior quadrant. Since most of the larger instantaneous QRS vectors are situated anterior and, in the case of the later vectors, to the right, tall R waves are projected on leads V_{3n} , V_1 , and V_2 and S waves on V_6 .

- b) Right sagittal QRS loop—Following an initial deflection anteriorly and slightly superiorly, the QRS sE loop in the sagittal projection is usually written in a counterclockwise direction anteriorly and at first inferiorly and later slightly superiorly. Occasionally the greater part of the sagittal QRS loop is situated superiorly.
- c) Frontal QRS loop—After inscription of the initial deflection, which can be directed to the right or left (see discussion of horizontal QRS loop, above), the frontal QRS loop is usually written in a clockwise direction to the left and inferiorly and then returns on the right and inferiorly or somewhat superiorly. Since the loop projects farther to the right than to the left in this pattern, lead I registers an rS deflection, and leads II, III, and aVF, R waves or RS deflections. Occasionally the QRS sE loop in the frontal pro-

jection is inscribed in a counterclockwise direction to the left and superiorly and then to the right. In this instance, all limb leads register rS deflections except lead aVR, which records a QR complex.

Vectorcardiographic RSR' Pattern

The theories as to the manner in which this vectorcardiographic pattern of right ventricular hypertrophy (and the corresponding electrocardiographic pattern) is produced are as varied as they are numerous. Some authorities attribute the terminal R' to delayed spread of activation through a right ventricular wall of normal thickness but with greatly hypertrophied trabeculae. Others consider the late rightward forces to be due to incomplete right bundle dilatation. Perhaps the most attractive theory, and certainly the theory favored by the weight of evidence, is that the late rightward and anteriorly directed forces in the RSR' pattern of right ventricular hypertrophy are produced by activation of hypertrophied basal regions of the right ventricle, including the crista supraventricularis, its parietal and septal bands, and the trabecular network of the right ventricle. Selective hypertrophy of these regions, mac-

the left and posteriorly (a not infrequent finding in right ventricular hypertrophy).

The diagnostic vectorcardiographic findings are: (1) The QRS sE loop is displaced anteriorly and to the right. (2) The

teriorly as is the maximal mean instantaneous

the usual QRS loop is rotated inferiorly and medially and lies at about $+75^\circ$.

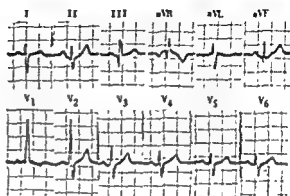
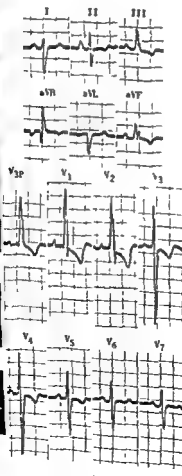
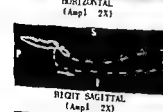


Fig. 104.—Electrocardiographic and vectorcardiographic tall R pattern of right ventricular hypertrophy recorded in a man, 30, with cyanotic congenital heart disease of unknown type.

Electrocardiographic findings supporting the diagnosis of right ventricular hypertrophy are: (1) There is right-axis deviation of A QRS ($+150^\circ$). (2) The terminal R of the QR deflection in aVR is greater than 5-mm amplitude. (3) There are small Q and tall R waves (18 mm) with late onset of intrinsoid deflection (0.07 second) in lead V₁ and a reversed precordial QRS transition. (4) The T waves are inverted in the precordial leads showing upright QRS deflections, which signifies an abnormally wide QRS-T spatial angle.

The diagnostic vectorcardiographic abnormalities are: (1) Alter the initial inscription of the QRS sE loop to the left, slightly posteriorly and inferiorly, the loop is written primarily anteriorly and to the right, in a clockwise direction in the horizontal projection and in a counterclockwise direction in the sagittal projection. The maximal mean instantaneous QRS spatial vector is situated to the right, anteriorly, and inferiorly. (2) There is a small S-T vector directed to the right. (3) The T sE loop is almost 150° discordant to the QRS sE loop. (4) The anterior orientation of the sE loop is suggestive of right atrial enlargement.



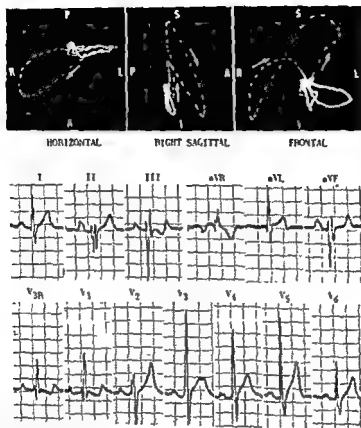


Fig 106—Electrocardiographic and vectorcardiographic patterns of right ventricular hypertrophy in a boy, 15, with surgically proved interatrial septal defect

clockwise in the loop
shaped The
se loop in t
medially

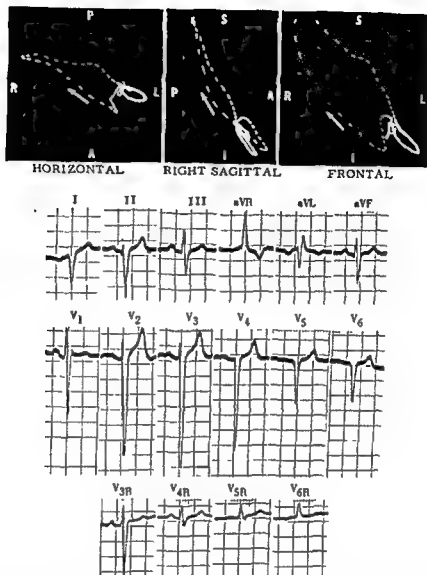


Fig. 107.—Electrocardiographic and vectorcardiographic patterns of right ventricular hypertrophy in a youth, 21, with undiagnosed cyanotic congenital heart disease. The electrocardiogram displays the $S_1-S_{II}-S_{III}$ pattern, which is most commonly observed in chronic cor pulmonale.

The electrocardiographic findings of significance are these. (1) $\Delta QRS = -150^\circ$ in the frontal plane, $\Delta T = +60^\circ$, $\Delta P = +120^\circ$. (2) All limb leads display resultant negative QRS deflections except for lead III, which shows an equiphasic RS deflection, and lead aVR, which records a tall R wave. (3) $\Delta QRS = -135^\circ$ in the horizontal plane. There is a reversed precordial QRS transition with resultant positivity on the right (leads V_{1R} to V_{6R}) and resultant negativity on the left.

for
insc

accompanied by more generalized hypertrophy of the right ventricular wall, has been observed pathologically in association with cardiac lesions which increase right ventricular stroke volume.

The essential characteristics of the RSR' type of QRS sE loop configuration (Figs. 101 and 102) are as follows.

1. The long axis or maximal mean instantaneous vector of the QRS sE loop is oriented to the left and slightly anteriorly or posteriorly and has much the same magnitude as normally.
2. The efferent limb of the QRS sE loop is inscribed more or less normally, but the entire afferent limb or the terminal half of the afferent limb is written to the right and anteriorly with a reversed direction of inscription in the horizontal and sagittal projections

The more detailed features of the planar QRS loops in the RSR' pattern of right ventricular hypertrophy are presented in the following paragraphs.

- a) *Horizontal QRS loop*—In the horizontal projection the QRS sE loop moves at first to the right and anteriorly, the initial deflection resembling that of the normal QRS sE loop. The loop is then written to the left, posteriorly or slightly anteriorly, and inferiorly. In general, the onset of right ventricular electrical predominance is signaled by a deflection of the QRS sE loop in an anterior, rightward, and superior direction. When the horizontal QRS loop reaches its turning point or maximal leftward extent, instead of turning in a counterclockwise direction posteriorly the loop rotates anteriorly and is then written in a clockwise direction from left to right. Thus, the afferent or returning limb of the loop is situated anterior to, and eventually to the right of, the efferent or outgoing limb. Generally the terminal segment of the loop is written farther to the right than the initial deflection, and it may even extend posteriorly. Sometimes the QRS

sE loop has a figure-of-eight configuration in the horizontal projection, in which case the first half of the loop is inscribed in a counterclockwise direction, and the second half, in a clockwise direction.

- b) *Right sagittal QRS loop*.—The QRS sE loop in this projection is usually written inferiorly and anteriorly along roughly the $+70^\circ$ to $+80^\circ$ axis. It may be written in a clockwise direction just as normally, but more often it has a figure-of-eight contour, the distal loop of which is inscribed in a counterclockwise direction.
- c) *Frontal QRS loop*.—The frontal projection of the QRS sE loop lies, for the most part, to the left of the midline and is usually situated within the $+30^\circ$ to $+90^\circ$ segment of the frontal reference frame. The loop is clockwise inscribed in most instances and exhibits a rightward and sometimes superiorly oriented terminal deflection.

S-T Vector and T sE Loop

(See discussion, in Chapter 8, of ventricular hypertrophy.)

In the absence of digitalis effect, an S-T vector is relatively uncommon in the vectorcardiographic RSR' pattern of right ventricular hypertrophy, although not infrequently an S-T vector is observed in the tall R pattern. In the latter pattern, the S-T vector can be ascribed, in part at least, to secondary repolarization changes consequent to the augmented depolarization forces produced by the right ventricle. When present in right ventricular hypertrophy, the S-T vector tends to be directed to the right, slightly posteriorly, and either superiorly or inferiorly.

The most consistent feature of the T sE loop in either type of vectorcardiographic right ventricular hypertrophy pattern is that it is almost invariably discordant to the terminal mean instantaneous QRS vectors (Figs. 103–107)

Combined Ventricular Hypertrophy; Ventricular Hypertrophy in Children

COMBINED VENTRICULAR HYPERTROPHY

Electrocardiographic Diagnosis

THE FREQUENCY with which significant hypertrophy of both ventricles is observed clinically and at post-mortem has evoked numerous attempts in the past to define criteria for the electrocardiographic diagnosis of this condition. That the electrocardiographic diagnosis of combined ventricular hypertrophy—if such a diagnosis can be made with any degree of certainty—very tenuous can be inferred from the wide variety of criteria which have been proposed. A résumé of some of the findings thought by different authorities to be indicative of combined hypertrophy follows

CRITERIA OF COSBY AND ASSOCIATES.—1. There is no significant reversal of the R/S ratio in V_1 , but the onset of the intrinsoid deflection in general occurs later than normally in this lead, but not later than its onset in V_6 .

2. The II wave of V_1 and/or the II wave of V_6 exceeds the normal amplitude.

LEPESCHIKIN'S CRITERIA.—1. Right ventricular dilatation accompanying left ventricular hypertrophy may cause the precordial QRS transitional point to shift far to the left, up to or beyond V_6 ; but the pattern of left ventricular strain* persists in the limb leads. A second suggestive finding consists of the presence of an S wave in lead I with a left ventricular strain pattern in the limb leads.

2. Combined right and left ventricular hypertrophy may produce a tall R wave followed by an inverted T wave in right and left ventricular leads with

a delayed intrinsoid deflection in leads V_1 and V_6 .

3. If there is a "perfect balance" of potentials from the two hypertrophied ventricles, the electrocardiogram may be normal.

CRITERIA OF SODI-PALLARES AND ASSOCIATES.—

1. A tall R wave may be present in lead V_1 with small or absent negative deflections. The T waves in right precordial leads may be upright or inverted.

2. Leads II, III, aVF, V_6 , and V_4 display tall, peaked symmetrical T waves, elevation of the S-T segments, which are upwardly concave, and tall R waves, which in lead V_6 have delayed onset of the intrinsoid deflection.

3. In combined ventricular hypertrophy due to ventricular septal defect, Sodi-Pallares and his associates have observed large diphasic complexes in leads V_2 , V_3 , and V_4 (Katz-Wachtel sign), persistent S waves in V_5 and V_6 , and a great shift to the right or upward of A QRS.

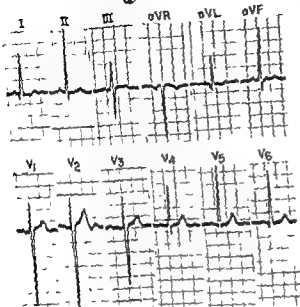
CRITERIA OF PAGNONI AND GOODWIN.—1. A finding which is considered suggestive of combined ventricular hypertrophy is the association of electrocardiographic vertical heart position with signs of left ventricular hypertrophy, such as delayed onset of the intrinsoid deflection in lead V_3 (0.05 second or longer after onset of the QRS interval) and S-T segment depression and T wave inversion in the same lead.

2. There are present an R wave greater than the Q wave in lead aVR, an S wave larger than the R wave in V_3 , and inversion of the T wave in V_1 , together with signs of left ventricular hypertrophy.

CRITERIA OF ROSENMAN AND KATZ.—1. There is electrocardiographic evidence of left ventricular hy-

*See the discussion of left and right ventricular strain on page 158

A



B

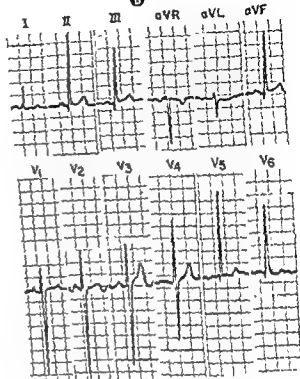


FIG. 11-1. ECG tracing A shows a normal QRS complex with a small rS pattern in the precordial leads and a small r wave in the limb leads. ECG tracing B shows a normal QRS complex with a small rS pattern in the precordial leads and a small r wave in the limb leads.

author

hypertrophy, as defined in the criteria of Sokolow and Lyon

2 This is accompanied by indirect evidence of right ventricular hypertrophy, such as "clockwise rotation," electrical heart positions other than horizontal or semihorizontal, or the P mitrale pattern of atrial hypertrophy and/or atrial fibrillation

Vectorcardiographic Findings

Crashman and his associates have not reported observing any vectorcardiographic pattern pathognomonic of combined ventricular hypertrophy. In certain forms of congenital heart disease which typically lead to biventricular hypertrophy (e.g., interventricular septal defects), these investigators have found vectorcardiographic manifestations of right ventricu-

lar hypertrophy in some cases and of left ventricular hypertrophy in others. However, in a considerable number of cases the vectorcardiogram shows

combined ventricular hypertrophy

THE VCG FINDINGS OF WHIFFLE, COSIO, AND LEVINE—In the horizontal projection of the vectorcardiogram recorded with the cube system of electrode placement, the QRS loop is long and very narrow, its length being at least 11 times its width. The QRS loop is oriented to the left, but not more than 20° posteriorly.

THE VCG FINDINGS OF RICHMAN AND WOLFF—1. The QRS ΔE loop lies inferiorly, slightly anteriorly, and to the left.

2. The initial QRS vectors are directed anteriorly, to the right, and slightly superiorly or inferiorly.

3. The subsequent QRS vectors of the centrifugal or efferent limb are directed anteriorly, inferiorly, and to the left.

4. The early QRS vectors of the centripetal or afferent limb point more to the left and less anteriorly and inferiorly than the preceding vectors.

5. The late QRS vectors are directed anteriorly or posteriorly, and superiorly and to the right.

6. The horizontal and frontal projections of the QRS sE loop have figure-of-eight configurations with the proximal loop counterclockwise inscribed and the distal loop clockwise inscribed.

7. The sagittal projection of the QRS sE loop has a figure-of-eight configuration with the proximal loop clockwise inscribed and the distal loop counterclockwise inscribed.

8. The T vectors are directed inferiorly, posteriorly, and to the left or away from the terminal QRS vectors.

9. The T loops are inscribed clockwise in the horizontal and frontal projections and counterclockwise in the sagittal projection.

In recording their vectorcardiograms, Richman and Wolff utilize the Duchosal-Sulzer double-cube system of electrode placement, which tends to magnify the vertical component of the cardiac vector. Otherwise their results can be applied to vectorcardiograms recorded with Grishman's cube modification of Duchosal-Sulzer's lead system.

Although we have observed vectorcardiographic patterns similar to those described by Whipple, Cosio and Levine and by Richman and Wolff, we have not been able to correlate these patterns specifically with combined ventricular hypertrophy. In fact, the QRS sE loop pattern described by Richman and Wolff has been recorded by us more frequently in cases of interatrial septal defect (a lesion not associated with biventricular hypertrophy) than in cases of patent ductus arteriosus or ventricular septal defect, which frequently produce anatomic hypertrophy of both ventricles.

At present, it would seem that both the electrocardiographic and the vectorcardiographic manifestations of combined ventricular hypertrophy require further delineation (Fig. 108).

VENTRICULAR STRAIN PATTERNS

In the original descriptions of ventricular strain patterns, the term *left ventricular strain* was applied to the pattern of left-axis deviation in the bipolar limb leads and T wave inversion in leads I and/or II, while right-axis deviation with T wave inversion in leads II and III was called *right ventricular strain*. To these patterns was later attached the inference that left ventricular strain was suggestive of left ventricular hypertrophy, and right ventricular strain, of right ventricular hypertrophy. As the science of electrocardiography developed and the precordial leads were added, the terminology of left and right ventricular strain was retained with various amendments and modifications. At present, left ventricular strain is applied by some to the findings of T wave inversion in leads I or II and in leads V_4 to V_6 with QRS complexes of normal size and configuration. The right ventricular strain pattern has been defined by Goldberger as consisting of "marked clockwise rotation of the heart" so that leads V_1 through V_3 or V_4 show rS or RS deflections accompanied by T wave inversion. Inverted T waves may also be present in leads aVL and aVF and in leads II and III.

The present status of these two patterns can be summarized as follows.

1. The early definitions of right and left ventricular strain patterns were based on the very limited information available, some of which was subsequently shown to be erroneous.

2. At present there is no agreement as to what constitutes these electrocardiographic patterns, nor agreement as to their implications.

3. There is agreement, however, that the term *strain* has unfortunate connotations which have no place in electrocardiography.

4. The so-called "left ventricular strain pattern" can appear in such widely diversified conditions as, for instance, coronary artery disease, myocarditis, and digitalis effect. Some argument can be raised as to whether the T wave inversion of the right ventricular strain pattern necessarily reflects changes in the right ventricle at all. Thus, posterior rotation of the QRS loop, due to various causes, with the T loop maintaining its normal position within 30° to 60° of the former, can produce T wave inversion over much of the precordium.

5. There seems to be a general trend toward abandoning entirely the terms "right ventricular strain" and "left ventricular strain."

VENTRICULAR HYPERTROPHY IN INFANCY AND EARLY CHILDHOOD

ular hypertrophy, the fact soon becomes apparent that these criteria pertain chiefly to adults and are quite unreliable in infants and young children. The factors responsible for the failure of the diagnostic criteria of left and right ventricular hypertrophy in the younger age group are primarily two (1) The

electrocardiogram and the criteria for the diagnosis of ventricular hypertrophy in this age group will be described.

The Normal Vectorcardiogram and Electrocardiogram

The concept of physiologic right ventricular preponderance during the neonatal period is well sup-

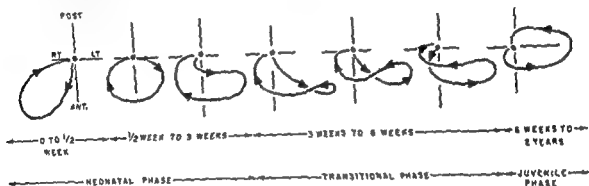


Fig 109.—A series of horizontal QRS loop diagrams showing the evolution of the vectorcardiogram from birth to 2 years of age. The loops are labeled with 'POST', 'RT', 'LT', and 'ANT'. Below the diagrams, a horizontal line is divided into three phases: NEONATAL PHASE (0 to 3 weeks), TRANSITIONAL PHASE (3 to 6 weeks), and JUVENILE PHASE (6 weeks to 2 years). The loops show a progression from a large, deep, and wide loop in the neonatal phase to a smaller, more compact loop in the juvenile phase.

electrocardiographic criteria for the diagnosis of right and left ventricular hypertrophy are based, for the most part, on data derived from studies of adults (2) The normal electrocardiogram in infants and

(a) right voltage of the QRS deflections in the left precordial leads or in all twelve leads of the routine electrocardiogram, (b) relatively tall R waves in the right precordial leads, (c) right-axis deviation of the mean manifest electrical axis of QRS, and (d) abnormally wide angular divergence of the mean QRS and T spatial vectors

Although vectorcardiographic studies of infants and young children are relatively limited in number to date, there is reason to believe that the vectorcardiogram will prove a useful adjunct to the electrocardiogram in the diagnosis of ventricular hypertrophy in this age group

After the discussion of the vectorcardiographic findings in infants and young children, the normal

ported by anatomic and electrocardiographic studies of the infant heart. Moreover, this concept is quite compatible with the fact that the fetal circulation burdens the right ventricle more than the left. With the birth of the infant, the left ventricle normally begins its lifelong performance of the greater proportion of the cardiac work, at birth the weight of the right ventricle usually exceeds that of the left ventricle, but after 2 weeks the left ventricle becomes slightly heavier than the right. After 4-6 weeks the left ventricle begins to grow more rapidly than the right, and within 7-12 months after birth the normal adult ratio of left ventricular weight to right ventricular weight is attained (approximately 2:1). There is preliminary evidence to indicate that the changing ratio of ventricular weights during the 12-month period following birth produces a characteristic sequence of vectorcardiographic changes. This sequence will be described in three phases: the neonatal, transitional, and juvenile phases (Fig. 109.)

For purposes of description, the neonatal phase is

2. The initial QRS vectors are directed anteriorly, to the right, and slightly superiorly or inferiorly.

3. The subsequent QRS vectors of the centrifugal or efferent limb are directed anteriorly, inferiorly, and to the left.

4. The early QRS vectors of the centripetal or afferent limb point more to the left and less anteriorly and inferiorly than the preceding vectors.

5. The late QRS vectors are directed anteriorly or posteriorly, and superiorly and to the right.

6. The horizontal and frontal projections of the QRS sE loop have figure-of-eight configurations with the proximal loop counterclockwise inscribed and the distal loop clockwise inscribed.

7. The sagittal projection of the QRS sE loop has a figure-of-eight configuration with the proximal loop clockwise inscribed and the distal loop counterclockwise inscribed.

8. The T vectors are directed inferiorly, posteriorly, and to the left or away from the terminal QRS vectors.

9. The T loops are inscribed clockwise in the horizontal and frontal projections and counterclockwise in the sagittal projection.

In recording their vectorcardiograms, Richman and Wolff utilize the Duchosal-Sulzer double-cube system of electrode placement, which tends to magnify the vertical component of the cardiac vector. Otherwise their results can be applied to vectorcardiograms recorded with Grishman's cube modification of Duchosal-Sulzer's lead system.

Although we have observed vectorcardiographic patterns similar to those described by Whipple, Cosio and Levine and by Richman and Wolff, we have not been able to correlate these patterns specifically with combined ventricular hypertrophy. In fact, the QRS sE loop pattern described by Richman and Wolff has been recorded by us more frequently in cases of interatrial septal defect (a lesion not associated with biventricular hypertrophy) than in cases of patent ductus arteriosus or ventricular septal defect, which frequently produce anatomic hypertrophy of both ventricles.

At present, it would seem that both the electrocardiographic and the vectorcardiographic manifestations of combined ventricular hypertrophy require further delineation (Fig. 108).

VENTRICULAR STRAIN PATTERNS

In the original descriptions of ventricular strain patterns, the term *left ventricular strain* was applied to the pattern of left-axis deviation in the bipolar limb leads and T wave inversion in leads I and/or II, while right-axis deviation with T wave inversion in leads II and III was called *right ventricular strain*. To these patterns was later attached the inference that left ventricular strain was suggestive of left ventricular hypertrophy, and right ventricular strain, of right ventricular hypertrophy. As the science of electrocardiography developed and the precordial leads were added, the terminology of left and right ventricular strain was retained with various amendments and modifications. At present, *left ventricular strain* is applied by some to the findings of T wave inversion in leads I or II and in leads V_1 or V_2 with QRS complexes of normal size and configuration. The right ventricular strain pattern has been defined by Goldberger as consisting of "marked clockwise rotation of the heart" so that leads V_1 through V_3 or V_4 show rS or RS deflections accompanied by T wave inversion. Inverted T waves may also be present in leads aVL and aVF and in leads II and III.

The present status of these two patterns can be summarized as follows:

1. The early definitions of right and left ventricular strain patterns were based on the very limited information available, some of which was subsequently shown to be erroneous.

2. At present there is no agreement as to what constitutes these electrocardiographic patterns, not agreement as to their implications.

3. There is agreement, however, that the term *strain* has unfortunate connotations which have no place in electrocardiography.

4. The so-called "left ventricular strain pattern" can appear in such widely diversified conditions as, for instance, coronary artery disease, myocarditis, and digitalis effect. Some argument can be raised as to whether the T wave inversion of the right ventricular strain pattern necessarily reflects changes in the right ventricle at all. Thus, posterior rotation of the QRS loop, due to various causes, with the T loop maintaining its normal position within 30° to 60° of the former, can produce T wave inversion over much of the precordium.

5. There seems to be a general trend toward abandoning entirely the terms "right ventricular strain" and "left ventricular strain."

loops are typified by a figure-of-eight configuration and an anterior orientation. At first, the distal loop of the "eight" is small because only a very small initial segment of the afferent limb lies relatively posterior to the efferent limb. Later, more and more of the afferent limb of the QRS loop comes to lie behind the efferent limb, until late in the transitional period the loop is written almost entirely in a counterclockwise direction in the right and anteriorly or slightly posteriorly.

RIGHT SAGITTAL QRS LOOP.—The loop is usually situated anteriorly and inferiorly and has a clockwise direction of inscription.

FRONTAL QRS LOOP.—Generally, the frontal loops are oriented mainly inferiorly and to the left and are written in a clockwise direction. They may display a terminal deflection to the right and superiorly.

The horizontal QRS loops described above may project R waves with slurred or notched upstrokes or rSR' complexes on lead V_1 .

JUVENILE PHASE

HORIZONTAL QRS LOOP.—Occasionally the QRS loop has a figure-of-eight configuration, but more often it is written entirely in a counterclockwise direction. In general, the loop tends to resemble the normal adult horizontal loop except for the following features, (a) the loop lies either entirely anteriorly or half anteriorly and half posteriorly, and (b) not infrequently the loop exhibits a terminal appendage (without conduction delay) directed to the right and posteriorly.

RIGHT SAGITTAL QRS LOOP.—The major portion of the loop usually lies inferiorly and either entirely anteriorly or half anteriorly and half posteriorly. It is written in a clockwise direction.

FRONTAL QRS LOOP.—Usually, the QRS loop is oriented to the left and inferiorly and is inscribed in a clockwise direction.

If the horizontal QRS loop lies entirely anteriorly, lead V_1 tends to register an R wave of greater amplitude than the following S wave. If the long axis of the loop parallels the positive axis of lead V_6 , there may appear in the precordial leads the electrocardiographic pattern of "counterclockwise rotation," an RS deflection being written in V_2 and resultant rSR' complex.

The upper age limit for the juvenile type of vectorcardiographic pattern is not well defined. Appar-

ently, horizontal QRS loops tending to display a more anterior orientation than the loops of normal adults have been recorded in children 11 years of age. Lamb and Dimond, who utilize their own system of electrode placement rather than the cube system, have observed horizontal QRS loops having a figure-of-

TABLE 9—NORMAL STANDARDS FOR THE R, S,* AND T WAVES IN CHILDREN ACCORDING TO AGE GROUP†

	NEWBORN TO 1 YEAR	1-10 YEARS	10-20 YEARS	20 YEARS AND OVER		
Lead aVR.						
R-Maximum	9.0	6.5	8.0	4.1		
Mean	2.32	1.6	1.39	0.91		
Lead aVL:						
R-Maximum	10.0	11.8	10.1	10.1		
Mean	3.33	3.15	2.21	2.61		
Lead V ₆ :						
R-Maximum		9.0	8.0			
Mean		4.18	3.8			
Lead V ₁ :						
R-Minimum	3.0	0.4	0.4	0		
Maximum	29	20.0	16.7	15.5		
Mean	13.61	7.15	5.29	3.09		
S-Minimum	0	0	0	0.8		
Maximum	28.0	36.5	30.6	26.2		
Mean	8.57	11.02	11.09	9.41		
Lead V ₄ :						
R-Minimum	0	5.0	3.5	2.0		
Maximum	24.0	23.0	25.0	22.6		
Mean	8.0	11.01	11.11	9.68		
T WAVES	V ₁	V ₄	V ₆	V ₆	V ₆	V ₆
Inverted	16 yr.	12 yr.	10 yr.	5 yr.	15 hr.	8 hr.
Diphasic	16 yr.	16 yr.	15 yr.	11 yr.	14 hr.	1 day

*The R and S waves are considered in terms of their minimum, maximum, and mean amplitude values (expressed in millimeters) for each age group in the scalar leads used to diagnose left and right ventricular hypertrophy.

†The T waves are described in terms of the average upper age limit at which they may be found to be inverted.

This nomenclature and criteria for diagnosis of Diseases of the Heart and Blood Vessels (5th ed., New York Heart Association, 1957), the data were compiled from authoritative sources.

eight configuration commonly in children up to 6 years of age but only rarely in normal adults over 20 years. It is evident that studies of larger series of infants and children are a necessity. However, several tentative conclusions seem warranted.

1 In the diagnosis of right ventricular hypertro-

here defined as the sequence of changes occurring during the first 3 weeks after birth; the *transitional phase*, during the second 3 weeks (fourth through sixth postnatal week); and the *juvenile phase*, from the age of 11 weeks to 2 years or older. Obviously, the age groups included in these phases are subject to future change as more information about the normal vectorcardiogram in the young is accumulated.

NEONATAL PHASE

HORIZONTAL QRS LOOP.—Early in this period, the QRS sE loop lies almost entirely anteriorly and to the right and is inscribed in a clockwise direction (Fig. 109). Later, the initial deflection and early portion of the loop are written to the left, and then to the left and anteriorly, the afferent limb passes anteriorly and to the right before returning to the point of origin. Late in the neonatal period, the QRS loop tends to lie more to the left than to the right. It displays an initial deflection to the right and anteriorly, and then the efferent limb of the loop is written somewhat anteriorly but more to the left than previously. Finally, the afferent limb is inscribed in a clockwise direction to the right and anteriorly, as illustrated in Figure 110

RIGHT SAGITTAL QRS LOOP.—The neonatal phase is characterized by an anteriorly oriented sagittal loop which usually, although not invariably, is written in a clockwise direction.

FRONTAL QRS LOOP.—Early in this phase the loop lies essentially to the right and inferiorly and is written in a counterclockwise direction. Subsequently the frontal QRS loop tends to be located less to the right and more to the left and is written in a clockwise direction.

The vectorcardiographic patterns described above, if recorded from adults, would be considered typical of right ventricular hypertrophy, as would the electrocardiographic findings. Thus, the first horizontal loop pattern described above projects a tall R wave on V_1 ; the second, a qR complex; and the third loop configuration, an rR' or rSR' complex.

TRANSITIONAL PHASE

HORIZONTAL QRS LOOP.—This projection best illustrates the transition from the neonatal loop configuration of physiologic right ventricular preponderance to the loop configuration observed in children 11 months of age and older. The transitional QRS

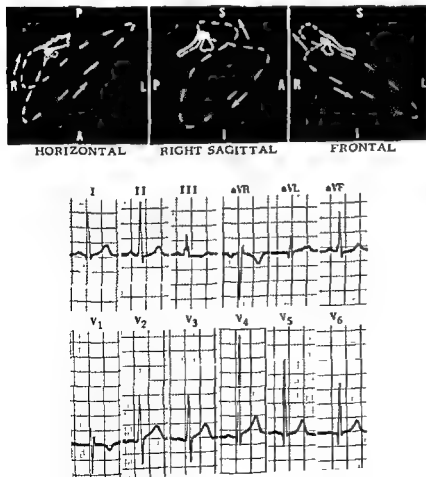


Fig. 110.—Normal electrocardiogram and vectorcardiogram in a boy.

limb and precordial leads and the RSR' deflection in lead V_1 . In the vectorcardiogram, the directions of inscription of the horizontal and sagittal QRS loops are normal except for the terminal portion of each loop, which is clockwise inscribed in the horizontal projection and counterclockwise inscribed in the sagittal projection. Both efferent and afferent limbs of the QRS sE loop are displaced anteriorly, the former more than the latter, in contrast to the adult pattern of right ventricular hypertrophy. Note also the prominent rightward, anterior, and inferior deflection of the early part of the QRS sE loop.

phy in infants and young children the electrocardiograph has obvious limitations.

2 It may be impossible to distinguish pathologic from physiologic right ventricular preponderance in the vectorcardiograms of infants less than 31 days old.

3 However, the diagnosis of pathologic right ventricular preponderance can probably be made in such infants by recording serial vectorcardiograms. According to Elek and his associates, the transitional vectorcardiographic pattern usually appears by the time an infant is 31 days old, or shortly thereafter. If serial vectorcardiograms fail to demonstrate the normal sequence of changes in the vectorcardiogram culminating in the appearance of the juvenile pattern, then pathologic right ventricular hypertrophy is probably present.

The sequence of vectorcardiographic patterns described above is compatible with the electrocardiographic studies of Ziegler in infants and young children of corresponding age groups. Ziegler found that the average amplitude of the R wave in lead V_1 exceeds that in V_6 from birth to approximately 6 months of age, that the two amplitudes are nearly equal in

less, a T wave inverted and preceded by an R wave 5 mm. or more in amplitude; an R/S ratio greater than 4 in children under 5 years and greater than 1 in children over 5 years, and ventricular activation time or pre-intrinsoid deflection time of 0.04 second or longer.

3. Lead V_5 shows an R wave amplitude of 4 mm. or less and an R/S ratio of 1 or less.

4. In leads V_1 and V_6 , $R_{V_1} + S_{V_6} = 10.5$ mm. or more in children over the age of 5 years; and

$$\frac{R}{S} \text{ ratio in } V_6 = 0.04 \text{ or less.}$$

5. In lead V_6 , the S wave has a depth of 7 mm. or more.

GOODWIN'S CRITERIA—1. In leads V_3R and V_1 , the QR complex has a Q/R ratio less than 1, or the R_s complex has an R/S ratio greater than 1, the ventricular activation times in both types of QRS configuration exceeding 0.03 second.

2. In lead aVR, the Q/R ratio is less than 1, or the ventricular activation time is 0.06 second or more.

Electrocardiographic criteria for right ventricular hypertrophy proposed by Goodwin and by Sokolow and Lyon were evaluated. It was found that Goodwin's criteria failed diagnostically in a significant percentage of the patients with right ventricular hypertrophy. The criteria of Sokolow and Lyon were fulfilled in virtually all the electrocardiograms of patients with right ventricular hypertrophy. However, Braunwald and his associates pointed out that application of these criteria to the large series of normal infants and children studied by Ziegler would result in many of these normals meeting the diagnostic requirements for right ventricular hypertrophy. It was the opinion of these investigators that the following approach to the electrocardiographic diagnosis of right ventricular hypertrophy may prove the most satisfactory.

Criteria of Sokolow and Lyon—(1) In lead aVR, the R wave has an amplitude of 5 mm. or more. (2) Lead V_1 is characterized by an R wave amplitude of 7 mm. or more, an S wave depth of 2 mm. or more, and (3) the R wave in lead V_5 exceeds the normal maximum values in Table 9, (b) the S wave in V_1 and the R wave in V_6 display voltages listed in Table 9, (c) the R wave in lead V_6 exceeds the normal maximum value listed in Table 9, (d) the R wave in lead V_1 exceeds the normal maximum value listed in Table 9, (e) the R wave in lead V_1 exceeds the normal maximum value listed in Table 9, (f) the R wave in lead V_1 exceeds the normal maximum value listed in Table 9, (g) the R wave in lead V_1 exceeds the normal maximum value listed in Table 9, (h) the R wave in lead V_1 exceeds the normal maximum value listed in Table 9, (i) the R wave in lead V_1 exceeds the normal maximum value listed in Table 9, (j) the R wave in lead V_1 exceeds the normal maximum value listed in Table 9, (k) the R wave in lead V_1 exceeds the normal maximum value listed in Table 9, (l) the R wave in lead V_1 exceeds the normal maximum value listed in Table 9, (m) the R wave in lead V_1 exceeds the normal maximum value listed in Table 9, (n) the R wave in lead V_1 exceeds the normal maximum value listed in Table 9, (o) the R wave in lead V_1 exceeds the normal maximum value listed in Table 9, (p) the R wave in lead V_1 exceeds the normal maximum value listed in Table 9, (q) the R wave in lead V_1 exceeds the normal maximum value listed in Table 9, (r) the R wave in lead V_1 exceeds the normal maximum value listed in Table 9, (s) the R wave in lead V_1 exceeds the normal maximum value listed in Table 9, (t) the R wave in lead V_1 exceeds the normal maximum value listed in Table 9, (u) the R wave in lead V_1 exceeds the normal maximum value listed in Table 9, (v) the R wave in lead V_1 exceeds the normal maximum value listed in Table 9, (w) the R wave in lead V_1 exceeds the normal maximum value listed in Table 9, (x) the R wave in lead V_1 exceeds the normal maximum value listed in Table 9, (y) the R wave in lead V_1 exceeds the normal maximum value listed in Table 9, (z) the R wave in lead V_1 exceeds the normal maximum value listed in Table 9.

The ECG Diagnosis of Right Ventricular Hypertrophy

It is not possible to list all of the many electrocardiographic criteria which have been proposed.

Criteria of Goodwin are widely used and are summarized below.

CRITERIA OF SOKOLOV AND LYON—1. In lead aVR, the R wave has an amplitude of 5 mm. or more.

2. Lead V_1 is characterized by an R wave amplitude of 7 mm. or more, an S wave depth of 2 mm. or

more, the ventric-

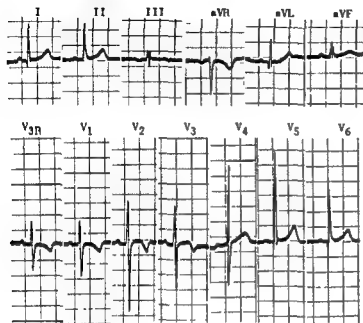
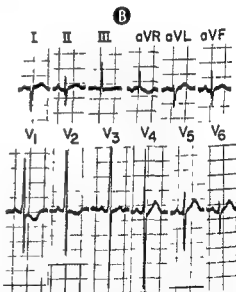
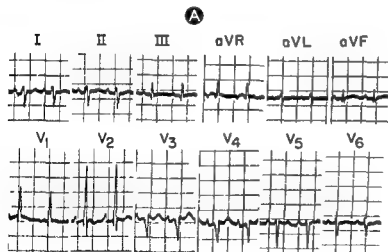


Fig. 111.—Normal electrocardiogram and vectorcardiogram in a boy, 4, without heart disease. Note, in the electrocardiogram, the almost equiphasic RS deflection in lead V_1 and the inverted T waves extending through lead V_4 . These findings are normal for this age group. In the vectorcardiogram, the QRS sE loop displays a prominent anterior and rightward early deflection which corresponds to the relatively tall R wave in lead V_1 of the electrocardiogram



probably reflect persistence of the physiologic right ventricular preponderance normally present in the fetus. B, normal electrocardiogram in girl, 1 month, also displaying the findings of physiologic right ventricular preponderance

phy in infants and young children the electrocardiograph has obvious limitations.

2. It may be impossible to distinguish pathologic from physiologic right ventricular preponderance in the newborn period.

infants by recording serial vectorcardiograms. According to Elek and his associates, the transitional vectorcardiographic pattern usually appears by the time an infant is 31 days old, or shortly thereafter. If serial vectorcardiograms fail to demonstrate the normal sequence of changes in the vectorcardiogram culminating in the appearance of the juvenile pattern, then pathologic right ventricular hypertrophy is probably present.

The sequence of vectorcardiographic patterns described above is compatible with the electrocardiographic studies of Ziegler in infants and young children of corresponding age groups. Ziegler found that the average amplitude of the R wave in lead V_1 exceeds that in V_4 from birth to approximately 6 months of age, that the two amplitudes are nearly equal in infants from 6 months to 1 year, but that after age 1 year the R wave in lead V_4 exceeds that in V_1 . He also observed that the R wave in V_1 decreases progressively throughout infancy and childhood.

When the R/S ratio in V_1 becomes, on the average, less than 1 Table 9 shows, according to age group the normal

lead:

vent. hypertrophy. See also Figures 121 and 122 for normal electrocardiographic and vectorcardiographic findings.

The ECG Diagnosis of Right Ventricular Hypertrophy

It is not possible to list all of the many electrocardiographic criteria which have been proposed for different types of right ventricular hypertrophy. Sokolow and Lyon and LA are summarized

CRITERIA OF SOKOLOW AND LYON.—1. In lead aVR, the R wave has an amplitude of 5 mm or more.

2. Lead V_1 is characterized by an R wave amplitude of 7 mm or more, an S wave depth of 2 mm or

less; a T wave inverted and preceded by an R wave 5 mm or more in amplitude, an R/S ratio greater than 4 in children under 5 years and greater than 1 in children over 5 years, and ventricular activation time or pre-intrinsicoid deflection time of 0.04 second or longer.

3. Lead V_4 shows an R wave amplitude of 4 mm, or less and an R/S ratio of 1 or less.

4. In leads V_1 and V_4 , $R_{V_1} + S_{V_4} = 10.5$ mm. or more in children over the age of 5 years; and

$$\frac{R/S \text{ ratio in } V_4}{R/S \text{ ratio in } V_1} = 0.04 \text{ or less.}$$

5. In lead V_4 , the S wave has a depth of 7 mm. or more.

GOODWIN'S CRITERIA.—1. In leads V_{3R} and V_1 , the QR complex has a Q/R ratio less than 1, or the RS complex has an R/S ratio greater than 1, the ventricular activation times in both types of QRS configuration exceeding 0.03 second.

2. In lead aVR, the Q/R ratio is less than 1, or the ventricular activation time is 0.06 second or more.

CRITERIA OF BRAUNWALD AND ASSOCIATES.—Braunwald and his co-workers have studied very thoroughly a large series of patients with congenital heart disease, the patients ranging in age from under 3 years to over 30 years (only two were less than 3 years old). The electrocardiographic criteria for right ventricular hypertrophy proposed by Goodwin and by Sokolow and Lyon were evaluated. It was found that Goodwin's criteria failed diagnostically in a significant percentage of the patients with right ventricular hypertrophy. The criteria of Sokolow and Lyon were fulfilled in virtually all the electrocardiograms of patients with right ventricular hypertrophy. However, Braunwald and his associates pointed out that application of these criteria to the large series of normal infants and children studied by Ziegler would result in many of these normals meeting the diagnostic requirements for right ventricular hypertrophy. It was the opinion of these investigators that the following approach to the electrocardiographic diagnosis of right ventricular hypertrophy may prove the most satisfactory.

Electrocardiographic findings diagnostic of right ventricular hypertrophy.—Right ventricular hypertrophy is almost certainly present if the electrocardiogram (1) satisfies the criteria of Sokolow and Lyon and (2) meets the following requirements. (a) the R waves in leads aVR, V_{3R} , and V_1 and the S waves in V_4 exceed in amplitude the normal maximum values in Table 9. (b) the S wave in V_1 and the R wave in V_4 display voltages less than the normal

ular activation time in V_1 meets the requirements of 0.04 second or more.

Electrocardiographic findings suggestive of right ventricular hypertrophy.—If the electrocardiogram meets only the requirements of Sokolow and Lyon, it can be considered merely suggestive of right ventricular hypertrophy and vectorcardiographic studies should be performed.

Electrocardiographic findings rendering the diagnosis of right ventricular hypertrophy unlikely.—If the electrocardiogram does not fulfill any of the above requirements, predominant right ventricular hypertrophy secondary to congenital heart disease is almost certainly ruled out.

RSR' complex in V_1 .—The preceding statements cannot be applied to electrocardiograms showing an RSR' complex in lead V_1 , with or without prolonged intraventricular conduction. It is in the clarification of electrocardiographic patterns such as this that the vectorcardiograph proves its diagnostic value. For example, right ventricular hypertrophy, incomplete right bundle branch block, and late depolarization of the pulmonary conus region in a normal heart, may all produce RSR' complexes in lead V_1 which may be quite difficult, if not impossible, to distinguish electrocardiographically one from another. However, the vectorcardiographic patterns of right ventricular hypertrophy and of incomplete right bundle branch

block can be readily differentiated. Moreover, it is possible to recognize as a normal variant the QRS loop which has a terminal deflection to the right and posteriorly and which produces a small terminal R' wave in V_1 in the absence of right ventricular hypertrophy and right bundle branch block, presumably as the result of late activation of the pulmonary conus region.

The ECG Diagnosis of Left Ventricular Hypertrophy

Braunwald and his associates, in their series of children and young adults with congenital heart disease, who ranged in age from 3 to over 30 years, evaluated the criteria of Sokolow and Lyon for the electrocardiographic diagnosis of left ventricular hypertrophy (see Chapter 9). They also utilized the amplitude standards which appear in Table 9. These investigators found that the requirements proposed by Sokolow and Lyon were met by about 54% of the patients with left ventricle hypertrophy, while only 32% of the patients presented electrocardiograms outside the limits of normal defined in Table 9. Thus, in children as well as in adults, the electrocardiographic diagnosis of left ventricle hypertrophy is undoubtedly marred by a significant percentage of false negative and false positive interpretations.

Congenital Heart Disease, Mitral Stenosis, and Cor Pulmonale: General Considerations

CLINICALLY, right ventricular hypertrophy occurs primarily in three types of heart disease—congenital heart disease, mitral stenosis, and chronic cor pulmonale. The first two are discussed in this paper.

in heart disease, but only recently has attention been called to the differences existing in the prominence of the electrocardiographic and vectorcardiographic manifestations of right ventricular hypertrophy in these conditions.

To illustrate the trend in the electrocardiographic findings of right ventricular hypertrophy in mitral stenosis, in chronic cor pulmonale, and in congenital heart disease, the electrocardiograms of a number of patients with vectorcardiographically diagnosed right ventricular hypertrophy (with postmortem or surgical confirmation in most of the mitral stenosis and congenital heart disease cases) were reviewed by us (see Table 10) to determine the following points:

3. The number of cases in the three groups in which the vectorcardiograms were diagnostic of right ventricular hypertrophy, and the frequency of each of the two vectorcardiographic patterns of right ventricular hypertrophy in these cases.

Attention must be called to the fact that the data presented below have no precise statistical significance because of the manner in which the patients were selected for study.

Table 10 does not present any statistically valid data as to the relative frequency of the electrocardiographic and vectorcardiographic findings of right ventricular hypertrophy in congenital heart disease, mitral stenosis, and chronic cor pulmonale. However, as the table indicates, there is ample evidence attesting to the lower incidence of these findings in mitral stenosis and their relative rarity in chronic cor pulmonale. Both the frequency of occurrence and the prominence of the electrocardiographic and vectorcardiographic patterns of right ventricular hypertrophy depend, in all probability, on such factors as the following:

1. The number of electrocardiograms in each of the above three groups in which diagnosis of right ventricular hypertrophy could be made, using—
 - a) The criteria of Barker and Valenzia for the diagnosis of right ventricular hypertrophy with complete and incomplete right bundle branch block—an R' deflection in V_1 exceeding 15 mm in complete right bundle branch block and an R' deflection exceeding 10 mm in incomplete right bundle branch block
 - b) The criteria of an R/S amplitude ratio in V_1 greater than 1 and an R wave in V_1 of 7 mm or more amplitude in the absence of an RSR' deflection in V_1
2. The average amplitude of the R wave or R' wave of an RSR' deflection in lead V_1 in the electrocardiograms
3. Factors affecting the manner in which the QRS forces are transmitted to and recorded by the lead electrodes.
 - a) The conductivity of the intrathoracic structures
 - b) Cardiac position and rotation and the location of the electrical center of the heart or electrical pull point.
2. The duration, degree, and type of right ventricular overloading (whether systolic, diastolic, or both—i.e., composite overloading).
3. The presence or absence of coexisting left ventricular overloading

Each of the above factors will be considered in some detail in the following paragraphs.

TABLE 10.—COMPARISON OF ECG AND VCG FINDINGS OF RIGHT VENTRICULAR HYPERTROPHY IN CONGENITAL HEART DISEASE, MITRAL STENOSIS, AND CHRONIC COR PULMONALE

	CONGENITAL HEART DISEASE*	MITRAL STENOSIS†	CHRONIC COR PULMONALE‡
Total number of cases	50	53	19
Cases with ECG right bundle branch block:	2	0	0
R' > 15 mm. in V ₁	0	0	0
Av. R' amplitude in V ₁	13 mm
VCG right ventricular hypertrophy (+ or - right bundle branch block)	2	0	0
Cases with RSR' in V ₁ less than 0.11-sec. duration:	14	28	5
R' > 10 mm in V ₁	7	0	0
Av. R' amplitude in V ₁	13 mm.	5 mm.	3 mm
VCG right ventricular hypertrophy	13	15	3
Cases with R/S amplitude ratio in V ₁ > 1:	26	18	0
R in V ₁ ≥ 7 mm.	25	9	0
R in V ₁ < 7 mm	1	9	0
Av. R amplitude in V ₁	19 mm	8 mm.	...
VCG right ventricular hypertrophy	26	15	0
Cases with R/S amplitude ratio in V ₁ < 1.	8	7	14
VCG right ventricular hypertrophy	0	2	1
Total number of cases with VCG right ventricular hypertrophy	41	32	4
VCG tall R QRS sE loop pattern of right ventricular hypertrophy	21	7	3
VCG RSR' QRS sE loop pattern of right ventricular hypertrophy	18	25	1
VCG right ventricular hypertrophy and right bundle branch block	2	0	0

*Includes only those congenital cardiac anomalies which, with varying frequency, produce right ventricular hypertrophy.

†Includes cases of pure mitral stenosis and cases of hemodynamically predominant mitral stenosis with mitral insufficiency and/or aortic valve disease.

‡Diagnosis was made on the basis of either postmortem proof of right ventricular hypertrophy or unequivocal radiologic evidence of chronic cor pulmonale.

FACTORS AFFECTING THE FREQUENCY AND PROMINENCE OF THE PATTERNS OF RIGHT VENTRICULAR HYPERTROPHY

Manner of Transmission of QRS Forces to the Lead Electrode

The transmission of QRS forces to the body surface electrodes is influenced by factors such as those to be described in the following paragraphs.

✓ *Conductivity of intrathoracic structures.*—The in-

fluence of this factor can be illustrated by the following examples:

1. *Chronic pulmonary emphysema* is responsible for virtually all cases of chronic pulmonary heart disease with right ventricular hypertrophy (chronic cor pulmonale). In pulmonary emphysema, the walls of

many of the alveoli in the lungs are ruptured and the affected alveoli coalesce to form abnormally large air sacs. The latter remain overdistended with air because of the poor respiratory exchange. Thus, the lungs contain more air than normally, and, since air is a poor conductor, the electrical forces produced by the heart are not transmitted to the chest electrode as well as normally. As a result, there may be low voltage of the electrocardiographic deflections in all leads, despite the presence of right ventricular hypertrophy, although this feature may be more marked in some leads than in others because of variations in the amount of air-filled lung between heart and electrode.

2. Rather marked degrees of right atrial dilatation are noted more commonly in congenital heart diseases than in mitral stenosis or pulmonary heart disease. If it is true, as some authorities believe, that right atrial dilatation facilitates transmission of the forces produced in the hypertrophied basal right ventricular wall and septum, then this factor may well play some part in determining the higher incidence of prominent right ventricular hypertrophy patterns in electrocardiograms of patients with congenital heart disease than in those of patients with acquired heart disease.

Cardiac position, rotation, and the location of electrical center of the heart.—The following examples illustrate the influence of this factor

1. In congenital heart disease with pulmonic stenosis, the long axis of the heart is believed by some investigators to be more horizontal than in any other type of right ventricular hypertrophy. As a result, the basal wall and outflow tract of the right ventricle (crista supraventricularis) and basal septum (the regions which undergo maximum hypertrophy in right ventricular hypertrophy) are oriented toward the positive half of the axis of derivation of lead V_1 . Hence, right precordial leads in this instance optimally record the augmented forces arising in the hypertrophied right ventricle.

2. In chronic cor pulmonale, according to Sodi-Pallares, the heart is located much lower in the chest than in either normal subjects or those with congenital or mitral stenotic heart disease. In addition, the heart is rotated clockwise on its longitudinal axis, and its apex is displaced posteriorly. Sodi-Pallares believes that, because of the lower position of the heart in the chest, the precordial electrode explores the atria rather than the hypertrophied right ventricle. He also postulates that the clockwise rotation of the heart displaces the left ventricle posteriorly, thereby causing all six precordial leads of the electrocardiogram to display low R waves with relatively deep S

waves, even though there may be anatomic right ventricular hypertrophy. As one might infer from the preceding explanation, Sodi-Pallares considers the electrocardiographic precordial leads to be semidirect leads which respond to proximity potentials arising in myocardium closest to the exploring electrode.

The frequent failure of the electrocardiogram and vectorcardiogram to present diagnostic evidence of right ventricular hypertrophy in chronic cor pulmonale can perhaps be explained somewhat differently in terms of the vector or equivalent dipole concept. It is probable that the marked changes in the anatomic position and rotation of the heart in chronic pulmonary emphysema are accompanied by a shift in the location of the electrical center of the heart. Since the effective axis of a given lead, or the direction of the lead vector, is a function of the location of the dipole center, its eccentricity, etc., a change in the site of the dipole center might be expected to alter the manner in which the lead in question responds to the transverse, sagittal, or vertical components of the cardiac vector. Thus, it is conceivable that a lead with an anteroposterior anatomic axis might have an effective axis which is so tilted that instantaneous vectors situated anteriorly are recorded by the lead as if they were located posteriorly. At present, such an explanation is purely conjectural, although certain observations which we have made (described later) provide some evidence to support this hypothesis.

Duration, Degree, and Type of Right Ventricular Overloading

In congenital heart disease, as a general rule, right ventricular overload is

Moreover, on the average, the hemodynamic burden imposed on the right ventricle is likely to be greater in congenital than in acquired cardiac lesions.

In order to interrelate better the anatomic, hemodynamic, and electrocardiographic changes accompanying the various congenital and acquired cardiac lesions, Cabrera and Monroy have categorized the latter according to whether a given cardiac lesion produces systolic, diastolic, or composite overload of the left ventricle.

As a result of an increased resistance to the ejection of blood during systole. Systolic overloading typically leads to concentric hypertrophy (i.e., muscular hypertrophy un-

TABLE 10—COMPARISON OF ECG AND VCG FINDINGS OF RIGHT VENTRICULAR HYPERTROPHY IN CONGENITAL HEART DISEASE, MITRAL STENOSIS, AND CHRONIC COR PULMONALE

	CONGENITAL HEART DISEASE*	MITRAL STENOSIS†	CHRONIC COR PULMONALE‡
Total number of cases	50	53	19
Cases with ECG right bundle branch block:	2	0	0
R' > 15 mm. in V ₁	0	0	0
Av. R' amplitude in V ₁	13 mm
VCG right ventricular hypertrophy (+ or - right bundle branch block)	2	0	0
Cases with RSR' in V ₁ less than 0.11-sec duration.	14	28	5
R' > 10 mm in V ₁	7	0	0
Av. R' amplitude in V ₁	13 mm.	5 mm	3 mm
VCG right ventricular hypertrophy	13	15	3
Cases with R/S amplitude ratio in V ₁ > 1:	28	18	0
R in V ₁ ≥ 7 mm.	35	9	0
R in V ₁ < 7 mm	1	9	0
Av. R amplitude in V ₁	19 mm	8 mm	...
VCG right ventricular hypertrophy	26	15	0
Cases with R/S amplitude ratio in V ₁ < 1.	8	7	14
VCG right ventricular hypertrophy	0	2	1
Total number of cases with VCG right ventricular hypertrophy	41	32	4
VCG tall R QRS sE loop pattern of right ventricular hypertrophy	21	7	3
VCG RSR' QRS sE loop pattern of right ventricular hypertrophy	18	25	1
VCG right ventricular hypertrophy and right bundle branch block	2	0	0

*Includes only those congenital cardiac anomalies which, with varying frequency, produce right ventricular hypertrophy

†Includes cases of pure mitral stenosis and cases of hemodynamically predominant mitral stenosis with mitral insufficiency and/or aortic valve disease

‡Diagnosis was made on the basis of either postmortem proof of right ventricular hypertrophy or unequivocal radiologic evidence of chronic cor pulmonale

FACTORS AFFECTING THE FREQUENCY AND PROMINENCE OF THE PATTERNS OF RIGHT VENTRICULAR HYPERTROPHY

Manner of Transmission of QRS Forces to the Lead Electrode

The transmission of QRS forces to the body surface

fluence of this factor can be illustrated by the following examples

1. Chronic pulmonary emphysema is responsible for virtually all cases of chronic pulmonary heart disease with right ventricular hypertrophy (chronic cor pulmonale). In pulmonary emphysema, the walls of

Congenital Heart Disease

ALTHOUGH THE CLINICIAN is quite cognizant of the fact that electrocardiography is not a substitute for angiocardiology and cardiac catheterization in the diagnostic study of congenital heart disease, he probably is less aware of, or tends to underestimate, the diagnostic value of the electrocardiogram and vectorcardiogram in this type of cardiac disease. Admittedly, the information provided by the electrocardiogram and vectorcardiogram is relatively nonspecific in most instances. Nevertheless, if used properly, it often has significant diagnostic and prognostic value. Moreover, complex diagnostic procedures like angiocardiology and cardiac catheterization ordinarily are not available to the physician who first examines a patient suspected of having congenital heart disease, and yet the physician must make the decision as to whether or not this diagnosis is a likely enough possibility to merit further study. Electrocardiography, on the other hand, is a diagnostic procedure which is readily available to most physicians and one that is easily performed.

The purpose of this chapter is to review briefly the anatomic and hemodynamic characteristics of certain congenital heart diseases and then to relate them

to the electrocardiogram and vectorcardiogram. When possible, the clinical implications of the electrocardiographic and vectorcardiographic findings will be cited. Since the number of cases of congenital cardiac anomalies which we studied was small (see Table 11), the findings will be supplemented with addi-

TABLE 11—CASES OF CONGENITAL HEART DISEASE STUDIED BY THE AUTHORS*

TYPE OF CONGENITAL HEART DISEASE	No. OF CASES	
	ECG	VCG
Isolated pulmonic stenosis with normal aortic flow	8	5
Interatrial septal defect	15	14
Interventricular septal defect	9	4
Patent ductus arteriosus	11	3
Tetralogy of Fallot (or pentalogy)	9	4

*Postmortem or surgical confirmation of the diagnosis was available in almost all cases.

normal and abnormal electrocardiograms and vectorcardiograms.

cause of their relatively greater frequency of occurrence and/or amenability to surgical correction.

TYPES OF CONGENITAL HEART DISEASE

The following classification emphasizes the hemodynamic effects of the cardiac abnormality.

- 1 Stenotic lesions causing systolic overloading of the right or left ventricle
 - a) Overloading of the left ventricle
 - 1 Coarctation of the aorta (adult type with closed ductus arteriosus)
 - b)

II Cardiac shunts

- 2 Patent ductus arteriosus with left-to-right shunt

- b) Diastolic overloading of the left ventricle and systolic overloading of the right ventricle
 - 1 Interventricular septal defect with right-to-left

accompanied by chamber dilatation). When there is diastolic overloading of one or the other ventricle, the volume of blood in the affected ventricle during diastole greatly exceeds that present normally. This causes eccentric hypertrophy of the affected ventricle, which is characterized by a lesser degree of muscular hypertrophy than in systolic overloading, but the hypertrophy is accompanied by dilatation of the affected chamber. *Composite overloading* is the term used when both systolic and diastolic overloading of one or the other ventricle are present. Cabrera and Monroy's concept of ventricular overloading resembles the classification of *right ventricular strain* proposed by Donzelot and his associates. Thus, systolic overloading corresponds to the term of Donzelot and his co-workers, *hypertrophy by barrier*, diastolic overloading, to their *hypertrophy by overload* (or *shunt*); and composite overloading is, in essence, what they designate as *hypertrophy by adaptation*.

Although the concept of ventricular overloading and the related concept of hypertrophy by barrier, overload, and adaptation have a certain degree of validity, nevertheless, Braunwald and his associates in Grishman's laboratory, the authors of this text, and other investigators have not noted as consistent a correlation of electrocardiographic findings with the type of congenital or acquired cardiac disease present as have been reported by Cabrera and Monroy and by Donzelot and his associates. An additional fact worthy of mention is that, in all probability, a high percentage of the incomplete right bundle branch block patterns observed by Cabrera and Monroy in cases with diastolic overloading of the right ventricle were actually right ventricular hypertrophy patterns of the RSR' type. This much is true, however, congenital or acquired cardiac lesions which cause systolic overloading of the left or right ventricle tend to be accompanied by concentric hypertrophy with marked thickening of the muscular wall of the affected ventricle. On the other hand, lesions which lead to diastolic overloading of the left or right ventricle are associated primarily with ventricular dilatation and relatively minimal hypertrophy of the ventricular wall (eccentric hypertrophy). In such instances, there may be selective hypertrophy of the crista supraventricularis and trabeculae of the right ventricle, the

electrical effects of which are much less prominent than the electrical effects of concentric hypertrophy.

Presence or Absence of Coexisting Left Ventricular Overloading

In the acquired mitral and pulmonary types of heart disease, prior to onset of right ventricular overloading, the left ventricle is almost invariably electrically predominant with reference to the right ventricle. Consequently, the electrical effects of anatomic right ventricular hypertrophy are, in varying degree, offset by the initial preponderance of left ventricular forces. If the anatomic right ventricular hypertrophy is relatively minimal, its electrical effects may not be sufficient to overcome the normal predominance of the left.

appear
this is o
incidence of electrocardiographic right ventricular hypertrophy in mitral stenosis than in congenital heart disease, since many of the cyanotic congenital anomalies, such as tetralogy of Fallot, are associated with hypoplasia of the left ventricle. In addition to the fact that mitral insufficiency, which causes left ventricular overloading, often coexists with mitral stenosis, it must be remembered that in rheumatic heart disease there frequently is multivalvular and myocardial involvement. For example, mitral stenosis may be accompanied by aortic stenosis and/or insufficiency, both of which produce left ventricular hypertrophy, or diffuse myocardial scarring consequent to rheumatic carditis can lead to dilatation and hypertrophy of the left ventricle. In the presence of left ventricular hypertrophy, the degree of anatomic

manifestations of right ventricular hypertrophy than would otherwise be the case; and—more often than not—the left ventricular hypertrophy prevents the appearance or obscures the electrocardiographic manifestations of right ventricular hypertrophy.

The three types of heart disease—congenital heart disease, mitral stenosis, and cor pulmonale—will be discussed fully and separately in the following three chapters

of blood to satisfy the demands of the fetal circulation

arteriosus ■ unable to maintain an adequate

velops in utero, in contrast with the situation in the infantile type.

Typically, in coarctation of the aorta there is hypertension in the upper extremities and weak or absent arterial pulsations in the lower extremities. The hypertension is usually systolic, although a varying

but two mechanisms have been entertained: (a) some authorities attribute the hypertension to mechanical obstruction of blood flow by the coarctation itself, while (b) others implicate renal ischemia secondary to the diminished blood flow to the kidneys. There is evidence for and against both mechanisms. In any event, depending on the degree of coarctation and the extent of the collateral circulation, there is systolic overloading of the left ventricle, whether this ■ attributable to the mechanical effects of the coarctation, to hypertension of renal origin, or to both factors. In addition, the hemodynamic burden imposed on the left ventricle is sometimes increased even further by associated cardiac malformations, the most common of which is a bicuspid aortic valve. In the presence of the latter anomaly, aortic insufficiency can result from incompetence of the aortic cusps due to hypertension and to dilatation of the aorta proximal to the coarctation.

In brief, if there is marked stenosis of the aorta or if the collateral circulation is poorly developed, coarctation of the aorta may produce severe systolic overloading of the left ventricle, which in turn may cause concentric hypertrophy of the left ventricle. On the other hand, if the coarctation is of a relatively mild degree or the collateral circulation well developed, there may be minimal left ventricular hypertrophy. Obviously, all degrees of anatomic left ventricular hypertrophy between the preceding two extremes may be encountered.

THE ECG AND VCG FINDINGS

To provide a more representative sampling of the reported electrocardiographic findings in the adult

type of coarctation of the aorta, data regarding various series of coarctation cases reported by a number of investigators were pooled, and the incidence of each of the principal electrocardiographic findings in coarctation was computed for the entire group collectively. The series from which the data were obtained includes those reported by the following: Braunwald, Kjellberg, Mettman, and Oglesby and their collaborators, and Landman, Ziegler, and Sokolow and Edgar. Their findings follow.

1. The electrocardiogram was normal in approximately one third of the cases. Braunwald and his associates report that normal vectorcardiograms were recorded in 4 of 11 cases of coarctation of the aorta.
2. Left ventricular hypertrophy was observed in slightly over half of the cases. By and large, in most cases the electrocardiographic features of left ventricular hypertrophy were not particularly prominent. It has been stated that the presence of marked evidence of left ventricular hypertrophy may be indicative of an associated aortic valvular lesion. Left ventricular hypertrophy was diagnosed vectorcardiographically in 7 of the 11 cases referred to above. Although Braunwald and his co-workers noted nothing unique about the vectorcardiographic pattern of left ventricular hypertrophy occurring in coarctation, the authors of this text were impressed, in the few cases they studied, by the fact that the T sE loop was concordant rather than discordant to the QRS sE loop, typical of the vectorcardiogram in left ventricular hypertrophy due to other cardiac lesions.
3. The mean manifest electrical axis of QRS (mean frontal plane QRS vector) was normally situated in about 60% of the cases, while about 30% of the cases showed left-axis deviation and about 10% right-axis deviation. Although the incidence of left-axis deviation is lower perhaps in coarctation of the aorta than in other conditions, these findings have been stated. However, there is much to be said for the contention of these authorities that left-axis deviation tends to occur in conditions causing both muscular hypertrophy and dilatation of the left ventricle (eccentric hypertrophy) and to be absent when concentric hypertrophy is present.

Hypertrophy

several types of cardiac disease which can give rise to concentric hypertrophy of the left ventricle. In all probability, the reason that acquired valvular

- shunt due to pulmonic stenosis or pulmonary hypertension (including Eisenmenger's complex)
- 2. Patent ductus arteriosus with right-to-left shunt due to pulmonary hypertension
- c) Diastolic overloading of the right ventricle
 - 1. Interatrial septal defect with left-to-right shunt (including Lutembacher's syndrome, consisting of congenital mitral stenosis and an interatrial septal defect)
- d) Diastolic and systolic (composite) overloading of the right ventricle
 - 1. Interatrial septal defect with right-to-left shunt due either to pulmonic stenosis (trilogy of Fallot) or to pulmonary hypertension
- III. Multiple cardiac anomalies associated with other developmental defects
 - a) Dextrocardia with and without situs inversus
 - b) Tetralogy of Fallot

According to Carbrera and Monroy, the electrocardiographic manifestations of systolic and diastolic overloading of the right and left ventricles are as follows:

- I. Right ventricle*
 - a) Diastolic overloading

- 1. Complete or incomplete right bundle branch block
- 2. Right-axis deviation
- b) Systolic overloading
 - 1. Increased voltage of the R wave in lead V_1 and sometimes initial slurring of the R wave in this lead
 - 2. Inverted T wave in lead V_1 if systolic overloading of the right ventricle is marked and of long duration
 - 3. The configuration of the QRS deflection in lead V_1 is usually monophasic or diphasic. However, if the systolic overloading is complicated by diastolic overloading, the QRS deflection may appear notched and polyphasic
 - 4. Right-axis deviation

II. Left ventricle*

- a) Diastolic overloading
 - 1. Tall R wave in V_5 and V_6 with delayed onset of the intrinscoid deflection
 - 2. Deep S wave in leads V_1 and V_4
 - 3. Tall upright T wave in leads V_5 and V_6 with-out opposition between Δ QRS and Δ T
- b) Systolic overloading
 - 1. Inverted T waves and/or depressed S-T segments in left precordial leads
 - 2. Opposition of Δ QRS and Δ T

STENOTIC LESIONS CAUSING SYSTOLIC LEFT VENTRICULAR OVERLOADING

Coarctation of the Aorta

Anatomically and hemodynamically, there are two types of coarctation of the aorta—the infantile type and the adult type.

In the *infantile type*, there is a marked elongated narrowing of the aortic segment between the origin of the left subclavian artery and the opening of a patent ductus arteriosus. After birth, a fetal type of circulation (pulmonoaortic shunt) through the patent ductus persists, and the right ventricle has to meet the circulatory demands of both the pulmonary circulation and the systemic circulation distal to the coarctation. Thus, at birth the right ventricle is suddenly burdened with a highly pathologic circulation, and, with rare exceptions, severe heart failure and death ensue within several days. The exceptional patients apparently have some other cardiac malformation and intracardiac shunt in addition to the infantile coarctation, but even in these cases, life seldom is prolonged beyond the juvenile period. In the few patients studied, the cardiac anomalies were found to be hemodynamically equivalent to a patent

ductus arteriosus with a pulmonoaortic shunt. The *infantile type* of coarctation of the aorta will not be considered in this text.

The *adult type* is the form of coarctation which is usually encountered clinically. It consists of a more localized and less severe narrowing of the aorta at, or just distal to, the insertion of the ductus arteriosus. Postnatally, the ductus arteriosus is often closed, however, if the ductus remains patent after birth, the ductal shunt is directed from left to right—that is, from aorta to pulmonary artery.

Hemodynamically and prognostically, the principal difference between the infantile and adult types of coarctation of the aorta is that a fully developed collateral circulation is present at birth in the adult type of coarctation and is absent in the infantile type. The development of a collateral circulation in utero depends on whether or not, despite the coarctation, the fetal circulation is adequate. Apparently, in the infantile type of coarctation an adequate fetal circulation is maintained, for either or both of the following reasons. (a) the ductus arteriosus inserts distal to the site of constriction of the aorta and therefore is able to shunt blood into the distal descending aorta, (b) the ductus arteriosus is malformed and greatly widened and therefore shunts a large-enough volume

*Composite overloading of the right or left ventricle is characterized electrocardiographically by the presence of signs of both diastolic and systolic overloading

of blood to satisfy the demands of the fetal circulation. In either case, in the infantile type of coarctation the stimulus is lacking for the development of a collateral circulation in utero. On the other hand, in the adult type of coarctation of the aorta the ductus arteriosus is unable to maintain an adequate fetal circulation, either because of its location proximal to the coarctation or because of its normal width. Thus, if the coarctation is severe, a collateral circulation develops in utero, in contrast with the situation in the infantile type.

Typically, in coarctation of the aorta there is hypertension in the upper extremities and weak or absent arterial pulsations in the lower extremities. The

type of coarctation of the aorta, data regarding various series of coarctation cases reported by a number of investigators were pooled, and the incidence of

Their findings follow.

1. The electrocardiogram was normal in approximately one third of the cases. Braunwald and his associates report that normal vectorcardiograms were recorded in 4 of 11 cases of coarctation of the aorta.
2. Left ventricular hypertrophy was observed in slightly over half of the cases. By and large, in most cases the electrocardiographic features of left ventricular hypertrophy were not particularly prominent. It has been stated that the presence of marked evidence of left ventricular hypertrophy may be indicative of an associated aortic valvular

but two mechanisms have been entertained (a) some authorities attribute the hypertension to mechanical obstruction of blood flow by the coarctation itself, while (b) others implicate renal ischemia secondary to the diminished blood flow to the kidneys. There is evidence for and against both mechanisms. In any event, depending on the degree of coarctation and the extent of the collateral circulation, there is systolic overloading of the left ventricle, whether this is attributable to the mechanical effects of the coarctation, to hypertension of renal origin, or to both factors. In addition, the hemodynamic burden imposed on the left ventricle is sometimes increased even further by associated cardiac malformations, the most common of which is a bicuspid aortic valve. In the presence of the latter anomaly, aortic insufficiency can result from incompetence of the aortic cusps due to hypertension and to dilatation of the aorta proximal to the coarctation.

In brief, if there is marked stenosis of the aorta or if the collateral circulation is poorly developed, coarctation of the aorta may produce severe systolic overloading of the left ventricle, which in turn may cause concentric hypertrophy of the left ventricle. On the other hand, if the coarctation is of a relatively mild degree or the collateral circulation well developed, there may be minimal left ventricular hypertrophy. Obviously, all degrees of anatomic left ventricular hypertrophy between the preceding two extremes may be encountered.

THE ECG AND VCG FINDINGS

To provide a more representative sampling of the reported electrocardiographic findings in the adult

cardiographic pattern of left ventricular hypertrophy occurring in coarctation, the authors of this text were impressed, in the few cases they studied, by the fact that the T_{SE} loop was concordant rather than discordant to the QRS_{SE} loop, typical of the vectorcardiogram in left ventricular hypertrophy due to other cardiac lesions.

3. The mean manifest electrical axis of QRS (mean frontal plane QRS vector) was normally situated in about 60% of the cases, while about 30% of the cases showed left-axis deviation and about 10% right-axis deviation. Although the incidence of

hypertrophy, nevertheless it would not seem to be as uncommon as Sodi-Pallares and his associates have stated. However, there is much to be said for the contention of these authorities that left-axis deviation tends to occur in conditions causing both muscular hypertrophy and dilatation of the left ventricle (eccentric hypertrophy) and to be absent when muscular hypertrophy is unaccompanied by dilatation (concentric hypertrophy). Coarctation of the aorta is one of several types of cardiac disease which can give rise to concentric hypertrophy of the left ventricle. In all probability, the reason that a

lar lesions, for example, produce eccentric hypertrophy of the left ventricle, and therefore exhibit electrocardiographic left-axis deviation, is that these lesions are often accompanied by myocardial disease, and so there is both systolic and diastolic overloading of the left ventricle.

4. Complete or incomplete right bundle branch block was present in about 30% of the cases of the combined series of Ziegler, Metianu and his co-workers, and Kjellberg and his associates. In the series of coarctation cases reported by Metianu and his collaborators, right bundle branch block was observed in about 15% of the cases and left bundle branch block in about 23%. However, left bundle branch block was not reported to have occurred in any of the other series of cases reviewed by us.

5. According to Landtman, depressed S-T segments appeared in leads II and V_3 in about one fourth of the cases he studied, but inverted T waves were never present in lead I and only exceptionally present in leads II and V_3 . The relative paucity of T wave abnormalities in left ventricular hypertrophy due to coarctation is in rather striking contrast to their frequency in left ventricular hypertrophy due to other cardiac lesions, and this fact does not seem consistent with Cabrera and Monroy's concept of the electrocardiographic changes attributable to systolic overloading of the left ventricle.

Congenital Aortic and Subaortic Stenosis

Congenital aortic (valvular) stenosis is the result of fusion of the valve cusps, while subaortic stenosis is due to a localized constriction of the infundibulum of the left ventricular outflow tract. Depending on the degree of stenosis, both lesions may fail to cause significant hypertrophy of the left ventricle, or, on the other hand, they may cause severe systolic overloading of the left ventricle with resulting concentric ventricular hypertrophy.

THE ECG AND VCG FINDINGS

The findings of Braunwald and Kjellberg and their associates follow:

1. In the combined series of cases reported by Braunwald and his co-workers and Kjellberg and his associates, approximately 85% of the cases showed normal electrocardiograms, while the remaining cases showed electrocardiographic left ventricular hypertrophy patterns.
2. Braunwald and his collaborators observed left-axis deviation in the electrocardiogram in only 1 of 12 cases of congenital aortic stenosis and subaortic stenosis.
3. Braunwald and his associates studied their 12 patients, and found that in 11 of 12 cases the electrocardiogram was normal.

say, vectorcardiographic studies of this type of cardiac anomaly are relatively few in number.

STENOTIC LESIONS CAUSING SYSTOLIC RIGHT VENTRICULAR OVERLOADING

Pulmonic Stenosis (Isolated with Normal Aortic Root)

Ordinarily, pulmonic stenosis is not an isolated anomaly but clinically is accompanied by other congenital defects, particularly septal defects and aortic overriding. But even when pulmonic stenosis occurs in company with other anomalies, in most instances it determines the severity of the hemodynamic burden imposed on the right ventricle. While pulmonic stenosis due to narrowing of the valvular ring or to stenosis of the pulmonary artery above the valve (supravalvular) may be encountered on rare occasions, the forms of pulmonic stenosis most frequently observed clinically fall into two main categories: valvular and infundibular stenosis.

Valvular stenosis, involving the cusps of the pulmonary valve, is the type said to predominate when

pulmonic stenosis is associated with atrial septal defect or when it occurs in the absence both of aortic overriding and of defects of the atrial and ventricular septa.

Infundibular stenosis, stenosis of the infundibulum of the right ventricle, may appear in either of the following two forms: (a) a general narrowing of the infundibulum from its ostium up to the pulmonary valve, which is found only with aortic overriding (see tetralogy of Fallot), (b) stenosis limited to the infundibular ostium, the form most frequently associated with ventricular septal defects (without aortic overriding).

Valvular stenosis may exist separately or in combination with infundibular stenosis, however, infundibular stenosis unaccompanied by valvular pulmonic stenosis is said to be a rare finding, although there is not universal agreement on this point.

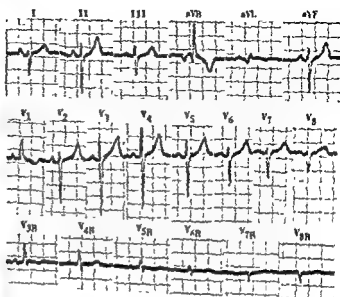


Fig. 113 — Fluoroscopic images of the heart.

Hemodynamically, isolated pulmonic stenosis may be of such a minimal degree as to impose little or no additional burden on the right ventricle, or, as is more often the case, it may greatly increase the resistance against which the right ventricle must eject blood during systole.

The resulting systolic overloading of the right ventricle can cause varying degrees of concentric right ventricular hypertrophy (without dilatation). Diastolic filling of the hypertrophied right ventricle requires increased pressure, and this is accompanied by a rise in pressure in the right atrium. Thus, in rather severe isolated pulmonic stenosis, there may occur both concentric hypertrophy of the right ventricle and hypertrophy and dilatation of the right atrium.

THE ECC AND VCG FINDINGS

The ECG and VCG findings were as follows:

- 1 The electrocardiogram was normal in a little over 20% of the 28 cases.
- 2 The P waves in lead II of the electrocardiogram were abnormally tall and/or wide in 16% of the cases.
- 3 In almost two thirds of the cases the electrocardiogram was diagnostic of right ventricular hypertrophy, but the vectorcardiogram was diagnostic of right ventricular hypertrophy in all 25 of the cases studied. In 21 of the vectorcardiograms, the QRS sE loop displayed the tall R type of right ventricular hypertrophy pattern, while the remaining 4 records showed RSR' right ventricular hypertrophy patterns.
- 4 Right bundle branch block was present in about 10% of the electrocardiograms.
- 5 Almost 60% of the electrocardiograms showed right-axis deviation, the remaining records were divided evenly in showing no axis deviation and left-axis deviation.
- 6 Although some authorities have reported a parallel relationship between the level of right ven-

tricular pressure in pulmonic stenosis and the prominence of the electrocardiographic and vectorcardiographic findings of right ventricular hypertrophy, Braunwald and his associates were unable to confirm this observation. However, the

authors of this text have observed a general relationship between the severity of the clinical manifestations of pulmonic stenosis and the prominence of the electrocardiographic and vectorcardiographic abnormalities.

CARDIAC SHUNTS CAUSING DIASTOLIC LEFT VENTRICULAR OVERLOADING WITH OR WITHOUT SYSTOLIC RIGHT VENTRICULAR OVERLOADING

Interventricular Septal Defect

Unlike atrial septal defects, ventricular septal defects occur more frequently in association with other congenital cardiac anomalies than as isolated lesions. A common combination is ventricular septal defect and pulmonic (usually infundibular) stenosis. At least 90% of isolated ventricular septal defects and virtually all such lesions combined with other cardiac malformations represent developmental anomalies of the membranous portion of the interventricular septum. All other ventricular septal defects result from im-

perfect development of the muscular septum (maladie de Roger) and are usually so small as to be hemodynamically insignificant. The severity of the clinical manifestations of ventricular septal defect is related to the direction and magnitude of the interventricular shunt, these factors in turn being influenced by the size of the septal patency and the pressure gradient between the two ventricles. In the absence of associated anomalies, such as severe pulmonic stenosis or an overriding aorta, the pressure gradient usually produces a left-to-right shunt. However, changes in the peripheral vascular resistance of the pulmonary

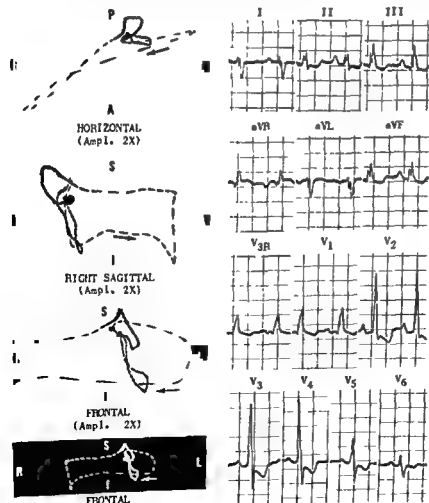


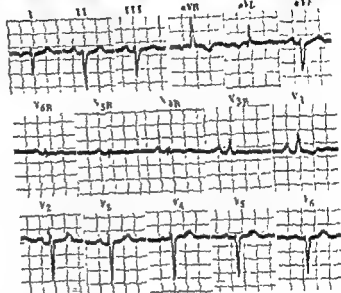
Fig. 114. — Electrocardiographic and vectorcardiographic tall R pattern of right ventricular hypertrophy in a woman, 28, with a large interventricular septal defect and pulmonary hypertension. The initial QRS forces, presumably due to septal ac-

tion and the absence of a Q wave in leads I and V₆ of the electrocardiogram. The corresponding abnormal S-T loop of the vector-

cardiogram is oriented slightly anteriorly, to the left, and inferiorly, and its terminus is displaced superiorly, to the right, and posteriorly. These findings are somewhat suggestive of right atrial enlargement (P pulmonale). Note, also, that the QRS sE loop remains open in each projection, indicating the presence of an S-T vector directed to the right and superiorly.



Fig. 115.—Electrocardiographic and vectorcardiographic tall R pattern of right ventricular hypertrophy in a woman, 30, with postmortem findings of cor triloculare biventriculare with common atrioventricular valve, corrected transposition of the great vessels, valvular pulmonic stenosis, totally anomalous pulmonary venous drainage, and situs inversus of liver, stomach, and pancreas. Note the inverted P wave in lead I which correlates with the rightward orientation of the P sE loop of the vectorcardiogram.



and systemic circulations also can alter the magnitude and direction of the shunt.

Sodi-Pallares and his associates have found the following relationships to hold true in ventricular septal defect (a) If the right ventricular pressure is less than 60 mm. Hg, there is systolic overloading of the right ventricle and diastolic overloading of the left ventricle (b) If the right ventricular pressure exceeds 60 mm. Hg, there is more marked systolic overloading of the right ventricle, but evidence for diastolic overloading of the left ventricle is lacking in the electrocardiogram

Kjellberg and his collaborators have pointed out that, if in a ventricular septal defect the peripheral resistance in the pulmonary circulation equals that in the systemic circulation, a significant interventricular shunt does not occur, and so the hemodynamic burden of the left ventricle is not increased, while that of the right ventricle is greatly increased. This leads to isolated right ventricular hypertrophy. However, with large interventricular septal defects there is a

large interventricular shunt despite a markedly elevated pulmonary vascular resistance, so that, more often than not, anatomic hypertrophy of both left and right ventricles occurs.

THE ECG AND VCG FINDINGS

The data presented below were derived from the combined series of cases reported by the following investigators. Braunwald, Hubbard, Marisco, and Kjellberg and their associates and includes 9 cases of the authors of this text. The combined series, which contains uncomplicated ventricular septal defects and septal defects with right-to-left shunts, totals 238 cases, but only 25 of the patients were studied vectorcardiographically.

- 1 The electrocardiogram was normal in 10% of all the cases. In the smaller group of patients studied vectorcardiographically, 40% of the vectorcardiograms were normal. However, this finding was confined entirely to those patients who had a

- ventricular septal defect without complications.
2. The P waves were abnormally tall and/or wide in leads I, II, or V₁ in almost 15% of the cases. Braunwald and his associates make no mention of the P sE loop findings in their reported series of congenital cardiac anomalies studied vectorcardiographically. None of the 5 patients with ventricular septal defect studied vectorcardiographically by us exhibited P sE loop findings unequivocally suggestive of atrial enlargement.
3. The diagnostic findings of left ventricular hypertrophy were present in 23% of the electrocardiograms and 12% of the vectorcardiograms.
4. The electrocardiogram was diagnostic of right ventricular hypertrophy in almost 35% of the cases, while 45% of the patients studied vectorcardiographically showed right ventricular hypertrophy patterns, primarily of the tall R type.
5. The electrocardiographic diagnosis of combined ventricular hypertrophy was made in 13% of the cases, and complete or incomplete right bundle branch block was present in 7%.
6. About 10% of the cases showed first-degree atrioventricular block (prolonged P-R interval), while over 45% exhibited the Katz-Wachtel sign, consisting of diphasic QRS complexes of great voltage in leads V₂, V₃, and V₄ as well as in the standard limb leads. Sodi-Pallares believes the Katz-Wachtel sign is relatively specific for ventricular septal defect, although occasionally it is observed in atrial septal defect and in patent ductus arteriosus.
7. The mean manifest electrical axis of QRS was normal in 34% of the cases. Right-axis deviation was present in 40% of the cases, and left-axis deviation in 26%.
8. Sodi-Pallares and his co-workers have observed deep Q waves in the left precordial leads of patients with ventricular septal defect and attribute this finding to septal hypertrophy. They regard deep Q waves in the left precordial leads as suggestive evidence favoring ventricular septal defect over other lesions (such as patent ductus arteriosus), which, like the septal defect can produce combined ventricular hypertrophy.

In general, the electrocardiographic and vectorcardiographic findings can be correlated with the clinical and hemodynamic features of a ventricular septal defect in the following way. (a) A normal electrocardiogram and vectorcardiogram suggests that, in the absence of pulmonary stenosis, the right ventricular pressure is probably normal, and either there is no interventricular shunt or there is a left-to-right shunt. (b) If the electrocardiogram or vector-

cardiogram shows isolated right ventricular hypertrophy or combined ventricular hypertrophy, then it is very likely that pulmonary hypertension exists (Figs 114 and 115).

Patent Ductus Arteriosus

During fetal life the ductus arteriosus performs the necessary function of carrying blood from the pulmonary artery to the aorta. This short vessel originates near the bifurcation of the main pulmonary artery or from the left pulmonary artery and joins the aorta just distal to the insertion of the left subclavian artery. During the first postnatal year it is estimated that about 95% of ducti become obliterated, although functional closure, as opposed to anatomic obliteration, probably occurs almost immediately following birth in normal infants. Carson and Burford feel that, if the ductus arteriosus has not been obliterated by the time the child is 3 years old, there is little likelihood of subsequent spontaneous closure. While asphyxia has been shown to delay closure of a normal ductus arteriosus, persistent patency of the ductus is thought probably to reflect an actual malformation of the vessel and not simply a failure of the normal ductus to close. A patent ductus may occur as an isolated abnormality or in combination with other congenital anomalies, such as septal defects, pulmonary or aortic stenosis, and malformations of the aortic arch system. Pulmonary hypertension may also complicate a patent ductus arteriosus and has been attributed to pulmonary vascular changes. However, more recent observations lend some credence to the belief that, in some instances at least, pulmonary hypertension may be related to hypoxia and may disappear when the latter condition is corrected.

A patent ductus arteriosus produces an arteriovenous shunt between the aorta and the pulmonary artery. This shunt leads to an increased pulmonary circulation and an increased pulmonary artery pressure, and, concomitantly, to a greater pulmonary venous return to the left heart. Thus, during a given time interval the left ventricle may expel 2-4 times the volume of blood ejected by the right ventricle. For this reason, an uncomplicated patent ductus arteriosus causes diastolic overloading of the left ventricle. If pulmonary hypertension supervenes in the course of a patent ductus, then, depending on the duration and severity of the resulting systolic overloading of the right ventricle, the electrocardiographic and vectorcardiographic findings of combined ventricular hypertrophy, or occasionally the findings of isolated right ventricular hypertrophy, may appear.

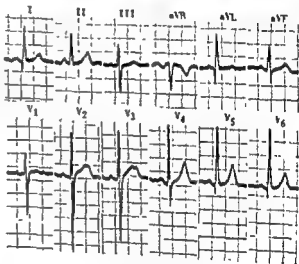
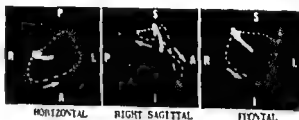
THE ECG AND VCG FINDINGS

The material presented below is based on the combined series of Braunwald and his co-workers, Sokolow and Edgar, Kjellberg and his associates, and the authors of this text. The total number of cases in the groups, which includes cases of uncomplicated patent ductus arteriosus and cases with pulmonary hypertension, was 139, 17 of the patients were studied vectorcardiographically.

presence of combined ventricular hypertrophy might be suspected from the electrocardiogram, and this interpretation would be consistent with patent ductus arteriosus with early and relatively minor degree of pulmonary hypertension.

In the vectorcardiogram

ated more anteriorly than normal, although inscribed in a normal direction in the horizontal projection. In addition, the QRS sE loops showed a prominent early deflection extending relatively far to the right and anteriorly. These early deflections were undoubtedly responsible for the tall R waves recorded in lead V_1 in the electrocardiograms of these 2 cases. In each case, the II wave exceeded 7 mm. even though the RS amplitude ratio in V_1 was less than 1. Parenthetically, one might add



1. The electrocardiogram was normal in about 60% of the cases, while approximately 45% of the vectorcardiograms were normal.
2. Almost one fourth of the cases presented electrocardiographic evidence of left ventricular hypertrophy, while 2 of the 17 vectorcardiograms were interpreted as left ventricular hypertrophy.
3. Eight per cent of the electrocardiograms showed right ventricular hypertrophy, and almost one third of the vectorcardiograms presented right ventricular hypertrophy.

4. In the vectorcardiograms recorded by us in patients with patent ductus arteriosus were unusual in that the QRS sE loops were situated

- that in the 2 cases in question the patients were adults. As will be recalled, the electrocardiogram of the juvenile typically displays much taller R waves in lead V_1 than does that of the adult. The authors consider the electrocardiographic and vectorcardiographic findings just described, when observed in an adult, to be strongly suggestive of combined ventricular hypertrophy.
5. Incomplete or complete right bundle branch block was noted in the electrocardiograms of only 3% of the cases.
6. The mean manifest electrical axis of QRS was normal in 60% of the cases (Fig. 116); right-axis deviation was present in 30% of the electrocardiograms and left-axis deviation was present in 10% of the tracings.

CARDIAC SHUNTS CAUSING DIASTOLIC RIGHT VENTRICULAR OVERLOADING

**Interatrial Septal Defect
(with Left-to-Right Shunt)**

When there is a congenital defect in the interatrial septum (other than a patent foramen ovale), the pressure gradient normally existing between the left and the right atria produces a left-to-right shunt of blood through the septal defect. Depending on the magnitude of the left-to-right shunt, the right ventricular output can rise to twice that of the left ventricle, and pulmonary blood flow may be increased to 3 times systemic blood flow. An atrial septal defect therefore leads to diastolic overloading of the right ventricle. According to Walker and his collaborators, the muscles of the basal portion of the right ventricle bear, for the most part, the hemodynamic burden imposed by an increase in stroke volume consequent to diastolic overloading of the right ventricle. This is to be contrasted with the concentric hypertrophy of the right ventricular wall which occurs in conditions increasing ventricular work—that is, in conditions causing systolic overloading. Thus, Walker and his associates postulate that a selective hypertrophy of basal right ventricular muscle occurs in atrial septal defects. In support of this hypothesis, Kjellberg and his co-workers have reported that on pathologic examination the right ventricular wall is of normal thickness in cases of atrial septal defect without pulmonary hypertension, however, characteristically there is marked hypertrophy of the crista supraventricularis, its parietal and septal bands, and the trabecular network of the right ventricle. With the development of pulmonary hypertension (and the resulting systolic overloading of the right ventricle) in some cases of atrial septal defect, the right ventricle undergoes concentric hypertrophy. The significance of these observations with reference to the electrocardiographic and vectorcardiographic features of atrial septal defect will be indicated later.

Because in an atrial septal defect the right atrium receives blood from the venae cavae as well as from the left atrium, the right atrium usually undergoes a variable degree of dilatation and hypertrophy. On the other hand, the left atrium is usually not enlarged even with large left-to-right shunts, such as those caused by an associated mitral stenosis (Lutembacher's syndrome), since the atrial septal defect functions somewhat like a safety valve, preventing any significant increase in the amount of blood in the left atrium.

THE ECG AND VCG FINDINGS

The percentages of cases of atrial septal defect showing each of the electrocardiographic and vectorcardiographic features cited below were calculated from the combined series of the following investigators. Braunwald, Kjellberg, Limon, Silverblatt, and Walker and their associates, Smull and Lamb, and the authors of this text. When these series were pooled, the number of cases totaled 239, but only 63 patients were studied vectorcardiographically.

1. The electrocardiogram was normal in about 6% of the 239 patients, while the vectorcardiogram was normal in none of the 63 patients studied vectorcardiographically.
2. Abnormally tall and/or wide P waves were recorded in lead II and/or lead V_1 in about one fourth of the cases. In our experience, abnormalities of the P sE loop were relatively uncommon in vectorcardiograms recorded in cases of atrial septal defect.
3. The electrocardiogram was diagnostic of right ventricular hypertrophy in about 30% of the cases, while the vectorcardiogram presented findings diagnostic of right ventricular hypertrophy in about 95% of the cases so studied. Approximately 65% of the vectorcardiograms showing right ventricular hypertrophy were found to have the RSR' pattern

vectorcardiographic pattern of right ventricular hypertrophy are atrial septal defect and mitral stenosis.

4. A right bundle branch block type of QRS configuration with a QRS duration of 0.10 second or longer was present in lead V_1 in about 13% of the cases, while RSR' deflections of shorter duration in lead V_1 were found in about 55% of the cases. Although QRS sE loops otherwise typical of right ventricular hypertrophy can occasionally display conduction delay localized to the terminal portion of the loop or involving the greater portion of the loop, the vectorcardiographic pattern of right bundle branch block unaccompanied by evidence of right ventricular hypertrophy was encountered relatively rarely. Thus, Braunwald and his associates observed the vectorcardiographic pattern of right bundle branch block in only 1 of 19 cases of interatrial septal defect, and we recorded this pat-

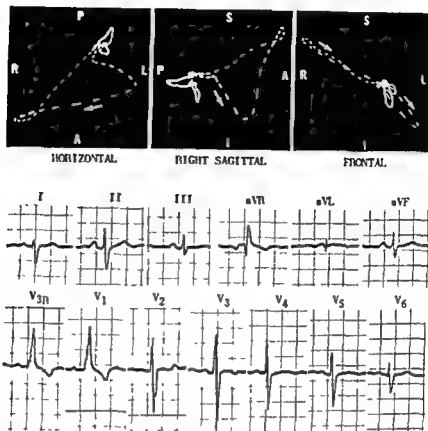


Fig. 118.—Electrocardiographic and vectorcardiographic tall R pattern of right ventricular hypertrophy in a youth, 19, with pulmonic stenosis and interatrial septal defect (trilogy of Fallot).

terminated by the degree of pulmonic stenosis. Generally, this condition is also accompanied by more prominent electrocardiographic and vectorcardiographic findings of right ventricular hypertrophy than occur in uncomplicated atrial septal defects (Fig 118).

Atrial septal defect with pulmonary hypertension—A reversed, or right-to-left, shunt produced by pulmonary hypertension is a much less common occur-

rence with atrial septal defect than with ventricular septal defect or patent ductus arteriosus. As in trilogy of Fallot, the degree of anatomic right ventricular

septal defect with pulmonary hypertension on the basis of pulmonary vascular disease than in uncomplicated septal defects.

MULTIPLE CARDIAC ANOMALIES OR CARDIAC ANOMALIES ACCOMPANIED BY OTHER DEVELOPMENTAL DEFECTS

Dextrocardia

When the heart is located in the right chest, any of the following abnormalities may be responsible:

Dextrocardia with situs inversus—In this condition, there is true or mirror-image dextrocardia, in which the left-sided chambers are situated to the right while the right-sided heart chambers are located to the left. The apex of the heart is formed by the left ventricle. This is the type of dextrocardia which, with chronic sinusitis and bronchiectasis, comprises Kartagener's triad (or syndrome).

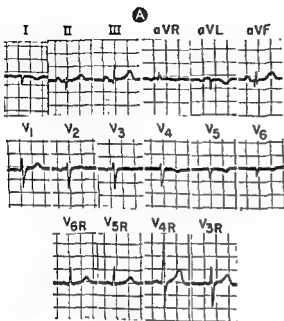
Isolated dextrocardia.—In this instance, mirror-

image or true dextrocardia is not accompanied by situs inversus of other body organs but tends to be associated with other cardiac anomalies, such as pulmonic stenosis, or cor triloculare batriatum.

Dextroversion of the heart—Mirror-image dextrocardia is not present in this condition. The heart is merely displaced and rotated so that it lies in the right chest, and there are usually associated cardiac abnormalities.

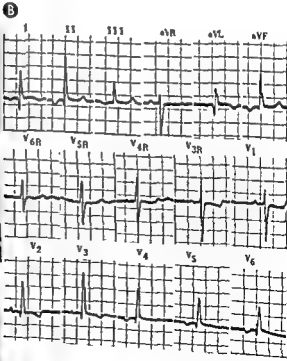
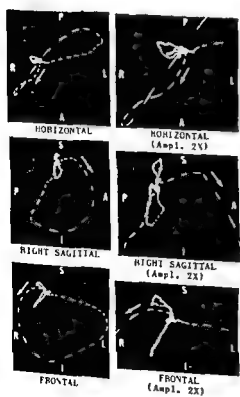
Dextroposition of the heart.—In this condition the heart is merely displaced into the right chest by some acquired disease of the lungs, pleura, or diaphragm.

Fig 119.—A, electrocardiographic features of



and the precordial leads were recorded from left

atrial hypertrophy in a woman, 20, with Eisenmenger's complex (large interventricular septal defect with overriding aorta and pulmonary hypertension) and total situs inversus. Here the electrocardiographic findings differ from those in



THE ECG AND VCG FINDINGS

In the following paragraphs the electrocardiographic and vectorcardiographic findings in mirror-image or true dextrocardia will be described. The electrocardiographic features of dextrocardia are as follows:

1. The electrical axis of P ($\bar{A}P$) is situated at about $+120^\circ$ in the frontal plane, with the result that lead I records an inverted P wave. This is the most typical finding in dextrocardia.
2. The QRS deflection in lead I and the T wave in this lead are mirror images of the corresponding normal deflections in this lead. Thus, there is usually a deep Q wave and an inverted T wave in lead I.
3. Leads II and III are interchanged.
4. The precordial transition is reversed, so that leads over the right precordium record upright QRS deflections and upright T waves, while leads over the left precordium record resultantly downwardly directed ventricular deflections.
5. If the left- and right-arm lead wires are reversed and the precordial leads are recorded from left to right over the right precordium, the electrocardiogram recorded should appear normal. If it does not, then associated cardiac abnormalities should be suspected (Fig. 119, A).

The vectorcardiographic findings in mirror-image or true dextrocardia are as follows

1. The P sE loop is usually directed to the right, inferiorly, and either slightly anteriorly or slightly posteriorly. The direction of the inscription of the P sE loop in the right sagittal projection is the reverse of normal, i.e., counterclockwise.
2. The QRS sE loop is generally situated to the right, inferiorly, and slightly anteriorly or slightly posteriorly. The direction of inscription of the spatial loop in each of its three projections is the reverse of normal (Fig. 119, B).

Tetralogy of Fallot

The familiar tetrad of abnormalities collectively designated *tetralogy of Fallot*, consists of three congenital anomalies—namely, pulmonic stenosis, aortic overriding, and high interventricular septal defect—which jointly produce the remaining acquired abnormality, right ventricular hypertrophy. This condition accounts for about 75% of all cases of cyanotic congenital heart disease. Fortunately, certain surgical

procedures achieve remarkably beneficial results in many patients with tetralogy of Fallot.

The basic hemodynamic disturbance produced by this combination of anomalies is a right-to-left shunt between the right ventricle and the aorta. Whether the clinical consequences of a tetralogy are minimal, lethal, or of some intermediate degree of severity is determined mainly by the magnitude of the shunt or, even more fundamentally, by the degree of pulmonic stenosis and overriding of the aorta. Thus the pulmonic stenosis may be mild, the aortic overriding minimal, and the hemodynamic disturbance relatively insignificant. The other extreme is represented by pulmonary atresia and complete transposition of the aorta, the latter arising entirely from the right ventricle. This combination is sometimes called *pseudo-truncus arteriosus*. In the less extreme cases of tetralogy of Fallot, there may be both systolic and diastolic overloading of the right ventricle, according to Cabrera and Monroy. These investigators state that the pulmonary stenosis and the overriding of the aorta determine the systolic overloading, while the blood shunted from the right ventricle to the aorta increases the diastolic loading of the right cavities. From the standpoint of the electrocardiogram, Sodi-Pallares and Marisco have found tetralogy of Fallot to behave much like a pure pulmonic stenosis.

THE ECG AND VCG FINDINGS

The percentages of cases of tetralogy of Fallot showing the various findings cited below were calculated from the combined series of Braunwald and his co-workers, Kjellberg and his associates, Woods, and the authors of this text. The number of cases in the combined series totaled 125, of which 30 were studied vectorcardiographically.

1. Both the electrocardiogram and vectorcardiogram were normal in about 3% of the cases.
2. In about 30% of the cases the P waves in lead II and/or lead V_1 were abnormally tall and/or wide.
3. In approximately 95% of the cases the electrocardiogram and vectorcardiogram presented the findings of right ventricular hypertrophy, the vectorcardiographic right ventricular hypertrophy pattern usually being of the tall R type.
4. The electrocardiographic pattern of complete or incomplete right bundle branch block was observed in about 3% of the cases.
5. There was right-axis deviation of the mean manifest electrical axis of QRS in almost 90% of the cases, left-axis deviation in about 7%, and no axis deviation in the remaining 3% of the cases.

Mitral Stenosis

ORDINARILY, in a discussion of the pathophysiologic factors responsible for the electrocardiographic and vectorcardiographic findings in mitral stenosis, chief and almost exclusive attention is given to the mechanical effects of the stenotic mitral valve and the associated rise in pulmonary capillary and arteriolar pressures. However, it should not be forgotten that invariably in rheumatic valvular lesions, such as mitral stenosis, antecedent rheumatic carditis has left residual myocardial damage of varying degree. Sometimes the myocardial damage may actually assume greater importance than the valvular lesion and may determine, among other things, the clinical course and the electrocardiographic manifestations of the patient's cardiac disease. Since the significance of the myocardial factor in a given case of mitral stenosis is difficult and usually impossible to assess before autopsy, the hemodynamic and related electrical effects of mitral stenosis will be considered in the following paragraphs only from the standpoint of the valvular lesion itself and the accompanying changes in the pulmonary circulation.

The train of pathophysiologic events in mitral stenosis can be described in brief as follows:

1. The increased resistance offered by the stenotic mitral valve leads to an elevated pressure in the left atrium, and, since there are no valves between the atrium and the pulmonary veins, the increased left intra-atrial pressure induces a rise in the pulmonary venous and capillary pressures.

2. Any increase in blood flow, such as that occurring during exercise, increases left atrial and pulmonary capillary pressures. Moreover, the stenotic mitral valve sometimes offers relatively little resistance to blood flow at rest, but with exercise its ability to adjust to the greater blood flow is limited, and this can be reflected by a marked rise in left atrial pressure.

3. The pulmonary arterial pressure for a given blood flow is a function of the pulmonary capillary pressure (measured as the so-called wedge pressure) and the resistance in the pulmonary arterioles. If an elevation of the pulmonary capillary pressure is of sufficiently long duration, pulmonary vascular changes develop, in which case the resulting increased arteriolar resistance in conjunction with the elevated pulmonary capillary pressure produces pulmonary hypertension.

4. To overcome the greater resistance to systolic ejection consequent to the increased pulmonary venous and capillary pressures, and thereby to maintain its normal output, the right ventricle must contract more forcefully. This in turn leads to a rise in pulmonary arterial and right ventricular systolic pressures. Concomitant elevation of the pulmonary arteriolar resistance has two contrasting hemodynamic consequences: (a) the higher pulmonary arteriolar resistance, on the one hand, protects the pulmonary capillaries from marked rises in pressure which otherwise might produce pulmonary edema, and (b) on the other hand, the greater arteriolar resistance imposes a more severe hemodynamic burden on the right ventricle.

In the presence of pulmonary hypertension, there is systolic overloading of the right ventricle, and, if cardiac failure supervenes, there may be added to this hemodynamic burden diastolic overloading of the right ventricle. In such cases, one not infrequently finds anatomic and electrocardiographic evidence of right ventricular hypertrophy of a degree comparable to that observed in some of the more severe types of congenital heart disease. On the other hand, the prominence of the electrocardiographic manifestations may fail to parallel the degree of the anatomically noted right ventricular hypertrophy because of the factors listed at the beginning of this section. Two

of the more important of these variables in mitral stenosis are: (a) changes in anatomic heart position and rotation which modify transmission of QRS potentials to the recording electrode; and (b) the presence of additional valvular or myocardial lesions causing left ventricular hypertrophy (which tends to offset the electrical effects of the right ventricular hypertrophy).

In a typical case of mitral stenosis, the right ventricle at postmortem examination shows little or no

thickening of its muscular wall, instead, there is hypertrophy of the crista supraventricularis and related structures and of the trabeculae of the right ventricle. This more or less selective hypertrophy of the right ventricle is usually accompanied by marked dilatation of the affected chamber. In addition, as one might anticipate, mitral stenosis characteristically leads to dilatation and hypertrophy of the left atrium, and sometimes of the right atrium. The left ventricle may be relatively unaffected pathologically.

ELECTROCARDIOGRAPHIC FINDINGS

The electrocardiographic findings most typical of mitral stenosis, which are to be described in the following paragraphs, are observed for the most part in pure mitral stenosis or in hemodynamically predominant mitral stenosis with coexisting mitral insufficiency of relatively minor significance. With more severe degrees of mitral insufficiency or when mitral stenosis is associated with aortic valvular disease, the electrocardiogram rarely displays the diagnostic findings of mitral stenosis.

Typically in mitral stenosis, the electrocardiographic manifestations are related etiologically to the two major anatomic effects of the valvular lesion, which are, as previously indicated, left atrial enlargement and right ventricular hypertrophy. To afford some estimate of the frequency of the various diagnostic features of pure or predominant mitral stenosis, the series of cases of mitral stenosis of Lewis, Biorek, Scott, and Donoso and their associates, and of Morris and Whitaker, and Trownce, including 47 cases of the authors of this text, were combined to form a study group totaling 435 cases. The percentage of electrocardiograms in this group showing each of the diagnostic features of mitral stenosis to be described will be cited at appropriate points in the following discussion.

Anatomic left atrial enlargement *per se* can alter the electrocardiogram in two ways, it can cause disturbances of the atrial rhythm, and it can produce the P wave pattern of P mitrale.

Cardiac Rhythm

Left atrial enlargement due to mitral stenosis frequently gives rise to paroxysmal or chronic atrial fibrillation or occasionally flutter. The manner in which these atrial arrhythmias are produced in mitral stenosis is not known for certain, although factors such as the following may be involved. (a) elevated

left atrial pressure, (b) left atrial dilatation, (c) intra-atrial conduction delay consequent to atrial dilatation and/or to residual myocardial fibrosis following acute rheumatic carditis, and (d) focal or diffuse fibrosis of atrial myocardium or acute "smoldering" subacute rheumatic carditis.

In the combined series of cases of mitral stenosis, 20% of the electrocardiograms showed atrial fibrillation, while 20% of the remaining cases with normal sinus rhythm in our own series displayed first-degree atrioventricular block. The latter finding is frequently noted electrocardiographically in patients with mitral stenosis before onset of atrial fibrillation and may persist indefinitely following conversion of atrial fibrillation to sinus rhythm. Apparently, in pure mitral insufficiency unaccompanied by mitral stenosis, sinus rhythm is far more common than atrial fibrillation, but in the great majority of cases of mitral stenosis with a significant degree of mitral insufficiency, there is a very high incidence of atrial fibrillation (15 out of 17 cases reported by Wierum and Glenn).

The ECG and VCG P Mitrale Pattern

The abnormalities of the electrocardiographic P waves characteristic of the P mitrale pattern (Fig. 130) are as follows.

1. The mean manifest electrical axis of P ($\bar{A}P$) or frontal plane mean P vector tends to assume a horizontal and leftward orientation, approximating the 0° axis of the frontal reference frame, in contrast with its normal average orientation along with $+60^\circ$ axis. This means that, by and large, the P waves in leads I and aVL in P mitrale are more prominent than those in leads III and aVF.
2. The P waves in leads I and aVL are abnormally wide, exceeding the normal upper limit of P

wave duration of 0.11 second. More often than not, the P waves, particularly in the leads just cited, display double-peaked, flattened summits. The notching and broadening of the P waves in P mitrale have been attributed by some authorities to an intra-atrial conduction disturbance or to a prolonged activation time of the left atrium. The conduction defect has been variously ascribed to stretching of the atrial wall as the left atrium dilates, to interstitial fibrosis, and to myocarditis. Sano and his associates believe that the characteristic widening and notching of the P waves in P mitrale supply reflect an exaggeration of the normal time lag of left atrial activation behind right atrial activation. Presumably, hypertrophy and dilatation of the left atrium increase the time required for activation, and since the onset of activation in the left atrium normally occurs later than in the right atrium, the result is an over-all lengthening of the time required for depolarization of both atria. Moreover, since activation

of the right atrium tends to be separated in time from activation of the left atrium, the electrical forces produced by activation of each atrium are manifested more or less separately in the electrocardiogram, as evidenced by the double-peaked P wave typical of P mitrale.

Occasionally in mitral stenosis the P waves in leads I and aVL, or, less commonly, in leads II and III, are abnormally tall, equaling or exceeding 2.5 mm. in amplitude.

- 3 The mean instantaneous P wave forces and the horizontal plane mean P vector in mitral stenosis tend to be rotated to the left and far posteriorly, probably reflecting the increased electrical predominance of the posteriorly situated left atrium. Alternatively, the early instantaneous P forces, which are attributed to right atrial activation, are directed anteriorly, but the subsequent and larger electrical P forces produced by left atrial activation are displaced abnormally far posteriorly. Thus the P waves in lead V_1 and V_2 may be large and downwardly di-

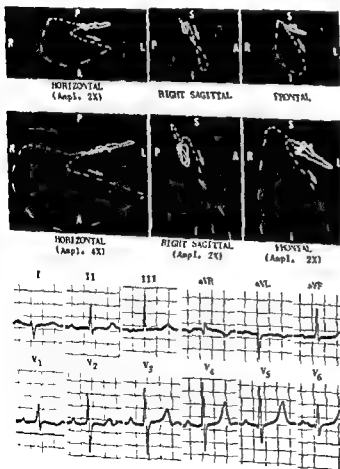


Fig 120.—Electrocardiographic and vectorcardiographic P mitrale pattern of left atrial enlargement and tall R pattern of right ventricular hypertrophy in a woman 21 years of age.

lated at about 60° in the frontal reference frame, while the width of the P wave in lead I is 0.13 second (upper limit of normal P wave duration, 0.11 second). The P sE loop in the vectorcardiogram is oriented almost directly to the left in the frontal projection and somewhat posteriorly in the horizontal projection. The vectorcardiographic findings characteristic of the tall R pattern of right ventricular hypertrophy are obvious in this figure and need not be described.

of the more important of these variables in mitral stenosis are: (a) changes in anatomic heart position and rotation which modify transmission of QRS potentials to the recording electrode; and (b) the presence of additional valvular or myocardial lesions causing left ventricular hypertrophy (which tends to offset the electrical effects of the right ventricular hypertrophy).

In a typical case of mitral stenosis, the right ventricle at postmortem examination shows little or no

thickening of its muscular wall, instead, there is hypertrophy of the crista supraventricularis and related structures and of the trabeculae of the right ventricle. This more or less selective hypertrophy of the right ventricle is usually accompanied by marked dilatation of the affected chamber. In addition, as one might anticipate, mitral stenosis characteristically leads to dilatation and hypertrophy of the left atrium, and sometimes of the right atrium. The left ventricle may be relatively unaffected pathologically

ELECTROCARDIOGRAPHIC FINDINGS

The electrocardiographic findings most typical of mitral stenosis, which are to be described in the following paragraphs, are observed for the most part in *pure mitral stenosis* or in hemodynamically predominant mitral stenosis with coexisting mitral insufficiency of relatively minor significance. With more severe degrees of mitral insufficiency or when mitral stenosis is associated with aortic valvular disease, the electrocardiogram rarely displays the diagnostic findings of mitral stenosis.

Typically in mitral stenosis, the electrocardiographic manifestations are related etiologically to the two major anatomic effects of the valvular lesion, which are, as previously indicated, left atrial enlargement and right ventricular hypertrophy. To afford some estimate of the frequency of the various diagnostic features of pure or predominant mitral stenosis, the series of cases of mitral stenosis of Lewis, Biorck, Scott, and Donoso and their associates, and of Morris and Whitaker, and Trounce, including 47 cases of the authors of this text, were combined to form a study group totaling 435 cases. The percentage of electrocardiograms in this group showing each of the diagnostic features of mitral stenosis to be described will be cited at appropriate points in the following discussion.

Anatomic left atrial enlargement per se can alter the electrocardiogram in two ways: it can cause disturbances of the atrial rhythm, and it can produce the P wave pattern of P mitrale.

Cardiac Rhythm

Left atrial enlargement due to mitral stenosis frequently gives rise to paroxysmal or chronic atrial fibrillation or occasionally flutter. The manner in which these atrial arrhythmias are produced in mitral stenosis is not known for certain, although factors such as the following may be involved: (a) elevated

left atrial pressure, (b) left atrial dilatation, (c) intra-atrial conduction delay consequent to atrial dilatation and/or to residual myocardial fibrosis following acute rheumatic carditis, and (d) focal or diffuse fibrosis of atrial myocardium or acute "smoldering" subacute rheumatic carditis.

In the combined series of cases of mitral stenosis, 20% of the electrocardiograms showed atrial fibrillation, while 20% of the remaining cases with normal sinus rhythm in our own series displayed first-degree atrioventricular block. The latter finding is frequently noted electrocardiographically in patients with mitral stenosis before onset of atrial fibrillation and may persist indefinitely following conversion of atrial fibrillation to sinus rhythm. Apparently, in pure mitral insufficiency unaccompanied by mitral stenosis, sinus rhythm is far more common than atrial fibrillation, but in the great majority of cases of mitral stenosis with a significant degree of mitral insufficiency, there is a very high incidence of atrial fibrillation (15 out of 17 cases reported by Wierum and Glenn).

The ECG and VCG P Mitrale Pattern

The abnormalities of the electrocardiographic P waves characteristic of the P mitrale pattern (Fig. 120) are as follows.

1. The mean manifest electrical axis of P ($\bar{A}P$) or frontal plane mean P vector tends to assume a horizontal and leftward orientation, approximating the 0° axis of the frontal reference frame, in contrast with its normal average orientation along with $+60^\circ$ axis. This means that, by and large, the P waves in leads I and aVL in P mitrale are more prominent than those in leads III and aVF.
2. The P waves in leads I and aVL are abnormally wide, exceeding the normal upper limit of P

wave duration of 0.11 second. More often than not, the P waves, particularly in the leads just cited, display double-peaked, flattened summits. The notching and broadening of the P waves in P mitrale have been attributed by some authorities to an intra-atrial conduction disturbance or to a prolonged activation time of the left atrium. The conduction defect has been variously ascribed to stretching of the atrial wall as the left atrium dilates, to interstitial fibrosis, and to myocarditis. Sano and his associates believe that the characteristic widening and notching of the P waves in P mitrale simply reflect an exaggeration of the normal time lag of left atrial activation behind right atrial activation. Presumably, hypertrophy and dilatation of the left atrium increase the time required for activation, and since the onset of activation in the left atrium normally occurs later than in the right atrium, the result is an over-all lengthening of the time required for depolarization of both atria. Moreover, since activation

of the right atrium tends to be separated in time from activation of the left atrium, the electrical forces produced by activation of each atrium are manifested more or less separately in the electrocardiogram, as evidenced by the double-peaked P wave typical of P mitrale.

Occasionally in mitral stenosis the P waves in leads I and aVL, or, less commonly, in leads II and III, are abnormally tall, equaling or exceeding 2.5 mm in amplitude.

- 3 The mean instantaneous P wave forces and the horizontal plane mean P vector in mitral stenosis tend to be rotated to the left and far posteriorly, probably reflecting the increased electrical predominance of the posteriorly situated left atrium. Alternatively, the early instantaneous P forces, which are attributed to right atrial activation, are directed anteriorly, but the subsequent and larger electrical P forces produced by left atrial activation are displaced abnormally far posteriorly. Thus the P waves in leads V_1 and V_2 may be large and downwardly di-

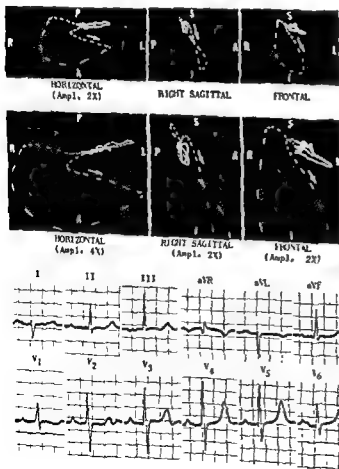


Fig. 120.—Electrocardiographic and vectorcardiographic P mitrale pattern of left atrial enlargement and tall R pattern of right ventricular hypertrophy in a woman, 31, with mitral stenosis. The electrocardiographic diagnosis of left atrial enlargement is based on the following findings: A P is located at about 0° in the frontal reference frame, while the width of the P wave in lead I is 0.12 second (upper limit of normal P wave duration, 0.11 second). The P sE loop in the vectorcardiogram is oriented almost directly to the left in the frontal projection and somewhat posteriorly in the horizontal projection. The vectorcardiographic findings characteristic of the tall R pattern of right ventricular hypertrophy are obvious in this figure and need not be described.

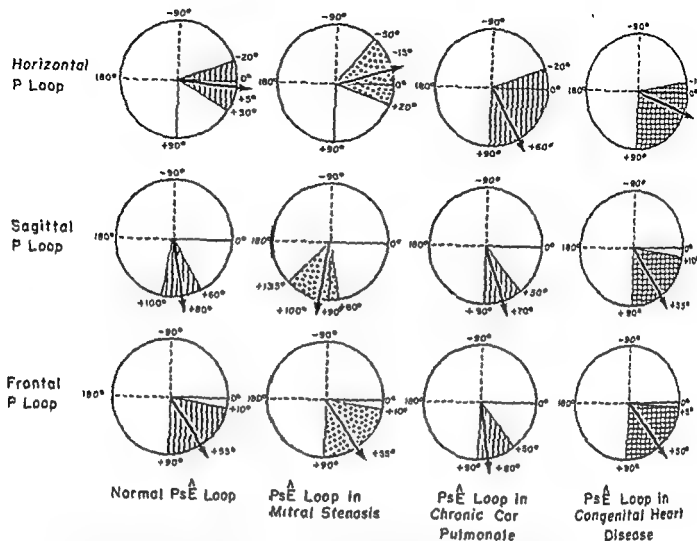


Fig. 121.—Extreme range of variation and average orientation of the maximal mean instantaneous vector of the P sE loop in normal subjects, in mitral stenosis, in chronic cor pulmonale, and in congenital heart disease.

rected, on the one hand, or they may be diphasic (plus-minus).

In the mitral stenosis cases with sinus rhythm in the combined series of Lewis and his co-workers, Scott and his associates, and the authors of this text, almost 65% of the electrocardiograms displayed abnormally wide and/or tall P waves in one or more leads. In our 30 cases with sinus rhythm, the P waves were normal in 9 cases, they were abnormally wide in lead I in 5 cases and in lead II in 9 cases, 4 electrocardiograms displayed abnormally tall P waves in lead II, and in 2 cases the P waves in lead II were both wide and tall. In 1 case the P waves were abnormally wide in lead I and abnormally tall in lead II. Notching of the P waves of varying degree was present in all 21 cases with other P wave abnormalities. The P wave amplitude in lead V₁ was not measured in our cases of mitral stenosis; but, as a general rule, the P

waves in this lead were usually relatively large and either inverted or diphasic (plus-minus), the initial upright component of the diphasic P wave being smaller than the following downwardly directed component. The mean manifest electrical axis of P in the electrocardiograms with P wave abnormalities averaged +48°, with a range of variation between 0° and +80°. It is worthy of note that left atrial enlargement resulting from mitral insufficiency is associated only infrequently with P wave abnormalities. Even when abnormal P waves are observed in mitral insufficiency, they tend to be less striking than those occurring in mitral stenosis. Bridgen and Leatham studied 30 patients with relatively pure mitral insufficiency and found that the P waves were normal in all cases. Thus, when the electrocardiogram shows prominent P wave abnormalities, the presence of mitral stenosis should be suspected.

The vectorcardiographic P sE loop abnormalities

TABLE 12 - ORIENTATION OF THE MAXIMAL MEAN INSTANTANEOUS VECTOR OF THE P SE LOOP IN MITRAL STENOSIS

	Horizontal			Right Sagittal			Frontal		
	Extreme Range	Av	Usual Range	Extreme Range	Av	Usual Range	Extreme Range	Av	Usual Range
30 cases with mitral stenosis and sinus rhythm	-50° to +20°	-15°	-30° to 0°	+80° to +135°	+100°	+80° to +100°	+10° to +90°	+55°	+30° to +80°
18 (of the above 30) cases with electrocardiographic p mitrale	-50° to 0°	-25°	-30° to 0°	+80° to 130°	+105°	+80° to +100°	+10° to +80°	+45°	+30° to +70°
(Normal cases*)	(-20° to +30°)	(+25°)	(0° to +5°)	(+80° to +100°)	(+80°)	(+80° to +90°)	(+10° to +90°)	(+55°)	(+20° to +60°)

*The normal values for P π loop orientation are enclosed in parentheses and are the same as those presented in Table 4 in Chapter V. They are included in the table as a basis for comparison with the values obtained in mutual steremia

corresponding to the electrocardiographic P mitrale pattern (Fig 121) are as follows.

1. The maximal mean instantaneous P vector or long axis of the P sE loop is of greater than normal magnitude.
2. In the horizontal projection, the P sE loop, in addition to its increased size, frequently has a bifid, or figure-of-eight, configuration, with the larger component of the loop being directed posteriorly and inscribed in a clockwise direction. The earlier portion of the P sE loop is written anteriorly in a counterclockwise direction. If the anterior component of the horizontal P loop equals or approaches in size the later posterior component, both left and right atrial enlargement may be present. The average orientation and range of variation of the P sE loop in our 30 cases of mitral stenosis are presented in Table 12 and in Figure 121. The average orientation of the P sE loop and range of variation were also determined in the 16 mitral stenosis cases with electrocardiographic P mitrale, and these results are also indicated in Table 12.
3. In the sagittal and frontal projections, the P sE loop is elongated and may have a figure-of-eight configuration, although far less frequently than in the horizontal projection. The direction of inscription of the sagittal and frontal loops is the same as normal—that is, clockwise and counterclockwise, respectively.

Right Ventricular Hypertrophy

If any one lead can be singled out as the diagnostic lead in right ventricular hypertrophy occurring in mitral stenosis, it is lead V_1 , because more often than not the electrocardiographic manifestations of right ventricular hypertrophy are most prominent and most easily recognized in this lead. The combined series of cases of mitral stenosis were grouped according to the type of QRS configuration and/or the R/S amplitude ratio in lead V_1 , and the following observations were made.

- 1 Lead V₁ recorded an rS or QS deflection in almost 45% of the cases, even though anatomic right ventricular hypertrophy could be demonstrated radiologically in many of these cases.
- 2 In approximately 25% of the cases, lead V₁ registered an RSR' deflection. The terminal R wave was of equal or smaller size than the initial R wave in 10% of the electrocardiograms, while in the remaining 15% the secondary R' wave was taller than the initial R wave. The first type of RSR'

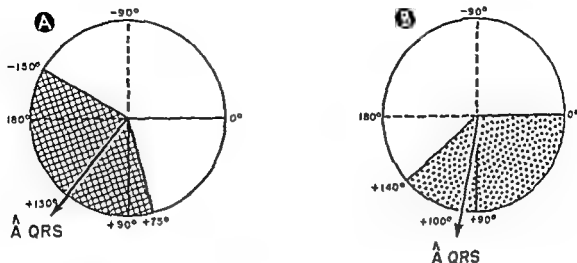


Fig. 122.—The extreme range of variation and average orientation of A QRS in the frontal plane in (A) congenital heart disease (with overloading of the right ventricle) and (B) mitral stenosis.

pattern is one that is frequently observed in normal electrocardiograms, while the second RSR' pattern has been considered in the past to represent incomplete right bundle branch block. As previously indicated, there is good reason to believe that in many cases the incomplete right bundle branch block pattern actually represents right ventricular hypertrophy. In our 21 cases with RSR' deflections in lead V_1 , the R' wave was smaller than 7 mm in amplitude in all but 1 case, which had an R' of 7 mm. Thus, none of the electrocardiograms fulfilled Barker and Valencia's criteria for the diagnosis of right ventricular hypertrophy in the presence of incomplete or complete right bundle branch block (R' > 10 mm or > 15 mm amplitude, respectively). Moreover, 9 of the 21 patients with RSR' deflections in lead V_1 failed to present vectorcardiographic evidence of right ventricular hypertrophy.

3 In the remaining 30% of the cases, lead V_1 dis-

played QRS complexes of various configurations other than RSR' (qR, qRs, Rs, R, etc.), but in

all of these cases if an R/S ratio greater than 1 in lead V_1 was the only requirement for making the diagnosis of right ventricular hypertrophy. Fifteen electrocardiograms in our series were placed in this category, but in only 8 of these did the R wave in V_1 equal or exceed 7 mm. In this group of electrocardiograms, the onset of the intrinsicoid deflection in lead V_1 occurred later than 0.03 second in almost 65% of the cases.

4 Right-axis deviation of the mean manifest electrical axis of QRS was present in 45% of the electrocardiograms in the combined series, left-axis deviation was noted in 5%, and no axis deviation in the remaining 50% (Fig. 122). Right-axis deviation of A QRS, when present, was not usually marked

VECTORCARDIOGRAPHIC FINDINGS

The QRS sE loop findings in patients with relatively pure mitral stenosis and with mixed mitral stenosis and insufficiency (and/or aortic valvular disease), presented below, were compiled from the series of Donoso and his co-workers, Scherlis and his associates, and the authors of this text. When these series were combined, the number of cases of relatively pure mitral stenosis totaled 81, while the total number of cases with mitral stenosis and insufficiency or other valvular lesions was 39.

1 In almost 75% of the pure mitral stenosis cases and 25% of the cases with other valvular lesions in addition to mitral stenosis, the QRS sE loop presented evidence of right ventricular hypertrophy. In our 36 cases of pure mitral stenosis, 23 vectorcardiograms (64% of the records) were diagnostic of right ventricular hypertrophy, 16 showing the RSR' pattern of right ventricular hypertrophy and 7 the tall R pattern of right ventricular hypertrophy. In the 17 cases of mitral stenosis accom-

panied by mitral insufficiency or aortic valve disease, 5 vectorcardiograms (29% of the records) were diagnostic of right ventricular hypertrophy, and all 5 showed the RSR' pattern of right ventricular hypertrophy.

2. Left ventricular hypertrophy patterns of the QRS sE loop were not observed in any cases of pure mitral stenosis but were present in 22% of the vectorcardiograms of patients with multivalvular lesions.

3. Eight of the 43 cases of pure mitral stenosis reported by Donoso and his associates presented the

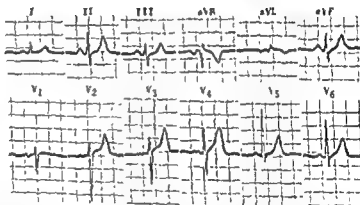
scribed only sketchily, since these patterns will be discussed in detail in the following chapter, on cor pulmonale. For descriptive convenience, the three QRS sE loop patterns will be referred to hereafter as "types A, B, and C" QRS sE loop patterns.

Type A QRS sE Loop Pattern

The QRS sE loop in this pattern (Fig 123) differs from the normal in that it displays a terminal deflection of varying size directed to the right, pos-



Fig 123.—Type A QRS sE loop pattern in mitral stenosis. The electrocardiogram is essentially normal. The planar QRS loops in the vectorcardiogram are normal in orientation and appearance with the exception of the large terminal deflection of the QRS sE loop to the right, posteriorly, and superiorly.



following vectorcardiographic pattern, which these investigators believe represents right ventricular hypertrophy. "The major portion of the QRS loop is located anterior to the isoelectric point, although the direction of inscription in the horizontal plane is counterclockwise."

4. In their series of mitral stenosis cases, Whipple and his co-workers observed QRS sE loops with posterior and superior terminal appendages without conduction delay in many vectorcardiograms not diagnostic of right ventricular hypertrophy, and we have had much the same experience in our mitral stenosis cases (and in cases of chronic cor pulmonale as well). The QRS sE loop findings in mitral stenosis without vectorcardiographic right ventricular hypertrophy can be reduced to three loop patterns, which, for the present, will be de-

scribed only sketchily, since these patterns will be discussed in detail in the following chapter, on cor pulmonale. For descriptive convenience, the three QRS sE loop patterns will be referred to hereafter as "types A, B, and C" QRS sE loop patterns.

Type B QRS sE Loop Pattern

For reasons to be discussed later, we believe this QRS sE loop pattern (Fig 124) to be very suggestive, if not diagnostic, of right ventricular hypertrophy. As in the type A pattern, the QRS sE loop in the type B pattern is characterized by a terminal deflection of varying size directed to the right, posteriorly, and superiorly. In the horizontal projection, the terminal deflection usually presents a spikelike appearance. Unless complicated by some other abnormality, neither this QRS sE loop pattern nor the other two patterns to be described are characterized by conduction delay.

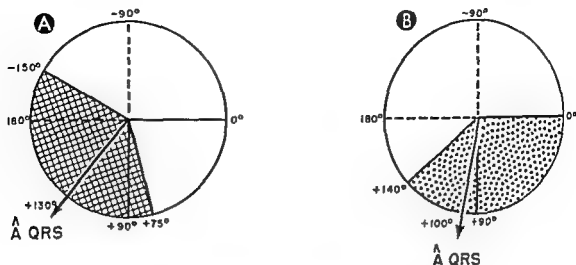


Fig. 122.—The extreme range of variation and average orientation of \bar{A} QRS in the frontal plane in (A) congenital heart disease (with overloading of the right ventricle) and (B) mitral stenosis.

pattern is one that is frequently observed in normal electrocardiograms, while the second RSR' pattern has been considered in the past to represent incomplete right bundle branch block. As previously indicated, there is good reason to believe that in many cases the incomplete right bundle branch block pattern actually represents right ventricular hypertrophy. In our 21 cases with RSR' deflections in lead V_1 , the R' wave was smaller than 7 mm in amplitude in all but 1 case, which had an R' of 7 mm. Thus, none of the electrocardiograms fulfilled Barker and Valencia's criteria for the diagnosis of right ventricular hypertrophy in the presence of incomplete or complete right bundle branch block (R' > 10 mm. or > 15 mm. amplitude, respectively). Moreover, 9 of the 21 patients with RSR' deflections in lead V_1 failed to present vectorcardiographic evidence of right ventricular hypertrophy.

3. In the remaining 30% of the cases, lead V_1 dis-

played QRS complexes of various configurations other than RSR' (qR, qRs, Rs, II, etc.), but in

all of these cases if an R/S ratio greater than 1 in lead V_1 was the only requirement for making the diagnosis of right ventricular hypertrophy. Fifteen electrocardiograms in our series were placed in this category, but in only 8 of these did the R wave in V_1 equal or exceed 7 mm. In this group of electrocardiograms, the onset of the intrinsoid deflection in lead V_1 occurred later than 0.03 second in almost 65% of the cases.

4. Right-axis deviation of the mean manifest electrical axis of QRS was present in 45% of the electrocardiograms in the combined series, left-axis deviation was noted in 5%, and no axis deviation in the remaining 50% (Fig. 122). Right-axis deviation of \bar{A} QRS, when present, was not usually marked

VECTORCARDIOGRAPHIC FINDINGS

The QRS sE loop findings in patients with relatively pure mitral stenosis and with mixed mitral stenosis and insufficiency (and/or aortic valvular disease), presented below, were compiled from the series of Donoso and his co-workers, Scherlis and his associates, and the authors of this text. When these series were combined, the number of cases of relatively pure mitral stenosis totaled 81, while the total number of cases with mitral stenosis and insufficiency or other valvular lesions was 39.

1. In almost 75% of the pure mitral stenosis cases and 25% of the cases with other valvular lesions in addition to mitral stenosis, the QRS sE loop presented evidence of right ventricular hypertrophy. In our 36 cases of pure mitral stenosis, 23 vectorcardiograms (64% of the records) were diagnostic of right ventricular hypertrophy, 16 showing the RSR' pattern of right ventricular hypertrophy and 7 the tall R pattern of right ventricular hypertrophy. In the 17 cases of mitral stenosis accom-

sE loop in the horizontal and sagittal projections occupies a less posterior or more anterior position than the type A pattern, so that characteristically it is directed slightly anterior or posterior, and the loop is clockwise inscribed far to the right and posteriorly. At times the sagittal QRS loop also displays a figure-of-eight configuration in which the distal loop of the "eight" is counterclockwise inscribed.

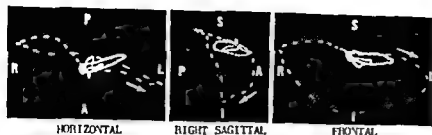
Type C QRS sE Loop Pattern

This type of QRS sE loop pattern (Fig. 125) is far less frequently encountered in mitral stenosis

than in chronic cor pulmonale and pulmonary emphysema and consists of marked posterior rotation of the entire QRS loop without any striking changes in its appearance otherwise. Usually the terminal QRS vectors are directed slightly to the left or right, far posteriorly and inferiorly. We believe that this QRS sE loop pattern reflects, more than either of the patterns already described, the effects of clockwise rotation of the heart on its longitudinal axis.

The frequency of these various QRS sE loop patterns in mitral stenosis, the manner in which they are produced, and their significance will be dealt with in parallel with the corresponding facts relating to the vectorcardiographic findings in chronic cor pulmonale in the following chapter.

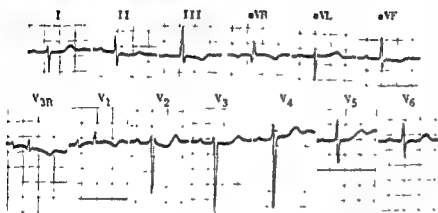
Fig. 124.—Type B QRS sE loop pat-



deflections in leads V_{3R} and V_1 are compatible with right ventricular hypertrophy. Since the horizontal QRS loop of the vectorcardiogram extends about equally to the left and right of the



HORIZONTAL
(Ampl. 2X)



trast with the horizontal QRS loop in the type A pattern, the type B horizontal QRS loop is characterized by anterior displacement of the left-to-right limb of the loop, which causes the horizontal loop to have a figure-of-eight configuration, the first half of the loop being written in a counterclockwise direction to the left and slightly anteriorly, and the second half, in a clockwise direction to the right and posteriorly. Unlike the frontal QRS loop in the type A pattern, which is frequently counterclockwise inscribed, the frontal loop in the type B pattern, as exemplified by the above vectorcardiogram, is generally written in a clockwise direction. On rare occasions the type B QRS sE loop pattern is observed in vectorcardiograms recorded from normal individuals, but as a rule, when it occurs in patients with mitral stenosis or chronic pulmonary disease, it is strongly suggestive of right ventricular hypertrophy.

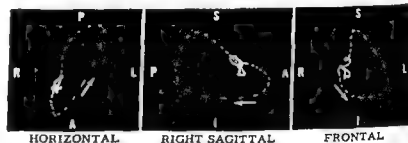
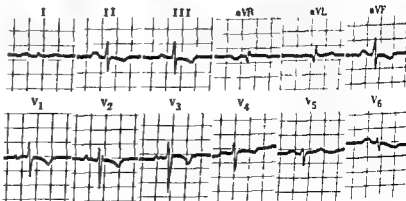


Fig. 125.—Type C QRS sE loop pattern in mitral stenosis. The terminal portion of the QRS sE loop in this pattern is located superiorly, but the most characteristic feature of the QRS loop is its posterior rotation. Significant rightward extension of the terminal part of the QRS sE loop in the type C pattern is uncommon in mitral stenosis but a relatively frequent finding in the corresponding QRS sE loop pattern in chronic pulmonary disease.



or, rarely, primary pulmonary hypertension. The discussion to follow—and, for that matter, the greater portion of this chapter—will be devoted to a consideration of the pathophysiology and electrocardiographic and vectorcardiographic manifestations of chronic cor pulmonale, particularly cor pulmonale occurring in patients with chronic obstructive emphysema.

No attempt will be made in this text to discuss the various types of lung disease or pulmonary vascular disease which may lead to cor pulmonale, nor will it be possible to describe all of the pathophysiologic mechanisms concerned. Instead, the discussion will center almost entirely on chronic cor pulmonale due to pulmonary emphysema, although for all intents and purposes the points developed during the discussion have equal relevance to chronic cor pulmonale resulting from other types of chronic lung or pulmonary vascular disease.

The attempt to establish or refute the diagnosis of chronic cor pulmonale is more than just an intellectual exercise serving no practical purpose. Chronic cor pulmonale complicating pulmonary emphysema

or some other type of chronic lung disease has important therapeutic and prognostic implications which profoundly influence the evaluation of a patient's clinical status. However, it sometimes proves a problem to establish the diagnosis of chronic cor pulmonale, for several reasons: (1) Neither radiologic evidence of severe chronic emphysema or fibrosis nor catheterization-proved pulmonary hypertension can be accepted as proof of the existence of chronic cor pulmonale. (2) The occurrence of congestive heart failure in a patient with chronic lung or pulmonary vascular disease may be related etiologically to some other type of heart disease, such as arteriosclerotic heart disease. (3) Right ventricular enlargement is particularly difficult to detect radiologically in patients with pulmonary emphysema. (However, there is sometimes indirect evidence of cor pulmonale, such as dilatation of the proximal portion of the main pulmonary artery.) Since other clinical studies may give, at times, equivocal results with reference to the diagnosis of chronic cor pulmonale, it can readily be appreciated that in some instances the electrocardiographic findings are of crucial importance.

GENESIS OF ECG FINDINGS IN CHRONIC COR PULMONALE DUE TO PULMONARY EMPHYSEMA

Chronic pulmonary emphysema may affect the electrocardiogram directly and indirectly in the following ways:

1. Emphysema decreases the conductivity of the lung and thereby impedes transmission of cardiac potentials to the body surface. As previously indicated, the emphysematous lung contains far more air than the normal lung, since there is poor respiratory exchange and trapping of air in the large air sacs formed by overdistended or coalescent alveoli. Because the lung tissue interposed between the heart and body surface contains more air than normally and because air is an extremely poor conductor, the electrical forces arising in the heart are poorly transmitted to the surface electrodes of the electrocardiograph. In this event, the electrocardiogram displays low-voltage deflections in all leads. The presence of low voltage is determined chiefly from the size of the QRS deflections, since corresponding criteria for low voltage of the P and T waves are lacking. (The significance of the latter finding would be almost impossible to assess anyway.) Certainly, low-voltage QRS deflections are not invariably observed in pulmonary emphysema, and their presence does not necessarily correlate with the severity of the lung disease. In our experience,

the more common finding in pulmonary emphysema is low QRS voltage which is limited to the extremity leads. In most cases, this finding can be attributed to the fact that the QRS forces are oriented almost directly posteriorly and therefore lie nearly perpendicular to the frontal plane.

2. Emphysema is accompanied by lowering of the diaphragm, and this in turn causes the heart to descend in the chest, to assume a more vertical position, and to rotate in a clockwise direction around its longitudinal axis. The clockwise rotation causes the left ventricle to be displaced posteriorly and the right ventricle to rotate to a more anterior position. The anatomic changes in the position and rotation of the heart are generally held responsible, in whole or in part, for the electrocardiographic findings of vertical electrical heart position, right-axis deviation of \bar{A} QRS, and the precordial lead QRS pattern of "marked clockwise rotation."

3. The... can lead to... hypertrophy and dilatation, and, in some cases, to cardiac failure. Thus, Mounsey and other investigators have observed right ventricular hypertrophy in approximately 60% of the

Cor Pulmonale and Pulmonary Emphysema

THE SYNONYMOUS TERMS *pulmonary heart disease* and *cor pulmonale* are utilized specifically to designate hypertrophy, dilatation, and/or failure of the right heart caused by an increased pulmonary vascular resistance, whether the latter is due to intrinsic disease of the lung or to pulmonary vascular disease. The

direct cause of *cor pulmonale* occurring in cases of lung disease or pulmonary vascular disease is pulmonary hypertension, however, not every patient with pulmonary hypertension has *cor pulmonale*, and so the terms *cor pulmonale* and *pulmonary hypertension* are not equivalent in meaning.

CLINICAL FORMS OF COR PULMONALE

Cor pulmonale may present clinically in three forms—*acute*, *subacute*, and *chronic cor pulmonale*—which differ according to the rapidity of onset and duration of the pulmonary hypertension and *cor pulmonale*.

Acute cor pulmonale—This form consists of acute and usually transient pulmonary hypertension resulting from sudden embolic occlusion of a major branch of the pulmonary artery or from widespread "seedling" and occlusion of smaller vessels by many small emboli. Pulmonary arteriospasm may also be an important factor in the genesis of the pulmonary hypertension and right ventricular dilatation. In occasional cases of recurrent pulmonary embolism, chronic *cor pulmonale* is the eventual outcome and has been attributed to pulmonary arteriosclerosis, which many authors believe is related in some way to organization of the emboli. The electrocardiographic and vectorcardiographic findings in acute *cor pulmonale* are described later in this chapter.

Subacute cor pulmonale—Since the subacute type of *cor pulmonale* is usually encountered in cases of diffuse carcinomatosis of the lungs, it is not surprising that the rapidity of onset and duration of the *cor pulmonale* are intermediate between the two extremes of acute and chronic *cor pulmonale*. In about 75% of the cases of diffuse carcinomatosis of the lung reported in the medical literature, the primary tumor

was gastric carcinoma. Tumors can spread to the lungs via the blood vessels and/or lymphatics. Retrograde spread of tumor from the hilar lymph nodes to the perivascular lymphatics of the lungs is referred to as *lymphangitic carcinomatosis*.

In 11 of the 78 reported cases of diffuse carcinomatosis of the lung, right ventricular hypertrophy was found at postmortem examination, and in 10 of the 11 cases, according to Morgan, obliterative lesions of the pulmonary arterioles, in the form of intravascular fibrosis or more recent thrombosis, were observed. Tumor cells were usually demonstrable in the blood vessels as well as in the perivascular lymphatics, and the resulting obliterative endarteritis was held responsible for the pulmonary hypertension and hypertrophy and/or eventual failure of the right ventricle, occurring in occasional patients with diffuse carcinomatosis of the lung. Since the electrocardiographic and, presumably, vectorcardiographic manifestations of this type of *cor pulmonale* are essentially similar to those occurring in chronic *cor pulmonale*, and because of the rarity of subacute *cor pulmonale*, the latter will not be considered individually in this text.

Chronic cor pulmonale—This form is seen most commonly in cases of long-standing obstructive emphysema but may also occur in patients with severe kyphoscoliosis, fibrotic or granulomatous disease of the lungs, chronic multiple pulmonary embolism,

THE ECG AND VCG FINDINGS IN CHRONIC COR PULMONALE AND IN PULMONARY EMPHYSEMA WITHOUT COR PULMONALE

The principal effects on the heart of the increased pulmonary vascular resistance in chronic cor pulmonale consist of (a) right atrial enlargement and (b) systolic overloading of the right ventricle, which is responsible, in whole or in part, for such electrocardiographic abnormalities as right-axis deviation of \bar{A} QRS, the precordial QRS pattern of "marked clockwise rotation," and the fully developed right ventricular enlargement patterns.

Right Atrial Enlargement

It will be recalled that the enlargement of the left atrium occurring in mitral stenosis is associated with disturbances of the atrial rhythm, the most common of which is atrial fibrillation, or with the electrocardi-

tion. Interestingly enough, each of the 3 cases with atrial fibrillation had generalized cardiac enlargement on roentgenographic study (1 patient from each group of the series making up the combined group), and 1 case was found to have systemic hypertension. Thus, the demonstration of atrial fibrillation or some other cardiac arrhythmia in a case with the clinical diagnosis of chronic cor pulmonale either should raise some question as to the correctness of this diagnosis or should suggest the possibility of coexisting heart disease of some other type.

The ECG and VCG in Pulmonale Pattern

ELECTROCARDIOGRAPHIC P PULMONALE PATTERN

The electrocardiographic features of the P pulmonale pattern occurring in chronic cor pulmonale (Fig 126) are as follows.

1. The mean manifest electrical axis of P (\bar{A} P) or the frontal plane mean P vector is situated to the right of its average normal location at $+60^\circ$ in

Fig. 126.—Electrocardiographic findings in chronic cor pulmonale. The P pulmonale pattern of right atrial enlargement is evidenced by the following: \bar{A} P in the frontal plane located at about $+60^\circ$, and a P wave amplitude in lead II of 2.5 mm. (average) instead of normal 1.5 mm.

does not militate against the diagnosis of right atrial enlargement in the frontal plane.

monale

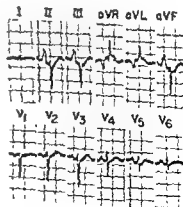


TABLE 13—CARDIAC RHYTHM IN CHRONIC COR PULMONALE

Study Group	No. of Cases		
	Total	Normal Sinus Rhythm	Atrial Fibrillation
Parkinson and Hoyle	60	79	1*
Scott and associates	28	27	1†
Authors' series	37	38	1‡
Total	145	142	3

* A patient with systemic hypertension and cardiomegaly.

† A patient with generalized cardiomegaly.

‡ A patient with predominant right ventricular hypertrophy by radiologic examination but with some left ventricular hypertrophy also.

ographic P wave pattern of P mitrale. In contrast, right atrial enlargement in chronic cor pulmonale rarely produces arrhythmias, although it frequently is accompanied by a characteristic P wave pattern, the P pulmonale pattern. In fact, the relative rarity of cardiac arrhythmias in patients with chronic cor pulmonale is rather impressive, particularly when the frequency of atrial fibrillation in patients with longstanding mitral valvular disease or arteriosclerotic heart disease is considered. In a combined series of chronic cor pulmonale cases of Parkinson and Hoyle, Scott and his associates, and the authors of this text (Table 13), 142 of the 145 cases exhibited sinus rhythm, the 3 exceptional cases showing atrial fibrilla-

cases of pulmonary emphysema which they studied. The different mechanisms in pulmonary emphysema which may sometimes increase pulmonary vascular resistance, and thereby cause systolic overloading of the right ventricle, are as follows:

a) The anatomic restriction of the pulmonary vascular bed may be one factor. Microscopic examination of the emphysematous lung reveals that the alveolar septi in many regions of the lung are atrophic, ruptured, or entirely absent; that many of the alveoli have coalesced to form large air sacs; and, finally, that there is rather extensive interstitial fibrosis. These pathologic changes in turn cause compression, narrowing, thrombosis, and obliteration of many of the pulmonary capillaries, with consequent restriction of the pulmonary vascular bed. As a result, the ability of the pulmonary vascular bed to adjust to increases in blood flow becomes greatly limited and exercise may lead to a rise in pulmonary artery pressure. Eventually, the restriction of the pulmonary vascular bed may become so marked that the pulmonary artery pressure is elevated even at rest.

b) Arterial hypoxemia may be a factor. The characteristic abnormality of respiratory function in pulmonary emphysema is poor aeration of perfused alveoli, which may lead to pronounced arterial hypoxemia and carbon dioxide retention. Systemic arterial hypoxemia in turn may produce in the following: (1) polycythemia and hypervolemia, (2) increased

cardiac output and pulmonary blood flow, and (3) possibly pulmonary vasoconstriction. All of these effects of hypoxemia tend to augment or exaggerate the effect of anatomic restriction of the pulmonary vascular bed and therefore tend to produce an even greater degree of pulmonary hypertension.

c) Additional factors, such as bronchopulmonary arterial shunts, pulmonary arteriosclerosis, increased bronchomotor tone, and increased alveolar pressure, probably play less important parts in the genesis of pulmonary hypertension than the factors described above.

From the foregoing, it is evident that the electrocardiographic features of chronic cor pulmonale are a composite of changes due to the mechanical effects of emphysema per se and to superimposed right ventricular hypertrophy, but the dividing line between the two types of electrocardiographic manifestations is exceedingly tenuous. In any event, the important thing is that the electrocardiographic features of right ventricular hypertrophy in chronic cor pulmonale are almost invariably modified by the coexisting abnormalities resulting solely from changes in cardiac position or rotation. More will be said later of the manner in which changes in heart position and cardiac rotation in chronic cor pulmonale influence the orientation and magnitude of the mean instantaneous QRS spatial vectors.

CHRONIC COR PULMONALE AND CHRONIC PULMONARY DISEASE WITHOUT DETECTABLE COR PULMONALE

The electrocardiographic findings in 37 patients hospitalized at Barnes Hospital with chronic lung or pulmonary vascular disease will be described in the following pages (see also Table 15). One or more electrocardiograms and vectorcardiograms were recorded from each patient. For purposes of comparison, the 37 cases were divided into two groups: one group having radiologically demonstrated or autopsy-proved cor pulmonale, and the other, chronic lung disease without detectable cor pulmonale. The two groups will be referred to hereafter as the "chronic cor pulmonale group" and "chronic pulmonary emphysema group," respectively. Even though the second group of cases presented no roentgenographic evidence of cor pulmonale, many of the patients had severe pulmonary emphysema, and a third of them were in congestive heart failure at the time of hospitalization. The types of lung disease in the two

groups and the number of cases in each group follow.

	No of Cases
I. Chronic cor pulmonale group	20
Pulmonary emphysema with or without fibrosis	15
Fibrocalfic tuberculosis	1
Cystic disease of the lungs	1*
Interstitial fibrosis of both lungs	1
Severe kyphoscoliosis	1
Minimal emphysema, pulmonary arteriosclerosis suspected	1
II. Chronic pulmonary emphysema group	17
Pulmonary emphysema with or without fibrosis	14
Pectus excavatum	1
Bronchiectasis	1
Pneumoconiosis	1

*Patient was a 20-year-old man

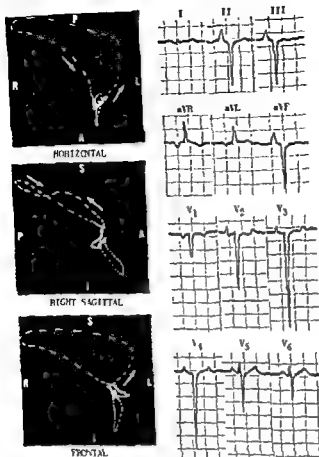


Fig. 127.—Electrocardiographic and vectorcardiographic P pulmonale pattern of right atrial enlargement and type A QRS sE loop pattern in a man, 53, with chronic cor pulmonale (secondary polycythemia, arterial oxygen saturation of 78%, congestive heart failure, and radiologic findings of right ventricular hypertrophy and of pulmonary emphysema and fibrosis)

the frontal reference frame and approaches, but, with rare exceptions, never exceeds, $+90^\circ$.

2. The magnitude of the mean instantaneous P vectors and $\bar{A}P$ is increased; and their average direction, as represented by the frontal and horizontal plane mean P vectors, tends to be more inferior, anterior, and less to the left than normally. The characteristic orientation of the mean instantaneous P vectors in P pulmonale is thought to reflect the electrical predominance of the enlarged right atrium, which is situated anteriorly, inferiorly, and to the right of the left atrium. Since the right atrium is normally the first to undergo activation, prolongation of its activation time as the result of dilatation and hypertrophy does not usually cause widening of the P waves, but, because of the greater magnitude of the P wave forces produced by the right atrium, the P waves are of increased amplitude.

Our diagnosis of P pulmonale is based on the presence of tall, peaked, or occasionally slurred or notched P waves of 2.5-mm or more amplitude in leads II, III, and/or aVF. The following findings support the diagnosis of P pulmonale but are not diagnostic in themselves

- a) Biphasic or inverted P waves of increased size in lead V_1 (a less common finding, but one more strongly favoring the diagnosis of P pulmonale, is the presence of tall upright P waves in lead V_1)
- b) Low, almost flat, P waves in lead I.

Occasionally, dilatation of a hypertrophied right atrium is said to prevent the appearance of the P pulmonale pattern, and the explanation usually given is that the increased mass of intra-atrial blood has an abnormally marked short-circuiting effect on atrial potentials. As a matter of fact, the exact mechanism responsible for the P pulmonale pattern remains in doubt. It seems unlikely that such a nontransient condition as right atrial hypertrophy could be responsible for this abnormality, since the electrocardiographic P pulmonale pattern has been observed to appear relatively fleetingly during acute episodes of pulmonary embolism, status asthmaticus, and acute pulmonary edema. The relative importance of right atrial dilatation and changes in anatomic heart position and rotation in the genesis of the P pulmonale pattern has not been established as yet. Myers has observed this P wave pattern occasionally in normal persons with asthenic body habitus and attributes its presence to a vertical heart position and a low diaphragm.

TABLE 14.—ORIENTATION OF THE MAXIMAL MEAN INSTANTANEOUS VECTOR OF THE P-R LOOP IN CHRONIC COR PULMONALE AND CHRONIC PULMONARY EMPHYSEMA WITHOUT COR PULMONALE

	Total No of Cases	% WITH VCC P Pul-MONALE	HORIZONTAL			RIGHT SAGITTAL			FRONTAL		
			Extreme Range	Av	Usual Range	Extreme Range	Av	Usual Range	Extreme Range	Av	Usual Range
Chronic cor pulmonale	20	82	-20° to $+90^\circ$	$+60^\circ$	$+40^\circ$ to $+80^\circ$	$+50^\circ$ to $+90^\circ$	$+70^\circ$...	$+50^\circ$ to $+90^\circ$	$+80^\circ$...
Chronic pulmonary emphysema without cor pulmonale	17	47	-10° to $+80^\circ$	$+35^\circ$	0° to $+60^\circ$	$+60^\circ$ to $+95^\circ$	$+75^\circ$...	$+50^\circ$ to $+90^\circ$	$+75^\circ$...
(Normal cases*)	(80)	(0)	$(-20^\circ$ to $+30^\circ)$	$(+5^\circ)$	$(0^\circ$ to $+5^\circ)$	$(+60^\circ$ to $+100^\circ)$	$(+80^\circ)$	$(+80^\circ$ to $+90^\circ)$	$(+10^\circ$ to $+100^\circ)$	$(+55^\circ)$	$(+20^\circ$ to $+60^\circ)$

*The normal values for P-R loop orientation are enclosed in parentheses and are the same as those presented in Table 4 in Chapter 7. They are included in the above table to provide a basis for comparison with the values obtained in chronic cor pulmonale and chronic pulmonary emphysema without cor pulmonale.

degrees of right axis deviation of A QRS (Fig. 138, right). In only 1 of our cases of chronic cor pulmonale was A QRS situated to the left of $+90^\circ$. In the electrocardiogram in this instance, A QRS was oriented along the -85° axis of the frontal reference frame, lead I recorded an R_s deflection of low voltage, and leads II and III displayed relatively deep QS deflections (there was no clinical history suggestive of myocardial infarction). However, the same electrocardiogram showed the precordial lead QRS pattern of "marked clockwise rotation," lead V₆ registering an R_s deflection. This would indicate that the horizontal plane mean QRS vector was situated posteriorly and to the right of -90° . The probable explanation for this discrepancy between the QRS configuration in leads I and V₆ is that, in this case, the lead vector or effective axis of lead I is canted downward in a left-to-right direction while the effective axis of lead V₆ is slanted in just the opposite direction. Thus, as Schaffer has pointed out, a cardiac vector directed almost vertically superiorly will be recorded in lead I as if rotated to the left and in V₆ as if rotated to the right of its actual position. In the above exceptional case, mean instantaneous QRS spatial vectors appearing during the second half of the QRS interval were probably directed superiorly and somewhat to the right, but because of the rotation of the effective axis of lead I, they projected on the positive half of the axis of derivation of this lead and therefore produced terminal QRS positivity rather than negativity. In support of this explanation is the fact that the frontal QRS loop of the patient's vectorcardiogram showed a maximal mean instantaneous QRS vector oriented along the -120° axis of the frontal reference frame. Consequently, in this case as probably also in similar cases of left-axis deviation in chronic cor pulmonale reported in the past, the apparent left-axis deviation is actually marked right-axis deviation.

The S₁-S_{1R}-S_{1II} pattern consists of predominantly downwardly directed QRS deflections (rS, qRS, QS) in leads I, II, and III and is associated with the precordial lead QRS pattern of "marked clockwise rotation," in which the transitional lead registering the transitional, equiphasic RS deflection lies to the left of lead V₆. There is a relatively high degree of correlation between the S₁-S_{1R}-S_{1II} pattern in the electrocardiogram and the presence of anatomic right ventricular hypertrophy. It is this pattern especially which is so frequently interpreted as indicating anterior, anteroseptal, diaphragmatic, or combined infarctions. In fact, the usual QRS criteria for the diagnosis of myocardial infarction are of limited value

in evaluating electrocardiograms presenting other evidence of chronic cor pulmonale.

Precordial QRS Pattern of "Marked Clockwise Rotation"

In the absence of electrocardiographic evidence of right ventricular hypertrophy, the precordial QRS pattern most characteristic of chronic cor pulmonale is that of "marked clockwise rotation." As will be recalled, in the normal electrocardiogram, the precordial lead which records the transitional, equiphasic RS deflection is usually V₄, or some lead to the right of this point, thus, the horizontal plane mean QRS vector is normally situated at or anterior to -30° in the horizontal reference frame. In chronic cor pulmonale, the mean QRS vector is often rotated as far posteriorly as -90° or more, and the equiphasic RS deflection is recorded by lead V₄ or some lead to the left of this point. As will be described later, this electrocardiographic pattern is frequently associated with

turn of the heart about its longitudinal axis, but a somewhat different mechanism may also be involved in cases with the electrocardiographic pattern of "marked clockwise rotation." This will be considered in detail in the discussion of the vectorcardiographic findings in chronic cor pulmonale.

Electrocardiographic Right Ventricular Hypertrophy Patterns

As will be noted in Table 15, showing the incidence of the various electrocardiographic findings in chronic cor pulmonale, the diagnosis of right ventricular hypertrophy was made in only 16-28% of the cases of chronic cor pulmonale in the several series, despite the fact that, in our series at least, the criteria used in making the diagnosis were far from strict. Some of the reasons for the failure of the electrocardiogram to detect right ventricular hypertrophy more frequently than it does in chronic cor pulmonale have already been considered and will not be repeated.

When right ventricular hypertrophy was diagnosable electrocardiographically in our patients, one of two QRS patterns was generally present in lead V₁—namely, an rSR' (or RS') with normal QRS interval, or a QR complex. In our series of chronic cor pulmonale cases, 4 out of 20 electrocardiograms showed right ventricular hypertrophy patterns, with two showing each of the above types of QRS configura-

According to Wood, the tall P wave of the P pulmonale pattern is "probably the earliest sign of cardiovascular disturbance resulting from emphysema, or at least competes in this respect with elevation of the right ventricular pressure and slight reduction of arterial oxygen saturation: it may develop several years before the onset of heart failure." Wood could find no correlation between the presence of the P pulmonale pattern in chronic cor pulmonale and such factors as anoxia, cardiac output, or right atrial pressure, although he felt that there was some relationship between this electrocardiographic finding and right ventricular pressure.

It is of some interest that Zuckermann and his co-workers concluded from their studies of patients with chronic cor pulmonale that a small or absent P wave in lead aVF excludes the possibility of chronic cor pulmonale more readily than a tall P wave in this lead establishes the same diagnosis. Moreover, they state that, when the voltage of the P waves in lead II or lead III is below 0.5 mm., the possibility of uncomplicated chronic cor pulmonale is practically excluded.

VECTORCARDIOGRAPHIC P PULMONALE PATTERN

Comparatively few vectorcardiographic studies of chronic cor pulmonale have been reported in the medical literature. The following description of the vectorcardiographic findings in this condition is based in large part on our observations in 37 cases of chronic lung or pulmonary vascular disease with and without chronic cor pulmonale. In 20 of the 37 cases there was postmortem proof or roentgenographic evidence of cor pulmonale.

The frequency of the vectorcardiographic finding of P pulmonale pattern in our study of cases of chronic cor pulmonale and of cases of chronic lung disease without roentgenographic cor pulmonale and the average orientation and range of variation in orientation of the P sE loop are shown in Table 14.

The P sE loop abnormalities corresponding to the electrocardiographic pattern of P pulmonale (Fig. 127) are as follows.

1. The maximal instantaneous P vector or long axis of the P sE loop is of increased magnitude
2. In the horizontal projection, the P sE loop frequently shows a figure-of-eight configuration which differs from that in mitral stenosis in that the initial anterior loop of the "eight" is larger

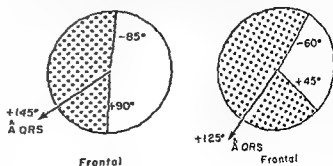
than the later posterior component. The two portions of P sE loops, with a figure-of-eight configuration can be inscribed in a counterclockwise direction, respectively or just the reverse. Occasionally, a horizontal P loop with a trapezoid-like configuration is written entirely in a clockwise direction. The corresponding sagittal and frontal P loops can be written in either a clockwise or a counterclockwise direction. However, the more common finding is that a P loop with a trapezoid-like configuration in the horizontal projection is entirely counterclockwise inscribed.

3. The sagittal P loop in P pulmonale is generally elongated but frequently presents a bifid configuration with the initial and larger portion of the loop lying anteriorly and the remainder of the loop situated posteriorly. Occasionally the sagittal P loop has a figure-of-eight configuration. The direction of inscription of the sagittal P loop is usually normal—that is, clockwise.
4. The frontal P loop tends to resemble the sagittal loop in configuration and to be directed almost vertically downward. The loop is usually written in a counterclockwise direction
5. As Sano and his associates have pointed out, the P sE loop in P pulmonale frequently remains open in all three projections, representing a displacement of the junction of P with the Ta component.

Right-Axis Deviation of \bar{A} QRS

Chronic cor pulmonale is one of the commonest causes of moderate to marked degrees of right-axis deviation of \bar{A} QRS unaccompanied by more obvious evidence of right ventricular hypertrophy (Fig. 128, left), while chronic pulmonary emphysema without cor pulmonale tends to be accompanied by lesser de-

Fig. 128.—Extreme range of variation and average orientation of \bar{A} QRS in the frontal plane in chronic cor pulmonale (left) and chronic pulmonary emphysema (without evident cor pulmonale) (right).



The outflow tract of the right ventricle and the crista supraventricularis is normally one of the last regions of the ventricles to undergo activation, and this fact has been related to the high incidence of QRS deflections in the R' usually = about the same size as the initial R wave and is said not to exceed 4 mm. Actually, many of the QR deflections recorded in lead V₁ in patients with chronic cor pulmonale or mitral stenosis are probably equivalent to RS' deflections in which the initial portion of the QRS complex is isoelectric. This certainly does not apply in every case, however, for the vectorcardiograms obtained in some patients display initial deflections of the QRS sE loop to the left and posteriorly. The explanations currently proposed for this finding have already been discussed in Chapter 10, dealing with the general diagnostic features of right ventricular hypertrophy in the electrocardiogram and vectorcardiogram. Parenthetically, it might be added that, in all probability, the high percentages of cases of chronic cor pulmonale with incomplete right bundle branch block patterns in lead V₁ reported by Scott and his co-workers and by Kilpatrick include many cases in which this electrocardiographic pattern is actually produced by a QRS sE loop right ventricular hypertrophy pattern of the RSR' type.

Right Ventricular Strain Pattern

Many investigators have placed considerable emphasis on the diagnostic finding of a right ventricular strain pattern in the electrocardiogram of patients

with chronic cor pulmonale. We have found this feature to be of little practical value in the electrocardiographic diagnosis of either chronic cor pulmonale or right ventricular hypertrophy, and the same experience has been reported by others. In approximately 60% of the cor pulmonale cases and 35% of the cases with chronic lung disease without cor pulmonale, there was either slight S-T segment depression or shallow T wave inversion in leads II, III, and aVF when these leads recorded primarily upright QRS deflections. However, the ST-T abnormalities in themselves are nonspecific so far as the diagnosis of cor pulmonale is concerned.

lead V₁. If one limits the diagnosis of right ventricular strain to electrocardiograms with inverted T waves in leads V₁ through V₃, only 20% of the cor pulmonale patients and about 5% of the patients with chronic lung disease without roentgenographic evidence of cor pulmonale showed this finding, and in some of these instances, the T wave inversion extended as far to the left as V₄ or V₆, which would indicate more generalized anterior myocardial ischemia. In short, we rarely use ST-T wave abnormalities to establish

what. The onset of intrinsoid deflection in lead V₁, the amplitude of the R wave in lead aVR, amplitude criteria pertaining to various combinations of R waves in right precordial leads and S waves in left precordial leads, etc.

VECTORCARDIOGRAPHIC QRS sE LOOP PATTERNS IN COR PULMONALE AND PULMONARY EMPHYSEMA

TYPE A QRS sE LOOP PATTERN

The type A QRS sE loop pattern was noted in approximately one quarter of the chronic cor pulmonale cases and in over half of the emphysema cases without radiologic evidence of cor pulmonale.

is 1
as 1
flec

and of brief duration. In rare instances the QRS loop is written almost straight anteriorly and slightly to the left, or to the left and posteriorly. The efferent limb of the horizontal QRS loop is next inscribed to the left and anteriorly, and

at about the time the loop reaches its maximal leftward extent, it turns in a counterclockwise direction posteriorly. The afferent limb of the horizontal

instead, the terminal part of the loop is written as a spikelike deflection far posteriorly and either slightly or far to the right. The QRS sE loop in this and the other

TABLE 15.—ELECTROCARDIOGRAPHIC FINDINGS IN CHRONIC COR PULMONALE*

	SCOTT AND ASSOCIATES	WOOD	KILPATRICK	ZUCKERMAN AND ASSOCIATES	AULTON'S SERIES	
					Chronic Cor Pulmonale	Chronic Pulmonary Emphysema
No of cases	28	100	20	50	20	17
P pulmonale pattern in bipolar limb leads	39%	85%	60%	28%	50%	18%
Av orientation of A P	+71°	+72°	+69°
Right-axis deviation of A QRS	...	46%	85%	96%	80%	20%
Av orientation of A QRS	+145°	+128°
S _c -S _u -S _m pattern	...	9%	20%	22%	20%	12%
Low QRS voltage†	...	40%	15%	...	40%—in limb leads only	12%—in limb lead only, and 6%—in limb and precor- dial leads
Precordial QRS pattern of "marked clockwise rotation"	..	16%	40%	60%	75%	59%
ECG right ventricular hypertrophy	28.5%	16%	25%	..	20%‡	18%
Right bundle branch block:						
Incomplete	28.5%	0	20%	...	0	0
Complete	3.6%	4%	0	...	0	0

*Data obtained from study series of cases of chronic cor pulmonale reported by the investigators cited in the column headings. (In the reports of Wood and of Kilpatrick, no information is given as to the specific leads of the electrocardiogram showing low QRS voltage.)

†The lead V₁ criteria used by the authors of this test in making the electrocardiographic diagnosis of right ventricular hypertrophy in adult patients with chronic cor pulmonale, mitral stenosis, and certain types of congenital heart disease, such as interatrial septal defects, are as follows: a QRS interval of 0.1" or exceeding 1", irrespective of the axis which the R' is obviously taller than R; R' is at least half the size of the S; (3) an RS deflection in lead V₁ in which the R wave approaches, equals, or exceeds the S wave in size and is of 0.04 second or longer duration.

tion. Of the 17 patients with chronic pulmonary emphysema without radiographic evidence of cor pulmonale, 2 had rsR' deflections in lead V₁ of their electrocardiograms. (These 2 cases in all likelihood belong in the chronic cor pulmonale group.) In all 6 cases with QR or RSR' deflections in lead V₁, the R/S or R'/S ratio in this lead equaled or exceeded 1. The average amplitude of the R waves of the QR deflections and the R' waves of the RSR' complexes was 4.6 mm.

As in many electrocardiograms recorded from patients with mitral stenosis, the electrocardiographic evidence of right ventricular hypertrophy in chronic cor pulmonale, even when present, is far from conspicuous, probably for the same reasons that the

electrocardiogram is less frequently diagnostic of right ventricular hypertrophy in these two types of heart disease than in congenital heart disease. The late terminal upright deflection in V₁, which is usually the only evidence of right ventricular hypertrophy in chronic cor pulmonale and is the commonest right ventricular hypertrophy pattern found in mitral stenosis, is probably attributable to the selective type of right ventricular hypertrophy present. Thus, in chronic cor pulmonale and in mitral stenosis, the earliest evidence of anatomic hypertrophy of the right ventricle consists of thickening of the muscle around the base of the outflow tract, particularly the crista supraventricularis, and thickening of the trabeculae carneae and papillary muscles of the right ventricle.

emphysema (Fig. 129). The average orientation of the maximal leftward mean instantaneous QRS vector was 0° in our cases of mitral stenosis, -35° in the chronic cor pulmonale cases, and -15° in the chronic emphysema cases. By the same token, the maximal terminal mean instantaneous QRS vector (the largest instantaneous vector situated to the right of the electrical null point) was located less posteriorly in mitral stenosis (average orientation, -145°) than in chronic cor pulmonale (average orientation, -120°) or chronic emphysema (average orientation, -125°). While in an occasional mitral stenosis case with this type of QRS sE loop pattern the maximal terminal mean instantaneous QRS vector may approach in magnitude the maximal leftward mean instantaneous QRS vector, this situation is observed far more frequently in the vectorcardiograms of patients with chronic cor pulmonale and/or pulmonary emphysema.

RIGHT SAGITTAL QRS LOOP.—In our cases of mitral stenosis with the type A pattern, the sagittal QRS loop tended, on the whole, to be oriented almost vertically inferiorly, the maximal mean instantaneous QRS vector lying, on the average, along the $+105^\circ$ axis of the sagittal reference frame. The QRS loop usually displayed terminally a well-defined and prominent superior deflection, the maximal superior mean instantaneous QRS vector having an average orientation of -125° .

The sagittal QRS loop in our cases of chronic cor pulmonale and pulmonary emphysema showed far more variability in appearance and orientation than in our cases of mitral stenosis. Thus, while sagittal loops of the type just described were sometimes observed in the chronic cor pulmonale-emphysema group, the following variant loop patterns were also frequently encountered:

- 1 A figure-of-eight sagittal loop, the proximal part of which was counterclockwise inscribed and the distal portion, clockwise inscribed. In sagittal loops of this type, the long axis of the loop was usually directed almost straight posteriorly, ranging in orientation between $+150^\circ$ and -150° .
- 2 A long narrow sagittal loop inscribed entirely in a counterclockwise direction. Sagittal loops of this type were less frequently observed by us than were the previous type but, when present, were

sagittal QRS loop of this type, although situated superiorly, does not form a well-defined deflection but simply is a continuation of the main body of the loop.

FRONTAL QRS LOOP.—In our cases of mitral stenosis with the type A QRS sE loop pattern, the frontal QRS loop was usually counterclockwise inscribed, only occasionally clockwise inscribed. The maximal leftward mean instantaneous QRS vector in these cases had an average orientation of $+30^\circ$, while the average orientation of the maximal terminal mean instantaneous QRS vector was about -135° in the frontal reference frame. On the other hand, there was an approximately equal distribution of clockwise- and counterclockwise-inscribed frontal loops in the vectorcardiograms of the chronic cor pulmonale cases. In the chronic cor pulmonale cases, the maximal leftward and maximal terminal mean instantaneous QRS vectors were oriented, on the average, along the -25° and -155° axes of the frontal reference frame, respectively, while the average orientations of the corresponding vectors in the emphysema group were $+10^\circ$ and -150° , respectively.

We are not certain as to the significance of this QRS sE loop pattern but are inclined to believe that in its fully developed form, with a prominent right, posterior, and superior terminal deflection, it may represent an early stage in the development of a more typical right ventricular hypertrophy QRS sE loop pattern. While it is true that the type A QRS sE loop pattern is sometimes observed in the vectorcardiograms of normal subjects, it is equally true that the frequency of this pattern varies inversely with the patient's age. Thus, the very frequency with which the type A pattern is encountered in early childhood would seem to argue in favor of its being a pattern of right ventricular hypertrophy.

In our cases of chronic cor pulmonale and pulmonary emphysema with this vectorcardiographic pattern, the electrocardiogram showed varying degrees of right-axis deviation in the limb leads and "clockwise rotation" in the precordial leads. It is evident that the terminal S waves in the left precordial leads in these cases do not reflect posterior rotation of the QRS sE loop itself but, rather, are attributable to the rightward terminal deflection of the loop. This is to be contrasted with the precordial lead QRS pattern of "clockwise rotation" observed with the type C QRS sE loop pattern (to be described shortly), for in the latter instance the QRS pattern in the chest leads is clearly related to the posterior rotation of the QRS sE loop as a whole. Interestingly

... in the frontal reference frame and a maximal superior mean instantaneous vector located at about -170° . Generally, the terminal part of a

TYPE A QRS sE LOOP PATTERN

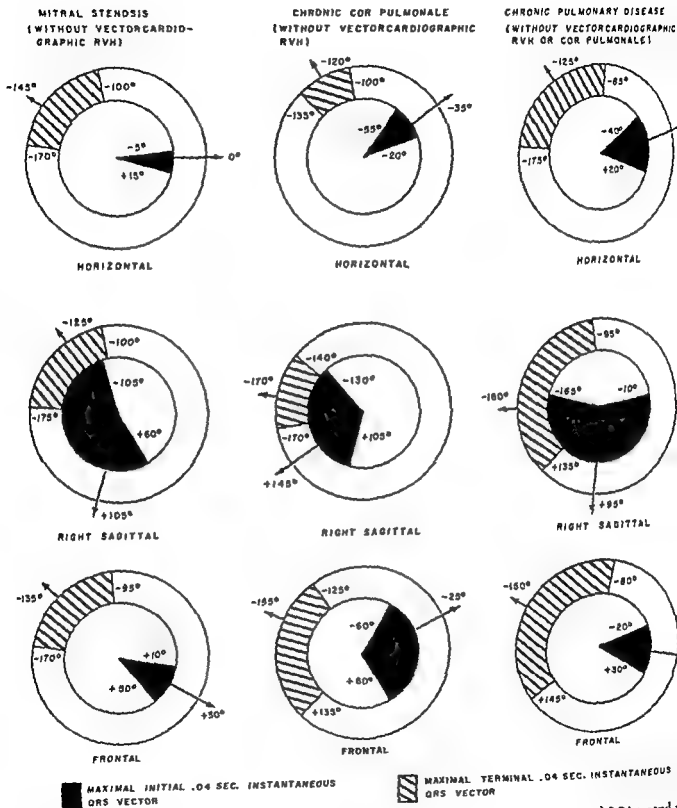
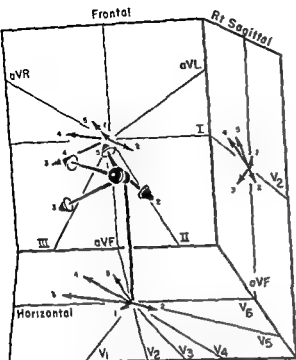
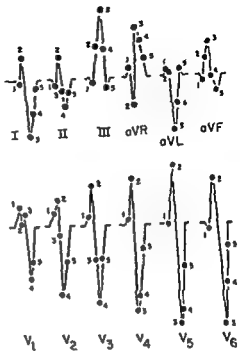


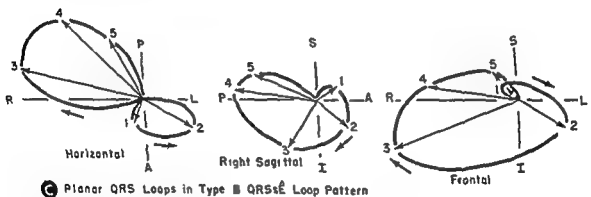
Fig. 129.—Extreme range of variation and average orientation of the maximal initial and terminal 0.04-second instantaneous QRS vectors in the type A QRS sE loop pattern in mitral stenosis, chronic cor pulmonale, and chronic pulmonary emphysema without evident cor pulmonale



A Instantaneous VA Vectors in the Type B QRS sE Loop Pattern in Mitral Stenosis and Chronic Cor Pulmonale



B QRS Deflections Projected on Scalar Leads



C Planar QRS Loops in Type B QRS sE Loop Pattern

Fig 130.—Instantaneous VA vectors in the type B QRS sE loop pattern in mitral stenosis and in chronic cor pulmonale. Note, in A, that the rightward VA vectors exhibit the posterior orientation of these larger vectors. In recording their planar projections or in significance of the large rightward late A vectors remains the same—that is, they are indicative of right ventricular hypertrophy. In B, the QRS deflections projected on the scalar leads by the VA vectors exhibit right-axis deviation of A QRS and the precordial QRS pattern of “marked clockwise rotation.”

enough, in about one half of our cases of mitral stenosis and about one third of our cases of chronic cor pulmonale emphysema, lead V_1 of the electrocardiogram recorded an RSR' deflection. The secondary R wave in these cases presumably corresponds to the terminal rightward deflection of the QRS sE loop, which evidently projects on the positive half of the axis of derivation of lead V_1 . Moreover, in approximately one half of all of our chronic cor pulmonale cases with RSR' deflections in lead V_1 , the R/S amplitude ratio in this lead exceeded 1. The average amplitude of the R' wave in these cases was 2.5 mm., although the range of variation extended from 0.7 mm. to 5 mm.

TYPE B QRS sE LOOP PATTERN

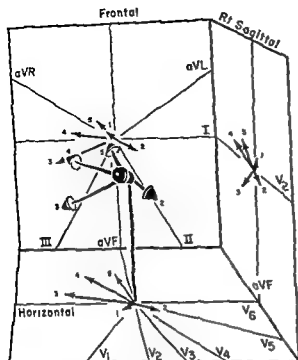
The type B QRS sE loop pattern (Fig. 130) was observed by us in only 6% of the vectorcardiograms of patients with mitral stenosis (i.e., only one third as frequently as the type A pattern), while the incidence of this pattern in the chronic emphysema cases was approximately twice as great. The type B pattern occurred most frequently in our cases of chronic cor pulmonale and was present in about 30% of the vectorcardiograms recorded. In fact, this and the type C QRS sE loop pattern (see p 209) were the two QRS sE loop patterns most commonly encountered in chronic cor pulmonale—at least in our experience.

HORIZONTAL QRS LOOP.—In the type B loop pattern, the horizontal QRS loop ordinarily exhibits a well-developed initial anterior and rightward deflection, however, this is not invariably true, since occasionally the horizontal loop will be found to proceed initially to the left and either anteriorly or posteriorly. In either case, the efferent limb of the loop is next written to the left and slightly anteriorly or posteriorly, although it usually does not extend as far laterally as the corresponding limb of the normal or type A horizontal loop. An anterior concavity in the efferent limb of the horizontal QRS loop is not an uncommon finding in vectorcardiograms showing the type B pattern. On reaching its maximal leftward extent, the horizontal QRS loop turns posteriorly, and the afferent limb is next inscribed rapidly in a counterclockwise direction from left to right. A characteristic feature of the horizontal loop in the type B QRS sE loop pattern is that the afferent limb of the loop is written only slightly posterior to the efferent limb and not infrequently curves slightly anteriorly late in its rightward course. Soon thereafter the loop turns posteriorly, and it continues for a time to be inscribed in a clockwise direction far to the right and far posteri-

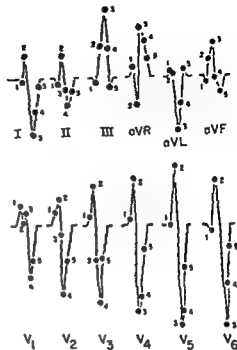
orly before returning eventually to its point of origin. In short, the horizontal QRS loop in the type B pattern typically presents a figure-of-eight configuration in which the early leftward loop of the "eight" is counterclockwise inscribed and the terminal rightward and posterior loop is clockwise inscribed. Generally, the terminal rightward and posterior component of the horizontal loop is larger and encloses a greater area than the earlier leftward component, this being especially true in vectorcardiograms of patients with chronic cor pulmonale. The average orientation of the maximal leftward mean instantaneous QRS vector in our cases of mitral stenosis was $+10^\circ$, in chronic cor pulmonale -10° , and in chronic emphysema $+5^\circ$, and the average orientation of the maximal terminal mean instantaneous QRS vector was, respectively, -165° , -125° , and -115° (Fig. 131).

RIGHT SAGITTAL QRS LOOP.—The sagittal loop in the type B pattern sometimes resembles that in the type A pattern but more frequently shows a triangular configuration. In other words, the sagittal loop displays two distinct maximal mean instantaneous vectors. The earlier of the two maximal mean instantaneous QRS vectors is usually directed inferiorly and slightly posteriorly, while the terminal maximal vector is oriented slightly superiorly and almost directly posteriorly. Depending on the magnitude and orientation of these two vectors, the limb of the loop extending between them is written either far posteriorly, in which case the sagittal loop is entirely clockwise inscribed, or more anteriorly. In the latter event, the sagittal loop may present a figure-of-eight configuration with the distal loop of the "eight" situated slightly anteriorly and having a counterclockwise direction of inscription, while the remainder of the loop is written in a clockwise direction slightly posteriorly. By and large, in our cases of mitral stenosis, chronic cor pulmonale, and emphysema with the type B QRS sE loop pattern, the average orientation of the earlier of the two maximal mean instantaneous vectors of the sagittal QRS loop varied between $+80^\circ$ and $+115^\circ$, while the average orientation of the second maximal vector ranged between 180° and -155° . In general, the early maximal instantaneous QRS vector tended to be directed more posteriorly, and the terminal maximal vector more superiorly, in the chronic cor pulmonale cases than in the mitral stenosis or chronic emphysema cases.

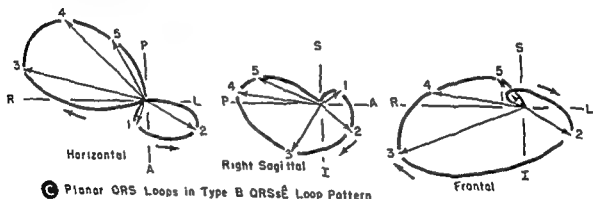
FRONTAL QRS LOOP.—The frontal loop in the type B QRS sE loop pattern usually extends, about equally, first to the left and then to the right of the electrical null point. In over 75% of the vectorcardiograms show-



A Instantaneous VA Vectors in the Type B QRSs Loop Pattern in Mitral Stenosis and Chronic Cor Pulmonale



B QRS Deflections Projected on Scalar Leads



C Planar QRS Loops in Type B QRSs Loop Pattern

Fig 130 Instantaneous VA vectors in the type B QRSs loop pattern

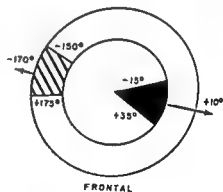
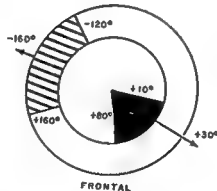
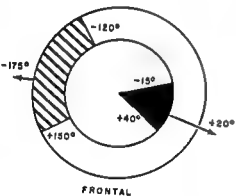
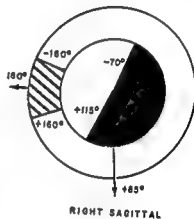
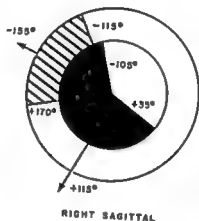
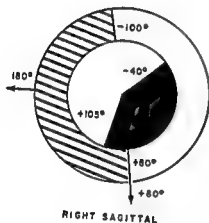
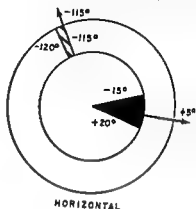
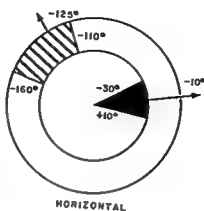
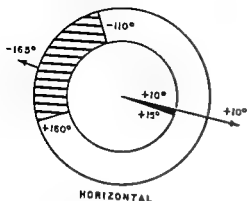
male
the p
recor
signif
hypertrophy In B, the QRS deflections pr
A QRS and the precordial QRS pattern o

TYPE B QRS sE LOOP PATTERN

MITRAL STENOSIS
(WITHOUT VECTORCARDIOGRAPHIC
RVH)

CHRONIC COR PULMONALE
(WITHOUT VECTORCARDIOGRAPHIC
RVH)

CHRONIC PULMONARY DISEASE
(WITHOUT VECTORCARDIOGRAPHIC
RVH OR COR PULMONALE)



MAXIMAL INITIAL .04 SEC. INSTANTANEOUS
QRS VECTOR

MAXIMAL TERMINAL .04 SEC INSTANTANEOUS
QRS VECTOR

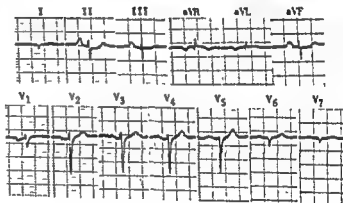
Fig. 131.—Extreme range of instantaneous QRS vectors in the coronary emphysema without evc

this pattern, we found the frontal loop to have a clockwise direction of inscription, while in less than a quarter of the cases a counterclockwise-inscribed frontal loop was noted. Occasionally the frontal loop may have a figure-of-eight configuration with a counterclockwise-inscribed leftward component and a clockwise-inscribed rightward component. The average orientation of the maximal leftward mean instantaneous QRS vector in our cases of mitral stenosis,

but such an event has been observed so rarely in our experience as to constitute an exception to the rule. The reasons for our believing that the type B pattern reflects right ventricular hypertrophy are

cases of mitral stenosis, -170° in chronic cor pul-

deflections in precordial leads V_1 through V_6 are directed primarily downward. A QRS in the horizontal plane is located to the right and posteriorly. A rightward, posterior, and superior orientation of sA QRS, as calculated from the electrocardiographic leads, correlates very well with the presence of chronic cor pulmonale. In the vectorcardiogram, the P sE loop is larger than normal and is situated abnormally anteriorly and almost vertically inferiorly. These findings are consistent with the vectorcardiographic diagnosis of P pulmonale. The QRS sE loop is written very briefly to the left but soon turns and is written to the right, posteriorly, and superiorly. The configuration of the QRS sE loop is compatible with the type B pattern of right ventricular hypertrophy. The T sE loop is discordant to the long axis of the QRS sE loop.



chronic cor pulmonale, and chronic emphysema ranged between $+10^\circ$ and $+30^\circ$, while the average orientation of the maximal rightward mean instantaneous vector varied between -175° and -160° (Fig. 131).

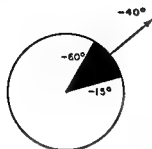
It is our belief that the type B QRS sE loop pattern, when observed in cases presenting other clinical findings suggestive of mitral stenosis or chronic cor pulmonale, represents a pattern of

monale, and $+125^\circ$ in chronic emphysema. By and large, in the mitral stenosis

played more marked right-axis deviation of A QRS than in the cases in which the vectorcardiograms showed the type A loop pattern. Although, in many cases, the QRS deflections in the bipolar limb leads approached the $S_I-S_{II}-S_{III}$ configuration in appearance, we observed the latter pattern only in the chronic cor pulmonale cases, but in this group the pattern appeared in approximately one half of the

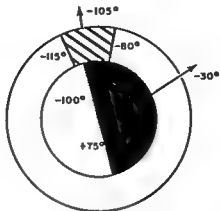
TYPE C QRS sE LOOP PATTERN

MITRAL STENOSIS
(WITHOUT VECTORCARDIOGRAPHIC RVH)



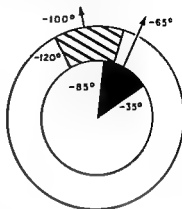
HORIZONTAL

CHRONIC COR PULMONALE
(WITHOUT VECTORCARDIOGRAPHIC RVH)



HORIZONTAL

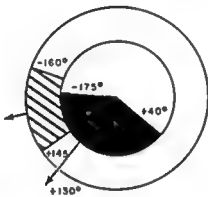
CHRONIC PULMONARY DISEASE
(WITHOUT VECTORCARDIOGRAPHIC RVH OR COR PULMONALE)



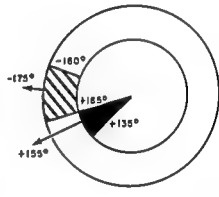
HORIZONTAL



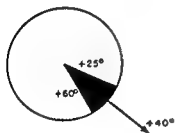
RIGHT SAGITTAL



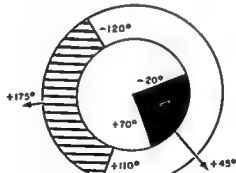
RIGHT SAGITTAL



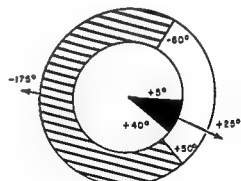
RIGHT SAGITTAL



FRONTAL



FRONTAL



FRONTAL



MAXIMAL INITIAL .04 SEC. INSTANTANEOUS QRS VECTOR



MAXIMAL TERMINAL .04 SEC. INSTANTANEOUS QRS VECTOR

Fig. 133.—Extreme range of variation and average orientation of the maximal initial and terminal .04-second mean instantaneous QRS vectors in the type C QRS sE loop pattern in mitral stenosis, chronic cor pulmonale, and chronic pulmonary emphysema without cor pulmonale

electrocardiograms. In addition, the electrocardiograms of most of the chronic cor pulmonale patients and of slightly fewer chronic emphysema patients showed the P pulmonale pattern. The QRS configuration in lead V_1 in our cases of mitral stenosis, chronic cor pulmonale, and chronic emphysema usually was of a vibratory $rSr's$, qR , rSr' , or rS type. Moreover, the precordial leads almost invariably displayed the

TYPE C QRS sE LOOP PATTERN

The type C QRS sE loop pattern appeared in about the same percentage of vectorcardiograms of our patients with mitral stenosis and chronic cor pulmonale as did the type II pattern, although it occurred much more frequently than the latter pattern in the cases of chronic emphysema, where it was present in

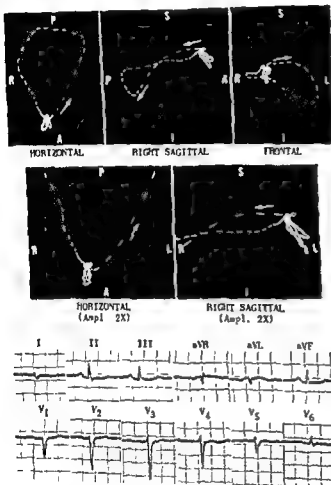


Fig. 134.—Vectorcardiographic type C QRS sE loop pattern in a man, 54, with severe obstructive emphysema and congestive heart failure but without radiologic evidence of cor pulmonale. The right-axis deviation of A QRS in the frontal plane scalar leads and the marked posterior rotation of A QRS in the horizontal scalar leads are compatible with chronic pulmonary disease. The entire QRS sE loop of the vectorcardiogram is rotated abnormally far posteriorly, so that the long axis of the horizontal QRS loop is directed along the -90° axis of the horizontal reference frame. The T sE loop is discordant to the QRS sE loop and is oriented almost directly anteriorly.

electrocardiographic pattern of "marked clockwise rotation." In occasional electrocardiograms, Q waves of such prominence as to raise the question of myocardial infarction were recorded in leads II, III, or aVF or in one or more of the right precordial leads, but in none of these cases was there historical or other clinical evidence suggesting antecedent infarction. Thus, one should be wary of making the erroneous electrocardiographic diagnosis of myocardial infarction in tracings compatible with chronic cor pulmonale.

almost one third of the vectorcardiograms studied.

HORIZONTAL QRS LOOP.—There were certain differences in the appearance of the QRS sE loop in the type C pattern in chronic cor pulmonale and emphysema as compared with the pattern in mitral stenosis. The dissimilarities were usually most striking in the horizontal projection. For example, in our few cases of mitral stenosis in which the vectorcardiograms displayed the type C QRS sE loop pattern, the horizontal QRS loop presented an essentially normal configuration but its long axis or maximal mean in-

stantaneous vector was simply rotated abnormally far posteriorly, its average orientation being about -40° . In contrast, the horizontal QRS loop in the chronic cor pulmonale and chronic emphysema cases displayed the following features:

1. The initial deflection of the loop was written almost straight anteriorly, or sometimes slightly to the right or left and anteriorly.

2. The loop then turned abruptly posteriorly, and the efferent limb of the loop was written as an almost straight line far posteriorly and to a varying degree to the left.

3. On reaching its maximal leftward and posterior extent, the loop then turned medially and proceeded rapidly from left to right.

4. The afferent limb and terminal part of the loop were often written in the form of a large rightward and posterior deflection, much like that occurring in the fully developed type A QRS sE loop pattern.

resemble that occurring in the type A pattern, although generally being oriented somewhat more inferiorly. If the frontal QRS loop should happen to be oriented almost vertically inferiorly, then the horizontal QRS loop may simulate that observed in the type A QRS sE loop pattern; however, this is simply the result of foreshortening of the loop in the horizontal projection (Fig. 134 and Table 16).

We are not certain as to the manner of production or the significance of the type C QRS sE loop pattern, although we have observed 2 patients with chronic cor pulmonale with this pattern who were found at postmortem to have marked right ventricular hypertrophy. Although there is no other evidence to support this impression, we nonetheless feel that the type C pattern as it appears in the chronic cor pulmonale cases—that is, with large rightward, posterior, and superior terminal mean instantaneous QRS vectors in addition to the abnormal posterior rotation of

TABLE 16—QRS sE LOOP PATTERNS IN MITRAL STENOSIS, CHRONIC COR PULMONALE, AND CHRONIC PULMONARY DISEASE WITHOUT COR PULMONALE

	TOTAL NO OF CASES	NORMAL QRS sE	RIGHT VENTRICULAR HYPERTROPHY	LEFT VENTRICULAR HYPERTROPHY	TYPE A QRS sE	TYPE B QRS sE	TYPE C QRS sE
Mitral stenosis	54	3	32	4	9	3	3
Chronic cor pulmonale	20	0	3	0	5	6	6
Chronic pulmonary disease	17	0	1	0	9	2	5

Thus, the horizontal QRS loop in chronic cor pulmonale and, to a lesser extent, in chronic emphysema displayed two maximal mean instantaneous QRS vectors. The first of these had an average orientation varying between -30° and -65° , while the second maximal vector was located, on the average, at about -105° (Fig. 133). Although the magnitudes of the two mean instantaneous vectors just referred to were often approximately equal, not infrequently in the chronic cor pulmonale cases the second instantaneous vector was the larger of the two.

RIGHT SAGITTAL QRS LOOP—The sagittal QRS loop in the type C pattern resembled that already described in the type A pattern with the exception that, by and large, the terminal mean instantaneous QRS vectors were situated superiorly less frequently than in the latter pattern. This difference was especially prominent in the vectorcardiograms of the mitral stenosis patients.

FRONTAL QRS LOOP—Like the sagittal loop, the frontal QRS loop in the type C pattern also tends to

the loop as a whole—may well reflect clockwise rotation of the heart on its longitudinal axis plus some degree of right ventricular preponderance. On the other hand, the type C QRS sE loop pattern in the vectorcardiograms of our cases of mitral stenosis would seem to represent primarily the electrical effects of anatomic cardiac rotation. Obviously, these conclusions are only tentative, and undoubtedly, they will be altered as further information becomes available.

As one might anticipate, the electrocardiographic findings in mitral stenosis with the type C QRS sE loop pattern consist, for the most part, of right-axis deviation of A QRS in the bipolar limb leads and the precordial lead QRS pattern of "moderate" or "marked clockwise rotation." In general, the electrocardiographic findings in the chronic cor pulmonale and chronic emphysema cases with the type C vectorcardiographic pattern were much the same as those just described except that the right-axis deviation and "clockwise rotation" were generally of more

marked degree than customarily observed in mitral stenosis

Genesis of Vectorcardiographic QRS sE Loop Patterns

In chronic cor pulmonale, just as in mitral stenosis, the earliest and most marked evidence of anatomic right ventricular hypertrophy consists of thickening of the trabecular and papillary muscles and the muscle around the base of the outflow tract of the right ven-

tricle. The from the posterior base of the fundibulum of the right ventricle to the right atrial ostium. According to Sodi-Pallares, the crista supraventricularis and adjacent regions of the outflow tract of the right ventricle belong to the interventricular septum at its higher level and, together with basal right septal myocardium, are normally the last portion of the right ventricle, and one of the last regions of the heart, to complete depolarization.

The QRS forces produced in the basal right ventricular myocardium are directed superiorly, to the right, and somewhat anteriorly, but algebraic summation of these forces with the larger leftward, posterior, and inferior or superior forces arising in the basal left ventricular wall normally yields terminal resultant or mean QRS vectors directed posteriorly, somewhat to the left, and either superiorly and inferiorly. However, because of the physiologic right ventricular preponderance existing in young children, the larger basal right ventricular forces may produce terminal mean QRS vectors directed to the right, superiorly, and posteriorly. If these vectors are situated within the 160° to -150° segment of the horizontal reference frame, they project small terminal R' deflections on lead V_1 and $V_{2,3}$. Since the component forces and the resultant terminal vectors are not normally of great magnitude, the R' deflections appearing in these instances in the right precordial leads are usually quite small, rarely exceeding 4 mm.

Inasmuch as any terminal mean instantaneous QRS spatial vector is the resultant of component left ventricular forces directed to the left, posteriorly, and superiorly or inferiorly, and of component right ventricular forces directed to the right, slightly anteriorly, and superiorly, it follows that, as the latter forces increase progressively in magnitude (assuming, for simplicity, that their direction remains unchanged, which is unlikely to be the case in right ventricular hypertrophy), the resultant or mean instantaneous QRS vectors must necessarily rotate in a counter-

clockwise direction from left, posterior, and superior or inferior, to right, posterior, and superior, and eventually to right, anterior, and superior. To a certain extent, this hypothetical sequence of changing orientation of the terminal QRS vectors is observed clinically in the electrocardiogram and vectorcardiogram, but certain discrepancies between fact and theory are noted, particularly in chronic cor pulmonale. For example, the anticipated rightward, superior, and anterior terminal QRS vectors reflecting selective hypertrophy of the right ventricle are rarely found in chronic cor pulmonale and pulmonary emphysema; instead, in these conditions the terminal QRS vectors are generally directed to the right, posteriorly, and superiorly or slightly to the left, posteriorly, and inferiorly. This may be due in no small part to the associated changes in heart position and cardiac rotation which are known to occur in emphysema. As previously indicated, the lowering of the diaphragm as the result of emphysema in turn causes the heart to descend in the chest, to assume a more vertical position, and to rotate in a clockwise direction around its longitudinal axis.

In the past it was accepted, without much question, that the electrocardiographic effects of cardiac positional and rotational changes in emphysema simply reflected orientation of the exploring lead electrode to an aspect of the heart different from normal. However, this explanation is based on the premise that the electrocardiographic leads respond primarily to "proximity potentials" produced by the region of the heart closest to the exploring electrode, and, as pointed out in Chapter 4, this concept is probably not valid when applied to body surface leads. In all likelihood, the correct explanation of the electrical effects of variations in anatomic heart position and rotation, such as those occurring in chronic emphysema, is to be sought in studies of the effects of these factors on the direction and magnitude of the lead vectors or effective axes. For the present, one can only speculate as to the manner in which positional and rotational changes of the heart may possibly be related to the terminal rightward, superior, and posterior QRS forces so frequently observed in chronic cor pulmonale. In the following paragraphs there is presented a purely hypothetical mechanism by which the changes in heart position and rotation in chronic cor pulmonale may account for the characteristic rightward, posterior, and superior terminal QRS forces.

As we indicated in the introduction to this section of the text (Chapter 13), the changes in heart position and rotation in pulmonary emphysema must

stantaneous vector was simply rotated abnormally far posteriorly, its average orientation being about -40° . In contrast, the horizontal QRS loop in the chronic cor pulmonale and chronic emphysema cases displayed the following features:

1. The initial deflection of the loop was written almost straight anteriorly, or sometimes slightly to the right or left and anteriorly.

2. The loop then turned abruptly posteriorly, and the efferent limb of the loop was written as an almost straight line far posteriorly and to a varying degree to the left.

3. On reaching its maximal leftward and posterior extent, the loop then turned medially and proceeded rapidly from left to right.

4. The afferent limb and terminal part of the loop were often written in the form of a large rightward and posterior deflection, much like that occurring in the fully developed type A QRS sE loop pattern.

resemble that occurring in the type A pattern, although generally being oriented somewhat more inferiorly. If the frontal QRS loop should happen to be oriented almost vertically inferiorly, then the horizontal QRS loop may simulate that observed in the type A QRS sE loop pattern; however, this is simply the result of foreshortening of the loop in the horizontal projection (Fig. 134 and Table 16).

We are not certain as to the manner of production or the significance of the type C QRS sE loop pattern, although we have observed 2 patients with chronic cor pulmonale with this pattern who were found at postmortem to have marked right ventricular hypertrophy. Although there is no other evidence to support this impression, we nonetheless feel that the type C pattern as it appears in the chronic cor pulmonale cases—that is, with large rightward, posterior, and superior terminal mean instantaneous QRS vectors in addition to the abnormal posterior rotation of

TABLE 16—QRS sE LOOP PATTERNS IN MITRAL STENOSIS, CHRONIC COR PULMONALE, AND CHRONIC PULMONARY DISEASE WITHOUT COR PULMONALE

	TOTAL NO OF CASES	NORMAL QRS sE	RIGHT VENTRICULAR HYPERTROPHY	LEFT VENTRICULAR HYPERTROPHY	TYPE A QRS sE	TYPE B QRS sE	TYPE C QRS sE
Mitral stenosis	54	3	32	4	9	3	3
Chronic cor pulmonale	20	0	3	0	5	6	6
Chronic pulmonary disease	17	0	1	0	9	2	5

Thus, the horizontal QRS loop in chronic cor pulmonale and, to a lesser extent, in chronic emphysema displayed two maximal mean instantaneous QRS vectors. The first of these had an average orientation varying between -30° and -65° , while the second maximal vector was located, on the average, at about -105° (Fig. 133). Although the magnitudes of the two mean instantaneous vectors just referred to were often approximately equal, not infrequently in the chronic cor pulmonale cases the second instantaneous vector was the larger of the two.

RIGHT SAGITTAL QRS LOOP—The sagittal QRS loop in the type C pattern resembled that already described in the type A pattern with the exception that, by and large, the terminal mean instantaneous QRS vectors were situated superiorly less frequently than in the latter pattern. This difference was especially prominent in the vectorcardiograms of the mitral stenosis patients.

FRONTAL QRS LOOP—Like the sagittal loop, the frontal QRS loop in the type C pattern also tends to

the loop as a whole—may well reflect clockwise rotation of the heart on its longitudinal axis plus some degree of right ventricular preponderance. On the other hand, the type C QRS sE loop pattern in the vectorcardiograms of our cases of mitral stenosis would seem to represent primarily the electrical effects of anatomic cardiac rotation. Obviously, these conclusions are only tentative, and undoubtedly, they will be altered as further information becomes available.

As one might anticipate, the electrocardiographic findings in mitral stenosis with the type C QRS sE loop pattern consist, for the most part, of right-axis deviation of A QRS in the bipolar limb leads and the precordial lead QRS pattern of "moderate" or "marked clockwise rotation." In general, the electrocardiographic findings in the chronic cor pulmonale and chronic emphysema cases with the type C vectorcardiographic pattern were much the same as those just described except that the right-axis deviation and "clockwise rotation" were generally of more

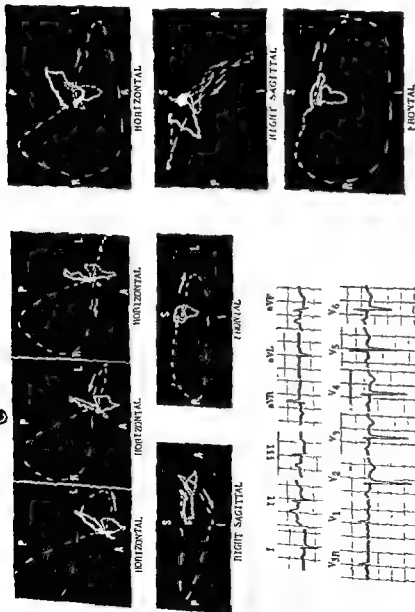


Fig. 125 (cont.)—Four months later (C) the electrocardiogram showed prominent P waves in leads II, III, and aVF, right-axis deviation of A QRS (-150°), low-amplitude QRS deflections in leads V₁ and V₂, orientation of A QRS in the horizontal plane to the right and posteriorly, and inverted T waves in leads II, III, aVF, and V₁ through V₄. The authors interpret this electrocardiogram as showing right ventricular hypertrophy and anterior myocardial infarction and/or digitalis effect. In the vectorcardiogram in C, the configuration of the horizontal QRS loop resembles that in B except that with respiration the left-to-right limb of the loop tended to shift progressively farther anteriorly, while the magnitude of the horizontal and frontal QRS loops was written to the right of the midline. The anterior and vertically inferior rather leftward vectors. Thus the greater part of the horizontal QRS loop is entirely clockwise for inscription and is situated anteriorly except for the terminal portion of the loop. One is the impression that the principal difference in QRS loop configuration between the vectorcardiogram in C and that in D is that the left-to-right limb of the QRS loop in C is displaced far anteriorly. In fact, if one compares the planar QRS loops in records B-D, it becomes apparent that they differ only to the extent that there is progressive anterior displacement of the inferior, left-to-right limb of the QRS loop, culminating with the fully developed right ventricular hypertrophy pattern in D.

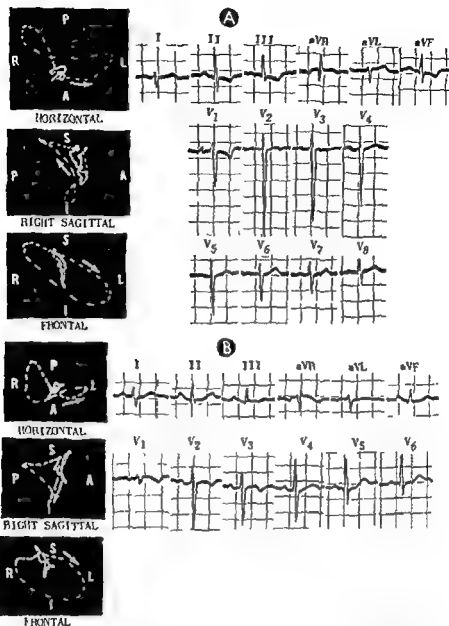


Fig. 135.—A, electrocardiographic and vectorcardiographic patterns of chronic cor pulmonale recorded from a man, 73, with congestive heart failure and pulmonary insufficiency due to bilateral far-advanced tuberculosis and bullous pulmonary emphysema. The horizontal QRS loop is located anteriorly, to the right, and posteriorly. In the horizontal plane, the horizontal QRS loop has left and posteriorly, and the second half inscribed clockwise equally far to the right and posteriorly. The terminal portions of the right sagittal and frontal QRS loops are located superiorly, to the right, and posteriorly. In the authors' opinion, the posteriorly directed QRS loop is characteristic of chronic cor pulmonale.

di
 the right middle and lower lobes and left lower lobe of the lungs. The patient had pulmonary emphysema, advanced saccular bronchiectasis of the right ventricular, and advanced congestive heart failure. He was recorded about 1 year before his death. The ECG shows a minor degree of right-axis deviation, which is considered, by the au

changes in the QRS sE loop. On the other hand, one can easily conceive of respiration producing instant-to-instant alteration in the direction of the effective axes of the vectorcardiographic leads by virtue of small shifts in the location of the equivalent cardiac dipole, changes in conductivity of the lungs, etc.

3 From a patient with severe chronic cor pulmonale we recorded serial electrocardiograms and vectorcardiograms at 2-4-month intervals over a period of about 1½ years, the last records being made shortly before the patient's death. Postmortem examination confirmed the presence of marked anatomic right ventricular hypertrophy. Of the many electrocardiograms obtained during the time the patient was

followed clinically, there were only two which showed diagnostic evidence of right ventricular hypertrophy, and these were recorded quite late in the course of the patient's illness (Fig. 135). The initial vectorcardiogram displayed the type B QRS sE loop pattern. As the patient's condition (chronic cor pulmonale) worsened clinically, the efferent left-to-right limb of the QRS sE loop, which was at first posteriorly situated, shifted steadily forward until finally it reached a point far enough anterior to cause a complete reversal in the direction of inscription of the horizontal QRS loop (the entire loop having a clockwise direction of inscription) and to produce a figure-of-eight configuration of the sagittal QRS loop. Despite the

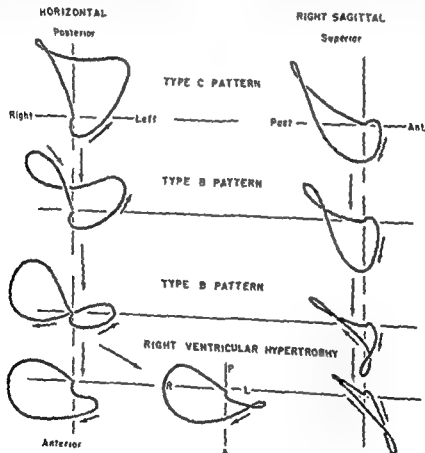


Fig. 136 — Cont.

this type

necessarily be accompanied by a shift in the location of the cardiac dipole center. The altered location of the dipole plus the decreased conductivity of the emphysematous lungs in turn lead to changes in the effective axes of the various leads. However, of these two factors, the more important is the location of the cardiac dipole. Schaffer has demonstrated that, with a shift in the location of the dipole center toward a given lead electrode, the image point of the electrode is shifted farther away from the dipole; on the other hand, if the dipole moves away from the electrode, the image point of the latter shifts closer to the dipole. Presumably, as the heart descends to a lower level in the chest in pulmonary emphysema, the dipole center also descends. In so doing, it approaches more closely the anterior electrode of the sagittal vectorcardiographic lead, lead Z, and therefore causes the effective axis of lead Z to rotate clockwise. If this supposition is correct, then it may well be that in chronic cor pulmonale (due to emphysema) the normal downward slant of lead Z in a posteroanterior direction is exaggerated. This being the case, the manifest vectors are recorded by lead Z as if rotated counterclockwise, vertically inferior vectors being rotated in an anterior direction and vertically superior vectors in a posterior direction. This effect of the increased downward slant of lead Z is all the more marked the more nearly perpendicular the cardiac vectors lie to the anatomic axis of lead Z. Thus, in chronic cor pulmonale with selective hypertrophy of the basal right ventricle, the late, rightward, anteriorly, and superiorly directed QRS forces of increased magnitude actually are recorded as if oriented posteriorly because of the marked downward tilt of the effective axis of lead Z, on the other hand, similarly directed QRS forces are more likely to be recorded in their true anterior orientation in mitral stenosis or congenital heart disease because of the less marked rotation of the effective axis of lead Z in these conditions.

In a small number of cases of chronic cor pulmonale with vectorcardiographic type A, type B, or type C QRS sE loop patterns, we tested the above premise in the following manner. After the control vectorcardiogram had been recorded in the customary way, a second record was obtained with the anterior electrode of lead Z applied at a higher level on the chest. This was done in an attempt to reverse the postulated exaggerated posteroanterior downward slant of lead Z produced by pulmonary emphysema. On comparing the two vectorcardiograms recorded in each of the cases of chronic cor pulmonale studied, it was found that in the second vectorcardiogram the terminal portion of the QRS sE loop originally located

to the right, superiorly, and posteriorly was found to lie anteriorly. It is highly probable that the deviation of the superiorly oriented vectors from posterior to anterior in the second vectorcardiogram reflected the upward slant of lead Z in a posteroanterior direction.

While the above observations do not prove, they at least suggest, the following: (a) that the mechanism by which cardiac positional and rotational changes in pulmonary emphysema influence the electrocardiogram and vectorcardiogram entails some alteration in the magnitude and, especially, in the direction of the effective axes of the leads utilized; and (b) that the unexpected posterior orientation of the terminal QRS forces in chronic cor pulmonale, representing, for the most part, the activation forces arising in the hypertrophied basal region of the right ventricle, may be related etiologically to clockwise rotation of the effective axis of lead Z. There are certain additional reasons for believing that the terminal right, posterior, and superior QRS forces in chronic cor pulmonale reflect selective right ventricular hypertrophy, some of these are as follows.

1. In almost all of the vectorcardiograms diagnostic of right ventricular hypertrophy with rightward and posterior terminal QRS vectors in our cases of mitral stenosis, chronic cor pulmonale, and congenital heart disease, as well as in the great majority of similar vectorcardiograms published in Grishman and Scherlis' textbook of vectorcardiography and in most of the vectorcardiograms of this type described in the report of Richman and Wolff, the terminal vectors were also oriented inferiorly. However, the converse of this did not hold true—that is, superiorly located terminal QRS vectors were by no means invariably directed posteriorly. Nevertheless, the consistency of the former association would seem to imply some relationship between the posterior orientation of the terminal QRS vectors in chronic cor pulmonale and the fact that these vectors are situated superiorly.

2. In a number of mitral stenosis cases, we have noted respiratory variation in QRS sE loop configuration between a typical RSR' pattern of right ventricular hypertrophy and an equally typical type B QRS sE loop pattern. Generally, this was accompanied by a changing orientation of the terminal QRS vectors from slightly inferior to slightly superior. Such a fleeting transition back and forth between the foregoing two QRS sE loop patterns can hardly be attributed to such a relatively permanent characteristic as the degree of anatomic right ventricular hypertrophy, nor would it seem likely that respiration alone could cause beat-to-beat variation in heart position and/or rotation of sufficient degree to produce the observed

seems reasonably certain that many instances of incomplete right bundle branch block pattern found in pulmonary embolism are not actually right bundle branch block at all—at least not in the sense that the term is used elsewhere in this text (see Chapter 17). As will be explained later in the description of the vectorcardiographic features of pulmonary embolism (pp. 219 and 220), in many of the cases in which a terminal R wave is recorded in lead V_1 of the electrocardiogram, the configuration of the QRS sE loop will

sometimes depressed, S-T segments and/or inverted T waves are recorded in leads V_1 and V_2 ; and depressed S-T segments and upright T waves appear in leads V_3 and V_6 .

ABNORMALITIES PROBABLY RELATED PRIMARILY TO CARDIAC ROTATION: Right-axis deviation of A QRS and the S_1 - Q_{III} pattern of McGinn and White—In all probability, anatomic cardiac rotation occurs in acute pulmonary embolism as the result of right ventricular and atrial dilatation. However, it is not certain

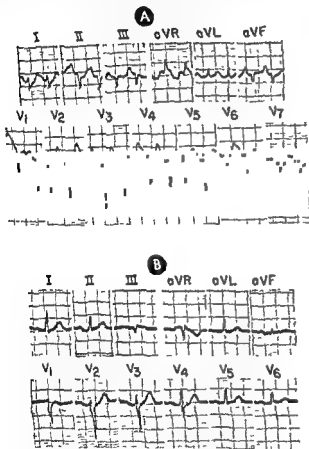


Fig 137.—Electrocardiograms recorded from a woman, 23, (A) 3 days post partum, shortly after clinical onset of acute cor pulmonale due to pulmonary embolism, and (B) 1 day later. The findings in A, quite typical of acute cor pulmonale, are: marked right-axis deviation of A QRS, producing an S_1 - S_1 - S_1 pattern, P pulmonale pattern in the limb leads, QS deflections in leads III and aVF, precordial leads showing the QRS pattern of "marked clockwise rotation," with low R waves and relatively deep S waves in all leads from V_1 through V_6 , and S-T segment depression in leads I, II, and V_1 through V_6 . The heart rate in A is approximately 160 beats per minute, and the rhythm is probably paroxysmal atrial tachycardia. Electrocardiogram B is within normal limits, the foregoing findings having disappeared.

not resemble right bundle branch block at all. Whether the electrocardiographic and vectorcardiographic abnormalities in these cases result from a local or focal intraventricular block, secondary to marked localized dilatation of the pulmonary outflow tract, or are produced by some other mechanism remains to be determined.

ACUTE CORONARY INSUFFICIENCY—As a result possibly of a fall in cardiac output, myocardial anoxemia may occur, particularly in older subjects and those patients with pre-existing coronary artery disease and left ventricular enlargement. Usually elevated,

whether rotation plays a major or a minor role in the etiology of the right-axis deviation of the instantaneous QRS vectors in the frontal plane and their posterior rotation in the horizontal plane. In any event, with moderate degrees of right-axis deviation, deep terminal S waves are projected on lead I and prominent Q waves of less than 0.03-second duration on leads III and aVF. This finding plus depressed S-T segments with "staircase ascent" to the T wave in lead I constitutes the S_1 - Q_{III} pattern of McGinn and White, which is considered quite characteristic of pulmonary embolism. If there is a marked degree of

appearance of typical features of right ventricular hypertrophy, the QRS sE loop continued to display terminal QRS vectors directed to the right, posteriorly, and superiorly. Obviously, the patient's anatomic right ventricular hypertrophy did not have its onset only during the final year and a half of life but must have long antedated the first vectorcardiogram recorded.

This finding and the close similarity of the QRS sE loop configuration in records displaying the type II pattern and those with the pattern of vectorcardiographic right ventricular hypertrophy would seem to suggest that the type B QRS sE loop pattern, in some cases at least, constitutes a third vectorcardiographic pattern of right ventricular hypertrophy, modified, however, by the distorted recording response of the vectorcardiographic leads. In fact, this opinion as to the significance of the type B QRS sE loop pattern does not originate with us but has been expressed by Fowler and Helm, Grishman and his associates, and others, although this same pattern has been considered a normal variant by other investigators. It must be admitted that we have, on rare occasion, observed a type II QRS sE loop pattern in vectorcardiograms of normal subjects, but, for that matter, the

same holds true for the RSR' pattern of right ventricular hypertrophy. Consequently, we do not feel that these rare exceptions to the rule can be regarded as evidence militating against the possibility that the type B pattern is indicative of right ventricular hypertrophy. As a matter of fact, it may well be that the type A and type C QRS sE loop patterns also signify either lesser degrees of anatomic right ventricular hypertrophy or right ventricular hypertrophy plus rotational and positional changes of the heart. The authors have observed the transition of a type C QRS sE loop pattern to a type B pattern as a respiratory variation in occasional patients and have also followed the evolution of a type B QRS sE loop pattern into a typical right ventricular hypertrophy pattern in other cases (Fig. 136). From a purely practical standpoint, the type B pattern in particular has the significance that, if it is eventually proved with certainty that the type B pattern is indicative of right ventricular hypertrophy, then the physician will be able to recognize right ventricular hypertrophy in a significant number of patients with chronic cor pulmonale whose electrocardiograms provide no clue as to the diagnosis.

ACUTE PULMONARY EMBOLISM WITH ACUTE COR PULMONALE: ECG AND VCG FINDINGS

When pulmonary embolism is suspected clinically, one of the most important decisions, which must be made promptly, is whether or not the clinical picture, although resembling pulmonary embolism, is actually due to myocardial infarction. For the electrocardiographer, the exclusion of myocardial infarction takes precedence over the diagnosis of pulmonary embolism. The electrocardiographic differentiation of infarction and pulmonary embolism ordinarily does not present too great a problem, but sometimes the distinction between the two can be quite difficult to make.

The most characteristic feature of the electrocardiogram in pulmonary embolism—the precipitant appearance and usually transient duration of the electrocardiographic changes—is also the chief reason why this condition has been so difficult to study adequately clinically. Nevertheless, it has been shown that one can produce in dogs, by compression of the pulmonary artery or by experimental pulmonary embolism, the same electrocardiographic abnormalities as those observed in patients with pulmonary embolism. In clinical pulmonary embolism, the electrocardiogram

may show no changes whatsoever, or it may display one or more of the following abnormalities:

TRANSIENT ATRIAL OR SUPRAVENTRICULAR ARRHYTHMIAS—These arrhythmias may take the form of premature atrial extrasystoles, paroxysmal atrial or nodal tachycardia, atrial fibrillation, or atrial flutter.

P PULMONALE.—The P pulmonale pattern of the P waves is not so common a finding in pulmonary embolism as was once thought. As will be recalled, P pulmonale can be diagnosed when tall P waves (≥ 2.5 mm) are present in leads II, III, and aVF, and low upright P waves in lead I. Presumably, pulmonary embolism causes dilatation of the right atrium, which brings the wall of the atrium closer to the chest wall, thereby increasing the voltage recorded by the lead electrodes. In addition, right atrial dilatation also causes the mean instantaneous P vectors to rotate inferiorly to a more vertical position.

TRANSIENT COMPLETE OR INCOMPLETE RIGHT BUNDLE BRANCH BLOCK—Right bundle branch block occurring with pulmonary embolism is probably due to injury sustained by the long trunk of the right bundle branch secondary to right ventricular dilatation. It

right-axis deviation, the instantaneous QRS vectors may come to lie in the right upper quadrant of the frontal reference frame, so that an $S_r-S_{II}-S_{III}$ pattern may appear in the standard bipolar limb leads while the remaining extremity leads record rS deflections, with the exception of lead aVR, which registers a Qr or QR deflection.

Pattern of "marked clockwise rotation" in the precordial leads—One of the commonest electrocardiographic findings in pulmonary embolism or acute cor pulmonale consists of a shift of the QRS transition point or lead (the lead registering an equiphasic RS deflection) farther to the left, sometimes beyond lead V_6 . This is simply an expression of the fact that the mean QRS vector in the horizontal plane is rotated

counterclockwise. A series of cases of pulmonary embolism and have reported their vectorcardiographic observations, by and large the general experience in the vectorcardiographic diagnosis of this condition is still somewhat limited. The reasons for this dearth of reported studies are multiple—for example, the abrupt onset and evanescence of the clinical manifestations of acute cor pulmonale due to pulmonary embolism,

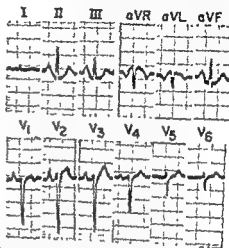


Fig. 139.—Electrocardiogram in acute pulmonary embolism, recorded shortly after onset of the embolism. The findings are characteristic.

Qr, qr, or QS deflection. The S-T segments in the right precordial leads may be either depressed or elevated, while the T waves are usually inverted in these leads. Grishman attributes the T wave inversion and the apparent subepicardial injury pattern in the right precordial leads to rotation of the T sE loop and the subendocardial injury vector along with the QRS sE loop. Consequently, inverted T waves and elevated S-T segments are projected on right precordial leads and on leads III and aVF, and depressed S-T segments and upright T waves are projected on left precordial leads. On the other hand, Sodi-Pallares attributes the S-T segment elevation and T wave inversion in right precordial leads to the effects of injured areas which may be present either on the right septal surface or on the free wall of the right ventricle. As a general rule, the S-T segment and T wave changes accompanying pulmonary embolism last only a few days, although they may be of even briefer duration, while the rotational QRS changes can persist for 1-3 weeks after the acute episode (Figs 137-139).

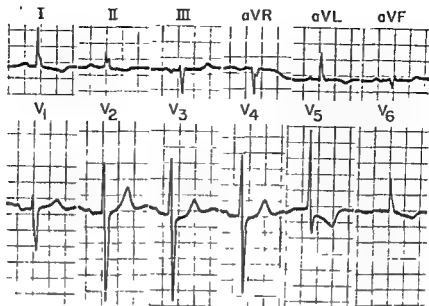
Although a few investigators have managed to ac-

the critical state of the patient, and the relative immobility of the cumbersome types of vector-

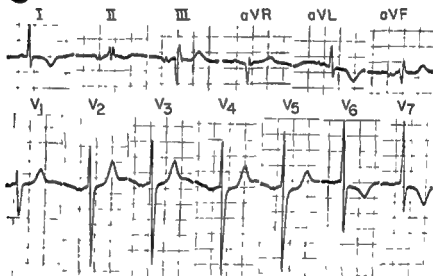
cardiographically 13 cases of pulmonary embolism. In some instances vectorcardiograms were available which had been recorded before the onset of the pulmonary embolism. The major vectorcardiographic findings, according to these investigators, were.

Fig 138.—Serial electrocardiograms recorded before and after pulmonary embolism. The changes in the QRS pattern and the S-T segment and T wave are characteristic.

A Before Pulmonary Embolism



B Shortly After Onset of Pulmonary Embolism



C Twenty-Four Hours After Onset of Pulmonary Embolism

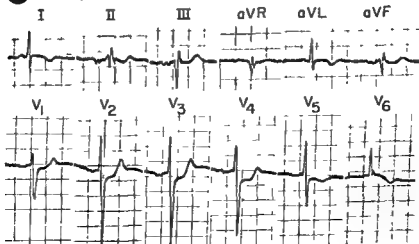


Fig. 138 — (Legend on facing page.)

Left Bundle Branch Block

GENERAL CONSIDERATIONS

MOST OF WHAT is known about the manner in which the septum and ventricles undergo activation in bundle branch block has been derived from studies of induced block in the dog heart, but how closely experimental block in the dog heart duplicates clinical block in the human heart is at present a moot question. In fact, there is growing suspicion that significant differences exist between experimental and clinical bundle branch block, but more will be said of this later during the discussion of right bundle branch block (Chapter 17). Even if one assumes the essential similarity of the clinical and experimental lesions, bundle branch block still retains most of its controversial aspects, since the observations made in experimental block have been interpreted differently by different authorities. For these reasons...

...activation block will be deferred, for individual discussion, along with discussion of other related aspects of each type of bundle branch block.

The normal intraventricular conducting pathways—in the normal heart, the bundle of His bifurcates

...in the septum, and branches profusely thereafter. In the dog heart, almost the entire thickness of the septal muscle mass is contributed by the left ventricle and normally is activated via the left bundle branch and its ramifications. By way of contrast, the right bundle branch is a long, slender, nonbranching stalk through most of its course down the right septal surface. Its first ramifications appear in the vicinity of the base of the right anterior papillary muscle—that is, on the endocardial surface of the anterior wall of the right ventricle near the interventricular septum. From this region, excitation spreads upward over the

right septal surface to activate the underlying thin layer of muscle in an apex-to-base direction.

The significance of the different anatomy and distribution of the two bundle branches lies in the fact that the slender cross-sectional dimension of the right bundle branch and its longer course prior to branching render it far more vulnerable to small focal, fibrotic, degenerative, or inflammatory lesions than the freely branching left bundle branch. This being the case, the incidence of right bundle branch block would exceed that of left bundle branch block were it not for the fact that the pathologic processes most likely to produce bundle branch block involve the left ventricle more often than the right. Thus, one predisposing factor tends to counterbalance the other, and, on the average, the electrocardiographic patterns of left bundle branch block and right bundle branch block are noted clinically with about equal frequency.

In clinical electrocardiography...

...intervals of less than 0.12 but greater than 0.08 second, incomplete. According to the terminology to be used in this text, the category of complete block will be referred to as "left or right bundle branch block," omitting the term "complete." Incomplete left bundle branch block will always be so designated, and is discussed separately later in this chapter.

Diffuse intraventricular block will not be discussed in any great detail in this text, since it is sufficient to state that this type of conduction defect is characterized by widening of the QRS complexes, often with relatively little change in their configuration. Diffuse intraventricular block can occur spontaneously but is more often a manifestation of severe myocardial damage, or of excess of quinidine, of pronestyl effect, or of hyperkalemia.

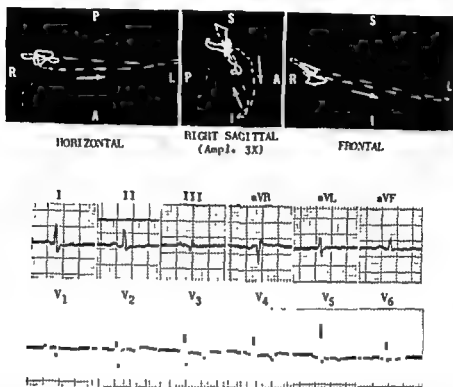


Fig. 140.—Electrocardiogram and vectorcardiogram recorded about 24 hours after clinical onset of acute pulmonary embolism. The electrocardiogram displays an S_1 - Q_m pattern of minor prominence and inverted T waves in leads V_1 through V_4 with flat or diphasic T waves in leads I and V_6 . These findings are not sufficient to justify an unequivocal diagnosis of acute pulmonary embolism. These features are the anterior displacement of the QRS sE vector to the right, posteriorly, and superiorly. These vectors are described by Karlen and Wolff in a number of cases of acute pulmonary embolism.

1. There is transient clockwise rotation of the QRS sE loop around its longitudinal axis. This is evidenced in the vectorcardiogram by the more superior and less rightward orientation of the initial vectors of the QRS sE loop. Occasionally the initial vectors are directed to the left.
2. The sagittal QRS loop is sometimes inscribed in a counterclockwise direction, although clockwise inscription occurs more often in pulmonary embolism.
3. The frontal QRS loop usually has a clockwise direction of inscription. The terminal instantaneous vectors of the frontal QRS loop are almost invariably oriented to the right.
4. When the initial deflection of the QRS sE loop is directed superiorly in pulmonary embolism, the magnitude and duration of the instantaneous vectors of this deflection are greater than normal but less than in diaphragmatic myocardial infarction.
5. The terminal instantaneous vectors of the QRS sE loop are almost always situated to the right and

posteriorly and, as often as not, lie superiorly. Moreover, the magnitude of these vectors also exceeds normal limits (Fig. 140).

We have obtained vectorcardiograms in a few cases of pulmonary embolism, but our experience is too limited to permit any conclusions concerning either the diagnostic findings or the usefulness of the vectorcardiogram in this condition. On the whole, the vectorcardiographic abnormalities in our cases were similar to those described by Karlen and Wolff. The most consistent vectorcardiographic finding in our cases was the presence of a terminal deflection of the QRS sE loop to the right, posteriorly, and superiorly, much like that observed in the types A and B loop patterns in mitral stenosis and chronic cor pulmonale (previously described). However, the terminal mean instantaneous QRS spatial vectors in our cases of acute cor pulmonale never attained a magnitude comparable to that of the terminal vectors in the types A and B QRS sE loop patterns.

left bundle branch block, and probably reflects the fact that both component vectors are exerting a significant effect on the direction of the resultant vector. As a consequence, the 0.01-second VA vector is situated at some point intermediate between the rightward and anteriorly directed right ventricular vector and the leftward and posteriorly directed septal vector, so that the VA vector generally is oriented slightly anteriorly and to the left. The components of the

plane and between $+10^\circ$ and -10° in the frontal plane. If one were to imagine these three vectors to be projected on the horizontal plane, they would be observed to develop in a clockwise direction.

Leads I and V_2 .—The major part of the upstroke of the R wave.

Leads aVF and V_1 .—The major part of the downstroke of the QS or rS deflection recorded in these leads.

0.08-SECOND VA VECTOR

The VA vector appearing at about 0.08 second after onset of the QRS interval is the largest instantaneous vector produced and is directed to the left and more superiorly and posteriorly than the other

Leads I and V_2 .—Beginning upstroke of a wide slurred or notched R wave.

Lead aVF.—Upstroke of a small R wave

Lead V_1 .—Small initial R wave. The peak of this R wave in lead V_1 coincides with the onset of the intrinsoid deflection and occurs at the normal time in left bundle branch block (normal, 0.015–0.035 second)

POSTERIOR, LEFTWARD, AND INFERIOR ORIENTATION.—This orientation of the initial VA vector is observed somewhat less frequently than that described above. Presumably, the leftward and posteriorly directed septal component vector dominates the electrical field of the heart from the very onset of the QRS interval. Whether the electrical predominance of the early leftward and posterior forces is due to their greater magnitude or to a delayed or slower development of the rightward and anterior forces of right ventricular activation is not known at present.

Leads I and V_2 .—Beginning upstroke of a wide slurred or notched R wave.

Lead aVF.—Upstroke of a small R wave

Lead V_1 .—Beginning downstroke of a broad deep QS deflection.

0.02-, 0.04-, AND 0.06-SECOND VA VECTORS

From about 0.02 to 0.06 second after onset of ventricular excitation, depolarization of the muscle mass of the septum continues in a right-to-left direction. Normally the septal musculature is activated so rapidly via the Purkinje fibers that the potentials generated are relatively negligible, however, in left bundle branch block, septal excitation probably occurs in an aberrant manner, so that the resulting forces have not only a different direction but also a greater magnitude. Thus, the 0.02-, 0.04-, and 0.06-second VA vectors appearing during this period increase in magnitude as they develop to the left, posteriorly, and superiorly. They tend to be located, on the average, between -30° and -80° in the horizontal

to fiber through the left ventricular myocardium along a broad activation front. The electrical forces produced are therefore of increased magnitude. As was pointed out in an earlier chapter, the Purkinje fibers penetrate deeply into the subendocardium, so that, normally, with the onset of ventricular excitation

... excitation wave spreads concentrically from each of these islands, with the result that activation of the inner muscle layers normally occurs in too many directions to give rise to measurable electrical forces. Once the islands of negativity merge to form a bounded wave front, measurable forces appear. Grant and Dodge speculate that, in left bundle branch block, left ventricular excitation may no longer begin as small islands of negativity but may begin as a wave front spreading from the right ventricle. This would account, at least in part, for the increased magnitude of the electrical forces in left bundle branch block, and therefore for the wide R waves recorded in leads I, aVL, and V_2 and the deep broad S waves registered in the right precordial leads.

2. There is reason to believe that in left bundle branch block in the human heart the posterobasal wall of the left ventricle is activated before the anterolateral wall. Thus, the thickest portion of the

... at the peak of the R wave or with the end of the slurred plateau-like peak of

MECHANISMS OF LEFT BUNDLE BRANCH BLOCK

The salient characteristic of left bundle branch block which differentiates it from other disturbances of intraventricular conduction is that septal and left ventricular activation, from onset to termination, is altered by the block. The manner in which excitation spreads through the septum and ventricles in left bundle branch block may be outlined as follows.

1. Since conduction down the left bundle branch is blocked at a high level in the conducting pathway, the excitation impulse first appears low on the right septal surface near the base of the anterior papillary muscle.
2. From this point, excitation spreads over the endocardial surface of the right ventricle and upward over the right septal surface.
3. As the activation wave moves transmurally through the apicolateral free wall of the right ventricle, the muscle mass of the septum undergoes activation in a right-to-left and apex-to-base direction. The excitation wave proceeds so slowly through the left septal muscle mass as to suggest that it spreads from muscle fiber to muscle fiber rather than via the specific conducting fibers of the Purkinje system.
4. The explanation for the QRS prolongation in left bundle branch block and the manner in which the wave of excitation spreads through the free wall of the left ventricle are the source of considerable controversy. There are perhaps three main schools of thought:
 - a) It is widely believed that the septum is the region of conduction delay, excitation spread-

ing either slowly over normal pathways or at a normal rate over abnormal and longer pathways. Once the excitation impulse reaches the left septal surface, it enters the left bundle branch below the block and is transmitted over normal pathways to the left ventricle.

- b) Rodríguez and Sodi-Pallares are in agreement with the above version with this exception, they believe that the main conduction delay in left bundle branch block is localized to a specific region of the septum, namely, the transition zone between regions of septum excited via the right branch and those excited via the left branch. Once the excitation impulse jumps this barrier and reaches the ramifications of the left bundle branch, it spreads over the left septal surface and through the left ventricle in a normal manner.
- c) The third school of thought, which seems to be gaining increasing support, holds that there is fiber-to-fiber transmyocardial spread of excitation not only through the septum but also through the left ventricle. Grant and Dodge, Kennamer and Prinzmetal, and Wener and his associates, among others, have produced evidence in support of this contention. The last-named investigators used esophageal and precordial leads to demonstrate that in clinical left bundle branch block the posterobasal wall of the left ventricle consistently undergoes activation from 0.01 to 0.08 second earlier than the anterolateral wall—just the reverse of the normal sequence.

THE INSTANTANEOUS VA VECTORS

The spread of activation through the interventricular septum and ventricles in left bundle branch block and the electrical forces produced can be presented in simplified manner in terms of the instantaneous VA vectors (see also Fig. 141).

0.01-SECOND VA VECTOR

In left bundle branch block, the 0.01-second VA vector may be considered the resultant of two component vectors. (a) a *septal vector*, directed to the left, posteriorly, and inferiorly, which represents the electrical forces produced by early activation of the septum in a right-to-left and apex-to-base direction, and (b) a *right ventricular vector*, directed anteriorly,

somewhat to the right and inferiorly, which represents the electrical forces generated during simultaneous activation of the apicoanterior wall of the right ventricle. Depending, in all probability, on the exact time sequence of excitation of the right septal surface and the apical right ventricular muscle, and on the relative magnitudes and directions of the component electrical forces arising in these two regions, the resultant 0.01-second VA vector may be oriented in either of two directions. (1) anterior, leftward, and inferior, or (2) posterior, leftward, and inferior.

ANTERIOR LEFTWARD, AND INFERIOR ORIENTATION.
—This is the more common of the two general directions which the 0.01-second VA vector may assume in

the R wave in leads V_4 and I. Because of the delayed onset of left ventricular excitation and the delayed appearance of the maximal instantaneous vector, onset of the intrascoid deflection in lead V_4 is likewise delayed to 0.08–0.10 second after the beginning of the QRS interval.

Leads aVF and V_1 .—The 0.08-second VA vector coincides with the nadir of the deep, wide S wave in these leads.

Precordial QRS transition.—Since the maximal instantaneous vector is oriented farther posteriorly than normal (and the maximal mean instantaneous QRS spatial vector corresponds roughly to the calculated mean QRS spatial vector), the transitional chest lead whose axis is perpendicular to the maximal vector is located farther to the left than in the normal precordial electrocardiogram. Thus, in left bundle branch block, leads V_1 through V_4 or V_5 usually register resultantly negative or downwardly directed QRS deflections, while lead V_6 records a broad R wave. Although the right precordial leads may show QS deflections in left bundle branch block, such deflections probably do not occur as often as previously thought. Grant and Dodge found that 45% of their patients with left bundle branch block had electrocardiograms showing initial R waves in leads V_1 through V_4 . The R waves were absent in lead V_1 in

only 35% of the electrocardiograms. In 15% the R waves were absent in leads V_1 and V_2 ; in only 5% were R waves absent in leads V_1 through V_3 , and in none of the electrocardiograms were R waves absent as far to the left as V_4 . This was in agreement with our observations in patients with left bundle branch block: 75% of the electrocardiograms showed initial R waves in all precordial leads, in the remaining 25% with QS deflections in lead V_1 , initial R waves were present in lead V_2 in about half of the cases. In our experience, QS deflections in lead aVF were noted relatively uncommonly.

0.10-SECOND VA VECTOR

This vector probably is related to activation of the anterolateral wall of the left ventricle and is therefore of smaller magnitude than the 0.08-second vector and is directed less posteriorly and superiorly.

Leads I and V_6 .—Downstroke of the broad R wave.

Leads aVF and V_1 .—Terminal limb of the S wave.

The late appearance of the 0.10-second and subsequent vectors because of delayed onset of left ventricular depolarization obviously leads to prolongation of the QRS interval, and so the QRS duration in left bundle branch block is 0.12 second or longer.

VENTRICULAR REPOLARIZATION

Shortly after the excitation impulse enters and begins to spread through the left ventricular myocardium, recovery commences in regions of the ventricles first activated, notably in the interventricular septum. (Repolarization potentials generated by the free wall of the right ventricle are negligible and may, for all

intents and purposes, be ignored.) Recovery starts first at the right septal surface, and then the repolarization wave spreads from right to left through the muscle mass of the septum. The septal repolarization forces thereby produced are directed to the right and anteriorly, just the reverse of the septal depolarization

Fig 141. — free wall is de-coded in an evidence has.



1. INITIAL ACTIVATION OF APICO-ANTERIOR RIGHT VENTRICULAR WALL
2. RIGHT-TO-LEFT SEPTAL ACTIVATION AND ACTIVATION OF RIGHT VENTRICULAR FREE WALL
3. COMPLETION OF SEPTAL AND RIGHT VENTRICULAR ACTIVATION
4. INITIAL ABERRANT ACTIVATION OF BASAL LEFT VENTRICULAR WALL
5. ACTIVATION OF POSTERIOR, LATERAL AND ANTERIOR LEFT VENTRICULAR WALL
6. COMPLETION OF ACTIVATION OF ANTERIOR WALL OF LEFT VENTRICLE

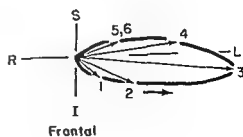
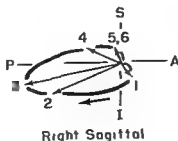
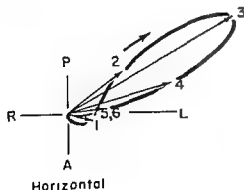
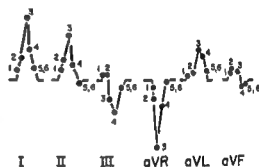
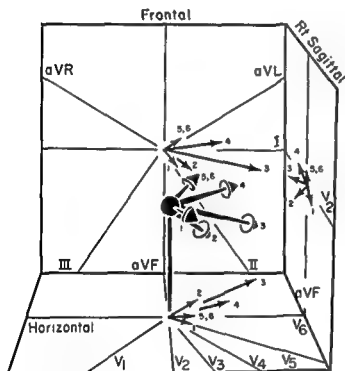


Fig. 141.—(Legend on facing page)

VECTOCARDIOGRAPHIC FINDINGS

QRS sE LOOP ABNORMALITIES

The following abnormal changes were noted in the vectorcardiogram (see also Fig. 142 and Table 17):

HORIZONTAL QRS LOOP.—In about one third of our cases of left bundle branch block, the horizontal QRS loop was written initially to the left and anteriorly, in an equal number of cases, the loop proceeded initially to the left and posteriorly, while in slightly less than a third of the cases the horizontal loop was inscribed anteriorly and slightly to the right. The rest of the horizontal QRS loop, whatever the direction of the initial deflection, was inscribed in a clockwise direction in the left and anterior

horizontal reference frame. In the afferent limb of the loop, or occasionally in its midportion, the time markings were closely spaced, indicating conduction delay. After its inscription the horizontal QRS loop did not return to its point of origin, instead, its junction with the T loop was displaced to the right and anteriorly, indicating a similarly directed ST vector.

Occasionally in left bundle branch block the horizontal QRS loop has a figure-of-eight configuration,

the distal loop of the "eight" usually being written in a clockwise direction. In loops of this contour, the initial and early vectors generally lie anteriorly and to the left.

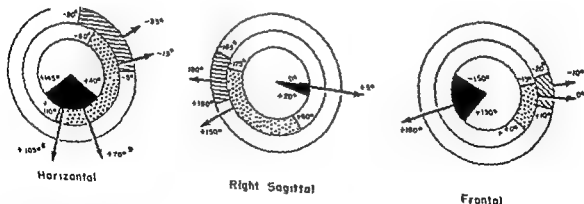
RIGHT SAGITTAL QRS LOOP.—The sagittal QRS loop is almost invariably written in a clockwise direction posteriorly and either slightly inferiorly or superiorly, its long axis ordinarily lying between $+170^\circ$ and -175° in the sagittal reference frame. The afferent limb, the midportion of the loop, or both are inscribed slowly, and the junction of the afferent limb with the T loop is displaced anteriorly and slightly inferiorly.

FRONTAL QRS LOOP.—The frontal QRS loop is usually written in a counterclockwise direction and situated within the -15° to 0° segment of the frontal reference frame. An S-T vector directed to the right and inferiorly is often present.

T sE LOOP

The spatial T loop is discordant to the QRS sE loop. Its general orientation is to the right, anteriorly, and either superiorly or inferiorly (Figs. 143-145).

Fig. 142—Extreme range of variation and an abnormal loop.



■ MAXIMAL MEAN INSTANTANEOUS QRS VECTOR OF AN ANTERIOR AND/OR RIGHTWARD INITIAL DEFLECTION OF QRS sE LOOP
 ▨ 2 SEC. MEAN INSTANTANEOUS QRS VECTOR OF QRS sE LOOPS WITHOUT ANTERIOR INITIAL DEFLECTION
 ▤ MAXIMAL MEAN INSTANTANEOUS QRS VECTOR

forces in left bundle branch block. Since the instantaneous T vectors make their appearance before the completion of left ventricular activation, the terminal limb of the QRS deflection does not stop at the base line but continues to rise or descend, as the case may be, until it merges with an elevated or depressed S-T segment. The S-T segment in a given lead is displaced in the direction of the abnormal T wave, since both abnormalities are manifestations of the same process, namely, altered ventricular repolarization. In effect, it is as if an S-T vector exists which is oriented parallel to the instantaneous T vectors.

Since the abnormal angular divergence of the instantaneous VA (or QRS) and T vectors in left bundle branch block is due fundamentally to the abnormal spread of excitation through the ventricle, the T waves and S-T segments of the electrocardiogram in left bundle branch block display *secondary changes* but the ventricular gradient remains normal. Other mechanisms (related to the gradient concept) which may contribute to the genesis of the secondary T wave

changes in left bundle branch block are as follows.

1. According to the ventricular gradient concept, $\bar{A} \text{ QRS} + \bar{A} \text{ T} = \bar{C}$, or $\bar{A} \text{ T} = \bar{C} - \bar{A} \text{ QRS}$. If the mean ventricular gradient vector \bar{C} remains normal, then $\bar{A} \text{ T} = -\bar{A} \text{ QRS}$.

In other words, every change in the area of the QRS complex causes a corresponding secondary change in the area of the ST-T complex which is equal in magnitude but opposite in direction to the QRS change. Therefore, the greater the positive area of the QRS complex in left precordial leads, the more marked will be the S-T segment depression and T wave inversion. Similarly, the greater the negative area of the QRS complexes in right precordial leads, the more prominent the S-T segment elevation and the taller the T waves.

2. If, as some authorities believe, in left bundle branch block there is aberrant spread of excitation through the left ventricular wall, then the direction of repolarization may be reversed in the left ventricle as well as in the septum.

ELECTROCARDIOGRAPHIC FINDINGS

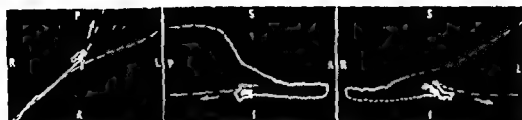
The electrocardiographic findings in left bundle branch block are listed below.

EXTREMITY LEADS

1. QRS interval prolongation to 0.12 second or longer
2. Leads I and aVL. Absent Q waves and slurred broad R waves.
3. Leads II, III, and aVF. rS deflections with deep, wide S waves (occasionally QS deflections).
4. Left-axis deviation of $\bar{A} \text{ QRS}$, the orientation of the latter ranging from -60° to 0° in the frontal reference frame
5. S-T vector and sA T are usually almost 180° discordant to sA QRS. Therefore:
 - a) Leads registering upright R waves (I, aVL, and V_6) generally display depressed S-T segments and inverted T waves
 - b) Leads recording predominantly downwardly directed ventricular deflections (II, III, aVF, and V_1 through V_4) ordinarily show upright T waves with a tendency to superior displacement of junction J of the S-T segment, particularly in right precordial leads.
 - c) The degree of S-T segment deviation and the size of the T waves vary directly with the area enclosed by the preceding QRS deflection.

PRECORDIAL LEADS

1. Delayed onset of the intrinsicoid deflection in lead V_4 (to 0.05 second or sometimes 0.08-0.10 second); normal intrinsicoid deflection time in lead V_1 .
2. Lead V_1 : Absent Q wave and slurred broad R wave
3. Leads V_1 and V_2 : rS deflections with deep, wide S waves (occasionally QS deflections)
Leads V_3 and V_4 : RS or RS (rarely QS) deflections. Usually there is a progressively increasing R/S amplitude ratio from right to left across the left precordium in left bundle branch block, but sometimes the R waves in the midprecordial leads may be relatively smaller than those in the right precordial leads
4. Posterior rotation of $\bar{A} \text{ QRS}$, the orientation of the latter tending to range from -60° to -30° in the horizontal reference frame



HORIZONTAL
(Ampl. 3X)

RIGHT SAGITTAL
(Ampl. 3X)

FRONTAL
(Ampl. 3X)



HORIZONTAL



RIGHT SAGITTAL



FRONTAL

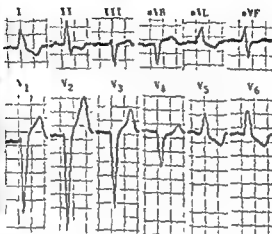


Fig 143 - Electrocardiogram
The standard

TABLE 17—VECTORCARDIOGRAPHIC FINDINGS IN LEFT BUNDLE BRANCH BLOCK

	HORIZONTAL		RIGHT SAGITTAL		FRONTAL	
	Extreme Range	Average	Extreme Range	Average	Extreme Range	Average
Orientation of the maximal mean instantaneous QRS vector	-60° to +110°	-15°	-60° to -30°		-15° to +40°	0°
Orientation of mean 0.02-second instantaneous QRS vector	-80° to -5°	-33°	-50° to -20°		-20° to +10°	-20° to 0°
Orientation of maximal vector of an anterior and/or rightward initial deflection of the QRS sE loop (when present)	+40° to +145°	+105° +70°†	+80° to +100°		+130° to -150°	+160°
Direction of inscription of:						
a) Initial deflection of QRS sE loop (if present)	1 Counterclockwise if initial deflection is directed to the left 2 Clockwise if initial deflection is directed to the right		Usually clockwise		Usually counterclockwise	
b) Effluent and afferent limbs of QRS sE loop						
Direction of S-T vector	Right, anterior		Anterior, inferior		Right, inferior	
Direction of initial inscription of QRS sE loop in horizontal projection	Anterior, leftward, 35%† Anterior, rightward, 30%† Posterior, leftward, 35%†				Counterclockwise	
Time of onset of maximal vector of horizontal QRS loop	Extreme Range 0 015-0 10 second	Average 0 065 second	Extreme Range 0 05-0 08 second			
Orientation of T sE loop	Usually approximately 180° discordant to the long axis or maximal mean vector of the QRS sE loop					

* Average orientation of rightward and anterior initial deflections of QRS sE loops in left bundle branch block.

† Average orientation of leftward and anterior initial deflections of QRS sE loops in left bundle branch block.

‡ The percentage of vectorcardiograms showing left bundle branch block in which the initial deflection of the QRS sE loop was as cited.

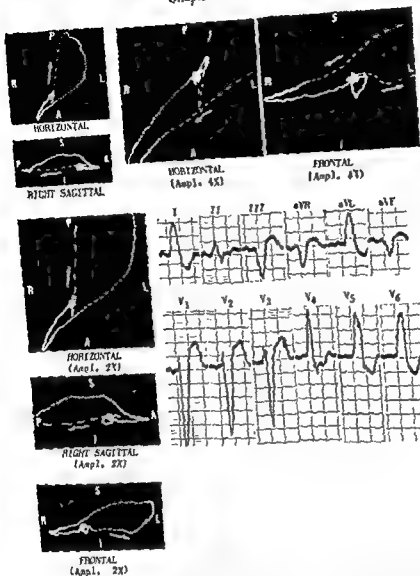


Fig 145—Electrocardiographic and vectorcardiographic patterns of left bundle branch block. Note, in the vectorcardiogram, the anterior, counterclockwise-inscribed initial deflection of the horizontal QRS loop. This deflection produces the relatively tall R waves in leads V_1 and V_2 of the electrocardiogram.

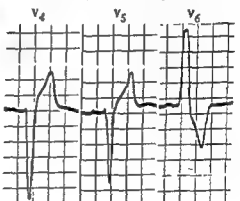
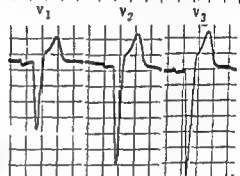
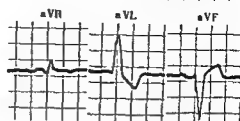
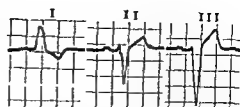
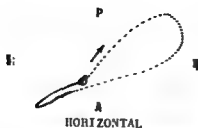
INCOMPLETE LEFT BUNDLE BRANCH BLOCK

Electrocardiographic Findings

It will be recalled that the principal point of distinction (arbitrary though it may be) which has been made in the past between complete and incomplete bundle branch block is that the QRS duration is 0.12 second or more in complete block and less than 0.12 second in incomplete block. Although there is some variation in the electrocardiographic criteria listed by different investigators for the diagnosis of incomplete

left bundle branch block, on the whole Barker's criteria can be considered representative. The features which Barker regards as suggestive of incomplete left bundle branch block are as follows:

- 1 The QRS interval is less than 0.12 second and at least 0.10 second in duration
- 2 The QRS complexes do not usually show high voltage.
- 3 There are no Q waves in leads V_4 and V_6



sis of left ventricular hypertrophy cannot be made in the presence of left bundle branch block. The increased QRS voltages are not necessarily related to the thickness of the left ventricular wall but may reflect aberrant spread of activation through the left ventricle.

uch the same
n, the diagno-
the increased

- 4 There is slurring or notching of the QRS complexes such as is seen in complete left bundle branch block.

Sodi-Pallares and his associates have extensively studied incomplete left bundle branch block produced experimentally in the dog heart, and from these investigations they have formulated a series of findings

which has already been discussed. The electrocardiographic characteristics of first- and second-degree (incomplete) left bundle branch block, as described by Sodi-Pallares and his co-workers, are as follows:

First-degree (incomplete) left bundle branch block. — This degree of block has the following characteristics (see also Fig 146)

- 1 Initial slurring of the R wave in leads V_3 , V_6 , and/or lead I, generally associated with absence of Q waves or with diminutive Q waves in these leads.
- 2 QRS duration ranging from 0.07 to 0.12 second, with the greater majority of cases having QRS in-

3

SECOND CASE

Second-degree (incomplete) left bundle branch block — Characterized as follows

1 Q_{II} - - -

- 2 QRS duration, from 0.12 to 0.15 second

In first-degree (incomplete) left bundle branch block, Sodi-Pallares and his associates postulate that the functional capacity of the left bundle branch is only slightly affected and that the excitation impulse is conducted down the left branch but at a slower rate than normally. The normal time lag of right septal activation after onset of excitation on the left septal surface tends, therefore, to be abolished in incomplete left bundle branch block, with the result

that the initial forces due to left-to-right septal depolarization are opposed and, in part at least, neutralized. This circumstance is responsible for the absence or decreased size of the Q wave in leads I and V_6 and the slurring of the early upstroke of the R wave in these leads. In second-degree (incomplete) left bundle branch block, Sodi-Pallares interprets the experimental findings as indicating that the left bundle branch is still functioning but at a very slow rate of conduction. Consequently, while the left branch activates some of the muscle mass of the left septum, the remainder receives the excitation impulse transiently from the right bundle branch.

Vectorcardiographic Findings

QRS sE LOOP ABNORMALITIES

The vectorcardiographic findings in incomplete left bundle branch block have not, as yet, been described in any great detail. According to Sodi-Pallares, in first-degree (incomplete) left bundle branch block the QRS sE loop in the horizontal projection is inscribed in the normal counterclockwise direction but with some delay in early portions of the loop, while in second-degree (incomplete) left bundle branch block the QRS sE loop in the horizontal projection can be inscribed in either a counterclockwise or a clockwise direction. From the brief descriptions of other investigators, it would seem that the vectorcardiographic findings in incomplete left bundle branch block resemble those in complete left bundle branch block except for the duration of the QRS sE loop.

The authors of this text studied the vectorcardiograms of a relatively small group of patients whose electrocardiograms provided the basis for selection. All of the following requirements were satisfied by the electrocardiograms of the cases selected:

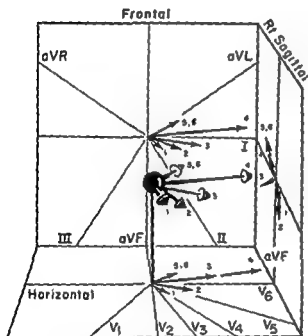
- 1 The R waves in leads I and V_6 showed no evidence of anterior infarction.
- 2
- 3

ing muscle, the apical portion of the

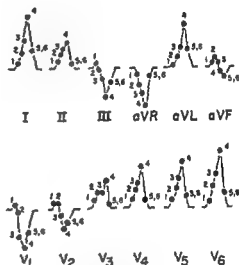


A Sequence of Septal-Ventricular Activation in Incomplete Left Bundle Branch Block

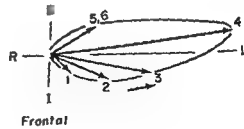
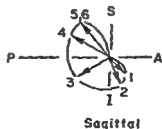
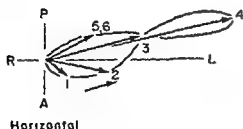
1. INITIAL EXCITATION NEAR BASE OF RIGHT ANTERIOR PAPILLARY MUSCLE VIA RIGHT BUNDLE BRANCH (RBB)
2. EXCITATION OF APICO-ANTERIOR VENTRICULAR FREE WALL AND PREDOMINANT RIGHT-TO-LEFT SEPTAL EXCITATION VIA RIGHT BUNDLE BRANCH
3. EXCITATION OF SEPTUM IN RIGHT-TO-LEFT DIRECTION AND APICO-ANTERIOR WALL ACTIVATION VIA BOTH BUNDLE BRANCHES
4. ACTIVATION OF ANTEROLATERAL LEFT VENTRICULAR WALL AND RIGHT VENTRICULAR WALL
5. ACTIVATION OF POSTEROLATERAL WALL OF LEFT VENTRICLE
6. ACTIVATION OF POSTEROBASAL LEFT VENTRICULAR WALL



B Instantaneous VA Vectors in Incomplete Left Bundle Branch Block



C QRS Deflections Projected On the Scalar Leads



D Planar QRS Loops in Incomplete Left Bundle Branch Block

4. There is slurring or notching of the QRS complex such as is seen in complete left bundle branch block.

Sodi-Pallares and his associates have extensively studied incomplete left bundle branch block produced experimentally in the dog heart, and from these investigations they have formulated a classification of left bundle branch block into three degrees, the third degree being complete left bundle branch block, which has already been discussed. The electrocardiographic characteristics of first- and second-degree (incomplete) left bundle branch block, as described by Sodi-Pallares and his co-workers, are as follows:

First-degree (incomplete) left bundle branch block.

—This degree of block has the following characteristics (see also Fig. 148):

1. Initial slurring of the R wave in leads V_3 , V_6 , and/or lead I, generally associated with absence of Q waves or with diminutive Q waves in these leads
2. QRS duration ranging from 0.07 to 0.12 second, with the greater majority of cases having QRS intervals between 0.08 and 0.11 second
3. Onset of intrinsicoid deflection in lead V_6 later than 0.045 second after start of QRS interval in most cases.

Second degree (incomplete) left bundle branch block—Characterized as follows.

1. Slurring involves not only the initial portion of the R wave but also the ascending limb of the R wave, and occasionally the descending limb.
2. QRS duration, from 0.12 to 0.15 second

In first-degree (incomplete) left bundle branch block, Sodi-Pallares and his associates postulate that the functional capacity of the left bundle branch is

activation after onset of excitation on the left septal surface tends, therefore, to be abolished in incomplete left bundle branch block, with the result

that the initial forces due to left-to-right septal depolarization are opposed and, in part at least, neutralized. This circumstance is responsible for the absence or decreased size of the Q wave in leads I and V_6 and the slurring of the early upstroke of the R wave in these leads. In second-degree (incomplete) left bundle branch block, Sodi-Pallares interprets the experimental findings as indicating that the left bundle branch is still functioning but at a very slow rate of conduction. Consequently, while the left branch activates some of the muscle mass of the left septum, the remainder receives the excitation impulse transseptally from the right bundle branch.

Vectorcardiographic Findings

QRS sE LOOP ABNORMALITIES

The vectorcardiographic findings in incomplete left bundle branch block have not, as yet, been described in any great detail. According to Sodi-Pallares, in first-degree (incomplete) left bundle branch block the QRS sE loop in the horizontal projection is inscribed in the normal counterclockwise direction but with some delay in early portions of the loop, while in second-degree (incomplete) left bundle branch block the QRS sE loop in the horizontal projection can be inscribed in either a counterclockwise or a clockwise direction. From the brief descriptions of other investigators, it would seem that the vectorcardiographic findings in incomplete left bundle branch block resemble those in complete left bundle branch block except for the duration of the QRS sE loop.

The authors of this text studied the vectorcardiograms of a relatively small group of patients whose electrocardiograms provided the basis for selection. All of the following requirements were satisfied by the electrocardiograms of the cases selected.

1. The R waves in leads I and V_6 showed slurred or notched upstrokes, while Q waves were absent
2. The QRS duration was less than 0.12 second.
3. The precordial leads showed no definite evidence of anterior infarction.

ing muscle, the apical portion of the interventricular septum, and the anterior free wall of the right ventricle are undergoing activation. The resultant of the electrical forces arising in the ascending limb of the left bundle branch and the anterior wall of the left

The requirements listed above contain some of the criteria both of Barker and of Sodi-Pallares for the diagnosis of incomplete left bundle branch block. The additional requirements were intended to exclude, insofar as possible, anteroseptal infarction, which may mimic incomplete left bundle branch block. The indication of left ventricular hypertrophy in the electrocardiogram was not considered a basis for excluding a case from the study series, since this condition seemed to be associated so frequently, in the electrocardiogram, with the features of incomplete left bundle branch block that there seemed to be some relationship between these two entities.

There was found to be surprising consistency in

the vectorcardiographic findings in our small group of patients, the salient abnormalities being as follows:

HORIZONTAL QRS LOOP.—The long axis of the QRS sE loop in the horizontal projection usually is situated between the -45° and -15° axes of the horizontal reference frame. The loop is written initially to the left and anteriorly. In about half of the vectorcardiograms showing incomplete left bundle branch block, the initial and early segments of the loop are inscribed somewhat slowly. The loop then is written to the left and posteriorly, in the form of a figure-of-eight, the proximal loop being counterclockwise inscribed. Occasionally there is conduction delay in the very terminal portion of the loop.

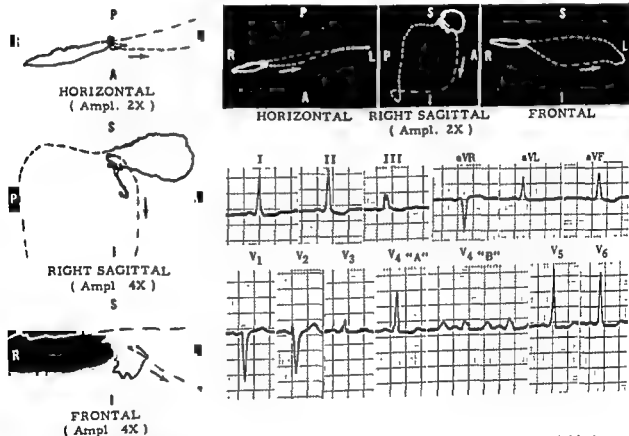


Fig. 147.—Electrocardiographic and vectorcardiographic patterns of incomplete left bundle branch block. The diagnostic abnormalities in the elec

Fig. 148.—Electrocardiographic and vectorcardiographic patterns of incomplete left bundle branch block. The QRS duration in the electrocardiogram is 0.12 second, but the configuration of the QRS deflections is more in keeping with incomplete than with complete left bundle branch block. The slurring of the S waves in leads I and aVL occurs on their upstrokes rather than at their summits, and terminal S waves are present in leads V_1 and V_2 . The QRS sE loop of the vectorcardiogram shows a left, posterior initial deflection with slowed inscription of this and the adjacent segment of the efferent limb of the loop. The horizontal QRS loop has a figure-of-eight configuration, and the frontal loop is situated superiorly and to the left.

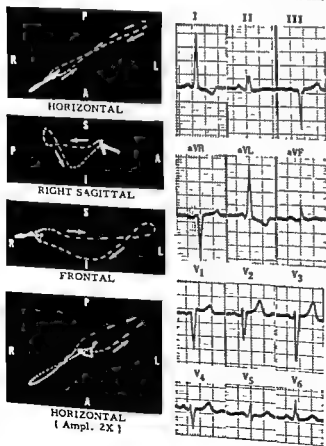
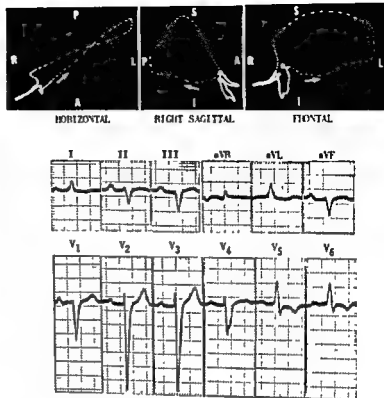


Fig. 149.—Electrocardiographic and vectorcardiographic patterns of incomplete left bundle branch block. In the vectorcardiogram, the counterclockwise inscription of the sagittal QRS loop and the clockwise inscription of the frontal loop are uncommon findings in incomplete left bundle branch block, the significance of which is not known.

RIGHT SAGITTAL QRS LOOP.—The sagittal loop is written posteriorly and slightly inferiorly or superiorly. The initial deflection of the loop is usually directed slightly anteriorly but sometimes posteriorly. In a small percentage of the vectorcardiograms, the sagittal loop is counterclockwise inscribed, although clockwise inscription is by far the more common finding. Conduction delay may be present in the early portion of the loop in some instances and in the afferent limb of the loop in others.

FRONTAL QRS LOOP.—The frontal QRS loop tends to lie almost horizontal and to the left. The direction of inscription varies, some loops being clockwise, and others counterclockwise, inscribed. By and large, counterclockwise inscription of the frontal loop is the usual finding.

VARIANT TYPE OF LEFT INTRAVENTRICULAR BLOCK

Vectorcardiographic Findings

A variant pattern, frequently encountered, which exhibits a high degree of consistency in its features, is the type described by Grishman and his associates. This pattern, they feel, is indicative of left ventricular hypertrophy with terminal conduction delay. As observed by us, this pattern was characterized in the vectorcardiogram by the following features

HORIZONTAL PROJECTION

QRS sE LOOP.—The horizontal QRS loop varied in orientation within the range of -75° to -30° (average orientation, -60°). There usually was an initial deflection of the loop to the right and anteriorly (occasionally to the left and anteriorly), and then the remainder of the loop was written in a counterclockwise direction to the left and farther posteriorly than normal. The returning or afferent limb of the loop invariably showed conduction delay and was often situated somewhat to the right. Frequently the QRS sE loop in the horizontal projection remained open, the S-T vector being directed to the right and anteriorly.

T sE LOOP.—The long axis of the horizontal T loop was almost invariably discordant to the long axis of the QRS loop. The average orientation of the T sE loop in the horizontal projection was along the $+95^{\circ}$ axis of the horizontal reference frame.

RIGHT SAGITTAL PROJECTION

QRS sE LOOP.—The sagittal loop was usually written in a clockwise direction anteriorly and inferiorly

S-T VECTOR

An S-T vector is observed frequently and is usually directed to the right, anteriorly, and superiorly or inferiorly.

T sE LOOP

The T sE loop is almost always discordant to the QRS sE loop and more or less parallel to the S-T vector (Figs. 147–149).

It should be stressed that the vectorcardiographic features ascribed above to left bundle branch block represent preliminary, tentative findings, the validity of which awaits further study.

and then posteriorly and superiorly. Again the afferent limb showed closely spaced dashes, indicating conduction delay. The orientation of the long axis of the sagittal QRS loop ranged between -170° and -120° (average orientation, -140°).

T sE LOOP.—The T loop was discordant to the QRS loop in this projection and was situated, on the average, along the $+30^{\circ}$ axis of the sagittal reference frame.

FRONTAL PROJECTION

QRS sE LOOP.—The major portion of the frontal QRS loop usually was located in the left upper quadrant, the long axis of the loop ranging between -75° and 0° (average orientation, -40°). The loop was usually written in a counterclockwise direction with the afferent limb showing conduction delay and frequently lying to the right of the midline.

T sE LOOP.—The T loop was discordant to the QRS loop, its average orientation being along the $+120^{\circ}$ axis of the frontal reference frame.

Electrocardiographic Findings

In cases with the vectorcardiographic variant pattern just described, the electrocardiogram typically showed the following findings

- 1 There is marked left-axis deviation of A QRS in the bipolar limb leads, the manifest electrical axis of QRS lying, on the average, along the -55° axis of the frontal reference frame.
- 2 The QRS duration varies between 0.11 and 0.15 second.

Fig. 150.—Electrocardiographic and vectorcardiographic findings in the variant type of left intraventricular block designated by Grishman and his associates as "left ventricular hypertrophy with terminal conduction delay."

The most characteristic feature of the electrocardiogram in this form of intraventricular block is the wide slurred terminal S wave in lead V₄. Additional findings usually observed are: left-axis deviation of A QRS, prolonged QRS interval, and secondary S-T segment and T wave changes.

The vectorcardiographic abnormalities are marked posterior, leftward, and superior rotation of the QRS sE loop, conduction delay involving all or only the terminal portion of the efferent limb of the QRS sE loop, and inscription of this part of the QRS sE loop to the right, posteriorly, and superiorly. The latter inscription is responsible for the terminal S wave in lead V₄. The direction of inscription of the QRS sE loop is normal in each projection. The initial deflection of the QRS sE loop in the above vectorcardiogram is to the left, but not infrequently in this form of left intraventricular block the initial deflection of the QRS sE loop can be written to the right and anteriorly.

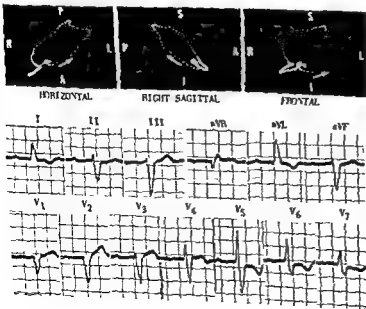
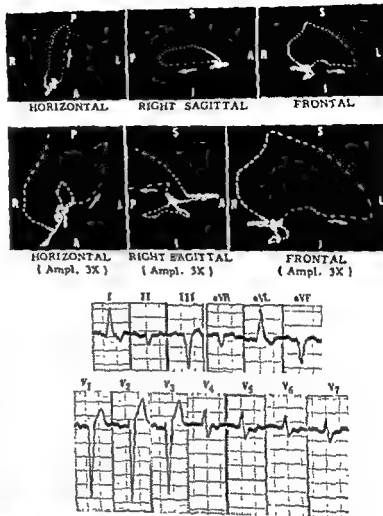


Fig. 151.—Electrocardiographic and vectorcardiographic patterns of the variant type of left intraventricular block ("left ventricular hypertrophy with terminal conduction delay").

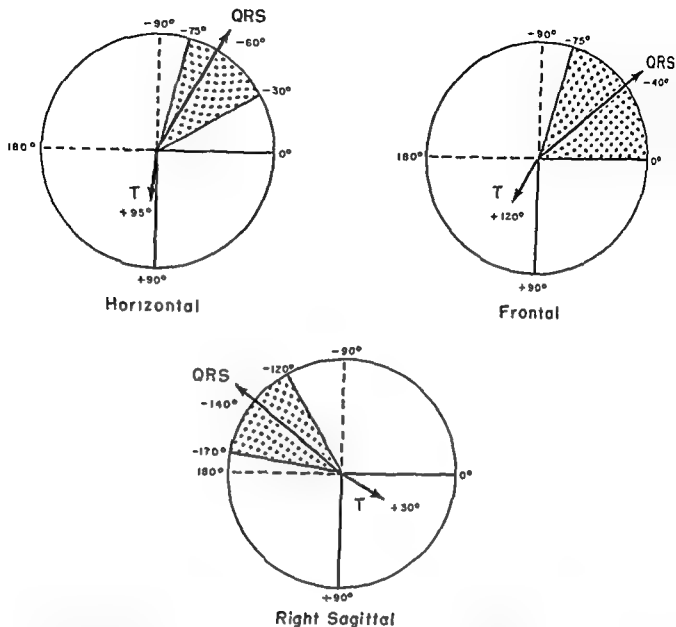


Fig 152.—Range of variation and average orientation of the maximal mean instantaneous QRS vector and maximal mean instantaneous T vector of the vectorcardiogram in the variant type of left intraventricular block ("left ventricular hypertrophy with terminal conduction delay").

- Because of the marked posterior rotation of the QRS sE loop, the precordial lead recording the transitional RS deflection is shifted far to the left, producing the electrocardiographic pattern of "marked clockwise rotation."

Thus, rS deflections are present in most leads to the right of lead V_6 , which usually shows an RS deflection, with the S wave being relatively wide. Occasionally rS deflections are recorded in leads as far to the left as V_4 , despite the fact that lead I displays a relatively taller R wave. Such cases as these in which leads I and V_6 register QRS deflections of differing configuration (qR or II in lead I, and RS in lead V_6) may be explained as follows.

Lead I—Typically in vectorcardiograms showing this type of intraventricular conduction disturbance, the frontal QRS loop is located almost entirely superiorly, and the terminal limb of the loop may even extend slightly to the right of the electrical null point. Despite this fact, lead I records terminal positivity, because its effective lead axis is slanted downward from left to right. Thus, as long as a vector is located superiorly, it may even be slightly to the right and still project on the positive half of the axis of derivation of lead I.

Lead V_6 —In contrast with lead I, lead V_6 has an effective axis which slants upward from left to right, and, thus being the case, superiorly oriented vectors.

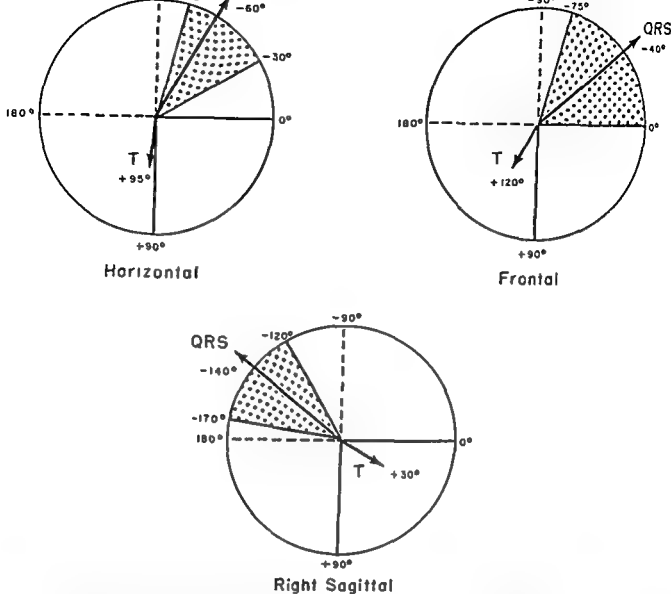


Fig. 152.—Range of variation and average orientation of the maximal mean instantaneous QRS vector and maximal mean instantaneous T vector of the vectorcardiogram in the variant type of left intraventricular block ("left ventricular hypertrophy with terminal conduction delay").

- Because of the marked posterior rotation of the QRS sE loop, the precordial lead recording the transitional RS deflection is shifted far to the left, producing the electrocardiographic pattern of "marked clockwise rotation."

Thus, rS deflections are present in most leads to the right of lead V_6 , which usually shows an RS deflection, with the S wave being relatively wide. Occasionally rS deflections are recorded in leads as far to the left as V_6 , despite the fact that lead I displays a relatively taller R wave. Such cases as these in which leads I and V_6 register QRS deflections of differing configuration (qR or R in lead I, and RS in lead V_6) may be explained as follows:

Lead I—Typically in vectorcardiograms showing this type of intraventricular conduction disturbance, the frontal QRS loop is located almost entirely superiorly, and the terminal limb of the loop may even extend slightly to the right of the electrical null point. Despite this fact, lead I records terminal positivity, because its effective lead axis is slanted downward from left to right. Thus, as long as a vector is located superiorly, it may even be slightly to the right and still project on the positive half of the axis of derivation of lead I.

Lead V_6 —In contrast with lead I, lead V_6 has an effective axis which slants upward from left to right, and, this being the case, superiorly oriented vectors,

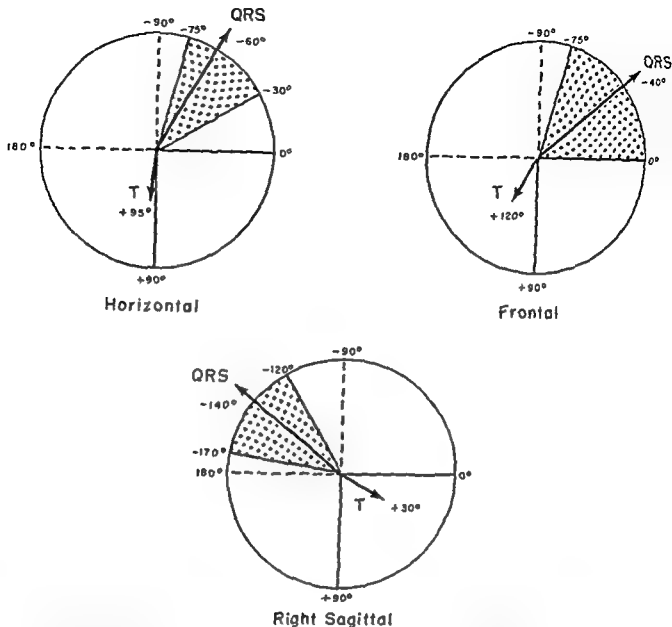


Fig. 152.—Range of variation and average orientation of the maximal mean instantaneous QRS vector and maximal mean instantaneous T vector of the vectorcardiogram in the variant type of left intraventricular block ("left ventricular hypertrophy with terminal conduction delay")

- 3 Because of the marked posterior rotation of the QRS sE loop, the precordial lead recording the transitional RS deflection is shifted far to the left, producing the electrocardiographic pattern of "marked clockwise rotation."

Thus, rS deflections are present in most leads to the right of lead V_6 , which usually shows an RS deflection, with the S wave being relatively wide. Occasionally rS deflections are recorded in leads as far to the left as V_6 , despite the fact that lead I displays a relatively taller R wave. Such cases as these in which leads I and V_6 register QRS deflections of differing configuration (qR or R in lead I, and RS in lead V_6) may be explained as follows

Lead I—Typically in vectorcardiograms showing this type of intraventricular conduction disturbance, the frontal QRS loop is located almost entirely superiorly, and the terminal limb of the loop may even extend slightly to the right of the electrical null point. Despite this fact, lead I records terminal positivity, because its effective lead axis is slanted downward from left to right. Thus, as long as a vector is located superiorly, it may even lie slightly to the right and still project on the positive half of the axis of derivation of lead I.

Lead V_6 —In contrast with lead I, lead V_6 has an effective axis which slants upward from left to right, and, this being the case, superiorly oriented vectors,

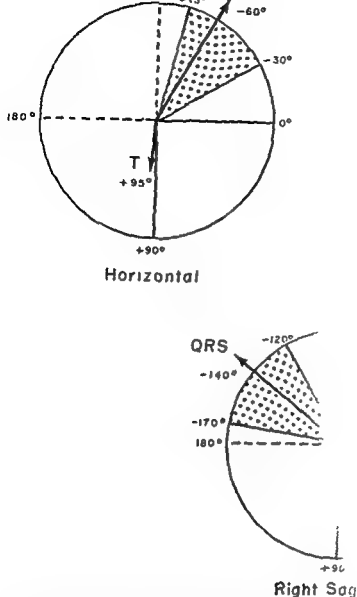


Fig. 152.—Range of variation and average orientation of the mean instantaneous T vector of the vectorcardiogram in the horizontal plane (hypertrophy with terminal conduction delay)

- 3 Because of the marked posterior rotation of the QRS sE loop, the precordial lead recording the transitional RS deflection is shifted far to the left, producing the electrocardiographic pattern of "marked clockwise rotation"

Thus, rS deflections are present in most leads to the right of lead V_6 , which usually shows an RS deflection, with the S wave being relatively wide. Occasionally rS deflections are recorded in leads as far to the left as V_6 , despite the fact that lead I displays a relatively taller R wave. Such cases as these in which leads I and V_6 register QRS deflections of differing configuration (qR or R in lead I, and RS in lead V_6) may be explained as follows

Lead I -

this type of the frontal QRS complex, and the leads extend slightly to the left. Despite this fact, because its effective lead axis is directed from left to right. Thus, as the vector is directed superiorly, it may even lie in the positive half of lead I.

Lead V_6 .—In contrast with lead I, the effective axis which slants upward from the left, and, this being the case, superiorly oriented.

Block located peripheral to the main right bundle branch.—The effects of a peripheral, or "focal," block of right intraventricular conduction on the ventricular activation process have been explained in two ways.

1. Segers and his associates and Vastesaeger propose that a localized region of the right ventricle receives the excitation impulse via the myocardial fibers rather than the Purkinje system. Activation of this region begins late in the QRS interval and proceeds slowly.

2. Dodge and Grant believe that in most (but not all) cases of right bundle branch block the site of the block is peripheral, and that not all of the right ventricle is affected by the block. These investigators postulate that "as soon as excitation reaches the site of the block it immediately spreads out into the surrounding regions of the right ventricle, as if the lesion were a 'leak' for excitation rather than a delaying or blocking mechanism. The remainder of the right ventricle is depolarized by abnormal routes and slower than normal velocities."

to 0.12 second or more, while the term *incomplete* is used when the QRS interval is 0.11 second or less. The authors of this text prefer not to attempt to describe incomplete right bundle branch block, for several reasons. (1) The electrocardiographic features of incomplete right bundle branch block can be duplicated by a wide variety of cardiac abnormalities, producing an equally wide range of QRS sE loop patterns in the vectorcardiogram. (2) We are not yet convinced that we can recognize incomplete right bundle branch block vectorcardiographically or electrocardiographically. In view of these facts, we will endeavor insofar as possible, to avoid use of the term *incomplete right bundle branch block*, since we consider it ambiguous. Thus, all instances of right bundle branch block which satisfy the criteria described later will be referred to as *right bundle branch block*, whether the QRS duration is 0.12 second or not (providing it is 0.10 second or longer).

In the past it was customarily stated in most textbooks that right bundle branch block could present in the electrocardiogram in either of two forms—namely, (1) the "Wilson," "common," or "atypical" form, or (2) the "classic," "uncommon," or "typical" form. The first of the right bundle branch block patterns cited (hereafter referred to either as the *common type of right bundle branch block*, or simply as *right bundle branch block*) is by far the more frequently observed pattern of the two; the *classic right bundle*

branch block pattern is encountered relatively rarely in clinical electrocardiography. Recently, several authorities in the field of vectorcardiography have expressed doubt as to whether the classic right bundle branch block actually represents right bundle branch block at all.

In fact, there is reason to believe that the pattern of classic right bundle branch block may be related etiologically to myocardial infarction involving several aspects of the left ventricle and occurring in company with an intraventricular conduction disturbance other than right bundle branch block. Thus, even aside from the rarity of the classic right bundle branch block pattern, the uncertainty regarding its mechanism and significance would seem to be reason enough for discussing it separately, apart from the bona fide right bundle branch block patterns to be described shortly. In its place, we have substituted what, for want of better terminology, will be referred to hereafter as the *right bundle branch block variant pattern*. While fundamentally the common and variant types of right bundle branch block exhibit essentially similar identifying features in the electrocardiogram and vectorcardiogram, nevertheless the two patterns differ sufficiently from each other, in their electrical effects as well as in their significance and the clinical circumstances in which they appear, to justify making a distinction between them. Moreover, as will be explained later, the level of the block in the right intraventricular conducting pathways in the right bundle branch block variant may not be the same as that in the common type of right bundle branch block.

The common type of right bundle branch block can be considered the electrocardiographic and vectorcardiographic prototype to which most of the pattern variations observed in clinical electrocardiography tend in general to conform. In the following pages, however, the instantaneous VA vectors and the electrocardiographic and vectorcardiographic findings in both the common and the variant types of right bundle branch block will be described in parallel. To avoid the confusion that might ensue from such a complicated presentation, the salient characteristics common to both types of right bundle branch block are herewith listed briefly.

1. Approximately the first half of ventricular activation is usually not altered significantly by the presence of right bundle branch block.

Thus: The first 0.06 second of the electrocardiographic QRS deflection and the vectorcardiographic QRS sE loop are relatively normal in appearance or show the same abnormalities as they

Block located peripheral to the main right bundle branch.—The effects of a peripheral, or "focal," block of right intraventricular conduction on the ventricular activation process have been explained in two ways:

1. Segers and his associates and Vastesaeger propose that a localized region of the right ventricle receives the excitation impulse via the myocardial fibers rather than the Purkinje system. Activation of this region begins late in the QRS interval and proceeds slowly.

2. Dodge and Grant believe that in most (but not all) cases of right bundle branch block the site of the block is peripheral, and that not all of the right ventricle is affected by the block. These investigators postulate that "as soon as excitation reaches the site of the block it immediately spreads out into the surrounding regions of the right ventricle, as if the lesion were a 'leak' for excitation rather than a delaying or blocking mechanism. The remainder of the right ventricle is depolarized by abnormal routes and slower than normal velocities."

In right bundle branch block, just as in left bundle branch block, the term *complete* is applied to right bundle branch block with QRS interval prolongation to 0.12 second or more, while the term *incomplete* is used when the QRS interval is 0.11 second or less. The authors of this text prefer not to attempt to describe incomplete right bundle branch block, for several reasons. (1) The electrocardiographic features of incomplete right bundle branch block can be duplicated by a wide variety of cardiac abnormalities, producing an equally wide range of QRS sE loop patterns in the vectorcardiogram. (2) We are not yet convinced that we can recognize incomplete right bundle branch block vectorcardiographically or electrocardiographically. In view of these facts, we will endeavor insofar as possible, to avoid use of the term *incomplete right bundle branch block*, since we consider it ambiguous. Thus, all instances of right bundle branch block which satisfy the criteria described later will be referred to as *right bundle branch block*, whether the QRS duration is 0.12 second or not (providing it is 0.10 second or longer).

In the past it was customarily stated in most textbooks that *right bundle branch block* could present in the electrocardiogram in either of two forms—namely, (1) the "Wilson," "common," or "atypical" form, or (2) the "classic," "uncommon," or "typical" form. The first of the right bundle branch block patterns cited (hereafter referred to either as the *common type of right bundle branch block*, or simply as *right bundle branch block*) is by far the more frequently observed pattern of the two, the *classic right bundle*

branch block pattern is encountered relatively rarely in clinical electrocardiography. Recently, several authorities in the field of vectorcardiography have expressed doubt as to whether the classic right bundle branch block actually represents right bundle branch block at all.

In fact, there is reason to believe that the pattern of classic right bundle branch block may be related etiologically to myocardial infarction involving several aspects of the left ventricle and occurring in company with an intraventricular conduction disturbance other than right bundle branch block. Thus, even aside from the rarity of the classic right bundle branch block pattern, the uncertainty regarding its mechanism and significance would seem to be reason enough for discussing it separately, apart from the bona fide right bundle branch block patterns to be described shortly. In its place, we have substituted what, for want of better terminology, will be referred to hereafter as the *right bundle branch block variant pattern*. While fundamentally the common and variant types of right bundle branch block exhibit essentially similar identifying features in the electrocardiogram and vectorcardiogram, nevertheless the two patterns differ sufficiently from each other, in their electrical effects as well as in their significance and the clinical circumstances in which they appear, to justify making a distinction between them. Moreover, as will be explained later, the level of the block in the right intraventricular conducting pathways in the right bundle branch block variant may not be the same as that in the common type of right bundle branch block.

The common type of right bundle branch block can be considered the electrocardiographic and vectorcardiographic prototype to which most of the pattern variations observed in clinical electrocardiography tend in general to conform. In the following pages, however, the instantaneous VA vectors and the electrocardiographic and vectorcardiographic findings in both the common and the variant types of right bundle branch block will be described in parallel. To avoid the confusion that might ensue from such a complicated presentation, the salient characteristics common to both types of right bundle branch block are herewith listed briefly

1. Approximately the first half of ventricular activation is usually not altered significantly by the presence of right bundle branch block

Thus, the first 0.06 second of the electrocardiographic QRS deflection and the vectorcardiographic QRS sE loop are relatively normal in appearance or show the same abnormalities as they

would were intraventricular conduction normal. During the second half of ventricular activation (i.e., during the terminal 0.04–0.06 second of the QRS interval), abnormal QRS forces directed to the right and anteriorly are produced for a period after the time when ventricular activation would normally have been completed.

Thus The...
nent, wide, a...
 V_{1a} and V_1 and a wide, abnormal...
on leads I and V_6 . The corresponding finding in the vectorcardiogram is the terminal finger-like appendage of the QRS sE loop, which is written slowly to the right and anteriorly.

THE INSTANTANEOUS VA VECTORS IN COMMON AND VARIANT TYPES OF RIGHT BUNDLE BRANCH BLOCK

The spread of activation through the interventricular septum and ventricles in right bundle branch block and the electrical forces produced can be presented in simplified manner in terms of the instantaneous VA vectors (see also Fig 154).

0.01-SECOND SEPTAL VA VECTOR

Since the left bundle branch is intact, the left septal surface and the greater thickness of the septal muscle mass are usually activated just as during normal intraventricular conduction. However, in occasional cases of right bundle branch block, the initial mean instantaneous spatial vectors of the vectorcardiographic QRS sE loop are found to be directed to the left and slightly anteriorly, or, less commonly, slightly posteriorly. While the abnormal orientation of the initial vectors in such cases can sometimes be attributed to antecedent myocardial infarction, this leaves unexplained the instances in which there is neither electrocardiographic nor clinical evidence of old or recent infarction. At present, information is too incomplete to permit anything other than speculation as to the mechanism responsible for the leftward

and slightly anterior or posterior initial vectors in some cases of right bundle branch block. One possible

this is not the usual finding in clinical right bundle

closely related to experimental block, in that the level of the block is relatively high in the right bundle branch. In our cases of right bundle branch block, an abnormal orientation of the initial QRS vectors occurred more frequently in association with the variant right bundle branch block pattern than with the common type of right bundle branch block. The 0.01 second instantaneous VA vector in right bundle branch block and the corresponding components of the QRS deflection recorded in leads I, V_6 , aVF, and V_1 are presented below.

Common Type of Right Bundle Branch Block		Variant Type of Right Bundle Branch Block	
	0.01-second VA vector directed to the right, anteriorly, and either inferiorly or superiorly		0.01-second VA vector directed to the right or, less frequently, to the left, inferiorly, and anteriorly
LEADS I AND V_6	Small Q waves		Small Q waves or, less often, beginning of upstroke of an initial R wave
LEAD aVF	Beginning of upstroke of an initial R wave or, less frequently, a small initial Q wave		Upstroke of small initial R wave
LEAD V_1	Upstroke of a small initial R wave		Upstroke of a small initial M wave, the beginning slurred upstroke of a large wide R wave or a small initial Q wave.

Block located peripheral to the main right bundle branch.—The effects of a peripheral, or "focal," block of right intraventricular conduction on the ventricular activation process have been explained in two ways:

1. Segers and his associates and Vastesaeger propose that a localized region of the right ventricle receives the excitation impulse via the myocardial fibers rather than the Purkinje system. Activation of this region begins late in the QRS interval and proceeds slowly.

2. Dodge and Grant believe that in most (but not all) cases of right bundle branch block the site of the block is peripheral, and that not all of the right ventricle is affected by the block. These investigators postulate that "as soon as excitation reaches the site of the block it immediately spreads out into the surrounding regions of the right ventricle, as if the lesion were a 'leak' for excitation rather than a delaying or blocking mechanism. The remainder of the right ventricle is depolarized by abnormal routes and slower than normal velocities."

In right bundle branch block, just as in left bundle branch block, the term *complete* is applied to right bundle branch block with QRS interval prolongation to 0.12 second or more, while the term *incomplete* is used when the QRS interval is 0.11 second or less. The authors of this text prefer not to attempt to describe incomplete right bundle branch block, for several reasons. (1) The electrocardiographic features of incomplete right bundle branch block can be duplicated by a wide variety of cardiac abnormalities, producing an equally wide range of QRS sE loop patterns in the vectorcardiogram. (2) We are not yet convinced that we can recognize incomplete right bundle branch block vectorcardiographically or electrocardiographically. In view of these facts, we will endeavor insofar as possible, to avoid use of the term *incomplete right bundle branch block*, since we consider it ambiguous. Thus, all instances of right bundle branch block which satisfy the criteria described later will be referred to as *right bundle branch block*, whether the QRS duration is 0.12 second or not (providing it is 0.10 second or longer).

In the past it was customarily stated in most textbooks that right bundle branch block could present in the electrocardiogram in either of two forms—namely, (1) the "Wilson," "common," or "atypical" form, or (2) the "classic," "uncommon," or "typical" form. The first of the right bundle branch block patterns cited (hereafter referred to either as the *common type of right bundle branch block*, or simply as *right bundle branch block*) is by far the more frequently observed pattern of the two, the *classic right bundle*

branch block pattern is encountered relatively rarely in clinical electrocardiography. Recently, several authorities in the field of vectorcardiography have expressed doubt as to whether the classic right bundle branch block actually represents right bundle branch block at all.

In fact, there is reason to believe that the pattern of classic right bundle branch block may be related etiologically to myocardial infarction involving several aspects of the left ventricle and occurring in company with an intraventricular conduction disturbance other than right bundle branch block. Thus, even aside from the rarity of the classic right bundle branch block pattern, the uncertainty regarding its mechanism and significance would seem to be reason enough for discussing it separately, apart from the bona fide right bundle branch block patterns to be described shortly. In its place, we have substituted what, for want of better terminology, will be referred to hereafter as the *right bundle branch block variant pattern*. While fundamentally the common and variant types of right bundle branch block exhibit essentially similar identifying features in the electrocardiogram and vectorcardiogram, nevertheless the two patterns differ sufficiently from each other, in their electrical effects as well as in their significance and the clinical circumstances in which they appear, to justify making a distinction between them. Moreover, as will be explained later, the level of the block in the right intraventricular conducting pathways in the right bundle branch block variant may not be the same as that in the common type of right bundle branch block.

The common type of right bundle branch block can be considered the electrocardiographic and vectorcardiographic prototype to which most of the pattern variations observed in clinical electrocardiography tend in general to conform. In the following pages, however, the instantaneous VA vectors and the electrocardiographic and vectorcardiographic findings in both the common and the variant types of right bundle branch block will be described in parallel. To avoid the confusion that might ensue from such a complicated presentation, the salient characteristics common to both types of right bundle branch block are herewith listed briefly.

1. Approximately the first half of ventricular activation is usually not altered significantly by the presence of right bundle branch block.

Thus The first 0.06 second of the electrocardiographic QRS deflection and the vectorcardiographic QRS sE loop are relatively normal in appearance or show the same abnormalities as they

would were intraventricular conduction normal.

- During the second half of ventricular activation (i.e., during the terminal 0.04–0.06 second of the QRS interval), abnormal QRS forces directed to the right and anteriorly are produced for a period after the time when ventricular activation would normally have been completed.

THE INSTANTANEOUS VA VECTORS IN COMMON AND VARIANT TYPES OF RIGHT BUNDLE BRANCH BLOCK

The spread of activation through the interventricular septum and ventricles in right bundle branch block and the electrical forces produced can be presented in simplified manner in terms of the instantaneous VA vectors (see also Fig 154).

0.01-SECOND SEPTAL VA VECTOR

Since the left bundle branch is intact, the left septal surface and the greater thickness of the septal muscle mass are usually activated just as during normal intraventricular conduction. However, in occasional cases of right bundle branch block, the initial mean instantaneous spatial vectors of the vectorcardiographic QRS sE loop are found to be directed to the left and slightly anteriorly, or, less commonly, slightly posteriorly. While the abnormal orientation of the initial vectors in such cases can sometimes be attributed to antecedent myocardial infarction, this leaves unexplained the instances in which there is neither electrocardiographic nor clinical evidence of old or recent infarction. At present, information is too incomplete to permit anything other than speculation as to the mechanism responsible for the leftward

Thus: These late QRS forces project a prominent, wide, and slurred terminal R' wave on leads V_{3R} and V_1 and a wide, shallow terminal S wave on leads I and V_6 . The corresponding finding in the vectorcardiogram is the terminal finger-like appendage of the QRS sE loop, which is written slowly to the right and anteriorly.

and slightly anterior or posterior initial vectors in some cases of right bundle branch block. One possible

initial QRS forces have an abnormal orientation, while this is not the usual finding in clinical right bundle branch block in human beings. Thus, it may be that right bundle branch block usually observed clinically is produced by a focal block in a peripheral portion of the right intraventricular conducting system, while the occasional cases of right bundle branch block with abnormally oriented initial QRS vectors may be more closely related to experimental block, in that the level of the block is relatively high in the right bundle branch. In our cases of right bundle branch block, an abnormal orientation of the initial QRS vectors occurred more frequently in association with the variant right bundle branch block pattern than with the common type of right bundle branch block. The 0.01 second instantaneous VA vector in right bundle branch block and the corresponding components of the QRS deflection recorded in leads I, V_6 , aVF, and V_1 are presented below.

Common Type of Right Bundle Branch Block		Variant Type of Right Bundle Branch Block	
0.01-second VA vector directed to the right, anteriorly, and either inferiorly or superiorly.		0.01-second VA vector directed to the right or, less frequently, to the left, inferiorly, and anteriorly.	
LEADS I AND V_6	Small Q waves	Small Q waves or, less often, beginning of upstroke of an initial R wave.	
LEAD aVF	Beginning of upstroke of an initial R wave or, less frequently, a small initial Q wave	Upstroke of small initial R wave	
LEAD V_1	Upstroke of a small initial S wave	Upstroke of a small initial R wave, the beginning slurred upstroke of a large wide R wave or a small initial Q wave	

Block located peripheral to the main right bundle branch.—The effects of a peripheral, or "focal," block of right intraventricular conduction on the ventricular activation process have been explained in two ways:

1. Segers and his associates and Vastesaeger propose that a localized region of the right ventricle receives the excitation impulse via the myocardial fibers rather than the Purkinje system. Activation of this region begins late in the QRS interval and proceeds slowly.

2. Dodge and Grant believe that in most (but not all) cases of right bundle branch block the site of the block is peripheral, and that not all of the right ventricle is affected by the block. These investigators postulate that "as soon as excitation reaches the site of the block it immediately spreads out into the surrounding regions of the right ventricle, as if the lesion were a 'leak' for excitation rather than a delaying or blocking mechanism. The remainder of the right ventricle is depolarized by abnormal routes and slower than normal velocities."

In right bundle branch block, just as in left bundle branch block, the term *complete* is applied to right bundle branch block with QRS interval prolongation to 0.12 second or more, while the term *incomplete* is used when the QRS interval is 0.11 second or less. The authors of this text prefer not to attempt to describe incomplete right bundle branch block, for several reasons. (1) The electrocardiographic features of incomplete right bundle branch block can be duplicated by a wide variety of cardiac abnormalities, producing an equally wide range of QRS sE loop patterns in the vectorcardiogram. (2) We are not yet convinced that we can recognize incomplete right bundle branch block vectorcardiographically or electrocardiographically. In view of these facts, we will endeavor insofar as possible, to avoid use of the term *incomplete right bundle branch block*, since we consider it ambiguous. Thus, all instances of right bundle branch block which satisfy the criteria described later will be referred to as *right bundle branch block*, whether the QRS duration is 0.12 second or not (providing it is 0.10 second or longer).

In the past it was customarily stated in most textbooks that right bundle branch block could present in the electrocardiogram in either of two forms—namely, (1) the "Wilson," "common," or "atypical" form, or (2) the "classic," "uncommon," or "typical" form. The first of the right bundle branch block patterns cited (hereafter referred to either as the common type of right bundle branch block, or simply as right bundle branch block) is by far the more frequently observed pattern of the two, the *classic right bundle*

branch block pattern is encountered relatively rarely in clinical electrocardiography. Recently, several authorities in the field of vectorcardiography have expressed doubt as to whether the classic right bundle branch block actually represents right bundle branch block at all.

In fact, there is reason to believe that the pattern of classic right bundle branch block may be related etiologically to myocardial infarction involving several aspects of the left ventricle and occurring in company with an intraventricular conduction disturbance other than right bundle branch block. Thus, even aside from the rarity of the classic right bundle branch block pattern, the uncertainty regarding its mechanism and significance would seem to be reason enough for discussing it separately, apart from the bona fide right bundle branch block patterns to be described shortly. In its place, we have substituted

ant types of right bundle branch block exhibit essentially similar identifying features in the electrocardiogram and vectorcardiogram, nevertheless the two patterns differ sufficiently from each other, in their electrical effects as well as in their significance and the clinical circumstances in which they appear, to justify making a distinction between them. Moreover, as will be explained later, the level of the block in the right intraventricular conducting pathways in the right bundle branch block variant may not be the same as that in the common type of right bundle branch block.

The common type of right bundle branch block can be considered the electrocardiographic and vectorcardiographic prototype to which most of the pattern variations observed in clinical electrocardiography tend in general to conform. In the following pages, however, the instantaneous VA vectors and the electrocardiographic and vectorcardiographic findings in both the common and the variant types of right bundle branch block will be described in parallel. To avoid the confusion that might ensue from such a complicated presentation, the salient characteristics common to both types of right bundle branch block are herewith listed briefly.

1. Approximately the first half of ventricular activation is usually not altered significantly by the presence of right bundle branch block.

Thus the first 0.06 second of the electrocardiographic QRS deflection and the vectorcardiographic QRS sE loop are relatively normal in appearance or show the same abnormalities as they

002-SECOND APICOAFTERIOR VA VECTOR

Because the excitation impulse is blocked (or delayed) in its passage down the right bundle branch, the septum continues to be activated from left to right. However, at the same time, excitation is transmitted in a normal fashion to the left ventricle, where it occurs after onset of ventricular de-

and direction as those produced during normal intraventricular conduction, at least in the common type of right bundle branch block. For one reason or another—whether due to concomitant ventricular hypertrophy and/or myocardial damage or to the site of the block in the right bundle branch system—the 002-second VA vector in the variant type of right bundle branch block is directed superiorly, to the left, and slightly anteriorly and may be of smaller than normal magnitude.

	Common Type of Right Bundle Branch Block	Variant Type of Right Bundle Branch Block
	002-second VA vector directed to the left, anteriorly, and inferiorly	002-second VA vector directed to the left, anteriorly, and superiorly.
LEADS I AND V_6	Beginning upstroke of an R wave.	Upstroke of an R wave.
LEAD aVF	Upstroke of an R wave.	Beginning downstroke of an S wave.
LEAD V_1	Completion of small initial R wave	Completion of small initial R wave; or the beginning upstroke of a slurred S wave or of an R wave following a small Q wave.

004-SECOND LEFT VENTRICULAR VA VECTOR

Activation of the free wall of the left ventricle gives rise to forces which dominate those produced by continuing left-to-right septal depolarization. In fact, the electrical predominance of the left ventricle is maintained for approximately the first 004 second of the QRS interval only, the 004-second VA vector being the maximal leftward mean instantaneous vector produced during ventricular activation in right bundle

branch block, just as normally. The orientation and magnitude of the 004-second VA vector may differ little from the normal, particularly in the common type of right bundle branch block; but often in the variant type of right bundle branch block, for reasons unknown, the 004-second vector is of lesser magnitude and more superior orientation than the corresponding normal vector or that occurring in the common type of right bundle branch block.

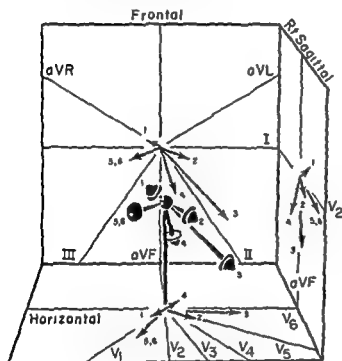
	Common Type of Right Bundle Branch Block	Variant Type of Right Bundle Branch Block
	004-second VA vector directed to the left, posteriorly, and inferiorly.	004-second VA vector directed to the left, superiorly, and usually posteriorly, occasionally anteriorly.
LEADS I AND V_6	Completion of upstroke of R wave. The 004-second VA vector roughly coincides with the peak of the R wave in lead V_6 , so that, of necessity, the time of onset of the intrascapular deflection in lead V_6 is normal despite the right bundle branch block.	Because of the marked superior orientation of the 004-second VA vector in this type of right bundle branch block pattern, the projection of the vector on the transverse lead axes of leads I and V_6 is much less than that of the corresponding vector in the common type of right bundle branch block. Thus, the peak of the R in leads I and V_6 is relatively low.

Fig 154.—Instantaneous VA vectors in right bundle branch block. In B, instantaneous VA vector 5.5 is so numbered to indicate that it actually represents several successive instantaneous vectors having much the same direction and magnitude. These combined vectors correspond to the late slowly inscribed R' wave of the RSR' deflection in lead V_1 of C.

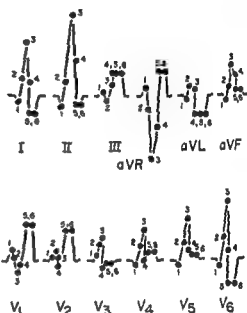


A Sequence of Septal-Ventricular Activation in Right Bundle Branch Block

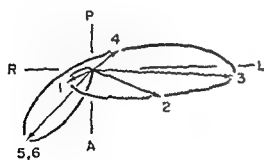
1. INITIAL ACTIVATION OF LEFT SEPTAL SURFACE
2. ACTIVATION OF MUSCLE MASS OF LEFT SEPTUM AND OF APICO-ANTERIOR LEFT VENTRICULAR FREE WALL
3. ACTIVATION OF ANTEROLATERAL WALL OF LT VENTRICLE
4. ACTIVATION OF BASAL LEFT VENTRICULAR WALL, CONTINUED LEFT-TO-RIGHT SEPTAL ACTIVATION AND ACTIVATION OF APICO-ANTERIOR OF RT VENTRICLE
5. COMPLETION OF SEPTAL ACTIVATION AND CONTINUED ACTIVATION OF RIGHT VENTRICULAR FREE WALL
6. ACTIVATION OF BASAL WALL OF RIGHT VENTRICLE AND/OR SEPTUM



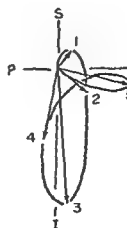
B Instantaneous VA Vectors in RBBB



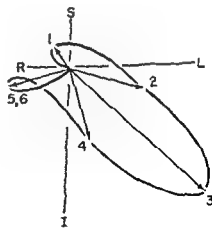
C QRS Deflections Projected on Scalar Leads



Horizontal



Right Sagittal



Frontal

D Planar QRS Loops in Right Bundle Branch Block

Fig. 154.—See legend on facing page

	Common Type of Right Bundle Branch Block	Variant Type of Right Bundle Branch Block
LEAD aVF	Completion of small terminal S wave or inscription of small secondary R wave.	Completion of S wave
LEAD V ₁	Downstroke of terminal R wave. (The peak of the terminal R wave in lead V ₁ coincides	Completion of R wave or terminal R wave.

val)

Thus, in summary, the four electrocardiographic leads whose QRS deflections were described above, and which can be considered to correspond to transverse, vertical, and anteroposterior leads of the vectorcardiogram, record QRS complexes with the following types of configuration in right bundle branch block

	Common Type of Right Bundle Branch Block	Variant Type of Right Bundle Branch Block
LEAD I:	qRs or qRS	Rs or RS, or qRs.
LEAD aVF:	RSR', rSR', qR, Rs, or RR'	rS
LEAD V ₁ :	rSR', rSR', or occasionally rR'	Slurred R, qR, rSR', or RR'
LEAD V ₂ :	Same as in lead I.	RS or rS.

VENTRICULAR REPOLARIZATION

Secondary changes in the S-T segments and the T waves usually accompany the altered QRS complexes in right bundle branch block. Because of the delay in right ventricular depolarization, the regions first activated (the free wall of the left ventricle and the septum, which project negative repolarization potentials on right precordial leads, for example) presumably begin to repolarize prior to the completion of the activation process in other areas of the heart, principally the free wall of the right ventricle. The direction of repolarization may also be reversed in the right ventricle itself, if it is true, as some believe, that in right bundle branch block there is an abnormal spread of the activation wave through the right ventricular wall. However, the ventricular gradient concept provides that every change in the area of the QRS complex causes a corresponding secondary change in the area of the ST-T complex which is equal in magnitude, but opposite in direction, to the former. Therefore, the greater the positive area of the QRS complex in right precordial leads, the more prominent will be the S-T segment depression and T

wave inversion. These several factors act to rotate the S-T and T vectors away from the terminal instantaneous QRS vectors and the corresponding mean vector for the terminal 0.04 second of the QRS interval. In the absence of primary T wave changes, such as those due to myocardial ischemia, the ventricular gradient remains normal. Repolarization forces produced early in ventricular diastole sometimes depress the S-T segments in right precordial leads, the T waves being inverted in these same leads. Because the mean instantaneous T spatial vectors in right bundle branch block tend to be almost 180° discordant to the terminal mean instantaneous QRS spatial vectors, not only are the T waves invariably inverted in leads V₁ and V₂, as indicated above, but they are equally invariably upright in leads V₃ and V₆, often despite the presence of severe coexisting myocardial disease. Thus, if an upright T wave following an RSR' deflection is noted in lead V₁, then the diagnosis of uncomplicated right bundle branch block should be questioned.

VECTORCARDIOGRAPHIC FINDINGS

Just as in the preceding discussion of the instantaneous VA vectors and related electrocardiographic findings in the common and variant types of right

bundle branch block, the description of the vectorcardiographic findings in these two pattern variants will be presented in parallel in the following pages.

*Common Type of Right Bundle
Branch Block*

*Variant Type of Right Bundle
Branch Block*

LEAD aVF:	Completion of upstroke of a small R wave	Completion of downstroke of a deep S wave.
LEAD V ₁ :	Nadir of S wave (following small initial R wave), which is of average, or less than average, depth in right bundle branch block.	Nadir of relatively shallow S wave or the lowest point of the incisura separating two R waves. When the 0.04-second VA vector is anteriorly placed, it sometimes contributes to the upstroke of an R wave.

0.06-SECOND VA VECTOR

As depolarization forces generated by the left ventricle begin to subside during the final 0.04–0.06 second of the QRS interval, those produced by continued left-to-right septal activation become increas-

ingly predominant. This is reflected in the fact that the 0.06-second VA vector is directed to the right, anteriorly, and either more or less horizontally or, in the case of the variant type of right bundle branch block pattern, superiorly.

*Common Type of Right Bundle
Branch Block*

*Variant Type of Right Bundle
Branch Block*

	0.06-second VA vector directed to the right, anteriorly, and horizontally.	0.06-second VA vector directed to the right, anteriorly, and superiorly
LEADS I AND V ₆ :	Downstroke of a broad terminal S wave	Downstroke of a broad and usually relatively deep terminal S wave
LEAD aVF:	Downstroke of R wave or beginning downstroke of shallow terminal S wave.	Continued downstroke of deep S wave
LEAD V ₁ :	Beginning upstroke of a secondary R wave which is wider and taller than the initial R wave.	Upstroke or continued upstroke of an R wave

0.08-SECOND AND SUBSEQUENT VA VECTORS

Late in the QRS interval, onset of right ventricular activation finally occurs, the excitation impulse having reached the right ventricular myocardium either via the Purkinje fibers or by direct muscle-fiber-to-muscle-fiber spread from the left ventricle. Whether the right ventricle depolarizes in a normal or abnormal manner, the fact remains that right ventricular activation occurs so late in the QRS interval that unopposed electrical forces are, in effect, "tacked on" at the end of ventricular activation. While the magnitude of these forces in the common type of right bundle branch block can be explained, perhaps, by the fact that they

are unopposed, this explanation is not applicable to the very large terminal QRS forces frequently observed in the variant pattern of right bundle branch block. The magnitude of these forces is such as to make almost inescapable the conclusion that they reflect totally aberrant activation of the right ventricle. The late instantaneous VA vectors lead to prolongation of the QRS interval to 0.11 second or longer and are directed toward the effective electrical site of the right ventricle—that is, to the right, anteriorly, and horizontally in the case of the common type of right bundle branch block and either horizontally or slightly superiorly in the case of the variant pattern of right bundle branch block.

*Common Type of Right Bundle
Branch Block*

*Variant Type of Right Bundle
Branch Block*

	0.08-second and subsequent instantaneous VA vectors directed to the right, anteriorly, and horizontally	0.08-second and subsequent VA vectors directed either horizontally or slightly superiorly, anteriorly and to the right
LEADS I AND V ₆ :	Completion of relatively shallow terminal S wave.	Completion of deep, wide terminal M wave.

Common Type of Right Bundle Branch Block

Variant Type of Right Bundle Branch Block

LEAD aVF.	Completion of small terminal S wave or inscription of small secondary R wave.	Completion of S wave
LEAD V ₁ .		Completion of R wave or terminal R wave.

val)

Thus, in summary, the four electrocardiographic leads whose QRS deflections were described above, and which can be considered to correspond to transverse, vertical, and anteroposterior leads of the vectorcardiogram, record QRS complexes with the following types of configuration in right bundle branch block

	Common Type of Right Bundle Branch Block	Variant Type of Right Bundle Branch Block
LEAD I:	qRs or qRS.	Rs or RS, or rRs.
LEAD aVF:	RSR', rSR', qR, Rs, or RR'	rS
LEAD V ₁ .	rSR', rSR', or occasionally rR'	Slurred R, qR, rSR', or RII'
LEAD V ₆ .	Same as in lead I	RS or rS

VENTRICULAR REPOLARIZATION

Secondary changes in the S-T segments and the T waves usually accompany the altered QRS complexes in right bundle branch block. Because of the delay in right ventricular depolarization, the regions first activated (the free wall of the left ventricle and the septum, which project negative repolarization potentials on right precordial leads, for example) presumably begin to repolarize prior to the completion of the activation process in other areas of the heart, principally the free wall of the right ventricle. The direction of repolarization may also be reversed in the right ventricle itself, if it is true, as some believe, that in right bundle branch block there is an abnormal spread of the activation wave through the right ventricular wall. However, the ventricular gradient concept provides that every change in the area of the QRS complex causes a corresponding secondary change in the area of the ST-T complex which is equal in magnitude, but opposite in direction, to the former. Therefore, the greater the positive area of the QRS complex in right precordial leads, the more prominent will be the S-T segment depression and T

wave inversion. These several factors act to rotate the S-T and T vectors away from the terminal instantaneous QRS vectors and the corresponding mean vector for the terminal 0.04 second of the QRS interval. In the absence of primary T wave changes, such as those due to myocardial ischemia, the ventricular gradient remains normal. Repolarization forces produced early in ventricular diastole sometimes depress the S-T segments in right precordial leads, the T waves being inverted in these same leads. Because the mean instantaneous T spatial vectors in right bundle branch block tend to be almost 180° discordant to the terminal mean instantaneous QRS spatial vectors, not only are the T waves invariably inverted in leads V₁ and V₂, as indicated above, but they are equally invariably upright in leads V₃ and V₆, often despite the presence of severe coexisting myocardial disease. Thus, if an upright T wave following an RSR' deflection is noted in lead V₁, then the diagnosis of uncomplicated right bundle branch block should be questioned.

VECTORCARDIOGRAPHIC FINDINGS

Just as in the preceding discussion of the instantaneous VA vectors and related electrocardiographic findings in the common and variant types of right

bundle branch block, the description of the vectorcardiographic findings in these two pattern variants will be presented in parallel in the following pages

COMMON TYPE OF RIGHT BUNDLE BRANCH BLOCK

VARIANT TYPE OF RIGHT BUNDLE BRANCH BLOCK

Horizontal QRS Loop

1. Initial deflection written to the right and anteriorly, just as normally.

2. The major part of the horizontal loop is usually written in a counterclockwise direction (rarely in a clockwise direction) to the left and at first anteriorly and later posteriorly (rarely is the efferent limb of the loop situated anterior to the efferent limb). The average orientation of the maximal leftward mean instantaneous QRS vector in our cases was at 0° in the horizontal reference frame.

3. In both patterns (common and variant), the efferent limb of the horizontal QRS loop does not return to the point of origin but continues in a rightward and predominantly anterior direction to inscribe a terminal, finger-like appendage, whose average orientation in the two patterns was exactly the same in our cases—i.e., along the $+120^\circ$ axis of the horizontal reference frame. On the whole, the terminal appendage to the QRS loop in the variant type of right bundle branch block differed from that in the common type in two respects: first, the maximal mean instantaneous vector of the appendage tended to be relatively quite large compared to the preceding leftward portion of the horizontal loop, and second, the conduction delay, as evidenced by the close spacing of the time dashes, was more prominent.

Right Sagittal QRS Loop

1. The sagittal QRS loop generally consists of two well-delineated components. Of these, the first inscribed resembles to some extent the normal sagittal QRS loop, in that it is written in a clockwise direction anteriorly and inferiorly and then returns posteriorly toward the electrical null point. The maximal mean instantaneous QRS vector of this part of the sagittal loop lies, on the average, at $+105^\circ$ in the sagittal reference frame.

2. Instead of returning to the electrical null point, the efferent limb of the sagittal loop turns anteriorly and inscribes a long finger-like appendage directed almost horizontally anteriorly. Conduction delay is present in the terminal appendage more often than not, but the delay is not usually striking. The average orientation of the maximal anterior mean instantaneous QRS vector tends to be about $+5^\circ$.

1. Although the initial deflection of the horizontal QRS loop in this (variant) pattern is frequently written to the right and anteriorly, in almost as many instances the horizontal QRS loop immediately moves to the left and anteriorly or, less commonly, to the left and slightly posteriorly (without electrocardiographic or clinical evidence of infarction).

2. In this pattern, the leftward portion of the horizontal loop is far more variable in appearance than in the common pattern. Thus the maximal leftward mean instantaneous QRS vector may not extend as far to the left as in the common type of right bundle branch block, however, the average orientation of this vector is 0° , like that in the common pattern. Often this part of the loop is entirely clockwise inscribed or presents a figure-of-eight configuration, with the proximal component counterclockwise inscribed and the distal component clockwise inscribed.

1. The sagittal QRS loop in the variant pattern of right bundle branch block does not exhibit the two components characterizing the sagittal loop in the common pattern. Generally, the sagittal loop is written briefly and initially inferiorly and anteriorly, but very quickly thereafter it turns in a clockwise direction superiorly and posteriorly or slightly anteriorly. The maximal mean instantaneous QRS vector for the first 0.04 second of the QRS interval was oriented, on the average, at -80° in our cases.

2. After the efferent limb of the sagittal loop has reached its maximally superior extent, it turns anteriorly in a clockwise direction and descends gradually. The maximal anterior mean instantaneous QRS vector in this pattern is usually directed essentially horizontally, its average orientation being at about -10° . Conduction delay in the terminal, anterior part of the sagittal loop is ordinarily more prominent than in the sagittal loop of the common pattern.

Frontal QRS Loop

1. As a general rule, the frontal QRS loop in the common type of right bundle branch block presents either of the following appearances:

a) The loop may be entirely clockwise inscribed despite a relatively horizontal orientation of its long axis.

1. The frontal loop is usually written initially inferiorly and to the right and/or to the left, but very quickly it moves superiorly. The remainder of the loop is inscribed in a counterclockwise direction superiorly and to the left and then superiorly and to the right, the latter segment of the loop displaying marked conduction delay.

COMMON TYPE OF RIGHT BUNDLE BRANCH BLOCK

The terminal part of the loop showing conduction delay is situated inferiorly and to the right.

b) The loop may be written with a more or less figure-of-eight configuration to the left and slightly inferiorly. The greater portion of the loop is counterclockwise inscribed, while the second component of the "eight" is clockwise inscribed to the right and inferiorly.

Instantaneous vector was $+165^\circ$

VARIANT TYPE OF RIGHT BUNDLE BRANCH BLOCK

Occasionally the frontal loop is inscribed superiorly and to the right or left initially, then inferiorly and to the left, and finally superiorly and to the right.

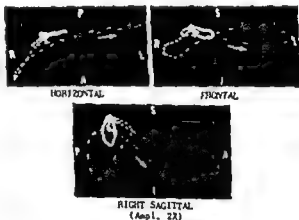
2. The average orientation of the maximal leftward mean instantaneous QRS vector in our cases was -10° that of the maximal rightward instantaneous vector, -160°

T sE Loop

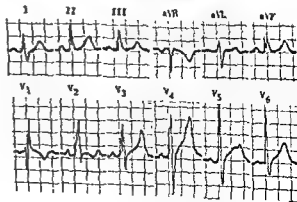
The most consistent feature of the T sE loop in right bundle branch block is that it is always directed away from the terminal vectors of the QRS sE loop.

S-T Vector

In contrast with left bundle branch block, uncomplicated right bundle branch block does not usually produce an S-T vector in the vectorcardiogram (Figs 155-158)



... in the electrocardiogram and the corresponding portion of the QRS sE loop of the vectorcardiogram appear essentially normal. The prominent terminal deflection of the QRS sE loop to the right, anteriorly, and slightly inferiorly is diagnostic of right bundle branch block and is related to the electrocardiographic findings in leads V_1 and V_6 . The T sE loop of the vectorcardiogram tends to parallel the long axis of the QRS sE loop but is directed away from the terminal deflection of the loop. Thus, leads I and V_6 record upright T waves, while lead V_1 registers an inverted T wave.



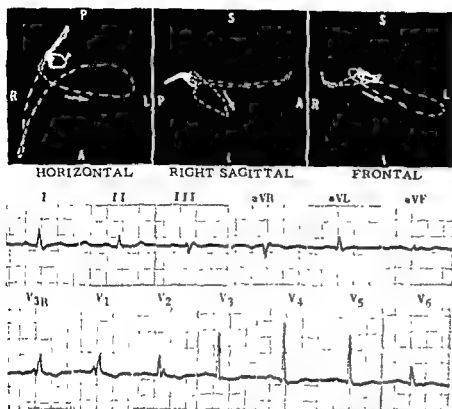
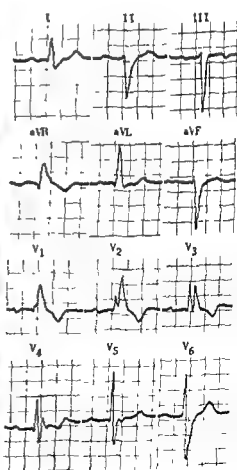
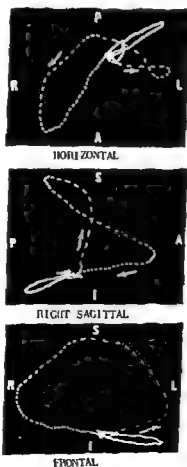


Fig. 156.—Electrocardiographic and vectorcardiographic findings in the common type of right bundle branch block. Note, in the electrocardiogram, that lead V_4 records only a minute terminal S wave. Moreover, the S waves of the RSR' deflections in leads $V_{1,2}$ and V_1 barely extend below the isoelectric base line. The explanation for these findings is evident in the vectorcardiogram. Thus, the first half of the QRS sE loop is situated anteriorly, and this is responsible for the diminutive S waves in the right precordial leads. In addition, the terminal deflection of the QRS sE loop is directed almost straight anteriorly and only slightly to the right. Consequently, the mean instantaneous QRS spatial vectors of the terminal part of the QRS sE loop project maximally on the axes of leads $V_{3,4}$ and V_1 and minimally on the negative half of the axis of lead V_6 . The terminal deflection of the QRS sE loop in this figure, as well as in Figure 155, displays no evidence of localized conduction delay.

Fig. 157.—Electrocardiographic and vectorcardiographic findings in the variant type of right bundle branch block.

In the electrocardiogram, the QRS interval is 0.18 second, there is marked left-axis deviation of \bar{A} QRS, lead V_1 displays a slurred, wide R wave, and lead V_6 registers an RS deflection, the terminal S wave being both deep and wide. Note the absence of a normal septal Q wave in lead V_4 .

The vectorcardiographic QRS sE loop in the variant right bundle branch block pattern differs from that in the common type of right bundle branch block as follows: there is an abnormal initial deflection of the loop to the left, anteriorly, and slightly inferiorly; the sagittal and frontal QRS loops are inscribed entirely superiorly, the latter usually having a counterclockwise inscription, the first part of the horizontal QRS loop written to the left is dwarfed by the large rightward and anterior terminal deflection subsequently inscribed, and the terminal limb of the QRS sE loop shows conduction delay.



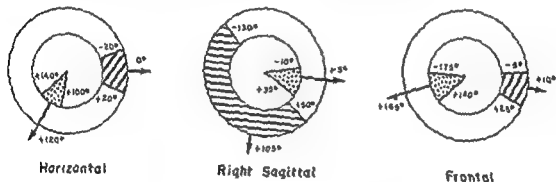
Grishman and his associates have described a pattern which is similar to the variant pattern of right bundle branch block discussed above, with this one and possibly all-important distinction: in the QRS sE loop pattern of Grishman and his co-workers, the sagittal and frontal QRS loops are situated markedly superiorly and the terminal mean instantaneous vectors are not directed to any significant degree anteriorly nor do they form a typical terminal rightward and anterior appendage in the horizontal projection (Fig. 153). These investigators believe the pattern to be the equivalent of that designated "left ventricular hypertrophy with terminal conduction delay" in Chapter 16. They point out that, since the terminal QRS forces are directed markedly superiorly in "left ventricular hypertrophy with terminal conduction de-

lay," minor differences in the position of these forces with respect to the anteroposterior (Ze) lead may result in the terminal portion of the QRS sE loop being inscribed anteriorly or posteriorly. If there is an anterior return of the loop, the electrocardiogram pre-

terminal S waves appears in the precordial leads.

None of the QRS sE loop patterns described so far in this chapter have been observed by the authors of this text to produce electrocardiographic findings of the type ascribed to classic right bundle branch block. This entity, which was described at a time when only scalar electrocardiograms were available, is said to present the following features:

Common Type of Right Bundle Branch Block



Variant Type of Right Bundle Branch Block

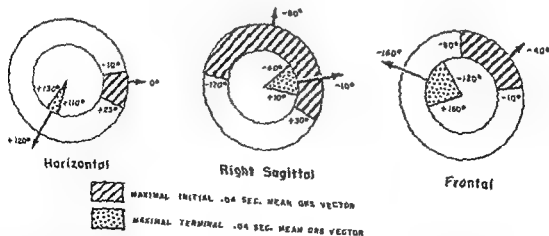


Fig. 158 - Range of variation and average orientation of the maximal mean initial 0.04-second QRS vector and the maximal mean terminal 0.04-second QRS vector of the vectorcardiographic QRS sE loop in the common and the variant types of right bundle branch block.

1. Lead I shows a small, narrow R wave and a deeper and wider S wave.
2. Leads II and III usually show narrow R waves taller than in lead I, which may be preceded by a small Q wave and followed either by a second up-right deflection or a smaller S wave.
3. Leads V_{1R} to V_2 record initial small Q waves and terminal large, slurred, and widened R waves, while, from right to left across the precordium, RS deflections are recorded with diminishing R wave amplitude and increasing depth of the S wave.

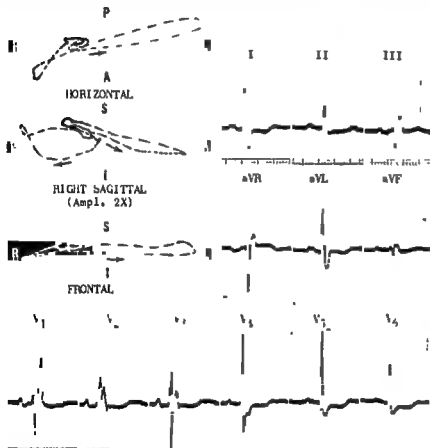


Fig. 159. — Electrocardiographic

ing left ventricular hypertrophy are: left-axis deviation of \bar{A} QRS in the frontal plane, tall R waves, depressed S-T segments, and diphasic T waves in leads I, aVL, V_5 and V_6 ; and the relatively deep S wave of the RSR' deflection in lead V_1 . In the vectorcardiogram, the findings suggestive of coexisting left ventricular hypertrophy are: increased magnitude of the leftward instantaneous vectors of the QRS sE loop, posterior and superior rotation of the long axis of the

terminus of the QRS sE loop), and the small T sE loop. The vectorcardiographic findings indicative of right bundle branch block are obvious and will not be described.

DIAGNOSIS OF COEXISTING VENTRICULAR HYPERTROPHY

The following electrocardiographic findings have been proposed by Barker and Valencia as suggestive of right bundle branch block plus right ventricular hypertrophy

1. If the secondary R wave in V_1 exceeds 10 mm. in amplitude in incomplete right bundle branch block and 15 mm. in complete right bundle branch block, right ventricular hypertrophy may be present.
2. The R and R' waves registered in right precordial leads should be clearly separated by the S wave

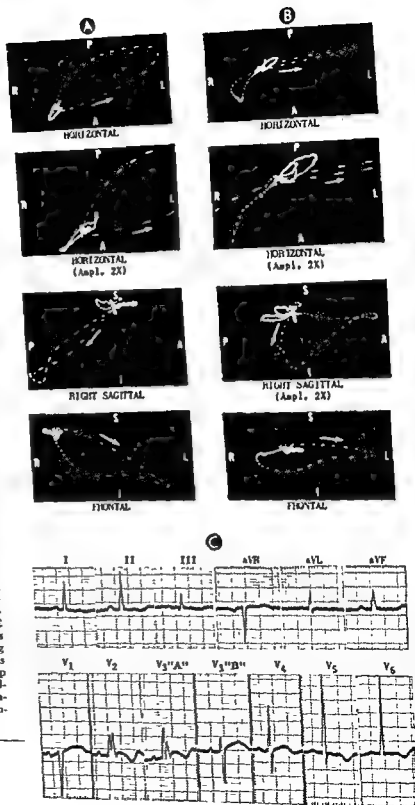
3. The R waves recorded in left precordial leads are relatively small in comparison with the increased size of the S waves.

The general experience has been that the above criteria are not of great value in detecting right ventricular hypertrophy in the presence of right bundle branch block. When we applied these criteria to the electrocardiograms of patients with mitral stenosis showing RSR' deflections in lead V_1 , we found that the diagnosis of right ventricular hypertrophy could not be made in a single case, even though the vector-

Fig. 160.—Electrocardiographic and vectorcardiographic findings in intermittent right bundle branch block and left ventricular hypertrophy

The electrocardiogram (C) is diagnostic of left ventricular hypertrophy, however, in leads V_1 and V_2 "A" the QRS complexes have widened to 0.14 second and consist of notched R waves with small terminal S waves. In lead V_1 "B" the intraventricular block has disappeared again. The appearance of the widened ventricular complexes in leads V_1 and V_2 "A" suggests right bundle branch block, which was verified by later electrocardiograms (not shown).

The two sets of vectorcardiographic loops (A and B) were obtained during the recording of a single vectorcardiogram from the patient whose electrocardiogram was just described. The planar QRS loops in A present the features of left ventricular hypertrophy. In B, note that, despite the appearance of right bundle branch block, the planar QRS loops show little change from those in A for about the first 0.03 second, but terminally a rightward and anterior deflection of the loop is written which shows closely spaced time markings. The vectorcardiogram is therefore diagnostic of right bundle branch block. Note, also, that the T sE loop in the vectorcardiogram in A is directed almost 180° away from the QRS sE loop, while the T sE loop in B is essentially concordant to the long axis of the QRS sE loop. This secondary change in T sE loop orientation reflects solely the alteration in ventricular depolarization consequent to the right bundle branch block.



cardiograms showed typical right ventricular hypertrophy patterns.

Braunwald and his associates have observed several instances in which vectorcardiographic loops diagnostic of right ventricular hypertrophy showed marked conduction delay in their terminal portions, probably due to right bundle branch block. These investigators were able to demonstrate in these cases a delayed onset of mechanical right ventricular systole such as m found in right bundle branch block but not in right ventricular hypertrophy alone. Burch and his associates and Wolff and his co-workers have also de-

scribed combined right ventricular hypertrophy and right bundle branch block as producing displacement anteriorly and to the right of a QRS sE loop otherwise typical of right bundle branch block.

Grishman and Scherlis have observed in some cases of combined left ventricular hypertrophy and right bundle branch block that the QRS loop is oriented more superiorly than is usually the case with right bundle branch block alone. This is in general agreement with our findings and those of Burch and his associates (Figs. 159-160).

OTHER TYPES OF INTRAVENTRICULAR BLOCK

Focal or Peri-infarction Intraventricular Block

This type of intraventricular block is thought to occur primarily as a complication of myocardial infarction. Accordingly, discussion of it will be deferred until later (Chapter 21).

Diffuse Intraventricular Block

Very rarely a marked intraventricular block without an associated complete interruption of the left bundle branch may result from left ventricular hypertrophy and dilatation, diffuse myocardial fibrosis, the use of quinidine, or hyperkalemia. Apparently, there is merely a diffuse slowing of conduction through the ventricular wall. Although the electrocardiographic pattern resembles that of left bundle branch block in some respects, the ability of the interventricular septum to depolarize from left to right usually produces normal Q waves in left precordial leads.

The vectorcardiographic counterpart of this type of intraventricular block has not been described. In fact, we studied vectorcardiographically only 1 case of diffuse intraventricular block. In this instance, the heart at postmortem examination was found to have endocardial fibroelastosis and marked ventricular

zarré appearance, while the vectorcardiogram displayed the following findings (1) marked conduction delay in the efferent limbs of the horizontal and frontal QRS loops and in the afferent limb of the sagittal loop, (2) abnormal initial deflection of the QRS sE loop to the left and posteriorly, (3) horizontal QRS loop entirely clockwise inscribed to the left and posteriorly, (4) frontal QRS loop almost linear and written almost directly to the left, and (5) T sE loop 180° discordant to the long axis of the QRS sE loop

Myocardial Ischemia, Injury, and Infarction:

General Considerations

EXPERIMENTAL OCCLUSION of the coronary artery in dogs produces electrocardiographic changes which correlate, in a general way, with the severity and reversibility of the histologic alterations in the myocardium. These electrocardiographic changes appear in three stages of increasing abnormality—namely, ischemia, injury, and necrosis. The ischemia and injury phases are not accompanied by irreversible alterations in the muscle cells, but once necrosis has supervened, the damage to the muscle fibers becomes irreversible. In addition to the reduction in blood

supply to the affected myocardium, other noxious influences sometimes produce the histologic and electrocardiographic changes of ischemia, injury, and necrosis. However, in the following chapters, the discussion will center primarily on ischemia, injury, and infarction secondary to reduced or absent blood supply to the involved myocardium, although the principles developed apply equally well to other conditions, such as myocarditis, pericarditis, etc (see Chapter 21).

ISCHEMIA

The distribution of the coronary arteries is such that normally the blood supply of the outer layers of ventricular musculature is relatively greater than that of the deeper subendocardial layers. This disparity in blood supply may be enhanced by the transmission of greater degrees of left intraventricular pressure to the subendocardium than to the outer layers of myocardium. The high pressure tends to collapse the blood vessels within the subendocardium. As a consequence of the foregoing two factors, myocardial ischemia appears first, and is more extensive, in the subendocardium.

Subendocardial Ischemia

Ischemia leads to a local delay in the onset of recovery and therefore to a local prolongation of the excited state. For reasons previously stated, ischemia secondary to diminished regional blood supply begins in the subendocardial layer of muscle. Since repolarization normally proceeds in an epicardial-to-endocar-

dial direction, delayed recovery in the subendocardial muscle does not reverse the direction of repolarization but merely lengthens its duration locally (thereby prolonging the Q-T interval). Thus the ischemic subendocardial muscle continues to repolarize for a time after opposing repolarization potentials from other regions have begun to subside. This circumstance tends to rotate the late instantaneous T vectors toward the effective site of the ischemia and to increase the magnitude of these vectors, since they are relatively unopposed. Consequently, leads over the involved myocardium record upright T waves of increased amplitude and duration.

Transmural (Epicardial) Ischemia

When ischemia extends transmurally to the epicardium, it apparently has a more profound effect on the recovery of epicardial cells than it has on recovery of endocardial cells. In the ischemic myocardium, onset of repolarization is delayed longer in the epicardium

than in the endocardium, with the result that the endocardial muscle fibers are the first to recover. The wave of repolarization then spreads through the involved muscle wall in an endocardial-to-epicardial direction, the reverse of normal. This local reversal in the direction of repolarization causes the repolarization forces generated by the involved myocardium to be directed just the opposite of normal. For example, at each instant during ventricular repolarization, transmural ischemia of the anterior wall of the left ventricle gives rise to T vectors directed posteriorly, which, added vectorially to the normal T vectors originating in unaffected portions of the left ventricle, yield mean instantaneous T vectors directed more or less away from the effective site of the ischemia. These instantaneous T vectors project on the negative portions of the axes of leads overlying the region of ischemia so that these leads record inverted T waves. Since ventricular depolarization and, therefore, the orientation of the mean instantaneous QRS vectors remain undisturbed by myocardial ischemia, the displacement of the instantaneous T vectors usually results in an increased angular divergence of the mean QRS and T vectors. If the QRS-T angle becomes sufficiently wide, leads registering upright QRS complexes may record inverted T waves, and vice versa. Inasmuch as transmural myocardial ischemia causes a local prolongation in the duration of the excited state, it is

associated with an abnormal ventricular gradient. For this reason, the T wave abnormalities of ischemia are primary in type.

The vectorcardiographic T sE loop has not been studied extensively as yet, and most of the available information pertains to its orientation with respect to the QRS sE loop. In transmural myocardial ischemia, the T sE loop tends to rotate away from the affected portion of the myocardium, and thus the angular deviation between the QRS sE and T sE loops usually, but not invariably, becomes abnormally increased (normally, the angle of deviation rarely exceeds 45°). An abnormal angle of deviation between the QRS sE and T sE loops may appear before T wave abnormalities become evident in the scalar electrocardiogram, since a relatively marked degree of angular deviation is generally required to produce abnormal T waves. The efferent limb of the normal T sE loop, like the upstroke of the normal T wave, is inscribed more slowly than the afferent limb of the loop and the downstroke of the T wave. Large, elongated T loops have been described in acute myocardial infarction, while old infarctions have been associated, by some investigators, with the presence of small round T loops. These variations in T loop configuration and inscription are not fully understood at present and require further study.

INJURY

Diastolic Current of Injury

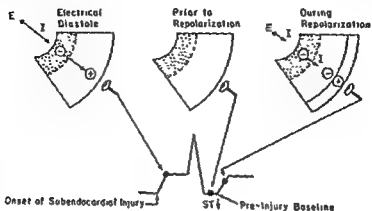
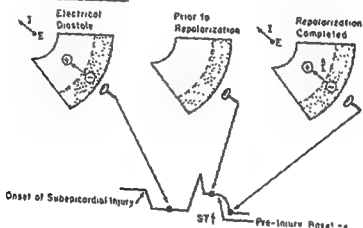
Injury of a resting myocardial cell has two effects (1) it decreases the degree of polarization so that there are fewer positive charges per unit surface area, and (2) it abolishes the selective permeability of the injured cell membrane so that negative ions are permitted to escape outside the cell, where they are neutralized by positive ions. As a result, during electrical diastole the injured membrane (Fig. 161) comes to be negatively charged relative to the intensely polarized and positively charged adjacent membrane, and a potential difference exists between the two regions. If the myocardial cell is situated in a volume conductor, a diastolic current of injury flows from the region of greater potential to the region of lesser positive, or more negative, potential—that is, from the outer to the inner surface of the cell membrane through the region of injury. The electrical field which is created in the surrounding conducting medium during electrical diastole can be represented by a vector directed from the injured area toward the intact cell membrane.

This vector, hereafter labeled “I”, depicts the electrical field of the diastolic current of injury, while a second vector, “-I,” discussed later (pp 258 and 259), represents the field of the systolic current of injury.

If it were possible to place an electrocardiographic lead electrode over the injured end of the resting muscle cell, the base line of the tracing would be deflected downward at the time of injury because I is directed away from the recording electrode. On the other hand, the precise instant at which the diastolic current of injury appears and depresses the electrocardiographic base line is never observed in clinical electrocardiography. Consequently, the direct effect of the diastolic current of injury on the electrocardiogram is never evident and will be ignored hereafter in this text.

Systolic Current of Injury

During electrical systole, a current of injury flows toward the injured cell membrane, and therefore in a

A SUBENDOCARDIAL INJURY**B SUBEPICARDIAL INJURY**

... myocardial injury
... assessed, while after de-

(Fig 181).—As noted before, the diastolic current of injury is present only during the diastolic phase of the cardiac cycle. The elevated S-T segment registered in the electrocardiogram and the apparent pres-

direction just the opposite of that of the diastolic current of injury. The mechanism responsible for this diastolic current of injury has been the subject of some dispute. The conflicting explanations which have been offered can be reduced, for the sake of simplicity, to the two mechanisms presented below: (a) disappearance of the diastolic current of injury and (b) blocking of depolarization.

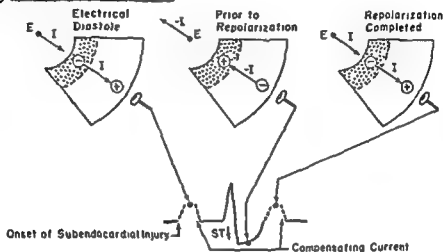
Disappearance of the diastolic current of injury

ence of a systolic current of injury therefore actually reflect the absence of the diastolic injury vector, according to the proponents of this concept. Repolarization of the cell restores the potential difference between injured and intact membrane, and so, following inscription of the T wave, the base line of the tracing descends once again.

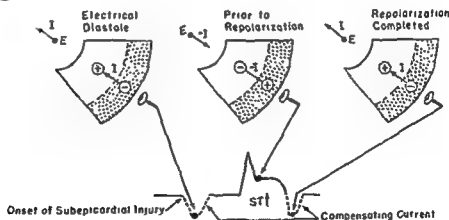
Blocking of depolarization (Fig. 162).—This concept is based on the premise that there is partial or complete blocking of the depolarization wave at the

borders of the region of injury. Thus, even though the injured membrane of the resting cell has fewer positive charges per unit surface area than adjacent intact membrane, with the completion of depolarization the injured membrane (where the activation wave has been completely or partially blocked) retains its positive charges and becomes positively charged with respect to the neutralized membrane surfaces. As a result, a systolic current of injury flows toward the injured cell membrane during the interval between

A SUBENDOCARDIAL INJURY



B SUBEPICARDIAL INJURY



F. 162

ary,
grap

However, it is postulated that the depolarization wave is blocked at the boundaries of the injured region so that the latter retains some of its dipoles at a time when uninjured muscle elsewhere has been completely discharged. Therefore, before repolarization, a systolic current of injury appears (represented by the vector $-I$) and projects negative voltage or a depressed S-T segment on the recording lead. With onset of repolarization the diastolic current of injury again appears, and it is immediately neutralized by the compensating current. In subepicardial injury (B), the systolic current of injury vector ($-I$) is directed toward the recording electrode, so that the S-T segment of the electrocardiogram is displaced upward. As the explanation for the S-T segment deviations observed clinically and experimentally in myocardial injury, the blocking of depolarization theory of the systolic current of injury is, in general, more widely accepted than the disappearance of the diastolic injury concept.

The electrical current surrounding the cell can be represented by a vector, the direction of which is directed just the reverse of the

toward the injured aspect of the cell.

In clinical electrocardiography, only the electrical field of the injured area is recorded, since the electrical field cannot be recorded. The authors of this text have chosen to accept the second mechanism outlined above as the explanation of the systolic current of injury.

Subendocardial and Subepicardial Injury

What has been indicated previously concerning the effects of injury of a single heart muscle cell holds true for injury of a region of the ventricular myocardium. When the injury involves the subendocardial layer of ventricular muscle, the activation wave can be considered to be blocked at the borders of the injured muscle. At the completion of electrical systole, the subendocardial muscle therefore retains some of its positive charges while outer muscle layers of the involved ventricular wall are completely depolarized. A potential difference exists between positively charged subendocardial muscle and relatively negatively charged epicardial muscle, and a systolic current of injury flows toward the injured muscle layer. The electrical field of the injury current resulting from subendocardial injury can be represented by an $-I$

vector originating at the electrical center of the heart and directed away from the effective site of the injured muscle. Thus, the $-I$ vector of subendocardial injury projects on the negative halves of the axes of leads overlying the region of the injury, with the result that these leads display depressed S-T segments.

When injury is limited to subepicardial muscle, the latter is positively charged (for the same reasons as described above) and the subendocardial muscle relatively negatively charged at the end of electrical systole. In this instance, the systolic injury vector ($-I$) is directed from the electrical center of the heart toward the effective site of the injured muscle and therefore projects elevated S-T segments on leads overlying the region of injury.

The $-I$ or S-T Vector of the Vectorcardiogram

If there is a significant systolic current of injury, the QRS SE loop of the vectorcardiogram does not, after its inscription, return to its point of origin because a potential difference continues to exist between one or both pairs of deflection plates. The fact that the QRS SE loop remains open indicates that a measurable S-T vector is present whose relative magnitude and direction can be depicted by a vector arrow drawn from the origin of the QRS SE loop to its terminus. In anterior subepicardial injury, this S-T vector is usually directed to the left, inferiorly, and to a varying degree anteriorly. In subendocardial injury, to the right posteriorly, and superiorly.

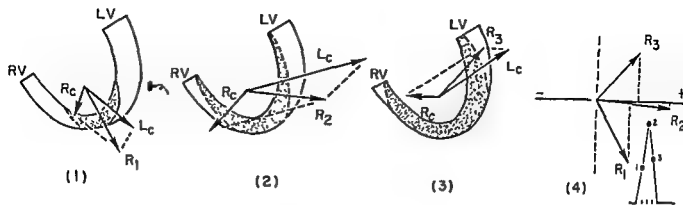
The T SE loop is inscribed from the termination of the open QRS SE loop to the point of origin.

INFARCTION

Infarction is the term used to designate necrosis of heart muscle secondary to a deficient blood supply. Clinical myocardial infarction occurs primarily as a complication of coronary artery disease (its immediate cause usually being coronary thrombosis) and can be considered the end-stage of the ischemia-injury-necrosis sequence described earlier in this chapter. Most infarctions are found, on pathologic study, to be situated in the left ventricular free wall and/or interventricular septum. The only exceptions to this rule are anteroseptal infarctions (which may involve a small strip of adjacent right ventricular wall), atrial infarctions, and right ventricular infarctions, although the latter two types of infarction are

recognized relatively rarely. Atrial infarction produces a shift of the P-Ta segment, but this effect is usually obscured by the larger ventricular deflections appearing at about the same time. Difficult as it may be to recognize an atrial infarction, it is virtually impossible to establish the diagnosis of right ventricular infarction. This is not surprising if one recalls that the right ventricle normally contributes only a quarter of the activation potentials producing the QRS complex. Thus the disappearance of some or all of these right ventricular forces as the result of infarction would not, in most instances, be likely to alter the QRS configuration significantly.

A NORMAL



B MYOCARDIAL INFARCTION

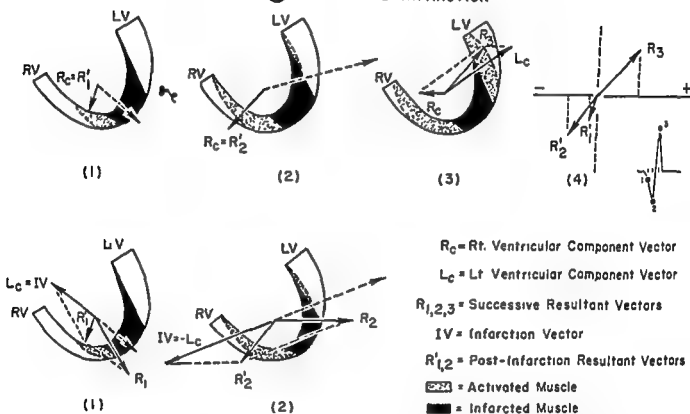


Fig. 163 —Genesis of the diagnostic Q waves and related QRS abnormalities in myocardial infarction. **A**, normal heart. The ventricular portion of the heart is depicted schematically, but with the omission of the septum. The activation wave front in each ventricle, the component vector representing the electrical force arising in each ventricle, and the resultant vector of the two component vectors are presented as they exist at three different stages in the activation process. In **A** (4), the three resultant or mean instantaneous vectors have been projected on the axis of derivation of a transverse lead, and the values obtained have been used to construct the ventricular complex recorded by the lead. **B**, myocardial infarct (solid black). The electrically inert infarcted muscle fails to produce component vectors L_c in stages 1 and 2 of the activation process. Consequently, the right ventricular component vectors are unopposed and are equivalent to the resultant vectors R_1 and R_2 , R_3 is unchanged. As demonstrated in the lower two figures in **B**, one can also determine the postinfarction resultant vector from the preinfarction vector, since the former is the resultant of the latter and the

Mechanism of the QRS Abnormalities of Infarction

A deep, wide Q wave appearing in a lead not normally recording Q waves of such prominence is perhaps the most typical QRS abnormality produced by infarction. Infarction Q waves were once ascribed to the transmission of negative cavity potentials through a "window" of necrotic myocardium to an overlying lead electrode. However, this explanation, like all others based on the localized potentials (or semidirect lead) concept of electrocardiography, is probably not valid when applied to body surface potentials. The mechanism outlined in the following paragraphs has as its basis the equivalent dipole or resultant vector concept, the validity of which seems, for the most part, established.

According to the theory currently accepted by most authorities, infarcted muscle may be considered electrically inert (Fig. 163, A and B). Therefore, the electrical effect of a transmural infarction equals the electrical forces normally produced by the infarcted muscle at a given instant of the QRS interval subtracted from the balance of cardiac forces normally existing at the same instant. Thus, from a given preinfarction mean instantaneous vector and from the vector representing the forces normally produced by the infarcted region of the ventricle (the infarction vector), it should be possible theoretically to calculate the corresponding postinfarction mean instantaneous vector (Fig. 164). This can be done simply by laying off the two vectors from the same point and then drawing a third vector, the postinfarction mean instantaneous vector, from the tip of the infarction vector to the tip of the preinfarction mean instantaneous vector. Since, clinically, the pre- and postinfarction mean instantaneous vectors can be obtained from the vectorcardiogram, it is also possible to calculate, by vector subtraction, the orientation of the infarction vector. In this instance the two mean instantaneous vectors are drawn from the same point, and the infarction vector is then drawn from the tip of the postinfarction vector to the tip of the preinfarction vector.

Since the infarction vector represents the electrical forces normally generated by the infarcted ventricular muscle, it necessarily points toward the effective electrical site of the infarction. As previously indicated, the electrical field of the heart at a given instant, or the corresponding mean instantaneous QRS spatial vector, is determined by the balance arrived at between opposing electrical forces acting simultane-

ously in many directions. The loss of forces normally generated by a region of infarcted myocardium leaves unbalanced forces of equal magnitude acting in the opposite direction. These unbalanced forces can be represented by an infarction vector like that described in the preceding paragraph but directed oppositely—that is, away from the effective electrical site of the infarction. (The term *infarction vector* will be used only in this sense hereafter in this text.) To determine the postinfarction direction and magnitude of a given preinfarction mean instantaneous vector, the latter and the infarction vector are plotted from the same point of origin, and lines are then drawn parallel to the two vectors to form a parallelogram. The diagonal from the point of origin of the two component vectors to the intersection of the two lines completing the parallelogram is the resultant of the infarction vector

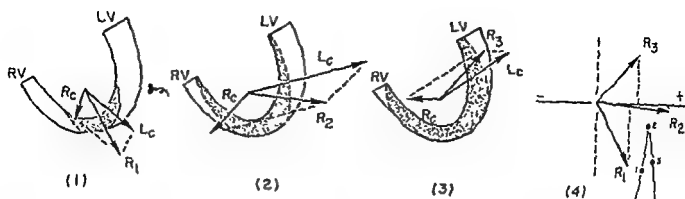
and the preinfarction instantaneous vector. It is obvious that the postinfarction instantaneous vector, like its component infarction vector, is shifted away from the effective electrical site of the infarction. For example, in anterior myocardial infarction, the 0.02-second mean instantaneous vector tends to be shifted posteriorly, whereas normally it usually lies somewhat anterior. As a consequence, lead V_1 , which before onset of the infarction

instantaneously projects

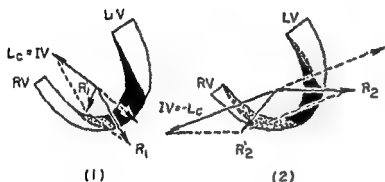
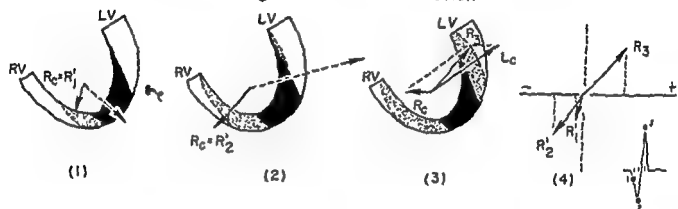
By way of example, the 0.02-second mean instantaneous vector may be displaced more anteriorly than normal. In this event, lead V_2 may register an abnormally tall R wave. The QRS abnormality in either type of infarction clearly reflects an over-all disturbance in the balance of cardiac forces and is not a manifestation of altered localized potentials.

It is evident, from the points developed in the preceding paragraphs, that the direction and magnitude of a given postinfarction mean instantaneous vector and, consequently, the electrocardiographic and vectorcardiographic changes produced by an infarction are functions of the following two variables: (1) the direction of the infarction vector (or the effective electrical site of the infarction) and (2) the orientation and magnitude of the preinfarction mean instantaneous QRS vectors. For example, the infarction vector in infarction of the anterior wall of the left ventricle is directed posteriorly. If the preinfarction mean instantaneous vectors during the initial 0.04 second of

A NORMAL



B MYOCARDIAL INFARCTION



$R_C = R_t$ Ventricular Component Vector

$L_C = L_t$ Ventricular Component Vector

$R_{1,2,3}$ = Successive Resultant Vectors

IV = Infarction Vector

$R'_{1,2}$ = Post-Infarction Resultant Vectors

 = Activated Muscle

 = Infarcted Muscle

front in each ventricle, the component vector representing the electrical force arising in each ventricle, and the resultant vector of the two component vectors are presented as they exist at three different stages in the activation process. In A (4), the three resultant or mean instantaneous vectors have been projected on the axis of derivation of a transverse lead, and the values obtained have been used to construct the ventricular complex recorded by the lead. In myocardial infarct (solid black). The electrically inert infarcted muscle fails to produce component vectors L_c in stages 1 and 2 of the activation process. Consequently, the right ventricular component vectors are unopposed and are equivalent to the resultant vectors R_1 and R_2 , R_1 is unchanged. As demonstrated in the lower two figures in B, one can also determine the postinfarction resultant vector from the preinfarction vector, since the former is the resultant of the latter and the

the QRS interval happen to be directed superiorly, the resultant of each of these instantaneous vectors is that of the infarction vector is a postinfarction instan-

II, III, and aVF. The electrocardiogram in such a case is usually interpreted as showing both anterior and inferior or diaphragmatic infarctions, whereas in reality the effective electrical site of the infarction is confined to the anterior wall of the left ventricle. By and large, however, the major features distinguishing one type of infarction from another are derived from differences in the direction of the infarction vector, or, in other words, from differences in the electrical location of the infarct. For this reason, the classification of myocardial infarction utilized in this text is based on the effective electrical site of the infarction or the direction of the infarction vector.

Criteria of Q Wave Abnormality

As a general rule, the recognition of acute myocardial infarction in the electrocardiogram seldom presents too great a problem, probably because in this stage of infarction the electrocardiogram displays not only QRS abnormalities but also characteristic shifts in the S-T segments and T wave changes. In contrast, it is quite difficult, and sometimes impossible, to distinguish the electrocardiographic residuals of a healed infarction from normal deflections. This is particularly true in the case of infarction Q waves when they occur as late residuals in leads normally inscribing septal Q waves. In evaluating Q waves to determine whether they represent an abnormality or not, the following criteria are often quite useful.

Lead I—Goldberger's criteria of abnormality are width of Q wave ≥ 0.04 second, depth of Q wave = 1 mm or more, provided the amplitude of the following

R wave is approximately 5 mm. According to Barker: depth of Q wave $\geq 10\%$ of the total QRS amplitude.

Leads III and aVF—The criteria of Barker, of Goldberger, and of Myers are: width of Q wave ≥ 0.01 second, depth of Q wave $> 25\%$ of the amplitude of the following R wave.

Lead aVL—Goldberger advocates that all of the following criteria be satisfied: width of Q wave ≥ 0.01 second, depth of Q wave $> 50\%$ of the amplitude of the following R wave, presence of upright P and T waves in lead aVL, and an rS deflection in lead aVL.

Leads V_1 through V_6 —Criteria of Sodi-Pallares: depth of Q wave > 3 mm. (if Q wave is followed by a small R wave); prolonged width of Q wave, and W-shaped QRS deflection. According to Goldberger: width of Q wave ≥ 0.04 second, depth of Q wave $> 25\%$ of amplitude of following R wave.

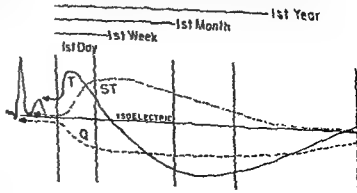
Leads V_1 and V_6 —Barker's criteria: width of Q wave ≥ 0.04 second, depth of Q wave $> 15\%$ of total QRS amplitude.

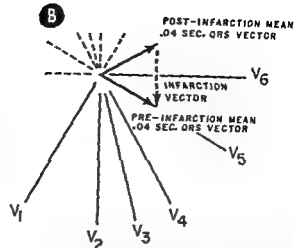
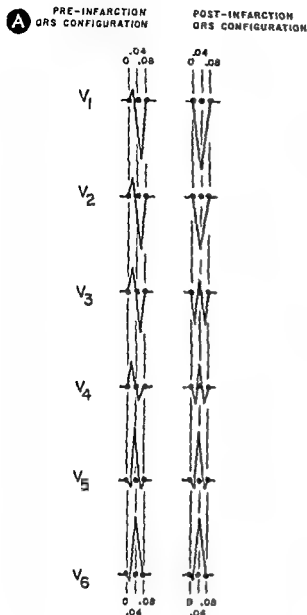
If in a given electrocardiogram there are Q waves in one or more leads satisfying the criteria listed above, the Q waves can ordinarily be considered a reliable indication of the presence of infarction. However, the converse of this does not necessarily hold true, that is, the failure of Q waves to meet the criteria for abnormality certainly cannot be regarded as incontrovertible evidence against the diagnosis of infarction. The application of the above criteria to the diagnosis of specific types of infarction and the limitations of the criteria in this regard are discussed later (p. 291).

Evolution of an Infarction

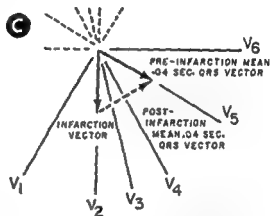
It will be recalled that in experimentally produced myocardial infarction there appear, in sequence, the electrocardiographic changes of myocardial ischemia, subepicardial injury, and, finally, myocardial necrosis

Fig. 165.—Development and evolution of the S-T segment and the Q and T wave changes accompanying myocardial infarction, as related to the time of onset of the infarction. The more a curve rises above the isoelectric line, the taller is the T wave or the greater the S-T segment elevation, while the greater the descent of the curve below the isoelectric line, the deeper is the Q wave or the inverted T wave. (After Lepschkin.)





Calculation of the Infarction Vector from the Pre-Infarction and Post-Infarction Mean .04 Sec. QRS Vectors in Horizontal Plane



Calculation of the Post-Infarction Mean .04 Sec. QRS Vector from the Corresponding Pre-Infarction QRS Vector and the Infarction Vector

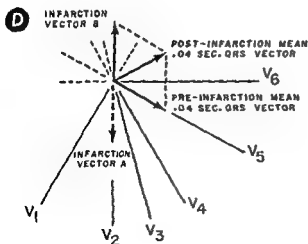


Fig. 164.—A-D, methods for calculating the infarction vector and the postinfarction mean instantaneous 0.04-second QRS vector. It should be noted that, strictly speaking, the infarction vector as depicted in **B** and **C** is defined as the vector representing the forces normally produced by the infarcted area of ventricular muscle. However, as

and it is therefore equal in magnitude to the latter forces but opposite in direction

... become smaller, in which case the normal Q wave.

tend to decrease

ap;
the
m
vi

3 The QRS loop, now distorted by the effect of the myocardial infarction, tends to close as the S-T vector disappears. The T loop becomes elongated and may be written at a constant rate of inscription. The long axis of the T loop tends to be directed away from the area of infarction.

In a strict sense, the diagnosis of myocardial infarction can only be made if there is electrocardiographic evidence of muscle necrosis in the form of abnormal Q waves or equivalent QRS changes. Nevertheless, if there is a strong clinical suspicion of infarction, S-T segment elevation of significant degree, although unaccompanied by QRS abnormalities, should be considered suggestive evidence, electrocardiographically, of infarction until proved otherwise by serial tracings. In most cases of infarction, Q waves and deeply and symmetrically inverted T waves will have appeared in the diagnostic leads within the first 24-48 hours, and the S-T segments will have begun their descent to the isoelectric base line. Once S-T segment elevation has disappeared after an infarction, it is no longer possible to date the infarction on the basis of the electrocardiographic findings in a single record, since QRS and T wave abnormalities resembling those present in the acute phase of infarction can persist indefinitely.

Terminology and Classification of Infarction Patterns

In the past, the terminology of infarction tended to stress the anatomic location of the infarction (e.g., anterior, posterior, lateral) because the infarction's site was believed to govern almost entirely the distribution of QRS abnormalities in the electrocardiographic leads. This method of designating the various infarction

patterns was in accord with the classic electrocardiographic-pathologic correlation studies of Myers. However, recent evidence and experience indicate that the electrical and anatomic locations of an infarction, although often approximately the same, frequently differ to a widely varying degree. That discrepancies should occur between electrocardiographic and pathologic localization of infarctions is probably less surprising than is the fact that the two studies correlate as frequently as they do. Two of the factors contributing to the inconsistencies in electrocardiographic and pathologic correlation are as follows:

a) The electrocardiogram is recorded with distant indirect leads which respond to the cardiac potentials as if the latter were actually a single equivalent dipole. This fact is not compatible with precise anatomic localization of a myocardial infarction.

b) Undoubtedly, factors other than the anatomic site of an infarction influence the distribution of QRS abnormalities in the electrocardiographic leads, as was pointed out in the preceding discussion of the mechanism of the Q waves of infarction. Thus the direction of the unbalanced forces produced by an infarction, and perhaps even the time they appear in the QRS interval, may well be modified by variations in intraventricular conduction, perifocal block, and/or co-existing abnormalities of ventricular muscle. In view of the uncertainty as to the mechanism of the QRS abnormalities of infarction, the meaning of these ab-

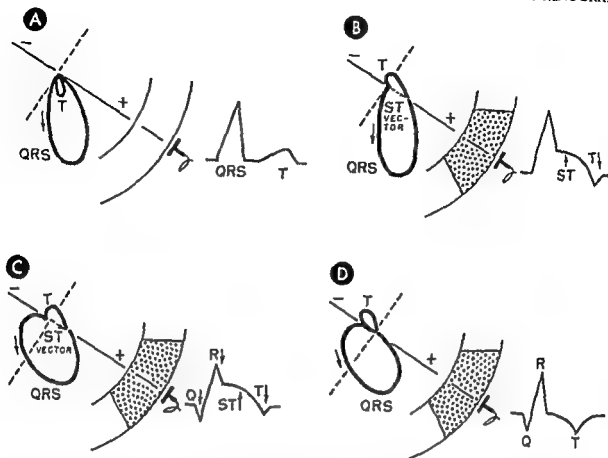


Fig. 166.—Evolution of a myocardial infarction. The related changes in the electrocardiogram and vectorcardiogram are depicted in A, before infarction, in B, during the subepicardial injury and ischemia stage of infarction, in C, during the stage of myocardial necrosis or infarction, and in D, during regression of the injury pattern. (See text for detailed description.)

or infarction. Clinically, myocardial infarction passes through much the same sequence. However, the initial stage, consisting of subendocardial ischemia, soon followed by transmural ischemia, is ordinarily so transient that the electrocardiographic abnormality first

detected is the S-T segment elevation of subepicardial injury. The evolution of electrocardiographic and related vectorcardiographic changes during a typical myocardial infarction may be summarized in general terms as follows (see also Figs. 165 and 166):

ELECTROCARDIOGRAM

1 S-T SEGMENT ELEVATION appears in diagnostic leads and is usually the first indication of a developing infarction. The T wave is often obscured by the S-T segment elevation, but, if it is discernible, it may show slight terminal inversion. The superimposition of S-T segment elevation on the pattern of an old infarction usually signifies fresh infarction in the region of previous involvement.

Duration. This stage may last only a few hours. However, it usually begins to subside after a week and disappears completely within 2 weeks to several months. Regression of the injury pattern heralds either the recovery or death of heart muscle. Thus, in the latter instance, the descent of the S-T segments is accompanied by developing electrocardiographic evidence of myocardial necrosis.

2 ABNORMAL Q OR QS WAVES usually make their appearance in diagnostic leads within several hours to sev-

VECTORCARDIOGRAM

1 This phase is reflected in the vectorcardiogram by failure of the QRS sE loop to close. The terminal portion of the loop does not return to its point of origin but tends to be displaced toward the effective site of subepicardial injury. The S-T vector which is directed from the point of origin of the loop to its terminus points toward the area of injury. The T loop may be small and directed away from the involved region.

2 Because the electrically inert infarcted myocardium disrupts the normal balance of electrical forces, the ini-

may become smaller, in a given case it may not invariably, preceded by an abnormal Q wave.

Duration The electrocardiographic and vectorcardiographic findings reflecting death of myocardial muscle may persist for months, years, or indefinitely. When these abnormalities persist indefinitely, as is commonly the case, they tend to become less prominent.

Steadily away from the involved area.

3 The QRS loop, now distorted by the effect of the myocardial infarction, tends to close as the S-T vector disappears. The T loop becomes elongated and may be written at a constant rate of inscription. The long axis of the T loop tends to be directed away from the area of infarction.

Duration The

away from the infarcted region

In a strict sense, the diagnosis of myocardial infarction can only be made if there is electrocardio-

theless, if there is a strong suspicion of infarction, S-T segment elevation of significant degree, although unaccompanied by QRS abnormalities, should be considered suggestive evidence, electrocardiographically, of infarction until proved otherwise by serial tracings. In most cases of infarction, Q waves and deeply and symmetrically inverted T waves will have appeared in the diagnostic leads within the first 24-48 hours, and the S-T segments will have begun their descent to the isoelectric base line. Once S-T segment elevation has disappeared after an infarction, it is no longer possible to date the infarction on the basis of the electrocardiographic findings in a single record, since QRS and T wave abnormalities resembling those present in the acute phase of infarction can persist indefinitely.

Terminology and Classification of Infarction Patterns

In the past, the terminology of infarction tended to stress the anatomic location of the infarction (e.g., anterior, posterior, lateral) because the infarction's site was believed to govern almost entirely the distribution of QRS abnormalities in the electrocardiographic leads. This method of designating the various infar-

ction patterns was in accord with the classic electrocardiographic-pathologic correlation studies of Myer. However, recent evidence and experience indicate that the electrical and anatomic locations of an infarction, although often approximately the same, frequently differ to a widely varying degree. That discrepancies should occur between electrocardiographic and pathologic localization of infarctions is probably less surprising than is the fact that the two studies correlate as frequently as they do. Two of the factors contributing to the inconsistencies in electrocardiographic and pathologic correlation are as follows.

a) The electrocardiogram is recorded with distant indirect leads which respond to the cardiac potentials as if the latter were actually a single equivalent dipole. This fact is not compatible with precise anatomic localization of a myocardial infarction.

b) Undoubtedly, factors other than the anatomic site of an infarction influence the distribution of QRS abnormalities in the electrocardiographic leads, as was pointed out in the preceding discussion of the mechanism of the Q waves of infarction. Thus the direction of the unbalanced forces produced by an infarction, and perhaps even the time they appear in the QRS interval, may well be modified by variations in intraventricular conduction, pericardial block, and/or co-existing abnormalities of ventricular muscle. In view of the uncertainty as to the mechanism of the QRS abnormalities of infarction, the meaning of these ab-

TABLE 18—CLASSIFICATION OF ELECTROCARDIOGRAPHIC AND VECTORCARDIOGRAPHIC INFARCTION PATTERNS

	EFFECTIVE ELECTRICAL LOCATION	DIRECTION OF INFARCTION VECTOR
A. Anterior infarctions	Anteroseptal Anterior Anterolateral Extensive anterior	Left posterior Posterior Right posterior Posterior, right
B. Inferoposterior infarctions	Inferior or diaphragmatic Posterolateral Strictly posterior	Superior, right Anterior, right Anterior
C. Infarctions in combined locations		
D. Infarction superimposed on bundle branch block		

normalities in terms of the localization of an infarction must remain in doubt for the time being.

For that matter, the actual anatomic site of an infarction is largely superfluous information from the standpoint of clinical significance, at least insofar as is presently known.

The system of nomenclature followed in this text labels an infarction according to its effective electrical position as indicated by the direction of the infarction vector or unbalanced forces created by the infarction (Table 18). As will be recalled, in myocardial infarction the unbalanced forces are directed away from the effective electrical site of the infarction. For example, in anterior myocardial infarction, the unbalanced forces created by the infarction, which, for descriptive convenience, can be represented by and referred to as an *infarction vector*, are directed posteriorly,

conversely, in a strictly posterior infarction the infarction vector is directed anteriorly. In the preceding examples, the effective electrical sites of the two infarctions are in anterior and posterior left ventricular wall, respectively, although this localization of the infarctions may or may not agree with their anatomic sites as determined at postmortem.

Since the ventricular activation process in each type of infarction will be described in terms of the schematic instantaneous VA vectors, the following general relationships should be kept in mind:

1. When myocardial infarction alters the 0.01-second VA vector, there is usually involvement of the apical portion of the interventricular septum.
2. When the 0.02-second VA vector is affected, there is involvement of apicoanterior or apicodiaphragmatic left ventricular wall (Fig. 167).
3. Infarction of anterolateral or diaphragmatic left ventricular free wall generally disturbs both the 0.02- and 0.04-second VA vectors.
4. Alterations in the terminal instantaneous vectors, such as the 0.06- and 0.08-second VA vectors, may well be indicative of infarction of posterior, posterobasal, or posterolateral left ventricular wall, the regions last activated in the left ventricle.

Similarly, the following general relationships can be considered to exist between the VA vectors and the QRS sE loop of the vectorcardiogram.

1. The 0.01-second VA vector can be related to the initial deflection of the QRS sE loop to the right and/or superiorly.
2. The 0.02-second VA vector corresponds roughly

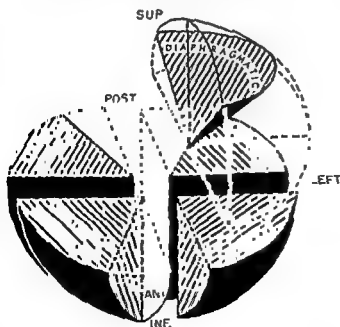


Fig. 167.—Approximate range of variation in orientation of the mean 0.02-second instantaneous QRS spatial vector in the normal vectorcardiogram and in vectorcar-

to the first half of the efferent limb of the QRS sE loop.

The 0.04-second VA vector is analogous to the long axis of maximal instantaneous vector of the QRS sE loop.

The 0.06-second VA vector can be regarded as representative of the instantaneous vectors forming the latter half of the efferent limb of the

VA vector, the

when necessary, to represent abnormal terminal QRS forces.

The relationships in mind, one can

The authors have found the original 0.02-second instantaneous spatial vector of the QRS sE loop to be of great value in the vectorcardiographic diagnosis of myocardial infarction (Fig 167).

TABLE 19—RELATIONSHIP BETWEEN THE ELECTRICAL SITE OF INFARCTION, THE VA VECTORS AFFECTED, AND THE RESULTING QRS CHANGES

ELECTRICAL SITE OF INFARCTION	DIRECTION OF INFARCTION VECTOR	INSTANTANEOUS VA VECTORS AFFECTED	RESULTING ABNORMALITIES OF QRS COMPLEX	RESULTING ABNORMALITIES OF QRS sE LOOP
Anteroseptal	Left, posterior	0.01-second septal and 0.02-second apicoanterior VA vectors	QS deflections or abnormal Q waves in leads V_1 , V_2 and sometimes V_3	Leftward and posterior inscription of the initial deflection and early efferent limb of the loop
Anterior	Posterior	0.02- and 0.04-second left ventricular VA vectors	QS deflections or abnormal Q waves in leads V_3 , V_4 , and V_5	Posterior displacement of the efferent limb and sometimes the long axis of the loop
Anterolateral	Right, posterior	0.02- and 0.04-second VA vectors	Abnormal Q waves in leads I, V_3 , and V_4	Posterior and rightward or medial displacement of the efferent limb and long axis of the loop
Extensive anterior	Right, posterior	0.01- to 0.06-second VA vectors	Abnormal Q waves in leads I and V_1 through V_5	Initial inscription of loop to the right and posterior and rightward or medial displacement of both efferent and afferent limbs and long axis of the loop
Diaphragmatic (inferior)	Superior	0.02- and 0.04-second VA vectors	Abnormal Q waves in leads II, III, and aVF	Superior displacement of efferent limb and sometimes the long axis of the loop
Posterolateral	Right, anterior	0.02- and 0.04-second VA vectors	Abnormally tall and/or wide R waves in lead V_1 and abnormal Q waves in leads I and V_4	Rightward and anterior displacement of the early efferent limb and anterior displacement of later efferent limb and long axis of loop
Strictly posterior	Anterior	0.04- and 0.06-second (or 0.08-second) VA vectors	Low, vibratory RR' deflection or rSR' deflection in leads V_{4R} and V_1	Anterior displacement of the long axis and afferent limb of the loop

Anterior Myocardial Infarction

SEVERAL DIFFERENT electrocardiographic and vectorcardiographic infarction patterns are included under the general designation of *anterior myocardial infarction*. In this text the following terms will be employed to label more specifically the various types of anterior infarction: *anteroseptal*, *strictly anterior*, *anterolateral*, and *extensive anterior*. Although the anterior

infarctions differ somewhat from one another as to their precise electrical position and consequently their electrocardiographic and vectorcardiographic features, nevertheless they have one characteristic in common—that is, each type of infarction gives rise to unbalanced forces directed to a varying degree posteriorly.

ANTEROSEPTAL INFARCTION

Anteroseptal infarction is usually caused by occlusion of one of the terminal ramifications of the descending branch of the left coronary artery and involves the anteroapical portion of the interventricular septum and adjacent anterior paraseptal wall of the left ventricle. In the past, two electrocardiographic infarction patterns were ascribed to anteroseptal infarction, one resulting from involvement of both the septum and the paraseptal aspect of the left ventricle and the other from paraseptal involvement only. In this text, the authors prefer to designate the first infarction variant “anteroseptal” and the second “strictly anterior,” since the vectorcardiographic findings in the two types of anterior infarction are quite distinctive.

The Instantaneous VA Vectors

As will be recalled, the apicoanterior, paraseptal portion of left ventricular wall and adjacent septum, which are the usual anatomic sites of involvement in anteroseptal infarction (see also Fig. 168), undergo activation within approximately the first 0.02 second of the QRS interval, so that this type of infarction typically alters the orientation and magnitude of the 0.01- and 0.02-second VA vectors.

0.01- AND 0.02-SECOND VA VECTORS

Both the 0.01-second septal VA vector and the 0.02-second apicoanterior VA vector are abnormally oriented to the left and posteriorly in anteroseptal myocardial infarction. This has been attributed to an abnormal spread of depolarization through the septum as the result of its involvement by infarction and to the loss of electromotive forces directed anteriorly consequent to apicoanterior wall involvement. Because of the loss of electrical forces directed to the right and anteriorly, the forces directed oppositely become preponderant early in the QRS interval. Thus, both 0.01- and 0.02-second VA vectors are displaced posteriorly and to the left. Sometimes it may happen that the loss of anteriorly directed forces produced by activation of apicoanterior left ventricular wall is not sufficient to displace the 0.02-second VA vector into the negative field of lead V_2 , even though the vector is located less anteriorly than is normally the case.

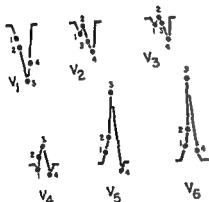
The postinfarction 0.01-second and 0.02-second VA vectors project the following deflections on the precordial leads.

Lead V_1 .—Beginning downstroke of a QS deflection.

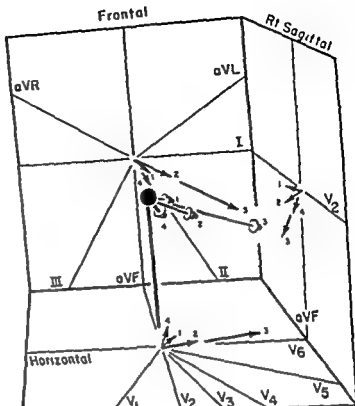
Lead V_2 .—Beginning downstroke of a QS deflection (if the 0.02-second VA vector is situated posteriorly, just like the 0.01-second VA vector), or a small



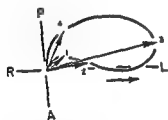
A Anteroseptal Myocardial Infarction



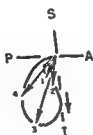
C QRS Deflections Projected on Scalar Leads



B Instantaneous VA Vectors in Anteroseptal Myocardial Infarction



Horizontal



Right Sagittal



Frontal

D Planar QRS Loops in Anteroseptal Myocardial Infarction

and to the left. The subsequent instantaneous vectors remain unaffected, for all intents and purposes. Because of the leftward and posterior deviation of the first two vectors, leads V_1 through V_6 record abnormal initial negativity in the form of QS or rS deflections (C). The scalar limb leads are not depicted in B because, as is characteristic in anteroseptal infarction, the abnormalities are confined to the precordial leads. In D, note the absence of the normal, initial rightward and anterior deflection of the QRS loop and the anterior concavity in the efferent limbs of the horizontal and sagittal loops.

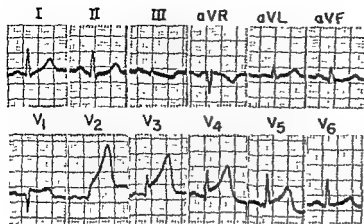


Fig. 169.—Electrocardiographic findings in the earliest phase of a developing acute antero-septal myocardial infarction. Although a QS deflection has appeared in lead V_1 and small Q waves in leads V_2 through V_4 , the most prominent findings at this stage of the evolution of the infarction pattern are the markedly elevated S-T segments in leads V_1 through V_4 and the very tall upright T waves in leads V_3 through V_6 . The S-T segment elevation in the anterior precordial leads is compatible with anterior subepicardial injury, while the tall upright T waves are probably indicative of subendocardial ischemia. If subsequent electrocardiograms had been available, leads V_1 through V_4 would probably have shown deepening Q waves and progressive T wave inversion as the S-T segments return to the isoelectric level.

initial Q wave followed by a minute R wave (if the 0.01-second vector lies posteriorly and the 0.02-second VA vector slightly anteriorly).

Lead V_1 , and sometimes lead V_2 .—Beginning downstroke of a QS deflection or a small initial Q wave followed by the beginning upstroke of a small or sometimes a larger R wave.

Leads V_4 and V_6 .—Beginning upstroke of an R wave.

0.04- AND 0.06-SECOND VA VECTORS

Inasmuch as anterolateral and basal regions of the left ventricle are not affected in antero-septal myocardial infarction, the orientation and magnitude of the electrical forces produced by these regions are normal, or at least essentially the same as before infarction, so that the precordial leads register the following deflections.

Leads V_1 through V_3 , or, sometimes, V_4 .—Comple-

tion of the S wave of a QS or a qRS complex, or of an R wave of a qR deflection.

Leads V_4 and V_6 .—Completion of the R wave, with or without a small terminal S wave.

The characteristic deviation of the S-T segments and the T wave abnormalities which accompany the different types of anterior myocardial infarction will be described, and the mechanism of these changes reviewed, in a separate section at the end of this chapter.

QRS Criteria for Diagnosis

The QRS criteria utilized by the authors in making the diagnosis of antero-septal myocardial infarction are as follows (see also Fig 169):

1. A small abnormal Q wave preceding an rS deflection in V_1 , or the presence of a QS deflection in V_1 and leads to the right.

TABLE 20—ORIENTATION OF THE MEAN 0.02-SECOND AND MAXIMAL MEAN INSTANTANEOUS VECTORS OF THE QRS sE LOOP IN ANTEROSEPTAL INFARCTION

	HORIZONTAL			RIGHT SAGITTAL			FRONTAL		
	Extreme Range	Av	Usual Range*	Extreme Range	Av	Usual Range*	Extreme Range	Av	Usual Range*
Mean 0.02-second instantaneous QRS vector	-15° to -5°	-10°	.	+100° to +150°	+120°		-10° to +30°	+5°	.
Maximal instantaneous QRS vector	-30° to -10°	-20°	.	+110° to +170°	+135°		+10° to +45°	+30°	...

*Usual range = range to 85% of cases

2. The presence of QS deflections or abnormal Q waves producing qRS, qR, or qRs deflections in one or more of the next three leads (V_2 , V_3 , and V_4).
3. An abnormal decrease in the relative amplitude of the R waves without their disappearance as the chest electrode is moved to the left of V_3 .
4. The absence of normal septal Q waves in leads I and V_6 .

Vectorcardiographic Findings

The average orientation and the extreme ranges of variation in orientation of the mean QRS-second and maximal mean instantaneous QRS vectors of the horizontal, sagittal, and frontal loops in antero-septal infarction are shown in Table 20.

HORIZONTAL QRS LOOP—In antero-septal infarction, the diagnostic abnormalities, if present, appear in the horizontal and right sagittal projections of the

vectorcardiogram. The distinctive feature of the horizontal QRS loop is the absence of the normal initial deflection of the loop to the right and anteriorly. Instead, with onset of ventricular activation, the horizontal QRS loop moves immediately to the left and posteriorly and usually remains in this quadrant during its counterclockwise inscription. In general, the long axis of the horizontal QRS loop (or, the maximal instantaneous QRS vector in the horizontal projection) tends to be slightly more posterior in antero-septal infarction than normally. Sometimes the efferent limb of the loop is displaced slightly posteriorly or may show minor posterior bowing in its early portion.

RI
in ar
normal
lim
for
are

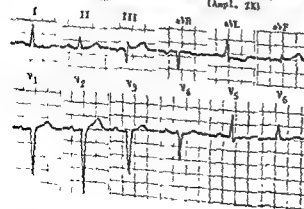
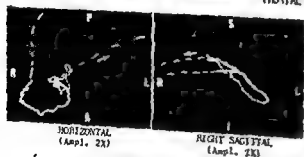
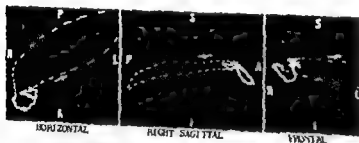


Fig. 170—Electrocardiographic and vectorcardiographic findings in healed antero-septal myocardial infarction.

In the electrocardiogram, the diagnostic findings are the QS deflections in leads V_2 , V_3 , and V_4 . The absence of the normal septal Q wave in leads I and V_6 and the fact that the S-T segments are isoelectric and the T waves upright in the right precordial leads are also diagnostic of the infarction is not

anterior concavity in the first half of the efferent limb of the horizontal QRS loop

partly to the left and partly to right—hence, the biphasic T wave in lead I, low upright T wave in lead V_6 , and upright T waves in the right midprecordial leads.

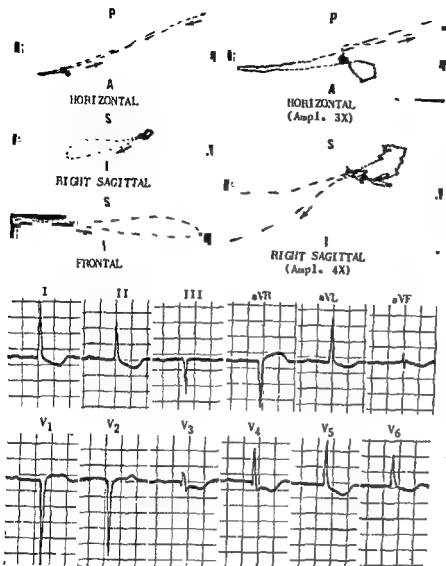


Fig. 171.—Electrocardiographic and vectorcardiographic findings in healed anteroapical myocardial infarction with coexisting left ventricular hypertrophy.

In the electrocardiogram, the presence of QS deflections in leads V_1 and V_2 and a small Q wave in lead V_3 is indicative of old anteroapical myocar-

...
existing left ventricular hypertrophy

In the vectorcardiogram, the initial deflection of the QRS sE loop posteriorly and then to the left is diagnostic of anteroapical infarction, while the elongated and posteriorly and superiorly oriented planar QRS loops and the discordant orientations of the T sE and QRS sE loops are consistent with left ventricular hypertrophy

a clockwise direction of inscription, if the sagittal loop is first inscribed superiorly, then it often presents a figure-of-eight configuration, the proximal component of which has a counterclockwise inscription and the larger distal component a clockwise direction of inscription. Figure-of-eight sagittal QRS loops have been a relatively common finding in anteroapical infarction in our experience.

FRONTAL QRS LOOP.—Since the unbalanced forces created by an anteroapical infarction are directed more or less perpendicular to the frontal plane, the frontal QRS loop does not show diagnostic changes. Although the frontal QRS loop is inscribed initially to the left, this finding has little diagnostic value because the normal frontal QRS loop often appears to proceed directly to the left (Figs 170 and 171).

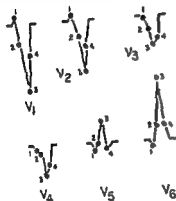
STRICTLY ANTERIOR INFARCTION

The unbalanced forces created by anterior myocardial infarction are oriented almost directly posteriorly, as if the site of the infarction were in paraseptal anterior left ventricular wall, which, more often than not, proves to be the case on pathologic study (However, as previously pointed out, the electrical and anatomic sites of an infarction need not invariably be

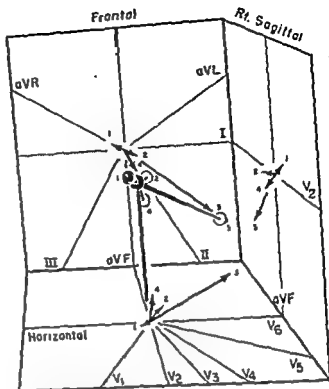
identical). The anterior wall of the left ventricle is activated relatively early in the QRS interval. Consequently, the failure of the infarcted anterior wall to generate potentials during the time it normally is undergoing activation permits oppositely directed electrical forces to become preponderant. For this reason, the electrical effects of an anterior infarction



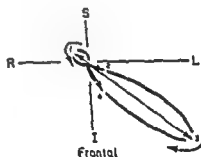
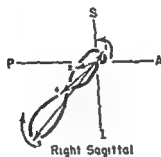
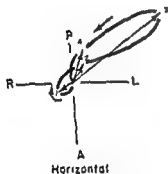
A Anterior Myocardial Infarction



C QRS Deflections Projected on Scalar Leads



B Instantaneous VA Vectors in Anterior Myocardial Infarction



D Planar QRS Loops in Anterior Myocardial Infarction

posteriorly. In fact, the long axis of the horizontal QRS loop is deviated farther posteriorly than normally. Note, also, that the direction of inscription of the sagittal QRS loop is counterclockwise for the initial part of the QRS interval.

are evidenced in the early part of the QRS deflection or QRS sE loop.

The Instantaneous VA Vectors

The electrical forces produced by septal and ventricular activation in strictly anterior myocardial infarction can be presented in simplified manner in terms of the instantaneous vectors (see also Fig. 172):

0.01-SECOND VA VECTOR

Infarction restricted to the anterior aspect of the left ventricle does not disturb the normal orientation of the 0.01-second VA vector to the right and anterior, in contrast with the situation in anteroseptal infarction. Thus, the appearance of the 0.01-second

only dominate the electrical field of the heart from 0.02 to 0.04 second or longer after onset of ventricular activation. The postinfarction 0.02- and 0.04-second VA vectors, which are the resultants of the corresponding preinfarction VA vectors and the posteriorly directed infarction vector, are both displaced farther posteriorly. The persisting leftward deviation of the 0.04-second VA vector probably reflects activation of uninvolved anterolateral and lateral walls of the left ventricle. The postinfarction 0.02- and 0.04-second VA vectors produce the following deflections in the precordial leads:

Leads V₁ and V₂.—Downstroke of a deep S wave. Inasmuch as the normal 0.02-second VA vector plays a more important role in the genesis of the initial R wave in lead V₂ than in lead V₁, the posterior displacement of this vector in anterior infarction fre-

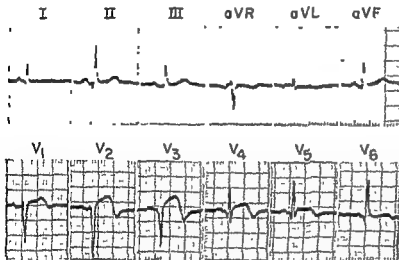


Fig. 173.—Electrocardiographic findings in acute anterior myocardial infarction. The salient features are a normal initial R wave in lead V₂ and a relatively smaller R wave in V₁, a QS deflection in lead V₁, a promi-

of myocardial necrosis, the S-T segment elevation of anterior subepicardial injury, and the T wave changes of transmural ischemia—all of which add up to acute anterior infarction

VA vector in strictly anterior myocardial infarction is accompanied in the precordial leads by inscription of the following deflections.

Lead V₁.—Upstroke of a small initial R wave.

Lead V₂.—Beginning upstroke of a small initial R wave.

Leads V₃ and V₄.—Depending on the anterior extent of the 0.01-second VA vector, these leads may record a small initial R wave, a Q wave, or an isoelectric segment

Leads V₅ and V₆.—Downstroke of a small initial Q wave.

0.02- AND 0.04-SECOND VA VECTORS

Normally, these vectors are determined largely by activation of left ventricular free wall. In anterior infarction, apicoanterior wall and adjacent anterior wall of the left ventricle are rendered electrically inert, with the result that opposing forces oriented posteri-

quently causes the R wave in lead V₂ to have a lower amplitude, relative to the total QRS amplitude, than that of the R wave in lead V₁.

Leads V₃ and V₄.—Downstroke of a deep S wave following a minute initial R wave, or the downstroke of a Q wave of 0.04-second duration. When these leads register a small initial R wave, its relative amplitude is less than that in leads V₂ and/or V₁. Occasionally, particularly in old anterior infarctions, leads V₁ through V₄ may all display rS deflections. In this event, the relative amplitude of the initial R wave decreases from right to left in two or more of the leads, in contrast with the normal progressive increase in the R/S ratio from right to left across the precordium. Sometimes the only evidence of an old infarction may be the presence of a small initial Q wave preceding a small R wave and a deep S wave (qrS deflection). In general, a Q wave (even if relatively small and narrow) which precedes the r wave of an rS deflection recorded in a right or midprecordial lead should be

viewed with suspicion, particularly if the Q wave is more prominent than the Q waves in lead V_3 or V_6 or

hypertrophy.

Leads V_3 and V_6 .—Completion of the Q wave and upstroke of the following R wave. Sometimes, particularly in lead V_3 , the Q wave may be suspiciously deep and/or wide and the R wave of somewhat low amplitude, but, typically in strictly anterior infarction, leads V_3 and V_6 do not show diagnostic changes involving the QRS deflections.

0.06-SECOND VA VECTORS

In the vast majority of anterior infarctions, the terminal QRS forces are not characteristically disturbed. However, occasionally the 0.06-second VA vector or subsequent instantaneous vectors may be directed to the right, away from the 0.04-second or maximal instantaneous vector. Grant has postulated that in some cases peri-infarction block may be the mechanism responsible for this variation. (Peri-infarction block is discussed in Chapter 21.)

Leads V_1 and V_2 .—Completion of the S wave of an rS deflection

Leads V_4 and V_5 .—Completion of the S wave of a QS or Qrs deflection, or completion of the II wave of a Qr or rSR' deflection.

Leads V_6 and V_6 .—Completion of the R wave of a qR deflection or the small S wave of a qRs deflection.

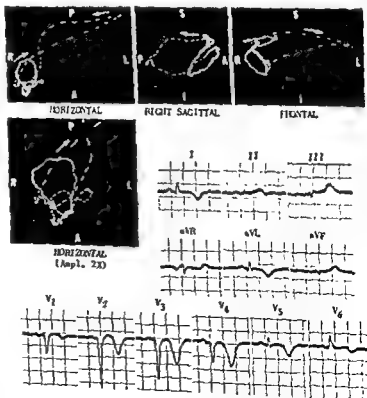
QRS Criteria for Diagnosis

1. The presence of initial R waves in leads V_1 or V_2 and of abnormal Q waves in one or more precordial leads to the left of V_1 (i.e., leads V_2 , V_3 , or V_4). The Q wave abnormality in the preceding leads can present in the form of QS deflections, small Q waves of at least 0.02-second width occurring in qRS deflections, or abnormally wide and/or deep Q waves of QR or QRS deflections.
2. A right-to-left decrease in the relative amplitudes of the R waves without their disappearance in precordial leads to the left of lead V_1 .
3. The presence of normal septal Q waves in leads I, V_3 , and V_6 . (As will be recalled, the absence of normal Q waves in the above leads is a common observation in anteroapical infarction. The absence of abnormally wide and/or deep Q waves in leads I, V_3 , and V_6 excludes the possibility of anterolateral, as opposed to strictly anterior, infarction [Fig. 173].)

Fig 174.—Electrocardiographic and vectorcardiographic findings in recent anterior myocardial infarction

In the electrocardiogram, lead V_1 shows an initial R wave and lead V_2 a small septal wave, but intervening leads, V_3 through V_6 , display QS deflections, isoelectric S-T segments, and deeply and symmetrically inverted T waves. This record represents a slightly later stage in the evolution of an anterior infarction than that in Figure 173.

In the vectorcardiogram, there is striking posterior displacement of the efferent limb of the QRS sE loop and a reversed direction of inscription of the sagittal QRS loop. Note the large, round, and posteriorly directed T loop in the horizontal projection. This is a typical finding in vectorcardiograms of patients with deeply and symmetrically inverted T waves of transmural ischemia.



are evidenced in the early part of the QRS deflection or QRS sE loop.

The Instantaneous VA Vectors

The electrical forces produced by septal and ventricular activation in strictly anterior myocardial infarction can be presented in simplified manner in terms of the instantaneous vectors (see also Fig. 172):

0.01-SECOND VA VECTOR

Infarction restricted to the anterior aspect of the left ventricle does not disturb the normal orientation of the 0.01-second VA vector to the right and anterior, in contrast with the situation in antero-septal infarction. Thus, the appearance of the 0.01-second

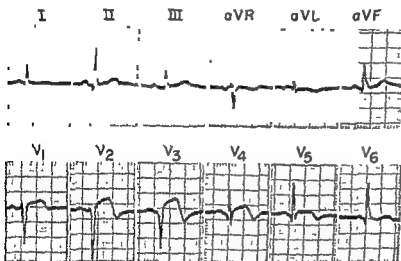


Fig. 173.—Electrocardiographic findings in acute anterior myocardial infarction. The salient features are: a normal initial R wave in lead V_1 and a relatively smaller R wave in V_2 , a QS deflection in lead V_3 , a prominent Q wave in lead V_4 , elevated S-T segments in leads V_5 through V_6 , and inverted T waves in leads V_5 through V_6 . Thus, the midprecordial leads show the QRS changes of myocardial necrosis, the S-T segment elevation of anterior subepicardial injury, and the T wave changes of transmural ischemia—all of which add up to acute anterior infarction.

VA vector in strictly anterior myocardial infarction is accompanied in the precordial leads by inscription of the following deflections

Lead V_1 .—Upstroke of a small initial R wave

Lead V_2 .—Beginning upstroke of a small initial R wave

Leads V_3 and V_4 .—Depending on the anterior extent of the 0.01-second VA vector, these leads may record a small initial R wave, a Q wave, or an isoelectric segment.

Leads V_5 and V_6 .—Downstroke of a small initial Q wave.

0.02- AND 0.04-SECOND VA VECTORS

Normally, these vectors are determined largely by activation of left ventricular free wall. In anterior infarction, apicoanterior wall and adjacent anterior wall of the left ventricle are rendered electrically inert, with the result that opposing forces oriented posteri-

orly dominate the electrical field of the heart from 0.02 to 0.04 second or longer after onset of ventricular activation. The postinfarction 0.02- and 0.04-second VA vectors, which are the resultants of the corresponding preinfarction VA vectors and the posteriorly directed infarction vector, are both displaced farther posteriorly. The persisting leftward deviation of the 0.04-second VA vector probably reflects activation of uninvolved anterolateral and lateral walls of the left ventricle. The postinfarction 0.02- and 0.04-second VA vectors produce the following deflections in the precordial leads:

Leads V_1 and V_2 .—Downstroke of a deep S wave. Inasmuch as the normal 0.02-second VA vector plays a more important role in the genesis of the initial R wave in lead V_2 than in lead V_1 , the posterior displacement of this vector in anterior infarction fre-

quently causes the R wave in lead V_2 to have a lower amplitude, relative to the total QRS amplitude, than that of the R wave in lead V_1 .

Leads V_3 and V_4 .—Downstroke of a deep S wave following a minute initial R wave, or the downstroke of a Q wave of 0.04-second duration. When these leads register a small initial R wave, its relative amplitude is less than that in leads V_2 and/or V_1 . Occasionally, particularly in old anterior infarctions, leads V_1 through V_4 may all display rS deflections. In this event, the relative amplitude of the initial R wave decreases from right to left in two or more of the leads, in contrast with the normal progressive increase in the R/S ratio from right to left across the precordium. Sometimes the only evidence of an old infarction may be the presence of a small initial Q wave preceding a small R wave and a deep S wave (qrS deflection). In general, a Q wave (even if relatively small and narrow) which precedes the r wave of an rS deflection recorded in a right or midprecordial lead should be

The average orientation and the extreme ranges of variation of orientation of the mean 0.02-second and maximal mean instantaneous QRS vectors of the horizontal, right sagittal, and frontal loops in anterior infarction are shown in Table 21.

HORIZONTAL QRS LOOP.—In anterior infarction, the horizontal QRS loop usually conforms in appearance to one of the following pattern variations.

1. The least prominent abnormality of the horizontal QRS loop may consist solely of an anterior concavity or posterior bowing of the efferent limb. The inscription of the loop is otherwise not too different from the normal. The long axis of the loop is situated posteriorly but not always to an abnormal degree. On the other hand, the posterior displacement of the 0.02-second instantaneous vector is a finding relatively rarely observed in normal vectorcardiograms.

2. Frequently in anterior infarction, the horizontal QRS loop is initially written in a clockwise direction to the right and anteriorly or sometimes posteriorly, and then the remainder of the loop is inscribed in a counterclockwise direction posteriorly and to the left. The efferent limb is displaced posteriorly and/or

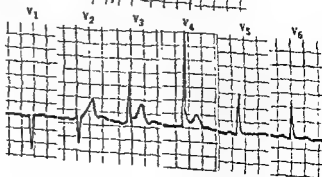
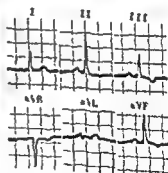
shows an anterior concavity. Both the long axis of the loop and the 0.02-second instantaneous vector tend to be oriented more posteriorly than in the pattern previously described.

3. Another variant loop pattern observed in anterior infarction is characterized by counterclockwise inscription of the initial deflection of the horizontal QRS loop to the right and anteriorly, and then clockwise inscription of the remainder of the loop to the left and far posteriorly. Thus, the horizontal QRS loop shows a figure-of-eight configuration, the initial deflection forming the smaller loop of the "eight," and the main body of the loop the larger component of the "eight." On the average, the maximal mean instantaneous vector and mean 0.02-second instantaneous vector of the horizontal QRS loop occupy a more posterior position in this pattern variant than in any of the others observed in strictly anterior infarction.

4. Finally, the horizontal QRS loop is sometimes written in a clockwise direction initially to the right and anteriorly or posteriorly but, in contrast with the QRS loop configuration described above in paragraph 2, the rest of the loop continues to be inscribed in a



Fig 176.—Well-localized anterior myocardial infarction which can be diagnosed only in the vectorcardiogram. The electrocardiogram shows no definite evidence of anterior myocardial infarction. The significance of the elevated S-T segments in leads V_4 and V_5 with reference to the diagnosis of infarction would be impossible to determine without serial tracings. However, the marked anterior concavity in the efferent limb of the QRS sE loop of the vectorcardiogram is indicative of a well-localized anterior infarction.



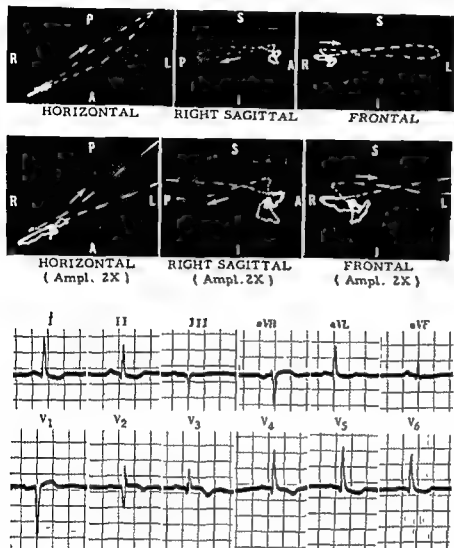


Fig. 175.—Electrocardiographic and vectorcardiographic findings in healed or old anterior myocardial infarction. The QRS abnormalities diagnostic of infarction are confined chiefly to leads V_1 and V_2 of the electrocardiogram. The horizontal QRS loop of the vectorcardiogram is strikingly abnormal in that its direction of inscription is completely reversed. Clockwise-inscribed horizontal QRS loops with normal rightward and anterior initial deflections are frequently observed in anterior myocardial infarction. There is an S-T vector which is best demonstrated in the sagittal and frontal projections. It is directed to the right and superiorly and therefore projects depressed S-T segments on leads I, aVL, and left precordial leads. The T sE loop is oriented almost 180° away from the QRS sE loop.

Vectorcardiographic Findings

Although the QRS sE loop in strictly anterior infarction tends to be variable in appearance, as will be described below, the loop in most instances will display at least the following two salient features. (1)

In contrast with the horizontal QRS loop in antero-septal infarction, the corresponding loop in anterior infarction is written initially to the right and usually anteriorly, or occasionally slightly posteriorly. (2) The efferent limb of the QRS sE loop, either in whole or in part, is written abnormally far posteriorly.

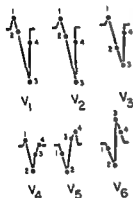
TABLE 21—ORIENTATION OF THE MEAN 0.02-SECOND AND MAXIMAL MEAN INSTANTANEOUS VECTORS OF THE QRS sE LOOP IN STRICTLY ANTERIOR INFARCTION

	HORIZONTAL			RIGHT SAGITTAL			FRONTAL		
	Extreme Range	Av	Usual Range*	Extreme Range	Av	Usual Range*	Extreme Range	Av	Usual Range*
Mean 0.02-second instantaneous QRS vector	-100° to -5°	-30°	-60° to -10°	$+100^\circ$ to -110°	$+170^\circ$	$+110^\circ$ to -150°	-120° to $+85^\circ$	$+15^\circ$	-70° to $+65^\circ$
Maximal mean instantaneous QRS vector	-60° to -10°	-30°	-35° to -10°	$+110^\circ$ to -170°	$+155^\circ$	$+130^\circ$ to 180°	-5° to $+45^\circ$	$+15^\circ$	$+5^\circ$ to $+35^\circ$

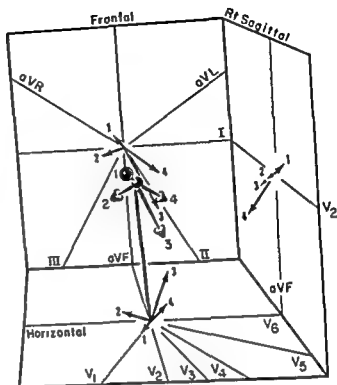
*Usual range = range in 85% of cases



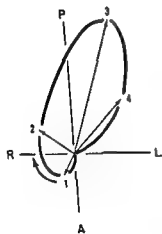
A Anterolateral Myocardial Infarction



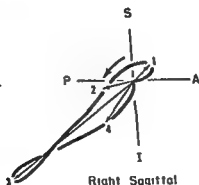
C QRS Deflections Projected on Scalar Leads



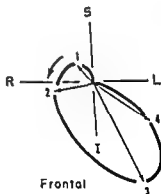
B Instantaneous VA Vectors in Anterolateral Myocardial Infarction



Horizontal



Right Sagittal



Frontal

D Planar QRS Loops in Anterolateral Myocardial Infarction

clockwise direction to the left and posteriorly. Thus the efferent limb of the horizontal loop is shifted posterior to the afferent limb. Both maximal mean and mean 0.02-second instantaneous vectors lie abnormally far posteriorly.

RIGHT SAGITTAL QRS LOOP.—In anterior infarction, the sagittal QRS loop confirms the marked posterior displacement of the long axis and mean 0.02-second instantaneous vector of the QRS Σ loop. In about 75% of the cases, the sagittal QRS loop is inscribed either

entirely or in part in a counterclockwise direction. In the latter event, the loop has a figure-of-eight, configuration, the proximal component being counterclockwise inscribed and the distal component clockwise inscribed. A figure-of-eight sagittal QRS loop is probably the most common configuration observed in anterior infarction.

FRONTAL QRS LOOP.—The frontal projection of the QRS Σ loop exhibits no characteristic abnormalities in localized anterior infarction (Figs. 174–176).

ANTEROLATERAL INFARCTION

By and large, infarctions of the lateral wall of the left ventricle can be placed in either of two categories: anterolateral infarction or posterolateral infarction. In *anterolateral infarction* the infarction vector (representing the unbalanced forces produced by the infarction) is directed somewhat posteriorly but for the most part to the right. Thus, abnormal Q waves are projected typically on leads I, aVL, V₅, and V₆ and sometimes on lead V₄. In *posterolateral infarction* the infarction vector is directed somewhat anteriorly but mainly to the right. In the electrocardiogram, leads V₆ and V₇ typically register abnormal Q waves, and leads V_{AR}, V₁, and V₂ record relatively tall R waves of 0.04 second or more duration. In our experience, virtually all lateral infarctions fall into one of these two groups, and it does not seem necessary to distinguish a third category of *strictly lateral infarction*. Posterolateral infarction is discussed in Chapter 20, dealing with inferoposterior myocardial infarctions.

The Instantaneous VA Vectors

The electrical forces produced during ventricular activation in anterolateral infarction can be presented in simplified manner in terms of the instantaneous VA vectors (see also Fig. 177).

0.01-SECOND VA VECTOR

Inasmuch as septal depolarization is ordinarily not affected in anterolateral infarction, the 0.01-second

VA vector is of the same order of magnitude and the same direction as normal. The 0.01-second VA vector is therefore directed to the right, anteriorly, and either superiorly or inferiorly and projects the following deflections on leads V₁, V₅, V₆, I and aVL.

Lead V₁.—Upstroke of an initial R wave.

Leads V₅, V₆, I, and aVL.—Beginning downstroke of a Q wave.

0.02- AND 0.04-SECOND VA VECTORS

The anterolateral wall of the left ventricle, which undergoes activation between 0.02 and 0.04 second of the QRS interval, is electrically inert and therefore no longer produces potentials to counterbalance oppositely directed electrical forces. The forces left unbalanced can be represented by an infarction vector, which is directed to the right and posteriorly. The postinfarction 0.02-second VA vector, which is the resultant of the infarction vector and the corresponding preinfarction 0.02-second vector (normally oriented to the left and anteriorly) is therefore displaced to the right and anteriorly or slightly posteriorly. Similarly, the postinfarction 0.04-second VA vector, which is the resultant of the infarction vector and the preinfarction 0.04-second vector situated to the left and posteriorly, assumes a more medial and posterior position in anterolateral infarction.

Lead V₁.—Completion of an initial R wave of increased amplitude and duration (if the 0.02-second VA vector lies to the right and anteriorly); or, as is more commonly the case, the beginning downstroke

Fig. 177.—Instantaneous VA vectors in the anterolateral myocardial infarction. The effective electrical site of the infarction is indicated in A. As shown in B, instantaneous VA vectors 1 and 3 are displaced to the right or medially and posteriorly. Displacement of vectors 2 and 3.

Fig 179.—Electrocardiographic and vectorcardiographic findings in acute anterolateral myocardial infarction.

Because the electrocardiogram was recorded quite early in the evolution of the infarction pattern, the Q waves in leads I, aVL, and V₁ are still relatively small, however,

vector in the horizontal projection directed to the left and posteriorly, and the rightward and anterior orientation of the T sE loop

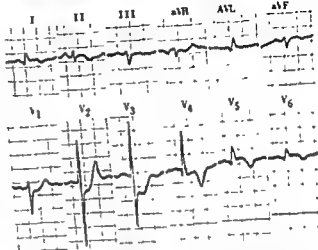
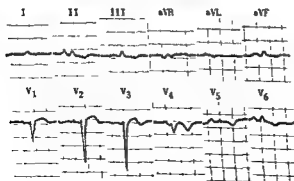


Fig 180—Electrocardiographic and vectorcardiographic findings in anterolateral infarction of uncertain duration. Although diagnostic Q waves do not appear in the electrocardiogram, the



diagram, the QRS sE loop is oriented directly posteriorly and inferiorly. The efferent limb of the horizontal QRS loop lies to the right of the afferent limb, while in the frontal QRS loop the efferent limb is inscribed irregularly, crossing the afferent limb at three points. It must be pointed out that the vectorcardiogram was recorded at maximal amplification, and so the planar QRS loops actually enclose extremely small areas compared with normal loops. The medial or rightward displacement of the efferent limb of the QRS sE loop and the greatly diminished magnitude of the instantaneous vectors of the QRS sE loop are diagnostic of anterolateral infarction. The T sE loop is oriented to the right, superiorly, and anteriorly, and there is no discernible S-T vector. Consequently, the age of the infarction cannot be determined from the vectorcardiogram. Note that the P sE loop in the frontal projection is almost as large as the frontal QRS loop.

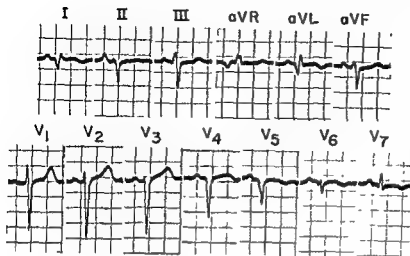


Fig. 178.—Electrocardiographic findings in anterolateral myocardial infarction of uncertain duration. The diagnostic features are: the wide, deep Q waves in leads I and aVL; the QS deflections in leads V₁ and V₂; the small, although significant, Q wave preceding the embryonic R wave in lead V₃; the relatively tall, wide R wave in lead V₄ with progressive diminution of relative R wave amplitude from right to left until the R wave disappears entirely, the slight coving of the S-T segments; and the inverted T waves in leads I, aVL, and V₁ through V₄. In the absence of definite S-T segment

the infarction.

of an \mathbf{M} wave (if the 0.02-second vector \mathbf{M} located to the right and posteriorly).

Leads I, aVL, V₅, and V₆.—Completion of abnormally deep and wide Q waves.

0.06-SECOND VA VECTOR

Since posterobasal areas of the left ventricle are usually spared in anterolateral infarction, the 0.06-second and subsequent instantaneous vectors generally occupy much the same position as they do normally, although occasionally they may be displaced farther posteriorly and sometimes to the right of the midline.

Lead V₁.—Completion of a terminal S wave.

Leads I, aVL, V₅, and V₆.—A terminal R wave of reduced amplitude (if the terminal vectors are situated to the left and posteriorly [Fig. 178]; or completion of a QS deflection (if all VA vectors after 0.01 second lie to the right of the midline)

Lead aVL in Diagnosis

Although occasionally the only diagnostic evidence of a high anterolateral infarction may consist of wide, deep Q waves in lead aVL, Q waves of equal prominence are frequently recorded in lead aVL in normal electrocardiograms. Proponents of the unipolar concept of electrocardiography attribute this finding in normal subjects to backward rotation of the cardiac apex and vertical heart position, which results in lead aVL recording initial negative potentials from the left ventricular cavity and later positive potentials from the epicardial surface of basal left ventricular wall. Since the right shoulder lead electrode also faces the back of the heart during atrial activation and

ventricular repolarization, lead aVL also displays inverted P and T waves. Consequently, the criteria recommended by Goldberger for Q wave abnormality in lead aVL stipulate that P and T waves must be upright before a prominent Q wave in this lead can be considered abnormal. In general, the experience of the authors has been that in the diagnosis of infarction the findings in lead aVL are often confusing. By and large, lead I and/or lead V₆ record the transverse (X) component of the cardiac vector more faithfully than does lead aVL. The reason for this is inherent in the direction of the lead axis of lead aVL. The axis of lead aVL is situated along the -30° to $+150^\circ$ axis of the frontal reference frame and obviously is neither transverse nor vertical but, rather, is a hybrid responding disproportionately to both X and Y (vertical) components of the cardiac vector. Consequently, lead aVL records Q waves when the initial and early instantaneous QRS vectors lie between $+60^\circ$ and $+90^\circ$, even though these vectors are situated to the left of the midline and project no Q waves on lead I. On the other hand, lead aVL fails to register Q waves when the initial and early instantaneous vectors are situated to the right between -90° and -120° , even though these vectors project Q waves on lead I. Thus, lead aVL fails completely to discriminate between vectors situated to the right or left when these vectors lie in either the $+60^\circ$ to $+90^\circ$ or the -90° to -120° segment of the frontal reference frame. Moreover, initial vectors oriented to the right and inferiorly (a common occurrence in normal persons) project more prominent Q waves on lead aVL than on lead I. In fact, it is difficult to differentiate such Q waves from those occurring in lead aVL in anterolateral infarction, as witnessed by the number of criteria which a Q wave in this lead must

TABLE 22—ORIENTATION OF THE MEAN 0.02-SECOND AND MAXIMAL MEAN INSTANTANEOUS VECTORS OF THE QRS sE LOOP IN ANTEROLATERAL INFARCTION

	HORIZONTAL			RIGHT SAGITTAL			FRONTAL		
	Extreme Range	Av.	Usual Range*	Extreme Range	Av.	Usual Range*	Extreme Range	Av.	Usual Range*
Mean 0.02-second instantaneous QRS vector	+95° to -60°	-100°	+95° to -110°	+130° to +10°	-100°	-165° to +10°	+90° to -90°	-155°	+90° to -120°
Maximal mean instantaneous QRS vector	-90° to -50°	-70°	-90° to -65°	+150° to -170°	+170°	+170° to -170°	-60° to +95°	+10°	+5° to +95°

*Usual range = range in 65% of cases.

the midline. In anterolateral infarction the long axis of the loop, or the maximal instantaneous QRS vector in the horizontal projection, ordinarily is situated between -90° and -50° in the horizontal reference frame.

- The mean 0.02-second instantaneous QRS vector in this projection usually lies well to the right and either anteriorly or posteriorly, in contrast with its normal orientation to the left and anteriorly. Occasionally in anterolateral infarction this vector is located to the left and far posteriorly.
- The horizontal QRS loop may have a clockwise or counterclockwise direction of inscription, depending apparently on the degree of posteromedial displacement of the efferent limb. Frequently, QRS loops inscribed in a counterclockwise direction present a figure-of-eight configuration.
- Occasionally in our series of anterolateral infarctions, moderate conduction slowing was observed in the afferent limb of the QRS sE loop in all three projections, although this was seldom of such a degree as to produce QRS prolongation to 0.12 second.

RIGHT SAGITTAL QRS LOOP.—The QRS sE loop in this projection confirms the marked posterior orientation already described in the horizontal projection. The direction of inscription may be either clockwise or counterclockwise.

FRONTAL QRS LOOP.—Unlike anteroapical and anterior infarctions, which cause no recognizable abnormalities of the frontal QRS loop, anterolateral infarction typically produces one or both of the following abnormalities in the frontal projection:

- The initial and early portion of the loop is written farther to the right than normal.
- The remainder of the loop is usually inscribed in a counterclockwise direction to the left and often somewhat superiorly. More often than not, the efferent limb of the loop, after moving for a time horizontally and to the left, then turns abruptly superiorly and medially. This sudden change in the course of the loop possibly reflects involvement of portions of the lateral ventricular wall activated relatively late in the QRS interval (Figs 170-181).

EXTENSIVE ANTERIOR INFARCTION

Extensive anterior infarction usually corresponds to occlusion of the anterior descending branch of the left coronary artery.

The Instantaneous VA Vectors

Extensive anterior myocardial infarction is essentially a combination of anteroapical, anterior, and anterolateral infarctions and is therefore accompanied by displacement of the 0.01-, 0.02-, and 0.04-second

VA vectors to the right and posteriorly (Fig 182). The 0.06-second VA vector and subsequent instantaneous vectors are situated posteriorly and either slightly to the right or left of the midline. Thus, leads I, aVL, and V₁ through V₄ record abnormal Q waves.

Vectorcardiographic Findings

The QRS sE loop in extensive anterior infarction typically shows the entire gamut of abnormalities de-

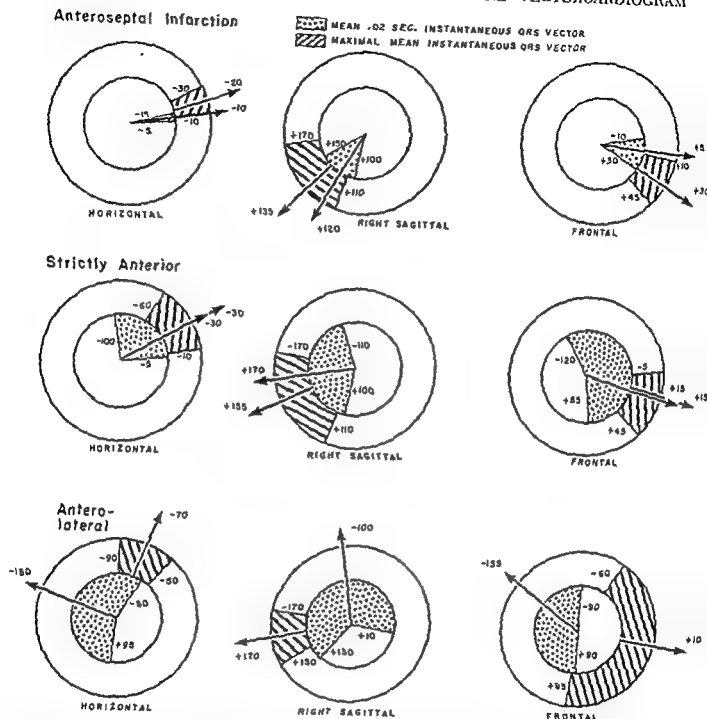


Fig. 181.—Range of variation and average orientation of the mean 0.02-second and the maximal mean instantaneous QRS vectors of the vectorcardiographic QRS sE loop in the various types of anterior myocardial infarction

satisfy to be considered abnormal (see Criteria of Q Wave Abnormality in Chapter 18)

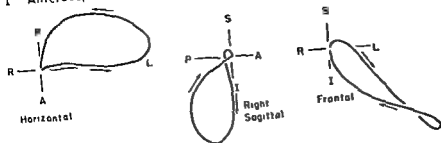
Vectorcardiographic Findings

The average orientation and the extreme ranges of variation in orientation of the mean 0.02-second and maximal mean instantaneous QRS vectors of the horizontal, right sagittal, and frontal loops in anterolateral infarction are shown in Table 22.

HORIZONTAL QRS LOOP—The salient diagnostic abnormalities presented by the QRS sE loop in the horizontal projection are as follows

1. The initial and early portions of the horizontal QRS loop extend farther to the right and anteriorly than normally is the case, and this initial deflection of the loop usually encloses a relatively large area
2. The body of the horizontal QRS loop is written far posteriorly and slightly to the left or right of

I Anteroseptal Infarction



II Strictly Anterior Infarction

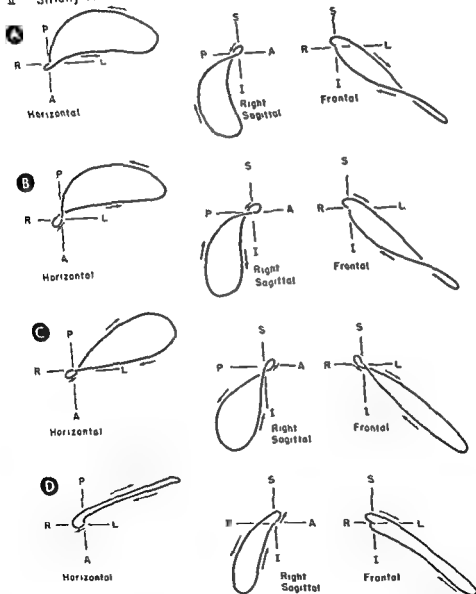
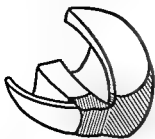
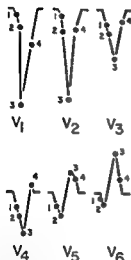


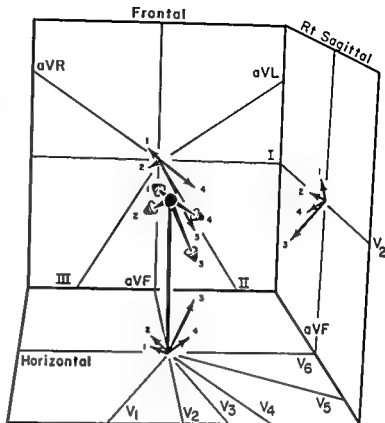
Fig 183.—Planar QRS loop patterns observed vectorcardiographically in the various types of anterior myocardial infarction (I) anteroseptal infarction, (II) strictly anterior infarction and its pattern variants (A-D) (continued).



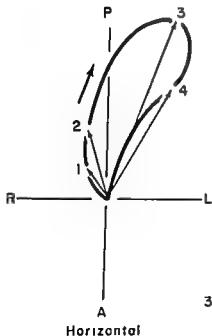
A Extensive Anterior Myocardial Infarction



B QRS Deflections Projected on Scalar Leads



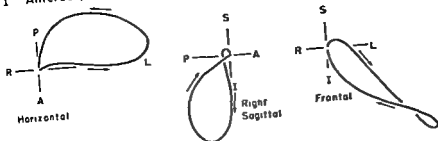
C Instantaneous VA Vectors in Extensive Anterior Myocardial Infarction



D Planar QRS Loops in Extensive Anterior Myocardial Infarction

in
ar
and to the right. Thus, an S₁ or S₂ in the precordial leads can be seen to present a combination of the features of anteroseptal and anterolateral infarction

I Anteroseptal Infarction



II Strictly Anterior Infarction

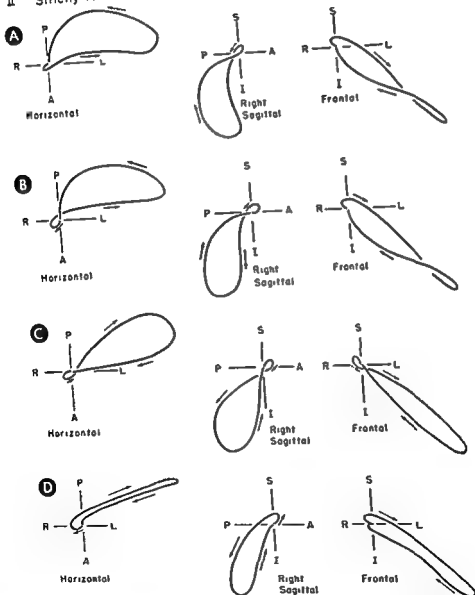
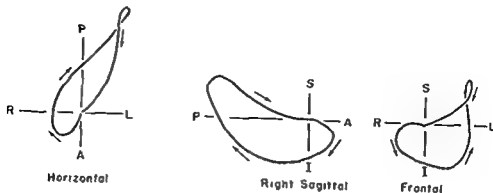


Fig. 183.—Planar QRS loop patterns observed vectorcardiographically in the various types of anterior myocardial infarction (I) anteroseptal infarction, (II) strictly anterior infarction and its pattern variants (A-D) (continued).

III Anterolateral Infarction



IV Extensive Anterior Infarction

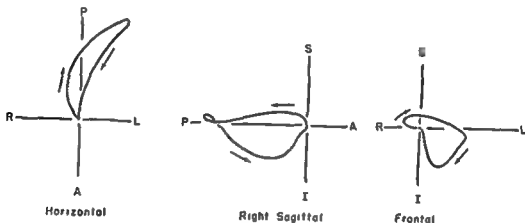


Fig. 183 (cont) —(III) anterolateral infarction; and (IV) extensive anterior infarction.

scribed for anteroapical, strictly anterior, and anterolateral infarctions (Fig. 183). Generally the initial deflection and efferent limb of the QRS sE loop are written to the right, posteriorly, and somewhat superiorly, and the loop then returns on the left posteriorly and inferiorly. Thus, abnormal Q waves are projected

on all six precordial leads and leads I and aVL.

The average orientation and the extreme ranges of variation in orientation of the mean 0.02-second and maximal mean instantaneous QRS vectors of the horizontal, sagittal, and frontal loops in extensive anterior infarction are shown in Table 23.

TABLE 23—ORIENTATION OF THE MEAN 0.02-SECOND AND MAXIMAL MEAN INSTANTANEOUS VECTORS OF THE QRS sE LOOP IN EXTENSIVE ANTERIOR INFARCTION

	HORIZONTAL			RIGHT SAGITTAL			FRONTAL		
	Extreme Range	Av.	Usual Range*	Extreme Range	Av.	Usual Range*	Extreme Range	Av.	Usual Range*
Mean 0.02-second instantaneous QRS vector	-50° to -30°	-40°	.	+110° to +130°	+120°	..	+50° to +70°	+60°	
Maximal mean instantaneous QRS vector	-60° to -45°	-50°	..	-170° to -160°	-165°	.	-50° to +10°	-20°	

*Usual range = range in 85% of cases

S-T VECTOR AND VENTRICULAR REPOLARIZATION IN ACUTE PHASE OF ANTERIOR INFARCTION

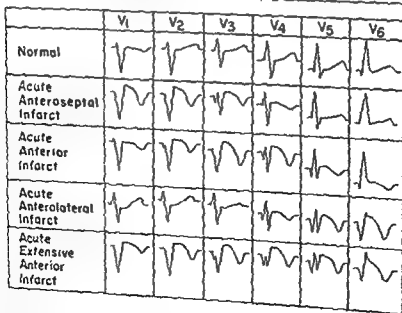
During the acute stage of an anterior myocardial infarction, the anterior wall is the site of subepicardial injury. Thus, as will be recalled, at the end of ventricular activation the subepicardial layer of ventricular muscle anteriorly retains some of its dipoles because the depolarization wave has been partially or wholly blocked at the boundaries of the injured region. The latter therefore comes to be positively charged with respect to deeper layers of muscle, and a systolic current of injury flows between the two. The electrical field established by the current of injury can be represented by an injury or S-T vector, which in anterior myocardial infarction is directed toward the effective electrical site of epicardial injury—that is, anteriorly. Consequently, the S-T vector projects positive voltages in the form of elevated S-T

segments on one or more of the anterior precordial leads. In the vectorcardiogram, the presence of an S-T vector in anterior infarction is evidenced by failure of the QRS sE loop to return to its point of origin in the horizontal and right sagittal projections, the terminus of the QRS sE loop being displaced anteriorly. The more exact orientation of the S-T vector in each of the four types of anterior infarction is indicated in Table 24.

As the intense current of injury subsides during the course of an anterior infarction, the effects of transmural ischemia begin to appear with increasing prominence in the electrocardiogram and vectorcardiogram. As indicated previously, transmural ischemia apparently delays recovery in subepicardial muscle to a greater degree than in subendocardial muscle,

TABLE 24—RELATIONSHIP BETWEEN THE EFFECTIVE ELECTRICAL SITE OF SUBEPICARDIAL INJURY AND TRANSMURAL ISCHEMIA AND THE DIRECTION OF THE S-T VECTOR AND THE T sE LOOP IN ANTERIOR MYOCARDIAL INFARCTION

EFFECTIVE ELECTRICAL SITE OF INJURY AND ISCHEMIA	DIRECTION OF S-T VECTOR	ORIENTATION OF T sE LOOP
Anteroseptal	Right, anterior	Left, posterior
Anterior	Anterior and slightly to the left	Posterior and slightly to the right
Anterolateral	Left, anterior	Right, posterior
Extensive anterior	Anterior or left and anterior	Posterior, right



thereby reversing the direction in which repolarization spreads through the ischemic ventricular wall. When the anterior wall of the left ventricle is the site of transmural ischemia, as is the case in an anterior infarction, repolarization forces produced in this region are directed posteriorly (just the opposite of normal) and continue to be generated for a time after repolarization elsewhere in the ventricles has been completed. The instantaneous T vectors which are the resultant of these abnormal forces arising in the anterior ventricular wall and of normal forces produced elsewhere tend to be displaced posteriorly away from the effective site of transmural ischemia. The specific orientation of the T sE loop in each of the four types of anterior infarction is presented in Table 24; but, in general, during the ischemic phase of an anterior infarction, the instantaneous T vectors project symmetrical and deeply inverted T waves

on one or more anterior chest leads and cause the T sE loop of the vectorcardiogram to rotate posteriorly.

Since the evolution of S-T segment and T wave changes in myocardial infarction has already been described in Chapter 18, it will not be described specifically for each type of infarction. Let it suffice to say that, early in an anterior infarction, the S-T segments are, for a time, elevated in one or more precordial leads, and that, as the S-T segments subsequently return to the isoelectric base line, the T waves in the same leads or lead become increasingly more deeply inverted. In the healed stage of an anterior infarction, the S-T segments are isoelectric, but the T waves may be of normal appearance, low upright, or asymmetrically inverted.

For a résumé of the electrocardiographic findings in the four types of anterior infarction, see Table 24.

Inferoposterior Myocardial Infarction

AN INFEROPOSTERIOR INFARCTION is usually due to an occlusion of the right coronary artery or circumflex artery and may have any of the following effective electrical locations. (1) inferior or diaphragmatic wall of the left ventricle, (2) posterolateral wall of the left ventricle, or (3) strictly posterior (postero-

basal or infra-atrial) wall of the left ventricle. Like the anterior infarctions, inferoposterior infarctions are distinguished one from another by their electrical location, as evidenced by the direction of the unbalanced forces they produce.

DIAPHRAGMATIC (INFERIOR) INFARCTION

Infarction of the diaphragmatic or inferior wall of the left ventricle abolishes the leftward and inferiorly directed QRS forces normally produced by this region, with the result that forces acting in the opposite direction become electrically preponderant. In effect, it is as if new forces of equal magnitude but opposite direction were added to the balance of cardiac forces. These new forces can be visualized as an infarction vector which, in diaphragmatic infarction, exerts its effect on the electrical field of the heart primarily in a superior direction—that is, along a vertical axis perpendicular to the horizontal plane. The abnormalities produced by diaphragmatic infarction are therefore confined to electrocardiographic and vectorcardiographic leads which record the vertical, or Y, component of the cardiac vector. Thus the precordial leads of the electrocardiogram and the horizontal projection of the vectorcardiogram do not show diagnostic changes, while leads II, III, and aVF and the frontal and sagittal projections of the vectorcardiogram typically display the abnormalities diagnostic of diaphragmatic infarction. While it may sometimes happen in diaphragmatic infarction that leads V₁ and V₂ record QRS deflections of increased resultant positivity, depressed S-T segments, and tall upright T waves, these changes are usually related to coexisting infarction of the strictly posterior or the posterolateral aspect of the left ventricle.

Although infarctions involving the inferior wall of the left ventricle continue to be referred to by many as *posterior infarctions*, this designation is being supplanted gradually by the terms *diaphragmatic* or *inferior*, both of which are used interchangeably in this text. The term "posterior" is reserved by the authors specifically for infarctions producing unbalanced forces directed anteriorly.

The Instantaneous VA Vectors

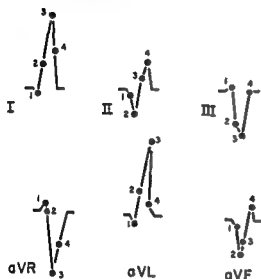
In describing the instantaneous VA vectors in diaphragmatic infarction (see also Fig. 184), only the vertical and transverse components of the vectors will be considered, since typically the anteroposterior component of the instantaneous vectors is not altered by the infarction and is therefore the same as in the normal electrocardiogram. Accordingly, in the discussion the instantaneous VA vectors will only be related to the lead deflections recorded in leads II, III, and aVF, which are the diagnostic leads in diaphragmatic myocardial infarction.

0.01-SECOND VA VECTOR

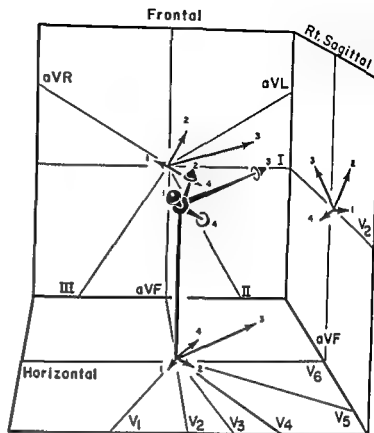
Although posterobasal septal involvement in diaphragmatic infarction is not uncommon, the initial septal forces usually retain their normal magnitude



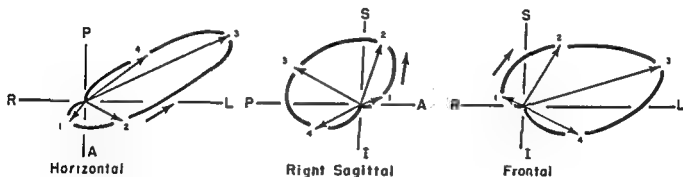
A Diaphragmatic Myocardial Infarction



C QRS Deflections Projected on Scalar Leads



B Instantaneous VA Vectors in Diaphragmatic Myocardial Infarction



D Planar QRS Loops in Diaphragmatic Myocardial Infarction

f., I.:

II and aVF (C). Since vector 1 is not affected by the infarction and, in the example depicted, happens to project on the positive half of the axis of derivation of lead III, this lead registers a minute R wave followed by a wide S wave. However this is the equivalent of a QS deflection. Inasmuch as the abnormal displacement of the VA vectors occurs pri-

and direction to the right and superiorly (or occasionally inferiorly)

Leads II, III, and aVF.—Beginning downstroke of a Q wave (or a small initial R wave if the 0.01-second VA vector is directed inferiorly).

0.02- AND 0.04-SECOND VA VECTORS

Transmural activation of the diaphragmatic wall of the left ventricle occupies approximately the period between 0.02 and 0.04 second of the QRS interval, during which time this region of the heart normally produces electrical forces directed to the left and inferiorly. In diaphragmatic infarction, these leftward and inferiorly directed forces are subtracted from the balance of cardiac forces existing at each instant of

but opposite direction, the latter being represented by an infarction vector directed superiorly and slightly to the right. As previously explained, the postinfarction 0.02- and 0.04-second vectors are resultants of the corresponding preinfarction vectors and the infarction vector.

Thus, in diaphragmatic myocardial infarction, the 0.02-second VA vector is displaced from its normal position (inferior, to the left, and slightly anterior) to a position far superior and more medial or slightly to the right. Similarly, there is usually upward displacement of the 0.04-second VA vector in this type of infarction. Although the 0.04-second VA vector ordinarily remains the maximal mean instantaneous vector, it generally does not extend as far superior as does the 0.02-second VA vector.

Leads II, III, and aVF.—Deep, wide Q waves (if the 0.01-second VA vector and the 0.02- and 0.04-second vectors are all oriented superiorly), or wide S waves following small initial R waves (if the 0.01-second vector is directed inferiorly and the 0.02- and 0.04-second vectors, superiorly).

0.06-SECOND VA VECTOR

If the basal diaphragmatic wall, which is activated relatively late in the QRS interval, is not involved by the infarction, the 0.06-second VA vector and subsequent instantaneous vectors have much the same magnitude and direction as normally, and therefore tend to be oriented more to the left and somewhat inferiorly or less superiorly than the preceding instantaneous vectors.

Leads II, III, and aVF.—Depending on the loca-

tion of the 0.06-second VA vector—and this can be variable—the vector projects a small terminal R wave or a terminal S wave on one or more of leads II, III, and aVF. When these leads record a terminal R wave, the latter is smaller than normal because the 0.04-second vector in diaphragmatic infarction is displaced superiorly and therefore contributes little or nothing to the formation of the terminal R wave. On the other hand, frequently there is displacement of the late instantaneous vectors in much the same direction as the vectors appearing during the first 0.04 second of the QRS interval, possibly reflecting extension of the infarction to the inferobasal area of the left ventricle. In such an instance, the 0.06-second VA vector and subsequent instantaneous vectors are directed almost as markedly superiorly as are the preceding vectors.

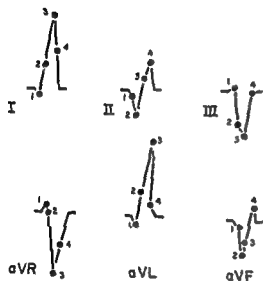
Before summarizing the various configurations of the QRS deflections recorded in leads II, III, and aVF in diaphragmatic myocardial infarction, the fact should be re-emphasized that typically in this type of infarction the 0.01-second VA vector is normal in direction and magnitude. Thus, if before infarction the 0.01-second vector was situated superiorly, then it remains so after infarction. In this event, the 0.01- to 0.04-second VA vectors all project negative potentials in the form of wide, deep Q waves on leads II, III, and aVF. On the other hand, if it should so happen that the preinfarction 0.01-second VA vector (and, therefore, the corresponding postinfarction vector) is directed inferiorly, then lead aVF and/or lead III record small initial R waves followed by S waves of larger size. Often, when this is the case, the 0.06-second VA vector projects a terminal R' on lead aVF and/or lead III, so that an rSR' or RS' complex is registered instead of an rS deflection. When the 0.01-second VA vector is located between +150° and 160° in the frontal reference frame, only lead II records a Q wave, while leads III and aVF show initial small R waves. Occasionally when the limb leads show apparent left-axis deviation of a QRS, with leads III and aVF recording rS deflections, the presence of a QS or qRS deflection in lead II may provide the clue to the correct diagnosis of diaphragmatic myocardial infarction, since this circumstance does not usually happen in left-axis deviation in the absence of infarction (but may occur occasionally in chronic pulmonary heart disease).

QRS Criteria for Diagnosis

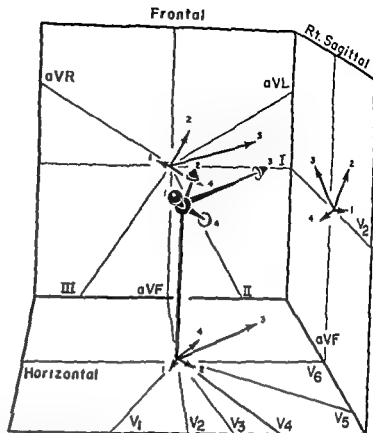
Ordinarily, the electrocardiographic recognition of an acute diaphragmatic myocardial infarction pre-



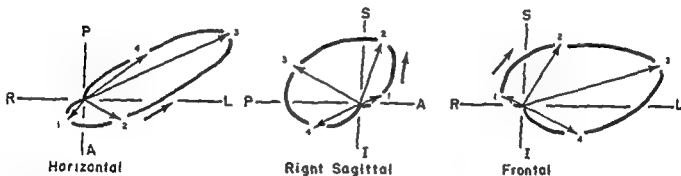
A Diaphragmatic Myocardial Infarction



C QRS Deflections Projected on Scalar Leads



B Instantaneous VA Vectors in Diaphragmatic Myocardial Infarction



D Planar QRS Loops in Diaphragmatic Myocardial Infarction

tion of the ically inert tantaneous waves on leads
 Note, in D, that the efferent limbs of the sagittal and frontal loops can be seen to be displaced abnormally superiorly, which in turn causes a reversed direction of inscription of these loops, on the other hand, the horizontal QRS loop is relatively normal in appearance. The schematic loops are quite characteristic for diaphragmatic infarction

dence of acute infarction plus vectorcardiographic abnormalities unmistakably indicative of diaphragmatic infarction). The qualifying terms "diagnostic" or "abnormal," when applied hereafter to Q waves appearing in leads II, III, and aVF, are meant to signify that the Q waves in question satisfy both width and depth criteria described above. The frequency of diagnostic Q waves in leads II, III, and aVF in our 45 cases of acute or old diaphragmatic myocardial infarction is summarized as follows.

	% OF ELECTROCARDIOGRAMS
No diagnostic Q waves in leads II, III, and aVF	39
Diagnostic Q waves in all three leads	12
Diagnostic Q waves in lead III only	20
Diagnostic Q waves in lead aVF only	8
(Note: No electrocardiogram displayed diagnostic Q waves in lead II alone.)	
Diagnostic Q waves in leads III and aVF	24
Relative frequency of diagnostic Q waves in the respective leads	
Diagnostic Q waves in lead III	56
Diagnostic Q waves in lead aVF	44
Diagnostic Q waves in lead II	12

Although the above percentages would seem to imply that lead III is the lead of diagnostic preference in diaphragmatic myocardial infarction, this is not entirely true, for lead III is more prone than either of the other two leads to yield false positive interpretations of infarction. This fact holds true especially if the electrocardiographer requires that the Q waves in lead III satisfy only one or the other of the width and depth criteria to be considered diagnostic. To illustrate this point, we shall turn once again to our own observations in a series of electrocardiograms recorded from patients of varying ages without evidence of cardiac disease. Diagnostic Q waves fulfilling both width and depth criteria of abnormality were noted in lead III alone in 4% of the electrocardiograms of these patients, while Q waves in lead III satisfying one of the criteria of abnormality and almost fulfilling the other criterion were observed in 12% of the records. Aside from the foregoing findings in normal electrocardiograms, it is well established that, in the absence of infarction, diagnostic Q waves may frequently occur in lead III and less frequently in lead aVF in chronic pulmonary emphysema with or without cor pulmonale, in acute cor pulmonale, in right bundle branch block, and even occasionally in left ventricular hypertrophy. From the over-all standpoint both of diagnostic sensitivity and reliability, if any

lead deserves to be considered the preferred diagnostic lead in diaphragmatic myocardial infarction, it is probably lead aVF. The explanation underlying this preference is presented in the following paragraphs.

The III in a transverse direction is the mean instantaneous vector in this type of infarction and the axis is derivation of leads II and III. As will be recalled, the infarction vector in diaphragmatic myocardial infarction causes superior displacement of the post-infarction mean instantaneous QRS spatial vectors, associated with little or no abnormal deviation of the vectors along the transverse axis. Obviously, the abnormal superiorly directed unbalanced forces created by the infarction are most accurately recorded by a vector "verticalizing" for all intents and purposes, only II and III. Lead aVF, on the other hand, and III are rotated at least 30° to either side of the vertical axis implies that these leads respond not only to the vertical component but also to the transverse component of a given cardiac vector. The possible inaccuracies which can be introduced by the foregoing deficiencies of leads II and III can be exemplified by the following.

1 Any mean instantaneous QRS vectors situated in the +150° to 180° segment of the frontal reference frame project negative voltages on lead II even though situated inferiorly, and the same holds true in the case of lead III for vectors located in the 0° to

vectors in question

2 Conversely, superiorly situated mean instantaneous QRS vectors which happen to lie in the 0° to -30° segment of the frontal reference frame project positive voltages on lead II, similarly, superiorly located vectors lying in the 150° to -150° segment of the frontal reference frame likewise project positive voltages on lead III. In either case, lead aVF registers negative voltages, signifying that the vectors are truly oriented superiorly.

3 In diaphragmatic myocardial infarction, the mean instantaneous QRS vectors which are displaced by the infarction vector are those appearing between 0.015 and 0.04 second—that is, vectors usually situated to the left. Consequently, the corresponding

sents little difficulty because sooner or later, in most instances, serial electrocardiograms not only will show diagnostic QRS abnormalities but—of equal, or even greater, importance—will also display characteristic evolutionary changes in the S-T segments and T waves in leads II, III, and aVF (Fig. 185). Quite another story is the healed or old diaphragmatic myocardial infarction, which so often poses a knotty diagnostic problem for the electrocardiographer, since his decision as to the presence or absence of infarction rests solely on a correct evaluation of the QRS deflections or Q waves (if present) in the diagnostic leads. (The same holds equally true for healed infarction involving other aspects of the left ventricular wall.) To say the least, the QRS residuals of healed diaphragmatic myocardial infarction are quite equivocal at times. Therefore, to do justice to the importance of this problem, obviously the QRS criteria for diagnos-

ing acute or old diaphragmatic myocardial infarction merit special attention.

From the very outset of the discussion, the fact must be kept in mind that the most reliable criteria of QRS abnormality in leads II, III, and aVF ($Q \geq 0.04$ second and $>25\%$ of the following R wave amplitude) are burdened with an inherent handicap, i.e., they pertain solely to Q wave abnormality in diaphragmatic infarction. Thus, the criteria ignore the significant percentage of electrocardiograms (about 15% in the series studied by the authors of this text) which exhibit rS or rSR' deflections in leads II, III, and aVF as the only residuals of infarction. Some idea of the value of the aforementioned criteria in recognizing old diaphragmatic myocardial infarction can be derived from our observations in 45 cases of acute and old infarction (all cases having either unequivocal clinical histories of old infarction or ancillary evi-

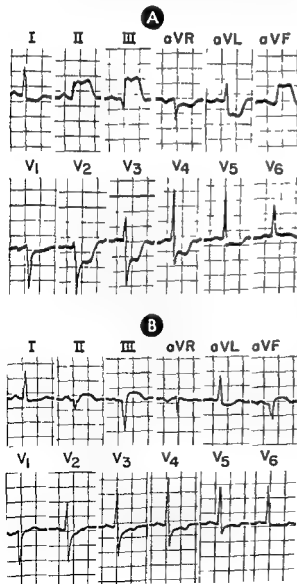
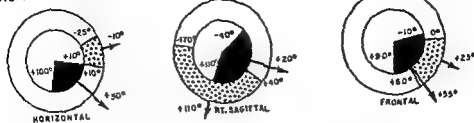
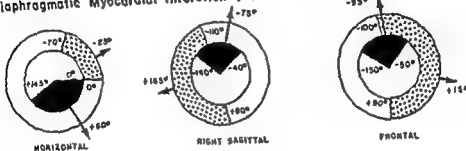


Fig. 185.—Evolution of electrocardiographic abnormalities diagnostic of acute diaphragmatic myocardial infarction. The findings in the initial record (A) are typical of the early phase of diaphragmatic myocardial infarction and consist of marked S-T segment elevation and upright T waves in leads II, III, and aVF. Although a diagnostic Q wave is present in lead III, significant Q waves have not yet appeared in leads II and aVF. The S-T segment depression in leads V₁ through V₆ may possibly represent anterior subendocardial myocardial injury but is far more likely to be reciprocal to the subepicardial injury involving the posterior or infra-atrial wall of the left ventricle. The second electrocardiogram (B) was recorded 24 hours later and differs from the preceding as follows: the S-T segment elevation in leads II, III, and aVF and the S-T segment depression in leads V₁ through V₆ are less marked than before, but inverted T waves are now present in these leads (with the exception of leads V₁ and V₂). Note that leads III and aVF now display QS deflections, and lead II, a Qr complex.

Normal (60 Cases)



Diaphragmatic Myocardial Infarction (25 Cases)



■ MEAN 0.02-SEC INSTANTANEOUS QRS VECTOR OF PLANAR QRS LOOP

▨ MAXIMAL MEAN INSTANTANEOUS QRS VECTOR OF PLANAR QRS LOOP

Fig. 186. Orientation of the mean 0.02-second instantaneous QRS vector in diaphragmatic myocardial infarction.

deviated superiorly on occasions. As a general rule,

FRONTAL QRS LOOP.—During the first 0.02–0.04 second of the QRS interval, the frontal QRS loop in diaphragmatic myocardial infarction is characterized

the orientation and perhaps the relative magnitude of the 0.02-second instantaneous QRS vector in the vectorcardiograms of patients suspected of infarction. The data we obtained from analyses of the vectorcardiograms of a series of patients with diaphragmatic infarction is summarized in Table 25 and Figure 186

also usually superiorly, although it may be inferiorly, and then the effluent limb is inscribed to the left and abnormally superiorly. The long axis of the loop (corresponding to the maximal mean instantaneous QRS vector in the frontal projection) may

TABLE 25.—ORIENTATION OF THE MEAN 0.02-SECOND AND MAXIMAL MEAN INSTANTANEOUS VECTORS OF THE QRS LOOP IN DIAPHRAGMATIC INFARCTION

	HORIZONTAL			RIGHT SAGITTAL			FRONTAL		
	Extreme Range	Av	Usual Range*	Extreme Range	Av	Usual Range*	Extreme Range	Av	Usual Range*
Mean 0.02-second instantaneous QRS vector	0° to +145°	+60°	+10° to +100°	-140° to -40°	-75°	-90° to -40°	-150° to -50°	-93°	-130° to -50°
Maximal mean instantaneous QRS vector	-70° to 0°	-25°	-45° to 0°	+50° to -110°	+165°	+130° to -140°	-100° to +90°	+15°	-40° to +30°

*Usual range = range in 85% of cases.

postinfarction vectors usually lie abnormally superiorly and to the left and tend, on the whole, to project deceptively small negative voltages on lead II because of their leftward orientation. By the same token, in diaphragmatic-lateral myocardial infarction, a common type of combined infarction, the mean instantaneous QRS vectors are displaced not only superiorly but also to the right. In this instance, lead III tends to register deceptively small negative deflections.

Other criteria, like the R_{III} peak interval (the interval from onset of the QRS to the peak of the R wave in lead III ≥ 0.06 second), for example, whether used singly or in combination with the Q width and depth criteria in lead aVF, have not increased the diagnostic accuracy of the electrocardiogram in diaphragmatic infarction. This problem has been approached somewhat differently by Grant and others, who utilize vector projection methods to determine the orientation of initial and early QRS vectors in diaphragmatic infarction. The method used by Grant to construct the mean 0.04-second QRS spatial vector from the electrocardiogram was described earlier, in Chapter 3. In the large series of normal subjects studied by Grant, the mean 0.04-second QRS spatial vector was found to be oriented invariably to the left, posteriorly, and inferiorly, while in diaphragmatic myocardial infarction this vector was usually directed markedly superiorly rather than inferiorly. Vector methods have been applied to the diagnosis of diaphragmatic infarction in a somewhat different way by Pearce and Chapman, who have recorded simultaneous leads aVF and V_R on a twin-channel electrocardiograph. Lead V_R was obtained by placing the exploring chest electrode just to the left of the seventh thoracic vertebra. The 0.01- and 0.02-second sagittal vectors were constructed by measuring the deflections at these intervals in the two leads, and the measurements were then utilized as the tangent of the angle of the vector. According to Pearce and Chapman, almost all of the autopsy-proved diaphragmatic infarcts in their series had 0.02-second sagittal vectors lying between -65° and -150° . The patients with prominent Q waves in lead aVF, who did not show diaphragmatic infarction at postmortem, uniformly had 0.02-second sagittal vectors situated inferior to -65° . Although there was a significant number of false positive interpretations, Pearce and Chapman found that these could be eliminated by combining the following two criteria (a) a 0.02-second sagittal vector situated between -65° and -150° , and (b) ΣQ_{aVF} interval of 0.04 second or longer.

Probably the most useful adjunct to the electrocardiogram in the diagnosis of inferior or diaphrag-

matic infarction is the vectorcardiogram, and this is particularly true in those cases in which leads III and aVF display rS or rSR' deflections.

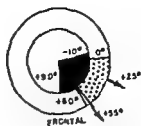
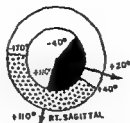
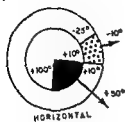
Vectorcardiographic Findings

Since the unbalanced forces created by infarction of the inferior aspect of the left ventricle are directed superiorly away from the electrically inert muscle, the resulting disturbance of the balance of cardiac forces occurs along the Y, or vertical, axis. Consequently, the vectorcardiographic abnormalities diagnostic of diaphragmatic infarction are to be sought in the two vectorcardiographic projections having a component lead which responds to the Y component of the cardiac vector—namely, the sagittal and frontal projections. Nevertheless, the horizontal projection of the QRS sE loop is included in the following description of the QRS sE loop findings in diaphragmatic infarction.

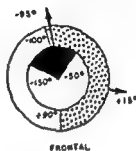
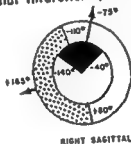
HORIZONTAL QRS LOOP—The horizontal QRS loop in diaphragmatic myocardial infarction ordinarily presents essentially a normal appearance, being counterclockwise inscribed and showing a normal initial deflection to the right and anteriorly. The mean 0.02-second instantaneous vector of the horizontal QRS loop is normally oriented, but the range of variation and average orientation of the maximal mean instantaneous vector of the loop tend to be situated farther posteriorly than the corresponding vector in the normal configuration.

RIGHT SAGITTAL QRS LOOP—The chief diagnostic abnormality of the sagittal QRS loop, and the feature most consistently present in diaphragmatic infarction, is that during the first 0.02–0.04 second of the QRS interval the loop is written markedly superiorly and usually slightly anteriorly. The pronounced superior displacement of the initial and early instantaneous vectors frequently causes counterclockwise inscription of the sagittal loop in its entirety or counterclockwise inscription of the proximal component of a figure-of-eight sagittal loop. Counterclockwise inscription was observed in over two thirds of the vectorcardiograms which we considered to be diagnostic of diaphragmatic infarction. Although the most striking evidence of diaphragmatic infarction in terms of superior displacement of the instantaneous vectors is usually seen in the initial and early portions of the QRS sE loop, the efferent limb, long axis of the sagittal QRS loop, and sometimes the afferent limb may, one or all, be

Normal (60 Cases)



Diaphragmatic Myocardial Infarction (25 Cases)



 MEAN 0.02-SEC. INSTANTANEOUS QRS VECTOR OF PLANAR QRS LOOP
 MAXIMAL MEAN INSTANTANEOUS QRS VECTOR OF PLANAR QRS LOOP

Fig. 186.—Range of variation and average orientation of the mean 0.02-second and maximal mean instantaneous vectors of the planar QRS loops in normal subjects and in patients with diaphragmatic myocardial infarction. The average orientation of a given instantaneous vector is indicated by a vector arrow.

deviated superiorly on occasions. As a general rule,

the orientation and perhaps the relative magnitude of the 0.02-second instantaneous QRS vector in the vectorcardiograms of patients suspected of infarction. The data we obtained from analyses of the vectorcardiograms of a series of patients with diaphragmatic infarction is summarized in Table 25 and Figure 186

FRONTAL QRS LOOP.—During the first 0.02–0.04 second of the QRS interval, the frontal QRS loop in diaphragmatic myocardial infarction is characterized by a prominent deflection extending abnormally superiorly. Initially the loop is written slightly to the right and usually superiorly, although occasionally inferiorly, and then the efferent limb is inscribed to the left and abnormally superiorly. The long axis of the loop (corresponding to the maximal mean instantaneous QRS vector in the frontal projection) may

TABLE 25.—ORIENTATION OF THE MEAN 0.02-SECOND AND MAXIMAL MEAN INSTANTANEOUS VECTORS OF THE QRS LOOP IN DIAPHRAGMATIC INFARCTION

	HORIZONTAL			RIGHT SAGITTAL			FRONTAL		
	Extreme Range	Av.	Usual Range*	Extreme Range	Av.	Usual Range*	Extreme Range	Av.	Usual Range*
Mean 0.02-second instantaneous QRS vector	0° to +145°	+60°	+10° to +100°	-140° to -40°	-75°	-90° to -40°	-150° to -50°	-95°	-130° to -50°
Maximal mean instantaneous QRS vector	-70° to 0°	-25°	-45° to 0°	+50° to -110°	+165°	+130° to -140°	-100° to +90°	+15°	-40° to +30°

*Usual range = range in 65% of cases.

sometimes lie above the 0° axis in diaphragmatic myocardial infarction, although in our cases the average orientation of the frontal QRS loop was essentially the same as that in normal subjects. After the appearance of the maximal instantaneous vector, the afferent limb returns inferiorly, in most instances, to complete inscription of the loop in a clockwise direction. However, sometimes the afferent limb may be situated above the efferent limb, the frontal loop in this event having a counterclockwise direction of inscription. As a general rule, when the frontal QRS loop in diaphragmatic myocardial infarction is written in a counterclockwise direction, the efferent limb of the loop is not only displaced superiorly but tends to be inferiorly concave, that is, to be bowed upward in

its midportion. In addition, frontal QRS loops with a figure-of-eight configuration are often observed in diaphragmatic myocardial infarction, the proximal loop of the "eight" having a clockwise direction of inscription and the distal component a counterclockwise direction of inscription. This variant type of frontal QRS loop configuration was observed by us more frequently in old healed diaphragmatic myocardial infarction than in more recent infarctions.

As Table 25 indicates, the orientation of the 0.02-second instantaneous vector of the frontal QRS loop would seem to be a better point of distinction between the normal frontal loop and the loop in diaphragmatic myocardial infarction than the orientation of the maximal instantaneous QRS vector or long axis of the

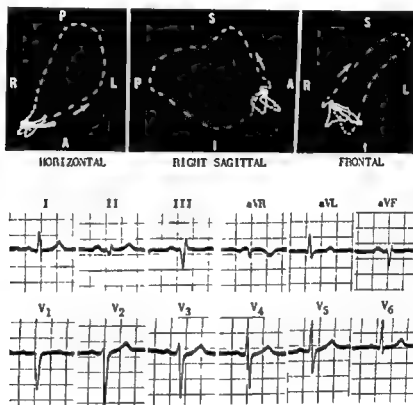


Fig. 187.—Electrocardiographic and vectorcardiographic findings in old or healed diaphragmatic myocardial infarction.

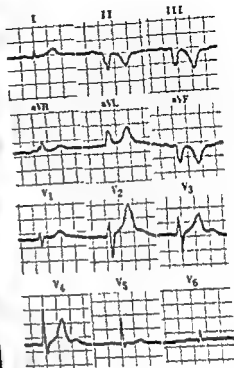
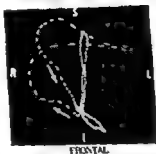
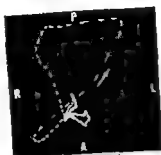
If one adheres to the conventional empiric criteria for the electrocardiographic diagnosis of diaphragmatic infarction, this diagnosis could not be made in the electrocardiogram in this figure because of the fact that leads II, III, and aVF register RSR' deflections. This electrocardiogram is a good case in point, illustrating the advantages of the vector approach to the electrocardiogram. On calculating the mean 0.04-second QRS spatial vector from the electrocardiogram, the vector will be found to lie at -50° in the frontal reference frame, in contrast with the inferior orientation of the normal mean 0.04-second QRS spatial vector. Thus, the electrocardiographic diagnosis of diaphragmatic infarction can be made by the vector method of analysis. (The limitations of this method are discussed in Chapter 7.)

leads II, III, and aVF of the electrocardiogram, while the superior displacement or subsequent portions of the QRS loop accounts for the pre-infarction would certainly diagram and the T SE loop, The in-

Fig. 188.—Electrocardiographic and vectorcardiographic findings in a recent diaphragmatic-antrolateral infarction.

In the electrocardiogram, the QRS duration is almost 0.12-second, QS deflections and deeply inverted T waves are recorded by leads II, III, and aVF. The QRS deflections in leads I and V_4 are of low amplitude, but the small Q waves in these leads are nondiagnostic of infarction. The width of the R wave in Lead V_3 is between 0.02 and 0.03 second, and so the R wave in V_4 cannot be considered indicative of antrolateral infarction.

The vectorcardiographic abnormalities diagnostic of diaphragmatic infarction are obvious and will not be described. Note the elongated, large, and superiorly directed T sE loop, indicative of diaphragmatic ischemia. The vectorcardiographic findings diagnostic of coexisting antrolateral infarction are as follows: the mean 0.02-second instantaneous QRS vectors in the frontal and horizontal QRS loops are directed much farther to the right and anteriorly (as well as superiorly) than normally, and the efferent limbs of the horizontal and frontal QRS loops are displaced to the right or medially, superiorly, and posteriorly. Note the reversed direction of inscription of the early deflection of the horizontal QRS loop. The prolonged QRS interval may reflect peri-infarction block (discussed on p. 335, Chapter 21).



loop. In normal subjects, we found the 0.02-second vector in the frontal plane to be located between 0° and $+60^\circ$ in three fourths of the cases, while in most cases of diaphragmatic myocardial infarction, the 0.02-second vector was situated between -40° and -140° . The average orientation of the mean 0.02-second instantaneous vector of the frontal QRS loop in diaphragmatic myocardial infarction was found, by us, to be -95° , while the orientation of the vector in normal subjects averaged $+55^\circ$. Over 80% of the frontal loops in the infarction series were inscribed in clockwise direction, a considerable increase in the frequency of this finding, as compared with normals.

S-T Vector and Ventricular Repolarization

In acute diaphragmatic myocardial infarction, there is present, for reasons previously cited, an S-T

vector which is directed toward the effective electrical site of subepicardial injury—that is, inferiorly, and this vector projects elevated S-T segments on leads II, III, and aVF. The corresponding abnormality of the QRS sE loop of the vectorcardiogram consists of a shift of the terminus of the loop inferiorly, a line drawn from the loop's point of origin to its terminus indicating the direction and magnitude of the S-T vector.

Subsequently, as the strong injury field subsides during the evolution of a diaphragmatic myocardial infarction, the changes due to transmural ischemia at the site of infarction make their appearance in the electrocardiogram and vectorcardiogram. The local reversal in the direction of repolarization consequent to the infarction-induced delay in subepicardial myocardial recovery tends to rotate the instantaneous T vectors away from the effective electrical site of the

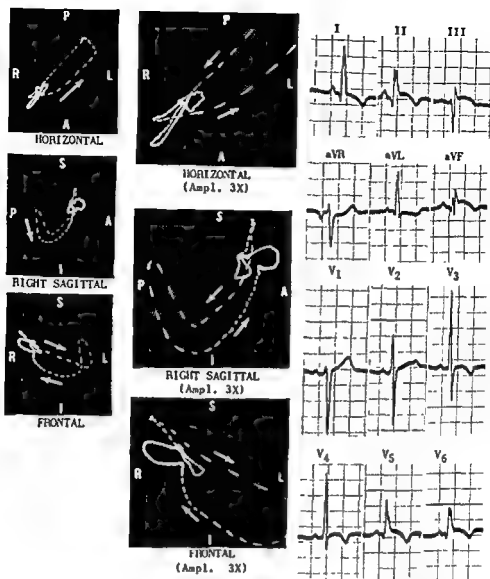


Fig. 189.—Electrocardiographic and vectorcardiographic findings at an early stage in the evolution of an acute diaphragmatic myocardial infarction. There is S-T segment elevation indicative of diaphragmatic-lateral subepicardial injury in leads II, III, aVF, V₄, and V₆ of the electrocardiogram, and in the same leads, inverted T waves of transmural ischemia are also present. The Q waves in leads II and aVF are, as yet, insignificant, while lead III registers an rSr' deflection. Thus, unequivocal evidence of actual muscle necrosis in the electrocardiogram has not appeared up to this point. In the vectorcardiogram, the terminus of the QRS sE loop is displaced anteriorly, inferiorly, and somewhat to the left, indicating a similarly directed S-T vector, while the T sE loop is oriented anteriorly, to the right, and somewhat superiorly. The right sagittal QRS loop exhibits a relatively prominent, markedly superiorly directed early deflection with a 0.02-second mean instantaneous vector lying at about -80° . In addition, there is a reversed direction of inscrip-

infarction—that is, superiorly and somewhat to the left. The T vectors project on the negative

T waves. These findings in the electrocardiogram are paralleled by the changes in the T sE loop of the vectorcardiogram. For example, in recent diaphragmatic infarction, the T sE loop is usually directed superiorly and slightly to the right and anteriorly. It tends to be greatly elongated, and the efferent and

afferent limbs of the loop may be inscribed at nearly the same rate (the time dashes being evenly spaced throughout). If the infarction is relatively old, the characteristics of the T sE loop are much more variable: the loop may have a normal appearance and orientation, it may be small, round, and oriented superiorly or away from QRS sE loop, or it may have a normal appearance but discordant orientation with respect to the long axis of the QRS sE loop (Fig. 157-159).

POSTEROLATERAL INFARCTION

The second type of inferoposterior infarction, posterolateral infarction, has received far less attention in the past than any of the other infarction patterns which have so far been described. In fact, the frequent, although not invariable, association of diaphragmatic and posterolateral infarctions led, in previous years, to grouping these two infarction patterns together under the common designation of posterior infarction. Since the latter term was also applied to diaphragmatic infarction unaccompanied by posterolateral involvement, this naturally resulted in considerable confusion in terminology and meaning (and tended to obscure the separate identity of posterolateral infarctions).

It will be remembered that during the description of the anterior myocardial infarctions the point was made that lateral infarctions are, for all intents and purposes, of two types, anterolateral infarction and posterolateral infarction. The anterolateral type of infarction is so designated because its electrical location is in the anterolateral wall of the left ventricle. Thus the infarction vector in anterolateral infarction is directed to the right and posteriorly (see preceding chapter). In contrast, posterolateral infarctions are placed, in terms of their effective electrical position, in the posterolateral or posterobasal wall of the left ventricle. The infarction vector representing the unbalanced forces created by the infarction is directed to the right and anteriorly.

In theory at least, one would expect the unbalanced forces resulting from posterolateral infarction to affect the electrocardiogram and vectorcardiogram during the time this region of the left ventricle normally undergoes activation—that is, from about 0.04 second after onset of the QRS interval until the end of this period. As will be indicated later, alterations of the terminal portion of the QRS sE loop of the vectorcardiogram and of the QRS deflection of the electrocardiogram in fact do frequently occur in pos-

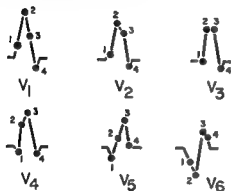
terolateral infarction, although they have not been extensively studied as yet. The electrocardiographic abnormalities generally accepted as being diagnostic of posterolateral infarction (tall, wide R wave in lead V₁ and deep, wide Q wave in leads V₆ and/or V₇) involve the earlier portion of the QRS deflection and therefore appear before activation of posterolateral left ventricular wall. In view of this fact, it is evident that, in addition to, or perhaps instead of, the mechanism of the QRS changes of infarction described earlier (Chapter 18), some other mechanism must be implicated to account for the early QRS abnormalities in posterolateral infarction, and this may well hold true for infarctions in other locations. Grant has summarized the problem of explaining the Q waves of infarction in the following way: "... whatever the anatomic location of the infarct, its electrical mechanism must be such that the very first part of the myocardium to generate electrical activity of sufficient magnitude to be recorded at the body surface is involved by the infarction process." He then goes on to speculate that "the early stages of ventricular depolarization being a nearly instantaneous process, it is possible to conceive of conduction relationships which could cause infarcts in various regions of the heart to be referred electrically to more proximate regions along the anterior and posterior subdivisions of the left bundle branch network." However, for the sake of simplicity, it will be assumed, in this text, that the QRS abnormalities in posterolateral infarction merely reflect a shift in the balance of cardiac forces resulting from loss of forces directed posteriorly and to the left.

The Instantaneous YA Vectors

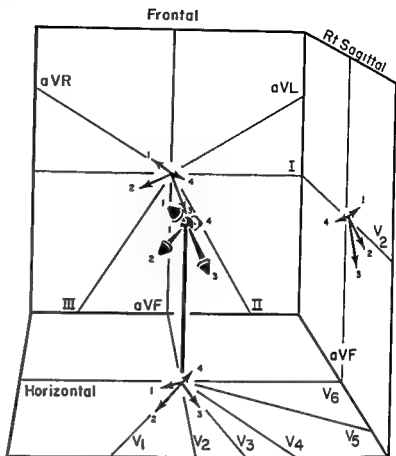
In the absence of concomitant diaphragmatic infarction, the unbalanced forces created by posterolateral infarction have two directional components: a



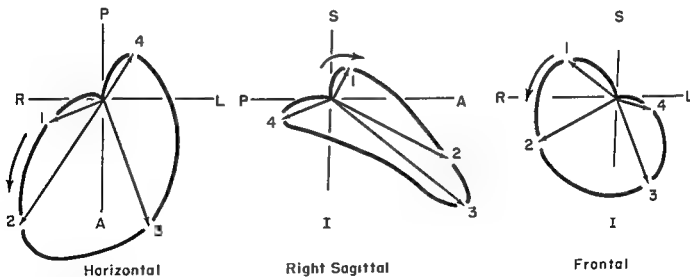
A Posterolateral Myocardial Infarction



C QRS Deflections Projected on Scalar Leads



B Instantaneous VA Vectors in Posterolateral Myocardial Infarction



D Planar QRS Loops in Posterolateral Myocardial Infarction

Fig. 190.—Inst
infarction is depicted
forces directed to
2 and 3 are deviat
derived from the
Note that, just as
R wave Lead V₄

right and transverse component (X) and an anterior sagittal (Z) component. Typically, the balance of cardiac forces is not altered along the vertical (Y) axis in posterolateral infarction. Thus, in describing the VA vectors in the following paragraphs, reference will be made only to the orientation of the vectors along the X and Z axes. For the same reason, in relating the instantaneous vectors to the electrocardiogram and vectorcardiogram (see Fig. 190), the precordial leads of the electrocardiogram and the horizontal projection of the vectorcardiogram will be emphasized for the most part. When diaphragmatic and posterolateral infarctions occur in combination, the infarction vector is directed not only to the right and anteriorly but also markedly superiorly. The presence of the diaphragmatic myocardial infarction does not, however, alter the features of the posterolateral infarction in the precordial electrocardiographic leads or in the horizontal vectorcardiogram but simply causes additional abnormalities (already described) to appear in limb leads II, III, and aVF and in the frontal and sagittal projections of the vectorcardiogram.

0.01-SECOND VA VECTOR

For reasons that are not clear at present, posterolateral infarction behaves electrically, first, as if its electrical location were in the posterolateral or posterobasal wall of the left ventricle, and, secondly, as if this region of the left ventricle were activated during the first 0.04 second of the QRS interval rather than later, as is actually the case. In other words, the infarction vector in posterolateral infarction makes its appearance early in the QRS interval and is directed to the right and somewhat anteriorly. While the basal portion of the septum may sometimes be involved in posterolateral infarction, in most cases initial septal depolarization from left to right is not disturbed, so that the 0.01-second VA vector is directed to the right and anteriorly, just as normally is the case, projecting the following deflections on the precordial leads and leads I and aVL.

Lead V₁.—Beginning upstroke of an R wave

Leads V₄ and V₅, and sometimes leads I, aVL, and V₆.—Beginning downstroke of a Q wave,

0.02-SECOND VA VECTOR

Although posterobasal left ventricular wall is activated later than 0.02 second after onset of the QRS interval, for some reason the unbalanced forces resulting from posterolateral infarction begin to affect the balance of cardiac forces at this time. The postinfarction 0.02-second VA vector, which is the resultant of the corresponding preinfarction vector (normally of relatively small magnitude and having a leftward and slightly anterior orientation) and the infarction vector, is displaced to the right and anteriorly and its magnitude is increased so that the following deflections are written in the electrocardiogram:

Lead V₁.—The 0.02-second VA vector coincides roughly with the peak of the tall R wave in this lead, since this vector lies well anteriorly and usually extends farther to the right than any other instantaneous vector.

Leads V₄ and V₅, and sometimes leads I, aVL, and V₆.—The 0.02-second VA vector coincides roughly with the nadir of the Q wave in these leads, since it usually projects maximally on the negative halves of the axes of derivation of these leads.

0.04-SECOND VA VECTOR

In a typical posterolateral infarction, the 0.04-second VA vector is situated to the left and well anteriorly, in contrast with its normal posterior location. Occasionally it may even lie to the right and anteriorly. Whether oriented to the left or right, the 0.04-second vector is in most instances, located sufficiently anteriorly to project on the positive half of the axis of derivation of lead V₁; that is, it is generally situated to the right of +30° in the horizontal reference frame. The less marked displacement of the 0.04-second vector in posterolateral infarction, in comparison with the 0.02-second VA vector, may perhaps be related to the greater magnitude of the preinfarction 0.01-second vector, which normally is directed to the left and posteriorly. Thus, the postinfarction 0.04-second vector tends, on the average, to conform in terms of its direction more nearly to the direction of the preinfarction 0.04-second vector than to the direction of the infarction vector. Consequently, the postinfarction 0.04-second vector usually retains its leftward orientation but shifts anteriorly and produces

ar to the right and anteriorly, while
ad in the horizontal and frontal QRS

the following deflections in the electrocardiogram:

Lead V_1 .—More often than not, the 0.04-second vector projects on the positive half of the axis of derivation of lead V_1 , which therefore completes the inscription of a tall R wave of 0.04-second (or longer) duration. Less frequently, the 0.04-second vector lies far enough to the left to contribute to the downstroke of a terminal S wave in lead V_1 .

Leads V_6 and V_7 , and sometimes leads I, aVL, and V_8 .—Beginning upstroke of a low R wave.

0.06-SECOND VA AND SUBSEQUENT INSTANTANEOUS VECTORS

The 0.06-second VA vector often has much the same orientation in posterolateral infarction as it has normally—that is, markedly posterior and slightly to the left. However, if anything, the orientation of the 0.06-second VA vector shows a wider range of variation in posterolateral infarction than it does normally. This and certain other dissimilarities between the

terminal vectors in the normal subject and in posterolateral infarction will be discussed more fully subsequently.

Lead V_1 .—Completion of a terminal S wave of varying size, which is usually smaller than the R wave in this lead.

Leads V_6 and V_7 , and sometimes leads I, aVL, and V_8 .—Completion of low terminal R wave.

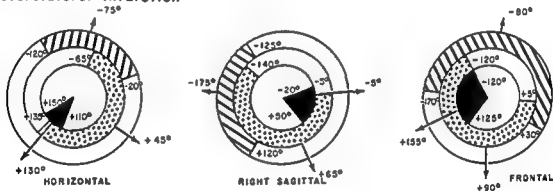
The electrocardiographic criteria for the diagnosis of posterolateral infarction will be outlined after the presentation of the vectorcardiographic findings in this type of infarction.

Vectorcardiographic Findings

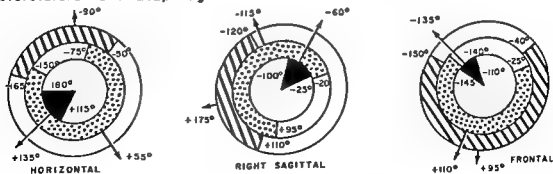
Since the unbalanced forces created by a posterolateral infarction are directed both to the right and anteriorly, they produce abnormal changes in the QRS sE loop in all three projections of the vectorcardiogram (Fig 191).

HORIZONTAL QRS LOOP—In the horizontal projec-

Posterolateral Infarction



Posterolateral and Diaphragmatic Infarction






-  .02 SEC. MEAN INSTANTANEOUS QRS VECTOR
-  MAXIMAL MEAN INSTANTANEOUS QRS VECTOR
-  MAXIMAL TERMINAL MEAN INSTANTANEOUS QRS VECTOR

Fig. 191.—Range of variation and average orientation of the 0.02-second mean, maximal mean, and maximal terminal mean instantaneous QRS vectors of the vectorcardiographic QRS sE loop in posterolateral and in diaphragmatic posterolateral infarctions

tion, the feature which is perhaps most characteristic of, and most consistently present in, posterolateral infarction is that the QRS loop for the first 0.04 second of the QRS interval is written abnormally far to the right and anteriorly. Thus, in our series of posterolateral infarctions, the mean 0.02-second instantaneous vector, as measured from the horizontal QRS loop, was oriented, on the average, along the $+130^\circ$ axis of the horizontal reference frame, while the maximal mean instantaneous QRS vector in this projection had an average orientation of $+45^\circ$. In general, the first half of the horizontal QRS loop is located anteriorly and at first to the right and then to the left of the midline and is inscribed in a counterclockwise direction. This portion of the QRS loop is therefore responsible for the abnormal Q waves which appear in the left lateral precordial leads and for the tall, wide R waves which are recorded in lead V_1 . The rest of the horizontal QRS loop is then written in a counterclockwise direction to the left (or sometimes to the right) and posteriorly. When the terminal portion of the QRS loop lies in the right posterior quadrant, it generally is clockwise inscribed and causes the QRS loop to have a figure-of-eight configuration. The average orientation of the mean 0.06-second instantaneous vector in the authors' cases was -75° . While the average orientation of the 0.06-second instantaneous vector in posterolateral infarction cited above does not differ significantly from that of the corresponding normal vector, exceptions occur in which the terminal 0.06-second vector is located farther to the right and more posteriorly than is observed normally. A more common difference between the terminal vectors in posterolateral infarction and those in the normal vectorcardiogram is that the former have a far greater magnitude, in many cases, than is ever observed normally. The reason for this is not apparent.

RIGHT SAGITTAL QRS LOOP—The sagittal QRS loop is clockwise inscribed in many cases of posterolateral infarction, but counterclockwise inscription of the entire loop or of one or the other component of a figure-of-eight sagittal loop is not an unusual finding. Typically, the sagittal loop tends to lie somewhat more anteriorly than posteriorly. In our cases, the mean 0.02-second instantaneous vector was oriented, on the average, at -5° , the maximal mean instantaneous vector, at $+65^\circ$, and the terminal mean 0.06-second instantaneous vector, along the -175° axis of the sagittal reference frame.

FRONTAL QRS LOOP—During the first 0.02–0.04 second of the QRS interval, the QRS sE loop in the frontal projection is generally written far to the right

—that is, provided the lateral component of the infarction vector is relatively large with respect to the anterior component. In this event, the rightward extent of the frontal QRS loop projects abnormal Q waves on lead I. However, if the major displacement of the QRS sE loop takes place in an anterior direction, the frontal QRS loop may fail to show diagnostic abnormalities (although it is unusual for the frontal loop, in cases such as this, to be entirely normal). More often than not, the frontal loop is inscribed in a counterclockwise direction, although clockwise inscription of the entire loop and, in the case of a figure-of-eight loop, clockwise-counterclockwise inscription of the initial and terminal components of the loop were found to occur with about equal frequency in our experience. On the average, in our cases, the mean 0.02-second instantaneous vector in the frontal projection was found to be situated at about $+155^\circ$; the maximal mean instantaneous vector, at about $+90^\circ$; and the terminal mean 0.06-second instantaneous vector, at about -80° . As a general rule, clockwise-inscribed frontal QRS loops frequently show abnormal superior deflections indicative of associated diaphragmatic involvement, while counterclockwise-inscribed frontal loops tend to display more striking evidence of lateral wall infarction.

Table 26 indicates the range and average orientation of the mean 0.02-second, maximal mean, and mean 0.06-second instantaneous vectors of the QRS sE loop in each projection in posterolateral infarction with and without concomitant diaphragmatic infarction (Fig. 191). It can be seen that diaphragmatic infarction alters the sagittal and frontal instantaneous vectors in a predictable way, that is, the mean 0.02-second and maximal mean instantaneous vectors are displaced superiorly and to the right and anteriorly.

S-T Vector and Ventricular Repolarization

In the vectorecardiographic study of posterolateral infarction, our experience has been greater with old infarctions than with acute infarctions. The QRS sE loop was, therefore, usually observed to be closed, an S-T vector not being present. For the same reason, the orientation and size of the T sE loop was

—however, in the vectorecardiogram—usually directed or anteriorly (the S-T vector being similarly directed), while the T sE loop was large and lozenge-shaped and directed to the right and

TABLE 26—ORIENTATION OF THE MEAN 0.02-SECOND, MAXIMAL MEAN, AND MEAN 0.06-SECOND INSTANTANEOUS VECTORS OF THE QRS IN POSTEROLATERAL MYOCARDIAL INFARCTION WITH AND WITHOUT ACCOMPANYING DIAPHRAGMATIC INFARCTION

	HORIZONTAL			RIGHT SAGITTAL			FRONTAL		
	Extreme Range	Av	Usual Range*	Extreme Range	Av	Usual Range*	Extreme Range	Av	Usual Range*
Posterolateral Infarction without Diaphragmatic Infarction									
Mean 0.02-second instantaneous QRS vector	+110° to +150°	+130°	+110° to +135°	-20° to +50°	-5°	-20° to 0°	+125° to -120°	+155°	+170° to -120°
Maximal mean instantaneous QRS vector	-65° to +135°	+45°	-15° to +120°	-5° to -140°	+65°	0° to +160°	+5° to -120°	+90°	+5° to +75°
Mean 0.06-second instantaneous QRS vector	-130° to -20°	-75°	-105° to -30°	+120° to -125°	-175°	+140° to -140°	-170° to +30°	-80°	-170° to -40°
Posterolateral Infarction with Diaphragmatic Infarction									
Mean 0.02-second instantaneous QRS vector	+115° to 160°	+135°	+120° to +155°	-100° to -25°	-60°	-70° to -35°	-145° to -110°	-135°	-145° to -130°
Maximal mean instantaneous QRS vector	-75° to -150°	+55°	-20° to -150°	+95° to -20°	-115°	-95° to -20°	-25° to -140°	+110°	+35° to -140°
Mean 0.06-second instantaneous QRS vector	-165° to -50°	-90°	-120° to -50°	+110° to -120°	+175°	+155° to -120°	-40° to -150°	+65°	+35° to -165°

*Usual range = range in 85% of cases.

anteriorly. We have found it surprisingly easy to recognize posterior ischemia vectorcardiographically, in contrast with the difficulties encountered electrocardiographically.

Electrocardiographic Criteria for Diagnosis

QRS ABNORMALITIES

The electrocardiographic abnormalities most characteristic of posterolateral infarction are (Fig. 192):

1. Abnormal Q waves in leads V_1 and/or V_2 , and sometimes in leads I, aVL , and V_6 .
2. An R wave in lead V_1 with a duration of 0.04 second or longer.

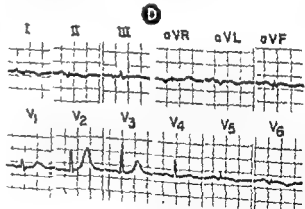
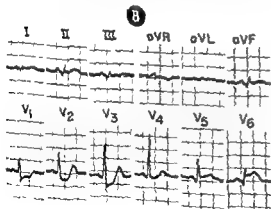
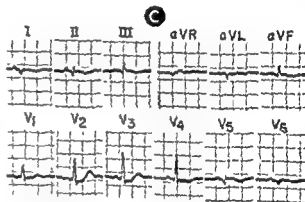
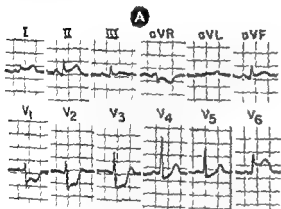
3. Increased amplitude of the R wave in V_1 with an R/S ratio equal to or greater than 1.

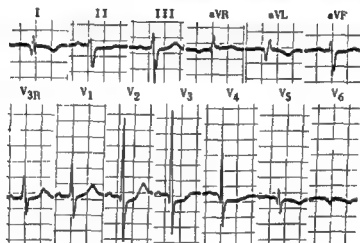
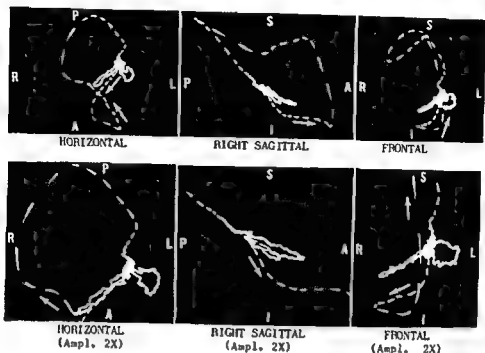
Pathologic cellular evidence of myocardial infarction, the incidence of the above electrocardiographic findings was as follows:*

Lead V_1 .—In 75% of the cases, $R/S \geq 1$ and width of R wave ≥ 0.04 second, in 25% of cases, $R/S < 1$ and width of R wave = 0.03–0.04 second.

Leads V_1 and/or V_2 .—Abnormal Q wave in 75% of cases.

*See Criteria of Q Wave Abnormalities in Chapter 18.





I . 111

Rv

QR

riorly and to the right, the sagittal QRS loop is counterclockwise inscribed, at first anteriorly and later posteriorly, while the frontal QRS loop is written almost entirely along the vertical axis. The T sE loop is directed anteriorly and to the right, indicating posterolateral ischemia

Lead I—Abnormal Q wave in 50% of cases.

Lead aVL—Abnormal Q wave in 15% of cases.

Leads I, aVL, V₆, and V₇—Equivocal, normal, or absent Q waves in all leads in 25% of cases.

Leads II, III, and aVF—Abnormal Q waves in 45% of cases (i.e., 45% of cases of posterolateral infarction selected by the authors for study evidenced associated diaphragmatic myocardial infarction)

It has been our experience that diagnostic findings in lead V₁ in posterolateral infarction tend, on the av-

erage, to be more prominent and more consistently present than those occurring in lead V₆, although it is equally true that the findings in lead V₁ are less specific for posterolateral infarction than those in lead V₆. For example, in some normal individuals with normal vectorcardiograms, the R/S ratio in lead V₁ may exceed 1, and the width of the R wave occasionally may approach or equal 0.04 second.

As Grishman has pointed out, the electrocardiographic features of healed posterolateral infarction

may resemble quite closely those of the so-called *classic* or *uncommon* type of right bundle branch block or may simulate right ventricular hypertrophy. In differentiating these conditions, one from the other, and in establishing the diagnosis of posterolateral infarction, the vectorcardiogram possesses unequivocal diagnostic advantages over the electrocardiogram.

S-T SEGMENT AND T WAVE CHANGES

In the subepicardial myocardial injury phase of acute posterolateral infarction, an S-T vector points toward the effective site of injury—that is, posteriorly and to the left. Thus, the S-T segments in leads V_1 and, usually, V_2 are upwardly displaced, while leads V_{3R} , V_1 , and V_2 , which are oriented to the negative aspect of the injury vector, record depressed S-T

V_2 in acute posterolateral infarction to the additive effects of posterior subepicardial injury and anterior subendocardial injury is conjectural.

Posterolateral transmural ischemia causes the instantaneous T vectors to rotate anteriorly and to the right. Inverted T waves are thus recorded in leads V_4 and V_7 , but the remaining routine precordial leads register upright T waves, usually larger. As a rule, the right precordial leads in posterolateral infarction display QRS, S-T, and T abnormalities which are inverted mirror images of the abnormalities in left posterior back leads: For example, the tall and wide R waves recorded in lead V_1 correspond to the deep and wide Q waves recorded in lead V_8 ; the depressed S-T segments in lead V_1 are reciprocally related to the elevated S-T segments in lead V_8 ; and the tall upright T waves registered in lead V_1 correspond to the deeply inverted T waves present in lead V_8 . The pattern for the evolution of the S-T segment and T wave abnormalities in posterolateral infarction is the same pattern as for myocardial infarction (see Chapter 18 and Figs. 193-195).

overlie the infarction. Whether one can attribute the pronounced S-T segment depression in leads V_1 and

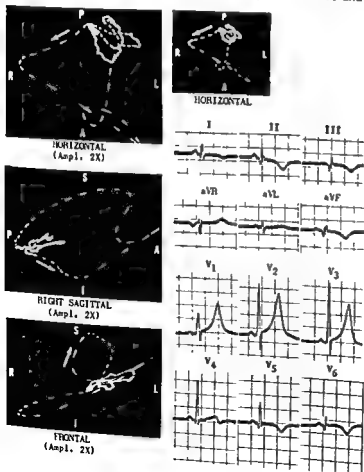


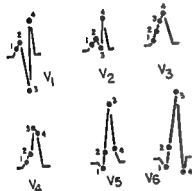
Fig. 194.—Electrocardiographic and vectorcardiographic findings in recent posterolateral myocardial infarction.

The electrocardiogram shows, an abnormal Q wave in lead V_6 , a tall, wide initial R wave in lead V_1 , tall upright T waves in leads V_1 through V_6 , and inverted T waves in leads I, II, III, aVF, V_4 , and V_6 . These findings are all compatible with posterolateral myocardial infarction and diaphragmatic-posterolateral ischemia.

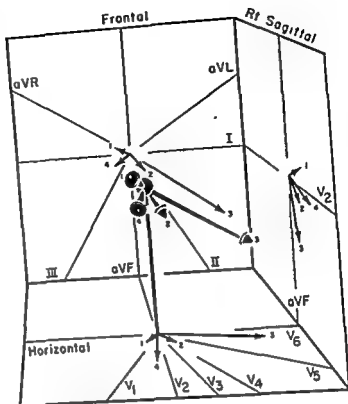
In the vectorcardiogram, the QRS sE loop displays an early deflection which extends abnormally far to the right and anteriorly. This signifies the presence of posterolateral myocardial infarction. There is a large S-T vector directed to the left and posteriorly, best demonstrated in the horizontal projection (as evidenced by the leftward and posterior displacement of the terminus of the QRS loop). This finding is indicative of posterolateral subepicardial injury, while the orientation of the T sE loop almost directly anteriorly is compatible with posterior ischemia.



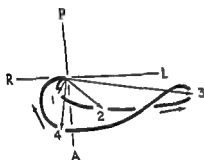
A Strictly Posterior Myocardial Infarction



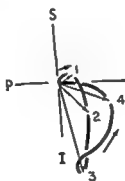
C QRS Deflections Projected on Scalar Leads



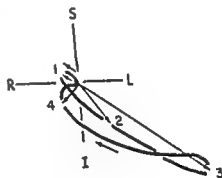
B Instantaneous VA Vectors in Strictly Posterior Myocardial Infarction



Horizontal



Right Sagittal



Frontal

D Planar QRS Loops in Strictly Posterior Myocardial Infarction

(D) show anterior displacement of their afferent or returning limbs, while the frontal QRS loop is normal.

based primarily on earlier observations of Crishman and his investigative group, supplemented by our observations in our own series of patients with this type of infarction.

The manner in which the diagnostic QRS abnormalities are produced by strictly posterior infarction is not known. However, strictly posterior infarction behaves electrically as if it were situated in some region of posterobasal left ventricular wall which is activated relatively late in the QRS interval. Thus, the most marked changes due to the infarction are relegated, for the most part, to the second half of the QRS deflection and QRS sE loop.

The Instantaneous VA Vectors

The electrical forces produced in strictly posterior infarction can be presented in simplified manner in terms of the instantaneous VA vectors (see also Fig. 196):

0.01- to 0.04-SECOND VA VECTORS

The 0.01- and 0.02-second VA vectors have essentially normal characteristics, since these vectors represent depolarization potentials arising in uninvolved regions of the septum and left ventricle which are activated early in the QRS interval. On the other hand, the 0.04-second VA vector is more variable in its orientation in that it is situated to the left and either posteriorly, or, as is more commonly the case, anteriorly.

Lead V.—The 0.01- to 0.04-second VA vectors project on this lead an initial small R wave followed by the downstroke of an S wave which is perhaps somewhat shallower than normal, or the initial R wave may be followed by an *incisura* not reaching the base line or by the slurred upstroke of a secondary R wave. The factor determining which of the preceding deflections is recorded is the degree of anterior displacement of the 0.04-second VA vector.

Leads I, aVL, V₁, and V₂.—The 0.01- to 0.04-second VA vectors produce small normal Q waves followed by relatively normal-appearing R waves in these leads.

0.06- AND 0.08-SECOND VA VECTORS

Following the appearance of the 0.04-second VA vector, subsequent instantaneous vectors in strictly posterior infarction tend to develop progressively to the right and anteriorly. Thus the 0.06-second VA vector usually extends more anteriorly than to the

right, while the 0.08-second VA vector projects more to the right than anteriorly (and not infrequently is situated somewhat posteriorly). Whether the anterior displacement of these vectors reflects simply the effect of an anteriorly directed infarction vector on the balance of cardiac forces existing during the second half of the QRS interval or whether an additional mechanism is involved (as, for example, conduction delay in some portion of the intraventricular conduction system consequent to the infarction) is not known at present.

Lead V₁.—Typically the 0.06- and 0.08-second VA vectors project on lead V₁ a relatively tall R wave which may or may not be followed by a small terminal S wave, depending on whether the 0.08-second VA vector is located anterior or posterior to the -150° axis of the horizontal reference frame. In summary, in strictly posterior infarction, lead V₁ typically records an RSR' deflection, a notched or slurred R wave (of lower amplitude than that occurring in right ventricular hypertrophy), or an RS deflection with an R/S amplitude ratio exceeding 1.

Leads I, aVL, V₃, and V₄.—These leads complete the inscription of an R wave, followed by a terminal S wave. Thus, the leads record qRs or qRS deflections in strictly posterior infarction. Unless there is concomitant diaphragmatic infarction, leads II, III, and aVF display normal QRS complexes.

Vectorcardiographic Findings

The average orientation and the extreme range of orientations of the mean 0.02-second, maximal mean, and mean 0.06-second instantaneous QRS vectors of the horizontal, sagittal, and frontal loops in strictly posterior myocardial infarction with and without diaphragmatic infarction are shown in Table 27 and Figure 197.

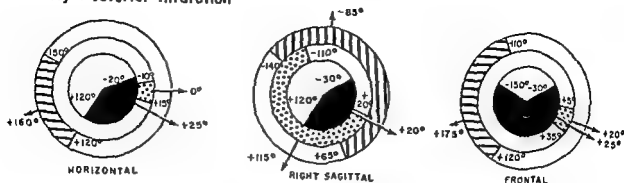
HORIZONTAL QRS LOOP.—The QRS sE loop in the horizontal projection is initially written to the right and anteriorly, just as normally, and then the efferent limb is inscribed to the left and anteriorly. After reaching its maximal leftward extent, the loop turns in a clockwise direction and moves medially toward the right. In strictly posterior infarction, the afferent limb is displaced anteriorly and may be anterior to the efferent limb throughout its entire course. In the latter situation, the horizontal QRS loop has a clockwise direction of inscription, and the terminal portion of the loop is situated to the right and anteriorly or occasionally posteriorly. In some cases, only the first portion of the afferent limb lies anterior to the efferent limb, and in this event, the crossing of the afferent

TABLE 27.—ORIENTATION OF THE MEAN 0.02-SECOND, MAXIMAL MEAN, AND MEAN 0.06-SECOND INSTANTANEOUS VECTORS OF THE QRS AS LOOP IN STRICTLY POSTERIOR MYOCARDIAL INFARCTION WITH AND WITHOUT DIAPHRAGMATIC INFARCTION

TABLE 27 —ORIENTATION OF THE MEAN 0.02-SECOND, MAXIMAL MEAN, AND MEAN 0.06-SECOND INSTANTANEOUS QRS VECTORS IN STRICTLY POSTERIOR MYOCARDIAL INFARCTION WITH AND WITHOUT DIAPHRAGMATIC INFARCTION									
	HORIZONTAL			RIGHT SAGITTAL			FRONTAL		
	Extreme Range	Av	Usual Range*	Extreme Range	Av	Usual Range*	Extreme Range	Av	Usual Range*
Strictly Posterior Infarction without Diaphragmatic Infarction									
Mean 0.02-second instantaneous QRS vector	-20° to +120°	+25°	-20° to +20°	-30° to +120°	+20°	-20° to +100°	-30° to -150°	+25°	-30° to +35°
Maximal mean instantaneous QRS vector	-10° to +15°	0°		+20° to -110°	+115°	+60° to -140°	+5° to +35°	+20°	.
Mean 0.06-second instantaneous QRS vector	+120° to -150°	+160°	+135° to -175°	-140° to +65°	-65°	-120° to +45°	+120° to -110°	+175°	+150° to -115°
Strictly Posterior Infarction with Diaphragmatic Infarction									
Mean 0.02-second instantaneous QRS vector	-25° to +120°	+60°	+50° to +120°	-110° to -40°	-65°	-60° to -40°	-70° to -50°	-60°	...
Maximal mean instantaneous QRS vector	+10° to +25°	+20°		0° to +70°	+35°	..	0° to +45°	+25°	...
Mean 0.06-second instantaneous QRS vector	+50° to -110°	160°	-175° to -110°	-30° to -175°	+80°	+50° to -175°	0° to +120°	+55°	+45° to +120°

*Usual range = range in 85% of cases.

Strictly Posterior Infarction



Strictly Posterior and Diaphragmatic Infarction

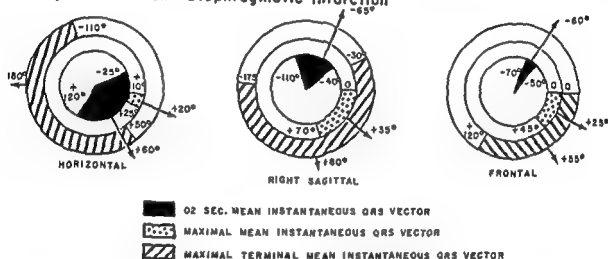


Fig. 197.—Range of variation and average orientation of the mean 0.02-second, the maximal mean, and the maximal terminal mean instantaneous QRS vectors in strictly posterior and diaphragmatic-strictly posterior myocardial infarctions

and efferent limbs of the horizontal QRS loop gives the latter a figure-of-eight configuration, the proximal loop of the "eight" being counterclockwise inscribed and the distal loop clockwise inscribed. Not uncommonly, loops of this configuration display a terminal deflection to the right and far posteriorly. In our experience, the mean 0.02-second instantaneous vector of the horizontal QRS loop in strictly posterior infarction was found to be oriented just as normally, while the maximal mean instantaneous QRS vector tended to shift abnormally far anteriorly. As a general rule, the mean 0.06-second instantaneous QRS vector in the horizontal projection is located abnormally far to the right and anteriorly, which is in striking contrast with the almost directly posterior orientation of the normal mean 0.06-second vector.

RIGHT SAGITTAL QRS LOOP—In strictly posterior infarction, the sagittal QRS loop confirms the anterior displacement of the long axis or maximal mean instantaneous vector of the QRS SE loop, already de-

scribed in the horizontal projection. In general, the sagittal loop presents either of the following configurations: (1) When the entire afferent limb of the horizontal QRS loop lies anterior to the efferent limb, the sagittal loop is written entirely in a counterclockwise direction. (2) When only a part of the afferent limb is situated anterior to the efferent limb in the horizontal projection, the same condition holds true in the sagittal projection. Thus the sagittal QRS loop will have a figure-of-eight configuration in which the proximal component of the loop is clockwise inscribed and the distal component counterclockwise inscribed. The mean 0.02-second instantaneous QRS vector in the sagittal projection, like that in the horizontal, does not differ from the normal in orientation unless there is associated diaphragmatic infarction. The maximal mean instantaneous QRS vector (long axis of the sagittal QRS loop) tends to be located somewhat more posteriorly than normal, while the mean 0.06-second instantaneous QRS vector is quite

distinctive in that it is directed anteriorly instead of posteriorly as is normally the case.

FRONTAL QRS LOOP—In the absence of combined diaphragmatic infarction, the frontal QRS loop in strictly posterior infarction does not show diagnostic abnormalities, since the unbalanced forces produced by this type of infarction are oriented primarily perpendicular to the frontal plane.

The T-E loop and the S-T vector in strictly posterior infarction are dealt with at the end of this chapter.

The ECG Criteria for Diagnosis

QRS ABNORMALITIES

(Although strictly posterior infarction fails to produce abnormal Q waves in any of the twelve routine

electrocardiographic leads, QRS changes do appear typically in one or more of the right precordial leads. (Needless to say, specific criteria for the electrocardiographic diagnosis of strictly posterior infarction have not been formulated as yet.) The electrocardiograms from patients with vectorcardiographically diagnosed old strictly posterior infarction which we reviewed displayed the following features:

Leads I, aVL, and V₆—Abnormal Q waves absent in all cases

Leads V_{1R} and V₂—RSR' configuration (rSR', rSR', or rSR') in 40% of the cases, notched or slurred R, or Rs with R/S ratio ≥ 1 in 35% of the cases, and QRS configuration of the rS type in lead V₁ in 25% of the cases.

It is evident from the description of the electrocardiogram and vectorcardiogram in strictly posterior infarction that the electrocardiographic QRS residuals

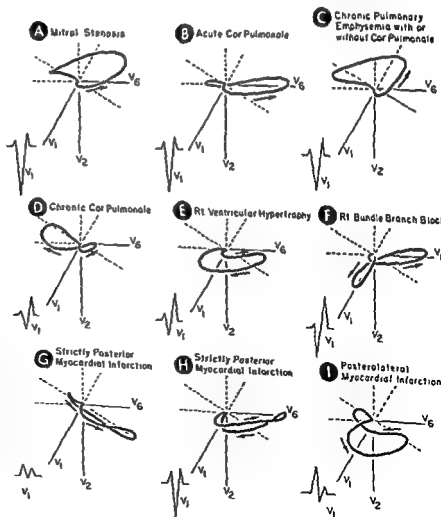


Fig 198.—Horizontal QRS loop patterns which may be accompanied by RSR' deflections in lead V₁ of the electrocardiogram. The schematic QRS loops in G and H represent two types of loop configurations observed in strictly posterior infarction. In all examples of QRS loop configuration except that in F, the QRS duration in the electrocardiogram is 0.10-second or less.

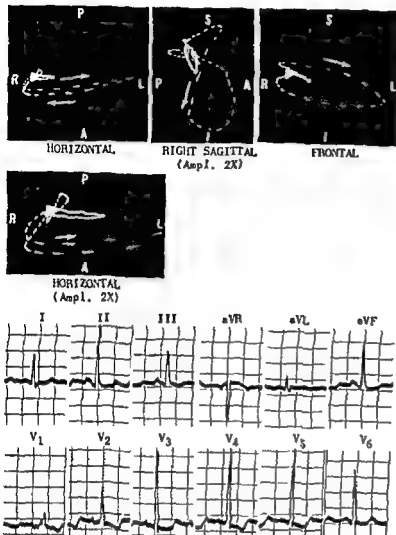


Fig. 199.—Electrocardiographic and vectorcardiographic findings in an old or healed strictly posterior infarction. One year before these recordings were taken, the patient was hospitalized for 6 weeks with a clinically typical picture of acute myocardial infarction. (The only finding in the above electrocardio-

graph was a deep Q wave in lead III.)

of this type of infarction can simulate incomplete right bundle branch block, right ventricular hypertrophy, the pattern of "counterclockwise rotation," or the juvenile precordial lead pattern, in which the R waves in right precordial leads are relatively large. Not only is the vectorcardiogram useful in differentiating these and other conditions producing RSR' deflections in lead V₁, but—of equal importance—it is free from the several handicaps which limit the value of the electrocardiogram in diagnosing strictly posterior infarction (Fig. 198). These electrocardiographic limitations are as follows: (a) The salient diagnostic feature of infarction, an abnormal Q wave or QS deflection, appears in none of the routine electrocardiographic leads. (b) More often than not, the increased amplitude of the R waves in right and midprecordial leads is not particularly striking. (c) Although esophageal leads or leads from the posterior thorax may occasionally show diagnostic changes, the recording of such leads is a time-consuming procedure and the results obtained are often quite difficult to interpret.

S-T VECTOR AND VENTRICULAR REPOLARIZATION

The authors of this text have rarely had the opportunity to study, vectorcardiographically or electrocardiographically, strictly posterior infarction in the acute stage. However, we might predict the abnormalities which would be present in an acute posterior infarction.

1. The terminus of the QRS sE loop would be displaced posteriorly, and so the right- and midprecordial leads of the electrocardiogram would register depressed S-T segments.
2. The T sE loop would probably be situated anteriorly and somewhat to the left or right. Thus the right- and midprecordial leads would display upright T waves during the stage of posterior transmural ischemia.

The vectorcardiographic and electrocardiographic findings in old or healed strictly posterior infarction are well exemplified in Figures 199 and 200.

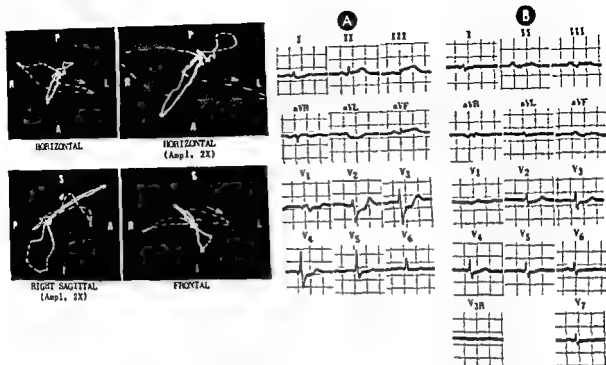


Fig 200.—Electrocardiographic and vectorcardiographic findings in acute diaphragmatic-strictly posterior myocardial infarction.

isoelectric level.

diagnostic of acute diaphragmatic-strictly posterior infarction. The large inferiorly oriented loop in the right sagittal projection is the M loop, whose size merely reflects the extreme diminution in QRS forces apparently consequent to the

a clockwise
t half of the
g at -50° in

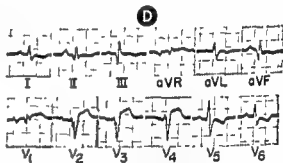
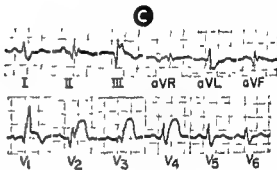
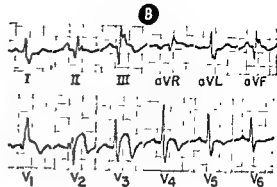
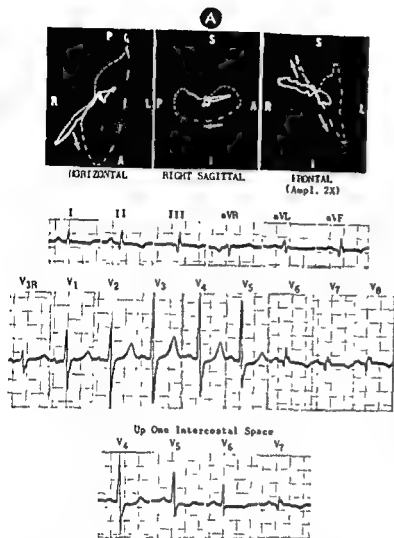


Fig. 201.—Electrocardiograms and vectorcardiogram in combined diaphragmatic-posterolateral and subsequent anterior myocardial infarctions

ab: V₁ up one intercostal space. In addition, the S-T segments are depressed in leads I, II, III, aVF, V₁ through V₄, and V₅ through V₇ up one intercostal space all register inverted T waves. These findings are compatible with diaphragmatic-posterolateral infarction in the recent past. Corresponding abnormalities in the vectorcardiogram are as follows: the horizontal QRS loop is written abnormally far anteriorly, over one half of the loop being situated anterior to the frontal plane, it written abnormally superiorly and slightly to the right, the QRS sE loop does not close, and the T loop is written abnormally far anteriorly and slightly to the right.

hos: terminal S waves have appeared in leads aVR and V₁. The inverted S-T segments and inverted T waves. The abnormalities previously described as being diagnostic of diaphragmatic infarction persist in this record, but the signs of posterolateral infarction have disappeared. The record can therefore be interpreted as showing an acute anterior myocardial infarction, an old diaphragmatic myocardial infarction, and right bundle branch block.

C: The Q waves have appeared in leads V₂ and V₃, confirming the initial impression of an acute anterior myocardial infarction.

D: second: The Q waves have appeared in leads V₂ and V₃, confirming the initial impression of an acute anterior myocardial infarction.

Miscellaneous Cardiac Abnormalities

- INFARCTIONS IN COMBINED LOCATIONS
- MYOCARDIAL INFARCTION WITH BUNDLE BRANCH BLOCK
- INFARCTION OF THE INTERVENTRICULAR SEPTUM

- FIBROSIS OF THE INTERVENTRICULAR SEPTUM
- SUBENDOCARDIAL MYOCARDIAL INFARCTION
- VENTRICULAR ANEURISM
- PERI-INFARCTION BLOCK
- PERICARDITIS AND MYOCARDITIS

INFARCTIONS IN COMBINED LOCATIONS

MYOCARDIAL INFARCTION frequently involves several different areas of the left ventricle concomitantly or may occur with an older infarction of a different location. As a general rule, the infarction vector in combined infarction is the resultant of the component infarction vectors of each aspect of the ventricular wall involved. For example, in diaphragmatic-anterolateral infarction, the infarction vector points superiorly, to the right, and posteriorly; in diaphragmatic-posterolateral infarction, it is directed superiorly, to the right, and anteriorly; and in diaphragmatic-anteroseptal infarction, it points to the left, posteriorly, and superiorly. In most instances, each of the components of a combined infarction produces changes individually recognizable in the electrocardiogram and vectorcardiogram, so that infarction in one region of the left

ventricle ordinarily does not interfere with the diagnostic changes produced by infarction of another region. Perhaps the major exception to this rule—but a rare one—is combined infarction of anterior and posterior walls of the left ventricle (Figs. 201 and 202). In a case of infarction of this type, the authors of this text were able to follow serial electrocardiograms recorded during the evolution of the two infarction patterns. The initial electrocardiograms showed the evolution of typical QRS complex, S-T segment, and T wave abnormalities of anterior infarction. A short time later, with a sudden deterioration in the patient's clinical status, the electrocardiographic precordial leads, which previously had displayed QS deflections or abnormally low R waves, showed R waves of relatively normal size and a normal precordial QRS transi-

notching on the downstroke of the S wave and the rS pattern. II, III, precor-

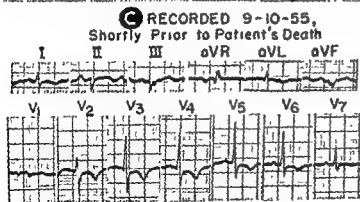
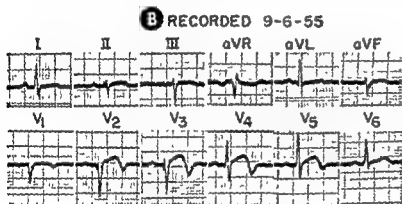
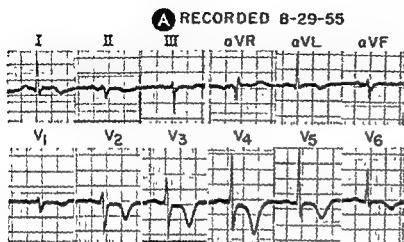


Fig. 202.—Electrocardiographic findings in a man, 53, with acute posterior myocardial infarction superimposed on recent anterior myocardial infarction. He was admitted to the hospital on August 19, 1955, after 5 hours of severe chest pain. His clinical course was stormy, and he died on September 10, 1955.

On August 19, 1955, the patient was admitted to the hospital with severe chest pain. His clinical course was stormy, and he died on September 10, 1955. The electrocardiographic findings are shown in Figure 202. The tracing shows a small Q wave in lead V1 and a small R wave in lead V6, which is compatible with anterior myocardial ischemia. On September 10, 1955, the following changes were noted. QS deflections in lead V1, small initial Q waves with abnormally low R waves in leads V2 and V3, elevated S-T segments in leads V2 through V6, and inverted T waves in leads V2 through V6—changes considered compatible with acute anterior or anteroseptal myocardial infarction. On September 10, he developed more severe chest pain and pulmonary edema and expired. Record C, obtained shortly before his death, showed a vibratory downward ventricular beat of low voltage in lead V1, on the other hand, the R waves in leads V2 through V6 were, if anything, larger than those in A. The S-T segments in these same leads were slightly depressed. On the basis of the trend toward "normalization" of the QRS deflections present in C as compared to B, record C was interpreted as suggestive of superimposed acute posterior myocardial infarction on an antecedent anteroseptal infarction. Postmortem examination disclosed a healing infarction of the apex and anterior wall of the left ventricle with mural thrombus, and recent infarction of what would correspond, in terms of electrical location, to the posterior wall and septum of the left ventricle, with terminal rupture of the posterior ventricular wall. Occlusions of the anterior descending branch of the left coronary artery and of the circumflex branch of the left coronary artery were noted. In summary, the anteroseptal infarction lessened or abolished anteriorly directed instantaneous QRS forces, causing the balance of forces to shift posteriorly and producing Q waves and low R waves in the anterior precordial leads. Subsequent posterior infarction removed posteriorly directed instantaneous forces so that the balance of electrical forces returned more nearly to the normal, and significant R waves reappeared in the anterior precordial leads as the only evidence of the later infarction. The S-T segment depression noted in C could well be reciprocal to the S-T segment elevation of posterior subepicardial injury in posterior chest leads.

tion. In addition, there was slight S-T segment depression in the precordial leads, and the T waves, previously inverted, had either become low upright or less deeply inverted. The electrocardiographic diagnosis of acute strictly posterior myocardial infarction superimposed on recent strictly anterior infarction was confirmed at postmortem. If the patient had lived,

electrocardiograms recorded at some future date conceivably might have shown no evidence of either infarction, since the electrical effects of one would tend to counterbalance the effects of the other. That such a course of events can occur (as illustrated in Figures 201 and 202) constitutes clinical evidence of the validity of the dipole or vector theory.

Fig. 203.—Electrocardiographic findings in right bundle branch block with a superimposed acute diaphragmatic-posterolateral myocardial infarction. The presence of right bundle branch block is indicated by the prolonged QRS interval, the wide terminal R' waves in leads V_{4a} and V_1 , and the wide terminal S waves in leads I and V_6 through V_8 . The QS deflection

in leads V_3 through V_6 are equally diagnostic of acute posterolateral infarction. The depressed S-T segments in leads V_3 and V_4 are probably related in a reciprocal manner to posterior subepicardial injury.

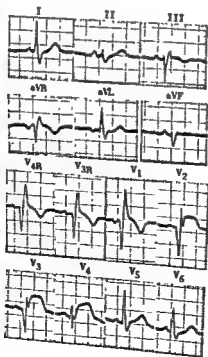
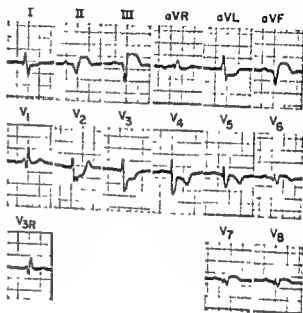


Fig. 204.—Electrocardiographic and vectorcardiographic findings in right bundle branch block with superimposed acute anteroseptal myocardial infarction. The vectorcardiographic QRS sE loop is written initially to the left, posteriorly, and inferiorly, indicating anteroseptal infarction, while the terminal portion of the QRS sE loop is slowly inscribed anteriorly, to the right, and slightly superiorly, signifying right bundle branch block. Although an anteriorly directed S-T vector is present in the vectorcardiogram, its magnitude is smaller than one might have expected in view of the marked S-T segment elevation in leads V_3 through V_6 of the electrocardiogram. The reason for this discrepancy is that the vectorcardiogram was recorded several days later than the electrocardiogram, when the subepicardial injury was subsiding.

MYOCARDIAL INFARCTION WITH BUNDLE BRANCH BLOCK

The single fact most important to understanding the electrocardiographic and vectorcardiographic abnormalities in coexisting myocardial infarction and bundle branch block is that infarction of the septum or left ventricular free wall manifests itself electrically, as a general rule, only at and during the time the involved myocardium would normally undergo activation. Since, normally, septal activation occurs during the first 0.02 second of the QRS interval, and activation of all but the basal portions of left ventricular free wall takes place between 0.02 and 0.04 second of the QRS interval, anteroseptal infarction, for example, alters the first 0.02 second of the QRS complex, while left ventricular free wall infarction (involving, as it frequently does, a portion of the septum as well) produces abnormalities of the first 0.04 second of the QRS deflection, in the form of abnormal Q waves or changes in the size of the

R waves. However, if onset of left ventricular activation is delayed and septal activation altered as the result of an intraventricular conduction defect, the electrical effect of a superimposed infarction is modified. In the case of left ventricular free wall infarctions, the effect of the infarction is shifted to a later part of the QRS complex and appears coincident with the delayed onset of free wall activation, whenever that occurs in the QRS interval. If activation of the left ventricle not only is delayed in onset but takes place in an abnormal or aberrant manner, then the QRS abnormalities are both late in onset and modified in appearance, in comparison with the QRS changes produced by the same type of infarction during normal intraventricular conduction. Inasmuch as most clinical infarctions involve interventricular septum and/or free wall of the left ventricle, the crucial factors determining the effect of coexisting bundle

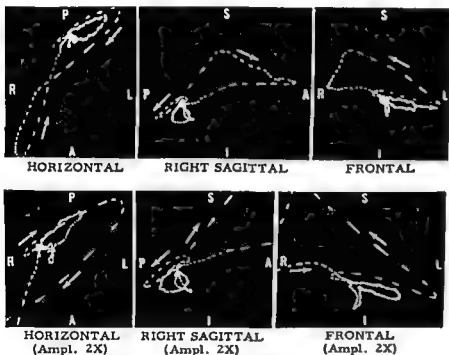


Fig. 205. — Electrocardiographic and vectorcardiographic findings in right bundle branch block and coexisting old anterior myocardial infarction

The sole electrocardiographic finding suggestive of an old anterior infarction is the low initial R wave in lead V₄.

In the vectorcardiogram, however, the horizontal QRS loop shows clockwise inscription of both its initial rightward and anterior deflection and subsequent leftward and posterior portion, both findings probably being related to posterior displacement of the efferent limb of the loop. The corresponding components of the sagittal QRS loop also exhibit a reversed direction of inscription. These early abnormalities of the QRS sE loop are diagnostic of anterior infarction. The large rightward and anterior terminal deflection of the horizontal QRS loop and the superior orientation of both sagittal and frontal QRS loops are typical of the variant right bundle branch block pattern described in Chapter 17.

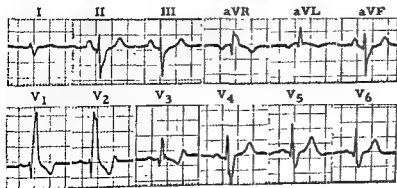
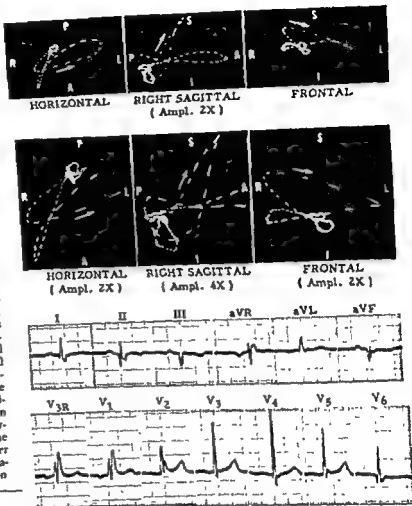


Fig 204.— Electrocardiographic and vectorcardiographic findings in right bundle branch block with coexisting old diaphragmatic-posterolateral myocardial infarction

In the electrocardiogram, the deep but slender Q waves in leads II and aVF and the QS deflection in lead III are compatible with diaphragmatic infarction. The presence of posterolateral involvement might be suspected from the prominent initial R waves and shallow S waves in leads V_{4R} and V_1 and the somewhat prominent Q wave in lead V_6 .

The vectorcardiographic abnormalities diagnostic of diaphragmatic-posterolateral infarction and right bundle branch block are obvious. There is a large initial deflection of the QRS sE loop abnormally far to the right, anteriorly, and superiorly. The mean 0.02-second instantaneous QRS vector lies at $+135^\circ$ in the horizontal plane, -50° in the sagittal plane, and -150° in the frontal plane. As will be recalled, the 0.02-second vector does not normally lie to the right of $+100^\circ$ in the horizontal plane or superior to -40° in the sagittal plane, and so the abnormal orientation of this vector in the above vectorcardiogram is further confirmation of the presence of diaphragmatic-posterolateral infarction.



branch block on the changes due to infarction are therefore dependent on the time and manner in which the septum and left ventricle are activated.

Right Bundle Branch Block

In right bundle branch block, left ventricular activation takes place just as it does when intraventricular conduction is normal. Accordingly, the presence of right bundle branch block in no way obscures the abnormal initial and/or early QRS forces characteristic of myocardial infarction. In turn, the electrocardiographic and vectorcardiographic features diagnostic of right bundle branch block, which, it will be remembered, alters the terminal mean instantaneous QRS vectors, are not disturbed by superimposed infarction. Thus, coexisting right bundle branch block and myocardial infarction are individually recognizable in the vectorcardiogram and electrocardiogram because the electrical effects of the two conditions ap-

pear at different times in the QRS interval. One possible exception to this rule is right bundle branch block with strictly posterior myocardial infarction. As will be recalled, this type of infarction typically affects the later instantaneous QRS vectors, causing them to be displaced anteriorly. Another common, although by no means invariable, abnormality in this type of infarction is anterior displacement of the long axis of the QRS sE loop. The only cases of strictly posterior infarction occurring with right bundle branch block which the authors of this text have been able to recognize with any assurance in the vectorcardiogram are those in which the long axis of the QRS sE loop was shifted farther anteriorly than is usually observed in uncomplicated right bundle branch block. In none of these cases was it possible to make the electrocardiographic diagnosis of strictly posterior infarction with any degree of certainty.

In the acute stage of infarction superimposed on right bundle branch block, the secondary S-T seg-

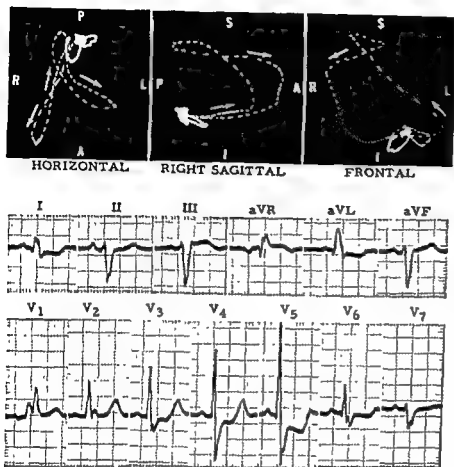


Fig. 207. — Electrocardiographic and vectorcardiographic findings in right bundle branch block with co-existing old posterolateral myocardial infarction.

The small Q waves in leads I, V₁, and V₂ in the electrocardiogram cannot be considered diagnostic of infarction. The broad initial R of the R-R' deflection in lead V₁ is perhaps the best electrocardiographic evidence of posterolateral infarction, but even this finding is somewhat equivocal.

The QRS sE loop of the vectorcardiogram presents the variant type of right bundle branch block pattern but, in addition, displays the following abnormalities diagnostic of posterolateral infarction: There is marked anterior displacement of both efferent and afferent limbs of the horizontal and sagittal QRS loops, causing a complete reversal in the direction of inscription of the first half of the horizontal loop. The frontal QRS loop is inscribed a short distance to the left and then turns abruptly superiorly and medially, reflecting medial displacement of the greater part of the efferent limb of the loop. An S-T vector directed to the right and inferiorly is probably representative of digitalis effect or lateral subendocardial injury. The T sE loop is situated anteriorly and slightly inferiorly, indicating posterior ischemia.

ment and T wave changes of the right bundle branch block modify to some extent, but rarely obscure, the S-T segment and T wave abnormalities characteristic of acute infarction.

In the cases of right bundle branch block with myocardial infarction studied by Dodge and Grant, the effective electrical location of the infarction was found to be diaphragmatic in almost 50% of the electrocardiograms. As Dodge and Grant pointed out, the right ventricle and a major portion of the right intraventricular conducting system lie within the distribution of the right coronary artery, and occlusion of this vessel is responsible for most cases of diaphragmatic myocardial infarction. Dodge and Grant found that the site of infarction in the remaining half of the patients (with right bundle branch block) was divided about equally between the several types of anterior infarction and posterior infarction (Figs.

203-207). Grant and Dodge also studied a series of cases with left bundle branch block in which electrocardiograms recorded before onset of the conduction disturbance showed myocardial infarction. Interestingly enough, over one half of the electrocardiograms showed diaphragmatic infarction, and the distribution of the site of infarction in the remaining differed from that in right bundle branch block only in that strictly anterior infarction was present less commonly than either anterolateral or posterior (strictly posterior and posterolateral) infarction. On the other hand, in the cases in which the electrocardiogram resembled left bundle branch block but in reality represented peri-infarction block, anterolateral infarction was the type of infarction most frequently present in tracings recorded before onset of intraventricular block. The explanation of Grant and his associates for this finding is given on page 337.

Left Bundle Branch Block

Unlike right bundle branch block, left bundle block is not as difficult, often impossible, to detect.

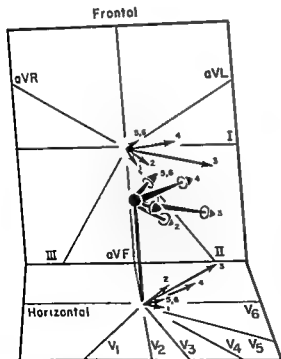
Diagnostic problem is somewhat less serious. S-T segment and T wave changes due to infarction can sometimes be detected despite the presence of

left bundle branch block. More will be said of this later (pp. 329 and 330). In the following pages, the discussion will center solely on the QRS findings in left bundle branch block, infarction of left ven-



A Sequence of Activation of Septum and Ventricles

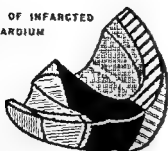
1. INITIAL ACTIVATION OF APICO-ANTERIOR RIGHT VENTRICULAR WALL
2. RIGHT-TO-LEFT SEPTAL ACTIVATION AND ACTIVATION OF RIGHT VENTRICULAR FREE WALL
3. COMPLETION OF SEPTAL AND RIGHT VENTRICULAR ACTIVATION
4. INITIAL ABERRANT ACTIVATION OF BASAL LEFT VENTRICULAR WALL
5. ACTIVATION OF POSTERIOR, LATERAL, AND ANTERIOR LEFT VENTRICULAR WALL
6. COMPLETION OF ACTIVATION OF ANTERIOR WALL OF LEFT VENTRICLE



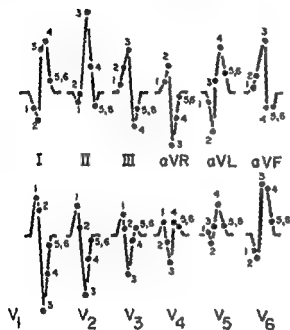
B Instantaneous VA Vectors in Uncomplicated Left Bundle Branch Block

Fig 208.—Instantaneous VA vectors in uncomplicated left bundle branch block. The septal-ventricular activation sequence, the VA vectors themselves, the QRS deflections projected on the scalar leads of the electrocardiogram, and the corresponding planar QRS loops were described in Figure 141, which is reproduced here (in part) mainly to serve as a basis for comparison with Figures 209 and 210.

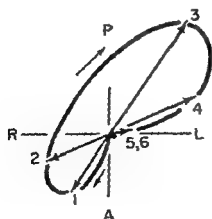
REGION OF INFARCTED MYOCARDIUM



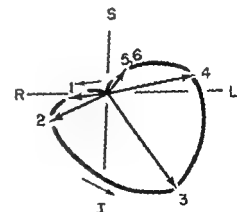
A Schematic Representation of a Septal Infarct



C QRS Deflections Projected on Scalar Leads

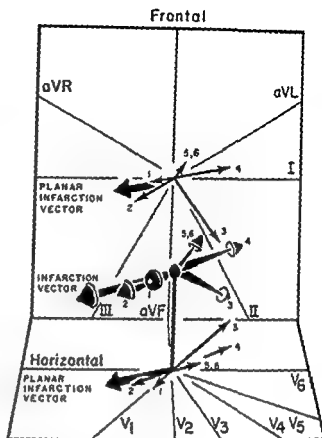


Horizontal



Frontal

D Planar QRS Loops in Left Bundle Branch Block Complicated by Extensive Septal Infarction



B Instantaneous VA Vectors in LBBB Complicated by Extensive Septal Infarction

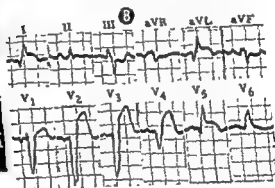
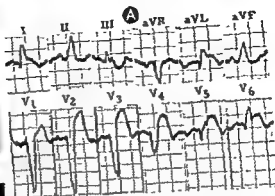
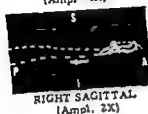


Fig. 210.—Electrocardiographic and vectorcardiographic findings in left bundle branch block complicated by acute

Electrocardiogram B, obtained from the same patient several days later, shows minor (cosmopolitan) changes in the

wave in lead V_1 is taller than the R waves in leads V_2 through V_4 . In B, the corresponding abnormality in the planar QRS loops consists of a large, anterior, rightward and inferior early deflection of the horizontal and frontal QRS loops.

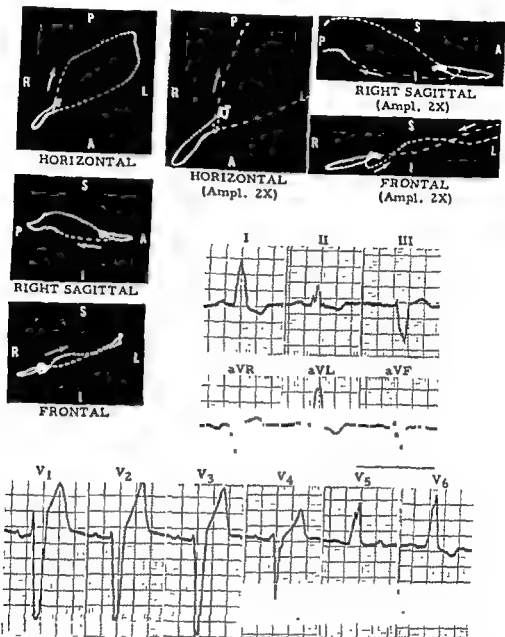


Fig 211.—Electrocardiographic and vectorcardiographic findings in left bundle branch block with coexisting old septal infarction

Although, in the electrocardiogram, minute Q waves are present in leads I, aVL, and V₆, a finding more suggestive of septal infarction is the relatively tall R wave in lead V₁ with diminishing R wave amplitude in leads V₂ through V₆.

In the vectorcardiogram, the QRS sE loop is characteristic of left bundle branch block except that there is an early deflection of the loop to the right, anteriorly, and inferiorly, indicative of septal infarction

in left bundle branch block, they are as follows (Fig. 208).

1. **Septal depolarization, from beginning to end,** occurs in a right-to-left direction and (at least in dogs with surgically produced left bundle branch block) requires about 0.04 second for completion. As a result, the instantaneous QRS vectors during the first 0.02 second of the QRS interval are oriented toward the left ventricle rather than away from it, while the instantaneous vectors appearing during the next 0.02

second are also directed to the left and posteriorly, whether the left ventricular free wall happens to be infarcted or not. Thus, in left bundle branch block, leads I and V₆ record positive voltages during the first 0.04 second of the QRS interval regardless of the presence or absence of a free wall infarction.

■ Since activation of left ventricular free wall does not commence in left bundle branch block until the second half of the QRS interval, the electrical effects of a free wall infarction likewise do not appear until

this portion of the QRS interval. Thus, free wall infarctions occurring in left bundle branch block are electrocardiographically "silent" during the first half of the QRS interval, on the other hand, it is only during this period that evidence of septal infarction complicating left bundle branch block is present in the electrocardiogram.

From the standpoint of their recognition, infarctions complicating left bundle branch block can therefore be separated into two general categories: (a) septal infarctions, which alter the first 0.04 second of the QRS deflection, and (b) left ventricular free wall infarctions, which affect the final 0.04-0.06 second of the QRS deflection.

Massive infarction of the interventricular septum.—An extensive infarction of the septum usually abolishes the instantaneous electrical forces caused by right-to-left septal depolarization, thereby allowing electrical forces (presumably arising in the right ventricle) to dominate temporarily the electrical field of the heart (Fig. 209). Consequently, the initial and early leftward-directed instantaneous vectors characteristic of left bundle branch block are rotated to the right, away from the left ventricle, and project Q

waves in leads I, aVL, and V₆. This Q wave diminishes in size from right to left across most of the precordium. The reversal in the R wave transition is related to the fact that, as the result of the infarction, the instantaneous vectors of the first 0.04 second of the QRS interval are directed to the right, while subsequent instantaneous vectors develop in a clockwise direction to the left and posteriorly in the horizontal plane—that is, away from the other precordial leads. When, finally, after considerable delay, left ventricular activation commences, the instantaneous vectors appearing after 0.04 second are oriented toward the left ventricle, just as is the case in uncomplicated left bundle branch block, and these vectors project terminal R waves on leads I, aVL, and V₆ and a terminal S wave on lead V₁ (Figs. 210 and 211).

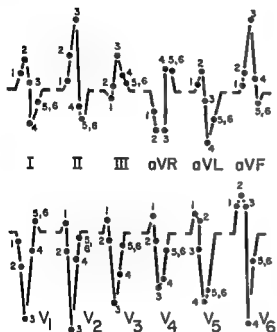
Infarction of left ventricular free wall.—Since the late instantaneous QRS vectors in left bundle branch block are determined by delayed left ventricular activation, it is these instantaneous vectors which are altered by infarction of the left ventricular free wall (Fig. 212). The failure of the infarcted portion of the free wall to generate QRS potentials during the terminal 0.04-0.06 second of the QRS interval allows oppositely directed forces to become preponderant, so

that the late instantaneous vectors are displaced away from the effective electrical site of the infarction. As it so happens, the displacement of the terminal vectors can ordinarily be recognized only if the vectors project negativity on a lead in which in left bundle branch block would otherwise be expected to register terminal positivity (or the converse—that is, terminal positivity on a lead ordinarily recording terminal negativity in left bundle branch block, a situation which will be discussed later). For this reason, free wall infarction in left bundle branch block usually can be detected only if it produces terminal S waves in leads I, aVL, V₃, and V₆. Lateral infarction is therefore more likely to be recognized than infarction of other portions of left ventricular wall, since all routine electrocardiographic leads other than those cited above can, and usually do, record terminal S waves in uncomplicated left bundle branch block. In lateral free wall infarction, electrocardiographic leads, which prior to infarction had recorded the wide slurred or notched R waves typical of left bundle branch block, afterward typically display RS deflections, the initial R wave resulting from undisturbed right-to-left septal depolarization and the terminal S wave reflecting the lateral wall infarction. If there is septal, as well as free wall, infarction, leads I, aVL, and V₆ may display notched QS deflections or qrs complexes. In addition, W-shaped deflections may appear in leads V₄ and V₅.

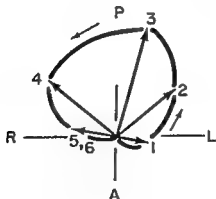
When lead V₄ and/or lead I record Q waves despite other electrocardiographic findings suggestive of complete left bundle branch block, diagnostic precedence should always be given to the possibility of septal infarction, not only because of the serious implications of the latter but also because of the frequency with which left bundle branch block and infarction occur together clinically. However, the following facts should be kept in mind in evaluating the significance of Q waves in leads I, aVL, and V₆ in the presence of left bundle branch block: (1) In uncomplicated left bundle branch block, leads I and V₆ can sometimes display Q waves, but the duration of the Q waves does not usually attain 0.02 second in the absence of infarction. On the other hand, it is not unusual for lead aVL to show deep, wide Q waves in uncomplicated left bundle branch block. (2) Grant and others have pointed out that diffuse intraventricular block and peri-infarction block, neither of which alters the initial QRS forces, can easily be mistaken for left bundle branch block. Since Q waves may be present in leads I and V₆ in diffuse intraventricular block (in which there is merely prolongation of the QRS interval with little change in QRS configuration) and peri-infarction block, these conditions may



A Schematic Representation of an Anterolateral Myocardial Infarct

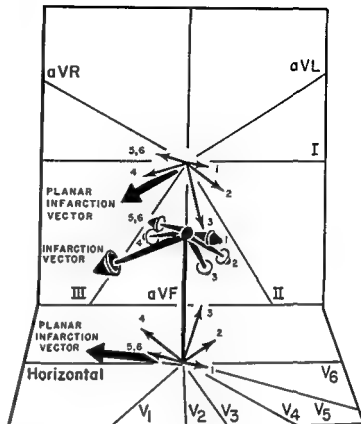


C QRS Deflections Projected on Scalar Leads

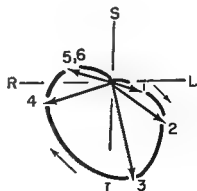


Horizontal

Frontal



B Instantaneous VA Vectors in LBBB Complicated by Anterolateral Myocardial Infarction



Frontal

D Planar QRS Loops in Left Bundle Branch Block Complicated by Anterolateral Myocardial Infarction

Fig. 212.—(Legend on facing page)

therefore occasionally simulate left bundle branch block with septal infarction.

The presence of terminal S waves in leads I and V_6 in what is otherwise a typical left bundle branch block is of more dubious reliability in establishing the diagnosis of free wall infarction, unless the change in QRS configuration is observed to develop in serial electrocardiograms recorded during an episode clinically suspicious of infarction or is accompanied by S-T segment and T wave changes compatible with acute infarction (S-T segment and T wave abnormalities of infarction superimposed on left bundle branch block are discussed at the end of this section.)

If the infarction is healed and only one electrocardiogram is available, it becomes quite difficult to evaluate the significance of terminal S waves in lead V_6 in particular. The reasons for this follow

1

in lead

bundle branch block

on two factors. First, the frontal QRS forces in left bundle branch block, as represented by the frontal QRS loop of the vectorcardiogram, tend to be oriented markedly superiorly and to the left and to develop in a counterclockwise direction, and second, as pointed out in an earlier chapter, the exploring electrode of lead V_6 is more or less routinely applied well below the horizontal plane through the cardiac dipole center. Since the indifferent electrode of lead V_6 is at the central terminal or, in effect, at the electrical center of the heart, the low position of the chest electrode causes the lead axis of lead V_6 to be tilted downward. This in turn may cause the terminal portion of the frontal QRS loop in left bundle branch block to project on the negative, rather than the positive, half of the lead axis of lead V_6 . To determine whether this factor is responsible for the presence of a terminal S wave in lead V_6 , the latter lead can be recorded up one intercostal space.

2. Another explanation for the terminal S waves sometimes observed in lead V_6 in uncomplicated left bundle branch block is that there may be a marked shift of the precordial QRS transition to the left in such cases. In this event, lead V_6 may still lie to the

right of the transition point. Precordial leads should be recorded farther to the left of lead V_6 to confirm or refute this possibility.

3. In our experience, the electrocardiographic findings which accompany the vectorcardiographic pattern of so-called "left ventricular hypertrophy with left bundle branch block" can readily be confused

QRS vectors are usually not disturbed. The terminal S wave in lead V_6 which characterizes "left ventricular hypertrophy with terminal conduction delay" is produced by a terminal return of the QRS S-E loop to the right, posteriorly, and superiorly. Hence the similarity of the electrocardiographic patterns of the conductive disturbances.

4. Grant has found that in a small percentage of strictly anterior infarctions, post-infarction block may lead to QRS interval prolongation and to displacement of the terminal QRS vectors to the right and superiorly. When this happens, the electrocardiogram tends to resemble left bundle branch block with S waves in lead V_6 .

S-T segment and T wave abnormalities in diagnosis of infarction with left bundle branch block.—Although an acute myocardial infarction involving the left ventricular free wall in left bundle branch block may or may not produce recognizable changes in the QRS deflection, the presence of an infarction may sometimes be suspected from the direction of displacement of the S-T segments. Specifically, when the S-T segments in a given lead in left bundle branch block are shifted in a direction just the opposite of that anticipated, subepicardial injury, and hence infarction, may be indicated. It will be recalled that, in uncomplicated left bundle branch block, leads recording upright QRS deflections characteristically display depressed S-T segments and inverted T waves, while downwardly directed QRS deflections are typically followed by upright T waves with S-T segment elevation. The mechanism of these S-T segment and T wave abnormalities (discussed in Chapter

6) consists, in brief, of reversal in the over-all direction of ventricular repolarization because of the altered depolarization process. Moreover, as was explained in the section dealing with ventricular gradient, in Chapter 6, the larger the area of the QRS deflection the greater the displacement of the S-T segment and T wave in the opposite direction. In uncomplicated left bundle branch block, the consistent relationship existing between the direction and area of the QRS complex and the direction and degree (area enclosed by the S-T segment) of S-T segment deviation and the direction and size of the T wave indicate that the S-T and T abnormalities in left bundle branch block are secondary in type. This being the case, if one were to find that the R waves of large area characteristically recorded in

leads V_5 and V_6 in left bundle branch block are followed by elevated S-T segments (or by isoelectric S-T segments, if the R wave area was very great) in these leads, one could infer from this that a large lateral subepicardial injury vector must be present to nullify or reverse the expected secondary shift in the S-T segment. This in turn would raise the question of acute infarction. By the same token, S-T segment depression in right precordial leads in left bundle branch block should raise the question of posterolateral subepicardial injury, possibly infarction.

THE VCG FINDINGS IN INFARCTION WITH LEFT BUNDLE BRANCH BLOCK

As yet, there have been few reports describing the vectorcardiographic findings in left bundle branch

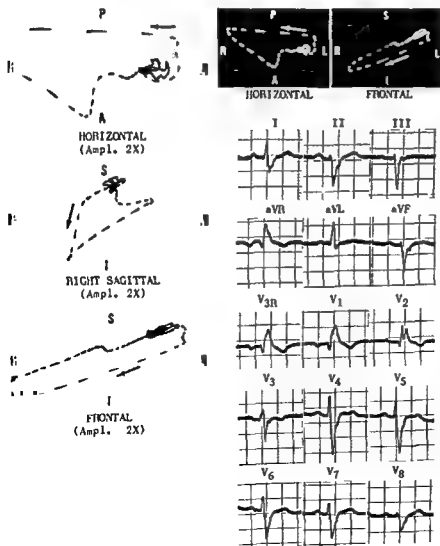


Fig. 213.—Electrocardiographic and vectorcardiographic findings in intraventricular block of unknown type.

In the electrocardiogram, the QRS

slurred terminal R' waves are present in leads V_{1R} through V_4 , and terminal S waves are present in the left precordial leads. The electrocardiogram presents many of the features which the authors of this text consider characteristic of the variant type of right bundle branch block, but the vectorcardiogram does not support this diagnosis.

In the vectorcardiogram, the QRS sE loop is written initially to the left, slightly anteriorly, and slightly superiorly. In the horizontal projection, the QRS loop is written in a counterclockwise direction, briefly to the left, and then the loop turns posteriorly and moves rapidly to the right. The afferent limb of the horizontal QRS loop is then written to the right and slightly anteriorly and shows some evidence of conduction delay. The greater portion of the sagittal QRS loop is written in a counterclockwise direction inferiorly, at first posteriorly and then anteriorly. The configuration of the QRS sE loop in each of its planar projections is not that usually observed in right bundle branch block. It is possible that this

block complicated by myocardial infarction. Richman and Wolff have described four cases of left bundle branch block masquerading as right bundle branch block in which the limb leads of the electrocardiogram were typical of left bundle branch block while the chest leads were suggestive of right bundle branch block. In the vectorcardiograms recorded in these cases, the QRS sE loop generally was located to the right, superiorly, and either slightly anteriorly or posteriorly. The initial vectors of the QRS sE loop in each case were directed anteriorly and inferiorly, with or without leftward deviation, while the terminal portion of the loop, which showed conduction delay, returned on the right, superiorly, and posteriorly. Richman and Wolff ascribed the electrocardiographic and vectorcardiographic abnormalities just cited to left bundle branch block complicated by septal, lateral, and diaphragmatic myocardial infarction.

Occasionally, we have observed electrocardiograms and vectorcardiograms which presented some of the features described by Richman and Wolff (Fig. 213). However, since preinfarction records were not available and postmortem correlation was lacking in our cases, we cannot be certain that these cases represented additional examples of left bundle branch block masquerading as right bundle branch block.

In the small series of cases having electrocardiograms compatible with the diagnosis of left bundle branch block and septal infarction which we studied vectorcardiographically, the principal findings were these (Figs. 210-211).

- 1 There was a prominent initial deflection of the horizontal QRS loop to the right and anteriorly, the maximal mean instantaneous vector of this portion of the loop lying between $+95^\circ$ and $+145^\circ$. In uncomplicated left bundle branch block, when an anteriorly directed initial deflection is

present, the maximal instantaneous vector is rarely situated to the right of $+90^\circ$, and never to the right of $+93^\circ$, and the initial deflection is usually in the counterclockwise direction. In con-

cluded by septal infarction generally shows a clockwise direction of inscription.

- 2 The duration of the early portion of the horizontal QRS loop situated to the right of the midline ranged from 0.02 to over 0.03 second in the cases of septal infarction with left bundle branch block. However, in the few instances of uncomplicated left bundle branch block with a rightward initial deflection of the horizontal QRS loop observed by us, the total duration of this part of the loop did not exceed 0.015 second, and usually was far less.
- 3 The maximal rightward mean instantaneous vector of the frontal QRS loop ranged in orientation between $+130^\circ$ and -175° , while in most cases of uncomplicated left bundle branch block it was impossible to distinguish a rightward initial deflection.
- 4 In one case of acute septal infarction with left bundle branch block, the electrocardiogram showed elevated S-T segments and inverted T waves in leads I, aVL, V_3 , and V_6 ; and corresponding abnormalities were present in the vectorcardiogram. The terminus of the QRS sE loop was displaced to the left, anteriorly, and slightly inferiorly, indicating the presence of a similarly directed S-T vector. The T sE loop was oriented to the right, anteriorly, and inferiorly.
- 5 Except for the findings just cited, the QRS sE loop in left bundle branch block with septal infarction otherwise resembled that in uncomplicated left bundle branch block.

INFARCTION OF THE INTERVENTRICULAR SEPTUM

Septal infarction occurs frequently in combination with infarction of left ventricular free wall, but rarely, if ever, is the septum the sole site of involvement. In the series of septal infarctions studied electrocardiographically and pathologically by Soda-Pallares and his associates and by Wolff, not a single case of septal infarction unaccompanied by free wall involvement was observed, although Myers apparently found several such cases in his series. Be that as it may, septal infarction is, for all intents and purposes, almost invariably associated with free wall infarction. Septal

involvement should be suspected if any of the following abnormalities appear in the electrocardiogram.

- 1 The presence of an extensive infarction of either anterior or inferoposterior walls of the heart.
- 2 The presence of both anterior and inferoposterior infarctions, particularly if bundle branch block appears temporarily or permanently at some time during the evolution of the infarction.
- 3 QS deflections in leads V_1 to V_4 or the absence of an R wave in any of leads V_2 , V_3 , or V_4 , if in adjacent leads to the right there is initial positivity.

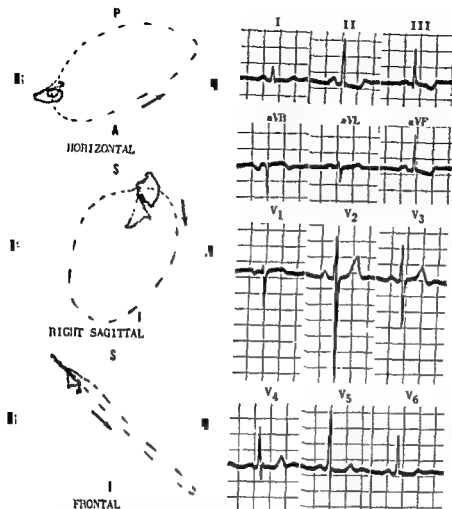


Fig. 214.—Electrocardiogram and vectorcardiogram in septal fibrosis.

Note, in the electrocardiogram, that normal, septal Q waves are absent in leads I, aVL, V₁, and V₂. This finding in conjunction with the lack of evidence of anteroseptal myocardial infarction is strongly suggestive of fibrosis of the interventricular septum.

The corresponding abnormality in the vectorcardiogram consists of the inscription of the initial portion of the QRS sE loop to the left, anteriorly, and slightly superiorly. There is nothing in the vectorcardiogram to suggest the presence of anteroseptal myocardial infarction or incomplete left bundle branch block. The abnormal direction

loop is discordant to the long axis of the QRS sE loop. The vectorcardiogram therefore corroborates the electrocardiographic impression of septal fibrosis and also displays a nonspecific T sE loop abnormality.

4. Q waves in leads V₅ and V₆ when there is complete left bundle branch block, or in leads V₁ and V₂ when there is complete right bundle branch block. Q waves in incomplete bundle branch

- block do not necessarily signify septal infarction.
- 5 The sudden onset of left or right bundle branch block or of atrioventricular block during an episode clinically compatible with myocardial infarction.

FIBROSIS OF THE INTERVENTRICULAR SEPTUM

Healed septal infarction can be simulated pathologically by coalescent foci of fibrosis in the septal muscle. The diagnostic electrocardiographic abnormality which Burch has observed in cases of septal fibrosis consists of absence of normal septal Q waves in leads I, V₅, and V₆. Normally the small Q waves in these leads reflect initial septal activation in a left-to-right direction more precisely than does the initial R wave in lead V₁, which also results from depolarization of paraseptal portions of the left and right ventricular free walls. Consequently, the presence or absence of an initial R wave in lead V₁ would not be expected to correlate as well with the presence or absence of septal fibrosis as the presence or absence of Q waves in leads I, V₅, and V₆. In occa-

sional vectorcardiograms, we have observed that the horizontal and sagittal QRS loops were written initially to the left, anteriorly, and inferiorly but were otherwise normal in configuration and orientation (Fig. 214). Whether or not these cases represent the vectorcardiographic counterpart of Burch's cases of septal fibrosis cannot be determined because post-mortem proof is lacking in the former. However, the electrocardiograms in our cases showed neither Q waves in leads I, aVL, V₅, and V₆ nor electrocardiographic or vectorcardiographic findings suggestive of incomplete left bundle branch block or anteroseptal infarction. The patients themselves were considered clinically to have coronary artery disease.

SUBENDOCARDIAL MYOCARDIAL INFARCTION

For reasons previously discussed, injury and ischemia limited solely to the anterior subendocardium produce an S-T vector pointing to the right, posteriorly, and superiorly and mean instantaneous T spatial vectors directed anteriorly to the left and inferiorly and therefore project depressed S-T segments and upright T waves on left precordial leads. In subendocardial infarction, myocardial ischemia may be subendocardial, as above, or transmural, in which case the mean instantaneous T spatial vectors are rotated posteriorly and cause anterior chest leads to register inverted T waves.

Since the S-T segment and T wave changes of subendocardial infarction are usually indistinguishable from those of chronic coronary insufficiency, the presence or absence of alterations in QRS configuration assumes critical diagnostic significance. Unfortunately, the association of QRS changes (particularly abnormal Q waves) with subendocardial myocardial

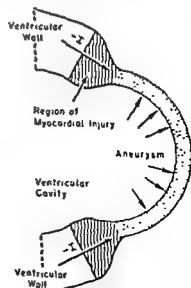
infarction has been the subject of some controversy. The many studies of this problem have been summarized thus: experimentally and clinically, pathologic Q waves have been recorded in anterior precordial leads in some instances of subendocardial infarction but not in others. Prinzmetal and his co-workers, who believe the inner one third to two thirds of the ventricular wall to be electrocardiographically "silent," did not observe abnormal Q waves in acute or chronic subendocardial infarctions produced experimentally in dogs. They concluded that "pure" subendocardial infarctions do not alter the QRS complex in the precordial electrocardiogram, an opinion which is gaining considerable support. The authors of this text are in agreement with Prinzmetal's conclusions. At present, the electrocardiographic status of subendocardial infarction remains unsettled, and, as far as is known, there have been no vectorcardiographic descriptions of such an entity.

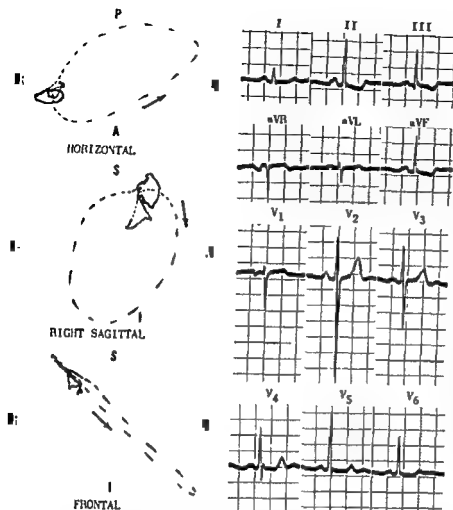
VENTRICULAR ANEURYSM

Following an acute myocardial infarction, the elevated S-T segments of the electrocardiogram ordinarily return to the isoelectric base line within several days to several months after onset of the acute episode. However, in a small number of cases the S-T segments remain upwardly displaced for many years or indefinitely and are usually associated with promi-

nent Q waves or QS deflections. Most of these patients are found to have had relatively massive infarctions previously. In many, but not all, of these patients ventricular aneurysms can be demonstrated; conversely, some patients with ventricular aneurysms do not display persistent S-T segment elevations. The mechanism responsible for the persistent injury

above. The $-I$ vectors project positive voltages on overlying leads during early electrical diastole, and so the electrocardiogram registers elevated S-T segments (See text for detailed discussion of this mechanism.)





4. Q waves in leads V_3 and V_6 when there is complete left bundle branch block, or in leads V_1 and V_2 when there is complete right bundle branch block. Q waves in incomplete bundle branch

- block do not necessarily signify septal infarction.
5 The sudden onset of left or right bundle branch block or of atrioventricular block during an episode clinically compatible with myocardial infarction.

FIBROSIS OF THE INTERVENTRICULAR SEPTUM

Healed septal infarction can be simulated pathologically by coalescent foci of fibrosis in the septal muscle. The diagnostic electrocardiographic abnormality which Burch has observed in cases of septal fibrosis consists of absence of normal septal Q waves in leads I, V_5 , and V_6 . Normally the small Q waves in these leads reflect initial septal activation in a left-to-right direction more precisely than does the initial R wave in lead V_1 , which also results from depolarization of paraseptal portions of the left and right ventricular free walls. Consequently, the presence or absence of an initial R wave in lead V_1 would not be expected to correlate as well with the presence or absence of septal fibrosis as the presence or absence of Q waves in leads I, V_5 , and V_6 . In occa-

normal, septal Q waves are absent in leads I, aVL, V_5 , and V_6 . This finding in conjunction with the lack of evidence of anterosseptal myocardial infarction is strongly suggestive of fibrosis of the interventricular septum.

The corresponding abnormality in the vectorcardiogram consists of the inscription of the initial portion of the QRS sE loop to the left, anteriorly, and slightly superiorly. There is nothing in the vectorcardiogram to suggest the presence of anterosseptal myocardial infarction or incomplete left bundle branch block. The abnormal direction of the initial segment of the QRS sE loop is best explained by the presence of septal fibrosis. In addition, the T sE loop is discordant to the long axis of the QRS sE loop. The vectorcardiogram therefore corroborates the electrocardiographic impression of septal fibrosis and also displays a nonspecific T sE loop abnormality.

sional vectorcardiograms, we have observed that the horizontal and sagittal QRS loops were written initially to the left, anteriorly, and inferiorly but were otherwise normal in configuration and orientation (Fig 214). Whether or not these cases represent the vectorcardiographic counterpart of Burch's cases of septal fibrosis cannot be determined because post-mortem proof is lacking in the former. However, the electrocardiograms in our cases showed neither Q waves in leads I, aVL, V_5 , and V_6 nor electrocardiographic or vectorcardiographic findings suggestive of incomplete left bundle branch block or anterosseptal infarction. The patients themselves were considered clinically to have coronary artery disease.

PERI-INFARCTION BLOCK

In 1950, for the first time, First, Bayley, and Bedford described a type of intraventricular conduction defect associated with myocardial infarction which they called *peri-infarction block*. The identifying features of peri-infarction block in the electrocardiogram are as follows (Fig. 217).

1. The QRS interval is prolonged to 0.11 or 0.12 second
2. Onset of the intrinsoid deflection in precordial leads overlying uninvolved portions of left ventricular wall occurs at the normal time but is delayed in leads overlying the peripheral zone of the infarction.
3. The electrocardiogram presents evidence of myocardial infarction. If the latter is an anterior infarction, the electrocardiogram often has a superficial resemblance to left bundle branch block.
4. As Grant has recently emphasized, the initial and terminal QRS forces in peri-infarction block are directed differently. The spatial angle subtended by the initial and terminal 0.04-second mean QRS spatial vectors usually exceeds 60° .

The mechanism of peri-infarction block is not known for certain, although the mechanism outlined by First, Bayley, and Bedford is generally, albeit tentatively, accepted by most authorities. These authors postulate the following. When myocardial infarction is accompanied or followed by onset of peri-infarction block, it is presumed that the infarction has involved an extensive portion of the subendocardial muscle and

Purkinje network. As a result, uninvolved muscle overlying the infarction cannot undergo activation in a direction perpendicular to the epicardial surface, as occurs normally, instead, the activation wave must spread by a circuitous route through unaffected muscle at the periphery of the infarction. The late activation of subepicardial muscle overlying the infarction is responsible, in peri-infarction block, for the QRS prolongation, for the delayed onset of the intrinsoid deflection in leads oriented to the infarction, and for the divergence of the initial and terminal instantaneous QRS vectors. Thus, for reasons previously explained, the initial instantaneous QRS vectors are displaced away from the site of infarction, and therefore away from the overlying exploring electrode of one or the other precordial lead. On the other hand, since the subepicardial muscle over the infarction is the last to be activated, the terminal instantaneous QRS vectors are directed toward the exploring electrode of the same precordial lead. Consequently, in peri-infarction block the lead in question records a QR or Qr deflection of prolonged duration.

More recently, Grant and his associates have described what they believe to be a type of peri-infarction block different from that described above. The principal point of distinction between the two types of peri-infarction block, according to Grant and his co-workers, is the absence of significant QRS prolongation in the second type. These investigators reviewed electrocardiograms recorded before and after onset of infarction in a large series of cases and found

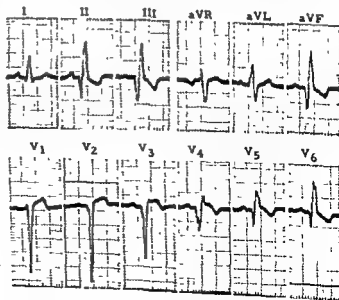


Fig 217.—Diaphragmatic and anterolateral myocardial infarctions in a man, 55, with coronary artery disease. The presence of peri-infarction block is suggested by the tall and wide R waves in leads II, III, aVF, V_4 and V_5 and the QRS duration of 0.12 second. Peri-

reference figure (the initial 0.04-second vector pointing away from the diaphragm and the terminal 0.04-second vector pointing toward the diaphragm) (From B S Lippman and M Massie, *Clinical Scalar Electrocardiography* [4th ed., Chicago Year Book Publishers, Inc., 1959], Fig 191.)

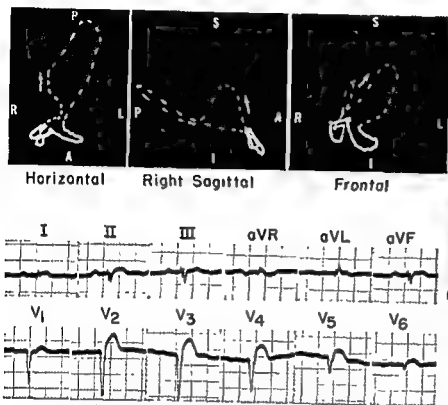


Fig. 216.—Electrocardiographic and vectorcardiographic findings in a man, 68, who later, at postmortem, was found to have had a ventricular aneurysm. He had a confirmed history of myocardial infarction, which occurred 1½ years before these recordings.

The electrocardiographic findings of significance are: a small Q wave followed by a small R wave in leads I and aVL,

this text have no ready explanation for this feature, although possibly it may reflect migration of the electrical point. The posteroanterior chest film of the patient is also reproduced above, the arrow indicating the location of the large ventricular aneurysm. The patient expired postoperatively, after attempted surgical correction of the aneurysm.

vector accompanying ventricular aneurysms is not definitely established, but several possibilities have been entertained

1. As the scarred, thin-walled aneurysm balloons outwardly with each ventricular systole, traction is exerted on the muscle to which it is attached. This gives rise to injury currents in the surrounding myocardium (Fig. 215)

2. In some cases, the S-T segment elevation may be secondary to deep QS deflections (see discussion of ventricular gradient in Chapter 6), since for every increase in the QRS area there must be an equal, but oppositely directed, increase in the area of the S-T interval and T wave.

3. Grishman explains the persistence of upwardly displaced S-T segments following myocardial infarction by postulating a shift in position of the dipole center during inscription of the QRS loop due to a markedly disturbed balance of activation potentials. Since, after writing the QRS loop, the electron beam of the vectorcardiograph does not return to its initial point of origin, the QRS loop remains open, the resulting S-T vector projecting S-T elevation on overlying leads. The shift in position of the dipole center is said also to occur in the presence of left bundle branch block. Here, also, the dipole shift is attributed to the marked imbalance of electrical forces produced by ventricular depolarization, just as is the case with myocardial infarction (Fig. 218).

PERI-INFARCTION BLOCK

In 1950, for the first time, First, Bayley, and Bedford described a type of intraventricular conduction defect associated with myocardial infarction which they called peri-infarction block. The identifying features of peri-infarction block in the electrocardiogram are as follows (Fig. 217):

- 1 The QRS interval is prolonged to 0.11 or 0.12 second.
- 2 Onset of the intrinsoid deflection in precordial leads overlying uninvolved portions of left ventricular wall occurs at the normal time but is delayed in leads overlying the peripheral zone of the infarction.
- 3
- 4 As Grant has recently emphasized, the initial and terminal QRS forces in peri-infarction block are directed differently. The spatial angle subtended by the initial and terminal 0.04-second mean QRS spatial vectors usually exceeds 60° .

The mechanism of peri-infarction block is not known for certain, although the mechanism outlined by First, Bayley, and Bedford is generally, albeit ten-

block, it is presumed that the infarction has involved an extensive portion of the subendocardial muscle and

Purkinje network. As a result, uninvolved muscle overlying the infarction cannot undergo activation in a direction perpendicular to the epicardial surface, as occurs normally; instead, the activation wave must spread by a circuitous route through unaffected muscle away from the infarction. The late activa-

tion of the muscle overlying the infarction, and the divergence of the initial and terminal instantaneous QRS vectors. Thus, for reasons previously explained, the initial instantaneous QRS vectors are displaced away from the site of infarction, and therefore away from the overlying exploring electrode of one or the other precordial lead. On the other hand, since the subepicardial muscle over the infarction is the last to be activated, the terminal instantaneous QRS vectors are directed toward the exploring electrode of the same precordial lead. Consequently, in

described what they believe to be a type of peri-infarction block different from that described above. The principal point of distinction between the two types of peri-infarction block, according to Grant and his co-workers, is the absence of significant QRS prolongation in the second type. These investigators reviewed electrocardiograms recorded before and after onset of infarction in a large series of cases and found

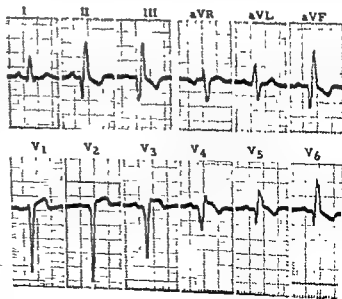


Fig 217.—Diaphragmatic and anterolateral myocardial infarctions in a man, 55, with coronary artery disease. The presence of peri-infarction block is suggested by the tall and wide R waves in leads II, III, aVF, V_1 , and V_2 and the QRS duration of 0.12 second. Peri-infarction block is also suggested by the wide angle between the initial and terminal 0.04-second vectors when plotted on the triaxial reference figure (the initial 0.04-second vector pointing away from the diaphragm and the terminal 0.04-second vector pointing toward the diaphragm). (From H S Lipman and E Masie, *Clinical Scalar Electrocardiography* [4th ed, Chicago Year Book Publishers, Inc, 1959], Fig 191.)

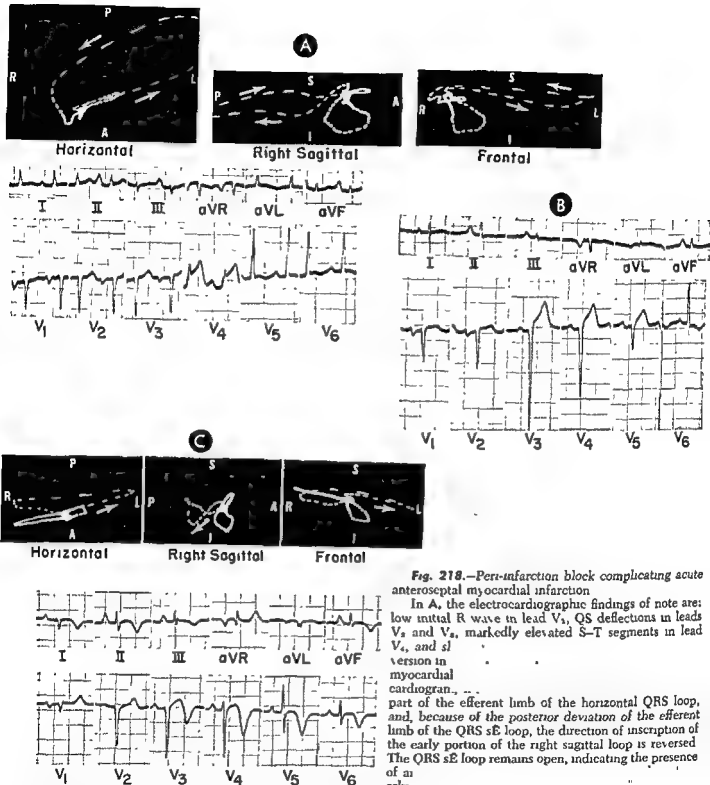


Fig. 218.—Perinfarction block complicating acute anteroseptal myocardial infarction

In **A**, the electrocardiographic findings of note are: low initial R wave in lead V₁, QS deflections in leads V₂ and V₃, markedly elevated S-T segments in lead V₄, and sl

version in myocardial

cardiogram. . . . part of the efferent limb of the horizontal QRS loop, and, because of the posterior deviation of the efferent limb of the QRS sE loop, the direction of inscription of the early portion of the right sagittal loop is reversed. The QRS sE loop remains open, indicating the presence of an

only,
ented slightly anteriorly and at first to the right and then to the left with the interpretation of the electrocardiographic abnormalities

In the electrocardiogram in **B**, recorded about deflections in leads V₂ through V₄ and low R wave, but the T waves are upright. Note that next

The electrocardiogram in **C** was recorded several days later. Leads I, II, III, and aVF show terminal R waves, and the T waves are inverted in leads I, II, III, and aVF. Leads aVR and V₁ show terminal R waves, while leads V₂ and V₃ both record deep terminal S waves. The diagnostic findings of recent anterior myocardial infarction persist, the T waves being deeply inverted in leads V₂ through V₄. The vectorcardiogram recorded at this time differs from that in **A** primarily in two respects: the QRS sE loop displays a which is responsible for the terminal S waves appearing in loop is large and directed to the right, slightly anteriorly,

that, in a significant percentage of the cases, anterolateral infarctions, and diaphragmatic infarctions in particular, produced alterations in the terminal, as well as the initial, QRS vectors. In most such cases, the initial vectors assumed relatively

infarctions, the altered terminal instantaneous vectors generally were rotated to the left, superiorly, and posteriorly. As Grant pointed out, anterolateral infarction may therefore be implicated in occasional cases, as the mechanism responsible for left-axis deviation of a QRS. Furthermore, if QRS interval prolongation is superimposed on this type of terminal

tion) (Fig 218), Grant found the altered terminal QRS vectors usually oriented to the right, posteriorly, and inferiorly. But sometimes the terminal vectors were directed to the right, superiorly, and anteriorly and projected terminal R' deflections on leads V_{2R} and V_1 . In such instances, if QRS prolongation to 0.12 second supervenes, the electrocardiogram may resemble right bundle branch block. Grant suggested that, possibly occasional infarctions may alter only the termi-

haps, to point out that strictly posterior infarction was not included in his study series. This type of infarction produces abnormalities which are manifested relatively late in the QRS interval, and the mechanism responsible for these findings may possibly be a form of peri-infarction block. The authors of this text and other investigators have noted vectorcardiographically that strictly posterior infarction quite characteristically alters either the initial and terminal or only the terminal instantaneous QRS vectors.

Grant and his associates believe that anterolateral infarction with peri-infarction block can usually be differentiated from left bundle branch block if the following facts are kept in mind:

1. A Q wave in lead I with a duration greater than 0.02 second occurs only in peri-infarction block, never in uncomplicated left bundle branch block.

2. A Q wave of less than 0.02-second duration may occasionally be present in lead V_4 in uncomplicated left bundle branch block, but Q waves of 0.03-second duration or longer in this lead occur only in peri-infarction block or in left bundle branch block with septal infarction.

3. In the large series of cases of uncomplicated left bundle branch block studied by Grant and his co-workers, an initial R wave was present in leads V_1 to V_4 in 45% of the cases, the R wave was absent in lead V_1 alone in 35% and absent in leads V_1 and V_2 in 15%. However, in only 5% of the cases of left bundle branch block was the initial R wave lost in leads V_1 through V_3 . In none of the cases of left bundle branch block were QS deflections recorded as far to the left as lead V_4 . In contrast, initial R waves were present in leads V_1 through V_4 in 100% of the cases of peri-infarction block.

5. In

R waves decrease systematically in magnitude between leads V_1 and V_4 , although this was not an unusual finding in peri-infarction block.

6. The best point of distinction between left bundle branch block and peri-infarction block, according to Grant and his associates, is the angle between the initial and terminal mean 0.04-second QRS spatial vectors. In left bundle branch block, the angle varies from 45° or less to 80°, but in peri-infarction block the angle is rarely less than 60° and usually exceeds 100°.

The primary difference between diaphragmatic myocardial infarction with peri-infarction block and the condition it may resemble, namely, right bundle branch block, is that the terminal 0.04-second mean QRS spatial vector, although directed to the right in both types of conduction disturbance, is situated as much as 90° more anterior in right bundle branch block than in peri-infarction block. In diaphragmatic myocardial infarction with peri-infarction block, the terminal mean vector lies slightly posterior and usually is directed more vertically than the corresponding vector in right bundle branch block.

Grant and Murray are of the opinion that the type of peri-infarction block observed in their infarction

series results from some mechanism other than that postulated by First, Bayley, and Bedford. The following is a quotation from Grant and Murray:

As a possible explanation for this type of peri-infarction block one may consider the conduction network in the left ventricle as consisting of two pathways which are effectively syncytial with one another over large areas of the myocardium. Under normal circumstances excitation spreads simultaneously 0.04 sec. of the t_r spread, perhaps,

of the left bundle branch for which there is considerable anatomic and some physiologic evidence. Anterolateral infarctions and diaphragmatic infarcts tend to lie in the distribution of the posterior subdivisions. An infarct in one region would, if it involved a large enough portion of the network, cause excitation to spread largely by way of the other pathway so that excitation of the myocardium adjacent to the infarct would be delayed by 0.04 sec., but there would be little or no prolongation of the QRS interval.

PERICARDITIS AND MYOCARDITIS

Pericarditis

Acute fibrinous pericarditis.—This condition injures the subepicardial myocardium and therefore produces an S-T vector directed toward the effective location of the epicardial injury. For example, pericarditis involving the anterior aspect of the left ventricle projects elevated S-T segments on anterior precordial leads. The T waves are usually upright during this phase. With subsidence of the acute pericarditis, the elevated S-T segments begin to return to the base line, and inverted T waves make their appearance.

In all probability, the latter are due to an abnormally delayed onset of repolarization in the subepicardial myocardium secondary to the myocardial inflammatory response. Accordingly, the T SE loop and SA T tend to swing away from the involved area. If there are no complications, all abnormalities disappear from the electrocardiogram within 4–8 weeks. When pericarditis occurs in adults within age groups prone to coronary artery disease, S-T segment deviation due to pericarditis and that occurring in early stages of developing myocardial infarction may be difficult to differentiate electrocardiographically, crucial as such a

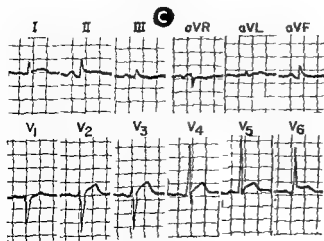
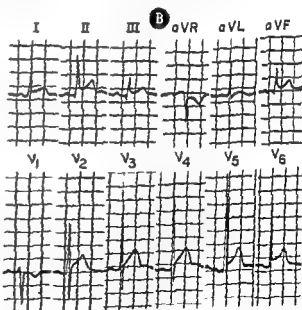
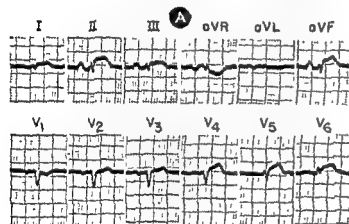
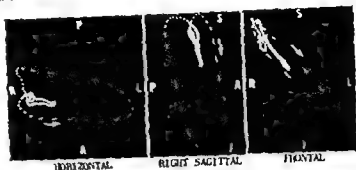


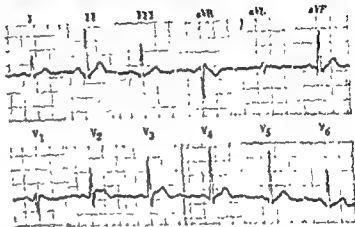
Fig 219.—A–C, three different electrocardiographic examples of a relatively early stage in the evolution of the pericarditis pattern. Note, in each record, the widespread S-T segment elevation occurring in leads I, II, III, aVF, and V₄ (or V₅) through V₆, and the normal T waves. Later in the evolution of changes, the S-T segments will return to the isoelectric lines, and, as they do so, the T waves will become progressively lower and finally inverted.

Fig. 220—Electrocardiographic and vectorcardiographic findings in subacute



from striking in these leads

In the vectorcardiogram, the QRS Σ loop remains open, its terminus being displaced slightly anteriorly and to the left. The S-T vector extending from the electrical null point to the terminus of the QRS Σ loop in each projection is compatible with anterolateral subepicardial injury, such as occurs in pericarditis.



distinction is to the prognosis and therapeutic management of the patient. Serial electrocardiograms are indicated, therefore, to distinguish between the two clinical possibilities. In interpreting the initial electrocardiogram recorded from such a patient, two features tend to summarize them:

1. Low voltage of all components of the ventricular complex, due possibly to a decreased volume of ventricular muscle secondary to prolonged reduction in work requirements.

2. Unusually wide angle between sA QRS and sA T.

- 1 Low voltage of all components of the ventricular complex, due possibly to a decreased volume of ventricular muscle secondary to prolonged reduction in work requirements
- 2 Unusually wide angle between sA QRS and sA T.

Myocarditis

Various forms of myocarditis, including acute rheumatic carditis, may produce one or more of the following abnormalities.

- 1 Conduction disturbances, such as prolonged Q-T intervals, atrioventricular block, and bundle branch block.
- 2 Disturbances in the cardiac rhythm, such as sinus tachycardia, atrioventricular nodal rhythms with atrioventricular dissociation, and occasionally atrial fibrillation.
- 3 An abnormally wide spatial angle between sA QRS and sA T.
- 4 The electrocardiographic abnormalities described in the discussion of acute fibrinous pericarditis or pericarditis with effusion.

carus than in myocardial infarction, in that the subepicardial injury pattern does not conform to a single area of involvement (in terms of the specific leads displaying elevated S-T segments). For example, one often observes S-T segment elevation in leads I, II, III, aVL, and aVF and in most of the precordial leads. Such a distribution of S-T segment elevation would be quite unusual in myocardial infarction (Figs 219 and 220).

- 2 The association of upright T waves and elevated S-T segments is more frequently encountered in pericarditis than in myocardial infarction. In the subepicardial injury phase of infarction, the T waves are usually difficult to separate from the S-T segments, or they are of low amplitude or are terminally inverted.

Pericarditis with effusion—This is characterized by lowered voltage of all components of the ventricular complex. The low amplitude QRS and T complexes

Myocardial Damage, Coronary Insufficiency, and Stress Tests

MYOCARDIAL DAMAGE AND CORONARY INSUFFICIENCY

WITH THE EXCEPTION of the rare infarctions resulting from congenitally aberrant or anomalous coronary arteries or from syphilitic involvement of the coronary ostia, a myocardial infarction generally indicates underlying coronary arteriosclerosis or atherosclerosis. However, many patients with coronary artery disease never sustain clinically recognizable infarctions, although after recurrent episodes of myocardial anoxia they may eventually suffer diffuse degenerative and fibrotic changes in the ventricular myocardium. In these patients, as well as in those who have had small, "subclinical" myocardial infarctions, the vectorcardiogram may display only minor deviations of the QRS sE loop from normal. For example, the contour of the QRS sE loop may be markedly irregular, with abrupt changes in course which reflect sudden changes in the direction and magnitude of the mean instantaneous QRS spatial vectors. Sometimes the direction of inscription of the QRS sE loop may be reversed in one or more projections of the vectorcardiogram, not infrequently, the QRS sE loop may have a markedly irregular contour and, or may not lie in a single plane of predilection; or, finally, S-T vector or T sE loop abnormalities may be present in the vectorcardiogram. With reference to the latter, the authors of this text consider an angular divergence of the long axes of the QRS sE and T sE loops greater than 45° to be the vectorcardiographic equivalent of "nonspecific T wave abnormalities" in the electrocardiogram. However, these vectorcardiographic abnormalities may or may not be accompanied by recognizable abnormalities of the QRS deflections, S-T segments, or T waves of the electrocardiogram (Figs. 221-223). When corresponding QRS changes are present in the electro-

cardiogram, they may take, for example, the form of notched or slurred QRS complexes, low R waves of equivocal significance in one or more precordial leads, or Q waves which are suspicious but not definitely abnormal. In general, the QRS sE loop abnormalities reflecting myocardial damage and corresponding abnormalities in the electrocardiogram have not been studied extensively as yet.

Much more attention has been given to the S-T segment and T wave or T sE loop changes in coronary artery disease. In some patients these abnormalities may remain as a persistent feature of the electrocardiogram or vectorcardiogram, while in others they may appear only during episodes of angina pectoris or after exercise or exertion. The S-T segment and T wave abnormalities may be grouped as follows.

Subendocardial ischemia and injury—The electrocardiographic and vectorcardiographic patterns of subendocardial ischemia and injury are considered to be most typical of coronary insufficiency. Subendocardial myocardial injury produces an S-T vector directed to the right, posteriorly, and superiorly, away from the effective electrical site of subendocardial injury in the left ventricle, while ischemia limited to subendocardial layers of muscle rotates the mean instantaneous T vectors in just the opposite direction—that is, toward the electrical location of the ischemic muscle. Thus, subendocardial injury and ischemia are evidenced in the electrocardiogram by the presence of depressed S-T segments and upright T waves in left precordial leads.

Transmural ischemia—When ischemia extends through the entire thickness of ventricular wall to the epicardial surface, the mean instantaneous T vectors

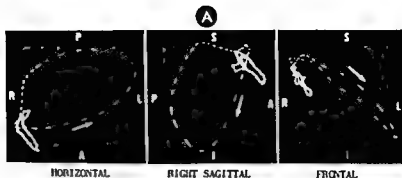
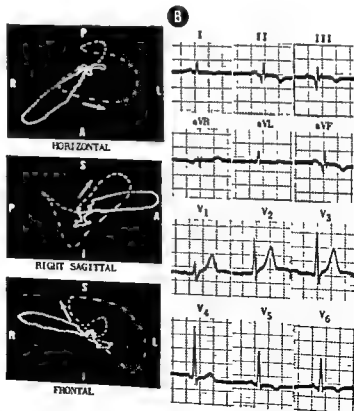


Fig. 221.—**A**, electrocardiogram and vectorcardiogram recorded from a patient with a history of angina pectoris. Although the electrocardiogram is within normal limits, the QRS \mathbf{sE} and T \mathbf{sE} loops of the vectorcardiogram are abnormally divergent. Thus, the spatial angle subtended by the long axes of the QRS \mathbf{sE} and T \mathbf{sE} loops (calculated by the method described in Chapter 7) is approximately 72° , while the upper limits of normal is 45° . This vectorcardiographic abnormality is compatible with myocardial disease or coronary artery disease. The foregoing interpretation of this vectorcardiogram is substantiated by the subsequent course of events, for 2 weeks later the patient was admitted to the hospital with the clinical picture of acute myocardial infarction.

B, electrocardiogram and vectorcardiogram recorded shortly after the patient's admission. Both are diagnostic of acute diaphragmatic and probable posterolateral myocardial infarction.



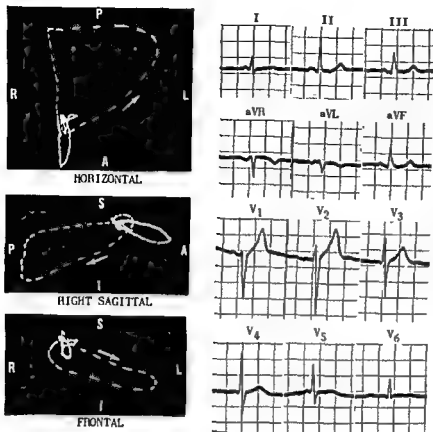


Fig. 222.—Electrocardiographic and vectorcardiographic findings in a patient with typical angina pectoris. The main abnormality in the electrocardiogram is the low T wave in lead I and the low to diphasic T wave in lead V₁. However, these findings are far from impressive. In contrast, in the vectorcardiogram the spatial angle subtended by the long axes of the QRS sE and T sE loops is approximately 110°, which is more than twice normal.

swing away from the electrical site of ischemia. Ordinarily this causes increased divergence of the mean instantaneous QRS vectors and mean instantaneous T vectors, with the result that leads registering upright QRS deflections tend to record T waves which become gradually lower, isoelectric, and then inverted with progression of the ischemia. In coronary artery disease, transmural ischemia may occur in company

with subendocardial injury or may be present in the absence of current of injury. This pattern may be persistent or evanescent.

Local transmural injury.—Occasionally a local subepicardial injury pattern, in the form of S-T segment elevations, may appear over one aspect of the heart. A temporary pattern of diaphragmatic wall injury is frequently observed.

STRESS TESTS

Unfortunately for the physician, the diagnosis of coronary artery disease is often difficult to establish, particularly in those patients who have atypical anginal pain and a normal resting electrocardiogram. In such situations it is frequently helpful diagnostically to utilize either the exercise test or the anoxemia test. The latter procedure is probably less widely used than the exercise test because it requires special equipment. However, neither test possesses any definite advantage over the other, although it is of some interest that patients having negative exercise tests may have positive anoxemia tests, and vice versa. These tests are undertaken only if control electrocardiographic tracings recorded just before commencing the tests show no significant abnormality, and provided

the patient is not receiving digitalis or other medications known to alter the duration of the excited state in heart muscle.

The Anoxemia Test

For the anoxemia test, Levy and his co-workers recommend the use of a mixture of 10% oxygen and 90% nitrogen, which is inspired by the patient at a rate comparable to that of normal pulmonary ventilation. A control electrocardiographic tracing is obtained before beginning the test. Thereafter, records are taken at 5-minute intervals during the test, which, unless chest pain or discomfort interrupts, usually lasts 25 minutes. The criteria of Levy and his associ-

ates for an abnormal test response are as follows:

1. Arithmetical sum of the S-T deviations in all four leads (I, II, III, and IV_r *) totaling 3 mm. or more.
2. Partial or complete reversal of the direction of the T wave in lead I accompanied by an S-T deviation of 1 mm. or more in this lead.
3. Complete reversal of the direction of the T wave in lead IV_r , with or without S-T segment deviations.

(For further information the reader is referred to the thorough review of this test by Stewart and Carr.)

The Exercise Test

The purpose of this procedure is to increase, by means of exercise, the demands placed on the coro-

*Lead IV_r is an obsolete bipolar precordial lead. The recording positive electrode is applied at the same point as the exploring electrode in lead V_4 , and the negative electrode is attached to the left leg.

nary blood supply of the myocardium. If the ability of the coronary blood flow to adjust to the increased needs of the heart is limited because of pathologic narrowing of the coronary arteries, relative ischemia and/or injury may be induced by exceeding this limit, and electrocardiographic abnormalities will then appear.

The recognition of an abnormal electrocardiographic response to exercise is made considerably more difficult by certain changes which normally occur with exercise. These changes principally involve the S-T segment and the T wave. With reference to the former, the normal S-T segment deviations which are observed in healthy subjects may be subdivided into two groups, which in this text will be called *apparent S-T deviations* and *physiologic S-T deviations*. These deviations will be discussed in the paragraphs to follow.

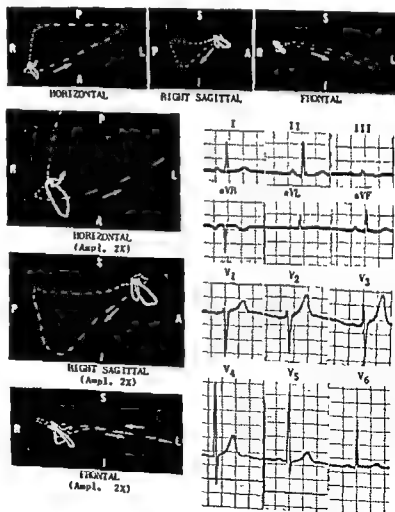


Fig. 223—Electrocardiographic and vectorcardiographic findings in a patient with typical angina pectoris. The electrocardiogram is within normal limits, although there is a tendency to high QRS voltage in lead V_1 , but in the vectorcardiogram, the spatial angle between the QRS and T loops is 85° , well above the upper limit of normal.

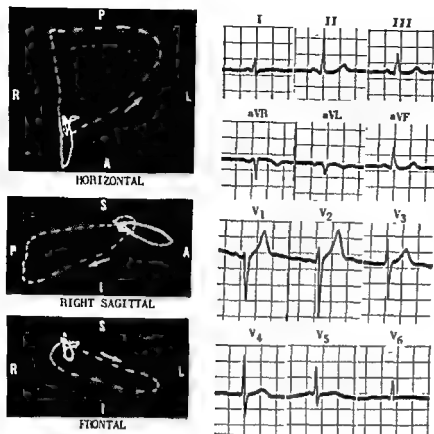


Fig. 222.—Electrocardiographic and vectorcardiographic findings in a patient with typical angina pectoris. The main abnormality in the electrocardiogram is the low T wave in lead I and the low to biphasic T wave in lead V₄. However, these findings are far from impressive. In contrast, in the vectorcardiogram the spatial angle subtended by the long axes of the QRS and T loops is approximately 110°, which is more than twice normal.

swing away from the electrical site of ischemia. Ordinarily this causes increased divergence of the mean instantaneous QRS vectors and mean instantaneous T vectors, with the result that leads registering upright QRS deflections tend to record T waves which become gradually lower, isoelectric, and then inverted with progression of the ischemia. In coronary artery disease, transmural ischemia may occur in company

with subendocardial injury or may be present in the absence of current of injury. This pattern may be persistent or evanescent.

Local transmural injury—Occasionally a local sub-epicardial injury pattern, in the form of S-T segment elevations, may appear over one aspect of the heart. A temporary pattern of diaphragmatic wall injury is frequently observed.

STRESS TESTS

Unfortunately for the physician, the diagnosis of coronary artery disease is often difficult to establish, particularly in those patients who have atypical anginal pain and a normal resting electrocardiogram. In such situations it is frequently helpful diagnostically to utilize either the exercise test or the anoxemia test. The latter procedure is probably less widely used than the exercise test because it requires special equipment. However, neither test possesses any definite advantage over the other, although it is of some interest that patients having negative exercise tests may have positive anoxemia tests, and vice versa. These tests are undertaken only if control electrocardiographic tracings recorded just before commencing the tests show no significant abnormality, and provided

the patient is not receiving digitalis or other medications known to alter the duration of the excited state in heart muscle.

The Anoxemia Test

For the anoxemia test, Levy and his co-workers recommend the use of a mixture of 10% oxygen and 90% nitrogen, which is inspired by the patient at a rate comparable to that of normal pulmonary ventilation. A control electrocardiographic tracing is obtained before beginning the test. Thereafter, records are taken at 5-minute intervals during the test, which, unless chest pain or discomfort interrupts, usually lasts 25 minutes. The criteria of Levy and his associ-

heart during exercise. This factor has been implicated, by some investigators, in the production of the tall upright T waves often seen after exercise. The presence or absence of sympathetic stimulation during an episode of tachycardia is probably important in deciding whether ST-T wave changes appear, although its influence in a given case is difficult to assess.

ABNORMAL ECG RESPONSES TO EXERCISE

The crux of the problem relating to the interpretation of the effects of exercise on the electrocardiogram lies in differentiating S-T segment and T wave

changes from evidence of abnormality. If the criteria employed are quite strict, then a positive response to the test constitutes strong evidence for coronary artery disease, but at the same time a large number of false negative test responses must be anticipated. On the other hand, if the test is to be used to eliminate the possibility of coronary artery disease, false negative responses must be excluded, in so far as possible, by utilization of less rigid criteria of abnormality. However, less rigid test criteria have the associated disadvantage of eliciting many false positive test responses in normal subjects. Thus the criteria selected should be those best suited to the purpose for which the stress test is being done. Scherf and Schaffer prefer for their purposes a rigid approach to the exercise test.

CRITERIA FOR ABNORMALITY—The electrocardiographic criteria for an abnormal exercise test proposed by different authorities are as follows:

1. An S-T segment depression greater than 2 mm in any lead is conceded, by all investigators, to be abnormal.
2. An S-T segment depression of 1.5–2 mm is considered probably abnormal, but if it is less than 1.5 mm, Scherf and Schaffer regard it as normal, realizing that in some instances false negative test responses result.
3. Twiss and Sokolow designate, as the upper limit of normal, an S-T segment depression of 1 mm in lead I, and of 1.5 mm in leads II and III. Biörck regards as normal those S-T segment depressions whose total sum in the three standard limb leads is less than 2 mm, while Master and his associates accept a 0.5-mm deviation of the S-T segments in any lead as the upper limit of normal.
4. The appearance of a pattern of local subepicardial

injury, as previously described, is abnormal.

5. Abnormal widening of the angle between SA QRS and SA T produces positive findings of T wave inversion in leads registering upright QRS complexes, such as leads I, II, and V₁ through V₆. If the T wave becomes lower or inverted at a time when the postexercise tachycardia is subsiding, this observation carries increased significance in terms of abnormality.
6. The occurrence of extrasystoles after exercise is thought to be definitely abnormal. They are usually ventricular in type and may be multifocal in origin. Occasionally, paroxysmal tachycardia may be precipitated by exercise.
7. Onset of significant atrioventricular or intraventricular conduction delay after exercise is a fairly reliable sign of coronary artery disease.

TECHNIQUE OF THE EXERCISE TEST

Inasmuch as strenuous exercise in normal subjects often elicits marked electrocardiographic changes, the criteria cited above are applicable only if the subject performs moderate exercise. Moderate exercise is considered equivalent to the work done by a person in one of three ways, as follows:

1. On the basis of the history obtained from the patient, Scherf and Schaffer prescribe an amount of exercise not exceeding that which the patient permits himself to perform daily, and approximating that which usually causes the patient to experience angina or its equivalent.

2. Other authorities have the patient exercise until he is stopped by pain, dyspnea, or fatigue. Scherf and Schaffer stress that this test inherently carries an increased danger to the patient and therefore should be reserved for cautious use in those patients with negative responses to more conservative testing.

3. Perhaps the most popular method at present is based on the two-step test of Master.

THE MASTER TEST

The Master steps usually consist of a wooden platform having two steps, 9 inches wide and 9 inches from the floor, placed on each side of a central step, 11 inches wide and 18 inches from the floor. When the patient climbs up one side of the steps and down the other, he has completed one trip. Master has devised tables which relate the number of trips to be taken

APPARENT S-T SEGMENT DEVIATIONS

In the presence of marked tachycardia, an apparent S-T depression may be due to an elevation of the T-P segment, which is itself the result of superimposition of the P wave on the T wave of the preceding complex.

Another cause of apparent S-T segment deviation after exercise is superimposition of a prominent auricular repolarization wave (Ta wave) on the ventricular S-T segment. The Ta wave lasts well beyond the end of the QRS complex even though the P-Ta interval is shortened by tachycardia. Therefore, an increase in the size of the Ta deflection may displace the ventricular S-T segment downward (or upward if the Ta wave follows an inverted P wave and is of positive polarity). Such an increase in the magnitude of the Ta deflection in exercise is probably caused by two factors:

1. The mean P wave vector becomes more vertical with exercise, and so there is an increased size of the P waves in leads II and III particularly. Since the area of the P wave is equal in size but opposite in polarity to the area of Ta, an increase in the size of an upright P wave causes an increase likewise in the size of the negative Ta wave.

2. More important is the fact that tachycardia shortens the monophasic action current of the atrial myocardium, affecting chiefly the recovery phase during which the Ta wave is written. As the Ta wave shortens, it must also deepen, in order to maintain an area equal and opposite to that of the P wave.

Some correction for the foregoing two mechanisms producing apparent S-T segment deviations can be accomplished in the following ways: (a) The level of the S-T segment can be compared to the level of the point of junction of the P-R segment with the QRS complex. (b) Occasionally, deviation of the S-T segment by a prominent Ta wave can be demonstrated more clearly by extending the downwardly sloping P-R segment into the S-T segment. If this sloping line descends to the level of the S-T segment, then apparent S-T segment deviation due to a large Ta wave is probably present. (c) The recording of lead V_4 or V_6 may often be helpful, since in this lead the P-Ta complex is usually small.

PHYSIOLOGIC S-T SEGMENT DEVIATIONS

In a previous section it was stated that normally there is a difference in the duration of the excited state between inner and outer areas of the ventricular myocardium, that is to say, normally there exists a

ventricular gradient. The vector representing this gradient, like the mean ST-T vector,* tends to parallel the mean QRS vector. Theoretically, if the duration of the excited state or the degree of repolarization delay were the same in all parts of the ventricular myocardium, the ventricular gradient would be zero and the mean QRS and ST-T vectors would be of equal amplitude and directed 180° away from each other. In reality, the ventricular gradient is never zero, but, as it decreases, the ST-T vector rotates away from the mean QRS vector. Thus, electrocardiographic leads registering upright QRS complexes may develop S-T segment depression and T wave flattening or inversion, which tend to increase as the ventricular gradient approaches zero. There are two factors related to the ventricular gradient which act to produce a physiologic S-T segment deviation after exercise in normal individuals:

1. Normally an increase in the heart rate results in a decrease in the ventricular gradient. Apparently, at faster heart rates the inner layers of the myocardium, normally the site of repolarization delay, tend to recover more promptly. Consequently, as their speed of recovery approaches that of the outer layers, the duration of the excited state becomes more nearly equal at the endocardial and epicardial surfaces of the heart, the ventricular gradient approaches zero, and the S-T segments and T waves descend.

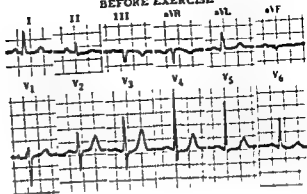
2. As with the P-Ta waves, in shortening the monophasic action current of the ventricular myocardium, tachycardia shortens mainly the recovery process, and this produces a shorter Q-T interval. In order to maintain its same area, the ST-T complex must increase its amplitude or area, becoming more positive or more negative depending on whether it follows a resultant upright or inverted QRS complex.

It should be added that an "effort" factor is also thought to be present in exercise which to a varying degree opposes the tendency of the above tachycardia factor to decrease the ventricular gradient. The effort factor possibly functions by delaying repolarization in the inner layers of the myocardium as the result of the more intense mechanical effort of the

*The electrical forces normally produced during both the S-T interval and the T interval result from ventricular repolarization. Consequently, factors such as those to be described, which influence the repolarization process, tend to manifest similar effects on both the S-T segment and the T wave. For this reason, these two components of the QRS-T complex will be referred to occasionally as the ST-T complex, or as being represented by an ST-T vector.

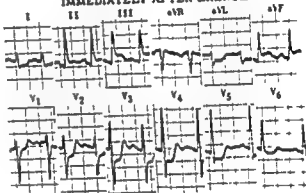
A

BEFORE EXERCISE



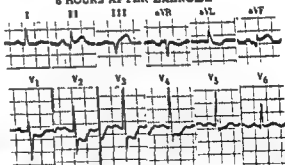
B

IMMEDIATELY AFTER EXERCISE



C

6 HOURS AFTER EXERCISE



HORIZONTAL

RIGHT SAGITTAL

FRONTAL

Fig 224—Electrocardiographic and vectorcardiographic findings during and after a double Master exercise test.

The control electrocardiogram in **A** is not entirely within normal limits, in that there is definite, although slight, S-T segment depression in leads V_1 through V_6 . Since the patient was not on digitalis medication, the S-T segment deviation in the electrocardiogram would have to be considered suggestive of subendocardial myocardial injury. With rare exceptions, an abnormal control electrocardiogram renders the exercise test purposeless and potentially hazardous.

The electrocardiogram in **B**, recorded immediately after exercise, displays marked S-T segment depression in leads I, aVL, and V_1 through V_6 and equally marked S-T segment elevation in leads II, III, and aVF. The latter finding is indicative of diaphragmatic-subepicardial myocardial injury. The S-T segment depression in the anterior precordial leads can be attributed to either or both of the following factors: anterior subendocardial myocardial injury and/or posterior subepicardial myocardial injury (the precordial leads recording reciprocal S-T segment deviation).

In the electrocardiogram in **C**, recorded 6 hours after the exercise stress test, abnormal Q waves have appeared in leads III and aVF, and S-T segment elevation persists in these leads and in lead II. The S-T segments in leads V_1 through V_6 remain depressed. The abnormalities present in this electrocardiogram are diagnostic of acute diaphragmatic myocardial infarction. The vectorcardiogram in **C** was recorded several days after the recording of the electrocardiogram appearing above it. The QRS sE loop displays a large, early, rightward and superior deflection, the mean 0.02-second instantaneous vectors of the right sagittal and frontal QRS loops being situated superior to -40° . These QRS sE loop abnormalities are diagnostic of diaphragmatic myocardial infarction, while the anterior, rightward, and superior orientation of the T sE loop is indicative of diaphragmatic-posterolateral myocardial ischemia.

TABLE 28.—NUMBER OF TRIPS PERFORMED DURING 1½ MINUTES IN THE MASTER TWO-STEP EXERCISE TEST*

Males (Females in Parentheses)

Weight	Age in years							
	5-9	10-14	15-19	20-29	30-39	40-49	50-59	60-69
<i>n</i>	♂ = ♀							
40-49	35	36 (33)	(33)					
50-59	31	35 (33)	12 (32)					
60-69	31	33 (32)	31 (30)					
70-79	28	12 (30)	30 (29)					
80-89	26	30 (23)	39 (26)	29 (28)	28 (27)	27 (24)	25 (22)	24 (21)
90-99	24	29 (27)	28 (26)	28 (27)	27 (25)	26 (23)	25 (21)	23 (20)
100-109	22	27 (25)	27 (25)	28 (26)	27 (25)	25 (23)	24 (21)	22 (19)
110-119	20	26 (23)	36 (33)	27 (25)	26 (24)	25 (22)	23 (20)	22 (18)
120-129	18	24 (22)	25 (22)	26 (24)	26 (24)	24 (21)	23 (19)	21 (18)
130-139	16	23 (20)	24 (20)	25 (23)	25 (22)	23 (20)	22 (19)	20 (17)
140-149		21 (18)	21 (19)	24 (22)	24 (21)	23 (19)	21 (18)	20 (16)
150-159		20 (17)	22 (17)	24 (21)	24 (20)	22 (19)	20 (17)	19 (16)
160-169		18 (15)	21 (16)	23 (20)	23 (19)	22 (18)	20 (16)	18 (15)
170-179		(13)	20 (14)	22 (19)	23 (18)	21 (17)	19 (16)	18 (14)
180-189			19 (13)	21 (18)	22 (17)	20 (16)	19 (15)	17 (14)
190-199			18 (12)	21 (17)	21 (16)	20 (15)	18 (14)	16 (13)
200-209				20 (16)	21 (15)	19 (14)	17 (13)	16 (12)
210-219				19 (15)	20 (14)	18 (13)	17 (13)	15 (11)
220-229				18 (14)	20 (13)	18 (13)	16 (12)	14 (11)

*Reproduced by permission from Master, M. A. The electrocardiogram after exercise. Standardized heart function test, U S Navy M Bull 40 346, 1942.

in a 1½-minute interval to the subject's sex, age, and weight (Table 28). Electrocardiographic tracings are taken before, immediately after, and at 2-, 4-, 8-, and 10-minute intervals after the test. If the response from the single Master two-step test is negative, a double test may be performed later by having the subject complete twice as many trips in a 3-minute interval. When the physician feels that the patient is able to

tolerate this amount of exercise, a double two-step Master test is often done initially. At the end of each trip, the subject should always turn in the same direction (e.g., toward the wall) to avoid dizziness. In addition, the subject should be instructed to notify the physician present at the first onset of chest pain or undue dyspnea or fatigue, because at this point the test should be terminated (Figs 224-227).

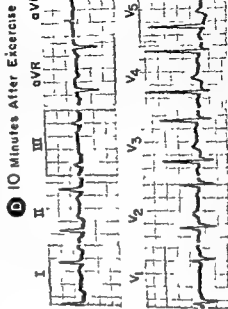
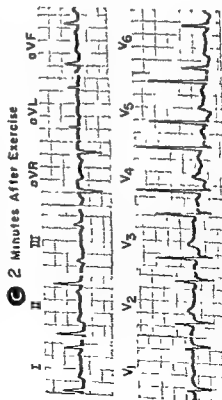
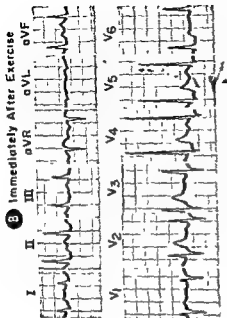
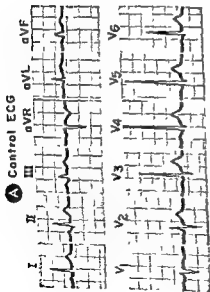


Fig 226.—Positive response to double Master test. Record A shows normal control electrocardiogram. Record B, made immediately after exercise, displays S-T segment depression in leads I, II, aVF, and V₁ through V₆. In leads

V₁ and V₂ particularly, the S-T segment depression exceeds 1.5 mm. These abnormalities persist, although diminished in degree, for 10 minutes after exercise. (records C and D)

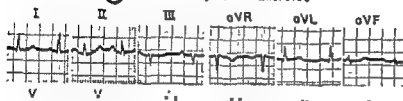
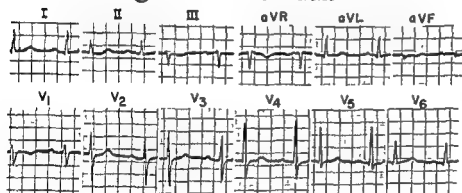
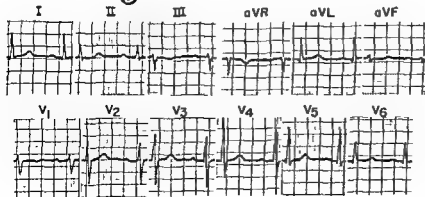
A Control ECG**B Immediately After Exercise****C 2 Minutes After Exercise****D 4 Minutes After Exercise**

Fig. 225.—Negative response to double Master test. The apparent depression of the S-T segments in lead II of record B can most certainly be attributed to a superimposed, deep, atrial T wave (Ta wave), since the downward slope of the P-R segment can be continued into the junction of the QRS deflections and S-T segments.

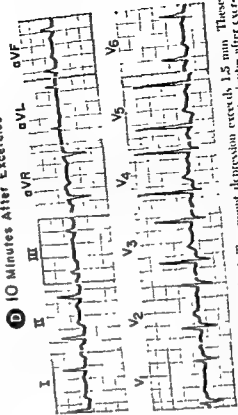
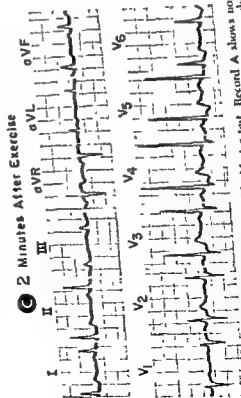
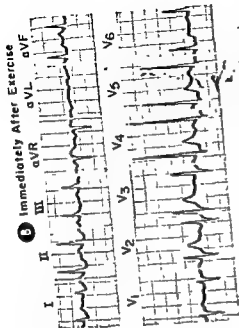
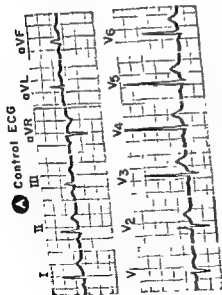
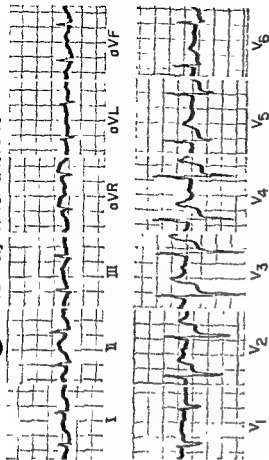
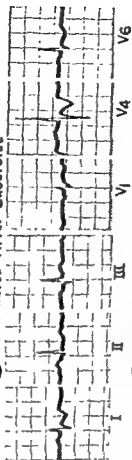
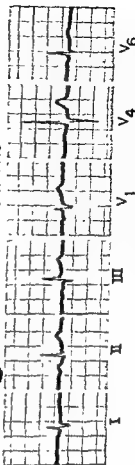


Fig. 226.—Positive response to double Master test. Record A shows normal control electrocardiogram. Record B, made immediately after exercise, displays S-T segment depression in leads I, II, aVF, and V₄ through V₆. In leads

V₁ and V₂, particularly, the S-T segment depression exceeds 1.5 mm. These abnormalities persist, although diminished in degree, for 10 minutes after exercise (records C and D).

B Immediately After Exercise**D 4 Minutes After Exercise****E 10 Minutes After Exercise**

cordial leads, while subsequent record **E** displays inverted T or diphasic T waves in leads V₁ through V₆, which finally disappear 10 minutes after exercise (**E**). An electrocardiogram and vectorcardiogram recorded from this patient several months after the exercise stress test showed diagnostic findings indicating diaphragmatic-posterolateral infarction in the past.

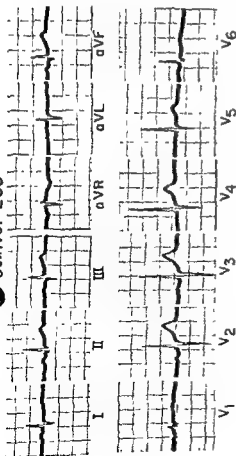
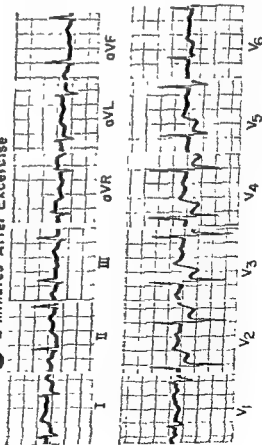
A Control ECG**C 2 Minutes After Exercise**

Fig. 227—Positive response to single Master test in a patient with a control electrocardiogram, which is probably abnormal. The electrocardiogram in **A** shows low T waves in leads I and V₆, suspiciously prominent O waves in leads III and aVF, and a low-amplitude, almost equiphasic RS deflection in lead V₁. The tracing in **B** shows marked S-T segment depression in the pre-

PART III

The Cardiac Arrhythmias

Disturbances of Impulse Formation and Conduction: General Considerations

GENERAL INTRODUCTION

THE PROPERTY OF automatic impulse formation is not confined to a single cardiac focus but is shared by nodal and Purkinje tissues scattered throughout the

charged, and conducted so rapidly through the heart that all other centers of slower impulse formation are kept in a discharged state.

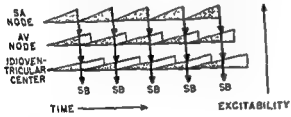


Fig. 228. Three time pacemakers discharges synchronously at the end of the period of time required by the atrio-

ward (in descending order, tail of the sinoatrial node, coronary sinus area; upper, middle, and lower portions of the atrioventricular node, bundle of His, and, finally, the more distal parts of the intraventricular conduction system and Purkinje network) (Fig. 228). The graded rhythmicity of the impulse-forming centers not only enables a single dominant pacemaker, normally the sinoatrial node, to drive the heart but also provides a mechanism by which suppression of one pacemaker calls into action the potential pace-

even slower than that in the atrioventricular node it follows, therefore, that the sinus node will keep in a state of suppression all other pacemaking centers in the heart,

be less susceptible to neurogenic depression than is the sinus node. As a result, widespread and uniform inhibition of all rhythm centers does not ordinarily occur except terminally.

heart Every focal collection of nodal or Purkinje cells has the potentiality of functioning as a cardiac pacemaker, but if all rhythmical centers were active simultaneously, the result would be chaotic heart action. Efficient cardiac function requires that all parts of the heart respond to a single rhythm, and this in turn implies that one potential pacemaker must dominate all others. For a rhythmical focus to emerge as dominant pacemaker, its impulses must be formed, dis-

Cardiac rhythms (often referred to as *ectopic rhythms*) which originate in some focus other than the sinoatrial node are divided, for purposes of discussion, into the two following groups, according to their manner of origin.

Escape beats or rhythms—Depressed impulse formation in, or blocked impulse conduction from, a higher pacemaker may permit a lower center to "escape" for one or more beats at its own inherent rhythmicity and rate (Fig. 229). Beats or rhythms so

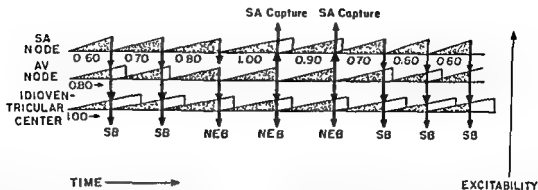


Fig. 229.—The mechanism of escape beats. This illustration differs from Figure 228 in that the time required by the sinoatrial node to reach its excitability threshold varies, sometimes being short and at other times much longer. As the rate of impulse formation slows in the sinoatrial node, it eventually falls below the inherent rate of impulse formation in the atrioventricular nodal pacemaker, at which time the atrioventricular node “escapes” to produce a nodal escape beat (NEB). In the present figure the atrioventricular nodal impulse not only prematurely discharges or “captures” the sinoatrial node (SA capture), and, in so doing, activates the atria, but it also activates the ventricles and discharges prematurely the idioventricular center. Consequently, for two cycles of the cardiac rhythm the atrioventricular nodal center is the dominant pacemaker. It should be noted that the atrioventricular node escapes at its own inherent rate of impulse formation because of slowing of impulse formation in a higher center. An entirely different situation exists in Figure 230

produced are called, in this text, escape beats or rhythms.

Ectopic beats or rhythms.—The term *ectopic*, as used hereafter, is applied only to those beats or rhythms arising as the result of some change in excitability locally in the region of impulse origin (Fig. 230).

The mechanism and electrocardiographic features of cardiac arrhythmias are related to the manner in which impulses are not only formed but also conducted. The following paragraphs are devoted to a preliminary discussion of the refractory period of heart muscle and its relationship to interference and dissociation and to blocked impulse conduction.

Once heart muscle has undergone excitation, it remains for a period of time completely nonresponsive to impulse stimuli. This interval, the *absolute refractory phase*, is followed by the *relative refractory phase*, during which the muscle cells gradually recover their excitability and conductivity (Fig. 231). Impulses entering the muscle tissue during the relative refractory phase may be conducted normally, slowly, incompletely, or not at all, depending on the following variables: (a) the time of arrival of the impulses, whether early or late in the relative refractory phase, and (b) the relationship between impulse strength and the excitability threshold of the muscle.

The absolute and relative refractory phases are of approximately the same duration, and their total length equals the duration of the refractory period. The length of the refractory period varies directly with the cycle length of the cardiac rhythm; the

longer the preceding cycle, the more prolonged the refractory period, and the shorter the cycle, the shorter the refractory period. However, there is a lower limit beyond which further shortening of the cycle is not accompanied by parallel changes in the refractory period.

The duration of the refractory period is normally longest in atrioventricular junctional tissues. Therefore, in a sense, the atrioventricular node is the weak link in the chain of conducting pathways between the sinus node and the Purkinje system in the ventricles. Because of their normally slow rate of conduction and subsequent recovery, the atrioventricular junctional tissues are readily depressed by drugs or disease processes which lengthen the refractory period of heart muscle, even though conduction elsewhere in the heart is not detectably disturbed. A fact to be kept in mind is that atrioventricular (and sinoatrial) junctional tissues are capable of bidirectional conduction. This property is best exemplified by beats originating in the atrioventricular node. The nodal impulse not only passes in a forward or antegrade direction to activate the ventricles but also travels up the atrioventricular node and spreads over the atria in a retrograde direction. That retrograde sinoatrial conduction may also occur is demonstrated whenever an ectopic atrial or nodal impulse prematurely discharges the sinus pacemaker. Inasmuch as variations in antegrade and retrograde atrioventricular conduction are encountered relatively frequently in clinical electrocardiography as manifestations of atrioventricular interference, or atrioventricular block, these

mechanisms will be briefly discussed in this chapter and developed later in more detail.

Atrioventricular Interference and Dissociation

The term *interference* is applied to the mechanism involved when conduction of one impulse delays or prevents conduction of another. Whether interference occurs in the sinoatrial junction, atria, ventricles, or, as described below, in the atrioventricular junction, it tends to appear under the following circumstances:

Rapid discharge of impulses by a single pacemaker

If, for example, two impulses are discharged by an atrial pacemaker in close succession, the second impulse may arrive at the atrioventricular node before it has recovered from the effects of the first (Fig. 232, A). In this event, the second atrial beat may be

conducted through the atrioventricular node more slowly than the preceding beat, it may penetrate without completely traversing the atrioventricular node, or it may not be conducted at all. The fact that the impulse either fails to be conducted or is conducted slowly is not a reflection of increased or prolonged refractoriness of the atrioventricular junctional tissues, it is a normal physiologic manifestation, called *interference*, and is due to arrival of the impulse during the normal refractory period of the atrioventricular node. Atrioventricular interference plays a prominent role in many of the arrhythmias described in later chapters.

Simultaneous activity of two pacemakers.—For atrioventricular interference to occur in this condition, a supranodal pacemaker (e.g., sinus node), and an atrioventricular nodal or ventricular center must be active simultaneously (Fig. 232, B). When a sinus

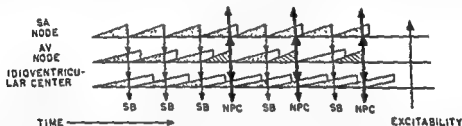
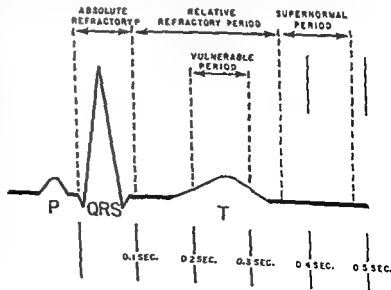


Fig. 230—The mechanism of premature ectopic beats (The conventions here are the same as those in Figures 228 and 229.) It can be seen that the sinoatrial node is the dominant pacemaker except on three occasions, when an atrioventricular nodal extrasystole or nodal premature contraction (NPC) is discharged early enough to discharge prematurely the sinoatrial node and idioventricular center, therefore capturing both the atria and the ventricles. Thus the atrioventricular node dominates the higher pacemaker, not by virtue of any slowing of the rate of impulse formation in the higher center, but rather because of a faster rate of impulse formation in the nodal center itself. Any pacemaker outside the sinoatrial node with an inherent rhythmicity so enhanced is called an *ectopic pacemaker*, and the beats (or rhythm) it produces are called *ectopic beats* (or an *ectopic rhythm*).

Fig. 231—Absolute refractory period, relative refractory period, and supernormal period of the atrioventricular and intraventricular conducting pathways and of ventricular muscle, shown in relation to the P-QRS-T deflections of the electrocardiogram. The vulnerable period cannot be placed in its exact time relationship but is approximately coincident with the peak of the T wave in the electrocardiogram. During the vulnerable period, any ectopic impulse which arrives in the ventricles is peculiarly predisposed to set off a series of ectopic beats and to produce an ectopic tachycardia.



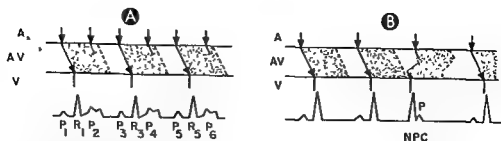


Fig. 232.—The two ways in which interference may occur in the atrioventricular junctional tissues. On the left of each diagram, the letter **A** indicates the atrial beats or P waves, the portion of the diagram enclosed by the two parallel and transverse lines (**AV**) represents the atrioventricular junctional tissues, and **V** refers to the ventricular beats. Stippled areas correspond to the refractory period of the atrioventricular node following conduction of an impulse. In **A**, it is assumed that the sinus node is firing off at a rapid rate and that, because of the sinus tachycardia, every other impulse arrives at the atrioventricular junction during the normal refractory period following conduction of the preceding sinus impulse. Therefore, since every other sinus beat fails to be conducted into the ventricles, the result is a 2:1 atrioventricular response. In **B**, the sinus node is discharging at a relatively slow rate. After the second sinus beat, an atrioventricular

Consequently, since the ventricles respond to the premature atrioventricular nodal extrasystole while the atria are activated by the sinus impulse, there results dissociation of the atria and ventricles for this one cycle. Atrioventricular interference occurring repeatedly between sinus impulse and impulses arising either in the atrioventricular node or in a lower center is called *atrioventricular dissociation*.

impulse and an atrioventricular nodal impulse are fired off almost synchronously, each impulse travels toward the other and leaves in its wake refractory muscle. When eventually the two impulses meet somewhere in the atrioventricular junctional tissues, their further spread is prevented by the refractory tissues ahead, so that each in effect cancels out or interferes with further propagation of the other. In this instance, atrioventricular interference results in the atria and ventricles responding independently to two separate pacemakers for a period of one cycle. If interference takes place repeatedly between successive sinus and nodal impulses, the two pacemakers continue to discharge independently and the atrial and ventricular rhythms become dissociated. This phenomenon is known as *atrioventricular dissociation*.

Sometimes it happens that the sinus and nodal impulses meet in the atria rather than in the junctional tissues (Fig 233). Before obliterating each other, each impulse activates a portion of the atrial myocardium and therefore contributes to the configuration of the resulting atrial beat. A P wave having a configuration intermediate between that of a sinus P wave and a retrograde P wave (an inverted P wave in leads II, III, and aVF which is produced by retrograde activation of the atria by an atrioventricular nodal or ventricular impulse) and appearing at about the expected time of onset of the next sinus beat is known as an *atrial fusion beat*, or a *fusion P wave*. Its configuration reflects the relative proportions of the atrial musculature activated by the sinus impulse

and by the nodal impulse. An atrial fusion beat is a manifestation of atrial interference. In a similar manner, ventricular fusion beats have a configuration intermediate between that of a conducted sinus beat and an ectopic ventricular beat and are produced by fusion of a supraventricular impulse and an impulse arising in an idioventricular focus. A ventricular deflection of this type is indicative of the occurrence of ventricular interference. Sinoatrial interference is perhaps observed most commonly with atrioventricular nodal beats. Thus, a premature nodal impulse may activate the atria and produce a retrograde P wave, but the next sinus P wave appears at the usual time, just as if the nodal beat had not occurred. From this it can be inferred that the nodal and sinus impulses interfered with each other at or near the sinoatrial junction, since the sinus impulse did not reach the atrial myocardium and the ectopic impulse failed to discharge prematurely the sinoatrial node and to interrupt its rhythm.

Atrioventricular Block

Atrioventricular interference and dissociation (Fig 234, A) are not to be confused with *atrioventricular block*, which is a manifestation of increased refractoriness of the junctional tissues. When an atrial impulse which is expected to pass through the atrioventricular node fails to do so, it can be assumed, usually correctly, that the refractory period of the node is prolonged and that atrioventricular block is therefore

present. In its various forms, atrioventricular block may occur as the single or most significant abnormality in the electrocardiogram, or it may appear as a complication of secondary importance during arrhythmias, owing to disturbed impulse formation.

In terms of severity or degree, atrioventricular block may be divided into the following types: incomplete atrioventricular block, of first and second degree, and complete (third-degree) atrioventricular block.

INCOMPLETE ATRIOVENTRICULAR BLOCK. First-degree block—In this type of atrioventricular block, each atrial impulse is conducted to the ventricles at a slower rate than normal. The P-R intervals of the

atrioventricular conduction of the atrial beats may be blocked at regular intervals, so that, for example, every sixth P wave fails to be followed by a QRS complex. On the other hand, blocking may occur irregularly, without a fixed pattern.

In the common type with the Wenckebach phenomenon, there is progressive lengthening of the P-R intervals of successive conducted beats until finally one is blocked completely in the atrioventricular node (Fig. 234, C). After this pause, the next atrial beat, which is conducted with a shorter P-R interval than subsequent beats, initiates another cycle of lengthening P-R intervals. Atrioventricular block showing the Wenckebach phenomenon is the common form of second-degree block and is due to progressively less complete recovery of the depressed junctional tissues after each conducted beat. Eventually an atrial impulse arrives during the absolute refractory phase, and its failure to be conducted permits the atrioventricular node to recover more completely before the next impulse appears.

the uncommon type and the common type with the Wenckebach phenomenon

In the uncommon type, the P-R intervals of the conducted beats remain constant (Fig. 234, B), also,

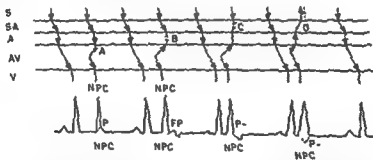


Fig. 233.—The various levels at which interference may occur between sinus and retrograde atrioventricular nodal impulses. (Symbols: S, impulses discharged by the sinoatrial node; SA, sinuatrial junction or conduction; A, atrial beats or P waves; AV, atrioventricular junction or conduction; V, ventricular beats or R waves; NPC, atrioventricular nodal premature contraction or extrasystole; FP, atrial fusion P wave; and P-, retrograde P wave produced by retrograde activation of the atria by an ectopic atrioventricular nodal impulse.) The levels at which interference takes place are as follows:

A, atrioventricular interference. The sinus and nodal impulses meet and obliterate each other in the atrioventricular junctional tissues (first NPC on the left).

B, atrial interference. When interference occurs in the atria between a sinus impulse and a retrograde atrioventricular nodal or ventricular impulse, an atrial fusion beat (FP) results, since the atria are activated in part by each impulse (second NPC, followed by a diphasic P wave).

C, sinuatrial interference. In this instance, the site at which interference takes place between the sinus and retro-

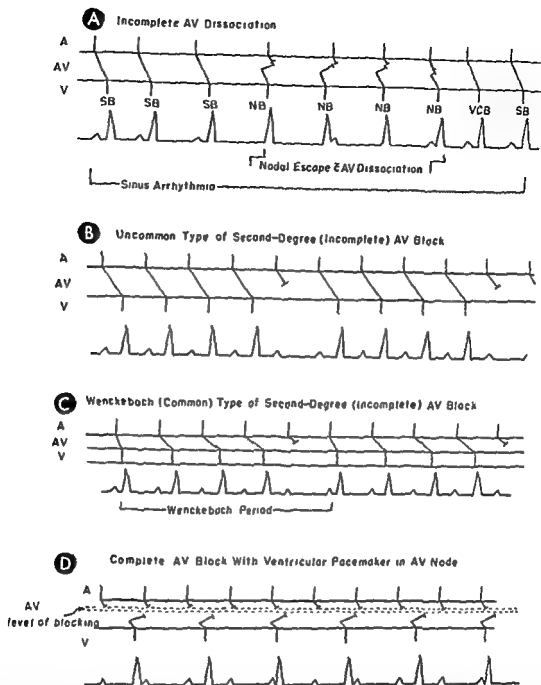


Fig. 234.—Mechanisms of atrioventricular nodal escape with atrioventricular dissociation and of incomplete and complete atrioventricular block. In **A**, sinus arrhythmia with marked variation in the sinus cycle length is demonstrated, the sinus beats being designated SB. At one point, the sinus pacemaker slows to such an extent that the atrioventricular node is able to escape for four cycles of the ventricular rhythm, the nodal beat being labeled NB. Atrioventricular interference occurs between the retrograde atrioventricular nodal impulses and the descending sinus impulses, and so the atrial P waves during this period are of sinus origin. The second to the last ventricular deflection is a ventricular capture beat (VCB). Such a beat occurs in atrioventricular dissociation whenever a sinus impulse is able to discharge prematurely the atrioventricular node and to be conducted into the ventricle to elicit a ventricular beat. In **B**, in contrast to atrioventricular interference, atrioventricular block entails an abnormal prolongation of the refractory period of the atrioventricular junctional tissues. There is prolonged atrioventricular conduction of the conducted sinus beats (first-degree atrioventricular block), while every fifth sinus beat fails completely to emerge from the atrioventricular junctional tissues into the ventricle. This diagram represents a rather uncommon type of second-degree or incomplete atrioventricular block. In **C**, the more frequently observed Wenckebach type of incomplete atrioventricular block is demonstrated. The lengths of the R-R cycles progressively shorten until the pause due to complete blocking of a sinus beat occurs, constituting a Wenckebach period. Characteristically in this type of block, the P-R interval of the first conducted beat following the pause is shorter than that of any subsequent beats. Also, there is a progressive increase in the

node (Fig. 234, D). The ventricular rhythm is produced by a pacemaker located below the site of the block. The atria and ventricles therefore beat independently, the former usually at a more rapid rate.

(See Chapter 27 for more detailed discussion of atrioventricular block.)

The varieties of atrioventricular block just described with reference to antegrade atrioventricular conduction may also involve retrograde atrioventricular conduction. Discussion of retrograde atrioventricular block will be deferred until later (Chapter 26). Most disturbances of sinoatrial conduction are, for all intents and purposes, impossible to recognize, with the exception of incomplete (second-degree) sinoatrial block, and even this may be difficult to diagnose

ramifies in the atrioventricular conducting tissues and upper portion of the bundle of His. The cardiac effects of vagal stimulation and increased vagal tone, which are dealt with later in more detail (see Chapter 28 for action of digitalis) include depression both of sinus and atrioventricular node rhythmicity and of sinoatrial and atrioventricular conductivity and prolongation of the refractory period of the junctional tissues

Classification of Disturbances of Impulse Formation

The authors of text utilize the following classification of disturbances of impulse formation.

- A Sinus bradycardia
- B Sinus tachycardia

2 Sinus arrhythmia

- C Escape beats and rhythms arising outside the sinus node because of depressed formation or blocked conduction of impulses originating in a higher pacemaker (as in sinus bradycardia, wandering supraventricular pacemaker, atrial extrasystoles, sinoatrial block, and atrioventricular block):

- 1 Atrioventricular nodal escape beats
- 2 Persistent atrioventricular nodal rhythms with complete capture of the atria
- 3 Transient atrioventricular nodal rhythms with intermittent atrial interference or incomplete capture of the atria
- 4 Atrioventricular nodal rhythms with atrioventricular dissociation (without atrial capture)
- 5 Ventricular escape beats
- 6 Idioventricular rhythm

D 1

- 1 Coupled ectopic beats (premature beats or extrasystoles) originating in an ectopic atrial, nodal, or ventricular focus and requiring a trigger impulse
- 2 Automatic ectopic beats and rhythms arising in a protected center capable of automatic, independent impulse formation (parasytote)
- 3 Paroxysmal ectopic tachycardia of supraventricular (atrial or nodal) or ventricular origin
- 4 Flutter and fibrillation of the atria or ventricles

Autonomic Nervous Tone

Impulse formation and conduction in the normal heart are affected by a variety of stimulating and depressing influences which are transmitted to the cardiac tissues by the autonomic nervous system and by the circulating blood. The hormones, mineral ions, and other constituents of the blood bear such a complicated and poorly defined relationship to the cardiac arrhythmias that, for the most part, they will not be considered in this review.

As will become evident, the fact that the vagus and sympathetic nerves maintain the sinoatrial and atrioventricular junctional tissues under a constant state of nervous tone is of fundamental importance in the genesis of many cardiac arrhythmias. The balance between sympathetic stimulation and vagal depression tends to fluctuate more or less continuously as nervous impulses, originating elsewhere in the body, augment or antagonize sympathetic or vagal

or decrease in vagal tone

The right vagus is distributed mainly to the sinoatrial node and junctional tissues, while the left vagus

length of the P-R interval of each conducted beat, but the maximal increment in the P-R interval occurs between the first and second conducted beats after the pause, while the increment in the P-R interval becomes shorter and shorter with each subsequent beat. The Wenckebach period then terminates with complete blocking of one sinus beat. As shown in D, in complete atrioventricular block none of the atrial beats are conducted into the ventricles. Consequently, the ventricular rhythm is produced by a secondary pacemaking center below the level of the atrioventricular block. The ventricular pacemaker is depicted as if situated low in the atrioventricular junctional tissues. Although the atria and ventricles may beat independently in complete atrioventricular dissociation as well as in complete atrioventricular block, the two mechanisms can usually be differentiated by the relative rates of the atrial and ventricular rhythms. Thus, in complete atrioventricular block, the atrial rhythm is more rapid than the ventricular, while the converse generally holds true in the case of complete atrioventricular dissociation.

NORMAL SINUS (SINOATRIAL) RHYTHM

Any cardiac rhythm arising in the sinoatrial node is a sinus rhythm, but a normal sinus, or sinoatrial, rhythm is differentiated from other rhythms, including variant types of sinus rhythm, by one or more of the following characteristics.

1. Each ventricular complex is preceded by a P wave which is upright in leads I and II and inverted in lead aVR.
2. The P-R interval of a conducted sinus beat is 0.12

second or longer.

3. The P and QRS deflections appear at a rate of 60–100 per minute (corresponding to a cycle length of 1.00–0.60 second) in adults.
4. The sinus rhythm may be slightly irregular, but the longest and shortest P-P cycles (or R-R cycles) differ by less than 0.12 second

Sinus rhythm failing to meet the latter two criteria are discussed below.

VARIANT TYPES OF SINUS RHYTHM

Sinus Tachycardia and Sinus Bradycardia

In adults, a sinus rhythm having a rate faster than 100 beats per minute is called *sinus tachycardia*. Although heart rates as fast as 230 beats per minute may be seen in children with sinus tachycardia, adults seldom exhibit rates of over 150 beats per minute. The few exceptions (i.e., sinus tachycardias with rates approaching 180 beats per minute) may be mistakenly diagnosed as paroxysmal atrial tachycardias, but the tachycardia can usually be identified as one of sinus node origin by the following characteristics.

1. The P-P intervals of a sinus tachycardia tend to vary in length, particularly when there are spontaneous or induced fluctuations in sympathetic and/or vagal tone, but the P-P cycles in paroxysmal atrial tachycardia remain strikingly constant
2. The P waves during sinus tachycardia generally resemble those present during slower sinus rhythm, although there may be some increase in their amplitude, for reasons previously cited in the discussion of exercise tachycardia (see Chapter 22). If identifiable, the P waves during paroxysmal atrial tachycardia often differ from the sinus P waves in configuration, but sometimes the difference may be too equivocal to use as a point of distinction.

A sinus rhythm with a rate less than 60 (but usually above 45) beats per minute is designated *sinus bradycardia*, the necessary assumption being that the atrial rate faithfully indicates the rate of sinus node discharge. Occasionally, slow sinus rhythms diagnosed as sinus bradycardia may actually be the result of 2:1 sinoatrial block. The correct identification of the mechanism is possible only if the onset and offset of the slow rhythm are observed to occur as an abrupt halving or doubling, respectively, of the atrial rate. On the other hand, slight irregularity of the slow rhythm favors the diagnosis of sinus bradycardia.

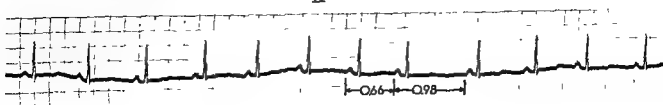
Sinus bradycardia is probably due to a high degree of vagal tone, which is thought to displace the cardiac pacemaker to the tail of the sinoatrial node. Any influence tending to reduce vagotonia, such as exercise, excitement, and atropine, speeds up the atrial rate. Sinus bradycardia is observed in many young adults, particularly in athletes, but is perhaps more commonly seen in older persons with arteriosclerosis.

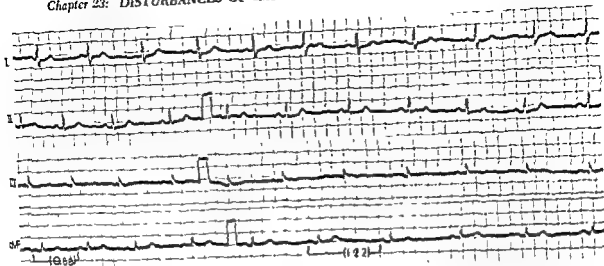
Sinus Arrhythmia

Normal sinus rhythm is ordinarily slightly irregular because of minor physiologic fluctuations in vagal tone. When this irregularity is such that the longest

Fig. 235.—Sinus arrhythmia in a 10-year-old child with rheumatic fever. The diagnosis of sinus arrhythmia can be made in lead II because the difference between the longest and the shortest P-P cycle exceeds 0.12 second. Note that, despite the changing sinus cycle length, the configuration of the P waves does not change, nor do the P-R intervals vary

II





rhythm and has no pathological significance.

and shortest P-P or R-R intervals differ by 0.12 second or more, sinus arrhythmia is said to be present (Figs 235 and 236), it may appear in two forms.

Phasic sinus arrhythmia—This form of arrhythmia is characterized by an alternate hastening and slowing of the heart rate which coincides with inspiration and expiration. The cyclic stimulation and depression of sinoatrial node rhythmicity are caused by fluctuations in vagal tone as reflex mechanisms in the lungs and blood vessels are activated during expiration and subside with inspiration. Presumably, vagal stimulation suppresses the head of the sinoatrial node so that the pacemaker next in order of rhythmicity (usually the tail of the sinus node) "escapes" and produces a slower rhythm. Subsequent lessening of vagal tone permits the higher center to take over once again.

Nonphasic sinus arrhythmia—In this rhythm, the periodic acceleration and deceleration of the heart is not related to the respiratory cycle. However, this type of sinus arrhythmia may sometimes be converted into the phasic form by forced deep breathing.

The P waves in sinus arrhythmia may become taller, and the P-R intervals slightly shorter, as the heart rate accelerates, while lower P waves and somewhat longer P-R intervals may accompany slowing of the heart. P-R intervals of less than 0.12-second duration and inverted P waves in leads II, III, and aVF, which characterize beats originating in the atrioventricular node, are not observed in sinus arrhythmia, as strictly defined, since migration of the pacemaker is limited to the confines of the sinoatrial node. When, as often happens, atrioventricular nodal

beats accompany an otherwise typical sinus arrhythmia, the diagnosis of wandering supraventricular pacemaker (see p. 373) is made (Fig. 237, A and B).

Phasic sinus arrhythmia is noted commonly in normal persons, particularly in children, adolescents, and some elderly adults. In contrast, nonphasic sinus arrhythmia is relatively uncommon and tends to occur mainly in older persons with, and sometimes without, heart disease. Occasionally the arrhythmia may be produced or accentuated by digitalis or other agents which increase parasympathetic nervous tone. However, neither form of sinus arrhythmia can be correlated with the presence or absence of cardiac disease.

"Coronary Nodal Rhythm"

Katz and Pick have applied the term "coronary nodal rhythm" to the electrocardiographic findings of a P-R interval of 0.02-0.10 second and upright P waves in leads I and II (in the absence of QRS changes indicating ventricular pre-excitation). Like Scherf, we do not believe that these findings reflect origin of the rhythm in the region of the coronary sinus but consider the rhythm to be sinoatrial, with the short P-R interval merely representing a normal variation. When the cardiac pacemaker lies in the region of the coronary sinus, the characteristic electrocardiographic findings consist of inverted P waves in leads II, III, and aVF, upright P waves in lead aVR, and a P-R interval longer than 0.12 second. (See p. 366)

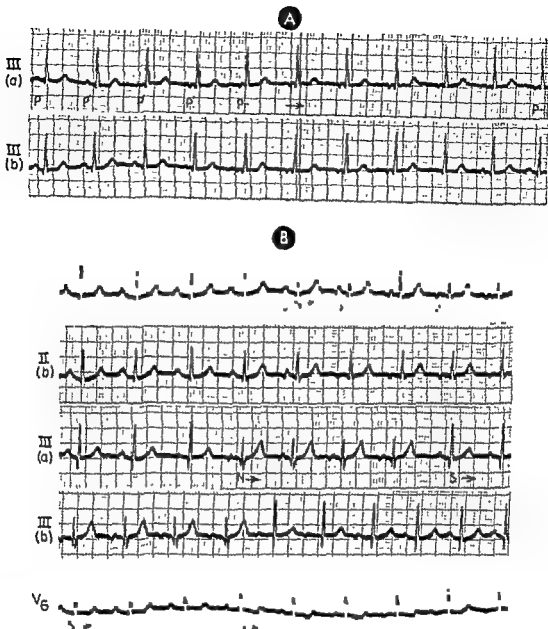


Fig. 237.—Two examples of wandering supraventricular pacemaker. In A, two interrupted strips of lead III are shown. Note that the first and second P waves in the top strip, lead III (a), are upright, although differing in appearance, while the third P wave is virtually isoelectric. The first P wave is a sinus beat (P), and the second to fourth P waves are atrial fusion beats (P'). The ventricular complexes after the first QRS deflection are of atrioventricular nodal origin. Subsequently, the mechanism of the rhythm is atrioventricular nodal with a retrograde P wave (P-) pre-

quent beats in this strip are of atrioventricular nodal origin, but there is atrioventricular nodal rhythm, and indicative of first-degree atrioventricular block, as is also suggested by the prolonged P-R intervals of the sinus beats elsewhere in the lead strips. The remaining leads demonstrate features already described, where the symbol S signifies sinus beats

with on-
last two
ts, those
all subse-

Atrioventricular Nodal and Idioventricular Escape Beats and Rhythms

ESCAPE BEATS or rhythms appear when impulse formation in a higher center is suppressed or when conduction of the impulses through the heart is blocked. Thus, prolonged sinus node inhibition or sinoatrial or

atrioventricular block frequently leads to the appearance of escape beats and rhythms arising in the atrioventricular node and, less frequently, in the ventricles.

THE ECG FEATURES OF ATRIOVENTRICULAR NODAL BEATS

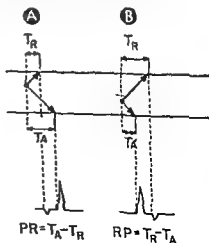
Whether atrioventricular nodal beats appear as escape beats or as premature ectopic beats, their electrocardiographic features (other than their effect on the cardiac rhythm and time of onset in the cardiac cycle) are essentially the same and can be summarized as follows:

1 An excitation impulse discharged by the atrioventricular node is distributed to the ventricles over the usual conducting pathways and therefore produces a QRS deflection resembling the QRS deflections present during sinus rhythm. Occasionally the

nodal beat may exhibit slight to moderate alterations in QRS configuration and duration (ventricular aberration), as will be described later in this chapter.

2 P waves may precede, follow, or coincide with the ventricular deflections of nodal beats. They result from retrograde atrioventricular conduction of the nodal impulses into the atria, which are then depolarized in a direction the reverse of that in sinus rhythm. Thus the frontal plane mean P vector, which is oriented approximately along the $+60^\circ$ axis in normal sinus rhythm, is rotated vertically upward

Fig. 238.—In A, the site of impulse formation is located relatively high in the atrioventricular node, and for this reason, forward conduction (T_A) of the nodal impulse into the ventricles takes a longer period of time than retrograde conduction (T_R) into the atria. Therefore, the retrograde P wave precedes the nodal ventricular beat by a P-R interval



duction minus the time required for forward or antegrade conduction of the nodal impulse

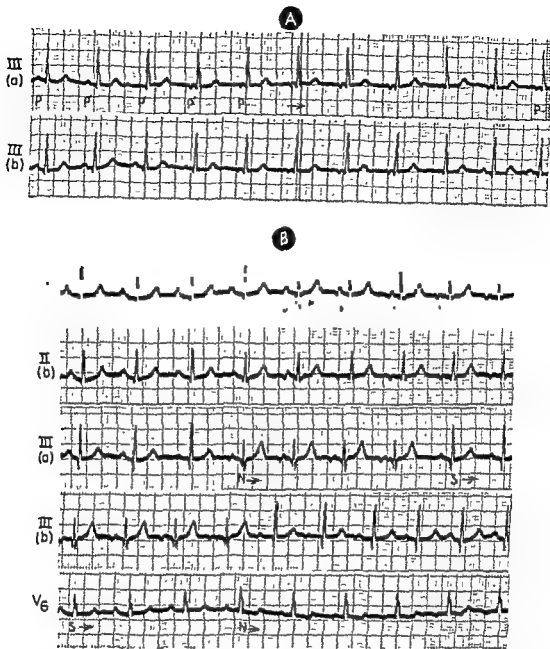


Fig. 237.—Two examples of wandering supraventricular pacemaker. In **A**, two interrupted strips of lead III are shown. Note that the first and second P waves in the top strip, lead III (a), are upright, although differing in appearance, while the third P wave is virtually isoelectric. The first P wave is a sinus beat (P), and the second to fourth P waves are atrial fusion beats (P'). The ventricular complexes after the first QRS deflection are of atrioventricular nodal origin. Subsequently, the mechanism of the rhythm is atrioventricular nodal with a retrograde P wave (P-) preceding each atrioventricular nodal ventricular beat. In lead strip III (b), sinus rhythm is present at first, then, with onset of atrioventricular nodal rhythm, atrial fusion P waves appear, followed by retrograde P waves. The last two complexes in the lower strip are of sinus node origin. In **B**, as in **A**, the P waves labeled P' are atrial fusion beats, those labeled P- are retrograde P waves. In lead strip II (a), the first nodal ventricular beat is indicated by N, and all subsequent beats in this strip are of atrioventricular nodal origin. In lead strip III (b), sinus rhythm is present at first, then, with onset of atrioventricular nodal rhythm, and also the relatively prolonged P-R interval of the nodal beat. The latter finding is indicative of first-degree atrioventricular block, as is also suggested by the prolonged P-R intervals of the sinus beats elsewhere in the lead strips. The remaining leads demonstrate features already described, where the symbol S signifies sinus beats.

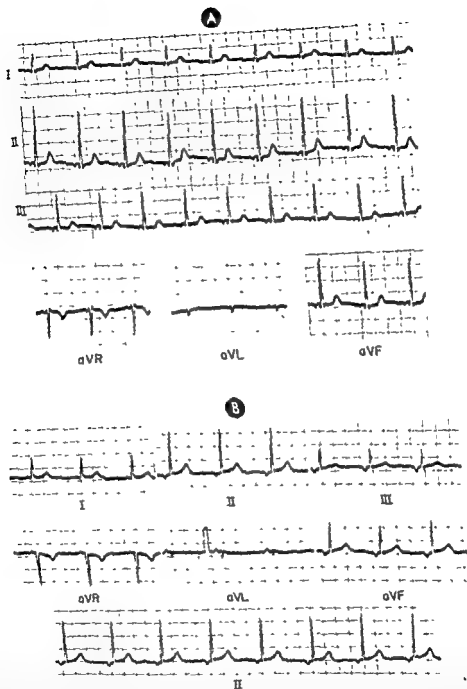
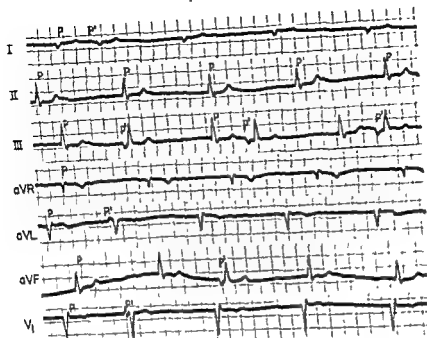


Fig. 240—A and B, electrocardiograms obtained from different persons but both demonstrating the typical features of an upper atrioventricular nodal rhythm—namely, inverted retrograde P waves in leads II, III, and aVF and upright P waves in lead aVR which precede the ventricular complexes by a very short P-R interval. The ventricular rate in A is 60 beats per minute



impulse conduction through the atrioventricular node is the same in both antegrade and retrograde directions. However, this is not always the case. As a generalization, it may be said that impaired retrograde conduction of a nodal impulse tends to shift the P wave behind the QRS complex, while disturbed antegrade conduction tends to shift the QRS complex behind the P wave (Fig. 239, B). Thus, an apparent lower nodal beat may actually be the result of prolonged retrograde conduction of an upper nodal im-

pulse. Conversely, the appearance of an upper nodal beat may be simulated by prolonged antegrade conduction of a lower nodal impulse. In summary, the P-QRS relationship in atrioventricular nodal beats is determined by two factors: (a) the site of impulse origin within the atrioventricular junctional tissues, and (b) the speed with which the atrioventricular tissues conduct the nodal impulse in a retrograde direction, as compared to the rate of conduction in an antegrade direction (Figs. 242 and 243).

ATRIOVENTRICULAR NODAL ESCAPE

It will be recalled that, normally, the sinus pacemaker keeps the atrioventricular node in a state of suppression, owing to the fact that each successive sinus impulse discharges the node prematurely—that

is, before the immature impulse forming there can be fired off spontaneously. Since the rhythmicity of the atrioventricular node or of any pacemaker is depressed by premature discharge, which in turn favors con-

coronary sinus beat appears relatively sooner, and the QRS complex much later, after discharge of the excitation impulse, than is the case with upper nodal beats. The major distinction between the two is that coronary sinus beats have P-R intervals longer than 0.12 second; and nodal beats, P-R intervals of 0.12 second or shorter. However, this point of differentiation is far from absolute, since upper atrioventricular nodal beats with prolonged forward conduction also exhibit P-R intervals in excess of 0.12 second. In any case, coronary sinus and upper atrioventricular nodal rhythms probably have the same clinical significance.

Middle atrioventricular nodal beats—Antegrade and retrograde conduction of a nodal impulse requires essentially the same amount of time, and so activation commences simultaneously in atrial and ventricular myocardium. Consequently, the characteristic feature of a middle nodal beat is that its

retrograde P wave is buried in the larger QRS complex and usually is not discernible.

Lower atrioventricular nodal beats.—In the case of an impulse arising lower in the atrioventricular node, the antegrade atrioventricular pathway is shorter than the retrograde pathway, and so ventricular excitation precedes that of the atrial myocardium. Ordinarily, the ventricular complex of a lower nodal beat is inscribed 0.10–0.20 second earlier than the retrograde P wave, provided there is no delay in retrograde conduction.

Inasmuch as atrioventricular nodal impulses pass toward the atria and ventricles simultaneously rather than sequentially, the P-R or R-P interval of a

that classification of atrioventricular nodal beats in the manner just described is valid only if the rate of

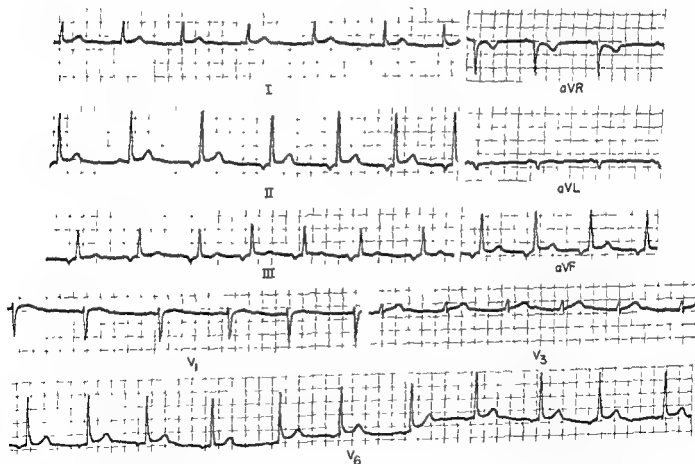


Fig. 241.—Electrocardiogram displaying a typical upper atrioventricular nodal rhythm in which the nodal pacemaker drives both the atria and the ventricles. The inverted retrograde P waves in leads II, III, and aVF and the upright P waves in lead aVR precede the ventricular complexes by a P-R interval of 0.13–0.14 second. This is slightly longer than the P-R interval usually observed in upper atrioventricular nodal rhythms. As an alternative interpretation, the electrocardiographic findings could, with equal validity, represent a coronary sinus rhythm. Note, in lead II, that there is definite arrhythmia of the atrioventricular nodal pacemaker and that one conducted sinus beat appears during the time when the atrioventricular nodal cycle length has lengthened.

relationships usually hold true in the electrocardiogram:

1 The interval between the last sinus beat and the nodal escape beat exceeds the basic cycle length of the sinus pacemaker (the average P-P interval) and corresponds to the cycle length of the nodal pacemaker.

2. In a given lead, the intervals preceding each of several nodal escape beats are essentially equal in length. This presupposes a constant rate of impulse formation in the atrioventricular node, which is usually the case. Some variation in the

atrial nodal arrhythmia, the nodal counterpart of sinus arrhythmia.

3. Ordinarily, the nodal escape beat fails to reach the atria and is not accompanied by a retrograde P wave. The reason for this is that in nodal escape the rates of the sinus and nodal pacemakers are usually so nearly the same that their impulses meet and cancel out each other in the atrioventricular junctional tissues (atrioventricular interference). The nodal beat either obscures a superimposed sinus P wave or is preceded by a nonconducted beat.

ATRIOVENTRICULAR NODAL ESCAPE RHYTHMS

When an atrioventricular nodal pacemaker escapes from the sinus node, it promptly takes over the ventricular rhythm. However, in the atria the outcome is more variable, in that the node may capture the atria completely, incompletely, or not at all. Since the

course of events in the atria following nodal escape may show this variation, the electrocardiographic features presented by nodal rhythms may also differ. This practical point of distinction makes it possible to arrange nodal rhythms into three overlapping cate-

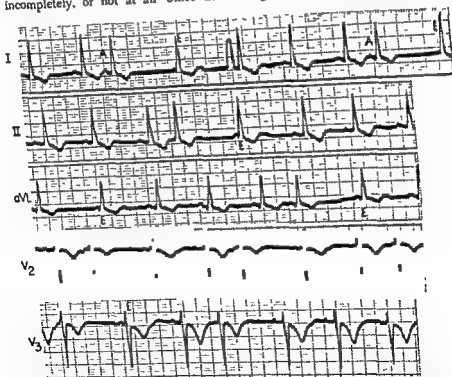


Fig 244—Lead strips showing frequent atrial premature beats (A) which are followed by atrioventricular nodal escape beats (E). The intervals between onset of the premature ventricular deflections and onset of the atrioventricular nodal escape beats are equal throughout. The P wave slightly preceding each nodal escape beat is of sinus node origin, and so atrioventricular interference has occurred in each instance. The atrial premature beats temporarily suppress the rhythmicity of the sinus node so that the atrioventricular node is permitted to escape at its own inherent rhythmicity for one beat. Note that the nodal escape beat has essentially the same configuration as QRS complexes of sinus node origin elsewhere in the same lead strip.

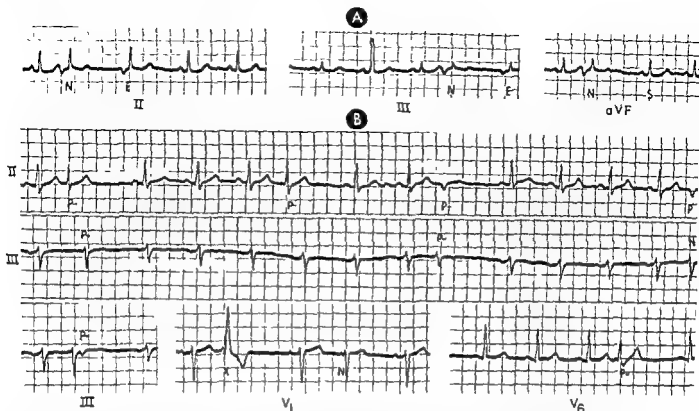


Fig. 243.—Electrocardiographic lead strips showing premature atrioventricular nodal beats of various types. In the lead strips of leads II, III, and aVF in A, the nodal extrasystoles (N) are preceded by inverted P waves, indicating, in all probability, an upper atrioventricular nodal origin of the premature beat. In leads II and III, the first beat following the premature extrasystole is a nodal escape beat (E) which is preceded by a retrograde P wave. This is somewhat unusual, in that nodal escape beats ordinarily appear at about the same time as the nonconducted sinus P waves, so that retrograde spread of the nodal impulse into the atria cannot occur. The symbol S denotes a conducted sinus beat. Leads II, III, V₁, and V₆ in B were all obtained from the same patient, and all contain premature supraventricular extrasystoles. The first two premature beats in lead II and the premature beats in the long strip of lead III show what appear to be terminal S waves but represent, in reality, fusion of S waves with retrograde inverted P waves (P-). Later in lead II, inverted P waves of atrioventricular nodal origin can be seen, and these are not accompanied by ventricular beats because of retrograde block of the nodal impulses. In lead III in the lower left corner, a typical lower atrioventricular nodal extrasystole is seen, the retrograde P wave following the nodal ventricular beat by an R-P interval of 0.14 second. In the adjacent strip of lead V₁, the extrasystole (X) is probably of ventricular origin. Shortly after, there appears an atrioventricular nodal extrasystole with a markedly prolonged coupling interval, preceded by a sinus P wave. In this instance, interference between the atrioventricular nodal impulse and the sinus impulse probably occurs in the atrioventricular junctional tissues.

tinued predominance of the sinus node, the suppressing effect of the latter is, in a sense, self-perpetuating. However, if it should so happen that a sinus impulse fails to reach the atrioventricular node in time to interrupt impulse formation, the nodal pacemaker discharges spontaneously and a nodal escape beat appears. Some of the circumstances in which nodal escape beats may be encountered are listed below:

1. One or more atrioventricular nodal escape beats often terminate a prolonged period of sinus node arrest or pause. Frequently, premature discharge of the sinoatrial node by an ectopic atrial beat is followed by a prolonged interval of sinus node inhibition, dur-

ing which one or more nodal escape beats are written (Figs 244 and 245).

2. Escape beats or a transient nodal rhythm may appear during sinus arrhythmia if the rate of the sinus pacemaker momentarily falls below the inherent rate of impulse formation in the atrioventricular node. This leads to the appearance of a rhythm called *wandering pacemaker* (Fig. 237).

3. Nodal rhythms often emerge during prolonged periods of blocked impulse conduction at the sinoatrial or atrioventricular junction. When the block is of relatively short duration, one or more nodal escape beats may appear before conduction is restored.

When nodal escape beats occur because of delayed arrival of a sinus impulse, the following rela-

Fig 24.5—This electrocardiogram like that in Figure 24.4, displays frequent atrial premature beats (A) followed by escape beats of atrioventricular nodal origin (E). Unlike the escape beats in Figure 24.4, those shown here differ in configuration from the conducted sinus beats, and in leads V_1 and V_2 give rise to a brief period of atrioventricular nodal escape rhythm. That the escape beats originate in the atrioventricular node is supported by the fact that the QRS interval in nodal escape beats is less than 0.12 second. One confining feature in this above electrocardiogram is the presence in lead I of what appears to be a ventricular fusion beat (FB), and the third beat from the end of lead V_2 is probably also a fusion beat. However, the presence in lead I of a ventricular fusion beat is generally considered indicative of an idioventricular origin of the ectopic beats. Nevertheless, the authors of this text have observed apparent ventricular fusion beats in other records in which the identity of atrioventricular nodal escape beats or atrioventricular nodal ectopic beats was unequivocally established.

groups. (1) persistent atrioventricular nodal rhythms with complete atrial capture, (2) transient or intermittent atrioventricular nodal rhythms with incomplete atrial capture, and (3) atrioventricular nodal rhythms without atrial capture (with atrioventricular dissociation).

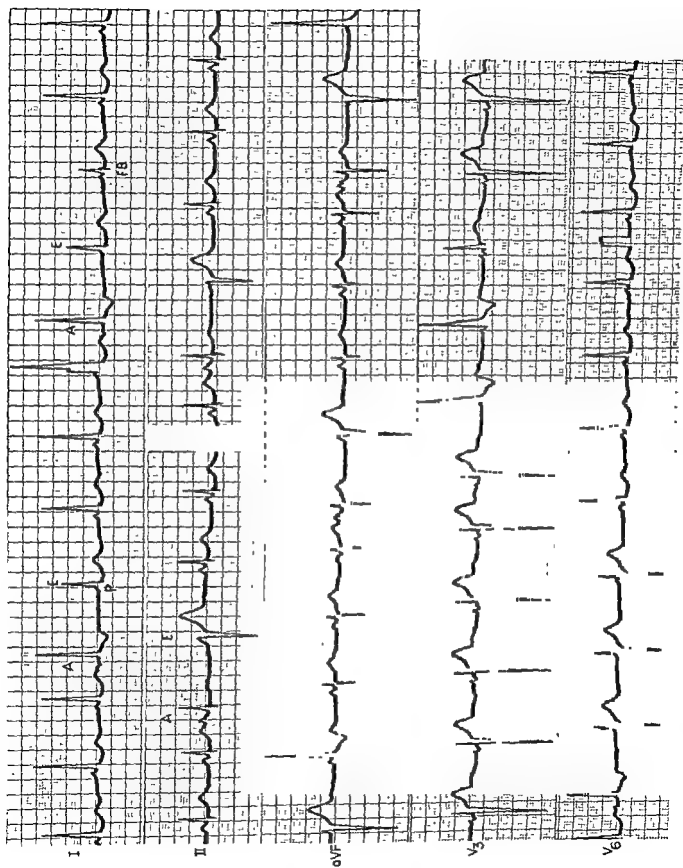
Persisting Atrioventricular Nodal Rhythm with Complete Atrial Capture

Nodal rhythms associated with complete sinoatrial block are included in this category, but their discussion will be deferred until later (Chapter 27), along with discussion of the associated conduction disturbances. With these exceptions, slow nodal rhythms which persist for long periods of time can generally be ascribed

to a primary nodal origin. In many cases, however, inhibition is secondary to marked vagotonia; but more frequently, perhaps, toxic agents, such as excess digitalis, quinidine, and potassium or inflammatory or degenerative processes, are culpable.

As previously explained, the electrocardiographic appearance of nodal beats depends on the site of the pacemaker in the junctional tissues and on the relative rates of retrograde and antegrade atrioventricular conduction. If the retrograde P wave precedes the ventricular deflection, the rhythm is said to be an upper atrioventricular nodal rhythm, if the P wave follows the QRS complex, a lower atrioventricular nodal rhythm is present, and, finally, nodal ventricular beats unaccompanied by retrograde P waves are indicative of a middle atrioventricular nodal rhythm. Because of its lower inherent rhythmicity, a nodal pacemaker generally drives the heart at a rate of 40–50 beats per minute, but, unlike the sinus node, it is relatively insensitive to variations in nervous tone. An atrioventricular nodal rhythm may remain quite regular despite exercise, carotid sinus stimulation, and similar maneuvers. On occasions, however, the rhythm may be accelerated and is analogous to the sinus tachycardia. If the heart rate is slow, and if the intervals, then the diagnosis of coronary sinus rhythm can be made.

When an atrioventricular nodal focus discharges at a rate of 100 beats per minute or more, the resulting rhythm is generally regarded as an ectopic (paroxysmal) atrioventricular nodal tachycardia. Presumably, the causative disturbance consists of increased excitability of the nodal focus itself, with or without concomitant sinus node inhibition. Opinions vary as to the proper classification of atrioventricular nodal



as progressive lengthening of the R-P intervals (Wenckebach phenomenon), reciprocal beats tend to follow the longest R-P interval of each sequence. Thus, a ventricular deflection with a normal or prolonged QRS interval (see discussion of ventricular aberration on page 381) which appears prematurely under these circumstances is likely to be a reciprocal beat.

4. The R-R interval of a reciprocal beat can be somewhat prolonged but does not ordinarily exceed the R-P interval. In fact, there seems to be an inverse relationship between the lengths of the R-P interval and the following P-R interval.

5. Generally, a reciprocal beat follows the preceding ventricular deflection by an interval of 0.50 second or less.

While it is theoretically possible for reciprocal beats to appear consecutively in the form of a reciprocal rhythm, the occurrence of such an arrhythmia in the human heart remains to be proved.

Atrioventricular Nodal Rhythms with Intermittent Atrial Interference (Wandering Supraventricular Pacemaker)

This disturbance is the equivalent of an exaggerated sinus arrhythmia in which vagal depression of the sinoatrial node becomes so marked that the sinus pacemaker fails to keep the atrioventricular node suppressed and the latter escapes for a short period. In keeping with the lower inherent rhythmicity of the atrioventricular node, compared to that of the sinus node, the nodal beats appear at the relatively slow rate of 40-50 per minute (corresponding to a cycle length of 1.5-2 seconds). As in sinus arrhythmia, the supraventricular pacemaker may wander or shift in phase with the respiratory cycle, or its movements are nonphasic. In either case, there is gradual slowing of the sinus rhythm until the upper atrioventricular node, the pacemaker next in descending order of rhythmicity, takes over. Occasionally the site of impulse formation may descend even lower in the atrioventricular node. Inasmuch as sinus node depression ordinarily is neither constant in degree nor persistent in duration in this arrhythmia, the nodal pacemaker remains active only for sporadic, brief periods. With the waning of vagal tone, impulse formation in the sinoatrial node gradually speeds up and in the process the sinus node regains its dominance over lower pacemakers. For the most part, the electrocardiographic features of wandering supraventricular pacemaker

have been described in previous paragraphs dealing with sinus arrhythmia and nodal escape rhythms and beats. Thus the discussion to follow will center on an additional finding not previously considered in detail, namely, atrial fusion beats.

ATRIAL FUSION BEATS

During the transition to and from atrioventricular nodal rhythm in wandering supraventricular pacemaker, one or more of the nodal beats frequently are preceded by an atrial fusion beat which appears at about the time the next sinus P wave is expected. The configuration of a fusion P wave is a compromise between that of a sinus P wave and of a retrograde P wave but may vary widely within these limits. Atrial fusion beats are produced in the following manner:

1. The nodal impulse passes in a retrograde direction and arrives in the atria at about the same time as the sinus impulse.

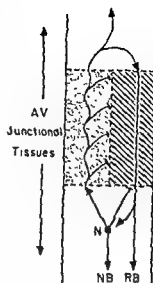
2. Thus two coexisting excitation processes are initiated in the atria. One wave of excitation spreads upward from the caudal part of the atria, and the other spreads downward from the sinus node.

3. If the two impulses happen to meet in the atria, as frequently is the case, there occurs a phenomenon known as *atrial interference*. By this is meant that each impulse cancels out the other because both have left refractory muscle in their wake. Thus, further spread of either impulse is prevented by the state of refractoriness ahead.

4. However, prior to their meeting, each impulse has activated a portion of the atrial myocardium. The magnitude of normally directed P wave potentials which are produced will depend on the amount of atrial muscle activated by the sinus impulse. Similarly, the more extensive the spread of retrograde excitation through the atria, the larger are the resulting retrograde P wave potentials. Variations in the relative times of onset of sinus and retrograde excitation may produce fusion P waves having a configuration intermediate between that of sinus and retrograde P waves or resembling closely one or the other. Thus, atrial fusion beats can be upright, low, diphasic, isoelectric, or inverted (Fig. 237).

As with sinus arrhythmia, the occurrence of wandering supraventricular pacemaker is usually secondary to marked vagotonia and is a common finding in normal subjects. It has no significance whatsoever in terms of the presence or absence of underlying cardiac disease.

Fig. 246.—Mechanism of reciprocal beats. According to Scherf, there is longitudinal dissociation of the atrioventricular conducting fibers; and so, theoretically, some of the fibers (diagonal lines) may be completely refractory and nonresponsive to retrograde spread of an atrioventricular nodal impulse originating at the nodal ectopic focus (N), while others (stippled) are only partially refractory and conduct the retrograde nodal impulse at a slower rate than normal. So slowly is the nodal impulse conducted by the partially refractory atrioventricular fibers that by the time the retrograde impulse reaches the atria, the previously refractory fibers of the atrioventricular conducting pathway have recovered. Consequently, as the nodal impulse enters the atria to activate them in a retrograde direction, it also turns backward and proceeds down the atrioventricular node to traverse the previously refractory atrioventricular fibers in an antegrade direction. This course of events is reflected in the electrocardiogram by the appearance of a P wave sandwiched between two ventricular complexes. The first P wave is induced by the original nodal impulse. The second P wave follows it by a period of time. This second P wave, produced by the re-entry impulse, is called a reciprocal beat (RB), the interval between onset of the initial nodal beat and onset of the reciprocal beat being 0.50 second or less.



rhythms with rates above 50, but less than 100, beats per minute. It has been suggested that these rhythms be considered the nodal counterpart of sinus tachycardia (nonparoxysmal nodal tachycardia) (Fig. 240).

RECIPROCAL BEATS IN ATRIOVENTRICULAR NODAL RHYTHM

In occasional atrioventricular nodal rhythms with initial excitation of the ventricles (and rarely in association with premature nodal or ventricular ectopic beats), a retrograde P wave may appear "sandwiched" between two closely spaced ventricular beats. The second of these is written prematurely with respect to the usual R-R interval of the prevailing nodal rhythm and is known as a reciprocal beat. The following explanation has been offered for the genesis of reciprocal beat (Fig. 246).

Above the site of impulse formation in the atrioventricular node there is a localized area of depression where some longitudinal fiber pathways are involved more severely than others. As a result, not only is there unidirectional blocking of retrograde impulse conduction in some fibers, but there is also delayed retrograde conduction throughout the entire area of refractoriness. As the nodal impulse producing the initial ventricular beat spreads through the ventricular myocardium, it also travels up the atrioventricular node in a retrograde direction and soon enters the area of depression. There the retrograde impulse is completely blocked in the severely depressed fibers but passes slowly up the remaining, less refractory, atrioventricular pathways. Because of this delay in retrograde conduction, the retrograde P wave follows the QRS complex of the nodal beat by a pro-

longed R-P interval (usually 0.20 second or longer). If the R-P interval is sufficiently prolonged, the longitudinal atrioventricular fibers, which were previously completely refractory to the retrograde nodal impulse, in the meantime recover their conductivity. In this event, the retrograde impulse splits before entering the atria, turns back, and passes down the atrioventricular node in an antegrade direction along the now responsive conducting fibers. The time required for retrograde conduction of the nodal impulse and subsequent forward conduction of the re-entry impulse is sometimes long enough to permit the ventricles to recover after their initial response to the nodal impulse. If such is the case, the re-entry impulse elicits a second ventricular response, or reciprocal beat (Fig. 249).

The electrocardiographic recognition of reciprocal beats encounters its chief obstacle in differentiating these beats from ventricular capture beats (or interference beats) which occur in nodal rhythms with atrioventricular dissociation. Both types of beats may appear in similar arrhythmias and, in fact, even in a single electrocardiogram, but ventricular capture beats are by far the more common finding. The points summarized below are useful in the identification of reciprocal beats.

- 1 The P wave preceding a reciprocal beat must have the configuration of a fusion P wave or, preferably, a retrograde P wave. Its contour must therefore differ from that of the sinus P wave.

- 2 Reciprocal beats are most likely to occur in nodal rhythms with delayed retrograde conduction, as shown by R-P intervals in excess of 0.20 second.

- 3 When the retrograde conduction delay occurs

as progressive lengthening of the R-P intervals (Wenckebach phenomenon), reciprocal beats tend to follow the longest R-P interval of each sequence. Thus, a ventricular deflection with a normal or prolonged QRS interval (see discussion of ventricular aberration on page 381) which appears prematurely under these circumstances is likely to be a reciprocal beat.

4. The P-R interval of a reciprocal beat can be somewhat prolonged but does not ordinarily exceed the R-P interval. In fact, there seems to be an inverse relationship between the lengths of the R-P interval and the following P-R interval.

5. Generally, a reciprocal beat follows the preceding ventricular deflection by an interval of 0.50 second or less.

While it is theoretically possible for reciprocal beats to appear consecutively in the form of a reciprocal rhythm, the occurrence of such an arrhythmia in the human heart remains to be proved.

Atrioventricular Nodal Rhythms with Intermittent Atrial Interference (Wandering Supraventricular Pacemaker)

This disturbance is the equivalent of an exaggerated sinus arrhythmia in which vagal depression of the sinoatrial node becomes so marked that the sinus pacemaker fails to keep the atrioventricular node suppressed and the latter escapes for a short period. In keeping with the lower inherent rhythmicity of the atrioventricular node, compared to that of the sinus node, the nodal beats appear at the relatively slow rate of 40-50 per minute (corresponding to a cycle length of 1.5-1.2 seconds). As in sinus arrhythmia, the supraventricular pacemaker may wander or shift in phase with the respiratory cycle, or its movements are nonphasic. In either case, there is gradual slowing of the sinus rhythm until the upper atrioventricular node, the pacemaker next in descending order of rhythmicity, takes over. Occasionally the site of impulse formation may descend even lower in the atrioventricular node. Inasmuch as sinus node depression is neither constant in degree nor persistent in duration in this arrhythmia, the nodal pacemaker remains active only for sporadic, brief periods. With the waning of vagal tone, impulse formation in the sinoatrial node gradually speeds up and in the process the sinus node regains its dominance over low rate pacemakers. For the most part, the electrocardiographic features of wandering supraventricular pacemaker

have been described in previous paragraphs dealing with sinus arrhythmia and nodal escape rhythms and beats. Thus the discussion to follow will center on an additional finding not previously considered in detail, namely, atrial fusion beats.

ATRIAL FUSION BEATS

During the transition to and from atrioventricular nodal rhythm in wandering supraventricular pacemaker, one or more of the nodal beats frequently are preceded by an atrial fusion beat which appears at about the time the next sinus P wave is expected. The configuration of a fusion P wave is a compromise between that of a sinus P wave and of a retrograde P wave but may vary widely within these limits. Atrial fusion beats are produced in the following manner.

1. The nodal impulse passes in a retrograde direction and arrives in the atria at about the same time as the sinus impulse.

2. Thus two coexisting excitation processes are initiated in the atria. One wave of excitation spreads upward from the caudal part of the atria, and the other spreads downward from the sinus node.

3. If the two impulses happen to meet in the atria, as frequently is the case, there occurs a phenomenon known as *atrial interference*. By this is meant that each impulse cancels out the other because both have left refractory muscle in their wake. Thus, further spread of either impulse is prevented by the state of refractoriness ahead.

4. However, prior to their meeting, each impulse has activated a portion of the atrial myocardium. The magnitude of normally directed P wave potentials which are produced will depend on the amount of atrial muscle activated by the sinus impulse. Similarly, the more extensive the spread of retrograde excitation through the atria, the larger are the resulting retrograde P wave potentials. Variations in the relative times of onset of sinus and retrograde excitation may produce fusion P waves having a configuration intermediate between that of sinus and retrograde P waves or resembling closely one or the other. Thus, atrial fusion beats can be upright, low, biphasic, isoelectric, or inverted (Fig. 237).

As with sinus arrhythmia, the occurrence of wandering supraventricular pacemaker is usually secondary to marked vagotonia and is a common finding in normal subjects. It has no significance whatsoever in terms of the presence or absence of underlying cardiac disease.

Atrioventricular Nodal Rhythms without Atrial Capture (with Atrioventricular Dissociation)

Nodal rhythms with atrioventricular dissociation differ from those previously described in that the nodal pacemaker produces only the ventricular rhythm, while the atria remain completely under the control of the sinoatrial node. Dissociation of the two pacemakers occurs within the atrioventricular junctional tissues at a level above the nodal center where one of two mechanisms prevents antegrade conduction of sinus impulses and retrograde conduction of nodal impulses. These mechanisms are atrioventricular interference and atrioventricular block.

Atrioventricular interference.—For atrioventricular interference to occur repeatedly, as it must in dissociation, the timing and rate of the two pacemakers must be such that each sinus impulse reaches the atrioventricular node in time for interference to occur between it and the retrograde nodal impulse.

Atrioventricular block.—The block may affect both antegrade and retrograde atrioventricular conduction, or it may be unidirectional and involve either. Dissociation of a faster nodal rhythm and a slower sinus

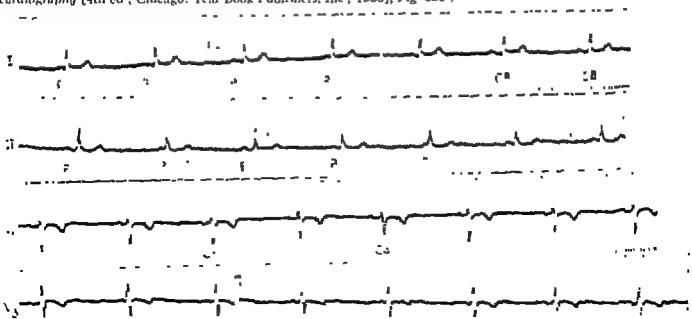
rhythm, the common form of persisting atrioventricular dissociation, is often accompanied by retrograde atrioventricular block.

Atrioventricular dissociation may be complete or incomplete. *Complete dissociation* is characterized by the fact that not a single sinus or nodal impulse passes completely through the atrioventricular node, the atrial and ventricular rhythms remaining absolutely independent of each other. *Incomplete dissociation* occurs when an occasional sinus impulse finds the atrioventricular node responsive and is conducted into the ventricles to produce a *ventricular capture beat*. By capturing the ventricles for one or more beats, the conducted impulse momentarily interrupts the nodal pacemaker. Rarely, incomplete dissociation is observed in which an occasional nodal impulse is conducted in a retrograde direction and captures the atria.

COMPLETE ATRIOVENTRICULAR DISSOCIATION

In the absence of atrioventricular block, physiologic interference alone may produce complete atrioventricular dissociation, provided the sinus and nodal

Fig. 247.—Atrioventricular dissociation. This electrocardiogram demonstrates the simplest, most common, and most benign form of atrioventricular dissociation. There is a slow sinoatrial rhythm with eventual atrioventricular nodal escape, the nodal pacemaker escaping at its inherent rate of impulse formation to produce a slow nodal rhythm in the ventricles. There are occasional ventricular capture beats (CB), occurring after slightly shorter R-R cycles than those of the atrioventricular nodal beats. In this record, the main clue to the presence of atrioventricular dissociation is the varying P-R relations. The preceding ventricular beats are conducted, indicating that there is no forward atrioventricular block, and (3) there is no evidence suggesting retrograde block. (From Lippman, H. S., and Massie, E. *Clinical Scalar Electrocardiography* [4th ed., Chicago: Year Book Publishers, Inc., 1959], Fig. 338.)



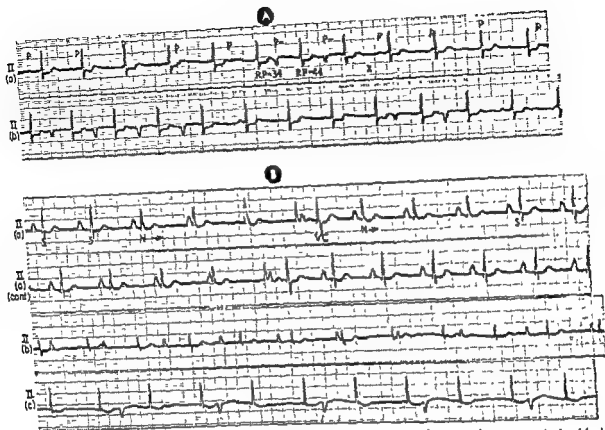


FIGURE 24-1. A, sinus rhythm with complete atrioventricular block followed by periods of transient atrioventricular dissociation. In B, the first two strips, continuous strips of lead II, show atrioventricular dissociation with ventricular capture beats (one of which is labeled VC) and short periods of sinus rhythm. Note the difference in the QRS configuration of the sinus beats (S) and of the atrioventricular nodal beats (N). In lead II (b) there is an atrioventricular nodal rhythm with complete atrioventricular dissociation and block, in lead II (c), atrioventricular nodal rhythm with 1:2 retrograde atrioventricular block.

pacemakers discharge at essentially the same rate. Rate equalization is accomplished by acceleration of the nodal pacemaker and/or slowing of the sinus node. Ordinarily, complete dissociation due to interference is an intermittent and transient phenomenon appearing during sinus bradycardia, sinus arrhythmia, or wandering pacemaker (Fig. 247). It is observed in a more persistent form in coexisting sinus and nodal tachycardia and more rarely in combined or double paroxysmal tachycardias.

Complete dissociation of a fast sinus rhythm and a slower nodal rhythm cannot be attributed solely to physiologic interference, which, as mentioned previ-

ously, requires equalization of the two pacemakers' rates. Antegrade atrioventricular block must therefore be implicated. Complete dissociation with antegrade atrioventricular block is described later in more detail, however, as a general rule, the degree of atrioventricular block required to produce dissociation increases as the difference in the rates of the sinus and nodal rhythms become greater.

INCOMPLETE ATRIOVENTRICULAR DISSOCIATION

Atrioventricular dissociation which tends to persist for a relatively long time commonly appears as incom-

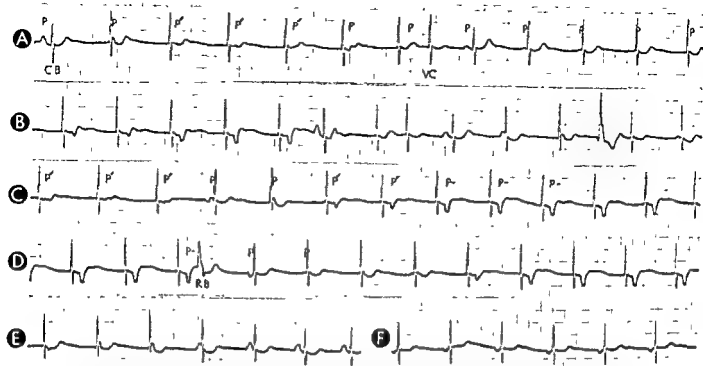


Fig. 249.—Atrioventricular nodal rhythm with alternating periods of atrioventricular dissociation and retrograde atrial activation with retrograde atrioventricular block. All lead strips are lead II. The ventricular complex (CB) is a conducted sinus beat; the ventricular deflection (VC) is a ventricular capture beat, and the QRS deflection (RB) is a reciprocal beat. P waves of sinus node origin are designated P, those of atrioventricular nodal origin, P_n, and those labeled P' are atrial fusion beats. Note that the configuration of the conducted sinus beat in A differs from that of atrioventricular nodal beats elsewhere in the same lead strip. In D, the retrograde P wave following the third nodal beat is followed in turn by a ventricular deflection showing aberration. The interval between the preceding nodal ventricular beat and the ventricular deflection following the retrograde P wave is 0.36 second, while the R-P interval of the nodal beat is 0.18 second. In lead strips B, C, and D, the alternating appearance of sinus and retrograde P waves suggests that retrograde atrioventricular block must be present at times. With the single exception of the relatively short R-P interval of the third nodal beat in D, all other features of the premature ventricular deflection (RB) are compatible with this beat being a reciprocal beat. In E, a mechanism is demonstrated which may tend either to perpetuate atrioventricular

ventricular nodal rhythm.

plete dissociation of a rapid nodal rhythm and a slower sinus rhythm. Incomplete dissociation may also occur intermittently, as will be indicated later in the discussion. Parenthetically, it should be pointed out that many texts apply the term *atrioventricular dissociation* only to the form of incomplete dissociation described above. However, in this text the term is used to designate a mechanism which occurs with various rhythms, although observed most frequently with nodal rhythm.

In incomplete dissociation of a faster nodal rhythm and slower sinus rhythm, the difference in the rates of the two pacemakers is usually due to an accelerated rate of impulse formation in the atrioventricular node, although slowing of the sinoatrial node may be a contributory factor. Thus, depending on the circumstances, incomplete dissociation may occur with nodal

rhythms whose rates range from 40 to 100 beats per minute, and sometimes even higher if paroxysmal nodal tachycardia is present. Since, in the electrocardiogram, the P-P intervals of the slower atrial rhythm are longer than the R-R intervals of the ventricular rhythm, successive P waves appear to march into and then emerge behind the QRS complexes. However, even though the relative positions of the sinus P waves and nodal R waves are constantly changing, the P-P intervals and R-R intervals may both be spaced off regularly.

The inability of the faster nodal center to take over the atrial rhythm is due to the fact that retrograde conduction of the nodal impulse is prevented either by physiologic atrioventricular interference or by retrograde atrioventricular block (Figs 248 and 249). Interference is the mechanism more likely to be in-

involved when the rates of the sinus node and nodal pacemaker do not differ greatly. If such proves to be the case, two additional factors may tend to favor the interference mechanism. (1) Retrograde atrioventricular conduction takes place less readily and more slowly than antegrade conduction. This fact may off-

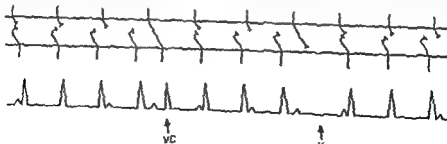
rapidly than the sinus impulses can arrive in the junctional tissues, most of the sinus impulses find the atrioventricular node refractory following excitation by a previous nodal beat. Nonetheless, because of the different timing of the two pacemakers, an occasional sinus impulse arrives at the atrioventricular node outside its absolute refractory phase and therefore is conducted into the ventricles. If the conducted impulse finds the ventricles responsive, it initiates ventricular excitation prematurely—that is, prior to onset of the expected nodal beat. The resulting ventricular deflection is called a ventricular capture beat and ordinarily presents much the same appearance as the nodal beats previously recorded. There is an inverse relationship between the P-R interval of the ventricular capture beat and the preceding R-P interval. When the R-P interval is short, the sinus impulse arrives earlier in the relative refractory phase of the atrioventricular node and is conducted to the ventricles more slowly than an impulse arriving later after a longer R-P interval. Sometimes onset of the ventricular capture beat occurs so prematurely that the recovery process in the ventricles is interrupted before its completion. Because of the partial refractoriness of the ventricular muscle, there is aberrant spread of excitation through the ventricles. This is manifested in the ventricular capture beat by the appearance of slight to marked changes in QRS configuration and/or duration. Ventricular aberration is the term used to refer to the QRS changes resulting from aberrant intraventricular conduction or from preferential atrioventricular conduction (discussed later, on page 381).

In passing through the atrioventricular node, the conducted atrial impulse of a ventricular capture beat

do not differ greatly, a form of sinus arrhythmia may be observed which resembles ventriculophase sinus arrhythmia occurring in complete atrioventricular block. As mentioned above, the P waves usually march into and through the QRS complexes. However, in the case of sinus arrhythmia, the first P wave to emerge behind the ventricular beat appears after a shorter P-P interval than those preceding, its earlier onset being related in some way to ventricular systole. Because of the shortened P-P interval, the P wave moves back in front of the QRS complex again, and the cycle repeats itself. This mechanism makes it possible for the sinus P wave to remain in close proximity to the nodal beat, thereby enabling the sinus impulse to interfere with the retrograde nodal impulse repeatedly.

More often than not in fast nodal rhythms, incomplete dissociation is maintained by a unidirectional blocking of retrograde atrioventricular conduction, as evidenced by failure of a retrograde P wave to appear when expected. (A retrograde P wave should follow within 0.20 second, or less, the QRS complex of the nodal beat whenever the next sinus P wave falls well outside the Q-T interval of the ventricular beat.)

Since the nodal impulses are discharged more



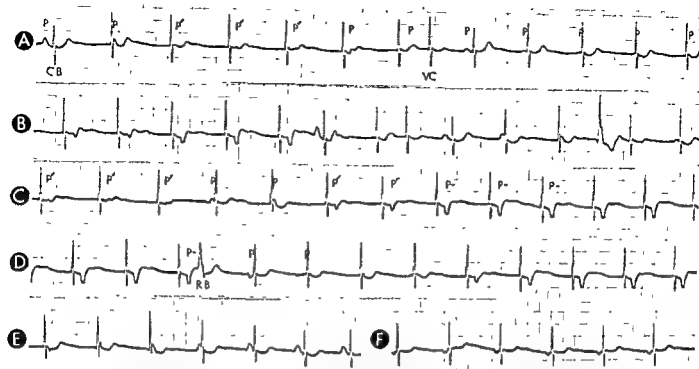


Fig. 249.—Atrioventricular nodal rhythm with alternating periods of atrioventricular dissociation and retrograde atrial activation with retrograde atrioventricular block. All lead strips are lead II. The ventricular complex (CB) is a conducted sinus beat, the ventricular deflection (VC) is a ventricular capture beat; and the QRS deflection (RB) is a reciprocal beat. P waves of sinus node origin are designated P, those of atrioventricular nodal origin, P⁻, and those labeled P⁺ are atrial fusion beats. Note that the configuration of the conducted sinus beat in A differs from that of atrioventricular nodal beats elsewhere in the same lead strip. In D, the retrograde P wave following the third nodal beat is

val of the third nodal beat in D, all other features of the premature ventricular deflection (RB) are compatible, with this beat being a reciprocal beat. In E, a mechanism is demonstrated which may tend either to perpetuate atrioventricular dissociation or to restore sinus rhythm. This mechanism is a form of ventriculophasic sinus arrhythmia. Thus, in E, the sinus P wave can be seen to emerge gradually behind the QRS deflection of the first three nodal beats, however, the third sinus cycle is shortened, causing the sinus P wave to move back in front of the fourth nodal ventricular beat. The last two QRS deflections in this lead strip are probably conducted sinus beats. In F, there is a persisting upper atrioventricular nodal rhythm.

plete dissociation of a rapid nodal rhythm and a slower sinus rhythm. Incomplete dissociation may also occur intermittently, as will be indicated later in the discussion. Parenthetically, it should be pointed out that many texts apply the term *atrioventricular dissociation* only to the form of incomplete dissociation described above. However, in this text the term is used to designate a mechanism which occurs with various rhythms, although observed most frequently with nodal rhythm.

In incomplete dissociation of a faster nodal rhythm and slower sinus rhythm, the difference in the rates of the two pacemakers is usually due to an accelerated rate of impulse formation in the atrioventricular node, although slowing of the sinoatrial node may be a contributory factor. Thus, depending on the circumstances, incomplete dissociation may occur with nodal

rhythms whose rates range from 40 to 100 beats per minute, and sometimes even higher if paroxysmal nodal tachycardia is present. Since, in the electrocardiogram, the P-P intervals of the slower atrial rhythm are longer than the R-R intervals of the ventricular rhythm, successive P waves appear to march into and then emerge behind the QRS complexes. However, even though the relative positions of the sinus P waves and nodal R waves are constantly changing, the P-P intervals and R-R intervals may both be spaced off regularly.

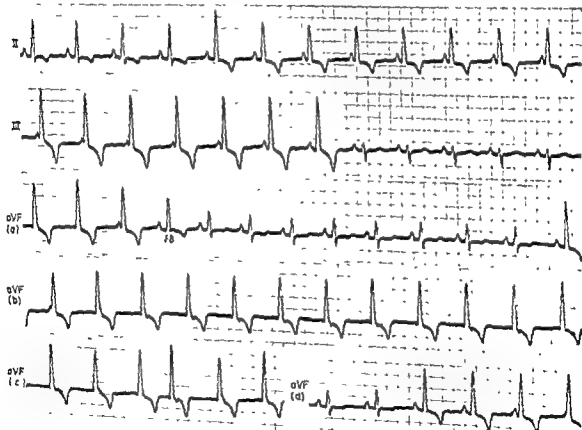
The inability of the faster nodal center to take over the atrial rhythm is due to the fact that retrograde conduction of the nodal impulse is prevented either by physiologic atrioventricular interference or by retrograde atrioventricular block (Figs 248 and 249). Interference is the mechanism more likely to be in-

the interval between two consecutive nodal beats, there frequently is a delay in conduction of the sinus impulse through the bundle of His. Inasmuch as the nodal pacemaker is discharged by the sinus impulse before it reaches the area of conduction delay, the next nodal impulse begins to form well in advance of onset of ventricular activation and is discharged sooner thereafter. Thus the VC-NB interval is shortened to the extent that ventricular excitation by the conducted atrial impulse is delayed. In the authors' experience, shortened VC-NB intervals are observed quite frequently. Occasionally the VC-NB interval is longer than a single-cycle R-R interval of the nodal rhythm. This has been attributed to transient depression of the nodal pacemaker resulting from its premature discharge by the conducted atrial beat (Figs. 250 and 251)

Clinical Significance of Atrioventricular Dissociation

cance of this finding. Thus, dissociation of sinus arrhythmia, sinus bradycardia, or wandering pacemaker is usually of little consequence, while its appearance under different circumstances may be of great diagnostic importance. In short, atrioventricular dissociation derives its clinical significance from the mechanisms and related factors responsible in a given instance for its appearance, with reference particularly to the following

1. *Rate of atrioventricular nodal rhythm*—As previously stated, atrioventricular dissociation occurring with slow nodal escape rhythms (rate of 40-50 beats



case, one is surprised to find what appears to be a ventricular fusion beat (FB) in lead aVF. The usual significance of a ventricular fusion beat (which is generally thought to indicate that other ectopic beats in the same record originate in the ventricles) cannot be applied to the above electrocardiogram (This subject is discussed in detail on page 381)

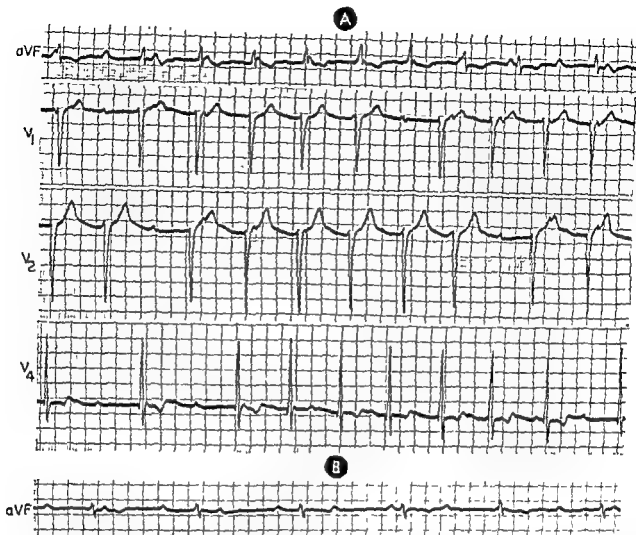


Fig. 251.—In A, the electrocardiographic lead strips show, for the most part, a relatively rapid atrioventricular nodal rhythm with a slower sinus rhythm in the atria. There are no definitely recognizable ventricular capture beats. However, there are frequent pauses in the ventricular rhythm. Possibly the best explanation for these pauses is that the sinus P wave, which either slightly precedes or is superimposed on the last nodal beat before the pause, is conducted almost through the atrioventricular node but does not emerge from it. In so doing, it discharges the immature atrioventricular nodal impulse (see Fig. 250). An alternative possibility is that the pauses in the ventricular rhythm are the result of an antegrade atrioventricular block of an atrioventricular nodal beat. This explanation is supported somewhat by the

There is complete atrioventricular dissociation. The QRS deflections resembles that of the pacemaker in III & almost exactly that of the atrioventricular node. The intervals are shorter than

discharges the immature impulse forming in the nodal pacemaker. If the nodal center is then able to reform and discharge a second impulse before arrival of the next sinus impulse at the atrioventricular junction, a nodal beat follows the ventricular capture beat. However, should the sinus impulse arrive first, the ventricular capture beat is followed by one or more conducted sinus beats, depending on how long the sinus node remains in control of the atria and ventricles. When ventricular capture beats initiate short periods

of sinus rhythm, incomplete dissociation is said to be intermittent rather than sustained.

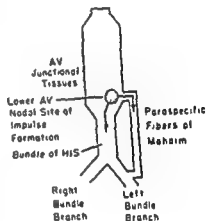
If a ventricular capture beat is followed by a nodal beat, the interval between the two (VC-NB interval*) sometimes corresponds to a single cycle of the nodal rhythm, since it represents the time required by the nodal pacemaker to mature and discharge its next impulse. Although the VC-NB interval often equals

*VC = ventricular capture beat, NB = nodal beat

per minute) in dissociation at tachycardia (rate of 50-100 per minute) is sometimes the first indication of inflammatory or degenerative myocardial disease. Later, in Chapter 26, paroxysmal atrioventricular nodal tachycardia (rate, above 100 beats per minute) with atrioventricular dissociation will be discussed, along with its clinical implications.

2. Mechanism affecting atrioventricular conduction—atrioventricular block versus atrioventricular interference—Because atrioventricular interference is a

excitation, the partial refractoriness of the intraventricular conducting pathways and myocardium may result in an abnormal spread of excitation through the ventricular muscle. This condition, called aberrant intraventricular conduction, is marked by changes in the QRS complex. Aberration of the ventricular complex is frequently observed in ectopic beats, or in ectopic tachycardia. The factor common to all these conditions is



parasympathetic fibers function as a conducting pathway and the explanation of ventricular aberration of atrioventricular nodal beats given here must be considered tentative until further information is available.

physiologic phenomenon, it does not in itself constitute an abnormality even when interference is the sole mechanism responsible for dissociation. Failure of ventricular or atrial capture beats to appear when expected establishes the presence of atrioventricular block (antegrade or retrograde block, respectively), which may have the same significance as nodal tachycardia occurring with atrioventricular dissociation.

3 Clinical background—Atrioventricular dissociation is sometimes produced by inflammatory and degenerative processes involving the myocardium, such as rheumatic myocarditis and arteriosclerotic heart disease, or by intoxication with certain drugs, particularly digitalis and quinidine. When dissociation is superimposed on a clinical background of suspected drug intoxication or cardiac disease, this finding has greater significance than would otherwise be the case.

Ventricular Aberration of Atrioventricular Nodal Escape Beats

If an excitation impulse arrives in the ventricles before they have recovered completely from previous

that two or more impulses reach the ventricles in

that of a right bundle branch block.

As indicated previously, nodal escape beats are characterized by delayed onset. This makes it all the more surprising that minimal to moderate degrees of ventricular aberration are frequently observed in nodal escape beats (Figs. 252-254). Obviously, the mechanism involved differs from that described for premature beats and rapid rhythms, since the late onset of the nodal escape beat would seem to preclude, as the causative factor, refractoriness of the intraventricular conducting pathways. Pick has recently advanced the hypothesis that aberration of nodal escape beats may be the result of preferential atrioventricular conduction of the nodal impulses (Fig. 255). This concept has its basis in the fact that irregular communications of the atrioventricular node, common bundle, and left bundle branch with the ventricular

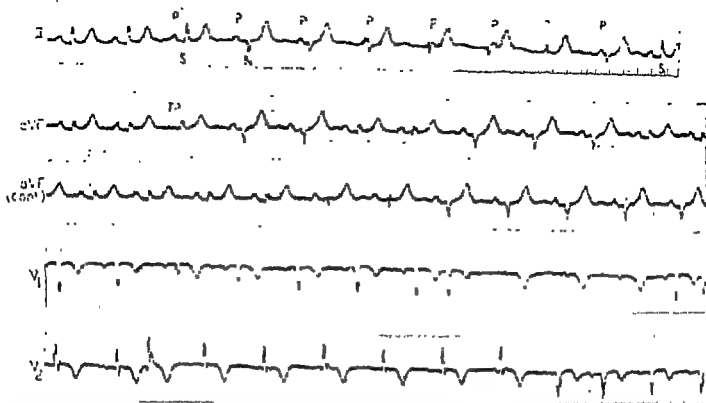


Fig. 253.—Electrocardiogram showing intermittent incomplete atrioventricular dissociation with atrioventricular nodal rhythm and occasional atrial extrasystoles. However, the most striking feature is the marked difference in the QRS configuration of the sinus beats and the atrioventricular nodal beats. Symbols: S, sinus beats; P, sinus P waves; N, atrioventricular nodal beats, and FP, atrial fusion beat (occurring in lead aVF).

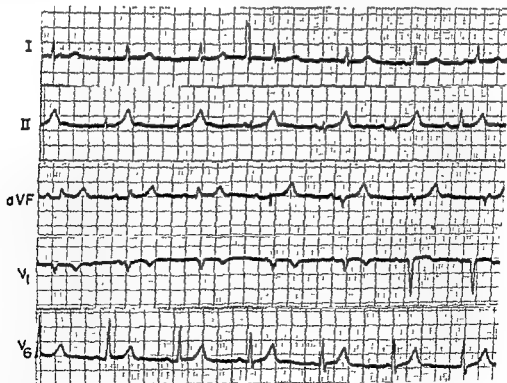


Fig. 254.—Intermittent atrioventricular nodal rhythm with incomplete atrioventricular dissociation and ventricular aberration of the nodal beats.

Ectopic Beats and Rhythms

TERMINOLOGY AND GENERAL CONSIDERATIONS

ECTOPIC BEAT—An ectopic beat is a beat which arises outside the sinoatrial node in an ectopic focus and results from some change in excitability, conductivity, or rhythmicity locally in the region of impulse origin. An ectopic beat may be one of two types. an automatic ectopic beat or a coupled ectopic beat.

a) **AUTOMATIC ECTOPIC BEATS (PARASYSTOLE).**—The focus producing beats of this type is unique in that, not only does it form and discharge impulses automatically and independently, but its rhythmical activity is "protected" against interruption by impulses originating in the sinus node or elsewhere. The mechanism giving rise to automatic beats is called *parasystole* and is described later.

Interectopic interval.—This term refers to the interval between two consecutive ectopic beats (see Fig. 256) whether or not one or more beats of different origin intervene.

b) **COUPLED PREMATURE ECTOPIC BEATS.**—In this type of ectopic beat, the impulse is not discharged automatically but requires a triggering excitation impulse. The initiating impulse may be a conducted sinus beat or another ectopic beat acting as a trigger impulse or a "re-entry" impulse whether the interval

Trigeminy and quadrigeminy.—Trigeminy consists of two coupled ectopic beats following each sinus beat, quadrigeminy, of three extrasystoles after each sinus beat. A series of four or more ectopic beats appearing in rapid succession may be regarded as a short run of paroxysmal tachycardia.

Multiple coupled ectopic beats.—To indicate the frequency with which extrasystoles occur in a given electrocardiogram, the following arbitrary scheme may be used (a) the term *rare extrasystoles* is used if only one ectopic beat occurs in a 10-second interval, (b) the term *occasional extrasystoles* signifies the occurrence of two or three extrasystoles in a 10-second interval, and (c) the term *frequent extrasystoles* is used when a 10-second interval in the electrocardiogram contains four or more ectopic beats.

Coupling interval.—The coupling interval is the interval between onset of an extrasystole and onset of the beat immediately preceding (see Fig. 256). In the case of atrioventricular nodal and ventricular ectopic beats, the coupling interval is measured from the QRS complex of the sinus beat to that of the extrasystole, and in atrial premature beats, from the sinus P wave to the ectopic P wave. The length of the coupling interval is a measure of the prematurity of the coupled beat and is determined in part by the length of the conduction pathway which must be traversed by the trigger impulse in order to reach the ectopic focus. The length of this pathway, and thus the length of the coupling interval, depends largely on the site of impulse origin. As a corollary to the preceding statement, the location of the ectopic focus has an important bearing on the way the excitation impulse spreads through the myocardium. The more abnormal the spread of excitation, the more the ectopic beat differs in appearance from the normal beat.

Bigeminy.—The term *bigeminy* is used to describe cardiac rhythms consisting of coupled beats, but the mechanism of the paired beats should always be indicated. While *bigeminy* is usually due to coupled ectopic beats, each of which is initiated by a preceding beat of the prevailing rhythm, it may also be produced by several other mechanisms, such as 3:2 Wenckebach atrioventricular block and nonconducted atrial extrasystoles following every second sinus beat.

myocardium (variously labeled *paraspecific fibers* or *preferential pathways*) have been demonstrated in normal fetal, neonatal, and young adult hearts. Hypothetically at least, it can be postulated that a nodal impulse may sometimes be transmitted via this accessory pathway to some part of the ventricular myocardium, instead of utilizing the normal atrioventricular conducting pathway, like impulses arising above the atrioventricular node. The degree of ventricular aberration displayed by the nodal beat would be related to the length of the preferential pathway and to the point at which excitation is introduced into the ventricular myocardium.

Pick has published records showing ventricular aberration of one or several nodal escape beats, and examples of this phenomenon appear in figures of this text. To these observations, we have added a small series of electrocardiograms which show ventricular aberration during relatively sustained rhythms occurring with wandering supraventricular pacemaker, with atrioventricular dissociation, and with complete atrial capture. In the latter instance, the aberration

was demonstrated during the recorded onset and offset of the nodal rhythm when on occasions, curiously enough, ventricular fusion beats were also noted. As a general rule, the aberration consisted primarily of slight changes in QRS configuration with little or no change in duration. Ventricular fusion beats might possibly reflect simultaneous activation of the ventricles by impulses passing down the usual conducting pathways and by impulses arriving via the atrioventricular preferential pathways.

The relative frequency with which nodal escape beats exhibit ventricular aberration, and the confusion which may arise in differentiating these beats from those originating in the ventricles have been emphasized by Pick. Moreover, one is tempted to speculate whether this innate predilection of nodal beats to show aberration may not also apply to nodal tachycardias. If so, then the question might be raised as to how frequently apparent ventricular tachycardias are actually atrioventricular nodal tachycardias with ventricular aberration. The answer to this question may be of therapeutic and prognostic significance.

IDIOVENTRICULAR ESCAPE RHYTHM

When a secondary pacemaker located in the ventricles is permitted to escape as the result of either blocking of impulses from higher pacemaking centers or depression of the rhythmicity of these centers, the ventricular rhythm produced is called an *idioventricular escape rhythm* (see Fig. 311). This type of escape rhythm is observed chiefly in complete atrioventricular block, when the site of the block is located relatively low in the atrioventricular junctional tissues, and in instances of marked cardiac depression induced by such factors as quinine intoxication, hyperkalemia, or terminal changes in the dying heart. Inasmuch as idioventricular rhythms are described in some detail in a later discussion of the electrocardiographic findings in complete atrioventricular block, only a brief preview of the electrocardiographic characteristics of idioventricular escape rhythms will be given at this point. The salient fea-

tures of this type of escape rhythm are as follows.

1. When the ventricular pacemaker is situated above the bifurcation of the common bundle, the ventricular deflections are generally indistinguishable from those produced by an atrioventricular nodal pacemaker.

2. Below the bifurcation of the common bundle, the generalization holds true that the more distal the location of the pacemaker in the intraventricular conduction system, the more aberrant is the spread of excitation through the ventricles, the greater is the distortion and widening of the idioventricular beats, and the slower is the idioventricular pacemaker.

3. As a general rule, idioventricular rhythms are characterized by rates of 40 beats per minute or less and by QRS deflections which are bizarre in appearance and widened to 0.12 second or more.

These interrelationships are responsible for the fact that coupled beats arising in the same ectopic focus (unifocal extrasystoles) tend to have the same appearance and essentially equal coupling intervals. Ectopic beats varying in configuration and coupling interval usually have different sites of origin and are called multifocal premature beats. However, it must be kept in mind that variation in conduction of the ectopic impulses may cause ectopic beats from a single focus to present the features of multifocal extrasystoles.

Postectopic interval.—The postectopic interval or pause extends from onset of the ectopic beat to onset of the following beat of the prevailing rhythm (see Fig. 256). Usually the first postectopic beat is a sinus beat, but occasionally the pause, if prolonged, is terminated by a nodal escape beat. In such a case, the postectopic interval corresponds to the time required for the atrioventricular node to mature and discharge an impulse.

Compensatory (postectopic) pause.—The postectopic interval is compensatory (see Fig. 257) if the combined coupling and postectopic intervals (that is, the interval between the sinus beat preceding and that following the ectopic beat) equal in length two cycles of the sinus rhythm (two R-R or P-P intervals).

Noncompensatory (postectopic) pause.—The post-

ectopic pause is noncompensatory (see Fig. 257) if the total length of the coupling and postectopic intervals is shorter than two sinus cycles but longer than a single R-R or P-P interval of the sinus rhythm.

Interpolated extrasystole.—An interpolated extrasystole (Fig. 258) does not prevent the following sinus beat from occurring in response, in contrast to the usual course of events. Interpolated beats are almost always of ventricular or atrioventricular nodal origin, interpolated atrial extrasystoles occurring only rarely.

The many factors which, in conjunction, determine if an ectopic beat is to be interpolated or followed by a compensatory or noncompensatory pause can be reduced to a single variable—namely, the effect of the ectopic impulse, if any, on the sinus pacemaker or on the following sinus impulse. A compensatory pause results when the ectopic impulse fails to reach the sinus node in time to discharge it prematurely. Instead it encounters the descending sinus impulse, and each impulse obliterates the other. As a result, the ectopic beat does not disturb the rhythm of the sinus pacemaker and the sinus impulse does not produce a conducted beat. The postectopic beat is therefore initiated by the next sinus impulse, the second P wave following the extrasystole, which appears at its expected

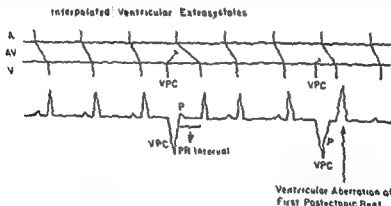


Fig. 258.—Mechanism of interpolated extrasystoles. An interpolated atrioventricular nodal or ventricular extrasystole (VPC) occurs that is not timed within a single sinus cycle. In other words, each sinus P wave (P) elicits a ventricu-

lary extrasystole. Because the sinus impulse arrives in the ventricle while the intraventricular conducting pathways are still partially refractory following conduction of the preceding ectopic beat, it is necessary to assume retrograde conduction of the ectopic impulse through a part of the atrioventricular junctional tissues, which are therefore rendered partially refractory. Thus, in contrast to the usual course of events following a ventricular extrasystole, the retrograde ectopic impulse of an interpolated ventricular extrasystole does not prevent atrioventricular conduction of the descending sinus impulse but simply delays it. This is a manifestation of concealed atrioventricular conduction. When the retrograde impulse of an interpolated ventricular extrasystole fails even to delay atrioventricular conduction of the first postectopic sinus beat, as in the second example above, the QRS deflection of the resulting conducted sinus beat generally shows aberration because the sinus impulse arrives in the ventricle while the intraventricular conducting pathways are still partially refractory following conduction of the preceding ectopic beat.

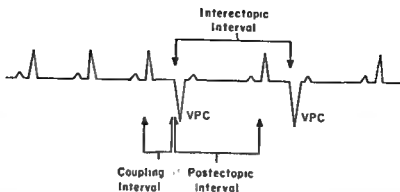


Fig. 256.—Diagrammatic electrocardiogram depicting interectopic, coupling, and postectopic intervals. The sinus beats are represented by upright P waves preceding upright R waves, while ventricular premature beats (VPC) following the third and fourth sinus beats are downwardly directed. The interval from onset of one ventricular premature beat to onset of the next ventricular premature beat is called the *interectopic interval*. (If the extrasystolic beats were of atrial origin, then the interectopic interval would extend from onset of the first premature ectopic P wave to onset of the next premature ectopic P wave.) The *coupling interval* of the ventricular extrasystole is the interval between onset of the ectopic beat and onset of the QRS deflection immediately preceding it. (In the case of an atrial extrasystole, the coupling interval extends from onset of the ectopic P wave to onset of the sinus P wave immediately preceding the ectopic P wave.) The *postectopic interval* extends from onset of the ventricular extrasystole to onset of the QRS deflection of the first postectopic sinus beat. (The postectopic interval of an atrial extrasystole is the interval extending from onset of the premature atrial P wave to onset of the first postectopic sinus P wave.)

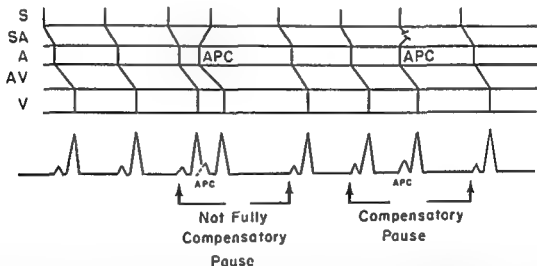


Fig. 257.—Mechanisms of compensatory and noncompensatory pauses following extrasystole (Symbols S, sinus node discharge, SA, sinoatrial conduction, A, atrial beat or P wave, AV, atrioventricular conduction, V, ventricular beat or QRS deflection, and APC, atrial premature contraction.) In the schematic lead strip below the diagram, the atrial premature beats (APC) are conducted into the ventricles to produce R waves having the same configuration as those of the sinus beats. In the first example, the atrial premature beat not only activates the ventricles but is able to spread in a retrograde direction and to discharge the sinus node prematurely. The premature discharge of the sinus pacemaker causes a transient depression of its rhythmicity so that the sinus cycle immediately following the APC is slightly longer than the usual sinus cycle. However, the lengthening of the postectopic sinus cycle is usually less in

pulse is discharged at the expected first postectopic sinus P wave is the compensatory.

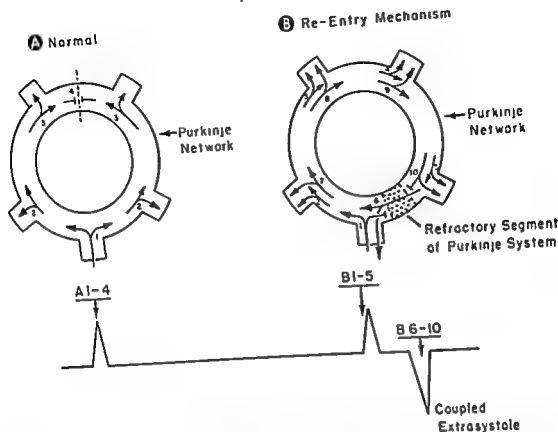


Fig 259.—Re-entry mechanism of premature ectopic beats. In A, a ring of conducting fibers and branches of the Purkinje network are depicted. The excitation impulse is assumed to enter the circular conducting pathway at point 1, where it splits, one impulse passing in a clockwise, and the other in a counterclockwise, direction. In their course around the ring of conducting tissue, the impulses split at points 2 and 3, from which excitation spreads, via adjoining branches, to the same time the original excitation impulses approach and

pulse re-enters the circular ring of conducting fibers and traverses it a second time to produce the coupled extrasystole (B 6-10)

of muscle distal to the site of blocking (this effect has been demonstrated in nerve preparations and has been termed *Wedensky facilitation* by neurophysiologists). Whether or not this is sufficient to produce suprathreshold excitability and discharge the ectopic focus is largely dependent on fluctuations in the sub-threshold background.

In the following discussion of coupled ectopic beats, the mechanism postulated by Scherf which was just described will provide the terminology and theo-

retical background, however, its selection in preference to the theory of re-entry is based on convenience alone and not on any difference in the relative validity of the two concepts. The fact is that neither the re-entry theory nor the theory of a single focus of sub-threshold activity has been proved to the exclusion of the other insofar as the genesis of coupled ectopic beats is concerned. (That re-entry is the mechanism responsible for reciprocal beats proves nothing as to its role in the causation of coupled ectopic beats.)

time. Thus the interval between the sinus beats preceding and following the ectopic beat equals two cycles of the sinus rhythm. Sometimes during a slow sinus rhythm, ventricular or nodal extrasystoles occurring early in diastole may be interpolated between two consecutive sinus beats. The reason for this is that the interval between onset of the ectopic beat and discharge of the next sinus impulse may be long enough to enable the conducting pathways and ventricular muscle to recover, at least partially. If such is the case, the sinus impulse produces a ventricular beat. Since the atrioventricular junctional tissues are still in the refractory phase following excitation by the ectopic beat, they conduct the sinus impulse more slowly than normally. Thus the P-R interval of the conducted sinus beat is prolonged, and to this extent the R-R interval containing the interpolated beat exceeds in length the usual R-R interval. These findings reflect incomplete atrioventricular interference between the ectopic and sinus impulses. If atrioventricular interference is complete, the sinus impulse is not conducted and the ventricular or nodal extrasystole is followed by a compensatory pause.

COUPLED ECTOPIC BEATS

Mechanisms

The mechanism of coupled ectopic beats is still debated. That a parasystolic center can, on rare occasions, produce both automatic and coupled beats is generally conceded. However, for all intents and purposes, only two postulated mechanisms need be considered, both of which assume focal origin of the ectopic impulse and its initiation by a preceding beat.

Re-entry.—This mechanism (see Fig 259) assumes a focal depression of conductivity involving certain peripheral fibers of the muscle syncytium. The initial sinus impulse finds these fibers still refractory from previous excitation. The excitation impulse therefore enters other branches of the syncytial network, which distribute it to muscle tissue elsewhere. Meanwhile, the depressed focus recovers its responsiveness. Thus, the sinus impulse, winding its way through the muscle syncytium, is led back into and passes along the previously blocked pathways. By the time the previously depressed focus has undergone activation, conducting fibers and muscle tissues excited initially may have emerged from the absolute refractory state, with the result that the excitation impulse is picked up and transmitted once again through the myocardium. Therefore, the ectopic beat that is produced appears prematurely—that is, it follows the preceding

A noncompensatory pause follows an extrasystole if the ectopic impulse is conducted in a retrograde direction to the sinoatrial node in time to discharge the immature sinus impulse before it can be fired off spontaneously. Premature discharge of the sinus pacemaker, which is the *sine qua non* for a noncompensatory pause, has two major effects on the length of the postectopic interval: (a) it shortens the sinus cycle preceding the ectopic beat, and (b) premature discharge of the sinus node—or, for that matter, any impulse-forming center—often depresses temporarily the rhythmicity of the pacemaker.

More often than not, sinus node depression produced in this manner lengthens the postectopic sinus cycle less than the preceding cycle is shortened. The total duration of these two cycles is therefore less than two normal sinus cycles, and so the postectopic interval is noncompensatory. When marked prematurity of an ectopic beat or the occurrence of a succession of ectopic beats leads to a relatively more severe degree of sinus node depression, the postectopic interval may be greatly prolonged and may be terminated by an atrioventricular nodal escape beat.

sinus beat by an interval which is shorter than a single cycle of the sinus rhythm.

Single focus of subthreshold activity.—According to Scherf, a coupled beat is produced when a trigger sinus impulse (or another ectopic impulse) initiates discharge of an ectopic focus of subthreshold activity. Presumably, a localized metabolic disturbance causes a subthreshold increase in focal excitability. If, on this subthreshold background, there is superimposed a further, albeit temporary, rise in focal excitability, induced by the trigger impulse, the level of excitability in the ectopic center becomes transiently suprathreshold. This precipitates discharge of the ectopic impulse.

The mechanism by which the trigger impulse increases excitability in the ectopic focus is not definitely known. One possible explanation is that the initial beat causes circulatory changes locally which alter the chemical environment of the ectopic center. On the other hand, it may be that the initial beat increases subthreshold excitability by a mechanism related to the phenomenon of Wenckebach facilitation. Thus it is conceivable that a small focus of scar tissue or depressed muscle blocks, completely or incompletely, the spread of the trigger impulse into a small area of muscle tissue beyond. Nevertheless, the blocked impulse causes a momentary increase in the excitability

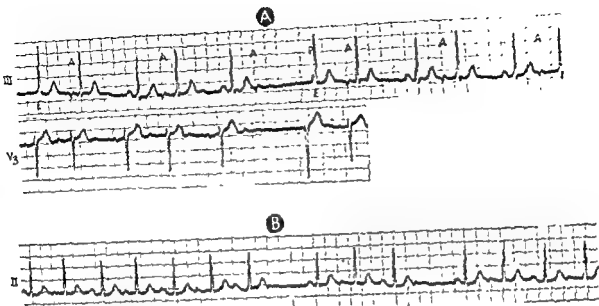


Fig. 261—Coupled atrial extrasystoles with

a coupled rhythm due to atrial extrasystoles. The coupled atrial extrasystoles just as in A, atrial extrasystoles and the conducted sinus beats

having the same configuration as the deflections initiated by sinus beats. The exceptions to this rule are discussed below.

VARIATIONS IN ATRIOVENTRICULAR AND INTRAVENTRICULAR CONDUCTION

An ectopic atrial beat with a short coupling interval sometimes may be of such premature onset that it appears in early ventricular diastole. At this time the atrioventricular and/or intraventricular conducting pathways may still be completely refractory from the preceding sinus beat. When this occurs, the premature atrial beat fails to produce a ventricular deflection. The atrial extrasystole, often referred to as a blocked extrasystole, is better described as "nonconducted" if it occurs within the Q-T interval of the preceding beat (that is, within the normal refractory period of the atrioventricular junctional tissues and/or intraventricular conducting pathways), since the failure of the ectopic atrial impulse to be transmitted into the ventricles can be ascribed, in this instance, solely to atrioventricular interference without the need of implicating pathologic blocking. If the atrial ectopic beat appears outside the Q-T interval of the preced-

ing beat and yet fails to be conducted, then the atrial premature contraction can justifiably be said to be blocked (Fig. 261). On the other hand, the atrioventricular and/or intraventricular pathways may have partially recovered before arrival of the ectopic atrial impulse. Although the impulse is transmitted, the refractoriness of the conducting tissues leads to prolonged atrioventricular conduction and/or aberrant intraventricular conduction. Generally, the longer the P-R interval of the atrial extrasystole, the less likely it is that the QRS complex will show ventricular aberration, or the less marked the aberration. The reason for this is that the prolonged atrioventricular conduction lengthens the time available to the intraventricular conducting fibers for recovery. When present, ventricular aberration may consist of either slight changes in duration and/or amplitude of the Q, R, and S waves or the appearance or disappearance of one of these waves. At the other extreme, the changes may sometimes be so striking that the QRS pattern resembles that of right bundle branch block (in 55% of the affected beats) (Fig. 262) or left bundle branch block. A ventricular deflection with aberration of this degree may be readily confused with a ventricular extrasystole if the preceding P wave of

Coupled Ectopic Atrial Beats

ELECTROCARDIOGRAPHIC APPEARANCE

The excitation impulse producing an atrial extrasystole or coupled beat originates in an ectopic focus in the atria (Fig. 260); and, in consequence, its spread through the atria differs from that of the impulses arising in the sinoatrial node. The abnormal spread of excitation and its early onset produces a premature P wave which differs from the sinus P wave in appearance. Moreover, ectopic atrial impulses arising from several foci spread through the atria differently and vary in P wave configuration one from another. The nearer their site of origin to the sinoatrial node, the more they resemble sinus P waves. Conversely, the nearer to the atrioventricular node the ectopic atrial beat arises, the greater its similarity to the retrograde P wave of a nodal beat. If leads II, III, and/or aVF

record a premature inverted P wave which is followed by a ventricular deflection after a P-R interval exceeding 0.12 second, the likelihood is that the P wave represents an ectopic atrial or coronary sinus beat, although a nodal premature systole with prolonged antegrade atrioventricular conduction cannot be excluded. Between these two extremes there can be seen atrial extrasystoles with a low, isoelectric, or diphasic P wave configuration. As a general rule, ectopic atrial beats originating in the same focus show essentially the same P wave configuration and have approximately equal coupling intervals (measured from sinus P wave to ectopic P wave). However, in a given instance, the correlation between the appearance of an ectopic atrial beat and its site of origin is uncertain, because variations in intra-atrial conduction may cause unifocal atrial extrasystoles to simulate ectopic beats of multifocal origin. Ordinarily, an atrial extrasystole produces a ventricular deflection

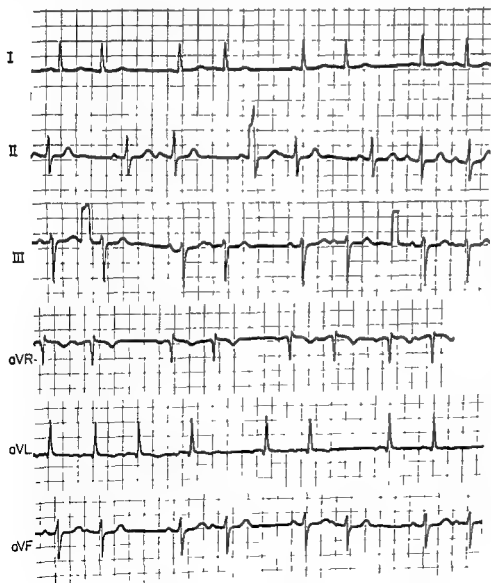


Fig. 260.—Bigeminal rhythm due to a coupled atrial extrasystole following every sinus beat. The close similarity of the ectopic and sinus P waves suggests that the atrial extrasystoles originate in a focus near the sinoatrial node. The ventricular complexes following the premature P waves do not show aberration.

the premature atrial beat is overlooked. Since the ectopic P wave is often buried in the previous T wave, the latter must be examined carefully for slurring, notching, or any other irregularity of its contour which might indicate a superimposed atrial beat. (Fig. 227)

tion can be attributed to the prematurity of the premature atrial beat. If these abnormalities accompany a premature atrial beat appearing late in electrical diastole—particularly if onset of the ectopic beat occurs well after the preceding T wave—a latent atrioventricular or intraventricular conduction defect may be implied. However, prolonged atrioventricular conduc-

the total duration of the pre- and postectopic P-P intervals is shorter than two sinus cycles. The postectopic pause is therefore noncompensatory.

Sometimes the impulse producing the first postectopic atrial beat originates elsewhere than in the sinus node. In fact, the W wave configuration of such a beat often resembles that of the previous atrial extrasystole. A postectopic beat of this type has been ascribed by some to a shift of the cardiac pacemaker to another site. Other investigators propose that the initial atrial extrasystole precipitates formation of another ectopic beat in the same or a different atrial focus, which then discharges spontaneously. In either case, postectopic intervals terminated by P waves which differ in appearance from sinus P waves tend to be slightly shorter than intervals terminated by sinus beats. If sinus node depression is quite marked, nodal escape may occur, but, in contrast to the postectopic atrial extrasystolic P wave described above, a P wave preceding the nodal escape beat, if present, is almost invariably a non-

by a lengthened refractory period, and so a coupled atrial beat may find the atrioventricular node and/or intraventricular conduction system only partially recovered. Thus, the QRS complex follows the ectopic P wave by a prolonged P-R interval or displays ventricular aberration. However, other atrial extrasystoles

responsible for conduction disturbances involving the first of a run of ectopic atrial beats. The remaining beats are conducted normally because the premature onset of the initial extrasystole decreases the cycle length and shortens the refractory period for the extrasystoles following. Similarly, only the second of two coupled atrial beats may evidence disturbed atrioventricular and/or intraventricular conduction, the reason being that its initiating sinus beat follows the postectopic pause of the preceding extrasystole.

THE POSTECTOPIC INTERVAL

Ectopic atrial impulses are conducted so rapidly to the sinoatrial node that ordinarily they discharge it prematurely. Premature discharge of the sinus node not only shortens the cycle preceding the extrasystole but also, by depressing the sinus pacemaker, slows formation of the next sinus impulse. Consequently, the first sinus P wave after the ectopic beat is delayed somewhat in onset, and the postectopic interval exceeds the length of a single sinus cycle. Nonetheless,

discharge spontaneously before the ectopic impulse can penetrate the sinoatrial junction. Such a condition may have any one of the following causes: (a) the atrial impulse may be discharged too late in diastole to reach the sinus node before it fires off spontaneously, (b) retrograde conduction of the ectopic impulse from its site of origin to the sinoatrial junction may proceed too slowly, in comparison with the rate of forward conduction of the sinus impulse from the sinoatrial node, or (c) the rate of impulse formation and discharge by the sinus pacemaker may be too rapid. Any of these factors may lead to sinus and ectopic atrial impulses meeting and interfering with each other in or near the sinoatrial junction, as evidenced by the fact that the ectopic impulse activates the atria without interrupting the sinus pacemaker. Thus, the postectopic sinus W wave appears at the expected time and follows a compensatory pause. Sometimes the sinus and ectopic impulses do not meet until each has excited a portion of the atria. In this event, interference occurs, not in the sinoatrial junction, but in the atrial muscle. Because of the occurrence of atrial interference, a fusion P wave is observed rather than the P wave of the ectopic atrial beat. The configuration of the fusion beat is intermediate between that of sinus P waves and ectopic P waves elsewhere in the same lead, and its onset approximates the expected time of onset of the next sinus P wave.

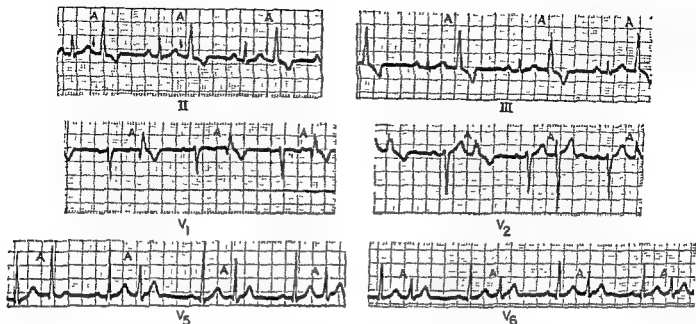
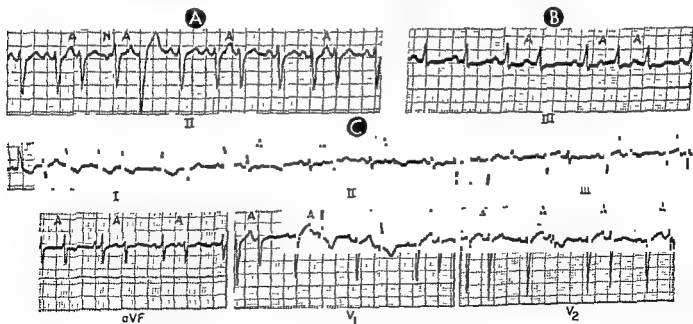


Fig. 262.—Coupled ectopic atrial beats giving rise to a bigeminal rhythm. In these lead strips, the premature ectopic atrial beats are indicated by A. The QRS deflections produced by the premature atrial beats show ventricular aberration in the form of a right bundle branch block type of configuration best demonstrated in lead V₁.

Fig. 263.—Coupled ectopic atrial beats (A) with and without ventricular aberration of the following QRS complexes. The inverted P wave labeled N in lead II of A is an atrioventricular nodal extrasystole.



the premature atrial beat is overlooked. Since the ectopic P wave is often buried in the previous T wave, the latter must be examined carefully for slurring, notching, or any other irregularity of its contour which might indicate a superimposed atrial beat. (Fig.

tion can be attributed to the prematurity of the ectopic atrial beat. If these abnormalities accompany a premature atrial beat appearing late in electrical diastole—particularly if onset of the ectopic beat occurs well after the preceding T wave—a latent atrioventricular or intraventricular conduction defect may be implicated.

ectopic impulse and the presence of a latent conduction defect. This mechanism is based on the fact that the recovery curve of heart muscle for a given cycle is the recovery curve of the preceding cycle. A

atrial beat may find the atrioventricular node or intraventricular conduction system only partially re-

with the same coupling interval are conducted normally because their initiating sinus beats are preceded by shorter R-R cycles. This mechanism is often responsible for conduction disturbances involving the first of a run of ectopic atrial beats. The remaining beats are conducted normally because the premature onset of the initial extrasystole decreases the cycle length and shortens the refractory period for the extrasystoles following. Similarly, only the second of two coupled atrial beats may evidence disturbed atrioventricular and/or intraventricular conduction, the reason being that its initiating sinus beat follows the postectopic pause of the preceding extrasystole.

THE POSTECTOPIC INTERVAL

Ectopic atrial impulses are conducted so rapidly to the sinoatrial node that ordinarily they discharge it prematurely. Premature discharge of the sinus node not only shortens the cycle preceding the extrasystole but also by depressing the sinus pacemaker, slows formation of the next sinus impulse. Consequently, the first sinus P wave after the ectopic beat is delayed somewhat in onset, and the postectopic interval exceeds the length of a single sinus cycle. Nonetheless,

the total duration of the pre- and postectopic P-P intervals is shorter than two sinus cycles. The postectopic pause is therefore noncompensatory.

Sometimes the impulse producing the first postectopic atrial beat originates elsewhere than in the sinus node. In fact, the P wave configuration of such a beat often resembles that of the previous atrial extrasystole. A postectopic beat of this type has been ascribed by some to a shift of the cardiac pacemaker to another site. Other investigators propose that the initial atrial extrasystole precipitates formation of another ectopic beat in the same or a different atrial focus, which then discharges spontaneously. In

sinus P waves are terminated by sinus beats. If sinus node depression is quite marked, nodal escape may occur, but, in contrast to the postectopic atrial extrasystolic P wave described above, a P wave preceding the nodal escape beat, if present, is almost invariably a nonconducted sinus P wave.

Occasionally an atrial extrasystole may be followed by a compensatory pause if the sinus node is able to discharge spontaneously before the ectopic impulse can penetrate the sinoatrial junction. Such a condition may have any one of the following causes: (a) the atrial impulse may be discharged too late in diastole to reach the sinus node before it fires off spontaneously; (b) retrograde conduction of the ectopic impulse from its site of origin to the sinoatrial junction may proceed too slowly, in comparison with the rate of forward conduction of the sinus impulse from the sinoatrial node; or (c) the rate of impulse formation and discharge by the sinus pacemaker may be too rapid. Any of these factors may lead to sinus and ectopic atrial impulses meeting and interfering with each other in or near the sinoatrial junction, as evidenced by the fact that the ectopic impulse activates the atria without interrupting the sinus pacemaker. Thus, the postectopic sinus P wave appears at the expected time and follows a compensatory pause. Sometimes the sinus and ectopic impulses do not meet until each has excited a portion of the atria. In this event, interference occurs, not in the sinoatrial junction, but in the atrial muscle. Because of the occurrence of atrial interference, a fusion P wave is observed rather than the P wave of the ectopic atrial beat. The configuration of the fusion beat is intermediate between that of sinus P waves and ectopic P waves elsewhere in the same lead, and its onset approximates the expected time of onset of the next sinus P wave.

Coupled Ectopic Atrioventricular Nodal Beats

ELECTROCARDIOGRAPHIC APPEARANCE

An ectopic impulse arising in the atrioventricular node is conducted through the junctional tissues in two directions simultaneously—namely, in a retrograde direction toward the atria, and in an antegrade or forward direction toward the ventricles. A nodal extrasystole therefore consists of a premature ventricular deflection which resembles, or differs only slightly in appearance from, conducted sinus beats, and which precedes, follows, or coincides with a retrograde P wave (inverted in leads II, III, and aVF and upright in lead aVR). The relative positions of the retrograde P wave and QRS complex of a nodal beat are determined by the time relationship between onset of ventricular excitation and onset of atrial excitation. Whether the ventricles receive the excitation impulse before the atria, or vice versa, is a function of two variables—namely, (a) the site of impulse origin in the atrioventricular node and (b) the comparative rates of antegrade and retrograde atrioventricular conduction. The general features of nodal beats were de-

scribed fully in the section on atrioventricular nodal rhythms (pp. 363–367) and will only be summarized at this point:

Upper atrioventricular nodal beats.—The retrograde P wave, which is inverted in leads II, III, and aVF and upright in lead aVR, precedes the ventricular deflection by a P–R interval of 0.12 second or less. (If the P–R interval is longer than 0.12 second, there may be delayed forward conduction of the upper nodal impulse, or the ectopic beat may originate near the coronary sinus area in the atria) (Fig. 264).

Middle atrioventricular nodal beats.—The retrograde P wave is buried in and obscured by the ventricular complex of the nodal beat.

Lower atrioventricular nodal beats.—The retrograde P wave follows the QRS complex by an R–P interval of 0.10–0.20 second.

VARIATIONS IN ATRIOVENTRICULAR AND INTRAVENTRICULAR CONDUCTION

Coupled atrioventricular nodal beats may show evidence of disturbed atrioventricular and/or intra-ventricular conduction for reasons previously cited—namely, (a) markedly premature onset of the nodal



beat, (b) latent atrioventricular and/or intraventricular conduction defects, unmasked by the shortened recovery period following the initial sinus beat, and (c) a prolonged refractory period after the initial sinus beat when this beat is preceded by a long R-R interval.

Variations in atrioventricular conduction of nodal impulses have been discussed previously and will not be considered in detail in this section. In brief recapitulation, disturbed retrograde and/or antegrade atrioventricular conduction of a nodal impulse may be accompanied by any of the following findings:

1. If retrograde atrioventricular conduction is completely blocked, the nodal impulse produces only a premature ventricular deflection which is not accompanied by a retrograde P wave, while a premature retrograde P wave without an associated QRS complex is indicative of blocked antegrade conduction.

2. Delayed retrograde or antegrade atrioventricular conduction of a nodal impulse may be suspected

if the P-QRS relationship present in other nodal extrasystoles, this may be a manifestation of disturbed atrioventricular conduction, or it may signify that the nodal extrasystole in question arises from a different focus. In general, prolonged retrograde conduction shifts the retrograde P wave behind, or farther behind, the ventricular deflection, so that the R-P interval lengthens. Delayed antegrade conduction causes the QRS complex to lag farther behind the retrograde P wave, the P-R interval increasing.

The previous discussion of ventricular aberration of ectopic atrial beats pertains equally well to aberrant intraventricular conduction of nodal extrasystoles and need not be repeated.

THE POSTECTOPIC INTERVAL

If the retrograde atrioventricular nodal impulse discharges the sinus node prematurely, the postectopic interval of the nodal extrasystole is longer than a single sinus cycle but is noncompensatory, as previously explained with reference to atrial extrasystoles. A compensatory postectopic pause is more frequently observed with nodal premature beats than with atrial beats and is particularly likely to occur with impulses originating low in the atrioventricular node or with delayed or blocked retrograde conduction. A retro-

grade nodal impulse may fail to discharge the sinus node for either of the following reasons: (1) there may be a unidirectional atrioventricular block which involves retrograde conduction but does not disturb antegrade conduction, and (2) the sinus impulse and the retrograde nodal impulse may interfere with each other at any of the following sites.

1. **Atrioventricular interference**—If interference occurs in the atrioventricular junctional tissues, the ventricular complex alone is produced by the nodal impulse, while the normal sinus P wave appears at its expected time but is not conducted.

2. **Atrial interference**—If the sinus and retrograde impulses do not meet until each has activated a portion of the atrial muscle, the QRS complex of the nodal beat is preceded or followed by a fusion P wave.

3. **Sinoatrial interference**—If the retrograde nodal impulse is able to complete activation of the atria before meeting the descending sinus impulse very near or in the sinoatrial junctional tissues, the only evidence that interference has occurred will be the compensatory postectopic pause. In short, the nodal beat controls both the atria and ventricles but does not interrupt the sinus pacemaker. Thus, the postectopic sinus P wave appears at the time anticipated.

Coupled Ectopic Ventricular Beats

ELECTROCARDIOGRAPHIC APPEARANCE

Ventricular extrasystoles appear in the electrocardiogram as premature QRS deflections which are widened to 0.12 second or more, are slurred and of large size, and are not preceded by either ectopic or conducted sinus P waves. These alterations in QRS configuration and duration reflect asynchronous onset of excitation in the two ventricles and aberrant spread of the excitation impulse subsequently through the myocardium. The more pronounced the disturbance of ventricular excitation, the more abnormal is the appearance of the ventricular deflection. The site of origin of the ectopic ventricular impulse relative to the location of the normal intraventricular conducting pathways affects the manner in which excitation spreads through the ventricles and therefore influences the appearance of the ventricular extrasystole. The following general relationships can be accepted with some reservations.

1. **Ectopic impulses arising in the bundle of His** above its bifurcation utilize the normal intraventricular conduction system. Consequently, they produce ventricular complexes which have the same appearance as conducted sinus beats.

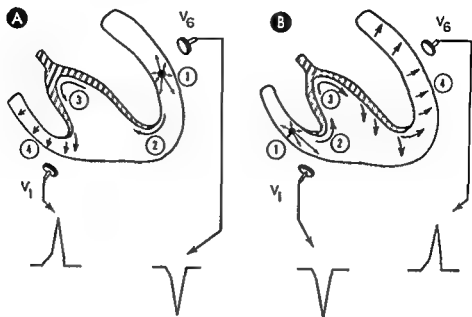


Fig. 265.—Localization of the site of origin of ventricular extrasystoles. In A, the site of ectopic impulse origin is assumed to be in the left ventricular wall at point 1. The ectopic impulse spreads in an aberrant manner through the left ventricular myocardium and eventually enters the left bundle branch at 2. It is transmitted in a retrograde direction up the left bundle branch and then turns down the right bundle branch (3) and is distributed to the right ventricle in a normal manner (4). Thus, the over-all spread of ectopic ventricular excitation occurs in a left-to-right direction, so that

Thus, when a ventricular extrasystole originates in the right ventricle, the over-all direction in which it spreads is from right to left, causing lead V_1 to record a downwardly directed ventricular beat and lead V_6 to register an upright ventricular extrasystole. It must be stressed that this explanation is greatly oversimplified and does not permit precise localization of the site of origin of a ventricular extrasystole.

2 An excitation impulse originating more distally in the conducting system first spreads through adjacent myocardium and the Purkinje network to activate initially the ventricle in which it arises (Fig. 265). In so doing, the ectopic impulse enters and traverses in a retrograde direction the ipsilateral bundle branch. On reaching the bifurcation, the excitation impulse then turns back into the opposite bundle branch and is distributed to and activates the other ventricle via the normal conducting pathways. Thus, the more distal in the conducting system the ectopic impulse originates, the more aberrant is the spread of excitation through the ipsilateral ventricle and the more delayed the onset of excitation in the contralateral ventricle. For example, ectopic impulses arising in the free wall of the left ventricle produce ventricular deflections of longer duration and more abnormal configuration than impulses originating in the interventricular septum. However, in addition to the site of impulse origin, other factors—such as myocardial disease, variations in intraventricular conduction, and heart position—may influence the appearance of

ventricular extrasystoles, according to some authorities. For example, ectopic ventricular beats with a QRS duration exceeding 0.16 second are thought to signify underlying cardiac disease. On the other hand, ectopic beats with QRS intervals less than 0.16 second neither support nor refute the possibility of cardiac pathology.

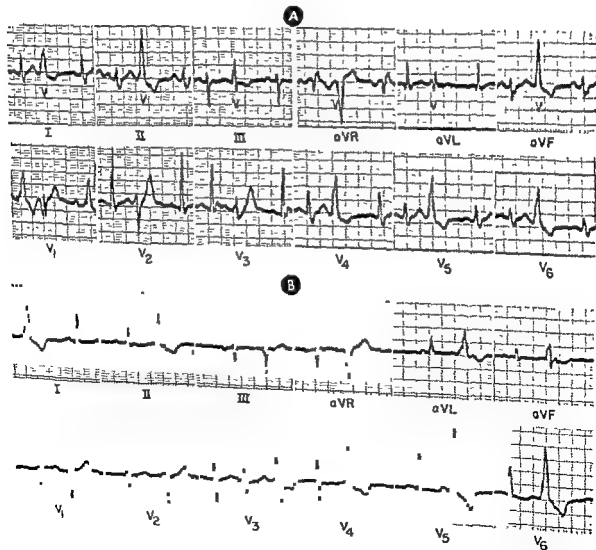
3. The excitation process in bundle branch block and that of ventricular extrasystoles are similar in at least one respect: each produces resultant electrical forces which, on the average, are directed toward the ventricle last activated. Thus, if the ectopic ventricular impulse is distributed first to the left ventricle, the QRS vectors are rotated toward the right ventricle and produce large positive deflections in right precordial leads and resultantly negative complexes in left precordial leads. If the ventricular extrasystole arises in the right ventricle, the QRS vectors of the ectopic beat are directed toward the left ventricle and project positivity on left precordial leads and negativity on right precordial leads. Inasmuch as the sequence of ventricular repolarization is altered be-

cause of changes in depolarization, the ST-T vectors tend to be directed away from the QRS vectors. Thus, ectopic ventricular beats which are resultant positive are usually followed by inverted T waves with S-T segment depression, and downwardly directed ventricular deflections, by upright T waves with S-T segment elevation. These findings represent so-called secondary T wave changes.

4. In a given lead, ventricular extrasystoles with the same site of origin generally have essentially equal

coupling intervals and usually exhibit much the same configuration. The term *multiform* has been suggested for ventricular extrasystoles which differ in configuration but have the same coupling intervals. Multiform extrasystoles may reflect variations in intraventricular conduction of impulses arising in a single focus. Ectopic ventricular beats induced by digitalis are frequently of the multiform type.

Fig 266.-1 The twelve leads of the standard 12-lead electrocardiogram while the conducted beats are diagnostic of right bundle branch block coupling intervals. The nonconducted sinus beats are of normal configuration.



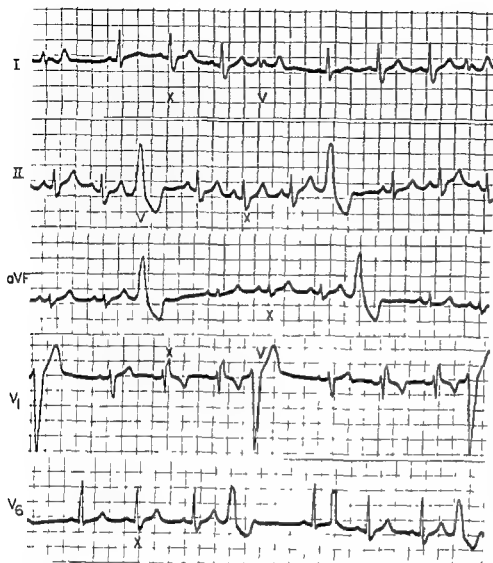


Fig. 267.—Quadrigeminy due to ventricular extrasystoles with conducted sinus beats showing intermittent right bundle branch block. Every third conducted sinus beat is followed by a ventricular extrasystole (V), probably originating in the right ventricle. The pauses following the extrasystoles are fully compensatory, and the first postectopic sinus beats are usually normal in appearance and duration. However, the second (X) and third postectopic sinus beats in each lead are diagnostic of right bundle branch block. Evidently, the compensatory pause following each ventricular extrasystole permits the intraventricular conducting pathways to recover completely, so that the first postectopic sinus beat is normal in appearance. But the following two sinus beats are preceded by shorter cycles and therefore arrive in the ventricles, while the right bundle branch block is refractory following conduction of the previous beat, the result being right bundle branch block.

RETROGRADE ATRIOVENTRICULAR CONDUCTION AND THE POSTECTOPIC INTERVAL

In the past, retrograde conduction of impulses originating in a ventricular focus was thought to be a rare occurrence. More recently, the fact has become apparent that retrograde activation of the atria by ectopic ventricular impulses occurs far more frequently than commonly realized. The reason this event is not more frequently recognized is that retrograde P waves are often difficult to detect because they are superimposed on some portion of the ectopic ventricular beat. On the other hand, a sinus P wave distorted by part of the ectopic ventricular beat can readily be mistaken for a retrograde P wave. As an aid to the correct identification of retrograde P waves accompanying ventricular extrasystoles, the following criteria have been proposed:

1. The P wave must be of premature onset with reference to the sinus P-P interval
2. The interval between retrograde P wave and the next sinus P wave must be longer than a single sinus P-P interval.
3. There must be unequivocal inversion of the P waves in lead II, preferably, and/or in leads III and aVF.
4. The retrograde P wave must follow the QRS complex of the ectopic beat by an interval which equals or exceeds the P-R interval of conducted sinus beats elsewhere in the electrocardiogram
5. If present in a given lead, retrograde P waves tend to follow the ventricular extrasystoles by R-P intervals of nearly equal length

That retrograde activation of the atria by an ectopic ventricular impulse does not occur more often than is noted is not surprising in view of the long pathway the impulse must traverse to reach the atria. Thus, an ectopic ventricular impulse, unlike a nodal impulse, must pass through the entire length of the

atrioventricular node, the most time-consuming part of the retrograde pathway. Consequently, it is not often that the ventricular impulse gets the opportunity to activate the atria before a sinus impulse can interfere, and even less often is the ventricular impulse able to discharge the sinus node prematurely. On the contrary, the next sinus impulse almost always interferes with retrograde spread of the ectopic impulse at one of the following levels.

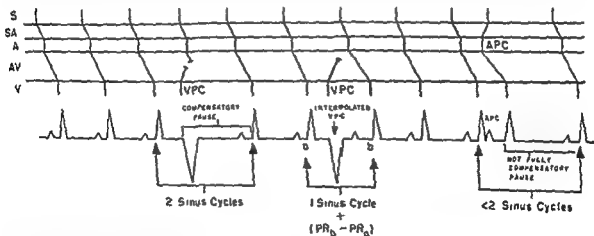
Sinoatrial interference—Interference between sinus and ectopic impulses in the sinoatrial junctional tissues can be inferred if the ventricular extrasystole is followed by a retrograde P wave and a compensatory pause.

Atrioventricular interference—In most instances, interference occurs between the two impulses in or near the atrioventricular junction (Figs. 268 and 269). The sinus impulse activates the atria, and the ectopic impulse activates the ventricles, but neither penetrates the atrioventricular node completely. The sinus P wave ordinarily is buried in the ventricular extrasystole, although sometimes it can be identified in the initial portion of the QRS deflection or superimposed on the S-T segment or T wave.

Atrial or ventricular interference—Interference in

the atria between a sinus impulse and a retrograde ventricular impulse is indicated in the electrocardiogram by the presence of a fusion P wave following a ventricular extrasystole. If either the coupling intervals of ventricular extrasystoles occurring late in diastole tend to vary or if there is sinus arrhythmia, an occasional sinus impulse may arrive in the ventricles at the approximate time an ectopic ventricular impulse is discharged. Each impulse activates part of the myocardium and, in so doing, leaves in its wake refractory muscle. When, finally, the two excitation impulses meet, they obliterate each other by the process of ventricular interference. The sinus-initiated excitation process, which spreads through the myocardium in a normal manner, and the ectopic excitation process, with its erratic, aberrant spread, both contribute to the configuration of the ventricular deflection, thereby producing a ventricular fusion beat.

Occasionally in slow sinus rhythms, the ectopic ventricular beat appears so early in diastole that the conducting pathways and ventricular muscle are able to recover sufficiently to respond to the next sinus impulse. The postectopic sinus impulse, which, as explained above, usually fails to be conducted, in this instance initiates ventricular excitation. The ventricu-



ventricular interference with the descending sinus impulse, the basic sinus rhythm is not disturbed. Consequently, the R-R interval containing the ventricular premature beat equals twice the basic R-R cycle length. The next ventricular extrasystole is interpolated. Thus, the retrograde ectopic ventricular impulse interferes with the descending sinus impulse in the atrioventricular junction only to the extent that it causes prolongation of atrioventricular conduction of the

interval containing the atrial extrasystole are less than two sinus cycles in length.

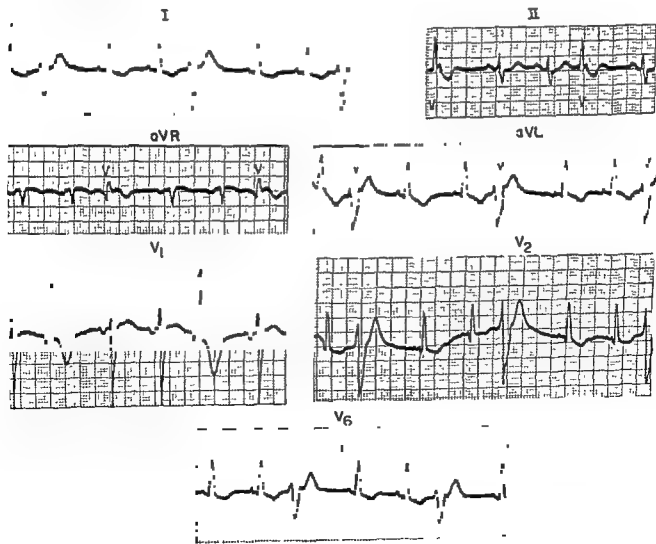
lar extrasystole is therefore included in a single R-R interval—that is to say, it is interpolated (Figs. 270 and 271). Because of the very short postectopic interval of the interpolated beat, the intraventricular conducting pathways and the myocardium may still be partially refractory when the sinus impulse arrives. As a result, the postectopic sinus beat may sometimes show ventricular aberration. Another and more common finding is prolongation of the P-R interval of the postectopic sinus beat. The partial refractoriness of the atrioventricular junctional tissues following an interpolated ventricular extrasystole, as evidenced by the slower rate of atrioventricular conduction, indicates that the retrograde ectopic impulse must have penetrated the atrioventricular node almost completely without emerging from it. In other words, *concealed atrioventricular conduction* of the ectopic beat has occurred. Since the sinus impulse discharged

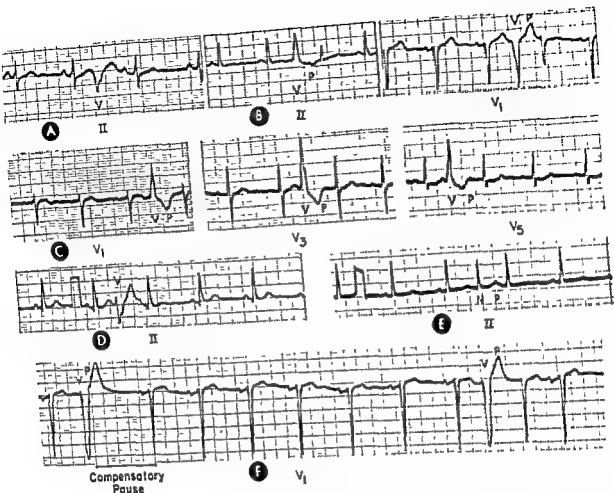
after the interpolated beat is conducted more slowly than the sinus impulse preceding the ectopic beat, the interval between them is generally longer than a single sinus cycle.

Postectopic T Wave Changes

Occasionally the T wave of a sinus beat terminating a long postectopic pause shows changes in configuration, voltage, and/or polarity. Less frequently, T wave changes are observed in as many as three or four of the conducted sinus beats following an extrasystole. Inverted T waves can become upright in the postectopic beat; upright T waves usually become low or inverted, or sometimes simply gain in amplitude. The mechanism of postectopic T wave alterations is not definitely known but seems to be related in some way to the long pause preceding the post-

Fig. 269.—Trigeminal rhythm due to single ventricular extrasystoles (V) of left ventricular origin following every two conducted sinus beats

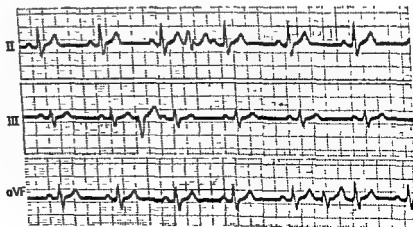




A, B, C, D, E, and F were recorded from different patients but all show

in the above lead strips originate in the ventricles in lead II and V1 and are followed by a normal sinus beat

Fig 271.—Interpolated ventricular extrasystoles with prolonged atrioventricular conduction of the first postectopic sinus beat



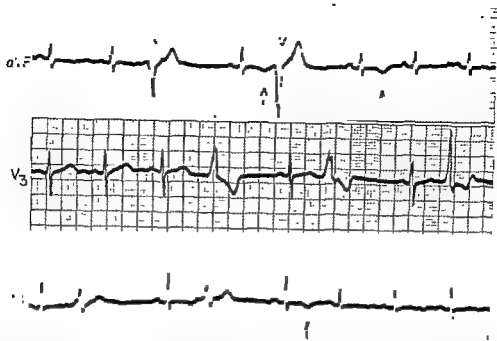


Fig. 272—Postextrasystolic T wave changes. In lead aVF, the T waves following the conducted sinus beats are generally biphasic or essentially isoelectric. However, the T waves of the first postectopic sinus beats following each of the ventricular extrasystoles (V) are inverted. This finding represents a postextrasystolic T wave change. In lead V₃, the T waves following the sinus beats in the right half of the lead strip are lower than the T waves following the consecutive sinus beats on the left. These changes, as well as the T wave inversion indicated by the arrow in lead V₃, also represent postextrasystolic T wave changes.

ectopic sinus beat. This association is demonstrated by the fact that interpolated extrasystoles (without a postectopic pause) never produce T wave changes, while, on the other hand, altered T waves may occasionally follow long pauses in atrial fibrillation or atrial premature beats. Various clinical studies of the phenomenon of postectopic T wave change are in general agreement as to its high incidence in patients with cardiac disease, in contrast to its relative rarity in normal subjects (Figs. 272–274).

Clinical Significance of Coupled Ectopic Beats

The sporadic occurrence of coupled ectopic beats in normal subjects is relatively common, particularly if predisposing influences are present (excess coffee, tea, and tobacco, emotional disturbances, etc.). Consequently, the greater frequency with which extrasystoles occur in patients with diseased hearts is of limited value in establishing the significance of ectopic beats in a given person. The presence of extrasystoles is not in itself indicative of underlying myocardial damage, but certain features of the premature beats have an approximate correlation with the cardiac status of the patient. For example

1. Extrasystoles which occur frequently and have a multifocal origin (based on their differing coupling intervals and appearance) are usually observed in patients with cardiac disease, sometimes as the result of digitalis toxicity.

2. If ectopic beats become more frequent during and immediately after exercise, coronary insufficiency and/or myocardial damage are likely to be present. Tachycardia, exercise induced or otherwise, tends to abolish ectopic beats in normal subjects, but its failure to do so cannot be construed as evidence of cardiac abnormality.

3. Some authorities attach much the same significance as the above to the occurrence of extrasystoles during rapid sinus rhythm or to the presence of both atrial and ventricular extrasystoles in the same electrocardiogram.

4. A bigeminal rhythm consisting of an ectopic beat, usually a ventricular extrasystole, coupled to every sinus beat, is commonly observed in digitalis intoxication. Myocardial disease is probably an additional causative factor in most instances, since it has been proved almost impossible to produce a bigeminal rhythm which is due to ventricular extrasystoles in a normal subject, even with large amounts of digitalis.

5. A finding considered almost pathognomonic of

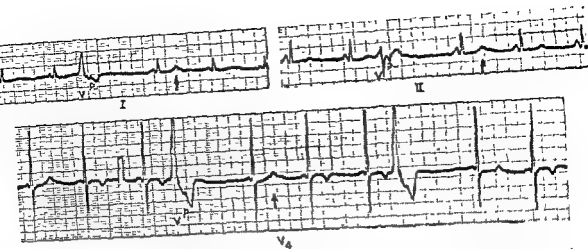
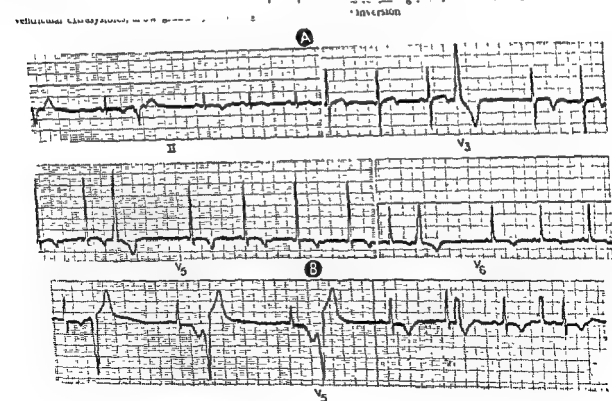


Fig. 273.—Postectrasystolic T wave changes In leads I and II, the upright T wave of the first postectopic sinus beats (indicated by an arrow) is of the ventricular type. The T wave of the first postectopic beat (indicated by an arrow) is of the ventricular type, the ectopic ventricular impulses into the atria

Fig. 274.—Postectrasystolic T wave changes in I In A, the postectrasystolic T wave changes in leads II and V3, the postectrasystolic T wave changes in leads II and V3 are present in sinus beats else



severe digitalis intoxication is the presence of bidirectional ventricular extrasystoles. These appear as paired, oppositely directed ectopic ventricular beats, the QRS complex of one being resultantly positive and the other resultantly negative.

6. Frequent multifocal ectopic beats arising in the atria may precede onset of supraventricular tachycardia, atrial flutter, or fibrillation. Similarly, extrasystoles of ventricular origin may herald onset of paroxysmal ventricular tachycardia, flutter, or fibrillation, particularly if the ectopic beats are super-

imposed on the preceding T waves. More will be said of this in a later discussion of ectopic ventricular tachycardia.

7. In other clinical syndromes, extrasystoles are sometimes an early sign of secondary cardiac involvement. Usually, however, such a wide variety of extracardiac factors are potentially involved, some capable of producing directly or indirectly, ectopic beats, that the significance of the extrasystoles in a given case cannot be clearly defined in the absence of other evidence as to the cardiac status of the patient.

AUTOMATIC ECTOPIC BEATS (PARASYSTOLE)

Parasystole consists of the simultaneous activity of two independent impulse-forming centers, one of which is "protected" from the other, and each competing with the other to activate the atria and/or ventricles. The ectopic parasystolic pacemaker is usually situated in the ventricles (rarely in the atria or atrioventricular node), while the competing rhythm generally emanates from the sinoatrial node. Atrial and

atrioventricular nodal types of parasystole will not be described (although examples are presented in subsequent figures), since the ventricular form is far more common and more clearly illustrates the parasystolic mechanism. Nevertheless, the general principles are the same, irrespective of the location of the parasystolic pacemaker.

Parasystolic ventricular beats differ from coupled

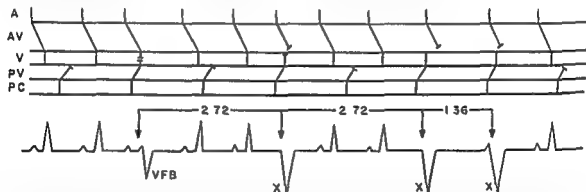


Fig. 275.—Mechanism of ventricular parasystole (Symbols A, atrial beats or P waves, AV, atrioventricular junctional tissues, PC, parasystolic center, PV, junctional tissues between the parasystolic center and the ventricular myocardium, V, ventricular beats, VFB, ventricular fusion beat, and X, ectopic ventricular beats produced by the parasystolic center).

tricular myocardium simultaneously with the sinus impulse, so that the resulting QRS complex is a fusion of the normal

the pacemaker and surrounding ventricular myocardium and to enter the ventricular myocardium before the arrival of the conducted sinus impulse

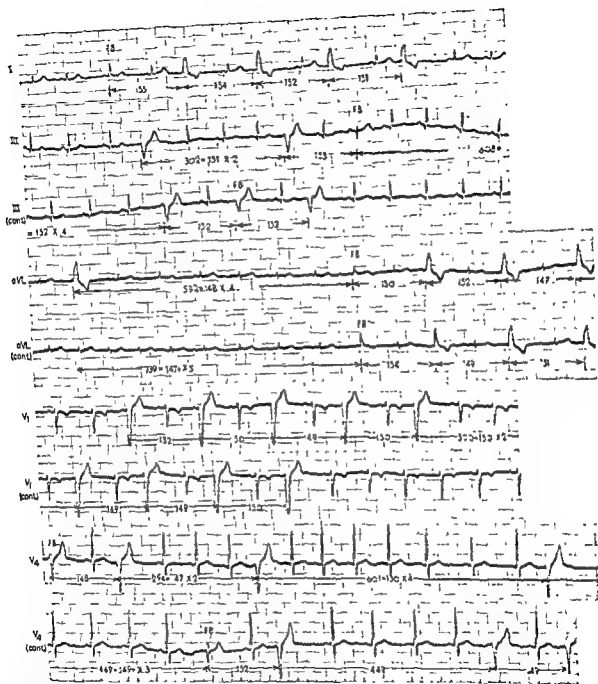


Fig 276.—Ventricular parasystole (Symbol, FB, ventricular fusion beat) In these lead strips, the ectopic ventricular beats show varying coupling intervals, but the interectopic intervals are equal to, or are whole-number multiples of, the basic parasystolic cycle length of approximately 1.52 second In the continuous leads strips of lead aVL, the parasystolic cycle length is shortened to 1.47–1.49 second Ventricular fusion beats are present in lead I and in both strips of lead III

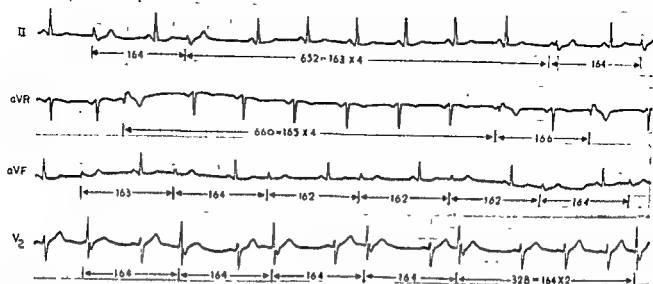
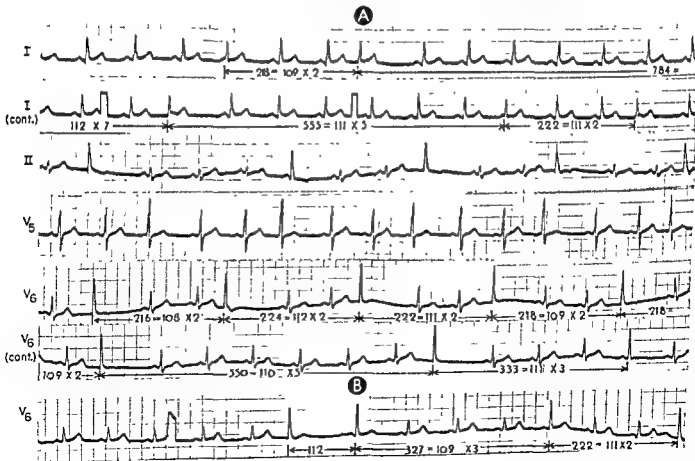


Fig. 277.—Ventricular parasystole. Note the w yet the relatively constant interectopic intervals all longer interectopic intervals are whole-number in lead aVR may possibly be a ventricular fusion beat.

Fig. 278.—Atrioventricular nodal parasystole. In atrioventricular nodal parasystole, ventricular fusion beats are, obviously, not seen. However, the varying coupling intervals and the relatively constant lengths of the measured or calculated parasystolic cycles are compatible with a parasystolic mechanism of the ectopic nodal ventricular beats. The lead strip in B was recorded several days after the lead strips in (A), but the parasystolic cycle length is relatively unchanged.



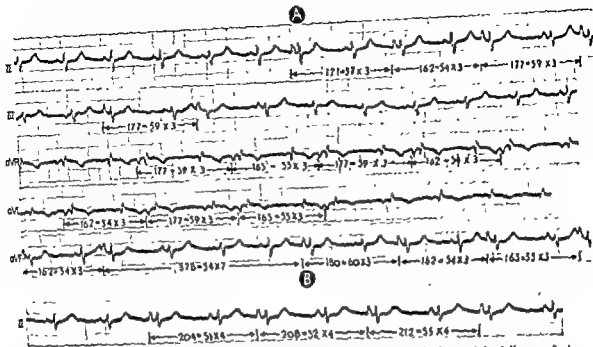


Fig 279—Presumed atrial parasystole. This presumptive diagnosis was made on the basis of the following findings: waves of ectopic origin with widely varying coupling intervals, and a calculated atrial parasystolic cycle length of approximately 0.54 second. The relatively wide variation in the calculated parasystolic cycle lengths may be ascribed to Wenckebach conduction of the parasystolic impulse through the surrounding atrial muscle. Thus, by and large, the longer the interectopic interval, the shorter the calculated parasystolic cycle length, and vice versa. The lead strip in B was recorded several days after the lead strips in A, but the calculated parasystolic cycle length is approximately the same in both.

ventricular beats in that discharge of the parasystolic center does not require a triggering impulse. Instead, the parasystolic pacemaker fires off automatically, rhythmically, and at its own inherent rate of impulse formation (Fig 275). Thus, the ectopic ventricular beats follow sinus beats by irregular intervals (a characteristic often referred to as *inconstant*, or *variable*, coupling) but bear a fixed relationship to one another from the standpoint of their interectopic intervals. In parasystole, all interectopic intervals in a given electrocardiogram can be demonstrated to be whole-number multiples of the shortest interectopic interval measured, or they can all be reduced to a common-denominator interval which corresponds to a single cycle of the ectopic pacemaker. This testifies to the striking regularity with which the parasystolic pacemaker forms and discharges impulses, even though many of the ectopic impulses fail to elicit a ventricular response. The regularity of the parasystolic rhythm indicates that the ectopic pacemaker is "protected" in some way against premature discharge by sinus impulses as they spread through the ventricular myocardium. The protective mechanism is generally believed to consist of an area of unidirectional entrance

block surrounding the parasystolic pacemaker, although this remains a controversial issue.

The number of parasystolic impulses which produce or fail to produce a ventricular beat is dependent on two factors. (1) the relative rates of the sinus and parasystolic rhythms (parasystolic rhythms are usually slow, but rates ranging between 20 and 200 per minute may be seen), and (2) the presence or absence of exit block (see below), or its equivalent, around the ectopic pacemaker. The faster the sinus rhythm and the slower the ectopic rhythm, the more likely it is that an ectopic impulse will be discharged while the ventricles are still refractory from previous excitation by a sinus beat. In other words, the sinus beat interferes with the parasystolic impulse in the ventricles. Sometimes the sinus and ectopic impulses arrive more or less simultaneously in the ventricles and each activates a part of the myocardium. Since two excitation processes jointly produce the ventricular deflection, the latter presents a configuration intermediate between that of parasystolic and sinus beats elsewhere in the record. This is called a *ventricular fusion beat*, and the presence of beats of this type is strongly suggestive of ventricular parasystole. Al-

though ventricular fusion beats are typical of parasystole, they may also be observed when ventricular extrasystoles with long coupling intervals occur during sinus arrhythmia.

Exit block surrounding the parasystolic pacemaker is suggested by the following: (1) a parasystolic impulse calculated to arrive outside the refractory period of the ventricular myocardium fails to produce a ventricular beat; and (2) the calculated rate of the parasystolic pacemaker exceeds that of the sinus node, but the expected paroxysmal ectopic tachycardia fails to appear. In either of the foregoing circumstances it must be assumed that some of the impulses discharged by the parasystolic center are prevented from entering and activating the ventricular myocardium. The specific mechanism responsible for the so-called exit block has not been established with certainty.

The electrocardiographic features of ventricular parasystole can be summarized as follows:

- 1 The ectopic ventricular beats are not coupled to a preceding beat—that is, they do not follow the initial sinus beat by a relatively fixed interval
- 2 Although the interectopic intervals may differ in

length, they are all whole-number multiples of a single common interval which corresponds to the cycle length of the parasystolic pacemaker.

3. The ectopic beats themselves display the widened, deformed appearance characteristic of beats arising in the ventricles below the bifurcation of the bundle of His. In addition to the conducted sinus beats and parasystolic beats, ventricular fusion beats of intermediate contour are usually observed in ventricular parasystole and constitute a finding of diagnostic significance. Very infrequently, ventricular fusion beats occur with coupled ventricular extrasystoles having long fixed coupling intervals, particularly if sinus arrhythmia is also present; ventricular fusion beats are sometimes observed in almost complete atrioventricular block with idioventricular pacemaker.

The identification of ventricular parasystole has been stressed because ectopic ventricular beats due to parasystole are almost always indicative of underlying cardiac disease, while coupled ectopic beats may occur in normal and abnormal hearts (Figs. 276–279)

Ectopic Tachycardias; Flutter and Fibrillation

PAROXYSMAL ECTOPIC TACHYCARDIA

Mechanisms

In its most abbreviated form, paroxysmal ectopic tachycardia may consist of as few as six ectopic beats appearing one after another in rapid succession. The first ectopic beat is triggered by the last sinus impulse or by the last beat of the prevailing rhythm, while each subsequent extrasystole is initiated by, and in turn initiates, another ectopic beat. In reality, paroxysmal tachycardia is composed of consecutive coupled ectopic beats, essentially the same as those occurring singly and sporadically or in bigeminal and trigeminal rhythms. There is abundant clinical and experimental evidence favoring the close affinity between paroxysmal tachycardia and isolated coupled ectopic beats. In fact, the theories relating to the mechanism of paroxysmal tachycardia, which are summarized below, are merely extensions of those previously described in the section on coupled extrasystoles in Chapter 25.

Re-entry—The theory of re-entry proposes that the initial sinus impulse, after exciting all responsive muscle, returns by a devious route to a focus of previous refractoriness. Here the excitation impulse is picked up by the now responsive tissues and introduced back again into conduction pathways traversed in the initial cycle. The re-entry impulse produces an ectopic beat which is coupled to the preceding sinus beat. If, instead of a single re-entry cycle, there occur repeated cycles of re-entry, it is thought that paroxysmal tachycardia may result.

Single focus of subthreshold activity—An ectopic focus of automatic impulse formation—that is, a parasystolic pacemaker—on rare occasions may give rise

to paroxysmal tachycardia. With this exception, most tachycardias are believed by Scherf to have the same underlying mechanism as coupled ectopic beats, the only difference being that each paroxysmal beat provides the triggering impulse for the next to follow. The ability of the ectopic focus to respond so rapidly and repetitively to initiating stimuli is probably related to the rapidity with which the focus, after discharge, regains its previous subthreshold state.

General Considerations

Paroxysmal tachycardias may arise in the atria, atrioventricular node, or ventricles. However, electrocardiographically it is frequently difficult, and sometimes impossible, to differentiate with any degree of certainty an atrial tachycardia from a nodal tachycardia. In this text, the terms *atrial* and *atrioventricular nodal* will not be used when the identity of a tachycardia is uncertain or when the facts under discussion are equally relevant to both types of tachycardia. Instead, paroxysmal tachycardias arising in the atrioventricular node or above will be referred to as *supraventricular tachycardias* and discussed under this general heading. In fact, there is little practical advantage to be gained from the differentiation of atrial and nodal tachycardias, since their clinical implications, therapy, and, as already mentioned, electrocardiographic features are often similar. On the other hand, clinically and in other respects, ventricular tachycardias are entirely different from supraventricular tachycardias. In short, the salient electrocardiographic fact to be established with reference to a tachycardia is its site of origin, whether supraventricular or ventricular.

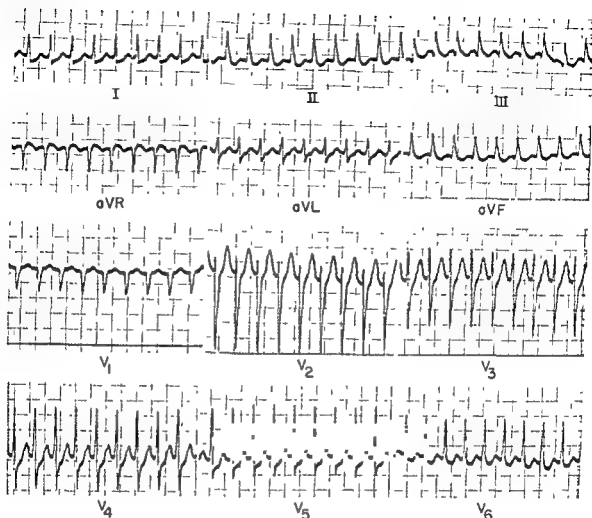


Fig. 280.—Paroxysmal supraventricular tachycardia, probably originating in the atria. The ventricular rate is 215 beats per minute. QRS deflections. The depre...

tricular (atrial or atrioventricular nodal) or ventricular.

Atrial, nodal, and ventricular tachycardias have the following features in common

1. The ectopic tachycardias occur in paroxysms of abrupt onset and offset.
2. The paroxysms tend to recur, the likelihood of such a recurrence being all the greater if there is a history of any previous attacks.
3. Before, after, and during intervals between attacks of paroxysmal tachycardia, the electrocardiogram frequently records single ectopic beats resembling those present during tachycardia and having the same coupling interval as the first beat of a paroxysm of tachycardia.
4. Occasionally, paroxysmal tachycardia persists only for a matter of minutes and passes without notice. Tachycardias which produce symptoms usually last several hours but may continue without interrup-

tion for days or, rarely, weeks. Sometimes, paroxysmal tachycardia takes the form of a *repetitive tachycardia*, which is characterized by persistently recurring paroxysms of approximately 20–200 extrasystoles, each paroxysm separated from the other by several sinus beats. These short, interrupted runs of tachycardia tend to be repeated over and over again, and in general are relatively refractory to therapy. Repetitive tachycardia may continue for months and then subside spontaneously, never to reappear.

5. Offset of a paroxysmal tachycardia is often followed by a long pause before the sinus pacemaker finally takes over, or there may be a period of slow sinus rhythm or of nodal escape. The reason for this is that the ectopic tachycardia depresses the sinus node. In a badly diseased heart this depression can be of such severe degree as to lead to prolonged cardiac standstill.

6. After a prolonged episode of paroxysmal tachy-

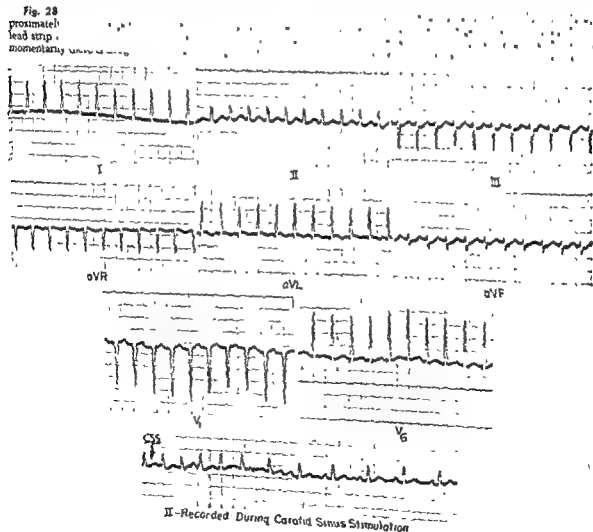
cardia, older patients with cardiac disease, and occasionally some persons without detectable heart disease, may show abnormal T wave changes in their electrocardiograms. The findings can persist from several hours or days to several weeks after termination of the tachycardia. This has been designated the post-tachycardia electrocardiographic syndrome. Several fatal cases of this type were found at autopsy to have "diffuse areas of subendocardial fibrosis."

Paroxysmal Supraventricular Tachycardia

In paroxysmal supraventricular tachycardia, the P waves, when identifiable, usually differ from those observed in the same patient during sinus rhythm. In tachycardias originating in the cephalic region of the atria, the ectopic P waves are upright in leads I and II. Tachycardias arising in the caudal aspect of the

atria or in the atrioventricular node are associated with inverted P waves in leads II, III, and aVF and upright P waves in leads I and aVR. In both atrial and nodal tachycardia

usually of normal duration from the same patient during sinus rhythm (Fig. 250). The exception to this rule is that ventricular aberration sometimes may alter the appearance of the QRS complexes in either type of tachycardia, as will be described later. Occasionally, nodal and atrial tachycardias can be differentiated from each other by the fact that in nodal tachycardia inverted P waves precede the QRS complexes by less than 0.12 second, while in atrial tachycardia upright or inverted P waves are followed by ventricular complexes after a P-R interval of 0.12 second or longer. However, it is often difficult to be certain whether the inverted P waves are associated with the preceding or following



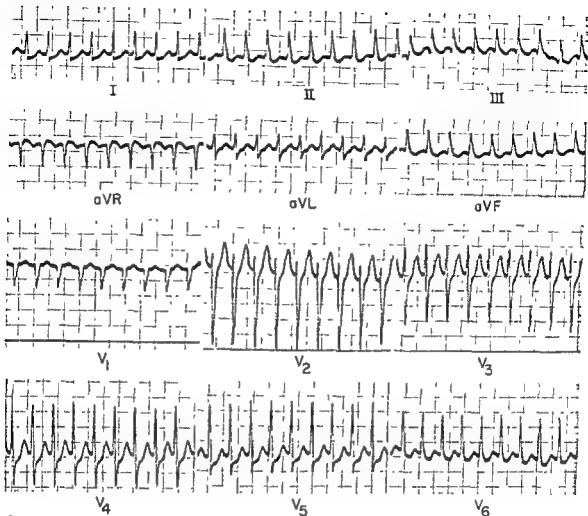


Fig. 280.—Paroxysmal tachycardia. Atrial tachycardia. QRS deflections are indicative of atrial tachycardia. The depressed S-T

tricular (atrial or atrioventricular nodal) or ventricular tachycardias have the following features in common:

1. The ectopic tachycardias occur in paroxysms of abrupt onset and offset
2. The paroxysms tend to recur, the likelihood of such a recurrence being all the greater if there is a history of any previous attacks.
3. Before, after, and during intervals between attacks of paroxysmal tachycardia, the electrocardiogram frequently records single ectopic beats resembling those present during tachycardia and having the same coupling interval as the first beat of a paroxysm of tachycardia.
4. Occasionally, paroxysmal tachycardia persists only for a matter of minutes and passes without notice. Tachycardias which produce symptoms usually last several hours but may continue without interrup-

tion for days or, rarely, weeks. Sometimes, paroxysmal tachycardia takes the form of a *repetitive tachycardia*, which is characterized by persistently recurring paroxysms of approximately 20–200 extrasystoles, each paroxysm separated from the other by several sinus beats. These short, interrupted runs of tachycardia tend to be repeated over and over again, and in general are relatively refractory to therapy. Repetitive tachycardia may continue for months and then subside spontaneously, never to reappear.

5. Offset of a paroxysmal tachycardia is often followed by a long pause before the sinus pacemaker finally takes over, or there may be a period of slow sinus rhythm or of nodal escape. The reason for this is that the ectopic tachycardia depresses the sinus node. In a badly diseased heart this depression can be of such severe degree as to lead to prolonged cardiac standstill.

6. After a prolonged episode of paroxysmal tachy-

during sinus rhythm, and their duration does not exceed 0.10 second. However, if the rate of the tachycardia is sufficiently rapid, the intraventricular conducting pathways and ventricular muscle may not have enough time to recover completely before arrival of each succeeding impulse. This can lead to

conduction disturbance is present during an atrial tachycardia, the abnormal appearance of the ventricular complexes may give the impression that the tachycardia originates in the ventricles, particularly if the ectopic P waves of the atrial tachycardia are poorly defined or obscured. Atrioventricular nodal tachycardia with ventricular aberration cannot ordinarily be differentiated from ventricular tachycardia, unless the recorded onset or offset of the paroxysm demonstrates frequent nodal extrasystoles.

Whenever the electrocardiogram shows a tachycardia of apparent supraventricular origin, an alternative diagnostic possibility—which should always be entertained and, if possible, excluded—is atrial flutter with persisting 2:1 atrioventricular response. Carotid sinus stimulation should always be attempted in such a situation, since the resulting vagal stimulation causes the ventricular rate to slow in atrial flutter, whereas it either abolishes or has no effect on a supraventricular tachycardia (Figs 281 and 282). The differential diagnosis of atrial flutter and supraventricular tachycardia is considered at greater length later in this chapter.

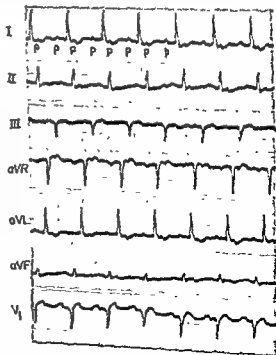
In the experience of some investigators, paroxysmal supraventricular tachycardias with very rapid rates seem less likely to be terminated by carotid sinus stimulation than those with slower rates. Although supraventricular tachycardia typically shows 1:1 atrioventricular response, variations in atrioventricular conduction may occur, running the gamut from interference phenomena such as P-R interval prolongation or 2:1 atrioventricular response (Fig. 283) to high degrees of atrioventricular block. In tachycardias with very rapid rates, diastole may be so shortened that the junctional tissues are never able to recover completely. This may lead to slower atrioventricular conduction of the supraventricular impulses or to 2:1 atrioventricular conduction in which every other impulse arrives at the atrioventricular node during its normal refractory period and is not conducted. In either case, one supraventricular impulse interferes with atrioventricular conduction of the following impulse (atrioventricular interference.). Failure of every second impulse to be conducted may occur in tachycardias with relatively

interference of atrioventricular block, is sometimes impossible to determine, but, in general, 2:1 atrioventricular response in tachycardias with rates below 200 beats per minute implies depressed atrioventricular conductivity. On the other hand, the atrioventricular junctional tissues cannot normally maintain a 1:1 response to more than 200–250 impulses per minute; and so, 2:1 conduction in tachycardias within this rate can be attributed to atrioventricular interference.

Three-to-one (or 4:1, 5:1, etc.) atrioventricular response or variable atrioventricular response in supraventricular tachycardia is usually indicative of impaired atrioventricular conductivity and may be produced by excess digitalis, by degenerative or in-

Fig. 283.—Paroxysmal atrial tachycardia with 2:1 atrioventricular response. The rate of the paroxysmal atrial tachycardia is 200 beats per minute, while the ven-

is not necessarily an indication of atrioventricular block in this instance, since the nonconducted P waves arrive at the atrioventricular junction during its normal refractory period. It will be recalled that the normal refractory period of the atrioventricular node coincides approximately with the Q-T interval of the electrocardiogram. In the tachycardia record shown here, the nonconducted P wave always falls within the Q-T interval of the preceding ventricular beat.



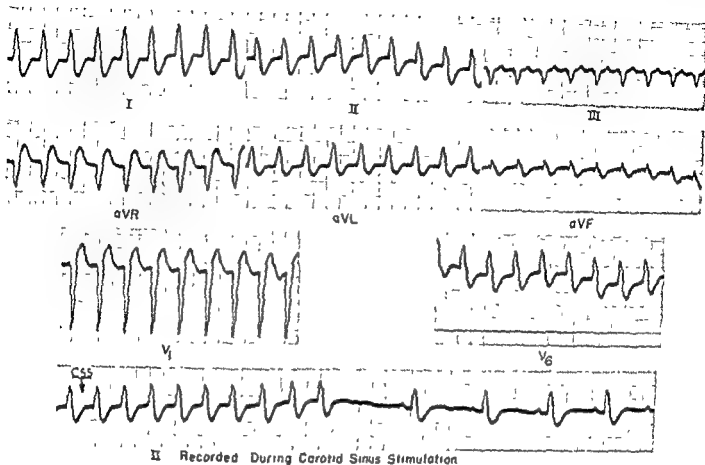


Fig 282 ~Paroxysmal tachycardia, with a ventricular rate of about 150 beats per minute. The ventricular rhythm is

QRS complexes, and so, in many instances the P-QRS relationship is not helpful in separating the two types of supraventricular tachycardia. When present, atrioventricular dissociation is perhaps the most reliable point of distinction between an atrial and an atrioventricular nodal tachycardia, provided, of course, the two do not coexist (combined paroxysmal tachycardias). Even though atrioventricular dissociation is present, the diagnosis of atrioventricular nodal tachycardia can only be made if the ventricular deflections have a duration of 0.10 second or less. If the QRS interval is wider than this, it usually is impossible to differentiate nodal tachycardia with aberration from ventricular tachycardia.

Paroxysmal supraventricular tachycardias can exhibit rates ranging from a little over 100 beats per minute in nodal tachycardias or 140 beats per minute in atrial tachycardias to as fast as 220 beats per minute, although rates of 150–190 beats per minute are commonly encountered. Once a supraventricular

tachycardia has become established, its rate remains constant and its rhythm strikingly regular, the cycle length varying only infrequently by more than 0.01 second from beat to beat. However, during onset of a paroxysm, the ectopic beats occur somewhat irregularly and with an accelerating rate until finally the tachycardia becomes established. This initial phase is referred to as the warm-up period of the tachycardia. Shortly before offset of a tachycardia, there is slowing of its rate, and, with the appearance of the last beat of the paroxysm, a noncompensatory pause follows. Whether the first postectopic beat proves to be a sinus beat, a supraventricular beat from a displaced pacemaker, or an atrioventricular nodal or ventricular escape beat is determined largely by the degree of sinus node depression induced by the supraventricular tachycardia as well as by the relative rhythmicity of the ectopic pacemakers.

In the usual supraventricular tachycardia, the configuration of the QRS complexes is the same as

during sinus rhythm, and their duration does not exceed 0.10 second. However, if the rate of the tachycardia is sufficiently rapid, the intraventricular conducting pathways and ventricular muscle may not have enough time to recover completely before arrival of each succeeding impulse. This can lead to aberrant intraventricular conduction of the supraventricular impulses or to the appearance of previously latent bundle branch block. When an intraventricular conduction disturbance is present during an atrial tachycardia, the abnormal appearance of the ventricular complexes may give the impression that the tachycardia originates in the ventricles, particularly if the ectopic P waves of the atrial tachycardia are poorly defined or obscured. Atrioventricular nodal tachycardia with ventricular aberration cannot ordinarily be differentiated from ventricular tachycardia, unless the recorded onset or offset of the paroxysm demonstrates frequent nodal extrasystoles.

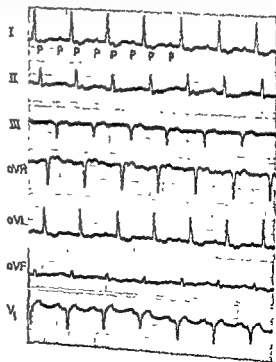
Whenever the electrocardiogram shows a tachycardia of apparent supraventricular origin, an alternative diagnostic possibility—which should always be entertained and, if possible, excluded—is atrial flutter with persisting 2:1 atrioventricular response. Carotid sinus stimulation should always be attempted in such a situation, since the resulting vagal stimulation causes the ventricular rate to slow in atrial flutter, whereas it either abolishes or has no effect on a supraventricular tachycardia (Figs. 281 and 282). The differential diagnosis of atrial flutter and supraventricular tachycardia is considered at greater length later in this chapter.

In the experience of some investigators, paroxysmal supraventricular tachycardias with very rapid rates seem less likely to be terminated by carotid sinus stimulation than those with slower rates. Although supraventricular tachycardia typically shows 1:1 atrioventricular response, variations in atrioventricular conduction may occur, running the gamut from interference phenomena such as P-R interval prolongation or 2:1 atrioventricular response (Fig. 283) to high degrees of atrioventricular block. In tachycardias with very rapid rates, diastole may be so shortened that the junctional tissues are never able to recover completely. This may lead to slower atrioventricular conduction of the supraventricular impulses or to 2:1 atrioventricular conduction in which every other impulse arrives at the atrioventricular node during its normal refractory period and is not conducted. In either case, one supraventricular impulse interferes with atrioventricular conduction of the following impulse (atrioventricular interference.) Failure of every second impulse to be conducted may occur in tachycardias with relatively

slower rates if the refractory period of the atrioventricular node is prolonged (atrioventricular block). The mechanism involved, whether atrioventricular interference or atrioventricular block, is sometimes impossible to determine, but, in general, 2:1 atrioventricular response in tachycardias with rates below 200 beats per minute implies depressed atrioventricular conductivity. On the other hand, the atrioventricular junctional tissues cannot normally maintain a 1:1 response to more than 200–250 impulses per minute, and so, 2:1 conduction in tachycardias within this rate can be attributed to atrioventricular interference.

Three-to-one (or 4:1, 5:1, etc.) atrioventricular response or variable atrioventricular response in supraventricular tachycardia is usually indicative of impaired atrioventricular conductivity and may be produced by excess digitalis, by degenerative or in-

Fig. 283.—Paroxysmal atrial tachycardia with 2:1 atrioventricular response. The rate of the paroxysmal atrial tachycardia is 200 beats per minute, while the ventricular rate is exactly one half as fast. The symbol P indicates the ectopic atrial beats in lead I. The failure of every other atrial beat to be conducted into the ventricles is not necessarily an indication of atrioventricular block in this instance, since the nonconducted P waves arrive at the atrioventricular junction during its normal refractory period. It will be recalled that the normal refractory period of the atrioventricular node coincides approximately with the Q-T interval of the electrocardiogram. In the tachycardia record shown here, the nonconducted P wave always falls within the Q-T interval of the preceding ventricular beat.



flammatory changes in the atrioventricular node, or by other influences. Sometimes, when the refractory period of the atrioventricular node is lengthened by one of the foregoing factors, recovery of the depressed junctional tissues after each conducted beat may be progressively less complete. Successive supraventricular beats are conducted, therefore, with gradually lengthening P-R intervals until one beat finally arrives during the absolute refractory period of the node and is blocked (Fig. 281). Because of the longer recovery period allotted the atrioventricular node by the resulting pause, the first conducted beat thereafter has a shorter P-R interval than those following, which show the same progressive increments in their P-R intervals as the beats of the preceding cycle. This cyclic change in the P-R intervals of successive beats, called the Wenckebach phenomenon, typifies the

common form of incomplete atrioventricular block (Figs. 285-287).

In addition to variations in forward atrioventricular conduction such as those just described (Fig. 288), nodal tachycardias frequently are accompanied by disturbances of retrograde conduction (Fig. 289), which may present electrocardiographically in the following forms:

Atrioventricular dissociation.—Failure of the nodal pacemaker to take over the atria can be due to retrograde atrioventricular block and/or interference (Fig. 290).

Incomplete retrograde atrioventricular block with Wenckebach phenomenon.—This form (see Fig. 248) is characterized by a shift of each successive retrograde P wave farther behind the QRS complex of the nodal beat until a retrograde P wave eventually

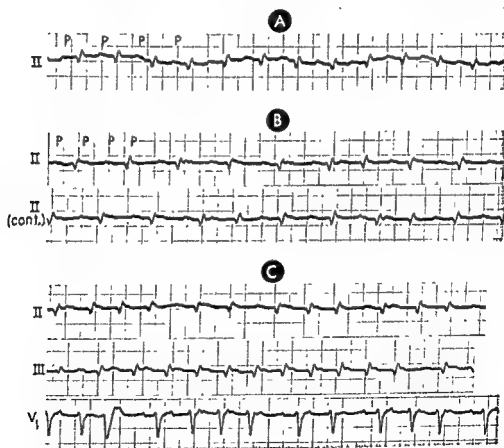


Fig. 281. Nodal atrial tachycardia with varying atrioventricular response. In A, lead II displays a sinus tachycardia and 3:2 response at other times. The ectopic atrial P waves are labeled P in this lead. During the periods of incomplete atrioventricular conduction, the P-R intervals of the conducted beats show the progressive lengthening characteristic of Wenckebach incomplete atrioventricular block. In B, there is 4:3 Wenckebach atrioventricular conduction, and at other times 3:2 conduction. The presence of varying ratios of atrioventricular response accompanied by the Wen-

and 3:2 response at other times. The ectopic atrial P waves are labeled P in this lead. During the periods of incomplete atrioventricular conduction, the P-R intervals of the conducted beats show the progressive lengthening characteristic of Wenckebach incomplete atrioventricular block. In B, there is 4:3 Wenckebach atrioventricular conduction, and at other times 3:2 conduction. The presence of varying ratios of atrioventricular response accompanied by the Wen-

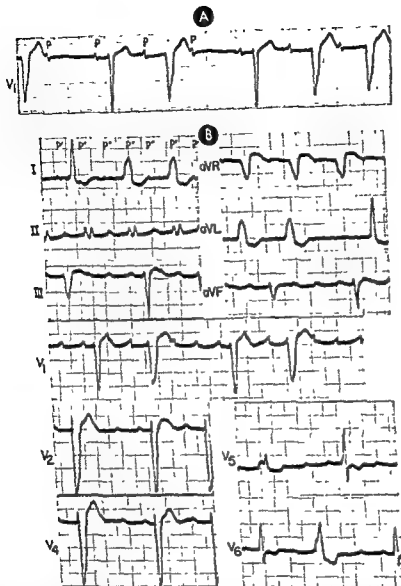


Fig. 285—Paroxysmal atrial tachycardia with Wenckebach incomplete atrioventricular block and intermittent left bundle branch block. In lead V_1 in A, sinus P waves (P') appear at a rate of about 60 per minute, and there is 3.2 Wenckebach incomplete atrioventricular block. Note that the QRS complex of the first conducted sinus beat after the blocked sinus beat is of normal duration, while the next conducted sinus beat produces a widened rS deflection, suggestive of complete left bundle branch block. Record B was made 1 day after record A. P waves (P') now appear at a rate of 160 per minute, and their configuration in lead V_1 differs from that in the same lead in A; thus, a paroxysmal atrial tachycardia is present.

flammatory changes in the atrioventricular node, or by other influences. Sometimes, when the refractory period of the atrioventricular node is lengthened by one of the foregoing factors, recovery of the depressed junctional tissues after each conducted beat may be progressively less complete. Successive supraventricular beats are conducted, therefore, with gradually lengthening P-R intervals until one beat finally arrives during the absolute refractory period of the node and is blocked (Fig. 284). Because of the longer recovery period allotted the atrioventricular node by the resulting pause, the first conducted beat thereafter has a shorter P-R interval than those following, which show the same progressive increments in their P-R intervals as the beats of the preceding cycle. This cyclic change in the P-R intervals of successive beats, called the Wenckebach phenomenon, typifies the

common form of incomplete atrioventricular block (Figs. 285-287).

In addition to variations in forward atrioventricular conduction such as those just described (Fig. 288), nodal tachycardias frequently are accompanied by disturbances of retrograde conduction (Fig. 289), which may present electrocardiographically in the following forms:

Atrioventricular dissociation.—Failure of the nodal pacemaker to take over the atria can be due to retrograde atrioventricular block and/or interference (Fig. 290).

Incomplete retrograde atrioventricular block with Wenckebach phenomenon.—This form (see Fig. 248) is characterized by a shift of each successive retrograde P wave farther behind the QRS complex of the nodal beat until a retrograde P wave eventually

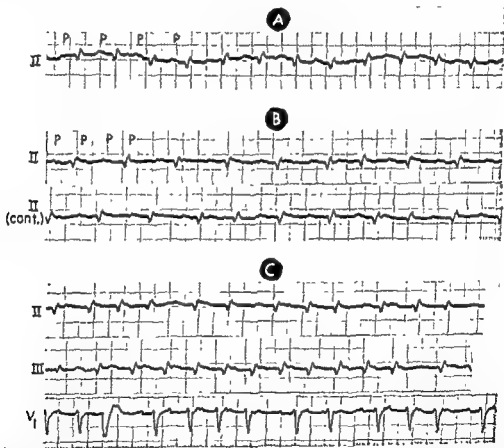


Fig. 284.—Paroxysmal atrial tachycardia with varying atrioventricular response. In A, lead II displays a sinus tachycardia with each atrial P wave (P) being conducted into the ventricles. However, in B, the continuous strip of lead II

shows incomplete atrioventricular block. In C, there is 4:3 Wenckebach atrioventricular conduction, and at other times 1:1 atrioventricular conduction. The presence of varying ratios of atrioventricular response accompanied by the Wenckebach phenomenon is usually indicative of an abnormal refractoriness of the atrioventricular junctional tissues, whether due to intrinsic atrioventricular node disease or to depression secondary to digitalis effect or vagal stimulation.



Fig. 299 Paroxysmal atrioventricular nodal tachycardia with retrograde activation of the atria and a 1:2 ventricular rate. Each ventricular complex is preceded by an R-P interval.

fails to appear or is replaced by a sinus P wave.

Incomplete retrograde atrioventricular block with constant R-P intervals—This type (Fig. 291) usually produces 1:2 atrioventricular response, every other retrograde P wave being absent. Sometimes the "dropping" of a retrograde P wave occurs at irregular intervals.

First-degree retrograde block, as evidenced by R-P intervals of 0.20 second or longer, undoubtedly occurs in nodal tachycardia but is usually impossible to establish with certainty, because the lengthened R-P interval makes it all the more difficult to determine whether the retrograde P wave accompanies the preceding or the following ventricular complex.

The frequency with which paroxysmal atrial tachycardia with atrioventricular block occurs as a mani-

festation of digitalis intoxication has been emphasized by many investigators. This form of supraventricular tachycardia is thought to resemble, physiologically, atrial flutter because of (a) the manner in which the paroxysmal atrial tachycardia with atrioventricular block responds to various therapeutic agents and (b) its refractoriness, in most instances, to carotid sinus stimulation. Therefore, it is not surprising that the differentiation of atrial tachycardia with atrioventricular block from a relatively slow atrial flutter often presents a difficult problem. As a general rule, an atrial rate above 200 beats per minute favors atrial flutter, while a slower atrial rate supports the diagnosis of atrial tachycardia. Other equally arbitrary

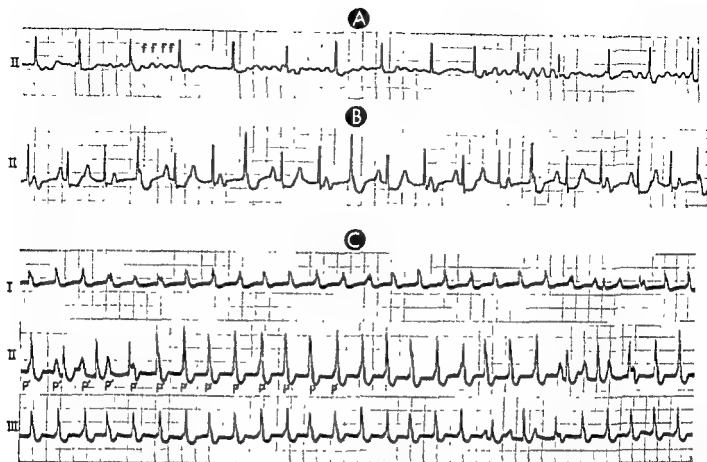


Fig. 286.—Transition from atrial fibrillation to paroxysmal atrial tachycardia with atrioventricular block occurring
s were recorded from the same patient during the

complete atrioventricular block with varying ratios of atrioventricular response. Consequently, the strip of lead II in B with atrioventricular block. (This lead strip was recorded strips in C were obtained about 1 hour later than those in B. The rate as previously, and the ectopic P waves (P') are best demonstrated in lead II. The P wave buried in the first QRS complex in lead II is nonconducted, while the next P wave is conducted. Finally, the 2-R intervals again. Thus, for the greater portion of the lead strip, there is 1:1 atrioventricular conduction.

points of distinction have been proposed, but none of the present criteria are entirely satisfactory. According to Lown, Wyatt, and Levine, the electrocardiographic features which tend to distinguish paroxysmal atrial tachycardia with atrioventricular block from atrial flutter are as follows:

1. In atrial flutter, the atrial rate generally exceeds 250 beats per minute, while in paroxysmal atrial tachycardia with atrioventricular block the atrial rate usually ranges from 150 to 250 beats per minute.
2. In atrial flutter, the atrial deflections in leads II and III are downwardly directed and are associated with an oscillating saw-tooth appearance of the base line. In paroxysmal atrial tachycardia with block, the atrial deflections are upright in leads II and III and are separated by an isoelectric base line (Fig. 283).
3. In pure atrial flutter, the atrial rhythm is perfectly regular, but in about one half of the cases of paroxysmal atrial tachycardia with block, the P-P intervals vary in length by 0.02-0.12 second.

CLINICAL SIGNIFICANCE OF SUPRAVENTRICULAR TACHYCARDIA

Supraventricular tachycardias, like single coupled atrial or nodal extrasystoles, may occur in normal or diseased hearts. In a large series of cardiac patients whose records were reviewed by Kissane and his associates, there was a 3.6% incidence of supraventricular tachycardia. Of the patients with electrocardiograms showing supraventricular tachycardia, about one third were considered to have normal hearts, another third had rheumatic heart disease; and about one sixth, arteriosclerotic heart disease. The remaining patients had thyrocardiac or hypertensive heart disease or other conditions. The association of supraventricular tachycardia with the Wolff-Parkinson-White syndrome and various forms of congenital heart disease, such as interatrial septal defect and Eisenmenger's complex, is also well recognized.

A person with a normal heart usually tolerates supraventricular tachycardia reasonably well unless the ventricular rate is very fast. Inasmuch as the car-



Supraventricular nodal tachycardia with retrograde activation of the atria and a ventricular rate of 150 bpm.

low the QRS deflections. Moreover in lead aVF, comparison of the QRS configuration with the first several sinus beats

inverted sinus waves (P). The reason for the variation in retrograde atrioventricular conduction of the atrioventricular nodal impulses in the above record is not clear.

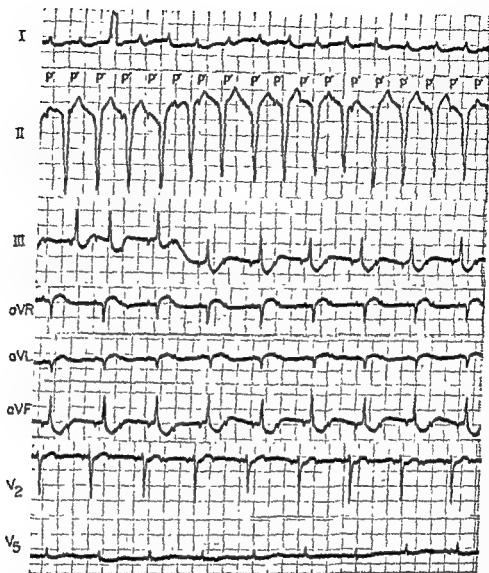


Fig. 288.—The mechanism and site of origin of the ectopic tachycardia present in this record cannot be established with certainty. In leads I and II, the ventricular rhythm is slightly irregular and has a rate of about 145 beats per minute, but ectopic P waves (P') can be identified which occur at a rate of about 170 beats per minute and are inverted in lead II. While it is possible that the inverted P waves in lead II are related to the ventricular beats occurring in this lead, the relatively minor variation in the R-R cycle length, as contrasted to the more marked variation in the P-R intervals, suggests that there is dissociation of the atrial and ventricular rhythms. Despite the aberration of the QRS deflections in leads I and II, their normal duration tends to exclude the possibility of ventricular tachycardia and favors tachycardia of atrioventricular nodal origin. One possible explanation for the findings in lead I and II is that the inverted P waves in lead II represent an atrial tachycardia originating low in the atria, while an atrioventricular nodal tachycardia is simultaneously present in the ventricle with incomplete or complete atrioventricular dissociation. In lead III, the first inverted P wave is not conducted, while the second and third P waves are transmitted into the ventricles with gradually lengthening P-R intervals. The fourth P wave is not conducted, and from that point on, throughout the remaining portion of lead III and the rest of the lead strips shown, there is supraventricular tachycardia with 2:1 atrioventricular conduction. If the findings in lead I and II were to be ignored, then the remaining leads of the electrocardiogram could be interpreted, alternatively, as atrioventricular nodal tachycardia, or as atrial tachycardia, with antegrade 2:1 atrioventricular block.

points of distinction have been proposed, but none of the present criteria are entirely satisfactory. According to Lown, Wyatt, and Levine, the electrocardiographic features which tend to distinguish paroxysmal atrial tachycardia with atrioventricular block from atrial flutter are as follows:

1. In atrial flutter, the atrial rate generally exceeds 250 beats per minute, while in paroxysmal atrial tachycardia with atrioventricular block the atrial rate usually ranges from 150 to 250 beats per minute.

2. In atrial flutter, the atrial deflections in leads II and III are downwardly directed and are associated with an oscillating saw-tooth appearance of the base line. In paroxysmal atrial tachycardia with block, the atrial deflections are upright in leads II and III and are separated by an isoelectric base line (Fig. 283).

3. In pure atrial flutter, the atrial rhythm is perfectly regular; but in about one half of the cases of paroxysmal atrial tachycardia with block, the P-P intervals vary in length by 0.02–0.12 second.

CLINICAL SIGNIFICANCE OF SUPRAVENTRICULAR TACHYCARDIA

Supraventricular tachycardias, like single coupled premature beats, may occur in normal or

associates, there was a 3.6% incidence of supraventricular tachycardia. Of the patients with electrocardiograms showing supraventricular tachycardia, about one third were considered to have normal hearts, another third had rheumatic heart disease, and about one sixth, arteriosclerotic heart disease. The remaining patients had thyrocardiac or hypertensive heart disease or other conditions. The association of supraventricular tachycardia with the Wolff-Parkinson-White syndrome and various forms of congenital heart disease, such as interatrial septal defect and Eisenmenger's complex, is also well recognized.

A person with a normal heart usually tolerates supraventricular tachycardia reasonably well unless the ventricular rate is very fast. Inasmuch as the car-



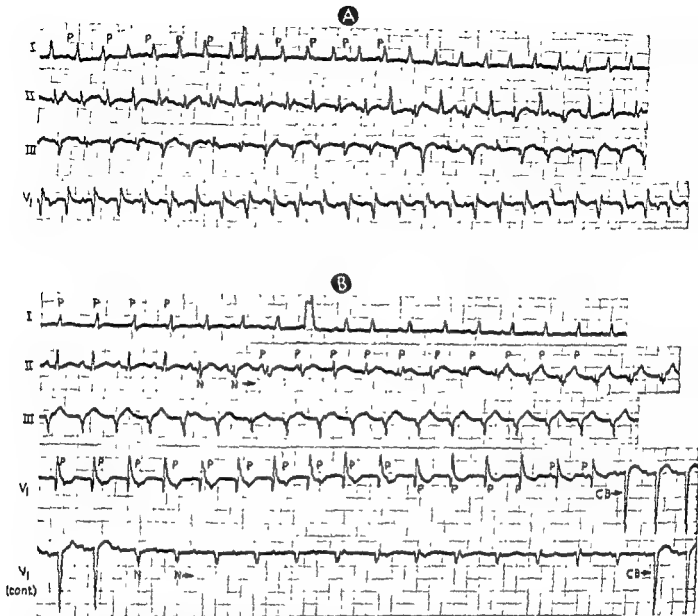


Fig. 290.—Paroxysmal atrioventricular nodal tachycardia with atrioventricular dissociation. The lead strips in A display a relatively regular tachycardia with a ventricular rate of about 150 beats per minute and QRS deflections of relatively normal duration. With some difficulty, upright sinus P waves (P) can be identified in all four lead strips shown, the P waves occurring at a slower rate and with a rhythm unrelated to the ventricular rhythm. In view of the latter findings, the diagnosis of atrioventricular dissociation (with sinoatrial rhythm in the atria) can be made, and the ventricular rate of the normal duration of the ion within a given lead strip may nodal beats to display ventricular aberration. The lead strips presented in B were recorded from the same patient a short time after those in A. The mechanism of the rhythm is best illustrated in leads II and V₁. The first four ventricular beats in lead II are produced by conducted sinus impulses, however, the fifth and subsequent ventricular complexes (N) are of atrioventricular nodal origin and occur at a rate of about 112 beats per minute. Sinus P waves (P) appearing at a slightly slower rate can be spaced off without interruption, indicating that there is atrioventricular dissociation. Note that, with onset of the atrioventricular nodal rhythm, there is an immediate change in QRS configuration, although there is only slight prolongation of the QRS duration. In lead V₁, there is a long period of dissociation, which, at the point indicated by the arrow and CB, anode of sinus rhythm in the ventricles. Note that, with onset of :

nodal tachycardia differs from that of the nodal beats present in the atrioventricular nodal tachycardia occurring in the first half of the lead strip of lead V₁.

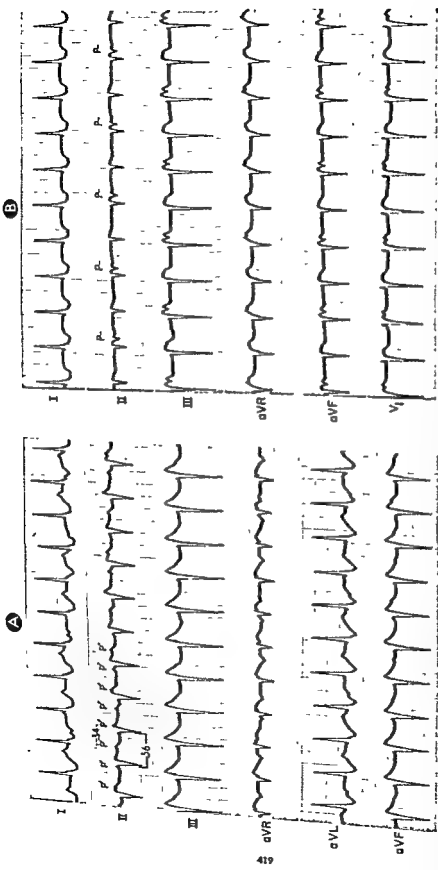


Fig. 291.—In A, there are present simultaneously a paroxysmal atrial tachycardia (atrial beats are labeled P') with an atrial rate of about 170–180 beats per minute and an atrioventricular nodal tachycardia with a ventricular rate of 108 beats per minute. The atrial tachycardia is completely unrelated to the atrioventricular nodal tachycardia, and so a diagnosis of combined or double paroxysmal supraventricular tachycardia with atrioventricular dissociation can be made. In this example, the double tachycardia is probably a manifestation of excess digitalis effect. Record B was obtained from the same patient several

hours later, following treatment with potassium chloride. Atrioventricular nodal tachycardia persists but exhibits a slower rate than was present in A. However, the P waves, which were upright in A and appeared at a rate and rhythm different from the ventricular deflections, are inverted in leads II, III, and aVF of B; therefore, they are retrograde P waves (P'). In addition, the inverted P waves follow every second ventricular beat, and so the mechanism of the rhythm in the electrocardiogram in B is atrioventricular nodal tachycardia with 1:2 retrograde atrioventricular block.

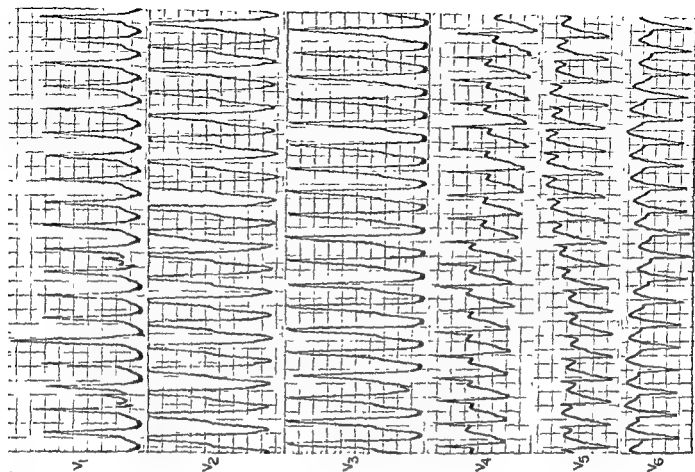
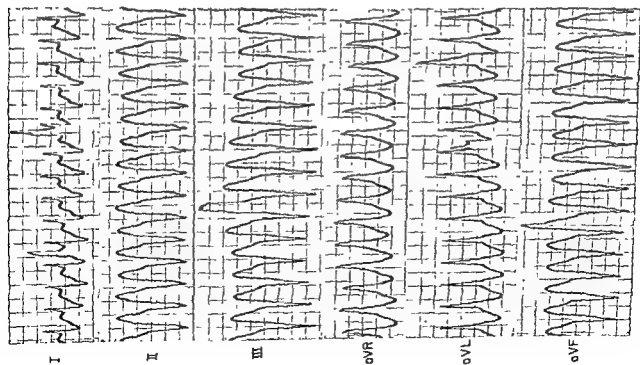


Fig 292.—A, paroxysmal ventricular tachycardia with a ventricular rate of

these features must be considered with great

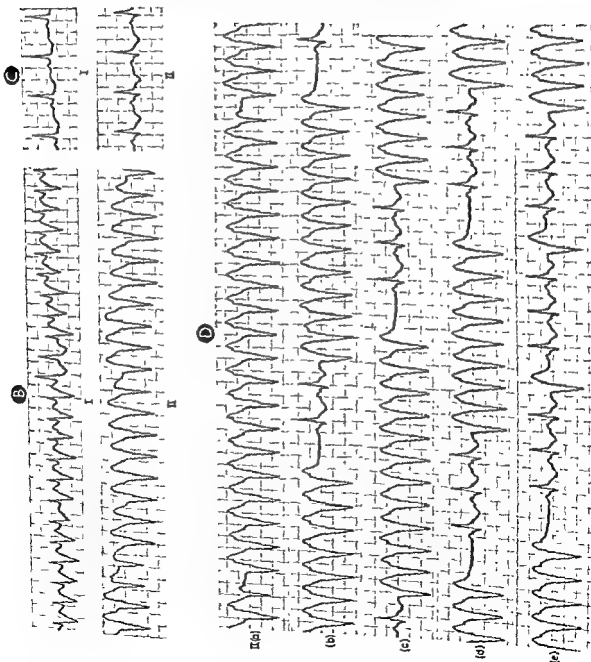


Fig. 292 (cont.)—B, strips of leads I and II showing short runs of ventricular tachycardia separated by QRS deflections of different configuration, which probably represent conducted sinus beats. C, sinus rhythm. Note the marked difference in the QRS configuration during sinus rhythm as compared to that previously noted during ventricular tachycardia. D, five-lead strips (continuous strips of lead II) recorded from the same patient as the preceding and demonstrating short recurring paroxysms of ventricular tachycardia as paroxysms of conducted sinus beats. This plane of the ventricular tachycardia displays some of the characteristics of a repetitive paroxysmal tachycardia (see Fig. 293).

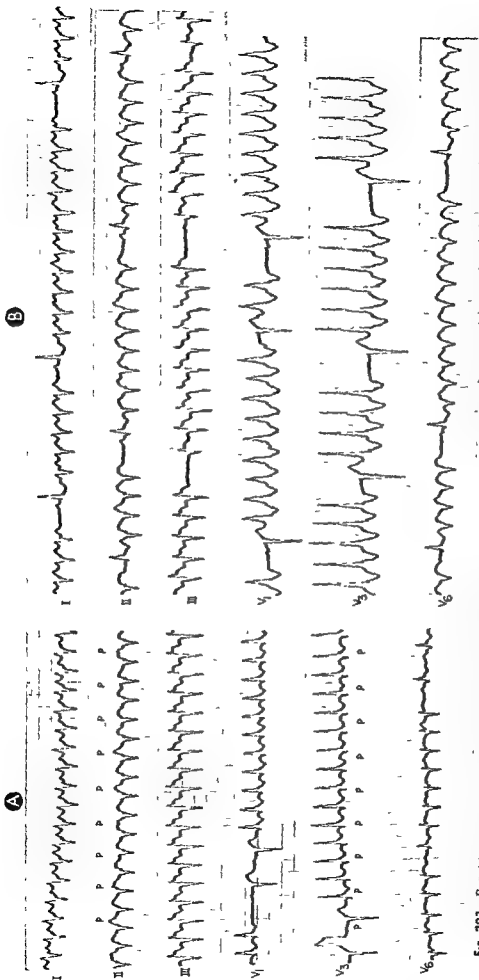


Fig. 293.—Repetitive paroxysmal ventricular tachycardia with atrioventricular dissociation. In A, there is ventricular tachycardia with a rate of about 170 beats per minute, which continues without interruption throughout leads I, II, and III. Although difficult to identify, P waves (P) can nevertheless be spaced off independent of the ventricular rhythm, so that there is complete atrioventricular dissociation of the sinoatrial rhythm in the atria and of the ectopic ventricular rhythm in the ventricles. In leads V₁, V₂, and V₆, the ventricular tachycardia begins to take on the characteristics of repetitive tachycardia, in that

one or two conducted sinus beats are inserted between paroxysms of tachycardia. In B, the electrocardiographic leads, recorded somewhat later from the same patient, display the characteristic features of a repetitive ventricular tachycardia. Thus, in each lead one can see short bouts of rapid ventricular beats which are separated from one another by one or two conducted sinus beats with a completely different QRS configuration. There is atrioventricular dissociation during each paroxysm of tachycardia.

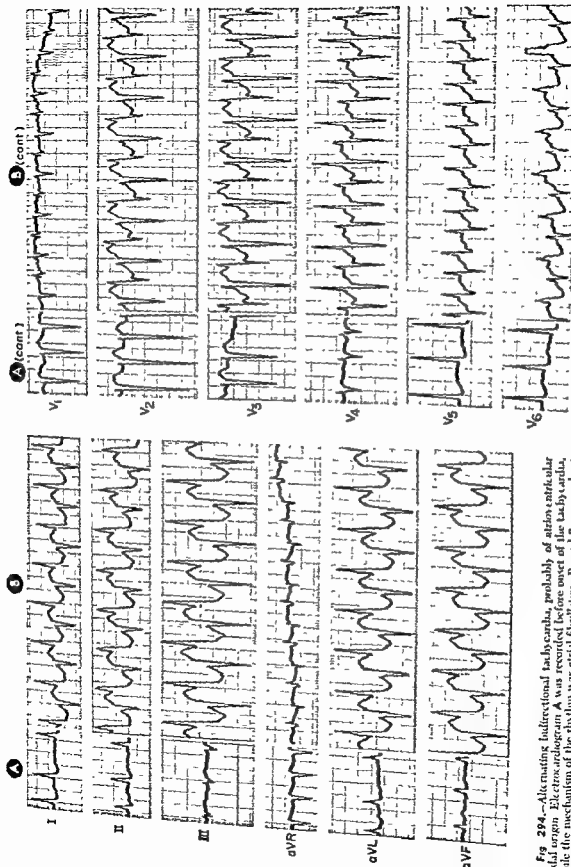


Fig 294.—Alternating bidirectional tachycardia, probably of atrioventricular nodal origin. Electrocardiogram A was recorded before onset of the tachycardia, while the mechanism of the rhythm was atrial fibrillation. Record B was made at the height of the episode of tachycardia. Note that not all of the leads record QRS deflections have much the same direction but certainly alternate in direction. The intervals between the beginning of the next QRS deflection is longer than the interval extending from the beginning of an R wave to the beginning of the next QRS deflection in leads V₁ and V₂ in particular, the right ventricular lead. However, the interval extending from the beginning of an R wave to the beginning of the next QRS deflection is longer than the interval extending from the beginning of the next QRS deflection to the following R wave (Continued)

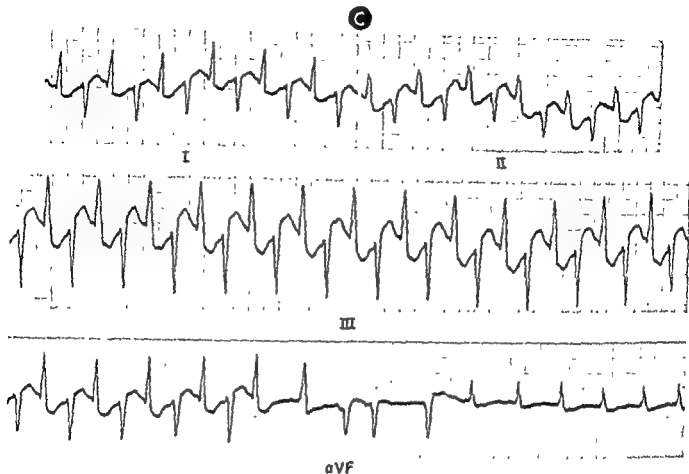


Fig. 294 (cont.)—The beats appearing in **C** were recorded after the patient had received intravenously 0.8 Gm of potassium chloride in an infusion. The termination of the bidirectional tachycardia was recorded in the final lead strip of lead aVF, the rhythm thereafter being atrial fibrillation with varying atrioventricular conduction.

diac output of normal hearts drops somewhat when the cardiac rate exceeds 180 beats per minute, vascular collapse occasionally may be experienced even by normal persons with such rapid rates. Fortunately, at least half the cases of supraventricular tachycardia occurring in normal hearts either subside spontaneously or can be terminated easily by such simple measures as the Valsalva procedure, carotid sinus stimulation, vomiting, etc. In older subjects, and par-

ticularly in patients with heart disease, paroxysms of supraventricular tachycardia displaying only moderately rapid ventricular rates (sometimes even less than 180 per minute) can effect a fall in cardiac output and coronary blood flow. Myocardial infarction, angina pectoris, or acute heart failure may rapidly ensue if the tachycardia is not soon abolished.

The theory of paroxysmal supraventricular tachycardia is discussed later.

Fig. 295.—The lead strips in **A** show ventricular tachycardia approaching ventricular flutter. In the two strips of lead II in **B**, recorded later (all strips in this figure from the same patient), there appears a typical ventricular tachycardia which does not resemble ventricular flutter, as did the previous tracing. Lead II (**b**) was recorded after lead II (**a**) and shows a change in the QRS configuration of the ventricular beats. For the first time, atrial deflections are definitely recognizable. The atrial waves appear at a rate and rhythm which are independent of the ventricular tachycardia. In **C**, ventricular tachycardia is still present, but the rate of the independent atrial rhythm (250 beats per minute) is consistent with the diagnosis of atrial flutter and complete atrioventricular dissociation. The presence of flutter is established in **D**, where the ventricular tachycardia has disappeared and there is predominantly atrial flutter (*F*, flutter waves) with 2:1 atrioventricular response. The final lead strip of lead II in **E** demonstrates a sinus rhythm with frequent atrial extrasystoles (*A*) and either occasional atrioventricular nodal extrasystoles (*N*) with prolonged P-R intervals or atrial extrasystoles originating low in the atria.

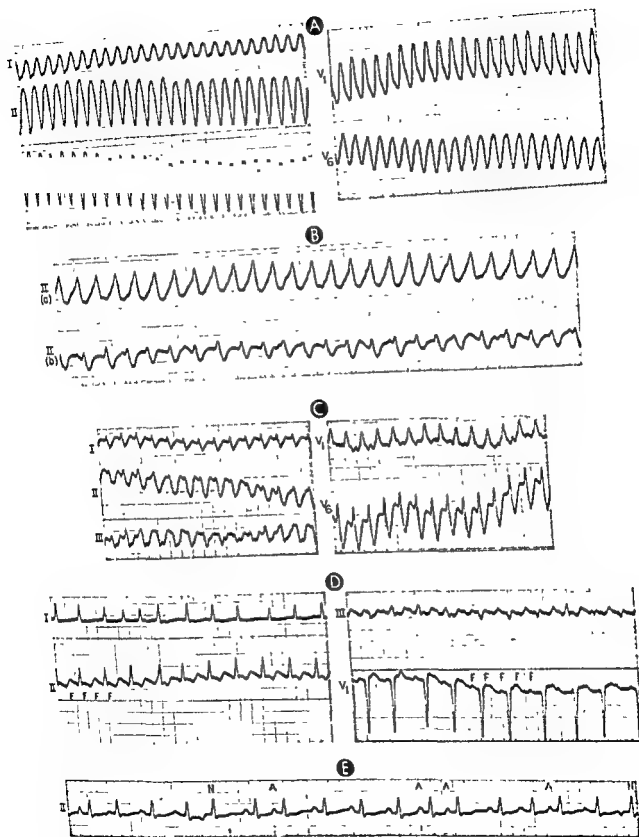


Fig. 295 —Legend on facing page.

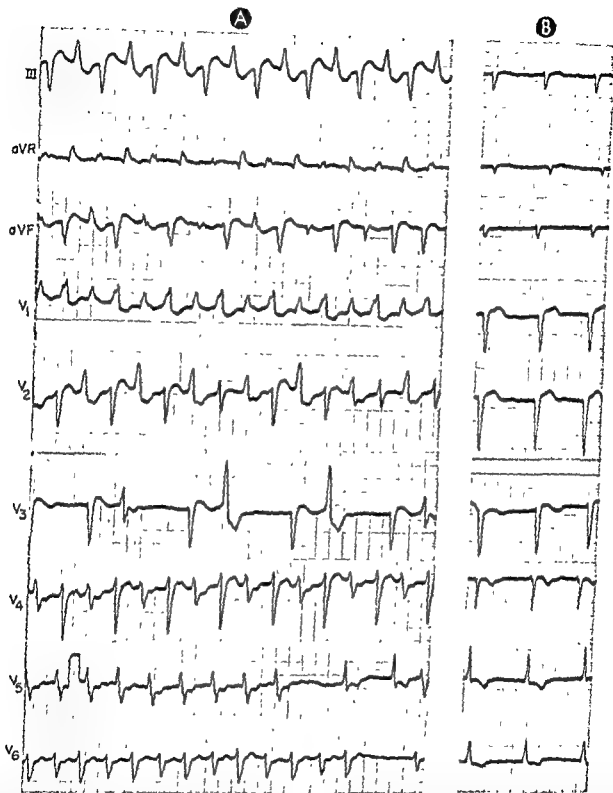


Fig. 296.—Alternating bidirectional tachycardia, possibly of atrioventricular nodal origin. In A, the electrocardiogram shows the characteristic features of an alternating bidirectional tachycardia but differs from that described in Figure 294 in that the QRS duration of the ventricular beats is 0.12 second. The record in B was made before onset of the bidirectional tachycardia, when the rhythm was atrial fibrillation. This record is presented simply to provide a basis for comparison of the QRS configuration present in the tachycardia and that present during fibrillation. (Continued)

Paroxysmal Ventricular Tachycardia

Ventricular tachycardia consists of

to the sinus rhythm. Ventricular tachycardia are widened (0.12 second or more) and deformed and appear at rates of 130-180 beats per minute (Fig. 292). However, faster or slower rates may be encountered in ventricular tachycardia. More often than not, there is some irregularity of the ventricular rhythm, but in many instances the variations in cycle length from beat to beat are no greater than those observed in supraventricular tachycardia. (In a typical supraventricular tachycardia, the R-R intervals vary by 0.01 second or less.)

Once established, a paroxysm of ventricular tachycardia may continue uninterruptedly until offset, more frequently, perhaps, the paroxysm is interrupted at irregular intervals by several sinus beats or by a short

of ectopic beats separated from one another by one or two sinus beats (Figs. 292 and 293). The first ectopic beat of each brief paroxysm appears prematurely

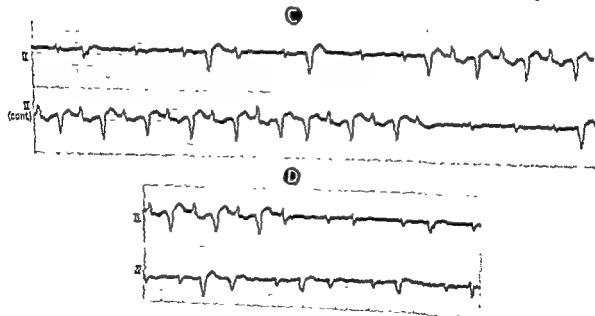
after the preceding sinus beat and is coupled to it by a short interval. The last beat of every

Paroxysmal ventricular tachycardias vary somewhat in their electrocardiographic features. The variations most commonly observed are those described below.

1. Sometimes the appearance of the ventricular beats is somewhat irregular, the R-R intervals being 130-140 msec.

2. On the other hand, some ventricular tachycardias are characterized by an irregular rhythm and by changes in the appearance of the ventricular deflections from beat to beat.

3. Sometimes the ectopic ventricular beats are so widened and distorted that the individual deflections of the QRS complex are difficult to distinguish from the T wave (Fig. 293). Moreover, the appearance of the ectopic beats and the intervals separating them often change from beat to beat. As the ventricular tachycardia approaches the fibrillatory stage, the ectopic beats gradually take the form of regular undu-



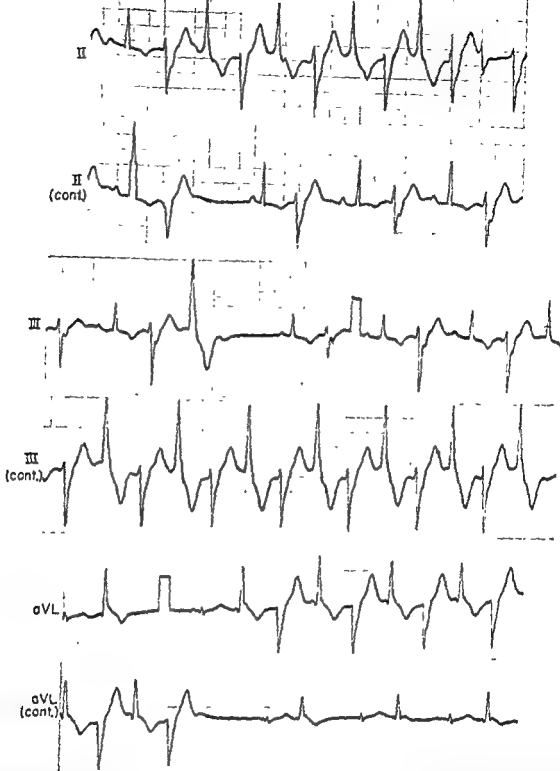
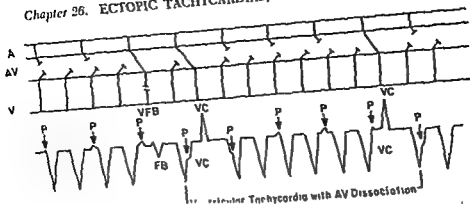


Fig. 297.—Alternating bidirectional tachycardia. This example is somewhat unusual in that sinus rhythm persists during the tachycardia as the result of atrioventricular dissociation. In addition, it can be seen in the two continuous strips of lead III, the continuous strip of lead III below, they are predominantly negative. Thus, it seems that the upright R wave originates above the bifurcation of the bundle branch. In summary, this and the preceding three examples of alternating bidirectional tachycardia suggest that this type of tachycardia actually represents a heterogeneous group of cardiac rhythms which may differ in mechanism and their site of origin.



not, it is impossible to do be made on the basis of normal duration (fusion beat (with produce the fusion with widened QR Ventricular aberr.

be assumed that the bizarre appearance of the ventricular tachycardia is due to the origin of the ectopic beats rather than defective intraventricular conduction of atrioventricular nodal impulses.

lating waves characteristic of prefibrillatory tachycardia or ventricular flutter

4 On rare occasions, particularly in severe digitalis intoxication, a form of ventricular tachycardia is encountered which is unique in that alternate ventricular complexes are oppositely directed. It is called *bidirectional ventricular tachycardia* (or, better, *alternating bidirectional tachycardia*) and, when present, is considered a poor prognostic sign. Carotid sinus stimulation has been noted at times to abolish all similarly directed deflections without affecting those oppositely directed. The mechanism underlying bidirectional ventricular tachycardia is not known, but the explanation currently favored is that the ectopic impulses arise above the bifurcation of the bundle and are conducted alternately down the left and right bundle branches. If this theory is correct, then a bidirectional tachycardia may have its origin in either the atrioventricular node or the ventricles, if the tachycardia has a ventricular origin, the ectopic focus is located in the common bundle and probably not below it (Figs 294, 296 and 297).

Retrograde activation of the atria by ectopic ventricular impulses is an unusual event in ventricular tachycardia, although the frequency with which it occurs is perhaps underestimated. The fact that retro-

grade activation of the atria during ventricular tachycardia is not always recognized is not surprising, in view of the difficulty experienced in ventricular tachycardias in identifying sinus P waves, much less retrograde P waves. When it is possible to recognize P waves, they are usually found to be sinus P waves which appear at a rate and rhythm independent of the rate and rhythm present in the ventricles. While sinus bradycardia or severe sinus inhibition or arrest may accompany ventricular tachycardia in the dying heart, the atrial rhythm in most instances is a relatively fast sinus rhythm or sinus tachycardia. The cause of the enhanced rhythmicity of the sinus pacemaker is not definitely established, but changes in the nutrition and oxygenation of the sinoatrial node have been implicated by some investigators. In any event, the result is that the sinus and ectopic impulses interfere with each other in or near the atrioventricular junctional tissues, and complete or incomplete atrioventricular dissociation is the outcome. On rare occasions in incomplete dissociation, a sinus impulse may be able to capture the ventricles and interrupt the tachycardia for a single beat. The ventricular capture beat which appears may provide one of the few reliable clues to the correct identification of a paroxysmal tachycardia characterized by abnormal, wide QRS complexes (Fig. 298). In such a tachycardia, the two

diagnostic alternatives to be differentiated are ventricular tachycardia and atrioventricular nodal tachycardia with ventricular aberration. The following electrocardiographic findings favor, in varying degree, the diagnosis of ventricular tachycardia (Fig. 298):

Complete ventricular capture without aberration of the conducted beat.—When a sinus impulse captures the ventricles completely, the ectopic impulse discharged shortly thereafter does not participate at all in ventricular excitation. For this to happen, it is evident that the sinus impulse must, of necessity, initiate ventricular excitation prematurely—that is, prior to discharge of the ectopic impulse. Thus the premature onset of the ventricular capture beat allows the ventricles a shorter recovery period than usual. If, despite this fact, the ventricular capture beat fails to show ventricular aberration, it is hardly likely that the abnormal duration and appearance of the ectopic ventricular beats elsewhere in the same lead strip are the result of aberrant intraventricular conduction of nodal impulses. Therefore, a ventricular capture beat with a QRS interval of 0.10 second or less strongly favors the diagnosis of ventricular tachycardia.

Incomplete ventricular capture with the appearance of a ventricular fusion beat—If ventricular capture by the sinus beat is incomplete, excitation processes initiated by the sinus and ectopic ventricular impulses proceed simultaneously in different directions through the myocardium. Since the ventricular fusion beat which results can be produced only by fusion of a supraventricular impulse with an impulse originating in the ventricles (the principal exception to this rule is ventricular pre-excitation occurring in the Wolff-Parkinson-White syndrome), the recognition of one or more ventricular fusion beats during a paroxysmal tachycardia establishes, as a general rule, its identity as a ventricular tachycardia and excludes

the possibility of atrioventricular nodal tachycardia.

Ventricular extrasystoles in antecedent or subsequent electrocardiograms.—If single ventricular extrasystoles are observed in an electrocardiogram recorded shortly before onset or after offset of a paroxysmal tachycardia, the probability is that the tachycardia is of ventricular origin.

Relatively slow rate and slight irregularity of the tachycardia.—In general, the slower and the more irregular the ventricular rhythm during the tachycardia, the more likely it is that ventricular tachycardia is present and the less likely is the diagnosis of atrioventricular nodal tachycardia with ventricular aberration.

CLINICAL SIGNIFICANCE OF VENTRICULAR TACHYCARDIA

Ventricular tachycardia is rarely observed in the absence of cardiac disease. It may appear as a complication of recent myocardial infarction, severe hypertensive or arteriosclerotic heart disease, congestive heart failure, and digitalis therapy if intoxication occurs. Paroxysmal ventricular tachycardia requires prompt therapy, for several reasons: (a) Since ventricular tachycardia occurs almost invariably in a severely damaged heart, the rapid ventricular rate is all the more likely to compromise cardiac function and lead to the onset of acute cardiac decompensation and pulmonary edema, or to Stokes-Adams attacks (consisting of shock and syncope, sometimes associated with convulsions). (b) An even greater hazard posed by ventricular tachycardia is that it is sometimes the precursor of ventricular fibrillation, which is, with few exceptions, a fatal arrhythmia. (c) A less frequent cause of Stokes-Adams attacks is cardiac standstill following abrupt offset of ventricular tachycardia.

ATRIAL FLUTTER AND ATRIAL FIBRILLATION

Ectopic atrial rhythms with rates exceeding the range of rates usually encountered in paroxysmal supraventricular tachycardia are of two closely related types, atrial flutter and atrial fibrillation. These two rhythms differ mainly in the following respects: (a) In atrial flutter, the configuration of the atrial flutter (F) waves and the F-F intervals remain constant from beat to beat, while fibrillation is characterized by undulating atrial (f) waves which vary widely in contour, amplitude, and timing. (b) Atrial flutter

waves appear at rates of 250–350 per minute, although slower rates are frequently observed during quinidine administration. In atrial fibrillation, the rate of the fibrillatory oscillations (f) is usually impossible to measure accurately but is certainly faster than 350 beats per minute.

The close interrelationship of atrial flutter and fibrillation has a firm foundation in clinical experience and experimental observations. Clinically, the two rhythms are often observed on different occasions in

the same individual, digitals commonly converts atrial flutter into fibrillation; and, finally, atrial fibrillation frequently passes through a period of flutter shortly before conversion to sinus rhythm by quinidine. Experimental evidence for such an affinity between atrial flutter and fibrillation is fairly extensive and will be summarized later, in discussing the mechanism of flutter and fibrillation, on pages 442 and 443.

The manner in which atrial flutter and fibrillation arise is one of the most controversial and complicated aspects of cardiac pathophysiology. From a strictly practical standpoint, it is not of great importance to the clinical electrocardiographer whether the specific mechanism involved is circus movement (pp. 442-443), rapid focal or multifocal impulse formation, or multiple re-entries of one or many impulses. In fact, none of these hypothetical mechanisms have as yet been irrefutably proved. For these reasons, consideration of the theories cited above will be limited to a brief recapitulation at the end of the chapter, but pertinent references listed in the bibliography may be consulted for more detailed presentations. In the following discussion it will, for simplicity and convenience, be assumed that atrial flutter and fibrillation originate in a single ectopic atrial focus, where impulses are formed and discharged much faster than in paroxysmal supraventricular tachycardia.

Because of their short refractory period, atrial muscle fibers are able to respond regularly to ectopic

atrial impulses discharged at rates approaching 350 beats per minute and can conduct the impulses just as rapidly as normally. Since the atria are therefore activated in an identical manner by each excitation impulse, the atrial deflections which are produced retain the same configuration and cycle length from beat to beat. Impulse formation in an ectopic atrial focus at a rate of 250 beats per minute or faster and an unchanging pattern of intra-atrial conduction of each ectopic impulse are the characteristics distinguishing atrial flutter from paroxysmal atrial tachycardia, on the one hand, and atrial fibrillation, on the other.

If an ectopic atrial focus fires off too rapidly and/or the refractory period of the atrial myocardium is abnormally prolonged, the fibers may not be able to recover completely from excitation by one impulse before the next is discharged. In this event, the refractory atrial muscle responds irregularly, or not at all, to excitatory stimuli. Successive ectopic impulses may be blocked in some areas and not in others; or they may spread slowly, erratically, and incompletely through the atrial myocardium. The end-result is that the atria remain in a state of continuous, chaotic electrical activity, which is reflected in the electrocardiogram by constant wavelike undulations of the base line. These fibrillatory waves vary markedly in contour and size and appear irregularly at a rate exceeding 350 beats per minute. Atrial fibrillation therefore represents failure of intra-atrial conduction in the

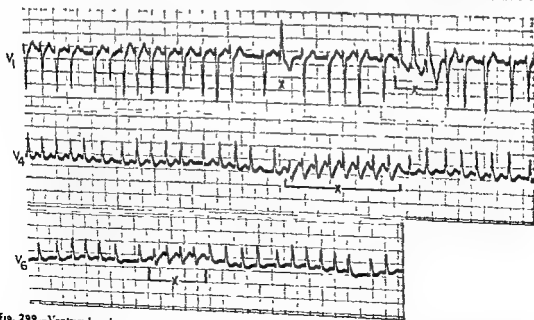


Fig. 299.—Ventricular aberration of conducted beats in atrial fibrillation, simulating paroxysms of ventricular tachycardia. Frequently, when there is aberrant intraventricular conduction, the ventricular beats (X) affected have a configuration resembling that observed in right bundle branch block.

presence of a very rapid ectopic atrial rhythm. Depressed atrial conductivity secondary to digitalis, myocardial disease, or other factors is frequently responsible for atrial flutter changing to fibrillation at less rapid rates of stimulation than would otherwise be the case.

Aberrant intraventricular conduction.—Just as may happen to any impulse arriving in the ventricles shortly after a previous impulse, flutter or fibrillatory impulses may sometimes be conducted to the ventricles in such close succession that recovery is not complete and excitation therefore spreads in an aberrant fashion through the myocardium. This leads to aberration of the ventricular deflection produced by the conducted supraventricular impulse so that the QRS complex differs from others in duration and/or configuration. Aberrant intraventricular conduction of flutter or fibrillatory impulses is the consequence of incomplete recovery of ventricular muscle and conducting pathways and usually involves beats which terminate a short cycle, particularly if the short cycle follows a relatively long one (see discussion of the effect of cycle length on the refractory period on p 354). Sometimes a long pause in the ventricular rhythm is terminated by a ventricular beat which may or may not show minimal to moderate aberration. This can usually be proved to be an escape beat by virtue of the fact that whenever a beat of this type appears in the record it follows the last conducted beat by the same constant interval. Ordinarily, the escape beat originates in the atrioventricular node.

It is frequently difficult to differentiate conducted beats with ventricular aberration from ectopic ventricular beats, especially in atrial fibrillation. This becomes particularly important when a rapid run of abnormal ventricular deflections is observed during atrial fibrillation (Fig. 299). The therapeutic approach is quite different if these beats are conducted supraventricular beats with ventricular aberration, as opposed to a short paroxysm of ventricular tachycardia. In attempting to differentiate the two types of abnormal ventricular beats, the following generalizations are sometimes helpful. (a) Ventricular aberration tends to produce a QRS configuration resembling that of right bundle branch block. (b) Conducted beats with aberrant intraventricular conduction are likely to vary in appearance as the degree of aberration fluctuates, while the configuration of ventricular extrasystoles originating in a single focus usually remains constant. (c) Unifocal ventricular extrasystoles typically are coupled to the preceding beat by a fixed interval, but the cycles preceding conducted beats

with aberration differ in length. (d) Ectopic ventricular beats in flutter and fibrillation are often followed by a pause, produced by retrograde penetration of the atrioventricular junctional tissues by the ectopic impulse.

Atrial Flutter

While clinically the rate and regularity or irregularity of the ventricular rhythm are justifiably stressed in the auscultatory diagnosis of atrial flutter and fibrillation, the electrocardiographic diagnosis of these two rhythms does not rest on these features. The contour, rate, and regularity of the atrial deflections provide the basis for the diagnosis of atrial flutter or fibrillation, regardless of the characteristics of the ventricular rhythm.

The flutter (F) waves appear at rates of 250–350 per minute, but rates below 200 waves per minute may be observed during the course of quinidine therapy (Fig. 300). The F waves can be recognized by their uniform configuration, amplitude, and timing in a given lead. Typically, every flutter wave consists of two oppositely directed components, corresponding to the P wave of atrial excitation and the following Ta wave of atrial repolarization. The prominence of the Ta waves, in particular, seems directly related to the atrial rate and increases as the rate accelerates. Thus the sawtooth or “picket-fence” oscillations of the base line characterizing flutter which is produced by relatively large, alternating upward and downward components of the F waves are a reflection of the rate of atrial excitation, and not the mechanism by which this occurs. Quinidine tends to widen the saw-tooth F waves and slows their rate until frequently they come to present more of a sine wave appearance.

In some leads, and occasionally in all leads, the flutter waves may be recorded as uniphasic deflections separated by isoelectric intervals and may be flat, upright, or inverted. Monophasic F waves are observed in slow atrial flutter chiefly. Leads II, III, aVF, V₁, and V₂ ordinarily register the most prominent F waves. However, it is not unusual for only one or two of these leads to show identifiable F waves, the atrial mechanism being poorly defined in all others.

Since the atrioventricular junctional tissues normally have a longer refractory period than either the atrial or ventricular myocardium, atrioventricular conductivity becomes the limiting factor governing the ventricular response in flutter. As a general rule, the atrioventricular conducting pathway cannot respond to more than 200–250 impulses per minute. Impulses



Fig 300.—Effect of quinidization on atrial flutter. Electrocardiogram A was recorded after the patient had been fully digitalized, and early in the course of quinidization. Before starting quinidine therapy, the electrocardiogram showed atrial flutter waves (F) with an atrial rate of 300 beats per minute, while the above electrocardiogram shows an atrial rate of about 200 beats per minute, illustrating the slowing effect of quinidine on the rate of atrial flutter. Note that there is varying atrioventricular response in A, presumably reflecting the depressant effect of digitalis on atrioventricular conduction. The strip of lead V₁ in B was recorded 24 hours later, when peak levels of quinidine had been attained. As a result of the marked quinidine effect, the atrial rate has slowed to 140 beats per minute but the basic configuration of the flutter waves in lead V₁ has not changed. Note, also, that there is now 2:1 atrioventricular response. The decreased ratio of atrioventricular response in this instance is probably related to two factors, (1) the general slowing of the rate of the atrial flutter, and (2) the vagolytic effect of quinidine, which tends to abolish the indirect effect of digitalis on atrioventricular conduction.

presence of a very rapid ectopic atrial rhythm. Depressed atrial conductivity secondary to digitalis, myocardial disease, or other factors is frequently responsible for atrial flutter changing to fibrillation at less rapid rates of stimulation than would otherwise be the case.

Aberrant intraventricular conduction.—Just as may happen to any impulse arriving in the ventricles shortly after a previous impulse, flutter or fibrillatory impulses may sometimes be conducted to the ventricles in such close succession that recovery is not complete and excitation therefore spreads in an aberrant fashion through the myocardium. This leads to aberration of the ventricular deflection produced by the conducted supraventricular impulse so that the QRS complex differs from others in duration and/or configuration. Aberrant intraventricular conduction of flutter or fibrillatory impulses is the consequence of incomplete recovery of ventricular muscle and conducting pathways and usually involves beats which terminate a short cycle, particularly if the short cycle follows a relatively long one (see discussion of the effect of cycle length on the refractory period on p. 354). Sometimes a long pause in the ventricular rhythm is terminated by a ventricular beat which may or may not show minimal to moderate aberration. This can usually be proved to be an escape beat by virtue of the fact that whenever a beat of this type appears in the record it follows the last conducted beat by the same constant interval. Ordinarily, the escape beat originates in the atrioventricular node.

It is frequently difficult to differentiate conducted beats with ventricular aberration from ectopic ventricular beats, especially in atrial fibrillation. This becomes particularly important when a rapid run of abnormal ventricular deflections is observed during atrial fibrillation (Fig. 299). The therapeutic approach is quite different if these beats are conducted supraventricular beats with ventricular aberration, as opposed to a short paroxysm of ventricular tachycardia. In attempting to differentiate the two types of abnormal ventricular beats, the following generalizations are sometimes helpful. (a) Ventricular aberration tends to produce a QRS configuration resembling that of right bundle branch block. (b) Conducted beats with aberrant intraventricular conduction are likely to vary in appearance as the degree of aberration fluctuates, while the configuration of ventricular extrasystoles originating in a single focus usually remains constant. (c) Unifocal ventricular extrasystoles typically are coupled to the preceding beat by a fixed interval, but the cycles preceding conducted beats

with aberration differ in length. (d) Ectopic ventricular beats in flutter and fibrillation are often followed by a pause, produced by retrograde penetration of the atrioventricular junctional tissues by the ectopic impulse.

Atrial Flutter

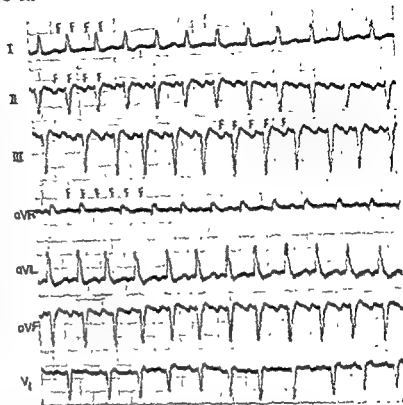
While clinically the rate and regularity or irregularity of the ventricular rhythm are justifiably stressed in the auscultatory diagnosis of atrial flutter and fibrillation, the electrocardiographic diagnosis of these two rhythms does not rest on these features. The contour, rate, and regularity of the atrial deflections provide the basis for the diagnosis of atrial flutter or fibrillation, regardless of the characteristics of the ventricular rhythm.

The flutter (F) waves appear at rates of 250–350 per minute, but rates below 200 waves per minute may be observed during the course of quinidine therapy (Fig. 300). The F waves can be recognized by their uniform configuration, amplitude, and timing in a given lead. Typically, every flutter wave consists of two oppositely directed components, corresponding to the P wave of atrial excitation and the following T_a wave of atrial repolarization. The prominence of the T_a waves, in particular, seems directly related to the atrial rate and increases as the rate accelerates. Thus the saw tooth or "picket-fence" oscillations of the base line characterizing flutter which is produced by relatively large, alternating upward and downward components of the F waves are a reflection of the rate of atrial excitation, and not the mechanism by which this occurs. Quinidine tends to widen the saw-tooth F waves and slows their rate until frequently they come to present more of a sine wave appearance.

In some leads, and occasionally in all leads, the flutter waves may be recorded as uniphasic deflections separated by isoelectric intervals and may be flat, upright, or inverted. Monophasic F waves are observed in slow atrial flutter chiefly. Leads II, III, aVF, V₁, and V₂ ordinarily register the most prominent F waves. However, it is not unusual for only one or two of these leads to show identifiable F waves, the atrial mechanism being poorly defined in all others.

Since the atrioventricular junctional tissues normally have a longer refractory period than either the atrial or ventricular myocardium, atrioventricular conductivity becomes the limiting factor governing the ventricular response in flutter. As a general rule, the atrioventricular conducting pathway cannot respond to more than 200–250 impulses per minute. Impulses

Fig. 302—Atrial Flutter with 2:1 atrioventricular response. The flutter waves (F) appear at a rate of about 260 beats per minute. The saw-tooth appearance of the flutter waves is best demonstrated in leads II, III, and aVF. Since the flutter waves are almost entirely upright in lead aVR, it is highly likely that in this instance the atrial flutter is originating low in the atria. (In this text, the single ectopic focus theory of the genesis of atrial flutter is followed.) Note that, in each lead strip, atrioventricular conduction occasionally changes from 2:1 to 3:1.



arriving at the atrioventricular node at a more rapid rate may find it in its normal refractory period and may not be conducted. Atrioventricular interference is the mechanism responsible for 2:1 atrioventricular response, the ratio so commonly observed in untreated atrial flutter (Fig. 301, A). This is an example of physiologic blocking, in that every second impulse arrives at the atrioventricular node before it has recovered from excitation by the preceding beat. The atrioventricular junctional tissues are just as responsive and recover just as rapidly as normally, but the atrial impulses follow each other in too close succession. Digitalis therapy, carotid sinus stimulation, inflammatory or degenerative changes in the atrioventricular node, and other such influences may depress atrioventricular conductivity and thereby superimpose a pathologic block on the pre-existing physiologic block. As a result, the 2:1 ratio of atrioventricular response is further modified at the level of the block, and a 4:1 or 6:1 ratio may appear, a 3:1 atrioventricular ratio being relatively uncommon (Fig. 301, A, B, and C). With a fixed ratio of atrioventricular response, the F-R intervals (the interval between corresponding points on the flutter waves and onset of the following ventricular complexes) remain of constant length. If the relationship between the flutter

waves and the ventricular beats varies but the R-R intervals remain constant, complete atrioventricular block is likely to be present.

Irregular atrioventricular response is far more common in digitalis-treated atrial flutter than is fixed atrioventricular response, the atrioventricular ratios in a given lead strip, for example, fluctuating erratically between the extremes of 2:1 and 0:1. Variations in atrioventricular conductivity are evidenced not only by changing ratios of atrioventricular response but also by the inconstant F-R intervals of the conducted beats. Generally, the interval between a conducted ventricular beat and the preceding F wave (either its apex or nadir) is longer following short cycles and shorter following long cycles. A Wenckebach type of progressive prolongation of the F-R intervals may be observed in successive cycles having the same conduction ratio (Fig. 301, C). With the occurrence of a longer R-R cycle, the F-R interval shortens and the sequence commences again. From the preceding facts it becomes evident that the ventricular rhythm in atrial flutter may sometimes be just as irregular as in fibrillation and that this finding does not differentiate the two atrial rhythms (Figs. 302-304).

To explain the irregularities in atrioventricular response, it has been postulated that some flutter

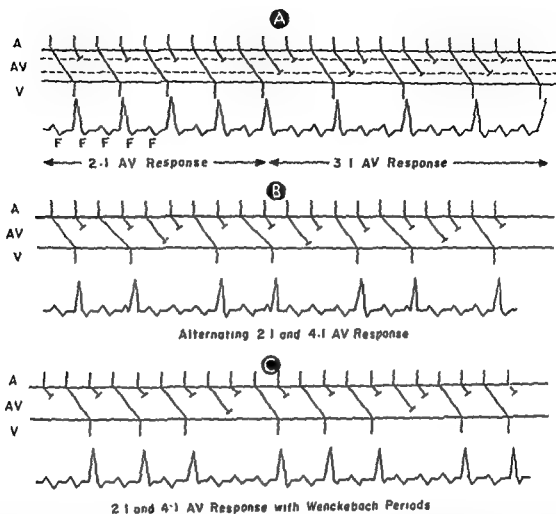
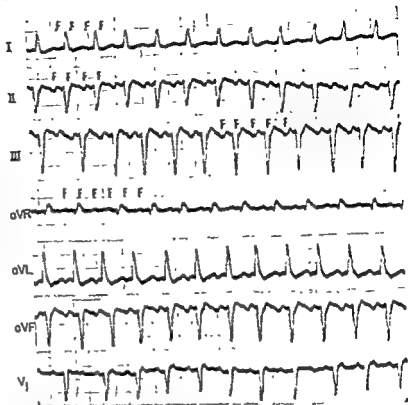


Fig. 301.—Mechanisms of atrioventricular response in atrial flutter. In the first half of diagram A, atrial flutter with 2:1 atrioventricular response is depicted. Because of the rapid atrial rate, every second flutter wave (F) arrives at the atrioventricular node in the refractory period of the previously conducted atrial beat and is therefore not conducted. It is commonly thought that the nonconducted atrial impulse is blocked at a relatively high level in the atrioventricular junctional tissues. In reality, 2:1 atrioventricular response in atrial flutter is not necessarily indicative of atrioventricular block but can be explained solely on the basis of physiologic atrioventricular interference. In the second half of the diagram, atrial flutter with 3:1 atrioventricular response is shown. Note that there is blocking at two levels within the atrioventricular node. The first atrial impulse following the conducted F wave penetrates the atrioventricular node far more deeply than does the following atrial beat. In atrial flutter, 3:1 atrioventricular response is relatively uncommon and is generally a manifestation of atrioventricular block due to prolonged refractoriness of the conducting tissues. In B, the mechanism of alternating 2:1 and 4:1 atrioventricular response in atrial flutter is illustrated. This mechanism frequently leads to a pseudobigeminal rhythm in the ventricles. Note that the atrioventricular conduction time of the second of each pair of conducted ventricular beats is longer than the atrioventricular conduction time of the first of these beats. The fifth, eleventh, and seventeenth atrial beats penetrate the atrioventricular junctional tissues more deeply than the other nonconducted beats, and in so doing they cause increased refractoriness of the conducting tissues so that the next atrial beat is not conducted. This is responsible for the 4:1 atrioventricular response. Varying 4:1 and 2:1 atrioventricular

beats can be seen to lengthen gradually until finally 4:1 atrioventricular response appears

Fig. 302.—Atrial flutter with 2:1 atrioventricular response. The flutter waves (F) appear at a rate of about 260 beats per minute. The saw-tooth appearance of the flutter waves is best demonstrated in leads II, III, and aVF. Since the flutter waves are almost entirely upright in lead aVR, it is highly likely that in this instance the atrial flutter is originating low in the atria (In this text, the single ectopic focus theory of the genesis of atrial flutter is followed.) Note that, in each lead strip, atrioventricular conduction occasionally changes from 2:1 to 3:1.



arriving at the atrioventricular node at a more rapid rate may find it in its normal refractory period and may not be conducted. Atrioventricular interference is the mechanism responsible for 2:1 atrioventricular response, the ratio so commonly observed in untreated atrial flutter (Fig 301, A). This is an example of physiologic blocking, in that every second impulse arrives at the atrioventricular node before it has recovered from excitation by the preceding beat. The atrioventricular junctional tissues are just as responsive and recover just as rapidly as normally, but the atrial impulses follow each other in too close succession. Digitalis therapy, carotid sinus stimulation, inflammatory or degenerative changes in the atrioventricular node, and other such influences may depress atrioventricular conductivity and thereby superimpose a pathologic block on the pre-existing physiologic block. As a result, the 2:1 ratio of atrioventricular response is further modified at the level of the block, and a 4:1 or 6:1 ratio may appear, a 3:1 atrioventricular ratio being relatively uncommon (Fig 301, A, B, and C). With a fixed ratio of atrioventricular response, the F-R intervals (the interval between corresponding points on the flutter waves and onset of the following ventricular complexes) remain of constant length. If the relationship between the flutter

waves and the ventricular beats varies but the R-R intervals remain constant, complete atrioventricular block is likely to be present.

Irregular atrioventricular response is far more common in digitalis-treated atrial flutter than is fixed atrioventricular response, the atrioventricular ratios in a given lead strip, for example, fluctuating erratically between the extremes of 2:1 and 1:1. Variations in atrioventricular conductivity are evidenced not only by changing ratios of atrioventricular response but also by the inconstant F-R intervals of the conducted beats. Generally, the interval between a conducted ventricular beat and the preceding F wave (either its apex or nadir) is longer following short cycles and shorter following long cycles. A Wenckebach type of progressive prolongation of the F-R intervals may be observed in successive cycles having the same conduction ratio (Fig 301, C). With the occurrence of a longer R-R cycle, the F-R interval shortens and the sequence commences again. From the preceding facts it becomes evident that the ventricular rhythm in atrial flutter may sometimes be just as irregular as in fibrillation and that this finding does not differentiate the two atrial rhythms (Figs. 302-304).

To explain the irregularities in atrioventricular response, it has been postulated that some flutter

impulses, although failing to emerge from the atrioventricular node into the ventricles, penetrate the atrioventricular junctional tissues more deeply than other block impulses. Thus, nonconducted flutter impulses may produce negligible or marked refractoriness of the atrioventricular junctional tissues, depending on whether they are blocked high in the atrioventricular node or penetrate more deeply before being blocked. If the latter event occurs, the prolonged refractory state may result in slower conduction of the next impulse or in failure of the following one or more flutter beats to be conducted. This phenomenon is called *concealed atrioventricular conduction* and is thought to be responsible for the variations in the atrioventricular response ratios and F-R intervals and for the appearance of 3:1 and 5:1 atrioventricular conduction in treated atrial flutter. The mechanism underlying this phenomenon is atrioventricular interference.

Impure Atrial Flutter or Atrial Flutter-Fibrillation

No definite boundary demarcates atrial flutter from fibrillation. Between the two there exists only a vague transitional stage in which the atrial rhythm exhibits features of both flutter and fibrillation. Impure atrial flutter, or *flutter-fibrillation*, the transitional rhythm linking typical flutter and typical fibrillation, is characterized by slight variations in the appearance and regularity of the F waves and an atrial rate approaching that of fibrillation. For all intents and purposes, impure atrial flutter and coarse atrial fibrillation are so closely related that there seems little practical value in distinguishing one from the other.

Atrial Fibrillation

In fibrillation, the atrial (f) waves are irregular in rhythm, dissimilar in appearance, and of lower ampli-

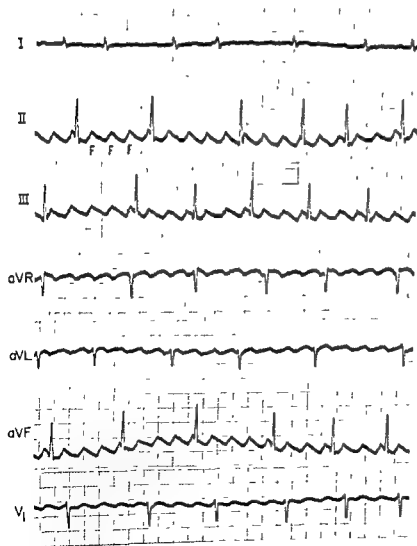


Fig 303.—Atrial flutter with ratios of atrioventricular response varying from 2:1 to 5:1. The rate of atrial flutter waves (F) is about 250 beats per minute.

tude, ordinarily, than flutter waves. The fibrillatory waves occur at rates varying between 400 and 700 per minute and may be prominent in some leads and not in others. As a general rule, very rapid fibrillatory rates are associated with low amplitude f waves, while coarse f waves tend to accompany slower rates. Sometimes there is so little disturbance of the base line that the fibrillatory waves cannot be differentiated, with any degree of certainty, from oscillations due to extraneous artefact. In such an instance, a presumptive diagnosis of atrial fibrillation can be made if P waves are not demonstrable and the ventricular rhythm is irregular. In atrial fibrillation the typical "irregular irregularity" of the ventricular rhythm results from the rapid irregular arrival of fibrillatory impulses at the atrioventricular junction and from the variations in atrioventricular conduction of the impulses. Some of the atrial impulses are conducted into the ventricles and others are blocked at different levels in the atrioventricular junction tissues. The variable depth of

penetration of the blocked impulses affects the manner in which subsequent impulses are conducted. Thus, concealed atrioventricular conduction is another factor contributing to the irregular ventricular rhythm in atrial fibrillation (Fig. 305).

The atrioventricular pathway is normally able to conduct only 200–250 impulses per minute, inasmuch as the fibrillatory impulses arrive at the node at a far more rapid rate, atrioventricular interference is always present in atrial fibrillation and may be the major mechanism regulating ventricular response when a rapid ventricular rate is encountered. Both interference and atrioventricular block, whether due to digitalis therapy or to pathologic changes in the nodal tissues, must be implicated when the ventricular rate in atrial fibrillation is within the range of 60–100 beats per minute (Fig. 306). Slower ventricular rhythms are usually indicative of higher degrees of atrioventricular block and, if perfectly regular, of complete atrioventricular block.



Fig. 304 — Atrial flutter with a rate of about 275 beats per minute and 4:1 atrioventricular response, the flutter waves being labeled F

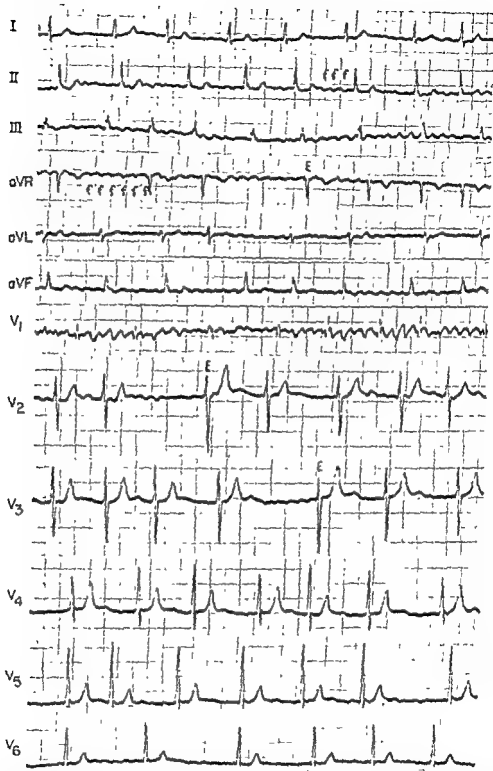


Fig. 305.—Atrial fibrillation. The basis for the diagnosis of atrial arrhythmia in this instance consists solely of the finding of rapid atrial oscillations (*f*) which are irregular in both appearance and rate of occurrence. The irregular ventricular response in atrial fibrillation can probably be ascribed to varying degrees of penetration of the atrioventricular nodal tissues by the fibrillatory impulses and the consequent variation in the rates of atrioventricular conduction of the atrial impulses producing ventricular beats. The ventricular complexes (*E*) in leads *aVR*, *V₁*, and *V₂* are preceded by an interval of the same length in each instance. These ventricular beats must therefore be atrioventricular nodal escape beats. Note, also, that the nodal escape interval is the longest R-R interval in the electrocardiogram. Parenthetically, it might be added that this electrocardiogram displays evidence of right ventricular enlargement (RSR' deflections in lead *V₁*) and was recorded from a patient known to have mitral stenosis.

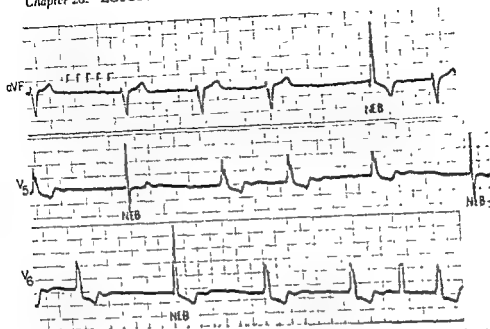


Fig. 206 Atrial fibrillation in which the conducted ventricular beats present the appearance of left bundle branch. The symbol *f* indicates the fibrillatory waves.

Effect of Vagal Stimulation in Flutter and Fibrillation

Carotid sinus stimulation, the Valsalva maneuver, or other measures increasing vagal tone may produce the following changes during atrial flutter and fibrillation.

In atrial flutter—(a) The atrial rate may increase, or, rarely, the flutter may be converted to fibrillation. (b) The main effect of vagal stimulation is to depress atrioventricular conductivity and, by so doing, to slow the rate of ventricular response. In atrial flutter, the ventricular rate falls abruptly and irregularly as the ratio of atrioventricular response shifts—for example, from 2:1 to 1:1 to 4:1 to 8:1, etc. This sequence is reversed so that there is an irregular return to the former rapid ventricular rate. Atrioventricular node depression persists only as long as carotid sinus stimulation is continued, although sometimes atrioventricular conductivity is restored before termination of the procedure.

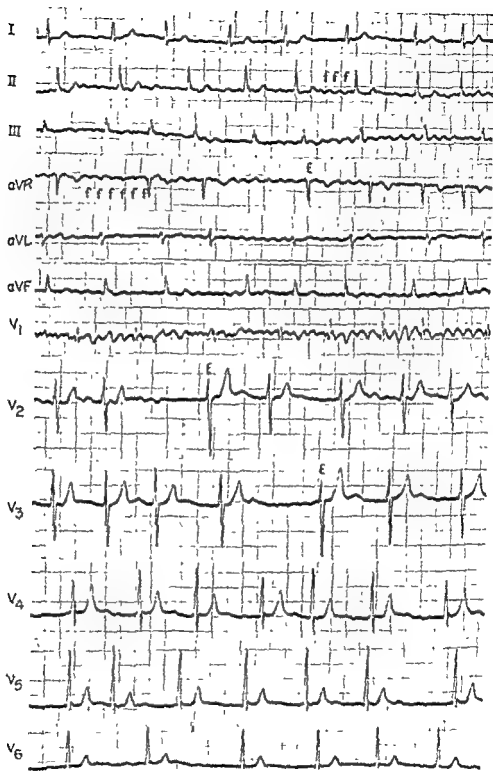
In atrial fibrillation—As in flutter, vagal stimulation depresses atrioventricular conduction and decreases the number of atrial impulses transmitted to the ventricles. Although there is irregular slowing of the ventricular rhythm, the abrupt jumps in ventricular rate observed in flutter as the atrioventricular rate is

halved, quartered, etc., are not characteristic of atrial fibrillation.

Measures increasing vagal tone—carotid sinus stimulation in particular—are important aids to the recognition of atrial flutter and fibrillation. In flutter with 2:1 atrioventricular response, every other flutter wave may be hidden in a ventricular deflection, so that the rhythm may be interpreted as paroxysmal supraventricular tachycardia. By slowing the ventricular rate, carotid sinus stimulation usually permits flutter waves obscured by QRS or T waves to be visualized. This holds equally for atrial fibrillation with fast ventricular rates. When the ventricular rhythm is very rapid in fibrillation, the R-R intervals sometimes vary little, if at all, in length. In the absence of an irregular ventricular rhythm and identifiable atrial deflections, the diagnosis of atrial fibrillation would be difficult to establish without resort to carotid sinus stimulation. This slows the ventricular rhythm and more clearly demonstrates the atrial mechanism, just as in flutter; in addition, the irregularity of the ventricular rhythm is accentuated (Figs. 307 and 308).

Clinical Aspects of Atrial Flutter and Fibrillation

Both atrial flutter and fibrillation may occur in a paroxysmal transient form or in an established chronic



... .. known to have mitral stenosis

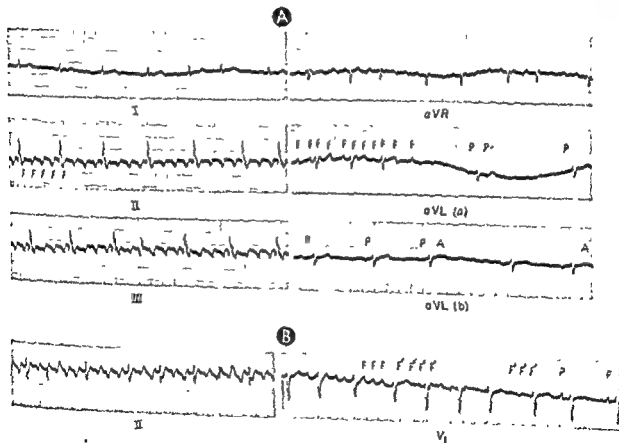
Q - ventricular enlargement (RSR' deflections in

form. Atrial fibrillation is one of the most commonly noted cardiac arrhythmias and is said to occur in about 70% of cases of severe heart failure. The incidence of atrial flutter is much lower, the ratio of atrial flutter to fibrillation being in the order of 1:10.

Both arrhythmias ordinarily are associated with cardiac disease—atrial flutter almost invariably so. However, many investigators have recorded cases of atrial fibrillation, usually of the paroxysmal type, occurring in the apparent absence of cardiac disease. In several series, such cases comprised approximately 10% of the total number of patients with atrial fibrillation. In general, atrial flutter and fibrillation tend to be superimposed on the same types of heart disease

(coronary arteriosclerosis, hypertension, and rheumatic mitral valvular disease.)

Prolongation of the P-R interval produced by these and other types of cardiac disease has been said to predispose to subsequent onset of atrial fibrillation. It is not surprising, therefore, that after reversion of atrial fibrillation to sinus rhythm, the P-R interval frequently remains prolonged, independently of any drug effect. Both arrhythmias may complicate myocardial infarction, but neither is ordinarily seen in systolic heart disease in the absence of coexisting diseases like those listed above. Thyrotoxicosis may precipitate either arrhythmia, but atrial fibrillation is the more commonly noted of the two. Atrial arrhythmias



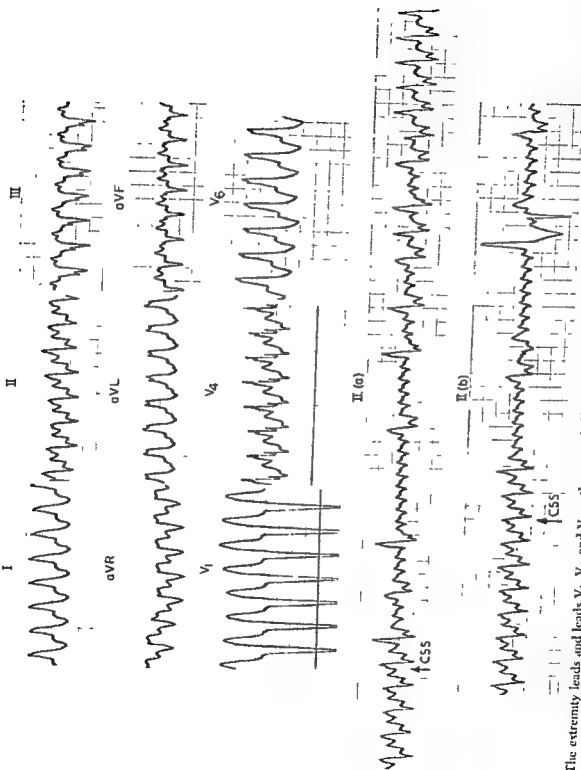


Fig 307.—The extremity leads and leads V_1 , V_4 , and V_6 in the upper half of the figure show a rapid ventricular rhythm, the rate being about 170 beats per minute. The ventricular complexes are deformed in a manner suggesting left bundle branch block, and there appear to be atrial deflections preceding each ventricular complex. Therefore, at this point the electrocardiogram might be interpreted as showing paroxysmal atrial tachycardia with left bundle branch block, or if the identification of the deflections preceding the ventricular complexes as atrial beats is not accepted, the rhythm would have to be interpreted as paroxysmal ventricular tachycardia. The two long strips of lead II shown at the bottom were recorded a short time later. In lead II (a), the

first portion of the lead shows a tachycardia identical with that in lead II above. However, with carotid sinus stimulation (CSS, at arrow), the resulting slowing of the ventricular rate due to decreased atrioventricular conduction reveals rapid atrial flutter waves. Note the irregular escape of atrioventricular conduction from the effects of carotid sinus stimulation later in the same strip. Lead II (b) demonstrates the same response to carotid sinus stimulation as was described in lead II (a). This electrocardiogram illustrates the value of carotid sinus stimulation in elucidating the mechanism of a paroxysmal tachycardia.

thway to initiate another cycle. As long as the action front is preceded by nonrefractory muscle, the circus movement continues without interruption. In short, the circus movement mechanism requires that there be a gap of nonrefractory, responsive muscle separating the head of the mother wave from its tail. The success of quinidine in terminating atrial flutter and fibrillation has been attributed to the fact that it prolongs the refractory period of atrial muscle (more precisely, to its slowing of conduction recovery), which, in effect, abolishes the indispensable "gap" of recovered myocardium preceding the mother wave. The circus movement subsides as soon as the mother wave encounters refractory myocardium.

In atrial flutter, the path traversed by the mother circus \square thought to be longer than in fibrillation, and thus the atrial oscillations are slower in flutter than in fibrillation. It \square also believed that the atria recover more rapidly in flutter than in fibrillation, so that the mother and daughter waves tend to follow a relatively constant pathway from cycle to cycle. This circumstance produces flutter waves of identical shape and timing in a given lead. On the other hand, the atrial recovery process is slower in atrial fibrillation. Consequently the pathways traversed by the mother and daughter circus waves vary from cycle \square cycle, and this is reflected in the variable appearance of the fibrillatory oscillations.

Multiple re-entry.—The mechanism of re-entry has already been described with reference to coupled ectopic beats occurring singly and to paroxysmal ectopic tachycardia. In flutter and fibrillation, according to Katz and Pick, the initiating sinus or ectopic impulse

by virtue of numerous interferences in the heart, and re-enters from a number of points, multiplies the number of daughter impulses to varying degrees. Each impulse continually wanders about the syncytium wherever it finds responsive muscle not yet stimulated by its sister impulses and each, in its turn, sets up new points of re-entry. If the pattern by which these multiple impulses

"When
term in

The multiple re-entries are sustained by subsequent impulses discharged by the dominant pacemaker or by impulses arising in multiple ectopic foci. The main

proponents of this theory at the present time are Katz and Pick, and Hecht.

Focal or multifocal impulse formation.—Lewis, in his experiments, stimulated the auricles with cardiac current to produce atrial flutter and fibrillation. Scherf and his associates were the first to induce atrial flutter by the injection of aconitine into the auricular wall. By cooling or clamping off the injected auricular appendix, they could abolish the aconitine-induced flutter; but when the clamp was released or the cooling discontinued, the flutter reappeared.

During aconitine-induced flutter, Scherf and his colleagues observed that fibrillation could be precipitated by stretching the wall of the auricle, and then could be abolished by cooling the site of aconitine application. However, fibrillation produced by electrical stimulation and topical application of drugs other than aconitine responded differently to cooling. This has also been noted by other investigators, as will be discussed below. Scherf has concluded from these and other observations that flutter probably results from rapid impulse formation in a single focus, while fibrillation is caused by rapid impulse formation in either a single center or in several centers. More recently, Prinzmetal and his associates have reached much the same conclusion concerning the mechanism of flutter and fibrillation.

the above theories, we can suggest that both mechanisms—circus movement and focal impulse formation—may cause atrial flutter and fibrillation. Brown and Acheson produced atrial flutter by the aconitine method of Scherf and of Prinzmetal and by the method of Ramos and Rosenbluth involving rapid electrical stimulation of the auricles. The latter method \square thought by its formulators to produce a circus movement. Not only did these two types of flutter respond differently to various agents, but it was also found that in aconitine-induced flutter a secondary mechanism existed simultaneously with the primary flutter. This secondary mechanism, which seemed able to maintain the flutter even when the aconitine focus was abolished, was thought to be due either to another spontaneous ectopic focus or to a circus movement.

VENTRICULAR FLUTTER AND FIBRILLATION

Ventricular flutter and fibrillation are, without doubt, the most serious of the cardiac arrhythmias. The theories relating to their mechanism of produc-

tion are essentially the same as were described for the corresponding atrial arrhythmias, atrial flutter, and fibrillation and are involved in the same controversy.

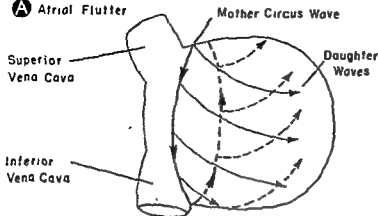
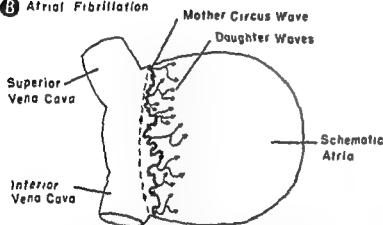
A Atrial Flutter**B Atrial Fibrillation**

Fig. 309.—The circus movement theory of atrial flutter and fibrillation. The regularity of the rhythm and similarity of the atrial flutter waves observed in the electrocardiogram have been ascribed to the fact that in atrial flutter (A) the mother circus wave enters, traverses, and re-enters the same pathway over and over again, while the daughter waves given off by the mother circus wave spread through the atrial myocardium in a constant and orderly way. On the other hand, in atrial fibrillation (B), the pathway of the mother wave is devious, prolonged, and variable, and the daughter waves are given off irregularly and proceed erratically through the atrial muscle. Consequently, the atria undergo fractional activation, and this is responsible for the varying

ence between the circus movement in atrial fibrillation and that in flutter are. (1) the more rapid atrial rate and (2) the occurrence of conduction failure in the atrial muscle in atrial fibrillation.

arrhythmias, including atrial fibrillation, are significant, albeit infrequent, manifestations of digitalis intoxication. In fact, atrial flutter, resulting from digitalis toxicity is observed very rarely. In all of the reported cases of atrial fibrillation or flutter secondary to digitalis intoxication, cardiac disease apparently was present in addition.

Mechanism of Atrial Flutter and Atrial Fibrillation

The mechanism producing atrial flutter and fibrillation has been the subject of lively controversy for half a decade, and the divergence of opinion is just as marked now as ever. Although investigations in recent years have provided new and important information concerning the genesis of these two rhythms, none of these data incontestably prove or refute any of the theories currently favored. These theories are three in number—namely, the concept of circus movement, the theory of multiple re-entries, and the theory of focal or multifocal impulse formation.

Circus movement.—While Lewis and his associates did not originate the circus movement concept, their extensive investigations seemed to establish it so firmly as the mechanism responsible for atrial flutter and fibrillation that for many years the concept (Fig. 309, A and B) was widely accepted and rarely challenged. However, there were some authorities who regarded this widespread acceptance of the circus movement theory as premature. More recently, the studies of Scherf and of others have raised new doubt as to the validity of the circus concept and at the same time have tended to favor the mechanism of ectopic focal or multifocal origin of atrial fibrillation and flutter.

In essence, the circus movement concept supposes that the activation wave called the *mother circus* follows a circular, unidirectional, and narrow path around the ostia of the two venae cavae. During its course, the mother circus gives rise to centrifugally directed *daughter waves*, which spread to all portions of the atria. When the mother wave completes its circus movement, it immediately re-enters the same

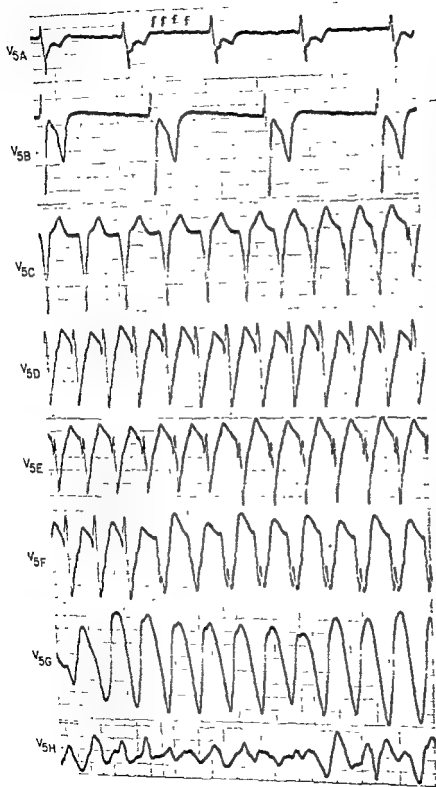
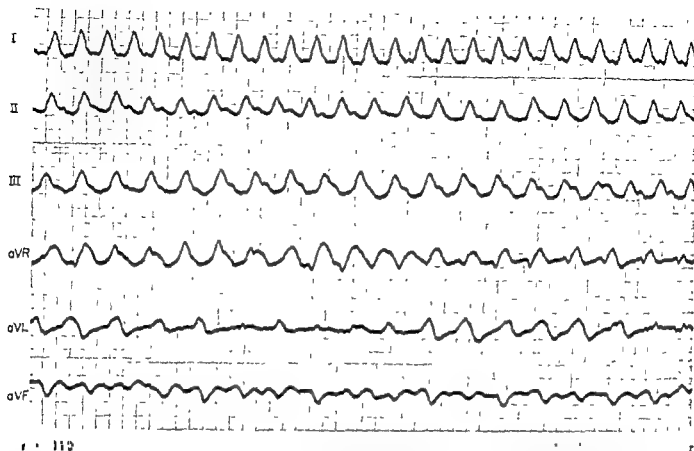


Fig. 311.—All of these lead strips are of lead V_5 and they are lettered in the order of their recording. In lead V_5 (A), fibrillatory waves (f) can be seen, and therefore atrial fibrillation is present in the atria. The ventricular rhythm is essentially regular despite variations in the f-QRS relationship. Thus, there must be complete atrioventricular dissociation and block with an idioventricular pacemaker (since the QRS duration exceeds 0.12 second). In lead V_5 (B), essentially the same abnormalities are present as in lead V_5 (A) except that the ventricular pacemaker has apparently descended lower in the ventricles, as evidenced by the fact that the QRS deflections are wider and the ventricular rate is slower than in lead V_5 (A). In lead V_5 (C), ventricular tachycardia has appeared, and thus continues with varying configurations of the ventricular complexes in lead V_5 (D and E) and in the early portion of lead V_5 (F). Later in lead V_5 (F), there is marked widening of the ventricular deflections, which culminates in the appearance in lead V_5 (G) of ventricular flutter. Finally, in lead V_5 (H), ventricular fibrillation supervenes.



can be seen, and there is atrioventricular dissociation and atrioventricular block. In the remaining leads, there is progressive deterioration of the ventricular pacemaker, and, finally, in lead aVF, ventricular fibrillation appears. In ventricular fibrillation, the ventricular beats are so distorted and appear so irregularly that the tracing presents an entirely chaotic appearance.

ELECTROCARDIOGRAPHIC FEATURES

Ventricular flutter and fibrillation consist of regular undulating continuous waves of large amplitude and marked widening. The normal components of the ventricular complex (QRS and T deflections) cannot usually be distinguished, one from the other. During ventricular flutter these waves vary in rate from 180 to 250 per minute, and all exhibit about the same configuration. When these waves become more bizarre and variable in appearance and occur with an irregular rhythm, ventricular fibrillation is present. In the

terminal stage of ventricular fibrillation, the ventricular rate may be slow and quite irregular, and the electrocardiogram may show only erratic oscillations of the base line (Figs. 310 and 311).

Ventricular fibrillation is often the terminal cardiac rhythm in patients dying from various causes, but especially in death following myocardial infarction or digitalis intoxication. This arrhythmia is frequently observed in Stokes-Adams attacks, when it is most likely to occur during change from a partial to a complete atrioventricular block or during the course of complete atrioventricular block.

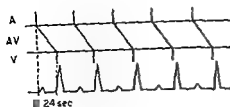


Fig. 312—First-degree atrioventricular block. The pur-

degree atrioventricular block, or *prolonged atrioventricular conduction*, can be diagnosed if every sinus P wave, without exception, is followed by a ventricular complex after a P-R interval of 0.21 second or longer (in adults) (see Figs. 312 and 313). This does not hold true when the sinus beat with prolonged atrioventricular conduction is preceded by an ectopic, atrial, nodal, or ventricular extrasystole. Thus, a premature atrial beat occurring late in the Q-T interval may penetrate the atrioventricular junction deeply without reaching the ventricles. The next sinus beat finds the atrioventricular pathways still refractory following concealed conduction of the ectopic impulse, and, as a result, the beat reaches the ventricles only after a long P-R interval. Similarly, retrograde penetration of the atrioventricular node by an ectopic nodal or ventricular impulse may also be responsible for the slower conduction of the post-ectopic sinus beat. In the examples cited, atrioventric-

ular interference is actually the mechanism producing the apparent first-degree atrioventricular block. The effect of concealed atrioventricular conduction is observed frequently with interpolated nodal or ventricular premature extrasystoles in the form of a prolonged P-R interval of the first postectopic conducted beat.

First-degree atrioventricular block is sometimes associated with such marked prolongation of the P-R interval that the latter exceeds the P-P interval in length. Thus, the sinus beat initiating each ventricular deflection is not the P wave immediately preceding the latter but the P wave before that.

Ordinarily in first-degree atrioventricular block, the P-R intervals remain constant in length unless the atrial rhythm shows some variation in cycle length or rate. In this event, the P-R intervals following longer R-R cycles tend to be shorter than those preceded by short R-R cycles. (Incomplete recovery of the atrioventricular conducting pathway after the beat terminating a short cycle is responsible for the lengthening P-R intervals.) It need hardly be mentioned that the 0.21-second value set for the upper limits of the normal P-R interval duration was selected because it applies to the majority of normal subjects. On the other hand, in occasional normal subjects, P-R intervals of 0.22 or 0.24 second may be observed.

SECOND-DEGREE ATRIOVENTRICULAR BLOCK.—This type of atrioventricular block is often designated *incomplete atrioventricular block* without indicating its degree, and, when so used, the term "incomplete atrioventricular block" implies that it is second-degree block. Second-degree atrioventricular block may be

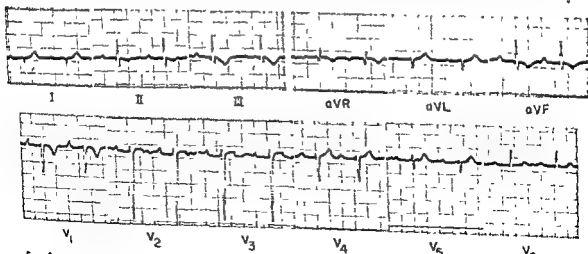


Fig. 313—First-degree atrioventricular block. The pur-

if the
The

...the patient's age group is less than 0.20 second

Atrioventricular Block and Sinoatrial Block

BLOCKED IMPULSE conduction at intra-atrial or intra-ventricular levels has been described previously in sections dealing with the electrocardiographic patterns of P mitrale and of bundle branch block and diffuse intraventricular block. In this chapter, only block occurring at or near the sinoatrial and atrioventricular junctions will be considered, that involving atrio-

ventricular conduction will receive the greater attention because of the frequency and clinical significance of atrioventricular block and because atrioventricular conduction, normal and abnormal, has been studied more extensively than sinoatrial conduction. However, the clinical cardiologist is becoming increasingly aware of the need for recognizing sinoatrial block.

ATRIOVENTRICULAR BLOCK

The fact that a sinus beat happens not to be conducted or is conducted slowly by the atrioventricular node does not in itself incriminate atrioventricular block as the causative mechanism to the exclusion of atrioventricular interference. There must also be indirect evidence that the refractory period of the atrioventricular junctional tissues is prolonged. If, for example, a ventricular deflection fails to appear after a sinus P wave which falls outside the Q-T interval of the preceding ventricular beat, or follows such a P wave by a P-R interval of 0.21 second or longer, it can usually be concluded that the refractory period of the atrioventricular junctional tissues extends beyond the Q-T interval—that is, beyond the approximate duration of the normal refractory period. In either case, the fact that prolonged refractoriness of the atrioventricular node is demonstrable substantiates the diagnosis of atrioventricular block.

The normal absolute refractory phase corresponds roughly to the initial one half of the Q-T interval, and the relative refractory phase of the atrioventricular junctional tissues, to the second half of the Q-T interval. Since atrial beats (for example, premature atrial extrasystoles), occurring shortly after the QRS complex, appear within the absolute refractory phase of the atrioventricular node, their failure to be con-

ducted is a normal physiologic event. Similarly, P waves falling near the end of the T wave—that is, in the relative refractory period—are conducted either slowly or normally, depending on how early or late in this period they arrive at the atrioventricular junction. The fact must be kept in mind that the length of the refractory period of the atrioventricular node (and of heart muscle in general) does not remain fixed but varies under the influence of many factors. One of the most important of these factors is the relationship between the length of the refractory period and the length of the preceding cycle. Within certain limits, the longer the preceding cycle length, the longer the duration of the refractory period of the beat terminating that cycle, and the shorter the preceding cycle, the shorter the refractory period.

Electrocardiographic Features

INCOMPLETE ATRIOVENTRICULAR BLOCK

The term *incomplete atrioventricular block* implies that some or all of the atrial beats are conducted into the ventricles abnormally slowly. Incomplete atrioventricular block can be divided into two types: first- and second-degree atrioventricular block.

FIRST-DEGREE ATRIOVENTRICULAR BLOCK.—First-

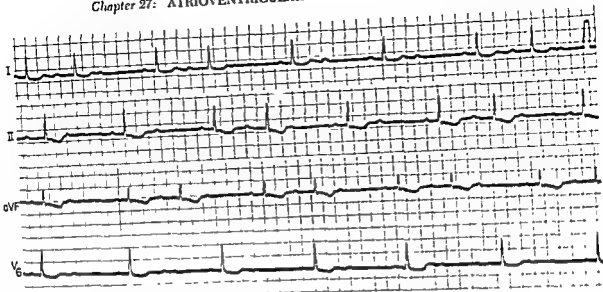


Fig. 316.—Incomplete atrioventricular block with periods of 3:2 atrioventricular block of the Wenckebach type and at other times 2:1 block in leads I, II and aVF. In lead V₆ there is 2:1 atrioventricular block throughout.

divided into two subtypes—the uncommon type, and the common, or Wenckebach, type.

Uncommon type—On rare occasions, a second-degree atrioventricular block may present the following features (see Figs 314, A and 315)

- 1 The P-R intervals of the conducted beats may be prolonged or of normal duration, but their lengths remain constant from beat to beat. However, the conducted beat following the ventricular pause may sometimes have a shorter P-R interval than the other beats.

- 2 Ventricular pauses due to blocked atrial beats usually occur at irregular intervals, so that the ratio of atrioventricular response varies. Sometimes, however, the ratio of atrial and ventricular beats is fixed.

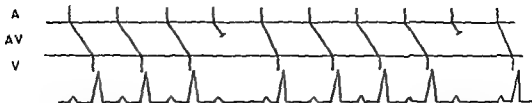
Common, or Wenckebach, type—In the common type of second-degree atrioventricular block (Figs. 314 B, 316 and 317), the P-R interval of each successive conducted beat lengthens progressively until finally one atrial beat is blocked. This is known as the *Wenckebach phenomenon*. The first conducted beat after the pause has a shorter P-R interval (sometimes of normal length) than any subsequent P-R interval, and, with its appearance, the cycle of lengthening P-R intervals begins once again. The electrocardiographic sequence starting with the conducted beat following the ventricular pause and ending with the next blocked atrial beat constitutes a *Wenckebach period*. The Wenckebach phenomenon is not a specific manifestation of atrioventricular block alone, for it can sometimes result from atrioventricular inter-

ference occurring with a rapid atrial rhythm. If the atrial rhythm is relatively slow, the presence of Wenckebach periods usually indicates depressed atrioventricular conductivity. The end-result of both of the foregoing mechanisms is that the first conducted atrial impulse of a Wenckebach period arrives at the atrioventricular node during its relative refractory phase. Each successive atrial impulse thereafter reaches the atrioventricular node earlier in its recovery period, with the result that atrioventricular conduction becomes more and more prolonged as recovery of the junctional tissues becomes progressively less complete. Eventually an atrial beat arrives when the junctional tissues are completely refractory, and it is blocked. Provided the blocked impulse does not penetrate the atrioventricular node deeply, the ensuing pause gives the node time to recover more completely. For this reason, the next atrial beat is conducted more rapidly to the ventricles than those which follow.

The explanation usually given for the characteristic features of Wenckebach atrioventricular block is as follows:

1. The maximal increment in the P-R interval occurs between the first and second conducted beats following the pause, on the other hand, although there is gradual lengthening of subsequent P-R intervals, the increment in the length of the P-R intervals between consecutive conducted beats becomes less and less. The fact that maximal increment in the P-R interval occurs between the first two conducted beats after the blocked atrial beat is probably an expression

(A) Uncommon Type of Second-Degree AV Block



(B) Common Type of Second-Degree AV Block with Wenckebach Periods

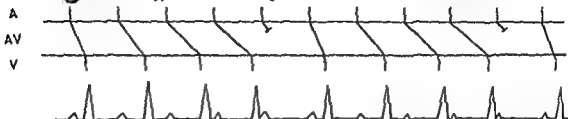
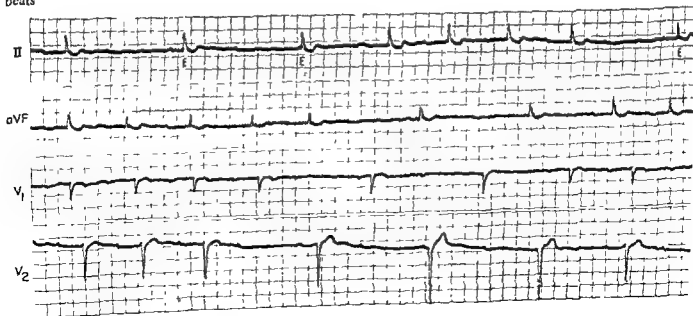


Fig. 314.—Uncommon type (A) and common type (B) of second-degree, or incomplete, atrioventricular block. In A, the P-R intervals of all conducted beats are of equal length. With this exception, the P-R intervals of all conducted beats are of equal length. In B, the P-R interval of the first conducted beat following the pause is shorter than the P-R interval of all subsequent conducted beats. The difference between the two types of incomplete atrioventricular block lies in the fact that in the common type of atrioventricular block there is gradual lengthening of the P-R intervals of subsequent conducted beats until finally one atrial beat fails to emerge from the atrioventricular node. The maximal increment in the P-R interval occurs between the first and second conducted beats following the pause. All subsequent conducted beats show a diminishing increment in the P-R interval length. Consequently, the R-R intervals of the conducted beats form what is known as *Wenckebach periods*. A Wenckebach period consists of a sequence of conducted beats starting with the first conducted beat following the ventricular pause and ending with the next blocked atrial beat. In such a sequence, the first R-R interval is the longest, shorter, and so on. The R-R intervals all exceed the P-P cycle length by the increment in the P-R interval of the conducted beats, while the ventricular pause due to the blocked atrial beat is less than the P-P cycle length by the decrement in the P-R intervals between the two conducted beats containing the pause.

Fig. 315
interval of
tricular con-
the remain-
beats



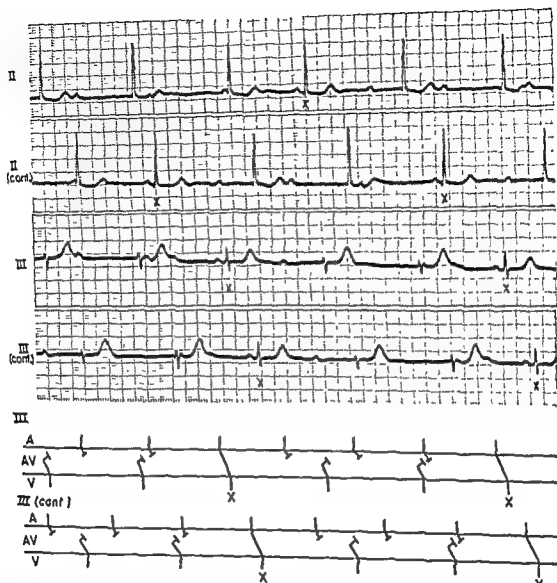


Fig 318.—Incomplete atrioventricular block with 4:1 atrioventricular response and atrioventricular nodal escape. In these continuous lead strips of leads II and III, the ventricular complexes (X) are produced by conducted sinus impulses, while all other ventricular deflections are atrioventricular nodal escape beats. Thus, for every one ventricular deflection produced by a conducted beat, there are four P waves. Therefore, 4:1 incomplete atrioventricular block is present with atrioventricular nodal escape. Notice the different QRS configuration but normal duration of the atrioventricular nodal escape beats, as compared with the conducted sinus beats. In the diagram of the two continuous strips of lead III, no attempt has been made to show the variation in depth of penetration of the atrioventricular junctional tissues by successive sinus impulses. Retrograde atrioventricular block must be assumed to be present to account for the failure of the retrograde impulses of the first, third, fifth, and seventh nodal escape beats to be transmitted to the atria before activation of the latter by sinus impulses.

of the parallel relationship existing between the refractory period of the atrioventricular junctional tissues and the length of the preceding R-R cycle. The first conducted beat after the pause follows the longest R-R cycle and therefore induces the greatest increase in the length of the refractory period of the atrioventricular node—hence the maximal increment occurs in the P-R interval of the second conducted beat. The R-R cycles shorten subsequently because the increments in atrioventricular conduction time become less and less, owing to the shortening cycle lengths. Actually, the shortening of the R-R cycles of the con-

ducted beats has two opposing effects on the degree of refractoriness of the atrioventricular pathway—namely, a shortening effect due to the shorter cycle lengths per se and a lengthening effect consequent to the increasing fatigue or less complete recovery of the junctional tissues.

2. It follows, from the above, that each consecutive R-R interval of a Wenckebach period is equal in length to the P-P interval plus the increment in the P-R interval between the two successive conducted beats. On the other hand, the R-R interval containing the blocked P wave equals in length two P-P cycles

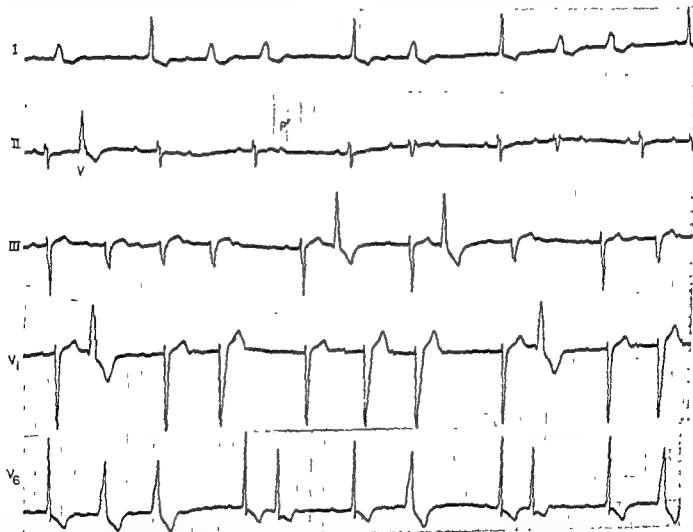


Fig. 317.—Three-to-two and 4:3 Wenckebach incomplete atrioventricular block with left bundle branch block in the ventricular beats following the first conducted beat after the pause. In lead III, at the beginning of the lead strip, a period of 5:4 incomplete atrioventricular block demonstrates Wenckebach periods. Thus, the first conducted beat has a shorter P-R interval than the following conducted beats, there is progressive lengthening of the P-R intervals of the conducted beats, the R-R cycle lengths decrease progressively. The first conducted beat after the pause shows a

Wenckebach type of configuration. In lead II, the P wave labeled P^* may be an atrial extrasystole but is probably a sinus P wave which is slightly distorted by artifact.



Fig.
mon. bil. univ. p. 1



Fig. 322—Complete atrioventricular block with idioventricular pacemaker. In contrast with the preceding figures, this electrocardiogram shows abnormally widened and deformed QRS deflections. Since there is complete dissociation of the faster atrial rhythm and slower ventricular rhythm, complete atrioventricular block must be present and the pacemaker producing the ventricular rhythm must be located in the ventricles, below the bifurcation of the common bundle. Note, also, that there is ventriculoatrial sinus arrhythmia, as indicated by the measured P-P cycles in lead V1.

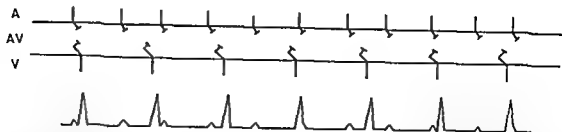


Fig. 319.—Third-degree, or complete, atrioventricular block with atrioventricular nodal pacemaker for the ventricle and ventriculophasic sinus arrhythmia. As a general rule, in ventriculophasic sinus arrhythmia the P-P cycles containing a ventricular beat are shorter than the P-P cycles not containing a QRS complex. It is thought that mechanical ventricular systole following shortly after the appearance of the electrocardiographic QRS complex causes, in some way, slightly premature discharge of the sinus pacemaker, so that the P-P cycle is shortened. This same phenomenon can be seen in incomplete atrioventricular block and in atrial flutter and paroxysmal supraventricular tachycardia with other than 1:1 atrioventricular response.

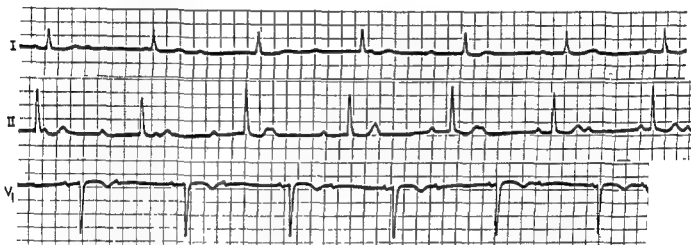


Fig. 320.—Complete atrioventricular block. Thus, sinus P waves can be spaced.

The pacemaker producing the ventricular rhythm must be such that the QRS deflections are not widened to 0.12 second.

minus the decrement in the P-R interval between the conducted sinus beats preceding and following the pause.

3. The Wenckebach phenomenon therefore consists of recurring series of progressively shorter ventricular cycles separated by long cycles. The long cycles or pauses are usually shorter than two short cycles or two P-P intervals, while the first cycle after a pause is longer than the last cycle preceding a pause.

4. The uncommon and common types of second-degree atrioventricular block seldom change from one to the other. The common, or Wenckebach, form tends to occur as a temporary complication of digitalis intoxication or as the result of acute damage to the atrioventricular node, as in myocarditis or infarction. The uncommon form is likely to persist more or less indefinitely and to eventuate in complete, or almost complete, atrioventricular block (Fig. 318)

COMPLETE (THIRD-DEGREE) ATRIOVENTRICULAR BLOCK

In complete (third-degree) atrioventricular block (Fig. 319), the atria beat with an independent rhythm and at a faster rate, usually, than the ventricles. The latter respond to a pacemaker located somewhere distal to the site of block. To facilitate discussion, the atrial rhythm will be assumed to be sinus rhythm in the following paragraphs, although, actually, complete atrioventricular block may occur with any type of atrial mechanism. The distinctive feature of complete atrioventricular block is that the sinus P waves and the QRS complexes may be spaced off regularly but the P-P intervals are usually shorter than the R-R intervals, and the P waves and QRS complexes bear no fixed relationship to one another. Thus the relative positions of the atrial and ventricular

P-P intervals, those containing QRS complexes generally being shorter than those not containing a ventricular deflection (Figs. 319 and 322). This effect of ventricular contraction on stimulus formation in the sinus node is peripheral vagal pressure, the influence of the right auricle. An additional factor may be changes in the blood supply of the sinus pacemaker owing to mechanical ventricular systole. The changing length of the sinus cycle, called *ventriculophasic sinus arrhythmia*, may tachycardia or ular response, or lar dissociation. Rarely, the relationship described above is reversed, so that the P-P intervals not containing a QRS complex are shorter than those which do (Fig. 323).

Clinical Aspects of Atrioventricular Block

Atrioventricular block of any degree may occur in inflammatory or degenerative diseases of the atrioventricular node or as a manifestation of digitalis, quinidine, or pronestyl effect. Sometimes it accompanies certain congenital cardiac anomalies, particularly high ventricular septal defects and patent atrioventricular communis. Stokes-Adams attacks may be produced during transition from an incomplete to a complete atrioventricular block by slowing of the ventricle by cardiac standstill, or by the appearance of a marked slowing of the ventricular rate owing to a shift of the ventricular pacemaker to an area of low rhythmicity (Fig. 311).

SINOATRIAL PAUSE, SINOATRIAL ARREST, AND SINOATRIAL BLOCK

SINOATRIAL PAUSE AND SINOATRIAL ARREST

Sinoatrial or sinus pause (Fig. 324, A) entails failure of the sinus node to discharge one or more impulses. Since sinus discharge per se produces no electrocardiographic deflection, sinus pause is manifested only indirectly by the unexpected absence of one or more atrial P waves. Obviously, sinus-initiated QRS-T deflections are likewise absent during the pause. Ordinarily, an atrioventricular nodal pacemaker becomes active fairly promptly and takes over the ventricular rhythm if the sinus pause is prolonged. In the depressed heart, the escape rhythm may originate in the ventricle, or there may be uniform failure of all pacemakers, with resulting cardiac asystole. This is almost invariably associated with sinoatrial arrest in which impulse formation in the sinus node presumably ceases completely for a prolonged period. Whether or not the outcome is fatal to the patient is determined almost entirely by the activity or inactivity of the secondary cardiac pacemakers. Sinus pause may follow an ectopic beat which is conducted retrograde to, prematurely discharges, and, as a consequence, depresses the sinus node, and not infrequently it is observed after offset of a paroxysmal tachycardia. Following some paroxysmal tachycardias—particularly if there is severe underlying cardiac disease—the sinus node depression induced by the ectopic impulses may be so severe as to lead to sinus arrest. Sinus pause occurs most commonly, and in its most benign form, in patients with vagotonia. It can

be differentiated from sinoatrial block (Fig. 324, B) by the fact that the duration of the pause is not a multiple of the usual sinus P-P interval but is widely variable.

SINOATRIAL BLOCK

In sinoatrial block (Fig. 324, B), the excitation impulse forms in the sinoatrial node just as normally in the case, but its conduction to the atria is blocked in the sinoatrial junction. Thus, a P-QRS-T complex does not appear for one or more cycles. Typically, the R-R interval containing the pause is *exactly* double (or exactly some other multiple of) the interval between two consecutive conducted sinus beats. Actually, the length of the pause is usually slightly shorter than an exact multiple of the basic sinus cycle, because the sinus impulse following the pause is conducted more rapidly through the sinoatrial junction into the atria than is the impulse immediately preceding the pause. This is a manifestation of the Wenckebach phenomenon which was previously described in terms of atrioventricular conduction. In fact, the P-P intervals in sinoatrial block sometimes form Wenckebach periods (Fig. 324, C). Sinoatrial block can be diagnosed only when it is a second-degree block of either the Wenckebach type or the type in which the pause is a multiple of the sinus cycle. In the presence of sinus arrhythmia, the diagnosis of sinoatrial block cannot be substantiated. A nonconducted atrial extrasystole almost obscured by

beats are constantly changing. Occasionally, however, the atrial rate may be so nearly a multiple of the slower ventricular rate that the P-QRS relationship remains virtually constant, and this causes the atrioventricular block to appear incomplete.

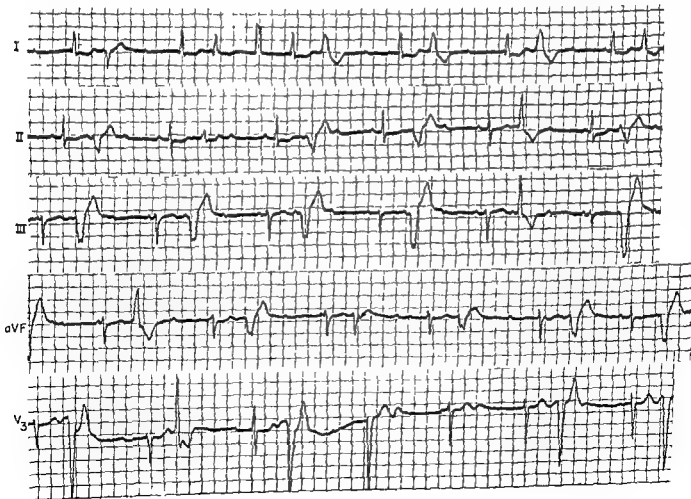
The approximate location of the ventricular pacemaker with respect to the normal conducting pathways is of more than esoteric interest to the clinician. If the rhythm center is situated above the bifurcation of the common bundle (or in the atrioventricular junctional tissues below the level of the block), the QRS complexes are essentially normal in appearance and duration. When the ventricular rhythm originates below the bifurcation of the common bundle, the excitatory impulse spreads in an abnormal fashion through the ventricles. The more distal the pacemaker is located in the conduction system, the more aberrant the spread of excitation and the greater the deformity and widening of the idioventricular beats.

In complete atrioventricular block, a ventricular pacemaker in the atrioventricular node or common bundle produces a regular ventricular rhythm with a rate of about 40 beats per minute, while rhythms emanating from more distant ventricular foci tend to be much slower. The most significant fact clinically in this: the lower in the conducting system is the pacemaker, the slower the ventricular rhythm and the greater the possibility that the pacemaker may fail, with resulting ventricular standstill. With idioventricular centers located above the bifurcation of the common bundle, there is much less likelihood of this occurring (Figs. 320 and 321).

VENTRICULOPHASIC SINUS ARRHYTHMIA IN ATRIOVENTRICULAR BLOCK

In complete and incomplete atrioventricular block, a frequent finding is variation in the lengths of the

Fig. 323.—Complete atrioventricular block with a ventricular rhythm originating above the bifurcation of the common bundle. Note that, despite the occurrence of extra P waves, the QRS complexes are quite regular. There is a tendency in this record for the P-P intervals to be longer than those P-P cycles not enclosing ventricular beats.



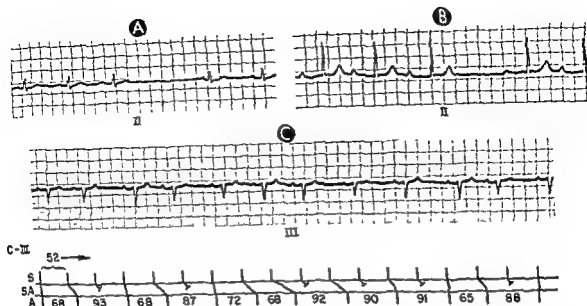
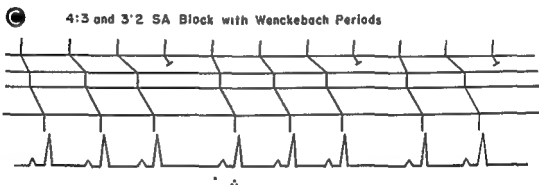
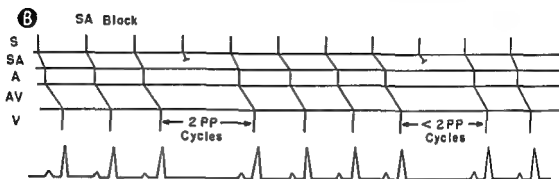
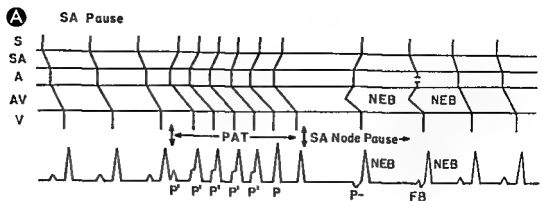


Fig. 325 —Incomplete sinoatrial block A, a short strip of lead II with a pause in the sinus rhythm due to sinoatrial block. The P-P interval containing the pause is twice the P-P interval of the preceding cycle. B, a strip of lead II from another patient. In this case, the pause in the atrial rhythm is less than two times the basic P-P cycle length. This may represent the effect of differences in the rate of sinoatrial conduction of the sinus impulses preceding and following the pause. C, a long strip of lead III obtained from still another patient. In this instance, there appears to be incomplete sinoatrial block with ratios of sinoatrial conduction varying between 4:3, 3:2, and 2:1. The period of 4:3 sinoatrial block appears in about the middle of the lead strip, and the P-P cycle lengths in this period show Wenckebach periods. Undoubtedly, some degree of sinus arrhythmia is present, but, in the diagram of lead III, the cycle length of sinus node discharge is represented as having a constant value of 0.52 second.



of the rhythmicity of the pacemaker, there ensues a long pause before the sinoatrial node initiates its first impulse after the tachycardia. However, before this impulse can be formed and discharged from the sinoatrial node, a retrograde atrioventricular nodal impulse is able to spread through the atria to produce a retrograde P wave (P-), to penetrate the sinoatrial junctional tissues, and to discharge prematurely the forming sinus impulse. Thus, the first atrioventricular nodal escape beat (NEB) following the bout of paroxysmal tachycardia captures ventricles, atria, and sinoatrial node. The second atrioventricular nodal escape beat initiates ventricular excitation, but, as it passes in a retrograde direction, it encounters the descending sinus impulse in the atria, and so an atrial fusion beat (FB) is recorded. Following this, the sinoatrial node takes over once again as dominant pacemaker. Thus, the sinoatrial pause extends from the last P

tion of the two sinus beats containing the blocked sinus impulse. In **C**, a more complicated form of sinoatrial block, namely, incomplete sinoatrial block with Wenckebach periods, is illustrated. This type of sinoatrial block can be recognized by the regularly recurring Wenckebach periods in the atrial rhythm. Thus, the P-P cycle length decreases progressively until finally a long pause ensues. Then the cycle of shortening P-P cycle lengths is repeated. The explanation for the Wenckebach periods in this form of sinoatrial block is exactly the same as was given in the corresponding type of atrioventricular block except that in this instance the variation in the rate of impulse conduction occurs in the sinoatrial junctional tissues.

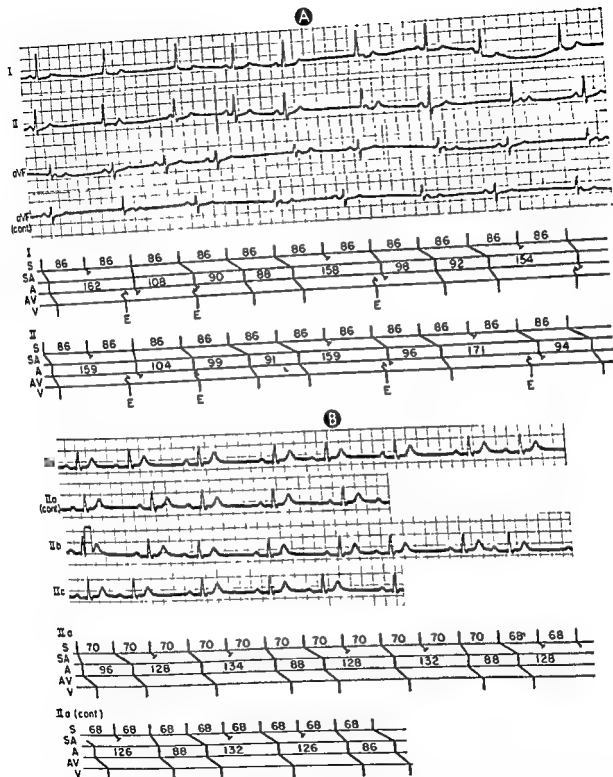


Fig 327.—A, strips of leads I and II and two continuous lead strips of lead aVF showing varying degrees of Wenckebach sinoatrial block with atrioventricular nodal escape beats (E). Note the regularly recurring pattern of decreasing P-P cycle lengths during the periods of 5.4 and 4.3 sinoatrial block (see diagrams of leads I and II). B, lead strips of lead II, recorded from a different patient and showing what probably is 2.1 and 3.2 Wenckebach sinoatrial block (see diagrams of the two strips of lead II, a). In addition, there is first-degree atrioventricular block.

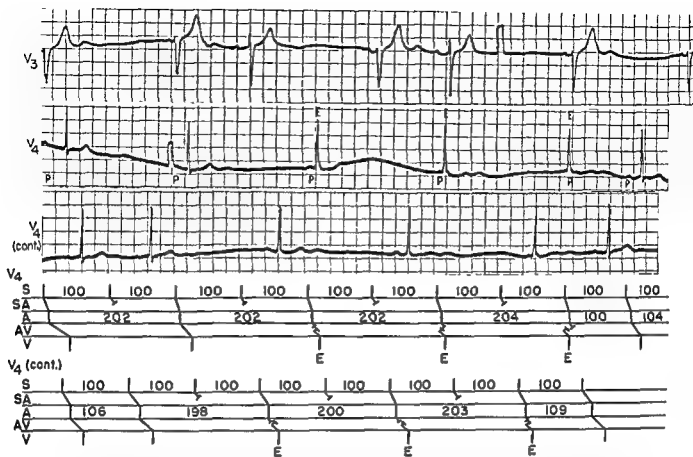


Fig. 326.—Varying degrees of sinoatrial block with atrioventricular nodal escape. In lead V₄, the first, second, fourth, sixth, and seventh ventricular complexes are atrioventricular nodal escape beats, but the P waves preceding them are sinus P waves (which are labeled P in lead V₄). The third and fifth QRS complexes are conducted beats. The longer P-P cycles (200 seconds) in this lead strip are almost twice the shorter P-P cycles (103 and 105 seconds), indicating 3:2 sinoatrial block. In the last portion of the lead, there is 2:1 sinoatrial block. Two continuous strips of lead V₄ show predominantly 2:1 sinoatrial block with the third, fourth, and fifth ventricular complexes being atrioventricular nodal escape beats (E) and the first, second, and sixth ventricular beats being conducted beats. In the second strip of lead V₄, the longer P-P cycles are slightly shorter than twice the shortest P-P cycles, but this can be attributed to variations in sinoatrial conduction of the sinus impulse preceding and the sinus impulse following the blocked beat. The two strips of lead V₄ are presented in diagram form to demonstrate the mechanisms responsible for the electrocardiographic findings.

PART IV

**Other Conditions Affecting
the Electrocardiogram**

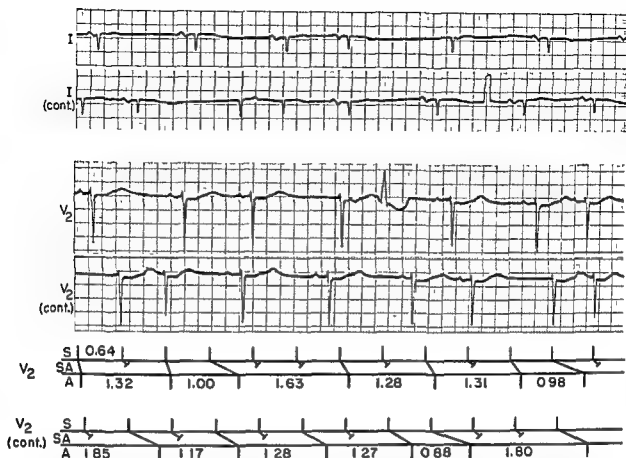


Fig. 328.—Varying degrees of sinoatrial block. The two continuous strips of lead V_2 are diagramed below the electrocardiogram. If it is assumed that the sinoatrial conduction times of the sinus impulses producing the second, third, and fourth P waves in the second strip of lead V_2 are probably the same, then the calculated cycle length of sinus node discharge is approximately 0.64 second, or one half the length of the P-P cycles of the aforementioned P waves. On spacing out this interval with reference to block is demonstrated. Note that the per- consecutive sinoatrial node discharges. A

a T wave may simulate sinoatrial block, and so a search should always be made for an ectopic P wave preceding the pause (Figs 325–328).

Clinical Aspects of Sinoatrial Pause, Sinoatrial Arrest, and Sinoatrial Block

Sinus node pause, sinus arrest, and sinoatrial block may be observed (a) in normal subjects with increased vagal tone or during infectious diseases, (b) in normal subjects with a hypersensitive carotid sinus,

(c) in patients with sinoatrial node involvement by coronary artery disease or myocarditis, or (d) as toxic manifestations of excess digitalis or quinidine, or of hyperkalemia. It has been stated that sinoatrial arrest, when due to toxic drug effects, may signify impending cardiac arrest.

For a detailed discussion of the effects of the drugs digitalis, quinidine, and pronestyl and of hyperkalemia on the heart and the electrocardiogram, see Chapter 28.

Digitalis, Quinidine, and Pronestyl; Electrolyte Imbalance

EFFECT OF DIGITALIS ON IMPULSE FORMATION AND TRANSMISSION

Digitalis Action

A comprehensive discussion of the effects of digitalis on the rhythm of the heart beat is beyond the scope of this text. Instead, the actions of digitalis are to be sketched only briefly in the following paragraphs, but the references listed in the bibliography may be consulted for a more detailed presentation of this subject.

The influence of digitalis on cardiac rhythmicity, excitability, and conductivity is mediated through two distinct actions—direct and indirect. In the direct action, the digitalis acts directly on heart muscle and produces myocardial depression qualitatively similar to, but quantitatively less intense than, that produced by quinidine. In the indirect action, the digitalis causes vagal stimulation. Thus, its indirect action is exerted through the intermediate agency of the vagal nerves and is equivalent in effect to increased vagal tone. Although the vagus nerves were not previously thought to extend as far as the ventricles, vagal stimulation recently has been demonstrated to influence the ventricular rhythm.

The actions of digitalis at different levels in the heart and their clinical implications are outlined below.

SINOATRIAL AND ATRIOVENTRICULAR NODAL PACEMAKERS

The rhythmicity of these centers is inhibited by both direct and indirect actions of digitalis. This is exemplified by sinus bradycardia, by sinus arrhythmia, or by the wandering supraventricular pacemaker which sometimes appears during digitalis therapy.

Fluctuating degrees of sinus node inhibition may, from time to time, permit an atrioventricular nodal pacemaker to escape at a slightly faster rate, and intermittent complete atrioventricular dissociation may appear.

SINOATRIAL AND ATRIOVENTRICULAR CONDUCTION PATHWAYS

The direct and indirect actions of digitalis have a synergistically depressive effect on sinoatrial and atrioventricular conductivity and prolong the refrac-

tation period. In the presence of digitalis-induced fibrillation, the depressant effect of digitalis on atrioventricular conduction is therapeutically desirable, while under other circumstances it may signify digitalis toxicity.

ATRIAL MYOCARDIUM

The influence of digitalis in the atria is complex, if not actually unpredictable to a certain degree. Sometimes the direct and indirect actions of digitalis augment, at other times antagonize, each other.

In general, the effects of digitalis on the atria are as follows:

Excitability.—Both directly and indirectly, digitalis depresses the excitability of atrial muscle and raises its excitability threshold to stimulation.

Refractory period.—The refractory period of atrial muscle is prolonged by digitalis.

Digitalis, Quinidine, and Pronestyl; Electrolyte Imbalance

EFFECT OF DIGITALIS ON IMPULSE FORMATION AND TRANSMISSION

Digitalis Action

A COMPREHENSIVE DISCUSSION of the effects of digitalis on the rhythm of the heart beat is beyond the scope of this text. Instead, the actions of digitalis are to be sketched only briefly in the following paragraphs, but the references listed in the bibliography may be consulted for a more detailed presentation of this subject.

The influence of digitalis on cardiac rhythmicity, excitability, and conductivity is mediated through two distinct actions—direct and indirect. In the *direct* action, the digitalis acts directly on heart muscle and produces myocardial depression qualitatively similar to, but quantitatively less intense than, that produced by quinidine. In the *indirect* action, the digitalis causes vagal stimulation. Thus, its indirect action is exerted through the intermediate agency of the vagal nerves and is equivalent in effect to increased vagal tone. Although the vagus nerves were not previously thought to extend as far as the ventricles, vagal stimulation recently has been demonstrated to influence the ventricular rhythm.

The actions of digitalis at different levels in the heart and their clinical implications are outlined below.

SINOATRIAL AND ATRIOVENTRICULAR NODAL PACEMAKERS

The rhythmicity of these centers is inhibited by both direct and indirect actions of digitalis. This is exemplified by sinus bradycardia, by sinus arrhythmia, or by the wandering supraventricular pacemaker which sometimes appears during digitalis therapy.

Fluctuating degrees of sinus node inhibition may, from time to time, permit an atrioventricular nodal pacemaker to escape at a slightly faster rate, and intermittent complete atrioventricular dissociation may appear.

SINOATRIAL AND ATRIOVENTRICULAR CONDUCTION PATHWAYS

The direct and indirect actions of digitalis have a synergistically depressive effect on sinoatrial and atrioventricular conductivity and prolong the refractory period of the junctional tissues. According to the dosage level, digitalis can produce all degrees of sinoatrial and atrioventricular block. In atrial flutter and fibrillation, the depressant effect of digitalis on atrioventricular conduction is therapeutically desirable, while under other circumstances it may signify digitalis toxicity.

ATRIAL MYOCARDIUM

The influence of digitalis in the atria is complex, if not actually unpredictable to a certain degree. Sometimes the direct and indirect actions of digitalis augment, at other times antagonize, each other.

In general, the effects of digitalis on the atria are as follows:

Excitability—Both directly and indirectly, digitalis depresses the excitability of atrial muscle and raises its excitability threshold to stimulation.

Refractory period—The refractory period of atrial muscle is greatly shortened by the vagal stimulating action of digitalis and, also, but to a lesser extent, by its direct muscular effect.

Conductivity.—Digitalis seems to depress the conductivity of atrial muscle. However, Scherf believes that the direct depressant action of digitalis or atrial conductivity is not yet supported by adequate proof.

Conversion of atrial flutter.—Ordinarily, the indirect action of digitalis, tending to shorten the refractory period of the atrial muscle, dominates its depressant effect on conductivity; and for this reason, digitalis often converts atrial flutter to fibrillation. In the occasional instances in which the reverse holds true—that is, the direct action being predominant—digitalis may cause atrial flutter to revert to sinus rhythm.

VENTRICULAR MYOCARDIUM

Although vagal fibers apparently reach the ventricular myocardium, the effects of vagal stimulation on the ventricles are rarely seen and, when present, are of minor importance. Consequently, the indirect action of digitalis in the ventricles is negligible, and the direct action, causing depressed conductivity and excitability, is predominant. It has been stated that, if digitalis lessens conductivity to a greater extent than it depresses excitability, it may convert ventricular tachycardia to ventricular fibrillation. As far as is known, digitalis does not affect the conductivity of the intraventricular conducting pathways, at least to a degree demonstrable in the electrocardiogram.

INTERRELATIONSHIP OF DIGITALIS AND POTASSIUM

Apparently, both the toxicity of digitalis and, perhaps even more fundamentally, its effect on the failing heart are involved in the complicated problem relating to the potassium metabolism of the myocardial cell. It is thought that the intracellular potassium ions surrounding the paired actin and myosin molecules prevent these proteins from uniting, owing to the mutually repelling action of ions having the same electrical charge. Excitation causes the cell membrane to become permeable to potassium ions, which diffuse out of the cell into the potassium-poor extracellular fluid. Loss of their potassium ion atmosphere permits actin and myosin to unite; and, after absorbing adenosine triphosphate, the resulting protein complex contracts. Thus the rapid migration of potassium ions to and fro across the cell membrane constitutes an important connecting link between electrical and mechanical cardiac systole and diastole.

Digitalis has been noted to improve the contractile dynamics of actomyosin solutions. Horvath and his associates feel that they have demonstrated a direct effect of digitoxin on the polymerization of

actin. However, it has been pointed out that, conceivably, these observed effects of digitalis may also reflect the effects of digitalis-induced alterations in the intracellular potassium ion concentration. The following additional observations by various investigators seem to imply a significant relationship between digitalis and the intracellular potassium of the heart:

1. Toxic doses of digitalis are said to liberate potassium from heart muscle. From a clinical standpoint, this is the explanation, presumably, for the reported effect of the toxic dose of digitalis in abolishing the electrocardiographic findings of hyperkalemia or lessening their prominence in patients with acute renal insufficiency. Several patients so treated and maintained on high doses of digitalis survived episodes of severe hyperkalemia.

2. Digitalis in therapeutic doses has been claimed by many investigators to increase the intracellular potassium ion concentration of the heart, but others have reported that digitalis lowers or has no effect on the potassium content of heart muscle. Clarke and Mosher found the potassium content of heart muscle obtained at autopsy to be lower than normal in undigitalized cardiac patients and normal or near normal in those who had received digitalis prior to death. In parallel with this observation, there is evidence suggesting that during the development of congestive heart failure there is a loss of body potassium, with a concomitant reduction in the cardiac intracellular potassium concentration, especially in those heart chambers which are failing. It has been proposed, without conclusive proof, that the beneficial effect of digitalis on the failing heart emanates from its action in restoring the heart muscle potassium to normal levels. Experimentally, digitalis in nontoxic doses has been found to prolong the life of adrenalectomized animals. This observation gives some substance, perhaps, to the belief that digitalis acts to maintain potassium within the heart cell.

3. Withdrawal of potassium from the body by dialysis or by mercurial diuresis has been shown experimentally and clinically to increase the sensitivity of the heart to digitalis. Thus, the removal of potassium from the body may precipitate digitalis intoxication despite an unchanged schedule of maintenance digitalis therapy. Conversely, most of the ectopic arrhythmias resulting from digitalis intoxication respond readily to potassium therapy. Sensitivity of the heart to digitalis is decreased, and resistance to the induction of digitalis intoxication increased, by the presence of elevated body potassium levels.

4. It has been shown that stimulation of the vagus nerve causes a loss of potassium from the heart. As was previously stated, the vagal-stimulating effect of digitalis is largely confined to the atria and to the junctional tissues of the sinoatrial and atrioventricular nodes. In view of the preceding facts, it is of interest that Sherrod noted significant potassium depletion in atrial muscle but no significant change in the potas-

Digitalis Effect on the Electrocardiogram

may be seen in the P-R-T segment, and T wave. The magnitude of

TABLE 29—DISTURBANCES OF IMPULSE FORMATION AND CONDUCTION DUE TO DIGITALIS

EXCESSIVE DIGITALIS EFFECT	DISTURBANCES OF IMPULSE FORMATION	DISTURBANCES OF IMPULSE CONDUCTION*
	<ol style="list-style-type: none"> Depressed rhythmicity of the sinoatrial node leading to sinus bradycardia, wandering supraventricular pacemaker, sinus arrhythmia, and atrioventricular nodal escape with atrioventricular dissociation and a ventricular rate less than 60 beats per minute Atrioventricular nodal rhythm with atrioventricular dissociation, a ventricular rate faster than 60 beats per minute, and retrograde atrioventricular block (occasionally with incomplete forward atrioventricular block) Rare in occasional premature ectopic ventricular beats (VPC's) (less commonly, atrial or nodal premature beats). Typically, ventricular extrasystoles induced by digitalis are multifocal in appearance but unifocal in origin, as evidenced by their constant coupling intervals 	<ol style="list-style-type: none"> First- or second-degree atrioventricular block Sinoatrial block with atrioventricular nodal escape High degree of atrioventricular block in the presence of atrial fibrillation, as evidenced by a slow, almost regular ventricular rhythm with frequent atrioventricular nodal escape
Therapeutic implications	Digitalis can be continued cautiously, preferably at a reduced dosage	
DIGITALIS INTOXICATION	The appearance of any of the following abnormalities in the electrocardiogram	
	<ol style="list-style-type: none"> Premature ectopic ventricular beats giving rise to a bigeminal rhythm, VPC's of multifocal origin or paired bidirectional VPC's, or VPC's occurring in short runs of consecutive beats Paroxysmal ectopic tachycardia <ul style="list-style-type: none"> Paroxysmal atrial tachycardia with atrioventricular block Paroxysmal atrioventricular nodal tachycardia with atrioventricular dissociation and retrograde atrioventricular block Simultaneous paroxysmal atrial and atrioventricular nodal tachycardias with complete atrioventricular dissociation Alternating bidirectional tachycardia Paroxysmal ventricular tachycardia Paroxysmal atrial or ventricular flutter or fibrillation 	<ol style="list-style-type: none"> Complete atrioventricular block
Therapeutic implications	Digitalis should be discontinued immediately. Oral or intravenous potassium chloride is the treatment of choice. Quinidine and pronestyl should not be given.	
	Therapy is the same as that used in complete atrioventricular block due to other causes	

*For all intents and purposes the conduction disturbances produced by digitalis are limited to the sinoatrial and atrioventricular conducting pathways. Intraventricular conduction abnormalities due to digitalis have not been reported, as far as the authors can determine.

TABLE 30—EFFECTS OF VAGAL STIMULATION, EXERCISE, AND DRUGS ON ECTOPIC TACHYCARDIAS, FLUTTER, AND FIBRILLATION

	SUPRAVENTRICULAR TACHYCARDIA (SVT) (Atrial or Atrioventricular Nodal)		ATRIAL FLUTTER (AFI)	ATRIAL FIBRILLATION (AF)	VENTRICULAR TACHYCARDIA (VT)
	Without Atrioventricular Block	With Atrioventricular Block			
Carotid sinus stimulation	1 Terminates SVT in 65% of cases 2 Alternatively, no effect	1 Rarely terminates SVT with atrioventricular block 2 Usually increases degree of atrioventricular block and slows ventricular rate	1 Usually temporarily increases degree of atrioventricular block and slows ventricular rate to $\frac{1}{2}$, $\frac{1}{3}$, etc. of the original rate. Despite continued vagal stimulation, there is usually an irregular return of ventricular rate to its former level. 2 Occasionally increases the atrial rate of AFI or converts flutter to fibrillation.	Increases degree of atrioventricular block with irregular slowing of ventricular rate	1. Usually no effect. 2. Rarely, decreases ventricular rate.
Exercise	No effect	May decrease degree of atrioventricular block and increase ventricular rate	Either no effect or decreases degree of atrioventricular block and increases ventricular rate.	Decreases degree of atrioventricular block temporarily, and temporarily increases ventricular rate. Apparently, these effects can occur despite adequate digitalis medication.	No effect.
Increased vagal tone produced by parasympathomimetic drugs	Often terminates SVT	Same effects as carotid sinus stimulation, but more marked and long lasting	Same effects as carotid sinus stimulation, but more marked and long lasting	Same effects as carotid sinus stimulation, although more marked and longer lasting	1. No effect 2 (?) May rarely convert VT to ventricular fibrillation.
Digitalis	Usually terminates SVT	1 When digitalis toxicity is not a causative factor, digitalis terminates SVT with atrioventricular block in less than 50% of the cases. 2 In over 50% of the cases, the degree of atrioventricular block is increased and ventricular rate is slowed.	1 Sometimes converts AFI to sinus rhythm directly 2 Usually converts AFI to atrial fibrillation, which in about 65% of such cases reverts to sinus rhythm on cessation of digitalis 3. Increases degree of atrioventricular block and slows ventricular rate.	1. Same effects as parasympathomimetic drugs. 2. Occasionally reverts AF directly to sinus rhythm, particularly if the AF is acute or paroxysmal rather than chronic, or if AF is secondary to congestive heart failure.	Occasionally may terminate VT not due to digitalis intoxication, when other measures have failed.

Quinidine and Procainyl 1) are similar in their effect on VT, but the relative efficacy are difficult to have as	1 Quinidine converts AF* to sinus rhythm in 80% of the cases. 2 Procainyl has same therapeutic efficacy as in AFL	1 Quinidine converts AF* to sinus rhythm in 30-50% of the cases 2 Procainyl sometimes reverts acute, paroxysmal AF* to sinus rhythm but has little effect in chronic AF* unless used in massive and potentially toxic doses.	1 Quinidine (a) has terminate S-VT or (b) alteratively, may increase ventricular rate by its vagolytic action 2 Procainyl terminate S-VT with atrioventricular block in 5 of 7 cases reported by Lewis and Levine	May terminate S-VT with or without atrioventricular block if the S-VT is due to digitalis intoxication
May terminate VT due to digitalis intoxication, but is less successful therapeutically in VT not due to digitalis excess		Effects of potassium on AFL and AF have not, as yet, been well studied, but potassium may terminate these arrhythmias when they are due to digitalis intoxication		Potassium

*Atrial and atrioventricular nodal tachycardias, with or without atrioventricular block, respond in essentially the same way to vagal stimulation, carotid, and so, no distinction is drawn between the two types of ectopic tachycardias in this table, both being grouped under the heading "supraventricular tachycardia"

these changes correlates, in only a very approximate and inconstant way, with the amount of digitalis administered. For this reason, the appearance of digitalis effect does not augur digitalis toxicity, nor does it indicate that a therapeutic dose of the drug has been given. In fact, the presence or absence of electrocardiographic digitalis effect affords no proof that a given patient has or has not received digitalis in the recent past. This point is illustrated by the occasional patients severely intoxicated with digitalis who display normal electrocardiograms, and their opposites—that is, patients not under digitalis therapy who show T wave and S-T segment changes which mimic digitalis effect but are due to other conditions. The electrocardiographic features of digitalis effect are as follows:

SHORTENING OF THE Q-T INTERVAL

of the heart, so that repolarization of the ventricular wall is accomplished more quickly than normally. The shortening of the Q-T interval is of little value clinically in the detection of digitalis effect unless previous electrocardiographic tracings are available for careful measurement and comparison of the Q-T intervals.

CHANGES IN THE S-T SEGMENT AND T WAVE

With mounting intensity of digitalis effect, the following two changes occur: (a) The S-T vector representing early repolarization forces tends to increase in magnitude as the T vector representing late repolarization potentials decreases. (b) The mean S-T vector is directed away from the mean QRS vector, while the mean T vector continues to parallel the QRS vector unless digitalis completely reverses the direction of repolarization. In this instance, the S-T and T vectors point away from the mean QRS vector.

In terms of the electrocardiogram, the above orientations of the mean QRS, S-T and T vectors relative to one another produce the digitalis effect pattern consisting of depressed S-T segments with small, upright terminal T waves or inverted T waves in leads registering resultant positive QRS complexes (see also Chapter 6, p 85).

1 T changes due leads recording result in the following manner (a) Minor degrees of digitalis effect may cause simultaneous repolarization both in the

normal epicardial to endocardial direction and in the reverse direction, the latter effect being due to more rapid recovery in the subendocardium. These two repolarization forces, directed oppositely, yield a resultant mean T vector of decreased magnitude whose orientation is not markedly altered. Because of the shortened Q-T interval, depolarization and repolarization tend to overlap, so that repolarization forces directed from endocardium to epicardium appear before inscription of the QRS is completed. The S-T segment and its point of junction with the ventricular complex (designated "J") are displaced downwardly as a result. Subsequently, the outer layers of myocardium, whose recovery process is less affected by digitalis, repolarize in the normal direction and a small, upright terminal T wave is written. (b) Often digitalis effect is so intense that the entire ventricular wall repolarizes in a reverse direction—that is, from endocardium to epicardium. In such a case, the S-T segment is depressed and the T wave is inverted.

Digitalis acts to abolish the subendocardial recovery delay which is present normally and is responsible for the normal ventricular gradient. The ventricular gradient becomes smaller as the variations in the duration of the excited state between inner and outer layers of heart muscle decrease with onset of digitalis effect. If the action of digitalis in reducing the ventricular gradient is coupled with another influence also likely to decrease the gradient—such as exercise, ventricular hypertrophy, transmural ischemia, or hypoxia—S-T and T wave changes which were not present previously may appear. Often the S-T segment depression secondary to digitalis is relatively distinctive because of its straight-line or downwardly bowed appearance. The S-T segment depression caused by other conditions more commonly exhibits upward bowing of the S-T segment. Unfortunately, the configuration of depressed S-T segments varies so widely that it is of little practical value in differentiating the S-T segment deviations of digitalis effect from changes due to other causes. It is interesting that the ST-T changes of digitalis can be nullified by potassium salts. However, intracellular potassium loss cannot be held responsible for the shortening of the Q-T interval observed in digitalis therapy.

The paradoxical effects of digitalis on impulse formation and conduction in the heart may be summarized in general terms as follows (see also Tables 29 and 30)

1. The depressant action of digitalis on atrioventricular conductivity, in particular, is sometimes therapeutically

desirable (e.g., when digitalis is used to slow the ventricular rate in atrial flutter or fibrillation) but at other times is a manifestation of digitalis toxicity. Thus, the significance of digitalis-induced atrioventricular block may depend, in a given instance, on the therapeutic objective of digitalis administration.

2. Digitalis is generally considered to be a cardiac depressant, and yet, on occasions, it apparently enhances the rhythmicity of secondary cardiac pacemakers. This effect is exemplified by the relatively rapid rate of atrioventricular nodal rhythms with atrioventricular dissociation which sometimes appear as manifestations of digitalis toxicity. By the same token, in complete atrioventricular block produced by toxic doses of digitalis, the rate of the ventricular pacemaker tends to be more rapid than that in complete atrioventricular block not related to digitalis.

3. Digitalis toxicity may be manifested by the appearance of rapid ectopic rhythms, which under other circumstances are abolished by administration of digitalis. Thus, digitalis may terminate paroxysmal supraventricular tachycardias, atrial flutter, and atrial fibrillation. Conversely, toxic levels of digitalis in the body may produce any of the preceding abnormal rhythms (including paroxysmal ventricular tachycardia).

A clinical observation familiar to all is the varying susceptibility of different patients to digitalis intoxication. This can be attributed, in some cases, to differences in the severity of the underlying cardiac disease, to the presence or absence of derangements of body electrolytes (notably potassium, sodium, calcium, and possibly magnesium), or to the existence of active myocarditis, myocardial ischemia, or some other disease process elsewhere in the body. However, the predilection of other patients to digitalis intoxication is not related to any factors which can be recognized in advance and for which allowances can be made during digitalization. Consequently, the effects of digitalis administration on impulse formation and conduction in the heart are somewhat unpredictable, and so, digitalization of a patient is, in a sense, an experiment which should be monitored by the electrocardiogram to avoid digitalis intoxication or to detect it at its earliest stage. The extracardiac manifestations of digitalis toxicity will not be described.

The terminology used in this text for designating the electrocardiographic manifestations of digitalis is as follows (see also Table 29)

Digitalis effect—Digitalis effect may be summarized as follows. Digitalis hastens the repolarization process in the ventricular muscle. This action is re-

ected in the electrocardiogram by a shortening of the Q-T interval, by S-T segment deviation, and by T wave depression or absence or the promi-

heart muscle

Excessive digitalis effect—This term is applied to

electrocardiographic findings which represent undesired or even toxic digitalis effects but are not contraindications to continued, cautious administration of the drug.

Digitalis intoxication—This is the designation given to those digitalis-induced abnormalities of impulse formation or conduction which preclude further digitalis therapy.

QUINIDINE AND PRONESTYL

Quinidine and pronestyl (procaine amide) differ in many respects besides their chemical structures, but in terms of their effect on the heart and electrocardiogram, the similarities of the two drugs far outnumber their dissimilarities. Comparison of the clinical value of quinidine and pronestyl has led to some controversy. However, at present it is believed that at comparable dosages (250 mg capsule of pronestyl is approximately 1 gr of quinidine), quinidine and pronestyl are of equal therapeutic efficacy in most of the arrhythmias, excluding chronic atrial fibrillation and flutter. In these arrhythmias, quinidine is more successful in effecting conversion to sinus rhythm than is pronestyl. Before considering the actions of these two drugs, it is well to point out that (a) procaine has the same effect on the heart as procaine amide (pronestyl) but is so rapidly hydrolyzed in the body that its effect is quite transient, and (b) quinine and atabrine apparently have cardiac effects resembling those of quinidine, but less marked.

Actions of Quinidine and Pronestyl

Vagal paralysis—Once quinidine or pronestyl has

effects depend on vagal stimulation. By decreasing the refractory period of the atrioventricular node and therefore lessening the degree of block in atrial fibrillation or flutter, the vagolytic action of quinidine and pronestyl can lead to a marked acceleration in the ventricular rate.

Decreased conductivity—Both drugs slow conduction recovery and lessen conductivity.

Depressed excitability—The excitability threshold for response to stimulation is raised, and irritability and excitability is depressed.

Slowing of rate of discharge of an ectopic focus—Prinzmetal and his co-workers believe this to be the

main antiarrhythmic action of quinidine, although it may not be separate and distinct from the two preceding drug effects. These investigators also tentatively suggest that the vagolytic action of quinidine may contribute to the depressant action on the ectopic pacemaker. Usually the ectopic focus is more sensitive to the depressant effect of quinidine than is the sinoatrial node. Therefore, when the ectopic pacemaker is slowed by quinidine to a rate below that at which the sinoatrial node is discharging, the arrhythmia is supplanted by a normal sinus rhythm. The occasional therapeutic failures of quinidine may stem from the fact that in these cases the ectopic focus has a resistance to quinidine equaling or surpassing that of the sinoatrial node.

While it is a common assertion that quinidine and pronestyl lengthen the refractory period of atrial and ventricular muscle, in actuality neither drug has this effect. Quinidine has even been demonstrated, in some cases, to shorten the refractory period. The antiarrhythmic properties of quinidine and pronestyl are derived chiefly from their depressant action on the conductivity and excitability of the heart, with perhaps an additional factor—namely, their tendency to slow the rate of discharge of the ectopic focus. The muscle and conductive tissues of all regions of the heart share, to a varying degree, the depressant effect of the two drugs—hence, the applicability of these drugs to both supraventricular and ventricular arrhythmias (Table 30). However, this widespread therapeutic action is accompanied by an equally widespread toxic action of the drugs, so that virtually any portion of the electrocardiographic complex may display drug-induced abnormalities.

The ECG Changes Due to Quinidine and Pronestyl

The following changes are probably within the limits of therapeutic effect.

1. Prolongation of the Q-T interval—the earliest manifestation of quinidine effect. This manifestation, although frequently observed during pronestyl therapy, may occasionally fail to be present. Moreover, myocardial disease, which is present more often than not in patients receiving quinidine, also causes Q-T interval prolongation.
2. Some widening and notching of the P waves.
3. Flattening or inversion of the T waves and slight depression of the S-T segments.

The changes which are probably representative of toxic drug effect are the following.

1. Possible increase in the duration of the P-R interval.
2. Slowing of the atrial rate, development of intra-atrial block, and atrial standstill in severe toxicity.
3. Progressive widening of the QRS complex with increasing blood levels of quinidine or pronestyl. Sokolow states that, ordinarily, the usual dose of 2-3 Gm. of quinidine orally per day does not cause significant widening of the QRS interval. Drug

therapy should be stopped if the QRS interval becomes widened by 50% of its control width, and caution should be exercised by recording an electrocardiogram before each dose of the drug when the drug-induced increment in the QRS interval approaches 25% of the control interval. Marked widening of the QRS deflections may precede onset of ventricular tachycardia or ventricular fibrillation.

4. According to Sokolow and others, the appearance of ventricular arrhythmias, such as ventricular extrasystoles and ventricular tachycardia, often represents toxic manifestations of quinidine (and presumably pronestyl).

Just as there is some disagreement over the respective therapeutic efficacies of pronestyl and quinidine, so also there is differing opinion concerning their comparative toxicities. While conclusive proof is lacking, many clinicians are of the conviction that pronestyl is a less toxic agent than quinidine, a view which Scherf does not accept.

ELECTROLYTE IMBALANCE

Only disturbances of body potassium and calcium will be described, since less is known of the cardiac effects of other electrolytes and since, in clinical electrocardiography, disturbances in body potassium and calcium are relatively frequent occurrences.

Potassium

Ninety-eight per cent of the body potassium resides intracellularly, but routinely it is possible to measure only the venous serum potassium concentration. It is evident that determination of the latter value can have only limited implications in terms of the total body potassium and intracellular potassium concentration because the extracellular potassium constitutes such a small fraction of the total. Hyperkalemia (hyperpotassemia) is said to be present when the serum potassium level exceeds 5.5 milliequivalents per liter (mEq./L.), while hypokalemia (hypopotassemia) exists when serum potassium levels are less than 3.5 mEq./L. This is not to say that serum potassium levels outside of the normal range must, of necessity, produce electrocardiographic or clinical manifestations. Moreover, identically abnormal serum potassium concentration in two persons need not be associated with the same degree of electrocardiographic change. In all probability, other electrolytes—sodium,

in particular—modify the effect of abnormal potassium levels on the heart. Sodium and potassium ions have a somewhat antagonistic relationship, in that hyponatremia (low serum sodium) exaggerates the electrocardiographic effects of an elevated serum potassium level, while a normal or high serum sodium level tends to antagonize the effects of hyperkalemia. Undoubtedly, the mechanism responsible for the interrelationship of body potassium and sodium is far more complicated than the term "antagonism" would infer.

ETIOLOGY OF ABNORMALITIES OF SERUM AND BODY POTASSIUM

Exogenous intake—Excessive or deficient dietary intake of potassium is important to the extent that it aggravates the primary defect causing abnormal potassium retention or loss. The oral administration of potassium to subjects with normal renal function rarely leads to hyperkalemia, but potassium chloride given too rapidly or in too high concentrations by intravenous infusion can produce transiently lethal potassium levels (greater than 10 mEq./L.) despite excellent kidney function.

Renal function—Chronically and severely diseased kidneys do not conserve potassium as well as do normal kidneys, and so, regardless of the intake of potas-

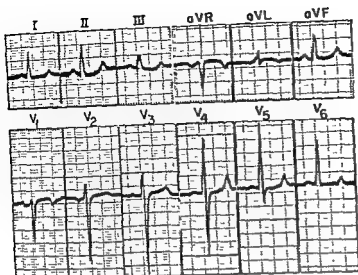
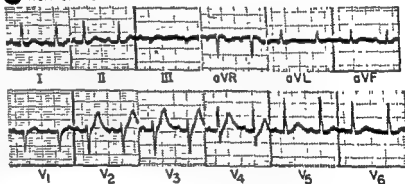


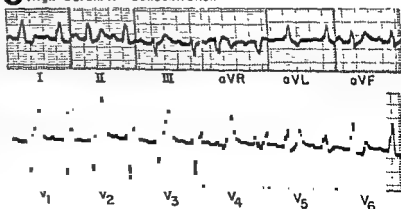
Fig. 329.—Electrocardiogram indicating hyperkalemia due to acute renal insufficiency. The principal abnormality is the presence of upright tented T waves in leads I, II, aVF, V₁, V₂, and V₃. (The "tenting" of the T waves refers to their symmetrical and peaked contour.) This finding occurs particularly when hyperkalemia is superimposed on pre-existing T wave abnormalities due to some other condition.

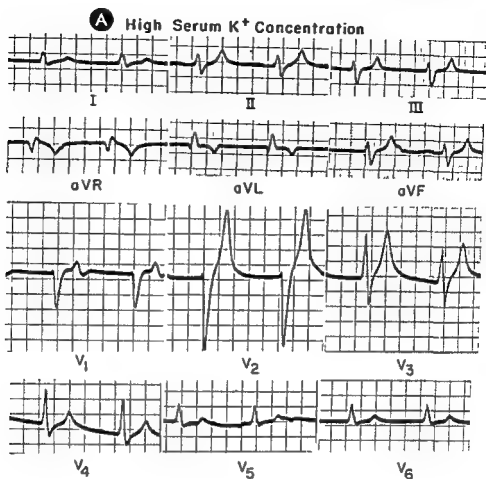
Fig 330.—**A**, electrocardiogram obtained shortly after onset of acute renal failure, before any change in the serum potassium ion concentration. This record is essentially within normal limits. **B**, record from same patient later in the course of acute renal failure, when the serum potassium ion concentration was quite high. The QRS interval is widened to 0.10–0.11 second, and the QRS configuration resembles that seen in left bundle branch block. The T waves are very tall in leads V₁ through V₆, and the S–T segments are depressed in leads I, II, aVF, V₁, and V₂. In addition, there is slight prolongation of the P–R interval in the second electrocardiogram, as compared to the first. These findings are compatible with hyperkalemia.

A Normal Serum K⁺ Concentration



B High Serum K⁺ Concentration





B Essentially Normal Serum K^+ Concentration

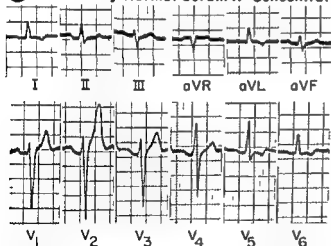
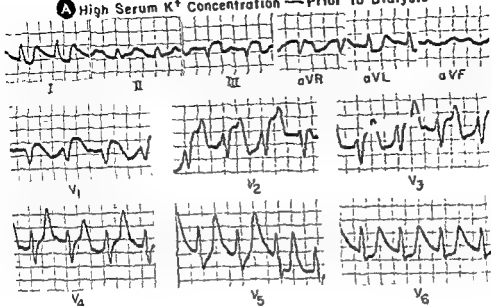


Fig. 331.—**A**, electrocardiogram from a patient with severe renal failure and a markedly elevated serum potassium ion concentration. This record shows a prolonged QRS interval (0.12 second) and tall peaked T waves in leads II, III, V₄, V₅, and V₆. The P waves cannot be identified with certainty, and so the mechanism of the rhythm may be atrioventricular nodal. **B**, later record from same patient. The previous intraventricular conduction defect and the tall T waves have disappeared, and the only abnormality present is T wave inversion in leads I, V₁, and V₂. The QRS interval is 0.08 second. Note that the general configuration of the QRS deflections is essentially the same in both records in corresponding leads despite the prolonged QRS interval in the former. Thus, in **A**, there probably is a diffuse intraventricular block rather than a block in one or the other bundle branch. The rhythm in **B** is sinus rhythm.

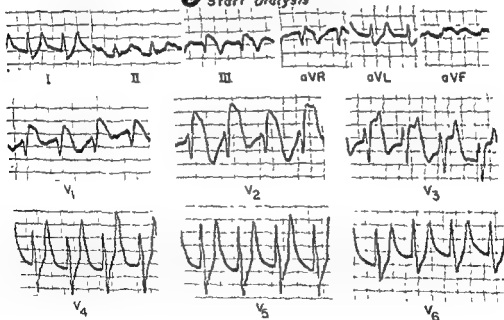
sium, the urinary concentration remains essentially constant. According to Elkinton and his associates, as well as other authorities, the renal tubules continue to secrete potassium whether the serum potassium level is high, normal, or low. This mechanism may be chiefly responsible for the low serum potassium concentrations often observed in patients with chronic renal disease. Inasmuch as the potassium clearance in

renal disease remains relatively constant, the amount of potassium excreted by the kidneys is largely dependent on the volume of urine output. It is generally accepted that either oliguria or anuria is necessary for the development of hyperkalemia. However, the extent of the potassium intake, protein catabolism, and potassium loss by other routes, as well as the serum sodium concentration, state of hydration, and

A High Serum K^+ Concentration — Prior to Dialysis



B Start Dialysis



through V_4 . The S-T segments are depressed and merge with terminal S waves in leads I, aVL, and V_4 through V_6 . Also, the T waves in most of the leads are larger than in corresponding leads in A. (Continued)

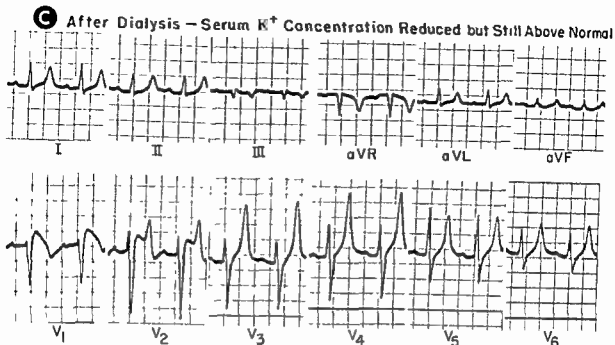


Fig. 332 (cont) — C, record after dialysis was completed, at which time the serum potassium ion concentration was greatly reduced from its previous high level but still above normal. The QRS interval in this electrocardiogram is 0.08 second. The P-R interval is only slightly prolonged, and the T waves are extremely tall and symmetrically peaked in leads I, II, and V_1 through V_6 . The S-T depression noted in A and B is much less striking in C, but the S-T segment elevation in leads V_1 and V_2 persists.

other factors, all influence the rapidity of onset and progression, as well as the degree of hyperkalemia resulting from the primary renal dysfunction.

Losses of potassium from the extracellular fluid — The common clinical examples of this mechanism which result in hypokalemia are excessive mercurial diuresis, chlorothiazide therapy, diabetic acidosis, severe vomiting or diarrhea, and the loss of gastrointestinal secretions through fistulas. Untreated diabetic acidosis initially causes a rise in the serum potassium levels because of intracellular potassium depletion. At a variable period after institution of therapy, hypokalemia often appears, probably owing to the following factors: (a) excessive urinary loss of potassium secondary to the diuretic effect of glycosuria, (b) dilution of the serum potassium by parenteral administration of large quantities of potassium-free fluids, and (c) the intracellular migration of potassium due to the acidosis per se and the intracellular deposition of potassium and glycogen promoted by insulin therapy.

THE ECG FEATURES OF HYPERKALEMIA

According to Merrill and his co-workers, the following general sequence of electrocardiographic changes develops as the serum potassium concentration becomes progressively more elevated.

1. The T waves, particularly in the precordial leads,

become tall, narrow, and peaked. They may be of normal amplitude but tent-shaped in the extremity and or the precordial leads in patients with a pre-existing tendency to T wave inversion due to underlying cardiac disease.

2. Prolongation of the Q-T interval may accompany the above finding.
3. Then S-T segment depression occurs, the S-T segment tending to form a more or less straight line from the nadir of the S wave to the peak of the T wave.
4. Atrioventricular block may next appear, usually in the form of a first-degree atrioventricular block.
5. There may be lowering and widening of the P waves with subsequent atrial standstill or atrial fibrillation.
6. Intraventricular block of increasing degree is usually observed.
7. Ventricular arrhythmia consisting of irregular bizarre undulations often presages terminal ventricular standstill.
8. Ectopic ventricular rhythms, such as extrasystoles, tachycardia, flutter, and fibrillation, may also be encountered in the advanced stages of hyperkalemia (Figs. 329-334).

THE ECG FEATURES OF HYPOKALEMIA

The electrocardiographic findings in hypokalemia

may reflect an intracellular deficit of potassium, although Surawicz and Lepschkin are of the opinion that the potassium gradient across the cell membranes may have a closer correlation with the changes in the electrocardiogram. The abnormalities observed in hypokalemia are as follows.

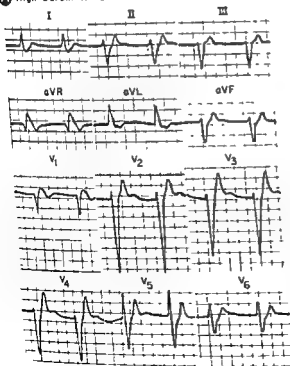
1. There is progressive lowering of the S-T segment. At first the ascending slope of the normal S-T segment changes to a straight, isoelectric line, and then S-T segment depression of increasing degree appears as the serum potassium falls.
2. There is lowering, and finally inversion, of the T wave.
3. An increased amplitude of the U wave may be noted in the precordial leads.
4. The Q-T interval is unchanged but often gives the appearance of being prolonged if the prominent U waves are confused for T waves.

5. Weller and his associates have called attention to the increased prominence of the P waves and to the prolongation of the P-R interval, which may often be seen in hypokalemia.

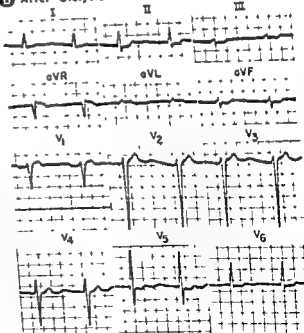
6. Surawicz and Lepschkin state that peaked P waves, atrioventricular conduction disturbances, and ectopic rhythms (particularly those of supraventricular origin) are helpful supportive evidence for hypokalemia when the electrocardiographic findings are otherwise equivocal (Figs 335 and 336).

Worthy of reiteration is the fact that, not uncommonly, the serum potassium concentration is found to be normal in the presence of an electrocardiogram typical of hyper- or hypokalemia. At the other extreme, abnormally elevated or depressed serum potassium levels may not be attended by any detectable electrocardiographic changes.

A High Serum K^+ Concentration



B After Dialysis



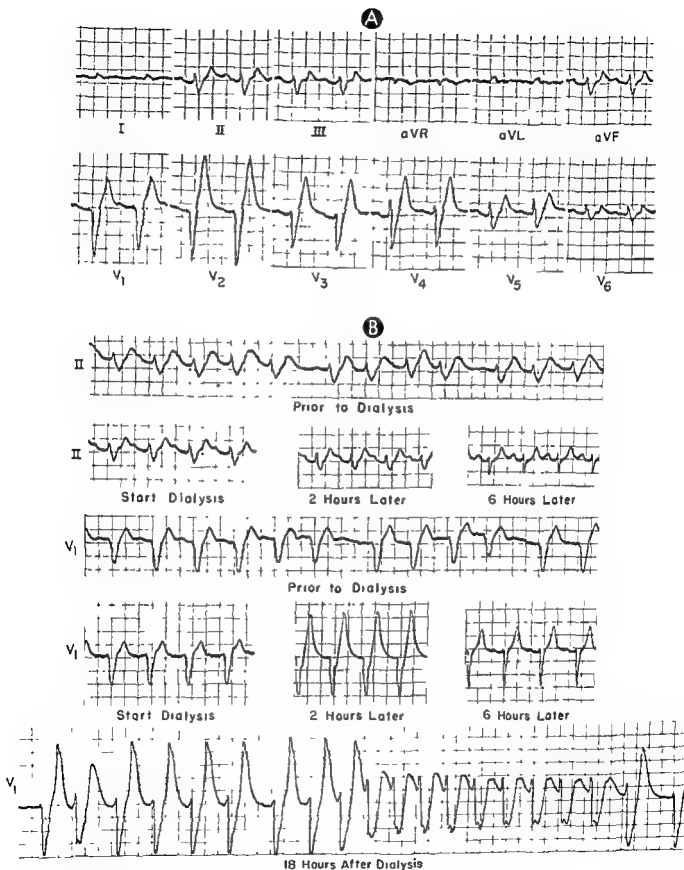
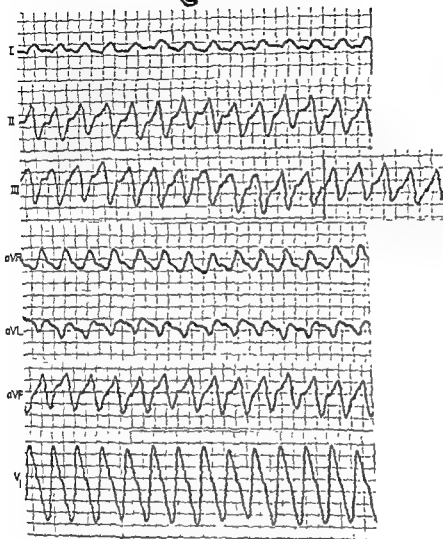
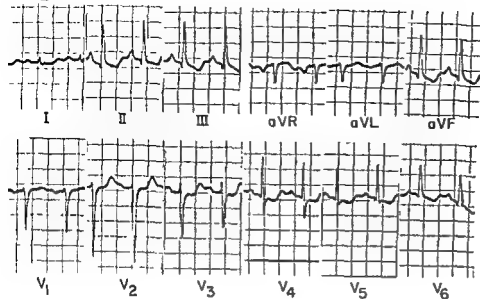


Fig. 334.—A, record from a patient in acute renal failure with greatly elevated serum potassium ion concentration. The electrocardiographic abnormalities diagnostic of hyperkalemia—prolonged intraventricular conduction, and extremely tall T strips recorded before, during, and after dialysis with the arti-

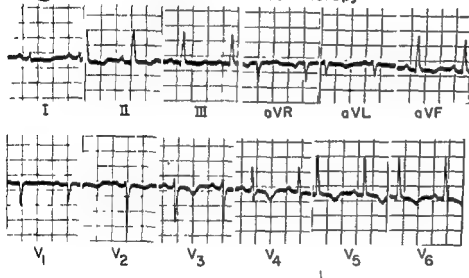


Terminal Record 36 Hours After Dialysis

A Low Serum K^+ Concentration



B Start Potassium Chloride Therapy



C Moderately High Serum K^+ Concentration After Therapy

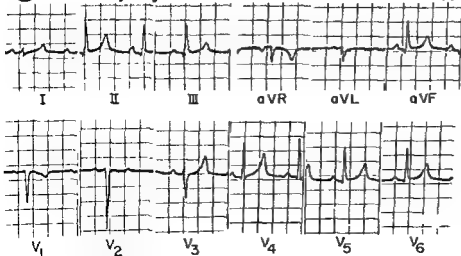
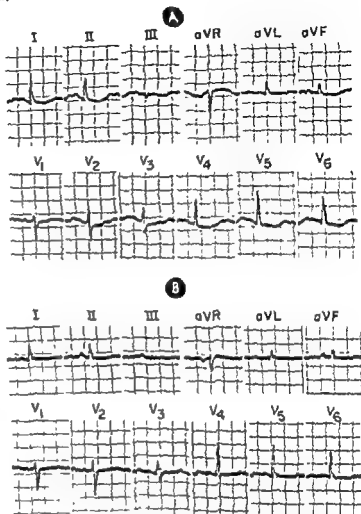


Fig. 335. — **A**, electrocardiogram from a patient with hypokalemia. The changes related to the low serum potassium ion concentration are S-T segment depression in leads I, II, III, and V_1 through V_4 , and inverted T waves in leads II, III, aVF, V_1 , and V_2 . **B**, record made about the time that parenteral potassium chloride therapy was begun. This electrocardiogram is also diagnostic of hypokalemia but shows certain additional changes, consisting of inversion of the T waves in leads I and V_5 through V_6 . The S-T segments are essentially isoelectric in most of the leads. The patient was treated vigorously with potassium chloride, and after therapy there was a moderately elevated serum potassium ion concentration. **C**, electrocardiogram consistent with moderately elevated serum potassium concentration, showing tall, peaked T waves in leads I, II, III, aVF, and V_1 through V_4 .

Fig. 336.—A, typical electrocardiographic findings of hypokalemia, consisting of depressed S-T segments and shallowly inverted T waves in leads I, II, III, aVF, and V₁ through V₆. In addition, prominent upright U waves can be seen shortly following the T waves in many of the leads. The latter finding is frequently observed in hypokalemia and may sometimes lead to erroneous results in measuring the Q-T intervals in this condition. B, record made after the patient had been treated with potassium chloride, and showing some improvement in the S-T segments and T waves compared with the first tracing. However, the T waves remain low in leads I, II, aVF, and V₁ through V₆, and the tracing, on the whole, is still suggestive of hypokalemia.



Calcium

Elevated serum calcium levels (hypercalcemia) rarely cause significant cardiac manifestations (other than shortening of the Q-T interval) unless they result from the intravenous infusion of calcium salts. The latter route of calcium administration has been attended by occasional deaths, particularly in patients with cardiac disease. It is said that the danger

of ventricular fibrillation resulting from elevated serum calcium levels is enhanced in digitalized patients, for reasons unknown. Transient ventricular ectopic rhythms have been described during intravenous infusion of calcium salts. Abnormally low serum calcium levels (hypocalcemia) may cause Q-T interval prolongation (primarily by virtue of lengthening of the S-T segment) and produce lowering or inversion of the T waves.

Ventricular Pre-Excitation (Wolff-Parkinson-White Syndrome)

THE Wolff-Parkinson-White syndrome is unique in that it is one of the few clinical cardiac syndromes—if not the only one—in which the diagnosis rests entirely on the electrocardiographic findings. This condition usually has a benign prognosis and is characterized by the following features (a) in the elec-

trocardiogram, normal sinus P waves are followed, after unusually short P-R intervals, by QRS complexes of abnormal configuration and usually of prolonged duration, and (b) patients with this condition are predisposed to recurrent episodes of paroxysmal ectopic rapid heart action.

MECHANISM

It is generally conceded that pre-excitation of a localized area of the ventricular musculature is responsible, in the final analysis, for the electrocardiographic features of this syndrome. However, the mechanism by which pre-excitation is accomplished has not been established conclusively. Two theories of the pre-excitation mechanism—the accessory atrioventricular pathway theory and the accelerated atrioventricular conduction theory—will be considered in the following paragraphs.

Accessory Atrioventricular Pathway Theory

The concept of accessory atrioventricular pathway proposes that one or more muscle bundles link atria to ventricles and serve as accessory conducting pathways, competing more or less, in this respect, with the atrioventricular node. (Such accessory pathways are presumed to be congenital in origin even though the clinical and electrocardiographic manifestations of ventricular pre-excitation may not appear for many years.) When the onset of pre-excitation occurs, it may be spontaneous or it may be the indirect result of disease of the normal conducting pathways. The anomalous conducting bundle provides a short cut for the activation impulse, enabling it to bypass the atrio-

ventricular node, which is normally the site of significant conduction delay.

The pre-excitation sequence may be summarized as follows:

1. The atrial impulse is divided between the atrioventricular node and the accessory pathway. However, because of rapid conduction through the anomalous pathway, the pre-excitation impulse arrives in a focal region of the ventricular myocardium in advance of the activation impulse traveling through the atrioventricular junctional tissues. Consequently, the P-R interval is shortened.

2. The depolarization wave may then pass from this one focus of pre-excitation throughout both ventricles. In this event, the ventricular activation process is analogous to that in unifocal ventricular premature contractions, in that depolarization spreads erratically from one ventricle to the other via the muscle fibers rather than along the conducting system. Thus the QRS complex is abnormally widened and deformed.

3. More often it happens that there is a synchronous activation of the ventricles by impulses passing through both (a) the accessory pathway and (b) the atrioventricular node and the bundle branch system. This circumstance produces an electrocardio-

graphic ventricular fusion beat, the initial slurred portion of which (the delta wave) results from pre-excitation of one area of ventricular myocardium. The rest of the QRS complex is produced largely by activation of remaining nonrefractory myocardium by the normally conducted impulse and may resemble somewhat the corresponding portion of a normally conducted beat in the same lead.

4. It has been postulated that the length of the accessory atrioventricular pathway may influence the electrocardiographic features of the pre-excitation beat. If the pathway is short, the short P-R interval may be followed by a QRS complex of essentially normal configuration (for example, the so-called "syndrome of the short P-R interval, normal QRS complex, and paroxysmal rapid heart action," which occurs predominantly in women). On the other hand, a long anomalous conducting bundle may cause marked slurring of the initial portion of a widened and deformed QRS complex.

Accelerated Atrioventricular Conduction Theory

Prinzmetal and his associates present an alternative explanation for the pre-excitation phenomenon, based on their interpretation of certain clinical and experimental observations. The fundamental tenets of their theory may be outlined as follows.

1. Certain elements of the atrioventricular node and the bundle of His deliver the excitation impulse to specific regions of the ventricular myocardium.

2. Pre-excitation is the manifestation of accelerated conduction by some, or all, of the conducting elements in the atrioventricular junctional tissues

at an accelerated rate, a ventricular fusion beat occurs, as previously described.

3. If all elements of the atrioventricular node evidence accelerated conduction, the P-R interval is shortened just as previously, but the QRS complex appears essentially normal, since excitation spreads through the ventricles in the usual way.

Validity of the Foregoing Theories of Ventricular Pre-excitation

It is not feasible to enumerate in this review all of the evidence for and against each of the foregoing concepts of pre-excitation. Some of the more perti-

nent observations may be presented in condensed form as follows:

Accessory atrioventricular pathway theory.—1. Accessory muscle bundles have been identified in about one half of the cases with antemortem ventricular pre-excitation studied pathologically and have not been observed in normal human hearts. (The frequent finding of conducting fibers between the atrioventricular node and the bundle of His or left bundle branch, the "paraspecific bundles" of Mahaim, has no etiologic relevance to the Wolff-Parkinson-White syndrome, and these conducting fibers are not to be

punctured directly into the ventricular myocardium by means of an artificial bypass or shunt, analogous to the accessory muscle bundle.

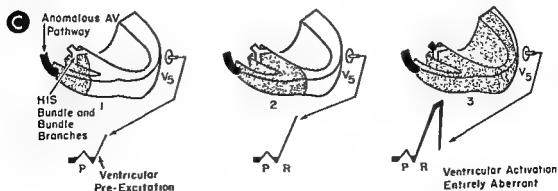
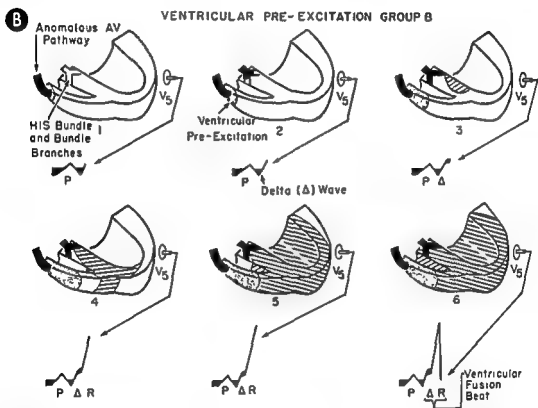
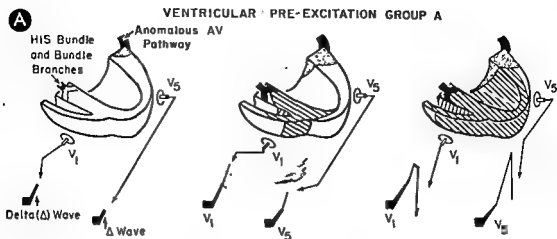
3. Atrioventricular node depressants, such as carotid sinus pressure, digitalis, and parasympatholytic drugs, promote the accessory bundle as the preferential pathway for atrioventricular conduction. The quantitatively different effects of these agents on normal and anomalous atrioventricular conduction seem to support, albeit indirectly, the existence of an alternate conduction pathway, entirely separate from the normal atrioventricular conducting system.

Accelerated atrioventricular conduction theory.—

1. A point emphasized by proponents of this theory is that ventricular pre-excitation beats have been produced by cardiac catheterization, by traction on the pulmonary artery or the left atricular appendage, by clinical and experimental coronary occlusion and

have that ventricular beats produced under the circumstances described do not represent pre-excitation beats. Thus, Scherf has observed that stimulation of the interventricular septum elicits ectopic ventricular beats which appear at essentially the same rate as the rate of sinus discharge. These beats may follow a short P-R interval and either may be totally distorted or may fuse with a normally conducted impulse to produce a ventricular fusion beat resembling that due to pre-excitation. According to other authorities, atrioventricular nodal rhythms with atrioventricular dissociation and other arrhythmias apparently can produce complexes which may be confused with ventricular pre-excitation beats.

2. An observation which has been considered as favoring the accelerated atrioventricular conduction



Aberrant Ventricular Pre-Excitation

Normal Ventricular Activation

Fig. 337.—Legend on facing page

theory rather than the accessory pathway concept is that clinical and experimental atrioventricular block has been noted to abolish the pre-excitation phenomenon or to prevent its experimental production. However, ventricular pre-excitation beats have been observed clinically in cases of first- and second-degree atrioventricular block.

3 To some extent, the validity of the accelerated atrioventricular conduction concept is indirectly compromised by the paradoxical effects of vagotonic and vagolytic drugs on the atrioventricular node and the

pre-excitation mechanism. For example, if ventricular pre-excitation is due to abnormal conduction by a part of the atrioventricular node, then it must be assumed that the region of the atrioventricular node conducting the pre-excitation impulse and the remaining portion of the node respond differently to carotid sinus stimulation and the vagotonic-cholinergic drugs, both of which tend to produce pre-excitation beats despite depressing nodal conductivity.

The authors of this text favor the accessory pathway concept of ventricular pre-excitation.

ELECTROCARDIOGRAPHIC FINDINGS

The characteristic features of ventricular pre-excitation and their incidences are cited below.

- 1 The P-R interval is 0.10 second or less in about 53% of the cases and is rarely greater than 0.12 second. A short P-R interval is significant, provided the P waves are those of a normal sinusoidal rhythm rather than retrograde P waves.
- 2 The QRS interval tends to be greater than 0.10 second, measuring 0.11-0.12 second in almost one half of the cases.

- 3 The P-J interval* typically remains normal (not over 0.20 second), since the QRS deflection is lengthened at the expense of the P-R interval.

the major deflection = downward.

*The P-J interval extends from the onset of the P wave to the junction (J) of the QRS complex with the S-T segment.



Fig. 338.—ECG and VCG findings in Group A pattern of ventricular pre-excitation.

In the ECG, the diagnostic abnormalities are: P-R interval of 0.12 sec, delta waves preceding upstrokes of II waves in leads II, III, aVF, and V_1 - V_6 ; downwardly directed delta wave in lead aVL, and QRS interval of 0.12 sec. Several findings—Q waves in leads I and V_6 and essentially normal T waves in all leads—are unusual in this pattern. Generally, the initial QRS forces in Groups A and II patterns are directed to the left and anteriorly, so that Q waves are not usually recorded in transverse leads such as leads I and V_6 .

In the VCG, the QRS sE loop is written almost entirely anteriorly, at first slightly to the right and then to the left and inferiorly. The anterior orientation of the QRS sE loop is responsible for the upright QRS deflections in all precordial leads of the ECG. The initial and earliest portion of the QRS sE loop corresponds to the delta waves of the QRS deflections in the ECG and is written irregularly and abnormally slowly to the right, anteriorly, and inferiorly. The closely spaced time markings in the initial and early portions of the QRS sE loop are pathognomonic of ventricular pre-excitation. The anterior location of the QRS sE loop is characteristic of the Group A pattern.

Fig. 339.—Electrocardiographic and vectorcardiographic findings in Group A ventricular pre-excitation.

The electrocardiogram shows the short P-R interval, prolonged QRS deflection, and slurred delta wave characteristic of pre-excitation, while the upright QRS deflections in the right precordial leads identify the pattern type as Group A. Note that leads III, aVF, and V_6 display QS deflections, a not infrequent finding in the Group A pre-excitation pattern and one which is not indicative of myocardial infarction for reasons cited in the text.

In the vectorcardiogram, the QRS sE loop is written entirely anteriorly, to the left and superiorly and displays the principal diagnostic feature of ventricular pre-excitation—namely, closely spaced time dashes in the initial and early portions of the efferent limb of the QRS sE loop. Note that the appearance of the QRS sE loop as a whole is distorted.

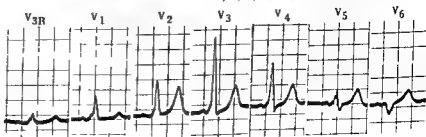


Fig. 340.—Electrocardiographic and vectorcardiographic findings in the Group B ventricular pre-excitation pattern.

The electrocardiograms shows diagnostic features of ventricular pre-excitation. The spatial angle between sA QRS and sA T is abnormally wide and represents a secondary T wave abnormality due to the altered ventricular activation process. The downwardly directed QRS deflections in leads V_{1-3} and V_i and the upright QRS deflections in precordial leads to the left of V_i are typical of the Group II ventricular pre-excitation pattern.

In the vectorcardiogram, the QRS sE loop is written entirely superiorly and to the left and in the horizontal projection lies along the 0° axis, a finding typical of the Group B pattern. Note the slowed and irregular inscription of the efferent limb of the QRS sE loop. The T sE loop is directed anteriorly and slightly to the right, and for this reason, lead I records an inverted T wave.

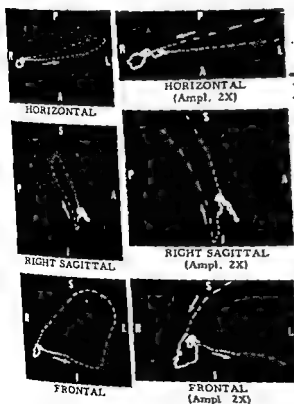
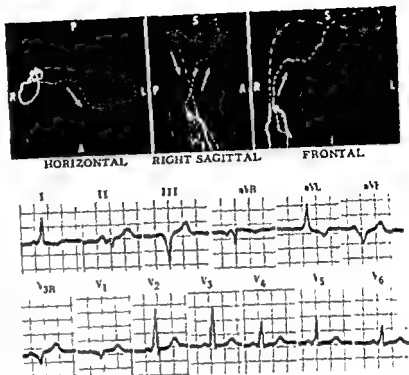
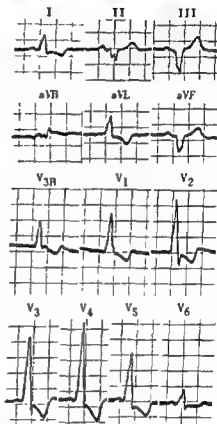
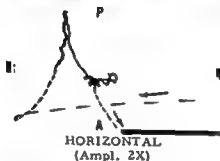
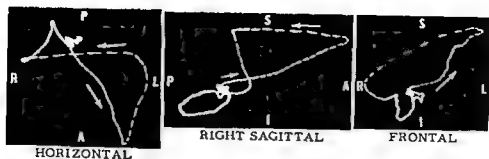


Fig. 341.—Electrocardiographic and vectorcardiographic findings in the Group B pattern of ventricular pre-excitation. The large QRS voltages present in the extremity and precordial leads should not be considered as signifying the absence of pre-excitation.



11, 12

effluent limb of the loop displays closely spaced time markings and an irregular inscription. Note the large S-T vector directed to the left, anteriorly, and slightly posteriorly as evidenced by the displacement of the terminus of the QRS

72, with a history of recurring episodes of paroxysmal tachycardia, the Group A ventricular pre-excitation pattern, the left, anteriorly, and superiorly, and the entire

5 The configuration of the QRS deflection in the precordial leads divides the ventricular pre-excitation syndrome into two groups, as follows:

In *Group A*, the premature component and the remainder of the QRS complex are primarily upright in both left and right precordial leads. In the left precordial leads, Q waves are absent, while the R waves in right precordial leads are large and often double peaked. The anterior direction of the activation forces has been interpreted as indicating that the accessory conducting bundle must be located posteriorly (Fig. 337, A).

In *Group B*, the left precordial leads register the type of QRS complexes described above. However, leads V_1 and V_2 show delta waves and QRS complexes which are resultant negative. QS deflections may be recorded in these right precordial leads as well as in leads II, III, and aVF. The electrocardiographic pattern has been attributed to location of the accessory bundle anteriorly, where it probably passes from the right atrium to insert on the epicardial sur-

face of the right ventricle (Fig. 337, B and C).

✓6. Secondary changes in the S-T segment and T wave may be observed in this syndrome, the extent of the change depending on the QRS area. Even though these changes may not be evident at times, there is, nonetheless, instability of the ST-T complex. Thus, secondary S-T and T changes tend to appear, for example, with exercise or onset of sinus tachycardia. This event, needless to say, does not indicate coronary insufficiency when aberrant atrioventricular conduction is known to exist.

✓7. A spontaneous and variable shift back and forth between normal and anomalous atrioventricular conduction takes place in about one half of the cases.

The features listed above apply to the recognition of the more typical cases of ventricular pre-excitation but may also be of some aid in the identification of the less typical variants of this syndrome, which have been catalogued by Ohnishi (Figs. 338-342).

PRODUCTION AND TERMINATION OF VENTRICULAR PRE-EXCITATION

The effects of various agents on the pre-excitation phenomenon in terms either of abolishing it, if it is

present, or precipitating it in a susceptible person, if it is not present, are summarized in Table 31. The

TABLE 31 —THE EFFECTS OF CAROTID SINUS STIMULATION AND VARIOUS DRUGS ON VENTRICULAR PRE-EXCITATION

AGENT	ACCESSORY PATHWAY	ATRIOVENTRICULAR NODE	RESULT
Carotid sinus (vagal) stimulation	Insignificant effect	Increased vagal tone depresses conductivity	This procedure may produce pre-excitation beats or an atrioventricular nodal rhythm with normal QRS complex.
Digitalis and parasympathomimetic drugs	Insignificant effect	Depress conductivity	Ventricular pre-excitation beats may result
✓Quinidine and procainamide	Usually these drugs have a greater depressant action on the accessory pathway than on the atrioventricular node		In about 30% of cases, quinidine regularly terminates ventricular pre-excitation
Sympathomimetic drug	Apparently the accessory pathway is not able to conduct above a certain critical rate of drug (or exercise) induced sinus tachycardia	These drugs tend to enhance conductivity by neutralizing parasympathomimetic effects	✓Ventricular pre-excitation tends to be abolished
Atropine	Insignificant effects	This drug enhances atrioventricular node conductivity by virtue of its vagolytic action	✓Ventricular pre-excitation may be replaced by normal conduction through the atrioventricular node.

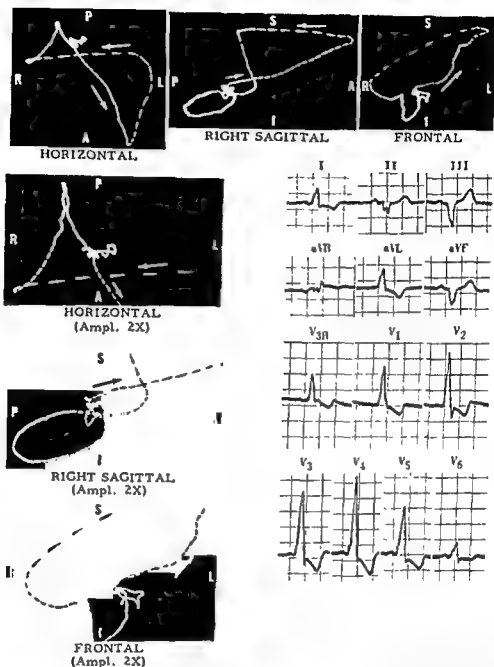


Fig. 342.—Electrocardiogram and vectorcardiogram from a man, 72, with a history of recurring episodes of paroxysmal tachycardia. The pre-excitation pattern is quite characteristic of the Group A ventricular pre-excitation pattern.

directed to the left inferiorly and slightly posteriorly as evidenced by the appearance of the pre-excitation pattern in Figure 343, observed in the

GROUP B

The following characteristics (see also Figs. 340-341) are typical of this group.

HORIZONTAL QRS LOOP.

In the vectorcardiographic pattern of Group B ventricular pre-excitation, the initial deflection of the horizontal QRS loop ordinarily is written to the left and anteriorly but occasionally is inscribed to the right and anteriorly or posteriorly.

The characteristic conduction delay and irregular inscription are noted in the early part of the QRS sE loop in each projection, as was described in the Group A pattern.

Generally the efferent limb of the horizontal QRS loop is written to the left and either slightly anteriorly, or first anteriorly and then slightly posteriorly. The loop then turns in a counterclockwise direction posteriorly and to the left, and it remains in this quadrant until its inscription is completed. The maximal mean instantaneous vector of the horizontal QRS loop lies between -35° and $+20^\circ$.

RIGHT SAGITTAL QRS LOOP

1. The orientation of the maximal mean instantaneous vector of the sagittal QRS loop ranges between $+150^\circ$ and -60° .
2. When the sagittal loop is oriented almost vertically superiorly, as is often the case, it usually has a counterclockwise direction of inscription. If the loop is inferiorly located, it usually is written in a clockwise direction. Figure-of-eight loops generally show counterclockwise inscription of their proximal components and clockwise inscription of their distal components.

FRONTAL QRS LOOP:

1. The maximal mean instantaneous vector of the frontal loop is generally situated between -45° and $+30^\circ$.
2. A figure-of-eight configuration of the frontal QRS loop is observed fairly commonly. The proximal and distal components show counterclockwise and clockwise inscription, respectively. When the frontal QRS loop does not have this configuration, it usually is written in a counterclockwise direction.

S-T VECTOR AND VENTRICULAR REPOLARIZATION

Although, in the series of patients with ventricular pre-excitation studied by us, the number of patients was too small to attach any statistical significance to the data, the findings may, nevertheless, represent the general trend, and this is sufficient for the purposes of this text.

Half of the vectorcardiograms both in Group A and in Group B showed displacement of the terminus of the QRS sE loop, indicative of an S-T vector. This vector was directed to the right in all cases in which it was present, but its vertical and anteroposterior orientations varied widely.

In Group A, the average orientations of the T sE loop in the horizontal, right sagittal, and frontal projections were $+70^\circ$, $+100^\circ$, and $+75^\circ$, respectively. The corresponding values for T sE loop orientation in Group B were $+130^\circ$, $+60^\circ$, and $+110^\circ$. In two vectorcardiograms in Group B, the horizontal T loop was either round or bifid, but in either case, the T loop showed two maximal instantaneous vectors of equal size but divergent duration. In a third vectorcardiogram, the frontal T loop presented the features just described.

PAROXYSMAL RAPID HEART ACTION IN THE WOLFF-PARKINSON-WHITE SYNDROME

Recurrent paroxysmal tachycardia accompanies

this condition. The paroxysmal tachycardias are almost invariably, if not always, of supraventricular origin. Atrial and atrioventricular nodal tachycardias are most commonly noted, followed in frequency by atrial fibrillation and atrial flutter (Figs. 343-345). Although the occurrence of paroxysmal ventricular tachycardia in cases of Wolff-Parkinson-White syndrome has been reported in the past, Wolff and other

investigators believe that most or all of the apparent ventricular tachycardias observed in uncomplicated cases of the Wolff-Parkinson-White syndrome are actually supraventricular tachycardias with persistent anomalous atrioventricular conduction (Fig. 344). Supportive evidence for this belief continues to accumulate.

Mechanism

The mechanisms proposed in explanation of the rapid abnormal heart rhythms occurring in the Wolff-

importance of these factors in the diagnosis and study of the Wolff-Parkinson-White syndrome is obvious. Moreover, Wolff and Richman emphasize that ventricular pre-excitation produces QRS complexes which may mimic myocardial infarction and, conversely, that it also may obscure the presence of myocardial infarction. In either case, the most reliable

diagnostic technique is to terminate the anomalous atrioventricular conduction long enough to evaluate the configuration of the QRS complexes in the absence of pre-excitation. Similarly, this procedure permits the diagnostic features of associated cardiac abnormalities, like right ventricular hypertrophy and right bundle branch block, to appear.

VECTOCARDIOGRAPHIC FINDINGS

The vectocardiographic features to be described below were observed by the authors of this text in 14 patients having the Wolff-Parkinson-White syndrome whose electrocardiograms and ancillary clinical data were quite typical of this condition. In 6 of these patients, the QRS configuration in the precordial electrocardiographic leads was that of the Group A type of ventricular aberration, while the remaining 8 patients could be placed in the Group B type. By and large, the vectocardiograms in these two groups were in keeping with the abnormalities present in the precordial electrocardiograms, so that the vectocardiograms like the electrocardiograms, could be divided into two general pattern types, which, for consistency, will be given the same designations as the corresponding electrocardiographic patterns. The salient feature diagnostic of ventricular pre-excitation and common to both types of QRS sE loop configuration was the fact that the initial and early portions of the spatial QRS loop were inscribed slowly, erratically, and in an abnormal direction. This abnormality, which corresponds to the delta wave or slurred initial limb of the QRS deflection of the electrocardiogram, is rarely, if ever, observed in the absence of ventricular pre-excitation. A more detailed description of the QRS sE loop in Groups A and B ventricular pre-excitation follows.

GROUP A

This entity presents the following characteristics (see also Figs. 338 and 339)

HORIZONTAL QRS LOOP

1. The initial deflection of the horizontal QRS loop is written to the left and usually anteriorly, although occasionally posteriorly.
2. In all three projections of the QRS sE loop, the earliest portion of the loop, and sometimes almost the entire efferent limb, shows conduction delay and an irregular or erratic inscription

3. In this type of QRS sE loop configuration, the efferent limb proceeds to the left and relatively far anteriorly, and then the loop turns in a counterclockwise direction, the afferent limb passing behind the efferent limb to return on the right and anteriorly. Occasionally the entire horizontal QRS loop is inscribed in a clockwise direction and lies anteriorly and to the left.
4. The maximal mean instantaneous vector of the horizontal QRS loop ranges in orientation between $+20^\circ$ and $+95^\circ$.

RIGHT SAGITTAL QRS LOOP

1. The QRS sE loop in the sagittal projection usually has a figure-of-eight configuration, the proximal and distal components of the loop being inscribed in counterclockwise and clockwise directions, respectively.
2. The initial deflection of the sagittal QRS loop is directed anteriorly and inferiorly in most instances.
3. The sagittal QRS loop is almost invariably situated anteriorly and either slightly superiorly or inferiorly. In our cases, the maximal mean instantaneous vector of the sagittal loop ranged in orientation between -30° and $+70^\circ$.

FRONTAL QRS LOOP

1. The frontal QRS loop tends to vary widely in configuration, although figure-of-eight loops were relatively common in the cases which we studied. In figure-of-eight frontal loops, the proximal component of the loop usually is written in a counterclockwise direction and the distal portion of the loop in a clockwise direction. When the efferent and afferent limbs of the frontal loop do not cross each other, the direction of inscription ordinarily is counterclockwise. Occasionally the frontal QRS loop has an almost linear configuration.
2. The maximal mean instantaneous vector (or long axis) of the frontal QRS loop usually is located between -30° and $+40^\circ$.

GROUP B

The following characteristics (see also Figs. 340 and 341) are typical of this group

HORIZONTAL QRS LOOP:

1. In the vectorcardiographic pattern of Group B ventricular pre-excitation, the initial deflection of the horizontal QRS loop ordinarily is written to the left and anteriorly but occasionally is inscribed to the right and anteriorly or posteriorly.
2. The characteristic conduction delay and irregular inscription are noted in the early part of the QRS sE loop in each projection, as was described in the Group A pattern.
3. Generally the efferent limb of the horizontal QRS loop is written to the left and either slightly anteriorly, or first anteriorly and then slightly posteriorly. The loop then turns in a counterclockwise direction posteriorly and to the left, and it remains in this quadrant until its inscription is completed.
4. The maximal mean instantaneous vector of the horizontal QRS loop lies between -35° and $+20^\circ$.

RIGHT SAGITTAL QRS LOOP

1. The orientation of the maximal mean instantaneous vector of the sagittal QRS loop ranges between $+150^\circ$ and -60° .
2. When the sagittal loop is oriented almost vertically superiorly, as is often the case, it usually has a counterclockwise direction of inscription. If the loop is inferiorly located, it usually is written in a clockwise direction. Figure-of-eight loops generally show counterclockwise inscription of their proximal components and clockwise inscription of their distal components.

FRONTAL QRS LOOP:

1. The maximal mean instantaneous vector of the frontal loop is generally situated between -45° and $+30^\circ$.
2. A figure-of-eight configuration of the frontal QRS loop is observed fairly commonly. The proximal and distal components show counterclockwise and clockwise inscription, respectively. When the frontal QRS loop does not have this configuration, it usually is written in a counterclockwise direction.

S-T VECTOR AND VENTRICULAR REPOLARIZATION

Although, in the series of patients with ventricular pre-excitation studied by us, the number of patients was too small to attach any statistical significance to the data, the findings may, nevertheless, represent the general trend, and this is sufficient for the purposes of this text.

Half of the vectorcardiograms both in Group A and in Group B showed displacement of the terminus of the QRS sE loop, indicative of an S-T vector. This vector was directed to the right in all cases in which it was present, but its vertical and anteroposterior orientations varied widely.

In Group A, the average orientations of the T sE loop in the horizontal, right sagittal, and frontal projections were $+70^\circ$, $+100^\circ$, and $+75^\circ$, respectively. The corresponding values for T sE loop orientation in Group B were $+130^\circ$, $+60^\circ$, and $+110^\circ$. In two vectorcardiograms in Group B, the horizontal T loop was either round or bifid, but in either case, the T loop showed two maximal instantaneous vectors of equal size but divergent duration. In a third vectorcardiogram, the frontal T loop presented the features just described.

PAROXYSMAL RAPID HEART ACTION IN THE WOLFF-PARKINSON-WHITE SYNDROME

Recurrent paroxysmal tachycardia accompanies such a high percentage of cases of Wolff-Parkinson-White syndrome (at least 70%) that it has come to be recognized as one of the principal clinical features of this condition. The paroxysmal tachycardias are almost invariably, if not always, of supraventricular origin. Atrial and atrioventricular nodal tachycardias are most commonly noted, followed in frequency by atrial fibrillation and atrial flutter (Figs. 343-345). Although the occurrence of paroxysmal ventricular tachycardia in cases of Wolff-Parkinson-White syndrome has been reported in the past, Wolff and other

investigators believe that most or all of the apparent ventricular tachycardias observed in uncomplicated cases of the Wolff-Parkinson-White syndrome are actually supraventricular tachycardias with persistent anomalous atrioventricular conduction (Fig. 344). Supportive evidence for this belief continues to accumulate.

Mechanism

The mechanisms proposed in explanation of the rapid abnormal heart rhythms occurring in the Wolff-

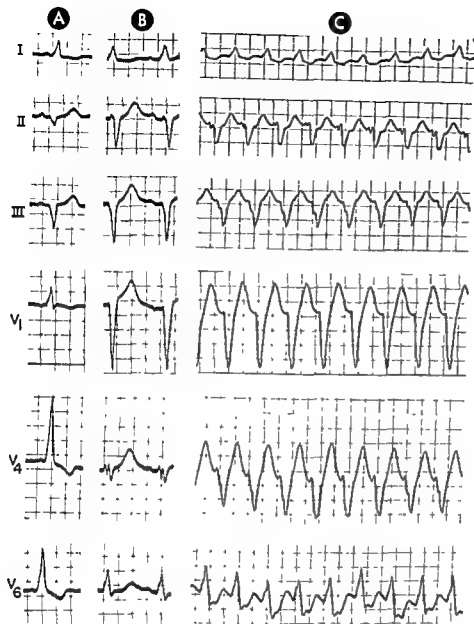
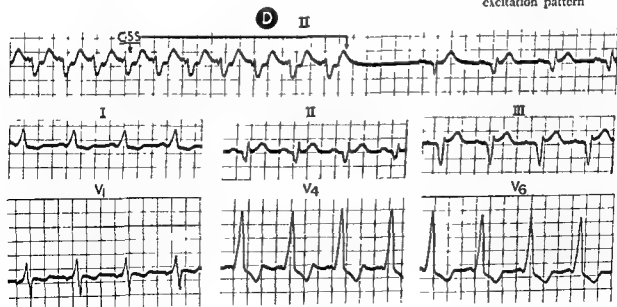


Fig. 343.—Electrocardiographic lead strips recorded from the patient with Wolff-Parkinson-White syndrome whose vectorcardiogram was shown in Figure 342. Leads I, II, III, V₁, V₄, and V₆ in column A were recorded before quinidine therapy. The leads in B were recorded after the patient had received quinidine, 0.2 Gm. at 2-hour intervals for 5 doses. Note the prolongation of both P-R and QRS intervals. Also note that, while the QRS configuration in leads I, II, and III has not changed significantly in B, as compared to A, the precordial leads in B display QRS deflections characteristic of the Group II pre-excitation pattern, whereas in A the Group A pre-excitation pattern was present. The lead strips in C were recorded shortly after those in B and demonstrate a paroxysmal tachycardia of supraventricular origin with a ventricular rate of 130 beats per minute. The Group B pre-excitation pattern persists despite onset of the tachycardia. In D, the lead strip of lead II was recorded during carotid sinus stimulation (CSS). During the period of carotid sinus stimulation there is gradual slowing of the rate of the ectopic tachycardia until it stops abruptly at the point indicated by the second arrow, fol-



lowing the termination of the tachycardia. Leads III, V₁, V₄, and V₆ were obtained shortly after the paroxysmal tachycardia was terminated and demonstrate return to the Group A pre-excitation pattern.

Parkinson-White syndrome will be described in the paragraphs to follow.

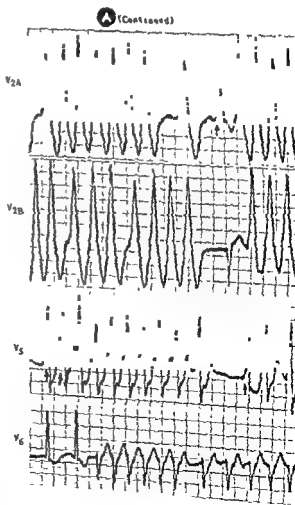
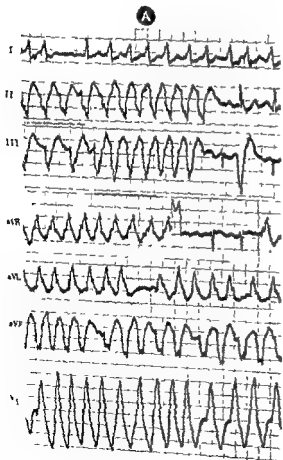
Paroxysmal atrial and atrio-ventricular nodal tachycardias—A paroxysm of rapid heart action may be precipitated by passage of the atrial or atrio-ventricular nodal activation impulse downward through the atrio-ventricular node and its subsequent return to the atria or atrio-ventricular node via the accessory pathway, thus constituting a form of re-entry. If the re-entry is repetitive, the paroxysmal tachycardia becomes established. Consistent with this explanation is the fact that the last ventricular beat preceding onset of an atrial or nodal tachycardia and also the ventricular

complexes written during the tachycardia are usually not of the pre-excitation type.

Paroxysmal atrial fibrillation and flutter—Unlike the preceding tachycardias, atrial fibrillation and flutter cannot be explained satisfactorily on the basis solely of cyclic re-entry of the impulse (into the atria) via the accessory pathway, since impossibly high ventricular rates would have to be assumed. However, some investigators postulate that the mechanism initiating the paroxysm may be re-entry but that the impulse is returned to the atria very early. If it arrives during the partial refractory or "vulnerable" period of atria, the re-entry impulse may cause onset of atrial

FIG. 344—Electrocardiogram and vectrocardiogram from patient hospitalized with clinical picture of acute con-

pre-excitation (Continued)



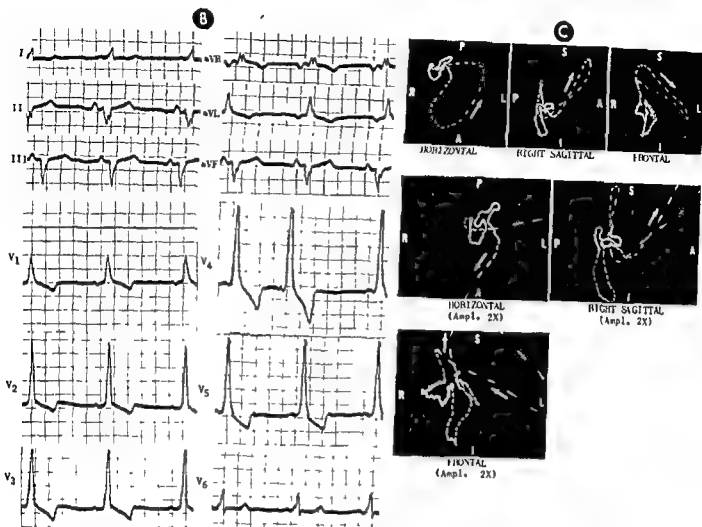


Fig. 344 (cont).—The ventricular pre-excitation to the left and superiorly the efferent limb of the C_{B} and the C_{A} have been reported in the past, most authorities feel, at present, that many, if not all, of these cases were actually atrial fibrillation with the pre-excitation type of aberration of the ventricular complexes

fibrillation or flutter. (During these arrhythmias a rapid, almost constant, stream of atrial impulses passes down either the accessory bundle or the atrioventricular node and bundle branch system, depending on which is less refractory at the time of onset of the tachycardia. Since one of these two conducting pathways continues to be used exclusively, the ventricular beats, if they are of the pre-excitation type, usually are greatly widened and deformed. If ventricular pre-excitation beats with marked ventricular aberration should occur during atrial fibrillation, the electrocardiogram may resemble ventricular tachycardia quite closely. The differentiation of the two rhythms assumes critical importance in this instance, since the patient may be treated unnecessarily with potentially hazardous drugs, such as quinidine, in the belief that ventricular

tachycardia is present. Actually, the rapid rhythm should be treated like any other atrial fibrillation with a rapid ventricular rate—that is, with digitalis. A paroxysm of pre-excitation beats occurring in atrial fibrillation will usually terminate when there is a ventricular pause of sufficient length to permit recovery of atrioventricular nodal conductivity. During the interval of transition from anomalous to normal atrioventricular conduction, ventricular fusion beats of the type observed commonly in ventricular pre-excitation with sinus rhythm may appear, and they are soon followed by the appearance of QRS deflections of normal configuration and duration.

Ventricular tachycardia—See comments concerning this type of tachycardia in the preceding three paragraphs.

CLINICAL ASPECTS OF WOLFF-PARKINSON-WHITE SYNDROME

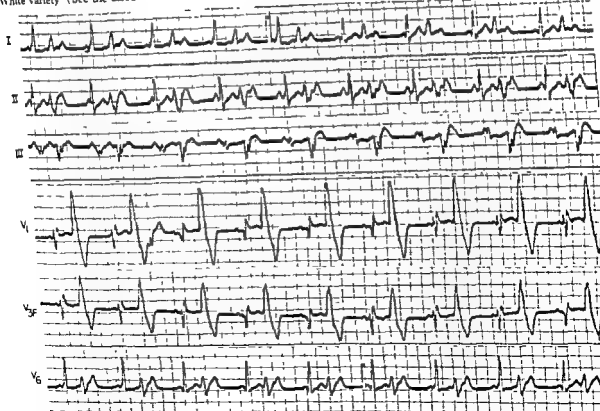
Wolff-Parkinson-White syndrome would be

over a period of time may produce irreversible changes in normal hearts or seriously compromise diseased hearts.

of ventricular pre-excitation is frequently erroneously as being indicative of heart disease. (b) Ventricular pre-excitation may obscure other abnormalities in the electrocardiogram. (c) The Wolff-Parkinson-White syndrome is accompanied by a high incidence of

However, in cases of the Wolff-Parkinson-White syndrome, ill effects have been encountered so infrequently that the benign nature of this condition is justifiably stressed. On the other hand, according to life insurance experience, the mortality rate among applicants with Wolff-Parkinson-White syndrome is about three times normal.

lar pre
point,
pre-excitation,
not infrequently
White variety



PART V

**Illustrative Vectorcardiograms
and Electrocardiograms**

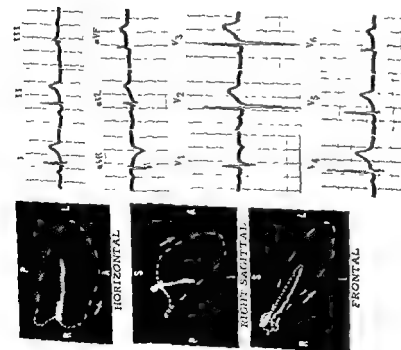


Fig. 346.—Electrocardiogram and vectorcardiogram recorded from a normal girl, 13.

In the electrocardiogram, the R/S amplitude ratios of I in lead V₁ is not abnormal in this age group.

In the vectorcardiogram, the corresponding finding is the anterior orientation of the first half of the QRS loop. Note that a parasagittal line through the midpoint of lead V₁ would bisect the horizontal QRS loop almost equally, the first half lying on the positive side of lead V₁ and the second half on the negative side of lead V₁. Hence the equiphasic RS deflection in lead V₁. Also note the right posterior terminal deflection of the horizontal QRS loop; this, too, is a normal vectorcardiographic finding in this age group.



Fig. 347.—Electrocardiogram and vectorcardiogram in a normal boy, 5. In the electrocardiogram, the right-axis deviation of A QRS and the terminal S waves in leads V₁ and V₂ are normal findings in this age group.

In the vectorcardiogram, the related features are: horizontal QRS loop showing a prominent rightward and posterior terminal deflection, and frontal QRS loop oriented almost vertically inferior, the first half of the loop being written to the left, and the second half to the right, of the midline.

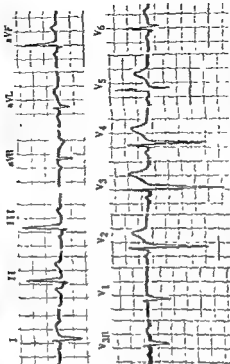


Fig. 348.—Electrocardiogram and vectorcardiogram in a normal boy, 5. In the electrocardiogram, the right-axis deviation of A QRS and the terminal S waves in leads V₁ and V₂ are normal findings in this age group.

In the vectorcardiogram, the related features are: horizontal QRS loop showing a prominent rightward and posterior terminal deflection, and frontal QRS loop oriented almost vertically inferior, the first half of the loop being written to the left, and the second half to the right, of the midline.

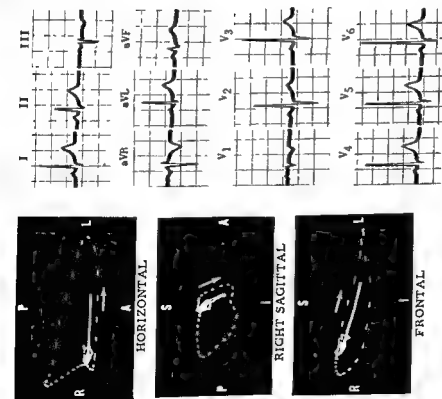


Fig. 348.—Electrocardiogram and vectorcardiogram in a normal woman. 24 Note the right posterior terminal deflection of the horizontal QRS loop of the vectorcardiogram. An unusual feature of the vectorcardiogram is that the frontal QRS loop, although directed almost horizontally to the left, is written in a clockwise direction. Usually, in frontal loops with this orientation, the direction of inscription is counterclockwise.

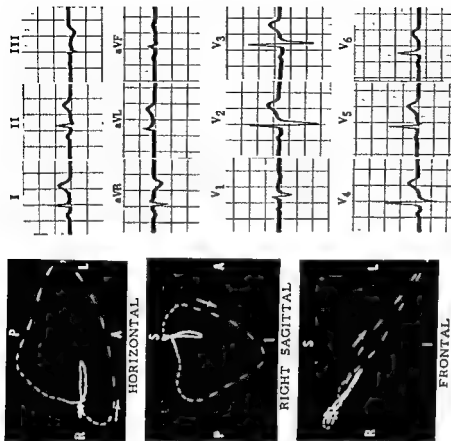


Fig. 349.—Electrocardiogram and vectorcardiogram in a normal man, 50. Note that the long axes of the planar QRS loops and planar T loops are directed almost parallel, although the spatial angle subtended by the long axes of the QRS sE and T sE loops can occasionally be as wide as 45° in normal persons.

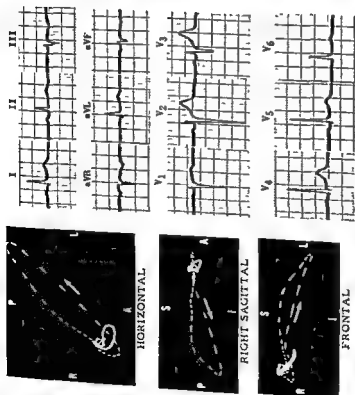


Fig 350.—Normal electrocardiogram and abnormal vectorcardiogram in *m. in. 88*, with angina pectoris

The electrocardiogram shows no definite S-T segment or T wave abnormalities. The exact width of the horizontal QRS-T angle cannot be determined precisely because none of six precordial leads records a transitional T wave, and therefore the orientation of A T can only be approximated. All that can be stated concerning the orientation of A T in the horizontal plane is that the vector lies between $+30^\circ$ and $+90^\circ$, while A QRS is situated at about -20° .

In the vectorcardiogram, the spatial angle subtended by the long axis of the QRS sE and T sE loops is 65° . This angle is abnormally wide, since the spatial angle of 45° represents the upper limits of normal in vectorcardiograms recorded with the cube lead system.

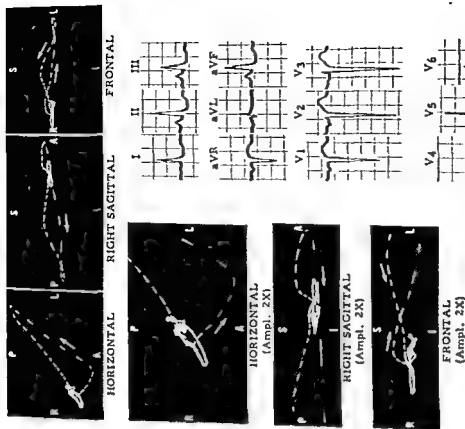


Fig. 351.—Electrocardiographic and vectorcardiographic patterns of left ventricular hypertrophy. Note, in the vectorcardiogram, the posterior rotation of the horizontal QRS loop, the left-axis deviation of the frontal QRS loop, and the discordant T sE loop

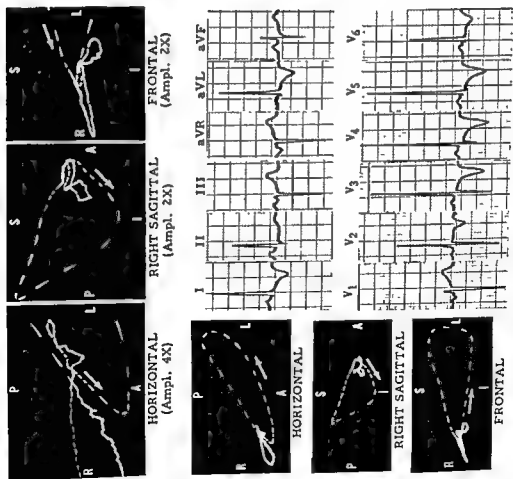


Fig. 352—Electrocardiographic and vectorcardiographic patterns of left ventricular hypertrophy. Note the leftward, posterior, and superior orientation of the QRS sE loop and the discordant T sE loop

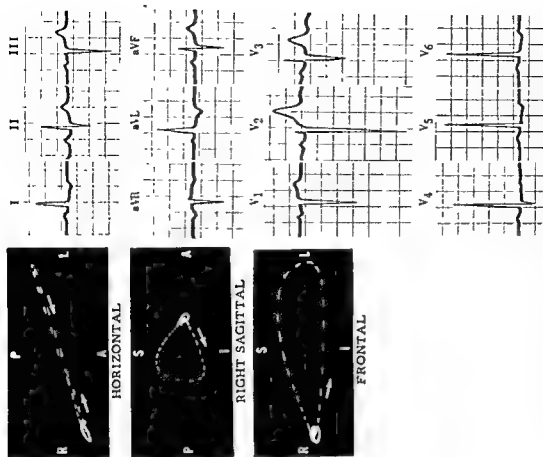


Fig. 353—Electrocardiographic and vectorcardiographic patterns of left ventricular hypertrophy. The above vectorcardiogram was recorded with much less amplification than the normal vectorcardiograms appearing in this text. Thus the mean instantaneous vectors of the QRS sE loop are of much greater magnitude than normal, and this is reflected in the electrocardiogram by the deep S waves appearing in leads V_1 and V_2 and the tall R waves in leads V_5 through V_6 . The T sE loop is discordant to the QRS sE loop in the vectorcardiogram

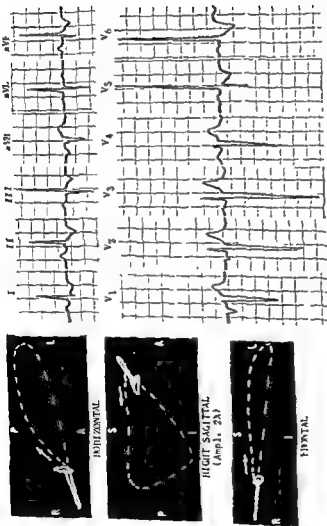


Fig. 354—Electrocardiographic and vectorcardiographic patterns of left ventricular hypertrophy in a youth, 15, with congenital aortic stenosis. Note, in the electrocardiogram, the deep Q waves in leads III and aVL. This finding is related in the vectorcardiogram to the clockwise inscription of the frontal QRS loop, which causes the early portion of the loop to be written superiorly. The diminished R wave amplitude in lead V₁ of the electrocardiogram is explained by the clockwise direction of inscription and posterior displacement of the efficient limb of the horizontal QRS loop of the vectorcardiogram. The electrocardiogram is otherwise quite typical of left ventricular hypertrophy. The explanation for the reversed direction of inscription of the QRS SE loop in its three planar projections is not known, but this finding has been observed by the authors of this text and by other investigators in occasional vectorcardiograms of patients with left ventricular hypertrophy. The vectorcardiogram otherwise is quite consistent with left ventricular hypertrophy.



Fig. 355 (left).—Electrocardiographic and vectorcardiographic patterns of right ventricular hypertrophy in a woman, 48, with interatrial septal defect.

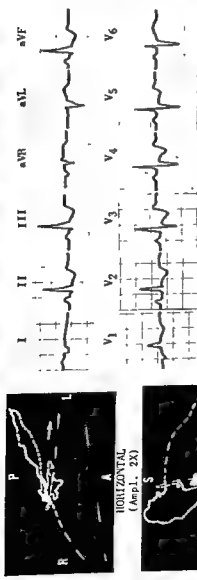
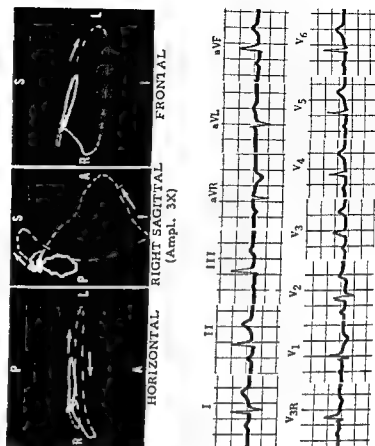


Fig. 356 (right).—Electrocardiographic and vectorcardiographic patterns of right ventricular hypertrophy in a woman, 33, with interatrial septal defect. Note the RSR' deflections in leads V_{1-2} and V_1 in the electrocardiogram. In the past, the electrocardiographic diagnosis of incomplete right bundle branch block would have been made on the basis of the QRS configuration in the right precordial leads. In the vectorcardiogram, the horizontal QRS loop is mainly clockwise inscribed and is located anterior, posterior, and to the right. In the sagittal plane, the QRS loop is mainly clockwise inscribed and is located anterior, posterior, and to the right. The authors of this text interpret the above electrocardiogram as being consistent with right ventricular hypertrophy. Their diagnostic criteria with particular reference to the RSR' deflection in lead V_1 are as follows: (1) the R' amplitude exceeds the amplitude of the initial R wave, and (2) the R/S amplitude ratio is equal to, or greater than 1.



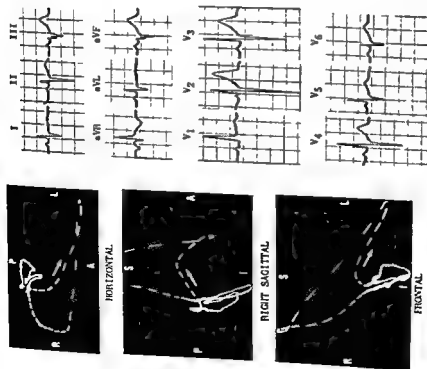


Fig. 357.—Electrocardiographic patterns of right ventricular hypertrophy in a woman, 30, with tetralogy of Fallot.

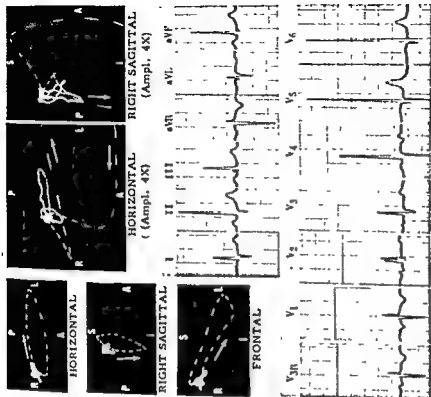


Fig. 358.—Electrocardiogram and vectorcardiogram in ventricular septal defect. The RSR' deflections in leads V_1 and V_2 of the electrocardiogram are suggestive of right ventricular hypertrophy, while the very tall R waves in leads V_5 and V_6 are equally suggestive of left ventricular hypertrophy. The horizontal QRS loop of the vectorcardiogram is inscribed in a clockwise direction and presents the type of configuration designated in the text as the RSR' pattern of right ventricular hypertrophy. However, the different limbs of the horizontal QRS loop is written farther to the left and somewhat more posteriorly than is usually the case in this QRS loop pattern of right ventricular hypertrophy. The counterclockwise direction of inscription of the right sagittal QRS loop is consistent with right ventricular hypertrophy, but the counterclockwise inscription and relatively horizontal orientation of the frontal QRS loop suggest coexisting left ventricular hypertrophy. The authors of this text interpret both the electrocardiogram and vectorcardiogram as being suggestive of combined ventricular hypertrophy.

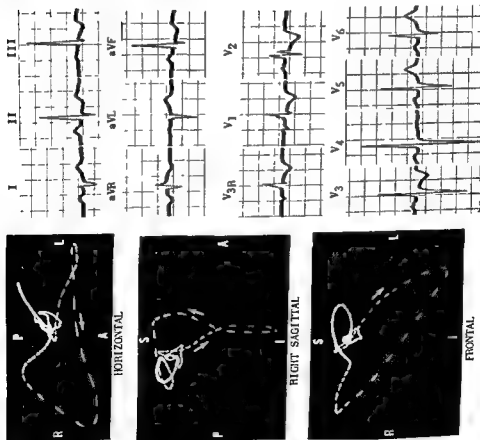


Fig 359.—Electrocardiographic and vectorcardiographic patterns of right ventricular hypertrophy in a patient with mitral stenosis

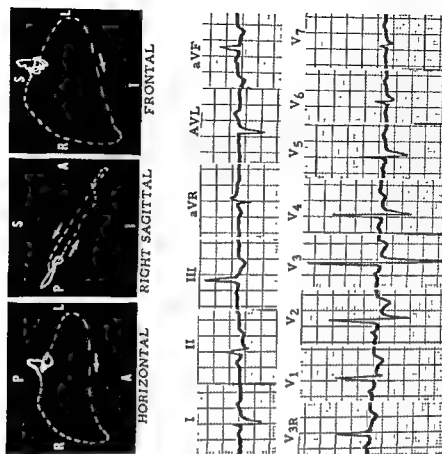


Fig. 360.—Electrocardiographic and vectorcardiographic patterns of right ventricular hypertrophy in a patient with mitral stenosis

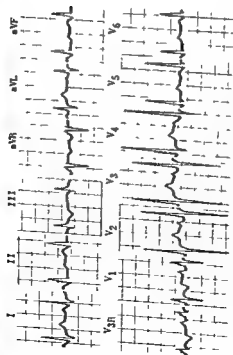


Fig. 361.—Electrocardiographic and vectorcardiographic patterns of right ventricular hypertrophy in a patient with mitral stenosis.

In the electrocardiogram, leads V_{4R} and V_5 display wide initial R waves, the R/S amplitude ratio in lead V_{4R} being greater than 1. These are the only electrocardiographic features suggestive of right ventricular hypertrophy.

In the vectorcardiogram, however, the horizontal QRS loop is written entirely in a clockwise direction anteriorly, a finding which is diagnostic of right ventricular hypertrophy.

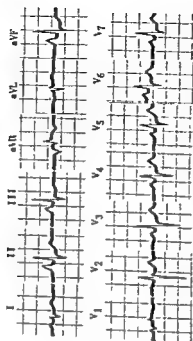
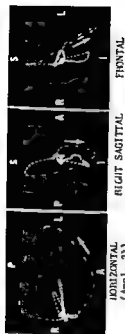


Fig. 362.—Electrocardiogram and vectorcardiogram in mitral stenosis. In the electrocardiogram, the tall P waves in leads II, III, and aVF are suggestive of right atrial enlargement, while the right-axis deviation of the QRS and the small but upright QRS deflection in lead V_1 are suggestive of right ventricular hypertrophy.

In the vectorcardiogram, however, the P sE loop is oriented for the most part posteriorly, and is otherwise consistent with the diagnosis of left atrial enlargement. The posterior and superior terminal deflection of the QRS sE loop and the inscription of the efficient limb of the QRS sE loop farther anteriorly than is usually the case in the normal vectorcardiogram are vectorcardiographic findings commonly seen in patients with mitral stenosis. These QRS sE loop findings cannot be considered indicative, per se, of right ventricular hypertrophy, although there is evidence suggesting that they may be related to enlargement of the pulmonary outflow tract.

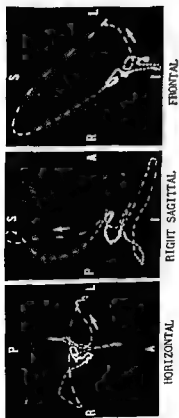


Fig. 363.—Electrocardiogram and vectorcardiogram in a woman, 69, with mitral stenosis, pulmonary hypertension, and congestive heart failure

In the electrocardiogram, the P waves are 0.12 second in duration and are notched or slurred—findings suggestive of the P mitrale pattern of left atrial enlargement. The marked right-axis deviation of the P mitrale pattern of left atrial enlargement in leads V_4 and V_5 are compatible with right ventricular hypertrophy. While the resultant positive QRS voltage in lead I, small as it is, might be thought to indicate marked left-axis deviation of a QRS, the more likely the possibility is that there is marked right-axis deviation of a QRS, the more likely the possibility is that the electrocardiogram as left-axis deviation because of the downward slant of the effective axis of lead I in a left-to-right direction (See Chapter 4 for detailed discussion)

In the vectorcardiogram, the P sE loop shows large instantaneous vectors directed both anteriorly and posteriorly, and so, combined atrial hypertrophy and enlargement is probably present. The planar QRS loops present the features of the type B QRS sE loop pattern observed in some patients with mitral stenosis or chronic cor pulmonale. Note the marked right-axis deviation of the frontal QRS loop. The above vectorcardiogram is interpreted by the authors of this text as being indicative of right ventricular hypertrophy

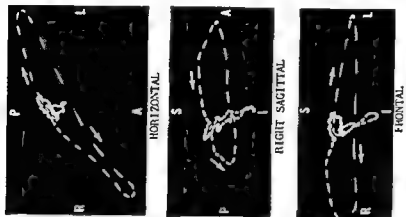


Fig. 364.—Electrocardiogram and vectorcardiogram in a patient with chronic cor pulmonale.

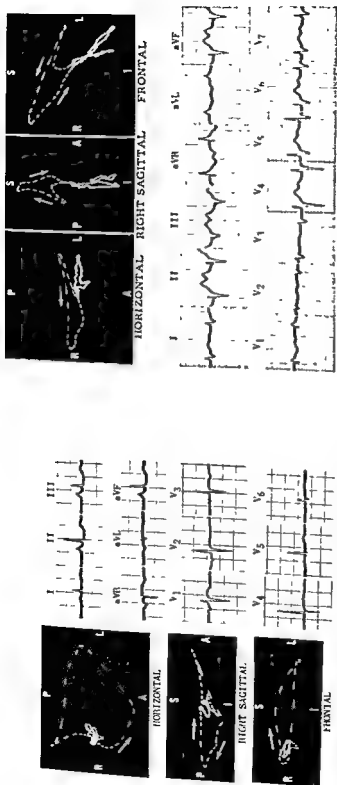


Fig 365—Electrocardiogram and vectorcardiogram in chronic pulmonary emphysema without evidence of chronic cor pulmonale.

In the electrocardiogram, the S-T segment depression in leads II, III, and aVF and the low T waves in leads I and V₁ through V₆ are probably related to digitalis effect. Otherwise the record is noncontributory with reference to the diagnosis of chronic pulmonary emphysema.

The vectorcardiogram shows the type A QRS ΣE loop pattern observed in patients with mitral stenosis or with chronic pulmonary emphysema without cor pulmonale and an S-T vector compatible with digitalis effect.

Fig 366—Electrocardiogram and vectorcardiogram in chronic cor pulmonale. The electrocardiogram shows first-degree atrioventricular block, the S-Sum pattern in the limb leads, QR deflections in lead V₁, and the precordial lead pattern of "clockwise rotation," findings compatible with chronic cor pulmonale.

The vectorcardiogram displays the type A QRS ΣE loop pattern, but, in contrast with the vectorcardiogram in Figure 365, here the large terminal instantaneous vectors of the QRS ΣE loop, directed to the right posteriorly and superiorly, are strongly suggestive of right ventricular hypertrophy. The anterior and vertically inferior orientation of the P ΣE loop and increased magnitude of the maximal mean instantaneous vector of the P ΣE loop are consistent with right atrial enlargement.

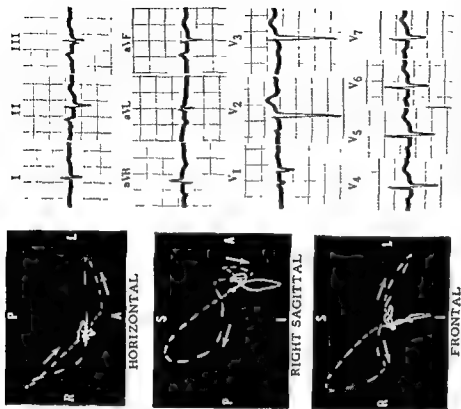


Fig. 368.—Electrocardiogram and vectorcardiogram recorded in chronic cor pulmonale. The electrocardiogram shows no evidence suggesting the presence of right ventricular hypertrophy, while the vectorcardiogram displays the type II QRS sE loop pattern considered by the authors of this text to be indicative of right ventricular hypertrophy. The large P sE loop directed somewhat anteriorly and vertically inferiorly is consistent with the vectorcardiographic diagnosis of right atrial enlargement.

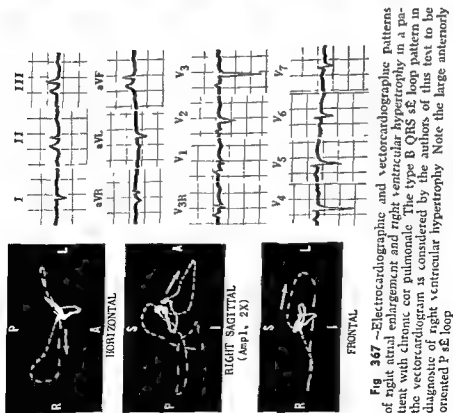


Fig. 367.—Electrocardiographic and vectorcardiographic patterns of right atrial enlargement and right ventricular hypertrophy in a patient with chronic cor pulmonale. The type B QRS sE loop pattern in the vectorcardiogram is considered by the authors of this text to be diagnostic of right ventricular hypertrophy. Note the large anteriorly oriented P sE loop.

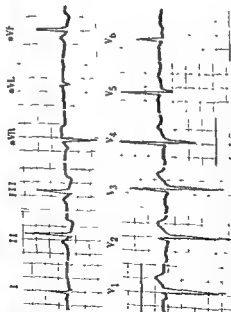


Fig 369.—The vectorcardiographic type C QRS Σ E loop pattern in chronic pulmonary emphysema. The S-T segment and T wave abnormalities in the electrocardiogram and the S-T vector and the T Σ E loop abnormalities in the vectorcardiogram are related—in part, at least—to digitalis effect.

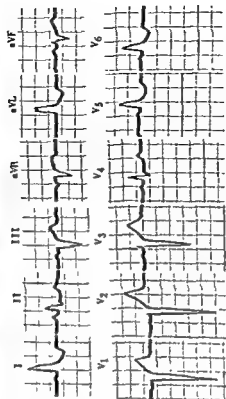
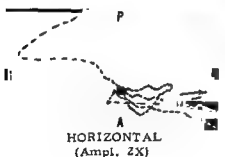
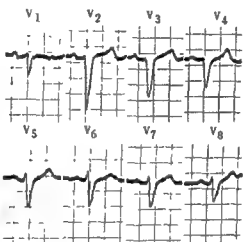
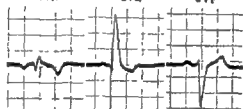
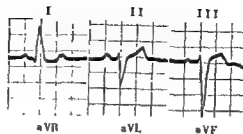
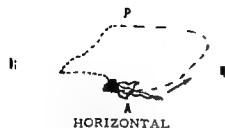


Fig 370.—Left bundle branch block. In the electrocardiogram, the QRS duration is 0.11 second. In the vectorcardiogram, the QRS Σ E loop is written initially slightly anteriorly and in the left and then is marked conduction delay to the entire anterior limb of the loop. The horizontal QRS loop has a figure-of-eight configuration.



WIDE TOLERANCE, LOW SLOPE AS SHOWN, WITH WIDE WAVES BEING RECORDED BY ALL SIX CHEST LEADS. There is marked left-axis deviation of A QRS in the frontal plane.

In the vectorcardiogram, the QRS sE loop is written initially to the right, anteriorly, and inferiorly and then to the left, posteriorly, and markedly superiorly. Terminally the QRS sE loop returns on the right, posteriorly, and superiorly, the afferent limb of the loop showing conduction delay.

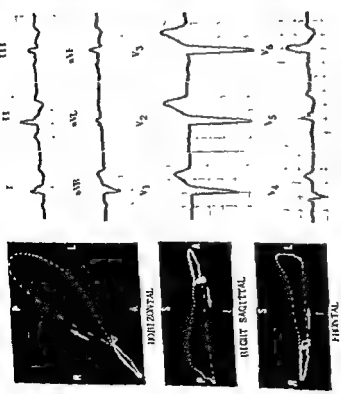


Fig 372.—Electrocardiogram and vectorcardiogram in left bundle branch block.
In the electrocardiogram, the QRS duration is 0.14 second.
In the vectorcardiogram, the QRS SE loop is written immediately to the left, posteriorly, and inferiorly and there is conduction delay in the entire afferent limb of the loop.

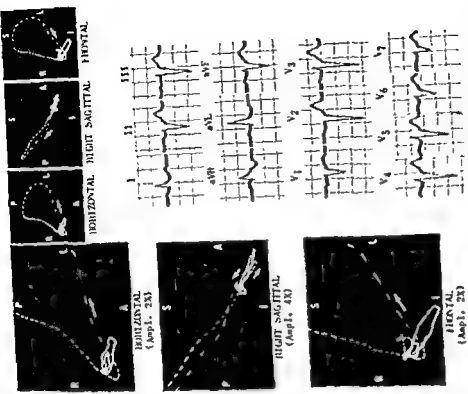


Fig 373.—Electrocardiogram and vectorcardiogram in a variant type of left intraventricular block (left ventricular hypertrophy with terminal conduction delay).

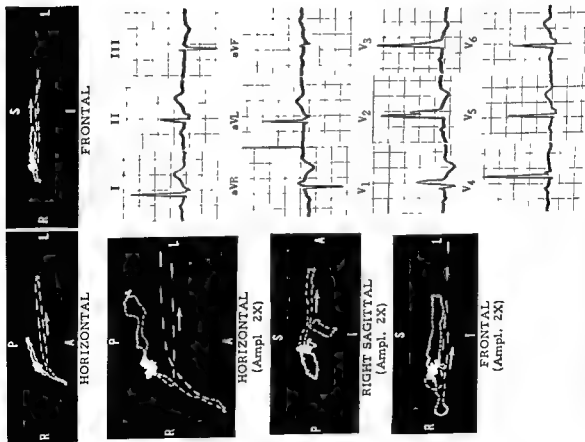


Fig 374.—Electrocardiogram and vectorcardiogram in the common type of right bundle branch block

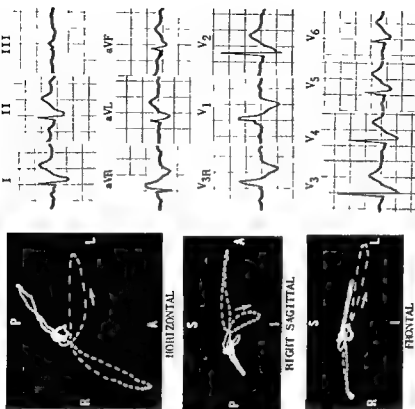


Fig. 375.—Electrocardiogram and vectorcardiogram in the common type of right bundle branch block.

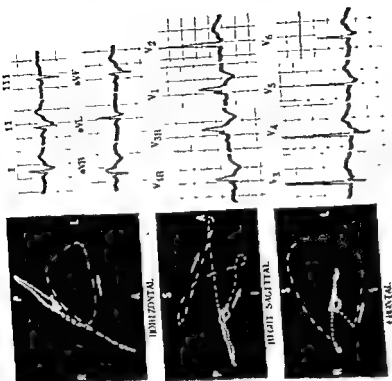


Fig 377.—Electrocardiogram and vectorcardiogram in the variant type of right bundle branch block.

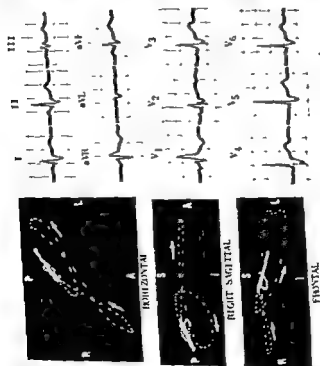


Fig 376.—Electrocardiogram and vectorcardiogram in the common type of right bundle branch block.

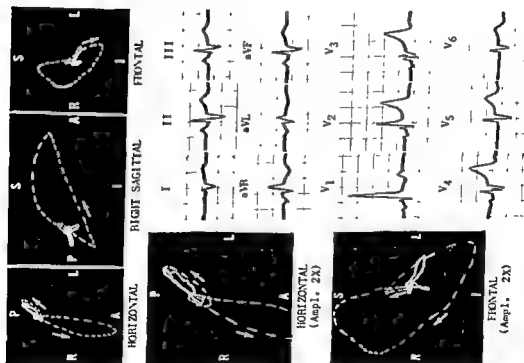


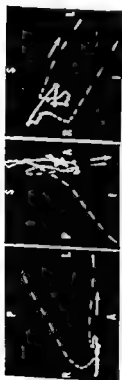
Fig. 378.—Electrocardiogram and vectorcardiogram in the variant type of right bundle branch block.



FRONTAL
(Ampl. 2X)

RIGHT SAGITTAL
(Ampl. 4X)

HORIZONTAL
(Ampl. 2X)



FRONTAL
(Ampl. 2X)

RIGHT SAGITTAL
(Ampl. 4X)

HORIZONTAL
(Ampl. 2X)

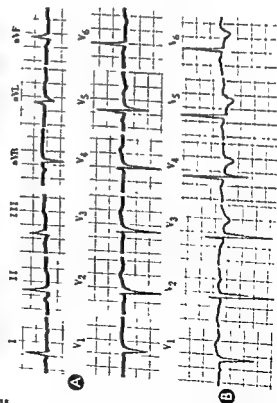


Fig. 379.—Electrocardiogram and vectorcardiogram from a woman, 68, with a history of myocardial infarction 1 year previously.

The two-lead electrocardiogram in **A** was obtained at the same time as the vectorcardiogram shown above, while the six precordial leads in **B** were recorded 2 months later. In **A**, there are inverted T waves in leads I, V₁, and V₂. Lead V₃ displays a QS deflection, and there are low initial R waves of increasing amplitude in leads V₄ through V₆. None of these findings constitute sufficient evidence to justify the diagnosis of anteroseptal myocardial infarction. The precordial leads in **B** show somewhat taller R waves in leads V₁, V₂, and V₃ and more marked T wave inversion in leads V₄ through V₆.

In the vectorcardiogram, the QRS sE loop is written initially to the left, posteriorly, and superiorly. There is an anterior concavity in the early portion of the efficient limb of the QRS sE loop in the horizontal and right sagittal projections. The initial portion of the right sagittal QRS loop is written in a direction the reverse of normal. These QRS sE loop findings are diagnostic of anteroseptal myocardial infarction. The T sE loop is discordant to the QRS sE loop, and there is an S-T vector directed predominantly to the right and superiorly. These findings are consistent with anterolateral subendocardial myocardial injury and ischemia. The vectorcardiogram is, therefore, diagnostic of old anteroseptal myocardial infarction and subendocardial injury and ischemia.

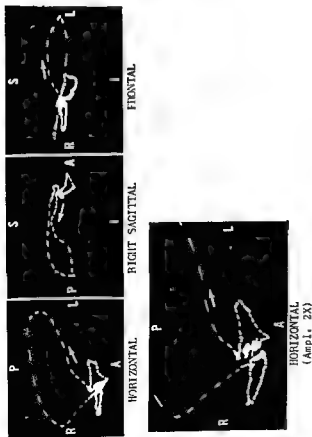


Fig 380.—Electrocardiogram and vectorcardiogram in a patient with recent anteroseptal myocardial infarction

Note, in the electrocardiogram, the QS deflections in leads V_1 through V_6 and the inverted T waves in these leads and in leads I, II, aVL, V_6 and V_7 . The terminal S waves in leads I, II, aVL, V_6 , and V_7 may reflect the type of perinfarction block described by Grant and associates in which the terminal instantaneous QRS vectors are directed away from the initial instantaneous vectors of the QRS sE loop.

In the vectorcardiogram, note that the QRS sE loop is written immediately to the left, posteriorly, and superiorly and that there is an anterior concavity in the outgoing limbs of the horizontal and sagittal loops. An S-T vector is directed to the right and anteriorly, and the T sE loop is directed to the right and slightly posteriorly. These findings are compatible with anteroseptal myocardial infarction and subepicardial myocardial injury

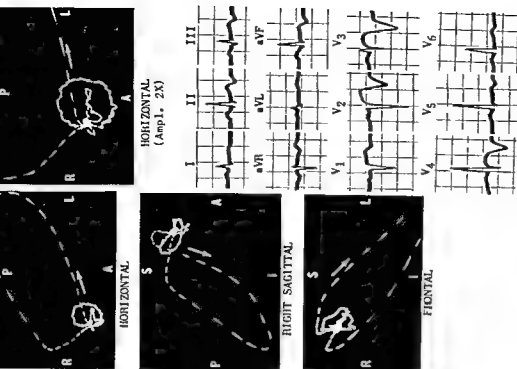


Fig 381.—Electrocardiogram and vectorcardiogram in acute anterior myocardial infarction

In the electrocardiogram, note the elevated S-T segments in leads V_1 through V_6 and the deeply inverted T waves in leads V_2 through V_6 . Leads V_1 and V_2 display QS deflections, and lead V_6 displays a small Q wave preceding a low R wave

In the vectorcardiogram, the QRS sE loop is written initially to the right, anteriorly, and superiorly and then is inscribed to the left, posteriorly, and inferiorly. This produces an anterior concavity in the early portion of the efferent limb of the QRS sE loop in its horizontal and sagittal projections and reverses the direction of inscription of the initial deflection of the sagittal QRS loop. A small S-T vector is directed almost straight anteriorly in the horizontal projection. The T sE loop is rounded in the horizontal projection and written with an almost uniform rate of inscription to the left and posteriorly. These findings are consistent with acute anterior myocardial infarction

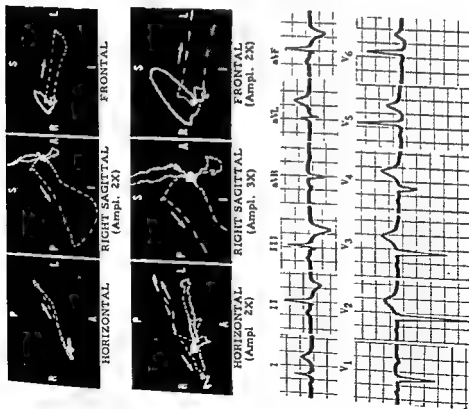


Fig 382—Electrocardiogram and vectorcardiogram in old, healed anteroseptal myocardial infarction.

Note, in the electrocardiogram, that leads II, III, and aVF display deeply inverted T waves, while leads V₁ through V₆ show low R waves and lead V₁ a QS deflection. These findings are interpreted as diaphragmatic myocardial ischemia and old anteroseptal myocardial infarction.

In the vectorcardiogram, the horizontal QRS loop is written initially to the left and posteriorly and shows posterior displacement of almost the entire inferior limb of the loop. In the sagittal projection, the posterior displacement of the inferior limb causes a complete reversal in the direction of inscription of the sagittal loop. The T-S loop is directed to the left, slightly posteriorly, and markedly superiorly, and there is an S-T vector directed to the right. Thus the vectorcardiogram is in agreement with the findings in the electrocardiogram.



FRONTAL

RIGHT SAGITTAL
(Amp 1, 2X)

HORIZONTAL



HORIZONTAL
(Amp 1, 4X)



RIGHT SAGITTAL
(Amp 1, 4X)



FRONTAL
(Amp 1, 4X)

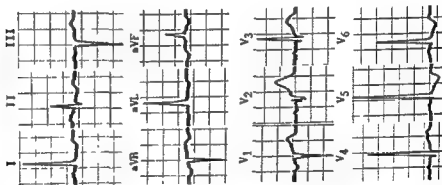


Fig. 383.—Electrocardiogram and vectorcardiogram in old strictly anterior myocardial infarction with coexisting left ventricular hypertrophy.

In the electrocardiogram, tall R waves and inverted T waves are recorded in leads I, aVL, V₄, and V₆. These findings are consistent with the diagnosis of left ventricular hypertrophy, while the small Q wave preceding the R wave in lead V₂ and the small Q wave in lead V₄ are suggestive of old strictly anterior myocardial infarction.

In the vectorcardiogram, the horizontal QRS loop is written initially to the right and anteriorly and then the loop turns in a clockwise direction and is written to the left and posteriorly. There is an anterior concavity in the early portion of the efferent limb of the horizontal QRS loop, and the long axis of the loop is displaced posteriorly. The right sagittal QRS loop is written briefly anteriorly, although not easily seen, and then is written almost directly posteriorly. There is left-axis deviation of the frontal QRS loop, the mean instantaneous vectors of the planar QRS loops are of greater than normal magnitude, and the T sE loop is discordant to the QRS sE loop. The latter vectorcardiographic findings are diagnostic of left ventricular hypertrophy, while the abnormalities initially described are diagnostic of old strictly anterior myocardial infarction.

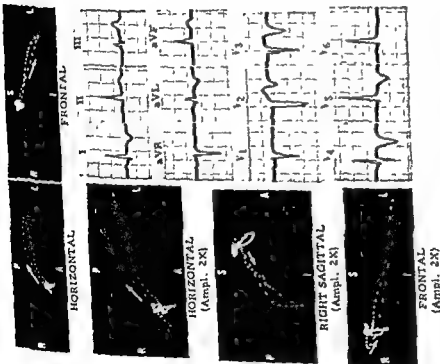


Fig. 384.—Electrocardiogram and vectorcardiogram in recent anterior myocardial infarction.

In the electrocardiogram, lead V_1 records a low initial R wave and an inverted T wave, while lead V_6 displays a QS deflection and a deeply inverted T wave. Inverted T waves also appear in leads I, aVL, V_4 , and V_5 . These findings are consistent with the diagnosis of anterior myocardial infarction and are suggestive of recent, as opposed to old, healed, infarction.

In the vectorcardiogram, the horizontal QRS loop is written initially to the right and anteriorly, and then the loop is inscribed in a clockwise direction posteriorly and to the left. There is posterior displacement of the efficient limbs of the horizontal and right sagittal QRS loops. The T wave loop is directed anteriorly, slightly to the left and inferiorly. It should be pointed out that the vectorcardiogram was recorded several days after the electrocardiogram, and so the T wave loop orientation is not consistent with the T wave abnormalities observed in the electrocardiogram.

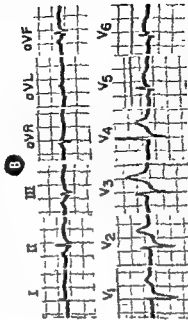
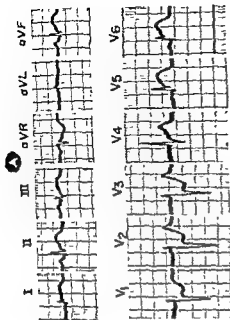


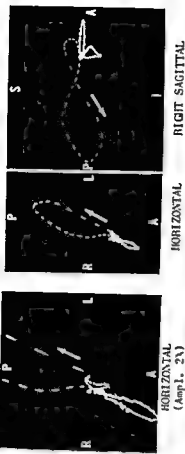
Fig. 385.—Acute anterolateral myocardial infarction. These two electrocardiograms were recorded 21 hours apart from the same patient. In A, the most prominent findings consist of marked S-T segment elevation in leads I, II, aVF, V_4 , and V_5 and marked S-T depression elevation in leads V_1 through V_3 . While small Q waves are present in leads I, V_4 , and V_5 , they are not sufficiently deep or wide to constitute reliable evidence of anterolateral infarction. However, the subprecordial injury pattern present in the left lateral leads is strongly suggestive of an early stage of developing anterolateral infarction. In B, the S-T segments are returning to the isoelectric level, and the Q waves are relatively more prominent.



Fig 384.—Electrocardiogram and vectorcardiogram in recent diaphragmatic or inferior myocardial infarction. In the vectorcardiogram, note the superior displacement of the effluent limb of the QRS sE loop and the superior orientation of the T sE loop in the right sagittal and frontal projections. As was the case in Figure 384, here, too, the fact that the vectorcardiogram was recorded several days after the electrocardiogram accounts for the more prominent abnormalities diagnostic of diaphragmatic infarction in the vectorcardiogram as compared to the electrocardiogram.



Fig 387.—Electrocardiogram and vectorcardiogram in old, healed diaphragmatic or inferior myocardial infarction and left ventricular hypertrophy. In the electrocardiogram, lead II and aVF record abnormal Q waves, but there is a small initial R wave in lead III. These findings suggest old diaphragmatic lateral myocardial infarction. The tall R wave in lead V₄ is consistent with the diagnosis of left ventricular hypertrophy. The findings are: QRS sE loop rotated abnormally posteriorly and superiorly, rightward and superior displacement of early portion of effluent limb of frontal QRS loop, and an inferior concavity in remaining portion of sE loop. The inscription of the first portion of the right sagittal QRS loop is reversed in direction, and in both frontal and right sagittal projections the mean Q-T second instantaneous QRS vector lies superior to -40° . The T sE loop is discordant to the QRS sE loop. These findings are diagnostic of old diaphragmatic lateral myocardial infarction and coexisting left ventricular hypertrophy.



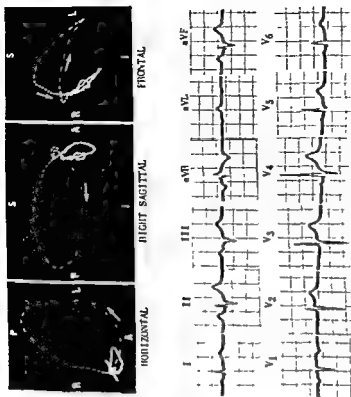


Fig. 389.—Electrocardiogram and vectorcardiogram in old diaphragmatic myocardial infarction. Note, in the electrocardiogram, that leads II and aVF register small Q waves, while lead III records a QS deflection. The corresponding finding in the vectorcardiogram is the superior displacement of the effluent and affluent limbs of the QRS sE loop. The significance of the posterior rotation of the QRS sE loop and the anterior concavity in the early portion of the effluent limb of the horizontal QRS loop is not apparent. Both the electrocardiographic and the vectorcardiographic findings are consistent with the diagnosis of old diaphragmatic infarction.

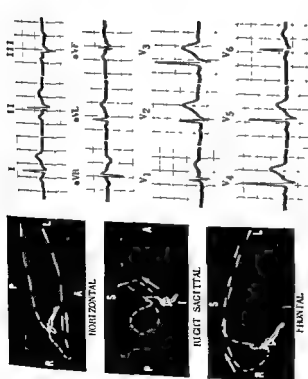


Fig. 388.—Electrocardiogram and vectorcardiogram in old or healed diaphragmatic myocardial infarction. Note that, in the electrocardiogram, lead II records an initial Q wave, while leads III and aVF register small initial R waves followed by S waves. The small initial R waves in leads III and aVF are produced by the brief initial deflection of the QRS sE loop directed inferiorly, while the S waves in the preceding leads reflect the rightward and/or superior displacement of the effluent limb of the QRS sE loop. Thus, the S waves preceded by small R waves in leads III and aVF are to be considered the equivalent of abnormal Q waves. The electrocardiographic and vectorcardiographic findings just described are consistent with the diagnosis of old healed diaphragmatic myocardial infarction.

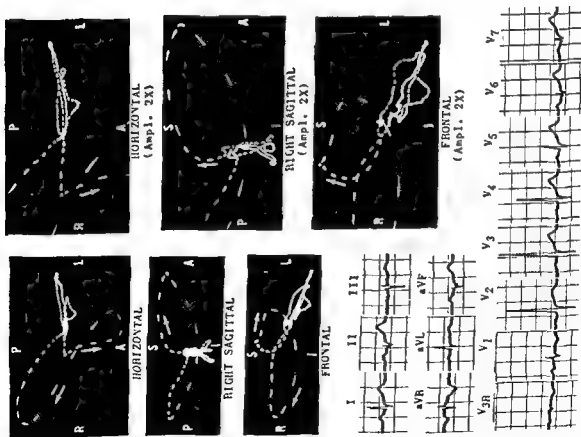


Fig 390.—Electrocardiogram and vectorcardiogram in old, healed diaphragmatic-posterolateral myocardial infarction

The electrocardiogram displays a small Q wave in lead II, while leads III and aVF register small initial R waves. In leads V₁ and V₂, the R/S amplitude ratio is greater than 1, while leads V₃ and V₄ register very low R waves preceded by small Q waves. These findings are somewhat suggestive of old diaphragmatic-posterolateral infarction

In the vectorcardiogram, however, the first half of the QRS sE loop is displaced abnormally far anteriorly, to the right, and superiorly, while the terminal portion of the QRS sE loop is written far to the right and posteriorly. The mean 0.02-second instantaneous QRS spatial vector calculated from the QRS sE loop lies well to the right and abnormally anteriorly and superiorly. The QRS sE loop abnormalities are quite diagnostic of diaphragmatic-posterolateral infarction, without evidence of recent onset of the infarction.

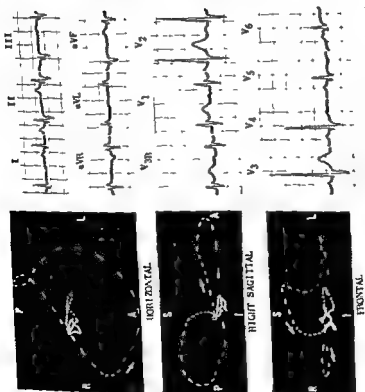


Fig 391.—Electrocardiogram and vectorcardiogram in old postmyocardial infarction

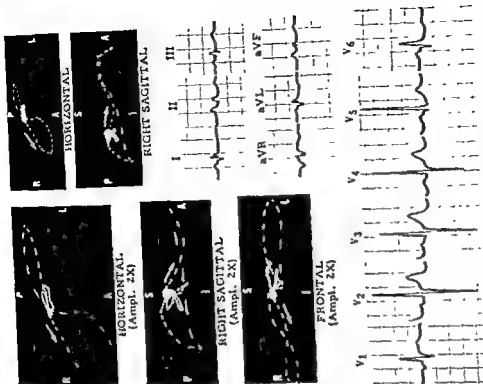


Fig. 392.—Electrocardiogram and vectorcardiogram in old posterior-lateral myocardial infarction. Note the relatively tall and wide R wave in lead V_1 , which is the counterpart of the deep, wide Q waves in leads I and V_6 .

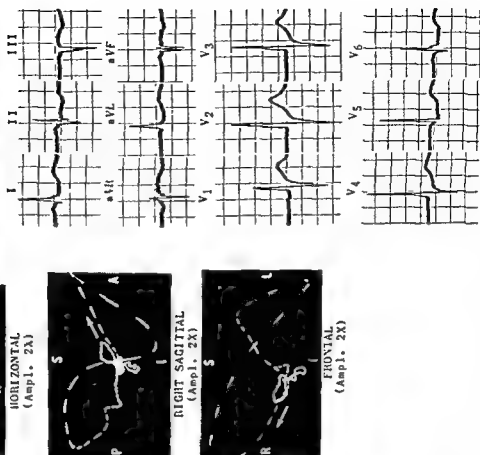
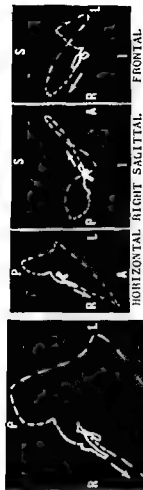
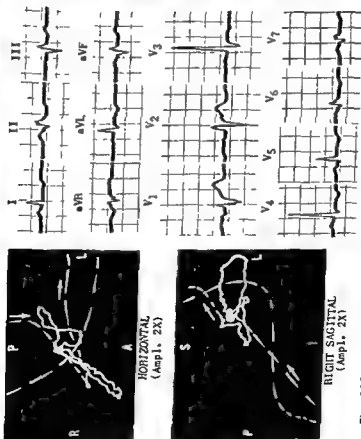


Fig. 393.—Electrocardiogram and vectorcardiogram in old diaphragmatic-posterolateral infarction. Note the abnormal Q waves in leads II, III, aVF, V₄, and V₇ in the electrocardiogram. In the vectorcardiogram, the initial portion of the QRS sE loop is written abnormally far to the right anteriorly and superiorly, while there is anterior and medial displacement of the afferent limb of the loop. The T sE loop is directed to the right and anteriorly. These vectorcardiographic findings are consistent with the diagnosis of diaphragmatic posterolateral infarction, probably old, with posterolateral myocardial ischemia.

Fig. 394.—Electrocardiogram and vectorcardiogram in old, healed diaphragmatic-posterolateral myocardial infarction.

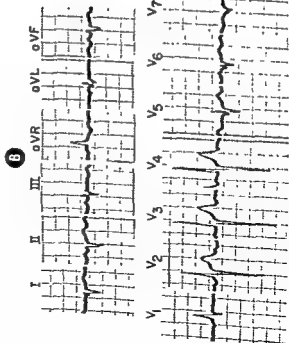
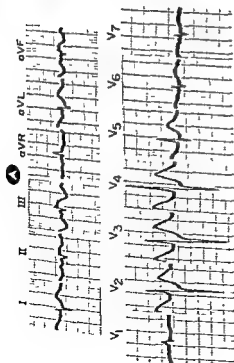


Fig. 395—Evolution of electrocardiographic changes in acute posterior-lateral infarction. Electrocardiograms **A** and **B** were recorded about 1 week apart.

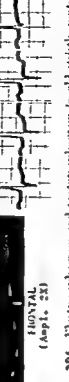


Fig. 396.—Electrocardiogram and vectorcardiogram in old strictly posterior myocardial infarction. Note the RSR' deflections in leads V_1 and V_2 in the electrocardiogram, the conventional interpretation of which would be "incomplete right bundle branch block." In the vectorcardiogram, however, there is marked anterior displacement of the apical limb of the QRS Σ loop consistent with the diagnosis of old strictly posterior infarction. (The patient had been hospitalized with the clinical diagnosis of myocardial infarction 1 year prior to these recordings.)



HORIZONTAL

RIGHT SAGITTAL
(Ampl. 2X)

FRONTAL



HORIZONTAL

RIGHT SAGITTAL

FRONTAL

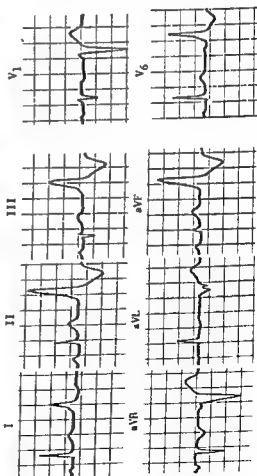


Fig. 397.—Electrocardiogram and vectorcardiogram in old diaphragmatic myocardial infarction.

In the electrocardiogram, only leads V_1 and V_6 of the precordial leads are shown in addition to the six routine extremity leads. Note that lead III displays an RSR' deflection, while lead aVF records an RR' deflection. In each of the limb leads, the conducted sinus beat is followed by a coupled ventricular extrasystole.

The vectorcardiogram shown in the top row corresponds to the conducted sinus beats in the electrocardiogram. Note the large superiorly directed early deflection of the right sagittal QRS loop and the superior displacement of the efferent limb of the frontal QRS loop. These findings plus the superior orientation of the T sE loop are compatible with diaphragmatic myocardial infarction and diaphragmatic ischemia. The electrocardiogram, in contrast, is not suggestive of infarction. The vectorcardiogram in the second row corresponds to the ventricular extrasystoles shown in the electrocardiogram. Note the closely spaced time dashes in the early portion of the efferent limb of the loop of the ventricular extrasystole.

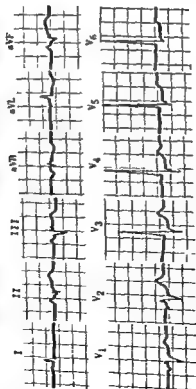


Fig. 398.—Electrocardiogram and vectorcardiogram in diaphragmatic myocardial infarction of uncertain duration.

In the electrocardiogram, abnormal Q waves are present in leads II, III, and aVF.

In the vectorcardiogram, recorded several days later, the QRS sE loop shows marked superior displacement of the efferent limb of the loop, which reverses the direction of inscription of the right sagittal planar loop and produces a crescent-shaped frontal QRS loop. The T sE loop is directed to the right, anteriorly, and slightly superiorly. The vectorcardiogram is compatible with the diagnosis of diaphragmatic myocardial infarction and post-lateral ischemia.

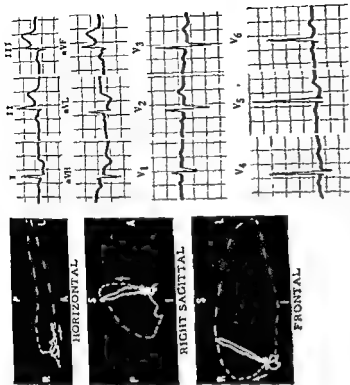


Fig. 399.—Electrocardiogram and vectorcardiogram in acute diaphragmatic myocardial infarction. The vectorcardiogram was recorded 4 days after the electrocardiogram, and so the two tracings are not entirely comparable. For example, in the electrocardiogram the diagnostic findings consist of elevated S-T segments in leads II, III, and aVF, and of small Q waves present in these leads. In the vectorcardiogram, however, there is marked superior displacement of the efferent limb of the QRS sE loop, which reverses the direction of inscription of both the right sagittal and frontal planar QRS loops. The T sE loop is directed almost straight superiorly. Thus the electrocardiogram represents an early stage (the stage of subepicardial myocardial injury) of a developing diaphragmatic myocardial infarction, while the vectorcardiogram corresponds to a somewhat later stage in the evolution of the infarction pattern, in that more prominent findings of muscle necrosis and ischemia are present. If an electrocardiogram had been recorded at the same time as the vectorcardiogram, it would probably have shown abnormal Q waves in leads II, III, and aVF and isolated S-T segments and deeply inverted T waves in these leads.

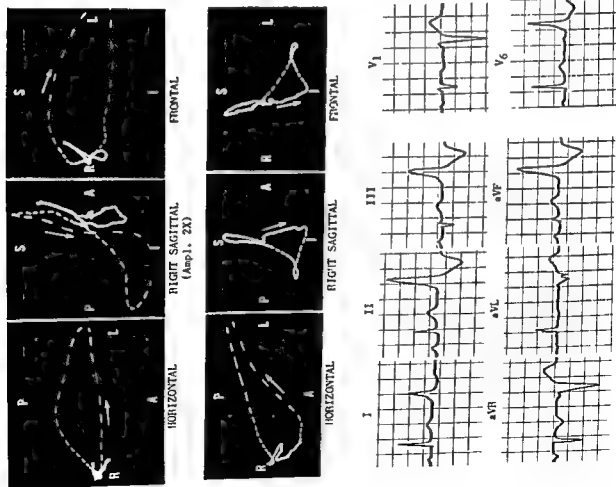


Fig. 397.—Electrocardiogram and vectorcardiogram in old diaphragmatic myocardial infarction.

In the electrocardiogram, only leads V_1 and V_6 of the precordial leads are shown in addition to the six routine extremity leads. Note that lead III displays an RSR' deflection, while lead aVF records an RR' deflection. In each of the limb leads, the conducted sinus beat is followed by a coupled ventricular extrasystole.

The vectorcardiogram shown in the top row corresponds to the conducted sinus beats in the electrocardiogram. Note the large superiorly directed early deflection of the right sagittal QRS loop and the superior displacement of the efferent limb of the frontal QRS loop. These findings plus the superior orientation of the T sE loop are compatible with diaphragmatic myocardial infarction and diaphragmatic ischemia. The electrocardiogram, in contrast, is not suggestive of infarction. The vectorcardiogram in the second row corresponds to the ventricular extrasystoles shown in the electrocardiogram. Note the closely spaced time dashes in the early portion of the efferent limb of the loop of the ventricular extrasystole.

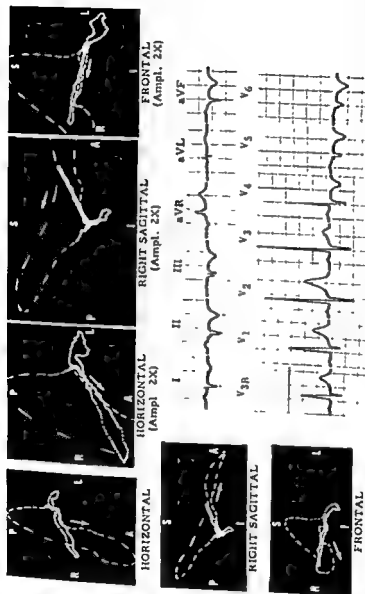


Fig. 402.—Electrocardiogram and vectorcardiogram in recent posterolateral myocardial infarction. Note, in the vectorcardiogram, that the QRS sE loop is written at first anteriorly and to the right, and then posteriorly, superiorly, and to the right, while the T sE loop is directed to the right and slightly anteriorly. Despite the abnormal Q waves in

leads II, III, and aVF of the electrocardiogram, which would suggest a posterolateral myocardial infarction, the vectorcardiogram shows no evidence of the lesion but is diagnostic of posterolateral infarction and posterolateral myocardial ischemia.

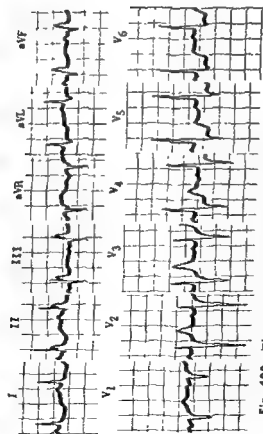


Fig. 400.—Electrocardiogram and vectorcardiogram in old diaphragmatic myocardial infarction. Note the marked S-T segment depression in leads V_1 through V_6 of the electrocardiogram and the corresponding S-T vector in the vectorcardiogram, which is directed primarily to the right. The S-T segment deviation and the S-T vector in the vectorcardiogram are compatible with anterolateral subendocardial myocardial injury.

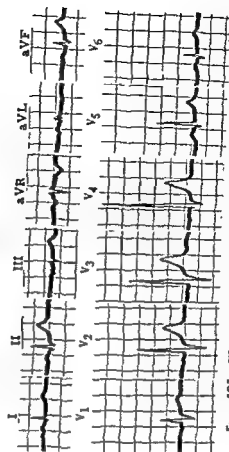


Fig. 401.—Electrocardiogram and vectorcardiogram in old, healed posterolateral myocardial infarction. Note the abnormal Q waves in leads V_1 and V_6 and the wide tall initial R wave in lead V_1 of the electrocardiogram. Corresponding findings in the vectorcardiogram consist of the large rightward and anterior early deflection of the QRS SE loop.

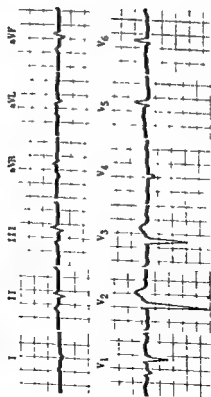
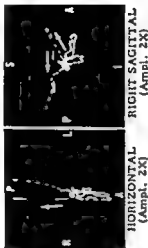


Fig 405.—Electrocardiogram and vectorcardiogram in old, healed diaphragmatic-antelateral (or apical) myocardial infarction

Fig 406.—Electrocardiogram and vectorcardiogram in old diaphragmatic-antelateral (apical) myocardial infarction. Note that abnormal Q waves are recorded by leads I, II, III, aVF, and V₁ through V₃ of the electrocardiogram. In the vectorcardiogram, the efficient limb of the QRS σ E loop is displaced markedly posteriorly, superiorly, and medially. Thus the directions of inscription of the horizontal and frontal QRS loops are reversed. Consequently, both the electrocardiogram and the vectorcardiogram are diagnostic of combined diaphragmatic-antelateral, or apical, myocardial infarction.

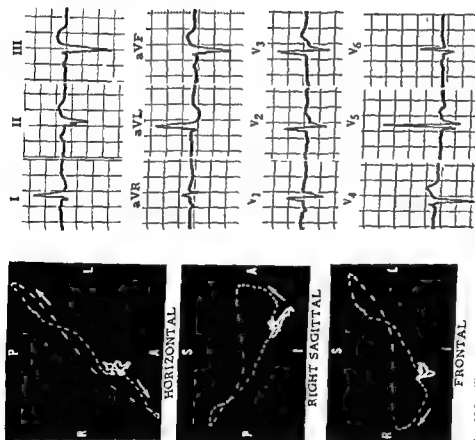


Fig. 403.—Electrocardiogram and vectorcardiogram in old, healed diaphragmatic-antrolateral myocardial infarction. Note the initial small R waves in leads II, III, and aVF which are related to the initial inferior inscription of the sagittal and frontal QRS loops. Thus the diagnosis of diaphragmatic infarction might be missed in the electrocardiogram, while the vectorcardiogram is clearly diagnostic of diaphragmatic-antrolateral infarction.

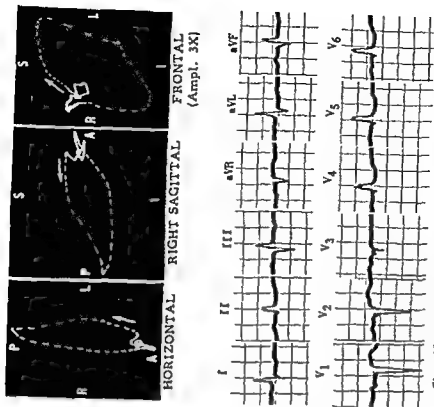


Fig. 404.—Electrocardiogram and vectorcardiogram in old, healed diaphragmatic-antroseptal myocardial infarction.

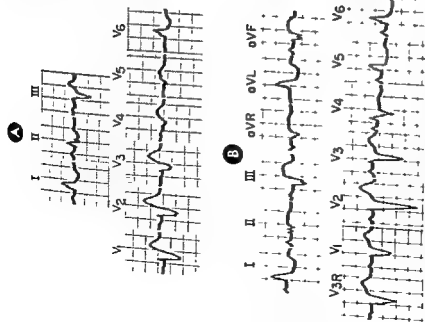


Fig 410.—A, electrocardiogram strongly suggestive of acute septal infarction complicating left bundle branch block. The initial R waves diminish in amplitude from right to left across the precordium and the S-T segments are elevated in leads V₁ and V₂. B, electrocardiogram strongly suggestive of acute diaphragmatic myocardial infarction complicating left bundle branch block. In this instance, the diagnosis of acute infarction rests primarily on the elevated S-T segments in leads II, III and aVF.

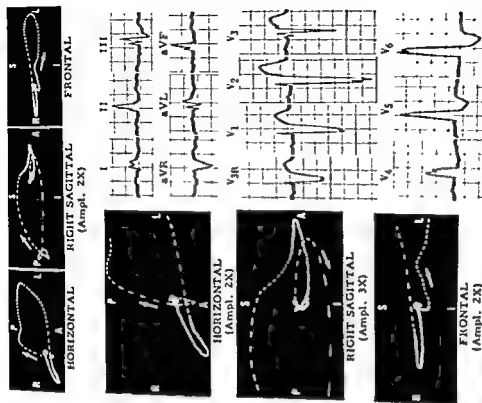


Fig 411.—Electrocardiogram and vectorcardiogram in left bundle branch block with old septal infarction. Note, in the electrocardiogram the small Q waves in leads I, aVL, V₁, and V₂. The corresponding finding in the vectorcardiogram is the rightward inscription of the initial portion of the QRS loop.

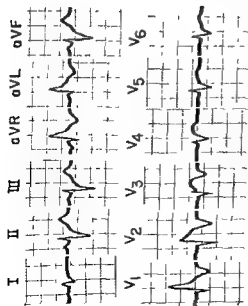


Fig. 407—Acute anteroseptal myocardial infarction with right bundle branch block. Note that the distinctive electrocardiographic features of both anteroseptal infarction and right bundle branch block are clearly evident.

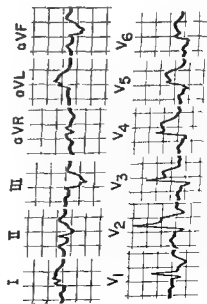


Fig. 408—Acute extensive anterior myocardial infarction with right bundle branch block.

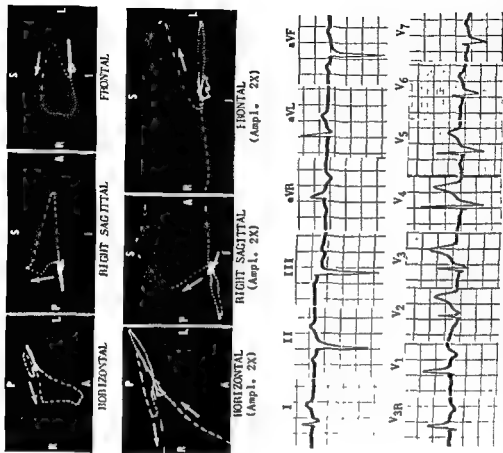


Fig. 409—Electrocardiogram and vectorcardiogram in old anterior myocardial infarction with right bundle branch block.

In the electrocardiogram, the main finding suggestive of old anterior infarction is the presence of Q waves in leads V₁ through V₆, although this is rather equivocal evidence for the diagnosis of infarction. In the vectorcardiogram, however, there is posterior displacement of the effluent limb of the QRS sE loop, while the remaining portion of the QRS sE loop is diagnostic of the variant type of right bundle branch block. The posterior shift in the effluent limb of the horizontal QRS loop is diagnostic of old anterior myocardial infarction.

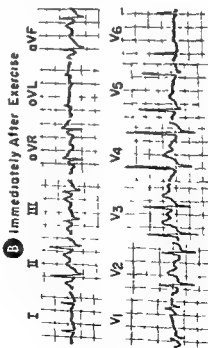
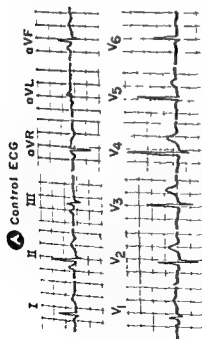
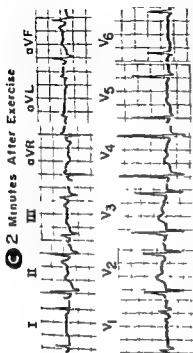


Fig. 416—An equivocal electrocardiographic response to the double Master stress test. The control electrocardiogram (**A**) is within normal limits. The record made immediately after exercise (**B**) shows a sinus tachycardia and apparent depression of the S-T segments in all leads except aVR, aVL, and V₁. The S-T segment depression persists, although less marked, at 2 minutes after exercise, as noted in **C**. Ten minutes after exercise, the electrocardiogram had returned to normal. There is a strong suspicion that the S-T segment depression in **B** may be related to the effects of tachycardia on the depth of the atrial T wave. Thus, if one were to continue the 1-10 segment through the QRS deflection, it would be found to intersect with the S-T segment at junction (J) in most leads. This would suggest that the S-T segment depression is actually produced by a superimposed deep atrial T wave. The above three electrocardiograms illustrate some of the difficulties which may be encountered in attempting to evaluate the significance of the electrocardiographic response to exercise.

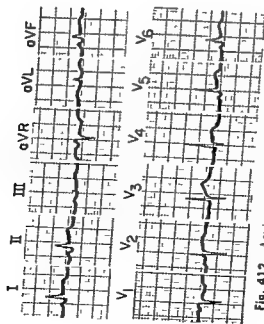


Fig. 412.—Acute pericarditis. Note the elevated S-T segments in leads I, II, aVF, and V_1 through V_4 .

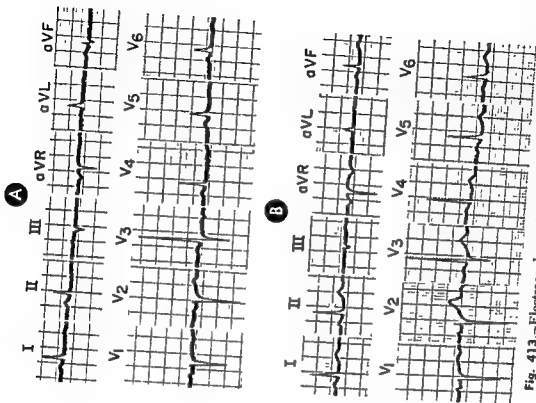


Fig. 413.—Electrocardiographic findings in a woman, 49, with myxedema treated with thyroid. A, record from the patient before administration of thyroid. Note the low upright or flat T waves in the limb leads and leads V_4 and V_5 , the inverted T wave in lead V_3 , and the diphasic T wave in lead V_1 . Shortly after record A was obtained, the patient was started on 15 mg thyroid daily. B, electrocardiogram recorded 1 month later. There is a general increase in T wave amplitude, and the T waves which previously were diphasic or inverted have become upright.

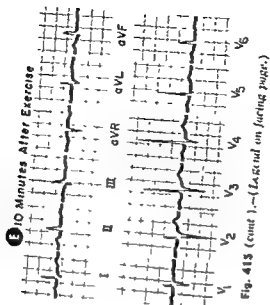
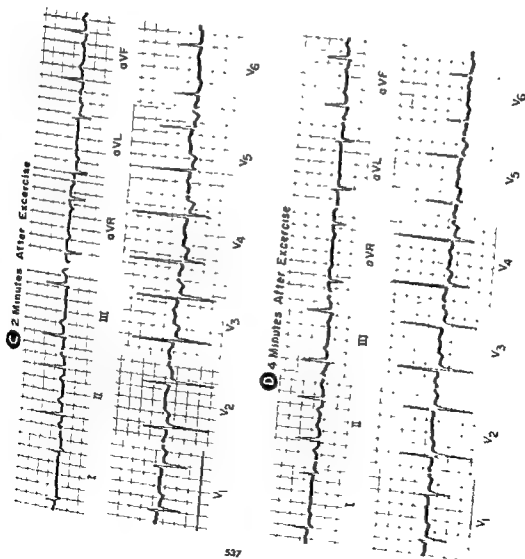


Fig. 413 (cont.)—(Lead on facing page.)

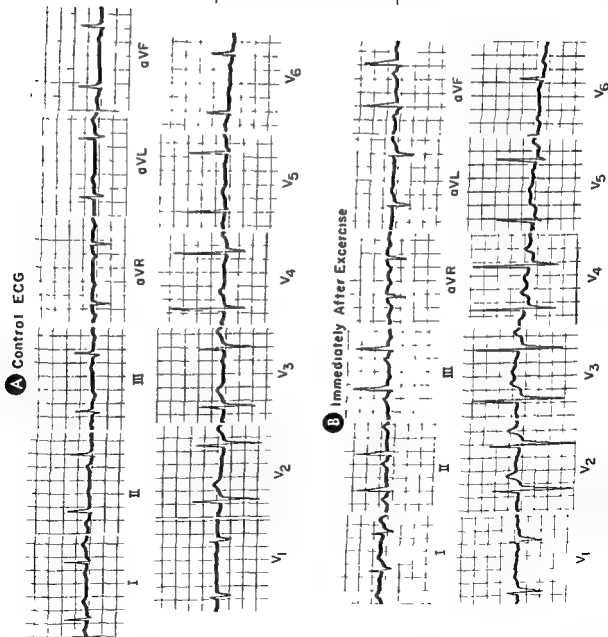


Fig. 415.—A positive electrocardiographic response to the double Master stress test. The control electrocardiogram (A) is within normal limits, while the electrocardiograms taken immediately after exercise (B) and 2 minutes after exercise (C) show widespread T wave changes and S-T segment deviation. In record D, made 4 minutes after exercise, inverted T waves persist in leads I and V₄ through V₆. Record E, obtained 10 minutes after exercise, has virtually returned to normal.

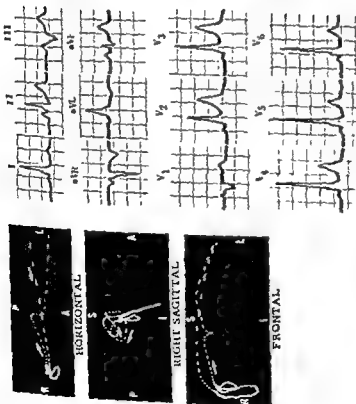


Fig. 418.—Electrocardiogram and vectorcardiogram in the Group B ventricular pre-excitation pattern

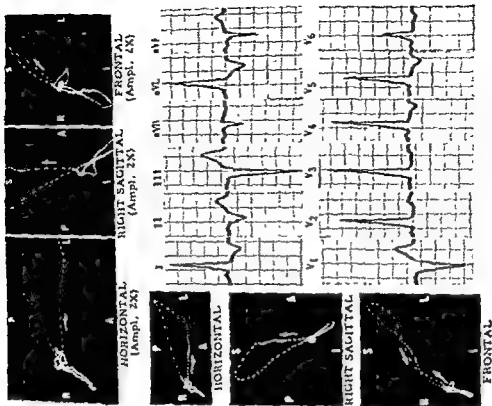


Fig. 419.—Electrocardiogram and vectorcardiogram in the Group B ventricular pre-excitation pattern

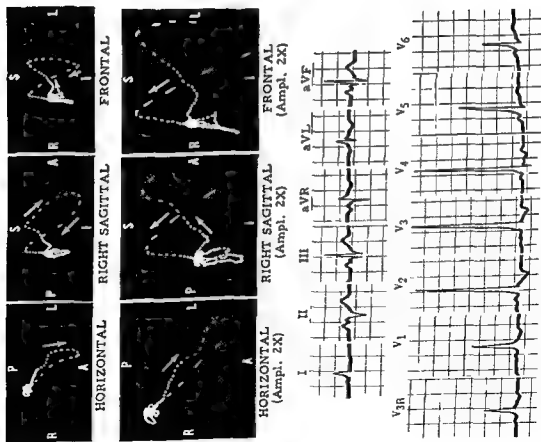


Fig. 416.—Electrocardiogram and vectorcardiogram in Group A ventricular pre-excitation pattern

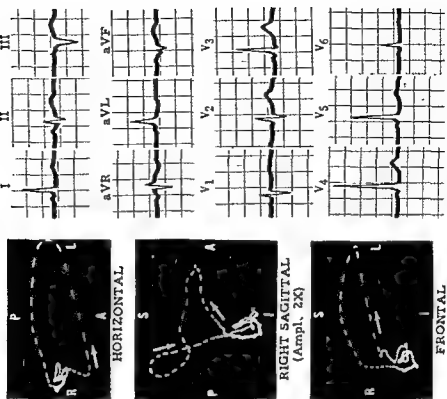


Fig. 417.—Electrocardiogram and vectorcardiogram in the Group B ventricular pre-excitation pattern

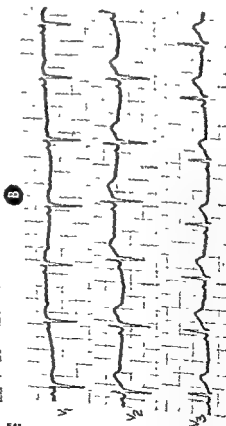
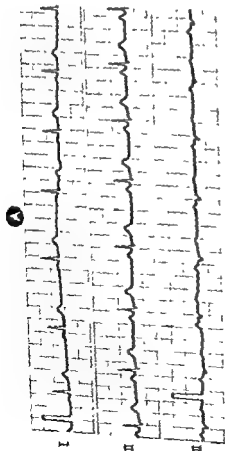


Fig 422—Sinus arrhythmia of various degree in two different patients

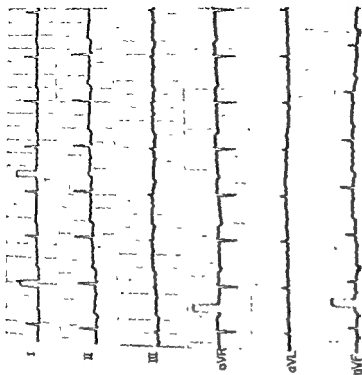


Fig 423—Upper atrioventricular nodal rhythm with prolonged ante-grade conduction, or, alternatively, coronary sinus rhythm. Retro-grade P waves precede each ventricular deflection by a P-R interval of about 0.17-0.18 second and are inverted in leads I, II, and aVF and upright in lead aVL. Typically in so-called upper atrioventricular nodal rhythm without ante-grade first-degree atrioventricular block, the P-R interval is 0.12 second or less, and so, prolonged forward or ante-grade conduction of the atrioventricular nodal impulse would have to be assumed in this record, or, as an alternative explanation, it might be postulated that the site of impulse origin is in the coronary sinus system, as at the atrial end of the atrioventricular node. Impulses arising in this area would be propagated in a retrograde direction through the atria, just like atrioventricular nodal impulses, but, unlike the latter, would have to traverse the entire length of the atrioventricular junctional tissues just as if they originated in the sinus atrial node—hence the longer P-R interval. These two possibilities cannot usually be distinguished.

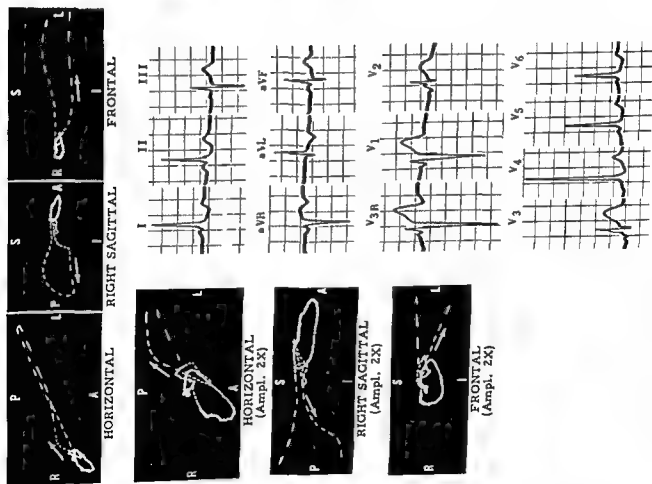


Fig 420 -Electrocardiogram and vectorcardiogram in the Group II ventricular pre-excitation pattern

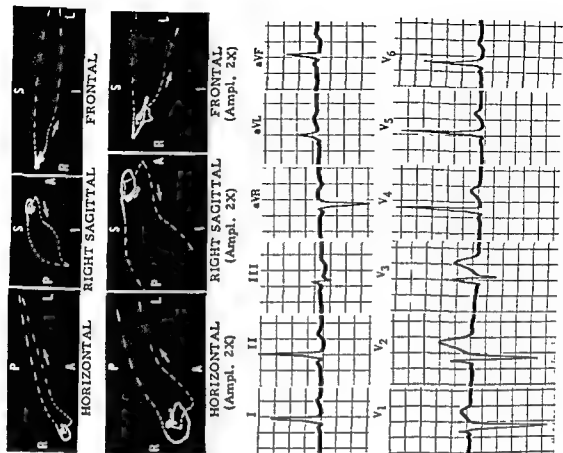


Fig. 421.-Electrocardiogram and vectorcardiogram in the Group II ventricular pre-excitation pattern.

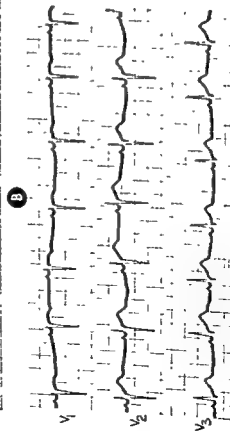
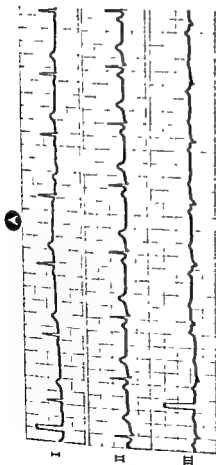


Fig 422.—Sinus arrhythmia with minor changes in two different patients

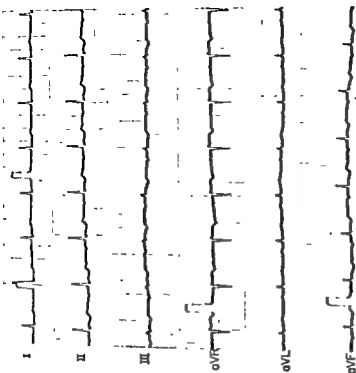


Fig 423.—Upper atrioventricular nodal rhythm with prolonged antegrade conduction or, alternatively, coronary sinus rhythm. Retrograde P waves precede each ventricular deflection by a P-R interval of about 0.17-0.18 second and are inverted in leads II, III, and aVF and upright in lead aVR. Typically in so-called upper atrioventricular nodal rhythm without antegrade first-degree atrioventricular block, the P-R interval is 0.12 second or less, and so, prolonged forward or antegrade conduction of the atrioventricular nodal impulse would have to be assumed in this record, or, as an alternative explanation, it might be postulated that the site of impulse origin is in the coronary sinus region, near the atrial end of the atrioventricular node. Impulses arising in this area would be propagated in a retrograde direction through the atria, just like atrioventricular nodal impulses, but, unlike the latter, would have to traverse the entire length of the atrioventricular functional tissues just as if they originated in the sinoatrial node—hence the longer P-R interval. These two possibilities cannot usually be distinguished.

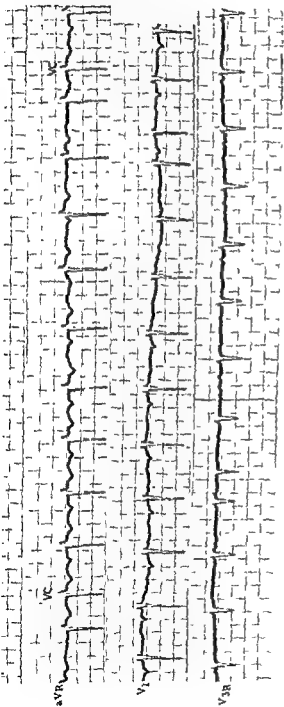


Fig. 424.—Intermittent atrioventricular nodal rhythm with complete atrioventricular dissociation and frequent ventricular capture beats (VC), recorded in a youth, 16, with acute rheumatic fever. Note the relatively rapid rate of the atrioventricular nodal rhythm. Conducted sinus beats are labeled S in lead III.



Fig. 425.—Atrioventricular nodal rhythm with complete atrioventricular dissociation, due to equalization of the atrial and ventricular rates. In lead III, some of the sinus P waves have been indicated by the symbol P.

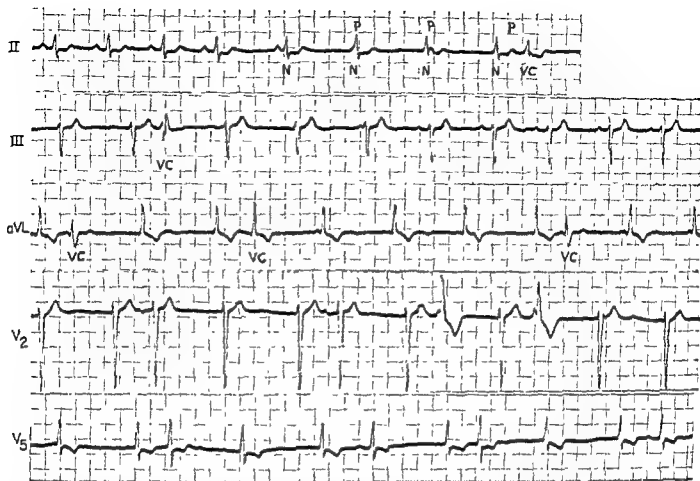


Fig. 427.—Intermittent atrioventricular nodal rhythm with incomplete atrioventricular dissociation. Note the differing QRS configuration of the ventricular capture beats (Key N, nodal beats, P, sinus P waves, and VC, ventricular capture beats). Coupled ventricular extrasystoles are also present in the second half of lead V₂.

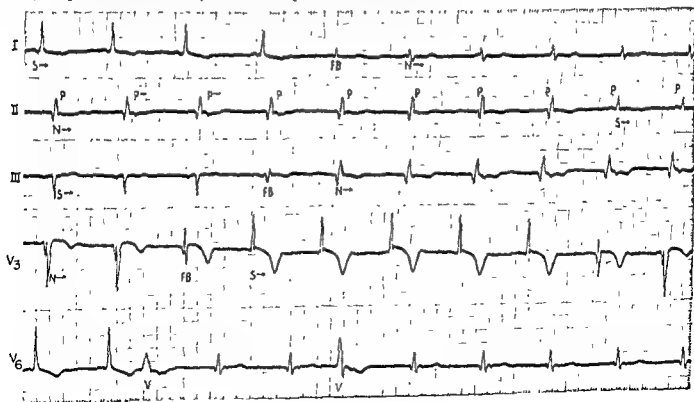
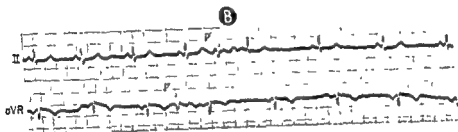
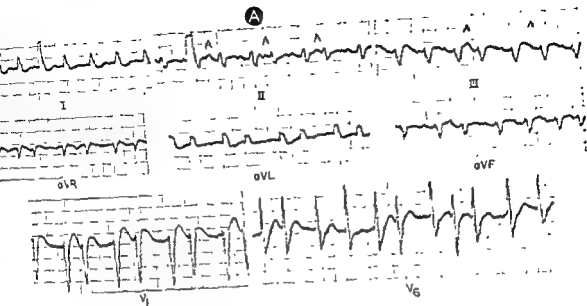


Fig. 428.—Legend on facing page



the P-P cycles in leads II and aVR containing the atrial escape beats and the intervals

lar aberration of the atrioventricular nodal escape beats and the presence of what appear to be ventricular fusion beats. The ventricular extrasystoles in lead V₆ are probably of multifocal origin, since they differ somewhat in appearance, possibly in their duration, and certainly in the lengths of their coupling intervals.

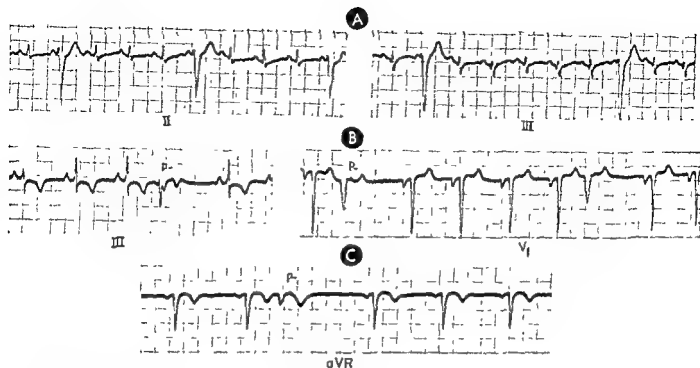


Fig. 430.—Coupled ventricular extrasystoles. The two lead strips in A show coupled ventricular extrasystoles appearing in lead II. In B, the retrograde P wave (P-) following the ventricular extrasystole in lead aVR of C. This wave appears prematurely with respect to the basic sinus cycle length and apparently discharges the sinus node prematurely, because the postextrasystolic pause in this instance is not fully compensatory.

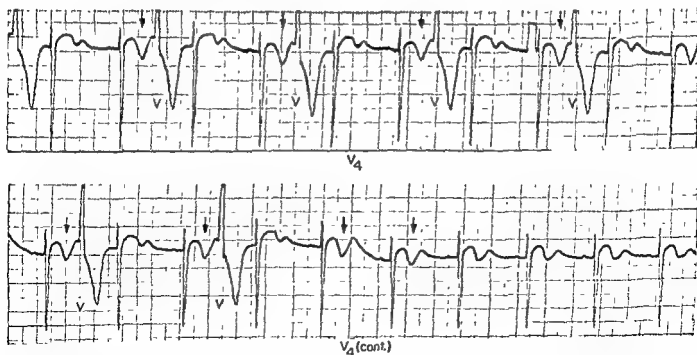


Fig. 431.—Interpolated ventricular extrasystoles (V) with postextrasystolic T wave changes. The T waves showing the postextrasystolic alteration are indicated by arrows. In this example, the T waves showing the postextrasystolic change

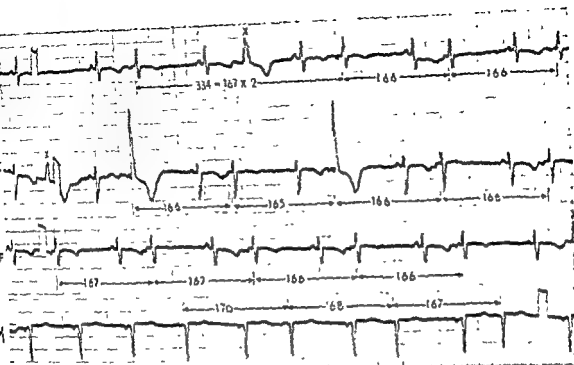


Fig. 412. Atrial extrasystole. The ectopic beats (X) are probably ventricular extrasystoles. The re-

calculated cycle length of the parasystolic atrioventricular nodal center. Note that ventricular fusion beats do not appear in this record. The two aberrant ectopic beats in lead III are probably atrioventricular nodal beats with ventricular aberration, however, this cannot be proved for certain.

follow the second postectopic QRS deflection (rather than the first, as is usually the case). This exception to the rule may be attributed to the fact that the ventricular extrasystoles are interpolated and therefore the first postectopic QRS deflection is not preceded by a compensatory pause. Since the pause following an extrasystole seems to be an essential requirement for the occurrence of postectopic T wave changes, the latter finding in this record appears later than usual and involves the second postectopic ventricular deflection.

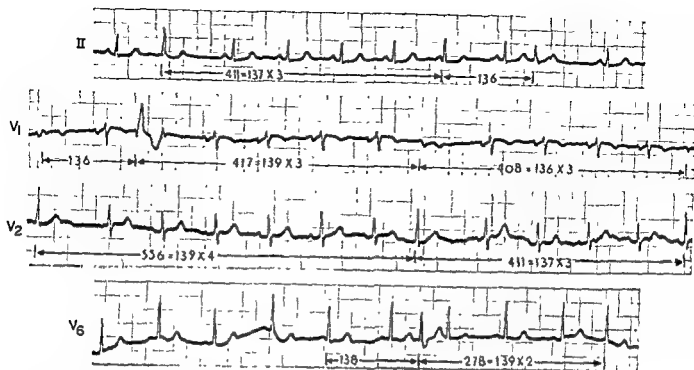


Fig. 433.—Atrioventricular nodal reentry.

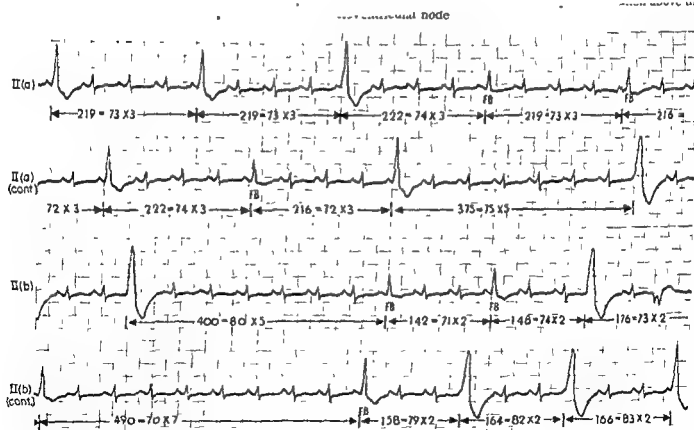
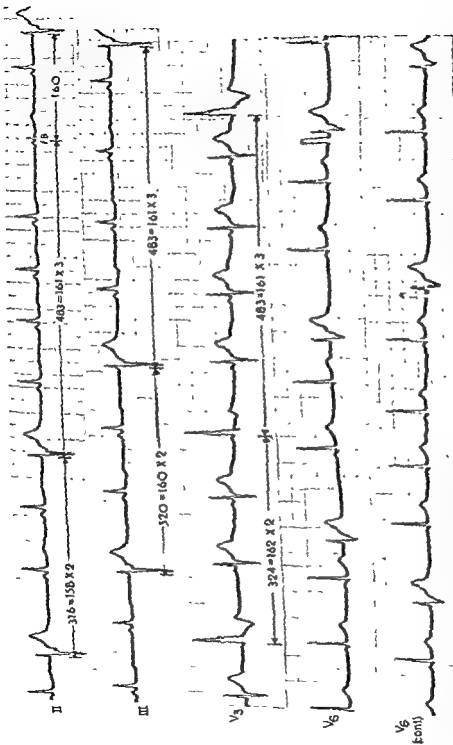


Fig. 434.—Ventricular parasystole. Note the varying coupling intervals of the widened bizarre ectopic ventricular beats. The interectopic intervals are whole-number multiples of intrinsic sinus cycle. (Note: In this case, the sinus cycle is 73 ms.) should be noted that, in this case, the ectopic beats are conducted retrogradely through the junctional tissues surrounding the parasystolic center. Fused ventricular beats (FB) are present.



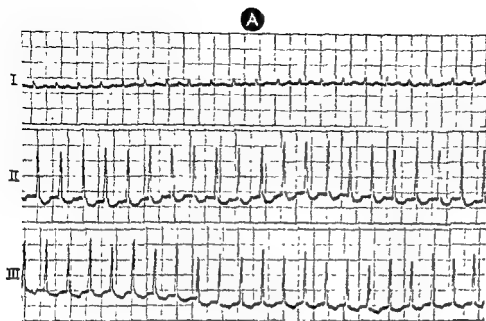


Fig. 436.—A, electrocardiogram showing a paroxysmal supraventricular tachycardia, probably originating in the atria. Record B, taken later from same patient, showing a return to normal sinus rhythm.

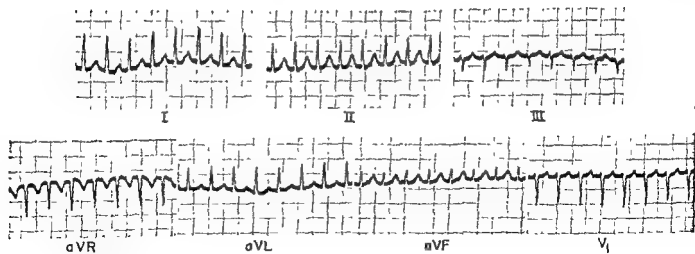
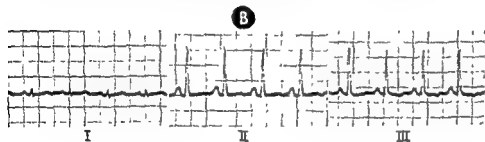


Fig. 437.—Paroxysmal supraventricular tachycardia, probably originating in the atria, with 1:1 atrioventricular response

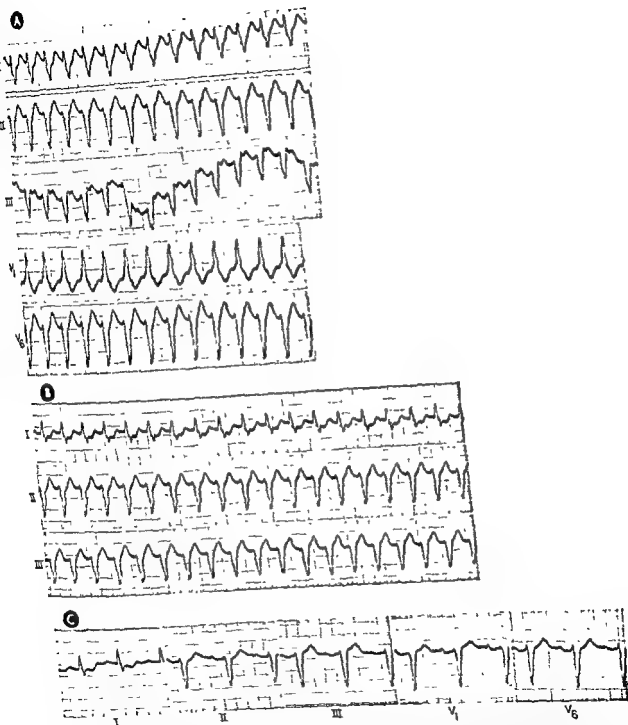


Fig 438—Electrocardiograms recorded about 1 hour apart from the same patient. Record A shows a paroxysmal tachycardia which might be identified erroneously as a ventricular tachycardia. However, there is no evidence of atrio-ventricular dissociation, and P waves are not clearly demonstrable. Record B shows findings somewhat similar to those in A. However the electrocardiogram in C, which was recorded after the patient had returned to normal sinus rhythm, displays ventricular deflections having essentially the same appearance and duration as those present during the paroxysmal tachycardia. Thus in retrospect, the paroxysmal tachycardia in A and B is obviously of supraventricular (probably atrial) origin, while the wide QRS interval and aberrant appearance of the QRS deflections during the tachycardia are probably related to a diffuse intraventricular conduction disturbance.

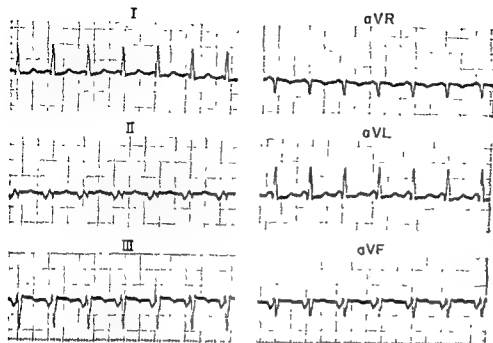


Fig. 439.—Paroxysmal atrioventricular nodal tachycardia. Note the inverted retrograde P waves preceding the ventricular deflections in leads II, III, and aVF and the upright retrograde P waves in lead aVR.

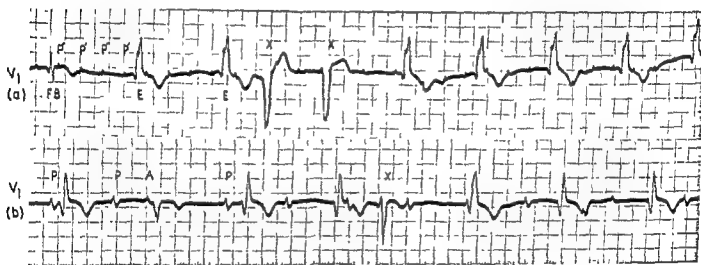


Fig. 440.—Both strips of lead V_1 were recorded from the same patient, the second record having been made about 24 hours after the first. (a) shows a sequence of beats with labels: P, P, P, P, E, E, X, X. (b) shows a sequence of beats with labels: P, P, A, P, X.

represent conducted atrial beats, while the first ventricular deflection in the lead strip is probably a ventricular fusion beat (FB). In lead V_1 (b), the atrial rhythm is of sinus node origin (sinus P waves are labeled P). There is almost complete atrioventricular block, and the ventricular rhythm arises in an idioventricular pacemaker. The P wave designated A is an atrial premature beat, and the QRS deflection following it is probably a ventricular fusion beat. The ventricular complex labeled X appears to be a conducted sinus beat.

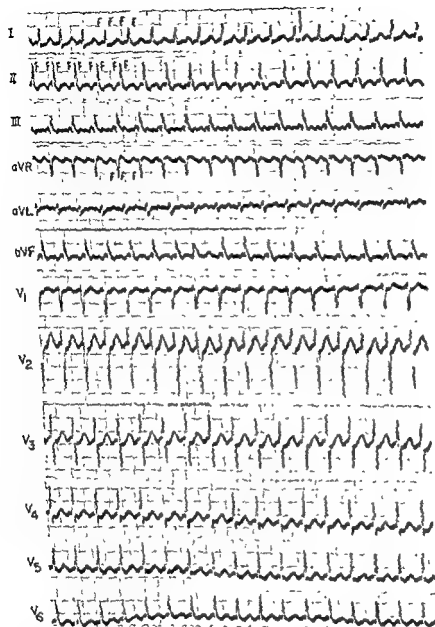


Fig. 441 - Atrial flutter with 2:1 atrioventricular response. The atrial flutter waves are labeled F.

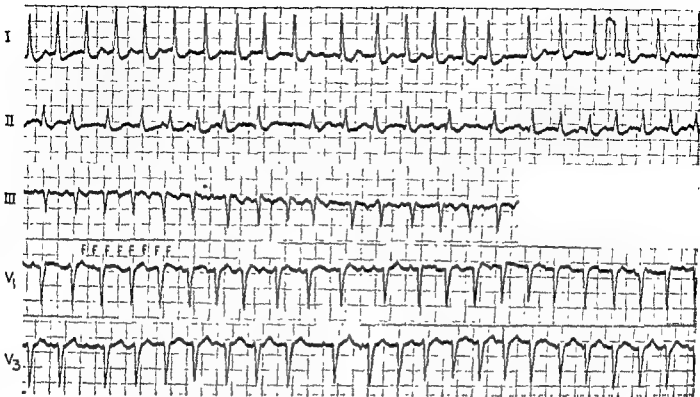


Fig. 442.—Atrial flutter approaching fibrillation (Key: F, atrial flutter waves.)



Fig. 443.—Atrial flutter with widely varying atrioventricular response and ventricular aberration of some of the QRS deflections (Key F, atrial flutter waves)



Fig. 444.—Impure atrial flutter with spontaneous transition to and from sinus rhythm in end of lead II, first part of lead aVF (a), and latter part of lead aVF (b)

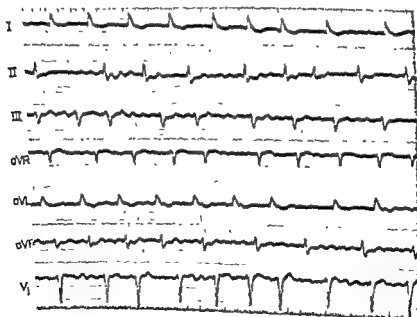


Fig. 445.—Atrial fibrillation.

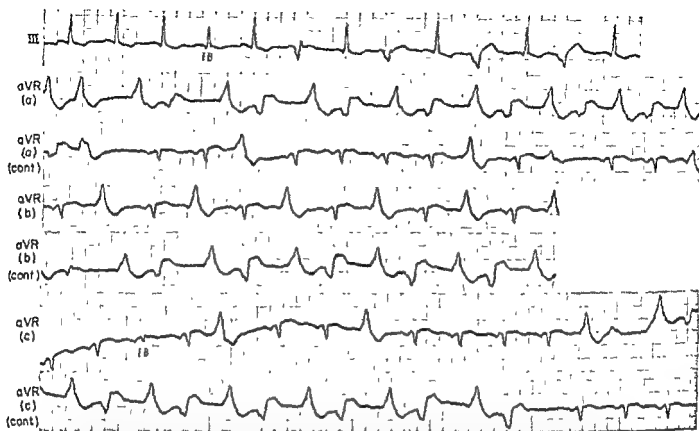


Fig 446.—Alternating bidirectional ventricular tachycardia. Shown are three continuous strips of lead aVR and a single strip of lead III containing periods of alternating bidirectional tachycardia. The deflections labeled FB are ventricular fusion beats. The presence of ventricular fusion beats, the marked widening and distortion of the QRS deflections, and the presence of atrioventricular dissociation are all compatible with a ventricular origin of the ectopic beats.



Fig . . .

ventricles
proachus
less and less clear cut In lead II (c), the ventricular tachycardia, shortly before its termination, consists of intermittent short paroxysms of tachycardia, between which are interspersed one to five ventricular beats of an atrioventricular nodal escape rhythm In lead II (d), there is a trigeminal rhythm, each group of three ventricular beats being composed of an atrioventricular nodal beat followed by two ventricular extrasystoles There is also atrioventricular dissociation In lead II (e), there is an atrioventricular nodal rhythm with complete atrioventricular dissociation

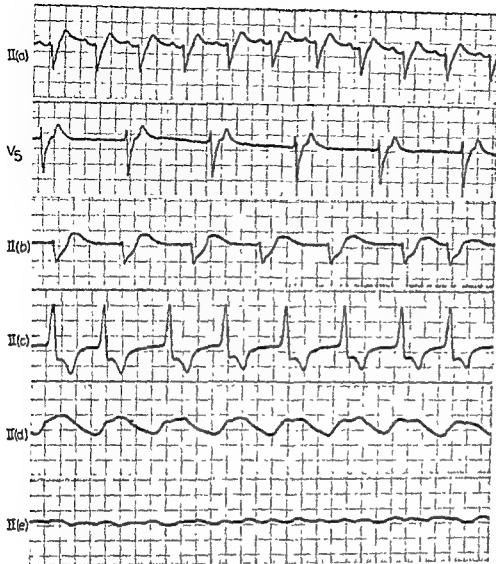
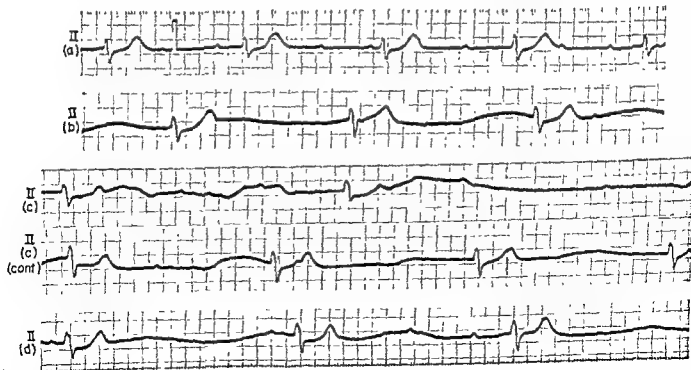
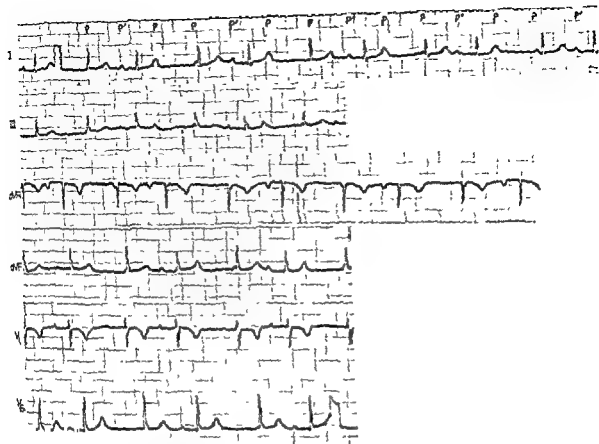


Fig. 448 (left).—Lead strips recorded from the same patient during a 2-hour period prior to his death. In lead II (a), there is a sinus tachycardia with a 1:1 atrioventricular conduction and slightly prolonged intraventricular conduction. In the next strip, of lead V₅, atrial deflections cannot be identified, and so the rhythm is either atrioventricular nodal or idioventricular in origin. In lead II (b), there is marked prolongation of the QRS interval and the QRS complexes are bizarre in appearance. The ventricular beats presumably arise in an idioventricular pacemaker. In lead II (c), there is a relatively slow ventricular tachycardia; while in lead II (d), the rhythm is ventricular flutter. Finally, in lead II (e), ventricular fibrillation appears.

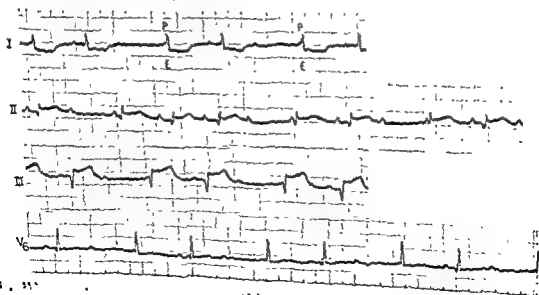
Fig. 449 (below)—Complete atrioventricular block with progressive deterioration of pacemaking



ity in the idioventricular center, the ventricular rate gradually slows and the QRS deflections progressively widen



escape beat and the second, a conducted escape beat. The remaining P waves are not conducted into the ventricles.



the escape beat is

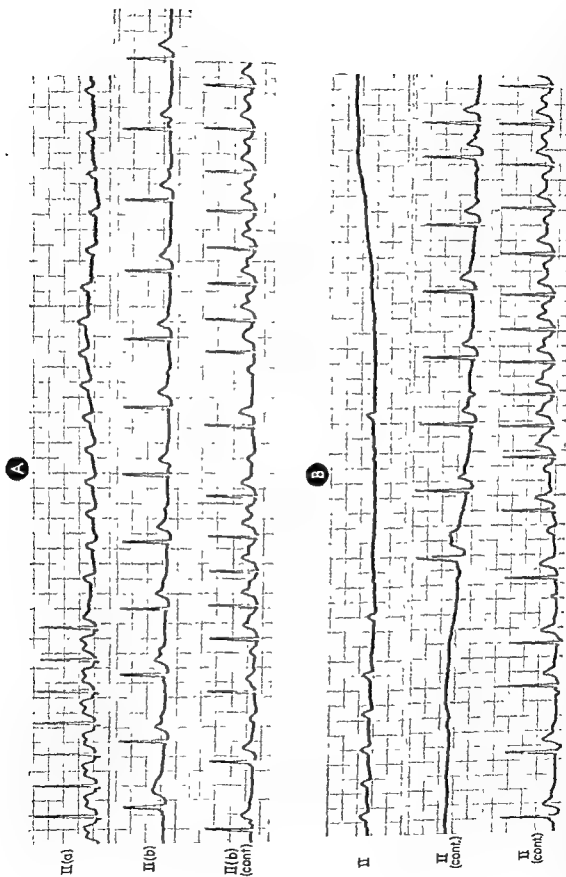


Fig. 452.—Lead strips recorded from the same patient on several occasions during Stokes-Adams attacks. In A, there can be seen rapid sinus tachycardia with onset of complete atrioventricular block, and prolonged ventricular stand-

still and finally appearance of atrioventricular nodal escape rhythm. In B, much the same sequence of events can be seen, except that here there is a long period of atrial, as well as ventricular, standstill (*Continued*)

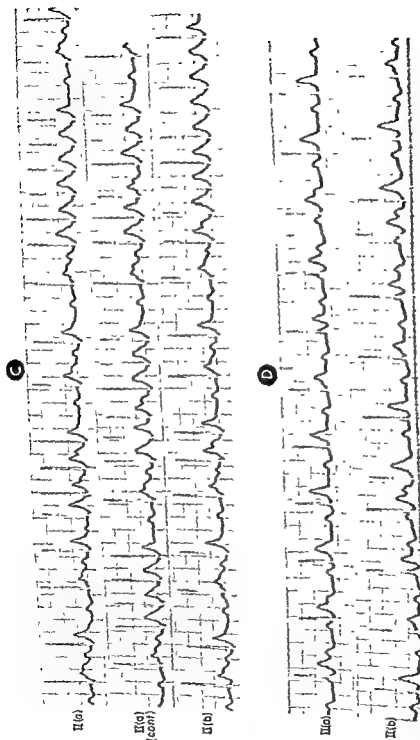


Fig. 452 (cont) —In C, there is rapid sinus tachycardia with short periods of 2:1 atrioventricular block. In D, the first strip shows complete atrioventricular block and dissociation with occasional ventricular captures, while the second strip shows almost complete atrioventricular block.

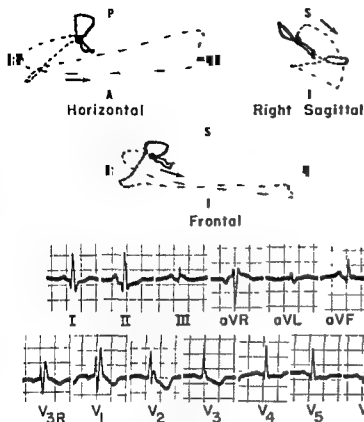


Fig. 453.—Electrocardiogram and vectorcardiogram in right bundle branch block and old, healed posterolateral myocardial infarction.

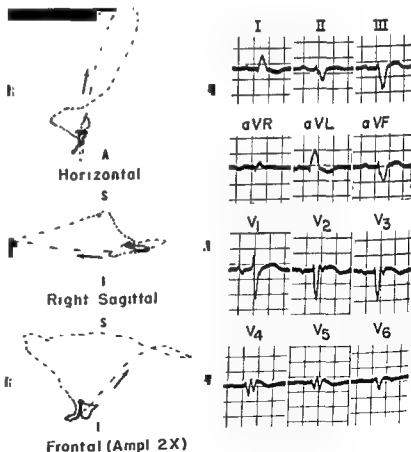
In the electrocardiogram, note the relatively deep Q wave in lead I and the relatively tall initial R wave in lead V₁. These findings are somewhat suggestive of an old posterolateral infarction, but they cannot be construed as being diagnostic of this condition.

In the vectorcardiogram, there is a large early deflection of the QRS sE loop to the right and anteriorly, and the efferent limb of the loop is displaced anteriorly. These findings are strongly suggestive of old posterolateral myocardial infarction.

The features of right bundle branch block are equally obvious in both the electrocardiogram and vectorcardiogram

Fig. 454.—Electrocardiogram and vectorcardiogram in left bundle branch block with recent infarction of the anterolateral wall of the left ventricle and interventricular septum. Autopsy confirmed the recent infarction of the lateral wall of the left ventricle and interventricular septum, but also demonstrated recent infarction of the posterior wall of the left ventricle, multiple healed infarcts of the entire left ventricle, and dilatation and hypertrophy of the heart, predominantly of the left ventricle.

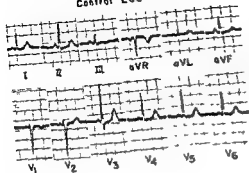
In the electrocardiogram, the QRS duration is 0.14 second, and there are broad slurred R waves in leads I and aVL. Additional findings which indicate septal and anterolateral infarctions superimposed on left bundle branch block are small Q waves in leads I and aVL, relatively tall R wave in lead V₁ with diminishing R wave amplitude from right to left, W-shaped ventricular deflections in leads V₁ and V₂, and QS deflection in lead V₃. There is minimal elevation of the S-T segments in leads V₁ through V₆.



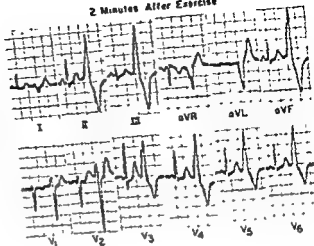
tive of coexisting septal and anterolateral infarction consist of the following: large early deflection of the QRS sE loop anteriorly and only

loop to the right and inferiorly, and the T sE loop is 180° discordant to the QRS sE loop

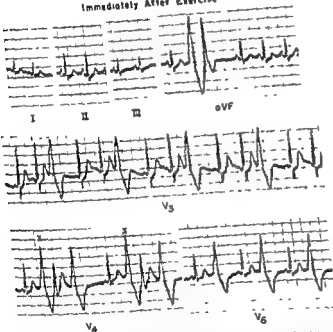
Control ECG



2 Minutes After Exercise



Immediately After Exercise



4 Minutes After Exercise

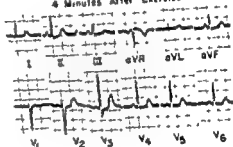


Fig 455—Positive electrocardiographic response to the Master exercise test. The control electrocardiogram appears to be entirely within normal limits. In the record made immediately after exercise, moderate depression of the S-T segments (leads I, II, III, and V₄ through V₆). A more striking finding in this electrocardiogram is the appearance of

constitutes equivocal evidence for interpreting the response to the test as positive, and the appearance of ST segment depression or extrasystoles in the postexercise tracings is, in itself, diagnostic of a positive response

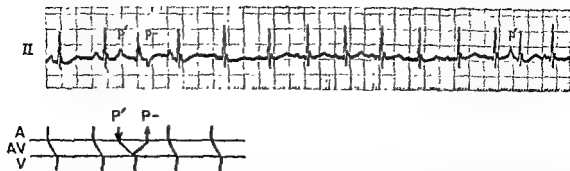


Fig. 456.—Reciprocal atrial beat following an atrial extrasystole. (Key: P', premature atrial extrasystoles, P—, reciprocal P wave following the first ectopic atrial beat.) The explanation for reciprocal ventricular beats has been discussed in the text and in Figure 246. The same mechanism, operating in a different direction, can explain the presence of a reciprocal atrial beat. Thus, the first ectopic atrial beat is transmitted through the atrioventricular node slowly, some fibers of the atrioventricular conducting pathways being entirely refractory to the ectopic beat. Shortly before emerging from the atrioventricular node, the ectopic atrial impulse splits, one impulse continuing into the ventricles and the other being propagated back up the atrioventricular node into the atria by the previously refractory conducting pathways.

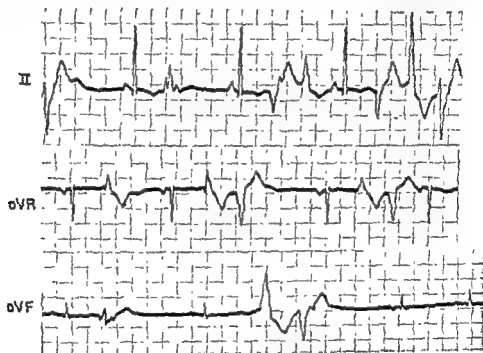


Fig. 457.—Multifocal and frequently bidirectional ventricular extrasystoles occurring in a patient intoxicated with digitalis.

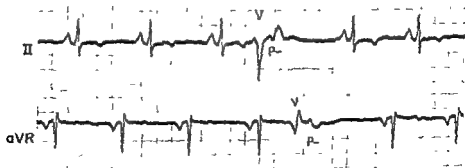


Fig. 458.—, the retrograde and interrupt ventricular extrasystoles.

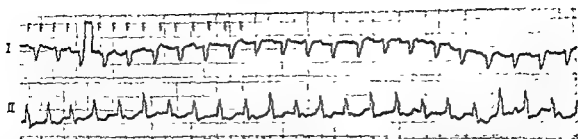


Fig. 459.—Simultaneous atrial flutter and atrioventricular nodal tachycardia with probably complete atrioventricular dissociation. In both lead strips, atrial flutter (F) waves can be identified, they appear at a rate of 250 per minute, with a rhythm which is independent of the ventricular rhythm. The ventricular complexes appear at a rate of 160 per minute and exhibit essentially regular cycles. Thus, there must be complete atrioventricular dissociation between the atria and the ectopic atrioventricular nodal pacemaker. This combination of rapid rhythms occurred in a patient with digitalis intoxication and is a rarely observed type of arrhythmia.

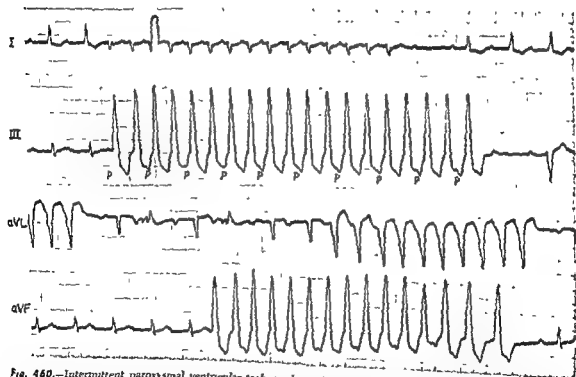


Fig. 460.—Intermittent paroxysmal ventricular tachycardia with atrioventricular dissociation occurring in the presence of first-degree atrioventricular block. Sinus P waves (P) can be identified superimposed on the S-T segment or T waves of the ectopic ventricular beats of the paroxysmal tachycardia.

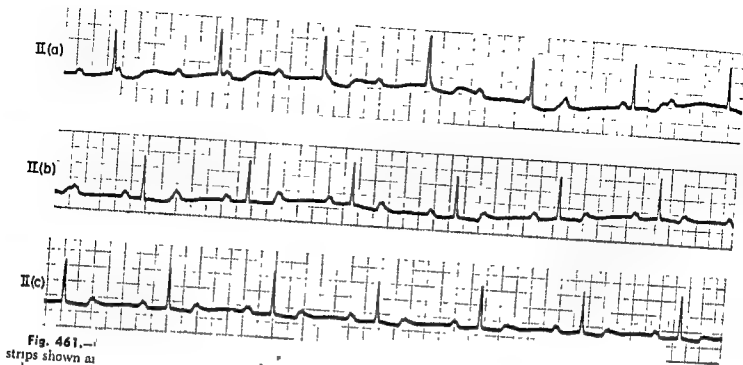


Fig. 461. —
strips shown at

The lead
thought that
However,
plete and that the R-R intervals in
the ventricular rhythm must have
nodal pacemaker

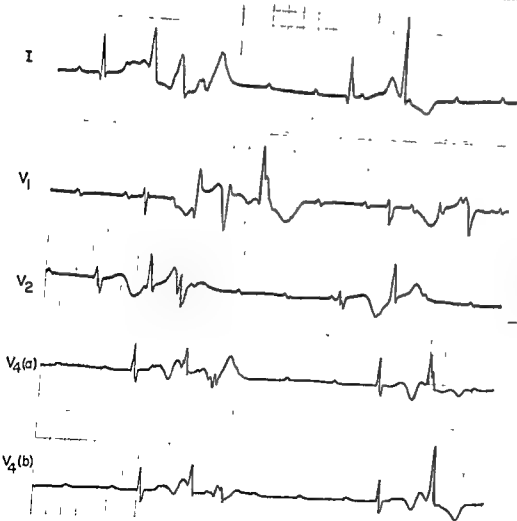


Fig. 462. — Multifocal ven-
tricular extrasystoles occurring
in the presence of complete
atrioventricular block. Note that
the ventricular extrasystoles are
bidirectional in some of the
leads

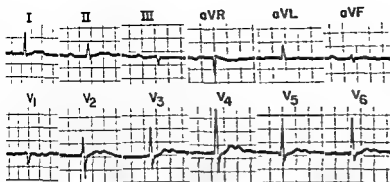
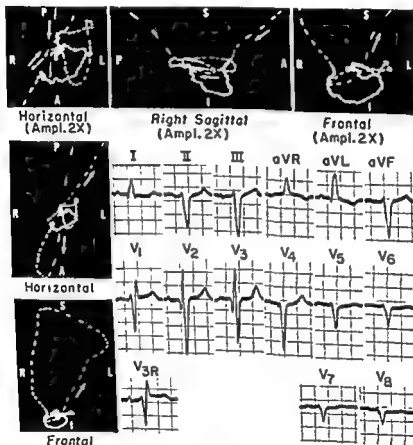


Fig. 463. — Hypokalemia. This electrocardiogram is compatible with the diagnosis of hypokalemia in that it displays strikingly prominent U waves in virtually all leads, slightly depressed S-T segments in leads V_2 through V_4 , and low T waves in most leads. An additional, and probably unrelated, finding is the presence of first-degree atrio-ventricular block.



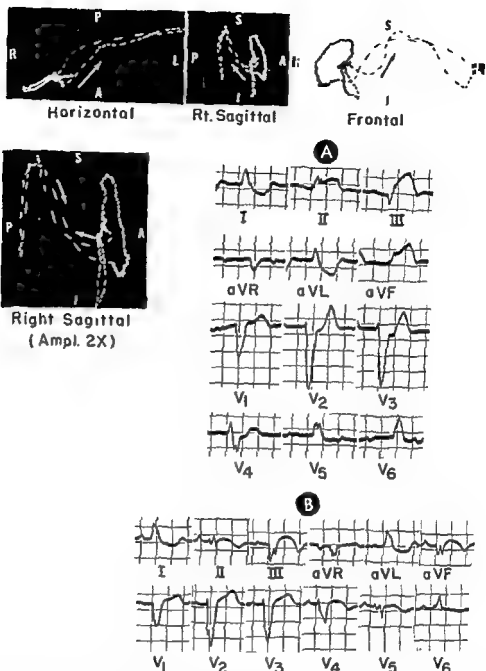


Fig. 465.—Electrocardiogram and vectorcardiogram in left bundle branch block with acute diaphragmatic myocardial infarction.

patient about 1 week later. The Q waves in leads III and aVF are deep and symmetrical. Note the change in the QRS configuration in these leads as compared to the configuration in A. Note also the change in configuration of the QRS deflections in leads V₄ and V₅. The latter findings may be related to septal involvement in addition to the diaphragmatic myocardial infarction.

In the vectorcardiogram, the QRS sE loop is markedly irregular in contour and shows striking superior displacement of the midportion of the QRS sE loop. The terminus of the loop's point of origin, while the T sE loop is large and is directed to the left and anteriorly. The above vectorcardiogram is, therefore, compatible with left bundle branch block and diagnostic of diaphragmatic myocardial ischemia, subepicardial injury, and infarction.

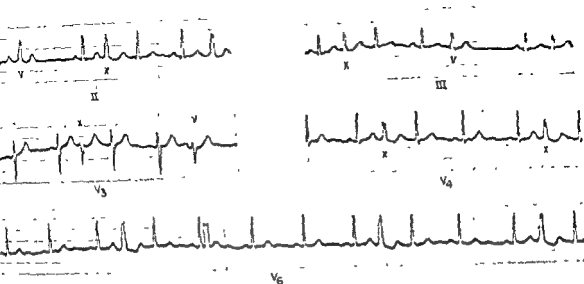


Fig 466.—Interpolated ventricular extrasystoles. The ectopic ventricular beats labeled X are interpolated, while those labeled V are not.

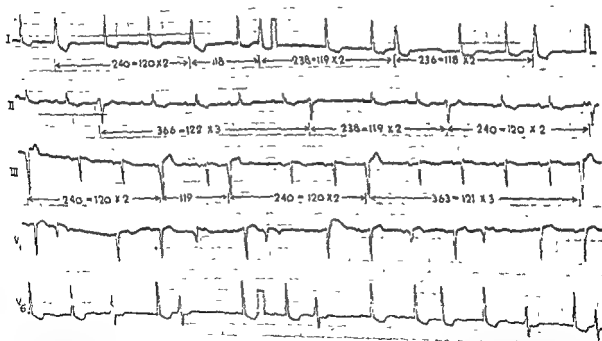


Fig 467.—Atrioventricular nodal parasytyle. The ectopic ventricular beats are less than 0.12 second in duration, they show varying coupling intervals, and yet their interectopic intervals are a whole-number multiple of approximately 1.20 seconds.

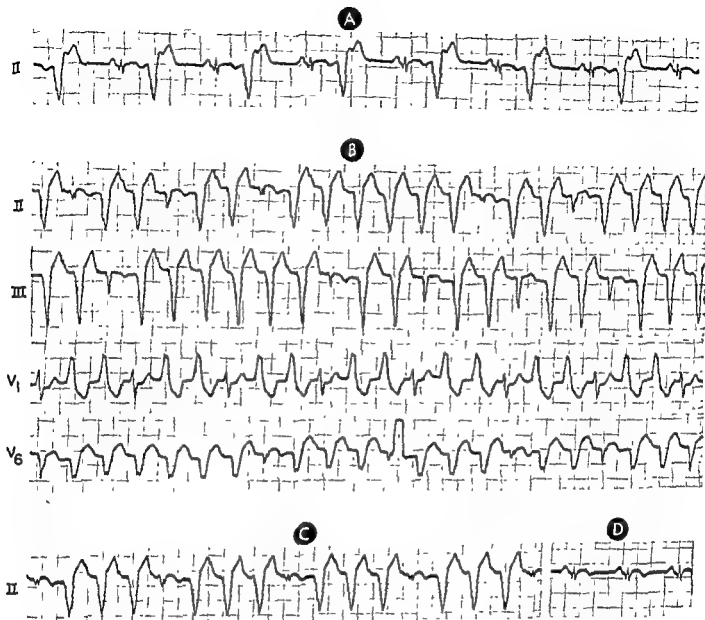


Fig. 468.—Ventricular tachycardia. In A, the strip of lead II shows a coupled rhythm, with each conducted sinus beat being followed by a ventricular extrasystole. In B, the lead strips of both leads II and III show ventricular extrasystoles. In C, the strip of lead II shows a coupled rhythm, with each conducted sinus beat being followed by a ventricular extrasystole. In D, the strip of lead II shows a normal sinus rhythm.

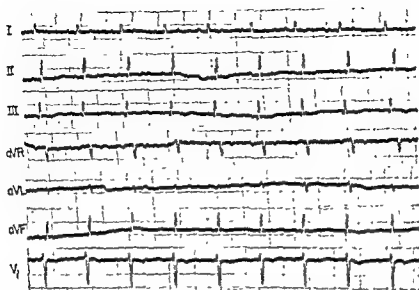


Fig 469.—Paroxysmal atrial tachycardia with 2:1 atrioventricular response. The atrial rate is approximately 175 beats per minute.

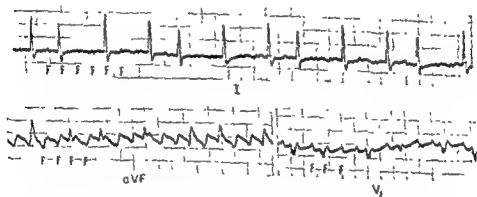


Fig 470 — Atrial flutter (F) with predominantly 2:1 and 3:1 atrioventricular response.

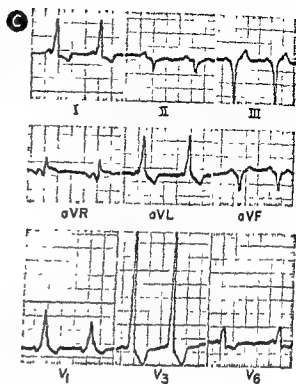
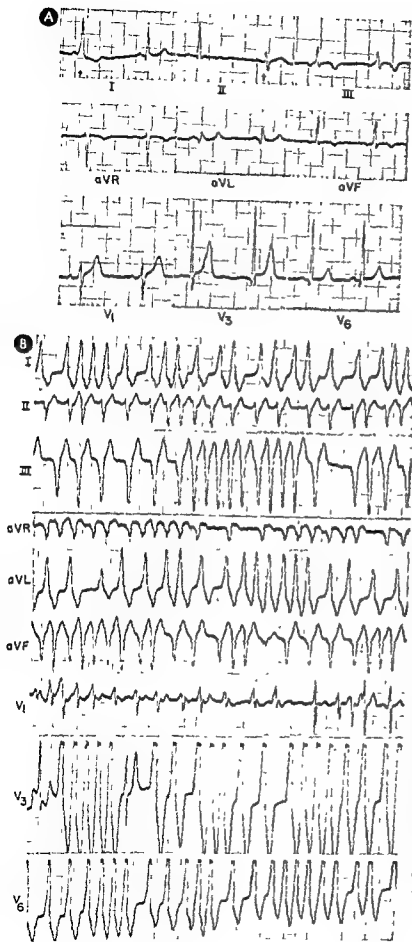


Fig. 471.—Wolf-Parkinson-White syndrome and rapid atrial fibrillation mimicking ventricular tachycardia. Electrocardiogram A shows a sinus rhythm with predominantly normal intraventricular conduction. However, the first ventricular complex in lead I shows a short P-R interval, a slurred upstroke of the R wave (delta wave indicated by an arrow), and an inverted T wave, while the second QRS deflection in lead II shows a minute embryonic R wave followed by the main upward component of the QRS deflection. These two findings, particularly the former, are strongly suggestive of intermittent ventricular pre-excitation. Electrocardiogram B was recorded from the same patient about 8 months later. At first glance, the rapid ventricular rate, the widened, bizarre QRS deflections, and the marked secondary ST-T changes would all suggest ventricular tachycardia if one were not aware of the findings in record A. However, the marked irregularity of the ventricular rhythm in B, the marked slurring of the early part of the upstroke of the R waves in leads I, aVL, V₁, V₄, and V₆, and the corresponding slurring of the downstroke of the QRS deflections in leads III, aVR, and aVF suggest the possibility that the rhythm represents atrial fibrillation with rapid ventricular response and ventricular aberration due to pre-excitation. Electrocardiogram C, recorded from the same patient after conversion of the atrial fibrillation to sinus rhythm, shows a typical example of Group A ventricular pre-excitation.

Bibliography

Childs, J. A., Burch, G. E., and Cronvich, J. A. Validity of equilateral tetrahedron as a spatial reference system, *Circulation* 2 122, 1950

Childs, J. A., Jackson, C. E., Burch, G. E., and Cronvich, J. A. Spatial vectorcardiogram in right bundle branch block, *Circulation* 3 600, 1951

Armbrust, C. A., Jr., and Levine, S. A. Paroxysmal ventricular tachycardia. A study of 107 cases, *Circulation* 1 28, 1950

Asman, R., and Byer, E. The normal human ventricular gradient I and II, *Am Heart J* 25 18, 38, 1943

Barker, J. M. *The Unipolar Electrocardiogram. A Clinical Interpretation* (New York: Appleton-Century-Crofts, Inc., 1952)

Barker, J. M., and Valencia, F. The precordial electrocardiogram in incomplete right bundle branch block, *Am Heart J* 38 378, 1949

Barker, P. S., Macleod, A. G., and Alexander, J. The excitatory process observed in the exposed human heart, *Am Heart J* 5 720, 1930

Barker, P. S., Wilson, F. N., Johnston, P. D., and Wishart, S. W. Auricular paroxysmal tachycardia with auriculo-ventricular block, *Am Heart J* 25 765, 1943

Bayley, R. H. The significance of the duration of Q3 with respect to coronary disease, *Am Heart J* 18 308, 1939

Bayley, R. H., and La Due, J. S. Electrocardiographic changes of impending infarction, and the ischemia-injury pattern produced in the dog by total and subtotal occlusion of a coronary artery, *Am Heart J* 28 54, 1944

Bazett, H. C. An analysis of the time relations of the electrocardiogram, *Heart* 7 353, 1918

Becker, R. A., Scher, A. M., and Erickson, R. D. Ventricular excitation in experimental left bundle branch block, *Am Heart J* 55 547, 1958

Bellet, S. *Clinical Disorders of the Heart Beat* (Philadelphia: Lea & Febiger 1951)

Bellet, S. Symposium on electrocardiography and vectorcardiography. The electrocardiogram in electrolyte imbalance. *AMA Arch Int Med* 96 618, 1955

Berliner, K., and Huppert, V. F. Benign ventricular premature beats, *Tr Am Heart A*, 1953

Burch, G. Anoxemia and exercise tests in the diagnosis of coronary disease, *Am Heart J* 32 889, 1946

Burck, C., Axen, O., Krook, H., Andrén, L., and Wolff, H. B. Studies in mitral stenosis, *Am Heart J* 45, 23, 1953

Blinder, H., Burstein, J., and Smolin, R. Drug effects in Wolff-Parkinson-White syndrome, *Am Heart J* 41, 268, 1952

Blumgart, H. L. The nature of auricular fibrillation and flutter. A symposium. Introduction, *Circulation* 7, 591, 1953

Bowen, W. J. Effect of digoxin upon rate of shortening of myosin B threads, *Fed. Proc.* 11:16, 1952. (Abstract.)

Boyer, P. K., and Poindexter, C. A. Influence of digitalis on electrolyte and water balance of heart muscle, *Am Heart J* 20 558, 1940

Braunwald, E., Donoso, E., Sapin, S. O., and Grishman, A. Hemodynamic, vectorcardiographic and electrocardiographic observations in right bundle branch block, *Proc. 25th Sc Sess Am Heart A*, Oct. 22-24, 1953 (New Orleans).

Braunwald, E., Donoso, E., Sapin, S. O., and Grishman, A. Right bundle branch block. Hemodynamic, vectorcardiographic and electrocardiographic observations, *Circulation* 13 668, 1956

Braunwald, E., Donoso, E., Sapin, S. O., and Grishman, A. A study of the electrocardiogram and vectorcardiogram in congenital heart disease, *Am Heart J* 50 591, 674, 823, 1955

Bremer, E. M., and Hillmuth, J. A. The electrocardiographic diagnosis of chronic cor pulmonale, *Tr. Am. Coll. Cardiol.* 7:120, 1957

Brill, I. C. Etiology and treatment of auricular fibrillation and auricular flutter, *Mod Concepts Cardiovas. Dis.*, vol 8, no 3, March, 1937.

Brill, S. A., and Blondeau, M. The spatial ventricular gradient, *Proc 25th Sc. Sess. Am. Heart A*, Oct. 22-24, 1953 (New Orleans).

Brill, S. A., Marchand, N., and Kossman, C. E. An electronic analogue computer for the automatic determination of the ventricular gradient in man, *Proc. 2d*

- World Cong. Cardiol. and 27th Sc. Sess. Am Heart A., 1954 (Washington, D.C.).
- Brody, D. A.: The meaning of lead vectors and the Burger triangle, *Am Heart J.* 48:730, 1954.
- Brody, D. A., and Romans, W. E.: A model which demonstrates the quantitative relationship between the electromotive forces of the heart and the extremity leads, *Am Heart J.* 45:263, 1953.
- Broomer, R. A., Jr., Estes, E. H., Jr., and Orgain, E. S.: Effects of digitoxin upon the twelve lead electrocardiogram, *Am. J. Med.* 21:237, 1956.
- Brown, H. H., and Acheson, G. H.: Aconitine-induced auricular arrhythmias and their relation to circus-movement flutter, *Circulation* 6:529, 1952.
- Burch, G. E.: An electrocardiographic syndrome characterized by absence of Q in leads I, V₁ and V₂, *Am Heart J.* 51:487, 1956.
- Burch, G. E., Abildskov, J. A., and Cronvich, J. A.: *Spatial Vectorcardiography* (Philadelphia: Lea & Febiger, 1953).
- Burch, G. E., Abildskov, J. A., and Cronvich, J. A.: A study of the spatial vectorcardiogram of the ventricular gradient, *Circulation* 9:267, 1954.
- Burch, G. E., Horan, L., Abildskov, J. A., and Cronvich, J. A.: A study of the spatial vectorcardiogram in subjects with posterior myocardial infarction, *Circulation* 12:418, 1955.
- Burchell, H. B., Essex, H. E., and Pruitt, R. D.: Studies on the spread of excitation through the ventricular myocardium II. The ventricular septum, *Circulation* 6:161, 1952.
- Burger, H. C., and van Milaan, J. B.: Heart vector and leads I, II, and III, *Brit Heart J.* 8:157, 1948, 9:154, 1947, 10:229, 1948.
- Burrows, B. A., and Sisson, J. H.: Measurement of total body potassium by radiisotope dilution technique, *J. Clin Invest* 29:801, 1950 (Abstract).
- Burstein, S. G., Bennett, L. L., Payne, F. E., and Hopper, J.: Effects of potassium and lanatoside-C in the failing heart in heart-lung preparations, *Fed Proc* 8:20, 1949. (Abstract).
- Cabrera, E., Garcia-Font, R., Gaxiola, A., and Pileggi, F.: Vectorcardiogram of ventricular activation in chronic coronary heart disease, *Am Heart J.* 55:557, 1958.
- Cabrera, E. C., and Monroy, J. R.: Systolic and diastolic loading of the heart I Physiological and clinical data, *Am Heart J.* 43:601, 1952.
- Calhoun, J. A., Cullen, C. E., Clarke, G., and Harrison, T. R.: Studies in congestive heart failure Effect of overwork and other factors on potassium content of cardiac muscle, *J. Clin Invest* 10:393, 1930.
- Calhoun, J. A., and Harrison, T. R.: Studies in congestive heart failure Effect of digitalis on potassium content of cardiac muscle of dogs, *J. Clin Invest* 10:139, 1931.
- Chapman, M. C., and Pearce, M. L.: Electrocardiographic diagnosis of myocardial infarction in the presence of left bundle branch block, *Circulation* 16:558, 1957.
- Clarke, N. E., and Mosher, H. E.: Water and electrolyte content of human heart in congestive heart failure with and without digitalization, *Circulation* 5:907, 1952.
- Cohen, B. M.: Digitalis poisoning and its treatment, *New England J Med* 246:225, 1952.
- Conway, J. P., Cronvich, J. A., and Burch, G. E.: Observations on the spatial vectorcardiogram in man, *Am Heart J.* 38:537, 1949.
- Cosby, R. S.; Levmon, D. C.; Zinn, W. J.; Dimittroff, S. P.; and Gruffith, G. C.: Congenital heart disease. An analysis of electrocardiographic patterns in forty-four patients with elevated right ventricular pressure, *Am Heart J.* 44:581, 1952.
- Criteria Committee of the New York Heart Association. *Nomenclature and Criteria for Diagnosis of Diseases of the Heart and Blood Vessels* (5th ed.; New York: Heart Association, 1953).
- Cudkowicz, L., and Armstrong, J. B.: Bronchial arteries in pulmonary emphysema, *Thorax* 8:46, 1953.
- Curtis, H. J., and Cole, K. S.: Membrane resting and action potentials of the squid giant axon, *Am. J. Physiol.* 133:254, 1941.
- Dahl, J. C., and Simonson, E.: Spatial vector analysis of early right ventricular preponderance, *Am Heart J.* 45:841, 1953.
- Decherd, C. M., Jr., Herrmann, G. R., and Schwab, E. H.: Paroxysmal supraventricular tachycardia with auroculoventricular block, *Am Heart J.* 28:446, 1943.
- Deeds, D., and Barnes, A. H.: The characteristics of the chest lead electrocardiograms of 100 normal adults, *Am Heart J.* 20:261, 1940.
- DenBoer, W.: *Vectorcardiographie* (Utrecht thesis, Rijks Universiteit, 1951).
- Dexter, L., Lewis, B. M., Haynes, F. W., Gorlin, R., and Housay, H. E. J.: Chronic cor pulmonale without hypoxia, *Bull. New England M Center* 14:69, 1952.
- Dimond, E. G.: *Electrocardiography* (St Louis: C. V. Mosby Company, 1954).
- Dix, H. H.: Various mechanisms in reciprocal rhythm, *Am Heart J.* 41:448, 1951.
- Dodge, H. T., and Grant, H. P.: Mechanisms of QRS complex prolongation in man Right ventricular conduction defects, *Am J Med* 21:534, 1956.
- Donoso, E.; Jick, S.; Braunwald, E.; Lamelas, M., and Grishman, A.: The spatial vectorcardiogram in mitral valve disease, *Am Heart J.* 53:760, 1957.
- Donoso, E., Sapin, S. O., Braunwald, E.; and Grishman, A.: A study of the electrocardiogram and vectorcardiogram in congenital heart disease II Vectorcardiographic criteria for ventricular hypertrophy, *Am Heart J.* 50:674, 1955.
- Donzelot, E., Methanu, C., and Durand, M.: Les hypertrophies ventriculaires droites dans les cardiopathies congénitales Essai de classification physiopathologique des modifications électrocardiographiques, *Arch mal. cœur* 45:97, 1952.
- Duchosal, P. W., and Grosgrun, J. R.: The spatial vectorcardiogram obtained by use of a trihedron and its scalar comparisons, *Circulation* 11:237, 1952.
- Duchosal, P. W., and Sulzer, R.: *La vectocardiographie* (Basel: S. Karger AG, 1949).
- Durrer, D., van der Tweel, L. H., and Blickman, J. H.: Spread of activation in the left ventricular wall of the dog III Transmural and intramural analysis, *Am Heart J.* 48:13, 1954.
- Einthoven, W., Fahr, G., and DeWaart, A.: Ueber die Richtung und die manifeste Groesse der Potentialschwankungen im menschlichen Herzen und ueber den Einfluss der Herzlage auf die Form des Elektrokardiogramme, *Arch ges Physiol* 150:275, 1913.

- Eli, S. R., Allenstein, B. J., and Griffith, C. C. The direct spatial vectorcardiogram in the infant. *Am. Heart J.* 47:369, 1954.
- Eli, S. R., Allenstein, B. J., Kornbluth, A. W., Griffith, C. C., and Levinson, D. C. The spatial vectorcardiogram in myocardial infarction typified by prominent R waves in leads aVR and V₁. *Am. Heart J.* 47:477, 1954.
- Elkington, J. R., Taras, R., and Peters, J. P. Transfers of potassium in renal insufficiency. *J. Clin. Invest.* 38:378, 1949.
- Elkington, J. R., and Taffel, M. Prolonged water deprivation in the dog. *J. Clin. Invest.* 21:787, 1942.
- Fehr, G. An analysis of the spread of the excitation wave in the human ventricle. *Arch. Int. Med.* 23:148, 1920.
- Fell, H. S., and Gilder, M. D. Regularity of simple paroxysmal tachycardia. *Heart* 8:1, 1921.
- Finn, S. B., Bayley, R. H., and Bedford, D. R. Perturbation block. Electrocardiographic abnormality occasionally resembling bundle branch block and local ventricular block of other types. *Circulation* 2:31, 1930.
- Fulman, A. P., and Richards, D. W. The management of cor pulmonale in chronic pulmonary disease with particular reference to the associated disturbances in the pulmonary circulation. *Am. Heart J.* 52:149, 1956.
- Fowler, N. O., and Helm, R. A. The spatial angle between the long axis of the QRS loop and the longitudinal axis of the ventricles. *Am. Heart J.* 48:621, 1953.
- Fowler, N. O., and Helm, R. A. The spatial QRS loop in right ventricular hypertrophy with special reference to the dominant R wave. *Circulation* 7:573, 1953.
- Fox, T. T., and Bobb, A. L. On the mechanism of the electrocardiographic syndrome of short PR interval with prolonged QRS complex. *Am. Heart J.* 28:311, 1944.
- Frank, E. Absolute quantitative comparison of instantaneous QRS equipotentials on a normal subject with dipole potentials on a homogeneous torso model. *Circulation* 11:243, 1955.
- Frank, E. An accurate clinically practical system for spatial vectorcardiography. *Circulation* 13:736, 1956.
- Frank, E. A comparative analysis of the eccentric double-layer representation of the human heart. *Am. Heart J.* 44:106, 1952.
- Frank, E. A direct experimental study of three systems of spatial vectorcardiography. *Circulation* 10:101, 1954.
- Frank, E. The image surface of a homogeneous torso. *Am. Heart J.* 47:757, 1954.
- Frank, E., and Kay, C. F. Frontal plane studies of homogeneous torso models. *Circulation* 9:724, 1954.
- Frau, G., Maggi, G. C., and Agostoni, A. An experimental study of AV conduction over fibers of the bundle of Kent. *Am. Heart J.* 8:775, 1953.
- Friedlander, R. D. and Butler, R. *Am. Heart J.* 1954.
- Friedman, M. St. *Am. Heart J.* 1954.
- Garcia Ramos, J., and Rosenbaum, M. The self-sustained activity in the isolated auricular muscle of mammals. *Arch. Inst. Cardiol. Mexico* 27:302, 1947.
- Gardberg, W. *Clinical Electrocardiography: Interpretation on a Physiologic Basis* (New York: Paul B. Hoeber, Inc., 1957).
- Gelland, D., and the presence with the spa. *Am. Heart J.* 1954.
- Glenister, D. L., and the cardiac conduction system in singularities, *Am. Heart J.* 20:389, 1954.
- Glenister, D. L., and the cardiac conduction system in singularities, *Am. Heart J.* 20:389, 1954.
- Goldberger, M. *Clinical Electrocardiography: Interpretation on a Physiologic Basis* (New York: Paul B. Hoeber, Inc., 1957).
- Goldberger, M., Lado, P., Roth, P. H., and Scherf, D. Changes of ventricular impulse formation during carotid sinus pressure in man. *Circulation* 10:735, 1954.
- Goldman, J. P. The electrocardiogram in normal children and in children with right ventricular hypertrophy. *Brit. Heart J.* 14:173, 1952.
- Gorlin, R., Lewis, D. M., Haynes, F. W., and Diller, L. Studies of the circulatory dynamics at rest in mitral valvular regurgitation with and without stenosis. *Am. Heart J.* 13:757, 1952.
- Grant, R. P., and Dodge, H. T. Mechanisms of QRS complex prolongation in man. Left ventricular conduction disturbances. *Am. J. Med.* 20:834, 1956.
- Grant, R. P., and Estes, E. H., Jr. *Spatial Vector Electrocardiography* (New York: Blakiston Company, 1951).
- Grant, R. P., Estes, E. H., and Doyle, J. T. Spatial vector electrocardiography. The clinical characteristics of S-T and T vectors. *Circulation* 3:152, 1951.
- Grant, R. P., and Murray, H. H. The QRS complex deformity of myocardial infarction in the human subject. *Am. J. Med.* 17:587, 1954.
- Grant, R. P., Sanders, R. J., Morrow, A. G., and Braunwald, E. Symposium on diagnostic methods in the study of left-to-right shunts. *Circulation* 16:791, 1957.

- Grishman, A.: *Lectures on Vectorcardiography*, presented at the Mount Sinai Hospital, New York, March, 1955.
- Grishman, A.: Spatial vectorcardiography, in W. Dock and I. Snapper: *Advances in Internal Medicine* (Chicago Year Book Publishers, Inc., 1954), vol. 6, pp. 91-131.
- Grishman, A., Borun, E. R.; and Jaffe, H. L.: Spatial vectorcardiography. Technique for the simultaneous recording of the frontal, sagittal and horizontal projections: I, *Am. Heart J.* 41:483, 1951.
- Grishman, A., and Scherlis, L.: *Spatial Vectorcardiography* (Philadelphia: W. B. Saunders Company, 1952).
- Grishman, A., Scherlis, L.; and Lasser, R. P.: Spatial vectorcardiography (review), *Am. J. Med.* 15:184, 1953.
- Hagen, P. S.: Effects of digitalin C in varying dosage on heart muscle, *Circulation* 14:265, 1956.
- Hecht, H. H.: The mechanism of auricular fibrillation and flutter, *Circulation* 7:594, 1953.
- Helm, R. A.: Theory of vectorcardiography. A review of fundamental concepts, *Am. Heart J.* 49:135, 1955.
- Helm, R. A.: The vectorcardiographic derivation of scalar leads, *Am. Heart J.* 48:519, 1953.
- Helm, R. A., and Fowler, N. O., Jr.: A simplified method for determining the angle between two spatial vectors, *Am. Heart J.* 45:835, 1953.
- Herrmann, W. F.: potassium patterns in anemia and oliguria, *Ann. Int. Med.* 38:933, 1953.
- Horan, L. G., Burch, G. E., Abildskov, J. A., and Cronvich, J. A.: The spatial vectorcardiogram in left ventricular hypertrophy, *Circulation* 10:728, 1954.
- Horvath, I., Kiraly, C., and Szerb, J.: Action of cardiac glycosides on the polymerization of actin, *Nature, London* 164:792, 1949.
- Howell, W. H.: Vagus inhibition of the heart in its relation to the inorganic salts of the blood, *Am. J. Physiol.* 15:280, 1906.
- Hurst, H. W., and Woodson, G. C., Jr.: *Atlas of Spatial Vector Electrocardiography* (New York: Blakiston Company, Inc., 1952).
- Johnson, J. B., Ferrer, M. I., West, J. R., and Courmand, A.: The relation between electrocardiographic evidence of right ventricular hypertrophy and pulmonary arterial pressures in patients with chronic pulmonary disease, *Circulation* 1:536, 1950.
- Johnston, F. D., Ryan, J. M., and Bryant, J. M.: The electrocardiogram and the position of the heart, *Am. Heart J.* 43:306, 1952.
- Karlen, W. S., and Wolff, L.: The vectorcardiogram in pulmonary embolism II, *Am. Heart J.* 51:839, 1956.
- Karlen, W. S., Wolff, L., and Young, E.: The vectorcardiogram in anterior myocardial infarction III, *Am. Heart J.* 52:45, 1956.
- Katz, L. N.: *Electrocardiography* (2d ed., Philadelphia: Lea & Febiger, 1916).
- Katz, L. N., and Pick, A.: *Clinical Electrocardiography The Arrhythmias* (Philadelphia: Lea & Febiger, 1956).
- Katz, L. N., and Pick, A.: The mechanism of auricular flutter and auricular fibrillation, *Circulation* 7:60, 1953).
- Kenamer, R., and Prinzmetal, M.: Depolarization of the ventricle with bundle branch block: X. Studies on the mechanism of ventricular activity, *Am. Heart J.* 47:76, 1954.
- Kent, A. F. S.: Illustrations of right lateral auriculoventricular junction in heart, *Proc. Physiol. Soc. London* 48:63, 1941.
- Kilpatrick, J. A.: Electrocardiographic changes in chronic pulmonary, *Brit. Heart J.* 13:309, 1951.
- Kissane, R. W., Brooks, R., and Clark, T. E.: Relation of supraventricular paroxysmal tachycardia to heart disease and the basal metabolism rate, *Circulation* 1:95, 1950.
- Kjellberg, S. R., Mannheimer, E.; Rudhe, U., and Jonsson, G.: Effects of myocardial and pericardial injury, *Bull. New York Acad. Med.* 28:61, 1952.
- Kossmann, C. E.: The normal electrocardiogram, *Circulation* 8:920, 1953.
- Kossmann, C. E., Berger, A. R., Rader, H., Brumlik, J., Briller, S. A., and Donnelly, J. H.: Intracardiac and intravascular potentials resulting from electrical activation of atrioventricular excitation, *Am. Heart J.* 33:308, 1947.
- Kossmann, C. E., and Johnston, F. D.: The precordial electrocardiogram I. The potential variations of the precordium and of the extremities in normal subjects, *Am. Heart J.* 10:925, 1935.
- Lamb, L. E., and Diamond, E. G.: The spatial vectorcardiogram during the first decade of life, *Am. Heart J.* 44:174, 1952.
- Landman, B.: Postoperative changes in the electrocardiogram in congenital heart disease II. Coarctation of the aorta and patent ductus arteriosus, *Circulation* 10:871, 1954.
- Langendorf, R.: Aberrant ventricular conduction, *Am. Heart J.* 41:700, 1951.
- Langendorf, R.: Concealed A-V conduction. The effect of blocked impulses on the formation and conduction of subsequent impulses, *Am. Heart J.* 35:542, 1948.
- Langendorf, R., and Pick, A.: Concealed conduction. Further evaluation of a fundamental aspect of propagation of the cardiac impulse, *Circulation* 13:381, 1956.
- Langendorf, R., and Pick, A.: Mechanisms of intermittent ventricular bigeminy II. Parasympole, and parasympole or re-entry with conduction disturbance, *Circulation* 11:431, 1955.
- Langendorf, R., Pick, A., and Winterhutz, M.: Mechanisms of intermittent ventricular bigeminy I. Appearance of ectopic beats dependent upon length of the ventricular cycle, the "rule of bigeminy," *Circulation* 11:422, 1955.
- Langner, P. H., Jr.: An octaxial reference system derived from a nonequilateral triangle for frontal plane vectorcardiography, *Am. Heart J.* 49:696, 1955.
- Langner, P. H., Jr., and Atkins, J. P.: Intrabronchial electrocardiography, *Circulation* 2:419, 1950.

- Langner, P. H., Jr., Dewees, E. J., and Moore, S. R.: A critical and comparative analysis of methods in electrocardiography employing mean QRS and T vectors, *Am. Heart J.* 46:455, 1953.
- Lasser, R. P., Borun, E. R., and Grishman, A.: Spatial vectorcardiography: VII. Right ventricular hypertrophy as seen in congenital heart disease, *Am. Heart J.* 42:370, 1951.
- Lasser, R. P., and Grishman, A.: Spatial vectorcardiography: VIII. Right bundle branch block, *Am. Heart J.* 42:513, 1951.
- Lasser, R. P., and Grishman, A.: Spatial vectorcardiography: children. An analysis of high R waves in right-
1. The
& Wil-
- Lepeschkin, E.: The U wave of the electrocardiogram, *AMA Arch. Int. Med.* 98:600, 1953.
- Levine, H. D., Lown, B., and Streeter, W. B.: Clinical significance of postextrasystolic T wave changes, *Circulation* 6:538, 1952.
- Levine, H. D., Vaziridar, J. P., Lown, B., and Merrill, J. P.: "Tent-shaped" T waves of normal amplitude in potassium intoxication, *Am. Heart J.* 43:437, 1952.
- Levine, S. A.: *Clinical Heart Disease* (5th ed., Philadelphia: W. B. Saunders Company, 1958).
- Levy, R. L., Williams, N. E., Bruenn, H. G., and Carr, A. A.: The "anoxemia test" in the diagnosis of coronary insufficiency, *Am. Heart J.* 21:634, 1941.
- Lewis, B. M., Corlin, R., Housay, H. E. J., Haynes, P. W., and Dexter, L. V.: Clinical and physiological correlation in patients with mitral stenosis, *Am. Heart J.* 19:105, 1929.
1. The
1. The
ion of
the Heart Beat (3d ed., London: Shaw & Sons, Ltd., 1925).
- Lewis, T.: Observations upon flutter and fibrillation, *Heart* 7:127, 293, 1918-20.
- Lewis, T., Drury, A. M., and Iliescu, C. C.: A demonstration of circus movement in clinical fibrillation of the auricles, *Heart* 8:381, 1921.
- Lewis, T., and Master, A. M.: Observations upon conduction in the mammalian heart: AV conduction, *Heart* 12:209, 1928.
- Lewis, T., and Rothschild, M. A.: The excitatory process in the dog's heart: II. The ventricles, *Phil. Tr. Roy. Soc.* 206:B:181, 1915.
- Limon, L. R., Esclavissat, M., Puech, P., De La Cruz, M. V., Rubio, V., Bouchard, F., and Soni, J.: El cateterismo intracardiaco: V. La comunicación interauricular. Correlación de los hallazgos hemodinámicos con los datos embriológicos, clínicos, radiológicos y electrocardiográficos en 50 casos, *Arch. Inst. Cardiol. México* 23:279, 1953.
- Lipman, H. S., and Masue, E.: *Clinical Unipolar Electrocardiography* (4th ed., Chicago: Year Book Publishers, Inc., 1959).
- Lipsett, M. B., and Zinn, W. J.: Anatomical and electrocardiographic correlation in combined ventricular hypertrophy, *Am. Heart J.* 45:68, 1953.
- Love, W. D.: The basis of quinidine therapy, *Am. J. Med. Sc.* 229:69, 1955.
- Love, W. S.: The effect of quinidine and strophanthidin upon the refractory period of the tortoise ventricle, *J. Pharmacol.* 1922.
- Lo
- Lown, B., and Levine, S. A.: Current concepts in digitalis therapy, *New England J. Med.* 230:819, 1954.
- Lown, B., and Levine, S. A.: Current concepts in digitalis therapy (Boston: Little, Brown & Company, 1954).
- Lown, B., Waller, J. M., Wyatt, N., Haigne, R., and Merrill, J. P.: Effects of alterations of body potassium in digitalis toxicity, *J. Clin. Invest.* 32:107, 1953.
- Lown, B., Wyatt, N., and Levine, S. A.: Tassium in auricular arrhythmias, *Am. Heart J.* 46:107, 1953.
- Lo
- Lo
- Lo
- Lo
- Mack, I., and Snider, G. L.: Respiratory insufficiency and chronic cor pulmonale, *Circulation* 13:419, 1950.
- Mahnow, M. R., and Langendorf, R.: Different mechanisms of fusion beats, *Am. Heart J.* 35:148, 1948.
- Mallov, S., and Robb, J. S.: Behavior of actomyosin
27:383, 1952.
- Mann, H. H., and Burchell, H. H.: The significance of T-wave inversion in sinus beats following ventricular extrasystoles, *Am. Heart J.* 47:504, 1954.
- Mansco, F., Penabaza, D., Tranchesi, J., Limon, R., and Sodi-Pallares, D.: The electrocardiogram in ventricular septal defect: Scalar and vector analysis of 32 cases, *Am. Heart J.* 49:188, 1955.
- Master, A. M., Nuzzi, E. S., Brown, B. C., and Parker, R. C., Jr.: Electrocardiogram and "two-step" exercise. A test of cardiac function and coronary insufficiency, *Am. J. Med. Sc.* 207:435, 1946.
- Master, A. M., Friedman, R., and Dack, S.: The electrocardiogram after standard exercise as a functional test of the heart, *Am. Heart J.* 24:777, 1942.
- de Melo, H. K.: Aspectos normais das derivações unipolares das extremidades, *Arq. bras. cardiol.* 1:237, 1948.
- Merrill, J. P., Levine, H. D., Somerville, W., and Smith, S.: Clinical recognition and treatment of acute potassium intoxication, *Ann. Int. Med.* 33:797, 1950.
- Metzner, C., Durand, M., and Dauzier, G.: L'electrocardiogramme dans la coarctation de l'aorte. Étude de 41 cas, *Cardiologia* 23:274, 1953.
- Muller, R., and Sharrett, R. H.: Interference dissociation, *Circulation* 16:603, 1957.

- Milnor, W. R.: Electrocardiogram and vectorcardiogram in right ventricular hypertrophy and right bundle branch block, *Circulation* 16:348, 1957.
- Milnor, W. R.: The normal vectorcardiogram and a system for the classification of vectorcardiographic abnormalities, *Circulation* 16:95, 1957.
- Milnor, W. R., and Bertrand, C. A.: The electrocardiogram in atrial septal defect. A study of 24 cases, with observations on the RSR'-V₁ pattern, *Am J. Med.* 22: 223, 1957.
- Milnor, W. R., Genecin, A., Talbot, S. A., and Newman, E. V.: A vectorcardiographic study of the "Q3" deflection in cases of myocardial infarction and in normal subjects, *Bull. Johns Hopkins Hosp.* 89:281, 1951.
- Milnor, W. R.; Talbot, S. A., and Newman, E. V.: A study of the relationship between unipolar leads and spatial vectorcardiograms, using the panoramic vectorcardiograph, *Circulation* 7:545, 1953.
- Miguel, C., Sodi-Pallares, D., Chencro, F., Pileggi, F., Medrano, G. A.; and Bisteni, A.: Right bundle branch block and right ventricular hypertrophy. Electrocardiographic and vectorcardiographic diagnosis, *Am J. Cardiol* 1:57, 1958.
- Morgan, A. D.: Pathology of subacute cor pulmonale in diffuse carcinomatosis of the lungs, *J. Path. & Bact.* 61. 75, 1949.
- Morris, T. L., and Whitaker, W.: The ventricular pattern in the right precordial leads in mitral stenosis, *Am Heart J* 52:738, 1956.
- Mounsey, J. W. D.: Emphysema heart disease, *Brit J. Tuberc.* 48:63, 1954.
- Myers, G. B. II.: The form of the QRS complex in bundle branch block and in anterolateral infarction, *Am Heart J* 39:817, 1950.
- Myers, G. B., Klein, H. A., and Hiratzka, T.: III. Correlation of electrocardiographic and pathologic findings in anteroposterior infarction, *Am Heart J* 37:205, 1949.
- Myers, G. B., Klein, H. A., and Hiratzka, T.: IV. Correlation of electrocardiographic and pathologic findings in infarction of the interventricular septum and right ventricle, *Am Heart J* 37:720, 1949.
- Myers, G. B., Klein, H. A., and Hiratzka, T.: II. Correlation of electrocardiographic and pathologic findings in large anterolateral infarcts, *Am Heart J* 36:838, 1948.
- Myers, G. B., Klein, H. A., and Stofer, B. E.: I. Correlation of electrocardiographic and pathologic findings in anteroapical infarction, *Am Heart J* 36:535, 1948.
- Myers, G. B., Klein, H. A., and Stofer, B. E.: VII. Correlation of electrocardiographic and pathologic findings in lateral infarction, *Am Heart J* 37:374, 1949.
- Myers, G. B., Klein, H. A., and Stofer, B. E.: The electrocardiographic diagnosis of right ventricular hypertrophy, *Am Heart J* 35:1, 1948.
- Myers, G. B., Klein, H. A., Stofer, B. E., and Hiratzka, T.: Normal variations in multiple precordial leads, *Am Heart J* 34:785, 1947.
- Nadler, C. S.: Recent advances in potassium metabolism, *Am J. M. Sc.* 226:88, 1953.
- Nastuk, W. L., and Hodgkin, A. L.: Electrical activity of single muscle fibers, *J. Cell and Comp. Physiol.* 35:39, 1950.
- Newburgh, L. H., and Leap, A.: *Significance of the Body Fluids in Clinical Medicine* (Springfield, Ill.: Charles C. Thomas, Publisher, 1950).
- Nyboer, J.: The ECG in practical risk appraisal, *Med. Section, Am. Life Convention, 34th Annual Meeting, 1946*, pp. 87-98.
- Oglesby, P.; Myers, G. S., and Campbell, J. A.: The electrocardiogram in congenital heart disease, *Circulation* 3:564, 1951.
- Ohnell, R. F.: Post-mortem examination and clinical report of a case of the short PR interval and wide QRS wave syndrome (WPW), *Cardiology* 4:249, 1940.
- Ohnell, R. F.: *Pre-excitation—A Cardiac Abnormality* (Stockholm: P. A. Norstedt & Soner, 1944); and *Acta med. Scandinav. supp.* 152, 1944.
- Orgain, E. S., Wolff, L., and White, P. D.: Uncomplicated auricular fibrillation and auricular flutter, frequent occurrence and good prognosis in patients without other evidence of cardiac disease, *Arch. Int. Med.* 57: 493, 1936.
- J. 14:451, 1952
- Papp, C., and Smith, K. S.: The changing electrocardiogram in Wilson block, *Circulation* 11:53, 1955.
- Parker, B. M., and Smith, J. R.: Pulmonary embolism and infarction, *Am J. Med.* 24:402, 1958.
- Parkinson, J., and Bedford, D. E.: The course and treatment of auricular flutter, *Quart. J. Med.* 21:21, 1927.
- Parkinson, J., and Hoyle, C.: The heart in emphysema, *Quart. J. Med.* 6:59, 1937.
- Pearce, M. L., and Chapman, M. G.: Evaluation of Q₁ by the initial sagittal QRS vectors in seventy autopsy cases, *Am. Heart J.* 53:782, 1957.
- Penalosa, D., and Tranchesi, J.: The three main vectors of the ventricular activation process in the normal human heart. I. Its significance, *Am Heart J* 49:51, 1955.
- Pick, A.: Aberrant ventricular conduction of escaped beats. Preferential and accessory pathway in the A-V junction, *Circulation* 13:702, 1956.
- Pick, A.: Digitals and the electrocardiogram, *Circulation* 15:603, 1957.
- Pick, A.: Parasympathetic, *Circulation* 8:243, 1953.
- Pick, A., and Katz, L. N.: Disturbances of impulse formation and conduction in the pre-excitation (WPW) syndrome: Their bearing on its mechanism, *Am J. Med.* 19:759, 1955.
- Pick, A., Langendorf, R., and Katz, L. N.: Depression of cardiac pacemakers by premature impulses, *Am Heart J* 41:49, 1951.
- Prinzmetal, M.: The mechanism of spontaneous auricular flutter and fibrillation in man, *Circulation* 7:607, 1953.
- Prinzmetal, M., Corday, E., Brill, I. C., Oblath, R. W., and Kruger, H. E.: *The Auricular Arrhythmias* (Springfield, Ill.: Charles C. Thomas, Publisher, 1952).
- Prinzmetal, M., Kennamer, R., Corday, E., Osborne, J. A., Fields, J., and Smith, L. A.: *Accelerated Conduction The Wolf-Parkinson-White Syndrome and Related Conditions* (New York: Grune & Stratton, Inc., 1952).
- Prinzmetal, M., Shaw, C. M., Jr., Maxwell, M. H., Flamm, E. J., Goldman, A., Kimura, N., Rakita, L., Borduas, J., Rothman, S., and Kennamer, R.: Studies on the mechanism of ventricular activity VI: The depolarization complex in pure subendocardial infarction, role of the subendocardial region in the normal electrocardiogram, *Am J. Med.* 16:469, 1954.

- disease, *Am. Heart J.* 54:161, 1957
- Ruchman, J. L., and Wolff, L.: Left bundle branch block masquerading as right bundle branch block, *Am. Heart J.* 47:383, 1954.
- Ruchman, J. L., and Wolff, L.: The spatial vectorcardiogram normal growth and hypertrophy, *Am. Heart J.* 21:617, 1941
- Rodriguez, M. I., Anselmi, A., and Sodi-Pallares, D.: The effect of digitalis on the spatial vectorcardiogram, *Heart J.* 44:715, 1952
- Rosenbaum, F. F., Hecht, H. H., Wilson, F. N., and Johnston, F. D.: The potential variations of the thorax and the esophagus in anomalous atrioventricular excitation (Wolff-Parkinson-White syndrome), *Am. Heart J.* 48:281, 1945
- Rosenbaum, M. B., and Lepeschkin, E.: The effect of ventricular systole on auricular rhythm in auriculoventricular block, *Circulation* 11:240, 1955
- Rosenbluth, A.: The mechanism of auricular flutter and auricular fibrillation, *Circulation* 7:612, 1953
- Ruskin, A., and Decherd, G. N.: Effect of strophanthine on the spatial vectorcardiogram in relation to digitalis glycosides, with special reference to blood serum, electrocardiogram and ectopic beats, *Am. Heart J.* 28:184, 1943
- Sano, T., Hellerstein, H. K., and Vayda, E.: P vector loop in health and disease as studied by the technique of electric dissection of the vectorcardiogram (differential vectorcardiography), *Proc. 28th Sc. Sess. Am. Heart A.*, Oct. 22-24, 1955 (New Orleans)
- Savilahti, M.: On normal and pathological PQ time of the electrocardiogram, *Acta med. scandinav.* 123:252, 1946
- Schaffer, A. I.: The body as a volume conductor in electrocardiography, *Am. Heart J.* 51:588, 1956
- Schaffer, A. I.: Posture, the manifest heart vector and the volume conductor, *Am. Heart J.* 53:695, 1957
- Schaffer, A. I.: Procaine amide compared with quinidine as a therapy for arrhythmias, *Am. Heart J.* 42:597, 1951
- Schaffer, A. I., and Beinfeld, W. H.: The vectorcardiogram of the newborn infant, *Am. Heart J.* 44:69, 1952
- Schaffer, A. I., Bergmann, P. C., Boyd, L. J., Markinson, A., and Beinfeld, W. H.: Eccentricity as a cause for the difference between the vectorcardiograms registered by the cube and the tetrahedral system, *Am. Heart J.* 45:148, 1953
- Schaffer, A. I., Dix, J. H., and Bergmann, P.: The effect of eccentricity on spatial vector analysis of the electrocardiogram of the newborn infant and on the correlation between the electrocardiogram and the vectorcardiogram, *Am. Heart J.* 43:735, 1952
- Scherf, D.: The atrial arrhythmias, *New England J. Med.* 252:928, 1955
- Scherf, D.: Studies on auricular tachycardia caused by acetonine administration, *Proc. Soc. Exper. Biol. & Med.* 64:233, 1947
- Scherf, D.: Treatment of cardiac arrhythmias, *Circulation* 8:756, 1953
- Scherf, D.; Romano, F. J., and Terranova, R.: Experimental studies on auricular flutter and fibrillation, *Am. Heart J.* 36:241, 1918
- Scherf, D., and Schaffer, A. I.: The electrocardiographic exercise test, *Am. Heart J.* 43:927, 1952
- Scherf, D., Schaffer, A. I., and Blumenfeld, S.: Mechanism of flutter and fibrillation, *A.M.A. Arch. Int. Med.* 91:333, 1953
- Scherf, D., and Schott, A.: *Extrasystoles and Allied Arrhythmias* (New York: Grune & Stratton, Inc., 1953)
- Scherf, D., and Terranova, R.: Mechanism of auricular flutter and fibrillation, *Am. J. Physiol.* 159:137, 1949
- Scherlis, L., Cowley, R. A., Richardson, A., Adams, C., and Love, W. S.: The spatial vectorcardiogram and electrocardiogram in mitral and aortic valvular disease
- Scherlis, L., and Grishman, A.: Spatial vectorcardiography Myocardial infarction: V, *Am. Heart J.* 42:24, 1951
- Schmitt, O. H., Levine, R. B., and Simonson, E.: Electrocardiography and vectorcardiography. The present status of vectorcardiography, *A.M.A. Arch. Int. Med.* 96:575, 1955
- Schreer, V., and Vogelpoel, L.: The clinical and electrocardiographic differentiation of supraventricular and ventricular tachycardia, *Am. Heart J.* 42:24, 1951
- Scott, R. C., Kaplan, S., Fowler, N. O., and Stiles, W. J.: The electrocardiographic pattern of right ventricular hypertrophy in mitral valve disease, *Circulation* 11:761, 1955
- Segers, M., Regnier, M., van Heerswynghe, J., and Hendrick, J.: Le vectorcardiogramme dans les troubles du rythme, *Acta cardiol.* 10:160, 1947
- Sherrod, T. R.: Effects of digitalis on electrolytes of heart muscle, *Proc. Soc. Exper. Biol. & Med.* 65:69, 1947
- Shmagranoff, G. L., and Jick, S.: Simultaneous atrial and nodal tachycardia, *Am. Heart J.* 54:417, 1957

- Silverblatt, M. L., Rosenfeld, I., Grishman, A., and Donoso, E.: The vectorcardiogram and electrocardiogram in interatrial septal defect, *Am. Heart J.* 53:380, 1957.
- Simonson, E., and Berman, R.: Differentiation between paroxysmal auricular tachycardia with partial A-V block and auricular flutter, *Am. Heart J.* 42:387, 1951.
- Smith, C. P., and Welden, J. E.: A clinical study of graphic findings in 15 cases, with special reference given to the electrocardiogram, *Am. Heart J.* 43:481, 1952.
- Sodi-Pallares, D.: *New Bases of Electrocardiography* (St. Louis. C. V. Mosby Company, 1956).
- Sodi-Pallares, D., Bisteni, A., and Herrmann, G. R.: Some views on the significance of QR and QR type complexes in right precordial leads in the absence of myocardial infarction, *Am. Heart J.* 43:710, 1952.
- Sodi-Pallares, D.; Bisteni, A.; Medrano, G. A., and Cusneros, F.: The activation of the free left ventricular wall in the dog's heart, *Am. Heart J.* 49:587, 1955.
- Sodi-Pallares, D., Brancato, R. W., Pileggi, F., Medrano, G. A., Bisteni, A., and Barbato, E.: The ventricular activation and the vectorcardiographic curve, *Am. Heart J.* 54:498, 1957.
- Sodi-Pallares, D., and Marisco, F.: The importance of electrocardiographic patterns in congenital heart disease, *Am. Heart J.* 49:202, 1955.
- Sodi-Pallares, D., and Rodriguez, M. I.: Morphology of the unipolar leads recorded at the septal surfaces: Its application to the diagnosis of left bundle branch block complicated by myocardial infarction, *Am. Heart J.* 43:27, 1953.
- Sodi-Pallares, D., Rodriguez, M. I., Chait, L. O., and Zucherman, R.: The activation of the interventricular septum, *Am. Heart J.* 41:569, 1951.
- Soffe, A. M., Wolff, L., Richman, J. L., Reimer, L., and Mazzoleni, A.: Comparative value of electrocardiographic and vectorcardiographic diagnosis. Pathologic correlation, Second World Cong. Cardiol. and 27th Sc. Sess., *Am. Heart A.* 1954 (Washington, D.C.).
- Sokolow, M.: The present status of therapy of the cardiac arrhythmias with quinidine, *Am. Heart J.* 42:771, 1951.
- Sokolow, M., and Edgar, A. L.: A study of the V leads in congenital heart disease, with particular reference to ventricular hypertrophy and its diagnostic value, *Am. Heart J.* 40:232, 1950.
- Sokolow, M., and Friedlander, H. D.: The normal unipolar precordial and limb lead electrocardiogram, *Am. Heart J.* 38:665, 1949.
- Sokolow, M., Katz, L. N., and Muscovitz, A. N.: Electrocardiogram in pulmonary embolism, *Am. Heart J.* 19:166, 1940.
- Sokolow, M., and Lyon, T. P.: The ventricular complex in left ventricular hypertrophy as obtained by unipolar precordial and limb leads, *Am. Heart J.* 37:161, 1949.
- Sokolow, M., and Lyon, T. P.: The ventricular complex in right ventricular hypertrophy as obtained by unipolar precordial and limb leads, *Am. Heart J.* 38:273, 1949.
- Stern, E. A., and Tenney, S. M.: Correlation of the spatial vectorcardiogram and the electrocardiogram in right ventricular hypertrophy, *Am. Heart J.* 51:53, 1956.
- Stewart, H. J., and Carr, H. A.: The anoxemia test, *Am. Heart J.* 48:293, 1954.
- Stutzman, J. W., and Pettinga, F. L.: Mechanism of cardiac arrhythmias during cyclopropane anesthesia, *Anesthesiology* 10:374, 1919.
- Surawicz, B., and Lepeschkin, E.: The electrocardiographic pattern of hypokalemia with and without hypocalcemia, *Circulation* 8:801, 1953.
- Swann, R. C., and Merrill, J. P.: The clinical course of leads and chest leads, *Am. J. Dis. Child.* 79:449, 1950.
- Szent-Gyorgyi, A.: Contraction in the heart muscle fiber, *Bull. New York Acad. Med.* 28:3, 1952.
- Tarai, R., and Elkinton, J. R.: Potassium deficiency and the role of the kidney in its production, *J. Clin. Invest.* 28:99, 1949.
- Thomas, A. J.: moconious of
- Trounce, J. R.: *Brit. Heart J.* 14:185, 1952.
- Twiss, A., and Sokolow, M.: Angina pectoris. Significant positions in three planes of space, *Am. Heart J.* 44:372, 1952.
- Vaquero, M., Limón, R., and Limón, A.: Electrocardiograma normal: Estudio de 500 casos en derivaciones standard y unipolares, *Mem. 2d Cong. Internat. Cardiol.* 2:887, 1948.
- Vastesaeger, M. M.: Les troubles de la conduction intraventriculaire chez l'homme, *Acta cardiol. supp.* 1, 1946.
- Vazifdar, J. P., and Levine, S. A.: Benign bundle branch block, *A.M.A. Arch. Int. Med.* 89:568, 1952.
- Velasquez, J., and Keiser, G. A., Jr.: Alternating bidirectional tachycardia, *Am. Heart J.* 54:440, 1957.
- Waldman, S., and Peltner, L.: Action of neostigmin in supraventricular tachycardias, *Am. J. Med.* 5:164, 1948 (Abstract).
- Walker, I. C., Jr., Helms, H. A., and Scott, R. C.: Right ventricular hypertrophy I Correlation of isolated right ventricular hypertrophy at autopsy with the electrocardiographic findings, *Circulation* 11:215, 1955. II Correlation of electrocardiographic right ventricular hypertrophy with the anatomic findings, *ibid.* p. 223.
- Walker, W. J., Mattingly, T. W., Pollack, H. E., Carmichael, D. B., Immon, T. W., and Forrester, R. H.: Electrocardiographic and hemodynamic correlation in atrial septal defect, *Am. Heart J.* 52:547, 1956.
- Wedd, A. M.: Influence of digoxin on potassium content of heart muscle, *J. Pharmacol. & Exper. Therap.* 65:268, 1937.
- Wedd, A. M., Blair, H. A., and Casselin, R. E.: The action of quinidine on the cold blooded heart, *J. Pharmacol. & Exper. Therap.* 75:251, 1942.
- Wedd, A. M.; Blair, H. A., and Warner, R. S.: The action of procaine amide on the heart, *Am. Heart J.* 42:399, 1951.
- Wegna, R., Geyer, J. H., and Brown, H. S.: Mechanism

- of ventricular fibrillation after digitalis, *Am J Physiol* 133:453, 1947.
- Wenbert, M. H., and Simonson, E. The diagnostic accuracy of Q3 and related electrocardiographic items for the detection of patients with posterior wall myocardial infarction, *Am Heart J* 50 82, 1955.
- Weller, J. M., Low, B., Hoigne, R. V., Wyatt, N. F.; Cuscinello, M., Merrill, J. P.; and Levine, S. A.: Effects of acute removal of potassium from dogs, *Circulation* 19:100, 1957.
- Wenger, R. A.: The effect of digitalis on the electrocardiogram, *Am Heart J* 44 106, 1953.
- Wessale, R. E., Schless, W. A.; Erlich, I. L., and Chiu, G. C. The effect of digitalis on the electrocardiogram, *Am Heart J* 44 106, 1953.
- Whipple, G. H., Cosio, G., and Levine, H. D. Vectorcardiographic patterns in rheumatic heart disease. Results in 56 autopsied cases (abstract), *Proc 26th Sc. Sess. Am Heart A.*, Oct. 22-24, 1955 (New Orleans), p. 122.
- Wierum, C., and Glenn, F. Electrocardiographic indications of significant mitral insufficiency in patients with mitral valve disease, *Am Heart J* 44 106, 1953.
- Williams, H. B. On the cause of the phase difference frequently observed between homonymous peaks of the electrocardiogram, *Am J Physiol* 35 292, 1914.
- Wilson, F. N., Bryant, J. M., and Johnston, F. D. On the possibility of constructing an Einthoven triangle for a given subject, *Am Heart J* 37 493, 1949.
- Wilson, F. N., and Herrmann, G. R. Relation of QRS-interval to ventricular weight, *Heart* 15 135, 1930.
- Wilson, F. N., and Herrmann, G. R. An experimental study of incomplete bundle branch block and of the refractory period of the heart of the dog, *Heart* 8 229, 1921.
- Wilson, F. N., Johnston, F. D., and Kossmann, C. E. The substitution of a tetrahedron for the Einthoven triangle, *Am Heart J* 33 584, 1947.
- Wilson, F. N., Johnston, F. D., Macleod, A. G., and Barker, P. S. Electrocardiograms that represent the potential variations of a single electrode, *Am Heart J* 9 447, 1934.
- Wilson, F. N., Kossmann, C. E., Burch, G. E., Goldberger, E., Grayhield, A., Hecht, H. H., Johnston, F. D., Lepeschkin, E., and Myers, G. H. (report of Committee on Electrocardiography American Heart Association) Recommendations for standardization of electrocardiographic and vectorcardiographic leads, *Circulation* 10 564, 1954.
- Wilson, F. N., Macleod, A. G., and Barker, P. S. Interpretation of initial deflections of the ventricular complex of the electrocardiogram, *Am Heart J* 6 637, 1933.
- Wilson, F. N., Macleod, A. G., and Barker, P. S. The potential variations produced by the heart beat at the apex of Einthoven's triangle, *Am Heart J* 7 207, 1931.
- Wilson, F. N., Macleod, A. G., Barker, P. S., and Johnston, F. D.: The determination and the significance of the areas of the ventricular deflections of the electrocardiogram, *Am Heart J* 10, 16, 1934.
- Wilson, F. N., Johnston, F. D., Rosenbaum, F. F.; Erlanger, H., Kossmann, C. E., Hecht, H. H., Curnin, N., Moores de Oliveira, R., Scarf, R.; and Barker, P. S.: Precordial electrocardiogram, *Am Heart J* 27, 19, 1944.
- Wilson, F. N.; Rosenbaum, F. F., and Johnston, F. D.: Interpretation of the ventricular complex of the electrocardiogram, in W. Dock and I. Snapper, *Advances in Internal Medicine* (New York: Interscience Publishers, Inc., 1947), vol. 2, pp. 1-63.
- Wunderlich, W., and Langendorf, R. Atrioventricular block with ventriculo-auricular response, *Am Heart J* 27, 301, 1914.
- Wolfe, L., and Richman, J. L.: The diagnosis of myocardial infarction in patients with anomalous atrioventricular excitation (Wolff-Parkinson-White syndrome), *Am Heart J* 45, 545, 1953.
- Wolfe, L., Richman, J. L., and Soffe, A. M.: The effect of heart position and rotation on the cardiac vector, *Am Heart J* 47, 101, 1954.
- Wolfe, L., Richman, J. L., and Soffe, A. M.: Spatial vectorcardiography: Review and critique, *New England J Med* 248 810, 1953.
- Wood, E. H., and Wood, G. K.: Blood electrolyte changes in the heart-lung preparation with special reference to the effects of the cardiac glycosides, *Am J Physiol* 137 6, 1942.
- Wood, E. H., and Wood, G. K.: Electrolyte and water content of ventricular musculature of heart-lung preparation with special reference to effects of cardiac glycosides, *Am J Physiol* 130 515, 1942.
- Wood, F. C., Wolfarth, C. C., and Gekeler, G. D.: Histological demonstration of accessory muscular connections between auricle and ventricle in a case of short P-R interval and prolonged QRS complex, *Am Heart J* 23 434, 1943.
- Wood, P. *Diseases of the Heart and Circulation* (2d ed., London: J. B. Lippincott Company, 1952).
- Wood, P.: Electrocardiographic appearance in acute and chronic pulmonary heart disease, *Brit Heart J* 10 67, 1952.
- Wood, P., McGregor, M., Magidson, O., and Whittaker, W.: The effort test in angina pectoris, *Brit Heart J* 12 363, 1950.
- of the literature, report of 16 cases with necropsy and of 6 cases with detailed histological study of the conduction system, *Arch Int Med* 62 1, 1938.
- Yu, P. N. C., Joss, H. A., and Katsampes, C. P.: Unipolar

- electrocardiograms in normal infants and children, *Am Heart J.* 41:91, 1951.
- Ziegler, R. F.: *Electrocardiographic Studies in Normal Infants and Children* (Springfield, Ill.: Charles C Thomas, Publisher, 1951).
- Ziegler, R. F.: The genesis and importance of the electrocardiogram in coarctation of the aorta, *Circulation* 9:371, 1954.
- Zimdahl, W. T., and Townsend, C. E.: Bidirectional ventricular tachycardia due to digitalis poisoning: Response to potassium therapy in evaluation of arrhythmia mechanism, *Am. Heart J.* 47:304, 1954.
- Zuckermann, R., Cabrera, E.; Fishleder, B. L.; and Sodi-Pallares, D.: The electrocardiogram in chronic cor pulmonale, *Am. Heart J.* 35:421, 1948.
- Zwemer, H. L., and Lowenstein, B. E.: Cortin-like effects of steroid glycosides on potassium, *Science* 91:75, 1940.

Index

[An asterisk (*) following a page number indicates reference to an illustration]

A

- ACETYLCHOLINE, 3
- esterase, 3
- ANISOTROPY, VENTRICULAR, 333-34
- persistent elevation S-T segment, 333-34
- ANGINA PECTORIS, 341-43*, 499*
- infarction in, 341*
- ANOREXIA MYOCARDIAL in pulmonary embolism, 217
- AORTA
 - coarctation, 170-72
 - ECC and VCG findings, 171-72
 - stenosis, *see* Stenosis
- ARRHYTHMIAS
 - see also* Atrial and Ventricular Flutter and Fibrillation
 - in pulmonary embolism, 216
 - auris, 360, 341*
 - "coronary nodal rhythm," 361, 366*
 - phasic and nonphasic, 361
 - ventriculophasic, 454
- ATRIAL FIBRILLATION*, 414*, 430-32, 436-39, 535*
 - clinical aspects, 439-42
 - digitalis effects, 460
 - effects of drugs, exercise and vagal stimulation, 460
 - in interatrial septal defect, 179
 - mechanism, 442-43
 - in mitral stenosis, 184
 - in Wolff-Parkinson-White syndrome, 489-91, 572*
- ATRIAL FLUTTER, 430-36, 437*, 553-54*, 565*, 571*
 - clinical aspects, 439-42
 - differentiation from ventricular tachycardia, 417
 - digitalis effect, 464, 466
 - effects of drugs and vagal stimulation, 466
 - exercise effects, 466

- impure, 430, 553*
- in interatrial septal defect, 179
- mechanism, 431, 442-43
- quasidominant effect, 432, 433*, 467
- in Wolff-Parkinson-White syndrome, 489-93
- ATRIAL FLUTTER-FIBRILLATION*, 430
- ATRIOVENTRICULAR BLOCK, 356-59, 374, 559-61*, 563*, 567*
- vs* atrioventricular interference, 381
- clinical aspects, 450
- complete, 357-59, 452-54, 558*, 566*
- incomplete, 357, 358*, 448-52, 559*
- retrograde, 412-15
- ventriculophasic sinus arrhythmia in, 454
- Wenckebach type, 357, 358*, 383, 449-52, 559*
- ATRIOVENTRICULAR DISSOCIATION, 356, 358*
 - in atrioventricular rhythm, 374, 542-44*, 557*, 563*
 - rate of rhythm and, 379
 - clinical significance, 379-81
 - complete, 374-75
 - incomplete, 374, 375-79
 - in tachycardia, 412, 418*
- ATRIUM
 - in chronic cor pulmonale, 195, 196, 197*, 207*, 508*
 - depolarization and repolarization, 17
 - digitalis effects, 163
 - infarction, 239
 - in mitral stenosis, 184, 185
- ATROPINE, effect on ventricular pre-excitation, 487
- AUTOVOMIC NERVOUS SYSTEM TONE and impulse formation and conduction, 379

AXES

- coordinate, of the body, 15
- electrical
 - mean and mean manifest, 23
 - see also* Mean Vector(s)
 - of cardiac rotation, 60
- AXIS DEVIATION
 - in chronic cor pulmonale and emphysema without cor pulmonale, 198-99
 - in coarctation of aorta, 171
 - no deviation, 39
 - in interatrial septal defect, 170
 - left, 39
 - in mitral stenosis, 188
 - in patent ductus arteriosus, 177
 - in pulmonary stenosis, 173
 - right, 39
 - in tetralogy of Fallot, 162

B

BEATS AND RHYTHMS

- atrial ectopic, *see* Atrial Flutter and Atrial Fibrillation
- atrial fusion beats, 358, 362*, 373
- atrioventricular nodal beats
 - ECC findings, 363-67, 368*
- atrioventricular nodal escape beats, 367-69
 - ventricular aberration of, 370-80*, 381-82
- atrioventricular nodal rhythms, 369-82, 511-42*, 557
 - without atrial capture, 374-79
 - with intermittent atrial interference, 373
 - persisting, with complete atrial capture, 371
 - rate, and atrioventricular dissociation, 379
 - reciprocal beats in, 372-73
 - "coronary nodal rhythm," 361, 366*

BEATS AND RHYTHMS (Cont.)

- coronary sinus rhythm, 541*
 - retrograde P waves in, 371
 - ectopic beats, 383-406
 - automatic, 383, 402-404
 - see also Parasystole
 - terminology, 383-88
 - ectopic beats, coupled premature, 383-402
 - see also Extrasystole(s)
 - atrial, 388-91
 - clinical significance, 400-402
 - coupling interval, 383
 - mechanisms, 386-87
 - pauses, 384*, 385
 - ectopic rhythms, 353, 354, 355*
 - escape, 353-54, 513*
 - extrasystole, see Extrasystole(s)
 - idioventricular escape rhythm, 382, 445*
 - multifocal premature beats, 385
 - sinus (sinuatrial) rhythm (normal), 360
 - variant types, 360-61
 - ventricular capture beat, 374, 377, 542*
 - followed by nodal beat—interval, 378
 - ventricular fusion beat, 404, 513*, 548-49*, 556*
- BIGEMINY, 383, 388*, 390*, 400, 559*
- BRADYCARDIA, SINUS, 360
- BUNDLE BRANCH BLOCK
- in coarctation of aorta, 172
 - with myocardial infarction, 320-31
 - in pulmonary embolism, 216
 - in pulmonary stenosis, 173
 - T wave in, 86-87
- BUNDLE BRANCH BLOCK, LEFT, 221-40, 509*, 511*
- anatomy of normal branch, 221
 - complete, 221
 - differentiation from infarction with per-infarction block, 337
 - ECC findings, 229-31, 509*, 511*
 - instantaneous VA vectors, 222-25
 - resumé, 226
 - S waves (terminal) in, 329
 - ventricular repolarization, 225-26
 - VCG findings, 227-31, 509*, 511*
 - QRS sE and T sE loops, 227, 231-31*
- diffuse, 221
- incomplete, 221, 231-36
- ECC findings, 231-33, 234-35*
 - instantaneous VA vectors, 232*, 233
 - first- and second-degree, 232*,

- 233
 - VCG findings, 233-36
 - QRS sE loop, 233-36
 - S-T vector, 234-35*, 236
 - T sE loop, 234-35, 236
 - mechanism, 222
 - with myocardial infarction, 323-31
 - ECC findings, 323-30, 533*, 562*, 568*
 - QRS, 323-29
 - S-T segment and T wave, 323, 327
 - free wall infarction, 327
 - “left ventricular hypertrophy with terminal conduction delay,” 329
 - septal, massive, 324-26*, 327, 331
 - VCG findings, 330-31, 533*, 562*, 568*
 - variant type, 236-40
 - ECC findings, 236-40
 - VCG findings, 236, 237-39*, 240
 - QRS sE and T sE loops, 236, 237-39*, 240
- BUNDLE BRANCH BLOCK, RIGHT, 241-254
- anatomy of normal branch, 221
 - classic type, 242
 - differentiation from healed infarction and ventricular hypertrophy, 306, 307
 - ECC findings, 251-52
 - complete, common and variant types
 - ECC findings, 242, 243-47, 249-51*, 512-14*
 - instantaneous VA vectors, 243-47
 - ventricular repolarization, 247
 - VCG findings, 247-53, 512-14*
 - QRS sE loops, 248-49, 250-51*
 - S-T vector, 249, 250-51*
 - T sE loop, 249
- differentiation from infarction with per-infarction block, 337
- incomplete, 242, 525*
- and “left ventricular hypertrophy with terminal conduction delay,” 236, 237-39*, 240, 251-52
- mechanisms, 241-43
- block in main branch, 241
 - peripheral block, 242
 - with myocardial infarction, 319-20*, 321-22, 532*, 567*
 - in patent ductus arteriosus, 177
 - uncommon, see classic type
 - variant type, 513-14*
 - see also common and variant types

with old posterolateral infarction, 322*

ventricular hypertrophy with, 252-54

BUNDLE OF HIS, 52

BURGER TRIANGLE, 48, 49*

C

- CALCIUM, ELEVATION IN SERUM, 479
- CARCINOMATOSIS OF LUNG: and cor pulmonale, 192
- CAROTID SINUS STIMULATION
 - see also Vagal Stimulation
 - in atrial flutter and fibrillation, 439, 440-41*, 466
 - in supraventricular tachycardia, 441, 466
 - in ventricular pre-excitation, 487
- CENTRAL TERMINAL OF WILSON: mathematical proof that it is zero potential, 23*
- CHILDREN AND INFANTS
 - ECC—normal, 159-163, 497*
 - R, S and T waves—normal standards in, 161
 - VCG—normal, 159-163, 497*
 - ventricular hypertrophy in, 159-64
- ECC diagnosis, 163-64
- CIRCUIT EQUATION, 118, 121*
- CIRCUS MOVEMENT, 42
- CONDUCTION (CARDIAC)
 - aberrant intraventricular, 381
 - atrioventricular prolonged, 447
 - digitalis effect, 463-69
 - normal, 353, 359, 381*
 - over paraspecific fibers, 381*, 382
 - pathways, 221
 - digitalis effects, 463
 - preferential, 381*, 382
 - ventricular, in extrasystole, 389, 392
- CORONARY ARTERY DISEASE
 - see also Angina Pectoris and Anoxemia, Myocardial
 - with infarction and per-infarction block, 335*
 - insufficiency
 - and myocardial damage, 340-42
 - in pulmonary embolism, 216
 - ischemia and injury in, 340
 - and myocardial damage, 340
- COR PULMONALE
 - acute, 192
 - with acute pulmonary embolism, 216-20
 - ECC findings, 216-19, 220*
 - precordial QRS pattern of “marked clockwise rotation,” 217-18*, 219, 220*, 507*, 510*
 - VCG findings, 219-20
 - and carcinomatosis of lung, 192
 - chronic, 192-216
 - cardiac position, rotation and

site of electrical center in, 167
ECG pattern of, 154°, 507°
P-E loop in, 166°, 507°
right ventricular hypertrophy in,
165-63, 199-201, 506°, 508°
chronic, due to emphysema, 166-
67, 193-216

ECG findings, 200
—genesis of, 193-94
—P pulmonale pattern, 195-98
—Q waves suggesting myocardial
infarction, 209
—QRS precordial "marked
clockwise rotation," 199,
203°, 207°

—right-axis deviation of A QRS,
197°, 198-99, 205°, 209°

QRS in E loop in, 201-216

—genesis of, 211-16

—type A, 201-204

—type B, 204-209

—type C, 208°, 209-11

right ventricular strain in, 201

S-Su pattern and, 207

clinical forms, 192

subacute, 192

CURRENT OF INJURY, *see* Injury

CURRENT MEMBRANE, 5

I

DEPOLARIZATION, 4°, 5-7

—*see also* Atrium, Septum, and Ven-

tricular Depolarization

blocking, in myocardial injury—

synthetic current of injury con-

cept, 258

equivalent dipole representation,

6°, 7

potential variations during, 11-12

DERMOGRAPHIA, 160-62

ECG and VCG in, 181°, 182

with sinus inversus, 160

DIGITALIS

effects, 463-69

on ECG, 463-69, 507°

on tachycardia (ectopic), 466

on VCG, 322°, 509°

on ventricular pre-excitation,

467

intoxication, 463, 469, 564-65°

and potassium—relationship, 464

DIPOLAR

axis, 5

definition, 3

equivalent dipole theory, 6°, 7, 13,

17, 43

equivalent (resultant), 6°, 8

moment (magnitude), 8, 13

polarized (hypothetical), potential

distribution in electrical field

of, 9°, 10-11

vector representation, 13-18

DRUG EFFECTS

see also specific drugs
on tachycardia, flutter and fibrilla-
tion, 468

on ventricular pre-excitation, 467

DUCTUS ARTERIOSUS, PATENT, 176-
77

ECG and VCG findings, 177

with pulmonary hypertension and

ECG suggesting biventricular

hypertrophy, 157°

E

EINSTEIN'S EQUILATERAL TRIAN-

GLE HYPOTHESIS, 20°, 21-23

EINSTEIN'S LAW, 21

EISENHENGEL'S COMPLEX, 181°

ELECTROCARDIOGRAM

in atrioventricular block, 357-59

in atrioventricular dissociation,

356, 358°

with atrioventricular nodal beats,

363-67, 365°

in bundle branch block

left, 222-26, 509°, 511°

—incomplete, 231-33, 234-35°

—variant type, 236-40

—ventricular repolarization, 225

right, 242, 243-47, 249-51°,

512-14

—ventricular repolarization, 247

in chronic cor pulmonale, 154°,

200, 507°

emphysema effects on, 193-94

P pulmonale pattern, 195-98

in coarctation of aorta, 171-72

deflections, 34°, 35

in dextrocardia, 181°, 192

digitalis effect, 465-69, 507°

after exercise—responses

abnormal, 345, 347°, 349-50°,

535-37°, 563°

normal, 343-45, 348°

in hyperkalemia, 470-77°, 474

in hypokalemia, 474-79

in interatrial defect with shunt,

178-79

in interventricular septal defect,

175

in mitral stenosis, 184-88, 504-

506°

in myocardial infarction, 260°,

261-63, 264-67

anterior, 283, 284°, 519°, 532°,

567°

anterolateral, 278-82, 287, 519°

anteroseptal, 268-70, 271°, 287,

515-17°, 532°

with bundle branch block, 320

—left, 323-30, 533°, 562°, 565°

—right, 319-20°, 321, 532°,

562°, 567°

diaphragmatic (inferior), 289-

94, 296-98°, 520-21°, 526-

25°, 568°
posterolateral, 299-302, 305-
308, 523°, 525°

Q wave abnormality—criteria,
203

QRS abnormalities—mechanism,
260°, 261-63

strictly anterior, 273°, 274-75,
276-77°, 576°

strictly posterior, 308-10, 313-
15, 525°

normal scalar, 52-70, 495°
characteristics, 64-69

in infants and children, 159-63,
497°

in patent ductus arteriosus, 177

in post-infarction block, 335

in pulmonary embolism with acute

cor pulmonale, 216-19, 220°

pulmonary emphysema effects on,

193

quinidine and procainamide effects,

469-70

in sinus (sinus) rhythm, 360-

62

in trilogy of Fallot, 180°

vector loops constructed from,

102-104

in ventricular hypertrophy, 123-24

left, 125-31, 499-501°

right, 132-47, 502-508°

—in chronic cor pulmonale,

165-68, 199-201

—in right bundle branch block,

253-54

in ventricular pre-excitation, 453-

99, 491°, 493

group A, 453-54°, 456°, 457,

490-92°, 538°

group B, 453, 455°, 457, 538-

40°

ELECTROCARDIOGRAPHY

amplifier and coil wire type, 32,

33°

direct-writing type, 32-34

oscilloscope tube type, 34, 92

string galvanometer type, 32, 33°

ELECTROCARDIOGRAPHY

equivalent dipole concept, 17, 43-

45

image vector concept, 17-51

lead field concept, 51

lead vector concept, 45-47, 48-50

semidirect lead hypothesis, 43-45

and cardiac rotation, 57

terminology, 34-38

ELECTRODES

of bipolar lead, 8

exploring (positive), 8

indifferent (negative), 8

vectorcardiographic

see also Leads (Vectorcardio-

graphic)

placement, 93-98

ELECTROLYTE IMBALANCE, 470-79
ELECTROMOTIVE FORCE OF MYOCARDIAL CELL
 membrane theory, 3-5°
 transmembrane flow of Na and K ions, 3, 4°
EMBOLISM, PULMONARY
 acute
 with acute cor pulmonale, 216-20
 —ECG findings, 216-19, 220°
 bundle branch block in, 216
 cardiac rotation, affecting ECG, 217
 coronary insufficiency (acute) in, 217
 ECG findings, 216-19, 220°
 —arrhythmias, transient, 216
 —axis deviation of A QRS, 217, 218°, 220°
 —P pulmonale pattern, 216, 217°, 219°
 —precordial QRS pattern of "marked clockwise rotation," 217-18°, 219, 220°
 —S₁-Q_m pattern, 217, 218°, 220°
 VCG findings, 219-20
 —QRS sE loop in, 220
 chronic, 509°
 in chronic cor pulmonale, 166-67
 chronic (without cor pulmonale), 194-216, 507°
 electrical effects of anatomic heart position and rotation on VCG, 211-15
 QRS sE loop in, 201-16, 507°
 —genesis of, 211-16
 —type A, 201-204
 —type B, 204-209
 —type C, 208°, 209-11
 right-axis deviation of A QRS, 198-99
 VCG P pulmonale pattern, 196
 effects on ECG, 193-94
EQUILATRAL TETRAHEDRON LEAD SYSTEM, 93-94
 see also Leads (Vectorcardiographic)
EQUILATRAL TRIANGLE HYPOTHESIS (Einthoven's), 21-23
EXERCISE, effects on tachycardia, flutter and fibrillation, 466
EXERCISE TESTS, 343-50
 ECG responses, 535°
 abnormal, 345, 536-37°, 563°
 normal, 343-45
 Master test, 345-50
EXIT BLOCK, 405, 406
EXTRASYSTOLE(S)
 see also Beats and Rhythms, ectopic
 atrial, 388-91, 545°

ECG in, 388
 postectopic interval, 391
 variations in ventricular conduction, 389
 atrioventricular, 392-93
 ECG findings, 392
 postectopic interval, 393
 variations in ventricular conduction, 392
 blocked, see atrial
 clinical significance, 400-402
 coupling interval, 383-85
 interpolated, 385
 mechanisms, 386
 re-entry, 386
 single focus of subthreshold activity, 387
 terminology, 383-86
 ventricular, 392-99, 526°, 546°, 564°, 566°, 570°
 ECG in, 393-95
 interpolated, 398, 399°, 546°, 569°
 retrograde conduction and postectopic interval, 396-98
EXTREMITY LEADS, 19-29
 reference frames, 23, 21°, 27-31
 standard bipolar, 19-21
 projections of cardiac vector on, equations for, 21°, 24-25
 unipolar
 calculation of correction factors, 25°, 26-27
 Goldberger's augmented (aVR, aVL, aVF), 22°, 24-25°, 26, 27
 precordial, 29-31
 Wilson's (VR, VL, VF), 22-25°, 26, 27

F

F WAVES, 430, 432, 433-37°
FOCAL BLOCK, see Peri-infarction Block
FORAMEN OVALE patent, 179

G

GALVANOMETER, definition, 7

H

HEART
 activation process—stages, 260°
 conduction pathways
 block, see specific conditions
 digitalis effects, 463
 normal, 221
 preferential, 381°, 382
 in dextrocardia, 180
 dextroversion and -position, 180
 excitation, sequence of, 52
 failure, acute congestive, 491°, 506°

position(electrical), 60-64
 and patterns of right ventricular hypertrophy, 167
 positions (electrocardiographic), 61°, 62-64
 rate—determination, 35-36
 refractory phase
 absolute, 354
 relative, 354, 355°
 rhythm
 see also Beats and Rhythms and Arrhythmias
 in chronic cor pulmonale, 195
 rotation (anatomic)
 in acute pulmonary embolism ECG, 217
 clockwise, in QRS sE pattern, type C, 191
 electrical axes of, 60
 electrical effects on chronic emphysema ECG and VCG, 211-15
 and precordial QRS transition, 57-58
 in ventricular hypertrophy, displacing QRS spatial vectors, 122
 shunts
 causing diastolic left ventricular overloading with or without systolic right ventricular overloading, 174-77
 causing diastolic right ventricular overloading, 178-80
 left-to-right, with interatrial septal defect, 178
 right-to-left, with atrial septal defect, 179-80
 vector representation of dipole, 13-16
 electrical forces, 17-19

HEART DISEASE, CONGENITAL, 169-82

cyanotic
 right ventricular hypertrophy in, 154°
 tall R pattern in, 151°
 P sE loop in, 152°, 186°
 with pulmonic stenosis, factors affecting patterns of right ventricular hypertrophy, 167
 with right ventricular overloading, 188
 types, 169

HYPERKALEMIA, 470
 ECG findings, 471-77°, 474

HYPERTENSION
 pulmonary
 with atrial septal defect, 180
 —causing right ventricular hypertrophy, 178
 differentiation from cor pulmonale, 192
 in mitral stenosis, 183, 506°

- with patent ductus arteriosus, 176
with ventricular septal defect, 174-75*, 176
vascular, with coarctation of aorta, 171
- HYPERTROPHY BY BARRIER, OVERLOAD AND ADAPTATION, 168**
- HYPOKALEMIA, 470**
ECG findings, 474-79, 567*
- I**
- IMPULSE FORMATION**
see also Pacemaker(s)
atrioventricular node, 363
and autonomic nervous tone, 359
digitalis effect, 463-69
disturbances, 353-62
classification, 359
- INFANTS, see Children and Infants**
- INFARCTION, see Atrium, Myocardial Infarction, Septum, and Ventricles**
- INJURY**
currents, 256-59
in ventricular aneurysm, 333*, 334
myocardial
diastolic current of injury, 256
—disappearance of, 257-58
—I vector of, 256, 257-58*
—S-T segment and, 257
subendocardial, 237*, 259, 333, 515*, 528*
subepicardial, 257*, 259, 318-19*, 518*
systolic current of injury, 256-59
—and blocking of depolarization, 258-59
—I (or S-T) vector of, 258*, 259
—vector loops with, 259
- INTERFERENCE**
atrial, with atrioventricular rhythms, 373
atrioventricular 335-56, 374
vs atrioventricular block, 381
- INTRAVENTRICULAR BLOCK, 510-11***
see also Bundle Branch Blocks
diffuse, 234
- INTRINSIC (OM) DEFLECTION, 13, 57***
58-59
time of onset, 67
- ISCHEMIA**
myocardial 507*
anterior, 515*
diaphragmatic, 517*
monophasic curves in, 87-88
posterior, 322*
subendocardial, 340
transmural, 340, 342

K

- KARLTAGNER'S SYNDROME, 160, 181***
- KATZ-WACHTEL SIGN, 176**
- KIDNEYS**
see also Renal Diseases
function and K imbalances, 470
- KIRCHHOFF'S LAW, 21, 23***

L

- LEAD AXES**
anatomic, 20*, 22
in lead vector concept, 49*
definition, 20*, 22
effective, 45, 47
in QRS-T angle calculations, 51*
precordial
QRS transitions in, 56-58
relation to horizontal plane, 29, 30*
reference frames, see Reference Frames
- LEADS**
bipolar, 8, 19, 20*
correction factors for, 50
definitions, 7-8
equivalent dipole hypothesis, 17, 43-45
extremity, see Extremity Leads
image vector concept, 47-51
lead field concept, 51
lead vector concept, 43-47, 48-50
scalar—deflections, 34*, 35
derivation from vectorcardiogram, 99-102
—electronic method, 99
—manual method, 100-101*, 102
semidirect, 43
semidirect lead hypothesis, 43-45
standardization factors
for unipolar leads, 25*, 26
for VCG leads, 94
transitional (RS), 57
unipolar, 8
unipolar precordial, 28*, 29-31
voltage in relation to
dipole moment and angle θ , 11, 16
vector projection on axis, 16
- LEADS (VECTOCARDIOGRAPHIC), 93-98**
corrected lead systems, 97-98
Frank's, 97-98
cube lead system (Crashman), 94-97
equilateral tetrahedron system, 93-94
in left ventricular hypertrophy, 134, 135*
standardizing factors, 94
for frontal, horizontal and sagittal projections, 93
orthogonal lead systems, 93, 94-97

LEADS (VECTOR)

- construction from ECG, 102-104
inscription, 92-93
P sE, 93, 105, 106*, 164
in chronic cor pulmonale, 160*, 507*
in congenital heart disease, 166*
—cyanotic, 151*
normal, 166*
planar projections, 108
of P mitrale, 152*, 165-66*, 167, 506*
of P pulmonale, 196, 198, 207*
QRS, construction from ECG, 103*, 104
QRS sE, 93, 105, 108-13
in chronic cor pulmonale, 201-16, 507*
in chronic emphysema without cor pulmonale, 201-16
figure-of-8, in ventricular hypertrophy
—left, 131
—right, 149, 153
frontal, 93, 113
horizontal, 111
in infants and children (normal), 159-61
in left bundle branch block, 227, 229-31*
—incomplete, 234-35*, 238
—variant, 236, 237-39*, 240
in mitral stenosis, 154-61, 210, 506*
—type A, 189, 201-204
—type B, 189-91, 204-209, 214
—type C, 190*, 191, 208*, 209-11
in myocardial infarction, 260-67
—anterolateral, 281*, 282-83
—anteroposterior, 270*, 271-72
—diaphragmatic, 294-99
—posterolateral, 302-304, 306-308*
—strictly anterior, 275*, 276-78
—strictly posterior, 310-13, 314-16
in myocardial ischemia, 250
planar, 109*, 111
planar projections, 107*, 108-13
projection on reference frames of
scalar leads, 100*, 102
in pulmonary embolism, 220
right sagittal, 111
terminology, 108
in ventricular hypertrophy
—left, 131-34, 135-37*
—right, 148-55
terminology, 92-93, 105
for planar projections, 93, 105
T sE, 93, 105, 106*
in left bundle branch block, 227, 229-31*

LOOPS (VECTOR) (Cont)

- incomplete, 234-35*, 236
- variant, 236, 237-39*, 240
- in myocardial infarction
 - diaphragmatic, 296-98*, 299
 - in myocardial ischemia, 256
 - and spatial QRS sE-T sE angle, 114
 - in ventricular hypertrophy
 - left, 134, 135-37*
 - right, 149, 151-54*, 155
- LUTEMBACHER'S SYNDROME, 178

M

MALADIE DE ROGER, 174

MASTER TEST (2-STEP), 345-50, 535-37*, 563*

MEAN INSTANTANEOUS VECTOR(s)

pre- and postinfarction, 260*, 261-63

QRS spatial, 54-59, 63

in ventricular hypertrophy, 118-22, 123-24

—left, 125-28

T spatial, in ventricular hypertrophy, 122-23, 124

of VCG—orientations (normal), 106*

ventricular activation (VA)

apicoanterior (0.02 second), 55, 56*

in bundle branch block

—left, 222-25, 229-31*

—left incomplete, 332*, 233

—right, 243-47

left ventricular (0.04 second), 55*, 56

in myocardial infarction, 266-67

—anterolateral, 278-80

—anteroseptal, 268-70

—diaphragmatic (inferior), 289-91

—posterolateral, 299-302

—strictly anterior, 273*, 274-75

—strictly posterior, 310

in normal heart, 54-59, 65

septal (0.01 second), 54, 55-56*

terminal, or basal (0.06 second), 55*, 56

in ventricular hypertrophy

—left, 125-28

—right, 138-45

MEAN VECTOR(s), 23

construction from ECG—methods

QRS, 20*, 36-41, 42

spatial, 40*, 41-42

ventricular gradient, 84*, 85-86

frontal plane (QRS)—construction, 36*, 37-39, 40*, 41-42

horizontal plane (QRS)—construction, 39-42

instantaneous, 23

planar QRS, 18*

construction from ECG, 20*, 24, 36-38, 42

reference frames, *see* Reference Frames

spatial

construction from ECG, 40*, 41-42

transitional contour or null pathway, 41

MEMBRANE THEORY (BEHNSTEIN'S), 3-5

MITRAL STENOSIS, 183-91, 504-506*

asymptomatic, 116*

cardiac rhythm in, 184

P mitral pattern, 184-87

QRS sE loop patterns, 188-91, 210

type A, 189, 201-204

type B, 189-91, 201-209, 214

type C, 190*, 191, 208*, 209-11

right ventricular hypertrophy in, 105-68, 504-505*

lead V, findings, 187

RSR' patterns, 152*

VCG in, 188-91, 201-11

MUSCLE FIBER, electrical effects of hypertrophy, 118-22

MYOCARDIAL CELL, SINGLE

electrical activity of, 7-11

emf production by, 3

MYOCARDIAL INFARCTION, 259-67

in angina pectoris, 341*

anterior, 266-67, 268-68, 519*

acute—S-T vector and ventricular repolarization in, 287-88

with right bundle branch block, 320*, 532*, 567*

anterior-posterior, 317-19

anterolateral, 266-67, 278-83, 299

ECC findings, 278-82, 287, 519*

—lead aVL, 280-82

—VA vectors, 278-80

with per-infarction block differentiated from left bundle branch block, 337

relation of electrical site, VA vectors and QRS changes, 266-67

VCG findings—QRS sE loops, 281*, 282-83, 286*

anteroseptal, 259, 266-67, 268-78

ECC findings 268-71, 272*, 287, 515-17*

—QRS criteria for diagnosis, 270

—VA vectors, 268-70

healed, 271, 515*, 517*

—with left ventricular hypertrophy, 272*

with per-infarction block, 336*, 337

with right bundle branch block, 319*, 532*

VCG findings, 271-72, 285*, 515-17*

—QRS sE loops, 270*, 271

—T sE loop, 271-72*

with bundle branch block, 266, 319*, 320-31

QRS abnormalities, 320

with bundle branch block—left, 323-31

ECC findings, 323-330, 562*

—QRS, 323-29

—S-T segment and T wave in, 323, 329-30

resembling right block, 331

with bundle branch block—right, 319-20*, 321-22, 562*

in combined locations, 317-19

and coronary insufficiency, 240-42

diaphragmatic (inferior), 266-67, 289-99

ECC findings, 289-94, 296-98*, 520-21*, 528-28*, 559*, 568*

—QRS criteria for diagnosis, 291-94

—VA vectors, 289-91

healed, 296*, 299

with per-infarction block differentiated from right bundle branch block, 337

VCG findings, 294-99, 520-21*, 528-28*, 568*

—QRS sE loops, 294-99

—S-T vector and ventricular repolarization, 296*, 297-99

—T sE loop, 296-98*, 299

diaphragmatic-anterolateral, 530-31*

with coronary artery disease, 335*

diaphragmatic-posterolateral, 302*, 303, 305*, 308*, 347*, 350*

with anterior infarction (later), 316*

with right bundle branch block, 319*, 321*

diaphragmatic—strictly posterior, 310-11, 312*, 315*

ECC findings, 260*, 261-63, 264-67

QRS abnormalities—mechanism of, 260*, 261-63

Q wave abnormality—criteria of, 263

S-T segment, 263*, 264

T wave, 263*, 265

electrophysiologic effects, 268-67

evolution, 263-65

extensive anterior, 266, 267, 283-284

ECC in, 287, 283, 284*

VCG in, 283-86, 287, 288*

inferoposterior, 268, 289-99

infra-apical, *see* strictly posterior

posterobasal, *see* strictly posterior

posterolateral, 266-67, 278, 299-308

ECG findings, 299-302, 305-308, 523*, 525*, 561*
 —criteria for diagnosis, 305-308
 —QRS abnormalities, 299, 305-307
 —S-T segment and T wave changes, 307-308
 healed—similarity to right bundle branch block and ventricular hypertrophy, 306-307
 VCG findings, 302-305, 306-308*, 523*, 525*
 —QRS sE loops, 302-304, 306-308*
 —S-T vector and ventricular repolarization, 303
 —T sE loop, 303, 306-308*
 Q waves in chronic cor pulmonale suggestive of, 209
 relation of electrical site, VA vectors and QRS changes, 266-67
 septal (interventricular), 331-32
 with free wall infarction, 331
 in left bundle branch block, 324-28*, 327, 331
 strictly anterior, 260, 268, 272-78
 ECG findings, 273*, 274-75, 276-77*, 518*
 —QRS criteria for diagnosis, 275
 —VA vectors, 273*, 274-75
 —VCG findings, 273*, 276-78, 285*, 518*
 strictly posterior, 266-67, 308-15, 525*
 ECG findings, 308-10, 313-15
 —criteria for diagnosis, 313-15
 —QRS abnormalities, 313-15
 —VA vectors, 310
 VCG findings, 310-13, 314-15, 525*
 —QRS sE loops, 310-13, 314-15
 —S-T vector and ventricular polarization, 314
 —T sE loop, 314
 subendocardial, 333
 terminology, 265-66
 VCG in, 264-65
 QRS sE loop and VA vectors, 266-67
 vectors
 infarction, 280*, 281, 262*
 pre- and postinfarction mean instantaneous, 260*, 281-63
 of ventricular free wall (left) in bundle branch block, 327-29
 Myocardial ischemia, 255-56
 monophasic curves in, 87-88
 subendocardial, 254
 repolarization in, 255
 transmural (epicardial), 255
 ECG in, 287
 VCG in, 250, 275*
 ventricular gradient in, 87-89

Myocarditis, 339
 Myxedema, with thyroid therapy, 534*

N

Null Contour, 41

O

Olm's Law: application to hypertrophied muscle fiber, 121*
 Oscilloscope, 92
 Overloading, see Ventricular Overloading

P

P Mitral Pattern, 184-88
 P Pulmonale Pattern, 195-98
 in chronic cor pulmonale, 196, 198, 207*
 in pulmonary embolism, 216, 217*, 219*
 P Wave(s), 53-54, 84-85
 ectopic, 409, 548*
 fusion, 356, 373
 mean vectors, 53
 P mitral, 152*, 184-88
 P pulmonale, 195-98
 retrograde, 375*, 412, 564*
 with atrioventricular nodal rhythm, 371, 547*
 with coronary sinus rhythm, 371
 P-J Interval, 483
 P-P Intervals, in sinoatrial block, 455, 459*, 459-60*
 P-R Interval, 54, 65
 prolonged in tachycardia, 411, 412
 Pacemaker(s), Cardiac
 ectopic, 355*
 normal sinus, 353
 single—rapid discharge by, 355
 sinoatrial, 353
 digitalis effect, 463
 two—simultaneous activity of, 355, 356*
 wandering supraventricular, 361, 362*, 368
 with atrioventricular rhythms, 373
 Paraspecific Fibers, 381*, 383
 Parastole, 383, 402-406
 atrial, 402, 405*
 atrioventricular, 402, 404*, 547-48*, 569*
 ventricular, 402-408, 548-49*
 Pericarditis
 acute fibrous, 338-39, 534*
 in adults, ECG differentiation from infarction, 338-39
 chronic constrictive, 339
 subacute, 339

Peri-infarction Block, 254, 335-38
 ECG findings, 335-38
 differentiation from bundle branch block, 337
 mechanism, 335
 Polarization, 3
 Polarized State, 3
 Potassium, 470-79
 and digitalis—relationship, 464
 effects on tachycardia, flutter and fibrillation, 467
 imbalance—causes, 470-74
 ions—transmembrane flow in myocardial cell, 3, 4
 Potential, 3
 during depolarization and repolarization—variations in, 11-13
 difference, 6*, 7
 in electrical field of polarized dipole, 9*, 10-11
 proximity potentials hypothesis, 43
 zero line, 7
 Pregnancy ECG and VCG of, 113*
 Preventive Effects
 on ECG, 409-70
 on tachycardia, flutter and fibrillation, 467
 on ventricular pre-excitation, 467
 Pseudotruncus Arterialis, 182
 Pulmonary Dilemmas
 chronic—QRS sE, type C, in, 190*
 embolism, see Embolism Pulmonary
 emphysema, see Emphysema
 infundibular stenosis, 172
 pulmonary heart disease, see Cor Pulmonale
 pulmonic stenosis
 with interatrial septal defect, 170-80
 isolated, with normal aortic root, 172-74
 valvular stenosis, 172
 Purkinje System or Fibers, 17
 in ventricular depolarization, 52

Q

Q Wave
 abnormality—criteria of, 263
 in myocardial infarction, 260*, 281-63
 normal, 67
 QRS Complex, 54-59, 65-67
 deflections, 34*, 35
 derivation from VCG, 99-101*, 102
 transitional, 38, 57
 and heart position
 in resultant vector concept, 62*, 64
 in semidirect lead concept, 61*, 62

QRS COMPLEX (Cont)

- mean instantaneous VA vectors,
see Mean Instantaneous Vectors
- in myocardial infarction
anteroseptal type, 268-70
with bundle branch block, 320, 323-29
- diaphragmatic, 291-94
mechanism, 260*, 261-63
posterolateral, 299, 305-307
relation to electrical site and VA vectors, 260-67
- strictly anterior, 274*, 275
strictly posterior, 313-15
- precordial pattern of "marked clockwise rotation," 193
in cor pulmonale
—acute, 217-18*, 219, 220*
—chronic, 199, 203*, 207*, 507*
in pulmonary embolism, 217-18*, 219, 220*
- precordial transition, 56-58
in left bundle branch block, 225
and regression T wave, 74*, 75
- Si-Ti-Sm pattern, 199
in chronic cor pulmonale, 207, 507*
- and right ventricular hypertrophy, 199
- in ventricular pre-excitation, 483-89
- QRS-T ANGLE
frontal plane—calculation, 50-51*
spatial, 68*, 69, 87*, 88-89
calculation, 89-91
- QRS VECTOR, MEAN MANIFEST, see Mean Instantaneous Vectors
- Q-T INTERVAL, 67
digitalis effects, 467
- QUADRILMINY, 383, 396*
- QUINIDINE, 469-70
effects, 467
on atrial flutter, 432, 433*, 467
on ECC, 469-70
on tachycardia and fibrillation, 467
on ventricular pre-excitation, 487, 490*

R

- R WAVE
see also Tall R Pattern
in children (normal), 161
- R-P INTERVALS: constant in retrograde atrioventricular block, 415, 419*
- RS COMPLEX, 13
- RSR' PATTERN
in ECC, 138-45, 502-503*
with mitral stenosis, 152*, 187-88
in VCG, 149, 150-55, 502-503*
- RS-T INTERVAL AND SEGMENT, see S-T Segment

REFERENCE FRAMES (OR SYSTEMS)

- hexaxial, 27-29, 38-39
corrected—application of, 50*
revised, based on lead vectors, 48, 49*
- horizontal or precordial, 19, 28-31
triaxial, 23, 24*
- vectorcardiographic, 98
expression in terms of scalar leads, 98
- RENAL FAILURE: acute, with hyperkalemia, 471-77*
- REPOLARIZATION, 5*, 7
see also Ventricular Repolarization
equivalent dipole representation, 7*
- opposition of effects, 71
potential variations during, 11-13
- RHEUMATIC FEVER: arrhythmias in, 360*, 512*
- RIGHT VENTRICULAR PREPONDERANCE
pathologic—VCG diagnosis, 163
physiologic, 159, 162*

S

- S WAVE(s)
in children (normal), 161
in chronic cor pulmonale, 154*, 507*
- terminal, in left bundle branch block, 329
- S-Qm PATTERN in pulmonary embolism (acute), 217, 218-20*
- Si-Sm-Sm PATTERN, 199, 507*
- S-T INTERVAL, 67, 70
- S-T SEGMENT, 67, 70
in bundle branch block
left, 226
—with infarction, 323, 329
right, 247
in coronary artery disease, 340-42
deviations with exercise, 343-44, 348*
- digitalis effect, 467, 507*
in myocardial infarction, 263*, 264, 323, 329, 526*
- posterolateral, 307-308
persistent elevation, in ventricular aneurysm, 333-34
and T wave, 70-71
in ventricular hypertrophy, 123
left, 128, 129, 130
- S-T VECTOR
injury vector, in myocardial injury, 258*, 259
in left bundle branch block, incomplete, 234-35*, 236
in myocardial infarction, 287-88
in myocardial injury, 257, 258*
in ventricular hypertrophy
left, 134, 135-37*
right, 151-52*, 155

in ventricular pre-excitation, 486, 489

SCALAR QUANTITY, 13

SEPTAL DEFECT(s)

- atrial
with pulmonary hypertension, 180
with right-to-left shunt, 179-80
- interatrial
with left-to-right shunt, 178-79
with pulmonary stenosis, 179
with right ventricular hypertrophy in, 153, 503*
- interventricular, 174-76
ECC and VCG findings, 175, 503*
- of septum primum, 179*
ventricular, 503*

SEPTUM

- see also Septal Defects
depolarization in left bundle branch block with infarction, 326
- interventricular
activation, 117
anatomy, 117
fibrosis, 332
infarction, 331-32
—with left bundle branch block, 324-26*, 327, 331

SINOATRIAL BLOCK, 455-60

SINOATRIAL PAUSE AND ARREST, 455, 460

SODIUM IONS transmembrane flow in myocardial cell, 3, 4

STENOSIS

- aortic congenital, 501*
and subaortic, 172
congenital, causing ventricular overload, 170-74
mitral, see Mitral Stenosis
pulmonic, see Pulmonary Diseases
- STOKES-ADAMS ATTACKS, 560-61*
- STRESS TESTS, 342-50
anoxemia test, 342
exercise test, 343-50

T

- T WAVE(s), 68
in bundle branch block, 86-87
left, with infarction, 323, 329
right, 247
changes
primary, 81*, 84-87
secondary, 84-87
in children (normal), 161, 162*
digitalis effects, 467
in myocardial infarction, 263*, 265
posterolateral, 307-308
"nonspecific abnormalities" in coronary insufficiency, 340
postectopic changes, 398-401
regression (T_R), 75
and QRS complex, 74*

and spatial QRS-T angle, 89
in ventricular extrasystole, 395
in ventricular hypertrophy, 123-23
left, 123, 129, 130
right, 146, 147

TACHICARDIAS

atrial, 407, 408, 411-12*, 414*,
419*, 532*, 571*

ectopic

atrioventricular nodal, 371, 552*,
563*

digitalis effect, 466, 565*

effects of vagal stimulation and
drugs, 468-67

exercise effects, 466

paroxysmal ectopic, 407-30, 458*

recurrent, in Wolff-Parkinson-
White syndrome, 489-93

supraventricular, 407, 408*, 409-
25, 550-51*

paroxysmal ventricular, 420-26*,
427-30, 565*, 570*

alternating bidirectional, 423*,
426-48*, 429, 556-57*, 564*

clinical significance, 430

differential diagnoses, 411, 420-
30

sinus, 360, 358*, 560-61*

TALL R PATTERN

in cyanotic congenital heart dis-
ease, 151*

in left bundle branch block, 231*

normal in infants and children, 159,
162*

in right ventricular hypertrophy
in ECG, 138-45

in VCG, 148-50, 183*

in tetralogy of Fallot, 151*

TA (Tp) Wave, 33, 54

TETRALOGY OF FALLOT, 151*, 182,
503*

TIME (ECG) measurements, 34-36

TRANSITIONAL (EQUIPHASE OR EQUI-
POTENTIAL) COMPLEX, 38, 57

TRANSITIONAL PATHWAY, 41

TRICEMINT, 383, 398*, 557*

TRILOGY OF FALLOT, 179-80

TRUNCUS ARTERIOSUS pseudo-, 182

U

U WAVES, 71, 567*

V

VAGAL STIMULATION

see also Carotid Sinus Stimulation

effects on

atrial fibrillation, 439, 440*, 466

atrial flutter, 439, 441*, 466

tachycardia, 466

VECTOR(S)

see also Mean Instantaneous Vec-
tor(s)

addition (composition), 13
parallelogram method, 13, 14*
simple consecutive—method, 13,
18*

triangle method, 13, 14*

components of, 15

determination of magnitude, 15-
16

current of injury

diastolic (I), 256, 257*

systolic (-I), 258*, 259

definition, 13

gradient, 77*, 79

infarction, 260*, 261, 262*

in left bundle branch block and
free wall infarction, 328*

injury, 256-59

in ventricular aneurysm, 333*,
334

length and direction of resultant of
2 vectors, method of determin-
ing, 15

pre- and postinfarction, 260*, 261,
262*

projection, trigonometry for, 15

quantity, 13

representation

of cardiac dipole, 13, 14*

of cardiac electrical forces, 17-
19

resultant, 13, 17

resultant vector concept, 13, 17

and cardiac positions (ECG),
62*, 64

spatial (cardiac), 15*, 19

vertical component, 49*, 50, 51*

X, Y and Z components, 15*, 19

subtraction—method, 14*, 15

VECTORCARDIOGRAMS

in acute cor pulmonale, 219-20

in chronic cor pulmonale

P pulmonale pattern, 196, 198,
207*

QRS sE loop patterns, 201-16

in chronic emphysema without cor

pulmonale, 507*, 509*

P pulmonale pattern, 196

QRS sE in, 201-16, 507*

in coarctation of aorta, 171-72

demonstration of scalar lead deflections
from, 99-102

in dextrocardia, 181*, 182

in interatrial defect with left-to-
right shunt, 178-79

in interventricular septal defect,
175

in left bundle branch block, 227-
31

incomplete, 233-34

—QRS sE loop, 233-36

—S-T vector, 234-35*, 238

—T sE loop, 234-35*, 236

—variant type, 236, 237-39*,
240

in mitral stenosis, QRS sE loop
patterns, 168-91, 201-11

in myocardial infarction, 264-65,
260-67

anterior, 283-60, 287, 519*,
532*, 567*

anterolateral, 281*, 282, 283

anteroseptal, 271-72, 515-17*,
532*

with bundle branch block, 320

—left, 325-28, 330-31, 533*,
562*

—right, 321-22, 562*, 567*

diaphragmatic, 294-99, 520-
21*, 526-29*

posterolateral, 302-305, 306-
308*, 523*, 525*

strictly anterior, 275*, 276-78

strictly posterior, 310-13, 314-
15, 525*

in myocardial injury, 258*, 259

in myocardial ischemia, 253, 256

normal, 105-15, 498*

in infants and children, 159-63,
497*

in patent ductus arteriosus, 177

in right bundle branch block, 247-
53, 512-14*

in trilogy of Fallot, 150

in ventricular hypertrophy

left, 131-37, 499-501*, 518*

right, 145-35, 503-506*

in ventricular pre-excitation, 484-
88*, 488-89

group A, 484*, 486*, 488, 538*

group B, 485, 489, 538-40*

VECTORCARDIOGRAPHY

electrode placement and lead sys-
tems, 93-98

corrected lead systems, 43-44,
97-98

cube lead system (Crishman),
94-97

equilateral tetrahedron, 93-94

orthogonal, 93, 94-97

instrumentation, 92

loops, 92-93

see also Loops

oscilloscope for, 92

VENTRICLES

digitalis effect, 464

effective sites, 117-18

free walls, 117

infarction

of free wall (left), 327-29

—with left bundle branch block,
327

right, 259

neonatal characteristics, 159

right ventricular preponderance

pathologic—VCG diagnosis, 163,
159, 162*

QRS COMPLEX (Cont.)

- mean instantaneous VA vectors, see Mean Instantaneous Vectors
 - in myocardial infarction
 - anteroseptal type, 268-70
 - with bundle branch block, 320, 323-29
 - diaphragmatic, 291-94
 - mechanism, 260*, 261-63
 - posterolateral, 299, 305-307
 - relation to electrical site and VA vectors, 266-67
 - strictly anterior, 274*, 275
 - strictly posterior, 313-15
 - precordial pattern of "marked clockwise rotation," 193
 - in cor pulmonale
 - acute, 217-18*, 219, 220*
 - chronic, 199, 205*, 207*, 507*
 - in pulmonary embolism, 217-18*, 219, 220*
 - precordial transition, 56-58
 - in left bundle branch block, 225
 - and regression T wave, 74*, 75
 - Si-SII-SIII pattern, 199
 - in chronic cor pulmonale, 207, 507*
 - and right ventricular hypertrophy, 199
 - in ventricular pre-excitation, 483-89
- QRS-T ANGLE
- frontal plane—calculation, 50-51*
 - spatial, 68*, 69, 87*, 88-89
 - calculation, 89-91
- QRS VECTOR, MEAN MANIFEST, see Mean Instantaneous Vectors
- Q-T INTERVAL, 67
- digitalis effects, 467
- QUADRIGEMINY, 383, 396*
- QUINIDINE, 469-70
- effects, 467
 - on atrial flutter, 432, 433*, 467
 - on ECG, 469-70
 - on tachycardia and fibrillation, 467
 - on ventricular pre-excitation, 467, 490*

R

R WAVE

- see also Tall R Pattern
- in children (normal), 161

R-P INTERVALS: constant in retrograde atrioventricular block, 415, 419*

RS COMPLEX, 13

RSR' PATTERN

- in ECG, 138-45, 502-503*
- with mitral stenosis, 152*, 187-88
- in VCG, 149, 150-55, 502-503*

RS-T INTERVAL AND SEGMENT, see S-T Segment

REFERENCE FRAMES (OR SYSTEMS)

- hexaxial, 27-29, 38-39
 - corrected—application of, 50*
 - revised, based on lead vectors, 48, 49*
- horizontal or precordial, 19, 28-31
- trial, 23, 24*
- vectorcardiographic, 98
 - expression in terms of scalar leads, 98
- RENAL FAILURE: acute, with hyperkalemia, 471-77*
- REPOLARIZATION, 5*, 7
 - see also Ventricular Repolarization
 - equivalent dipole representation, 7*
 - opposition of effects, 71
 - potential variations during, 11-13
- RHEUMATIC FEVER: arrhythmias in, 360*, 542*
- RIGHT VENTRICULAR PREPONDERANCE
 - pathologic—VCG diagnosis, 163
 - physiologic, 159, 162*

S

S WAVE(S)

- in children (normal), 161
- in chronic cor pulmonale, 154*, 507*
- terminal, in left bundle branch block, 329

SI-QIII PATTERN in pulmonary embolism (acute), 217, 218-20*

SI-SII-SIII PATTERN, 199, 507*

S-T INTERVAL, 67, 70

S-T SEGMENT, 67, 70

- in bundle branch block
 - left, 226
 - with infarction, 323, 329
 - right, 247
- in coronary artery disease, 340-42
- deviations with exercise, 343-44, 348*
- digitalis effect, 467, 507*
- in myocardial infarction, 263*, 264, 323, 329, 526*
- posterolateral, 307-308
- persistent elevation, in ventricular aneurysm, 333-34
- and T wave, 70-71
- in ventricular hypertrophy, 123
- left, 128, 129, 130

S-T VECTOR

- injury vector, in myocardial injury, 258*, 259
- in left bundle branch block, incomplete, 234-35*, 236
- in myocardial infarction, 287-88
- in myocardial injury, 257, 258*
- in ventricular hypertrophy
 - left, 134, 135-37*
 - right, 151-52*, 155

in ventricular pre-excitation, 486*, 489

SCALAR QUANTITY, 13

SEPTAL DEFECT(S)

- atrial
 - with pulmonary hypertension, 160
 - with right-to-left shunt, 179-80
- interatrial
 - with left-to-right shunt, 178-79
 - with pulmonary stenosis, 179
 - with right ventricular hypertrophy in, 153, 502*
- interventricular, 174-76
- ECG and VCG findings, 175, 503*
- of septum primum, 179*
- ventricular, 503*

SEPTUM

- see also Septal Defects
- depolarization in left bundle branch block with infarction, 326
- interventricular activation, 117
- anatomy, 117
- fibrosis, 332
- infarction, 331-32
 - with left bundle branch block, 324-26*, 327, 331

SINOATRIAL BLOCK, 455-60

SINOATRIAL PAUSE AND ARREST, 455, 460

SODIUM IONS: transmembrane flow in myocardial cell, 3, 4

STENOSIS

- aortic congenital, 501*
- and subaortic, 172
- congenital, causing ventricular overload, 170-74
- mitral, see Mitral Stenosis
- pulmonic, see Pulmonary Diseases
- STOKES-ADAMS ATTACKS, 560-61*
- STRESS TESTS, 342-50
 - anovemia test, 342
 - exercise test, 343-50

T

T WAVE(S), 68

- in bundle branch block, 68-87
- left, with infarction, 323, 329
- right, 247
- changes
 - primary, 81*, 84-87
 - secondary, 84-87
- in children (normal), 161, 162*
- digitalis effects, 467
- in myocardial infarction, 263*, 265
- posterolateral, 307-308
- "nonspecific abnormalities" in coronary insufficiency, 340
- postectopic changes, 398-401
- regression (T_R), 75
- and QRS complex, 74*

and spatial QRS-T angle, 88
in ventricular extrasystole, 395
in ventricular hypertrophy, 122-23
left, 128, 129, 130
right, 146, 147

TACHYCARDIAS

atrial, 407, 408, 411-12*, 414*,
419*, 552*, 571*

ectopic

atrioventricular nodal, 371, 552*,
563*

digitalis effect, 466, 565*
effects of vagal stimulation and
drugs, 466-67

exercise effects, 466
paroxysmal ectopic, 407-30, 488*

recurrent, in Wolff-Parkinson-
White syndrome, 459-93

supraventricular, 407, 408*, 409-
25, 550-51*

paroxysmal ventricular, 420-26*,
427-30, 565* 570*

alternating bidirectional, 423*,
428-48*, 429, 556-57*, 564*

clinical significance, 430
differential diagnoses, 411, 429-
30

sinus, 560, 558*, 560-61*

TALL R PATTERN

in cyanotic congenital heart dis-
ease, 151*

in left bundle branch block, 231*
normal in infants and children, 159,
162*

in right ventricular hypertrophy
in ECG, 138-45
in VCG, 148-50, 185*

in tetralogy of Fallot, 151*

Ta (Tp) wave, 35, 54

TETRALOGY OF FALLOT, 151*, 182,
503*

TIME (ECG) measurements, 34-36

TRANSITIONAL (EQUIPHASIC OR EQUI-
POTENTIAL) COMPLEX, 38, 57

TRANSITIONAL PATHWAY, 41

TRICUSPID, 383, 398*, 557*

TRILEAF OF FALLOT, 179-80

TRICUSPID ARTERIOSUS pseudo-, 182

U

U WAVES, 71, 567*

V

VAGAL STIMULATION
see also Carotid Sinus Stimulation
effects on

atrial fibrillation, 439, 440*, 466

atrial flutter, 439, 441*, 466

tachycardia, 466

VECTOR(S)
see also Mean Instantaneous Vec-
tor(s)

addition (composition), 13
parallelogram method, 13, 14*

simple consecutive—method, 13,
18*

triangle method, 13, 14*

components of, 15
determination of magnitude, 15-
16

current of injury
diastolic (I), 258, 257*

systolic (-I), 258*, 259

definition, 13
gradient, 77*, 79

infarction, 260*, 261, 262*

in left bundle branch block and
free wall infarction, 328*

injury, 258-59
in ventricular aneurysm, 333*,
334

length and direction of resultant of
2 vectors, method of determin-
ing, 15

pre- and postinfarction, 260*, 261,
262*

projection, trigonometry for, 15
quantity, 13

representation
of cardiac dipole, 13, 14*

of cardiac electrical forces, 17-
19

resultant, 13, 17
resultant vector concept, 13, 17
and cardiac positions (ECG),
62*, 64

spatial (cardiac), 15*, 19
vertical component, 49*, 50, 51*

X, Y and Z components, 15*, 19

subtraction—method, 14*, 15

VECTOCARDIOGRAMS
in acute cor pulmonale, 219-20

in chronic cor pulmonale
P pulmonale pattern, 196, 198,
207*

QRS sE loop patterns, 201-16
in chronic emphysema without cor
pulmonale, 507*, 509*

P pulmonale pattern 196
QRS sE in, 201-16, 507*

in coarctation of aorta, 171-72
determination of scalar lead deflections
from, 99-102

in dextrocardia, 181*, 182

in intracardiac defect with left-to-
right shunt, 178-79

in interventricular septal defect,
175

in left bundle branch block, 227-
31

incomplete, 233-34
—QRS sE loop, 233-38

—S-T vector, 234-35*, 236

—T sE loop, 234-35*, 236
—variant type, 236, 237-39*,
240

in mitral stenosis, QRS sE loop
patterns, 188-91, 201-11

in myocardial infarction, 261-65,
266-67

anterior, 263-66, 267, 519*,
532*, 567*

anterolateral, 281*, 282, 283

anteroseptal, 271-72, 515-17*,
532*

with bundle branch block, 320
—left, 325-28, 330-31, 533*,
562*

—right, 321-22, 562*, 567*

diaphragmatic, 291-99, 520-
21*, 526-28*

postrolateral, 302-303, 306-
308*, 523*, 525*

strictly anterior, 275*, 276-78

strictly posterior, 310-13, 314-
15, 525*

in myocardial injury, 258*, 259

in myocardial ischemia, 253, 250

normal, 105-15, 498*

in infants and children, 159-63,
497*

in patent ductus arteriosus, 177

in right bundle branch block, 247-
53, 512-14*

in tetralogy of Fallot, 180

in ventricular hypertrophy
left, 131-37, 499-501*, 516*

right, 149-55, 502-506*

in ventricular pre-excitation, 464-
68*, 468-69

group A, 464*, 466*, 468, 535*

group B, 463, 469, 538-40*

VECTOCARDIOGRAPHY
electrode placement and lead sys-
tems, 93-98

corrected lead systems, 43-44,
97-98

cube lead system (Crashman),
91-97

equilateral tetrahedron, 93-94

orthogonal, 93, 94-97

instrumentation, 92

loops, 92-93
see also Loops

oscilloscope for, 92

VENTRICLES

digitalis effect, 464

effective sites, 117-18

free walls, 117

infarction
of free wall (left), 327-29
—with left bundle branch block,
327

right, 259

neonatal characteristics, 159

right ventricular preponderance
pathologic—VCG diagnosis, 163

physiologic, 159, 162*

VENTRICULAR ABERRATION(s), 377
 in atrial extrasystole, 389-91
 in atrial fibrillation, 431*, 432
 of atrioventricular nodal escape beats, 379-80*, 381-82
 in supraventricular tachycardia, 409

VENTRICULAR ACTIVATION TIME, 58, 67
 in hypertrophy, 122, 124

VENTRICULAR DEPOLARIZATION, 17

VENTRICULAR FLUTTER AND FIBRILLATION, 443-45, 558*

VENTRICULAR GRADIENT, 71-88
 constriction from ECG, 84*, 85-86
 in myocardial ischemia, 87-88

VENTRICULAR HYPERTROPHY
 activation time in, 122, 124
 combined, 150-56
 ECG diagnosis, 156, 503*
 in patent ductus arteriosus, 177
 QRS sE loop suggestive of, 177, 503*
 VCG findings, 157, 503*
 ECG in, 123-24
 electrical effects, 118-24
 in infancy and childhood, 159-61
 left—ECG diagnosis, 184
 right—ECG diagnosis, 163
 left
 with anteroseptal infarction (healed), 272*
 in coarctation of aorta, 171
 ECG in, 125-31, 135-37*, 499-501*, 518*
 —evaluation, 130
 —résumé, 129-30
 figure-of-8 pattern, 131
 mean instantaneous QRS spatial vectors in, 125-28
 QRS sE loop in, 131
 S-T segment in, 128, 129, 130
 "with terminal conduction delay," 510-11*
 —and left bundle branch block with free wall infarction, 329
 —and right bundle branch block, 236, 237-39*, 240, 251-52
 T wave in, 128, 129, 130
 T sE and S-T vector in, 134, 135-37*
 VA vectors in, 125-28
 VCG in, 131-37, 499-501*, 518*
 ventricular repolarization in, 128
 mean instantaneous QRS spatial vector in, 118-22, 123-24
 right
 in chronic cor pulmonale, 165-68

—ECG patterns, 197*, 199-201, 506*, 508*

—factors affecting ECG patterns, 166-68

concentric, of wall, in atrial septal defect, 178

in congenital heart disease, 163-68

differentiation from healed posterolateral infarction and classic right bundle branch block, 306-307

ECG in, 138-47, 174-75*, 502-506*

—résumé, 146-47

in Eisenmenger's complex, 181*

in emphysema with cor pulmonale, 193-94

figure-of-8 pattern, 149, 152*, 155

in interatrial septal defect, 178, 179*

in mitral stenosis, 165-68, 184, 185-86*, 187-88

in patent ductus arteriosus, 176-77

in pulmonary stenosis, 173

QRS in preordial leads in tall R and RSR' patterns, 143-45

QRS sE loops in, 148-55
 —transition from type C to type B, 215*, 216
 —type B in, 189, 190*, 207, 212-13*, 215*, 216
 RSR' pattern (ECG) in, 138-45, 187-88
 RSR' pattern (VCG) in, 149, 150-55
 S-Su-Su pattern, 199
 T wave and S-T segment in, 146, 147
 tall R pattern (ECG) in, 138-45
 tall R pattern (VCG) in, 148-50, 185*
 in tetralogy of Fallot, 162
 VA vectors in, 138-45
 VCG in, 148-55, 502-506*
 ventricular repolarization in, 149
 with right bundle branch block, 252-54
 T wave and S-T segment in, 122-23

VENTRICULAR OVERLOADING
 composite, 168, 170n
 diastolic left, 174-77
 diastolic right, 178-80
 effect on patterns of right ventricular hypertrophy in congenital heart disease, mitral stenosis and chronic cor pulmonale, 167-68

systolic left, 170-72
 systolic right, 172-74

VENTRICULAR PRE-EXCITATION, 480-83
 see also Wolff-Parkinson-White Syndrome
 ECG findings, 483-88, 491*, 493*
 group A, 483-84*, 486*, 487, 490-92*, 538*, 572*
 group B, 483*, 485*, 487, 538-40*
 effects of carotid sinus stimulation and drugs on, 487
 mechanism—theories of, 480
 VCG findings, 484-88*, 488-49
 group A, 484*, 486*, 488, 538*
 group B, 485*, 489, 538-40*

VENTRICULAR REPOLARIZATION, 17
 in bundle branch block
 left, 225
 right, 247
 in myocardial infarction
 acute anterior, 287-88
 diaphragmatic, 206*, 297-99
 posterolateral, 303
 in ventricular hypertrophy
 left, 126
 right, 146
 in ventricular pre-excitation, 489

VENTRICULAR STRAIN
 patterns, 158
 right, 168
 in chronic cor pulmonale, 201

VOLTAGE
 in lead
 inverse relation to cube of distance between heart and electrode, 19
 relation to dipole moment and angle θ , 11, 18
 relation to vector projection on lead axis, 18
 measurements, 34-36

IV

WEDENSKY FACILITATION, 386, 387

WEDGE PRESSURE, 183

WENCKEBACH PHENOMENON, 357, 358*, 375*, 383, 412, 413-15*
 in atrioventricular block, 449-52, 559*
 in sinoatrial block, 455, 456-60*

WOLFF-PARKINSON-WHITE SYNDROME, 480-93, 572*
 see also Ventricular Pre-excitation
 clinical aspects, 493
 heart action in, 486*, 489-93

